

Organometallic Chemistry

SECOND EDITION

Gary O. Spessard

Gary L. Miessler

St. Olaf College

Northfield, Minnesota

Oxford New York

OXFORD UNIVERSITY PRESS

2010

Oxford University Press, Inc., publishes works that further Oxford University's objective of excellence in research, scholarship, and education.

Oxford New York
Auckland Cape Town Dar es Salaam Hong Kong Karachi
Kuala Lumpur Madrid Melbourne Mexico City Nairobi
New Delhi Shanghai Taipei Toronto

With offices in
Argentina Austria Brazil Chile Czech Republic France Greece
Guatemala Hungary Italy Japan Poland Portugal Singapore
South Korea Switzerland Thailand Turkey Ukraine Vietnam

Copyright © 2010 by Oxford University Press, Inc.

Published by Oxford University Press, Inc.
198 Madison Avenue, New York, New York 10016
<http://www.oup.com>

Oxford is a registered trademark of Oxford University Press

All rights reserved. No part of this publication may be reproduced, stored in a retrieval system, or transmitted, in any form or by any means, electronic, mechanical, photocopying, recording, or otherwise, without the prior permission of Oxford University Press.

Library of Congress Cataloging-in-Publication Data

Spessard, Gary O.

Organometallic chemistry / Gary Spessard, Gary Miessler.—2nd ed.
p. cm.

Includes bibliographical references and index.

ISBN 978-0-19-533099-1 (hardcover : alk. paper) 1. Organometallic chemistry. I. Miessler, Gary L., 1949– II. Title.

QD411.S65 2010

547'.05—dc22 2009019010

Printing number: 9 8 7 6 5 4 3 2 1

Printed in the United States of America
on acid-free paper

FIGURES

Chapter 1		
Figure 1-1	Examples of Sandwich Compounds	2
Figure 1-2	Examples of Cluster Compounds	3
Figure 1-3	Anion of Zeise's Compound	4
Figure 1-4	Conformations of Ferrocene	7
Figure 1-5	Vitamin B ₁₂ Coenzyme	10
Chapter 2		
Figure 2-1	<i>s</i> , <i>p</i> , and <i>d</i> Orbitals	16
Figure 2-2	Interactions between Waves	19
Figure 2-3	Molecular Orbitals of H ₂	22
Figure 2-4	Molecular Orbitals of O ₂	23
Figure 2-5	Molecular Orbitals of CO	25
Figure 2-6	Molecular Orbitals of Linear H ₃ ⁺	30
Figure 2-7	Molecular Orbitals of CO ₂	33
Figure 2-8	π Molecular Orbitals for π -C ₃ H ₅	35
Figure 2-9	Construction of π Orbitals of Butadiene from Group Orbitals of Ethylene	37
Figure 2-10	Molecular Orbitals of Cyclic H ₃ ⁺	38
Figure 2-11	Molecular Orbitals for Cyclic π Systems	41
Figure 2-12	π Molecular Orbitals of Benzene	42
Chapter 3		
Figure 3-1	Molecular Orbitals of Cr(CO) ₆ (Only interactions between ligand (σ and π^*) orbitals and metal <i>d</i> orbitals are shown.)	65
Figure 3-2	A <i>t</i> _{2g} Orbital of Cr(CO) ₆	66
Figure 3-3	An <i>e</i> _g [*] Orbital of Cr(CO) ₆	68
Figure 3-4	Exceptions to the 18-Electron Rule	69

Figure 3-5	Relative Energies of Metal d Orbitals for Complexes of Common Geometries	70
Figure 3-6	Examples of Square Planar d^8 Molecules	70
Figure 3-7	Molecular Orbitals of Square Planar Complexes (Only σ donor and π acceptor interactions are shown.)	71
Chapter 4		
Figure 4-1	Selected Molecular Orbitals of N_2 and CO	76
Figure 4-2	σ and π Interactions between CO and a Metal Atom	76
Figure 4-3	Bridging versus Terminal Carbonyls in $Fe_2(CO)_9$	81
Figure 4-4	Bridging CO in $[(\eta^5-C_5H_5)Mo(CO)_2]_2$	82
Figure 4-5	Binary Carbonyl Complexes	83
Figure 4-6	Oxygen-Bonded Carbonyls	87
Figure 4-7	Linear and Bent NO	89
Figure 4-8	Covalent and Ionic Approaches to Bonding in NO Complexes	90
Figure 4-9	Examples of NO Playing Multiple Roles	91
Figure 4-10	P_4 , $[Ir(CO)_3]_4$, $P_3[Co(CO)_3]$, and $Co_4(CO)_{12}$	98
Chapter 5		
Figure 5-1	Bonding in Ethylene Complexes	104
Figure 5-2	Examples of Allyl Complexes	105
Figure 5-3	Bonding in η^3 -Allyl Complexes	105
Figure 5-4	Examples of Molecules Containing Linear π Systems	106
Figure 5-5	Bonding in <i>s-cis</i> -Butadiene Complexes	107
Figure 5-6	Group Orbitals for the C_5H_5 Ligands of Ferrocene	110
Figure 5-7	Bonding Molecular Orbital Formed from d_{yz} Orbital of Iron in Ferrocene	111
Figure 5-8	Antibonding Molecular Orbital Formed from d_{yz} Orbital of Iron in Ferrocene	112
Figure 5-9	Molecular Orbital Energy Levels in Ferrocene	113
Figure 5-10	Molecular Orbitals of Ferrocene Having Greatest d Character	114
Figure 5-11	Reaction of Cobalticinium with Hydride	115
Figure 5-12	Electrophilic Substitution with Acylium Ion on Ferrocene	116
Figure 5-13	Structure of $[Ti(\eta^5-P_5)_2]^{2-}$	116
Figure 5-14	Complexes Containing C_5H_5 and CO	117
Figure 5-15	Examples of Chromium Complexes Containing Linked and Fused Six-Membered Rings	123
Figure 5-16	Half Sandwich Complexes Containing $\eta^6-C_6H_6$	123

Figure 5-17	Examples of Bonding Modes of Cyclooctatetraene	125
Figure 5-18	Bonding in Uranocene	126
Figure 5-19	Multiple–Decker Sandwich Compounds	127
Figure 5-20	Proposed Isomer of Ferrocene	127
Figure 5-21	Ring Whizzer Mechanism	132
Chapter 6		
Figure 6-1	Structure of $\text{Re}(\text{CH}_3)_6$	139
Figure 6-2	π Bonding in Carbene Complexes and in Alkenes	142
Figure 6-3	Delocalized π Bonding in Carbene Complexes (E designates a highly electronegative heteroatom such as O, N, or S.)	143
Figure 6-4	Resonance Structures and <i>cis</i> and <i>trans</i> Isomers of $\text{Cr}(\text{CO})_5[\text{C}(\text{OCH}_3)\text{C}_6\text{H}_5]$	144
Figure 6-5	Bonding in Carbyne Complexes	146
Figure 6-6	Complexes Containing Metal–Carbon Single, Double, and Triple Bonds	147
Figure 6-7	Carbide and Alkylidyne Complexes	148
Figure 6-8	Metallacumulene Complexes	151
Figure 6-9	Bonding in Dihydrogen Complexes	153
Figure 6-10	Examples of Agostic Interactions	155
Figure 6-11	Bonding between Phosphines and Transition Metals (traditional view)	155
Figure 6-12	Pi Acceptor Orbitals of Phosphines (revised view)	156
Figure 6-13	Ligand Cone Angle	158
Figure 6-14	C_{60} and C_{70}	161
Figure 6-15	Fullerene Complex of Platinum	162
Figure 6-16	Bonding of C_{60} to Metal	163
Figure 6-17	$[(\text{Et}_3\text{P})_2\text{Pt}]_6\text{C}_{60}$	164
Figure 6-18	$(\eta^2\text{-C}_{70})\text{Ir}(\text{CO})\text{Cl}(\text{PPh}_3)_2$	165
Figure 6-19	$(\mu_3\text{-}\eta^2\text{:}\eta^2\text{:}\eta^2\text{-C}_{60})\text{Ru}_3(\text{CO})_9$	165
Figure 6-20	Mass Spectrum of $(\eta^5\text{:}\eta^5\text{-C}_{10}\text{H}_8)\text{Mo}_2(\text{CO})_6$	167
Figure 6-21	Isotope Patterns of Mo and Mo_2	168
Figure 6-22	APCI Spectrum of $[\text{Cp}(\textit{tfd})\text{W}(\mu\text{-S})_2\text{W}(=\text{O})\text{Cp}]$ (Upper: Actual spectrum; lower: calculated spectrum based on molecular formula and isotope distributions.)	169
Chapter 7		
Figure 7-1	Spectral and Structural Characteristics of Pt(II) Complexes	180

Figure 7-2	Activation Energy and the <i>trans</i> Effect (The depth of the energy curve for the intermediate and the relative heights of the two maxima will vary with the specific reactants.)	183
Figure 7-3	HOMO–LUMO Interactions of Hard and Soft Acids and Bases	187
Figure 7-4	Ligand Substitution of a Square Planar Complex	188
Figure 7-5	Intermediates in the Substitution of $M(\text{CO})_5\text{X}$ Complexes	193
Figure 7-6	The Relationship of Transition State to Reaction Coordinate—The Hammond Postulate	195
Figure 7-7	Reaction Progress–Energy Diagram for the Addition of H_2 to Vaska’s Compound	206
Figure 7-8	Interactions of Frontier Orbitals and H_2 Molecular Orbitals	207
Figure 7-9	“Perpendicular” Approach of H_2 to Metal Complex	207
Figure 7-10	Interactions of Frontier Metal and C–H Molecular Orbitals	211
Figure 7-11	Stereochemical Probes	224
Figure 7-12	Pd(II) Complexes Used for Reductive Elimination Studies	231
Chapter 8		
Figure 8-1	Possible Mechanisms for CO Insertion Reactions	246
Figure 8-2	Mechanisms of Reverse Reactions for CO Migration and Alkyl Migration Related to Experiment II	248
Figure 8-3	Mechanisms of Reverse Reactions for CO Migration and Alkyl Migration Related to Experiment III	249
Figure 8-4	Classification of π Ligands	271
Figure 8-5	Relative Reactivity of π Ligands	271
Figure 8-6	π MOs of Allyl and 1,3-Butadiene	273
Figure 8-7	π -MOs of Unsymmetrical Allyl Ligands	277
Figure 8-8	Reactivity at Different Sites on Metal–Arene Complexes	281
Chapter 9		
Figure 9-1	Reaction Progress versus Energy Diagrams for a Catalyzed and Uncatalyzed Reaction	313
Figure 9-2	A Schematic View of the Mechanism of Chymotrypsin-Catalyzed Amide Hydrolysis Occurring at the Enzyme Active Site	319
Figure 9-3	Stereoisomer of Metolachlor	379
Chapter 10		
Figure 10-1	Molecular Orbital Diagram for Triplet and Singlet Free Carbene	396

Figure 10-2	Influence of a Heteroatom Substituent on the Electronic State of a Free Carbene	397
Figure 10-3	(a) Interaction between a Singlet Free Carbene and a Metal; (b) Interaction between a Triplet Free Carbene and a Metal	401
Figure 10-4a	Molecular Orbital Picture of a Fischer Carbene Complex	402
Figure 10-4b	Molecular Orbital Picture of a Schrock Carbene Complex	403
Figure 10-5	π Donation in <i>N</i> -Heterocyclic Carbenes	405
Figure 10-6	Some Important <i>N</i> -Heterocyclic Carbenes	406
Figure 10-7	Reactive Sites of Transition Metal–Carbene Complexes	420
Figure 10-8	Frontier Orbital Interactions in Nucleophilic Attack on Fischer Carbene Complexes	421
Figure 10-9	The LUMOs of (a) Methyl Acetate and (b) Acetone	422
Figure 10-10	The HOMO of $F_3Nb=CH_2$	427
Figure 10-11a	Molecular Orbital Bonding Scheme for a Fischer Carbyne Complex	442
Figure 10-11b	Molecular Orbital Bonding Scheme for a Schrock Carbyne Complex	443
Figure 10-12a	LUMO of a Cationic Fischer Carbyne Complex	447
Figure 10-12b	LUMOs of a Neutral Fischer Carbyne Complex Showing Only the $M-C_{\text{carbyne}}$ Interactions	448
Chapter 11		
Figure 11-1	Possible Dyad Tacticity and Double Bond Configurations Associated with ROMP of Norbornene	482
Figure 11-2	<i>Cis</i> -Syndiotactic and <i>trans</i> -Isotactic Configuration during ROMP of Norbornene	482
Figure 11-3	Some Common Stereochemistries Resulting from <i>Z</i> - <i>N</i> Polymerization of Propene and Other 1-Alkenes	501
Figure 11-4	Modes of Approach and Insertion of Prochiral Propene onto a Metal Site and Growing Polymer Chain	503
Figure 11-5	Primary and Secondary Insertion of Propene in a Growing Polymer Chain	503
Figure 11-6	Molecular Orbital Correlation Diagram for σ Bond Metathesis	511
Chapter 12		
Figure 12-1	Chiral Diphosphine Ligands	529
Figure 12-2	Free-Energy versus Reaction Progress Diagram for the Rate-Determining Step of Asymmetric Hydrogenation	531
Figure 12-3	Ru(II)-BINAP/Diamine Catalysts	540

Figure 12-4	A Predictive Model for Enantioselection in Asymmetric Oxidation of Secondary Alcohols	551
Figure 12-5	The Relationship of Enantioselective Desymmetrization to Sense of Phosphine Orientation in C_2 -Symmetric Bisphosphine–Bisamide Ligands	562
Figure 12-6	Chiral Ligands That Promote Asymmetric Hydroformylation	573
Figure 12-7	Regioselectivity of Addition of an Aryl Halide to Various Alkenes during Heck Olefination	578
Chapter 13		
Figure 13-1	Octahedral and Tetrahedral Fragments	641
Figure 13-2	Orbitals of Parent Structures CH_4 and ML_6	641
Figure 13-3	Seven- and 17-Electron Fragments	642
Figure 13-4	Six- and 16-Electron Fragments	642
Figure 13-5	Molecules Resulting from the Combination of Isolobal Fragments	643
Figure 13-6	Isolobally Related Three-Membered Rings	644
Figure 13-7	Isolobally Related Tetrahedral Molecules	644
Figure 13-8	Isolobal $Au(PPh_3)_3$ and H	648
Figure 13-9	Coordinate System for Bonding in $B_6H_6^{2-}$	651
Figure 13-10	Bonding in $B_6H_6^{2-}$	652
Figure 13-11	<i>Closo</i> , <i>Nido</i> , and <i>Arachno</i> Borane Structures	654
Figure 13-12	Structures of <i>Closo</i> , <i>Nido</i> , and <i>Arachno</i> Boranes	654
Figure 13-13	Examples of Heteroboranes	657
Figure 13-14	Organometallic Derivatives of B_5H_9	659
Figure 13-15	Orbitals of Isolobal Fragments BH and $Fe(CO)_3$	659
Figure 13-16	Comparison of $C_2B_9H_{11}^{2-}$ with $C_3H_5^-$ (Each B and C atom also has a terminal H atom, not shown.)	660
Figure 13-17	Carborane Analogues of Ferrocene	661
Figure 13-18	Carbon- and Nitrogen-Centered Clusters	666
Figure 13-19	Bonding Interactions between Central Carbon and Octahedral Ru_6	667

PREFACE

Organometallic chemistry is an exciting and rapidly-expanding field that has changed considerably over the 12 years intervening between the first edition of our textbook and the appearance of this new edition. Since 1997, six organometallic chemists have been honored as Nobel Laureates because their work has had such an enormous impact, not only on the field but also to related areas of the chemical sciences, especially organic synthesis. The first edition indicated that π -bond metathesis would have significant bearing on the course of organometallic chemistry. We now realize that the applications of metathesis to organic synthesis constitute one of the most significant advances in the ability to construct complex molecules to occur in the past 50 years. The ready availability of user-friendly software and high-speed computers has made computational chemistry and molecular modeling important and routinely used tools for the elucidation of organometallic reaction mechanisms. High-level molecular orbital calculations have helped unravel the mysteries of catalytic cycles and allowed chemists to develop new chemistry based on the results and predictions of these computations. Recent developments in organometallic chemistry have been highly beneficial to practitioners of materials science, who produce exciting new substances, often through organotransition metal-catalyzed polymerization reactions.

DISTINCTIVE FEATURES OF THE SECOND EDITION

Written with both undergraduate and graduate students in mind, *Organometallic Chemistry* introduces both audiences to their first in-depth study of the subject. The undergraduate audience will appreciate the logical progression of topics in the early chapters that results in a careful and rigorous, but gentle introduction to concepts of structure and bonding of organometallic compounds. We anticipate that the graduate audience will find these early chapters a useful review of organic and inorganic chemistry concepts now applied specifically to organotransition metal complexes. Later chapters build on this foundation and take both undergraduates and graduates to new levels of understanding

by introducing rigorous coverage of organometallic reaction mechanisms and more advanced topics of catalysis, carbene complexes, metathesis, applications of organometallic chemistry to organic synthesis, and cluster compounds. Both audiences will benefit from the careful explanations, numerous exercises, clear illustrations, and coverage of key experiments.

Numerous in-chapter worked examples and expansive end-of-chapter problem sets reinforce fundamental concepts covered in the chapters. End-of-chapter problems cover a wide range of difficulty, from basic practice problems to more advanced analytical types of problems, and many of these are referenced directly to the current chemical literature.

An experimental approach is employed to teach students not only what is known about organometallic chemistry, but also how we know what we know. Therefore, the text includes discussions of both classic and contemporary experiments that have revealed the fundamental concepts underlying the subject.

Real-world applications are highlighted throughout the text to engage students and reveal the relevance of organometallic chemistry to everyday life, especially as it impacts the world of industry.

WHAT IS NEW IN THE SECOND EDITION

The focus of our second edition remains organotransition metal chemistry, and the order of topics is substantially the same as that found in the first edition. As a thematic overview, readers will benefit from the following changes:

- **Updated and expanded coverage** of the latest developments from the field, including IR, NMR, and mass spectroscopy; catalysis; carbene complexes; metathesis and polymerization; and applications to organic synthesis.
- **Increased presentation of industrial applications**, including hydroformylation; Grubbs and Schrock metal carbene catalysts; SHOP; palladium-catalyzed cross-couplings; and more.
- **New emphasis on green chemistry** reveals how well the principles of organotransition metal catalysis meld with the principles of green chemistry.
- **New computational approaches** to molecular orbital calculations.
- **Increased number and variety of end-of-chapter problems and worked examples.** The new edition includes over 80% more end-of-chapter problems and 50% more in-chapter worked examples than the previous edition. The problems cover a broad range of difficulty, and many of the end-of-chapter exercises are referenced directly to the original literature.

- **More molecular model illustrations.** The text now includes over 600 illustrations and structures, a 25% increase over the previous edition. A total of 120 figures are brand new, and all preexisting figures have been revised for clarity and consistency.

Detailed Chapter-by-Chapter Revisions

Chapter 2 retains its emphasis on a qualitative approach to molecular orbital theory; however, we have also added a section on computational chemistry. The thrust of this new section introduces readers to approaches to molecular orbital and molecular mechanics calculations employed by readily available commercial software packages. We make no attempt to thoroughly explain the theory behind these approaches, but instead we emphasize what each method can do and how it is applied to real chemical systems. Both qualitative and computational approaches to MO theory appear again throughout the text.

Chapter 3 introduces the 18-electron rule as a basis to help understand the bonding of several types of ligands to transition metals. These ligand types are covered in Chapters 4–6, where readers will discover how ligands combine with metals to form many unique and exquisitely beautiful structures that are quite distinct from those found in organic chemistry.

We have expanded coverage of spectroscopy in several ways. **Chapter 4** introduces the use of infrared spectroscopy, especially its applications to carbonyl complexes. C-13 and H-1 nuclear magnetic resonance spectroscopy are emphasized in **Chapter 5** and P-31 NMR is introduced in **Chapter 6**. New to the second edition is the inclusion of a section on mass spectroscopy in Chapter 6. Chapters 4–6 contain numerous end-of-chapter problems, where spectroscopic information is an essential part of the exercise. Subsequent chapters have additional spectroscopy problems.

Once readers understand the basic tenets of structure and bonding, they are ready to become acquainted with several kinds of reactions that involve organotransition metal complexes. **Chapter 7** covers reactions that occur primarily at the metal. It has been expanded to include new material on C–H and C–C bond activation, an exciting area of organometallic chemistry with applications to the petrochemical industry and organic synthesis. **Chapter 8** examines reactions that occur primarily on ligands attached to the metal, and the material in this chapter has been updated from the first edition. The reactions discussed in these two chapters appear again extensively in Chapters 9–12. We have tried wherever possible in Chapters 7 and 8 to point out obvious parallels of organometallic reactions to reactions in organic chemistry.

Catalysis plays an increasingly important role in all areas of chemistry. One of the major tenets of green chemistry is the use of catalysts instead of stoichiometric reagents wherever possible. Reactions catalyzed by organotransition

metals play key roles in industrial processes and in the laboratories of synthesis chemists. **Chapter 9** has been expanded to include information on hydrocyanation and the use of catalysis in the production of specialty chemicals. Since the publication of our first edition, green chemistry has become an increasingly important area. Originating in the industrial sector, green chemistry now plays an important role in the teaching laboratory, where significant efforts to make experiments more environmentally friendly are ongoing and bearing fruit. Chapter 9 (Catalysis) introduces some of the basic tenets of green chemistry, and green applications to organometallic chemistry are mentioned often, especially in Chapter 12, where applications of organometallic chemistry to organic synthesis are covered.

Chapter 10 in the first edition covered metal carbene complexes, metathesis, and polymerization reactions. The chapter has now been split into two chapters. **Chapter 10** now emphasizes the chemistry of carbene complexes; new material on *N*-heterocyclic carbene complexes, with applications in synthesis, has been introduced. **Chapter 11** now considers metathesis and polymerization. The sections on the discovery and elucidation of π -bond metathesis have been rewritten and expanded. The discussion of both metathesis and Ziegler–Natta polymerization reactions has been considerably enhanced and brought up to date.

Application of organometallic chemistry to the synthesis of complex organic molecules continues to be one of the most interesting and exciting areas of organotransition metal chemistry. **Chapter 12** updates material on asymmetric hydrogenation by considering Ir-catalyzed hydrogenation and new developments in Ru-catalyzed asymmetric hydrogenation. Asymmetric oxidation, which may have broader applications than hydrogenation, is now covered. Most of Chapter 12 emphasizes the use of organotransition metal compounds to catalyze the formation of new C–C bonds, often under asymmetric conditions. The chapter now includes enhanced sections on the Tsuji–Trost reaction, Heck olefination, and cross-coupling reactions. Whereas the first edition only considered Stille cross-coupling, Chapter 12 now includes material on the Suzuki, Sonogashira, and Negishi cross-coupling reactions, which have had enormous impact on synthesis in recent years.

Chapter 13 in the first edition covered a variety of topics relating to applications of organometallic chemistry to other areas of science. This material has been eliminated with the exception of material on fullerenes, which now appears in Chapter 6. Chapter 13 updates the discussion of the isolobal analogy and cluster chemistry, which was the purview of Chapter 12 in the first edition.

Organometallic compounds are unique, useful, and esthetically pleasing. We hope readers of our book will also find this to be true and will learn much about a most important and interesting field of chemistry.

SUPPLEMENTS

The following supplementary items are available to instructors who adopt the second edition:

Instructor's Resource CD-ROM includes all figures from the text in electronic format and the solutions manual files containing the solutions to all exercises and problems from the textbook in editable Word file format. Please contact your publisher sales representative.

ACKNOWLEDGMENTS

Production of the second edition was a huge project, and it could not have been possible without the help of many individuals. First and foremost, we thank our families (Carol, Sarah, Aaron, Becky, Naomi, and Rachel) for their forbearance and constant support during countless hours the authors spent at the computer and in the library over the past two years. We would also like to express appreciation to everyone at Oxford University Press, including Jason Noe, Chemistry Editor, and Melissa Rubes, Editorial Assistant, for all their hard work. In addition, we thank Patrick Lynch, Editorial Director; John Challice, Vice President and Publisher; Adam Glazer, Director of Marketing; Preeti Parasharami, Product Manager; Steven Cestaro, Production Director; Lisa Grzan, Managing Editor; Paula Schlosser, Art Director; and Dan Niver and Binbin Li, Designers. We were aided at St. Olaf College by Karen Renneke, Chemistry Department Administrative Assistant, and student Stephanie Harstad, who provided valuable editorial contributions. Gary S. sincerely thanks the University of Arizona for allowing him full use of their library facilities.

We were privileged to have a distinguished group of educators review all or part of our manuscript for the second edition. These individuals provided extremely helpful feedback and numerous suggestions for improvement. The reviewers pointed out several errors in the manuscript that we had overlooked and have since corrected, and we are indeed grateful for their acumen. Most of the suggestions they made have been incorporated into this new edition; even if they were not, their comments forced us to refine our approach to the writing process. In addition to two reviewers who wish to remain anonymous, we specifically acknowledge the following individuals for their substantial contributions to our efforts in creating the second edition:

Merritt B. Andrus, Brigham Young University
E. Kent Barefield, Georgia Institute of Technology
Laurance G. Beauvais, San Diego State University
Holly D. Bendorf, Lycoming College
Byron L. Bennett, Idaho State University *(list continues on next p.)*

Steven M. Berry, University of Minnesota–Duluth
Paul Brandt, North Central College
Ferman Chavez, Oakland University
Kenneth M. Doxsee, University of Oregon
Eric J. Hawrelak, Bloomsburg University of Pennsylvania
Adam R. Johnson, Harvey Mudd College
Kevin Klausmeyer, Baylor University
Jay A. Labinger, California Institute of Technology
Man Lung (Desmond) Kwan, John Carroll University
Robin Macaluso, University of Northern Colorado
Joel T. Mague, Tulane University
James A. Miranda, Sacramento State University
Katrina Miranda, Arizona State University
Louis Messerle, The University of Iowa
Chip Nataro, Lafayette College
Joseph O’Connor, University of California, San Diego
Jodi O’Donnell, Reed College
Stacy O’Reilly, Butler University
Oleg Oszerv, Texas A&M University
Daniel Rabinovich, University of North Carolina–Charlotte
Seth C. Rasmussen, North Dakota State University
Kevin Shaughnessy, University of Alabama
Robert Stockland Jr., Bucknell University
Joshua Telser, Roosevelt University
Klaus H. Theopold, University of Delaware
Rory Waterman, University of Vermont
Anne M. Wilson, Butler University
Deanna L. Zubris, Villanova University

Furthermore, we are truly grateful to all our reviewers of the first edition and those individuals who provided much needed support:

Mitsuru Kubota, Harvey Mudd College
Charles P. Casey, University of Wisconsin–Madison
Philip Hampton, California State University Channel Islands
Robert Angelici, Iowa State University
Louis Hegedus, Colorado State University

Gary O. Spessard, Sierra Vista, Arizona
Gary L. Miessler, Northfield, Minnesota

BRIEF CONTENTS

Figures		xi
Preface		xvii
Chapter 1	An Overview of Organometallic Chemistry	1
Chapter 2	Fundamentals of Structure and Bonding	13
Chapter 3	The 18-Electron Rule	53
Chapter 4	The Carbonyl Ligand	75
Chapter 5	Pi Ligands	103
Chapter 6	Other Important Ligands	136
Chapter 7	Organometallic Reactions I: <i>Reactions That Occur at the Metal</i>	176
Chapter 8	Organometallic Reactions II: <i>Reactions Involving Modification of Ligands</i>	244
Chapter 9	Homogeneous Catalysis: <i>The Use of Transition Metal Complexes in Catalytic Cycles</i>	311
Chapter 10	Transition Metal–Carbene and –Carbyne Complexes: <i>Structure, Preparation, and Chemistry</i>	393
Chapter 11	Metathesis and Polymerization Reactions	456
Chapter 12	Applications of Organometallic Chemistry to Organic Synthesis	522
Chapter 13	Isolobal Groups and Cluster Compounds	640
Appendix A	List of Abbreviations	A-1
Appendix B	Answers to Exercises	A-5
Index		I-1

CONTENTS

Figures		xi
Preface		xvii
Chapter 1	An Overview of Organometallic Chemistry	1
1-1	Striking Difference	1
1-2	Historical Background	4
Chapter 2	Fundamentals of Structure and Bonding	13
2-1	Atomic Orbitals	13
2-2	Molecular Orbitals	21
2-3	Computational Organometallic Chemistry	42
Chapter 3	The 18-Electron Rule	53
3-1	Counting Electrons	53
3-2	Why 18 Electrons?	60
3-3	Square Planar Complexes	69
Chapter 4	The Carbonyl Ligand	75
4-1	Bonding	75
4-2	Binary Carbonyl Complexes	83
4-3	Oxygen-Bonded Carbonyls	86
4-4	Ligands Similar to CO	87
4-5	IR Spectra	92
4-6	Main Group Parallels with Binary Carbonyl Complexes	96
Chapter 5	Pi Ligands	103
5-1	Linear Pi Systems	103
5-2	Cyclic π Systems	107
5-3	Nuclear Magnetic Resonance Spectra of Organometallic Compounds	127

Chapter 6	Other Important Ligands	136
6-1	Complexes Containing M–C, M=C, and M≡C Bonds	136
6-2	Hydride and Dihydrogen Complexes	152
6-3	Phosphines and Related Ligands	155
6-4	Fullerene Ligands	160
6-5	Mass Spectra	165
Chapter 7	Organometallic Reactions I: <i>Reactions That Occur at the Metal</i>	176
7-1	Ligand Substitution	178
7-2	Oxidative Addition	202
7-3	Reductive Elimination	226
Chapter 8	Organometallic Reactions II: <i>Reactions Involving Modification of Ligands</i>	244
8-1	Insertion and Deinsertion	244
8-2	Nucleophilic Addition to the Ligand	267
8-3	Nucleophilic Abstraction	285
8-4	Electrophilic Reactions	289
Chapter 9	Homogeneous Catalysis: <i>The Use of Transition Metal Complexes in Catalytic Cycles</i>	311
9-1	Fundamental Concepts of Homogeneous Catalysis	312
9-2	The Hydroformylation Reaction	322
9-3	The Wacker–Smidt Synthesis of Acetaldehyde	340
9-4	Hydrogenation	350
9-5	Carbonylation of Methanol	361
9-6	Hydrocyanation	367
9-7	Specialty Chemicals	375
Chapter 10	Transition Metal–Carbene and –Carbyne Complexes: <i>Structure, Preparation, and Chemistry</i>	393
10-1	Structure of Metal Carbenes	394
10-2	Synthesis of Metal Carbene Complexes	407
10-3	Reactions of Metal–Carbene Complexes	419
10-4	Metal–Carbyne Complexes	439

Chapter 11	Metathesis and Polymerization Reactions	456
11-1	π Bond Metathesis	456
11-2	Alkyne Metathesis	486
11-3	Ziegler–Natta and Related Polymerizations of Alkenes	492
11-4	σ Bond Metathesis	507
Chapter 12	Applications of Organometallic Chemistry to Organic Synthesis	522
12-1	Enantioselective Functional Group Interconversions	524
12-2	Carbon–Carbon Bond Formation via Nucleophilic Attack on an η^3 - π Ligand: The Tsuji–Trost Reaction	555
12-3	Carbon–Carbon Bond Formation via Carbonyl and Alkene Insertion	567
12-4	Carbon–Carbon Bond Formation via Transmetalation Reactions (Cross-Coupling Reactions)	584
12-5	Carbon–Carbon Bond Formation through Cyclization Reactions	613
Chapter 13	Isolobal Groups and Cluster Compounds	640
13-1	The Isolobal Analogy	640
13-2	Cluster Compounds	650
Appendix A	List of Abbreviations	A-1
Appendix B	Answers to Exercises	A-5
Index		I-1

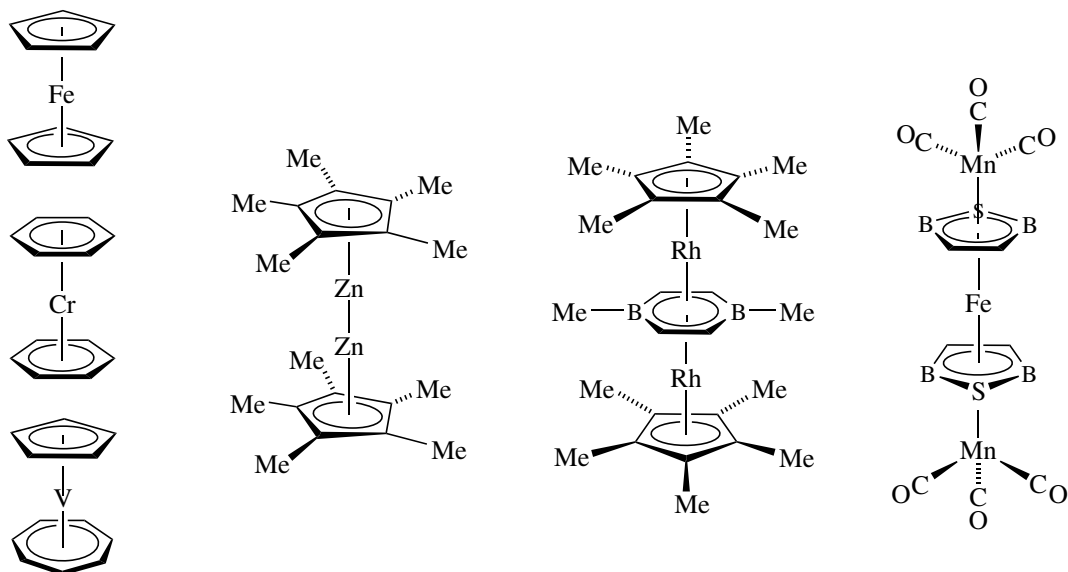
An Overview of Organometallic Chemistry

Organometallic chemistry, the chemistry of compounds containing metal–carbon bonds, is one of the most interesting and certainly most rapidly growing areas of chemical research. It encompasses a wide variety of chemical compounds and their reactions: compounds containing both sigma (σ) and pi (π) bonds between metal atoms and carbon; many cluster compounds, containing two or more metal–metal bonds; molecules containing carbon fragments that are unusual or unknown in organic chemistry; and reactions that in some cases bear similarities to known organic reactions and in other cases are dramatically different. Aside from their intrinsically interesting nature, many organometallic compounds form useful catalysts and, consequently, are of significant industrial interest. Over the past several years, organometallic reagents have played the role of promoting key steps in the total synthesis of numerous molecules, many of which are biologically active.

1-1 STRIKING DIFFERENCE

Several examples illustrate how organometallic molecules are strikingly different from those encountered in classical inorganic and organic chemistry. Ligands¹ of cyclic delocalized π systems (e.g., benzene or cyclopentadienyl) can team up with metal atoms to form “sandwich” compounds with a metal sandwiched between them. Sometimes atoms of other elements, such as phosphorus or sulfur, can be included as well. Examples of these double- and multiple-decker sandwich

¹A ligand is a molecule, ion, or molecular fragment bound to a central atom, usually a metal atom.

**Figure 1-1**

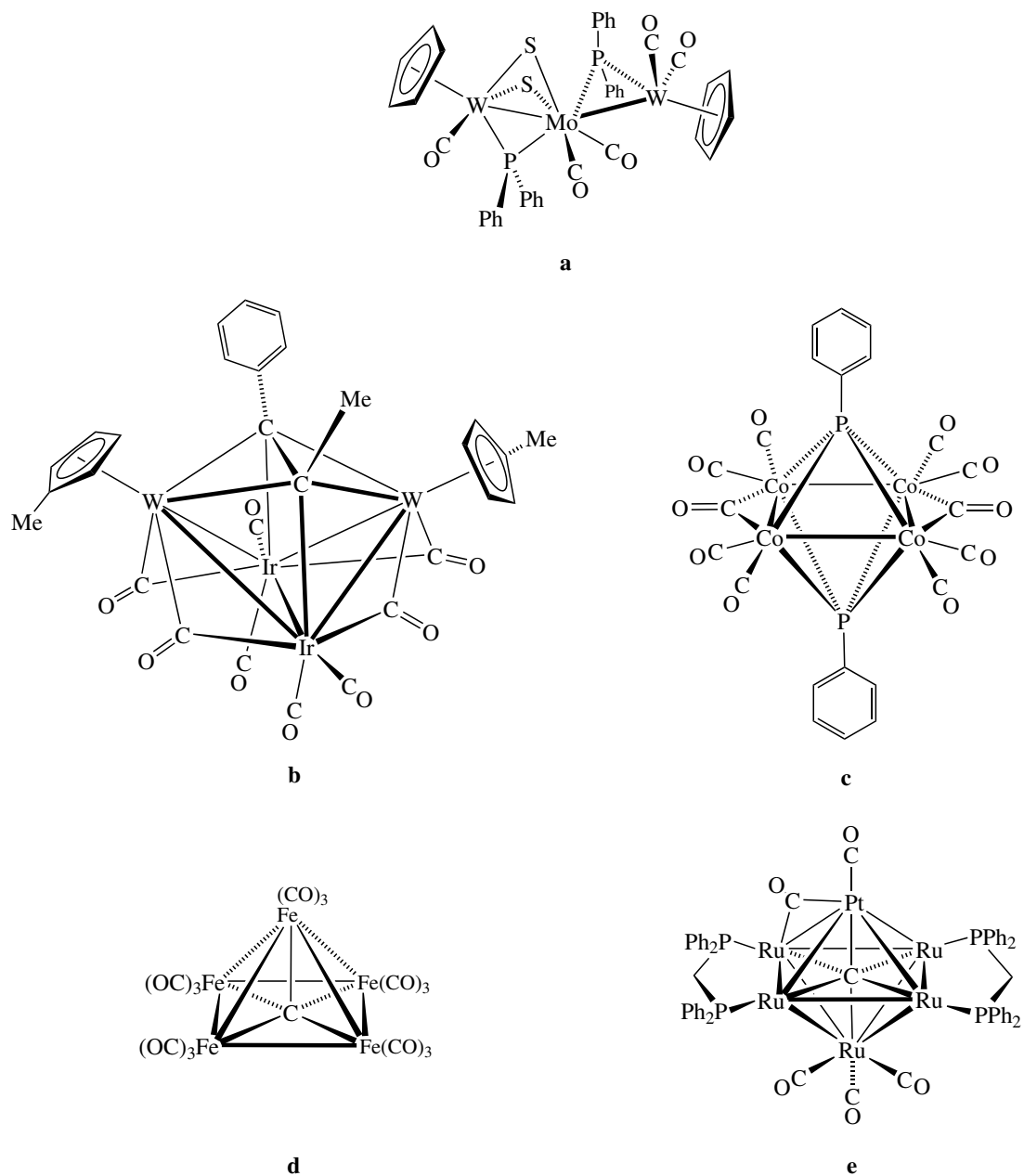
Examples of
Sandwich
Compounds

compounds are shown in Figure 1-1. The structure and bonding of sandwich compounds will be discussed in Chapter 5.

A characteristic of metal atoms bonded to organic ligands, especially CO (the most common of all ligands in organometallic chemistry), is that they often exhibit the capacity to form covalent bonds to other metal atoms to form dinuclear complexes and polynuclear *cluster compounds* (some known cluster compounds contain no organic ligands). These clusters may contain only three metal atoms or as many as several dozen; there is no limit to their size or variety. Dinuclear complexes may contain single, double, triple, or even quadruple bonds between the metal atoms and may in some cases have ligands that bridge two or more of the metals. Examples of metal cluster compounds containing organic ligands are shown as structures **a**, **b**, and **c** in Figure 1-2; cluster complexes will be encountered again in Chapter 13.

Carbon itself may play quite a different role than commonly encountered in organic chemistry. Certain metal clusters encapsulate carbon atoms; the resulting molecules, called *carbide clusters*, in some cases contain carbon bonded to five, six, or more surrounding metals.² Figures 1-2d and e illustrate two examples of carbide clusters.

²The traditional notion of carbon forming bonds to at most four additional atoms must be reconsidered (a few examples of carbon bonded to more than four atoms are also known in organic chemistry).

**Figure 1-2**Examples of Cluster
Compounds

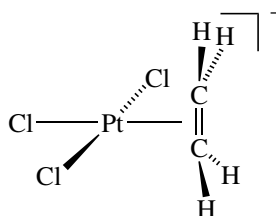
Strictly speaking, the only compounds classified as organometallic are those that contain metal–carbon bonds, but in practice complexes containing several other ligands similar to CO in their bonding, such as NO and N₂, are frequently included. Other ligands, such as phosphines (PR₃) and dihydrogen (H₂), often occur in organometallic complexes, and their chemistry is closely associated with the chemistry of organic ligands. We will include examples of these and other non-organic ligands as appropriate in our discussion of organometallic chemistry.

1-2 HISTORICAL BACKGROUND

The first organometallic compound to be reported was synthesized in 1827³ by W.C. Zeise, who obtained yellow needle-like crystals after refluxing a mixture of PtCl₄ and PtCl₂ in ethanol, followed by the addition of KCl solution.⁴ Zeise correctly asserted that this yellow product (subsequently dubbed “Zeise’s salt”) contained an ethylene group. This assertion was questioned by other chemists, most notably J. Liebig, and was not verified conclusively until experiments performed by K. Birnbaum in 1868. The structure of the compound proved extremely elusive, however, and was not determined until more than 140 years after Zeise’s discovery!⁵ Zeise’s salt proved to be the first compound containing an organic molecule attached to a metal using the π electrons of the former. It is an ionic compound of formula K[Pt(C₂H₄)Cl₃] · H₂O; the structure of the anion, shown in Figure 1-3, is based on a square plane, with three chloro ligands occupying corners of the square and the ethylene occupying the fourth corner, but perpendicular to the plane defined by the Pt and Cl atoms.

Figure 1-3

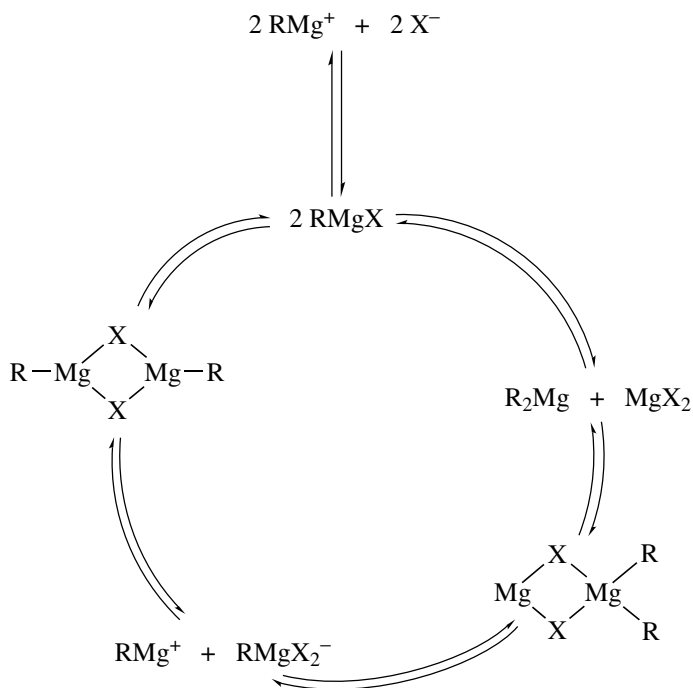
Anion of Zeise’s
Compound



³To place this in historical perspective, John Quincy Adams was the U.S. President at the time. The following year, Friedrich Wöhler reported that the organic compound urea could be made from the inorganic reagents HOCN and NH₃—the “birth” of organic chemistry.

⁴W. C. Zeise, *Ann. Phys. Chem.*, **1831**, 21, 497. A translation of excerpts from this paper can be found in *Classics in Coordination Chemistry, Part 2*, G. B. Kauffman, Ed., Dover: New York, 1976, pp. 21–37.

⁵R. A. Love, T. F. Koetzle, G. J. B. Williams, L. C. Andrews, and R. Bau, *Inorg. Chem.*, **1975**, 14, 2653.

**Scheme 1.1**Grignard Reagent
Equilibria

The first compound containing carbon monoxide as a ligand was another platinum chloro complex, reported in 1867. In 1890, Mond⁶ reported the preparation of $\text{Ni}(\text{CO})_4$, a compound that became commercially useful for the purification of nickel. Other metal CO (“carbonyl”) complexes were soon obtained; particularly notable was the work on iron carbonyls beginning around 80 years ago by Hieber.⁷

Reactions between magnesium and alkyl halides performed by Barbier⁸ in 1898 and 1899, and subsequently by Grignard,⁹ led to the synthesis of alkyl magnesium complexes now known as Grignard reagents. These complexes contain magnesium–carbon σ bonds; they are multifaceted in their structure and function. In solution they participate in a variety of chemical equilibria, some of which are summarized in Scheme 1.1. Their synthetic utility was recognized early; by 1905, more than 200 research papers had appeared on the topic. Grignard reagents and other reagents containing metal–alkyl σ bonds (such as organolithium, organozinc,

⁶L. Mond, *J. Chem. Soc.*, **1890**, 57, 749.

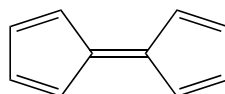
⁷W. Hieber and S. Fritz, *Chem. Ber.*, **1928**, 61B, 558.

⁸P. Barbier, *Compt. Rend.*, **1899**, 128, 110.

⁹V. Grignard, *Comp. Rend.*, **1900**, 130, 1322; *Ann. Chim.*, **1901**, 24, 433. An English translation of most of the latter paper appeared in *J. Chem. Ed.*, **1970**, 47, 290.

organocadmium, and organomercury reagents) have proven of immense importance in the development of organic chemistry.

From the discovery of Zeise's salt in 1827 to approximately 1950, the field of organometallic chemistry developed rather slowly. Some organometallic compounds, such as the Grignard reagents (RMgX), found utility in organic synthesis, but there was little study of compounds containing metal–carbon bonds as a distinct research area. In 1951, in an attempt to synthesize fulvalene (shown below) from cyclopentadienyl bromide, Kealy and Pauson allowed C_5H_5MgBr to react with $FeCl_3$ using anhydrous diethyl ether as solvent (equation 1.1).¹⁰ This reaction did not yield the desired fulvalene, but rather an orange solid of formula $(C_5H_5)_2Fe$ that was later named ferrocene.



Fulvalene

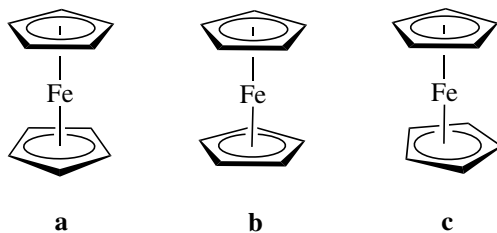


The product was surprisingly stable: it could be sublimed in air without decomposition and was resistant to catalytic hydrogenation and Diels–Alder reactions. In 1956, X-ray diffraction indicated the structure consisted of an iron atom “sandwiched” between two parallel C_5H_5 rings.¹¹ The details of the structure of ferrocene proved somewhat controversial, with the initial study indicating the rings to be in a staggered conformation (Figure 1-4a). Electron diffraction studies of gas phase ferrocene, however, showed the rings to be eclipsed (Figure 1-4b), or very nearly so. More recent X-ray diffraction studies of solid ferrocene have identified several crystalline phases, with an eclipsed conformation at 98 K and conformations with slightly twisted rings (a skew conformation) in higher-temperature crystalline modifications (Figure 1-4c).¹²

¹⁰T. J. Kealy and P. L. Pauson, *Nature* **1951**, 168, 1039. A report of the synthesis of “dicyclopentadienyliron” by Miller in 1952 showed a structure for $C_{10}H_{10}Fe$ as two cyclopentadienyl groups attached to Fe by single bonds. Because Miller's laboratory work occurred in 1948, he may have been the first to synthesize ferrocene without knowing its true structure. See S. A. Miller, J. A. Tebboth, and J. F. Tremaine, *J. Chem. Soc.*, **1952**, 632.

¹¹J. D. Dunitz, L. E. Orgel, and R. A. Rich, *Acta Crystallogr.*, **1956**, 9, 373.

¹²E. A. V. Ebsworth, D. W. H. Rankin, and S. Cradock, *Structural Methods in Inorganic Chemistry*, 2nd ed., Blackwell Scientific Publications: Oxford, 1991, pp 414–417.

**Figure 1-4**Conformations of
Ferrocene

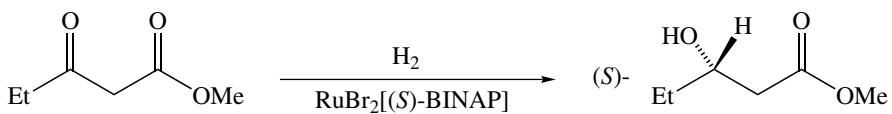
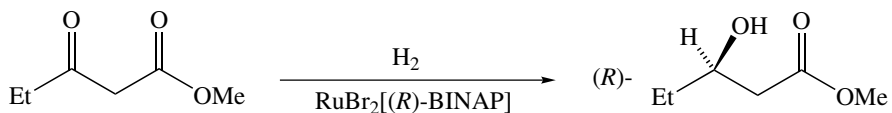
The discovery of the prototype sandwich compound ferrocene rapidly led to the synthesis of other sandwich compounds, other compounds containing metal atoms bonded to cyclic organic ligands, and a vast array of additional transition metal complexes containing other organic ligands. It is therefore often stated, with justification, that the discovery of ferrocene began the era of “modern” organometallic chemistry, an area that has grown with increasing rapidity in succeeding decades.

Over the past 30 years, a major area of growth in organotransition metal chemistry has been the discovery and use of complexes containing chiral ligands. These compounds can catalyze the selective formation of specific enantiomers of chiral molecules. In some cases, the enantioselectivity of these reactions has even equaled that of enzymatic systems. A striking example is the catalytic reduction of β -ketoesters to β -hydroxyesters using ruthenium(II) complexes containing the chiral ligands (*R*)-BINAP and (*S*)-BINAP, as shown in Scheme 1.2.¹³ Selective synthesis of a single enantiomer in greater than 99% enantiomeric excess over the opposite enantiomer has been achieved. These results are comparable with the enantioselectivity achieved using enzymes from baker’s yeast!¹⁴ Chiral syntheses using organotransition metal complexes will be discussed in Chapters 9 and 12. Chapter 12 will also explore the incredible utility of organotransitionmetal reagents in promoting the formation of C–C bonds, the most important type of reaction in organic synthesis.

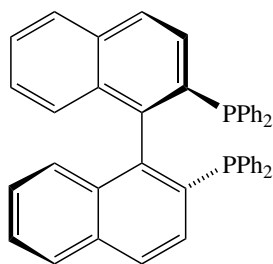
Already in this century, six chemists have received the Nobel Prize for seminal work in organometallic chemistry. Noyori, Knowles, and Sharpless became Nobel Laureates in 2001 as a result of their work on the use of organometallic complexes to catalyze asymmetric hydrogenation and oxidation reactions of organic compounds. More details of this work will appear in Chapter 12. Just four years later, Chauvin, Grubbs, and Schrock were honored

¹³R. Noyori, T. Ohkuma, M. Kitamura, H. Takaya, N. Sayo, H. Kumobayashi, and S. Akutagawa, *J. Am. Chem. Soc.*, **1987**, *109*, 5856.

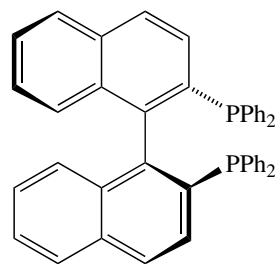
¹⁴Stereoselective reductions of β -ketoesters are of great importance in the biosynthesis of antibiotics and other biologically-active compounds.

**Scheme 1.2**

Enantioselective
Synthesis Using
Chiral Ru-BINAP
Catalysts

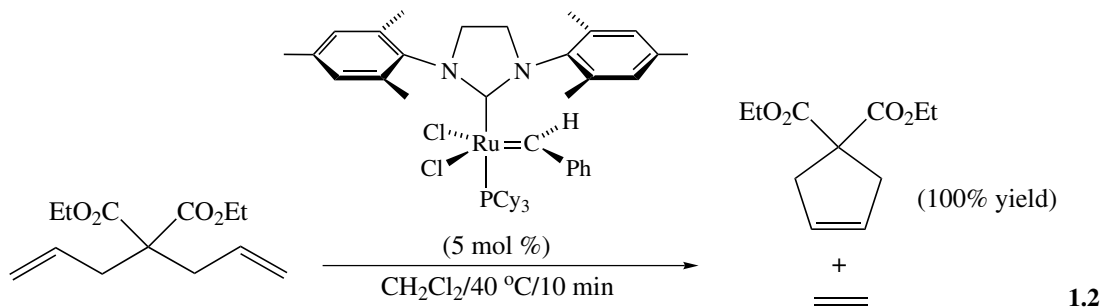


(R)-BINAP



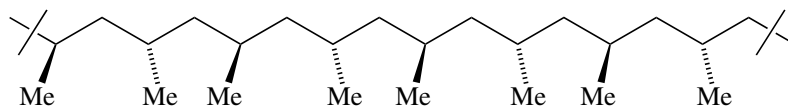
(S)-BINAP

with the Nobel Prize for their fundamental studies on the mechanism of π -bond metathesis, an example of which is shown in a catalytic ring-closing metathesis reaction (equation 1.2).¹⁵ We will explore the impact of their research in Chapter 11.



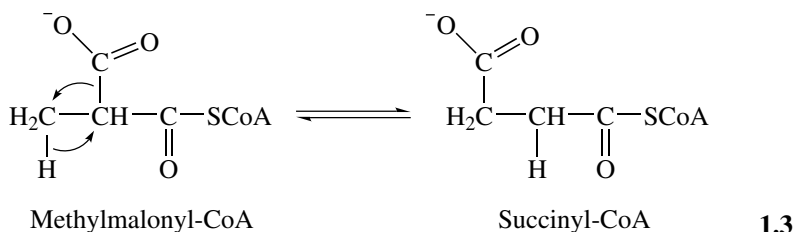
¹⁵M. Scholl, S. Ding, C. W. Lee, and R. H. Grubbs, *Org. Lett.*, **1999**, *1*, 953.

Chapter 11 also explores polymerization reactions that are used to make giant molecules with many practical uses. Organotransition metal complexes play key roles in these transformations. Ziegler and Natta (who shared the 1963 Nobel Prize in Chemistry) were pioneers in the use of early transition metal compounds to catalyze the polymerization of ethene and propene. Stereoregular polymers resulted in the latter case, such as syndiotactic polypropene.



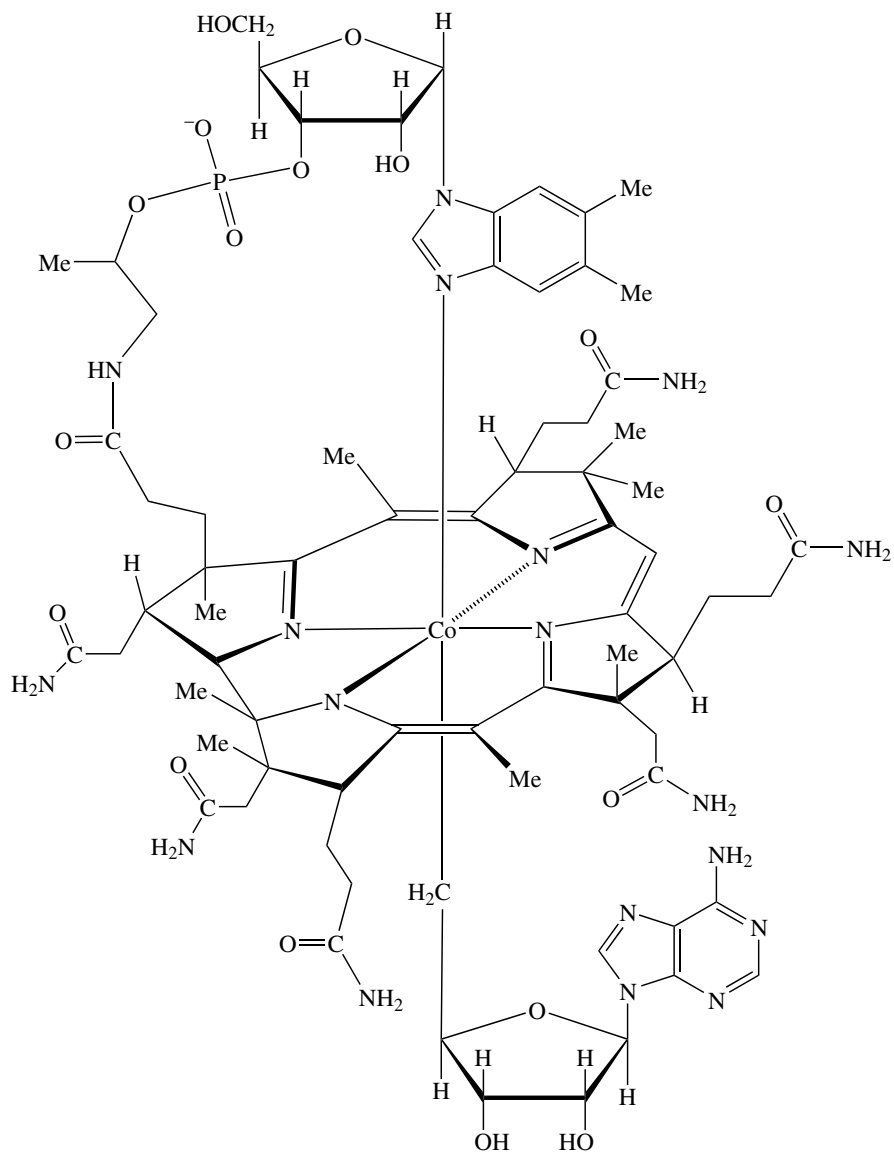
Syndiotactic Polypropene

Finally, a discussion of the historical background of organometallic chemistry would be incomplete without mention of what surely qualifies as the oldest known organometallic compound, vitamin B₁₂ coenzyme (Figure 1-5). This naturally occurring cobalt complex contains a cobalt–carbon σ bond. It is a cofactor in a number of enzymes that catalyze 1,2-shifts in biochemical systems, such as the interconversion of methylmalonyl–CoA to succinyl–CoA (equation 1.3).



Chapter 1 has provided a mere glimpse of the huge number of compounds and numerous reaction types that encompass the area of science called organometallic chemistry. In the following chapters, we will focus on these compounds and the transformations they undergo, confining the treatment primarily to the structure and chemical reactivity of molecules where a bond exists between carbon and a transition metal.¹⁶

¹⁶For a good discussion of main-group organometallic chemistry, see C. Elschenbroich, *Organometallics*, 3rd ed., Wiley-VCH: Weinheim, Germany, 2006, Chapters 4–11.

**Figure 1-5**

Vitamin B₁₂
Coenzyme

Suggested Reading

The following articles by Dietmar Seyferth, listed in reverse chronological order, have appeared in the journal *Organometallics* over the past several years. Each gives a nice historical account of some key areas of organometallic chemistry.

1. "Alkyl and Aryl Derivatives of the Alkali Halides: Useful Synthetic Reagents as Strong Bases and Potent Nucleophiles. 1. Conversion of Organic Halides to Organoalkali-Metal Compounds," **2006**, 25, 2.
2. "Uranocene. The First Member of a New Class of Organometallic Derivatives of the *f* Elements," **2004**, 23, 3562.
3. "(Cyclobutadiene)iron Tricarbonyl—A Case of Theory before Experiment," **2003**, 22, 2.
4. "Bis(benzene)chromium. 2. Its Discovery by E. O. Fischer and W. Hafner and Subsequent Work by the Research Groups of E. O. Fischer, H. H. Zeiss, F. Hein, C. Elschenbroich, and Others," **2002**, 21, 2800.
5. "Bis(benzene)chromium. 1. Franz Hein at the University of Leipzig and Harold Zeiss and Minoru Tsutsui at Yale," **2002**, 21, 1520.
6. "Zinc Alkyls, Edward Frankland, and the Beginnings of Main-Group Organometallic Chemistry," **2001**, 20, 2940.
7. "[$(C_2H_4)PtCl_3$]⁻, the Anion of Zeise's Salt, $K[(C_2H_4)PtCl_3] \cdot H_2O$," **2001**, 20, 2.

In addition, several articles appearing in the journal *Pure and Applied Chemistry* placed the development of organometallic chemistry in historical perspective.

1. Volume 78, issue 1 (2006), was dedicated to the theme of the application of organometallic chemistry to organic synthesis. Individual articles in this issue provide useful historical background.
2. A. Yamamoto, "Organometallic Chemistry. Past, Present, and Future," **2001**, 73, 205.
3. J. Halpern, "Organometallic Chemistry at the Threshold of a New Millenium. Retrospect and Prospect," **2001**, 73, 209.

Other Readings

G. Wilkinson, "The Iron Sandwich. A Recollection of the First Four Months," *J. Organomet. Chem.*, **1975**, 100, 273. This article is a nice account of the history of the discovery of ferrocene. Wilkinson, along with E. O. Fischer, won the Nobel Prize in Chemistry for his pioneering work on sandwich compounds.

For a series of more modern articles by several authors on the history of the early research on ferrocene and other metallocenes, see *J. Organomet. Chem.*, **2001**, 637–639, 3–26. See also P. Laszlo and R. Hoffmann, "Ferrocene: Ironclad History or Rashomon Tale," *Angew. Chem. Int. Ed.*, **2000**, 39, 123, for a short, interesting article on the discovery of the structure of ferrocene.

For an early article on the historical background of organometallic chemistry, see J. Thayer, *Adv. Organomet. Chem.*, **1975**, 13, 1.

For a historical perspective on the development of modern organometallic chemistry from one of its most active participants, see F. A. Cotton, "A Half-Century of

Nonclassical Organometallic Chemistry: A Personal Perspective,” *Inorg. Chem.*, **2002**, *41*, 643.

The following article discusses the history of Natta’s discovery of stereoregular polymers: P. Corradini, “The Discovery of Isotactic Polypropylene and Its Impact on Pure and Applied Science,” *J. Polym. Sci., Part A, Polym. Chem.*, **2004**, *42*, 391.

Fundamentals of Structure and Bonding

An essential objective of organometallic chemistry is to understand how organic ligands can bond to metal atoms. An examination of the interactions between metal orbitals and orbitals on these ligands can provide valuable insight into how organometallic molecules form and react; such an examination may also indicate future avenues of study and potential uses for these compounds.

Before considering how ligands bond to metals, it is useful to look at the types of orbitals involved in such bonds. Chapter 2 includes a brief review of atomic orbitals, followed by a discussion of the ways in which atomic orbitals can interact to form molecular orbitals. Aspects of computational chemistry are introduced and discussed in terms of their relevance to organometallic chemistry. In subsequent chapters, we will consider how molecular orbitals of a variety of ligands can interact with transition metal orbitals. In these cases, we will pay particular attention to how metal *d* orbitals are involved.

2-1 ATOMIC ORBITALS

The modern view of atoms holds that although atoms are composed of three types of subatomic particles—protons, neutrons, and electrons—the chemical behavior of atoms is governed by the behavior of the electrons. Furthermore, the electrons do not behave according to the traditional concept of “particles,” but rather exhibit the characteristics of waves. In a single atom these waves can be described by the Schrödinger wave equation:

$$\mathcal{H}\psi = E\psi$$

where

\mathcal{H} = Hamiltonian operator

E = energy of the electron

ψ = wave function

The wave function ψ can be represented by a mathematical expression describing the wave characteristics of an electron in an atom. The Hamiltonian operator, \mathcal{H} , is a set of mathematical instructions to be performed on ψ in such a way as to give a result that is a numerical value (the energy of the electron) multiplied by ψ . The details of the Hamiltonian operator need not concern us here; elaborate discussions can be found in a variety of physical chemistry texts. The characteristics of the wave function ψ , however, are essential background for understanding the discussion of chemical bonding that will follow.

The wave function ψ has the following important characteristics:

1. ψ is a mathematical description of a region of space (an **orbital**) that can be occupied by up to two electrons.
2. For any atom, there are many solutions to the wave equation. Each solution describes one of the orbitals of the atom.
3. ψ describes the *probable* location of electrons; it is not capable of predicting exactly where an electron is at a given place and time.
4. The square of the wave function, ψ^2 , evaluated at a given set of coordinates (x , y , z), is proportional to the probability that an electron will be at that point.
5. The mathematical expression of ψ incorporates **quantum numbers**, which are related to the energy, size, and shape of atomic orbitals.

Solutions to the Schrödinger equation are described by quantum numbers, as summarized in Table 2-1. Values for the first of these quantum numbers, n , l , and

Table 2-1 Quantum Numbers

Symbol	Name	Possible values	Description
n	Principal	1, 2, 3, ...	Describes size and energy of orbitals. (In older terminology, defined <i>shell</i> of electrons.)
l	Azimuthal (angular momentum)	0, 1, 2, ..., ($n-1$) $l = 0$ <i>s</i> orbitals $l = 1$ <i>p</i> orbitals $l = 2$ <i>d</i> orbitals $l = 3$ <i>f</i> orbitals	Describes shape of orbitals; plays secondary role (after n) in determining energy. (In older terminology, defined <i>subshell</i> of electrons.)
m_l	Magnetic	0, ± 1 , ± 2 , ..., $\pm l$ (integer values from $-l$ to $+l$)	Describes orientation of orbitals. (The number of values of m_l is the number of orbitals in a subshell.)
m_s	Spin	$\frac{1}{2}$, $-\frac{1}{2}$	Describes spin of electron in orbital.

m_l , are obtained by solving the Schrödinger equation and define an atomic orbital; the fourth, m_s , describes electron spin within an orbital.

The quantum number l gives the classification of an orbital (s , p , d , etc.) and determines the orbital's shape. The number of values of the quantum number m_l is equal to the number of orbitals having that classification, as shown below.

	<i>Classification</i>	<i>Number of orbitals</i>
$l = 0$ $m_l = 0$ (one value)	s	1
$l = 1$ $m_l = -1, 0, 1$ (three values)	p	3
$l = 2$ $m_l = -2, -1, 0, 1, 2$ (five values)	d	5

The shapes and orientations of s , p , and d orbitals are extremely important in organometallic chemistry and are shown in Figure 2-1.

An atomic orbital is defined by its set of quantum numbers n , l , and m_l . For example, a $2p_z$ orbital has $n = 2$, $l = 1$, and $m_l = 0$. Within an orbital, individual electrons may have quantum number $m_s = \frac{1}{2}$ or $-\frac{1}{2}$. Because each electron in an atom must have its own unique set of all four quantum numbers (according to the Pauli exclusion principle), if an orbital is filled, one electron must have $m_s = \frac{1}{2}$ and the other must have $m_s = -\frac{1}{2}$. Quantum number m_s is often designated by arrows:

\uparrow represents $m_s = \frac{1}{2}$

\downarrow represents $m_s = -\frac{1}{2}$

- a. Determine the possible values of quantum number l for a shell having $n = 4$.
- b. What values of quantum number m_l are possible for a $3p$ orbital?
- c. How many electrons, at most, can occupy a $4p$ orbital?

Example 2-1

Solutions:

- a. Quantum number l can have integer values beginning with 0 and going up to $n - 1$. Therefore, $l = 0, 1, 2, 3$.
- b. Values of m_l are limited by the value of quantum number l . For any p orbital, $l = 1$. Therefore, $m_l = -1, 0, +1$ (integer values between $-l$ and $+l$).
- c. No orbital, regardless of label, can be occupied by more than 2 electrons—so the answer is 2.

- a. How many electrons, at most, can occupy a shell having $n = 2$?
- b. What values of quantum number m_l are possible for a d electron?
- c. At most, how many electrons in a p subshell can have $m_s = \frac{1}{2}$?

Exercise 2-1¹

¹Solutions to all exercises are given in Appendix B.

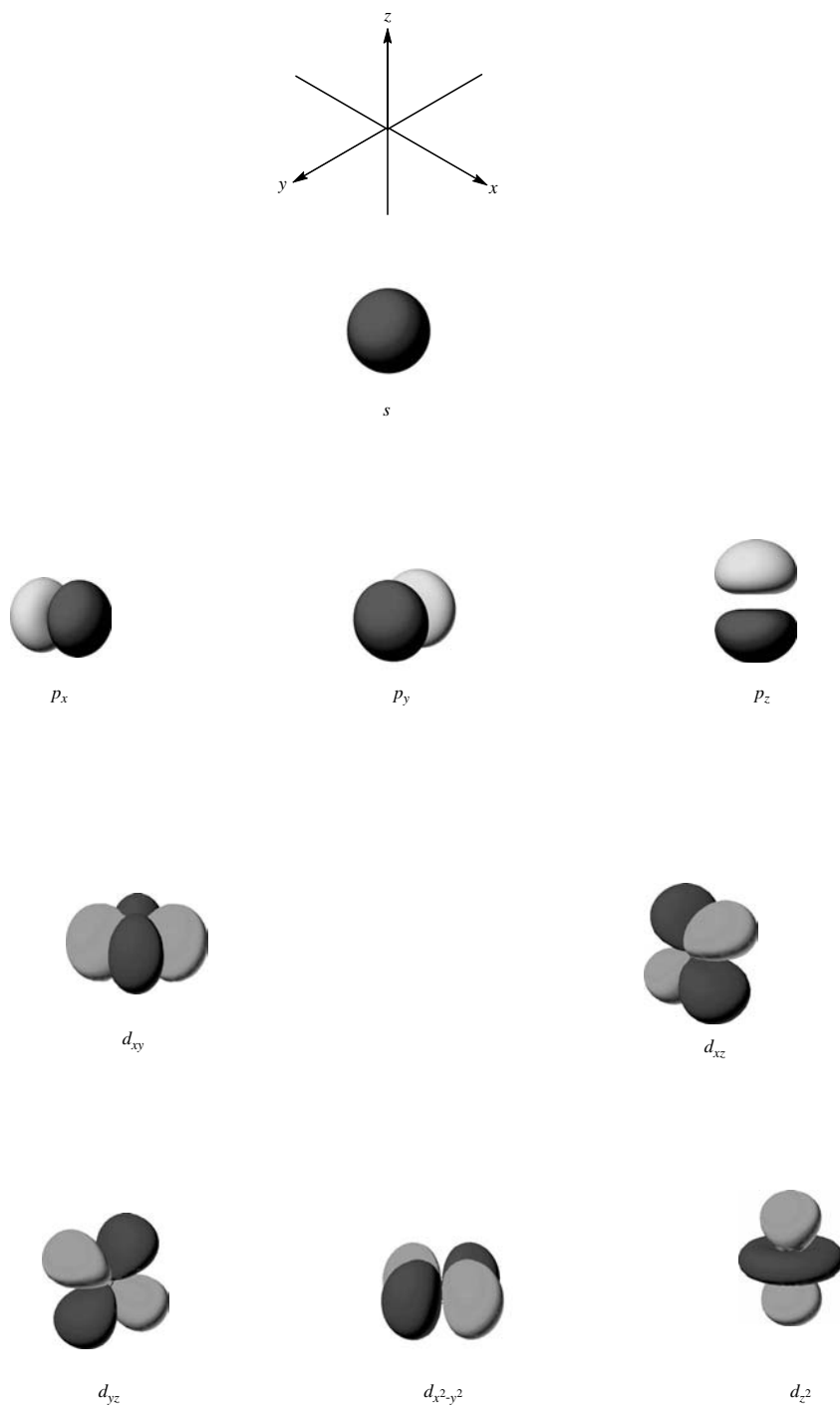


Figure 2-1
 s , p , and d Orbitals

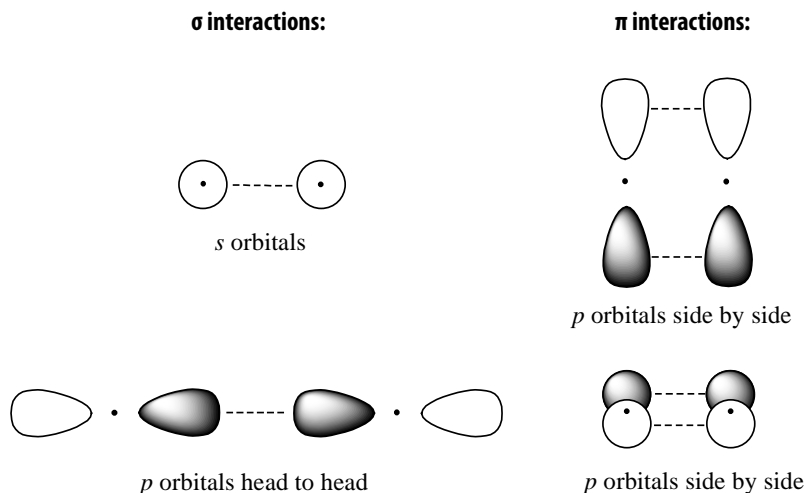
Interactions between Atomic Orbitals

Atomic orbitals on neighboring atoms may interact with each other—if certain conditions are satisfied:

- Atomic orbitals must have an appropriate orientation with respect to each other and be close enough to interact.
- For such an interaction to be strong, the atomic orbitals should have similar energies.

The **molecular orbital** (MO) concept of chemical bonding is based on these fundamental assumptions. As the name implies, MOs are similar in concept to atomic orbitals; in fact, molecular orbitals are derived from atomic orbitals. Both types of orbitals are based on the wave nature of electrons; therefore, all five characteristics listed previously for atomic orbitals also apply to molecular orbitals.

As stated, atomic orbitals on two atoms may interact if they are oriented appropriately with respect to each other.² In general, if atomic orbitals point toward each other and interact directly between the nuclei, they participate in a σ interaction; if atomic orbitals are oriented such that they interact in two regions off to the side, they participate in a π interaction. Examples of these interactions follow.

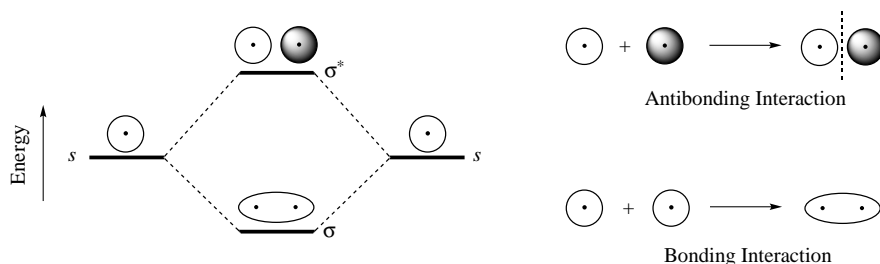


²In other words, the orbitals must have the same symmetry to interact. Background on chemical symmetry may be found in S. F. A. Kettle, *Symmetry and Structure*, Wiley: New York, 1995, and in G. L. Miessler and D. A. Tarr, *Inorganic Chemistry*, 3rd ed., Pearson Prentice Hall: Upper Saddle River, NJ, 2004, pp. 139–157.

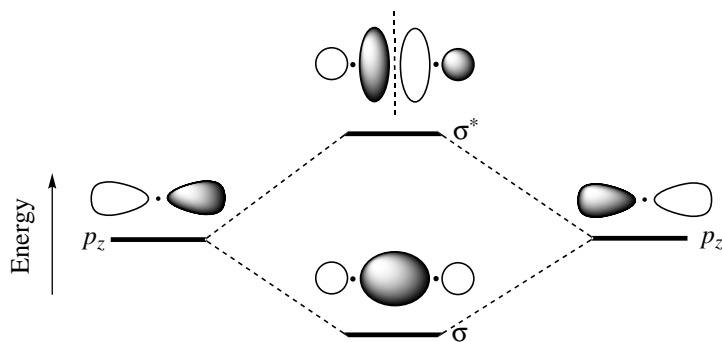
In addition, whenever orbitals on two atoms interact, they do so in two ways: in a **bonding** fashion, in which the signs of the orbital waves match up, and in an **antibonding** fashion, in which the signs of the orbital waves are opposite. In a bonding interaction, electrons are concentrated between the nuclei and tend to hold the nuclei together; in an antibonding interaction, electrons avoid the region of space between the nuclei and therefore expose the nuclei to each other's positive charges, tending to cause the nuclei to repel each other. Thus, a bonding interaction stabilizes a molecule, and an antibonding interaction destabilizes it.

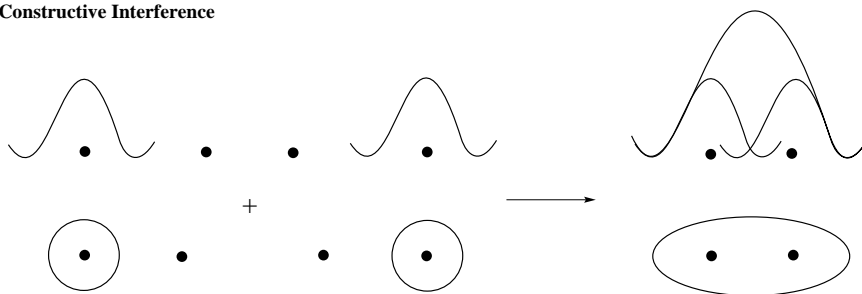
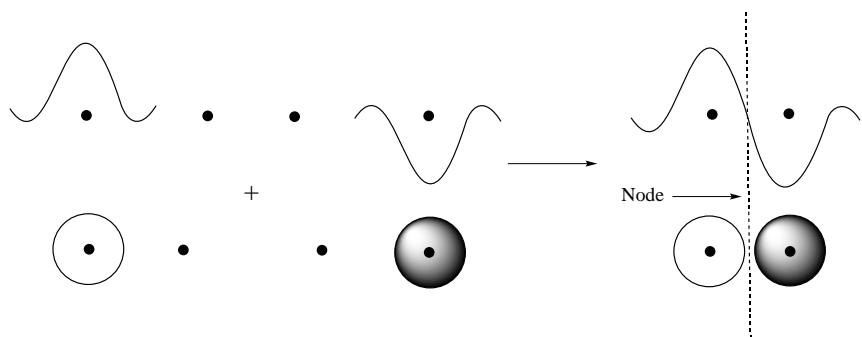
2-1-1 σ Interactions

The simplest case of a σ interaction is between s orbitals on neighboring atoms. Two types of interaction occur: bonding and antibonding. The bonding interaction leads to a molecular orbital (a bonding orbital, designated σ) that is lower in energy than the atomic orbitals from which it is formed; the antibonding interaction gives rise to a molecular orbital (an antibonding orbital, designated σ^* ; an asterisk is commonly used to indicate antibonding) that is higher in energy than the atomic orbitals from which it is formed. These interactions are shown below.



Similarly, p orbitals on adjacent atoms can interact. If the p orbitals are pointed directly toward each other, the interaction is classified as σ , and bonding and antibonding molecular orbitals are formed.

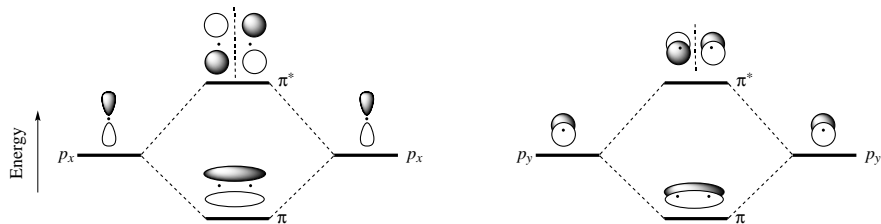


Constructive Interference**Destructive Interference****Figure 2-2**Interactions
between Waves

These interactions may be compared conceptually with the way in which overlapping waves interact (Figure 2-2). If (electron) waves on neighboring atoms overlap in such a way that their signs are the same, the result is constructive interference of the waves; the resulting wave, representing a bonding interaction, has a greater amplitude in the region between the nuclei. If the waves overlap such that their signs are opposite, the waves cancel each other out in the middle, creating a node of zero amplitude. This is an example of destructive interference and corresponds to an antibonding interaction.

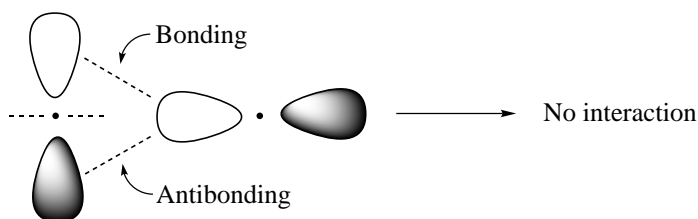
2-1-2 π Interactions

Similarly, parallel p orbitals on neighboring atoms can interact. In this case, the interaction occurs—not directly between the nuclei, as in the σ case—but in two regions off to the side. When the signs on the neighboring orbital lobes match, the interaction is a bonding one, leading to the formation of a π molecular orbital lower in energy than the p orbitals from which it is derived; when the signs on the neighboring lobes are opposite, an antibonding (π^*) orbital is formed that is of higher energy than the original atomic orbitals. These are shown for p orbitals in two orientations on the next page.



2-1-3 Nonbonding

If the orientations of atomic orbitals are such that a bonding interaction would be canceled by an equal antibonding interaction, there is no net interaction, and the orbitals are designated **nonbonding**. For example, a p_x orbital on one atom is not oriented suitably to interact with a p_z orbital on a neighboring atom, as shown below.³



Example 2-2

Classify the interactions between orbitals on two adjacent atoms as σ , π , or nonbonding (assign the z axis to pass through the atomic nuclei).

	<i>Atom 1</i>	<i>Atom 2</i>	<i>Diagram</i>	<i>Classification</i>
Example:	s	p_z		σ
a.	p_x	p_x		
b.	p_x	p_y		
c.	p_z	d_{z^2}		

Solutions:

- Two p_x orbitals: These orbitals interact in two regions; therefore, the classification is π .
- A p_x orbital on the first atom, p_y on the second: Because there is no match of orbital lobes, these orbitals are *nonbonding*.
- A p_z orbital on the first atom, d_{z^2} on the second: There is one region of overlap; the classification is σ .

³In general, we will choose the z axis to be the axis joining the atomic nuclei.

Classify the interactions between orbitals on two adjacent atoms as σ , π , or nonbonding.

Exercise 2-2

- a. Atom 1: s ; atom 2: p_y
- b. Atom 1: d_{xz} ; atom 2: d_{xz}
- c. Atom 1: d_{z^2} ; atom 2: d_{z^2}

2-2 MOLECULAR ORBITALS

When all possible orbital interactions between neighboring atoms are considered, the result is a molecular orbital energy level diagram. In Chapter 2 we will consider first the simplest case: interactions between the orbitals of two atoms in diatomic molecules and ions. We will then extend this approach to consider the bonding in polyatomic organic π systems. Diatomic species and organic π systems represent many of the most important ligands in organometallic chemistry.

2-2-1 Diatomic Molecules

Diatomic molecules are among the most important ligands occurring in organometallic compounds. We will therefore give special attention to the bonding in diatomics, considering first the **homonuclear** cases, such as H_2 and O_2 , and then **heteronuclear** diatomics, such as CO.

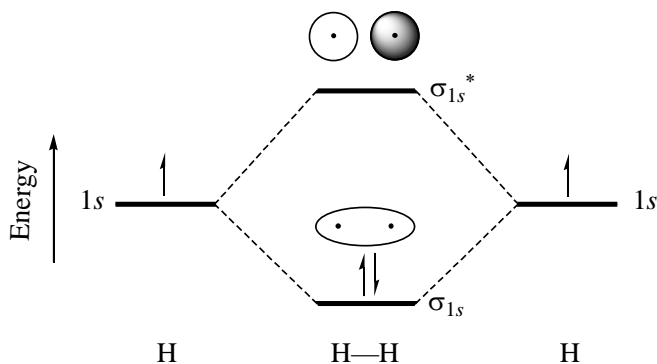
In general, the atomic orbitals of the interacting atoms will be shown on the far left and far right of these diagrams and the molecular orbitals themselves in the middle. Relative energies of the orbitals will be indicated on the vertical scale of the diagrams.

Homonuclear Diatomics

Molecular Orbitals of H_2 . The simplest example of a diatomic molecule is H_2 . For this molecule, the only atomic orbitals available are the $1s$ orbitals of the hydrogens. These orbitals interact to yield bonding σ_{1s} and antibonding σ_{1s}^* molecular orbitals; the molecular orbital energy level diagram is shown in Figure 2-3. (Subscripts are often used to designate the atomic orbitals from which the molecular orbitals are derived.)

Electrons occupy the molecular orbitals beginning with the lowest energy orbital, in this case the σ_{1s} . Consequently, H_2 has one pair of electrons in a bonding molecular orbital; this is the same as saying that it has a single bond. Since H_2 has only two electrons, it has no electrons left to occupy the higher energy antibonding orbital.

This picture of bonding can be compared with the Lewis dot structure, $H : H$, in which a single bond is designated by a pair of electrons shared between two atoms. In terms of molecular orbitals, a single bond is defined in H_2 as a pair of electrons occupying a bonding molecular orbital.

**Figure 2-3**

Molecular Orbitals
of H_2

Bond Order

In the molecular orbital model, the number of bonds between two atoms is designated as the bond order and depends not only on the number of bonding electrons, but also on the number of antibonding electrons. In general, the bond order can be determined from the following equation.⁴

$$\text{Bond order} = \frac{1}{2} (\text{number of bonding electrons} \\ - \text{number of antibonding electrons})$$

In the example of H_2 , the bond order = $\frac{1}{2} (2 - 0) = 1$ (a single bond). In diatomic molecules, a bond order of 1 corresponds to a single bond, a bond order of 2 to a double bond, and so forth.

Suppose one wanted to consider whether He_2 is likely to be a stable molecule. This molecule, if it existed, would have a similar molecular orbital energy level diagram to H_2 (in both cases, only 1s atomic orbitals are involved) but it would have four electrons: two in the bonding σ_{1s} molecular orbital and two in the antibonding σ_{1s}^* orbital. Its bond order would be = $\frac{1}{2} (2 - 2) = 0$, or no bond. In other words, He_2 would have no bond at all; not surprisingly, molecules of He_2 have not been observed except under demanding experimental conditions.⁵

Magnetic Behavior

The magnetic behavior of molecules is related to the presence or absence of unpaired electrons. Molecules such as H_2 that have no unpaired electrons (both electrons are paired in the same orbital) are classified as **diamagnetic**; they are not attracted by magnetic

⁴In general, it is sufficient to consider only the valence electrons in the calculation of the bond order; inner electrons may be assumed to belong to individual atoms rather than participating significantly in bonding.

⁵F. Luo, G. C. McBane, G. Kim, C. F. Giese, and W. R. Gentry, *J. Chem. Phys.*, **1993**, 98, 3564. See also L. L. Lohr and S. M. Blinder, *J. Chem. Educ.*, **2007**, 84, 860.

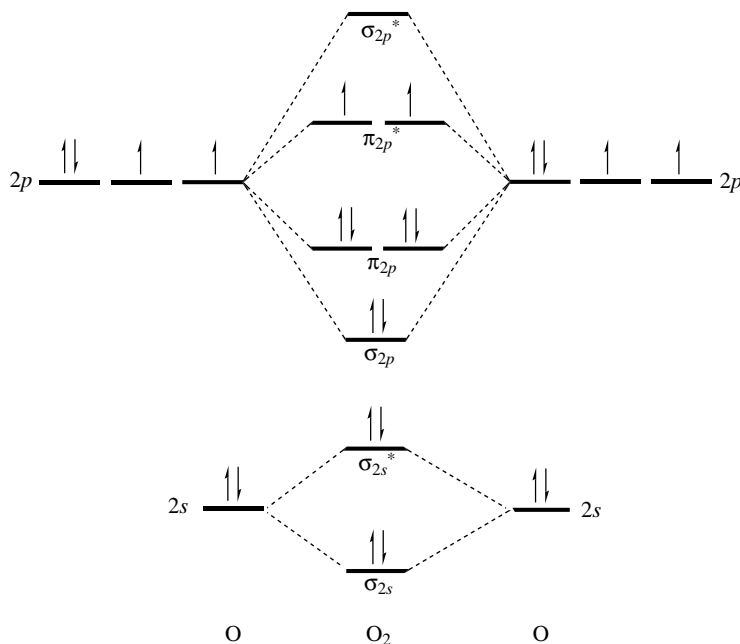


Figure 2-4

Molecular
Orbitals of O₂

fields. Other molecules, as we will soon see, have unpaired electrons and are strongly attracted by magnetic fields. Such molecules are classified as **paramagnetic**.

Second-Row Homonuclear Diatomic Molecules

Second-row elements have $2s$ and $2p$ valence orbitals. Interactions between these orbitals give the molecular orbital energy level diagram shown in Figure 2-4. The molecule O₂ is an example of this arrangement.

In O₂, the $2s$ orbital interactions are similar to the $1s$ interactions in H₂ and form σ_{2s} and σ_{2s}^* molecular orbitals. The $2p$ orbitals of the oxygens interact in both σ and π fashions.

- One set of σ interactions (involving $2p_z$ orbitals) forms σ_{2p} and σ_{2p}^* molecular orbitals.
- Two sets of π interactions (one involving $2p_x$ orbitals and the other involving $2p_y$ orbitals) form two π_{2p} orbitals and two π_{2p}^* orbitals. Because the p_x and p_y interactions are equivalent, the π_{2p} orbitals have the same energy (are **degenerate**), and the π_{2p}^* orbitals also have the same energy).

In general, σ interactions between $2p$ orbitals are stronger than π interactions; the σ interaction occurs directly between the atomic nuclei and has a somewhat stronger effect than the π interactions, which occur off to the side. Consequently,

Table 2-2 Examples of Heteronuclear Diatomics of the Second-Row Elements

Formula	Name	Name as ligand
CO	Carbon monoxide	Carbonyl
CN ⁻	Cyanide	Cyano
NO ⁺	Nitrosyl	Nitrosyl ^a
NO	Nitric oxide	Nitrosyl

^aThe charge on the ligand when NO is bonded to a metal can be a matter of uncertainty. The name “nitrosyl” is used in general for NO ligands, without implications for the charge on the ligand or the oxidation state of the metal.

the σ_{2p} orbital is lower in energy than the π_{2p} orbitals, and the σ_{2p}^* is higher in energy than the π_{2p}^* orbitals, as shown.⁶

When the electrons are placed in the orbitals in order of increasing energy for O₂, the first ten electrons fill the five lowest energy orbitals. The next highest orbitals in energy are the π_{2p}^* . The final two electrons must occupy these orbitals in accordance with Hund’s rule, which states that electrons in such cases tend to occupy degenerate orbitals separately (to minimize electron–electron repulsion by occupying separate regions in space) and with parallel spins (matching values of quantum number m_l). The result is that the final two electrons in O₂ occupy separate π_{2p}^* orbitals and have parallel spins. Because these electrons are unpaired, O₂ is paramagnetic; it behaves like a tiny magnet. Experiments have shown that O₂ is, indeed, attracted by magnetic fields, lending support to the molecular orbital picture. The Lewis dot picture of O₂, illustrated below, does not provide a way of predicting these unpaired electrons.

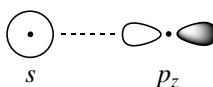
The bond order in O₂ = $\frac{1}{2}(8 - 4) = 2$ (a double bond). $\text{:}\ddot{\text{O}}=\ddot{\text{O}}\text{:}$

The oxygen–oxygen distance of 120.7 pm in O₂ is comparable to the distance expected for a double bond.

Heteronuclear Diatomics

Many diatomic molecules and ions contain two different elements; several play crucial roles in organometallic chemistry. Table 2-2 provides examples.

⁶The molecular orbital diagram illustrated in Figure 2-4 considers only interactions between atomic orbitals of identical energy: $2s$ with $2s$ and $2p$ with $2p$. Interactions also occur between s and p_z orbitals, however, as illustrated below. When these interactions are taken into account, the net effect is to raise the energy of the σ_{2p} orbital relative to the π_{2p} . In some cases, this interaction may be strong enough to push the σ_{2p} higher than the π_{2p} .



Molecular orbital energy level diagrams for these second-row heteronuclear diatomics can be drawn rather easily by modifying the homonuclear pattern slightly (as described for O_2 , Figure 2-4). The relative energies of the atomic orbitals should be shown, indicating that the more electronegative element has lower energy orbitals.

For example, in CO (Figure 2-5) the atomic orbitals of the more electronegative oxygen are lower, a reflection of the greater effective nuclear charge (oxygen has two more protons than carbon) pulling its orbitals to lower energy. The relative energies of the molecular orbitals of CO are similar to those of O_2 .⁷

The shapes of the molecular orbitals should also be noted, especially because they have great chemical significance. In carbon monoxide, the bonding π orbitals are skewed toward the more electronegative oxygen; the antibonding (and empty) π^* orbitals are skewed toward the carbon. The large, empty lobes on carbon have immense importance in the numerous compounds containing CO bonded to metals (the order of atoms in these cases is almost always M–C–O), as

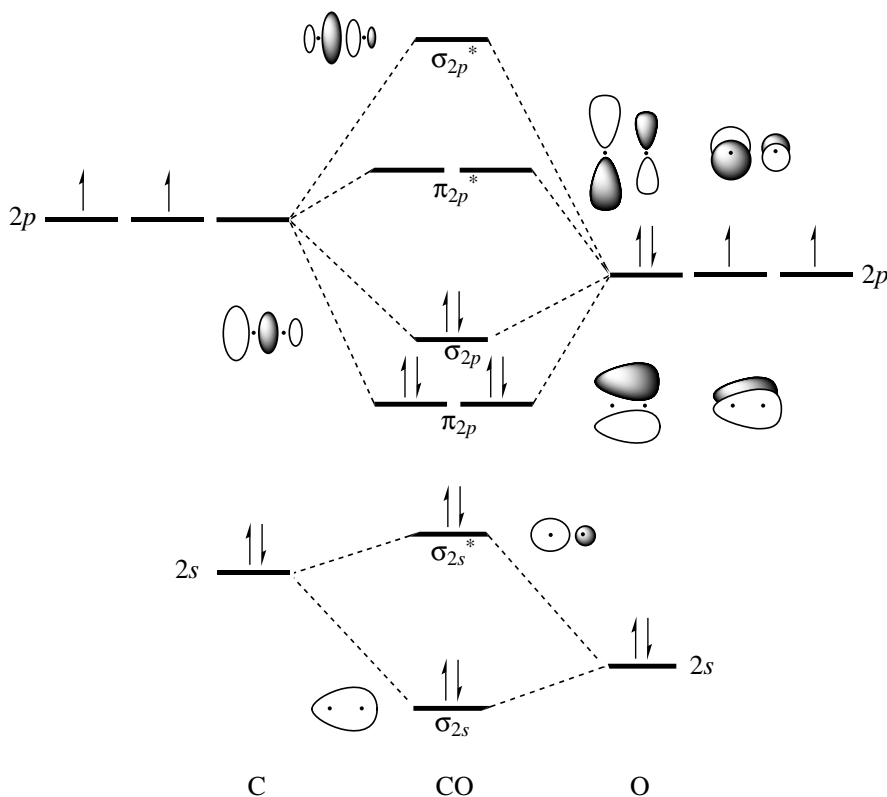


Figure 2-5
Molecular Orbitals
of CO

⁷The one exception: the σ_{2p} orbital is higher in energy than the π_{2p} orbitals in CO; the opposite is true in O_2 —see Footnote 6.

Table 2-3 Valence Orbital Potential Energies^a

Atomic number	Element	Orbital potential energy (eV)				
		1s	2s	2p	3s	3p
1	H	-13.6				
2	He	-24.6				
3	Li		-5.4			
4	Be		-9.3			
5	B		-14.0	-8.3		
6	C		-19.4	-10.7		
7	N		-25.6	-13.2		
8	O		-32.4	-15.9		
9	F		-40.2	-18.7		
10	Ne		-48.5	-21.6		
11	Na				-5.1	
12	Mg				-7.6	
13	Al				-11.3	-6.0
14	Si				-15.9	-7.8
15	P				-18.8	-9.6
16	S				-22.7	-11.6
17	Cl				-25.2	-13.7
18	Ar				-29.2	-15.8

^aJ. B. Mann, T. L. Meek, and L. C. Allen, *J. Am. Chem. Soc.*, **2000**, 122, 2780.

will be discussed in Chapter 4. In addition, the highest energy pair of electrons, in the σ_{2p} orbital, is concentrated on the carbon; it also plays an important role in bonding to metals.

A useful reference is provided by the valence orbital potential energy; this is a measure of average potential energy of atomic orbitals. Valence orbital potential energies are negative, representing attractions between valence electrons and the nuclei; the more negative the value, the stronger the attraction and the lower the energy of the orbital. Valence orbital potential energies for the first 18 elements are given in Table 2-3.

In general, the more electronegative the element, the lower (more negative) the potential energies of the corresponding valence orbitals. For example, in CO the 2p orbitals of oxygen (-15.9 eV) are lower in potential energy than the 2p orbitals of carbon (-10.7 eV); this is shown in the molecular orbital diagram of CO (Figure 2-5) by indicating that the energies of the 2p atomic orbitals are lower in energy for oxygen than for carbon. The 2s orbital of oxygen is also much lower in energy than the 2s orbital of carbon.

Comparison of Atomic Orbitals with Molecular Orbitals

In many ways molecular orbitals are like atomic orbitals.

1. Both types of orbitals have a definite energy and shape.
2. Both types of orbitals can be occupied by up to two electrons; if two electrons occupy the same orbital, they must have opposite spin (the Pauli exclusion principle applies).
3. In filling orbitals of the same energy (degenerate levels), electrons in both types of orbitals tend to occupy separate orbitals and have parallel spins (Hund's rule applies).
4. Both types of orbitals describe probable locations of electrons, rather than exact locations (an orbital does not designate an orbit).
5. Both types of orbitals describe the wave nature of electrons; in some cases, a single orbital may have positive and negative portions (lobes) representing positive and negative values of the corresponding wave functions (like peaks and valleys of waves on an ocean). For example, this is the case for π molecular orbitals and p atomic orbitals.

Molecular orbitals differ from atomic orbitals only in that the former arise from interactions between the latter, and molecular orbitals therefore describe the behavior of electrons in molecules rather than in single atoms.

A Suggested Procedure for Writing Molecular Orbital Diagrams

The molecular orbital concept is fundamental to organometallic chemistry. The exercises that follow provide useful practice in drawing MO energy level diagrams. The following steps outline a recommended procedure:

1. Using valence orbital potential energies, indicate the relative energies of the atomic orbitals from which the molecular orbitals are derived. These are ordinarily shown on the far left and on the far right of the diagram (see Figures 2-3, 2-4, and 2-5). Generally, it is sufficient to use only the valence orbitals, especially in homonuclear diatomic molecules; the core electrons are located much closer to the nuclei than the valence electrons and, consequently, these inner electrons have only minor effects on the bonding (they are also filled with electrons and generate an equal number of bonding and antibonding electrons, giving no net effect on the bond order).
2. Show the bonding and antibonding molecular orbitals that result from interactions of the atomic orbitals. These are placed in the center of the diagram. (For convenience, the axis joining the nuclei is generally chosen as the z axis.)
3. Identify the molecular orbitals with appropriate labels:

σ for sigma interactions

π for pi interactions

4. Antibonding MOs are designated by an asterisk superscript. For example, an antibonding sigma orbital resulting from overlap of $2s$ atomic orbitals is designated σ_{2s}^* .
5. Place the appropriate number of electrons in the molecular orbital energy levels by first determining the total number of valence electrons in the molecule or ion and then placing these in the molecular orbitals, starting with the lowest energy MO. Hund's rule and the Pauli exclusion principle should be followed.
6. Check: Be sure that the total number of molecular orbitals is equal to the sum of the number of atomic orbitals used and that the total number of valence electrons in the molecular orbitals is correct.

Exercise 2-3

Prepare a molecular orbital energy level diagram of N_2 . Include labels for the molecular orbitals and all valence electrons. Predict the bond order for N_2 .

Diatomic Ions

Homonuclear diatomic ions can be treated in a manner similar to that used for neutral molecules. Although the relative energies of molecular orbitals in such ions may be somewhat different than in the neutral molecules, in general the molecular orbital diagram for the molecules may be used for the ions simply by adjusting the electron count. For example, the molecular orbitals of the ions O_2^+ , O_2^- , and O_2^{2-} may be described using the orbitals for neutral O_2 in Figure 2-4.

Example 2-3

Prepare a molecular orbital energy level diagram of the peroxide ion, O_2^{2-} , and predict the bond order of this ion.

Solution: The molecular orbital diagram is similar to that for O_2 , shown in Figure 2-4. The peroxide ion has two more antibonding electrons than neutral O_2 , giving a bond order of 1.

$$\text{Bond order} = \frac{1}{2}(8 - 6) = 1 \text{ (a single bond)}$$

The results of this approach for O_2 and its ions are shown in Table 2-4. As the number of electrons increases, the bond order decreases (the additional electrons occupy antibonding π^* orbitals), and the oxygen–oxygen bond length increases.

Table 2-4 Dioxygen Species

Formula	Name	Bonding electrons	Antibonding electrons	Bond order	Bond length (pm)
O_2^+	Dioxygenyl	8	3	2.5	112
O_2	Dioxygen	8	4	2.0	121
O_2^-	Superoxide	8	5	1.5	128
O_2^{2-}	Peroxide	8	6	1.0	149

Fractional bond orders are possible, as in the cases of O_2^+ and O_2^- , when the number of antibonding electrons is odd.

Prepare a molecular orbital energy level diagram for the acetylide ion, C_2^{2-} , and predict its bond order.

Exercise 2-4

2-2-2 Polyatomic Molecules: The Group Orbital Approach

Most molecules, of course, have far more than two atoms, and the method used for diatomic species is not sufficient to devise an appropriate molecular orbital picture. However, the assumptions fundamental to diatomics still apply: orbitals interact if their lobes are oriented appropriately with respect to each other, and interactions are stronger if the orbitals interacting are closer in energy.

One way to view interactions between atomic orbitals in polyatomic molecules and ions is to consider separately the orbitals on a central atom and the orbitals on surrounding atoms. In this approach, the orbitals on surrounding atoms, considered a group, are labeled **group orbitals**.⁸

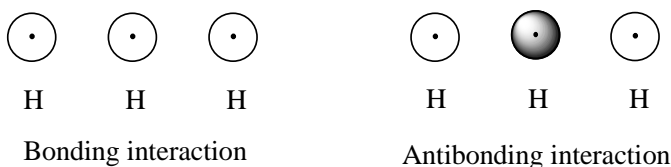
Examples

Molecular Orbitals of H_3^+ . As a simple example, we will consider the orbitals of H_3^+ , a known (although unstable) ion. One possible structure of H_3^+ would be linear: H—H—H. In this ion we have only the $1s$ orbitals to consider. There are two outer hydrogens (to contribute the group orbitals) plus the central hydrogen. The $1s$ orbitals of the outer hydrogens may have the same sign of their wave functions (group orbital 1) or opposite signs (group orbital 2).

⁸The designation “group orbital” does not imply direct bonding between the orbitals involved in the group; group orbitals should rather be viewed as collections of similar orbitals. For more information on the group orbital approach, see E. V. Anslyn and D. A. Dougherty, *Modern Physical Organic Chemistry*, University Science Books: Sausalito, CA, 2006, pp. 26–61.



In linear H_3^+ , the only orbital available on the central hydrogen is its $1s$. This orbital is capable of interacting, in both a bonding and an antibonding fashion, with group orbital 1.



The $1s$ orbital on the central hydrogen, however, cannot interact with group orbital 2; a bonding interaction on one side would be canceled by an antibonding interaction on the opposite side.

When sketching the molecular orbitals of polyatomic species, we begin by placing the valence orbitals of the central atom on the far left and the group orbitals of the surrounding atoms on the far right. We then show the resulting molecular orbital diagram in the middle. For H_3^+ the molecular orbital energy level diagram is shown in Figure 2-6.⁹

In this ion, the single pair of electrons occupies the lowest-energy molecular orbital, a bonding orbital distributed over all three atoms. This implies a bond

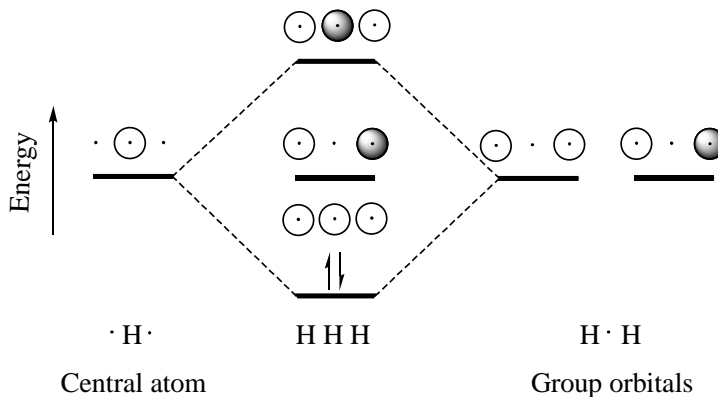


Figure 2-6
Molecular Orbitals
of Linear H_3^+

⁹Note that the MO at the middle energy level in Figure 2-6 is group orbital 2. This MO is *nonbonding*. The nonbonding MO in this case is energy equivalent to a situation in which two $1s$ orbitals are positioned an infinite distance apart and incapable of interacting. Nonbonding energy levels typically result when an odd number of orbitals interact to form MOs.

order of approximately one-half (half an electron pair per bond) and would be consistent with the observation that H_3^+ is known, but not stable.¹⁰

Molecular Orbitals of CO_2 . In most cases of polyatomic molecules, p orbitals cause the orbital analysis to be much more complex than in the case of H_3^+ . Carbon dioxide is such a situation, involving valence p orbitals on both the central and the surrounding atoms. The group orbitals are on the oxygens and are of three types.

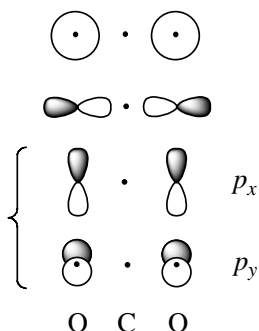
Type of group orbital

s

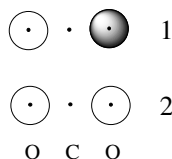
p_z (atomic orbitals pointed toward each other)

p_x and p_y (atomic orbitals parallel to each other)

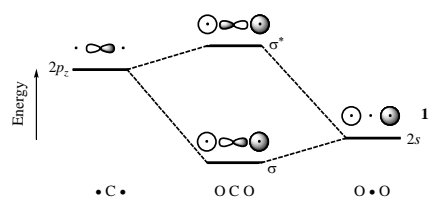
Diagrams



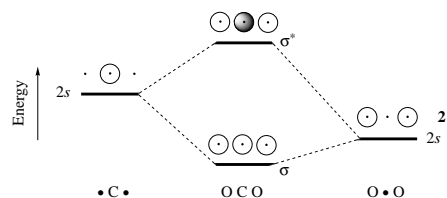
To determine the types of interactions possible between the central carbon and the group orbitals, we must consider each of the types of group orbitals in turn.



Group Orbitals

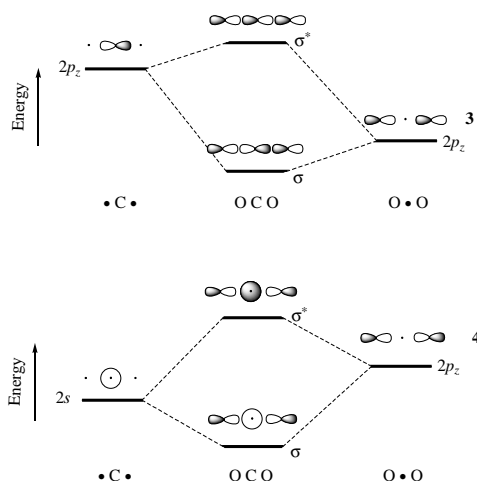
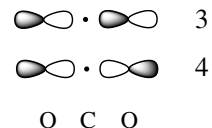


Group orbital 1 can interact with the $2p_z$ orbital of carbon. (This interaction is likely to be weak, because the $2s$ orbitals of oxygen are much lower in energy than the $2p$ orbitals of carbon.)

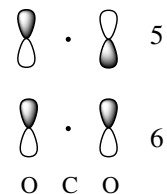


Group orbital 2 can interact with the $2s$ orbital of carbon.

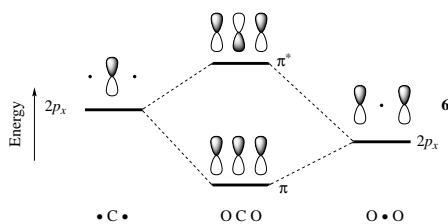
¹⁰ H_3^+ is actually believed to be cyclic rather than linear, as will be discussed later in Chapter 2.

p_z Group Orbitals

The interactions of the p_z group orbitals are similar to those in the case of the s group orbitals. Group orbital 3 can interact with the $2p_z$ orbital of carbon, and group orbital 4 can interact with the $2s$ orbital of carbon.

 p_x and p_y Group Orbitals

The p_x and p_y interactions differ only in their orientation. The p_x group orbitals are as follows:

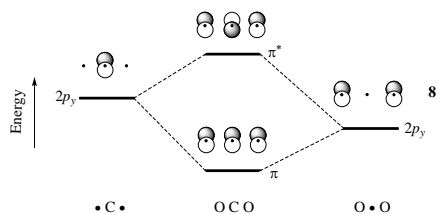
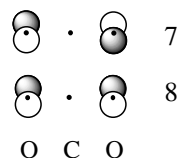


No orbital on the central carbon can interact with group orbital 5; this group orbital is nonbonding.

The $2p_x$ orbital of carbon, however, can interact with group orbital 6, as shown on the left.

The p_y interactions are similar to the p_x .

The group orbitals are as follows:



Because no atomic orbital on carbon is capable of interacting with group orbital 7, this group orbital is nonbonding. Group orbital 8 can, however, interact with the $2p_y$ orbital of carbon in an interaction similar (except for orientation) to that of group orbital 6.

The overall molecular orbital energy level diagram of CO_2 is shown in Figure 2-7. The molecular orbital picture of other linear triatomic species, such

For the linear ion FHF^- , sketch the group orbitals on the fluorines and determine which of these orbitals can interact with the $1s$ orbital of hydrogen. Sketch a molecular orbital energy level diagram.

Exercise 2-5

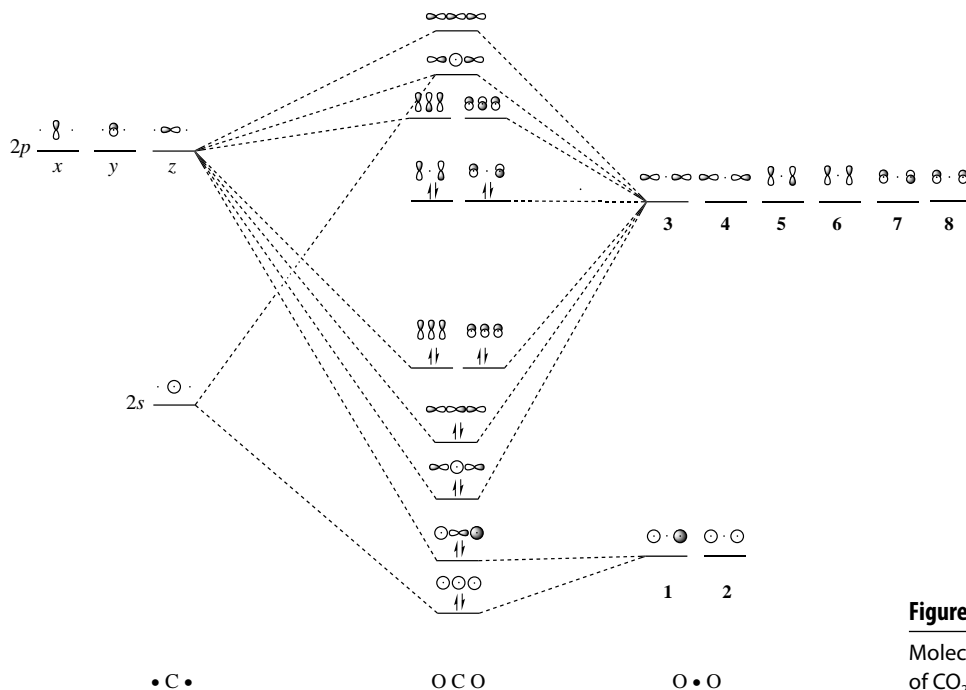


Figure 2-7

Molecular Orbitals
of CO_2

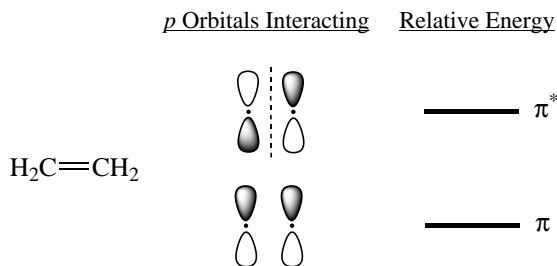
as N_3^- , and CS_2 , can be determined similarly. A similar approach can also be used in “linear” π systems, as described later in Chapter 2.

2-2-3 Ligands Having Extended π Systems

Whereas it is a relatively simple matter to describe pictorially how σ and π bonds occur between pairs of atoms, it is a somewhat more involved process to explain bonding between metals and organic ligands having extended π systems. How, for example, are the C_5H_5 rings attached to Fe in ferrocene (Figure 1-5) and how can such molecules as benzene and 1,3-butadiene bond to metals? To understand the bonding between metals and π systems, it is necessary to first consider the π bonding within the ligands themselves. Fortunately, the group orbital approach can be adapted to simplify these situations. In the following discussion, we first describe linear and then cyclic π systems; in later chapters we consider the question of how such systems can bond to metals.

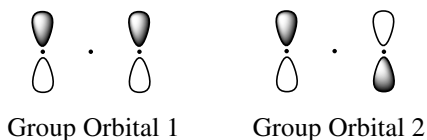
Examples

Linear π Systems. The simplest case of an organic molecule having a linear π system is ethylene, which has a single π bond resulting from the interactions of two $2p$ orbitals on its carbon atoms. Interactions of these p orbitals result in one bonding and one antibonding π orbital, as shown.



The antibonding interaction has a nodal plane perpendicular to the internuclear axis, while the bonding interaction has no such nodal plane.

Next is the three-atom system, π -allyl, C_3H_5 . In this case, there are three $2p$ orbitals to be considered, one from each of the carbon atoms participating in the π system. This situation can be viewed using the group orbital approach. The group orbitals here are derived from the parallel $2p$ orbitals on the terminal carbon atoms.



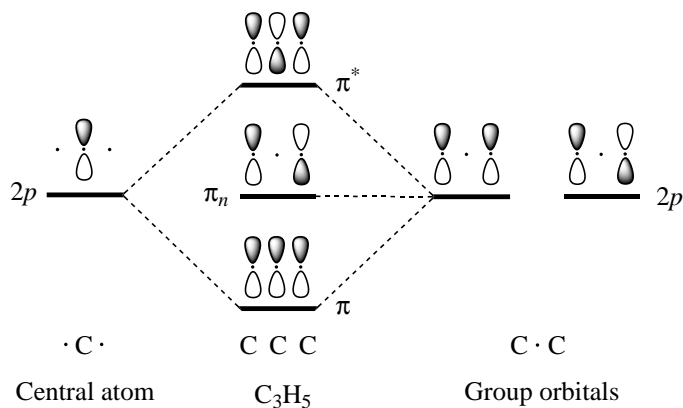
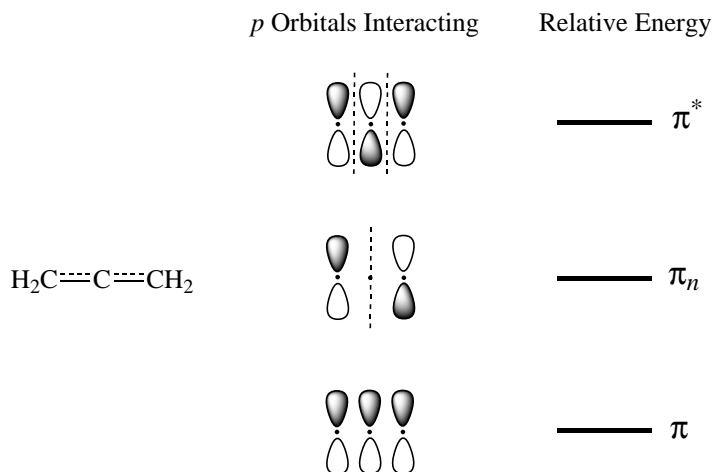


Figure 2-8
 π Molecular Orbitals
 for π - C_3H_5

Group orbital 1 can interact, in both a bonding and an antibonding fashion, with the corresponding $2p$ orbital on the central carbon. Group orbital 2, on the other hand, is not suitable for interacting with any of the central carbon orbitals; this group orbital is nonbonding. The resulting molecular orbital energy level diagram for this three-atom π system is shown in Figure 2-8.

To extend this approach, we will find it useful to view these π interactions in a slightly different way. For the π -allyl system the possible interactions are as follows.

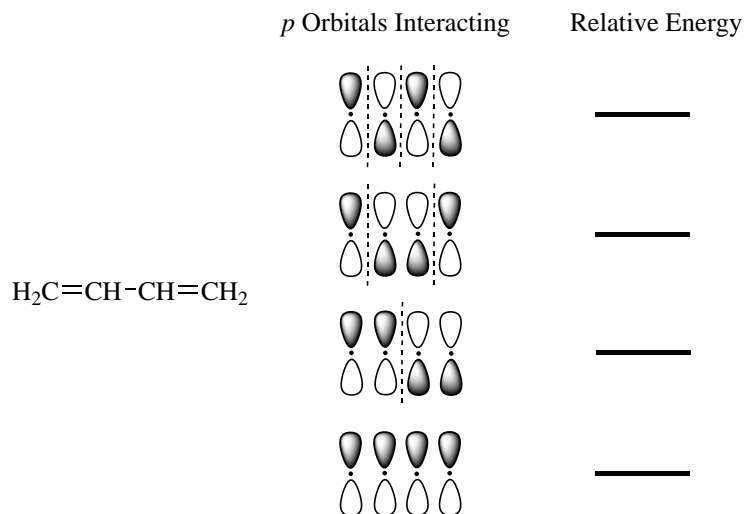


The lowest energy π molecular orbital for this system has all three p orbitals interacting constructively, to give a bonding molecular orbital. The nonbonding situation (π_n), in which a nodal plane bisects the molecule, cutting through the

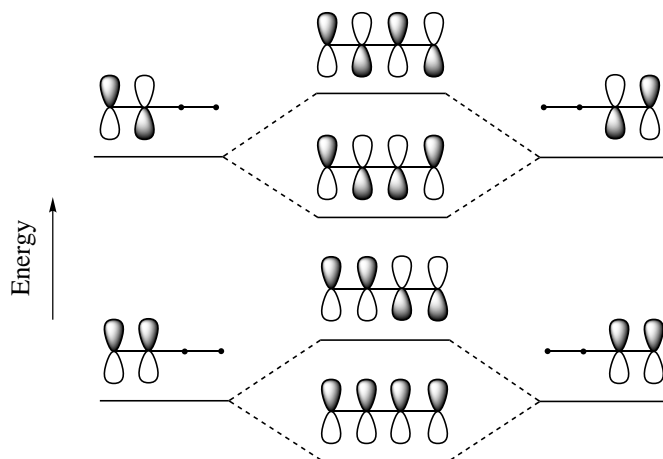
central carbon, is higher in energy. In this case, the p orbital on the central carbon does not participate in the molecular orbital (in general, nodal planes passing through the center of p orbitals and perpendicular to internuclear axes will “cancel” these orbitals from participation in the π molecular orbitals). The antibonding π^* orbital, in which there is an antibonding interaction between each neighboring pair of carbon p orbitals, is highest in energy. This can be compared with the π^* orbital of ethylene, in which an antibonding interaction also occurs.

In these π systems, there is an increase in the number of nodes in going from lower energy to higher energy orbitals—for example, in the π -allyl system, the number of nodes increases from zero to one to two, from the lowest energy to the highest energy orbital.¹¹ This is the same pattern of nodes as for linear H_3^+ (Figure 2-6). This is a trend that will also occur in more extended π systems.

One additional example should suffice to illustrate this procedure. 1,3-Butadiene may exist in *s-cis* or *s-trans* forms (where *s* designates the central C–C σ bond). For our purposes, it will be sufficient to treat both as “linear” systems; the nodal behavior of the molecular orbitals will be the same in each case as in a linear π system of four atoms. As for ethylene and π -allyl, the $2p$ orbitals of the carbon atoms in the chain may interact in a variety of ways, with the lowest energy π molecular orbital having all constructive interactions between neighboring p orbitals and the energy of the other π orbitals increasing with the number of nodes between the atoms.



¹¹This does not include the nodal plane that is coplanar with the carbon chain, bisecting each p orbital participating in the π system.

**Figure 2-9**

Construction of π Orbitals of Butadiene from Group Orbitals of Ethylene

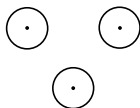
This picture can also be derived by a group orbital approach, beginning with the π and π^* orbitals of ethylene, as shown in Figure 2-9.¹² The π orbitals of two interacting ethylenes form the two lowest energy π orbitals of butadiene and, similarly, the π^* orbitals of the ethylenes can form the two highest energy π orbitals of butadiene.

Similar patterns can be obtained for longer π systems.

Sketch the π molecular orbitals for linear C_5H_7 and predict the relative energies of these orbitals.

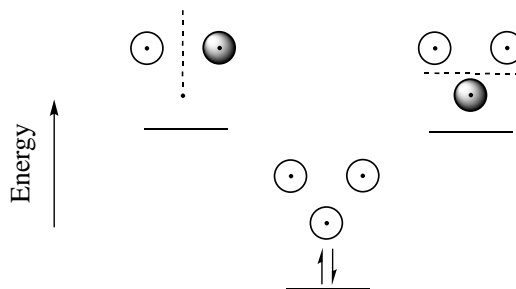
Exercise 2-6

Cyclic π Systems. The procedure for obtaining a pictorial representation of the orbitals of cyclic π systems of hydrocarbons is similar to the procedure for the linear systems described in the preceding section. Before discussing cyclic π systems, however, let us consider again the simple case of H_3^+ , now examining a possible cyclic structure for this ion. One possible interaction for *cyclo*- H_3^+ would have a bonding interaction between each participating $1s$ orbital.

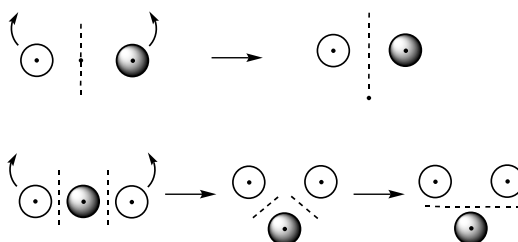


¹²T. H. Lowry and K. S. Richardson, *Mechanism and Theory in Organic Chemistry*, Harper & Row: New York, 1987, p. 79.

Figure 2-10
Molecular Orbitals
of Cyclic H_3^+



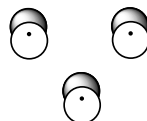
Three atomic orbitals are involved; three molecular orbitals must also be formed. What are the other two? In the linear case, the middle molecular orbital had a single node and the highest energy molecular orbital had two nodes (Figure 2-6). Suppose the linear arrangement is wrapped into an equilateral triangle, with the nodes maintained.



The result is a pair of molecular orbitals in cyclic H_3^+ , each with a single node. Because they have the same number of nodes, they have the same energy (are degenerate), as illustrated in Figure 2-10. One pair of electrons occupies a bonding orbital, giving rise to the equivalent of a one-third bond between each pair of hydrogen atoms. This is believed to be the correct geometry of the highly reactive H_3^+ .

Cyclic Hydrocarbons

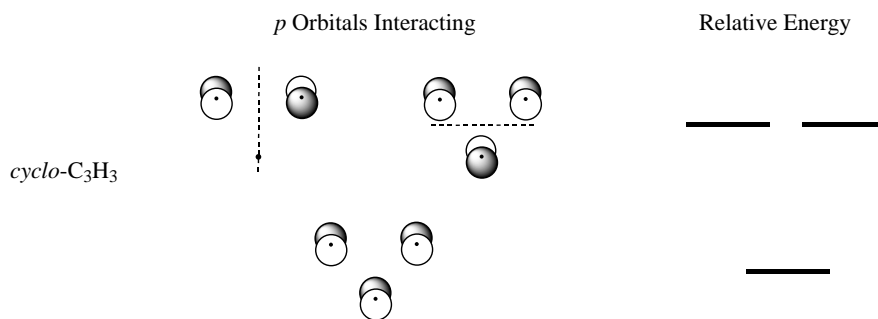
The smallest cyclic hydrocarbon having an extended π system is the cyclopropenyl system, *cyclo*- C_3H_3 . The lowest energy π molecular orbital for this system is the one resulting from constructive interaction between each of the $2p$ orbitals in the ring (top view).



Two additional π molecular orbitals are needed (because the number of molecular orbitals must equal the number of atomic orbitals used). Each of these has a single nodal plane that is perpendicular to the plane of the molecule and bisects the molecule; as in *cyclo*-H₃⁺, the nodes for these two molecular orbitals are perpendicular to each other:



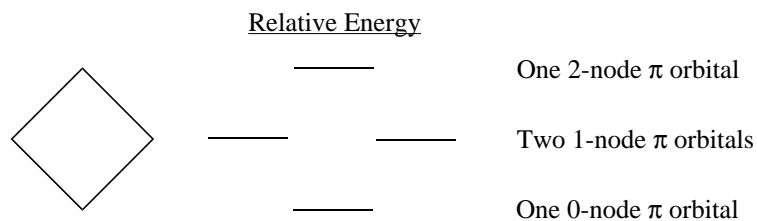
These molecular orbitals have the same energy; in general, π molecular orbitals having the same number of nodes in cyclic π systems of hydrocarbons are degenerate. The total π molecular orbital diagram for *cyclo*-C₃H₃ can therefore be summarized as follows.



A simple way to determine the p orbital interactions and the relative energies of the cyclic π systems having regular polygonal geometry is to inscribe the polygon inside a circle with one vertex pointed down; each vertex tangent to the circle then corresponds to the relative energy of a molecular orbital.¹³ Furthermore, the number of nodal planes bisecting the molecule (and perpendicular to the plane of the molecule) increases with higher energy, with the bottom orbital having zero nodes, the next pair of orbitals a single node, and so on. For example, the next cyclic π system, *cyclo*-C₄H₄ (cyclobutadiene), would be predicted by this scheme to have molecular orbitals as follows.¹⁴

¹³This operation is called the Frost–Hückel mnemonic or simply the *circle trick*.

¹⁴This approach would predict a diradical for cyclobutadiene (one electron in each 1-node orbital). Although cyclobutadiene itself is very reactive (P. Reeves, T. Devon, and R. Pettit, *J. Am. Chem. Soc.*, **1969**, *91*, 5890), complexes containing derivatives of cyclobutadiene are known. Cyclobutadiene itself is rectangular rather than square (D. W. Kohn and P. Chen, *J. Am. Chem. Soc.*, **1993**, *115*, 2844) and at 8 K it has been isolated in a solid argon matrix (O. L. Chapman, C. L. McIntosh, and J. Pacansky, *J. Am. Chem. Soc.*, **1973**, *95*, 614; A. Krantz, C. Y. Lin, and M. D. Newton, *ibid.*, **1973**, *95*, 2746).



Similar results are obtained for other cyclic π systems, as shown in Figure 2-11. In these diagrams, nodal planes are disposed symmetrically. For example, in *cyclo*- C_4H_4 the single node molecular orbitals bisect the molecule through opposite sides; the nodal planes of these molecular orbitals are oriented at 90° angles to each other. The 2-node orbital for this molecule also has the nodal planes at 90° angles.

This method may seem oversimplified, but the nodal behavior and relative energies are the same as that obtained from molecular orbital calculations. Throughout this discussion, we have shown in some cases not the actual shapes of the π molecular orbitals, but rather the p orbitals used. The nodal behavior of both sets (the π orbitals and the p orbitals that are used to generate the π orbitals) is identical and therefore sufficient to discuss how these ligands can bond to metals. Additional diagrams of numerous molecular orbitals for linear and cyclic π systems can be found in the reference in footnote 15.

Benzene. In the molecular orbital approach for benzene, each carbon in the ring is considered to use sp^2 hybrid orbitals. These orbitals are involved in carbon-carbon σ bonding (from overlap of sp^2 hybrids on adjacent carbons) and carbon-hydrogen σ bonding (from overlap of an sp^2 hybrid on each carbon with the $1s$ orbital of hydrogen). This leaves on each carbon a p orbital *not* participating in the hybrids and available to participate in a cyclic π system. When these six p orbitals interact, six π molecular orbitals are formed, as illustrated in Figure 2-12.

Benzene has six π electrons (equivalent to the six electrons used in double bonding in the Lewis structure); these occupy the three lowest-energy π molecular orbitals. The lowest-energy orbital is bonding with respect to each carbon-carbon bond (and corresponds to one bonding pair distributed over six bonds). The next two molecular orbitals are degenerate and are principally bonding, but each has a node bisecting the molecule and adding a degree of antibonding character. Overall, six electrons, or three pairs, occupy bonding orbitals spread over six bonds. The net effect is an approximate π bond order of one-half (actually

¹⁵W. L. Jorgenson and L. Salem, *The Organic Chemist's Book of Orbitals*, Academic Press: New York, 1973.

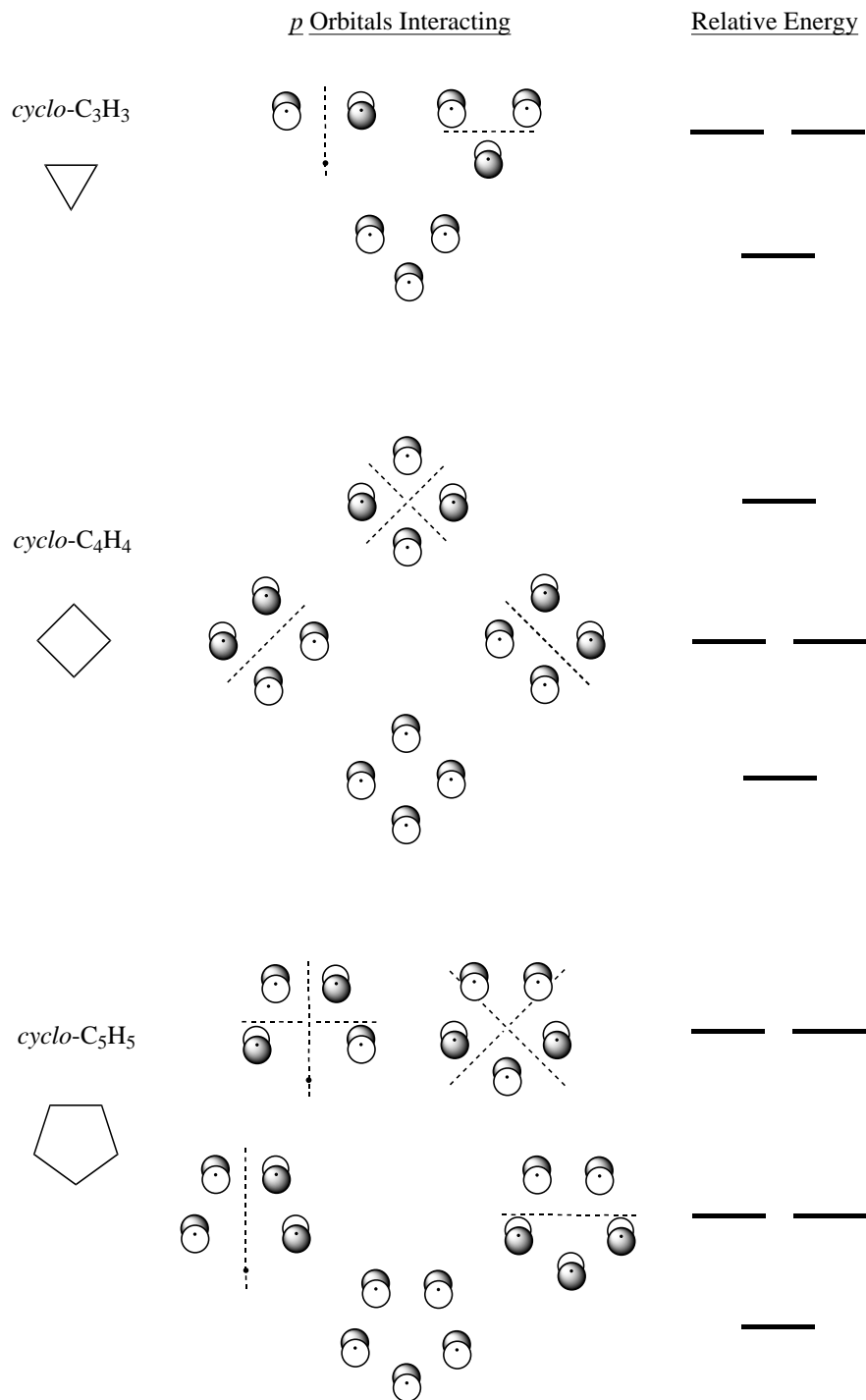


Figure 2-11
Molecular Orbitals
for Cyclic π Systems

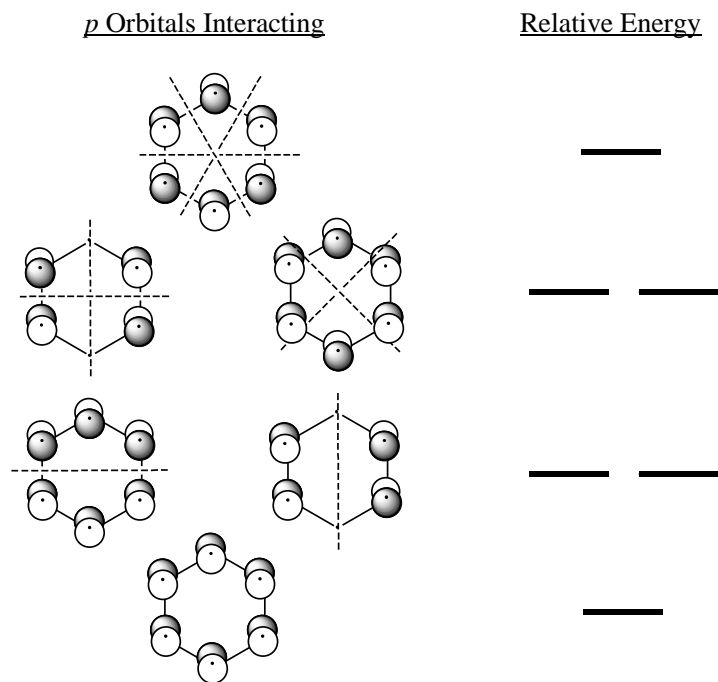


Figure 2-12
 π Molecular
 Orbitals of
 Benzene

slightly less because of the nodes in the second and third orbitals), similar to the prediction of the Lewis model.

Many other cyclic molecules like benzene are known. Some of these are involved in another “classic” family of molecules: the sandwich compounds, in which atoms, most commonly of metals, are sandwiched between rings. These remarkable compounds have proven extraordinarily interesting since the prototype, ferrocene, was synthesized in the 1950s. Examples of sandwich compounds are given in Chapter 1 (Figure 1-1); these are discussed further in Chapter 5.

2-3 COMPUTATIONAL ORGANOMETALLIC CHEMISTRY

Chemists have increasingly used computational chemistry to study aspects of organometallic chemistry. Although Chapter 2 and subsequent chapters make good use of qualitative molecular orbital theory, the ready availability of easy-to-use computational chemistry software and the powerful capability of modern desktop computers allow chemists to effectively model complex systems to obtain minimum energy geometry of molecules, determine transition state energies, and predict the course of chemical reactions, particularly if two or more isomeric products could form. Researchers have modeled entire catalytic cycles, which

is especially useful because intermediates in these cycles can be difficult to isolate and characterize. Such studies have provided compelling evidence to support certain mechanistic hypotheses and have also allowed chemists to exclude other postulated mechanisms.

Computational chemistry can be divided into two major parts: (1) molecular mechanics (MM) and (2) MO theory. The MM approach is based on classical physics; MO theory is based on quantum mechanics. MM calculations are much less mathematically intensive than computations used for most MO methods; therefore, the former method is suitable for treating large molecules containing up to thousands of atoms. MM calculations are not suitable for locating transition states, however, because the parameters used in these calculations are derived from stable, isolable molecules. The MO approach is suitable for determining the energy and structure of a transition state because the method is designed to examine electron configurations of any molecular species.

2-3-1 Molecular Mechanics

MM is based on the assumption that atoms in a molecule in the ground state adopt positions that will minimize the strain energy. Strain energy is caused by a number of factors, including: (1) bond deformation (the deviation of bond lengths in a molecule from “ideal” values; (2) angle deformation (the deviation of bond angles from “ideal” values; (3) torsional strain (dihedral angles that differ from “ideal” values give rise to torsional strain); (4) van der Waals strain (repulsion), which is also called steric hindrance; and (5) electrostatic repulsion (dipole–dipole interactions within a molecule are sometimes unfavorable). These factors comprise what is known as a *force field*.

Thus, the key part of a MM calculation is a systematic determination of the steric energy (E_{steric}) of a molecule, which is the sum of the five factors mentioned above as well as other components defined in the force field. The calculation uses equations derived from classical physics to either determine E_{steric} of the molecule, based on the input geometry, or compute this energy by systematically moving the atoms in the molecule and calculating the energy obtained after each movement. The latter process, called energy minimization, is an iterative procedure that uses mathematical criteria to determine when the minimum energy is reached.¹⁶ The higher the value of E_{steric} , the greater the deviation of the various factors, such as bond deformation, from ideal values. These ideal values are obtained from so-

¹⁶It must be pointed out that an energy minimum may be local, that is, it does not reflect the lowest energy geometry of the molecule, which is called the global minimum. Oftentimes MM calculations reach a local minimum according to preset criteria and then calculation ceases. Special efforts are then needed to prod the calculation to explore other geometries.

called strain-free molecules and are entered into the computation as parameters. For example, an sp^3 -hybridized methyl carbon atom in an alkane has a different set of force field parameters than a methylenic carbon ($=CH_2$). Thus, to perform a successful MM calculation, every atom in the molecule must have standard parameters of the force field assigned to it.

Different MM methods are available to chemists and abbreviations reminiscent of the approach used to develop them are associated with each of them. Some of the methods suitable for use in organometallic chemistry are known as augmented MM2 and MM3, as well as UFF, which stand for *molecular mechanics* version 2 or 3 and *universal force field*, respectively. The force fields for each of these methods are parameterized for the transition metals as well as the ligands attached.

E_{steric} has no direct relationship to thermodynamic constants such as heat of formation ($\Delta_f H^\circ$). On the other hand, the difference in E_{steric} between two conformational isomers or two diastereomers is similar to $\Delta\Delta_f H^\circ$ for those isomers. This suggests that the application of MM to the prediction of which of two isomeric products is more likely to form is thermodynamically meaningful. MM serves as a quick method for determining minimum energy geometries of organometallic complexes as long as the user of such a method keeps in mind that sometimes the results are not in accord with experiment because improper parameters were used for the constituent atoms. MM has also been used to determine a quantity called the natural bite angle (β_n) for bidentate ligands. The β_n has been used to assess the efficacy of bidentate ligands involved in transition metal catalyzed reactions, which will be discussed in Chapter 9.

2-3-2 MO Theory

The MO approach to molecular energy and other properties is fundamentally different than that of MM. In MM we assume that nuclei move and electrons are essentially “stationary,” that is, they are not explicitly considered in the force field calculations. Most MO approaches use the Born–Oppenheimer approximation, which considers nuclei relatively stationary compared with fast-moving electrons. Thus, the MO approach must somehow address electron motion and energy. Because the motion of electrons is governed by the Heisenberg Uncertainty Principle, quantum mechanical rather than classical physical calculations must be used.

An MO calculation is a many-body problem that cannot be solved exactly. Thus, various levels of approximation must be applied to determine MO energy levels and contours, molecular energy, and other characteristics of molecules. We will consider briefly these levels of approximation, which manifest themselves as MO methods that have acronyms associated with them, and also discuss how these methods can be applied to organometallic chemistry.

Ab initio MO Theory

All MO calculations attempt to solve the Schrödinger equation ($\mathcal{H}\Psi = E\Psi$) by setting up a Hamiltonian operator (\mathcal{H}) that contains terms for the potential and kinetic energy of the electrons in the molecule. The wave function Ψ is derived from a linear combination of basis set orbitals (typically atomic orbitals) from each atom in the molecule. The *ab initio* approach¹⁷ is the purest form of MO calculation, using the least degree of approximation, and it tries through iterative calculations to determine MO energy levels and other electronic molecular parameters by including the interactions of all atomic orbitals for the atoms in the molecule. The complexity of the calculation is a function of the completeness of the basis set of atomic orbitals. Most *ab initio* MO calculations divide pure atomic orbitals into a linear combination of wave functions such that even a simple molecule such as H₂O can have a basis set as large as over 30 basis orbital wave functions.¹⁸ Clearly, the greater the complexity of the basis set of orbitals, the more intensive the calculation.¹⁹ *Ab initio* MO calculations using large, expanded basis sets are so computationally intensive that they are limited to molecules containing fewer than perhaps 50 atoms. On the other hand, high-level *ab initio* calculations can yield results for such characteristics as bond distance and dipole moment that are very close to experimental values.

Semi-empirical MO Theory

Before the ready availability of high-speed computers, theoreticians realized that for them to perform MO calculations on anything but the very smallest molecules, they would need to reduce the mathematical intensity of the computation. They did this not only by making approximations that greatly reduced the size of the basis set (typically only the outer atomic orbitals are included in the calculation), but they also ignored the interaction of some of these basis set orbitals, which often turned out to be small and thus could be neglected. To make the computation yield results that were close to experimental values, numerical parameters were added that were derived empirically by experiment, hence the term “semi-empirical.”

¹⁷Also known as Hartree–Fock (H–F) theory.

¹⁸If only pure atomic orbitals were used for H₂O, the basis set would consist of two 1s orbitals for hydrogen and the 1s, 2s, and three 2p orbitals for oxygen, a total of seven orbitals.

¹⁹*Ab initio* calculations scale by a factor of n^4 , where n is equal to the total number of basis orbitals. Contrast this with MM calculations, which scale by a factor of m^2 , where m is equal to the number of atoms in the molecule. The computational cost difference between these two methods is enormous for molecules containing 20 or more non-hydrogen atoms.

Associated with semi-empirical MO theory are acronyms that indicate the various levels of approximation used. Some of these acronyms include CNDO, MINDO, MNDO, AM1, and PM3. These acronyms describe the level of mixing interactions of different atomic orbitals, not only on the same atom but also on adjacent atoms. The last three methods listed are most useful to organic chemists because, in addition to determining MO energy levels and providing chemists with pictorial representations of MOs, these procedures calculate $\Delta_f H^\circ$ directly. To do this, calculations are performed on “training sets” of organic molecules. Semi-empirical parameters are adjusted so that the calculation yields results that are equal to experimental heats of formation. If the semi-empirical calculations give reasonable heats of formation for every molecule in the training sets and if the training sets comprise a broad range of organic compounds, then semi-empirical calculations performed on almost any organic molecule, even those not included in the training sets, should yield accurate thermodynamic information. Work has continued to update training sets and modify semi-empirical parameters so that AM1 and PM3 calculations are generally quite reliable. Semi-empirical MO calculations can also be used as input for *ab initio* calculations, thus saving computation time overall. Until quite recently, however, semi-empirical MO methods were not parameterized to include most of the transition metals. Thus, this approach has historically had limited value to organometallic chemistry.

Extended Hückel Theory

Extended Hückel Theory (EHT) uses the highest degree of approximation of any of the approaches we have already considered. The Hamiltonian operator is the least complex and the basis set of orbitals includes only pure outer atomic orbitals for each atom in the molecule. Many of the interactions that would be considered in semi-empirical MO theory are ignored in EHT. EHT calculations are the least computationally expensive of all, which means that the method is often used as a “quick and dirty” means of obtaining electronic information about a molecule. EHT is suitable for all elements in the periodic table, so it may be applied to organometallic chemistry. Although molecular orbital energy values and thermodynamic information about a molecule are not accessible from EHT calculations, the method does provide useful information about the shape and contour of molecular orbitals.

2-3-3 Electron Correlation

All the MO methods that we have seen so far fail to consider explicitly the concept of electron correlation. Electron correlation addresses the tendency of electrons to repel one another and thus move about so that electron–electron repulsion is minimized. It accounts systematically for electrostatic interaction of electrons,

particularly those that are spin-paired in the same orbital. Thus, energies calculated by *ab initio* MO methods give electronic energy levels that are too high. The difference between the calculated value and the true value is called the correlation energy. The *ab initio* approach does not address electron correlation directly, but instead treats one electron at a time in the presence of an average field composed of the remaining electrons in the molecule. Failure to account for electron correlation can lead to poor results, especially in the calculation of transition state energies.

Semi-empirical MO methods address electron correlation implicitly; they simply adjust parameters until the calculations give the “correct” answer compared with experiment. EHT does not address electron correlation at all, so quantitative results from such calculations are almost always wrong unless fortuitous. There are, however, several approaches to explicitly account for electron correlation. One approach is to perform post-*ab initio* (post-H–F) calculations that in effect mix different electronic configurations involving the ground state and several excited states of the molecule. Such calculations are quite computationally intensive and can be performed only on relatively small molecules. Two commonly-seen acronyms associated with the post H–F approach to electron correlation are MP2 and CI, which stand for *M*øller–*P*lesset theory at the level of second-order and configuration *i*nteraction, respectively.

2-3-4 Density Functional Theory

Density Functional Theory (DFT) is similar in some respects to high-level MO theory, but its approach is fundamentally different. DFT states that the total energy of a molecule and other useful properties can be derived from precise knowledge of the electron density (ρ) of a molecule. Instead of using wavefunctions that are comprised of basis atomic orbitals, DFT in principle can employ a function that describes the electron density at every point in a molecule. Although the concept is relatively simple, the derivation of appropriate functions that describe electron density and also thereby relate to total energy is not trivial. It turns out that ρ is a function of spatial coordinates (r). To relate $\rho(r)$ to energy, DFT uses the mathematical concept of a *functional*, which is a function of a function. In other words, if $f(r) = \rho$ (i.e., ρ is a function of r), then the functional that gives the energy is $F[f(r)]$.

The exact form of $F[f(r)]$ is impossible to determine exactly, but it can be approximated according to equation 2.1.

$$E = F[f(r)] = E^T + E^V + E^J + E^{XC} \quad 2.1$$

E^T is a functional representing kinetic energy, E^V gives the potential energy (nuclear–electron attraction and nuclear–nuclear repulsion), and E^J is a coulombic functional that represents electron–electron repulsion. The sum of the

first three terms of equation 2.1 represents the classical energy of the charge distribution of the molecular system. The exchange-correlation term is given by E^{XC} , which is not so straightforward to describe. Usually DFT calculations divide E^{XC} into two parts, one representing exchange interactions of electrons based on the Pauli Exclusion Principle and the other representing electron correlation effects. The exchange functional is not based on classical notions, such as kinetic and potential energy, but instead derives from the quantum mechanical treatment of electron behavior. Because DFT explicitly includes an electron correlation term, the answers it provides automatically reflect the effects of electron correlation.

Now that we have a theoretically sound basis for determining molecular energy and other parameters on the basis of electron density, the task remains to put this theory into practice. Unfortunately, the functional E^{XC} cannot be explicitly described and its value is not known. Theoreticians Kohn and Sham derived a set of equations that allows the evaluation of E^{XC} .²⁰ The exact procedure they developed goes beyond the scope of this text, but it can be described qualitatively. The Kohn–Sham equations use a basis set of orbitals, very similar to those employed for *ab initio* MO theory, to determine a suitable representation of E^{XC} . The process involves using a functional that incorporates the basis orbitals and first guessing at a trial solution. Then the result obtained using the trial solution is used to determine a new solution, and the process continues iteratively until self-consistency is reached. To augment the Kohn–Sham approach and make it more practical for actual computer calculations, approximations to E^{XC} have been developed by several theoreticians using empirical data. Thus, DFT contains elements of a semi-empirical approach in these cases. Two acronyms attached to DFT calculations are B3LYP and PW91, where the letters refer to the individuals who developed the method. Often the DFT method chemists apply is abbreviated to indicate the method employed to determine E^{XC} and the basis set of Kohn–Sham orbitals used, for example, B3LYP/6–31G.

A major advantage of DFT theory is its relatively low computational intensity compared with post-*ab initio* electron correlation calculations.²¹ Because DFT calculations can be augmented with empirical data relevant to the transition metals, they are now the preferred approach to theoretical studies of organotransition metal chemistry. We must point out, however, that theoreticians still cannot know ahead of time which DFT method will work best for a particular situation;

²⁰W. Kohn and I. J. Sham, *Phys. Rev. A*, **1965**, *140*, 1133.

²¹The computational cost of most DFT calculations is approximately the same as that for *ab initio* methods using large basis sets of orbital functions.

Table 2-5 Comparison of Computational Chemistry Methods

Method	Accuracy	Utility	Suitability for organometallic chemistry	Computational cost	Molecular scale
Molecular Mechanics (MM)	Fair to good; depends on atom parameterization	Energy comparison of conformers and diastereomers	Good if augmented parameters for transition metals are used	Low	Up to thousands of atoms
<i>Ab initio</i> MO Theory	Good if large basis sets of orbitals are used and post-H-F calculations are performed	Equilibrium and transition state geometries; reaction energy calculations	Poor	Medium to high; depends on basis set; if post-H-F calculations are done, cost is very high	Up to 50 atoms
Semi-empirical MO Theory ^a	Now good for most organometallic molecules	Same as <i>ab initio</i> MO theory; $\Delta_r H^\circ$ values	Good; most transition metals are now parameterized	Medium	Up to thousands of atoms
Extended Hückel Theory (EHT)	Poor	Determining shapes of MOs	Good	Low	Up to 100 atoms or more
Density Functional Theory (DFT)	Generally good; depends on method	Same as <i>ab initio</i> MO theory	Good	High	Up to 50 atoms

^aA new edition of semi-empirical MO software (PM6 from MOPAC2009™) is available that is much more powerful than older editions, which were not suitable for calculations on organotransition metal complexes.

often, more than one brand of calculation must be used for comparison purposes. Efforts to improve DFT by introducing variations that will behave in a predictable fashion are ongoing.

Table 2-5 compares the characteristics and utility of all of the methods we have just considered.

Suggested Reading

Atomic and Molecular Orbitals

H. B. Gray, *Chemical Bonds: An Introduction to Atomic and Molecular Structure*, Benjamin: Menlo Park, CA, 1973.

Y. Jean, F. Volatron, and J. Burdett, *An Introduction to Molecular Orbitals*, Oxford University Press: New York, 1993.

- J. G. Verkade, *A Pictorial Approach to Molecular Bonding and Vibrations*, 2nd ed., Springer-Verlag: New York, 1997.
- J. K. Burdett, *Chemical Bonds: A Dialog*, Wiley: Chichester, England, 1997.

Computational Chemistry

- E. G. Lewars, *Computational Chemistry: Introduction to the Theory and Applications of Molecular and Quantum Mechanics*, Kluwer Academic: Boston, 2003.
- C. J. Cramer, *Essentials of Computational Chemistry: Theory and Models*, Wiley: Chichester, England, 2002.
- A. Leach, *Molecular Modeling: Principles and Applications*, 2nd ed., Prentice Hall: Upper Saddle River, NJ, 2001.
- Computational Organometallic Chemistry*, T. R. Cundari, Ed., Dekker: New York, 2001.
- W. Koch and M. C. Holthausen, *A Chemist's Guide to Density Functional Theory*, Wiley-VCH: Weinheim, Germany, 2000.
- F. Jensen, *Introduction to Computational Chemistry*, Wiley: Chichester, England, 1999.
- A. K. Rappe and C. J. Casewit, *Molecular Mechanics across Chemistry*, University Science Books: Sausalito, CA, 1997.
- W. J. Hehre, L. Radom, P. v. R. Schleyer, and J. Pople, *Ab Initio MO Theory*, Wiley: New York, 1986.

Problems

- 2-1** What are possible values of the following?
- Quantum number l for a shell having $n = 3$
 - Quantum number m_s for two electrons occupying the same orbital
 - Quantum number m_l for p electrons
 - Quantum number m_l for electrons in a $4d$ subshell
- 2-2** Classify the interactions between orbitals on two adjacent atoms as σ , π , or nonbonding. Assume that the two atoms aligned along the horizontal axis (z -axis), and the y -axis is the vertical axis.
- Atom 1: d_{yz} ; atom 2: d_{yz}
 - Atom 1: p_y ; atom 2: d_{xz}
 - Atom 1: d_z^2 ; atom 2: s
- 2-3** Classify the interactions between orbitals on two adjacent atoms as σ , π , or nonbonding. Assume that the two atoms aligned along the horizontal axis (z -axis), and the y -axis is the vertical axis.
- Atom 1: s ; atom 2: p_y
 - Atom 1: p_z ; atom 2: d_{xy}
 - Atom 1: p_y ; atom 2: p_y

- 2-4 Prepare a molecular orbital energy level diagram for nitric oxide (NO) and predict the bond order of this molecule. On the basis of the molecular orbital diagram, what do you predict for the bond orders of NO^+ and NO^- ? Which of these diatomic species would you expect to have the shortest bond length? Why?
- 2-5 The shapes of the π and π^* orbitals of diatomic ligands are important in organometallic chemistry.
- Sketch the expected shapes of the π and π^* orbitals of the following:
 N_2 CN^- CO BO^-
 - What trends do you predict in the shapes of these orbitals? Why do you expect such trends? (Hint: Consider relative electronegativity.)
- 2-6 Now use molecular modeling software to generate the shapes of the π and π^* orbitals of the molecules and ions listed in the preceding problem. What trends do you observe? Are these consistent with trends in electronegativities?
- 2-7 On the basis of molecular orbitals, predict the shortest bond in each set.
- H_2^+ H_2
 - NO^+ NO NO^-
 - CO^+ CO
- 2-8 Is H_4 a plausible molecule? Using the approach described in Chapter 2, sketch the molecular orbitals (show interacting orbitals, nodes of molecular orbitals, and relative energies of molecular orbitals) for the following geometries:
- Linear
 - Square
- Which, if either, would you expect to be a more likely structure?
- 2-9 For the linear azide ion, N_3^- , sketch the group orbitals and determine which of these orbitals can interact with the valence orbitals of the central nitrogen. Classify the possible interactions as σ , π , or nonbonding.
- 2-10 Sketch the π orbitals of 1,3,5-hexatriene, C_6H_8 , and predict the relative energies of the orbitals. Indicate clearly the locations of the nodes.
- 2-11 Sketch the π orbitals of *cyclo*- C_7H_7 and predict the relative energies of these orbitals. Indicate clearly the locations of the nodes.
- 2-12 Now use molecular modeling software to calculate and display the π molecular orbitals of the following molecules:
- π -Allyl, C_3H_5 . Compare your results with Figure 2-8.

- b. 1,3,5-Hexatriene, C_6H_8 . Compare your results with your sketches in problem **2-10**.
- c. Cyclobutadiene, C_4H_4 . Compare your results with the diagrams shown for this molecule in Figure **2-11**.
- d. *cyclo*- C_7H_7 . Compare your results with your sketches in problem **2-11**.

The 18-Electron Rule

In main group chemistry, electron counts in molecules are often described by the octet rule, in which electronic structures can be rationalized on the basis of a valence shell requirement of 8 electrons (two valence *s* electrons plus six valence *p* electrons). Similarly, in organometallic chemistry the electronic structures of many compounds are based on a total valence electron count of 18 on the central metal atom (ten valence *d* electrons in addition to the *s* and *p* electrons of the “octet”). As in the case of the octet rule, there are many exceptions to the **18-electron rule**,¹ but the rule nevertheless provides some useful guidelines to the chemistry of many organometallic complexes. In Chapter 3 we first examine how electrons are counted according to this rule. We then consider the basis for its usefulness (and some of the reasons why it is not always valid).

3-1 COUNTING ELECTRONS

Several schemes exist for counting electrons in organometallic compounds. We will describe two of these using several examples. The first two examples are of classic 18-electron species.

3-1-1 Method A: Donor Pair Method

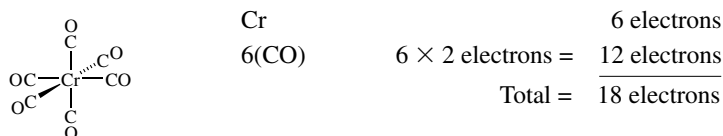
This method considers ligands to donate electron pairs to the metal. To determine the total electron count, one must take into account the charge on each

¹Also called the effective atomic number (EAN) rule.

ligand and determine the formal oxidation state of the metal. We will demonstrate this method using two examples of classic 18-electron complexes, $\text{Cr}(\text{CO})_6$ and $(\eta^5\text{-C}_5\text{H}_5)\text{Fe}(\text{CO})_2\text{Cl}$.

$\text{Cr}(\text{CO})_6$

A chromium atom has six electrons outside its noble gas core. For transition metals the only electrons that are counted are the *s* and *d* electrons beyond the noble gas core. Each CO is considered to act as a donor of 2 electrons (from an electron dot standpoint, $:\text{C}\equiv\text{O}:$, the donated electrons correspond to the lone pair on carbon). Thus, the total electron count is



$\text{Cr}(\text{CO})_6$ is therefore considered an 18-electron complex. It is thermally stable; for example, it can be sublimed without decomposition. $\text{Cr}(\text{CO})_5$, a 16-electron species, is much less stable and known primarily as a reaction intermediate;² 20-electron $\text{Cr}(\text{CO})_7$ is not known. Likewise, the 17-electron $[\text{Cr}(\text{CO})_6]^+$ and 19-electron $[\text{Cr}(\text{CO})_6]^-$ are much less stable than the neutral, 18-electron $\text{Cr}(\text{CO})_6$. The bonding in $\text{Cr}(\text{CO})_6$, which provides a rationale for the special stability of many 18-electron systems, is discussed in Section 3-2.

$(\eta^5\text{-C}_5\text{H}_5)\text{Fe}(\text{CO})_2\text{Cl}$

As usual, CO is counted as a two-electron donor. Chloride is considered Cl^- , also a donor of two electrons (one of the four valence electron pairs in $:\ddot{\text{Cl}}:^-$). Pentahapto- C_5H_5 (see diagram on next page) is considered by this method as C_5H_5^- , a donor of three electron pairs; it is a six-electron donor. Therefore, because this complex³ is considered to contain the two negative ligands Cl^- and C_5H_5^- , the oxidation state of iron in $(\eta^5\text{-C}_5\text{H}_5)\text{Fe}(\text{CO})_2\text{Cl}$ is 2⁺. In this case, iron (II) has six such electrons:⁴

Iron(0) has the electron configuration $[\text{Ar}] 4s^2 3d^6$

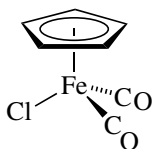
Iron(II) has the electron configuration $[\text{Ar}] 3d^6$

²J. Kim, T. K. Kim, J. Kim, Y. S. Lee, and H. Ihee, *J. Phys. Chem. A*, **2007**, *111*, 4697, and references cited therein.

³The η^5 notation (read “pentahapto” and signifying that the ligand has a *hapticity* of 5) designates that all five carbon atoms in the C_5H_5 ring are bonded to the iron (in general, the superscript in this notation indicates the number of atoms in a ligand bonded to a metal; this type of notation is discussed further in Chapter 5).

⁴Oxidation states may be indicated by charges (2+) or by Roman numerals in parentheses (II).

The electron count in the molecule $(\eta^5\text{-C}_5\text{H}_5)\text{Fe}(\text{CO})_2\text{Cl}$ is therefore



Fe(II)	6 electrons
$\eta^5\text{-C}_5\text{H}_5^-$	6 electrons
2 (CO)	4 electrons
Cl ⁻	<u>2 electrons</u>
Total =	18 electrons

3-1-2 Method B: Neutral Ligand Method

This method uses the number of electrons that would be donated by ligands *if they were neutral*. For neutral ligands such as CO, donated electrons are counted in the same way as in method A. For monatomic ligands derived from ions, ligands are considered to donate the number of electrons equal to their negative charge as free ions. For example,

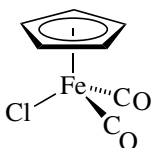
<i>Free ion</i>	<i>Electron count by neutral ligand model</i>	
Cl ⁻	Cl	1-electron donor
O ²⁻	O	2-electron donor
N ³⁻	N	3-electron donor

To determine the total electron count by this method, one does not need to determine the oxidation state of the metal.

Cr(CO)₆

Because the only ligand in this compound is the neutral CO, the electron count by this method is identical to the count by method A.

$(\eta^5\text{-C}_5\text{H}_5)\text{Fe}(\text{CO})_2\text{Cl}$ In this method, $\eta^5\text{-C}_5\text{H}_5$ is now considered as if it were a neutral ligand (or radical), in which case it would contribute five electrons; *the electron count is identical to the hapticity (superscript)*. CO again is a two-electron donor and Cl (counted as if it were a neutral species) is a one-electron donor. An iron atom (considered neutral) has eight electrons beyond its noble gas core. The electron count is as follows:



Fe atom	8 electrons
$\eta^5\text{-C}_5\text{H}_5$	5 electrons
2 (CO)	4 electrons
Cl	<u>1 electron</u>
Total =	18 electrons

Method B therefore gives the same result as method A: $(\eta^5\text{-C}_5\text{H}_5)\text{Fe}(\text{CO})_2\text{Cl}$ is an 18-electron species.

3-1-3 Other Considerations

Charge

Many organometallic complexes are charged, and this charge must be included when determining the total electron count. We can verify, by either method of electron counting, that $[\text{Mn}(\text{CO})_6]^+$ and $[(\eta^5\text{-C}_5\text{H}_5)\text{Cr}(\text{CO})_3]^-$ are both 18-electron ions.

$[\text{Mn}(\text{CO})_6]^+$

Method A: Mn^+ has the configuration $[\text{Ar}]3d^6$: 6 electrons outside the Ar core:

Mn(I):	6 electrons
6 CO	12 electrons
Total =	<u>18 electrons</u>

Method B:	Mn	7 electrons
	6 CO	12 electrons
	+ charge	- 1 electron (subtract electron for each + charge)
	Total =	<u>18 electrons</u>

$[(\eta^5\text{-C}_5\text{H}_5)\text{Cr}(\text{CO})_3]^-$

Method A:	Cr(0):	6 electrons
	3 CO	6 electrons
	$(\eta^5\text{-C}_5\text{H}_5)^-$	6 electrons
	Total =	<u>18 electrons</u>

Method B:	Cr	6 electrons
	3 CO	6 electrons
	$\eta^5\text{-C}_5\text{H}_5$	5 electrons
	- charge	1 electron (add electron for each - charge)
	Total =	<u>18 electrons</u>

Metal–Metal Bonds

A metal–metal bond is equivalent to an electron pair. In general, these electrons are assigned equally to the metal atoms.

M–M	2 electrons in bond	1 electron per metal
M=M	4 electrons in bonds	2 electrons per metal
M≡M	6 electrons in bonds	3 electrons per metal

For example, in the dimeric complex $(\text{CO})_5\text{Mn–Mn}(\text{CO})_5$, the electron count per manganese atom is (by both methods)

Mn	7 electrons
5 (CO)	10 electrons
Mn–Mn bond	1 electron
Total =	18 electrons

For future reference, the electron counts for common ligands according to both schemes are given in Table 3-1.

The electron counting method used is a matter of individual preference. Method A has the advantage of including the formal oxidation state of the metal but may tend to overemphasize the ionic nature of some metal–ligand bonds. Counting electrons for some otherwise simple ligands (such as O^{2-} and N^{3-}) may seem cumbersome and unrealistic. Method B is often quicker, especially for ligands having extended π systems; for example, η^5 ligands have an electron count of 5, η^3 ligands an electron count of 3, and so on (see Footnote 2). Also, method B has the advantage of not requiring that the oxidation state of the metal be assigned. Other electron counting schemes have also been developed. It is generally best to select one method and to use it consistently.

Table 3-1 Electron Counting Schemes for Common Ligands

Ligand	Method A	Method B
H	2 (:H ⁺)	1
F, Cl, Br, I	2 (:X ⁻)	1
OH	2 (:OH ⁻)	1
CN	2 (:C≡N: ⁻)	1
CH ₃	2 (:CH ₃ ⁻)	1
NO (bent M–N–O)	2 (:N=O: ⁻)	1
CO, PR ₃	2	2
NH ₃ , H ₂ O	2	2
=CRR' (carbene)	2	2
H ₂ C = CH ₂	2	2
=O, =S	4 (:O ²⁻ , :S ²⁻)	2
NO (linear M–N–O)	2 (:N≡O: ⁺)	3
η^3 -C ₃ H ₅ (allyl)	2 (C ₃ H ₅ ⁺)	3
≡CR (carbyne)	3	3
≡N	6 (N ³⁻)	3
η^4 -C ₄ H ₆ (butadiene)	4	4
η^5 -C ₅ H ₅ (cyclopentadienyl)	6 (C ₅ H ₅ ⁻)	5
η^6 -C ₆ H ₆ (benzene)	6	6
η^7 -C ₇ H ₇ (tropylium ion)	6 (C ₇ H ₇ ⁺)	7

Example 3-1

Both methods of electron counting are illustrated for the following complexes.

<i>Complex</i>	<i>Method A</i>		<i>Method B</i>	
[Fe(CO) ₂ (CN) ₄] ²⁻	Fe(II)	6 e ⁻	Fe	8 e ⁻
	2 CO	4 e ⁻	2 CO	4 e ⁻
	4 CN ⁻	8 e ⁻	4 CN ⁻	4 e ⁻
	2 - charge	^a		2 e ⁻
		18 e ⁻		18 e ⁻
(η ⁵ -C ₅ H ₅) ₂ Fe (ferrocene)	Fe(II)	6 e ⁻	Fe	8 e ⁻
	2 η ⁵ -C ₅ H ₅ ⁻	12 e ⁻	2 η ⁵ -C ₅ H ₅	10 e ⁻
		18 e ⁻		18 e ⁻
[Re(CO) ₅ (PF ₃)] ⁺	Re(I)	6 e ⁻	Re	7 e ⁻
	5 CO	10 e ⁻	5 CO	10 e ⁻
	PF ₃	2 e ⁻	PF ₃	2 e ⁻
	+ charge	^a	+ charge	-1 e ⁻
		18 e ⁻		18 e ⁻

^aCharge on ion is accounted for in assignment of oxidation state to Re.

Electron counting (by any method) does *not* imply anything about the degree of covalent or ionic bonding; it is strictly a bookkeeping procedure, as are the metal oxidation numbers that may be used in the counting. Physical measurements are necessary to provide evidence about the actual electron distribution in molecules. Linear and cyclic organic π systems interact with metals in more complicated ways, as discussed in Chapter 5.

Exercise 3-1

Determine the valence electron counts for the metals in the following, not all of which are 18-electron complexes.

- [Fe(CN)₆]³⁻
- (η⁵-C₅H₅)Ni(NO) (has linear Ni-N-O)
- cis*-Pt(NH₃)₂Cl₂
- W(CH₃)₆

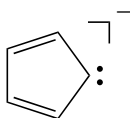
Exercise 3-2

Identify the first-row transition metal for the following 18-electron species.

- [M(CO)₃(PPh₃)]⁻
- HM(CO)₅
- (η⁴-C₈H₈)M(CO)₃
- [(η⁵-C₅H₅)M(CO)₃]₂ (assume single M-M bond)

Covalent Bond Classification (L–X Notation)⁵

It is useful to introduce some symbolism that will appear often in later chapters in this book. Most ligands may be classified as “L-type” or “X-type.” L-type ligands are neutral, two-electron donors such as CO or PR₃. Ligands such as Cl or CH₃ are designated X-type ligands. X-type ligands typically carry a negative charge and would be two-electron donors according to the Donor Pair Method (method A) and one-electron donors according to the Neutral Ligand Method (method B). Some ligands, such as η⁵-C₅H₅, contain both types of classifications. If we consider the structure of η⁵-C₅H₅ to have the following structural representation, it would be symbolized in L–X notation as L₂X.



In general, any organometallic complex containing L- and X-type ligands may be represented by the general formula



where

a = the number of X-type ligands,

b = the number of L-type ligands,

and

c = the charge.

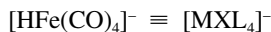
Several useful relationships result from this notation.

1. Electron count (EAN):

$$\text{EAN} = N + a + 2b - c$$

where N = the group number of the metal in the periodic table.

Example:

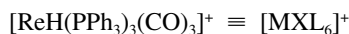


$$\text{EAN} = 8 + 1 + 2(4) - (-1) = 18 \text{ electrons}$$

2. Coordination number (CN):

$$\text{CN} = a + b$$

⁵For further details of the CBC (L–X) system and additional examples, see M. L. H. Green, *J. Organomet. Chem.*, **1995**, 500, 127.

Example:

$$\text{CN} = 1 + 6 = 7$$

3. Oxidation state of the metal (OS):

$$\text{OS} = a + c$$

Example:

$$\text{OS} = 3 + 0 = 3$$

4. Number of
- d
- electrons (
- d^n
-):

$$d^n = \text{N} - \text{OS} = \text{N} - (a + c)$$

Example:

$$d^n = 4 - (4 + 0) = 0$$

Exercise 3-3

Represent the complex $[\text{Ir}(\text{CO})(\text{PPh}_3)_2(\text{Cl})(\text{NO})]^+$ in L-X notation. Calculate the electron count, coordination number, oxidation state of the metal, and number of d electrons for the metal.

3-2 WHY 18 ELECTRONS?

An oversimplified rationale for the special significance of 18 electrons can be made by analogy with the octet rule in main group chemistry. If the octet represents a complete valence electron shell configuration (s^2p^6), then the number 18 can be considered to correspond to a filled valence shell for a transition metal ($s^2p^6d^{10}$). This analogy, although perhaps a useful way to relate the electron configurations to the idea of valence shells of electrons for atoms, does not explain why many complexes violate this “rule.” In particular, the valence shell rationale does not distinguish among types of interactions that may occur between metal

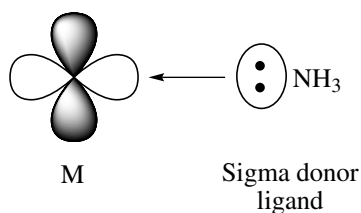
and ligand orbitals; this distinction is an important consideration in determining which complexes obey the rule and which ones violate it.

3-2-1 Types of Metal–Ligand Interactions

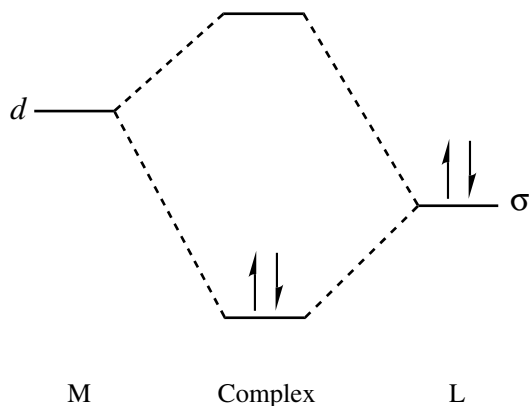
Metal and ligand orbitals can interact in several ways. The type of interaction depends on the orientation of the orbitals with respect to each other. Most of these interactions can be classified into three types, based on the role of the ligands: σ donor, π donor, and π acceptor. These classifications are discussed in the following sections.

σ Donor Ligands

These ligands have an electron pair capable of being donated directly toward an empty (or partly empty) metal orbital. The following is an example of the interaction of a donor orbital of NH_3 , occupied by a lone pair of electrons, and an empty d orbital of suitable orientation on a metal.

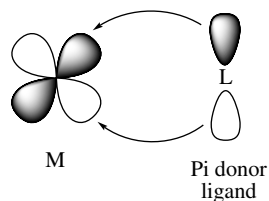


In a σ donor interaction, the electron pair on the ligand is stabilized by the formation of a bonding molecular orbital, and the empty metal orbital (a d orbital in the example above) is destabilized in the formation of an antibonding orbital, as shown below.

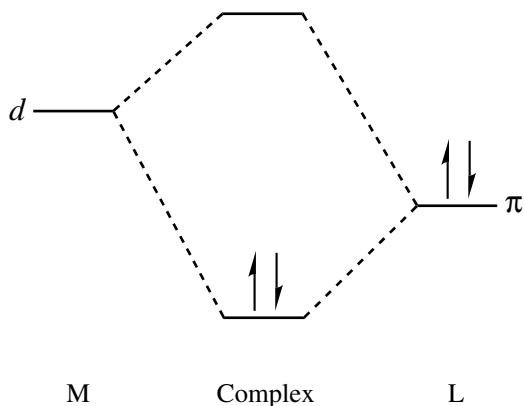


π Donor Ligands

In some cases, ligands may donate electrons in a π fashion, for example, using a filled p orbital as indicated below. Halide ions may participate in this type of interaction, with an electron pair donated in a π fashion to an empty metal d orbital (this d orbital must have a different orientation than the d orbital used in σ interactions).

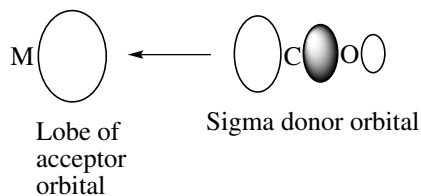


The π donor interaction is in one respect similar to the σ donor case; the electron pair on the ligand is stabilized by the formation of a bonding molecular orbital, and the empty metal d orbital is destabilized in the formation of an antibonding orbital.

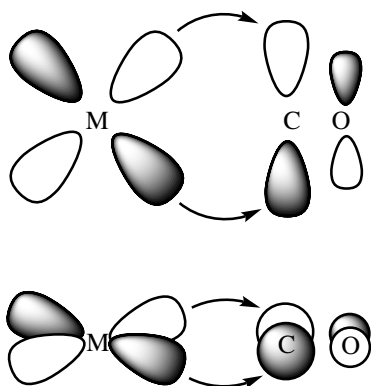


π Acceptor Ligands

Although ligands are often thought of as donating electron pairs to metals, such is not always the case. For example, many types of ligands are known in which σ donation is complemented by the ability of a ligand to accept electron density from a metal using suitable acceptor orbitals. The classic example of such a ligand is CO, the carbonyl ligand. The CO ligand can function as a σ donor using an electron pair in its highest occupied molecular orbital (HOMO), as shown on the next page.



At the same time, CO has empty π^* orbitals of suitable orientation to accept electron density from the metal.



The effect of the π acceptor interaction is the opposite of the σ interactions; an electron pair on the metal is now stabilized when a molecular orbital is formed, whereas the energy of the (empty) ligand orbital is *destabilized* as it becomes a higher energy (antibonding) molecular orbital.

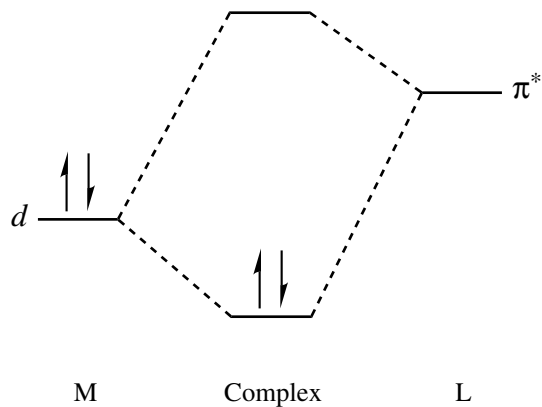
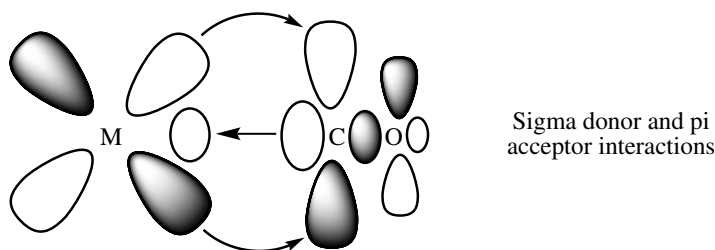


Table 3-2 Examples of Donor and Acceptor Ligands.

σ Donor	π Donor ^a	π Acceptor ^a
NH ₃	OH ⁻	CO
H ₂ O	Cl ⁻	CN ⁻
H ⁻	RCO ₂ ⁻	PR ₃

^aThese ligands also act as σ donors.

These two ligand functions, σ donor and π acceptor, are synergistic. The more effective the σ donation, the greater the electron density on the metal. The resulting electron-rich metal in turn is capable of donating electrons back to the ligand,⁶ which then acts as a π acceptor.



Examples of common ligands of all three types are given in Table 3-2. In many instances, ligands behave in more than one way. Hydroxide, for example, can be considered both a σ donor and a π donor, whereas a phosphine (PR₃) is both a σ donor and a π acceptor.

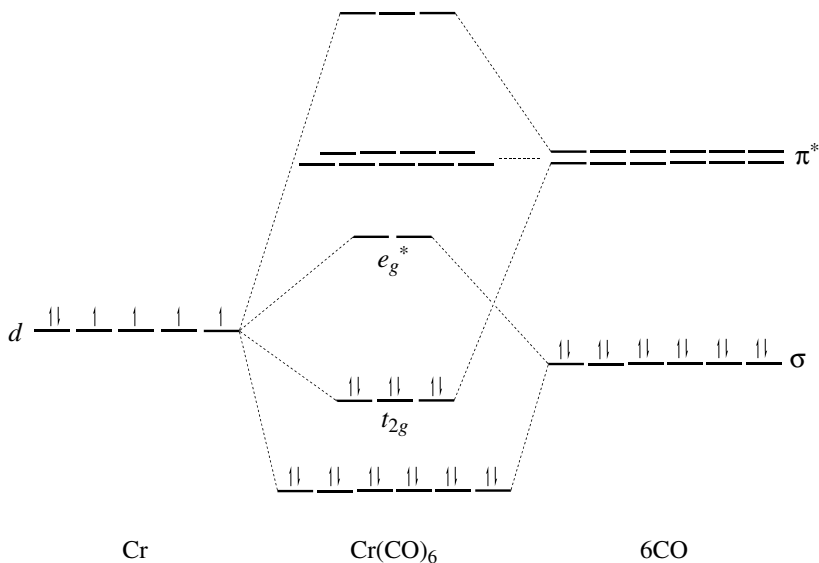
3-2-2 Molecular Orbitals and the 18-Electron Rule

Octahedral Complexes

As we pointed out earlier in Chapter 3, Cr(CO)₆ is a good example of a complex that obeys the 18-electron rule. The molecular orbitals of interest in this molecule are those that result primarily from interactions between the *d* orbitals of Cr and the σ donor (HOMO) and π acceptor orbitals (LUMO) of the six CO ligands. The molecular orbitals corresponding to these interactions are shown in Figure 3-1.⁷ (See Chapter 2, Figure 2-5, for a molecular orbital picture of CO.)

⁶This phenomenon is sometimes called “back-bonding” or “back-donation.”

⁷Molecular orbitals are often designated by symmetry labels, such as the *t*_{2g} and *e*_g* labels describing orbitals with significant *d* character in Figure 3-1. The method of assigning these labels is beyond the scope of this text. For further information on symmetry labels,

**Figure 3-1**

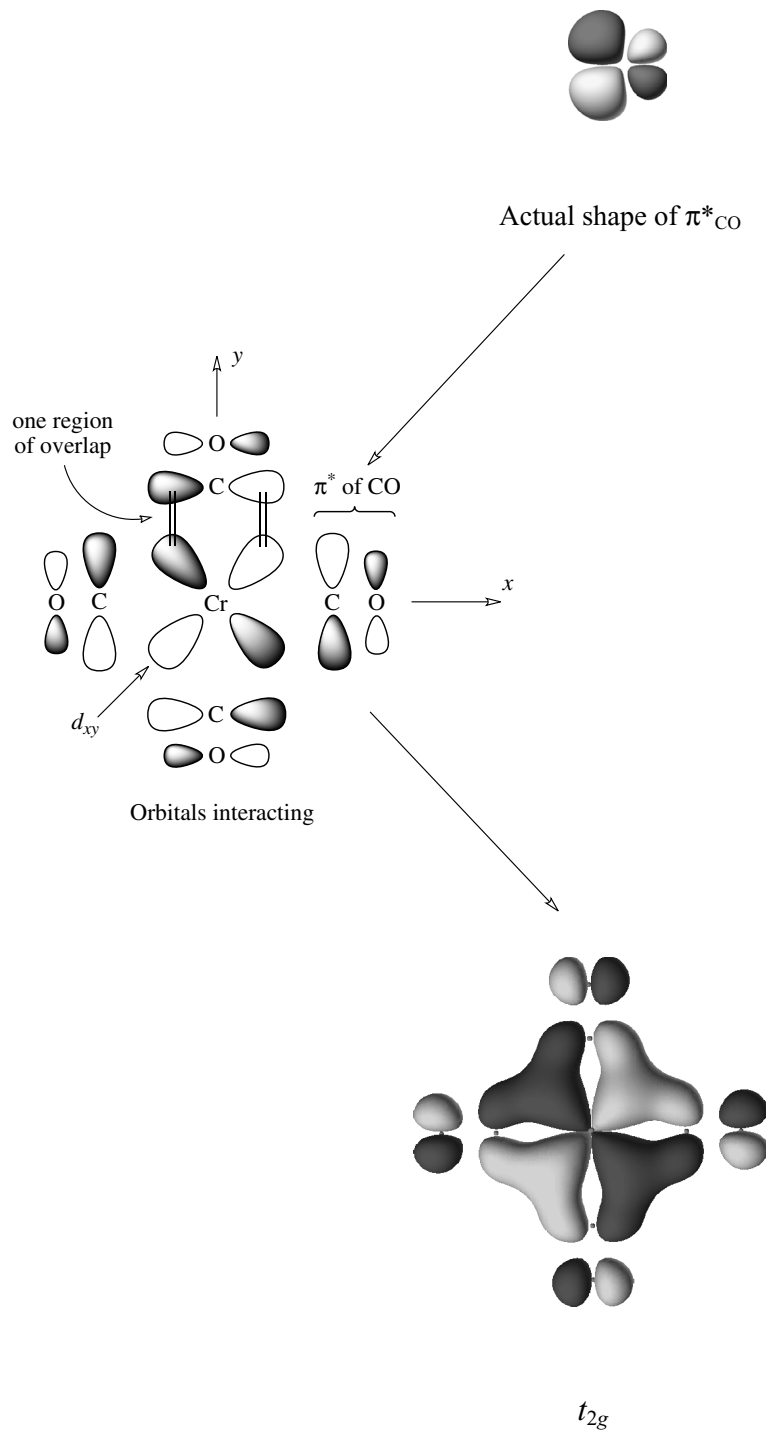
Molecular Orbitals of $\text{Cr}(\text{CO})_6$ (Only interactions between ligand (σ and π^*) orbitals and metal d orbitals are shown.)

Chromium(0) has six electrons outside its noble gas core. Each of the six CO ligands contributes a pair of electrons to give a total electron count of 18. In the molecular orbital energy level diagram these 18 electrons appear as the 12 σ electrons (the σ electrons of the CO ligands, stabilized by their interaction with the metal orbitals) and 6 metal–ligand bonding electrons (these electrons occupy orbitals having the symmetry label t_{2g}).

Adding one or more electrons to $\text{Cr}(\text{CO})_6$ would populate metal–ligand antibonding orbitals (symmetry label e_g^*); the consequence would be destabilization of the molecule. Removing electrons from $\text{Cr}(\text{CO})_6$ would depopulate the t_{2g} orbitals. These are bonding in nature as a consequence of the strong π acceptor ability of the CO ligands; a decrease in electron density in these orbitals would also tend to destabilize the complex. The result is that the 18-electron configuration for this molecule is the most stable.

The shapes of the t_{2g} and e_g^* orbitals support this description of bonding in $\text{Cr}(\text{CO})_6$. One of the t_{2g} orbitals is shown in Figure 3-2. An electron pair in this orbital spends the majority of its time in one of the four regions of overlap near the chromium as indicated in Figure 3-2 (these regions result from interaction of the d_{xy} orbital of Cr with four π^* orbitals of CO). Electrons in each of these regions would be expected to be attracted strongly by three nuclei, the chromium

see F. A. Cotton, *Chemical Applications of Group Theory*, 3rd ed., Wiley: New York, 1990, pp. 90–91.

**Figure 3-2**

A t_{2g} Orbital
of $\text{Cr}(\text{CO})_6$

and two carbons; the resulting effect would be to hold these nuclei together, in effect keeping the CO ligands attached to the metal. The two other t_{2g} orbitals have the same shape, but different orientations, than the one shown in Figure 3-2; these orbitals involve the d_{xz} and d_{yz} orbitals of the metal. Collectively, the electron pairs in the three t_{2g} orbitals are crucial in bonding the six carbonyls to the chromium; in the absence of these electrons, the carbonyls would readily dissociate.

One of the e_g^* orbitals of $\text{Cr}(\text{CO})_6$ is shown in Figure 3-3. The principal interaction in this case is antibonding between the σ orbitals of the carbonyls and the d orbital lobes of the chromium. Electrons in this orbital, or in the other e_g^* orbital, would therefore destabilize the molecule, weakening Cr–CO bonds.

Continuing for the moment to consider 6-coordinate molecules of octahedral geometry, we can gain some insight as to when the 18-electron rule can be expected to be most valid. $\text{Cr}(\text{CO})_6$ obeys the rule because of two factors: the strong σ donor ability of CO raises the e_g^* orbitals in energy, making them strongly antibonding; and the strong π acceptor ability of CO lowers the t_{2g} orbitals in energy, making them strongly bonding. Ligands that are both strong σ donors and π acceptors, therefore, should be the most effective at forcing adherence to the 18-electron rule. Other ligands, including some organic ligands, do not have these features and, consequently, their compounds may or may not adhere to the rule.

Examples of exceptions may be noted. $[\text{Zn}(\text{en})_3]^{2+}$ is a 22-electron species; it has both the t_{2g} and e_g^* orbitals filled. Although en (ethylenediamine = $\text{NH}_2\text{CH}_2\text{CH}_2\text{NH}_2$) is a good σ -donor, it is not as strong a donor as CO. As a result, the e_g^* orbital is not sufficiently antibonding to cause significant destabilization of the complex, and the 22-electron species, with 4 electrons in e_g^* orbitals, is stable. An example of a 12-electron species is TiF_6^{2-} . In this case, the fluoride ligand is a π donor as well as a σ donor. The π donor ability of F^- destabilizes the t_{2g} orbitals of the complex, making them slightly antibonding. The ion TiF_6^{2-} has 12 electrons in the bonding σ orbitals and no electrons in the antibonding t_{2g} or e_g^* orbitals.

These examples of exceptions to the 18-electron rule are shown schematically in Figure 3-4.⁸

Other Geometries

The same type of argument can be made for complexes of geometries other than octahedral; in most, but not all cases there is an 18-electron configuration of special stability for complexes of strongly π accepting ligands. Examples include trigonal bipyramidal geometry [for example, $\text{Fe}(\text{CO})_5$] and tetrahedral geometry

⁸P. R. Mitchell and R. V. Parish, *J. Chem. Ed.*, **1969**, 46, 311.

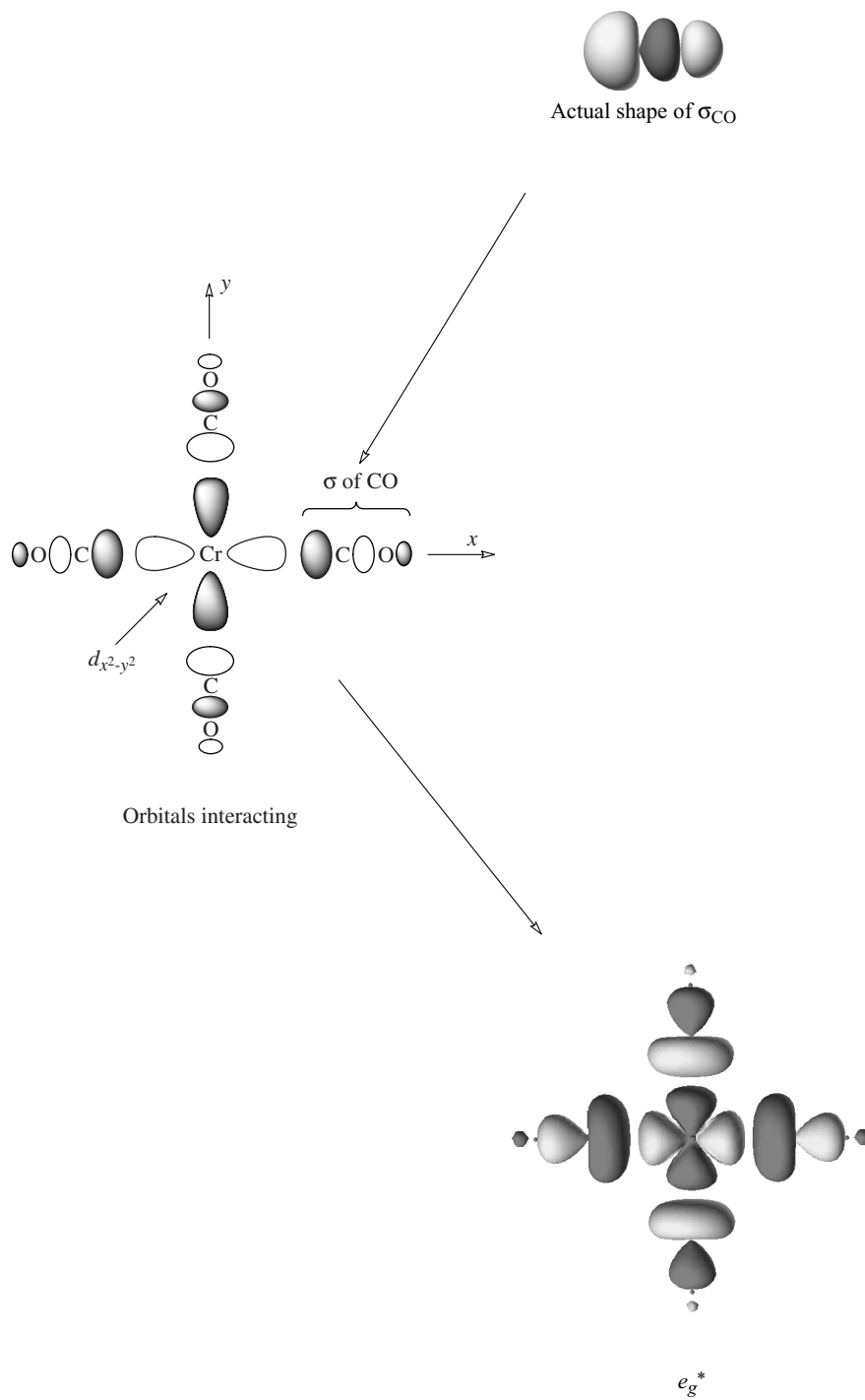
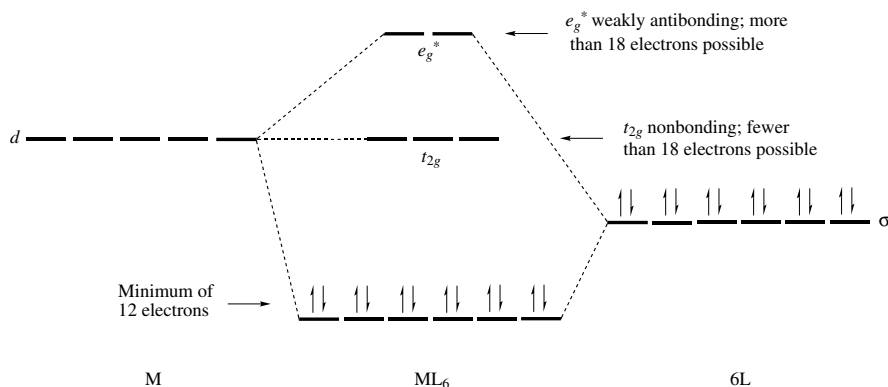


Figure 3-3
 An e_g^* Orbital
 of $\text{Cr}(\text{CO})_6$

**Figure 3-4**

Exceptions to the 18-Electron Rule (Although the six lowest energy MOs are shown as degenerate in the figure, this is an approximation that does not take into account interactions *s* and *p* orbitals of the metal.)

[for example, $\text{Ni}(\text{CO})_4$]. The most common exception is square planar geometry, in which a 16-electron configuration may be the most stable, especially for complexes of d^8 metals.

The relative energies of *d* orbitals of transition metal complexes can be predicted approximately by the *crystal field approach*, a model of bonding that considers how the orbitals on a metal would interact with negative charges located at the sites of the ligands. By this model, the metal *d* orbitals pointing most directly toward the ligands will interact most strongly; electron pairs on the ligands will be stabilized, and a metal *d* orbital will be destabilized by such interactions. As a result, the more directly a *d* orbital points toward the ligands, the higher the energy of the resulting antibonding orbital.

For example, in octahedral geometry, the two *d* orbitals pointing most directly toward the ligands are the $d_{x^2-y^2}$ and d_{z^2} . These metal orbitals interact more strongly with the ligands than the other *d* orbitals and give rise to the highest energy (antibonding) molecular orbitals (labeled e_g^* ; see Figure 3-1). Similar reasoning can predict the relative energies of molecular orbitals derived from metal *d* orbitals for other geometries; examples of common geometries are shown in Figure 3-5.⁹

3-3 SQUARE PLANAR COMPLEXES

Chapter 9 discusses square planar complexes, which are particularly important in the field of catalysis. Examples include the d^8 , 16-electron complexes illustrated in Figure 3-6.

⁹Symbols such as a_1 , a_{1g} , and b_{2g} are additional symmetry labels useful in describing MOs with significant *d* character. See Footnote 7 in Chapter 3.

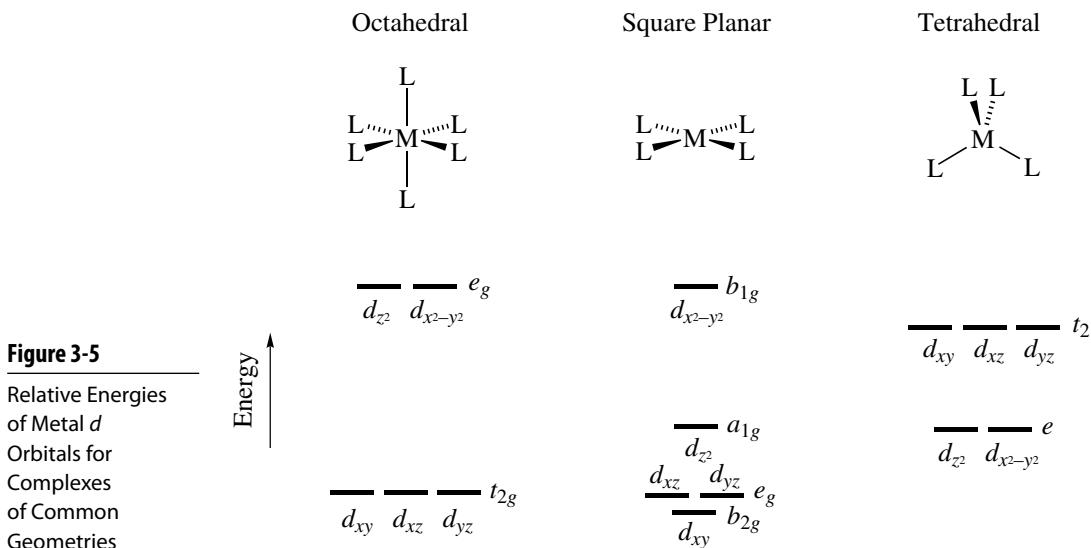
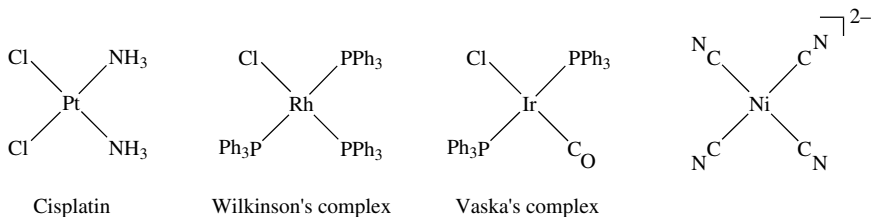
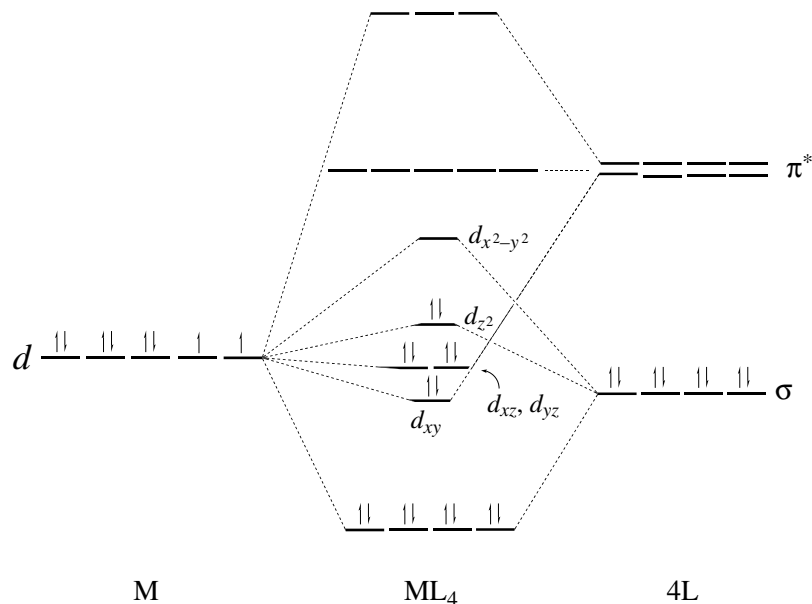


Figure 3-6
Examples of Square Planar d^8 Molecules



To understand why 16-electron square planar complexes might be especially stable, it is useful to examine the molecular orbitals of such a complex. An example of a molecular orbital energy level diagram for a square planar molecule of formula ML_4 ($\text{L} =$ ligand that can function as both σ donor and π acceptor) is shown in Figure 3-7.

Four molecular orbitals of ML_4 are derived primarily from the σ donor orbitals of the ligands; electrons occupying such orbitals are bonding in nature. Three additional orbitals are slightly bonding (derived primarily from d_{xz} , d_{yz} , and d_{xy} orbitals of the metal) and one is essentially nonbonding (derived primarily from the d_{z^2} orbital of the metal). These bonding and nonbonding orbitals can be filled by 16 electrons. Additional electrons would occupy an antibonding orbital derived from the antibonding interaction of a metal $d_{x^2-y^2}$ orbital with the σ donor orbitals of the ligands. Consequently, for square planar complexes of ligands having both σ donor and π acceptor characteristics, a 16-electron configuration may

**Figure 3-7**

Molecular Orbitals of Square Planar Complexes (Only σ donor and π acceptor interactions are shown.)

be significantly more stable than an 18-electron configuration. Sixteen-electron square planar complexes may also be capable of accepting one or two ligands at the vacant coordination sites (along the z axis), thereby achieving an 18-electron configuration. As will be demonstrated in Chapter 7, this is a common reaction of 16-electron square planar complexes.

Verify that the complexes in Figure 3-6 are 16-electron species.

Exercise 3-4

Sixteen-electron square planar complexes are most commonly found for d^8 metals, in particular those metals having formal oxidation states of 2+ (Ni^{2+} , Pd^{2+} , Pt^{2+}) and 1+ (Rh^+ , Ir^+). Some of these complexes have important catalytic behavior, as discussed in Chapter 9.

Suggested Reading

General Background on the 18-Electron Rule

P. R. Mitchell and R. V. Parish, *J. Chem. Ed.*, **1969**, *46*, 811.

W. B. Jensen, *J. Chem. Ed.*, **2005**, *82*, 28.

More Recent Perspective and Related Concepts

P. Pyykkö, *J. Organomet. Chem.*, **2006**, 691, 4336.

C. R. Landis, T. Cleveland, and T. K. Firman, *J. Am. Chem. Soc.*, **1998**, 120, 2641.

D. Mingos and P. Michael, *J. Organomet. Chem.*, **2004**, 689, 4420.

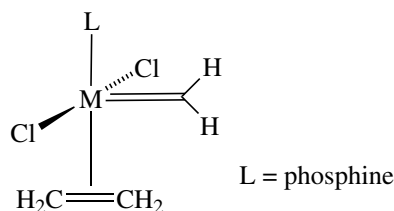
Problems

- 3-1** Octahedral transition metal complexes containing strong π acceptor ligands obey the 18-electron rule much more often than complexes containing π donor ligands. Why?
- 3-2** Determine the valence electron counts on the transition metals.
- $[(\eta^5\text{-C}_5\text{H}_5)_2\text{Co}]^+$
 - $\text{Ir}(\text{CO})\text{Cl}(\text{PMe}_3)_2$
 - $[\text{Fe}(\text{CO})_4]^{2-}$
 - $\text{Rh}(\text{CO})(\text{CS})(\text{PPh}_3)_2\text{Br}$
- 3-3** Identify the first-row transition metal in the following 18-electron species.
- $(\eta^4\text{-C}_4\text{H}_4)\text{M}(\text{CO})_3$
 - $[(\eta^3\text{-C}_3\text{H}_5)\text{M}(\text{CN})_4]^{2-}$
 - $(\eta^3\text{-C}_3\text{H}_5)(\eta^5\text{-C}_5\text{H}_5)\text{M}(\text{CO})$
 - $(\eta^5\text{-C}_5\text{H}_5)\text{M}(\text{NO})$ (has linear M–N–O)
- 3-4** Identify the second-row transition metal in the following 18-electron species.
- $[(\eta^5\text{-C}_5\text{H}_5)\text{M}(\text{CO})_3]_2$ (has single M–M bond)
 - $[(\eta^5\text{-C}_5\text{H}_5)\text{M}(\text{CO})_2]_2$ (has double M=M bond)
 - $[(\eta^5\text{-C}_5\text{H}_5)\text{M}(\text{CO})_2(\text{NO})]^+$ (has linear M–N–O)
 - $(\eta^4\text{-C}_8\text{H}_8)\text{M}(\text{CO})_3$
 - $[\text{M}(\text{CO})_3(\text{PMe}_3)]^-$
- 3-5** Identify the transition metal in the following 16-electron square planar species:
- $\text{MCl}(\text{CO})(\text{PPh}_3)_2$ (M = second-row transition metal)
 - $(\text{CH}_3)_2\text{M}(\text{PPh}_3)_2$ (M = second-row transition metal)
 - $[\text{MCl}_3(\text{NH}_3)]^-$ (M = third-row transition metal)
- 3-6** What charge, z , would be necessary for the following to obey the 18-electron rule?
- $[(\eta^6\text{-C}_6\text{H}_6)_2\text{Ru}]^z$

- b. $[\text{Co}(\text{CO})_3(\text{CH}_3\text{CN})]^z$
 c. $[\text{NiCl}(\text{PF}_3)_3]^z$
 d. $[\text{Ru}(\text{CO})_4(\text{SiMe}_3)]^z$ (suggestion: look at the position of Si in the periodic table)

3-7 Determine the specified quantity.

- a. The metal–metal bond order in $[(\eta^5\text{-C}_5\text{Me}_5)\text{Rh}(\text{CO})_2]$
 b. The expected charge on $[\text{W}(\text{CO})_5(\text{SnPh}_3)]^z$
 c. The identity of the second-row transition metal in the 16-electron complex $(\eta^5\text{-C}_5\text{H}_5)(\eta^1\text{-C}_3\text{H}_5)(\eta^3\text{-C}_3\text{H}_5)_2\text{M}$
 d. The number of CO ligands in $[(\eta^5\text{-C}_5\text{H}_5)\text{W}(\text{CO})_x]_2$, which has a tungsten–tungsten triple bond
 e. The number of CO ligands in $\text{Mn}(\text{CO})_x\text{Cl}$
 f. The identity of the second-row transition metal in the catalytically important 16-electron species (reference: B. F. Straub, *Angew. Chem.*, **2005**, *44*, 5974)



3-8 Represent the following complexes in L–X notation. Calculate the electron count, coordination number, oxidation state of the metal, and number of d electrons for the metal.

- a. $\text{RhCl}(\text{PPh}_3)_3$
 b. $[\text{Fe}(\text{CO})(\text{CN})_5]^{3-}$
 c. $(\text{CH}_3)\text{Ir}(\text{CO})(\text{PEt}_3)_2\text{ClBr}$
 d. $(\eta^5\text{-C}_5\text{H}_5)_2\text{Co}$

3-9 For a square planar complex ML_4 where L is a σ donor and π acceptor, sketch the following interactions (assume that the z axis is perpendicular to the plane of the molecule).

- a. Interaction of d_{xy} orbital on M with π^* orbitals on ligands
 b. Interaction of d_{xz} orbital on M with π^* orbitals on ligands
 c. Interaction of $d_{x^2-y^2}$ orbital on M with σ orbitals on ligands
 d. Interaction of d_z^2 orbital on M with σ orbitals on ligands

- 3-10** What is the valence electron count for the blue ion NiCl_4^{2-} ? Why does this tetrahedral ion not obey the 18-electron rule?
- 3-11** What is the valence electron count in $(\text{CH}_3)_3\text{Re}(=\text{O})_2$? Suggest a reason why this compound does not obey the 18-electron rule. (See A. Haaland, W. Scherer et al., *Organometallics*, **2000**, 19, 22.)

The Carbonyl Ligand

The carbonyl ligand, CO, is the most common ligand in organometallic chemistry. It may serve as the only ligand in **binary carbonyls**, such as $\text{Ni}(\text{CO})_4$, $\text{W}(\text{CO})_6$, and $\text{Fe}_2(\text{CO})_9$, or, more commonly, in combination with other ligands, both organic and inorganic. CO may bond to a single metal or it may serve as a bridge between two or more metals. In Chapter 4 we consider the bonding between metals and CO, the synthesis and some reactions of CO complexes, and examples of the various types of CO complexes that form.

4-1 BONDING

It is useful to begin by reviewing the bonding in CO itself. As described in Chapter 2 (Figure 2-5), the molecular orbital picture of CO is similar to that of N_2 (Exercise 2-3); the molecular orbitals derived primarily from the $2p$ atomic orbitals of these molecules are illustrated in Figure 4-1.

4-1-1 CO as a Terminal Ligand

Two features of the molecular orbitals of CO deserve particular attention. First, the highest energy occupied orbital (the HOMO) has its largest lobe on carbon. It is through this orbital, occupied by an electron pair, that CO exerts its σ donor function, donating electron density directly toward an appropriate metal orbital (such as an unfilled p , d , or hybrid orbital). At the same time, CO has two empty π^* orbitals (LUMOs); these also have larger lobes on carbon than on oxygen. As a consequence of the localization of π^* orbitals on carbon, the carbon acts as the principal

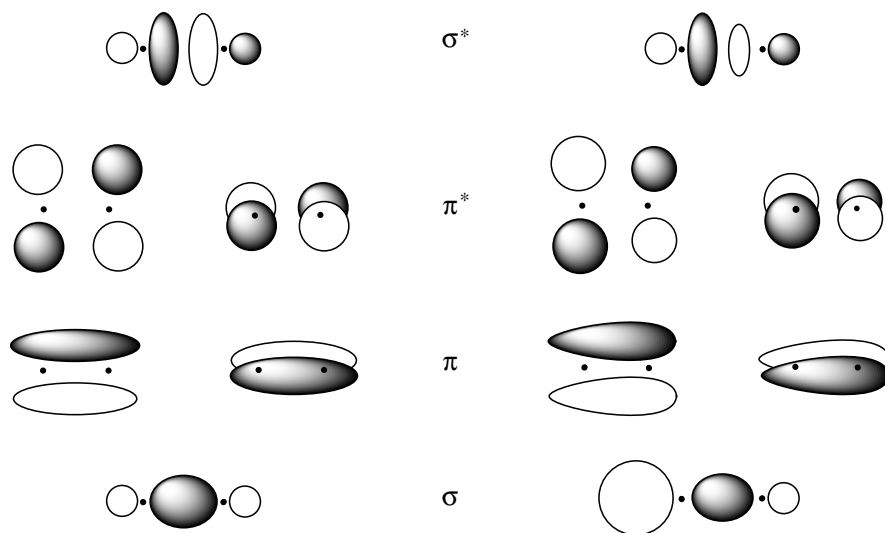


Figure 4-1
Selected Molecular
Orbitals of
 N_2 and CO

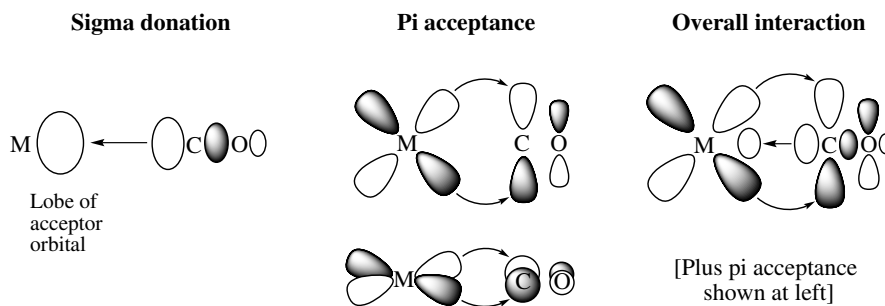


Figure 4-2
 σ and π Interactions
between CO
and a Metal Atom

site of the π acceptor function of the ligand: a metal atom having electrons in a d orbital of suitable symmetry can donate electron density to these π^* orbitals. These σ donor and π acceptor interactions are illustrated in Figure 4-2.

The overall effect is synergistic: CO can donate electron density via a σ orbital to a metal atom; the greater the electron density on the metal, the more effectively it is able to return electron density to the π^* orbitals of CO. The net effect can be rather strong bonding between the metal and CO; however, as described later, the strength of this bonding is dependent on several factors, including the charge on the complex and the ligand environment of the metal.

Exercise 4-1

N_2 has molecular orbitals slightly different from those of CO, as shown in Figure 4-1. Would you expect N_2 to be a stronger or weaker π acceptor than CO?

If this picture of bonding between CO and metal atoms is valid, it should be supported by experimental evidence. Two sources of such evidence are infrared spectroscopy (IR) and X-ray crystallography. First, any change in bonding between carbon and oxygen should be reflected in the C–O (carbonyl) stretching vibration as observed by IR. As in organic compounds, the C–O stretch in organometallic compounds is often intense (stretching the C–O bond results in a substantial change in dipole moment), and its energy often yields valuable information about the molecular structure. Free carbon monoxide has a C–O stretch at 2143 cm^{-1} ; $\text{Cr}(\text{CO})_6$, on the other hand, has its C–O stretch at 2000 cm^{-1} . The lower energy for the stretching mode means that the C–O bond is weaker in $\text{Cr}(\text{CO})_6$.

The energy necessary to stretch a bond is proportional to $\sqrt{\frac{k}{\mu}}$, where

k = force constant, a measure of the rigidity of a bond
 μ = reduced mass; for atoms of mass m_1 and m_2 the reduced mass is given by

$$\mu = \frac{m_1 m_2}{m_1 + m_2}.$$

The stronger the bond between two atoms, the larger the force constant; consequently, the greater the energy necessary to stretch the bond and the higher the energy of the corresponding band (the higher the wave number, cm^{-1}) in the infrared spectrum. Similarly, the more massive the atoms involved in the bond, as reflected in a higher reduced mass, the less energy necessary to stretch the bond and the lower the energy of absorption in the infrared spectrum.

Both σ donation (which donates electron density from a bonding orbital on CO) and π acceptance (which places electron density in CO antibonding orbitals) would be expected to weaken the C–O bond and to decrease the energy necessary to stretch that bond.

The charge on a carbonyl complex is also reflected in its infrared spectrum. Three isoelectronic hexacarbonyls have the following C–O stretching bands:^{1,2}

<i>Complex</i>	<i>$\nu(\text{CO}), \text{cm}^{-1}$</i>
$[\text{V}(\text{CO})_6]^-$	1858
$[\text{Cr}(\text{CO})_6]$	2000
$[\text{Mn}(\text{CO})_6]^+$	2095
(Free CO)	2143)

¹K. Nakamoto, *Infrared and Raman Spectra of Inorganic and Coordination Compounds*, 4th ed., Wiley: New York, 1986, pp. 292–293.

²Positions of infrared absorptions may vary slightly depending on solvent, counterions, or other factors.

Of these three, $[\text{V}(\text{CO})_6]^-$ has the metal with the smallest nuclear charge. Consequently, vanadium has the weakest ability to attract electrons and the greatest tendency to “back” donate electron density to CO. The consequence is strong population of the π^* orbitals of CO and reduction of the strength of the C–O bond. In general, the more negative the charge on organometallic species, the greater the tendency of the metal to donate electrons to the π^* orbitals of CO and the lower the energy of the C–O stretching vibrations.

Exercise 4-2

On the basis of the carbonyl complexes shown in the preceding table, predict the approximate position (in cm^{-1}) of the C–O stretching band in $[\text{Ti}(\text{CO})_6]^{2-}$.

Infrared Spectra of Carbonyl Cations

Let’s examine one more series of isoelectronic transition metal carbonyl complexes:

<i>Complex</i>	<i>$\nu(\text{CO}), \text{cm}^{-1}$</i>
$[\text{W}(\text{CO})_6]$	1977
$[\text{Re}(\text{CO})_6]^+$	2085
$[\text{Os}(\text{CO})_6]^{2+}$	2190
$[\text{Ir}(\text{CO})_6]^{3+}$	2254

The same trend occurs as seen before: the more positive the charge in the complex, the less C–O backbonding and the higher the energy necessary to stretch C–O bonds. But how is it possible for C–O bands in carbonyl complexes to be stronger (have higher energy C–O stretches) than free CO, as in the cases of $[\text{Os}(\text{CO})_6]^{2+}$ and $[\text{Ir}(\text{CO})_6]^{3+}$? When the metal ion and CO interact in such metal carbonyls, the positive charge of the metal is believed to reduce the polarization of C–O molecular orbitals.³ The σ and π orbitals of CO in the free molecule are strongly polarized toward the much more electronegative oxygen atom. When a positively charged metal atom interacts with the carbon end of this molecule, the positive charge attracts electron density from the oxygen atom toward the carbon atom. The result is more covalent character in the carbon–oxygen bond and a stronger bond for the cationic complex than in free CO. The stronger this effect, the stronger the bond and the higher the energy of the C–O stretching vibration.

³A. J. Lupinetti, S. Fau, G. Frenking, and S. H. Strauss, *J. Phys. Chem. A*, **1997**, *101*, 9551 and R. K. Szilagy and G. Frenking, *Organometallics*, **1997**, *16*, 4807. Additional aspects of bonding between transition metals and CO, using statistical data on metal–carbon and carbon–oxygen bond distances, are discussed in R. K. Hocking and T. W. Hambley, *Organometallics*, **2007**, *26*, 2815.

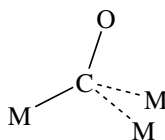
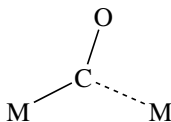
Bond Distances

Additional evidence on carbonyl ligand bonding to metals is provided by X-ray crystallography, which gives information on relative positions of atoms in molecules. In carbon monoxide the C–O distance has been measured as 112.8 pm. Weakening of the C–O bond in carbonyl complexes by σ donation and π acceptance would be expected to cause this distance to increase. Such an increase in bond length is found in complexes containing CO, with C–O distances of approximately 115 pm for many neutral carbonyl complexes. Although such measurements provide definitive measures of bond distances, in practice it is far more convenient to use infrared spectra to obtain data on the strength of C–O bonds.⁴

4-1-2 Bridging Modes of CO

Although CO is most commonly found as a “terminal” ligand attached to a single metal atom, many cases are known in which CO forms bridges between two or more metals. Many such bridging modes are known; the most common are shown in Table 4-1 (on next page). Bridging ligands are designated using the Greek letter μ (mu), followed by a subscript indicating the number of atoms bridged. For example, μ_2 indicates that a ligand bridges two atoms.

In addition to the symmetrical bridging modes of CO shown in Table 4-1, CO sometimes bridges metals asymmetrically; in these cases CO is considered *semibridging* (shown below).



Semibridging Modes of CO

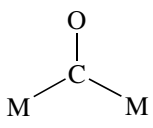
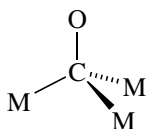
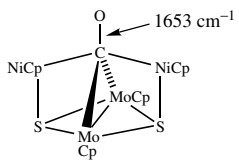
A variety of factors can result in an asymmetric carbonyl bridge, including inherent asymmetry in molecules (such as CO bridging two or three different metals) and crowding (where moving of a CO away from a symmetrically bridging position would help reduce crowding in part of a molecule).⁵

The bridging mode is strongly correlated with the position of the C–O stretching band (Table 4-1). In cases where CO bridges two metal atoms, both metals can contribute electron density into π^* orbitals of CO to weaken the C–O bond and lower the energy of the stretch. Consequently, the C–O stretch for doubly bridging

⁴Additional trends involving bond distances and charges in carbonyl complexes are discussed in R. K. Hocking and T. W. Hambley, *Organometallics*, **2007**, *26*, 2815.

⁵For a discussion of various factors involved in asymmetrically bridging CO ligands, see F. A. Cotton and G. Wilkinson, *Advanced Inorganic Chemistry*, 5th ed., Wiley–Interscience: New York, 1988, pp. 1028–1032.

Table 4-1 Bonding Modes of CO

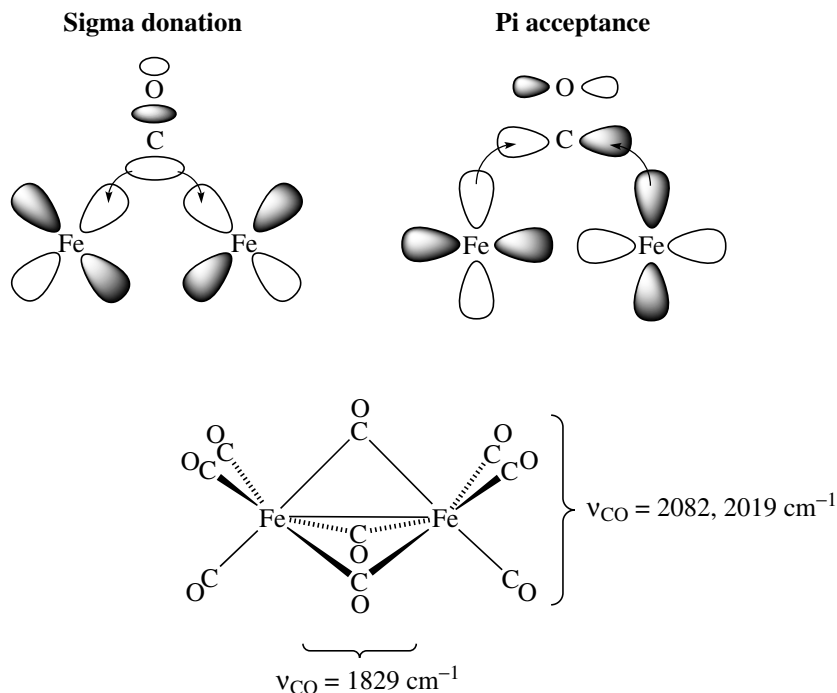
Type of CO	Approximate range for $\nu(\text{CO})$ in neutral complexes (cm^{-1})
Terminal M–CO	1850–2120
Bridging	
Symmetrical μ_2 -CO	1700–1860
	
Symmetrical μ_3 -CO	1600–1700
	
μ_4 -CO	Few examples are known; one is shown below. ³
	

³P. Li and M. D. Curtis, *J. Am. Chem. Soc.*, **1989**, *111*, 8279.

CO is at a much lower energy than that for terminal carbonyls. For example, in $\text{Fe}_2(\text{CO})_9$, there are three bridging and six terminal CO ligands (Figure 4-3). Infrared absorption caused by bridging carbonyls in this molecule occurs approximately 200 cm^{-1} lower than for terminal CO ligands; the bands for the terminal CO ligands in $\text{Fe}_2(\text{CO})_9$ are similar to those reported for $\text{Fe}(\text{CO})_5$, 2034 and 2013 cm^{-1} .⁶

Because the C–O bond is weaker in bridging CO ligands than in terminal COs, the carbon–oxygen bond in the bridging ligands is expected to be longer. This expectation is supported by the C–O bond distances in $\text{Fe}_2(\text{CO})_9$: 117.6 pm for the bridging ligands in comparison with an average of 115.6 pm for the terminal ligands.

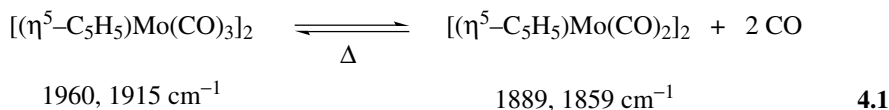
⁶The infrared spectra and structures of Fe carbonyl complexes, with references to the original data, are discussed in J. H. Jang, J. G. Lee, H. Lee, Y. Xie, and H. F. Schaefer III, *J. Phys. Chem. A*, **1998**, *102*, 5298.

**Figure 4-3**

Bridging versus Terminal Carbonyls in $\text{Fe}_2(\text{CO})_9$

Interaction of three or four metal atoms with a triply or quadruply bridging CO further weakens the C–O bond; the infrared band for the C–O stretch in μ_3 -CO or μ_4 -CO is still lower than that in the doubly bridging case.

A particularly interesting situation is that of the nearly linear bridging carbonyls, such as in $[(\eta^5\text{-C}_5\text{H}_5)\text{Mo}(\text{CO})_2]_2$. When a sample of $[(\eta^5\text{-C}_5\text{H}_5)\text{Mo}(\text{CO})_3]_2$ is heated, some carbon monoxide is driven off; the product, $[(\eta^5\text{-C}_5\text{H}_5)\text{Mo}(\text{CO})_2]_2$, reacts readily with CO to reverse this reaction, as shown in equation 4.1.⁷

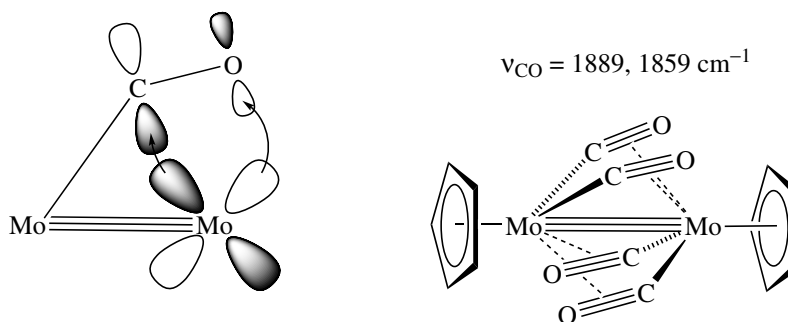


This reaction is accompanied by a shift of the infrared bands in the carbonyl region to lower energies, as shown. The Mo–Mo bonds also shorten by approximately 80 pm, consistent with an increase in the metal–metal bond order from one to three. Although it was originally proposed that the “linear” CO ligands may donate some electron density to the neighboring metal from π orbitals,

⁷D. S. Ginley and M. S. Wrighton, *J. Am. Chem. Soc.*, **1975**, 97, 3533 and R. J. Klingler, W. Butler, and M. D. Curtis, *J. Am. Chem. Soc.*, **1975**, 97, 3535.

Figure 4-4

Bridging CO in
 $[(\eta^5\text{-C}_5\text{H}_5)\text{Mo}(\text{CO})_2]_2$



subsequent calculations have indicated that a more important interaction is the donation from a metal d orbital to the π^* orbital of CO, as shown in Figure 4-4.⁸ Such donation weakens the C–O bond in the ligand and results in the observed shift of the C–O stretching bands to lower energy.

For purposes of electron counting, symmetrically bridging carbonyls, like terminal carbonyls, can most conveniently be counted as donating two electrons overall, with the electrons apportioned equally among the atoms bridged.⁹ For example, in $\text{Fe}_2(\text{CO})_9$ (Figure 4-3) the electrons on either of the iron atoms can be counted as follows:

Fe		8 electrons
Fe–Fe bond		1 electron
3 terminal COs	3×2 electrons =	6 electrons
3 μ_2 -CO	$3 \times \frac{1}{2} \times 2$ electrons =	3 electrons
		<hr/> 18 electrons

Exercise 4-3

Determine the electron count of Co in the solid form of $\text{Co}_2(\text{CO})_8$ (Figure 4-5 in the following section).

Additional examples of the utility of infrared spectra in characterizing carbonyl complexes are included in Section 4-5.

⁸A. L. Sargent and M. B. Hall, *J. Am. Chem. Soc.*, **1989**, *111*, 1563, and references therein.

⁹Triply bridging carbonyls also function as two-electron donors, formally two thirds of an electron per metal. In such cases it is often best to consider the two electrons donated to the complex as a whole rather than to specific metal atoms.

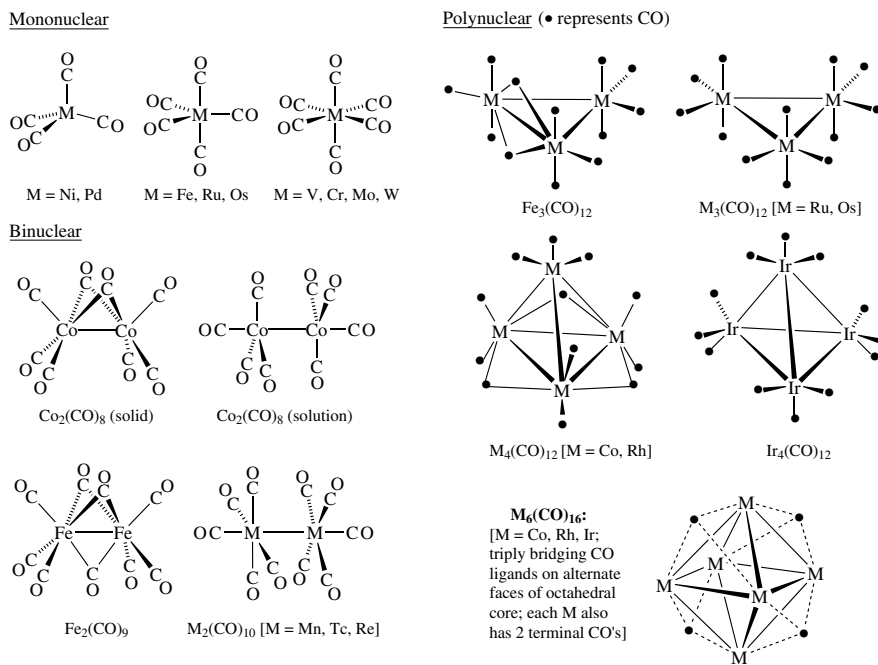


Figure 4-5
Binary Carbonyl
Complexes

4-2 BINARY CARBONYL COMPLEXES

Binary carbonyls, containing only metal atoms and CO, are fairly numerous. Structures of some representative binary carbonyl complexes are shown in Figure 4-5.

Most of these complexes obey the 18-electron rule. The cluster compounds $\text{Co}_6(\text{CO})_{16}$ and $\text{Rh}_6(\text{CO})_{16}$ do not obey the rule, however; more detailed analysis of the bonding in cluster compounds is necessary to satisfactorily account for the electron counting in these and other cluster compounds. This question is considered in Chapter 13.

One other binary carbonyl does not obey the rule: the 17-electron $\text{V}(\text{CO})_6$. This complex, which is pyrophoric and much less thermally stable than the 18-electron $\text{Cr}(\text{CO})_6$, is one of a few cases in which strong π acceptor ligands do not succeed in requiring an 18-electron configuration. In $\text{V}(\text{CO})_6$ the vanadium is apparently too small to permit a seventh coordination site; hence, no metal-metal bonded dimer [which might potentially yield 18-electron $(\text{CO})_6\text{V}-\text{V}(\text{CO})_6$] is ordinarily possible.¹⁰ However, $\text{V}(\text{CO})_6$ is easily reduced to $[\text{V}(\text{CO})_6]^-$, a well-studied 18-electron complex.

¹⁰In rare gas matrices and experiments involving laser photolysis, evidence has been reported for species that may contain two vanadiums and bridging carbonyls. See Z. Liu, Q. Li, Y. Xie, R. B. King, and H. F. Schaefer III, *Inorg. Chem.*, **2007**, *46*, 1803, and references therein.

Exercise 4-4

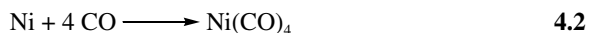
Verify the 18-electron rule for five of the binary carbonyls [other than $\text{Co}_6(\text{CO})_{16}$ and $\text{Rh}_6(\text{CO})_{16}$] shown in Figure 4-5.

An interesting feature of the structures of binary carbonyl complexes is that the tendency of CO to bridge transition metals tends to decrease in moving down the periodic table from smaller metals to larger. For example, in $\text{Fe}_2(\text{CO})_9$, there are three bridging carbonyls, but in $\text{Ru}_2(\text{CO})_9$ and $\text{Os}_2(\text{CO})_9$, there is a single bridging CO. Examples of the tendency of CO to act as a bridging ligand in first row transition metal complexes are also cited in later chapters.

4-2-1 Synthesis

Binary carbonyl complexes can be synthesized in many ways. Several of the most common methods are described below.

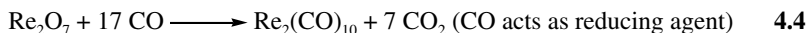
- 1. Direct reaction of a transition metal with CO.** The most facile of these reactions involves nickel, which reacts with CO at ambient temperature and 1 atm:



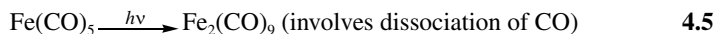
$\text{Ni}(\text{CO})_4$ is a volatile, toxic liquid that must be handled with great caution. It was first observed by Mond, who found that CO reacted with nickel valves.¹¹ The reverse reaction, involving thermal decomposition of $\text{Ni}(\text{CO})_4$, can be used to prepare nickel of high purity. Coupling of the forward and reverse reactions has been used commercially in the Mond process for obtaining purified nickel from ores.

Other binary carbonyls can be obtained from the direct reaction of metal powders with CO, but elevated temperatures and pressures are necessary.

- 2. Reductive carbonylation.** In this procedure, a transition metal compound (with the metal in a positive oxidation state) is allowed to react with CO and a reducing agent. Examples:



- 3. Thermal or photochemical reaction of other binary carbonyls.** Examples:



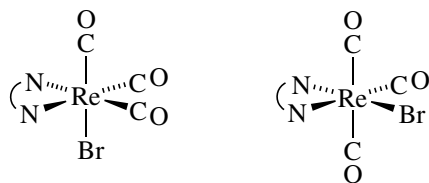
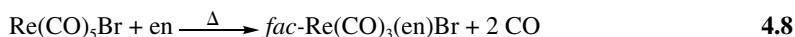
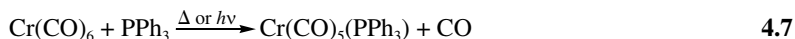
¹¹The original report by Mond [L. Mond, C. Langer, and F. Quincke, *J. Chem. Soc. (London)*, **1890**, 57, 749] is reprinted in *J. Organomet. Chem.*, **1990**, 383, 1.



4-2-2 Reactions

Dissociation of CO

The most common reaction of carbonyl complexes is CO dissociation. This reaction, which may be initiated thermally or by absorption of ultraviolet light, characteristically involves a loss of CO from an 18-electron complex to give a 16-electron intermediate, which may react in a variety of ways depending on the nature of the complex and its environment. A common reaction is replacement of the lost CO by another ligand to form a new 18-electron species as product—a substitution reaction. The following are examples:¹²



fac-ReBr(CO)₃(en)

mer-ReBr(CO)₃(en)

This type of reaction, therefore, provides a pathway in which CO complexes can be used as precursors for a variety of complexes of other ligands. Additional aspects of CO dissociation reactions are discussed in later chapters.

Formation of Metal Carbonyl Anions

Transition metal carbonyl anions having charges of 1– through 4– are known. Originally such anions were prepared by the reaction of neutral metal carbonyls with bases, for example,¹³



¹²The prefix *fac* designates a *facial* stereoisomer—in this case an octahedron with three CO groups at the corners of the same triangular face. *Meridional* isomers (abbreviated *mer*) correspond to stereoisomers in which three identical groups (*e.g.*, COs) lie in the same plane.

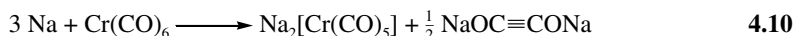
¹³The history of transition metal carbonyl anion synthesis, with extensive references, is described in J. E. Ellis, *Organometallics*, **2003**, 22, 3322.

Table 4-2 Positions of Strong C–O Absorptions in Binary Anionic Carbonyl Complexes

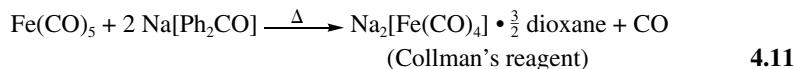
Charge	Examples	Range of C–O bands (cm ⁻¹)
1–	[Co(CO) ₄] ⁻ , [Fe(CO) ₅] ⁻	1852–1911
2–	[Fe(CO) ₄] ²⁻ , [Ti(CO) ₆] ²⁻	1730–1775
3–	[Co(CO) ₃] ³⁻ , [V(CO) ₃] ³⁻	1560–1690
4–	[Cr(CO) ₄] ⁴⁻ , [Mo(CO) ₄] ⁴⁻	1462–1478

Source: J. E. Ellis, *Organometallics*, **2003**, 22, 3322.

Transition metal carbonyl anions are now synthesized primarily by the reduction of transition metal carbonyl compounds in donor solvents. For example, in liquid ammonia solvent Cr(CO)₆ can be reduced by sodium to form the disodium salt of [Cr(CO)₅]²⁻ plus the explosive compound disodium acetylenediolate:



The most commercially important metal carbonyl anion, [Fe(CO)₄]²⁻, contained in Collman's reagent (shown below), can be prepared from the following reaction in dioxane solvent.¹⁴



In solution, Na₂[Fe(CO)₄] can dissociate to yield anions such as [NaFe(CO)₄]⁻ and species in which solvent molecules are attached to the anions. Collman's reagent has broad applications in chemical synthesis.

The infrared spectra of transition metal carbonyl anions provide an excellent illustration of the effect on the charge of the π acceptor ability of CO; as expected, the more negative the charge, the stronger the π acceptance and the lower the energy of the C–O stretching vibrations (Table 4-2).

4-3 OXYGEN-BONDED CARBONYLS

This chapter would be incomplete without the mention of one additional aspect of CO as a ligand: it can sometimes bond through oxygen as well as carbon. This phenomenon was first noted in the ability of the oxygen of a metal carbonyl complex to act as a donor toward Lewis acids such as AlCl₃, with the overall function of CO serving as a bridge between the two metals. Numerous examples are now known in which CO bonds through its oxygen to metal atoms, with

¹⁴J. P. Collman, R. G. Finke, J. N. Cawse, and J. I. Brauman, *J. Am. Chem. Soc.*, **1977**, 99, 2515.

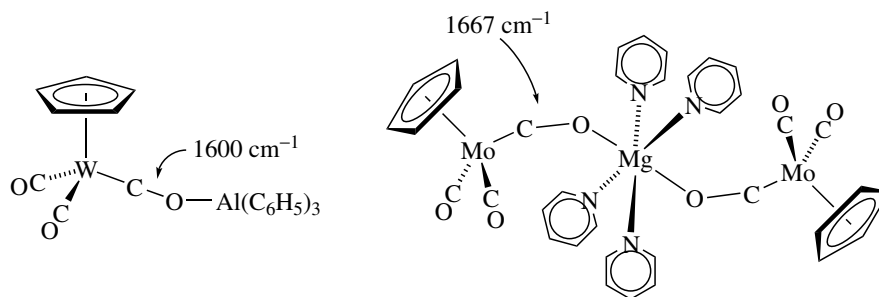


Figure 4-6

Oxygen-Bonded Carbonyls

the C–O–metal arrangement generally bent. Attachment of a Lewis acid to the oxygen results in significant weakening and lengthening of the C–O bond. The result is a shift of the C–O stretching vibration to lower energy in the infrared. The magnitude of this shift is frequently between 100 and 200 cm^{-1} but may be greater. Examples of O–bonded carbonyls (sometimes called isocarbonyls) are shown in Figure 4-6. The physical and chemical properties of O–bonded carbonyls have been reviewed.¹⁵

4-4 LIGANDS SIMILAR TO CO

Several diatomic ligands similar to CO are worth brief mention. Two of these, CS (thiocarbonyl) and CSe (selenocarbonyl), are of interest in part for purposes of comparison with CO. Several other common ligands are isoelectronic with CO and, not surprisingly, exhibit structural and chemical parallels with CO. Two examples are CN^- (cyanide) and N_2 (dinitrogen). In addition, the NO (nitrosyl) ligand deserves discussion because of its similarities with CO. NS (thionitrosyl) and other ligands isoelectronic with NO also are considered briefly.

4-4-1 CS, CSe, and CTe Complexes

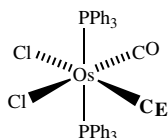
In most cases, synthesis of CS (thiocarbonyl), CSe (selenocarbonyl), and CTe (tellurocarbonyl) complexes is somewhat more difficult than that for analogous CO complexes, since CS, CSe, and CTe do not exist as stable, free molecules and do not, therefore, provide a ready ligand source.¹⁶ Consequently, the comparatively small number of such complexes should not be viewed as an indication of their stability; the chemistry of complexes of these three ligands may eventually rival that of CO complexes in breadth and utility. CS complexes are also of interest as possible intermediates in certain sulfur-transfer reactions in the removal of sulfur from natural fuels. In recent years, the chemistry of complexes containing

¹⁵C. P. Horwitz and D. F. Shriver, *Adv. Organomet. Chem.*, **1984**, 23, 219.

¹⁶E. K. Moltzen, K. J. Klabunde, and A. Senning, *Chem. Rev.*, **1988**, 88, 391.

Table 4-3 Osmium Complexes Containing CO and Isoelectronic Ligands

Formula	$\nu(\text{C-E})$ (cm^{-1})
(1) $\text{OsCl}_2(\text{CO})_2(\text{PPh}_3)_2$	2040, 1975
(2) $\text{OsCl}_2(\text{CO})(\text{CS})(\text{PPh}_3)_2$	1315
(3) $\text{OsCl}_2(\text{CO})(\text{CSe})(\text{PPh}_3)_2$	1156
(4) $\text{OsCl}_2(\text{CO})(\text{CTe})(\text{PPh}_3)_2$	1046



these ligands has developed more rapidly as avenues for their synthesis have been devised.

CS, CSe, and CTe are similar to CO in their bonding modes; they behave as both σ donors and π acceptors and can bond to metals in terminal or bridging modes. Of these three ligands, CS has been studied the most closely. CS usually functions as a stronger σ donor and π acceptor than CO.¹⁷ The CTe ligand is rare, with only a handful of examples known. Nevertheless, a series of isoelectronic and isostructural complexes containing all four ligands, CO through CTe, was synthesized as early as 1980.¹⁸ These complexes and their C–E (E = element from group 16) stretching bands are listed in Table 4-3.

The decrease in C–E stretching energy in moving down this list is partly a consequence of increased reduced mass (Section 4-1-1) in going from oxygen to more massive outer atoms. In addition, the C–E bonds become progressively weaker moving down this series, a consequence of the general phenomenon that bonds between main group atoms tend to become weaker in descending the periodic table. In particular, π bonding is typically much weaker for elements found lower in the table (for example, Si=Si bonds are much weaker than C=C bonds). Consequently, C–S bonds are typically weaker than C–O bonds, and C–Se and C–Te bonds are even weaker. The C–O stretching bands in the series shown in Table 4-3 do not change significantly (complexes 2–4 all have bands near 2040 cm^{-1}), suggesting that the overall interactions of these ligands with the osmium result in similar concentrations of electrons on the metal.

¹⁷P. V. Broadhurst, *Polyhedron*, **1985**, 4, 1801.

¹⁸G. R. Clark, K. Marsden, W. R. Roper, and L. J. Wright, *J. Am. Chem. Soc.*, **1980**, 102, 1206.

	Linear	Bent	
	$M \leftarrow :N \equiv O:$	$M \leftarrow :N \begin{array}{l} \diagup \\ \diagdown \end{array} \begin{array}{l} \ddot{O} \\ \ddot{O} \end{array}$	
M-N-O angle	165-180°	119-140°	
$\nu(N-O)$ in neutral molecules	1620-1830 cm^{-1}	1520-1720 cm^{-1}	
Electron donor count	2 (as NO^+) 3 (as NO)	2 (as NO^-) 1 (as NO)	Figure 4-7 Linear and Bent NO

4-4-2 CN^- and N_2 Complexes

Cyanide is a stronger σ donor and a somewhat weaker π acceptor than CO; overall, it is similar to CO in its ability to interact with metal orbitals. Unlike most organic ligands, which bond to metals in low formal oxidation states, cyanide bonds readily to metals with higher oxidation states. As a good σ donor, CN^- interacts strongly with positively charged metal ions; as a weaker π acceptor than CO (largely a consequence of the negative charge of CN^- and the lower electronegativity of N in comparison with O), cyanide is not as able to stabilize metals in low oxidation states. Therefore, its compounds are often studied in the context of “classical” coordination chemistry rather than organometallic chemistry. Dinitrogen is a weaker σ donor and π acceptor. However, N_2 complexes are of great interest, especially as possible intermediates in reactions that may simulate natural processes of nitrogen fixation.¹⁹

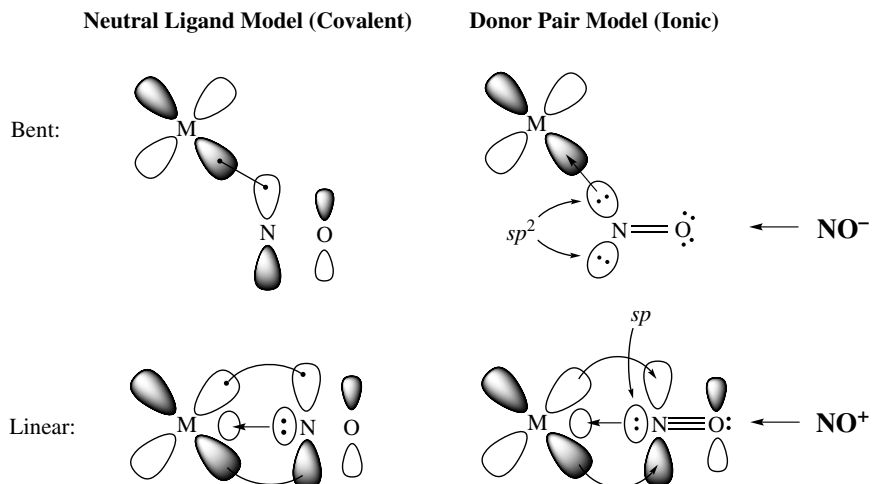
4-4-3 NO Complexes

Like CO, the NO (nitrosyl) ligand is both a σ donor and a π acceptor and can be a terminal or bridging ligand; useful information can be obtained about its compounds by analysis of its infrared spectra. Unlike CO, however, terminal NO has two common coordination modes: linear (like CO) and bent. Useful information about the linear and bent bonding modes of NO is summarized in Figure 4-7.

A formal analogy is often drawn between the linear bonding modes of both ligands: NO^+ is isoelectronic with CO; therefore, in its bonding to metals linear NO is considered NO^+ , a two-electron donor, by the donor pair (ionic) method (method A, Chapter 3). By the neutral ligand method (method B), linear NO is a three-electron donor (it has one more electron than the two-electron donor, CO).

The bent coordination mode of NO is often considered to arise formally from NO^- , with the bent geometry suggesting sp^2 hybridization at the nitrogen. By

¹⁹R. A. Henderson, G. J. Leigh, and C. J. Pickett, *Adv. Inorg. Chem. Radiochem.*, **1983**, 27, 197.

**Figure 4-8**

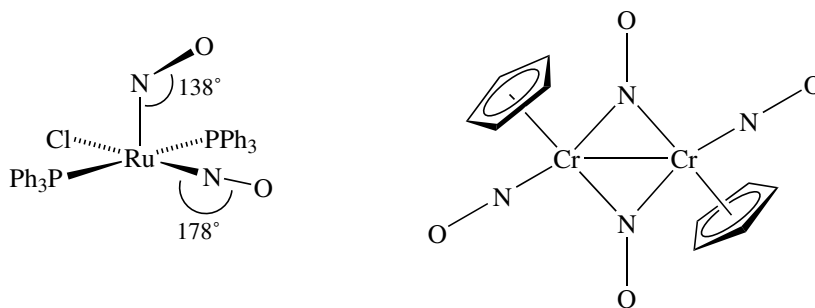
Covalent and Ionic Approaches to Bonding in NO Complexes

electron counting method A, therefore, bent NO is considered the two-electron donor NO^- ; by the neutral ligand method it is considered a one-electron donor.

These views of bonding can be illustrated, as in Figure 4-8. In the neutral ligand model, which may be described as emphasizing the covalent nature of metal–ligand bonds, the electron configuration of NO is the starting point. NO has similar molecular orbitals to CO and one more electron, which occupies a π^* orbital. When NO bonds in a bent fashion to a metal, the π^* orbital interacts with a metal d orbital; if each of these orbitals has a single electron, a covalent bond between the ligand and metal is formed. In the linear coordination mode, the σ bonding orbital of NO, occupied by a pair of electrons, can donate this pair to a suitable empty orbital on the metal. In addition, the singly occupied π^* orbital of NO can participate in covalent bonding with another d orbital on the metal. The result is the same type of synergistic σ donor- π acceptor bonding common in CO complexes.

In the donor pair model (method A), NO in the bent coordination mode is considered NO^- . The nitrogen in NO^- is considered sp^2 hybridized and can donate an electron pair to a metal d orbital, as shown in Figure 4-8. In the linear mode, the ligand is considered NO^+ , with sp hybridization on nitrogen.²⁰ An electron pair is donated through this hybrid. The metal (which is formally considered to have one more electron than in the covalent, neutral ligand case) can then donate an electron pair to an empty π^* orbital on the ligand.

²⁰In L–X notation, NO in a linear case is considered an LX ligand and in a bent case an X ligand. See M. L. H. Green, *J. Organomet. Chem.*, **1995**, 500, 127, for a discussion of this classification scheme.

**Figure 4-9**

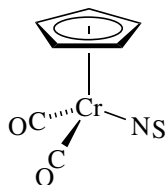
Examples of NO
Playing Multiple
Roles

Numerous complexes containing each mode are known, and examples are also known in which both linear and bent NO occur in the same complex. Whereas linear coordination usually gives rise to N–O stretching vibrations at higher energy than in the bent mode, there is enough overlap in the ranges of these bands that infrared spectra alone may not be sufficient to distinguish between the two. Furthermore, the manner of packing in crystals may give rise to considerable bending of the metal–N–O bond from 180° in the “linear” coordination mode.

One compound containing only a metal and NO ligands is known:²¹ Cr(NO)₄, a tetrahedral molecule isoelectronic with Ni(CO)₄. Complexes containing bridging nitrosyl ligands are also known, with the bridging ligand generally considered formally a 3-electron donor.

Sometimes NO plays more than one role in the same molecule; examples are shown in Figure 4-9.

4-4-4 NS and NSe Complexes



In recent years, several dozen compounds containing the isoelectronic NS (thionitrosyl) ligand have been synthesized. Infrared data have indicated that, like NO, NS can function in linear, bent, and bridging modes. In general, NS is stronger than NO in its ability to act as a π acceptor ligand; the relative abilities of NO and NS to accept π electrons depend on the electronic environment of

²¹The term *homoleptic* has been coined to describe complexes in which all ligands are identical. Cr(NO)₄, Ni(CO)₄, and W(CH₃)₆ are examples of homoleptic complexes.

the specific compounds being compared.²² Only a single NSe (selenonitrosyl) complex has been reported.²³ Theoretical calculations are consistent with increasing metal–N bond order and decreasing N–E bond order in the series M–NO through M–NTe.²⁴

4-5 IR SPECTRA

IR spectra can be useful in two respects. The number of IR bands depends on molecular symmetry; consequently, by determining the number of such bands for a particular ligand (such as CO), one may be able to decide among several alternative geometries for a compound—or at least reduce the number of possibilities. In addition, as we have seen, the position of the IR band can indicate the function of a ligand (for example, terminal vs. bridging modes) and, in the case of π acceptor ligands, can describe the electron environment of the metal.

4-5-1 Number of IR Bands

Vibrational modes, to be IR-active, must result in a change in the dipole moment of the molecule. Not all vibrations give rise to a change in dipole moment; these consequently do not appear in the IR spectrum.

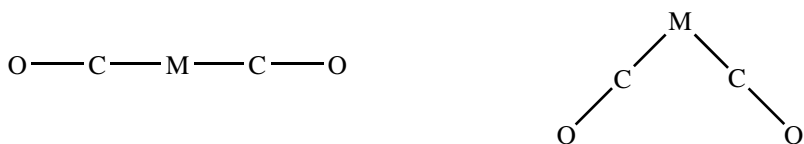
Carbonyl complexes provide convenient examples of vibrations that are visible and invisible in the IR spectrum. Identical reasoning applies to other linear monodentate ligands (such as CN^- and NO), and also to more complex ligands. We begin by considering several simple cases.

Monocarbonyl Complexes

These complexes have a single possible C–O stretching mode. Consequently, they show a single band in the IR.

Dicarbonyl Complexes

Two geometries, linear and bent, must be considered.

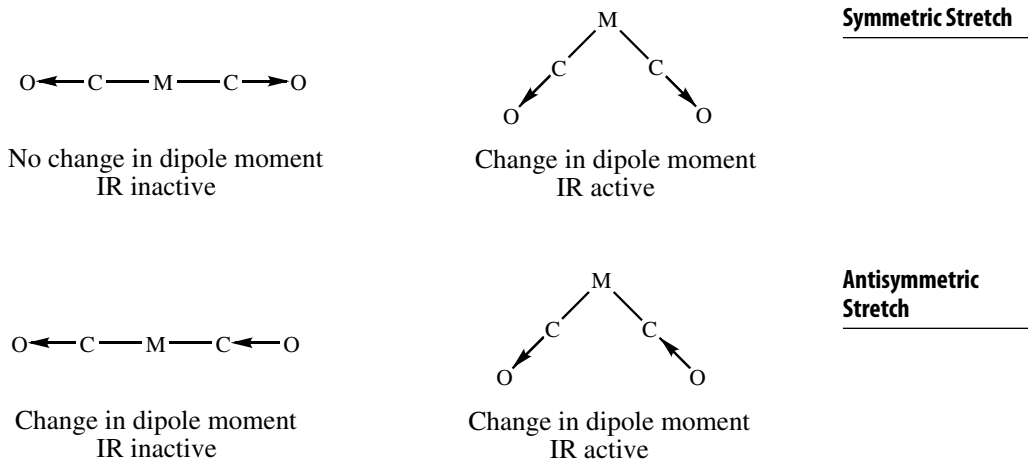


²²H. W. Roesky and K. K. Pandey, *Adv. Inorg. Chem. Radiochem.*, **1983**, 26, 337.

²³T. J. Crevier, S. Lovell, J. M. Mayer, A. L. Rheingold, and I. A. Guzei, *J. Am. Chem. Soc.*, **1998**, 120, 6607.

²⁴C. M. Teague, T. A. O'Brien, and J. F. O'Brien, *J. Coord. Chem.*, **2002**, 55, 627, using the complexes $\text{CpCr}(\text{CO})_2(\text{NE})$, E = O, S, Se, and Te.

In the case of two CO ligands arranged linearly, only an antisymmetric vibration of the ligands is IR-active; a symmetric vibrational mode results in no change in dipole moment and hence is inactive. If two COs are oriented in a nonlinear fashion, however, both symmetric and antisymmetric vibrations result in changes in dipole moment, and both are IR-active. These modes are shown below.



Therefore, an infrared spectrum can be a convenient tool for determining the structure for molecules known to have exactly two CO ligands: a single band indicates linear orientation of the carbonyls; two bands indicates nonlinear orientation.

Complexes Containing Three or More Carbonyls

The predictions in these cases are not quite so simple. The exact number of carbonyl bands can be determined by the methods of group theory.²⁵ For convenient reference, the numbers of bands expected for a variety of CO complexes are given in Table 4-4.

Several additional points relating to the number of infrared bands are worth noting. First, although one can predict the number of IR-active bands using Table 4-4, fewer bands may sometimes be observed. In some cases, bands may overlap to such a degree that they become indistinguishable; alternatively, one or more bands may have very low intensity and be difficult to observe. In some cases, isomers may be present in the same sample, and it may be difficult to sort out which

²⁵G. L. Miessler and D. A. Tarr, *Inorganic Chemistry*, 3rd ed., Pearson Prentice Hall: Upper Saddle River, NJ, 2004, pp.103–110 and F. A. Cotton, *Chemical Applications of Group Theory*, 3rd ed., Wiley: New York, 1990, pp. 304–317 and 328–337.

Table 4-4 Carbonyl Stretching Bands^a

Number of CO ligands	Coordination number		
	4	5	6
3			
IR bands	2	1	2
IR bands		3	3
IR bands		3	
4			
IR bands	1	3	1
IR bands		4	4
5			
IR bands		2	3
6			
IR band			1

^aL = ligand other than CO.

IR absorptions belong to which compound. In carbonyl complexes the number of C–O stretching bands cannot exceed the number of CO ligands. The alternative is possible in some cases (more CO groups than IR bands) when vibrational modes are not IR active (do not cause a change in dipole moment). Examples can be found in Table 4-2. The highly symmetric tetrahedral $[M(CO)_4]$ and octahedral $[M(CO)_6]$ complexes have a single carbonyl band in the IR spectrum. For a detailed survey of vibrational frequencies of transition metal carbonyl complexes, including cations and anions as well as neutral species, see footnote 26.

4-5-2 Positions of Infrared Bands

In this chapter we have already encountered two examples in which the position of the carbonyl stretching band provides useful information. In the case of the isoelectronic species $[Mn(CO)_6]^+$, $Cr(CO)_6$, and $[V(CO)_6]^-$, an increase in negative charge on the complex causes a significant reduction in the energy of the C–O band as a consequence of additional π back bonding from the metal to the ligands. The bonding mode is also reflected in the infrared spectrum, with energy decreasing in the order

terminal CO > doubly bridging CO (μ_2) > triply bridging CO (μ_3).

The positions of infrared bands are also a function of other ligands present, as shown in the following examples.

<i>Complex</i>	<i>$\nu(CO)$, cm^{-1}</i>
<i>fac</i> -Mo(CO) ₃ (PF ₃) ₃	2074, 2026
<i>fac</i> -Mo(CO) ₃ (PCl ₃) ₃	2041, 1989
<i>fac</i> -Mo(CO) ₃ (PPh ₃) ₃	1937, 1841

Moving down this series, the σ donor ability of the phosphine ligands (PR₃) increases, and the π acceptor ability decreases. PF₃ is the weakest of the donors (as a consequence of the highly electronegative fluorines) and the strongest of the acceptors. As a result, the molybdenum in Mo(CO)₃(PPh₃)₃ carries the greatest electron density; it is the most able to donate electron density to the π^* orbitals of the CO ligands. Consequently, the CO ligands in Mo(CO)₃(PPh₃)₃ have the weakest C–O bonds and the lowest energy stretching bands. Many comparable series are known.

The important point is that the position of the carbonyl bands can provide important clues to the electronic environment of the metal. The greater the electron density on the metal (and the greater the negative charge), the greater the back bonding to CO and the lower the energy of the carbonyl stretching

²⁶M. Zhou, L. Andrews, and C. W. Bauschlicher, Jr., *Chem. Rev.*, **2001**, 101, 1931.

vibrations. Similar correlations between metal environment and infrared spectra can be drawn for a variety of other ligands, both organic and inorganic. NO, for example, has an infrared spectrum that is strongly correlated with environment in a manner similar to that of CO.²⁷ In combination with information on the number of infrared bands, the positions of such bands for CO and other ligands can therefore be extremely useful in characterizing organometallic compounds.

4-6 MAIN GROUP PARALLELS WITH BINARY CARBONYL COMPLEXES

Chemical similarities occur between main group and transition metal species that are “electronically equivalent” (i.e., species that require the same number of electrons to achieve a filled valence configuration).²⁸ For example, a halogen atom, one electron short of a valence shell octet, may be considered electronically equivalent to Mn(CO)₅, a 17-electron species one electron short of an 18-electron configuration. In this section we discuss briefly some parallels between main group atoms and ions and electronically equivalent binary carbonyl complexes.

Much of the chemistry of main group and metal carbonyl species can be rationalized from the way in which these species can achieve closed-shell (octet or 18-electron) configurations. These methods of achieving more stable configurations are illustrated for the following electronically equivalent species.

<i>Electrons short of filled shell</i>	<i>Examples of electronically equivalent species</i>	
	<i>Main group</i>	<i>Metal carbonyl</i>
1	Cl, Br, I	Mn(CO) ₅ , Co(CO) ₄
2	S	Fe(CO) ₄ , Os(CO) ₄
3	P	Co(CO) ₃ , Ir(CO) ₃

Halogen atoms, one electron short of a valence shell octet, exhibit chemical similarities with 17-electron organometallic species; some of the most striking are the parallels between halogen atoms and Co(CO)₄, as summarized in Table 4-5. Both can reach filled-shell electron configurations by acquiring an electron or by dimerization to form either a Co–Co or a Cl–Cl bond. The neutral dimers are capable of adding across multiple carbon–carbon bonds and can undergo disproportionation by Lewis bases. Anions of both electronically equivalent species have a 1– charge and can combine with H⁺ to form acids: both HX (X = Cl, Br, or I) and

²⁷Interpretation of infrared spectra of NO complexes is made more complicated, however, by the possibility of both bent and linear coordination modes of NO.

²⁸J. E. Ellis, *J. Chem. Ed.*, **1976**, 53, 2.

Table 4-5 Parallels between Cl and $\text{Co}(\text{CO})_4$

Characteristic	Cl	$\text{Co}(\text{CO})_4$
Electron short of closed shell	1	1
Ion with closed-shell configuration	Cl^-	$[\text{Co}(\text{CO})_4]^-$
Neutral dimer	Cl_2	$\text{Co}_2(\text{CO})_8$
Interhalogen compound formation	BrCl	$\text{ICo}(\text{CO})_4$
Hydrohalic acid	HCl	$\text{HCo}(\text{CO})_4$
Insoluble heavy metal salts	AgCl	$\text{AgCo}(\text{CO})_4$
Addition across multiple bonds	$\text{Cl}_2 + \begin{array}{c} \text{F} & & \text{F} \\ & \diagdown & / \\ & \text{C}=\text{C} \\ & / & \diagdown \\ \text{F} & & \text{F} \end{array} \longrightarrow \begin{array}{c} \text{F} & \text{F} \\ & \\ \text{Cl}-\text{C}-\text{C}-\text{Cl} \\ & \\ \text{F} & \text{F} \end{array}$	$\text{Co}_2(\text{CO})_8 + \begin{array}{c} \text{F} & & \text{F} \\ & \diagdown & / \\ & \text{C}=\text{C} \\ & / & \diagdown \\ \text{F} & & \text{F} \end{array} \longrightarrow (\text{CO})_4\text{Co}-\begin{array}{c} \text{F} & \text{F} \\ & \\ \text{C}-\text{C} \\ & \\ \text{F} & \text{F} \end{array}-\text{Co}(\text{CO})_4$
Disproportionation by Lewis bases	$\text{Cl}_2 + \text{Me}_3\text{N} \longrightarrow \text{Me}_3\text{NCl}^+ + \text{Cl}^-$	$\text{Co}_2(\text{CO})_8 + \text{C}_5\text{H}_{10}\text{NH} \longrightarrow [\text{C}_5\text{H}_{10}\text{NHCo}(\text{CO})_4]^+ + [\text{Co}(\text{CO})_4]^-$

$\text{HCo}(\text{CO})_4$ are strong acids in aqueous solution. Both types of anions form precipitates with heavy metal ions such as Ag^+ in aqueous solution. The parallels between seven-electron halogen atoms and 17-electron binary carbonyl species are sufficiently strong to justify applying the label *pseudohalogen* to these carbonyls.²⁹

Similarly, six-electron main group species show chemical similarities with 16-electron organometallic species. As for the halogens and 17-electron organometallic complexes, many of these similarities can be accounted for on the basis of ways in which the species can acquire or share electrons to achieve filled-shell configurations. Some similarities between sulfur and the electronically equivalent $\text{Fe}(\text{CO})_4$ are listed in Table 4-6.

The concept of electronically equivalent groups can also be extended to five-electron main group elements [Group 15 (VA)] and 15-electron organometallic species. For example, phosphorus and $\text{Ir}(\text{CO})_3$ both form tetrahedral tetramers, as shown in Figure 4-10. The 15-electron $\text{Co}(\text{CO})_3$ [which is isoelectronic with $\text{Ir}(\text{CO})_3$] can replace one or more phosphorus atoms in the P_4 tetrahedron, as also shown in this Figure 4-10.

The parallels between electronically equivalent main group and organometallic species are interesting and summarize a considerable amount of their chemistry. The limitations of these parallels should also be recognized, however. For example, main group compounds having valence electron counts greater than

²⁹The label *pseudohalogen* is also applied to main group species having electronic similarities to halogen atoms. Examples include CN and SCN .

Table 4-6 Parallels between Sulfur and $\text{Fe}(\text{CO})_4$

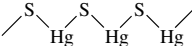
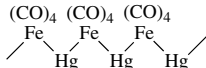
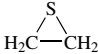
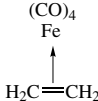
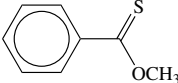
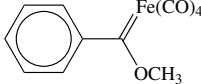
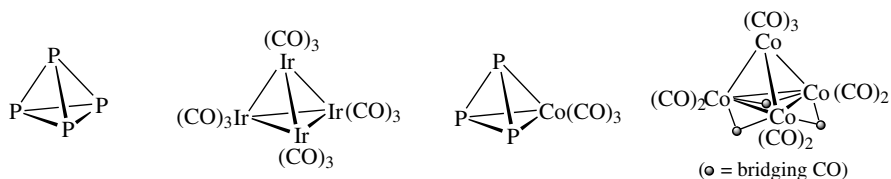
Characteristic	S	$\text{Fe}(\text{CO})_4$
Electrons short of closed shell	2	2
Ion with closed-shell configuration	S^{2-}	$[\text{Fe}(\text{CO})_4]^{2-}$
Neutral molecule	S_8	$\text{Fe}_3(\text{CO})_{12}$
Acid	H_2S	$\text{H}_2\text{Fe}(\text{CO})_4$
Dissociation constants		
K_1	5.7×10^{-8}	3.6×10^{-5}
K_2	1.2×10^{-15}	1×10^{-14}
Polymeric mercury compound		
Compound with ethylene		
Esters and carbene complexes		
	Thiol ester	Carbene complex

Figure 4-10

P_4 , $[\text{Ir}(\text{CO})_3]_4$,
 $\text{P}_3[\text{Co}(\text{CO})_3]_4$, and
 $\text{Co}_4(\text{CO})_{12}$



8 (sometimes called “expanded octets”) may not have organometallic parallels; organometallic analogues of such compounds as IF_7 and XeF_4 are not known. Organometallic complexes of ligands that do not interact with metal atoms as strongly as CO may not follow the 18-electron rule. These complexes may consequently behave differently than electronically equivalent main group species. In addition, the reaction chemistry of organometallic compounds may differ significantly from that of main group chemistry. For example, the loss of ligands such as CO is far more common in organometallic chemistry than in main group

chemistry. Therefore, as in any scheme based on a framework as simple as electron counting, the concept of electronically equivalent groups, although useful, has its limitations. It serves as valuable background, however, for a potentially more versatile way to seek parallels between main group and organometallic chemistry—the concept of isolobal groups—to be discussed in Chapter 13.

Suggested Reading

Carbonyl and Other Complexes with Metals in Negative Oxidation States

J. E. Ellis, *Inorg. Chem.*, **2006**, *45*, 3167.

Parallels with Main Group Chemistry

J. E. Ellis, *J. Chem. Ed.*, **1976**, *53*, 2.

Bonding in CO Complexes

D. M. P. Mingos, “Bonding of Unsaturated Organic Molecules to Transition Metals,” In *Comprehensive Organometallic Chemistry*, G. Wilkinson, F. G. A. Stone, and E. W. Abel, Eds., Pergamon Press: Oxford, 1982, Vol. 3, pp. 2–27.

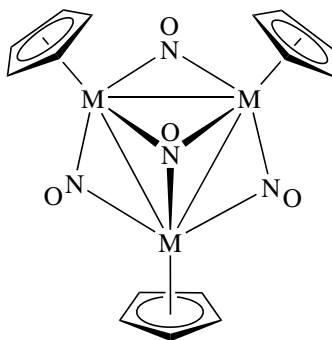
NO Complexes

J. A. Olabe and L. D. Slep, “Reactivity and Structure of Complexes of Small Molecules: Nitric and Nitrous Oxide,” In *Comprehensive Coordination Chemistry II*, J. A. McCleverty and T. J. Meyer, Eds., Pergamon Press: Oxford, 2004, Vol. 1, pp. 603–623.

Problems

- 4-1** $\text{V}(\text{CO})_6$ and $[\text{V}(\text{CO})_6]^-$ are both octahedral. Which has the shorter carbon–oxygen distance? The shorter vanadium–carbon distance?
- 4-2** Predict the metal-containing products of the following reactions.
- $\text{Mo}(\text{CO})_6 + \text{ethylenediamine} \longrightarrow$ [In this reaction two moles of gas are liberated for every mole of $\text{Mo}(\text{CO})_6$ reacting.]
 - $\text{V}(\text{CO})_6 + \text{NO} \longrightarrow$ [to give an 18-electron V complex]
- 4-3** Select the best choice in each of the following and briefly justify the reason for your selection.
- Shortest C–O bond: $\text{Ni}(\text{CO})_4$ $[\text{Co}(\text{CO})_4]^-$ $[\text{Fe}(\text{CO})_4]^{2-}$
 - Highest C–O stretching frequency: $\text{Ni}(\text{CO})_3(\text{PH}_3)$ $\text{Ni}(\text{CO})_3(\text{PF}_3)$

- c. Strongest π acceptor ligand: NO^- O_2 O_2^- O_2^{2-}
 d. Shortest M–C bond: $\text{W}(\text{CO})_6$ $[\text{Re}(\text{CO})_6]^+$ $[\text{Os}(\text{CO})_6]^{2+}$ $[\text{Ir}(\text{CO})_6]^{3+}$
- 4-4 In contrast to NO, few complexes of the phosphorus monoxide (PO) ligand have been reported.³⁰ On the basis of what you know about NO as a ligand and on the relevant electron configurations, discuss possible ways in which PO might be likely to interact with transition metals. Be sure to include in your discussion the specific classification(s) of ligand–metal interactions most likely to occur.
- 4-5 When heated at low pressure, the compound $(\eta^5\text{-C}_5\text{Me}_5)\text{Rh}(\text{CO})_2$ reacts to give a gas and another product having a single peak in the $^1\text{H-NMR}$ and a single band near 1850 cm^{-1} in the infrared. Suggest a structure for this product.
- 4-6 The following questions concern the complex shown below.

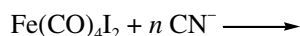


- a. Identify the first-row transition metal.
 b. This complex shows infrared absorptions at 1320 and 1495 cm^{-1} . Account for these bands.
 c. Suppose each C_5H_5 ligand was replaced by C_5Me_5 . Would you expect the IR bands described in part **b** to shift to higher or lower energies? Why?
- 4-7 The ion $[\text{Ru}(\text{Cl})(\text{NO})_2(\text{PPh}_3)_2]^+$ has N–O stretching bands at 1687 and 1845 cm^{-1} . The C–O stretching bands of dicarbonyl complexes are typically much closer than this in energy. Why are the N–O band frequencies so much farther apart?
- 4-8 Account for the observation that only a single carbonyl stretching band is observed for the ion $[\text{Co}(\text{CO})_3(\text{PPh}_3)_2]^+$.
- 4-9 Remarkably, not until after more than a century of carbonyl chemistry were stable salts isolated containing the cations $[\text{M}(\text{CO})_2]^+$ ($\text{M} = \text{Ag}, \text{Au}$)

³⁰A. Bérces, *et. al. Organometallics* **2000**, *19*, 4336, and references therein.

and $[\text{M}(\text{CO})_4]^{2+}$ ($\text{M} = \text{Pd}, \text{Pt}$).³¹ Where would you predict the carbonyl stretching bands in these ions to occur relative to other cationic carbonyl complexes?

- 4-10** An unusual bonding mode of the carbonyl ligand has carbon bridging two metals, whereas oxygen is bonded to a third.³² Would you predict the carbonyl stretching frequency in this bridging mode to be higher or lower than for ordinary doubly bridging CO ligands?
- 4-11** Photolysis of $\text{Fe}_2(\text{CO})_9$ gives a product having IR bands at 2055, 2032, 2022, 1814, and 1857 cm^{-1} . The product is less massive than $\text{Fe}_2(\text{CO})_9$. Suggest a structure for this product.³³
- 4-12** Predict the transition metal-containing product, an 18-electron species, of the following reaction.



The product has two intense infrared bands. In addition, two weaker bands are also observed. No iodine is found in the product, and iron remains in its 2+ oxidation state. Finally, the product has the same number of nitrogen and oxygen atoms.³⁴

- 4-13** When molybdenum hexacarbonyl is refluxed in butyronitrile, $\text{C}_3\text{H}_7\text{CN}$, product **X** is formed first. Continued reflux converts **X** to **Y**, and very long reflux (several days) converts **Y** to **Z**.³⁵ However, even refluxing for many weeks does not convert compound **Z** into another product. In addition,

- In each step of reaction, a colorless gas is liberated.
- **X**, **Y**, and **Z** all follow the 18-electron rule.
- The following infrared bands are observed (cm^{-1}):

X:	2077	Y: ³⁶	2107	Z:	1910
	1975		1898		1792
	1938		1842		

- a. Propose (sketch) structures of **X**, **Y**, and **Z**.
- b. Suggest a reason why **Z** does not react further when refluxed in butyronitrile.

³¹L. Weber, *Angew. Chem. Int. Ed. Engl.*, **1994**, *33*, 1077.

³²R. D. Adams, Z. Li, J. C. Lii, and W. Wu, *J. Am. Chem. Soc.*, **1992**, *114*, 4918.

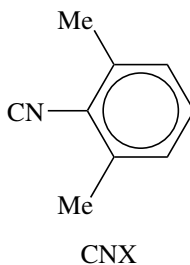
³³S. C. Fletcher, M. Poliakoff, and J. J. Turner, *Inorg. Chem.*, **1986**, *25*, 3597, provides original spectra of $\text{Fe}_2(\text{CO})_9$ and this product.

³⁴J. Jiang and S. A. Koch, *Inorg. Chem.*, **2002**, *41*, 158.

³⁵G. J. Kubas, *Inorg. Chem.* **1983**, *22*, 692.

³⁶A weak band in **Y** may be obscured by the other bands.

- 4-14** The complexes $\text{TpOs}(\text{NE})\text{Cl}_2$ [Tp = hydrotris(1-pyrazolyl)borate, a tridentate ligand; E = O, S, and Se] have N–E stretching bands at 1157, 1832, and 1284 cm^{-1} .
- Match the three complexes with their infrared bands, and explain the reasons for your match.
 - If ^{15}N is used in place of ^{14}N in these complexes, would you predict the N–E bands to be shifted to higher or lower energies? Why?³⁷
- 4-15** $\text{W}_2(\eta^5\text{-C}_5\text{H}_5)_2(\text{CO})_6$ has strong infrared bands at 1956 and 1908 cm^{-1} , and $\text{W}_2(\eta^5\text{-C}_5\text{H}_5)_2(\text{CO})_4$ has strong bands at 1892 and 1833 cm^{-1} . Why does the latter compound have its bands at lower energy than the former?
- 4-16** The first reported isocyanide analogue of $[\text{Fe}(\text{CO})_4]^{2-}$ was $[\text{Fe}(\text{CNX})_4]^{2-}$ (see structure of CNX below).³⁸
- $[\text{Ta}(\text{CNX})_6]^-$ has a carbon–nitrogen stretch at 1812 cm^{-1} . Would you expect $[\text{Fe}(\text{CNX})_4]^{2-}$ to have a C–N stretch at higher or lower energy? Explain briefly.
 - $[\text{V}(\text{CNX})_6]^-$ has a carbon–nitrogen distance of 120 pm. Would you expect $[\text{Fe}(\text{CNX})_4]^{2-}$ to have a longer or shorter C–N distance? Explain briefly.



³⁷T. J. Crevier, S. Lovell, J. M. Mayer, A. L. Rheingold, and I. A. Guzei, *J. Am. Chem. Soc.*, **1998**, *120*, 6607.

³⁸W. W. Brennessel and J. E. Ellis, *Angew. Chem. Int. Ed.*, **2007**, *46*, 598.

Pi Ligands

Among the most distinctive aspects of organometallic chemistry is the ability of a wide variety of ligands containing π electron systems to form bonds to metals. The most common of these π ligands are hydrocarbons, both linear (such as ethylene and butadiene) and cyclic (such as benzene and derivatives of the cyclopropenyl group, C_3H_3); many π ligands containing “heteroatoms” such as sulfur, boron, and nitrogen are also known. In some cases, these π bonded ligands are far more stable when attached to metals than when free (some ligands are essentially unknown in the free state). In general, the ability of π ligands to undergo reactions is quite different than when these ligands are unattached to metals. Finally, the structures of many of these metal– π ligand complexes are striking, lending an almost artistic interest to this realm within organometallic chemistry.

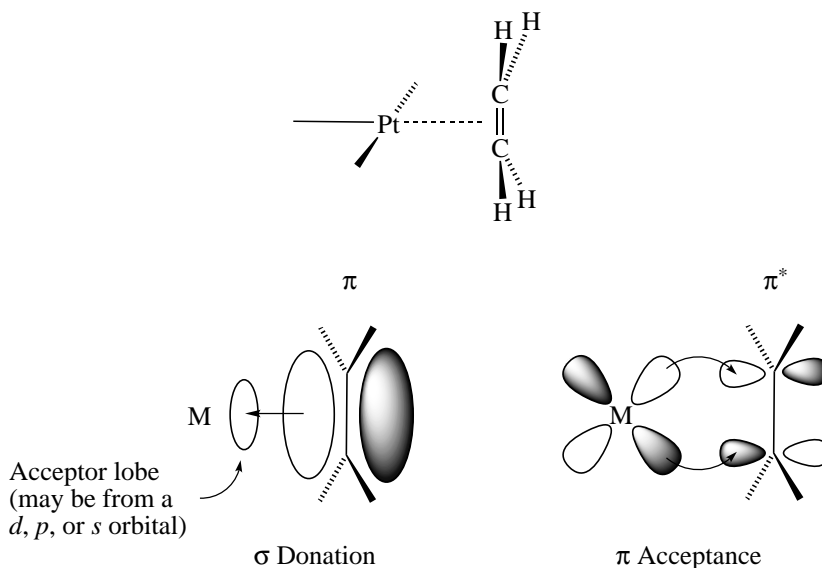
In Chapter 5 we consider interactions between ligand π systems and metals, beginning with the simplest of the linear systems—ethylene—and then proceeding with more complex linear and cyclic systems. During this discussion, we pay special attention to the classic example of the compound ferrocene.

5-1 LINEAR PI SYSTEMS

5-1-1 π -Ethylene Complexes

Many complexes involve ethylene (C_2H_4) as a ligand, including the anion of Zeise’s salt, $[Pt(\eta^2-C_2H_4)Cl_3]^-$ (Figure 1-3)—one of the earliest organometallic compounds to be synthesized. In such complexes, ethylene most commonly acts as a *sidebound* ligand with the following geometry with respect to the metal.

Figure 5-1
Bonding in Ethylene
Complexes



Ethylene donates electron density to the metal in a σ fashion, using its π bonding electron pair, as shown in Figure 5-1. At the same time, electron density can be donated back to the ligand in a π fashion from a metal d orbital to the empty π^* orbital of the ligand. This is another example of the synergistic effect of σ donation and π acceptance encountered earlier with the CO ligand.

This picture of bonding is in agreement with measured C–C distances. Free ethylene has a C–C distance of 133.7 pm, whereas the corresponding distance in the anion of Zeise’s salt is 137.5 pm. The lengthening of this bond can be explained by a combination of the two factors involved in the synergistic σ donor– π acceptor nature of the ligand: (a) donation to the metal in a σ fashion reduces the electron density in a filled π bonding orbital within the ligand, weakening the C–C bond; (b) the back-donation from the metal to the π^* orbital of the ligand also reduces the C–C bond strength by populating this antibonding orbital. The net effect weakens and hence lengthens the C–C bond in the C_2H_4 ligand.

5-1-2 π -Allyl Complexes

The allyl group can function as a trihapto ligand: using delocalized π orbitals as described previously; as a monohapto ligand, primarily σ bonded to a metal; or as a bridging ligand. Examples of these types of coordination are shown in Figure 5-2.

Bonding between $\eta^3-C_3H_5$ and a metal atom is shown schematically in Figure 5-3. The lowest energy π orbital (Figure 2-8) can donate electron density to a suitable orbital on the metal (the bottom interaction illustrated in Figure 5-3). The next orbital, nonbonding in free allyl, can act as a donor or acceptor, depending on the electron distribution between the metal and the ligand; frequently, its

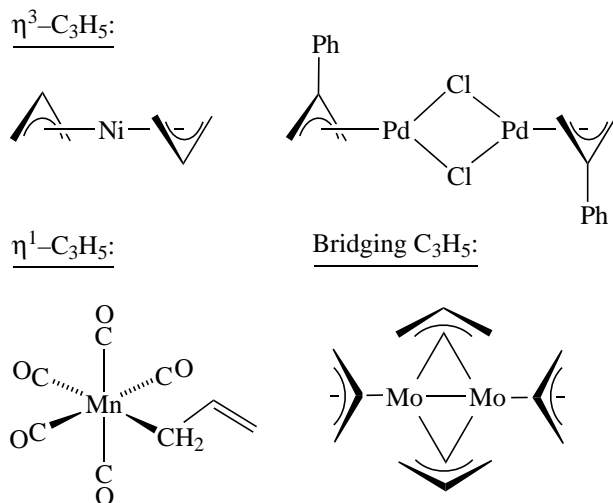
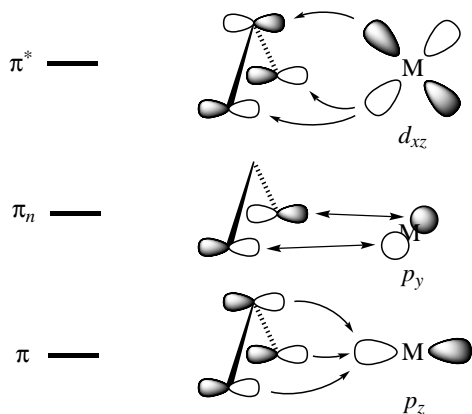


Figure 5-2
Examples of Allyl
Complexes

**Relative energy
of allyl orbitals**



**Other metal orbitals
with suitable symmetry**

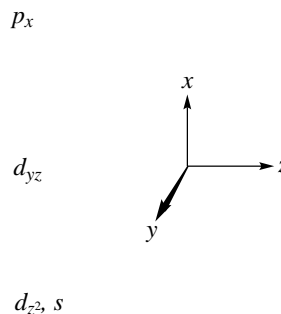
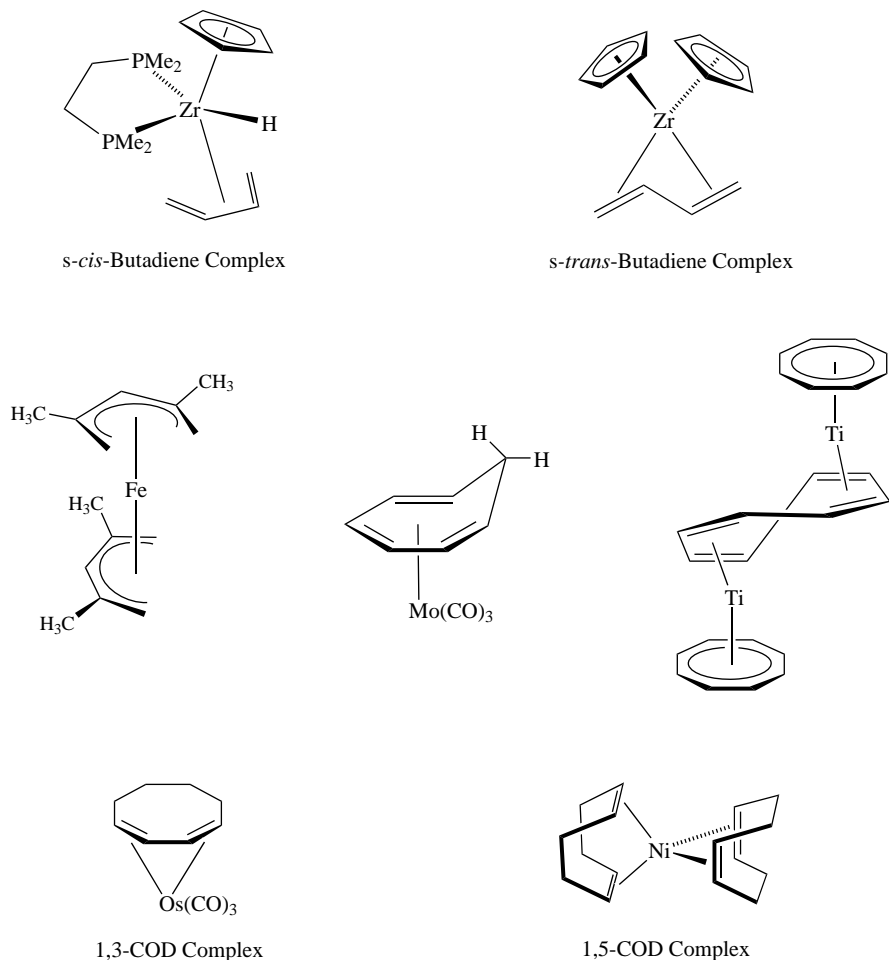


Figure 5-3
Bonding in $\eta^3\text{-Allyl}$
Complexes

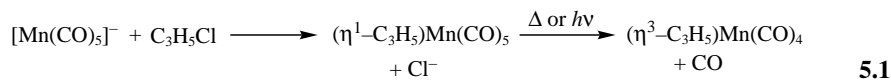
primary function is as a filled donor orbital. The empty, highest energy π orbital acts as an acceptor; thus, there can be synergistic σ and π interactions between allyl and the metal. In π -allyl complexes the carbon-metal distances reflect the overall environment of the metal. Whereas in the majority of cases the central carbon is closer to the metal than the end carbons, in some cases the reverse is true. The C-C-C angle within the ligand is generally near 120° , consistent with sp^2 hybridization on the central carbon.

Allyl complexes (or complexes of substituted allyls) are intermediates in many reactions—some of which take advantage of the capacity of this ligand to function

**Figure 5-4**

Examples of
Molecules
Containing Linear
 π Systems

in both an η^3 and an η^1 fashion. Loss of CO from carbonyl complexes containing η^1 -allyl ligands often results in conversion of η^1 - to η^3 -allyl. For example,



(Note that all manganese-containing species in this sequence of reactions are 18-electron species. The mechanism of this reaction is discussed in Chapter 7, Section 7-2-2.)

5-1-3 Other Linear π Systems

Many other such systems are known. Several examples of organic ligands having longer π systems are shown in Figure 5-4. Butadiene and longer conjugated

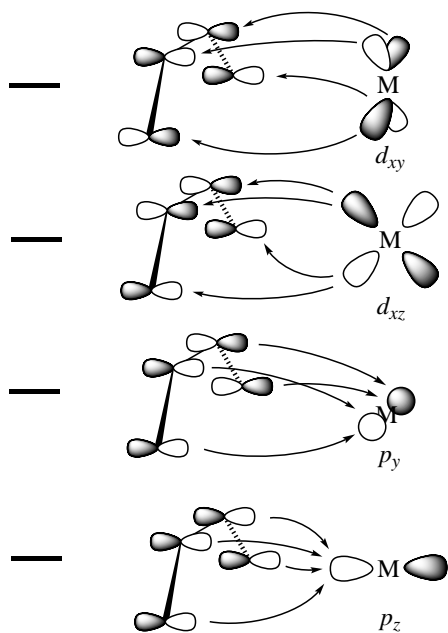
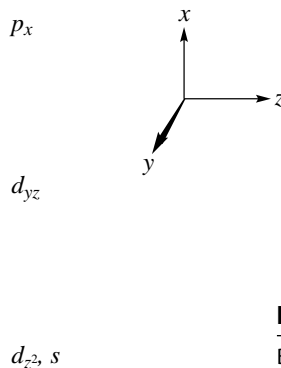
Relative energy
of butadiene orbitalsOther metal orbitals
with suitable symmetry

Figure 5-5

Bonding in
s-cis-Butadiene
Complexes

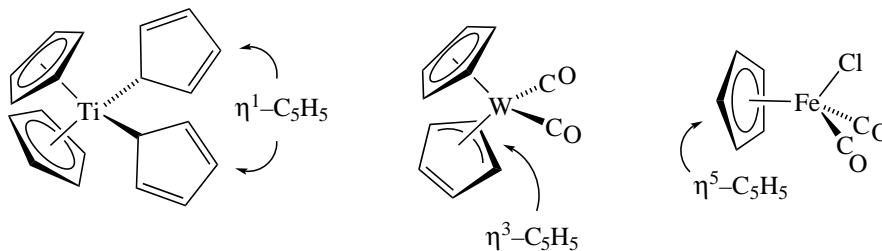
π systems have the possibility of isomeric ligand forms (*s-cis* and *s-trans* for butadiene). Larger cyclic ligands may have a π system extending through part of the ring. An example is cyclooctadiene (COD): the 1,3-isomer has a four-atom π system comparable to butadiene; 1,5-cyclooctadiene has two isolated double bonds, one or both of which may interact with a metal in a manner similar to ethylene. A schematic diagram outlining the metal–ligand interactions for a *cis*-butadiene complex is shown in Figure 5-5.

5-2 CYCLIC π SYSTEMS

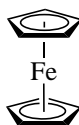
5-2-1 Cyclopentadienyl (Cp) Complexes

The cyclopentadienyl group, C_5H_5 , may bond to metals in a variety of ways, with examples known of the η^1 - and η^3 - modes, as well as the most common η^5 -bonding mode, shown below. As described in Chapter 1, the discovery of the first cyclopentadienyl complex, ferrocene, was a landmark in the development of organometallic chemistry and stimulated the search for other compounds containing π -bonded organic ligands. Numerous substituted cyclopentadienyl ligands are also known, such as $C_5(CH_3)_5$ (often abbreviated Cp*) and $C_5(\text{benzyl})_5$.¹

¹Common abbreviations for cyclopentadienyl ligands include Cp = C_5H_5 , Cp* = C_5Me_5 , and Cp' = C_5EtMe_4 .



Ferrocene



Ferrocene is the prototype of a series of sandwich compounds, called the **metalloenes**, with the formula $(C_5H_5)_2M$. The bonding in ferrocene can be viewed in a variety of ways. One possibility is to consider it an iron(II) complex with two cyclopentadienide ($C_5H_5^-$) ions, while another is to view it as iron(0) coordinated by two neutral C_5H_5 ligands. The actual bonding situation in ferrocene is much more complicated and requires an analysis of the various metal–ligand interactions in this molecule. As usual, orbitals on the central Fe and on the two C_5H_5 rings interact if they are of appropriate symmetry; furthermore, we expect interactions to be strongest if they are between orbitals of similar energy.

Figure 2-11 in Chapter 2 illustrates sketches of the molecular orbitals of a C_5H_5 ring; two of these rings are arranged in a parallel fashion in ferrocene to “sandwich in” the metal atom. The following discussion is based on the eclipsed conformation of ferrocene, the conformation consistent with gas phase and low-temperature data on this molecule.^{2,3} Theoretical calculations also indicate that the eclipsed conformation has slightly lower energy than the staggered form.⁴ Descriptions of the bonding in ferrocene based on the staggered geometry are common in the chemical literature, because this was once believed to be the molecule’s most stable conformation.⁵

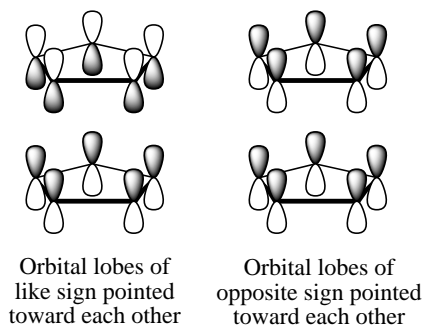
²A. Haaland and J. E. Nilsson, *Acta Chem. Scand.*, **1968**, 22, 2653; see also A. Haaland, *Acc. Chem. Res.*, **1979**, 12, 415.

³P. Seiler and J. Dunitz, *Acta Crystallogr. Sect. B*, **1982**, 38, 1741.

⁴S. Coriani, A. Haaland, T. Helgaker, and P. Jørgensen, *ChemPhysChem*, **2007**, 7, 245, and references cited therein.

⁵The $C_5(CH_3)_5$ and $C_5(\text{benzyl})_5$ analogs of ferrocene do have staggered geometries, as do several other metallocenes; see M. D. Rausch, W-M. Tsai, J. W. Chambers, R. D. Rogers, and H. G. Alt, *Organometallics* **1989**, 8, 816, for some examples.

The group orbitals are derived from the π orbitals of the two C_5H_5 rings by pairing C_5H_5 orbitals of the same energy and same number of nodes, for example, pairing the zero-node orbital of one ring with the zero-node orbital of the other.⁶ The molecular orbitals must be paired in such a way that *the nodal planes are coincident*. Furthermore, in each pairing there are two possible orientations of the ring molecular orbitals: one in which lobes of like sign are pointed toward each other and one in which lobes of opposite sign are pointed toward each other. For example, the zero-node orbitals of the C_5H_5 rings may be paired in the following ways to generate two of the group orbitals.



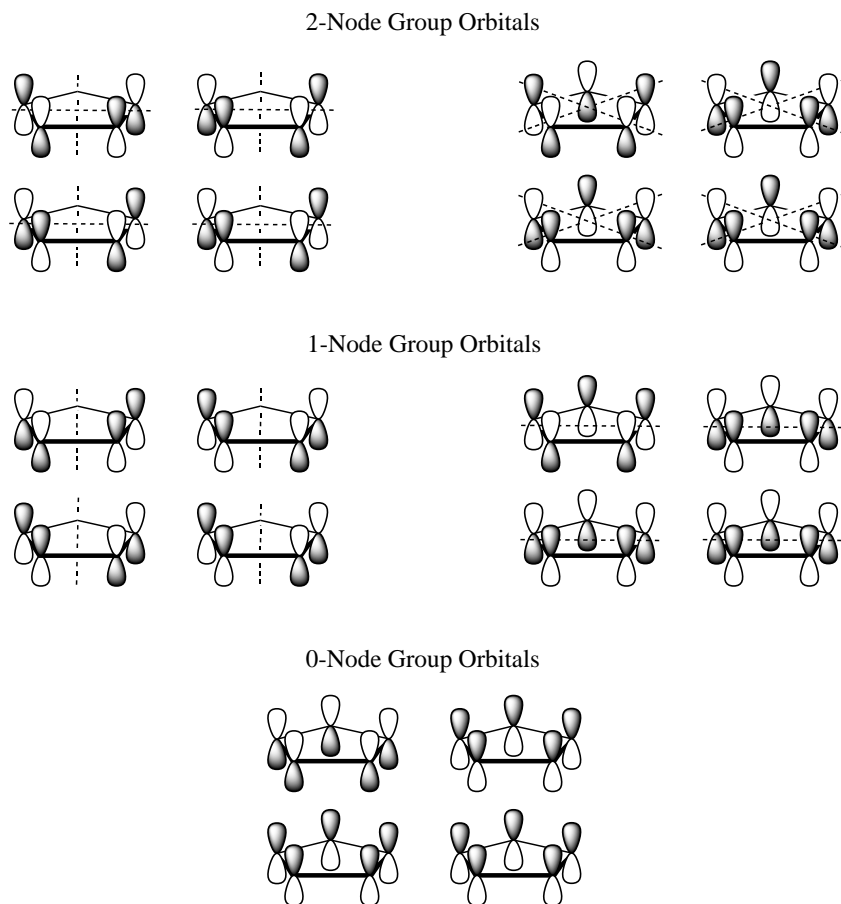
The ten group orbitals arising from the C_5H_5 ligands are shown in Figure 5-6. Note that the two π systems for each group orbital do not interact directly with each other.

The process of developing the molecular orbital picture of ferrocene now becomes one of matching the group orbitals with the s , p , and d orbitals of appropriate symmetry on Fe.

Determine which orbitals on Fe are appropriate for interaction with each of the group orbitals in Figure 5-6.

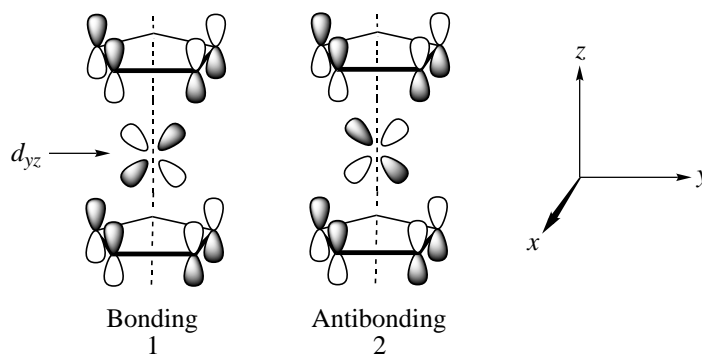
Exercise 5-1

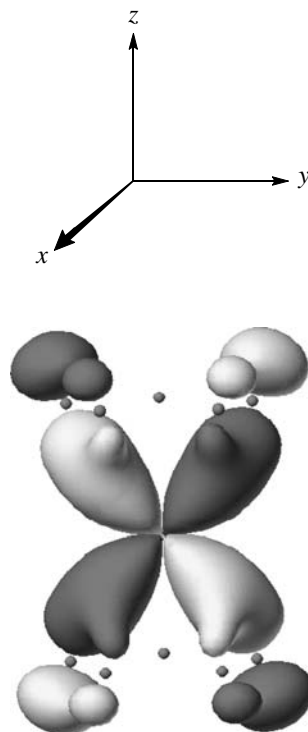
⁶Not counting the nodal planes that are coplanar with the C_5H_5 rings.

**Figure 5-6**

Group Orbitals for
the C_5H_5 Ligands of
Ferrocene

We illustrate one of these interactions: the interaction between the d_{yz} orbital of Fe and its appropriate group orbital (one of the one-node group orbitals shown in Figure 5-6). This interaction can occur in a bonding and an antibonding fashion, as shown below.



**Figure 5-7**

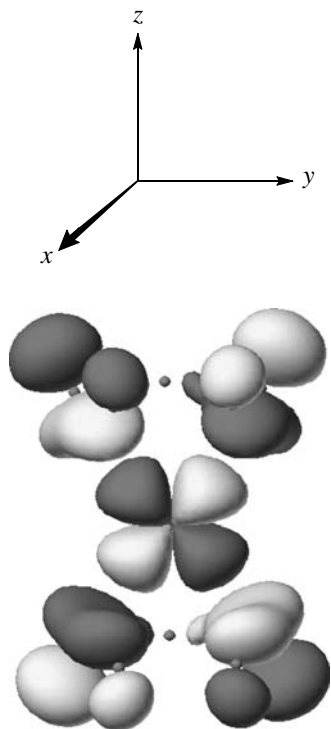
Bonding Molecular
Orbital Formed
from d_{yz} Orbital of
Iron in Ferrocene

In the bonding orbital resulting from interaction 1, the lobes of the d_{yz} orbital of iron merge with the lobes of the group orbital to which they point, giving the striking appearance illustrated in Figure 5-7.

The nodal behavior of the interacting metal and group orbitals must be preserved in the molecular orbitals that result. Thus, the molecular orbital in Figure 5-7 must have two nodal planes, the same as those of the original d_{yz} orbital: the xy plane (shown horizontally in Figure 5-7) and the xz plane (cutting vertically through the molecule in Figure 5-7). The antibonding interaction 2 gives the molecular orbital shown in Figure 5-8.

The complete energy-level diagram for the molecular orbitals of ferrocene is shown in Figure 5-9. The molecular orbital resulting from the d_{yz} bonding interaction, labeled 1 in Figure 5-9, contains a pair of electrons. Its antibonding counterpart, 2, is empty. It is a useful exercise to match the other group orbitals from Figure 5-6 with the molecular orbitals in Figure 5-9 to verify the types of metal–ligand interactions that occur.

The most interesting orbitals of ferrocene are those having the greatest d orbital character; these are highlighted in the box in Figure 5-9. Two of these orbitals, having largely d_{xy} and $d_{x^2-y^2}$ character, are weakly bonding and are occupied by electron pairs; one, having largely d_{z^2} character, is essentially non-bonding and occupied by one electron pair; and two, having primarily d_{xz} and d_{yz} character,

**Figure 5-8**

Antibonding
Molecular Orbital
Formed from d_{yz}
Orbital of Iron in
Ferrocene

are empty. The relative energies of these orbitals and their d orbital–group orbital interactions are illustrated in Figure 5-10.^{7,8}

The overall bonding in ferrocene can now be summarized. The occupied orbitals of the cyclopentadienyl ligands—the zero-node and one-node group orbitals—are stabilized by their interactions with iron. In addition, six electrons occupy molecular orbitals that are largely derived from iron d orbitals (as one would expect for d^6 iron(II)), but these occupied orbitals, displayed in Figure 5-10, have significant ligand character too. The molecular orbital picture in this

⁷The relative energies of the lowest three orbitals shown in Figure 5-10 have been controversial. UV photoelectron spectroscopy indicates that the order is as shown, with the orbital having largely d_{z^2} character slightly higher in energy than the degenerate pair having substantial d_{xy} and $d_{x^2-y^2}$ character. This order may be reversed for some metallocenes. (See A. Haaland, *Accts. Chem. Res.*, **1979**, *12*, 415.) A recent report (Z. Xu, Y. Xie, W. Feng, and H. F. Schaefer III, *J. Phys. Chem. A*, **2003**, *107*, 2716) places the orbital having d_{z^2} character lower in energy than the degenerate pair and discusses the energy levels for the metallocenes $(\eta^5\text{-C}_5\text{H}_5)_2\text{V}$ through $(\eta^5\text{-C}_5\text{H}_5)_2\text{Ni}$.

⁸J. C. Giordan, J. H. Moore, and J. A. Tossell, *Acc. Chem. Res.*, **1986**, *19*, 281; E. Rühl and A. P. Hitchcock, *J. Am. Chem. Soc.*, **1989**, *111*, 5069.

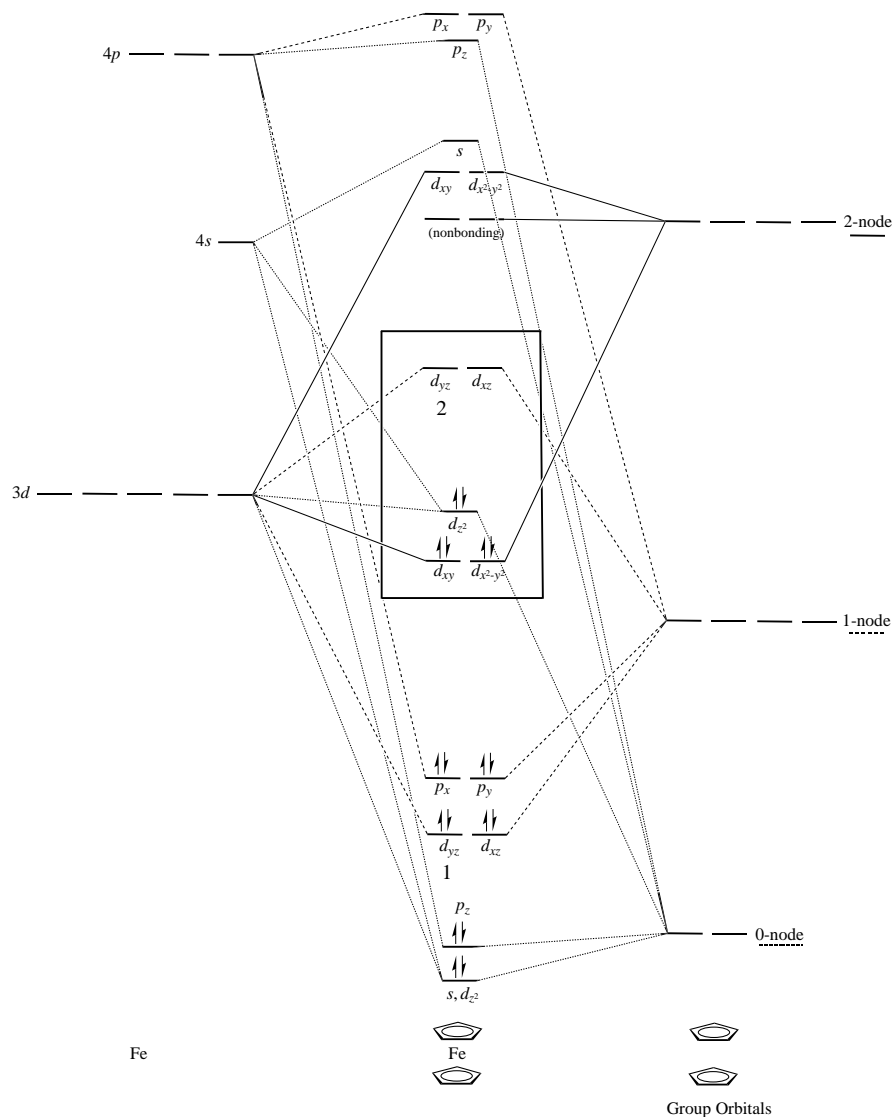
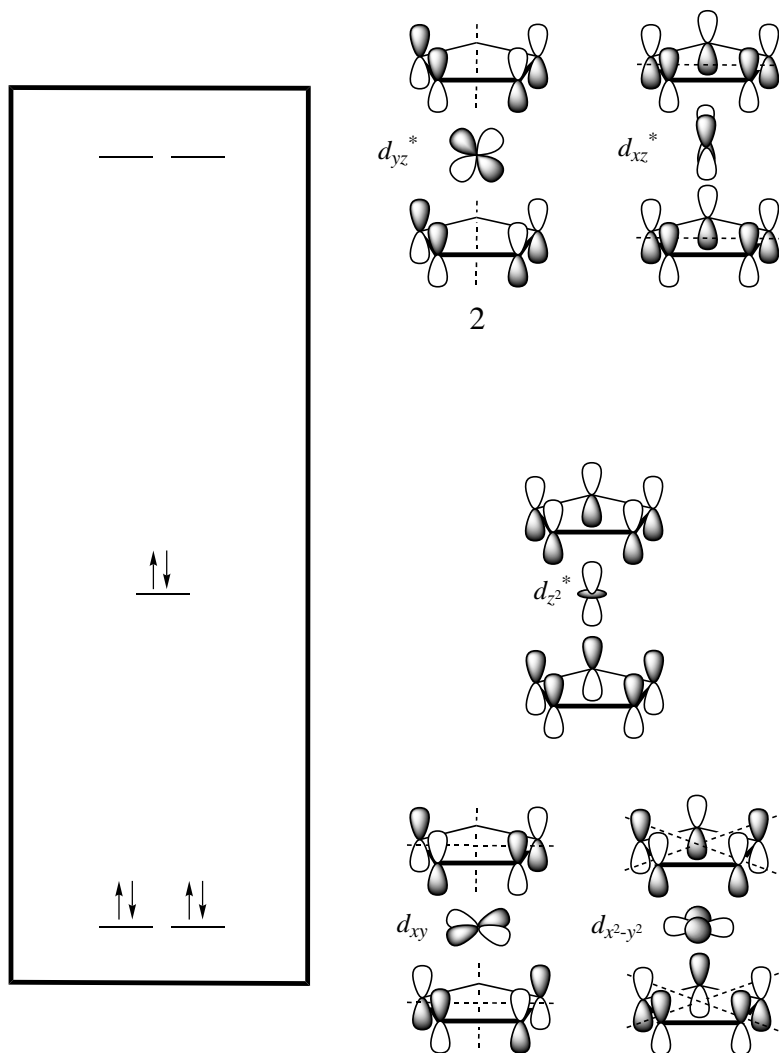


Figure 5-9
Molecular Orbital
Energy Levels in
Ferrocene

case is consistent with the 18-electron rule; however, as is evident in other metallocenes, the cyclopentadienyl ligand is not as effective as other ligands, notably CO, at favoring the 18-electron arrangement.

Other Metallocenes

Other metallocenes have similar structures but do not necessarily obey the 18-electron rule. For example, cobaltocene, $(\eta^5\text{-C}_5\text{H}_5)_2\text{Co}$, and nickelocene, $(\eta^5\text{-C}_5\text{H}_5)_2\text{Ni}$, are structurally similar 19- and 20-electron species. The “extra”

**Figure 5-10**

Molecular Orbitals of Ferrocene Having Greatest d Character
 *The three highest energy orbitals are antibonding; the corresponding bonding interactions have lower energy; see Figure 5-9.

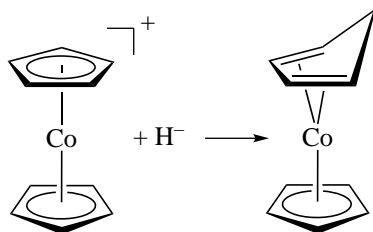
electrons have important chemical and physical consequences, as seen in comparative data in Table 5-1.⁹

The increase in metal–carbon distance in moving down this series is important because it is counter to the trend that radii of transition metal atoms and ions decrease from Sc through Ni. The explanation is that the 19th and 20th electrons of the metallocenes occupy antibonding orbitals (Figure 5-9). As a consequence, the metal–ligand distance increases (the ligands in cobaltocene and nickelocene are less tightly held to the metal), and ΔH for metal–ligand dissociation decreases.

⁹See Footnote 2.

Table 5-1 Ferrocene, Cobaltocene, and Nickelocene

Complex	Color	Count	Unpaired electrons	M–C Distance (pm)	ΔH for $M^{2+} - C_5H_5^-$ Dissociation (kcal/mol)
$(\eta^5-C_5H_5)_2Fe$	Orange	18	0	206.4	351
$(\eta^5-C_5H_5)_2Co$	Purple	19	1	211.9	335
$(\eta^5-C_5H_5)_2Ni$	Green	20	2	219.6	315

**Figure 5-11**

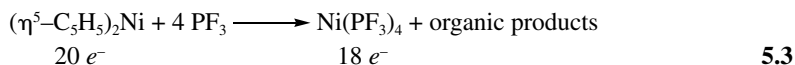
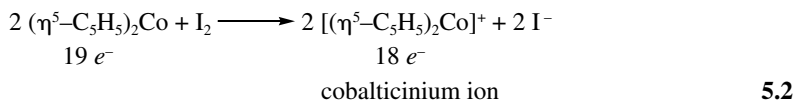
Reaction of
Cobalticinium with
Hydride

The number of unpaired electrons in these three metallocenes is also consistent with the picture of bonding shown in Figure 5-9.

Would you predict the metal–carbon distances in $(\eta^5-C_5H_5)_2V$ and $(\eta^5-C_5H_5)_2Cr$ to be longer or shorter than in ferrocene?

Exercise 5-2

Ferrocene itself shows much more chemical stability than cobaltocene and nickelocene; many of the chemical reactions of the latter are characterized by a tendency to yield 18-electron products. For example, ferrocene is unreactive toward iodine and rarely participates in reactions in which other ligands substitute for the cyclopentadienyl ligand. However, cobaltocene and nickelocene undergo the following reactions to give 18-electron products.

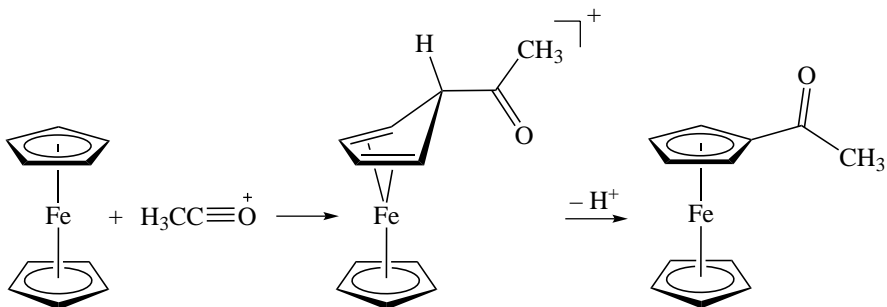


Interestingly, cobalticinium, $[(\eta^5-C_5H_5)_2Co]^+$, reacts with hydride to give a neutral, 18-electron sandwich compound in which one cyclopentadienyl ligand has been modified into $\eta^4-C_5H_6$, as shown in Figure 5-11.

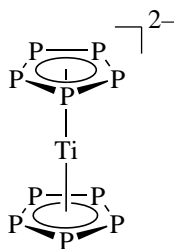
Ferrocene, however, is by no means chemically inert. It undergoes a variety of reactions, including many on the cyclopentadienyl rings. A good example is

Figure 5-12

Electrophilic
Substitution with
Acylium Ion on
Ferrocene

**Figure 5-13**

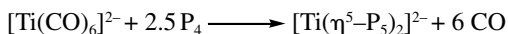
Structure of
 $[\text{Ti}(\eta^5\text{-P}_5)_2]^{2-}$



electrophilic acyl substitution (Figure 5-12), a reaction paralleling Friedel–Crafts acylation of benzene and its derivatives. In general, electrophilic aromatic substitution reactions are much more rapid for ferrocene than for benzene, an indication of a greater concentration of electron density in the rings of the sandwich compound than in benzene.

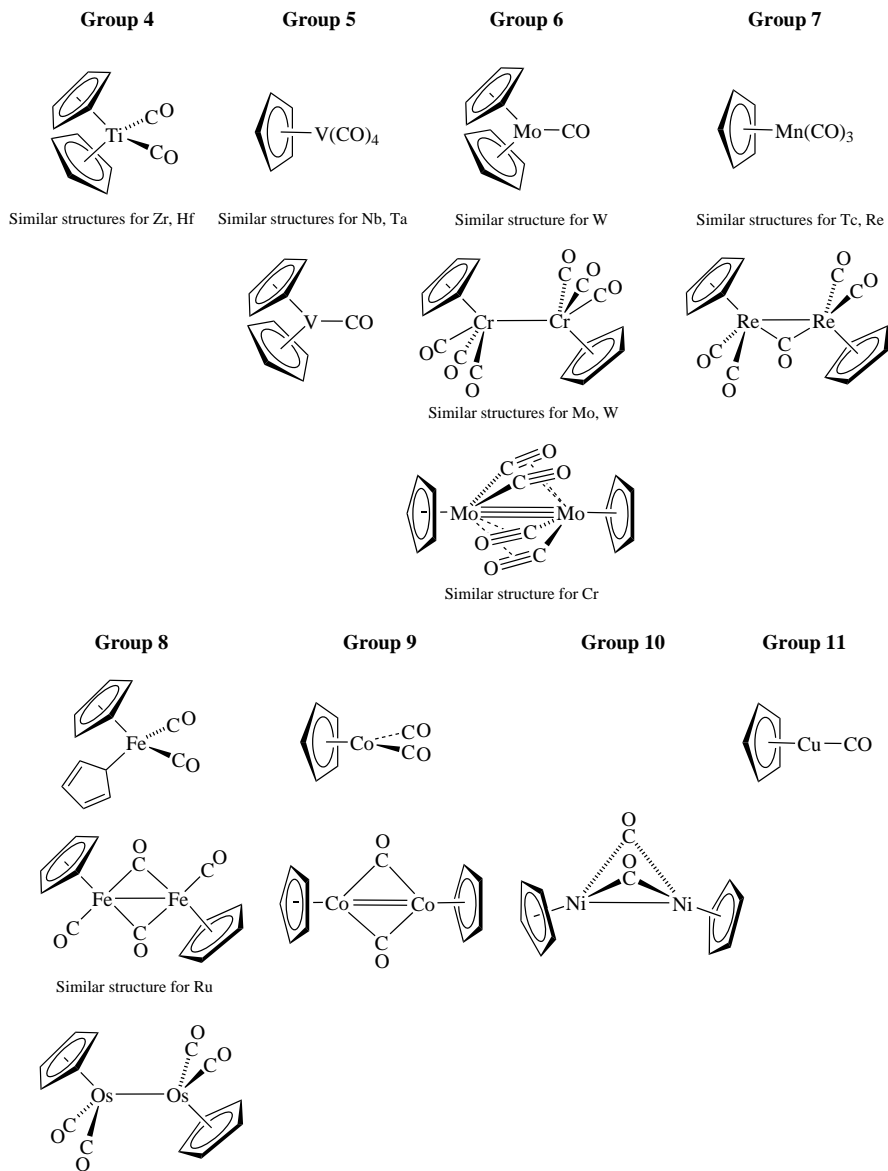
Manganocene, $(\eta^5\text{-C}_5\text{H}_5)_2\text{Mn}$, has an unusually long metal–carbon distance, 238.0 pm. This is because manganocene is a high spin complex; each orbital in the box in Figure 5-10 has a single unpaired electron. Because two of these electrons are in antibonding orbitals and each bonding orbital is just singly occupied, the manganese–carbon bonds are longer and weaker than that of the other metallocenes in the series $(\eta^5\text{-C}_5\text{H}_5)_2\text{V}$ through $(\eta^5\text{-C}_5\text{H}_5)_2\text{Ni}$.

One of the most remarkable of all metallocenes is an ion that does not contain carbon at all! This complex, $[\text{Ti}(\eta^5\text{-P}_5)_2]^{2-}$, illustrated in Figure 5-13, was synthesized by reacting $[\text{Ti}(\text{CO})_6]^{2-}$ with white phosphorus, P_4 ; it represents the first “all-inorganic” metallocene.¹⁰



5.4

¹⁰E. Urnezius, W. W. Brennessel, C. J. Cramer, J. E. Ellis, and P. v. R. Schleyer, *Science*, **2002**, 295, 832.

**Figure 5-14**

Complexes
Containing C_5H_5
and CO

5-2-2 Complexes Containing Cyclopentadienyl and CO Ligands

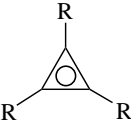


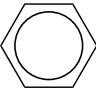
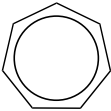
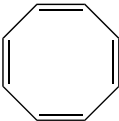
Not surprisingly, many complexes containing both Cp and CO ligands are known. These include “half sandwich” compounds such as $(\eta^5-C_5H_5)Mn(CO)_3$ and dimeric and larger cluster molecules. Selected examples are illustrated in Figure 5-14. As

for the binary CO complexes, complexes of the second- and third-row transition metals demonstrate a decreasing tendency of CO to act as a bridging ligand.

5-2-3 Other Cyclic π Ligands

Many other cyclic π ligands are known. The most common cyclic hydrocarbon ligands are listed in Table 5-2. Depending on the ligand and the electron requirements of the metal (or metals), these ligands may be capable of bonding in a monohapto or polyhapto fashion, and they may bridge two or more metals. The different sized rings have interesting features and are worth a brief survey.

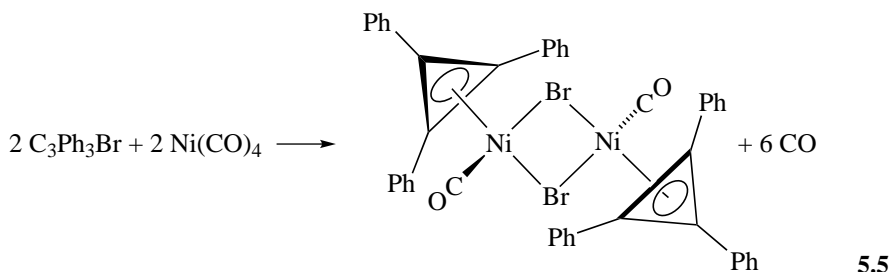
Table 5-2 Cyclic π Ligands

Formula	Structure	Name	Electron count	
			Method A ^a	Method B
C ₃ H ₃		Cyclopropenyl R = alkyl, phenyl	2 (C ₃ R ₃ ⁺)	3
C ₄ H ₄		Cyclobutadiene	6 (C ₄ H ₄ ²⁻)	4
C ₅ H ₅		Cyclopentadienyl (Cp)	6 (C ₅ H ₅ ⁻)	5
C ₆ H ₆		Benzene	6 (C ₆ H ₆)	6
C ₇ H ₇		Tropylium	6 (C ₇ H ₇ ⁺)	7
C ₈ H ₈		Cyclooctatetraene (COT)	10 (C ₈ H ₈ ²⁻)	8

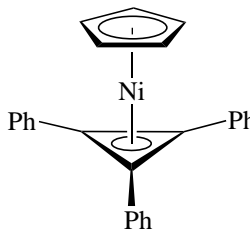
^aMethod A counts these cyclic π systems by assigning them the number of π electrons (2, 6, or 10) they would have as aromatic rings.

Cyclo- C_3R_3

The number of cyclopropenyl complexes has remained relatively small; principally, these are of the phenyl derivative C_3Ph_3 .¹¹ The difficulty in synthesizing these complexes has paralleled the difficulty in preparing the parent aromatic ions because they are small, highly strained ring systems. The first complex containing $\eta^3-C_3Ph_3$ ligand was the dimeric nickel complex $[(\eta^3-C_3Ph_3)Ni(CO)Br]_2$, prepared by the following reaction.¹²



Sandwich compounds involving $\eta^3-C_3Ph_3$ and larger rings are also known, and the rings may have different sizes; one example is shown at right.



Although the initial cyclopropenyl complexes reported were with first-row transition metals, second- and third-row transition metals are now known to also form $\eta^3-C_3R_3$ complexes.¹³ In addition, second- and third-row transition metals can form unsymmetrical complexes with C_3R_3 in which the metal-carbon distances differ significantly.

Cyclo- C_4H_4

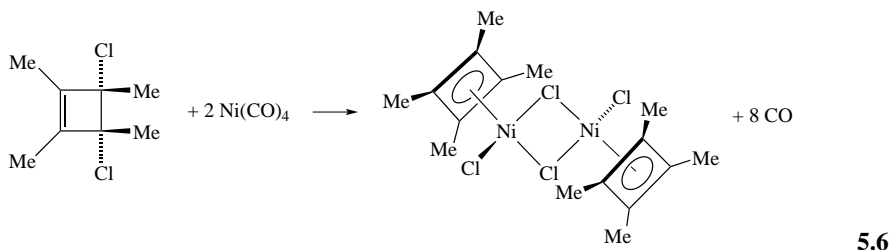
Cyclobutadiene transition metal complexes were actually synthesized long before cyclobutadiene itself.¹⁴ Interestingly, one of these complexes was also a halogen-bridged dimeric nickel complex, as shown on the next page.

¹¹A. Efraty, *Chem. Rev.*, **1977**, 77, 691.

¹²S. F. A. Kettle, *Inorg. Chem.*, **1964**, 3, 604.

¹³K. Komatsu and T. Kitagawa, *Chem. Rev.*, **2003**, 103, 1371, and references cited therein.

¹⁴R. Criegee, *Angew. Chem.*, **1959**, 71, 70.

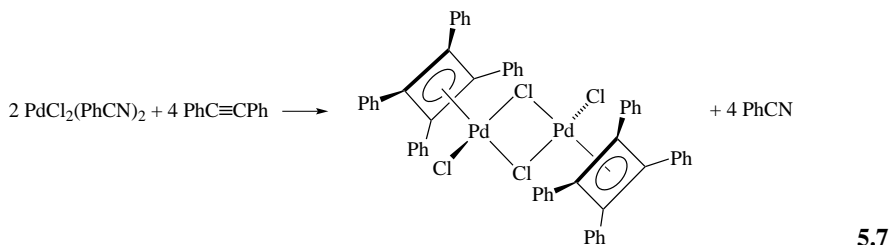


The $\eta^4\text{-C}_4\text{H}_4$ ligand is ordinarily square;¹⁵ its bonding to metals may be viewed in a manner similar to that observed in ferrocene, with the principal interaction between the π orbitals of the ring and d orbitals of the metal.

Exercise 5-3

Sketch the group orbitals on the ligands¹⁶ for the sandwich compound $(\eta^4\text{-C}_4\text{H}_4)_2\text{Ni}$. Identify the metal s , p , and d orbitals suitable for interaction with each of the group orbitals. (Assume that the rings are parallel and eclipsed.)

One of the more intriguing ways to synthesize $\eta^4\text{-C}_4\text{H}_4$ complexes is by the coupling of two acetylenes via a “template” reaction, such as that given below.¹⁷



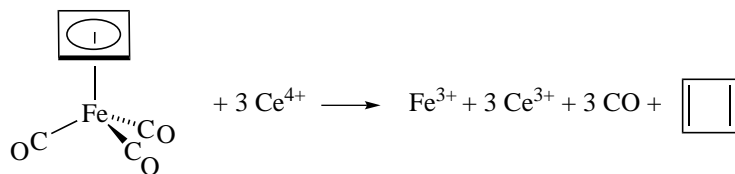
Like ferrocene, $\eta^4\text{-C}_4\text{H}_4$ complexes readily undergo electrophilic substitution at the ring; this is undoubtedly a consequence of significant electron donation from the metal to the ring. A particularly useful feature of $\eta^4\text{-C}_4\text{H}_4$ complexes is that they undergo decomposition reactions that can be used as a source of free cyclobutadiene for organic synthesis, as illustrated on the next page.¹⁸

¹⁵This is in contrast to the rectangular shape of free cyclobutadiene.

¹⁶Reference to Figure 2-11 in Chapter 2 may be helpful.

¹⁷P. M. Maitlis, *Acc. Chem. Res.*, **1976**, 9, 93.

¹⁸J. C. Barborak, L. Watts, and R. Pettit, *J. Am. Chem. Soc.*, **1966**, 88, 1328.

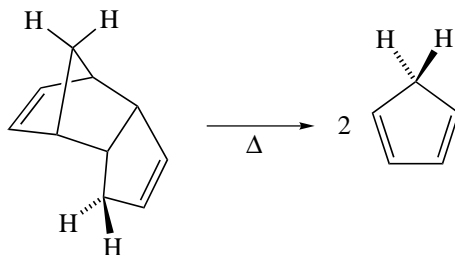


5.8

Cyclo- C_5H_5

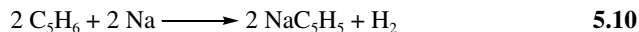
Cyclopentadienyl complexes, as previously discussed, are exceptionally numerous and have been the subject of extensive study. Several routes are available for introducing this ligand into a metal complex. One approach is to react a metal compound with the cyclopentadienide ion, C_5H_5^- . This ion can be purchased as the sodium salt in solution; it can also be prepared by the following two-step process.

1. Cracking of dicyclopentadiene (Diels–Alder dimer of cyclopentadiene). This is an example of a retro Diels–Alder reaction.

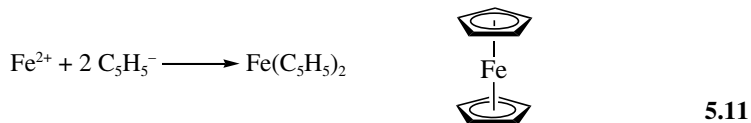


5.9

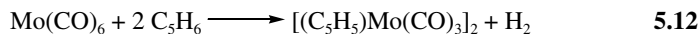
2. Reduction of cyclopentadiene by sodium.



The sodium salt can then react with the appropriate metal complex or ion.



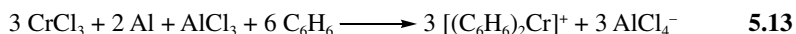
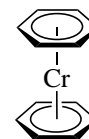
A second method is by direct reaction of a metal or metal complex with the cyclopentadiene monomer. For example,



Many examples of cyclopentadienyl complexes will be found later in this text.

Cyclo-C₆H₆ (Benzene)

Benzene and its derivatives are among the better known of the many η^6 -arene complexes. The best known of these is dibenzenechromium, (C₆H₆)₂Cr. Like other compounds of formula (C₆H₆)₂M, dibenzenechromium can be prepared by the Fischer–Hafner synthesis, using a transition metal halide, aluminum as a reducing agent, and the Lewis acid AlCl₃:



The cation is then reduced to the neutral (C₆H₆)₂Cr using a reducing agent, for example, dithionite, S₂O₄²⁻.

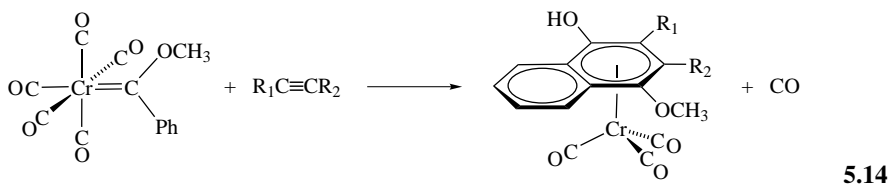
Dibenzenechromium, like ferrocene, exhibits eclipsed rings in its most stable conformation. The metal–ligand bonding in this compound may be interpreted using the group orbital approach applied to ferrocene earlier in Chapter 5.

Exercise 5-4

Show how the d_{xy} orbital of chromium can interact with a two-node group orbital derived from the benzene rings (see Figure 2-12) to form bonding and antibonding molecular orbitals. Sketch the shape of the bonding molecular orbital that would result from this interaction.

Dibenzenechromium is less thermally stable than ferrocene. Furthermore, unlike ferrocene, (C₆H₆)₂Cr is not subject to electrophilic aromatic substitution; the electrophile oxidizes the chromium(0) to chromium(I) instead of attacking the rings.

In some cases cyclization reactions occur in which three two-membered π systems fuse into a η^6 six-membered ring. An example of this very interesting phenomenon is shown below;¹⁹ this type of mechanism is discussed in Chapter 12.



5.14

¹⁹K. H. Dötz, *Angew. Chem. Int. Ed. Engl.*, **1984**, 23, 587.

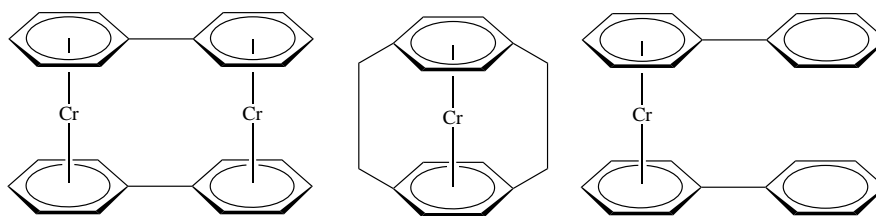


Figure 5-15

Examples of Chromium Complexes Containing Linked and Fused Six-Membered Rings

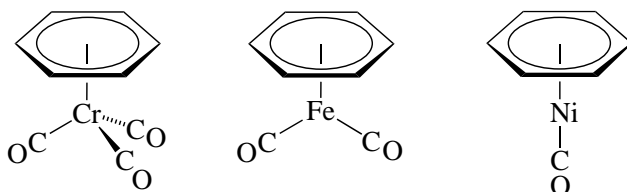


Figure 5-16

Half Sandwich Complexes Containing $\eta^6\text{-C}_6\text{H}_6$

Chromium and other metals also form 18-electron complexes containing linked and fused hexahapto six-membered rings with a variety of geometries; examples are illustrated in Figure 5-15. Many sandwich complexes containing $\eta^6\text{-C}_6\text{H}_6$ and rings of other hapticity [for example, $(\eta^6\text{-C}_6\text{H}_6)(\eta^5\text{-C}_5\text{H}_5)\text{Mn}$] and half sandwich complexes containing $\eta^6\text{-C}_6\text{H}_6$ and carbonyl ligands are also known (Figure 5-16). The structure of $(\eta^6\text{-C}_6\text{H}_6)\text{Cr}(\text{CO})_3$ is sometimes referred to as a “piano stool.”

Predict the charges of the following 18-electron complexes containing $\eta^6\text{-C}_6\text{H}_6$:

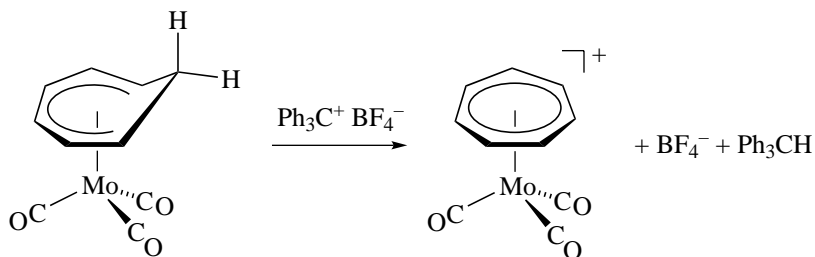
- a. $[(\text{C}_6\text{H}_6)_2\text{Ru}]^z$ b. $[(\text{C}_6\text{H}_6)\text{V}(\text{CO})_4]^z$ c. $[(\text{C}_6\text{H}_6)(\eta^5\text{-C}_5\text{H}_5)\text{Co}]^z$

Exercise 5-5

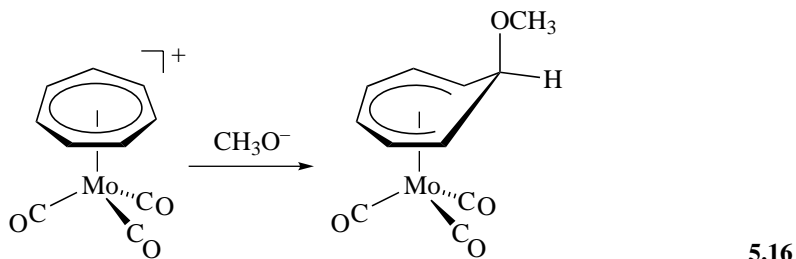
Cyclo- C_7H_7 (Tropylium²⁰)

Hexahapto cycloheptatriene complexes ($\eta^6\text{-C}_7\text{H}_8$) can be treated with $\text{Ph}_3\text{C}^+\text{BF}_4^-$ to abstract a hydrogen and yield the $\eta^7\text{-C}_7\text{H}_7$ ligand. A well-studied example is the synthesis of $[(\eta^7\text{-C}_7\text{H}_7)\text{Mo}(\text{CO})_3]^+$, as shown below.

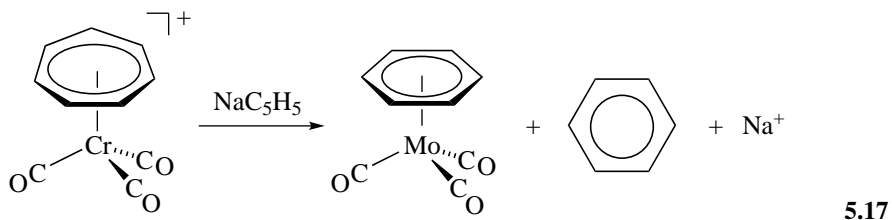
²⁰“Tropylium” is the name of the aromatic cation, C_7H_7^+ .



A cation is produced in this reaction, making the ring susceptible to nucleophilic addition by methoxide.



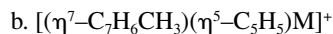
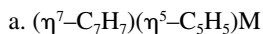
In some cases, the seven-membered ring is subject to contraction, as in the example below.²¹



Few complexes containing a metal sandwiched between two $\eta^7\text{-C}_7\text{H}_7$ rings are known. One example is $[(\eta^7\text{-C}_7\text{H}_7)_2\text{V}]^{2+}$. Several sandwich complexes have, however, been synthesized containing $\eta^7\text{-C}_7\text{H}_7$ in combination with rings of other sizes.

Exercise 5-6

Identify the first-row transition metal in the following 18-electron sandwich complexes.



²¹J. D. Munro and P. L. Pauson, *J. Chem. Soc., Dalton Trans.*, **1960**, 3479.

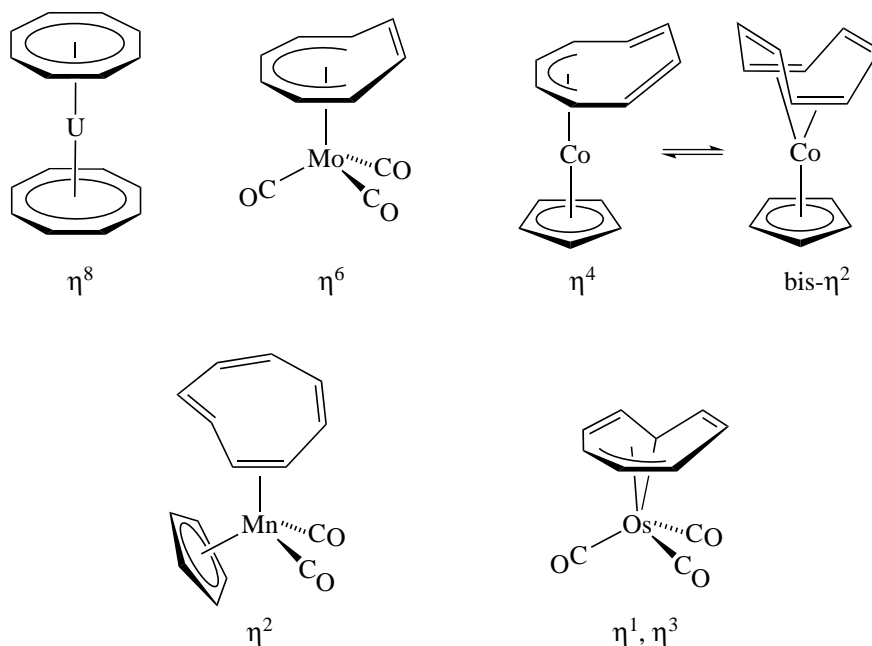
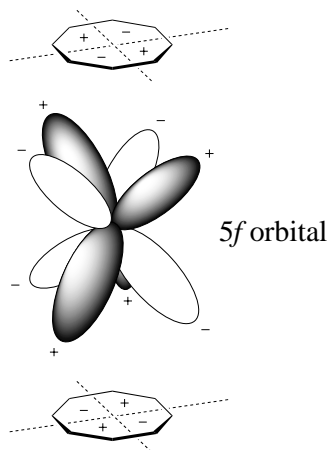


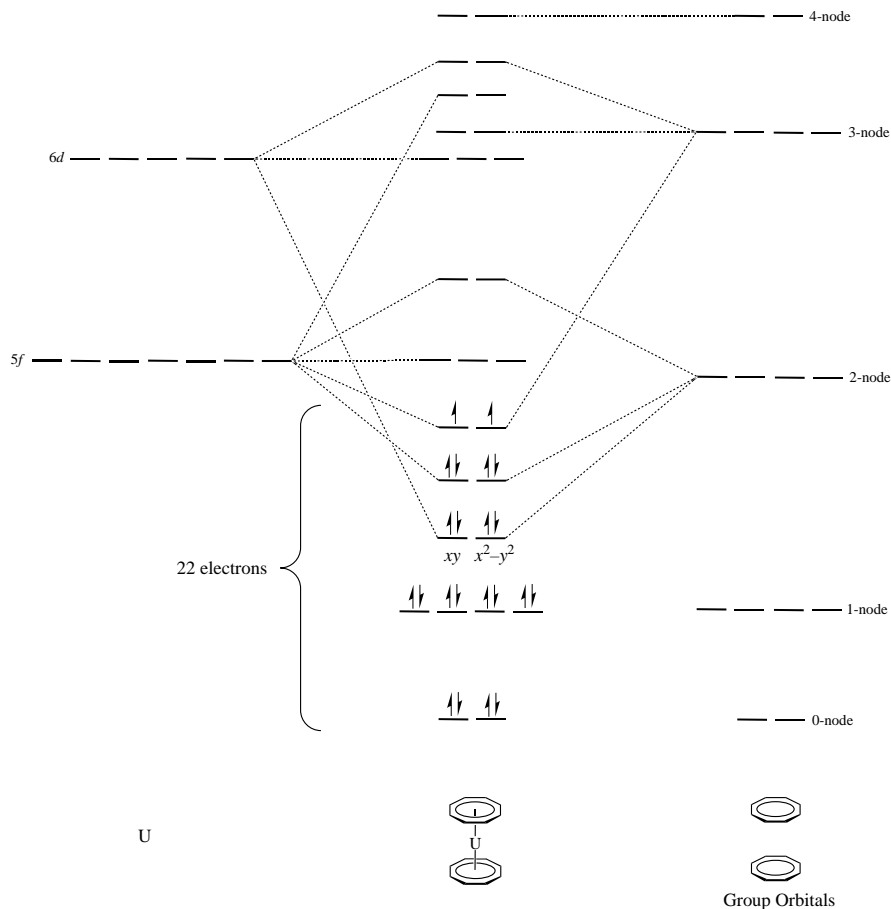
Figure 5-17
Examples of
Bonding Modes of
Cyclooctatetraene

Cyclo- C_8H_8 (Cyclooctatetraene, COT)

COT has the most diverse array of bonding modes of any of the cyclic hydrocarbons of formula C_nH_n . In addition to the η^8 - mode of principal interest in Chapter 5 (formally involving $C_8H_8^{2-}$), this ligand can also function in η^2 -, η^4 -, and η^6 - modes and sometimes modes of odd hapticity; in addition, it can form a variety of bridges between metals. Examples of bonding modes of *cyclo*- C_8H_8 are illustrated in Figure 5-17.

Although examples of molecules containing planar C_8H_8 ligands are known for some d block transition metals, the most interesting complexes of this ligand are with the actinide elements. These elements have $5f$ orbitals suitable for interaction with some π orbitals on the ligand rings. Among the most important interactions in these complexes are those between f orbitals and two-node group orbitals, as illustrated at right; in addition, weaker interactions may occur between other f orbitals and three-node group orbitals.



**Figure 5-18**

Bonding in Uranocene

Exercise 5-7

Sketch the π orbitals for cyclooctatetraenide, $C_8H_8^{2-}$, and indicate the positions of the nodal planes cutting through the ring.

The most famous of the sandwich compounds of cyclic C_8H_8 is uranocene, $(\eta^8-C_8H_8)_2U$. This air-sensitive compound is actually a 22-electron species—clearly the 18-electron rule does not apply in the realm of the actinides. A schematic diagram of selected orbital interactions in uranocene is given in Figure 5-18. Similar metallocenes are also known for other actinides, although their study is inhibited somewhat by the radioactivity of these elements.

Particularly interesting are the cases in which cyclic ligands can bridge metals resulting in “triple-decker” and higher-order sandwich compounds (Figure 5-19).

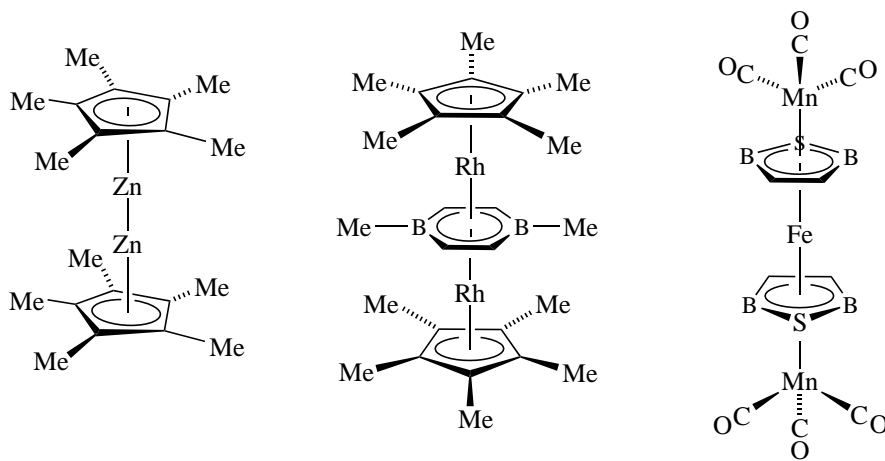


Figure 5-19
Multiple-Decker
Sandwich
Compounds



Figure 5-20
Proposed Isomer of
Ferrocene

Complexes containing delocalized rings with hapticities higher than eight have not been reported. However, an interesting alternative would have a transition metal at the center of a cyclic polyene coordinating system. Calculations have suggested that the 10-carbon ring all-*trans*-cycloclodeca-1,3,5,7,9-pentaene might form a stable complex with iron(0) in the center of the ring (Figure 5-20).²² If synthesized, this complex would have the formula $\text{FeC}_{10}\text{H}_{10}$ and therefore be an isomer of ferrocene.

5-3 NUCLEAR MAGNETIC RESONANCE SPECTRA OF ORGANOMETALLIC COMPOUNDS

Nuclear magnetic resonance (NMR) is one of the most valuable tools in characterizing organometallic complexes. The advent of high-field NMR instruments using superconducting magnets has in many ways revolutionized the study of these compounds. Convenient NMR spectra can now be taken using many metal nuclei as well as the more traditional nuclei, such as ^1H , ^{13}C , ^{19}F , and ^{31}P ; the combined spectral data of several nuclei make it possible to identify many compounds by their NMR spectra alone.

As in organic chemistry, chemical shifts, splitting patterns, and coupling constants are useful in characterizing the environments of individual atoms in

²²K. Mashima, T. Oshima, and A. Nakamura, *J. Organomet. Chem.*, **2005**, 690, 4375.

organometallic compounds. The reader may find it helpful to review the basic theory of NMR as presented in an organic chemistry text. More advanced discussions of NMR, especially relating to ^{13}C , have been surveyed elsewhere.²³

5-3-1 ^{13}C NMR

^{13}C NMR has become increasingly useful with the advent of modern instrumentation. Although the isotope ^{13}C has a low natural abundance (approximately 1.1 %) and low sensitivity for the NMR experiment (about 1.6% the sensitivity of ^1H), Fourier transform techniques now make it possible to obtain useful ^{13}C spectra for a wide range of organometallic complexes. Nevertheless, the time necessary to obtain a ^{13}C spectrum may still be an experimental difficulty for compounds present in very small amounts or those having low solubility. Rapid reactions may also be inaccessible by this technique. Some useful features of ^{13}C spectra include the following:

- An opportunity to observe organic ligands that do not contain hydrogen (such as CO and CF_3)
- Direct observation of the carbon skeleton of organic ligands. This possibility is enhanced when a spectrum is acquired with complete proton decoupling because decoupled spectra show singlets for atoms in each environment.
- ^{13}C chemical shifts are much more widely dispersed than ^1H shifts. Thus, proton decoupled ^{13}C spectra may give well-separated singlets and lend themselves to more straightforward analysis than proton spectra, which are much more likely to have overlapping peaks. The consequence is that more complex structures may be elucidated by ^{13}C than by ^1H spectra. In addition, the wide dispersion of chemical shifts often makes it easy to distinguish different ligands in compounds containing several types of organic ligands.
- ^{13}C NMR is also a valuable tool for observing rapid intermolecular rearrangement processes.²⁴ Because ^{13}C peaks are typically more widely dispersed than ^1H peaks, faster exchange processes can be observed by ^{13}C NMR.

Approximate ranges of chemical shifts for ^{13}C spectra of some categories of organometallic complexes are listed in Table 5-3.²⁵ Several features of these data deserve comment. The wide ranges of chemical shifts should be noted, a reflection

²³(a) B. E. Mann, *Adv. Organomet. Chem.*, **1974**, *12*, 135; (b) P.W. Jolly and R. Mynott, *Adv. Organomet. Chem.*, **1981**, *19*, 257; and (c) E. Breitmaier and W. Voelter, *Carbon 13 NMR Spectroscopy*, VCH: New York, 1987.

²⁴E. Breitmaier and W. Voelter, *Carbon 13 NMR Spectroscopy*, VCH: New York, 1987.

²⁵For extensive tables of chemical shifts for organic ligands, see Footnote 23a.

Table 5-3 ^{13}C Chemical Shifts for Organometallic Compounds

Ligand	^{13}C Chemical shift range ^a
M—CH ₃	-28.9 to +23.5
M=CR ₂	190 to 400
M≡CR	235 to 401
M—CO	177 to 275
in neutral binary CO complexes	183 to 223
M—(η^5 -C ₅ H ₅)	-790 to +1430
Fe—(η^5 -C ₅ H ₅)	69.2
M—(η^3 -C ₃ H ₅)	C ₂ : 91 to 129 C ₁ and C ₃ : 46 to 79
M—C ₆ H ₅	M—C: 130 to 193 <i>ortho</i> : 132 to 141 <i>meta</i> : 127 to 130 <i>para</i> : 121 to 131

^aParts per million relative to Si(CH₃)₄

of the dramatic effect that the molecular environment can have. In addition, the following aspects of ^{13}C spectra should be noted.

- Terminal carbonyl peaks are frequently in the range δ 195 to 225 ppm, a range sufficiently distinctive that the CO resonances are usually easy to distinguish from those of other ligands.
- One factor correlated with the ^{13}C chemical shift is the strength of the C–O bond; in general, the stronger the bond, the lower the chemical shift.²⁶
- Bridging carbonyls have slightly greater chemical shifts than terminal carbonyls and consequently may lend themselves to easy identification (however, infrared spectra are usually better able to distinguish between bridging and terminal carbonyls).
- Cyclopentadienyl ligands have a wide range of chemical shifts, with the value for ferrocene nearer the low end for such values. Other organic ligands may also have wide ranges in chemical shifts.

5-3-2 Proton NMR

The ^1H spectra of organometallic compounds containing hydrogens can also provide useful structural information.²⁷ For example, protons bonded directly to metals (hydride complexes, discussed in Chapter 6) are strongly shielded, with chemical shifts commonly in the approximate range -5 to -20 ppm relative to Si(CH₃)₄ (tetramethylsilane, commonly abbreviated TMS). Such protons are easy to detect, because few other protons typically appear in this region.

²⁶P. C. Lauterbur and R. B. King, *J. Am. Chem. Soc.*, **1965**, 87, 3266.

²⁷The ranges mentioned are for diamagnetic complexes. Paramagnetic complexes may have much larger chemical shifts, sometimes several hundred parts per million relative to tetramethylsilane.

Table 5-4 Examples of ^1H Chemical Shifts for Organometallic Compounds

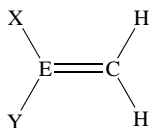
Complex	^1H Chemical shift ^a
$\text{Mn}(\text{CO})_5\text{H}$	-7.5
$\text{W}(\text{CH}_3)_6$	1.80
$(\eta^2\text{-C}_2\text{H}_4)_3\text{Ni}$	3.06
$(\eta^5\text{-C}_5\text{H}_5)_2\text{Fe}$	4.04
$(\eta^6\text{-C}_6\text{H}_6)_2\text{Cr}$	4.12
$(\eta^5\text{-C}_5\text{H}_5)_2\text{Ta}(\text{CH}_3)(=\text{CH}_2)$	10.22

^aParts per million relative to $\text{Si}(\text{CH}_3)_4$.

Protons in methyl complexes ($\text{M}-\text{CH}_3$, also discussed in Chapter 6) typically have chemical shifts between 1 and 4 ppm, similar to their positions in organic molecules. Cyclic π ligands such as $\eta^5\text{-C}_5\text{H}_5$ and $\eta^6\text{-C}_6\text{H}_6$ most commonly have ^1H chemical shifts between 4 and 7 ppm and, because of the relatively large number of protons involved, may lend themselves to easy identification. Protons in other types of organic ligands also have characteristic chemical shifts; examples are given in Table 5-4.

As in organic chemistry, integration of the various peaks in organometallic compounds can provide the ratio of atoms in different environments; it is usually accurate, for example, to assume that the area of a ^1H peak (or set of peaks) is proportional to the number of nuclei giving rise to that peak. However, for ^{13}C this approach is somewhat less reliable. For instance, relaxation times of different carbon atoms in organometallic complexes vary widely, which may lead to inaccuracy in the correlation of peak area with number of atoms (the correlation between area and number of atoms is dependent on rapid relaxation).²⁸ The addition of paramagnetic reagents may speed up relaxation and thereby improve the validity of integration data; one compound often used is $\text{Cr}(\text{acac})_3$ [acac = acetylacetonate = $\text{H}_3\text{CC}(\text{=O})\text{CHC}(\text{=O})\text{CH}_3^-$].

5-3-3 Molecular Rearrangement Processes



Under certain conditions, NMR spectra may change significantly as the temperature is changed. As an example of this phenomenon, consider a molecule having two hydrogens in nonequivalent environments, as shown at left. In this example, the carbon to which the hydrogens are attached is bonded to

²⁸For more information on the problems associated with integration in ^{13}C -NMR, see J. K. M. Sanders and B. K. Hunter, *Modern NMR Spectroscopy*, Saunders: New York, 1992.

another atom by a bond that has hindered rotation as a result of π bonding.

At low temperature, rotation about this bond is very slow, and the NMR shows two signals: one for each hydrogen. Because the magnetic environments of these hydrogens are different, their corresponding chemical shifts are different.



As the temperature is increased, the rate of rotation about the bond increases. Instead of showing the hydrogens in their original positions, the NMR now shows the peaks beginning to merge, or “coalesce.”



At still higher temperatures, the rate of rotation about the bond becomes so rapid that the NMR can no longer distinguish the individual environments of the hydrogens; instead, it now shows a single signal corresponding to the average of the two original signals.



One of the most interesting of the complexes in Figure 5-14 is $(C_5H_5)_2Fe(CO)_2$. This compound contains both η^1- and $\eta^5-C_5H_5$ ligands (and consequently obeys the 18-electron rule). The 1H NMR spectrum at $30^\circ C$ exhibits two singlets of equal area. A singlet would be expected for the five equivalent protons of the $\eta^5-C_5H_5$ ring but is surprising for the $\eta^1-C_5H_5$ ring, since the protons are not all equivalent. A “ring whizzer” mechanism (Figure 5-21) has been proposed by which the five ring positions of the monohapto ring interchange via 1,5-hydride shifts extremely rapidly, so rapidly that the NMR can see only the average signal for this ring.²⁹ At lower temperatures this process is slower, and the different resonances for the protons of $\eta^1-C_5H_5$ become apparent.

A more detailed discussion of NMR spectra in organometallic complexes, including nuclei not mentioned here, is available.³⁰

²⁹C. H. Campbell and M. L. H. Green, *J. Chem. Soc. A*, **1970**, 1318.

³⁰C. Elschenbroich, *Organometallics*, 3rd ed., Wiley-VCH: Weinheim, Germany, 2005.

Figure 5-21
Ring Whizzer
Mechanism



Suggested Reading

Bonding between Transition Metals and π Systems

Metallocenes, A. Togni and R. L. Halterman, Eds., Wiley-VCH: Weinheim, Germany, 1998 (a two-volume set).

Sandwich complexes: D. M. P. Mingos, "Bonding of Unsaturated Organic Molecules to Transition Metals," In *Comprehensive Organometallic Chemistry*, G. Wilkinson, F. G. A. Stone, and E. W. Abel, Eds., Pergamon Press: Oxford, 1982, Vol. 3, pp. 28–47.

Alkene, alkyne, and polyene complexes: D. M. P. Mingos, "Bonding of Unsaturated Organic Molecules to Transition Metals," In *Comprehensive Organometallic Chemistry*, G. Wilkinson, F. G. A. Stone, and E. W. Abel, Eds., Pergamon Press: Oxford, 1982, Vol. 3, pp. 47–67.

Structural Determinations of Cyclopentadienyl Complexes

E. A. V. Ebsworth, D. W. H. Rankin, and S. Cradock, *Structural Methods in Inorganic Chemistry*, 2nd ed., Blackwell: Oxford, 1991, pp. 414–425.

Pentadienyl Complex Review

L. Stahl and R. D. Ernst, *Adv. Organomet. Chem.*, **2008**, 55, 137.

NMR Techniques

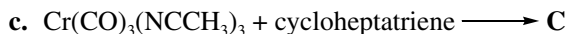
E. A. V. Ebsworth, D. W. H. Rankin, and S. Cradock, *Structural Methods in Inorganic Chemistry*, 2nd ed., Blackwell: Oxford, 1991, pp. 28–105.

Problems

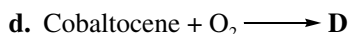
5-1 Homoleptic complexes of the ethylene ligand are not common. The simplest of these involving a transition metal observed to date is $(\eta^2\text{-C}_2\text{H}_4)_2\text{Ni}$, which can be trapped in cold matrices when $(\eta^2\text{-C}_2\text{H}_4)_3\text{Ni}$ is photolyzed.

- a. Assuming that the ethylene ligands are parallel (along the horizontal axis), sketch the group orbitals of these ligands. For each group orbital, list the atomic orbitals of Ni of appropriate shape and orientation for interaction (consider s , p , and d orbitals of Ni).

- b. Sketch the shape of a bonding molecular orbital involving one of the d orbitals of Ni.
- c. Is the C–C distance in $(\eta^2\text{-C}_2\text{H}_4)_2\text{Ni}$ likely to be longer or shorter than in free ethylene? Why?
- 5-2** Using molecular modeling software, draw $(\eta^2\text{-C}_2\text{H}_4)_2\text{Ni}$ and generate and display its molecular orbitals. Compare your results for this problem with your answers for problem **5-1**.
- a. Identify the molecular orbitals that result from interactions between the Ni orbitals and the orbitals on the rings.
- b. Which molecular orbitals involve bonding interactions between d orbitals of Ni and π orbitals on the rings?
- c. Sketch a molecular orbital energy level diagram. Compare your results with the diagram for ferrocene (Figure **5-9**) and comment on the similarities and differences.
- 5-3** Suppose a metal is bonded to a $\eta^3\text{-C}_3\text{H}_3$ ligand. For each of the π orbitals of this ligand, determine which s , p , and d orbitals of a metal atom would be suitable for interaction. (For convenience, assign the z axis to join the metal to the center of the triangle of the ligand.)
- 5-4** When the positions of hydrogen atoms in cyclic $\eta^n\text{-C}_n\text{H}_n$ are analyzed, in some cases they are above the plane of the carbon atoms (away from the metal) and in some cases below. As the size of the ring increases, is the “up” or “down” orientation of the hydrogens likely to be favored? Why?
- 5-5** The Fe–C distance in $[(\eta^5\text{-C}_5\text{H}_5)_2\text{Fe}]^+$ is approximately 6 pm longer than that in $(\eta^5\text{-C}_5\text{H}_5)_2\text{Fe}$, but the Co–C distance in $[(\eta^5\text{-C}_5\text{H}_5)_2\text{Co}]^+$ is approximately 6 pm shorter than that in $(\eta^5\text{-C}_5\text{H}_5)_2\text{Co}$. Account for this phenomenon.
- 5-6** Determine the value of the unknown quantity in the following 18-electron complexes:
- a. $[(\eta^6\text{-C}_6\text{H}_6)\text{Mn}(\text{CO})_2]^z$
- b. $(\eta^6\text{-C}_6\text{H}_6)\text{M}(\text{CO})_3$ (M = second-row transition metal)
- c. $[(\eta^6\text{-C}_6\text{H}_6)\text{Co}(\text{CO})_x]^+$
- 5-7** Predict the products of the following reactions.
- a. $\text{Co}_2(\text{CO})_8 + \text{H}_2 \longrightarrow \mathbf{A}$
 \mathbf{A} is a strong acid, has a molecular weight less than 200, and has a single ^1H NMR resonance.
- b. $(\eta^4\text{-C}_4\text{H}_6)\text{Fe}(\text{CO})_3 + \text{HBF}_4 + \text{CO} \longrightarrow \mathbf{B}$
 \mathbf{B} has four infrared bands near 2100 cm^{-1} . The hapticity of the hydrocarbon ligand in \mathbf{B} is different than that of the butadiene ligand in the reactant. BF_4^- is a product of this reaction.



The number of infrared bands near 2000 cm^{-1} in the product is the same as in the reactant.



The molecular weight of **D** is more than double that of cobaltocene. **D** has protons in four magnetic environments with relative NMR intensities of 5:2:2:1. One half of **D** is a mirror image of the other half. **D** has an infrared band in the C–O single bond region.

5-8 Ferrocene reacts with the acylium ion, $\text{H}_3\text{C}-\text{C}\equiv\text{O}^+$, to give complex **X**, a cation; base extracts H^+ from **X** to give **Y**, which has the formula $\text{C}_{12}\text{H}_{12}\text{FeO}$. **Y** reacts further with the acylium ion, followed by base, to give **Z**. Suggest structures for **X**, **Y**, and **Z**.

5-9 Heating $[(\eta^5-\text{C}_5\text{H}_5)\text{Fe}(\text{CO})_3]^+$ with NaH gives **A**, which has formula $\text{FeC}_7\text{H}_6\text{O}_2$, plus colorless gas **B**. Molecule **A** reacts rapidly at room temperature to eliminate colorless gas **C**, forming solid **D**, which has empirical formula $\text{FeC}_7\text{H}_5\text{O}_2$. Compound **D** has two strong IR bands, one near 1850 cm^{-1} and the other near 2000 cm^{-1} . Treatment of **D** with iodine generates solid **E** of empirical formula $\text{FeC}_7\text{H}_5\text{O}_2\text{I}$. Reaction of NaC_5H_5 with **E** yields solid **F** of formula $\text{FeC}_{12}\text{H}_{10}\text{O}_2$. Upon heating, **F** gives off **B**, leaving a sublimable, orange solid **G** of formula $\text{FeC}_{10}\text{H}_{10}$. Propose structures for **A** through **G**.

5-10 Photolysis of $(\eta^5-\text{C}_5\text{H}_5)(\eta^2-\text{C}_2\text{H}_4)_2\text{Rh}$ in the presence of benzene in an unreacting solvent such as pentane yields a remarkable product having the following characteristics.

- It has the empirical formula RhC_8H_8 .
- It has a metal–metal bond and follows the 18-electron rule.
- Although the ^1H NMR spectrum has not been reported, it is likely to have the following characteristics:
 - Three types resonances, with relative intensities 5:2:1
 - The largest peak should have a chemical shift similar to that of the ring protons in the starting material.

Finally, those who like to sail on the the sea might be particularly fond of this molecule! Propose a structure for this product.³¹

5-11 The ring whizzer mechanism of rearrangement of $(\eta^4-\text{C}_8\text{H}_8)\text{Ru}(\text{CO})_3$ is substantially slower than that for $(\eta^4-\text{C}_8\text{H}_8)\text{Fe}(\text{CO})_3$ and can be observed by ^1H NMR as well as ^{13}C NMR. Suggest a reason for the slower rearrangement in the ruthenium compound.³²

³¹J. Müller, P. E. Gaede, and K. Qiao, *Angew. Chem. Int. Ed. Engl.*, **1993**, 32, 1697.

³²F. A. Cotton and D. L. Hunter, *J. Am. Chem. Soc.*, **1976**, 98, 1413, and references therein.

- 5-12** Both the ^1H and ^{13}C variable temperature NMR spectra of $(\eta^4\text{-C}_8\text{H}_8)\text{Fe}(\text{CO})_3$ have been reported. What information could be determined using ^{13}C NMR that could not be determined using ^1H NMR?³³
- 5-13** Whereas the compound $[(\eta^5\text{-C}_5\text{H}_5)\text{Fe}(\text{CO})]_2$ has bands in the infrared at 1904 and 1958 cm^{-1} , $[(\eta^5\text{-C}_5\text{Me}_5)\text{Fe}(\text{CO})]_2$ (Me = methyl) has bands at 1876 and 1929 cm^{-1} .³⁴
- Account for the differences in position of these bands for the two compounds.
 - What does the appearance of two bands rather than a single band imply about the structures of these compounds?
- 5-14** $(\eta^5\text{-C}_5\text{H}_5)_2\text{Co}(\text{CO})_3$ has IR bands at 1965 and 1812 cm^{-1} , but $(\eta^5\text{-C}_5\text{H}_5)_2\text{Co}(\text{CO})_2$ has only a single band, at 1792 cm^{-1} . Account for this difference and provide sketches of both molecules that are consistent with the IR data and the 18-electron rule.

³³F. A. Cotton, *Acct. Chem. Res.*, **1968**, *1*, 257 and F. A. Cotton and D. L. Hunter, *J. Am. Chem. Soc.*, **1976**, *98*, 1413.

³⁴M. Vitale, M. E. Archer, and B. E. Bursten, *Chem. Commun.* **1998**, 179–180.

Other Important Ligands

We have by no means exhausted the types of ligands encountered in organometallic chemistry. On the contrary, several additional classes of ligands are of immense importance. Three types of ligands containing metal–carbon σ bonds deserve particular attention: alkyl ligands; carbenes (containing metal–carbon double bonds), and carbynes (containing metal–carbon triple bonds). The latter two contain metal–carbon π interactions as well as σ interactions. In addition, several nonorganic ligands play important roles in organometallic chemistry. Examples include hydrogen atoms, dihydrogen (H_2), phosphines (PR_3), and the related arsenic and antimony compounds. In some cases these ligands exhibit behavior paralleling that of organic ligands; in other instances, their behavior is significantly different. In addition, complexes containing these ligands serve important functions in organometallic reactions, including catalytic processes.

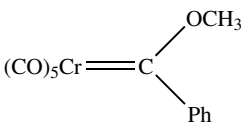
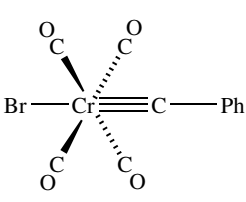
6-1 COMPLEXES CONTAINING M–C, M=C, AND M \equiv C BONDS

Complexes containing direct metal–carbon single, double, and triple bonds have been studied extensively; the most important ligands having these types of bonds are summarized in Table 6-1.

6-1-1 Alkyl and Related Complexes

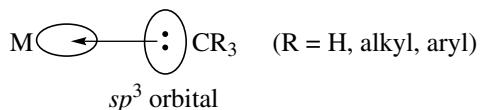
Some of the earliest known organometallic complexes were those having σ bonds between main group metal atoms and alkyl groups. Examples include

Table 6-1 Complexes Containing M–C, M=C, and M≡C Bonds

Ligand	Formula	Example
Alkyl	—CR ₃	(CO) ₅ Mn — CH ₃
Carbene (alkylidene)	=CRR'	(CO) ₅ Cr = C 
Carbyne (alkylidyne)	≡CR	

Grignard reagents, which have magnesium–alkyl bonds, and alkyl complexes with alkali metals, such as methyllithium. The syntheses and reactions of these main group compounds are typically discussed in detail in organic chemistry texts.

The first stable transition metal alkyls were synthesized in the first decade of the 20th century; many such complexes are now known. Examples of stable transition metal alkyls include Ti(CH₃)₄, W(CH₃)₆, and Cr[CH₂Si(CH₃)₃]₄. The metal–ligand bonding in these compounds may be viewed as primarily involving covalent sharing of electrons between the metal and the carbon in a σ fashion, as shown below.



In terms of electron counting, the alkyl ligand may be considered the two-electron donor, :CR₃[−] (method A), or the one-electron donor, ·CR₃ (method B). Significant ionic contribution to the bonding may occur in complexes of highly electropositive elements such as the alkali metals and alkaline earths.

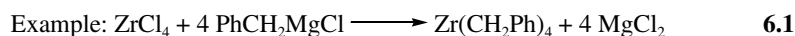
Exercise 6-1

Identify the transition metal in the following 18-electron complexes:

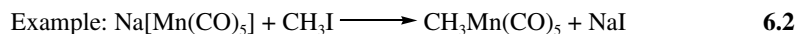
- a. $\text{CH}_3\text{M}(\text{CO})_4$ M = First-row transition metal
 b. $(\eta^5\text{-C}_5\text{H}_5)\text{CH}_3\text{M}(\text{CO})_2$ M = First-row transition metal
 c. $\text{CH}_3\text{M}(\text{CO})_2(\text{PMe}_3)_2\text{Br}$ M = Third-row transition metal

Many synthetic routes to transition metal alkyl complexes have been developed. Four of the most important of these methods are as follows.

1. Reaction of transition metal halides with organolithium, organomagnesium, or organoaluminum reagent.

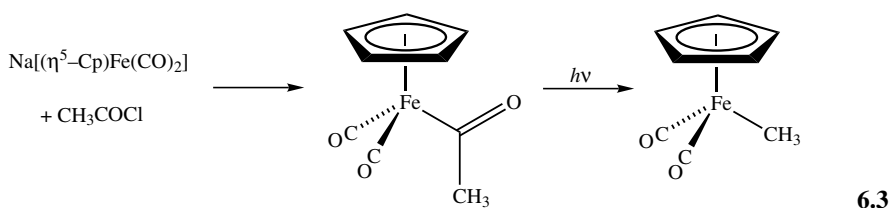


2. Reaction of metal carbonyl anion with alkyl halide.



3. Reaction of metal carbonyl anion with acyl halide.

Example:



4. Reaction of metal halide with other non-transition metal alkyls.

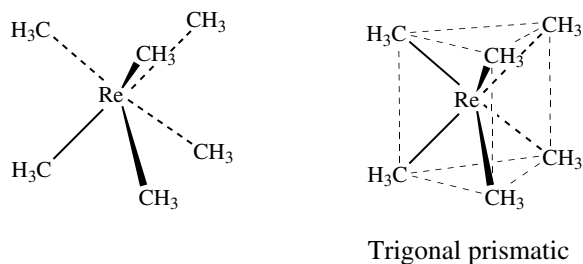


Although many complexes contain alkyl ligands, complexes containing alkyl groups as the only ligands¹ are relatively few and have a tendency to be kinetically unstable and difficult to isolate;² their stability is enhanced by structural crowding, which protects the coordination sites of the metal by blocking pathways to decomposition. For example, the six-coordinate $\text{W}(\text{CH}_3)_6$ can be melted at 30 °C without decomposition, whereas the four-coordinate $\text{Ti}(\text{CH}_3)_4$ is subject to decomposition at approximately – 40 °C.³

¹As previously mentioned, the term *homoleptic* has been coined to describe complexes in which all ligands are identical.

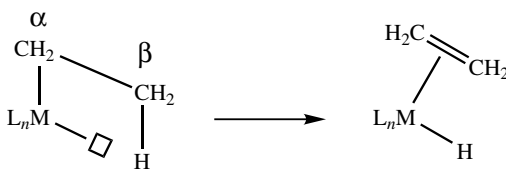
²An interesting historical perspective on alkyl complexes is in G. Wilkinson, *Science*, **1974**, *185*, 109.

³A. J. Shortland and G. Wilkinson, *J. Chem. Soc., Dalton Trans.*, **1973**, 872.

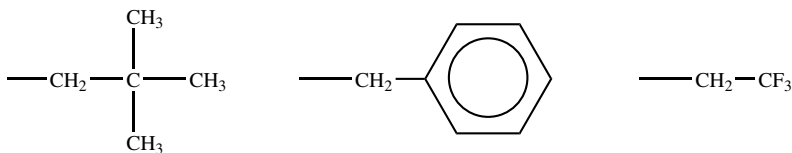
**Figure 6-1**Structure of
 $\text{Re}(\text{CH}_3)_6$

Interestingly, homoleptic transition metal complexes of the methyl ligand and its derivatives tend to have geometries that are strikingly different from those of many other transition metal complexes. $\text{Re}(\text{CH}_3)_6$, for example, has trigonal prismatic geometry (Figure 6-1), and other six-coordinate methyl complexes, including $\text{W}(\text{CH}_3)_6$, have distorted trigonal prismatic geometry.^{4,5}

In addition, alkyl complexes having β hydrogens tend to be *much* less stable (kinetically) than complexes lacking β hydrogens. Complexes with β hydrogens are subject to a method of decomposition called **β -elimination**, as illustrated in the following diagram.



To provide stability, the β positions of alkyl ligands can be blocked in a variety of ways, for example:



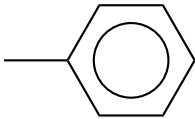
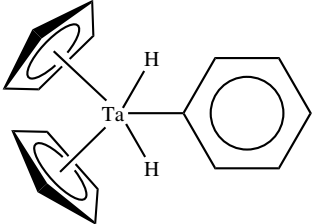
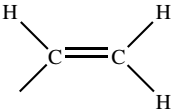
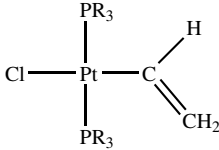

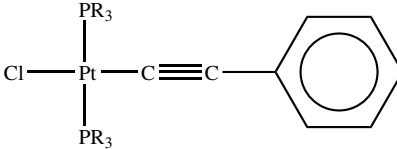
β -Elimination reactions will be discussed in more detail in Chapter 8.

Sometimes the kinetic instability of complexes containing β hydrogens can be put to good use. As discussed in Chapter 9, the instability of alkyl complexes

⁴S. Kleinhenz, V. Pfennig, and K. Seppelt, *Chem. Eur. J.*, **1998**, *4*, 1687.

⁵For a discussion of the shapes of alkyl complexes related to the VSEPR model of molecular geometry, see G. S. McGrady and A. J. Downs, *Coord. Chem. Rev.*, **2000**, *197*, 95.

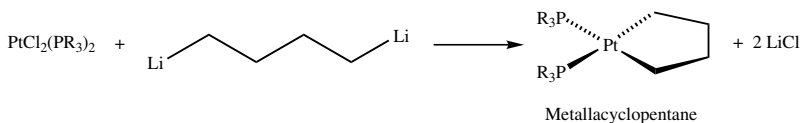
Table 6-2 Other Organic Ligands Forming σ Bonds to Metal

Ligand	Formula	Example
Aryl		
Alkenyl (vinyl)		
Alkynyl		

having β hydrogens can be a useful feature in catalytic processes, where the rapid reactivity of an intermediate can be crucial to the effectiveness of the overall process. Many alkyl complexes, therefore, are important in catalytic cycles.

Several other ligands involve direct metal–carbon σ bonds. Examples are given in Table 6-2.

There are also many known examples of **metallacycles**, complexes containing metals incorporated into rings.⁶ The following equation is an example of the synthesis of one metallacycle.

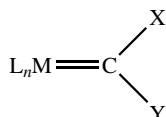
**6.5**

⁶B. Blom, H. Clayton, M. Kilkenny, and J. R. Moss, *Adv. Organomet. Chem.*, **2006**, 54, 149.

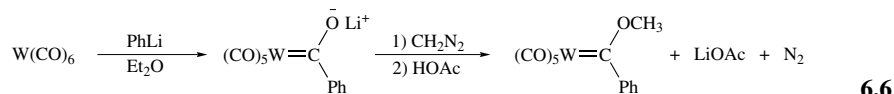
In addition to being interesting in their own right, metallacycles are proposed as intermediates in a variety of catalytic processes. More examples of metallacycles are provided in later chapters.

6-1-2 Carbene (Alkylidene) Complexes

Carbene complexes contain metal–carbon double bonds;⁷ they have the general structure shown below (X, Y = alkyl, aryl, H, or highly electronegative atoms such as O, N, S, or halogens). First synthesized in 1964 by Fischer and Maasböl,⁸ carbene complexes are now known for the majority of transition metals and for a wide range of ligands, including the prototype carbene :CH₂.



The original 1964 synthesis of a carbene complex was a classic in organometallic chemistry and generated the prototype of what are now known as Fischer carbene complexes. In this synthesis, W(CO)₆ was allowed to react with phenyllithium in diethylether to form the anion [W(CO)₅COC₆H₅][−]. Reaction of this ion with diazomethane (CH₂N₂) yielded the carbene complex shown below in equation 6.6.



The chromium and molybdenum analogs to this tungsten carbene complex have subsequently been prepared.

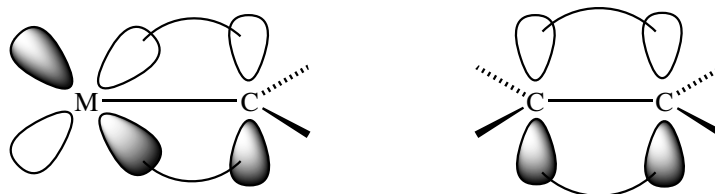
The majority of carbene complexes, including those first synthesized by Fischer, contain one or two highly electronegative *heteroatoms* such as O, N, or S directly attached to the carbene carbon. These are commonly designated *Fischer-type* carbene complexes and have been studied extensively over the past four decades. Other carbene complexes contain only carbon and/or hydrogen attached to the carbene carbon. First synthesized several years after the initial Fischer

⁷IUPAC has recommended that the term “alkylidene” be used to describe all complexes containing metal–carbon double bonds and that “carbene” be restricted to free :CR₂. For a detailed description of the distinction between these two terms (and between “carbyne” and “alkylidyne,” described later in this chapter), see W. A. Nugent and J. M. Mayer, *Metal–Ligand Multiple Bonds*, Wiley–Interscience: New York, 1988, pp. 11–16.

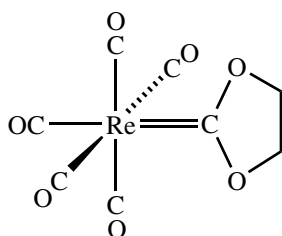
⁸E. O. Fischer and A. Maasböl, *Angew. Chem. Int. Ed. Engl.*, **1964**, *3*, 580.

Figure 6-2

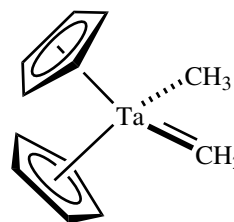
π Bonding in
Carbene Complexes
and in Alkenes



carbenes, these have been studied extensively by Schrock's research group as well as by many others; they are sometimes designated *Schrock-type* carbene complexes, commonly referred to as alkylidenes.⁹



Fischer Carbene Complex

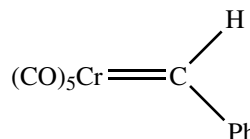
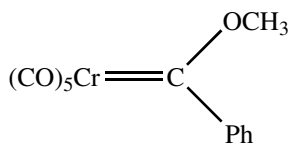


Schrock Carbene (Alkylidene) Complex

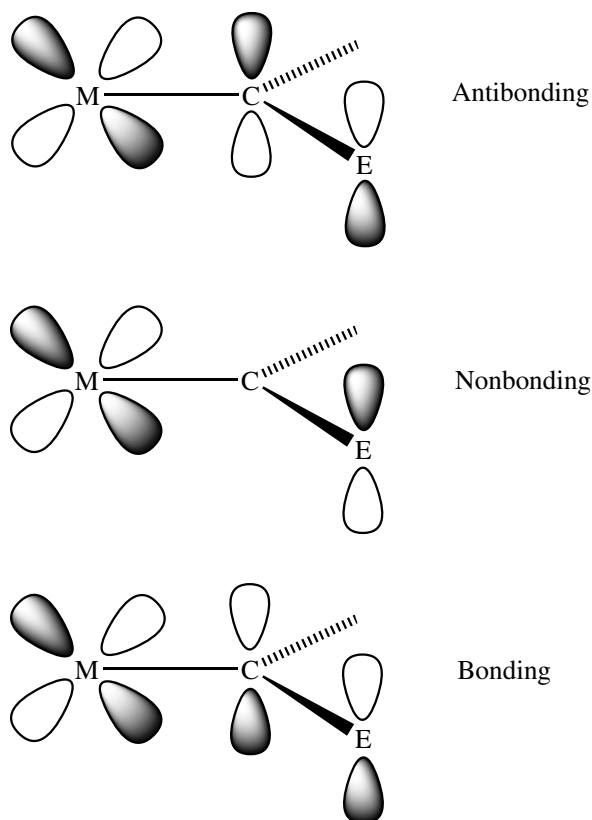
In Chapter 6 we confine the discussion to a very qualitative view of the bonding in carbene complexes; more detail on the structure, bonding, and reaction chemistry of these complexes is discussed in Chapter 10.

The formal double bond in carbene complexes may be compared with the double bond in alkenes; in the case of the carbene complex, the metal must use a *d* orbital (rather than a *p* orbital) in forming the π bond with carbon, as illustrated in Figure 6-2.

Another important aspect of bonding in carbene complexes is that complexes having a highly electronegative "heteroatom" such as O, N, or S attached to the carbene carbon tend to be more stable than complexes lacking such an atom.



⁹R. R. Schrock, *J. Am. Chem. Soc.*, **1974**, 96, 6796; *Acc. Chem. Res.*, **1979**, 12, 98.

**Figure 6-3**

Delocalized π Bonding in Carbene Complexes. E Designates a Highly Electronegative Heteroatom such as O, N, or S.

For example, $\text{Cr}(\text{CO})_5[\text{C}(\text{OCH}_3)\text{C}_6\text{H}_5]$, with an oxygen on the carbene carbon, is much more stable than $\text{Cr}(\text{CO})_5[\text{C}(\text{H})\text{C}_6\text{H}_5]$. The stability of the complex is enhanced if the highly electronegative atom can participate in the π bonding, with the result a delocalized, three-atom π system (analogous to the π -allyl system described in Chapter 2) involving a d orbital on the metal and p orbitals on carbon and on the heteroatom.¹⁰ An example of such a π system is illustrated in Figure 6-3. Such a delocalized three-atom system provides more stability than would a simple metal-carbon π bond. As discussed in Chapter 10, the presence of a highly electronegative atom can stabilize the complex by lowering the energy of the M–C–heteroatom bonding orbital.

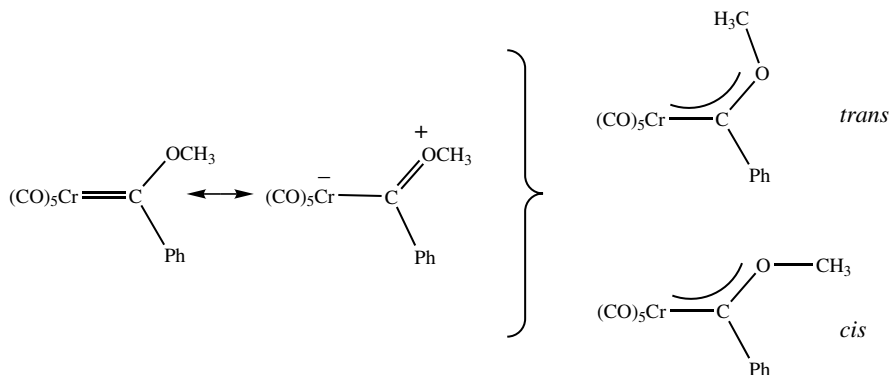
The methoxycarbene complex $\text{Cr}(\text{CO})_5[\text{C}(\text{OCH}_3)\text{C}_6\text{H}_5]$, Figure 6-4, illustrates some important characteristics of bonding in transition metal carbene complexes.¹¹ Evidence for double bonding between chromium and carbon is provided by X-ray

¹⁰In some cases, d orbitals on the heteroatom can also participate.

¹¹E. O. Fischer, *Adv. Organomet. Chem.*, **1976**, *14*, 1.

Figure 6-4

Resonance Structures and *cis* and *trans* Isomers of $\text{Cr}(\text{CO})_5[\text{C}(\text{OCH}_3)\text{C}_6\text{H}_5]$



crystallography, which measures this distance at 204 pm, compared with a typical Cr–C single bond distance of approximately 220 pm.

One interesting aspect of this complex is its ability to exhibit a proton NMR spectrum that is temperature dependent. At room temperature a single resonance is found for the methyl protons; however, as the temperature is lowered, this peak first broadens and then splits into two peaks. How can this behavior be explained?

A single methyl proton resonance, corresponding to one magnetic environment, is expected for the carbene complex as illustrated, with a double bond between chromium and carbon and a single bond (permitting rapid rotation about the bond) between carbon and oxygen. The room temperature NMR is therefore as expected, with a single methyl signal. The splitting of this peak at lower temperature into two peaks, however, suggests two different proton environments.¹² Two environments are possible if there is hindered rotation about the C–O bond. A resonance structure for the complex can be drawn, showing some double bonding between carbon and oxygen; such double bonding is significant enough for *cis* and *trans* isomers, as illustrated in Figure 6-4, to be observable at low temperatures.

Evidence for double bond character in the C–O bond is also provided by crystal structure data, which exhibit a C–O bond distance of 133 pm, compared with a typical C–O single bond distance of 143 pm.¹³ The double bonding between carbon and oxygen, although weak (typical C=O bonds are much shorter, approximately 116 pm), is sufficient to slow down rotation about the bond so that at low temperatures proton NMR detects the *cis* and *trans* methyl protons separately. At higher temperature, there is sufficient energy to cause rapid rotation about the

¹²C. G. Kreiter and E. O. Fischer, *Angew. Chem. Int. Ed. Engl.*, **1969**, 8, 761.

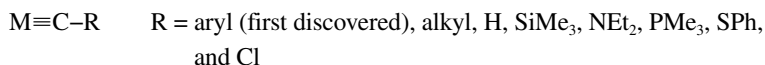
¹³O. S. Mills and A. D. Redhouse, *J. Chem. Soc. A*, **1968**, 642.

C–O bond so that the NMR sees only an average signal, which is observed as a single peak.

X-ray crystallographic data, as mentioned, show double bond character in both the Cr–C and C–O bonds. This supports the statement made early in the discussion of carbene complexes that π bonding in complexes of this type (containing a highly electronegative atom—in this case oxygen) may be considered delocalized over three atoms. Although not absolutely essential for all carbene complexes, the delocalization of π electron density over three or more atoms provides an additional measure of stability to many of these compounds.¹⁴

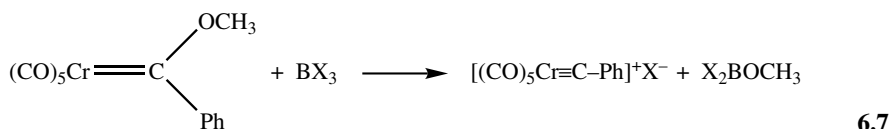
6-1-3 Carbyne Complexes

Nine years after Fischer's report of the first stable transition metal–carbene complex, the first report was made of the synthesis of complexes containing a transition metal–carbon triple bond; fittingly this report was also made by the Fischer group.¹⁵ Carbyne complexes have metal–carbon triple bonds, and they are formally analogous to alkynes.¹⁶ Many carbyne complexes are now known; examples of carbyne ligands include the following.



In Fischer's original synthesis, carbyne complexes were obtained fortuitously as products of the reactions of carbene complexes with Lewis acids. For example, the methoxycarbene complex $\text{Cr}(\text{CO})_5[\text{C}(\text{OCH}_3)\text{C}_6\text{H}_5]$ reacts with the Lewis acids BX_3 ($\text{X} = \text{Cl, Br, or I}$).

First, the Lewis acid attacks the oxygen, the basic site on the carbene.

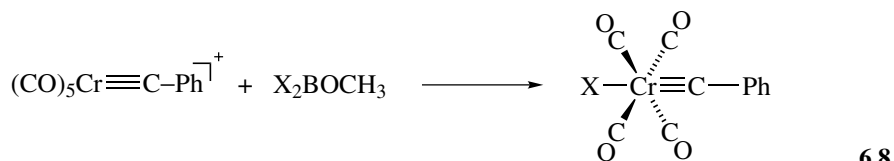


Subsequently, the intermediate loses CO, with the halogen coordinating in a position *trans* to the carbyne.

¹⁴*Transition Metal Carbene Complexes*, Verlag Chemie: Weinheim, Germany, 1983; pp 120–122.

¹⁵E. O. Fischer, G. Kreis, C. G. Müller, G. Huttner, and H. Lorentz., *Angew. Chem. Int. Ed. Engl.*, **1973**, *12*, 64.

¹⁶Complexes containing metal–carbon triple bonds in which the metal is in a relatively high formal oxidation state are frequently designated *alkylidyne*s. Carbyne complexes are also sometimes classified as *Fischer-type* or *Schrock-type*, as in the case of carbene complexes. The distinction between these is discussed in Chapter 10.



The best evidence for the carbyne nature of the complex is provided by X-ray crystallography, which gives a Cr–C bond distance of 168 pm (for X = Cl), considerably shorter than the comparable distance for the parent carbene complex. The Cr≡C–C angle is, as expected, 180° for this complex; however, slight deviations from linearity are observed for many complexes in crystalline form—in part a consequence of the manner of packing in the crystal.

Bonding in carbyne complexes may be viewed as a combination of a σ bond plus two π bonds, as illustrated in Figure 6-5.

The carbyne ligand has a lone pair of electrons in an sp hybrid on carbon; this lone pair can donate to a suitable hybrid orbital on Cr to form a σ bond. In addition, the carbon has two p orbitals that can accept electron density from d orbitals on Cr to form π bonds. Thus, the overall function of the carbyne ligand is as both a σ donor and a π acceptor. For electron counting purposes a $:\text{CR}^+$ ligand can be considered a two-electron donor (an L ligand by method A); it is usually more convenient to count neutral CR as a three-electron donor (an LX ligand by method B).

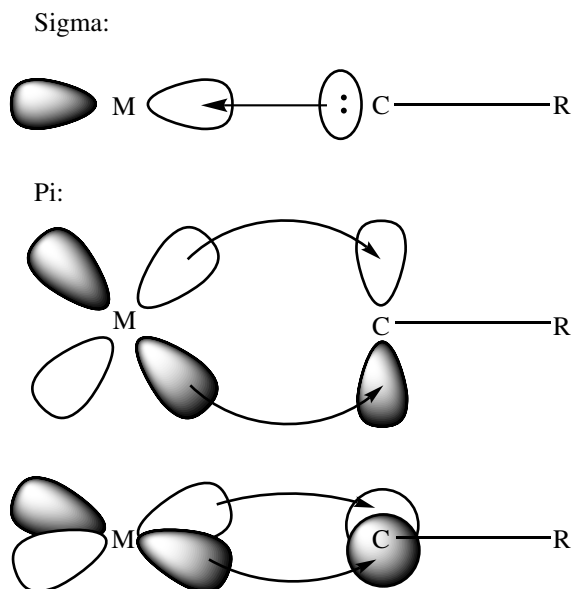


Figure 6-5
Bonding in Carbyne
Complexes

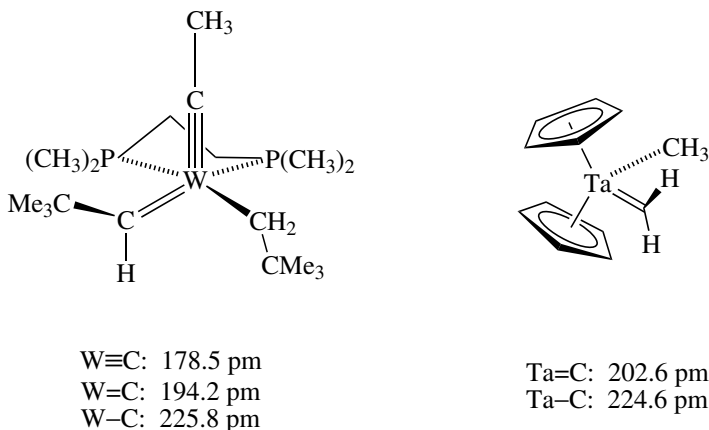


Figure 6-6

Complexes
Containing
Metal–Carbon
Single, Double, and
Triple Bonds

Verify that $Cr(CO)_4Br(\equiv CPh)$ satisfies the 18-electron rule.

Example 6-1

Method A

Cr	6 electrons
4 CO	8 electrons
:Br ⁻	2 electrons
:CC ₆ H ₅ ⁺	2 electrons
	18 electrons

Method B

Cr	6 electrons
4 CO	8 electrons
Br	1 electron
$\equiv CC_6H_5$	3 electrons
	18 electrons

Identify the third-row transition metal in the following carbyne complexes.

Exercise 6-2

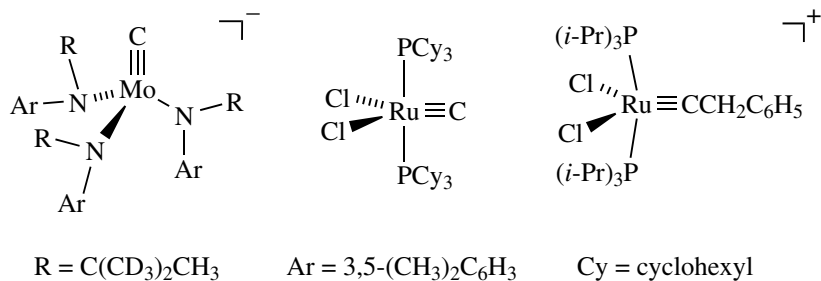
- $(\eta^5-C_5Me_5)M(CCM_3)(H)(PR_3)_2$
- $M(C-o\text{-tolyl})(CO)(PPh_3)_2Cl$

Carbyne complexes can be synthesized in a variety of ways in addition to Lewis acid attack on carbenes, as described previously. Synthetic routes for carbynes and the reactions of these compounds have been reviewed in the literature.¹⁷ Reactions of carbynes will be discussed in more detail in Chapter 10.

In some cases molecules have been synthesized containing two or three of the types of ligands discussed in this section: alkyl, carbene, and carbyne. Such molecules provide an opportunity to make direct comparisons of lengths of metal–carbon single, double, and triple bonds, as shown in Figure 6-6.

¹⁷H. P. Kim and R. J. Angelici, "Transition Metal Complexes with Terminal Carbyne Ligands," *Adv. Organomet. Chem.*, **1987**, 27, 51 and H. Fischer, P. Hoffmann, F. R. Kreissl, R. R. Schrock, U. Schubert, and K. Weiss, *Carbyne Complexes*, VCH Publishers: Weinheim, Germany, 1988.

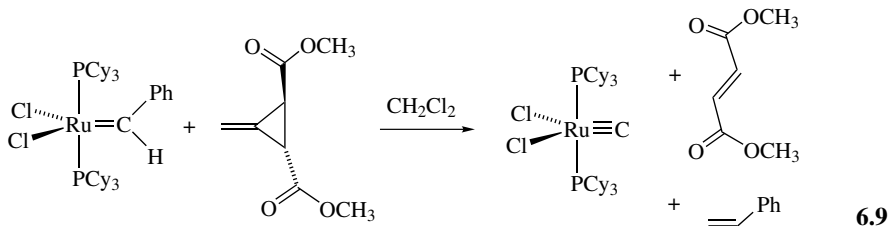
Figure 6-7

Carbide and
Alkyldiynes
Complexes

6-1-4 Carbide Complexes

The ultimate member of the series alkyl ($-CR_3$), carbene ($=CR_2$), and carbyne ($\equiv CR$) is the carbide¹⁸ ligand, C. Although it is tempting to represent this, by extension, as quadruply bonded $\equiv C$, this ligand, when attached to transition metals, is probably best considered $\equiv C^-$. The first transition metal carbide complex to be reported was the anion $[C\equiv Mo\{N(C(CD_3)_2Me)(3,5-Me_2(C_6H_3))\}_3]^-$, shown in Figure 6-7.¹⁹

Subsequent research eventually led to the preparation of neutral carbide complexes. The first of these to be reported was the trigonal bipyramidal ruthenium complex illustrated in Figure 6-7, prepared from a carbene complex via the following reaction:²⁰



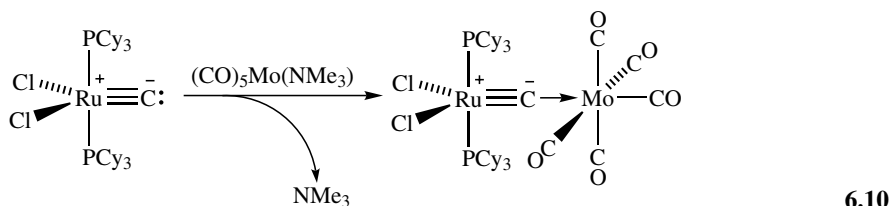
The metal–carbon bond distance in carbide complexes is generally quite similar to the comparable distances in alkyldiynes complexes. For example, the Ru–C distance in the ruthenium carbide complex in Figure 6-7, 165.0 pm, is nearly identical to that in $[RuCl_2(\equiv CCH_2Ph)(PR_3)]^+$ (R = isopropyl), 166.0 pm, also shown in Figure 6-7.

¹⁸Or carbido.

¹⁹J. C. Peters, A. L. Odom, and C. C. Cummins, *J. Chem. Soc., Chem. Commun.*, **1997**, 1995.

²⁰R. G. Carlson, M. A. Gile, J. A. Heppert, M. H. Mason, D. R. Powell, D. Vander Velde, and J. M. Vilain, *J. Am. Chem. Soc.*, **2002**, *124*, 1580.

Carbide complexes themselves can act as σ donors, with this function carried through the carbon atom. In such circumstances the carbido carbon functions as a two-electron donor, for example:²¹



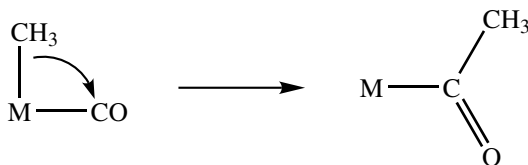
One of the interesting characteristics of carbide complexes that can be useful in their characterization is their very large downfield ¹³C chemical shift, typically near 500 ppm.

Theoretical calculations on transition metal carbide complexes suggest that, as expected, both *s* and *p* components exist in the metal–C bonds and the π bonding component of the bonds is stronger than the σ bonding component.²²

6-1-5 Other Organic Ligands

The list of ligands capable of bonding to metals through carbon is still in complete. Examples of several other important ligands not yet considered are given in Table 6-3.

Acyl complexes can be formed from migration of alkyl groups to CO ligands, as in the following example.



The formation of acyl complexes is an important step in carbonyl insertion reactions,²³ as described in Chapter 8 (Section 8-1-1).

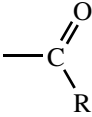
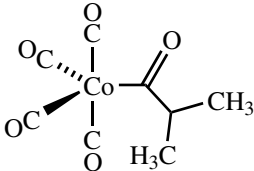
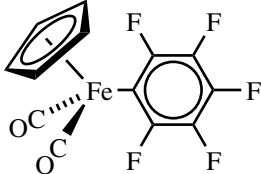
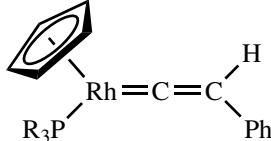
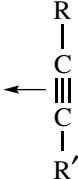
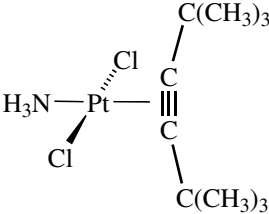
Trifluoromethyl, –CF₃, and other perfluoroalkyl and perfluoroaryl complexes are, in general, much more thermally stable than their alkyl and aryl counterparts.

²¹A. Hejl, T. M. Trnka, M. W. Day, and R. H. Grubbs, *J. Chem. Soc., Chem. Commun.*, **2002**, 2524.

²²A. Krapp, K. K. Pandey, and G. Frenking, *J. Am. Chem. Soc.*, **2007**, 129, 7596.

²³As we will see, this name for this reaction is misleading!

Table 6-3 Other Organic Ligands

Ligand	Formula	Example
Acyl		
Perfluoroalkyl, perfluoroaryl	$-\text{CF}_3$ $-\text{C}_6\text{F}_5$	
Vinylidene	$=\text{C}=\text{CH}_2$	
Alkyne		

For example, $\text{CF}_3\text{Co}(\text{CO})_4$ can be distilled without decomposing at its boiling point, 91°C , while $\text{CH}_3\text{Co}(\text{CO})_4$ decomposes even at temperatures as low as -30°C . The reasons for this enhanced stability in the perfluoro complexes are complex, but a major factor is clearly the greater bond dissociation energy of the M–ligand bond in the fluorine-containing ligands. In the perfluoroalkyl complexes, the highly electronegative fluorines cause the ligands to pull electrons away from the metal, inducing significant polarity into the M–C bond, a polarity that increases the bond strength. In the perfluoroaryl complexes, low-lying π^* orbitals on the ligands are available to participate in back-bonding with the metal, likewise strengthening the M–C bond.

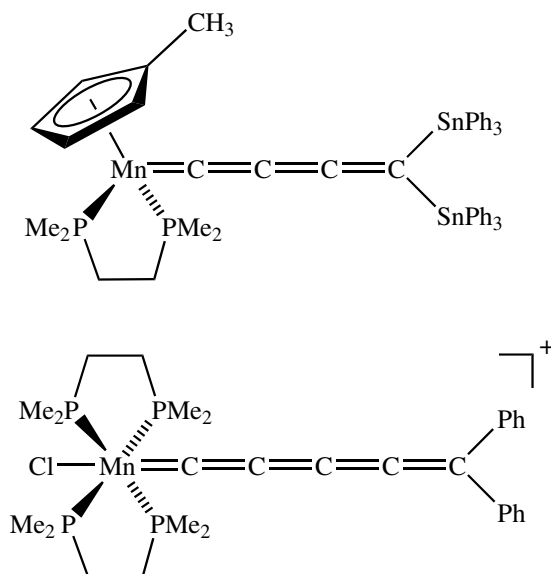


Figure 6-8
Metallacumulene
Complexes

Vinylidene complexes are examples of carbene complexes having cumulated (consecutive) double bonds. Ligands with longer cumulated double bonds are called cumulenylidene ligands, and their complexes are called metallacumulenes. These ligands, with their long rod-like carbon chains, have been of considerable interest in recent years, partly because of possible applications as molecular wires and nonlinear optical materials in nano-devices.^{24,25} Metallacumulene complexes of general formula $L_nM(=C)_mCR_2$ are well known for $m = 1$ (vinylidenes) and $m = 2$ (allenyldenens), but longer chains, especially for $m = 3$, have been more challenging. Examples having four and five carbon atoms in the chain have, however, been prepared. Selected examples of metallacumulene complexes are shown in Figure 6-8.

Many complexes containing alkyne ligands are known. Most commonly, these ligands act as two-electron donors, with a π orbital donating an electron pair in a manner analogous to a sidebound alkene. Bridging alkynes may be considered to donate an electron pair to each of two metals (one pair from each of the alkyne's two occupied π orbitals), acting as a two-electron donor to each. Alkyne complexes have been the subject of immense interest in the study of alkyne methathesis reactions, to be discussed in Chapter 11.²⁶

²⁴M. I. Bruce, *Coord. Chem. Rev.*, **2004**, 248, 1603.

²⁵K. Venkatesan, O. Blacque, and H. Berke, *Organometallics*, **2006**, 25, 5190.

²⁶A. Fürstner and P. W. Davies, *Chem. Commun.*, **2005**, 2307.

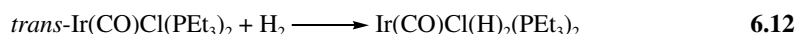
6-2 HYDRIDE AND DIHYDROGEN COMPLEXES^{27,28}

The simplest of all possible ligands is the hydrogen atom, H; similarly, the simplest possible diatomic ligand is the dihydrogen molecule, H₂. It is perhaps not surprising that these ligands have gained attention, by virtue of their apparent simplicity, as models for bonding schemes in coordination compounds. Moreover, both ligands have played immense roles in the development of applications of organometallic chemistry to organic synthesis, especially catalytic processes. Although the hydrogen atom (ordinarily designated the *hydride* ligand) has been recognized as an important ligand for many years, the significance of the *dihydrogen* ligand has become recognized relatively recently, and its chemistry is now developing rapidly.

6-2-1 Hydride Complexes

Although hydrogen atoms form bonds with nearly every element in the periodic table, we will specifically consider coordination compounds containing H atoms bonded to transition metals. Because the hydrogen atom has only a 1s orbital of suitable energy for bonding, the bond between H and a transition metal must, by necessity, be a σ interaction, involving metal *s*, *p*, and/or *d* orbitals (or a hybrid orbital). As a ligand, H may be considered a two-electron donor as hydride (:H⁻, method A) or a one-electron neutral donor (H atom, method B).

Although some homoleptic transition metal complexes of the hydride ligand are known—an example that is structurally interesting is the nine-coordinate [ReH₉]²⁻ ion²⁹—we are principally interested in complexes containing H in combination with other ligands. Such complexes may be made in a variety of ways, as discussed in succeeding chapters. Probably the most common synthesis is by reaction of a transition metal complex with H₂. The following are examples.



The hydride ligand can often be readily recognized by ¹H NMR because the H experiences strong shielding. Typical chemical shifts of hydrides are between ca. -2 and -12 ppm for terminal hydrides, with bridging hydrides absorbing at a still higher field.

²⁷G. J. Kubas, *Comments Inorg. Chem.*, **1988**, 7, 17; R. H. Crabtree, *Acc. Chem. Res.*, **1990**, 23, 95; G. J. Kubas, *Acc. Chem. Res.*, **1988**, 21, 120.

²⁸J. K. Burdett, O. Eisenstein, and S. A. Jackson, "Transition Metal Dihydrogen Complexes: Theoretical Studies," In *Transition Metal Hydrides*, A. Dedieu, Ed., VCH Publishers: New York, 1992.

²⁹S. C. Abrahams, A. P. Ginsberg, and K. Knox, *Inorg. Chem.*, **1964**, 3, 558.

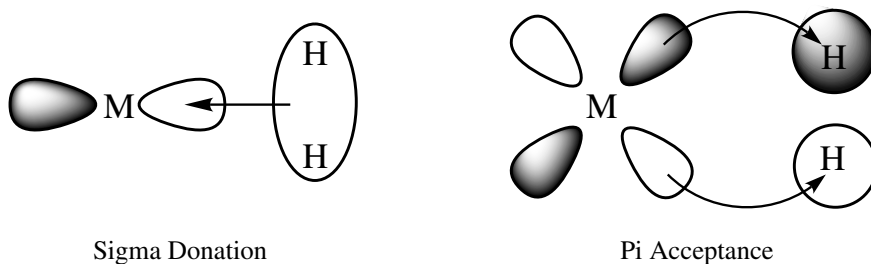


Figure 6-9
Bonding in
Dihydrogen
Complexes

One of the most interesting aspects of transition metal hydride chemistry is the relationship between this ligand and the rapidly developing chemistry of the dihydrogen ligand, H_2 .

6-2-2 Dihydrogen Complexes

Although complexes containing H_2 molecules coordinated to transition metals had been proposed for many years and many complexes containing hydride ligands had been prepared, the first structural characterization of a dihydrogen complex did not occur until 1984, when Kubas and co-workers synthesized the complexes $M(CO)_3(PR_3)_2(H_2)$ ($M = Mo, W$; $R = \text{cyclohexyl, isopropyl}$).³⁰ Subsequently, many H_2 complexes have been identified, and the chemistry of this ligand has developed rapidly.

The bonding between dihydrogen and a transition metal can be described as shown in Figure 6-9. The σ electrons in H_2 can be donated to a suitable empty orbital on the metal (such as a d orbital or a hybrid orbital), whereas the empty σ^* orbital of the ligand can accept electron density from occupied d orbitals of the metal. The result is an overall weakening and lengthening of the H–H bond in comparison with free H_2 . Typical H–H distances in complexes containing coordinated dihydrogen are in the range 82–90 pm, in comparison with 74.14 pm in free H_2 .

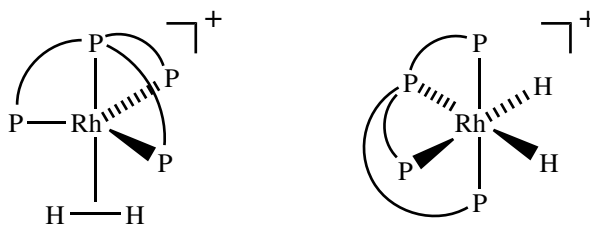
This bonding scheme leads to interesting ramifications that are distinctive from other donor–acceptor ligands such as CO and cyclic π systems that are held together by multiple bonds. If the metal is electron rich and donates strongly to the σ^* of H_2 , the H–H bond can rupture, giving separate H atoms as hydride ligands. Consequently, the search for stable H_2 complexes has focused on metals likely to be relatively poor donors, such as those in high oxidation states or those surrounded by ligands that function as strong electron acceptors. In particular, good π acceptors such as CO and NO can be effective at stabilizing the dihydrogen ligand.

³⁰G. J. Kubas, R. R. Ryan, B. I. Swanson, P. J. Vergamini, and H. J. Wasserman, *J. Am. Chem. Soc.*, **1984**, *106*, 451.

Exercise 6-3

Explain why $\text{Mo}(\text{PMe}_3)_5\text{H}_2$ is a dihydride (contains two separate H ligands), whereas $\text{Mo}(\text{CO})_3(\text{PR}_3)_2(\text{H}_2)$ contains the dihydrogen ligand (R = isopropyl).

The dividing line between whether an $\text{M}(\text{H})_2$ or $\text{M}(\text{H}_2)$ structure will be favored is a narrow one, and subtle differences in environment can be important. For example, in $\{\text{Rh}[\text{P}(\text{CH}_2\text{CH}_2\text{PPh}_2)_3](\text{H}_2)\}^+$, two isomers are found, as illustrated below. If hydrogen occupies an apex of the trigonal bipyramidal isomer, it is present as H_2 ; if hydrogen occupies *cis* positions of the octahedral isomer, it is present as separate H atoms.³¹ Calculations have demonstrated that there is less donation from the metal to the ligand at the apical site of the trigonal bipyramid than in the *cis* positions of the octahedral isomer.³²



Dihydrogen complexes have frequently been suggested as possible intermediates in a variety of reactions of hydrogen at metal centers. Some of these reactions are steps in catalytic processes of significant commercial interest.

6-2-3 Agostic Hydrogens

In some cases hydrogen atoms may form “bent” linkages between carbon atoms on ligands and metal atoms; such interactions have come to be described as *agostic*. Examples are illustrated in Figure 6-10.³³ In the first structure, the Ti–C–C angle in the ethyl ligand is over 20° less than the regular tetrahedral angle for sp^3 hybridized carbon. This has been interpreted as the consequence of a β hydrogen approaching the metal closely, forming a bridge between the β carbon and the metal.

Some such interactions have been substantiated by neutron diffraction; many others have been proposed, especially in reaction intermediates. The second

³¹C. Bianchini, C. Mealli, M. Peruzzini, and F. Zanobini, *J. Am. Chem. Soc.*, **1987**, *109*, 5548.

³²F. Maseras, M. Duran, A. Lledos, and J. Bertran, *Inorg. Chem.*, **1989**, *28*, 2984.

³³F. A. Cotton, *Inorg. Chem.*, **2002**, *41*, 643 and M. Brookhart, M. L. H. Green, and G. Parkin, *Proc. Nat. Acad. Sci.*, **2007**, *104*, 6908, and references cited therein.

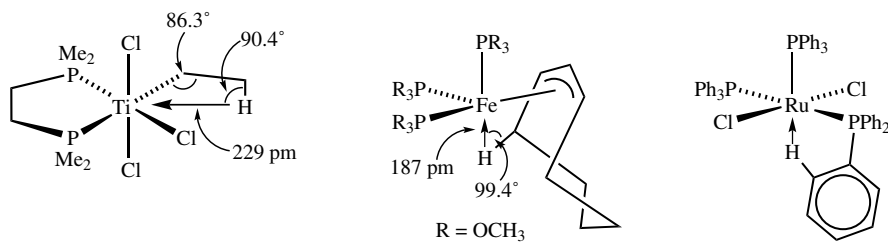


Figure 6-10
Examples of Agostic Interactions



Figure 6-11
Bonding between Phosphines and Transition Metals (traditional view)

molecule in Figure 6-10 shows the first agostic interaction to be supported in this way.³⁴ Because the hydrogen involved in an agostic interaction with a metal is, in effect, acting as a donor to form a weak bond with the metal, the C–H bond becomes elongated and the bond is weakened. The result is a tendency to “activate” the C–H bond as a step toward further reaction. Several examples of these types of interactions are discussed in later chapters.

6-3 PHOSPHINES AND RELATED LIGANDS

Among the most important of all ligands are the phosphines, PR_3 .³⁵ Together with other phosphorus-containing ligands and related compounds of arsenic and antimony, phosphines parallel the CO ligand in many ways. Like CO, phosphines are σ donors (via a hybrid orbital containing a lone pair on phosphorus) and π acceptors. For many years it was thought that empty $3d$ orbitals of phosphorus functioned as the acceptor orbitals, as shown in Figure 6-11. By this view, as the R groups attached to phosphorus become more electronegative, they withdraw electrons from phosphorus, making the phosphorus more positive and better able to accept electrons from the metal via a d orbital. The nature of the R groups, therefore, determines the relative donor/acceptor ability of the ligand. $\text{P}(\text{CH}_3)_3$, for example, is a strong σ donor by virtue of the electron-releasing

³⁴R. K. Brown, J. M. Williams, A. J. Schultz, G. D. Stucky, S. D. Ittel, and R. L. Harlow, *J. Am. Chem. Soc.*, **1980**, *102*, 981.

³⁵The IUPAC recommends that these compounds be called phosphanes, but the name phosphine is well established and commonly used.

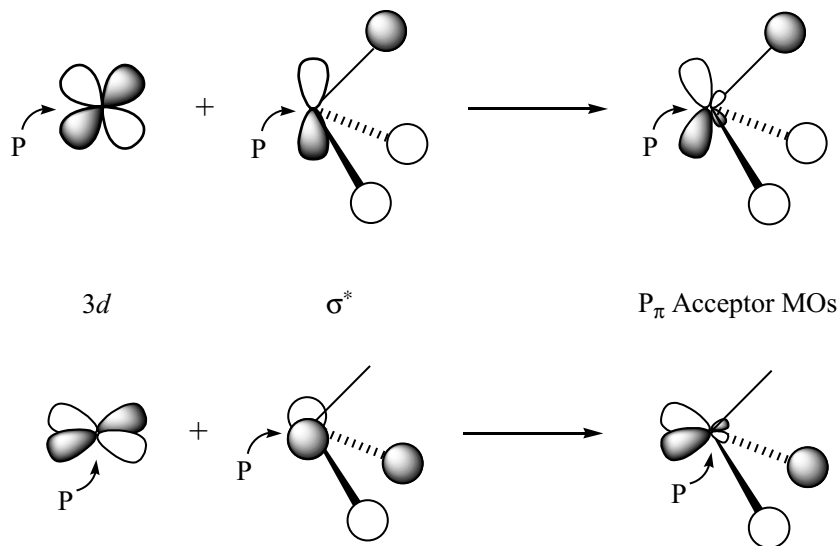


Figure 6-12
Pi Acceptor Orbitals
of Phosphines
(revised view)

nature of the methyl groups; at the same time, it is a relatively weak π acceptor. PF_3 , on the other hand, is a strong π acceptor (and weak σ donor) and rivals CO in the overall strength of its interaction with metal d orbitals. Not surprisingly, complexes containing PF_3 tend to obey the 18-electron rule. By changing the R groups, one can therefore “fine tune” the phosphine to be a donor/acceptor of a desired strength.

In 1985, a revised view of the bonding in phosphines was proposed.³⁶ According to this proposal, the important acceptor orbital of the phosphine is not a pure $3d$ orbital, but rather a combination of a $3d$ orbital with a σ^* orbital involved in the P–R bonding, as shown in Figure 6-12. This orbital has two acceptor lobes, similar to those of a $3d$ orbital, but is antibonding with respect to the P–R bond. To test this scheme, crystal structures of a variety of phosphine complexes in different oxidation states were compared. In most of these cases, as the charge on the metal became more negative, the P–R distance increased—as

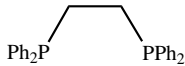
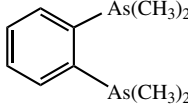
Exercise 6-4

The M–P distance in $(\eta^5\text{-C}_5\text{H}_5)\text{Co}(\text{PEt}_3)_2$ is 221.8 pm and the P–C distance is 184.6 pm. The corresponding distances in $[(\eta^5\text{-C}_5\text{H}_5)\text{Co}(\text{PEt}_3)_2]^+$ are 223.0 pm and 182.9 pm.³⁷ Account for the changes in these distances as the former complex is oxidized.

³⁶A. G. Orpen and N. G. Connelly, *J. Chem. Soc., Chem. Commun.*, **1985**, 1310.

³⁷R. L. Harlow, R. J. McKinney, and J. F. Whitney, *Organometallics*, **1983**, 2, 1839.

Table 6-4 Selected Ligands of Phosphorus, Arsenic, and Antimony

Name	Formula
Phosphine	PR_3
Phosphite	P(OR)_3
dppe ^a (diphenylphosphinoethane)	
diars	
Arsine	AsR_3
Stibine	SbR_3

^aThere are many similar ligands with four-letter acronyms to summarize their structures. For example: **dmpe** = dimethylphosphinoethane; **depp** = diethylphosphinopropane.

would be expected if additional electron density were pushed into an orbital having P–R antibonding character.

Similar interactions occur in other phosphorus-containing ligands and related ligands containing arsenic and antimony. Names and formulas of some of these ligands are given in Table 6-4.

Steric Considerations

An additional factor important in phosphine chemistry is the amount of space occupied by the R group. This factor is important in a variety of contexts; for example, the rate at which phosphine dissociates from a metal is related to the amount of space occupied by the phosphine and the resultant crowding around the metal. To describe the steric effects of phosphines and other ligands, Tolman has defined the **cone angle** as the apex angle θ of a cone that encompasses the van der Waals radii of the outermost atoms of a ligand, as shown in Figure 6-13.³⁸ If the R group has substituents, these are folded back away from the metal. Values of cone angles of selected ligands are given in Table 6-5.³⁹

³⁸C. A. Tolman, *J. Am. Chem. Soc.* **1970**, 92, 2953; *Chem. Rev.* **1977**, 77, 313.

³⁹Values of cone angles have been revised on the basis of analysis of crystal structure information in the Cambridge Structural Database. For a review of these results and other

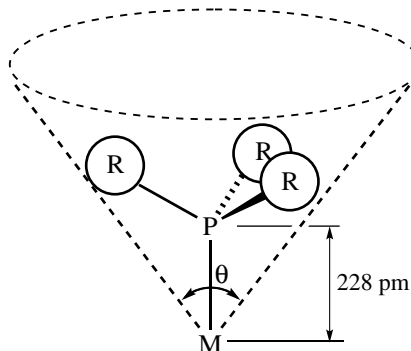
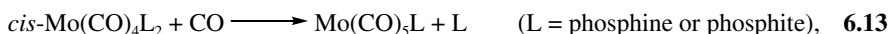


Figure 6-13
Ligand Cone Angle

Table 6-5 Ligand Cone Angles

Ligand	θ	Ligand	θ
PH_3	87°	$\text{P}(\text{CH}_3)(\text{C}_6\text{H}_5)_2$	136°
PF_3	104°	$\text{P}(\text{CF}_3)_3$	137°
$\text{P}(\text{OCH}_3)_3$	107°	$\text{P}(\text{O}-o\text{-C}_6\text{H}_4\text{CH}_3)_3$	141
$\text{P}(\text{OC}_2\text{H}_5)_3$	109°	$\text{P}(\text{C}_6\text{H}_5)_3$	145°
$\text{P}(\text{CH}_3)_3$	118°	$\text{P}(\text{cyclo-C}_6\text{H}_{11})_3$	170°
PCl_3	124°	$\text{P}(t\text{-C}_4\text{H}_9)_3$	182°
$\text{P}(\text{CH}_3)_2(\text{C}_6\text{H}_5)$	127°	$\text{P}(\text{C}_6\text{F}_5)_3$	184°
PBr_3	131°	$\text{P}(o\text{-C}_6\text{H}_4\text{CH}_3)_3$	194°
$\text{P}(\text{C}_2\text{H}_5)_3$	132°	$\text{P}(\text{mesityl})_3$	212°

As might be expected, the presence of bulky ligands can lead to more rapid ligand dissociation as a consequence of crowding around the metal. For example, the rate of the reaction



which is first order in $\text{cis-Mo}(\text{CO})_4\text{L}_2$, increases with increasing ligand bulk, as shown by the cone angles in Table 6-6.⁴⁰

Numerous other examples of the effect of ligand bulk on the dissociation of ligands have been reported in the chemical literature.⁴¹ We will see additional

considerations related to the steric effects of ligands on rates of substitution reactions, see K. A. Bunten, L. Chen, A. L. Fernandez, and A. J. Poë, *Coord. Chem. Rev.*, **2002**, 233–234, 41 and C. H. Suresh, *Inorg. Chem.*, **2006**, 45, 4982.

⁴⁰D. J. Darensbourg and A.H. Graves, *Inorg. Chem.*, **1979**, 18, 1257.

⁴¹For example, M. J. Wovkulich and J. D. Atwood, *Organometallics*, **1982**, 1, 1316 and J. D. Atwood, M. J. Wovkulich, and D. C. Sonnenberger, *Acc. Chem. Res.*, **1983**, 16, 350.

Table 6-6 Rates of Reaction of *cis*-Mo(CO)₄L₂^a

Ligand	Rate constant ($\times 10^{-5} \text{s}^{-1}$)	Cone angle
P(OPh) ₃	< 1.0	128°
PMePh ₂	1.3	136°
P(O- <i>o</i> -tolyl) ₃	16	141°
PPh ₃	320	145°
PPh(cyclohexyl) ₂	6400	162°

^aReactions were performed at 70 °C in CO-saturated tetrachloroethylene.

examples of this effect as we examine reactions of organometallic complexes in later chapters.

Electronic Effects

In addition to considering the steric bulk of phosphines and related ligands, Tolman developed a system for describing the electronic effects of such ligands. He based this system on the strong absorption band of *A*₁ symmetry⁴² of complexes having the formula Ni(CO)₃(PRR'R''), where the identity of the R, R', and R'' groups had a strong influence on the position of this band.⁴³ Considering a series of 70 ligands, Tolman chose P(*t*-Bu)₃, the strongest donor ligand, as a reference. Because the carbonyl ligands in Ni(CO)₃[P(*t*-Bu)₃] consequently exhibited the strongest back-bonding, the *A*₁ absorption band of this complex occurred at the lowest energy, 2056.1 cm⁻¹. Tolman defined a parameter χ_i to represent the effect of individual substituents (R, R', R'') on this band:

$$\nu_{\text{CO}} = 2056.1 \text{ cm}^{-1} + \sum_{i=1}^3 \chi_i \text{ cm}^{-1}.$$

On the basis of spectra observed for complexes having particular ligands, a value of χ_i for each R substituent could then be determined. For example, the poorest donor ligand considered by Tolman was PF₃. The *A*₁ absorption band of Ni(CO)₃(PF₃) was at 2110.8 cm⁻¹. Using this value for ν_{CO} in the equation above,

$$2110.8 \text{ cm}^{-1} = 2056.1 \text{ cm}^{-1} + \sum_{i=1}^3 \chi_i \text{ cm}^{-1}$$

$$54.7 \text{ cm}^{-1} = \sum_{i=1}^3 \chi_i \text{ cm}^{-1} = 3 \times \chi_i \text{ (for F)} ; \chi_i = 18.2 \text{ cm}^{-1}.$$

⁴²This designates the totally symmetric vibration, in which all metal–ligand bonds stretch simultaneously.

⁴³C. A. Tolman, *J. Am. Chem. Soc.*, **1970**, 92, 2953.

Table 6-7 Substituent χ Factors for Phosphine and Related Ligands

Substituent	χ_i (cm ⁻¹)	Substituent	χ_i (cm ⁻¹)
- <i>t</i> -Bu	0.0	-OEt	6.8
-Cyclohexyl	0.1	-OMe	7.7
- <i>i</i> -Pr	1.0	-H	8.3
-Et	1.8	-OPh	9.7
-Me	2.6	-C ₆ F ₅	11.2
-Ph	4.3	-Cl	14.8
- <i>p</i> -C ₆ H ₄ F	5.0	-F	18.2
- <i>m</i> -C ₆ H ₄ F	6.0	-CF ₃	19.6

For phosphine ligands in which R, R', and R'' are not identical, the values of χ_i for the individual R groups are summed to give the total effect on the A₁ absorption band.

Because the effect of different ligands on the position of the absorption band of the nickel complex is inherently related to the donor strength of the phosphorus-containing ligand, a list of substituent groups R, R', and R'' also shows the relative electron donating and accepting nature of these groups. Strongly donating groups therefore have small values of χ_i (with the strongest donor, *t*-Bu, having $\chi_i = 0$), and strongly electron withdrawing groups such as halogen atoms have large values. Representative values of χ_i are provided in Table 6-7.

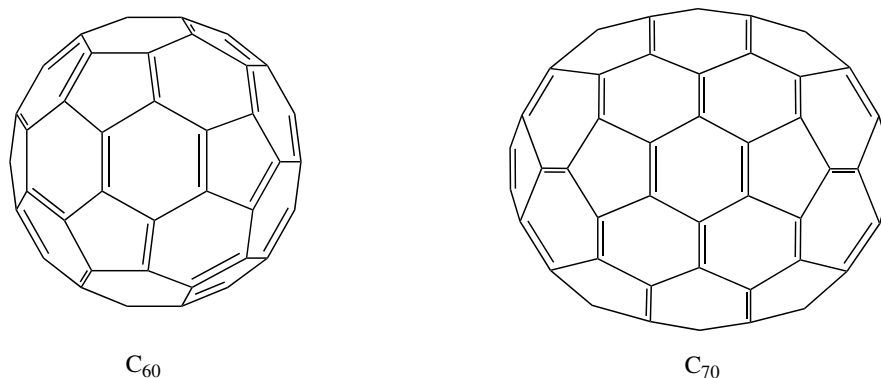
³¹P NMR

Like ¹H and ¹³C, the ³¹P nucleus has a spin of 1/2. It is also the only stable isotope of phosphorus. Furthermore, the ³¹P chemical shift is highly sensitive to chemical structure and its chemical shift range is broad. As a consequence of these features, ³¹P NMR spectroscopy has had broad applications in the study of complexes of phosphines and other phosphorus-containing ligands. A recent review provides a variety of examples, including spectral analyses, of applications of ³¹P and ¹³C NMR to transition metal complexes with phosphorus-containing ligands.⁴⁴

6-4 FULLERENE LIGANDS

One of the most fascinating developments in modern chemistry has been the synthesis of buckminsterfullerene, C₆₀, and the related fullerenes ("buckyballs") with their geodesic dome-like shapes. First reported as synthesized in the gas phase

⁴⁴P. S. Pregosin, *Coord. Chem. Rev.*, **2008**, 252, 2156.

**Figure 6-14** C_{60} and C_{70}

by Kroto, Smalley, and co-workers in 1985,⁴⁵ C_{60} , C_{70} , and a variety of related species were soon synthesized; structures of C_{60} and C_{70} are shown in Figure 6-14. Subsequent work has been extensive, and many attempts have been made to coordinate fullerenes to metals.

6-4-1 Structures of Fullerenes

The prototype fullerene, C_{60} , consists of fused 5- and 6-membered carbon rings. Each 6-membered ring is surrounded, alternately, by hexagons and pentagons of carbons; each pentagon is fused to five hexagons. The consequence of this structural motif is that each hexagon is like the base of a bowl; the three pentagons fused to this ring and linked by hexagons force the structure to curve (in contrast to graphite, in which each hexagon is fused to six surrounding hexagons in the same plane). This phenomenon, best seen by assembling a model, results in a dome-like structure that eventually curves around on itself to give a structure resembling a sphere, the same shape as a soccer ball (which has an identical arrangement of pentagons and hexagons on its surface).⁴⁶ All 60 atoms are equivalent and give rise to a single ^{13}C NMR resonance.

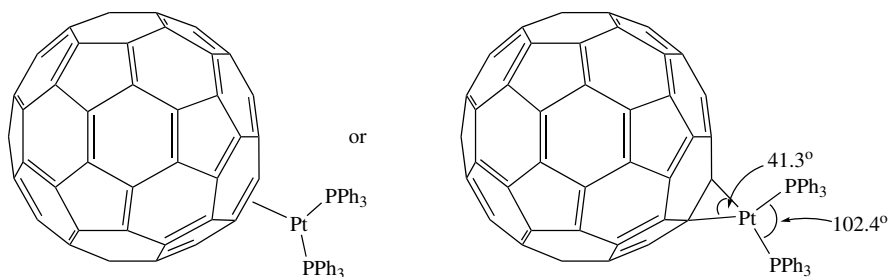
Although all atoms in C_{60} are equivalent, the bonds are not. Two types of bonds occur (best viewed using a model): at the fusion of two 6-membered rings and at the fusion of 5- and 6-membered rings. X-ray crystallographic studies on C_{60} complexes have indicated that the C–C bond length at the fusion of two 6-membered rings in these complexes is shorter, 135.5 pm, in comparison with the comparable distance at the fusion of 5- and 6-membered rings, 146.7 pm.⁴⁷

⁴⁵H. W. Kroto, J. R. Heath, S. C. O'Brien, R. F. Curl, and R. E. Smalley, *Nature (London)*, **1985**, 318, 162.

⁴⁶The structure of C_{60} has the same symmetry characteristics as an icosahedron.

⁴⁷S. Liu, Y. Lu, M. M. Kappes, and J. A. Ibers, *Science*, **1991**, 254, 408.

Figure 6-15
Fullerene Complex of Platinum



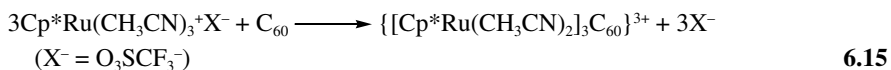
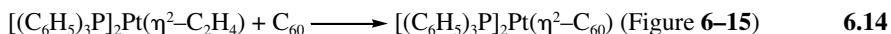
This is indicative of a greater degree of π bonding at the fusion of the 6-membered rings.

Surrounding each 6-membered ring with two pentagons (on opposite sides) and four hexagons (with each pentagon, as in C_{60} , fused to five hexagons) yields a slightly larger, somewhat prolate structure with 70 carbon atoms. C_{70} is often obtained as a byproduct of the synthesis of C_{60} and is among the most stable of the fullerenes. Unlike C_{60} , five different types of carbon are present in C_{70} , giving rise to five ^{13}C NMR resonances.⁴⁸

6-4-2 Fullerene–Metal Complexes⁴⁹

Although several types of compounds involving fullerenes and metals are known, we will focus on just one: complexes in which the fullerene itself behaves as a ligand. As a ligand, C_{60} appears to behave most commonly as an electron-deficient alkene (or arene) and to bond in a dihapto fashion. This type of bonding was observed in the first complex to be synthesized in which C_{60} acts as a ligand toward a metal, $[(\text{C}_6\text{H}_5)_3\text{P}]_2\text{Pt}(\eta^2\text{-C}_{60})$,⁵⁰ illustrated in Figure 6-15.

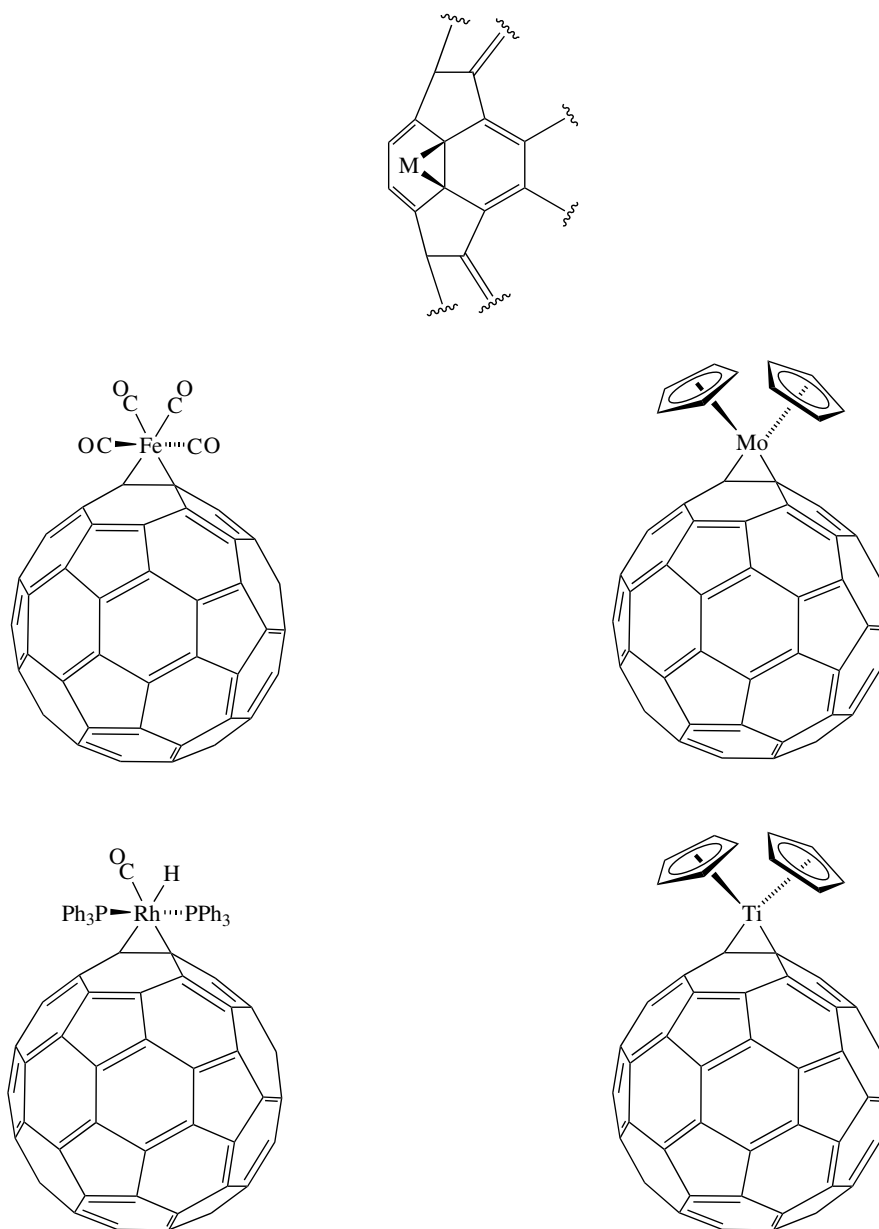
A common route to the synthesis of fullerene complexes is by displacement of other ligands, typically those weakly coordinated to metals. Examples of such ligands include ethylene (equation 6.14) and CH_3CN (equation 6.15).



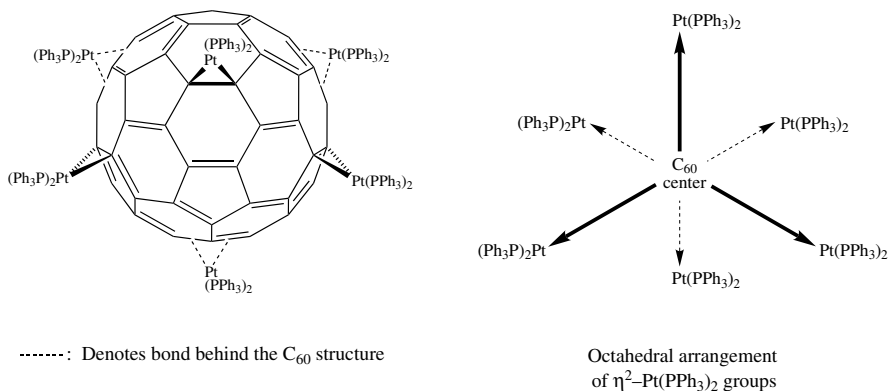
⁴⁸R. Taylor, J. P. Hare, A. K. Abdul-Sada, and H. W. Kroto, *J. Chem. Soc., Chem. Commun.*, **1990**, 1423.

⁴⁹For a recent review of fullerene complexes, see A. Hirsch and M. Brettreich, *Fullerenes*, Wiley-VCH: Weinheim, Germany, 2005, pp. 231–250.

⁵⁰P. J. Fagan, J. C. Calabrese, and B. Malone, *Science*, **1991**, 252, 1160.

**Figure 6-16**Bonding of C_{60} to Metal

The C_{60} ligand typically bonds to metals in a dihapto fashion, involving the carbon–carbon bond at the fusion of two 6-membered rings, as shown in Figure 6-16. Such a carbon–carbon bond is shorter, and thus has more π bonding character, than a bond at the fusion of 5- and 6-membered rings. Examples of complexes having this type of bonding mode are also shown in Figure 6-16.

**Figure 6-17**

$$[(\text{Et}_3\text{P})_2\text{Pt}]_6\text{C}_{60}$$

Bonding of a fullerene to a metal leads to distortion at the site of attachment (also shown in Figure 6-16). This is similar to what happens when alkenes bond to metals: the four groups attached to the C=C bond of the alkene bend back away from the metal as *d* electron density from the metal is donated into the π* orbital of the alkene. Similarly, the *d* electron density of the metal can donate to an empty antibonding orbital of a fullerene and cause distortion. The effect is to pull the two carbons involved slightly away from the C₆₀ surface. In addition, the distance between these carbons is elongated slightly as a consequence of this interaction. This increase in C–C bond distance is analogous to the elongation that occurs when ethylene and other alkenes bond to metals, as discussed in Chapter 5.

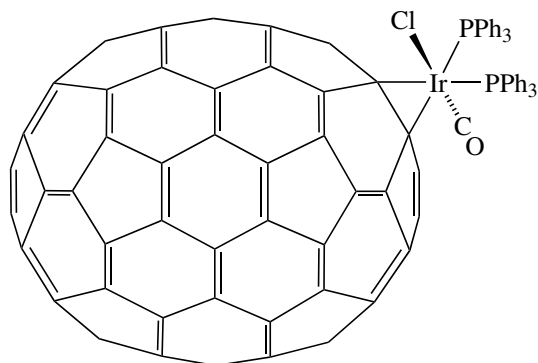
In some cases more than one metal can become attached to a fullerene surface. A spectacular example is $[(\text{Et}_3\text{P})_2\text{Pt}]_6\text{C}_{60}$, illustrated in Figure 6-17.⁵¹ In this structure, the six (Et₃P)₂Pt units are arranged octahedrally around the C₆₀. As usual, each platinum is bonded to two carbons at the juncture of two 6-membered rings; each of these pairs of carbons is pulled out slightly from the C₆₀ surface.

Although complexes of C₆₀ have been studied most extensively, some complexes of other fullerenes have also been prepared. An example is (η²-C₇₀)Ir(CO)Cl(PPh₃)₂, shown in Figure 6-18.⁵² As in the case of the known C₆₀ complexes, bonding to the metal occurs at the fusion of two 6-membered rings. The C₇₀ ligand is prolate, elongated along the axis pointing toward the metal.

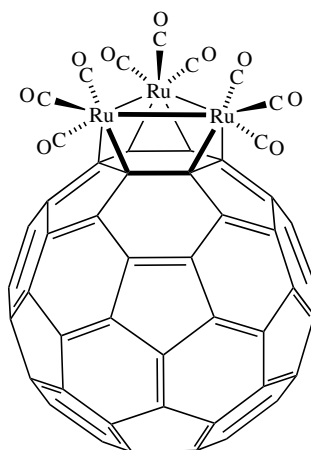
With its 5- and 6-membered rings, can C₆₀ ever act as a pentahapto or hexahapto ligand? When Ru₃(CO)₁₂ and C₆₀ are heated to reflux, the product shown in Figure 6-19 is formed, in which all three rutheniums are coordinated to a 6-membered ring of the fullerene. The C₆₀ cannot satisfactorily be labeled as

⁵¹P. J. Fagan, J. C. Calabrese, and B. Malone, *J. Am. Chem. Soc.*, **1991**, *113*, 9408.

⁵²A. L. Balch, V. J. Catalano, J. W. Lee, M. M. Olmstead, and S. R. Parkin, *J. Am. Chem. Soc.*, **1991**, *113*, 8953.

**Figure 6-18**

$(\eta^2\text{-C}_{70})\text{Ir}(\text{CO})$
 $\text{Cl}(\text{PPh}_3)_2$

**Figure 6-19**

$(\mu_3\text{-}\eta^2:\eta^2:\eta^2\text{-C}_{60})$
 $\text{Ru}_3(\text{CO})_9$

η^6 -, however, because the C–C distances in the ring are alternatively longer and shorter; the compound is better described as $(\mu_3\text{-}\eta^2:\eta^2:\eta^2\text{-C}_{60})\text{Ru}_3(\text{CO})_9$.⁵³

6-5 MASS SPECTRA

With the evolution of new types of mass spectrometers, coupled with steady advances in the technology associated with earlier techniques, mass spectrometry has become an increasingly useful tool for studying organometallic molecules. In some cases, relatively gentle ionization techniques generate spectra of intact molecular ions, in essence mass “fingerprints” of molecules. In other cases, ligands may readily dissociate, yielding spectra of molecular fragments, which may still provide useful information; carbonyl complexes are in this category.

⁵³H.-F. Hsu and J. R. Shapley, *J. Am. Chem. Soc.*, **1996**, *118*, 9192.

Table 6-8 Ionization Techniques in Mass Spectrometry

Type	Ionization process	Notes
Electron impact (EI)	Collision of electron beam with molecule, causing ejection of electrons	“Hard” technique tends to cause fragmentation; samples must be vaporized
Fast atom bombardment (FAB)	Collision of beam of neutral atoms with solid sample	Less fragmentation than EI; spectra may include peaks from solid matrix
Atmospheric pressure ionization (API)		Continuous spray of sample solution at atmospheric pressure
Electrospray ionization (ESI)	High voltage yields aerosol of electrically charged droplets	Very soft technique, little fragmentation; useful for molecules of very high mass
Atmospheric pressure chemical ionization (APCI)	Plasma created by corona discharge causes gas phase ion–molecule reactions	Soft technique, little fragmentation
Matrix-assisted laser desorption ionization (MALDI)	UV laser pulse applied to solid matrix containing sample	Soft technique, little fragmentation; used extensively for large biomolecules

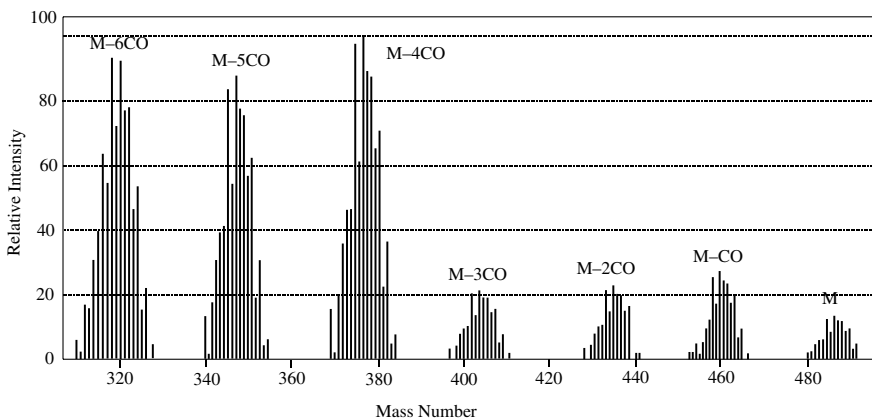
In still other cases, structures may rearrange and/or fragment rapidly, yielding spectra that may be a true challenge to interpret. Sometimes compounds are not sufficiently volatile, do not ionize readily or decompose rapidly, or have other problems that result in their showing no mass spectra at all.

Our purpose is not to focus on the methods of mass spectrometry but rather to provide illustrations of some of the types of situations that may occur when this technique is used to characterize organometallic compounds. A brief but useful description of some of the techniques used in the mass spectrometry of coordination compounds, including organometallic compounds, is available.⁵⁴ Because mass spectrometry relies on the interaction of ions rather than neutral molecules with magnetic fields, the selection of ionizing techniques is an important consideration. Some of the most common ionizing techniques are listed in Table 6-8.

6-5-1 Fragmentation

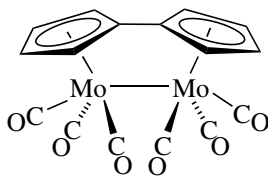
Many organometallic complexes are subject to fragmentation during mass spectrometry, especially if ionization occurs by a high-energy process such as electron impact. The most common type of fragmentation is the loss of one or more ligands.

⁵⁴E. A. V. Ebsworth, D. W. H. Rankin, and S. Craddock, *Structural Methods in Inorganic Chemistry*, CRC Press: Boca Raton, FL, 1991, pp. 378–391.

**Figure 6-20**

Mass Spectrum
of $(\eta^5:\eta^5\text{-C}_{10}\text{H}_8)$
 $\text{Mo}_2(\text{CO})_6$

For example, carbonyl complexes typically are subject to fragmentation to yield spectra showing consecutive loss of one or more carbonyls. This phenomenon is readily recognized in spectra that exhibit clusters of similar peaks differing by 28 mass units. An example, the electron impact spectrum of the fulvalene complex $(\eta^5:\eta^5\text{-C}_{10}\text{H}_8)\text{Mo}_2(\text{CO})_6$, is illustrated in Figure 6-20. The parent molecular ion, a cluster of peaks matching the isotope pattern of Mo_2 , is centered at a mass of 488 Da. Each loss of CO gives a decrease in mass of 28. In this example, clusters appear for the loss of all possible numbers of carbonyls; loss of all six CO ligands leaves a fragment with the mass of Mo_2 plus fulvalene. A very small peak of mass 128, matching that of fulvalene, also occurs in the spectrum.



6-5-2 Isotope Patterns

In the analysis of mass spectra of organometallic compounds, advantage can often be taken of the characteristic isotope patterns of many metals. For example, the clusters in Figure 6-20 are similar to the isotope pattern of Mo_2 , which is distinctively different from the pattern for Mo, as illustrated in Figure 6-21.

Isotopic distributions of the elements are available in many sources. These have been published by the IUPAC, and updated values are published periodically and available online.⁵⁵ In addition, modern mass spectrometers typically are

⁵⁵IUPAC, *Quantities, Units, and Symbols in Physical Chemistry*, I. Mills, Blackwell: Oxford, 1988, pp. 90–98 and M. E. Wieser, *Pure Appl. Chem.*, **2006**, 78, 2051, and references cited

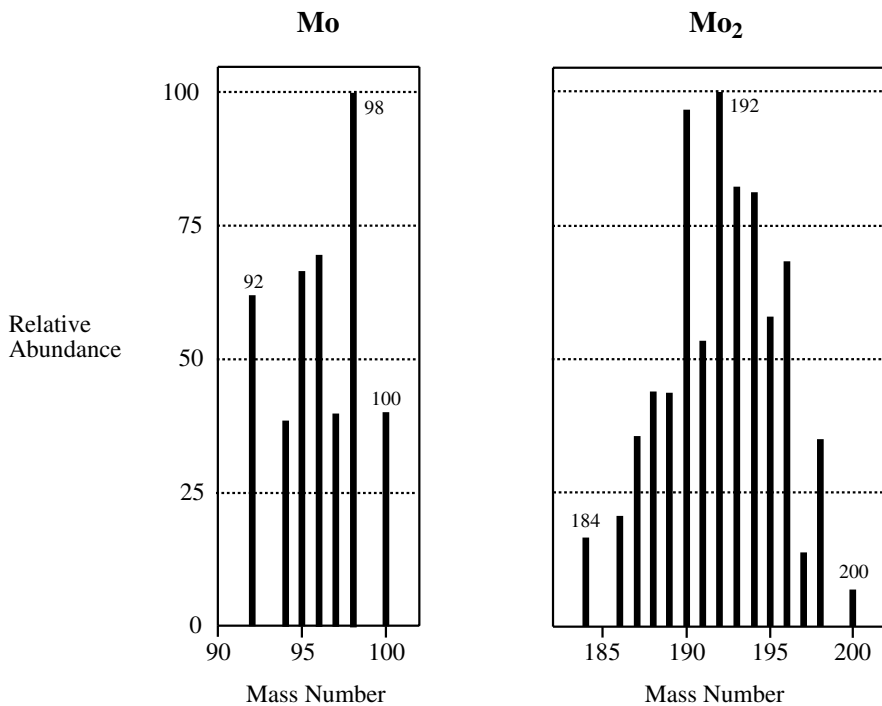


Figure 6-21
Isotope Patterns of
Mo and Mo₂

equipped with software to calculate simulated spectra based on distributions of isotopes. Mass spectra simulators are also available online.⁵⁶

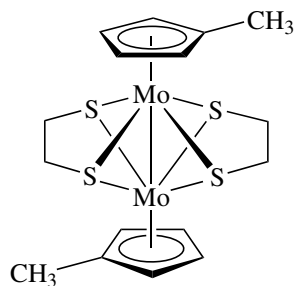
Many other ligands, especially those weakly bound and subject to dissociation, can be lost during mass spectrometry; examples include phosphines, N₂, H₂, and η^2 -C₂H₄. Cyclic π systems may also be lost, but often to a lesser extent; for example, the fulvalene ligand in Figure 6-20 remains attached to the metals, whereas the CO ligands are lost. In complexes containing both η^5 -Cp and CO ligands, the cyclopentadienyl ligands typically show a much stronger tendency to remain attached to transition metals than CO ligands.

Sometimes ligands themselves may fragment. For example, the electron impact spectrum of the dithiolate-bridged compound illustrated on the next page exhibits only a trace of a parent molecular ion cluster centered at m/z 534, but has an intense cluster at 478 corresponding to loss of ethylenes (mass of 28 each)

therein. Isotopic compositions of the elements and relative atomic masses of the isotopes can be found at http://physics.nist.gov/cgi-bin/Compositions/stand_alone.pl?ele=&ascii=html&isotope=some.

⁵⁶For example, <http://www2.sisweb.com/mstools/isotope.htm>.

from the dithiolate bridges. There are no peaks corresponding to loss of the methylcyclopentadienyl ligands.



6-5-3 Observing Molecular Ions

Comparatively “soft” ionization techniques such as electrospray and atmospheric pressure chemical ionization (APCI) may yield parent molecular ions with little or no fragmentation when other techniques fail. Clearly, such a technique is the method of choice to determine the molecular mass in many situations. An example of an APCI spectrum of a compound, $[\text{Cp}(\text{tfd})\text{W}(\mu\text{-S})_2\text{W}(=\text{O})\text{Cp}]$, shown below, that does not give a useful electron impact spectrum is shown in Figure 6-22.

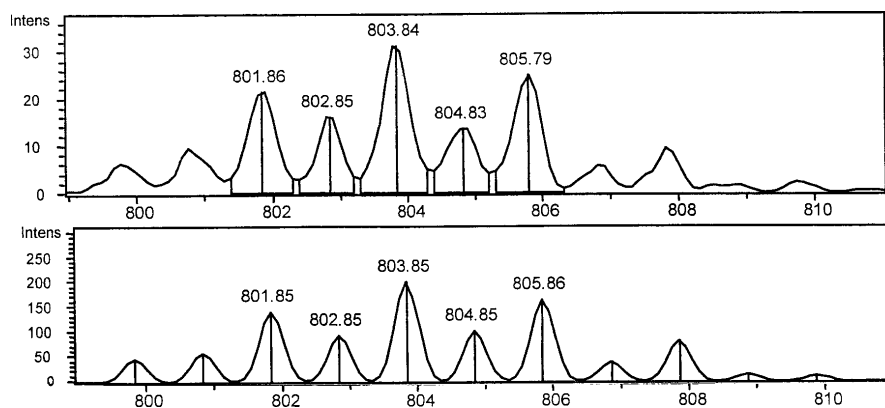
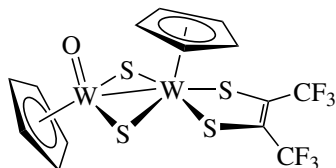


Figure 6-22

APCI Spectrum of $[\text{Cp}(\text{tfd})\text{W}(\mu\text{-S})_2\text{W}(=\text{O})\text{Cp}]$ (Upper: Actual spectrum; lower: Calculated spectrum based on molecular formula and isotope distributions.)

Suggested Reading

Carbene (Alkylidene) Complexes

K. H. Dötz, H. Fischer, P. Hoffman, F. R. Kreissl, D. Schubert, and K. Weiss, *Transition Metal Carbene Complexes*, Verlag Chemie: Weinheim, Germany, 1983.

Carbyne (Alkylidyne) Complexes

H. P. Kim and R. J. Angelici, "Transition Metal Complexes with Terminal Carbyne Ligands," *Adv. Organomet. Chem.*, **1987**, 27, 51.

H. Fischer, P. Hoffman, F. R. Kreissl, R. R. Schrock, U. Schubert, and K. Weiss, *Carbyne Complexes*, VCH: Weinheim, Germany, 1988.

Metallacycles

B. Blom, H. Clayton, M. Kilkenny, and J. R. Moss, "Metallacycloalkanes," *Adv. Organomet. Chem.*, **2006**, 54, 149.

Metallacumulenes and Other Molecules Containing C_n Chains

M. I. Bruce and P. J. Low, "Transition Metal Complexes Containing All-Carbon Ligands," *Adv. Organomet. Chem.*, **2004**, 50, 179.

Dihydrogen Complexes

G. J. Kubas, *Proc. Natl. Acad. Sci. USA*, **2007**, 104, 6901.

Agostic Interactions

M. Brookhart, M. L. H. Green, and G. Parkin, *Proc. Natl. Acad. Sci. USA*, **2007**, 104, 6908.

W. Scherer, G. S. McGrady, *Angew. Chem., Int. Ed.*, **2004**, 43, 1782.

Phosphines and Cone Angles

K. A. Bunten, L. Chen, A. L. Fernandez, and A. J. Poë, *Coord. Chem. Rev.*, **2002**, 233–234, 41.

³¹P NMR

P. S. Pregosin, *Coord. Chem. Rev.*, **2008**, 252, 2156.

Fullerenes and Fullerene Complexes

A. Hirsch and M. Brettreich, *Fullerenes*, Wiley–VCH: Weinheim, Germany, 2005.

Mass Spectrometry

E. Rosenberg, *J. Chromatogr. A*, **2003**, 1000, 841.

E. A. V. Ebsworth, D. W. H. Rankin, and S. Cradock, *Structural Methods in Inorganic Chemistry*, CRC Press: Boca Raton, FL, 1991, pp. 378–391.

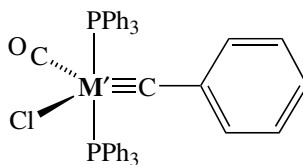
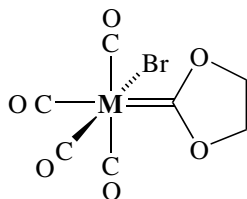
Problems

6-1 Identify the first-row transition metal.

- $\text{H}_3\text{CM}(\text{CO})_5$
- $\text{M}(\text{CO})(\text{CS})(\text{PF}_3)(\text{PPh}_3)\text{Br}$
- $(\text{CO})_5\text{M}=\text{C}(\text{OCH}_3)\text{C}_6\text{H}_5$
- $(\eta^5\text{-C}_5\text{H}_5)(\text{CO})_2\text{M}=\text{C}=\text{C}(\text{CMe}_3)_2$
- $\text{M}(\text{CO})_5(\text{COCH}_3)$

6-2 Identify:

- The third-row transition metal **M**:
- The second-row transition metal **M'**:

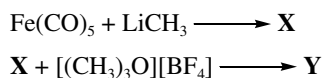


6-3 Predict the transition metal-containing products of the following reactions.

- $[(\eta^5\text{-C}_5\text{H}_5)\text{W}(\text{CO})_3]^- + \text{C}_2\text{H}_5\text{I} \longrightarrow$
- $\text{Mn}_2(\text{CO})_{10} + \text{H}_2 \longrightarrow$
- $\text{Mo}(\text{CO})_6 + \text{PPh}_3 \longrightarrow$
- $\text{TaF}_5 + 5 \text{LiCH}_3 \longrightarrow \text{A}; \quad \text{A} + \text{LiCH}_3 \longrightarrow \text{B}^{57}$
- $\text{cis-Mo}(\text{CO})_4(\text{PPh}_3)_2 + \text{CO} \longrightarrow \quad +$

Would you predict that this reaction would be faster or slower if $\text{cis-Mo}(\text{CO})_4(\text{PMe}_2\text{Ph})_2$ were used instead of $\text{cis-Mo}(\text{CO})_4(\text{PPh}_3)_2$? Explain.

- Which complex would you predict to have the longer Fe–P bonds, $(\eta^4\text{-C}_4\text{Ph}_4)\text{Fe}(\text{CO})(\text{PR}_3)_2$ or $[(\eta^4\text{-C}_4\text{Ph}_4)\text{Fe}(\text{CO})(\text{PR}_3)_2]^+$, where $\text{R} = \text{OCH}_3$? Explain.
- Diphenylphosphinoethane (Table 6-4) reacts with $\text{W}(\text{CO})_6$ to yield a product having four infrared bands near 2000 cm^{-1} . Provide a likely structure for this product.
- Give likely structures for **X** and **Y**.



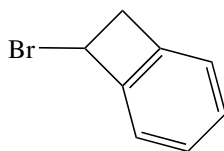
⁵⁷S. Kleinhenz, V. Pfennig, and K. Seppelt, *Chem. Eur. J.*, **1998**, *4*, 1687.

- 6-7** The complex $\text{Ir}(\text{CO})\text{Cl}(\text{PEt}_3)_2$ reacts with H_2 to give a product having two Ir–H stretching bands in the infrared and a single ^{31}P NMR resonance. Suggest a structure for this product.
- 6-8** $\text{NaMn}(\text{CO})_5$ reacts with $\text{H}_2\text{C}=\text{CHCH}_2\text{Cl}$ to give **A** + **B**. Compound **A** obeys the 18-electron rule and shows protons in three distinct magnetic environments. Water-soluble compound **B** reacts with aqueous AgNO_3 to form a white precipitate that turns gray on exposure to light. When heated, **A** gives off gas **C** and converts to **D**, which has protons in two distinct magnetic environments. Identify compounds **A** through **D**.
- 6-9** The complex $[(\eta^5\text{-C}_5\text{H}_5)\text{Mo}(\text{CO})_3]_2$ reacts with I_2 to give a product **A** having three infrared bands near 2000 cm^{-1} . This product reacts with triphenylphosphine to give **B**, which has two bands near 2000 cm^{-1} . Identify **A** and **B**.
- 6-10** Reaction of $[\eta^5\text{-C}_5(\text{CH}_3)_5]\text{Ru}(\text{PR}_3)\text{Br}$ with H_2 in toluene at 25°C yields a square pyramidal product with the $\eta^5\text{-C}_5(\text{CH}_3)_5$ ligand at the top of the pyramid. ^1H NMR shows two peaks near $\delta = -6$ ppm but no evidence of H–H coupling or other indication of a bond between hydrogens [$\text{PR}_3 = \text{P}(\text{isopropyl})_2(\text{C}_6\text{H}_5)$].
- Propose a reasonable structure for the product.
 - Suppose you wanted to prepare a dihydrogen complex using a similar reaction. What type of phosphine would you use in your reactant and why?
- 6-11** For complexes having the formula *trans*- $\text{Rh}(\text{CO})\text{ClL}_2$ (L = phosphine), arrange the following phosphines in order of decreasing energy of the carbonyl stretching band in the IR for their corresponding complexes: PPh_3 , $\text{P}(t\text{-C}_4\text{H}_9)_3$, $\text{P}(p\text{-C}_6\text{H}_4\text{F})_3$, $\text{P}(p\text{-C}_6\text{H}_4\text{Me})_3$, $\text{P}(\text{C}_6\text{F}_5)_3$.
- 6-12** Equilibrium constants for the reaction $\text{Co}(\text{CO})\text{Br}_2\text{L}_2 \rightleftharpoons \text{CoBr}_2\text{L}_2 + \text{CO}$ are given below. All values of K were measured at the same temperature.

L	K
PEt_3	1
PEt_2Ph	2.5
PEtPh_2	24.2

- Account for this trend in equilibrium constants.
- Of these three phosphines, which will give the cobalt complex with the lowest energy carbonyl stretch in the infrared spectrum? Explain briefly.

- 6-13** Tolman's cone angles for the phosphite ligands $\text{P}(\text{OMe})_3$, $\text{P}(\text{OEt})_3$, and $\text{P}(\text{O}^i\text{Pr})_3$ are, respectively, 107° , 109° , and 130° . However, examination of crystal structures of complexes containing these ligands in the Cambridge Structure Database gave average angles, in the same order, of 124° , 125° , and 137° .⁵⁸ Suggest why the Tolman angles may underestimate the steric requirements of these ligands.
- 6-14** The compound $[\eta^5\text{-C}_5\text{Me}_5]\text{Cr}(\text{CO})_2$ obeys the 18-electron rule. Exposure of this compound to ultraviolet light leads to the formation of **X**, which has the following characteristics.⁵⁹
- A single IR band at 1788 cm^{-1}
A single ^1H NMR resonance
- What is the bond order between the Cr atoms?
 - Propose a structure for **X**.
- 6-15** A Grignard reagent can be prepared from 1-bromobenzocyclobutene, shown below. When this Grignard reagent is allowed to react with $\text{Cp}_2\text{Zr}(\text{CH}_3)\text{Cl}$, the 16-electron complex **1** is formed. In the presence of $\text{P}(\text{CH}_3)_3$, **1** eliminates methane, forming 18-electron complex **2**. Proton NMR of **2** shows resonances at δ 5.09 (relative area 5), 5.02 (5), 0.82 (9), multiple peaks at 6.31–6.78 (4), 3.40 (1), and 2.64–2.68 (1). The resonances at 5.09 and 5.02 are doublets, with the splitting attributable to P–H coupling. Elemental analysis of **2** indicated 63.12% carbon and 6.31% hydrogen. Propose structures for **1** and **2**.⁶⁰



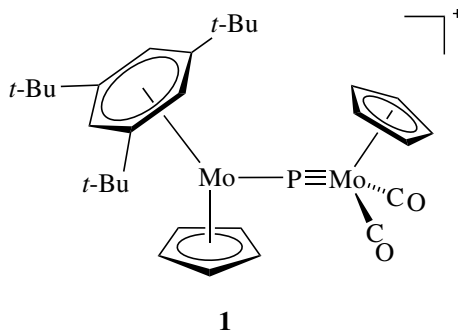
- 6-16** In a reaction that may have only one other example in the literature, the cation **1** reacts with the ion $\text{HB}(\text{sec-C}_4\text{H}_9)_3^-$ (a potential source of hydride) to form **2**, a red–orange compound. The following data are reported for **2**.⁶¹

⁵⁸J. M. Smith and N. J. Coville, *Organometallics*, **2001**, *20*, 1210.

⁵⁹I. G. Virrels, T. F. Nolan, M. W. George, and J. J. Turner, *Organometallics*, **1997**, *16*, 5879.

⁶⁰T. V. V. Ramakrishna, S. Lushnikova, and P. R. Sharp, *Organometallics*, **2002**, *21*, 5685–5687.

⁶¹I. Amor, D. García-Vivó, M. E. García, M. A. Ruiz, D. Sáez, H. Hamidov, and J. C. Jeffery, *Organometallics*, **2007**, *26*, 466.



IR: strong bands at 1920, 1857 cm^{-1} .

^1H NMR: chemical shift (relative area):

5.46 (2)

5.28 (5)

5.15 (3)

4.22 (2)

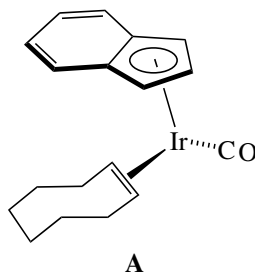
0.7–2.0 (2)

1.31 (27)

^{13}C NMR: resonance at 236.9 ppm,
seven additional peaks and clusters of
peaks between 32.4 and 115.7 ppm.

Propose (sketch) a structure for **2**.

- 6-17** Reaction of Ir complex **A** with C_{60} yielded a black solid residue **B** with the following spectral characteristics: mass spectrum: M^+ ($m/z = 1056$); ^1H NMR: δ 7.65 (multiplet, 2H), 7.48 (multiplet, 2H), 6.89 (triplet, 1H, $J = 2.7$ Hz), and 5.97 ppm (doublet, 2H, $J = 2.7$ Hz); IR: $\nu_{\text{CO}} = 1998 \text{ cm}^{-1}$.⁶²



⁶²R. S. Koefod, M. F. Hudgens, and J. R. Shapley, *J. Am. Chem. Soc.*, **1991**, *113*, 8957.

-
- a. Propose a structure for **B**.
 - b. The carbonyl stretching frequency of **A** was reported as 1954 cm^{-1} . How does the electron density at Ir change in going from **A** to **B**? Explain.
 - c. When **B** was treated with PPh_3 , a new complex **C** rapidly formed along with some C_{60} . What is the structure of **C**?
 - d. When **B** was treated with $\text{H}_2\text{C}=\text{CH}_2$, a new complex **D** formed along with C_{60} . This time, however, the rate of formation of **D** was much slower than that for **C**. What is the structure of **D**? Why does it form much more slowly than **C**?

Organometallic Reactions I

Reactions That Occur at the Metal

The diversity of the transition metals and also that of organic ligands indicates that the chemistry of organotransition metal complexes is indeed diverse, so much so that trying to understand the reactions of organotransition metal compounds would seem a daunting task. Over the past 40 years, much progress has been made in the study of organometallic reaction mechanisms. The good news from these investigations is that organometallic compounds undergo relatively few different kinds of reactions. Moreover, many of these reaction types have direct parallels with organic chemistry. We will try to point out these similarities during our discussion of basic kinds of reactions in this chapter and the next. Comprehension of these reaction types at this point in the text should greatly assist readers in grasping later topics in the textbook, such as catalysis and applications of organometallic chemistry to organic synthesis.

In Chapter 7, we will consider reactions where the center of action occurs primarily at the metal and not the ligands. Reactions that occur mainly at the ligands will be discussed in Chapter 8.

Table 7-1¹ shows briefly several important kinds of organometallic reactions. Note that some of these reactions really are the same, although the forward reaction and the reverse reactions have different names (i.e., oxidative addition and

¹A note on symbolism used throughout the remainder of the text is in order. Recall from Chapter 3 that the symbol L represents a ligand that donates two electrons to a complex (e.g., CO or phosphine). X (or sometimes Y or Z) represents a one-electron donor such as Cl or alkyl. To indicate a collection of unspecified L-type ligands (or sometimes L and X ligands) attached to a metal, the symbol L_n is used.

Table 7-1 Common Reactions of Organotransition Metal Complexes

Reaction type	Schematic example	Δ Oxidation state of M	Δ Coordination number of M	Δe^- count	Text section
Ligand substitution	$L'' + L_n ML' \longrightarrow L_n ML'' + L'$	0	0	0	7-1
[Oxidative addition Reductive elimination	$L_n M + X-Y \longrightarrow L_n M(X)(Y)$	+2	+2	+2	7-2
	$L_n M(X)(Y) \longrightarrow L_n M + X-Y$	-2	-2	-2	7-3
[1,1-Insertion ^a 1,2-Insertion ^a	$L_n M - \overset{Y}{\underset{ }{\text{C}}} - \overset{1}{\text{X}} = \overset{Z}{\text{Z}} \longrightarrow L_n M - \overset{Z}{\underset{ }{\text{C}}} - \overset{1}{\text{X}} - \overset{1}{\text{Y}}$	0	-1	-2	8-1-1
	$L_n M - \overset{Y}{\underset{ }{\text{C}}} - \overset{1}{\text{X}} = \overset{2}{\text{Z}} \longrightarrow L_n M - \overset{1}{\text{X}} - \overset{2}{\text{Z}} - \overset{1}{\text{Y}}$	0	-1	-2	8-1-1
[Nucleophilic addition ^b Nucleophilic abstraction ^b	$L_n M - \overset{Y}{\underset{ }{\text{C}}} - \overset{X}{\underset{ }{\text{Z}}} + \text{Nuc}^- \longrightarrow [L_n M - \overset{Y}{\underset{ }{\text{C}}} - \overset{X}{\underset{ }{\text{Z}}} - \text{Nuc}]^-$	0 ^c	0	0	8-2
	$L_n M - \overset{O}{\underset{ }{\text{C}}} - \text{R} + \text{Nuc-H} \longrightarrow L_n M - \text{H} + \text{Nuc} - \overset{O}{\underset{ }{\text{C}}} - \text{R}$	0	0	0	8-3
[Electrophilic addition ^b Electrophilic abstraction ^b	$L_n M - \text{X} = \text{Z} + \text{E}^+ \longrightarrow [L_n M = \text{X} - \text{Z} - \text{E}]^+$	0	0	0	8-4
	$L_n M - \text{X} - \text{Z} - \text{Y} + \text{E}^+ \longrightarrow L_n M^+ - \overset{X}{\underset{ }{\text{Z}}} + \text{E-Y}$	0	0	0	8-4
π - and σ -Bond metathesis ^d	$\begin{array}{c} \text{R} \\ \\ \text{C} \\ \\ \text{C} \\ \\ \text{R}' \end{array} + \begin{array}{c} \text{R} \\ \\ \text{C} \\ \\ \text{C} \\ \\ \text{R}' \end{array} \text{ or } \begin{array}{c} \text{X} \\ \\ \text{Y} \end{array} + \begin{array}{c} \text{W} \\ \\ \text{Z} \end{array} \longrightarrow \begin{array}{c} \text{R} - \text{C} = \text{C} - \text{R} \\ + \\ \text{R}' - \text{C} = \text{C} - \text{R}' \end{array} \text{ or } \begin{array}{c} \text{X} - \text{W} \\ + \\ \text{Y} - \text{Z} \end{array}$				11-1 and 11-4

^aThe reverse reaction, called *deinsertion* or elimination, is also possible.

^bThere is no one general reaction; several variations are possible.

^cDepends upon change in hapticity; e.g., X=Z going from η^3 to η^2 results in a 2 e^- reduction.

^d Δ oxidation state, coordination number, and e^- count are not applicable here, especially in π -bond metathesis where the metal complex is a catalyst.

reductive elimination). Note also the change in electron count and oxidation state during the course of these reactions.²

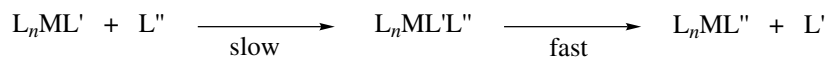
7-1 LIGAND SUBSTITUTION

Sometimes the first (and last) step in a catalytic cycle (to be discussed in Chapter 9), for example, ligand substitution is a common reaction type. This reaction is comparable in many ways to substitutions that occur at the carbon atom in organic chemistry. Equation 7.1 shows the general reaction.

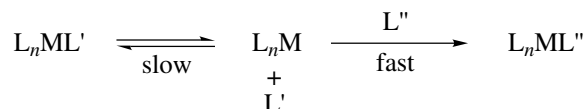


Much of the work on ligand substitution of organometallic complexes has involved metal carbonyls with a trialkyl or a triarylphosphine serving as the replacement ligand. Two main mechanistic pathways exist by which substitution may occur—associative (**A**) and dissociative (**D**).

Associative (**A**):



Dissociative (**D**):



The **A** pathway is characterized by a bimolecular rate-determining step involving the substrate and incoming ligand (L''). Sixteen-electron complexes usually undergo ligand substitution by an **A** mechanism. **D** mechanisms, typically involving 18-electron complexes, show a rate-limiting step in which one ligand on the substrate must depart before another can bind to the metal. Although there are clear-cut examples of dissociative and associative reactions, several ligand substitutions do not fit neatly into either type. The pathways of these reactions seem to lie between the mechanistic extremes of **A** and **D**. These mechanisms are called interchange (**I**) pathways, specifically labeled **I_a** (associative interchange) and **I_d** (dissociative interchange), where, for example, **I_a** stands for *interchange with an increase in coordination number in the rate-determining step*. As in S_N2 substitution at carbon, **I** pathways go through no discrete, detectable intermediates.

²For a good discussion of a number of common types of organometallic reactions, see C. A. Tolman, *Chem. Soc. Rev.*, **1972**, 1, 337.

The spectrum of pathways from **D** through **I** to **A** is analogous to the S_N1 – S_N2 manifold found in organic chemistry.³

Another characteristic of ligand substitution reactions is the order of reactivity with respect to the metal in a triad such as Cr, Mo, W or Ni, Pd, Pt. The second-row transition metal complexes are usually more reactive than either of those containing first- or third-row elements. It is not completely clear why this trend exists, but certainly it must be a function of atomic covalent radius (for example, Cr < Mo ~ W; steric crowding among ligands decreases as one goes down the periodic table), nuclear charge (Cr < Mo < W; the incoming ligand is more attracted to the metal with higher nuclear charge), and M–L bond energy (bond dissociation energy for M–CO: Cr < Mo < W; the weaker the M–L bond, the more facile the substitution). The first two factors favor heavier atoms and the last favors the lightest atom in the triad. Considering these and possibly other grounds discussed later in Chapter 7, complexes containing the middle triad element are most reactive.

7-1-1 The *trans* Influence and *trans* Effect

Before we consider the mechanistic types of substitution reactions in more detail, it is worthwhile to consider a factor that can direct the course of ligand substitution known as the *trans effect*. It has long been known⁴ that, in square planar transition metal complexes especially, certain ligands seem to direct substitution preferentially to a position *trans* to themselves. Both thermodynamics and kinetics provide the basis for this tendency. When the reaction is controlled primarily by factors influencing the ground state energy of the complex, the *trans effect* is more correctly termed the *trans influence*.⁵ The *kinetic trans effect* is associated with reactions where factors affecting the transition state energy control the product outcome. Over the years, both phenomena have been lumped together as the *trans effect*. We will discuss in this section the two factors that govern the product distribution, dividing them into the *trans influence* and the kinetic *trans effect*.

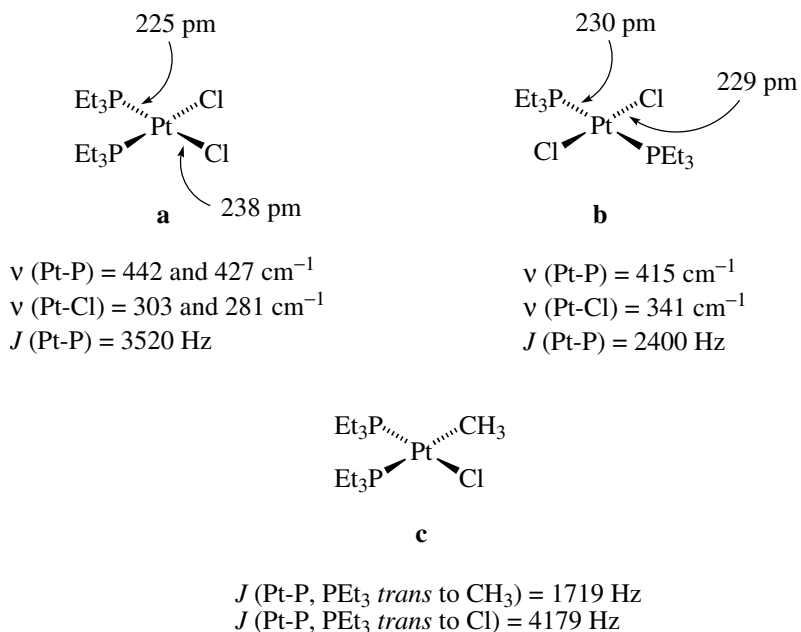
Trans Influence

Ligands that form strong σ bonds, such as hydride and alkyl, or π acceptor ligands, such as CN^- , CO, and PR_3 , which also bond strongly to the metal, tend

³D. T. Richens, *Chem. Rev.*, **2005**, *105*, 1961. Although the review referenced here concerns ligand substitution in transition metal complexes that are more traditionally inorganic than organometallic in nature, it contains useful information on the mechanism of ligand substitution that is relevant to organometallic chemistry.

⁴I. I. Chernyaev, *Ann. Inst. Platine*, **1926**, *4*, 261.

⁵Also called a *structural trans effect*. For a thorough discussion of the measurement and significance of the *trans influence* of ligands, see T. G. Appleton, H. C. Clark, and L. E. Manzer, *Coord. Chem. Rev.*, **1973**, *10*, 335.

**Figure 7-1**

Spectral and
Structural
Characteristics of
Pt(II) Complexes

to weaken the metal–ligand bond *trans* to the first ligand. In the ground state, this is a thermodynamic property called the *trans influence*. Studies of square planar platinum complexes have demonstrated that a ligand does weaken the metal–ligand bond of the group situated *trans* to it.⁶ These investigations have indicated that a ligand with a strong *trans influence* causes, in the infrared region of the electromagnetic spectrum, a decrease in M–L stretching frequency of the ligand *trans* to it (thus indicating a weakening of the M–L bond).

Moreover, NMR studies have measured the coupling constant $J_{\text{Pt-P}}$ of a number of trialkylphosphine platinum complexes. Trialkyl phosphines, as shown in Figures 7-1a⁷ and b,⁸ have a greater *trans influence* than Cl, and this is reflected in the higher coupling constant ($J_{\text{Pt-P}}$) and *lower* IR Pt–Cl stretching frequency

⁶A. Pidcock, R. E. Richards, and L. M. Venanzi, *J. Chem. Soc. A*, **1966**, 1707; L. M. Venanzi, *Chem. Brit.*, **1968**, 162; and F. Basolo, In *Mechanisms of Inorganic Reactions*, R. F. Gould, Ed., Advances in Chemistry Series, Vol. 49, American Chemical Society: Washington, D. C., 1965.

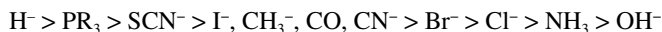
⁷(a) Bond lengths (For PMe_3 complex instead of PEt_3) from X-ray data: G. G. Messner, E. L. Amma, and J. A. Ibers, *Inorg. Chem.*, **1967**, 6, 725; (b) IR stretching frequencies: P. L. Goggin and R. J. Goodfellow, *J. Chem. Soc. A*, **1966**, 1462; NMR coupling constants ($J_{\text{Pt-P}}$): S. O. Grim, R. L. Keiter, and W. McFarlane, *Inorg. Chem.*, **1967**, 6, 1133.

⁸(a) Bond lengths from X-ray data: G. G. Messner and E. L. Amma, *Inorg. Chem.*, **1966**, 5, 1775; (b) IR stretching frequencies: P. L. Goggin and R. J. Goodfellow, *J. Chem. Soc. A*,

($\nu_{\text{Cl-Pt}}$) present when Cl is *trans* to the phosphine rather than when PEt_3 is *trans* to itself. The higher coupling constant in the *cis* isomer reflects the higher *s* character of the ligand–metal bond. The methyl group (Figure 7-1c), on the other hand, has a higher *trans* influence than Cl, as reflected in the small $J_{\text{Pt-P}}$ of 1719 Hz, when methyl is *trans* to the phosphine, and a $J_{\text{Pt-P}}$ equal to 4179 Hz when phosphine is *trans* to Cl.⁹

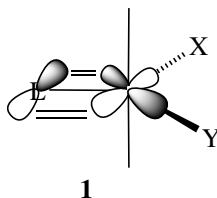
Since the methyl group is a strong σ bonding ligand, it causes the σ bonding character of the Pt–P bond to decrease, thus decreasing the coupling constant. Phosphines in general have a high *trans* influence because they exert both strong σ donation and π acceptance from the metal, thereby weakening the bond *trans* to the phosphine.

Ligands that have a strong σ electron donating ability are listed¹⁰ in approximate descending order of their effect.



Kinetic *trans* Effect

The tendency of certain ligands to direct incoming groups to the *trans* position also occurs with reactions under kinetic control. This case is known as the *kinetic trans effect*, whereby the influence of the ligand *trans* to the incoming one is felt due to the difference in energy between the ground state and the transition state in the rate-determining step. The σ donation effects are important, as well as the effect of π donation from the metal to the ligand. When a ligand forms strong π acceptor bonds with platinum, for instance, charge is removed from the metal. The effect on the energy of the ground state is relatively small, but it is significant on the transition-state energy because, during ligand substitution of a square planar Pt complex, we usually expect an increase in coordination to trigonal bipyramidal geometry in the transition state (see Section 7-1-2). A π bonding ligand originally present in the substrate (the complex undergoing substitution) can contribute to stabilizing the transition state, **1**, via the d_{xz} orbital from the metal.



1966, 1462; NMR coupling constants ($J_{\text{Pt-P}}$): S. O. Grim, R. L. Keiter, and W. McFarlane, *Inorg. Chem.*, **1967**, 6, 1133.

⁹F. H. Allen and A. Pidcock, *J. Chem. Soc. A*, **1968**, 2700.

¹⁰F. R. Hartley, *Chem. Soc. Rev.*, **1973**, 163.

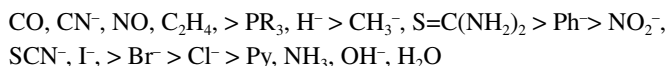
Table 7-2 Effect of *trans* Ligand on Rate at 25 °C for the Reaction $\text{trans-Pt}(\text{Cl})(\text{R})(\text{PEt}_3)_2 + \text{Py} \rightarrow [\text{trans-Pt}(\text{Py})(\text{R})(\text{PEt}_3)_2]^+ + \text{Cl}^-$

R	k ($\text{M}^{-1}\text{s}^{-1}$)
H ⁻	4.2
CH ₃ ⁻	6.7×10^{-2}
Ph ⁻	1.6×10^{-2}
Cl ⁻	4×10^{-4}

Overall, this effect increases the rate of reaction *trans* to the strong π acceptor ligand. The order of π bonding effects for various ligands is as follows.¹¹



When σ donation and π acceptance effects are combined, the overall *trans effect* list is as follows.¹²



Ligands highest in the series are strong π acceptors, followed by strong σ donors. Ligands at the low end of the series possess neither strong σ nor π bonding abilities. The *trans* effect can be very large—rates in platinum complexes may differ as much as 10^4 between complexes with strong *trans* effect ligands and those with weak ones. Table 7-2 presents the relative rate of substitution of chloride(Cl) by pyridine (Py) on *trans*-Pt(PEt₃)₂(Cl)R when R is varied.¹³

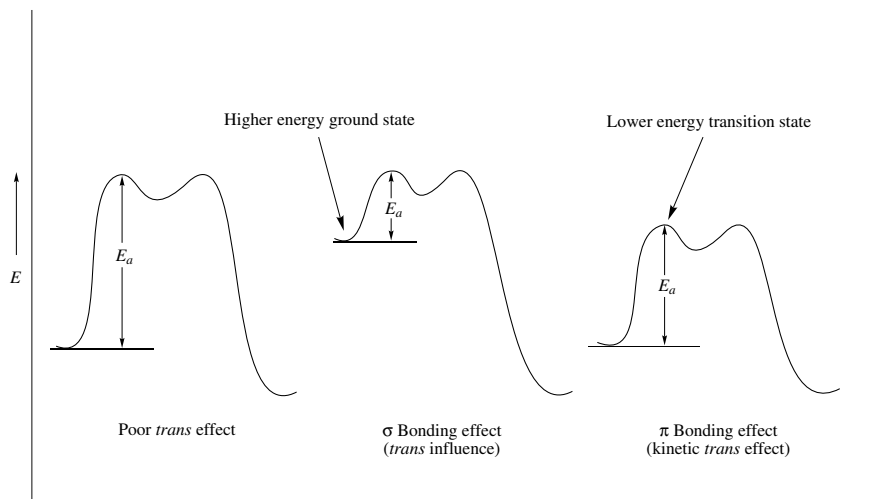
To assess the nature of the *trans* effect, one must investigate the influence of a ligand in destabilizing the ground state (really the *trans* influence) and in stabilizing the transition state (the *kinetic trans effect*). Groups such as alkyl and hydride do not have π -acceptor orbitals and thus are unable to form π bonds to the metal that could effectively stabilize the trigonal bipyramidal transition state in an associative reaction involving a coordinatively unsaturated¹⁴ square planar complex. Presumably, these ligands are effective solely by lowering the bond energy of the M–X bond and destabilizing the reactant. Ligands such as CO and the phosphines can stabilize the trigonal bipyramidal transition state through π bonding and can also decrease the energy of the M–X bond in the ground state through

¹¹See Footnote 10.

¹²See Footnote 10.

¹³F. Basolo, J. Chatt, H. B. Gray, R. G. Pearson, and B. L. Shaw, *J. Chem. Soc.*, **1961**, 2207.

¹⁴A coordinatively unsaturated complex possesses less than 18 electrons and has sites available for ligand bonding (e.g., a 16-electron square planar Pt complex). An octahedral, 18-electron complex, such as Cr(CO)₆, is deemed coordinatively saturated.

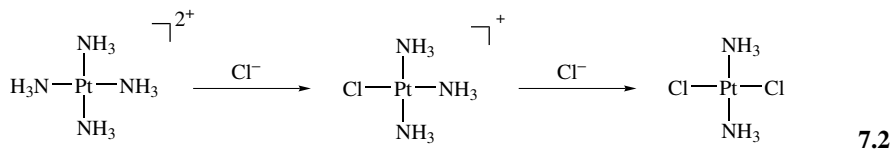
**Figure 7-2**

Activation Energy and the *trans* Effect
The depth of the energy curve for the intermediate and the relative heights of the two maxima will vary with the specific reactants.

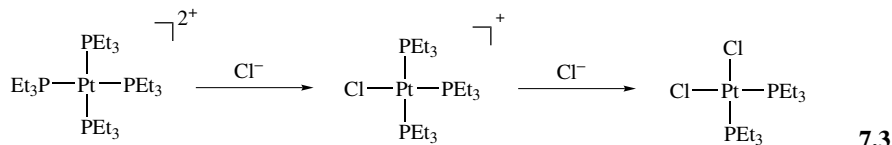
strong σ donation. It is sometimes difficult to determine the dominant effect, but Figure 7-2 summarizes the possible situations that could occur. When all is said and done, however, the phenomenon of selective labilization of ligands *trans* to other ligands is usually called the *trans effect* regardless of whether the reason for the effect of the directing ligand is kinetic or thermodynamic in origin.

The *trans effect* is somewhat different in octahedral complexes due to the smaller *s* character of each bond and possibly due to steric effects caused by the relatively greater crowding found in octahedral versus square planar environments. In general, however, it appears that *trans effects* are related to the ability of the ligand to stabilize the transition state during rate-limiting dissociation. Studies on octahedral Cr complexes¹⁵ indicate that the order of the *trans effect* is rather similar and follows the general trend as shown above.

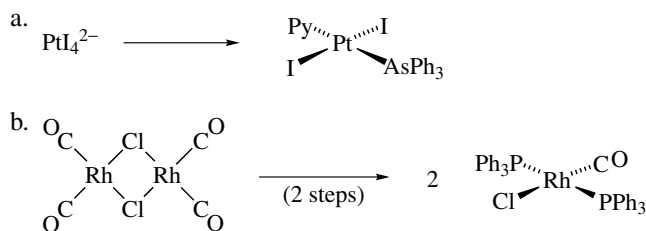
Equations 7.2 and 7.3 provide two examples showing how one could perform a synthesis taking advantage of the *trans effect*. Equation 7.2 shows that Cl has a larger *trans effect* than NH_3 , but PET_3 has a larger *trans effect* than Cl according to equation 7.3.



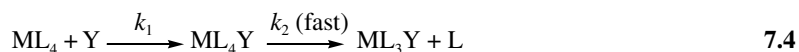
¹⁵J. D. Atwood, M. J. Wovkulich, and D. C. Sonnenberger, *Acc. Chem. Res.*, **1983**, *16*, 350 and B. J. Coe and S. J. Glenwright, *Coord. Chem. Rev.*, **2000**, *203*, 5.

**Exercise 7-1**

Using the structure to the left of the reaction arrow as the starting material, propose a synthesis route to the structure on the right. You may use any reasonable reagents for your synthesis route.

**7-1-2 Associative substitution**

Coordinatively-unsaturated 16-electron complexes typically undergo associative substitution. Here the mechanism involves a slow bimolecular step where the incoming ligand and 16-electron complex combine to form a coordinatively saturated 18-electron intermediate. The intermediate rapidly expels the leaving group to give the new substituted 16-electron product. This is outlined in equation 7.4.



A two-term rate law lends support to the mechanism outlined above and often takes the following general form:

$$\text{Rate} = k_s[\text{ML}_4] + k_1[\text{ML}_4][\text{Y}]$$

The k_s term arises because the solvent may also act as a nucleophile. Because a large excess of solvent is usually present in a reaction, the first term is called *pseudo* first order. The rate law expression is identical to that for an $\text{S}_{\text{N}}2$ reaction in organic chemistry. These reactions typically have highly negative entropies of activation, which provides additional support for the associative nature of the reaction.¹⁶

¹⁶J. D. Atwood, *Inorganic and Organometallic Reaction Mechanisms*, 2nd ed., Brooks/Cole: Monterey, CA, 1997; pp. 55–66.

Transition State Theory and Activation Volumes

The enthalpy of activation (ΔH^\ddagger) and the entropy of activation (ΔS^\ddagger), both derived from rate studies on reactions, are useful in providing information about the mechanism of a reaction. Both arise from transition-state theory (also known as absolute rate theory), which treats the activated complex at the transition state as a discrete entity in equilibrium with reactants. The value for ΔH^\ddagger corresponds to E_a from the Arrhenius equation according to $E_a = \Delta H^\ddagger + RT$. Its magnitude is a measure of bond energy changes in going from reactants to the transition state. The entropy of activation indicates the change in order as the reaction proceeds to the transition state. A highly negative value for ΔS^\ddagger implies that order increases on the way to the transition state, as exemplified by a bimolecular transformation such as the Diels–Alder reaction. A reaction that gives a positive value for ΔS^\ddagger indicates that the path to the transition state leads to greater disorder. Dissociative processes, such as the S_N1 reaction, exhibit large positive values of ΔS^\ddagger .¹⁷

Another measure of the associative or dissociative nature of reactions is the activation volume (ΔV^\ddagger). The following equation shows the approximate relationship between the rate constant (k_p or k_{obs}) and the applied pressure.

$$\ln k_p \approx \ln k_o - \Delta V^\ddagger P/RT, \text{ where } k_o \text{ is the rate constant at zero pressure}$$

Since measurable volume changes in solution require rather large changes in pressure, a special apparatus is required to measure ΔV^\ddagger . By plotting $\ln k_{obs}$ vs. P , one can determine ΔV^\ddagger from the slope. If k_{obs} increases with increasing pressure (indicating that increasing pressure favors compaction of a transition state involving bond making), then the sign of ΔV^\ddagger is negative. Dissociative reactions, on the other hand, resist increases in pressure. By increasing pressure, k_{obs} should decrease because ΔV^\ddagger is positive. Measurements of ΔV^\ddagger have become increasingly common as a means of obtaining information about transition-state structure.¹⁸

Associative substitution is usually found with square planar d^8 metal complexes such as those of Ni(II), Pd(II), Pt(II), Ir(I), and Au(III). Substitution reactions of these complexes have been thoroughly investigated.¹⁹ As in the

¹⁷For more information on absolute rate theory, see F. A. Carey and R. J. Sundberg, *Advanced Organic Chemistry, Part A*, 5th ed., Springer Science: New York, 2007, pp. 270–276.

¹⁸See Footnote 3 and A. Drljaca, C. D. Hubbard, R. van Eldik, T. Asano, M. V. Basilevsky, and W. J. leNoble, *Chem. Rev.*, **1998**, 98, 2167.

¹⁹A. Peloso, *Coord. Chem. Rev.*, **1973**, 10, 123; R. J. Cross, *Chem. Soc. Rev.*, **1985**, 14, 197; and J. P. Collman, L. S. Hegedus, J. R. Norton, and R. G. Finke, *Principles and Applications of Organotransition Metal Chemistry*, University Science Books: Mill Valley, CA, 1987, pp. 241–244, and references therein.

case of S_N2 reactions, the rate of substitution depends upon several factors, including nucleophilicity (*soft* nucleophiles such as SCN^- and PR_3 are particularly effective when the metal center is *soft* [e.g., $Pt(II)$]), leaving group ability (a function of $M-L$ bond strength or Brønsted–Lowry base strength; the weaker the base, the better the leaving group), the solvent,²⁰ and the *trans* effect.

Hard and Soft Acids and Bases

The concept of hard and soft acids and bases needs some explanation here. We are really talking about the hardness or softness of *Lewis* acids or bases. Hard acids tend to be small in size, have a large positive charge, and possess an electron cloud that is not capable of significant distortion (non-polarizable). Examples of hard acids are H^+ , Al^{3+} , or BF_3 . Soft acids are just the opposite, in that they tend to be of large size with respect to their charge and possess polarizable electron clouds. Species such as Hg^{2+} , Tl^+ , and low-valent transition metals typify soft acids.

Hard and soft bases are similar to their acid counterparts except that they are electron rich species instead of electron poor. Hard bases would include F^- , OH^- , or NH_3 . Species such as I^- , R_2S , CO , or R_3P constitute examples of soft bases. A good rule of thumb to apply when assessing the softness of an acid or base is to assume that softness increases as one proceeds down a column or group in the periodic table. Reactions between hard acids and hard bases readily occur because the two reacting partners have a strong coulombic attraction for each other. Soft acids and soft bases tend to react rapidly for a more subtle reason. Figure 7-3 indicates that soft acids and bases interact well because the HOMO (highest occupied molecular orbital) of the base is close in energy to the LUMO (lowest unoccupied molecular orbital) of the acid, assuming that these orbitals have appropriate symmetry. Since the HOMO is filled with two electrons and the LUMO lacks electrons, the interaction between the two orbitals gives a doubly occupied bonding orbital and an empty antibonding orbital. Overall, the interaction of the two orbitals results in a significant energy lowering. This would not be the case if the acid were hard (the LUMO would be quite high in energy) and the base also hard (the HOMO is relatively low in energy). Then the HOMO and LUMO would be so far apart in energy that effective interaction between them would be negligible, resulting in very little energy lowering.

It is difficult to quantify the “hardness” or “softness” of a Lewis acid or base. We cannot measure a pK_a value, as is the case when assessing the strength of Brønsted–Lowry acids.

²⁰Solvents can have a profound effect on the rate of ligand substitution. For a recent article detailing the effect that ionic liquids (salts that are liquid at room temperature) can have on the rate of substitution, especially when the incoming ligand is anionic, see M. D. Singer, S. J. P’Pool, R. A. Taylor, J. McNeill III, S. H. Young, N.W. Hoffman, M. A. Klingshirn, R. D. Rogers, and K. H. Shaughnessy, *J. Organomet. Chem.*, **2005**, 690, 3540.

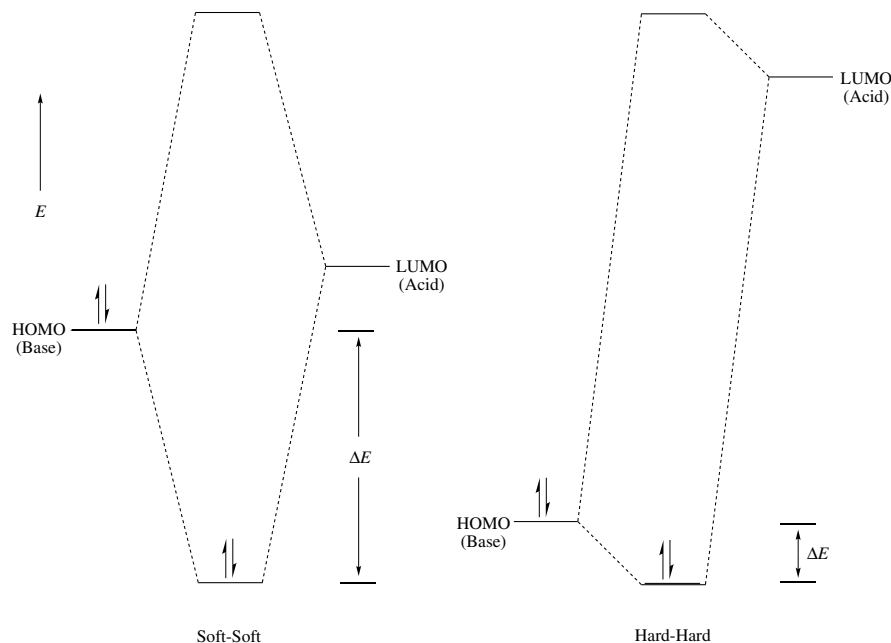


Figure 7-3
HOMO–LUMO
Interactions of Hard
and Soft Acids and
Bases

R. G. Pearson has reported a scale of absolute hardness for acids and bases, defining hardness to be one-half the difference between the ionization potential and the electron affinity of an atom or species.²¹ He has obtained good agreement in many cases between the calculated values for hardness and the experimental behavior of the acid or base.

Unlike S_N2 reactions in organic chemistry, associative substitution of square planar complexes usually results in *retention* of configuration and not inversion. Figure 7-4 indicates that the reaction is thought to proceed by attack of the incoming nucleophile **Y** (or solvent) from the top or up from the bottom to give a square-pyramidal intermediate that rearranges to a trigonal bipyramid. Note that the *trans*-directing ligand, **T_d**, and the incoming and leaving ligands, **Y** and **X**, are all equatorial substituents of the trigonal bipyramid. Finally, the leaving group leaves and the final product is a square planar complex with the incoming ligand *trans* to **T_d**. Equations 7.2 and 7.3 show typical associative ligand substitution reactions.²²

²¹R. G. Pearson, *Inorg. Chem.* **1988**, *27*, 734. See also G. L. Miessler and D. A. Tarr, *Inorganic Chemistry*, 3rd ed., Prentice Hall: Upper Saddle River, NJ, 2004; pp. 183–192.

²²Not all square planar complexes of Pt undergo associative ligand substitution. *Cis*-(dimethyl)(dimethylsulfoxide)(triarylphosphine)platinum(II) undergoes displacement of DMSO by pyridine via dissociation of DMSO in the rate-determining first step. Retention of configuration is observed, presumably via a T-shaped intermediate. See R. Romeo, L. M. Scolaro, M. R. Plutino, F. F. de Biani, G. Bottari, and A. Romeo, *Inorg. Chim. Acta.*, **2003**, *350*, 143.

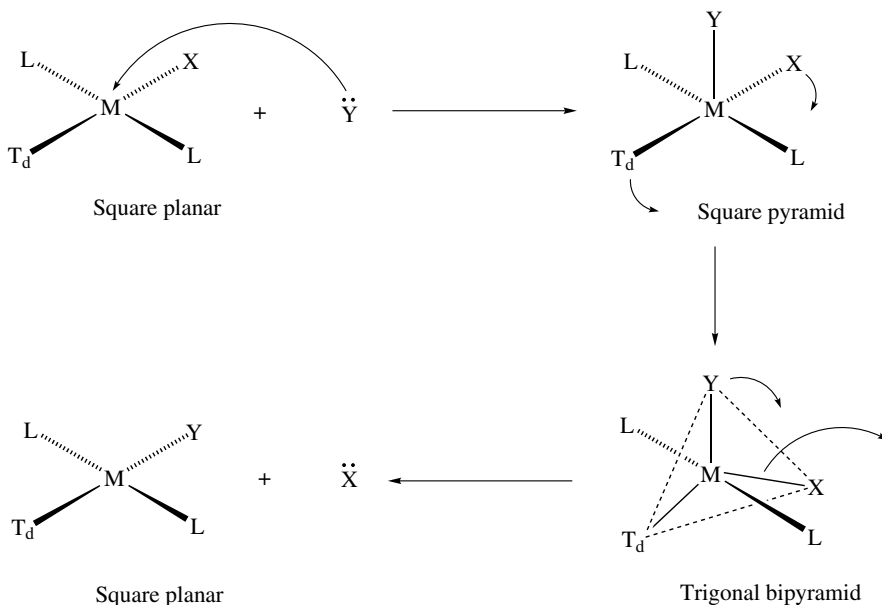
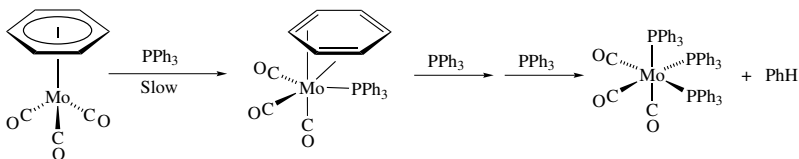


Figure 7-4
Ligand Substitution
of a Square Planar
Complex

Associative Substitution with 18-Electron Systems

The 18-electron rule makes it unlikely that coordinatively-saturated, 18-electron complexes would undergo substitution by an **A** mechanism. An exception to this conventional wisdom was formulated by Basolo,²³ who postulated that substitution in 18-electron complexes may occur associatively if the metal complex can delocalize a pair of electrons onto one of its ligands.

For example, equation 7.5 shows substitution of an 18-electron molybdenum complex by phosphine ligand,²⁴ which proceeds with a rate law first order in starting complex and first order in incoming ligand—exactly as would be demonstrated in an associative substitution of a 16-electron square planar complex as discussed earlier in Section 7-1-2. Note that the rate-determining step of this reaction involves a change in hapticity of the arene ligand from η^6 to η^4 , coincident with attachment of the incoming phosphine ligand.



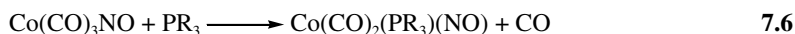
7.5

²³F. Basolo, *Inorg. Chim. Acta*, **1981**, 50, 65.

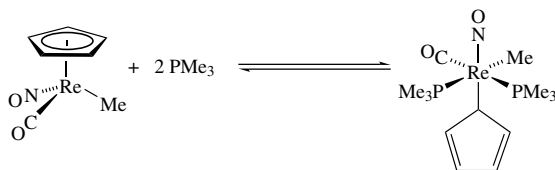
²⁴F. Zingales, A. Chiesa, and F. Basolo, *J. Am. Chem. Soc.*, **1966**, 88, 2707.

Such a change preserves the electron count in the coordination sphere when the extra incoming ligand is attached. Studies on similar molybdenum–triene complexes have resulted in the isolation of 18-electron η^4 –(triene)Mo(CO)₃(PR₃); moreover, an η^4 –arene complex has been isolated and characterized in the solid state.²⁵

Equations 7.6–7.9 provide examples of associative substitution reactions on 18-electron complexes. In all cases, modification of the electron contribution of one of the ligands occurs. In reaction 7.6 the nitrosyl group rearranges from its 3-electron, linear form (an 18 e[−] complex) to a 1-electron, bent form (a 16-e[−] complex).²⁶ This allows the phosphine to attack to give the 18 e[−] complex Co(CO)₃(PR₃)(NO). Finally, CO departs to give the product. The overall rate of the reaction is related to the nucleophilicity of the phosphine and follows the order PEt₂Ph ~ PPh₃ > P(OPh)₃ (see Section 6–3).



Reaction 7.7 involves conversion from η^5 to η^1 –Cp (via η^3),²⁷ and reaction 7.8 shows “slippage” of η^5 to η^3 –indenyl. Such slippage is quite rapid compared with the η^6 to η^4 change observed with comparable metal complexes of η^6 –benzene or the η^5 to η^3 transformation when η^5 –Cp is the π ligand. This “indenyl ligand effect” was noted by Basolo, who attributed the enhanced reactivity to the greater resonance stabilization of the η^3 –indenyl group (with one aromatic ring intact) compared with η^4 –benzene or η^3 –Cp, which are no longer aromatic.²⁸ One of the most interesting examples of this type involves reorganization of electrons in a tetrazole ligand attached to iron, shown in equation 7.9. The tetrazole changes from ligand-type L₂ to X₂ and finally back to L₂. The ΔH^\ddagger of 6.9 kcal/mol and ΔS^\ddagger of −31.4 eu clearly support a rapid associative mechanism for the reaction.²⁹



7.7

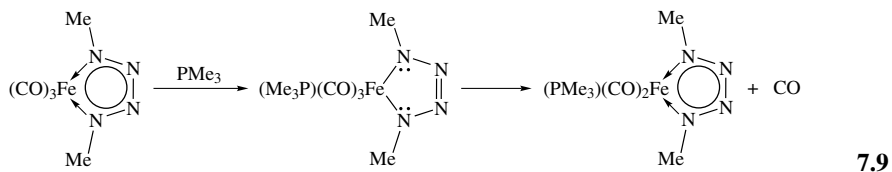
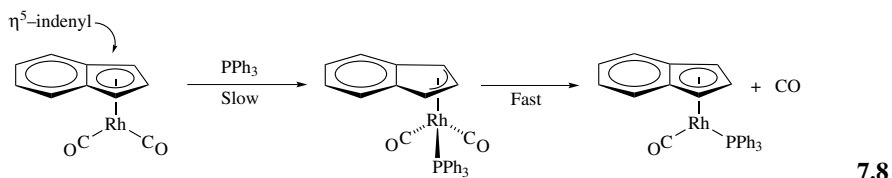
²⁵D. J. Darensbourg, “Ligand Substitution in Metal Carbonyls,” In F. G. A. Stone and R. West, Eds., *Advances in Organometallic Chemistry*, Academic Press: New York, 1982, Vol. 21, p. 123.

²⁶J. S. Howell and P. M. Burkinshaw, *Chem. Rev.*, **1983**, 83, 557.

²⁷C. P. Casey and J. M. O’Connor, *Organometallics*, **1985**, 4, 384 and C. P. Casey, J. M. O’Connor, and K. J. Haller, *J. Am. Chem. Soc.*, **1985**, 107, 1241.

²⁸M. E. Rerek, L. N. Ji, and F. Basolo, *J. Chem. Soc., Chem. Commun.*, **1983**, 1208 and L. N. Ji, M. E. Rerek, and F. Basolo, *Organometallics*, **1984**, 2, 740.

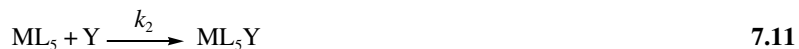
²⁹C. Y. Chang, C. E. Johnson, T. G. Richmond, Y. T. Chen, W. C. Trogler, and F. Basolo, *Inorg. Chem.*, **1981**, 20, 3167 and Q. Z. Shi, T. G. Richmond, W. C. Trogler, and F. Basolo, *Organometallics*, **1982**, 1, 1033.

**Exercise 7-2**

- Propose a structure for the starting material in equation 7.6.
- Calculate the electron count for each complex in equation 7.9.

7-1-3 Dissociative Displacements

The **D** mechanism requires the formation of an intermediate with reduced coordination number, and it is the most common pathway for 18-electron complexes, as outlined in equations 7.10 and 7.11.



Application of the steady state approximation³⁰ produces a rate law for this mechanism as

³⁰The steady-state approximation assumes that, in a multistep reaction, the concentration of intermediates is small and constant because the rate of their formation equals their rate of destruction. Application of the steady-state approximation for equations 7.10 and 7.11 proceeds as follows:

We first write the rate law as

$$\text{Rate} = k_2[\text{ML}_5][\text{Y}].$$

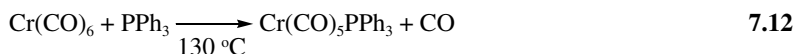
Since we do not know the concentration of the fleeting intermediate, ML_5 , we apply the steady-state approximation to find its concentration in terms of variables that are measurable. We assume that the change in concentration of ML_5 with time is equal to zero (that is, the rate of

$$\text{Rate} = \frac{k_1 k_2 [\text{ML}_6][\text{Y}]}{k_{-1}[\text{L}] + k_2[\text{Y}]}$$

If the concentration of leaving group (L) is relatively small compared with that of the incoming nucleophile or if k_{-1} is small, then the rate law reduces to

$$\text{Rate} = k[\text{ML}_6],$$

which is much like the rate law for a limiting $\text{S}_{\text{N}}1$ reaction in organic chemistry. Studies have shown, however, that the resulting 16-electron intermediates, formed upon ligand dissociation, are highly reactive and show little selectivity toward achieving coordinative saturation. Thus, k_{-1} is often comparable in magnitude to k_2 ,³¹ and the more complicated rate law holds unless the incoming ligand is in large concentration. Studies on the kinetics of ligand substitution reactions of metal carbonyl complexes have yielded significant information on the mechanism of displacement of other neutral ligands (e.g., phosphines, alkenes, and amines) from low-valent metal centers. A typical example of a substitution that occurs by a **D** mechanism is shown in equation 7.12.³²



formation of intermediate is equal to the rate of disappearance; this is the approximation). Thus,

$$d[\text{ML}_5]/dt = 0 = k_1[\text{ML}_6] - k_{-1}[\text{ML}_5][\text{L}] - k_2[\text{ML}_5][\text{Y}].$$

Rearranging terms in order to solve for $[\text{ML}_5]$, we have

$$[\text{ML}_5]\{k_{-1}[\text{L}] + k_2[\text{Y}]\} = k_1[\text{ML}_6]$$

and

$$[\text{ML}_5] = k_1[\text{ML}_6]/\{k_{-1}[\text{L}] + k_2[\text{Y}]\}.$$

Plugging the value for $[\text{ML}_5]$ back into the original rate law expression, we have a new equation:

$$\text{Rate} = k_1 k_2 [\text{ML}_6][\text{Y}]/\{k_{-1}[\text{L}] + k_2[\text{Y}]\}.$$

For more discussion of the steady-state approximation, see I. N. Levine, *Physical Chemistry*, 3rd ed., McGraw-Hill: New York, 1988, pp. 532–533; and F. A. Carey and R. J. Sundberg, *Advanced Organic Chemistry, Part A*, 5th ed., Springer Science: New York, 2007, pp. 282–283.

³¹D. J. Darensbourg, "Ligand Substitution in Metal Carbonyls," In F. G. A. Stone and R. West, Eds., *Advances in Organometallic Chemistry*, Academic Press: New York, 1982, Vol. 21, p. 115.

³²J. A. S. Howell and P.M. Burkinshaw, *Chem. Rev.*, **1983**, 83, 559, and references therein.

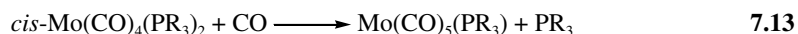
Relative Rates

Rates of substitution for various ML_6 complexes (the carbonyl complexes have been the most studied) differ considerably depending on the metal and the ligands present. The 18-electron species $[V(CO)_6]^-$ is resistant to substitution by even molten PPh_3 .³³ Group 6 hexacoordinate complexes typically show k_1 values ranging from 10^{-12} to 10^{-3} sec^{-1} .³⁴

As mentioned in Section 7-1, second-row complexes tend to react faster than first- or third-row complexes in simple ligand substitutions that occur by a dissociative mechanism.³⁵ This trend has been well studied for Group 6 complexes and is often observed with d^9 and d^{10} metals. For the series of metal carbonyls $M(CO)_6$ where $M = Cr, Mo, \text{ and } W$, the observed order of reactivity does not mirror the order of $M-C$ bond energies, which are $W > Mo > Cr$. The order does seem to correspond to the calculated values for the force constants of $M-C$ bonds in Group 6 metal carbonyls.³⁶

Steric Effects

Steric effects play a role in the rate of ligand displacement. The rate of reaction for equation 7.13 has been measured for a number of phosphine ligands (PR_3), and the results indicate that the rate of substitution is accelerated by bulky phosphines. A good correlation between cone angle (see Section 6-3) of the phosphine (or phosphite) ligand and rate of displacement by CO was obtained, as shown in Table 7-3.



The cis Effect

Octahedral complexes of the general formula $M(CO)_5X$ often exhibit a tendency to lose a CO substituted *cis* to the X ligand (Group 6 and 7 metal complexes have

³³A. Davidson and J. E. Ellis, *J. Organomet. Chem.*, **1971**, 31, 239.

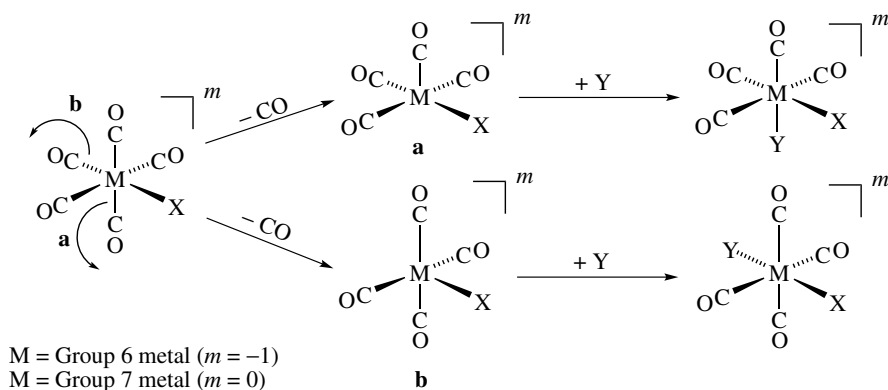
³⁴D. J. Darensbourg, "Ligand Substitution in Metal Carbonyls," In F. G. A. Stone and R. West, Eds., *Advances in Organometallic Chemistry*, Academic Press: New York, 1982, Vol. 21, p. 117.

³⁵D. J. Darensbourg, "Ligand Substitution in Metal Carbonyls," In F. G. A. Stone and R. West, Eds., *Advances in Organometallic Chemistry*, Academic Press: New York, 1982, Vol. 21, p. 116.

³⁶Force constants (k) of bonds directly relate to the IR stretching frequency: the higher the value for k , the higher the value for the stretching frequency. See J. A. S. Howell and P. M. Burkinshaw, *Chem. Rev.*, **1983**, 83, 559, and references therein.

Table 7-3³⁷ Rates of Ligand (L) Replacement by CO at 70 °C

L	Cone angle (°)	Rate constant (sec ⁻¹)	ΔH^\ddagger (kcal/mol)	ΔS^\ddagger (eu) ^a
Phosphines				
PMe ₂ Ph	122	<1.0 x 10 ⁻⁶		
PMePh ₂	136	1.33 x 10 ⁻⁵		
PPh ₃	145	3.16 x 10 ⁻³	29.7	14.4
PPhCy ₂ ^b	162	6.40 x 10 ⁻²	30.2	21.7
Phosphites				
P(OPh) ₃	128	<1.0 x 10 ⁻⁵		
P(O- <i>o</i> -tol) ₃ ^c	141	1.60 x 10 ⁻⁴	31.9	14.4

^aeu = cal/mol-K.^bCy = cyclohexyl.^c*o*-tol = *ortho*-toluyl (*o*-methylphenyl).**Figure 7-5**Intermediates in the Substitution of $M(CO)_5X$ Complexes

been well investigated).³⁸ This phenomenon of *cis* labilization is termed the *cis* effect.³⁹ Loss of a carbonyl group from an octahedral complex provides two distinct square pyramidal intermediates, **a** and **b** (Figure 7-5), depending on whether the CO is lost from a position *cis* (**a**) or *trans* (**b**) to X.

³⁷D. J. Darensbourg, "Ligand Substitution in Metal Carbonyls," In F. G. A. Stone and R. West, Eds., *Advances in Organometallic Chemistry*, Academic Press: New York, 1982, Vol. 21, p. 119.

³⁸J. D. Atwood and T. L. Brown, *J. Am. Chem. Soc.*, **1976**, 98, 3160.

³⁹*Cis* effects occur with square planar Pt complexes, but these are very small and the order of the effect with respect to ligand is variable. For a discussion, see J. D. Atwood, *Inorganic and Organometallic Reaction Mechanisms*, 2nd ed., VCH: New York, 1997, pp. 51–52.

Calculations show⁴⁰ that a ligand such as a halogen (a poor σ donor and π acceptor) stabilizes the geometry shown in **a** more than **b** and thus as a consequence of the Hammond postulate (see below), the transition state leading to **a** is more stable than that leading to **b**. When *cis* ligands are present that do not share the electronic properties of the halogens (i. e., they are better σ donors and/or have the capacity for π acceptance), the preference for *cis* labilization is reduced. Ligands that are stronger π acceptors than CO (such as $F_2C=CF_2$) actually labilize preferential loss of the *trans* CO.

The Hammond Postulate

A mechanism is a description of events—primarily bond breaking and making—that occur during the transformation of reactant to product. It is important to have knowledge about the structure of transition states, especially the one involved in the rate-determining step. Such knowledge assists the chemist in predicting what effects different substituents will have on the rate of the reaction and the product distribution (if more than one product is possible) and in understanding the role of stereochemistry on the transformation of reactant to product.

Careful application of the Hammond postulate allows us to ascertain the structure of the transition state under certain conditions if we know something about the structure and energy of the next prior or later consecutive species, which could be an unstable intermediate, reactant, or product. Proposed originally by George Hammond,⁴¹ the postulate declares, “if two states, as for example, a transition state and an unstable intermediate, occur consecutively during a reaction process and have nearly the same energy content, their interconversion will involve only a small reorganization of molecular structure.”

We can apply this postulate by looking at three cases described in Figure 7-6. Figure 7-6a shows a highly exothermic overall reaction or step in a reaction coordinate-energy diagram. The energy of the reactant is very similar to that of the transition state. In this case, we can say that the transition state comes early in the reaction coordinate and the structure of the starting material closely resembles that of the transition state. Figure 7-6b shows the opposite situation where a highly endothermic step occurs. The transition state comes late in the reaction pathway and thus resembles that of the product. A good example here would be the ionization step that occurs in an S_N1 reaction where a substrate undergoes dissociation to yield a leaving group and a carbocation intermediate (equation 7.14).

⁴⁰M. Elian and R. Hoffmann, *Inorg. Chem.*, **1975**, *14*, 1058 and J. K. Burdett, *J. Chem. Soc., Faraday Trans. 2*, **1974**, *70*, 1599.

⁴¹G. S. Hammond, *J. Am. Chem. Soc.*, **1955**, *77*, 334. The Hammond postulate is also discussed in most organic chemistry textbooks and in F. A. Carey and R. J. Sundberg, *Advanced Organic Chemistry, Part A*, 5th ed., Springer Scientific: New York, 2007, pp. 289–293.

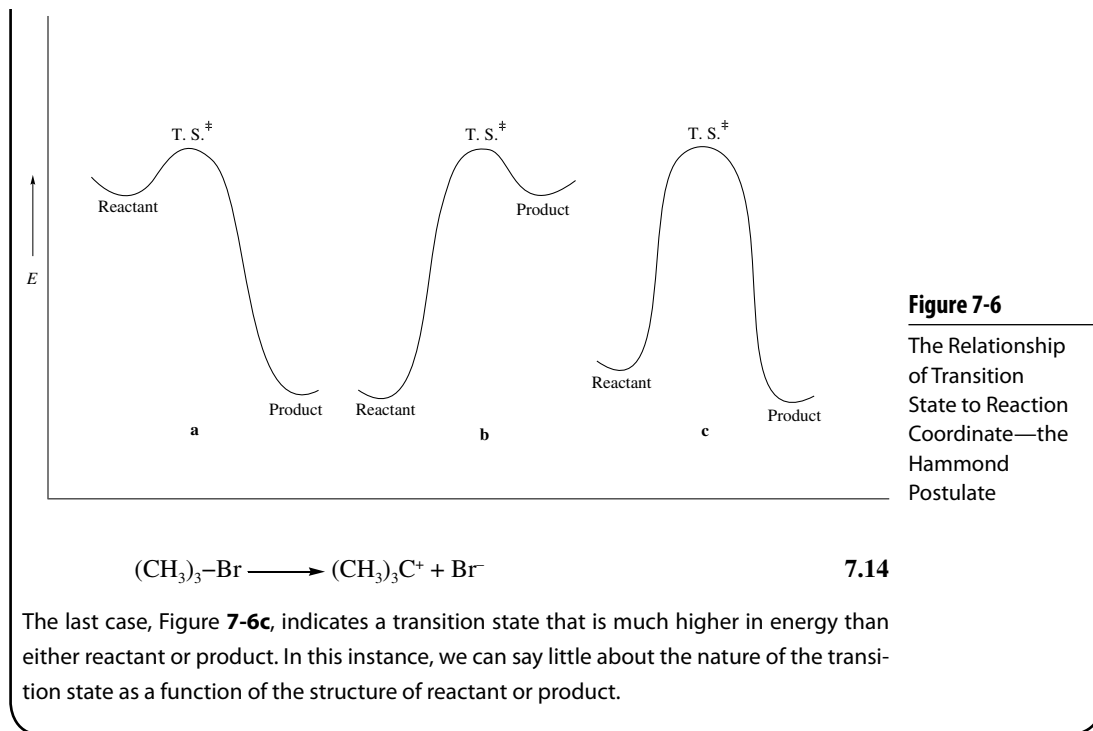


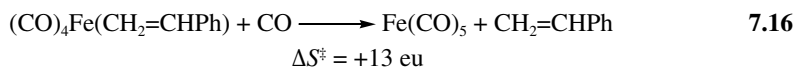
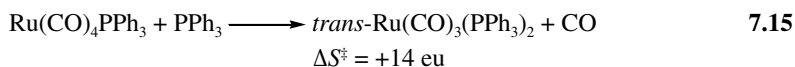
Figure 7-6
The Relationship of Transition State to Reaction Coordinate—the Hammond Postulate

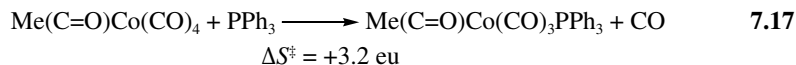
Other Ligands

The rate of substitution of a particular ligand is a function of ligand type. Carbon-donor L-type ligands, such as CO or arene, dissociate rather easily because they are neutral in the free state. L_nX groups (such as Cp), on the other hand, dissociate more reluctantly as radicals or ions that are less stable.

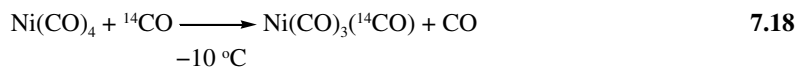
ML_5 and ML_4 Complexes

ML_5 d^8 systems involving Group 8 and 9 metals are typically trigonal bipyramidal in structure and, because of this, they have low energy barriers to exchange and interconversion between square-pyramidal and trigonal bipyramidal forms. The facility of these isomerizations makes mechanistic conclusions on the basis of product stereochemistries rather meaningless. Nevertheless, many ML_5 complexes undergo substitution reactions, and kinetic parameters often demonstrate a **D** mechanism. Equations 7.15 to 7.17 serve as examples for ML_5 substitutions.





The dissociative substitution of d^{10} ML_4 complexes has been well studied, particularly with regard to $\text{M} = \text{Ni}$ (equation 7.18).



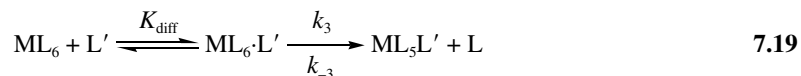
Here the geometry of the starting complex is invariably tetrahedral. $\text{Ni}(\text{CO})_4$ also reacts readily with phosphines to give mono- and disubstituted complexes. These then react incrementally more slowly than $\text{Ni}(\text{CO})_4$ toward further ligand exchange due to the stabilizing influence of phosphine ligands.

The rate of ligand dissociation of ML_4 ($\text{L} = \text{PR}_3$) complexes to give ML_3 correlates strongly with the cone angle. Also, as we have seen previously, the dissociation is slower when phosphite ligands with the same cone angle as the corresponding phosphine are compared. This is due to the greater π -acceptance ability of phosphites compared with phosphines and results in ground state metal stabilization. For the Group 10 d^{10} ML_4 series, the rate of substitution typically varies in the order $\text{Pd} > \text{Pt} \sim \text{Ni}$.

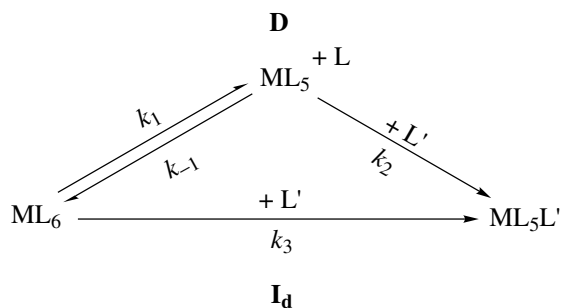
A picture emerges from several lines of investigation on the displacement of ligands from coordinatively saturated species. That is, *the reaction appears to proceed by rate-determining loss of ligand to produce a highly reactive 16-electron intermediate*. This intermediate probably closely resembles the transition state occurring during the rate-determining step, according to the Hammond postulate. The intermediate then captures a new nucleophile to complete the process of substitution.

7-1-4 The Interchange Pathway

We would not expect coordinatively saturated 18-electron complexes to increase coordination number or electron count during ligand substitution processes. Earlier in Chapter 7, the interchange (**I**) pathway was mentioned as a mechanistic possibility for ligand substitution. There is evidence that indicates that something like an **I** pathway can happen, in which there is an apparent increase in coordination number on the way from coordinatively saturated reactant to product. This is illustrated in outline form in equation 7.19.



The best studied cases where interchange pathways may occur are those in which there is competition between **I** (actually an **I_d**, dissociative interchange) and **D** mechanisms (Scheme 7.1)



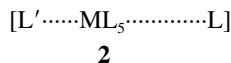
Scheme 7.1

Competing **D** and **I_d** Pathways

In the **I_d** mechanism (as shown in equation 7.19), the substrate and **L'** combine under diffusion control⁴² to give a “cage” complex (**ML₆·L'**) in which **ML₆** and **L'** are loosely bound together and confined inside a “cage” of solvent molecules. **ML₆·L'** then undergoes rate-determining formation of **ML₆L'**, followed by rapid loss of leaving group, **L**. According to this scheme and using the steady-state approximation, the rate law would be

$$\text{Rate} = K_{\text{diff}}k_3[\text{ML}_6][\text{L}'].$$

The **I_d** mechanism may be further described as a process that proceeds through a transition state, **2**:



Here the rate-determining step occurs when both the incoming and the departing ligand are loosely held in the coordination sphere. The **I_d** mechanism distinguishes itself from the **I_a** in that there is considerable rupture of the M–L bond of the departing ligand and very little bond making between the metal and the incoming **L'** group in the transition state. It is difficult to find hard evidence for such a mechanism because isolation of the intermediates **ML₆·L'** and **ML₆L'** would be problematic indeed. In fact, the inability to detect such intermediates is cause for chemists to suggest the possibility of the existence of an **I** mechanism, especially if there is a linear relationship detected between the observed rate and ligand concentration.

Kinetic evidence suggests that competing **D** and **I_d** pathways (Scheme 7.1) can occur under some conditions. When **L** = amines, phosphines, or nitriles, experiments indicate that a two-term rate law applies:

$$\text{Rate} = k_1[\text{ML}_6] + k_3[\text{ML}_6][\text{L}'].$$

⁴²Diffusion-controlled rate processes are very rapid and are influenced solely by the rate at which molecules can diffuse toward one another and collide.

Table 7-4^a Activation Parameters for Ligand Substitution of $M(\text{CO})_6$ with PBu_3

M	$\Delta H_1^{\ddagger b}$	$\Delta S_1^{\ddagger c}$	ΔH_3^{\ddagger}	ΔS_3^{\ddagger}
Cr	40.2	22	25.5	-15
Mo	31.6	6.7	21.7	-15
W	39.9	14	29.2	-6.9

^aR. J. Angelici and J. R. Graham, *J. Am. Chem. Soc.*, **1966**, 88, 3658 and R. J. Angelici and J. R. Graham, *Inorg. Chem.*, **1967**, 6, 2082.

^bkcal/mol.

^cEntropy units (eu), cal/mol-K.

In this expression, k_1 refers to the rate constant for rate-determining dissociation (equation 7.10) and k_3 to that for the rate-determining step in an I_d process (equation 7.19). Table 7-4 gives a few examples of Group 6 metal complexes that seem to undergo simultaneous **D** and I_d substitutions. Note that the enthalpy of activation, ΔH_3^{\ddagger} , for the I_d pathway is less than that for the corresponding purely dissociative process, ΔH_1^{\ddagger} . The ΔS^{\ddagger} terms for the two pathways, moreover, are vastly different—the purely dissociative process shows a highly positive entropy of activation, whereas ΔS^{\ddagger} for I_d processes is clearly negative, as would be expected for a transition state that increases in order upon going from reactants to products.

The data in Table 7-4 also indicate that the activation enthalpy for both pathways is lowest when $M = \text{Mo}$, consistent with the general trend in rate of ligand substitution of first row, third row < second row for reasons discussed earlier in this Chapter.

Scheme 7.2, which describes another case where an I_d process may occur, involves substitution on complexes containing a polyhapto ligand, such as a diene or triene. Application of the steady-state approximation with respect to the two intermediates, **A** and **B**, gives a rate law of the following form:

$$\text{Rate} = \{k_1 k_2 [\text{M}(\text{CO})_4 \text{diene}][\text{L}] / (k_{-1} + k_2[\text{L}])\} + k_3 [\text{M}(\text{CO})_4 \text{diene}][\text{L}].$$

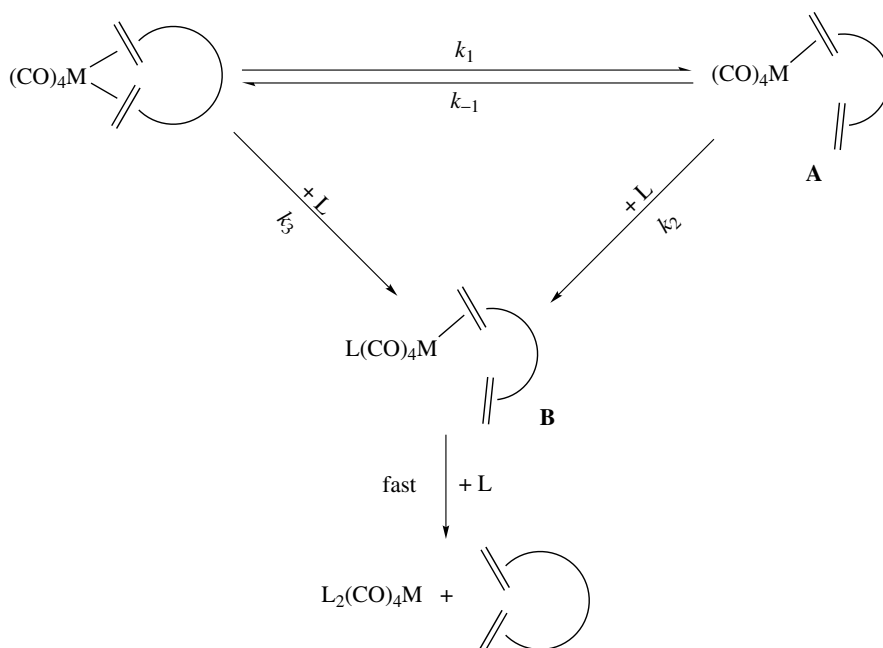
If $k_2[\text{L}]$ is large (i.e., there is a large concentration of incoming ligand), then the rate law reduces to

$$\text{Rate} = k_1 [\text{M}(\text{CO})_4 \text{diene}] + k_3 [\text{M}(\text{CO})_4 \text{diene}][\text{L}],$$

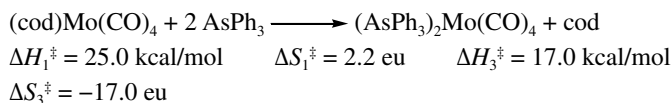
an expression that corresponds to simultaneous **D** and I_d pathways.

A specific example of such a reaction, using 1,5-cyclooctadiene (cod) as the polyhapto ligand, is shown in equation 7.20.⁴³

⁴³F. Zingales, M. Graziani, and U. Belluco, *J. Am. Chem. Soc.*, **1967**, 89, 256.

**Scheme 7.2**

Substitution
Involving a
Substrate with a
Polyhapto Ligand

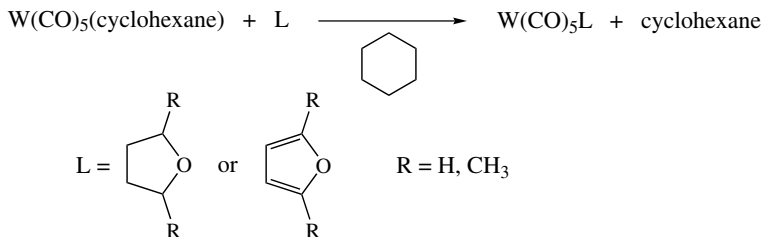
**7.20**

Again, the ΔS_1^\ddagger represents the entropy of activation for the **D** pathway, while ΔS_3^\ddagger corresponds to the **I_a** process.⁴⁴

There is likely a fine line between **I_d** and **I_a** mechanisms. Reaction of $\text{W}(\text{CO})_5(\text{cyclohexane})$ with methylated and unmethylated tetrahydrofurans and furans (Equation 7.21) indicates evidence of an operative **I_a** pathway because ΔH^\ddagger is low compared with the $(\text{CO})_5\text{W-CyH}$ bond dissociation energy, ΔS^\ddagger is negative, and the reaction rate changes not only as a function of the electronic and steric properties of the tetrahydrofuran and furan incoming ligands but also as a function of the ligand concentration. Although readers might consider the cyclohexane solvent ligand to be very weakly attached to the metal, making the tungsten complex actually coordinatively unsaturated, Schultz pointed out that such metal–solvent complexes have a weakly bound (bond dissociation energy of 10–15 kcal/mol) solvent ligand and may represent the true “coordinatively unsaturated” species found in many catalytic cycles. Such species and the reactions

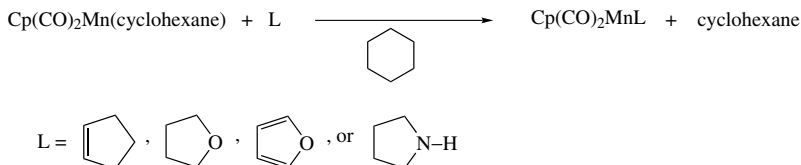
⁴⁴For a more recent example of apparent competing **D** and **I_d** pathways involving diphosphine substitution on $\text{M}(\text{CO})_4(\text{norbornadiene})$ ($\text{M} = \text{Cr}, \text{Mo}, \text{W}$), see A. Tekkaya and S. Özkaz, *J. Organomet. Chem.*, **1999**, 590, 208.

they undergo can be studied by a variety of spectroscopic methods on the nano- and picosecond time scale.⁴⁵



7.21

Reaction of $\text{CpMn(CO)}_2(\text{cyclohexane})$ with $\text{L} = \text{cyclopentene}$, THF, furan, and pyrrolidine (equation 7.22), on the other hand, appears to proceed by a mechanistically ambiguous route that seems best described by an I_d pathway. Again, fast kinetic methods were used to determine that there was not a strong dependence of the rate on the electronic and steric properties of different ligands, expected with A-type reactions (ΔH^\ddagger was relatively constant regardless of ligand), yet there was a linear dependence on ligand concentration. Although ΔS^\ddagger was negative with all ligands investigated, it was not highly so.⁴⁶



7.22

7-1-5 17-Electron Complexes

In contrast to the 18-electron V(CO)_6^- , which is extremely sluggish in its reaction with even molten PPh_3 , V(CO)_6 , a 17- e^- complex, reacts with PPh_3 readily at -70°C !⁴⁷ $(\text{MeCp})\text{Mn(CO)}_3$ is unreactive to substitution by PPh_3 after heating at 140°C for over three days,⁴⁸ yet it reacts with P(OEt)_3 completely in milliseconds

⁴⁵R. Krishnan and R. H. Schultz, *Organometallics*, **2001**, 20, 3314, and references therein.

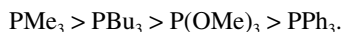
⁴⁶L. Lugovsky, J. Lin, and R. H. Schultz, *Dalton Trans.*, **2003**, 3103, and references therein.

⁴⁷J. E. Ellis, R. A. Faltynek, G. L. Rochfort, R.E. Stevens, and G. A. Zank, *Inorg. Chem.*, **1980**, 19, 1082.

⁴⁸R. J. Angelici and W. Loewen, *Inorg. Chem.*, **1967**, 6, 682.

after 1-electron oxidation to $[(\text{MeCp})\text{Mn}(\text{CO})_3]^+$.⁴⁹ Corresponding 17- e^- complexes generally seem to react much faster toward ligand substitution than their 18- e^- analogs.⁵⁰ Although dissociative or radical pathways are possible, more recent evidence points to an associative mechanism taking place in a number of cases involving Group 5 and 7 metals.

For example, in the substitution of $\text{V}(\text{CO})_6$ with phosphines, the rate of reaction varied with respect to change in phosphine nucleophile according to the order⁵¹



If the reaction mechanism involved a **D** pathway, a change in nucleophile would be expected to have little effect on the overall reaction rate, analogous to the $\text{S}_{\text{N}}1$ reaction in organic chemistry. The trend in reaction rate with respect to phosphine probably reflects a combination of steric and electronic factors. Trialkylphosphines are more electron rich and thus better σ bases (σ donors) than triarylphosphines or phosphites. Steric effects seem to play a role, and we would expect this to be the case since an associative reaction would involve a sterically congested ML_7 (19- e^-) intermediate or transition state. That is apparently why PMe_3 reacts faster than PBu_3 when both have about the same σ basicity. The reaction also shows negative values for the ΔS^\ddagger regardless of the nucleophile, consistent with an **A** mechanism. Finally, 19- e^- complexes, which typically have rather short lifetimes, have been generated electrochemically⁵² and their geometries calculated theoretically.⁵³ Substitution reactions that have been documented for 19- e^- complexes show a **D** mechanism.

Equation 7.23⁵⁴ demonstrates another example of an associative ligand substitution involving a 17- e^- substrate; the resulting 17- e^- substituted product then rapidly dimerizes.

⁴⁹Y. Huang, G. B. Carpenter, D. A. Sweigert, Y. K. Chung, and B. Y. Lee, *Organometallics*, **1995**, *14*, 1423.

⁵⁰M. C. Baird, *Chem. Rev.*, **1988**, *88*, 1217.

⁵¹Q.-Z. Shi, T. G. Richmond, W. C. Troglor, and F. Basolo, *J. Am. Chem. Soc.*, **1984**, *106*, 71.

⁵²For example, see C. C. Neto, S. Kim, Q. Meng, D. A. Sweigert, and Y. K. Chung, *J. Am. Chem. Soc.*, **1993**, *115*, 2077 and Y. Huang, C. C. Neto, K. A. Pevear, M. M. Banaszak Holl, D. A. Sweigert, and Y. K. Chung, *Inorg. Chim. Acta.*, **1994**, *226*, 53.

⁵³One of the problems in characterizing 19- e^- complexes is accounting for the location of the extra electron. Does it reside on the metal, or do the ligands “absorb” it? For more information on recent theoretical studies of 19- e^- complexes, see D. A. Braden and D. R. Tyler, *Organometallics*, **2000**, *19*, 3762.

⁵⁴T. R. Herrinton and T. L. Brown, *J. Am. Chem. Soc.*, **1985**, *107*, 5700.

Table 7-5 Characteristics of Ligand Substitution Reactions

Mechanism	Substrate Type	Rate Law ^a	ΔS [‡] (ΔV [‡])	Stereochemistry
A	16-e ⁻ square planar ^b	2 nd order	Negative	Retention
D	18-e ^{-c,d}	1 st order	Positive	Not well-defined
I _d	18-e ^{-c}	Complex	Negative	Not well-defined
I _a	18-e ^{-c}	Complex	Negative	Not well-defined

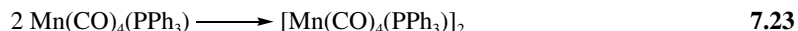
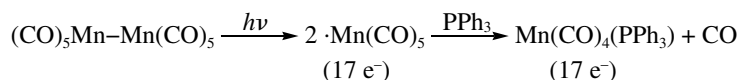
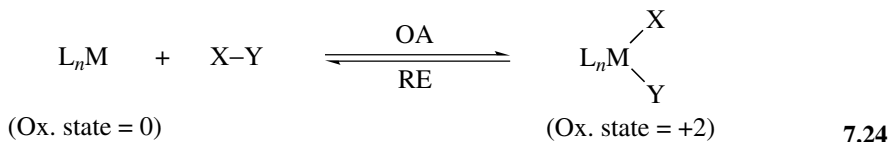
^aLimiting cases.^b17-e⁻ complexes also undergo associative substitution.^cDifferent geometries; octahedral is most common.^d19-e⁻ complexes undergo dissociative substitution.

Table 7-5 summarizes some of the characteristics of the types of ligand substitution reactions we have covered in Section 7-1.

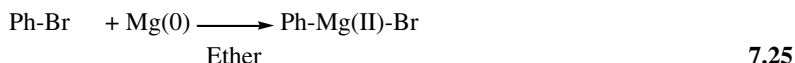
7-2 OXIDATIVE ADDITION

Oxidative addition (OA) and its reverse-reaction counterpart, reductive elimination (RE), play important roles as key steps in catalytic cycles (see Chapter 9) and in synthetic transformations (see Chapter 12). In the broadest sense, OA involves the attachment of two groups X–Y to a metal complex of relatively low oxidation state. This produces a new complex with an oxidation state two units higher than before, an increase in coordination number of two, and an electron count two higher than present in the starting material. Equation 7.24 outlines the essential changes present in an OA (and, of course, in the reverse direction, RE).

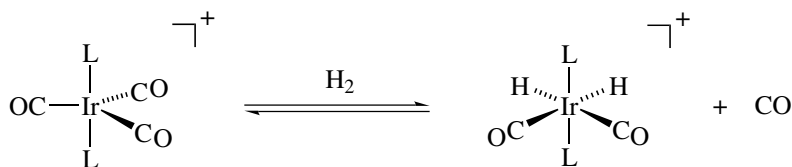


Readers familiar with organic chemistry will recognize that the formation of a Grignard reagent is really an OA, as illustrated in equation 7.25. Here phenyl magnesium bromide forms when the phenyl group and bromide add to elemental magnesium. Note that the oxidation state of the metal changes from zero to +2. Group 1 and 2 metals are capable of undergoing OA in the metallic state and

differ from the mid to late transition metals, which require the prior association of ligands to the metal atom before reaction occurs.



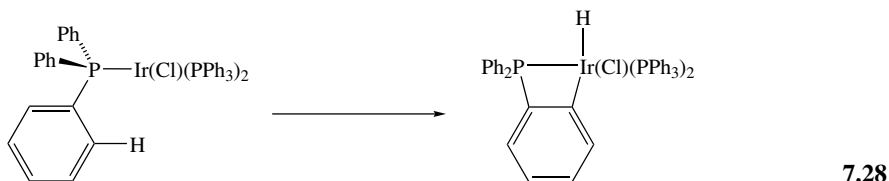
Oxidative additions typically occur on transition metal complexes with counts of 16 electrons or fewer. Addition is possible to 18-electron complexes; however, loss of a ligand (dissociation) must occur first (equation 7.26).⁵⁵



A binuclear variant of OA may occur where each metal increases in oxidation state by one unit. Equation 7.27 shows one such example.⁵⁶



Finally, OA may occur intramolecularly, as equation 7.28 demonstrates. Intramolecular additions of this type are called *cyclometallations* or, more specifically, an *orthometallation* in the case shown.

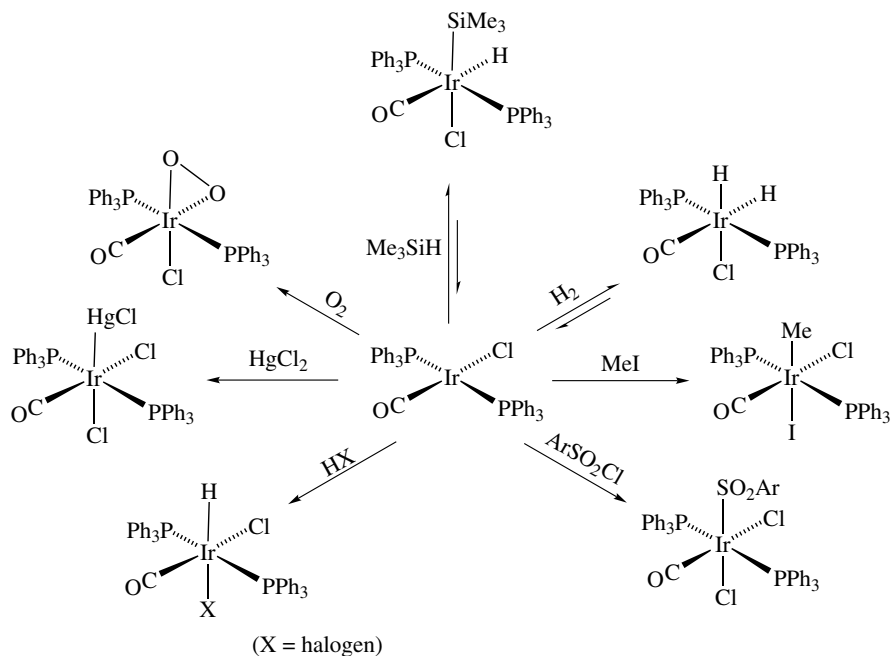


Verify that equations 7.26 and 7.28 are oxidative additions.

Exercise 7-3

⁵⁵M. J. Church, M. J. Mays, R. N. F. Simpson, and F. P. Stephanini, *J. Chem. Soc. A*, **1970**, 2909.

⁵⁶It should be pointed out that in equation 7.27 the metal undergoes oxidation, but the coordination number of the metal does not change.



Scheme 7.3
Oxidative Addition
Reactions of Vaska's
Compound

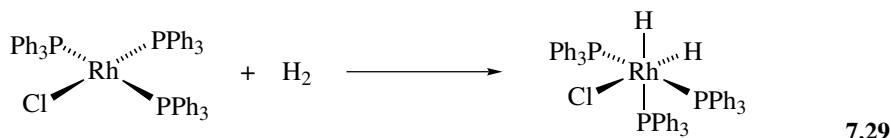
One of the first detailed studies of OA was performed by L. Vaska⁵⁷ on 16-electron square planar iridium complexes, the most notable of which is currently known as Vaska's compound, the central compound in Scheme 7.3. The reactions portrayed in Scheme 7.3 indicate that several different kinds of molecules react with the iridium complex. Mechanistic pathways leading to the products shown and to products resulting from other metal complexes are many and varied. We will consider a few of these mechanistic types, trying to point out as we go along similarities to other reactions from the realm of organic chemistry.

7-2-1 3-Center Concerted Addition

Addition of H₂

The addition of dihydrogen to Vaska's compound (Scheme 7.3) is an excellent example of concerted, 3-center, *syn* addition in which the transition state is a three-membered ring consisting of the metal and the two hydrogen atoms. Addition of H₂ to Wilkinson's catalyst, an early step in the homogeneous catalytic hydrogenation of alkenes (to be discussed in Chapter 9), serves as another well-known example (equation 7.29).

⁵⁷L. Vaska and J. W. Diluzio, *J. Am. Chem. Soc.*, **1962**, 84, 679.



Addition of dihydrogen to Vaska's compound is feasible thermodynamically when one compares the bond dissociation energy of dihydrogen (104 kcal/mol) with the energy released when two Ir–H bonds form (ca. 120 kcal/mol total). Because the reaction is of the associative type, the entropy change ought to be negative; experiment indicates $\Delta_r S^\circ = -30$ eu. Thus, the free energy change turns out to be slightly negative ($\Delta_r G^\circ = -7$ kcal/mol at 25 °C), implying that the reaction could be reversible under suitable conditions.

Rate studies of H_2 addition to square–planar complexes have been conducted.⁵⁸ Measurements at room temperature in several aromatic solvents yield a bimolecular rate law:

$$\text{Rate} = k_{\text{obs}}[(PPh_3)_2(CO)(Cl)Ir][H_2].$$

The ΔH^\ddagger is low (10–12 kcal/mol), the entropies of activation are negative ($\Delta S^\ddagger = -20$ to -23 eu), and the reaction is exergonic, all of which suggest an early transition state (according to the Hammond postulate) and an OA reaction in the rate-determining step. Figure 7-7 shows a reaction coordinate–energy profile for concerted addition of dihydrogen to a metal complex.

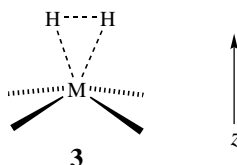
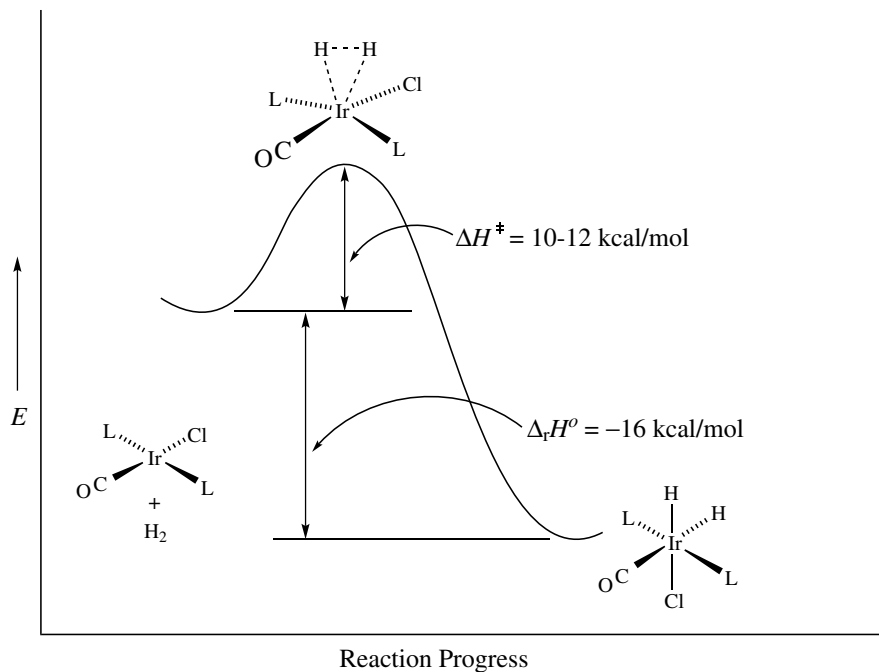
Several theoretical investigations of dihydrogen addition have employed MO theory to show the interaction of H_2 with the orbitals on the metal complex.⁵⁹ Calculations involving square–planar molecules show that two interactions are most connected with the breaking of the H–H bond and the formation of two M–H bonds as dihydrogen approaches the metal in a “parallel” manner. Detailed analysis indicates that, when the square–planar geometry distorts to an angular geometry **3**,⁶⁰ two important interactions may occur that lower the energy of the pathway to the transition state as the dihydrogen molecule approaches the metal complex.

⁵⁸P. Zhou, A. A. Vitale, J. San Filippo, Jr., and W. H. Saunders, Jr., *J. Am. Chem. Soc.* **1985**, *107*, 8049.

⁵⁹J. J. Low and W. A. Goddard, III, *J. Am. Chem. Soc.*, **1984**, *106*, 6928. A recent study of H_2 addition to a bis(2,2'-bipyridine)rhodium(I) complex yielded similar results for the structure of the transition state as well as values for ΔH^\ddagger , ΔS^\ddagger , $\Delta_r H^\circ$, and $\Delta_r S^\circ$ comparable to those found for H_2 addition to Vaska's compound. See E. Fujita, B. S. Brunschwig, C. Creutz, J. T. Muckerman, N. Sutin, D. Szalda, and R. van Eldik, *Inorg. Chem.*, **2006**, *45*, 1595.

⁶⁰A. Didieu and A. Strich, *Inorg. Chem.*, **1979**, *18*, 2940.

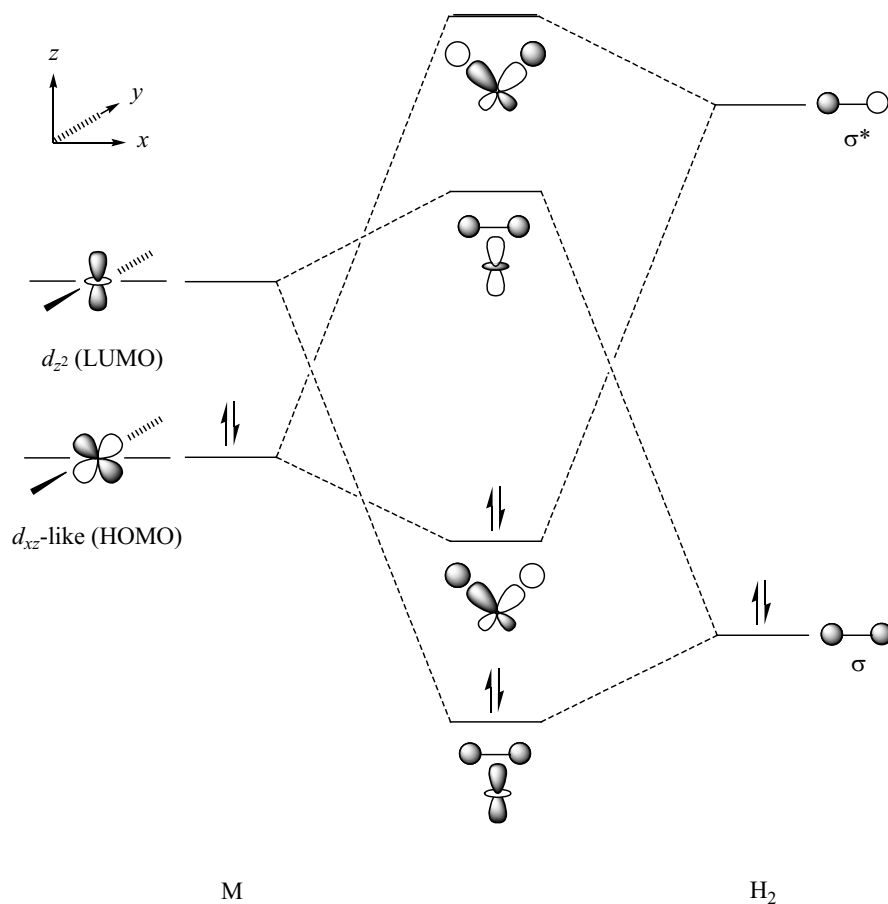
Figure 7-7
Reaction Progress-
Energy Diagram
for the Addition
of H₂ to Vaska's
Compound



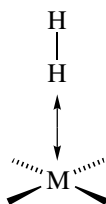
1. The LUMO of the metal (d_{z^2} , also known as a d_σ orbital), possessing a symmetry compatible with the σ bonding orbital of H_2 (HOMO), interacts in a bonding manner.
2. The HOMO becomes much the same as a d_{xz} (or d_π) orbital, allowing a bonding interaction with the σ^* orbital of H_2 , which possesses the same symmetry.

Building on the discussion in Sections 6-2-1 and 6-2-2, we see that the interaction between the σ orbital of H_2 and the LUMO of the metal in Figure 7-8 represents σ electron donation from H_2 to the metal, and it is bonding.⁶¹ The second interaction is that between the HOMO of the metal and the σ^* orbital of H_2 . This corresponds to a back-bonding π donation from the metal to H_2 , thus weakening the H-H

⁶¹Net repulsive interactions of the H_2 σ orbital with filled metal orbitals are also possible and these would lower the overall effectiveness of the bonding; see J-Y. Saillard and R. Hoffmann, *J. Am. Chem. Soc.* **1984**, 106, 2006.

**Figure 7-8**

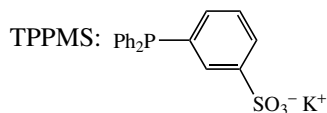
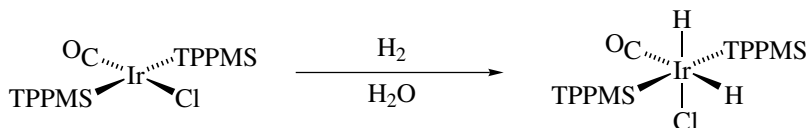
Interactions of Frontier Orbitals and H₂ Molecular Orbitals

**Figure 7-9**

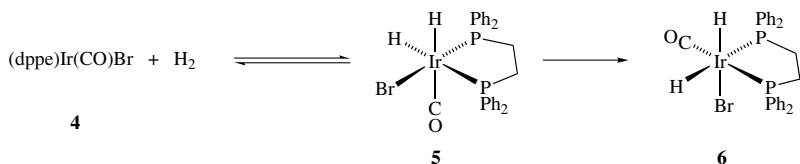
"Perpendicular" Approach of H₂ to Metal Complex

bond. A "perpendicular" approach of dihydrogen to the metal complex (Figure 7-9) seems to require a much higher energy transition state based on MO theory.

By now, such donor–acceptance ligand bonding interactions should be quite familiar (recall that in Chapter 6 it was established that the dividing line between a true dihydride and a dihydrogen–metal complex is a subtle one). Equations 7.30 and 7.31 show other examples of OA of dihydrogen.



7.30



7.31

Equation 7.30 demonstrates the increasing use of the green solvent H_2O (see Section 9-1-5 for more discussion on green chemistry) as a reaction medium for organometallic reactions; in this case the product is the result of *syn* addition of H_2 , which is exactly the same result observed in organic solvents.⁶² The TPPMS (triphenylphosphine *m*-monosulfonate) group attached to phosphorus makes both the phosphine and the resulting Ir complex water soluble.

The addition of H_2 to complex **4** to yield **5** is interesting (equation 7.31). Originally, it was thought that **5** formed under kinetic control by parallel addition of H_2 along the P–Ir–CO axis. Rearrangement of **5** to its thermodynamically more stable diastereomer **6** occurred via reversible loss of H_2 , followed by OA again of H_2 parallel to the P–Ir–Br axis. Closer examination of the reaction revealed that the rearrangement of **5** to **6** also involved a bimolecular reaction between **4** and **5**.⁶³

Exercise 7-4

- Verify that compound **5** forms by parallel addition of H_2 along the P–Ir–CO axis and **6** forms as a result of H_2 adding parallel to the P–Ir–Br axis.
- Why is compound **6** more stable than **5**?

⁶²D. R. Paterniti, P. J. Roman, Jr., and J. D. Atwood, *Organometallics*, **1997**, *16*, 3371.

⁶³C. E. Johnson and R. J. Eisenberg, *J. Am. Chem. Soc.*, **1985**, *107*, 3148; and A. J. Kunin, C. E. Johnson, J. A. Maquire, W. D. Jones, and R. Eisenberg, *J. Am. Chem. Soc.*, **1987**, *109*, 2963; for recent work involving addition of H_2 to Ir complexes with chiral diphosphine ligands, see A. Ç. Atesin, S. B. Duckett, C. Flaschenriem, W. W. Brennessel, and R. Eisenberg, *Inorg. Chem.*, **2007**, *46*, 1196.

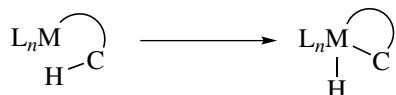
Addition of C–H

Although intra- or intermolecular OA of a C–H bond to a metal (equation 7.32) is not, strictly speaking, the addition of a symmetrical addendum,⁶⁴ it is a reaction where the C–H bond of the oxidizing agent possesses electronic characteristics similar to that of the H–H bond.



or

R = alkyl, aryl, vinyl, alkynyl



7.32

The study of C–H bond OA, also called *C–H bond activation*, represents an area of research that has seen an enormous increase in activity over the past 20 years. These efforts have given us numerous examples of the addition of a C–H bond (especially intermolecular addition) to a transition metal and have increased our understanding of the reaction mechanisms involved.⁶⁵ C–H activation is important because it allows direct binding to occur between a metal and a relatively abundant and normally unreactive organic molecule (e.g., methane, ethane, or benzene). Subsequent transformations of the resulting C–M bond lead to substituted hydrocarbons containing a variety of functional groups that would be difficult to introduce directly on the free hydrocarbons themselves by conventional organic chemistry (for example, the conversion of CH₄ to CH₃OH). We will see several examples of such transformations in later chapters. Moreover, if C–H bond activation and subsequent transformation are catalytic in transition metals, then the process could become chemically selective, economical, and green.

Examples of intramolecular C–H activation (or cyclometallation) were initially more common than intermolecular cases, probably due to the favorable entropy effect of having both the metal and the C–H group within the same molecule, but work in recent years has provided numerous intermolecular C–H activation transformations. Regardless of the mode of addition, C–H activation is inherently more difficult than OA of dihydrogen for several reasons.

Table 7-6 shows that transition metal–hydrogen bonds are typically stronger (but not always significantly stronger) than M–C bonds, and both types of bonds

⁶⁴The group, X–Y, adding to the metal is called the *addendum* or the oxidizing agent.

⁶⁵For reviews that give examples of C–H bond activation, see R. H. Crabtree, *J. Chem. Soc. Dalton Trans.*, **2001**, 2437; V. Ritleng, C. Sirlin, and M. Pfeffer, *Chem Rev.*, **2002**, 102, 1731; and C.-H. Jun and J. H. Lee, *Pure Appl. Chem.*, **2004**, 76, 577.

Table 7-6 Selected Experimentally Derived M–H and M–C Bond Dissociation Energies (kcal/mol) Compared with Those of C–H and C–C Bonds^{a,b}

C–H 85 → 105 (H-allyl → CH ₃ -H)					
Ti–H ^c	45	Cp(CO) ₃ Cr–H	62	(CO) ₄ Co–H	66
Cp ⁺ (H)Zr–H	78	Cp(CO) ₃ Mo–H	69	Cp(CO) ₂ Rh ⁺ –H	69
Cp ⁺ (H)Hf–H	80	Cp(CO) ₃ W–H	72	(CO)(PPh ₃)Cl ₂ Ir–H	59
C–C 75 → 93 (C-allyl → C-Ph)					
Ti–CH ₃ ^c	42	Cr–CH ₃ ^c	34	Co–CH ₃ ^c	42
Cp ⁺ (CH ₃) ₂ Zr–CH ₃	66	Cp(CO) ₃ Mo–CH ₃	48	Rh ⁺ –CH ₃ ^c	34
Cp ⁺ (CH ₃) ₂ Hf–CH ₃	70	W ⁺ –CH ₃ ^c	53	Ir ⁺ –CH ₃ ^c	75

^aData taken from J. Uddin, C. M. Morales, J. H. Maynard, and C. R. Landis, *Organometallics*, **2006**, *25*, 5566.

^bDetermined at 298 K unless otherwise specified.

^cDetermined at 0 K by ion beam mass spectrometry.

usually increase in strength as one goes down a column in the periodic table.⁶⁶ Because the H–H bond (BDE = 104 kcal/mol) and a C–H bond (BDE is up to 105 kcal/mol) are roughly comparable in energy, the resulting L_nM(H)(H) adduct typically possesses more bond energy than the comparable L_nM(R)(H) product. The former process is thus usually more feasible thermodynamically.

As the C–H bond approaches the metal, steric hindrance is greater than that from the approach of dihydrogen, so one might expect that steric hindrance may cause C–H activation to be kinetically less feasible than OA of H₂. Indeed, workers have shown that it is the bond between a primary alkane carbon and hydrogen that is more likely to add to the metal rather than bonds between hydrogen and secondary or tertiary carbons.

From a molecular orbital standpoint, it is possible to do an analysis of C–H OA similar to that for addition of H₂ (Figure 7-8). The non-spherical nature of the σ C–H bonding orbital, however, makes its overlap with the metal's empty d_{z²}-like orbital or dsp-hybridized orbital (d_σ) of comparable symmetry less favorable than that of the σ (H₂) orbital (Figure 7-10). Also, the interaction of the filled d_{xz}-like metal orbital (d_π) with the C–H σ* orbital (back-bonding) is weaker because the latter orbital is unsymmetrical, not directed toward the metal, and less spherical in nature than the comparable dihydrogen orbital;

⁶⁶The following two papers compare M–C and H–C bond strengths on the basis of high-level MO calculations: E. Clot, C. Mégret, O. Eisenstein, and R. N. Perutz, *J. Am. Chem. Soc.*, **2006**, *128*, 8350 and M. Mitoraj, H. Zhu, A. Michalak, and T. Ziegler, *Organometallics*, **2007**, *26*, 1627.

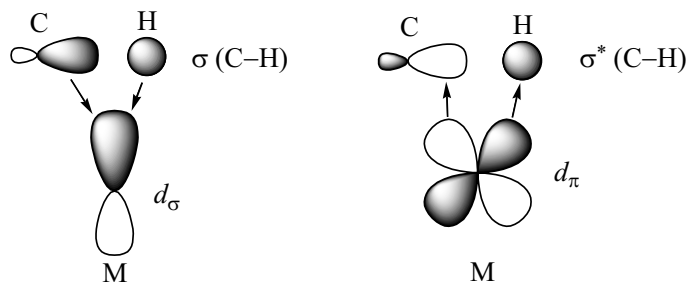
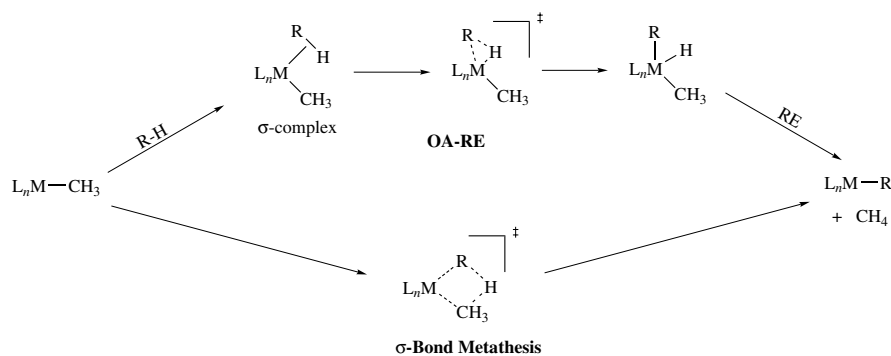


Figure 7-10

Interactions of Frontier Metal and C-H Molecular Orbitals



Scheme 7.4

C-H Activation Mechanistic Pathways

overall, therefore, C-H bonds tend to be weaker σ donors and π acceptors than H-H bonds.⁶⁷

Based on the simple MO analysis described above and analogous to the addition of H₂, the simplest mechanism for C-H activation would be a one-step, concerted three-center addition of the C-H bond to a metal complex. Calculations and experiment, however, suggest a more complicated picture. As the C-H bond approaches the metal, a σ -complex intermediate forms, which then goes through a three-center transition state to give the adduct (Scheme 7.4).⁶⁸ If another *hydrocarbyl* group⁶⁹ is already attached to the metal, an exchange of R groups

⁶⁷K. Krogh-Jespersen and A. S. Goldman, "Transition States for Oxidative Addition to Three-Coordinate Ir(I): H-H, C-H, C-C, and C-F Bond Activation Energies," In *Transition State Modeling for Catalysis*, D. G. Truhlar and K. Morokuma, Eds., ACS Symposium Series 721, American Chemical Society: Washington, D. C., 1999, pp. 151-172.

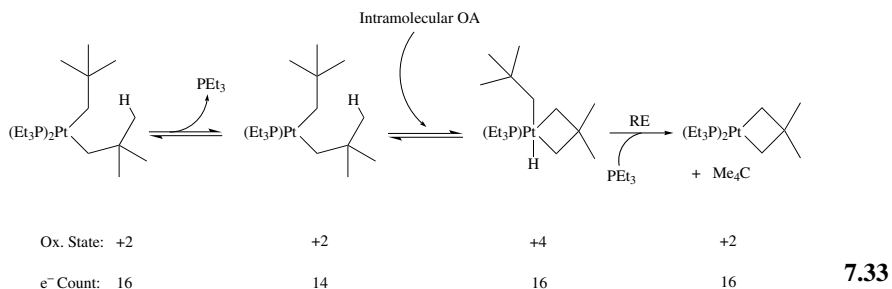
⁶⁸S. Sakaki, *Topics in Organomet. Chem.*, **2005**, 12, 31; E. S. Xavier, W. B. De Almeida, J. C. S. da Silva, and W. Rocha, *Organometallics*, **2005**, 24, 2262; and S. Bi, Z. Zhang, and S. Zhu, *Chem. Phys. Lett.*, **2006**, 431, 385.

⁶⁹The word "hydrocarbyl" is used to describe a σ -bonded hydrocarbon ligand that may be an alkyl, aryl, or vinyl group, for example.

can occur via a reductive elimination reaction (Section 7-3). Other mechanistic paths are possible, and one in particular is also shown in Scheme 7.4— σ -bond metathesis. Note that this mechanism does not require a change in oxidation state of the metal. This latter pathway is likely for early d^0 transition metal complexes, where the OA mechanism is not available, but it has also been suggested as a mechanistic possibility for some C–H activations involving middle to late transition metals.⁷⁰ Sigma bond metathesis is a very important fundamental organometallic reaction, which we will see again in Chapter 11.

The reaction described in equation 7.33 exemplifies intramolecular C–H activation (cyclometallation) followed by reductive elimination (see Section 7-3) of neopentane.⁷¹ Another more recent example (equation 7.34) was designed to demonstrate intramolecular competition between aryl C–H and alkyl C–H bond activation.⁷² Interestingly, in this case, alkyl C–H addition to the metal occurred to the exclusion of aryl C–H addition, although other experimental work and theoretical investigations indicate that the preference for either intra or intermolecular C–H activation is to be C–H (sp^2 aryl or vinyl) > I° C–H (sp^3) > II° C–H (sp^3) > III° C–H (sp^3) > I° C–H (sp^3 allyl or benzyl), a trend that is in accord with decreasing C–H bond dissociation energy.⁷³ Relief of steric crowding when a C–H bond from the bulky *tert*-butyl group reacts rather than the aryl C–H group was offered as a possible explanation for the unusual preference shown.

The years 1982 and 1983 saw exciting new developments in direct intermolecular C–H activation when three research groups independently reported similar alkane C–H additions to electron-rich 16-electron Ir(I) and

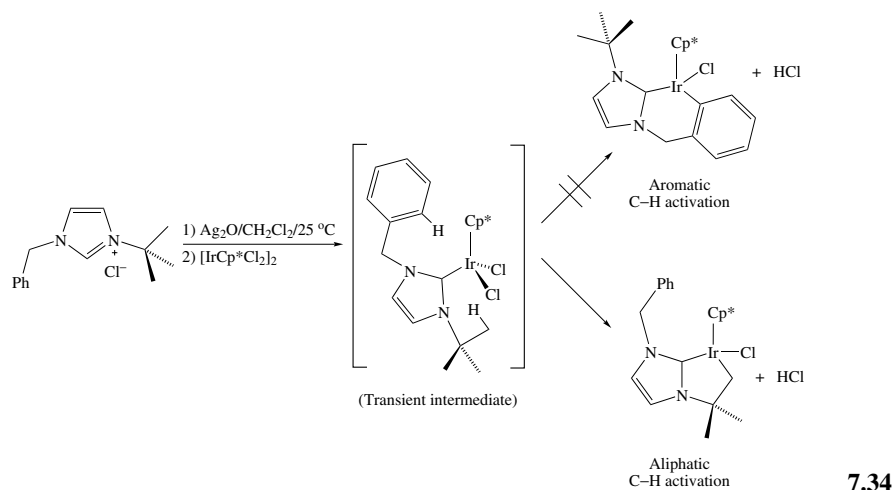


⁷⁰For a review and discussion of various C–H activation mechanisms, see M. Lersch and M. Tilset, *Chem. Rev.*, **2005**, *105*, 2471; R. N. Perutz, B. A. Vastine and M. B. Hall, *J. Am. Chem. Soc.*, **2007**, *129*, 12068; and S. Sabo-Etienne, *Angew. Chem. Int. Ed.*, **2007**, *46*, 2578.

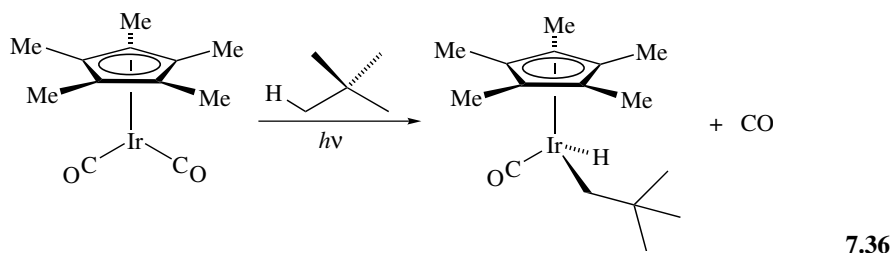
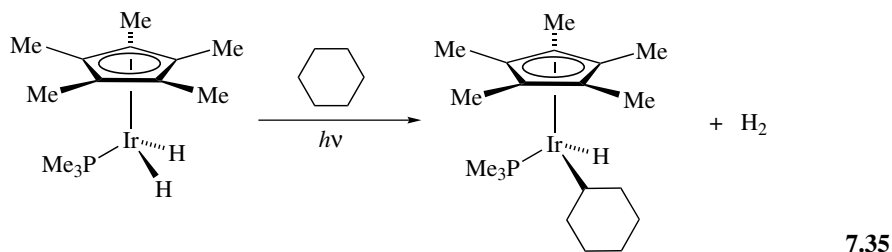
⁷¹J. A. Ibers, R. DiCosimo, and G. M. Whitesides, *Organometallics*, **1982**, *1*, 13.

⁷²R. Corberán, M. Sanaú, and E. Peris, *Organometallics*, **2006**, *25*, 4002.

⁷³J. S. Owen, J. A. Labinger, and J. E. Bercaw, *J. Am. Chem. Soc.*, **2006**, *128*, 2005 and M. Mitoraj, J. Zhu, A. Michalak, and T. Ziegler, *Organometallics*, **2007**, *26*, 1627.



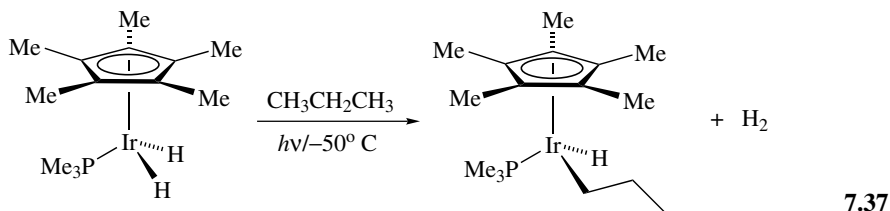
Rh(I) complexes. Equations 7.35,⁷⁴ 7.36,⁷⁵ and 7.37⁷⁶ show these results. All the examples first involve production of a reactive, electron-rich, 16-electron complex by photoactivated reductive elimination of H₂ or loss of a neutral ligand. This is a rather general reaction for a variety of alkanes and arenes that react not only with Ir and Rh complexes, but also with low-valent Ru, Pt, and Os complexes.



⁷⁴A. H. Janowisz and R. G. Bergman, *J. Am. Chem. Soc.*, **1982**, 104, 352.

⁷⁵J. K. Hoyano and W. A. G. Graham, *J. Am. Chem. Soc.*, **1982**, 104, 3723.

⁷⁶W. D. Jones and F. J. Feher, *Organometallics*, **1983**, 2, 562.



More recently, Bergman's group has expanded the scope of C–H activation using Ir(III) complexes, which are not as electron rich as the Ir(I) complexes, as illustrated in Scheme 7.5. The starting material contains a weakly coordinating ligand (CF_3SO_2^- , also known as triflate and abbreviated OTf), which is easily lost, producing a 16- e^- reactive intermediate. The presence of a CH_3 ligand in the starting material allows for loss of CH_4 by reductive elimination, which is a driving force for the overall reaction whose last step is 1,2-elimination. Despite the lack of electron richness of the Ir(III) complex, the reaction produces a strong M–C bond because third-row transition metals tend to form the strongest M–C and M–H bonds (*vide supra*—Table 7-6). This is another driving force for the reaction. The initial oxidative addition product is not observed, but its existence is implied by the nature of the products obtained. Detailed experimental⁷⁷ and theoretical investigations⁷⁸ showed that the mechanism most likely goes through an Ir(V) intermediate after OA, which is followed by a reductive elimination to form CH_4 . The alternate pathway involving a σ bond metathesis probably does not occur.

Exercise 7-5

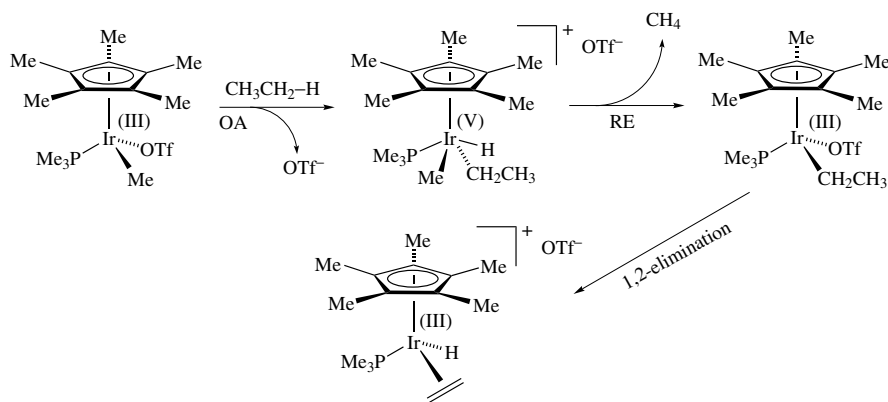
Propose a structure for the final product in Scheme 7.5 if the hydrocarbon added in the first step were benzene instead of ethane.

In general, intermolecular C–H OA is favorable if (1) the metal complex is coordinatively unsaturated, (2) the metal complex is relatively sterically uncongested, (3) the metal is a second- or preferably a third-row element, (4) electron-rich PR_3 ligands are attached to the metal such that the R groups on the phosphine are resistant to cyclometallation (e.g., $\text{R} = \text{CH}_3$, and (5) the metal has a filled orbital capable of interacting with the σ^* antibonding orbital of the C–H bond.⁷⁹ C–H activation continues to be a very active area of research, and a major goal

⁷⁷S. R. Klei, T. D. Tilley, and R. G. Bergman, *J. Am. Chem. Soc.*, **2000**, *122*, 1816 and P. Burger and R. G. Bergman, *J. Am. Chem. Soc.*, **1993**, *115*, 10462.

⁷⁸S. Niu and M. B. Hall, *J. Am. Chem. Soc.*, **1998**, *120*, 6169.

⁷⁹R. H. Crabtree, *Chem. Rev.*, **1985**, *85*, 245.

**Scheme 7.5**

C-H Activation of an Ir(III) complex

is now to make this reaction both specific for particular C-H bonds and catalytic with regard to the transition metal complex. The reactions above are stoichiometric, but we will see examples of transition metal-catalyzed C-H bond activations in later chapters.⁸⁰

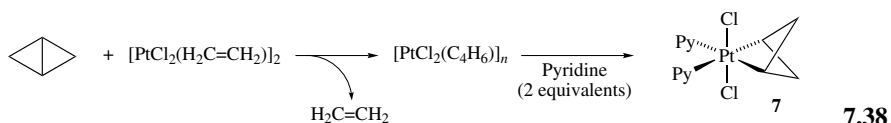
Addition of C-C

Oxidative addition of a C-C bond (C-C bond activation) to a metal, like C-H addition, is potentially very important on both a laboratory and an industrial scale. If a metal complex were available that could react via OA with a specific alkane C-C bond, for example, the ultimate result would be exclusive functionalization of a normally unreactive carbon atom. Once that occurs, there are numerous transformations available to convert the M-C bond to other functionalities. Catalytic activation of C-C bonds in long-chain hydrocarbons found in petroleum could provide low-energy, efficient routes to production of compounds that are useful in gasoline refining. Unfortunately, unstrained C-C bonds—the type found in saturated hydrocarbons—typically do not readily undergo OA for the same reasons associated with lack of reactivity of C-H bonds. In fact, the situation ought to be worse with C-C bond activation, because OA now produces not one but two M-C bonds at the expense of breaking a robust C-C bond. There should, moreover, be more steric hindrance created when a C-C bond approaches

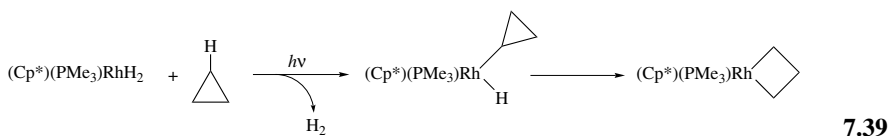
⁸⁰It must be pointed out that there are other complications regarding the addition of alkyl C-H bonds to a metal. The resulting metal alkyl complex could undergo either reductive elimination back to starting material (Section 7-3) or, if a β C-H bond is present, rapid 1,2-elimination (see Scheme 7.5, Section 6-1-1, and Chapter 8). The latter outcome may not be so bad, however, if the goal of C-H activation is to convert an alkane to an alkene, a compound possessing a functional group associated with a rich chemistry. See O. Eisenstein and R. H. Crabtree, *New J. Chem.*, **2001**, 25, 665, for a discussion of the interplay between 1,2-elimination and RE after C-H activation has occurred.

a metal complex compared with a C–H bond. Finally, the orbital interactions between a $C(sp^3)$ – $C(sp^3)$ bond and a metal are either not as favorable or about as favorable as those existing with the approach of $C(sp^3)$ –H to a metal complex. Most examples of C–C OA have involved the reaction of cyclic hydrocarbons with at least one highly strained, relatively weak C–C bond. Here, relief of ring strain is a driving force in the reaction. Several such examples follow.

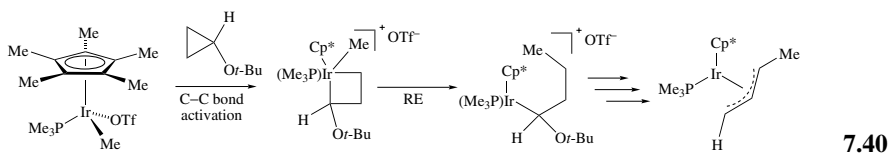
Reaction of the platinum complex known as Zeise's dimer with bicyclo[1.1.0]butane, which contains a highly strained bridging bond, gives the corresponding platinabicyclo[1.1.1]pentane (**7**) (equation 7.38) as a stable, crystalline solid.⁸¹



Equation 7.39 describes a transformation with first the C–H bond of cyclopropane adding to the Rh complex, followed by RE of H_2 , and then rearrangement to give the rhodacyclobutane.⁸² Metallacyclobutanes are thought to be intermediates in some alkene polymerization and metathesis reactions; these compounds will appear again in Chapter 11.



Using the same Ir(III) complex shown in Scheme 7.5, Bergman was able to demonstrate that direct C–C bond activation occurred (equation 7.40).⁸³



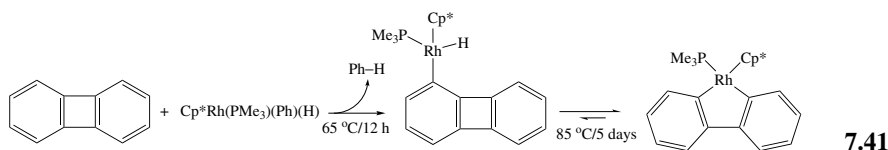
Although readers might expect that C–H bond activation would lead to a more stable adduct than OA of a C–C bond, and thus always be preferred in systems where there is a choice between the two modes of activation, that is not

⁸¹A. Miyashita, M. Takahashi, and J. Takaya, *J. Am. Chem. Soc.*, **1981**, 103, 6257.

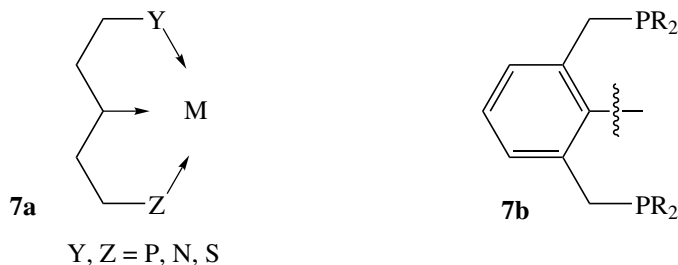
⁸²R. A. Periana and R. G. Bergman, *J. Am. Chem. Soc.*, **1986**, 108, 7346.

⁸³M. R. Anstey, C. M. Yung, J. Du, and R. G. Bergman, *J. Am. Chem. Soc.*, **2007**, 129, 776.

always the case. The last 10–15 years have seen many more examples of C–C bond activation, some of which do not involve reaction of strained C–C bonds. The following two cases indicate that C–C bond activation is not only competitive with OA of C–H, but may even be preferred. Equation 7.41 shows the Rh complex first undergoing OA of an aryl C–H bond to give the first product. Further heating over time produces the thermodynamically-more-stable, five-membered ring metallacycle that resulted from C–C bond activation.⁸⁴



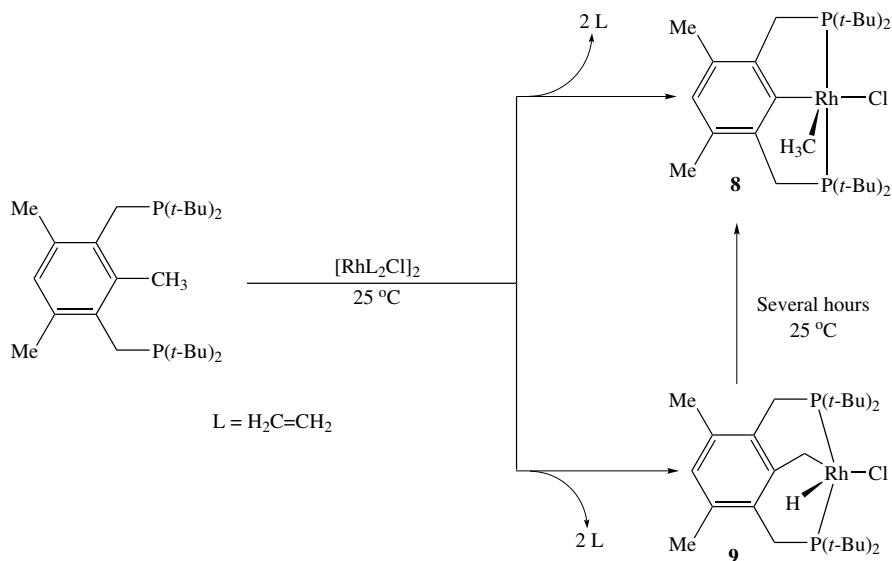
Milstein and co-workers⁸⁵ have studied OA and RE reactions of Rh and Ir complexes containing tridentate pincer ligands, which are generalized as structure **7a**; **7b** shows a specific pincer ligand type called PCP (two phosphorous atoms and a carbon bond to the metal). Such ligands resist degradation at relatively high temperatures and possess a huge variety of steric and electronic properties as a result of varying the substituents on the heteroatom Y and Z groups.⁸⁶ The high steric bulk of the *tert*-butyl groups on phosphorus of the particular *t*-BuPCP ligand used in Scheme 7.6 brings the substituted benzene into close proximity to the metal and allows direct comparison of the OA of a benzylic C–H bond and an aryl–CH₃ bond.



⁸⁴C. Perthuisot and W. D. Jones, *J. Am. Chem. Soc.*, **1994**, *116*, 3647.

⁸⁵B. Rybtchinski and D. Milstein, *Angew. Chem. Int. Ed.*, **1999**, *38*, 870 and B. Rybtchinski, A. Vialok, Y. Ben-David, and D. Milstein, *J. Am. Chem. Soc.*, **1996**, *118*, 12406.

⁸⁶For a recently-published book containing numerous examples of C–H and C–H activation as well as several other organometallic reactions involving pincer ligands, see D. Morales-Morales, *The Chemistry of Pincer Compounds*, Elsevier: Amsterdam, 2007.

**Scheme 7.6**

C–C Bond
Activation with a
PCP–Rh Complex

Even at room temperature, product **8**, the result of C–C bond activation, formed along with compound **9** (C–H activation). Continued reaction after several hours resulted in conversion of **9** to **8**. The experiment suggested that the kinetic barriers to C–H and C–C activation were indeed similar, and that overall there was a thermodynamic preference for C–C activation.

In addition to the stoichiometric C–C OA reactions discussed so far, there are now numerous examples of catalytic transformations where at some point in the catalytic cycle a C–C bond activation occurs. Some of these are quite useful to synthesis chemists.⁸⁷

Exercise 7-6

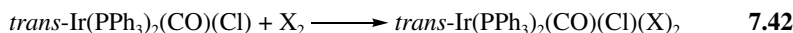
Suggest two reasons why the reactions described in Equation 7.41 and Scheme 7.6 might be favorable thermodynamically compared with addition of a relatively unstrained C(sp³)–C(sp³) bond to the same metals.

⁸⁷For a review of catalytic C–C bond activation, see C.-H. Jun, *Chem. Soc. Rev.*, **2004**, 33, 610.

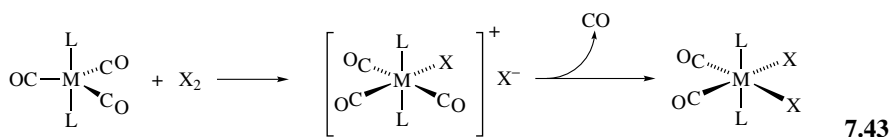
7-2-2 Polar Oxidative Addition Pathways

Addition of X_2

The OA of halogens, X_2 ($X = \text{Cl}, \text{Br}, \text{or I}$), to square-planar complexes involving such d^8 metals as Rh(I) or Ir(I) typically gives *trans* addition, as illustrated in equation 7.42.⁸⁸



The mechanism probably involves a two-step process in which the relatively electron-rich metal abstracts X^+ from X_2 (much like addition of halogen to a double bond in organic chemistry) followed by capture of the positively charged metal complex by the remaining X^- . Interestingly, the stereochemistry resulting from halogen attack on d^8 trigonal bipyramidal complexes ($M = \text{Fe}, \text{Ru}, \text{or Os}$; $L = \text{phosphine}$) is *cis* (equation 7.43). This apparently results from a two-step mechanism in which the complex attacks the halogen to form an octahedral cation complex, which is followed by loss of a neutral ligand and, finally, collapse of the outer sphere halide ion to give overall *cis* stereochemistry.⁸⁹



Why does the *cis*-dihalo product form in equation 7.43 and not the *trans*-dihalo isomer? [Hint: See Section 7-1-1.]

Exercise 7-7

Oxidative Addition of $R-X$

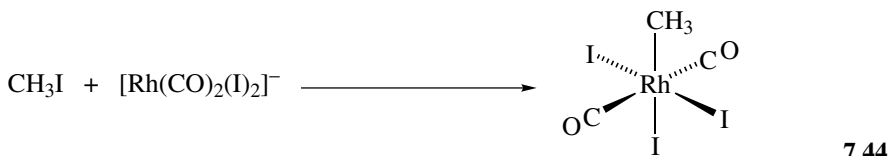
When $R = \text{alkyl}$ (especially CH_3), the metal complex can behave as a nucleophile attacking an alkyl or acyl halide. Such reactions, occurring typically on 16-e^- square planar complexes, have been well studied.⁹⁰ The first step involves

⁸⁸J. P. Collman and C. T. Sears, Jr., *Inorg. Chem.*, **1968**, 7, 27; see also A. Yahav, I. Goldberg, and A. Vigalok, *Organometallics*, **2005**, 24, 5654, for a more modern example of addition of X_2 , which in this case involves reaction of I_2 with *cis*- and *trans*-(Et_3P) $_2$ (*p*-fluorophenyl) $_2$ Pt complexes to give initial *trans* addition of I_2 followed by rearrangement to the same *cis*-diiodo Pt complex.

⁸⁹J. P. Collman and W. R. Roper, "Oxidative-Addition Reactions of d^8 Complexes," in *Advances in Organometallic Chemistry*, F. G. A. Stone and R. West, Eds., Academic Press: New York, 1968; Vol. 7, pp. 53–94.

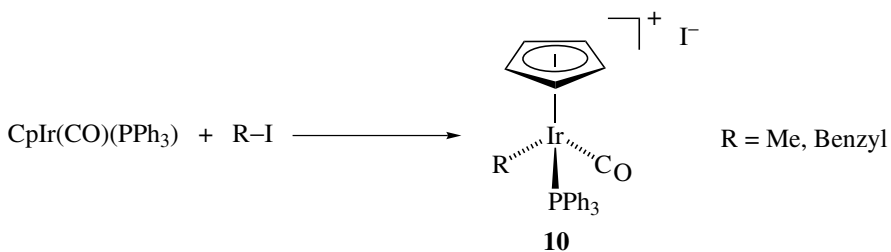
⁹⁰R. J. Cross, *Chem. Soc. Rev.*, **1985**, 14, 197.

nucleophilic displacement of the leaving group followed usually (but not always) by combination of the leaving group and substituted metal complex, the prototypical example of which appeared in Scheme 7.3 (Section 7-2), where CH_3I adds to Vaska's compound. Another excellent example of OA of CH_3I to a metal occurs as a key step in the Monsanto acetic acid synthesis (to be discussed in Chapter 9), shown in equation 7.44.

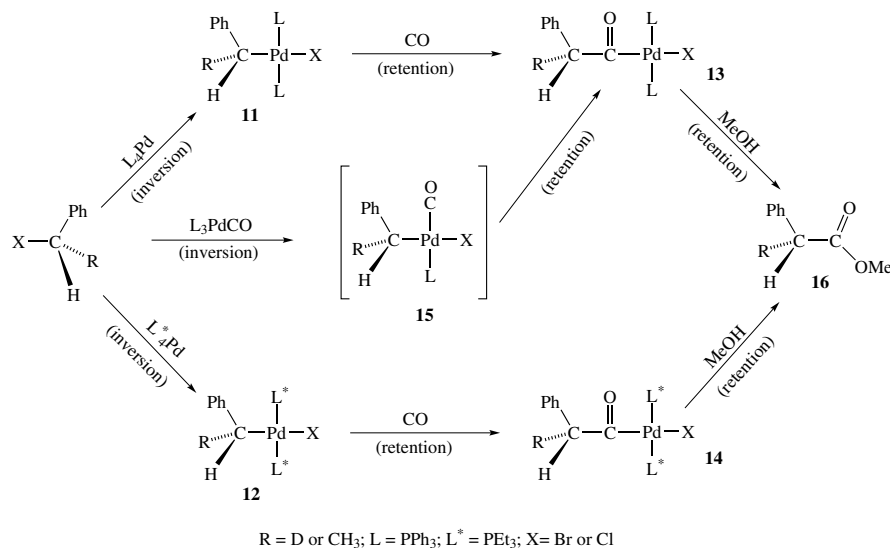


The overall effect of the reaction results in the addition of R-X to the metal. Substrate types that will undergo this mode of OA are generally limited to $\text{R} = \text{benzyl}$, allyl, and methyl. Some acyl compounds $[\text{R}(\text{C}=\text{O})-\text{X}]$ also readily undergo OA. These are the same substrates that are most reactive in $\text{S}_{\text{N}}2$ displacements or in nucleophilic acyl substitution. Other characteristics of these OA reactions associated with the $\text{S}_{\text{N}}2$ pathway include the following:

- second-order kinetics (first order with respect to metal complex and first order in alkyl halide);
- dependence of rate on leaving group ability: $\text{X} = \text{CF}_3\text{SO}_3 > \text{I} > \text{tosylate} \sim \text{Br} > \text{Cl}$;
- large negative entropies of activation (-40 to -50 eu);
- increase in rate when phosphine ligands are present and modified to be more electron releasing (e.g., PMe_3 or PET_3);
- dependence of rate on solvent (polar solvents increase the rate);
- retardation of the rate of reaction due to increasing steric bulk of ligands already attached to the complex; and
- isolation, in certain instances, of ionic intermediates such as **10**,⁹¹ the result expected after the nucleophilic displacement of the leaving group.



⁹¹J. W. Kang and P. M. Maitlis, *J. Organometal. Chem.*, **1971**, 26, 393 and A. J. Oliver and W. A. G. Graham, *Inorg. Chem.*, **1970**, 9, 2653.

**Scheme 7.7**

Stereospecific
Reactions of
Palladium
Complexes

The evidence described above is strongly suggestive of an S_N2 displacement mechanism exactly analogous to its counterpart in organic chemistry. The one piece missing from this mechanistic puzzle is an examination of the stereochemistry at the carbon atom of the substrate. Probably the most convincing evidence for an S_N2 pathway would be the unambiguous demonstration of the occurrence of inversion of configuration at the carbon bearing the leaving group. Until about 30 years ago, clear-cut examples of inversion of configuration taking place upon OA of R-X were lacking. Making up for this deficiency, the detailed studies by Stille *et al.*⁹² on OA of substituted benzyl halides onto palladium complexes provided the first unambiguous examples of inversion of configuration taking place during attack on the substrate by a metal.

Scheme 7.7 illustrates the reactions carried out by the Stille group. Up to the time of the study, the stereochemistry of all steps in the reaction sequences, except that of OA, had been established. Thus, inversion of configuration to yield **11** or **12** must have occurred in the first step, since (1) the next step going to **13** or **14** is carbonyl insertion (to be discussed in detail in Chapter 8), known to occur with retention of configuration, and (2) the final step, called methanolysis, proceeds without disturbing a bond at the carbon stereogenic center. The alternate sequence through the middle of the scheme shows a carbonylated complex, **15**, reacting with the alkyl halide, producing an intermediate that already has a carbonyl ligand on the metal. Rearrangement involving carbonyl

⁹²J. K. Stille and K. S. Y. Lau, *Acc. Chem. Res.*, **1977**, *10*, 434.

insertion resulting in retention of configuration of the migrating alkyl group followed by methanolysis yields the same product, **16**. By comparing the optical purity and absolute configuration of the starting alkyl halides to those of **16**, the change at the stereogenic center was clearly inversion of configuration. These studies also found that the order of reactivity of benzyl halides was $\text{PhCH}_2\text{Br} > \text{PhCH}_2\text{Cl} > \text{PhCHBrCH}_3 > \text{PhCHClCH}_3$. This is consistent with the order expected for an $\text{S}_{\text{N}}2$ reaction, because Br is a better leaving group than Cl and primary substrates react faster than secondary substrates. Stille also reported that the more electron-rich the metal, the faster the reaction, again consistent with an $\text{S}_{\text{N}}2$ pathway.

Within the past 10 years, there have been several reports on high-level molecular orbital calculations (mainly at the DFT level) being used to investigate the pathway of OA of CH_3I to a variety of transition metal complexes. This work corroborates the work of Stille's group by indicating that the $\text{S}_{\text{N}}2$ mechanism is the lowest energy pathway.⁹³

What about unactivated C–X bonds, such as those found in aryl halides, which also readily undergo OA? In Chapter 12 we will see many useful synthetic transformations where OA of an aryl C–X bond is the first step in a catalytic cycle. The $\text{S}_{\text{N}}2$ pathway is not available for aryl halides, so another mode of addition must occur. Especially informative studies have been reported on the OA of Ar–X to L_2Pd (L = phosphine), which is often involved in the catalytic cycles mentioned above. These investigations⁹⁴ have shown that OA occurs after dissociation of one of the L ligands, and calculations⁹⁵ not only corroborate the experimental work, but also suggest that the step involving OA is probably more like the three-centered, concerted step found with C–H and C–C addition.

7-2-3 Radical Pathways

Mechanistic pathways that involve radical intermediates may accompany $\text{S}_{\text{N}}2$ -type polar oxidative additions. Under certain conditions, such pathways may

⁹³M. Feliz, Z. Freixa, P. W. N. M. van Leeuwen, and C. Bo, *Organometallics*, **2005**, *24*, 5718; T. R. Griffin, D. B. Cook, A. Haynes, J. M. Pearson, D. Monti, and G. E. Morris, *J. Am. Chem. Soc.*, **1996**, *118*, 3029; and M. Cheong, R. Schmid, and T. Ziegler, *Organometallics*, **2000**, *19*, 1973.

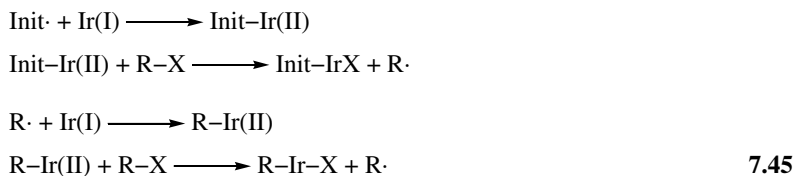
⁹⁴A. H. Roy and J. F. Hartwig, *Organometallics*, **2004**, *23*, 1533 and F. Barrios-Landeros and J. F. Hartwig, *J. Am. Chem. Soc.*, **2005**, *127*, 6944.

⁹⁵M. Ahlquist, P. Fristrup, D. Tanner, and P.-O. Norrby, *Organometallics*, **2006**, *25*, 2066 and K. C. Lam, T. B. Marder, and Z. Lin, *ibid.*, **2007**, *26*, 758.

even be the dominant route between reactant and product. Metal complexes with an odd number of d electrons, including Co(II) and Rh(II), are good candidates for radical oxidative additions. For example, the binuclear complex, $(\text{CO})_5\text{Mn}-\text{Mn}(\text{CO})_5$, reacts with Br_2 to yield $\text{BrMn}(\text{CO})_5$ via a pathway involving radicals in which each atom of Mn undergoes a one-electron change in oxidation state. Complexes with an even number of d electrons, such as the much-studied d^8 Vaska's complex, can also react via radical mechanisms during OA of R-X.

We will consider two types of radical pathways—the chain and non-chain mechanisms. Although other mechanisms are possible, these two routes have been well investigated. Our consideration of them allows us not only to exemplify OA pathways common to a number of metal complexes, but also to introduce some useful and generally applicable techniques for examining mechanisms. At this time, unfortunately, there are no real guidelines for predicting which metal complexes will undergo a particular type of pathway involving radical intermediates.

Iridium complexes, such as Vaska's compound, can undergo OA of R-X (where R \neq methyl, allyl, or benzyl) by a radical chain pathway according to equations 7.45.⁹⁶



Evidence for a radical pathway includes the observation that the reaction is accelerated by radical initiators (such as oxygen or peroxides) and the presence of UV light. Moreover, the order of reactivity for the R group is $\text{III}^\circ > \text{II}^\circ > \text{I}^\circ$, which is inconsistent with a direct displacement mechanism, but is in accord with the stability of alkyl radicals. Radical inhibitors (such as sterically hindered phenols) retard the rate of reaction with sterically-hindered alkyl halides, but not when R = methyl, allyl, and benzyl. When stereoisomerically pure alkyl halides are used, OA results in the formation of a 1:1 mixture of stereoisomeric alkyl iridium complexes, consistent with the formation of an intermediate radical $\text{R}\cdot$.

⁹⁶J. A. Labinger and J. A. Osborn, *Inorg. Chem.* **1980**, *19*, 3230 and J. A. Labinger, J. A. Osborn, and N. J. Colville, *Inorg. Chem.* **1980**, *19*, 3236.

Stereochemical Probes

The stereochemical outcome of a reaction can suggest much about its mechanistic pathway. If a molecular fragment, whose stereochemistry is clearly defined, can be attached to the reactant and remain attached during the course of the reaction without affecting the chemistry, then determination of product stereochemistry can be straightforward using spectroscopic means.

For example, the two primary alkyl bromides, **17** and **18** (Figure 7-11), are diastereomerically related, the former is called *erythro* and the latter *threo*. The designations *erythro* and *threo* arise from the corresponding simple sugars, erythrose and threose, **19** and **20**. These bromides serve as useful probes, because the possible stereochemical outcomes of retention, inversion, or racemization at the carbon bearing the bromide may be readily determined by NMR spectroscopy without requiring the use of optically active compounds. Starting with **18** ($R = D$, $R' = \textit{tert}$ -butyl), we would expect the stereochemistry found in **21** if retention of configuration occurred upon OA. Note that the only reasonable conformation for product requires that the bulky *tert*-butyl group be *anti* to the metal. Inversion of configuration would give **22**. We can distinguish between **21** and **22** by the measuring the magnitude of the coupling constant between the two vicinal protons H_1

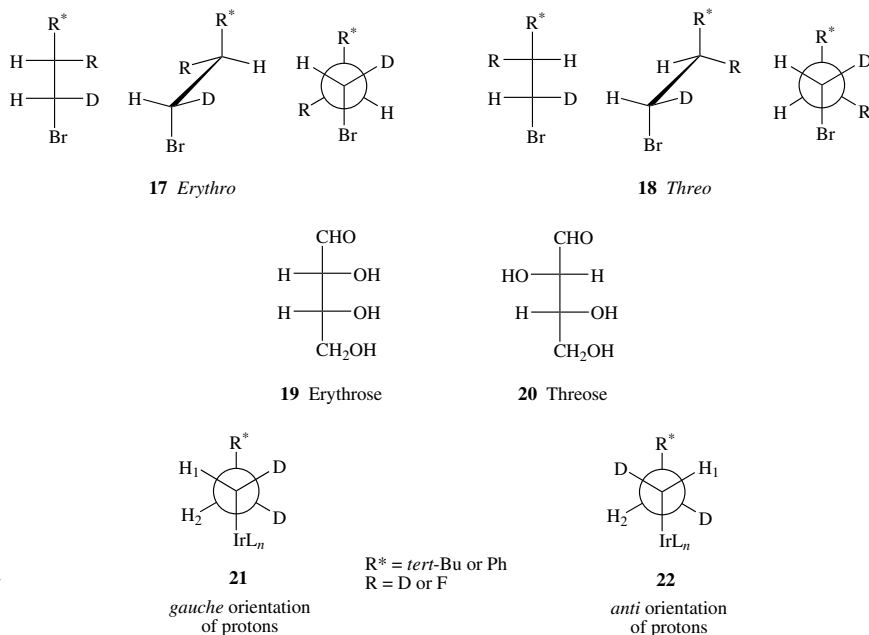


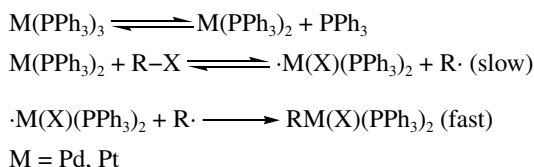
Figure 7-11

Stereochemical Probes

and H₂ and then applying the Karplus⁹⁷ relationship. Finally, if racemization occurs, the NMR spectra of product will be identical, regardless of whether we start from **17** or **18**, because equal molar amounts of **21** and **22** will be present.

Variations of **17** and **18** have also been used as probes where R = F and R' = phenyl. Fluorine, like hydrogen, has a spin of 1/2 and couples with the vicinal proton. Fluorine-hydrogen coupling constants are significantly larger than those for vicinal hydrogens. Using the Karplus relation, it is relatively easy to discern *anti* versus *gauche* orientation of adjacent protons.

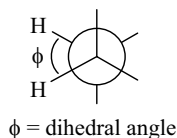
Another mechanistic possibility involving radical intermediates is the non-chain mechanism as outlined in equations **7.46**.⁹⁸

**7.46**

Two observations suggest a mechanism involving radical intermediates. First, a stereorandomization occurs at R. For instance, if R is chiral and one starts with the *S* enantiomer, the resulting product, RMXL_{n-1} , is racemic. Second, the rates of reaction as a function of the structure of R decrease according to $\text{R} = \text{III}^\circ > \text{II}^\circ > \text{I}^\circ$. Since this also corresponds to the order of stability of alkyl radicals, the observation is consistent with the presence of radical intermediates. On the other hand, we can distinguish non-chain pathways from chain mechanisms because the former are not subject to rate change resulting from the addition of radical scavengers or initiators.

Oxidative addition is complex in terms of the mechanistic possibilities available. Subtle variations in reaction conditions can result in a change in mechanism. Some symmetrical addenda (H₂) or those with nonpolar bonds involving electropositive non-metals (C-H or C-C) seem to undergo addition by a concerted

⁹⁷M. Karplus, *J. Am. Chem. Soc.*, **1963**, 85, 2870. Karplus reported a relationship between the coupling constant of vicinal protons and the dihedral angle described by these adjacent nuclei. Coupling is maximal when the dihedral angle (ϕ) = 0° or 180° and minimal when ϕ = 90°.



⁹⁸A. V. Kramer, J. A. Labinger, J. S. Bradley, and J. A. Osborn, *J. Am. Chem. Soc.*, **1974**, 96, 7145 and A. V. Kramer and J. A. Osborn, *J. Am. Chem. Soc.*, **1974**, 96, 7832.

Table 7-7 Oxidation Addition Pathways

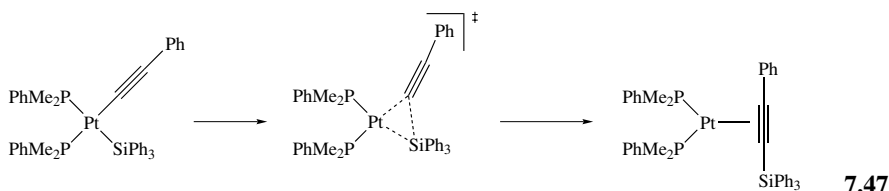
Mechanism Type	Species Adding to ML_n	Number of steps	Stereochemistry at carbon	Stereochemistry of new ligands on the metal
3-Center Concerted ^a	H-H, C-H, C-C, Ar-X, Vinyl-X	One	Retention of configuration	<i>cis</i>
Polar	X-X	Two	N/A	<i>trans</i>
S_N2 -like	Me-X, Allyl-X, Benzyl-X	Two	Inversion of configuration	<i>trans</i> (usually)
Radical	R-X (R ≠ Ar, vinyl, Me, allyl, benzyl)	Multiple	Racemization	Variable

^aOther concerted mechanisms are possible (see Section 7-2-1).

three-center process; others involving electronegative nonmetals—whether symmetrical or non-symmetrical [e.g., C-O, C(sp^3)-X, H-X, or X-X]—undergo OA via polar or radical pathways. Table 7-7 provides a summary of characteristics of some OA reactions that are classified on the basis of mechanism type.

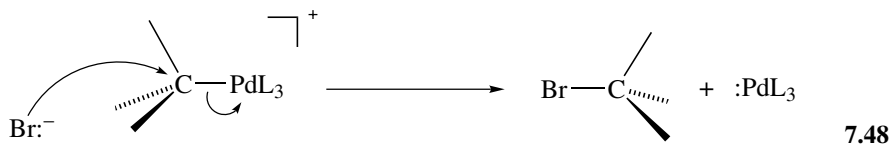
7-3 REDUCTIVE ELIMINATION

RE is the reverse of OA, whereby oxidation state, coordination number, and electron count all decrease, usually by two units. According to the principle of microscopic reversibility, the mechanistic pathways for RE are exactly the same as those for OA, only now in the reverse sense (this principle corresponds to the idea that the lowest pathway over a mountain chain must be the same regardless of the direction of travel). Equation 7.47 shows an example of RE from a platinum complex to give a silylalkyne.⁹⁹ RE here likely goes through a concerted, three-centered transition state with both M-Si and M-C(alkynyl) bonds breaking and the new Si-C bond starting to form.



⁹⁹F. Ozawa and T. Mori, *Organometallics*, **2003**, 22, 3593.

The schematic reaction shown in equation 7.48 could be considered a RE, although the halide attacks the CH_3 ligand in an $\text{S}_{\text{N}}2$ manner to give the alkyl halide and reduced metal complex. We saw the reverse of this reaction in Section 7-2-2.¹⁰⁰



Reductive elimination is favored in complexes with bulky ligands (due to relief of steric hindrance upon ligand loss), a low electron density at the metal (high oxidation state), and the presence of groups that can stabilize the reduced metal fragment upon ligand loss (such as CO or $\text{P}(\text{OR})_3$). It is a reaction type that is perhaps more difficult to study than OA, because complexes that are susceptible to RE are often unstable. The reaction seems particularly facile for complexes of the late transition metals in Groups 8–10, particularly d^8 nickel(II) and palladium(II), as well as for d^6 platinum (IV), palladium (IV), rhodium (III), and iridium (III). Copper triad (Cu, Ag, or Au) complexes also have a tendency to undergo RE; indeed, some of the first compounds observed to do so were d^8 gold (III) complexes.¹⁰¹

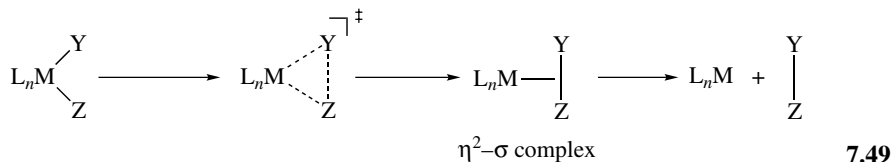
As chemists seek to discover new methods of producing C–C bonds, RE stands out as one of the best ways of accomplishing this task. Carbon–carbon coupling methods involving RE of transition metals complexes with two carbon fragments attached are now routinely used in synthesis and have largely supplanted C–C bond-forming reactions involving Grignard reagents. Often the last step in a catalytic cycle designed to join two different carbon fragments, RE is part of the overall process of the synthesis of several different molecules with industrial or biological significance, as we shall see in Chapters 9 and 12. In addition to producing hydrocarbons, $\text{R}-\text{R}'$ (R = alkyl or aryl and R' = alkyl, aryl, or vinyl), RE also provides a pathway to compounds with bonds of the following types: $\text{R}-\text{H}$ (R = alkyl, aryl), $\text{RC}(=\text{O})-\text{H}$ (aldehydes), $\text{R}(\text{C}=\text{O})-\text{R}'$ (ketones), and $\text{R}-\text{X}$ (alkyl halides).

¹⁰⁰Equation 7.48 could also be considered an example of a nucleophilic abstraction; this type of reaction is described in Section 8-3.

¹⁰¹A. Burway, C. S. Gibson, and S. Holt, *J. Chem. Soc.*, **1935**, 1024; W. L. G. Gent and C. S. Gibson, *J. Chem. Soc.*, **1949**, 1835; and M. E. Foss and C. S. Gibson, *J. Chem. Soc.*, **1949**, 3063. A more recent discussion of RE from Au complexes may be found in A. Tamaki, S. A. Magennis, and J. Kochi, *J. Am. Chem. Soc.*, **1974**, 96, 6154.

7-3-1 *cis*-Elimination

Most synthetically-useful reductive eliminations occur by a concerted three-centered process (the reverse of three-center OA) outlined in equation 7.49.



Such a mechanism requires that the two leaving groups, Y and Z, be attached to the metal in a *cis* manner and strongly suggests, moreover, that retention of stereochemistry occurs at the leaving group atoms. Theoretical investigations on RE of alkanes from gold and palladium complexes indicate that *cis*-1,1-elimination is allowed by symmetry and takes place from either a tricoordinate Y-shaped (Au^{102} or Pd^{103}) activated complex or transient intermediate **23** or a T-shaped (Pd) intermediate, **24**, where the leaving groups are *cis* to each other. The T- or Y-shaped species forms upon prior dissociation of a ligand, typically a phosphine.



For RE of d^8 , 16-e^- *cis*-dihydrocarbyl complexes of the type $\text{L}_n\text{M}(\text{R})(\text{R}')$, where metals in the group 10 triad have been most studied, there are three reasonable mechanistic paths:¹⁰⁴

1. Loss of an L ligand (usually a phosphine) to give a 14-e^- complex (T- or Y-shaped), followed by concerted reductive elimination to form $\text{R-R}'$ (see preceding paragraph);
2. Direct loss of R and R' from a 16-e^- complex without first loss of L; and
3. Association of an L ligand to the 16-e^- complex, followed by formation of $\text{R-R}'$.

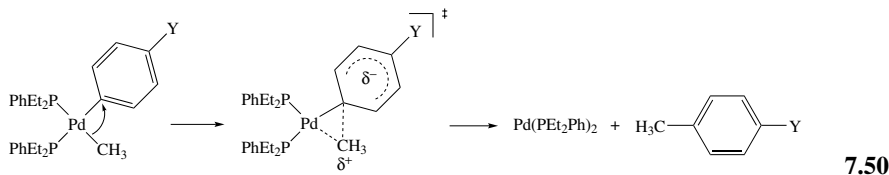
¹⁰²S. Komiya, T. A. Albright, R. Hoffmann, and J. Kochi, *J. Am. Chem. Soc.*, **1976**, 98, 7255.

¹⁰³K. Tatsumi, R. Hoffmann, A. Yamamoto, and J. K. Stille, *Bull. Chem. Soc. Jpn.*, **1981**, 54, 1857.

¹⁰⁴R. K. Merwin, R. C. Schnabel, J. D. Koola, and D. M. Roddick, *Organometallics*, **1992**, 11, 2972.

From the standpoint of thermodynamics, mechanism **3** is probably the most favorable, followed by mechanism **2** and then **1**. Mechanism **3** involves an increase in steric hindrance, so RE involving second- and third-row transition metal complexes via that mechanism is less likely than those involving nickel, for example. For *cis*-NiMe₂L_{*n*} (*n* = 1, 2, and 3) calculations demonstrated that the activation energy barrier for RE was lowest for mechanism **1**, followed by mechanism **3** and then **2**.¹⁰⁵

An interesting variation of mechanism **2** is akin to migratory insertion, which is discussed in Chapter 8. Such reactions seem to occur when alkyl groups and unsaturated hydrocarbyl groups eliminate from L₂Pd(R)(R') complexes, R is alkyl and R' is vinyl or aryl. Experimental results and calculations suggest that the Pd–alkyl bond breaks before the Pd–C(*sp*²) bond.¹⁰⁶ The three-center transition state also shows significant bonding of the relatively electron-rich alkyl group to the relatively electron-deficient *sp*²-hybridized carbon of the other leaving group. Equation 7.50 shows an example of such a reaction.¹⁰⁷



What kind of substituents (Y) at the *para* position of the phenyl group in Equation 7.50 should increase the rate of RE? Electron donating or withdrawing? Explain briefly why.

Exercise 7-8

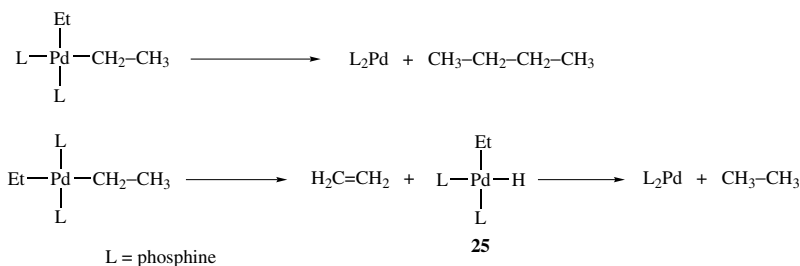
In addition to the considerations above, early, definitive experimental work clearly indicated that leaving groups must have a *cis* relationship for RE to occur. Equation 7.51 provides experimental evidence consistent with *cis*-elimination. The *cis*-ethyl complex gives butane directly, whereas the *trans*-isomer undergoes

¹⁰⁵K. Tatsumi, A. Nakamura, S. Komiya, T. Yamamoto, and A. Yamamoto, *J. Am. Chem. Soc.*, **1984**, *106*, 8181.

¹⁰⁶This is not too surprising based on relative M–C bond energies. See M. J. Calhorda, J. M. Brown, and N. A. Cooley, *Organometallics*, **1991**, *10*, 1431 and D. S. McGuinness, N. Saendig, B. F. Yates, and K. J. Caldwell, *J. Am. Chem. Soc.*, **2001**, *123*, 4029.

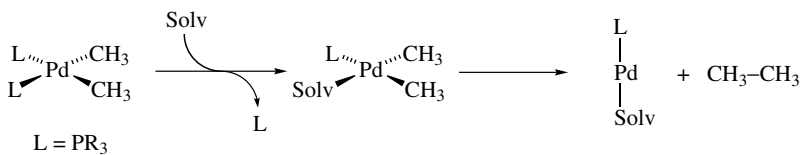
¹⁰⁷F. Ozawa, K. Kurihara, M. Fujimori, T. Hidaka, T. Toyoshima, and A. Yamamoto, *Organometallics*, **1989**, *8*, 180.

facile 1,2-elimination to produce ethene and the ethylhydridopalladium complex, **25**, which finally yields ethane¹⁰⁸ after RE.



7.51

The seminal investigations of Stille and co-workers,¹⁰⁹ however, provided substantial information on the mechanism of RE. These studies established that, for the palladium complexes shown in Figure 7-12, the stereochemical relationship between the leaving groups was necessarily *cis*. The rates of reductive elimination of these compounds were measured; those rates for the *cis* series are listed in Table 7-8. Two of the *trans* compounds, **27** and **29**, were obliged to isomerize to the *cis* isomer before reductive elimination could occur, and their overall rates of RE were retarded. Addition of Ph₃P retarded the rates of reaction of the *cis* complexes, because Stille's group reported that ligand dissociation (mechanism I) was required before reductive elimination could occur, with a solvent molecule (Solv) taking up the empty coordination site (equation 7.52). The order of reactivity of the *cis* complexes reflects the chelate effect¹¹⁰ (**28** > **30**) and the increased electron density of phosphine ligands upon alkyl substitution (**26** > **28**). Polar solvents seemed to enhance the rate of reductive elimination by assisting in the *trans* to *cis* isomerization (via pseudorotation through five-coordinate species) and in stabilizing the reduced coordination product formed, as shown in equation 7.53.

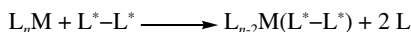


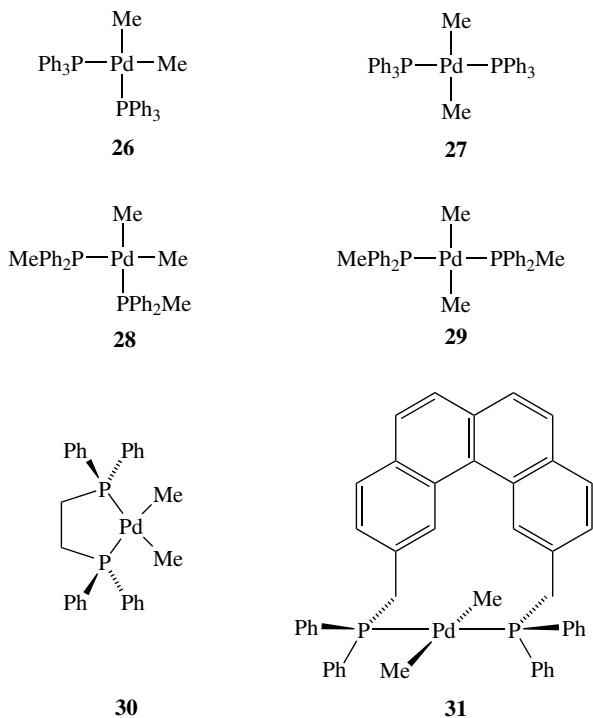
7.52

¹⁰⁸F. Ozawa, T. Ito, Y. Nakamura, and A. Yamamoto, *Bull. Chem. Soc. Jpn.*, **1981**, 54, 1868.

¹⁰⁹For a good example of this work, see A. Gillie and J. K. Stille, *J. Am. Chem. Soc.*, **1980**, 102, 4933.

¹¹⁰Bidentate or chelating ligands tend to bind tightly to transition metals. A general ligand substitution reaction, involving displacement by a bidentate ligand (shown below), should have a positive $\Delta_r S^\circ$, which therefore makes $\Delta_r G^\circ$ tend to be negative. A subsequent reaction of losing a bidentate ligand then becomes unfavorable thermodynamically.



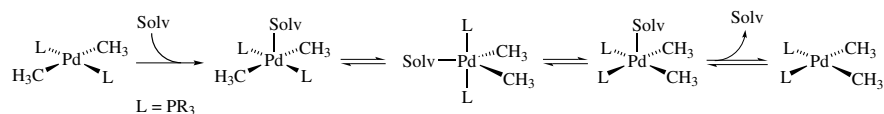
**Figure 7-12**

Pd(II) Complexes
Used for Reductive
Elimination Studies

Table 7-8 Relative Rates of RE of *Cis*
Complexes at 60 °C

<i>cis</i> -Complex	<i>k</i> (sec ⁻¹)
26	1.041×10^{-3}
28	9.625×10^{-5}
30^a	4.78×10^{-7}

^aRun at 80 °C.

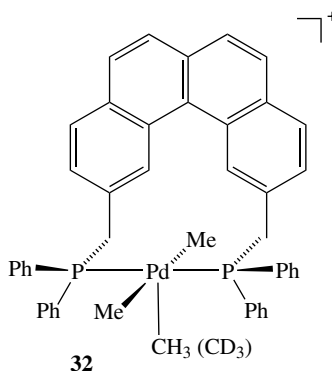


7.53

One of the *trans* compounds, **31**, substituted with the *TRANSPHOS* ligand, did not undergo reductive elimination, even at 100°, because isomerization to the *cis* isomer would be difficult. Not only does the presence of a bidentate ligand

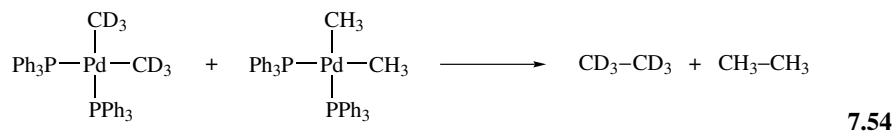
tend to retard isomerization due to the chelate effect, but also the rigidity of the *TRANSPHOS* group makes requisite first-step phosphine dissociation unlikely.

Although **31** did not undergo reductive elimination, the addition of methyl iodide immediately produced ethane. This suggested that methyl iodide underwent OA with the Pd(II) complex to yield **32**, which then underwent RE of the adjacent *cis* methyl groups. The observation that CD_3I reacts with **31** to give only $\text{CD}_3\text{-CH}_3$ lends further support to this hypothesis and to the overall notion of *cis*-elimination (via **32**, shown below).

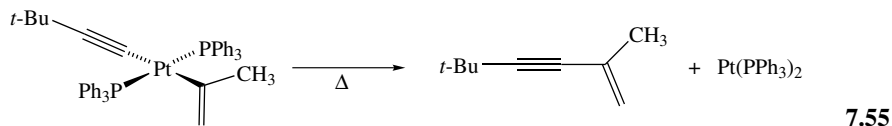


Crossover Experiments

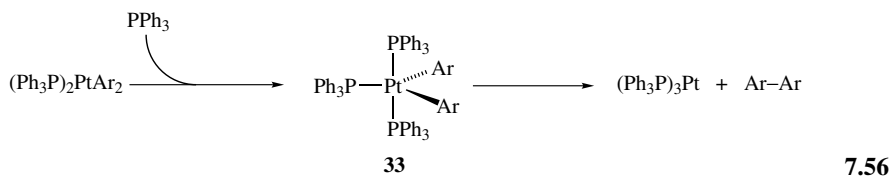
Crossover experiments are helpful in determining whether a mechanistic pathway is intramolecular or intermolecular. In this type of experiment, two forms of the same reactant are used—one unlabeled and the other labeled with isotopes of atoms found in the original compound (e.g., hydrogen vs. deuterium). If the reaction is intermolecular, products should show scrambling of the label, such that some products will be completely labeled, some completely unlabeled, and some partially labeled. Intramolecular pathways should show no such scrambling. Crossover experiments performed by Stille's group (equation **7.54**) showed that, when equimolar mixtures of **26**, **28**, or **30** and their hexadeuterio counterparts were allowed to react, *only ethane and CD_3CD_3 were produced*. The absence of the crossover product, CD_3CH_3 , and the presence of products that seemingly could form only via an intramolecular pathway gave strong support to the now well-accepted view that RE is a concerted, intramolecular reaction involving leaving groups that are *cis* with respect to each other.



Another example of dissociative *trans* to *cis* isomerization followed by RE occurs in a vinylic cross-coupling reaction, such as that illustrated in equation 7.55.¹¹¹ Here again, addition of phosphines retards the rate of elimination.



Although the dissociative pathway for RE seems quite common (certainly those where the metals are from Groups 8–10), in some instances phosphine dissociation is not required for RE to occur.¹¹² The addition of phosphines actually accelerates the rate of RE of biaryls (Ar = Ph or CH₃Ph) from *cis*-Pt(II) complexes,¹¹³ as shown in equation 7.56. It is possible that added phosphine coordinates with the Pt to give a 5-coordinate activated complex or intermediate that can rearrange to a *cis*-diaryl trigonal bipyramidal species, **33**. RE from such 5-coordinate species is facile if the leaving groups are *cis*.¹¹⁴



The contrast between the dissociative (mechanism 1) nature of RE from Pd(II) complexes and the apparent associative pathway (mechanism 3) for Pt(II) deserves comment. Palladium seems to have less of a tendency to form 18-electron

¹¹¹P. J. Stang and M. H. Kowalski, *J. Am. Chem. Soc.*, **1989**, *111*, 3356.

¹¹²See J. P. Collman, L. S. Hegedus, J. R. Norton, and R. G. Finke, *Principles and Applications of Organotransition Metal Chemistry*, University Science Books: Mill Valley, CA, 1987 pp. 329–330, for examples.

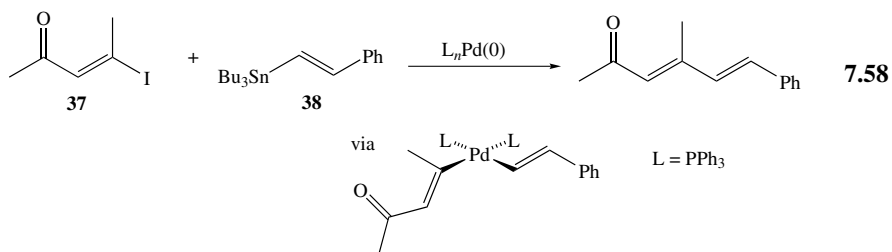
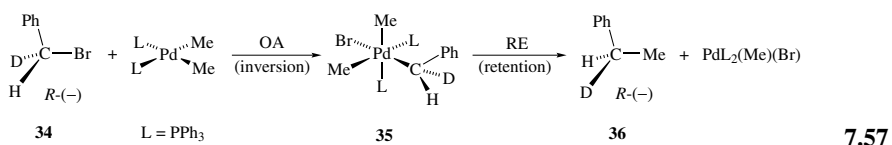
¹¹³P. S. Braterman, R. J. Cross, and G. B. Young, *J. Chem. Soc. Dalton*, **1977**, 1892.

¹¹⁴See Footnote 105.

complexes than either Pt or Ni.¹¹⁵ Therefore, 16-electron Pd(II) complexes such as **26** will usually undergo dissociation before acquiring more electrons through ligand addition.

7-3-2 Stereochemistry at the Leaving Group

When determination of stereochemistry at the leaving carbon stereocenter is possible, retention of configuration is observed during the RE step. In the example shown in equation 7.57, Milstein and Stille¹¹⁶ found a net inversion of configuration for OA followed by RE using a Pd(II) complex. The pathway requires, first, inversion of configuration of **34** during the OA step (see Section 7-2-2) to give **35** and, second, retention of configuration during the RE step to produce **36**. Equation 7.58 depicts another example of RE with retention of configuration, this time at an sp^2 center.¹¹⁷



This reaction represents the last step in a Pd-catalyzed coupling of two fragments, **37** and **38**, which are bound to Pd in a mechanism that features RE as the last step. Coupling reactions of this sort will be discussed more fully in Chapter 12.

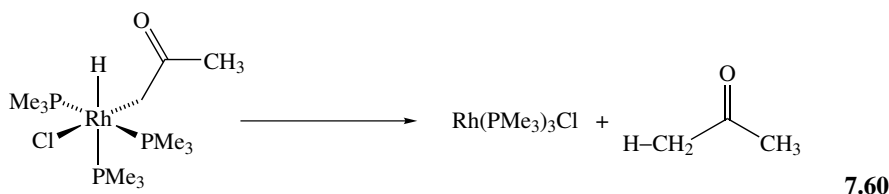
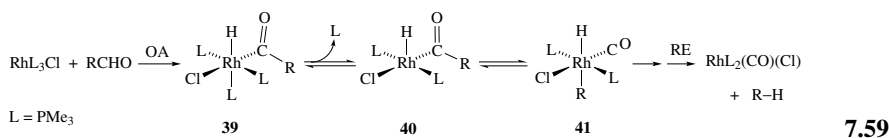
¹¹⁵See J. K. Stille, In *The Chemistry of the Metal–Carbon Bond*, F. R. Hartley and S. Patai, Eds., Wiley: London, 1985, Vol. 2, Chapter 9, and references therein.

¹¹⁶D. Milstein and J. K. Stille, *J. Am. Chem. Soc.*, **1979**, *101*, 4981.

¹¹⁷J. K. Stille, *Angew. Chem. Int. Ed. Engl.*, **1986**, *25*, 508.

7-3-3 C–H Elimination

Examples of elimination of C–H are increasingly cited in the literature, and investigations of C–H RE elimination are used to help elucidate pathways of C–H bond activation, taking advantage of the principle of microscopic reversibility. Research with d^8 rhodium and iridium complexes¹¹⁸ indicates that RE in these cases is concerted, intramolecular, and involves the loss of carbon and hydrogen that have a *cis* relationship to each other. In these cases, the now-familiar rate-determining loss of phosphine ligand (mechanism **1**) occurs before a new C–H bond can form. In a simple way, we can view the loss of phosphine as both effectively reducing electron density at the metal (thus forcing the need for lowering the oxidation state through RE) and providing a less stable stereochemical configuration. RE of this unstable configuration is thus energetically favorable. Equations **7.59** and **7.60** provide two examples of C–H elimination.



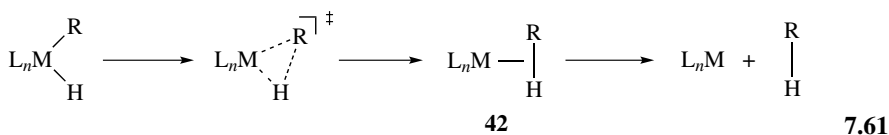
As shown in equation **7.59**, OA of the aldehyde yields the *cis*-hydridoacylrhodium complex, **39**. Heating results in ligand dissociation to give **40**, which undergoes migratory deinsertion (to be discussed in Chapter 8) to produce **41**. Isomerization of **41** to a *cis*-hydridoalkyl complex presumably occurs before the final RE step to yield the C–H elimination product. These reactions have applications in catalytic industrial process known as olefin hydroformylation (Section **9-2**). Equation **7.60** illustrates straightforward RE to form a new C–H bond.

¹¹⁸D. Milstein, *Acc. Chem. Res.*, **1984**, *17*, 223.

Exercise 7-9

Propose a mechanism for the conversion of **41** to $\text{RhL}_2(\text{CO})\text{Cl}$ in equation 7.59. [Hint: Consider a mechanism involving loss of L to produce five-coordinate intermediates followed by addition of L.]

The timing of the breakage of the M–C and M–H bonds and the formation of the C–H bond is of interest to chemists. Equation 7.61¹¹⁹ illustrates the commonly accepted and now-familiar pathway for RE to form C–H bonds, which first involves a three-centered transition state, followed by an η^2 -C–H metal complex **42** and finally production of the free alkane and reduced metal.

**7-3-4 Dinuclear Reductive Eliminations**

RE is also possible when two complexes react according to equation 7.62.



One well-known example (equation 7.63) involves the formation of dihydrogen from the reaction of two equivalents of $\text{HCo}(\text{CO})_4$. A radical mechanism appears to be operative in this case involving hydrogen atom transfer.¹²⁰



Several other examples of this type of elimination have been discovered and a variety of mechanisms postulated. It is beyond the scope of this book to provide a

¹¹⁹For a discussion with extensive references of C–H bond formation involving reductive elimination of alkanes, see W. D. Jones, A. J. Vetter, D. D. Wick, and T. O. Northcutt, "Alkane Complexes as Intermediates in C–H Bond Activation Reactions," In *Activation and Functionalization of C–H Bonds*, K. I. Goldberg and A. S. Goldman, Eds., ACS Symposium Series 885, American Chemical Society: Washington, D. C., 2004, pp. 56–69. See also another chapter in the same volume: "Kinetic and Equilibrium Deuterium Isotope Effects of C–H Bond Reductive Elimination and Oxidative Addition Reactions Involving the *Ansa*-Tungstencene Methyl-Hydride Complex $[\text{Me}_2\text{Si}(\text{C}_5\text{Me}_4)_2]\text{W}(\text{Me})\text{H}$," pp. 86–104.

¹²⁰H. W. Sternberg, I. Wender, R. A. Friedel, and M. Orchin, *J. Am. Chem. Soc.*, **1953**, 75, 2717.

detailed investigation of these reactions, but the reader should be aware that they do occur.¹²¹

Suggested Reading

Trans Influence and trans Effect

F. R. Hartley, *Chem. Soc. Rev.*, **1973**, 2, 163.

F. Basolo and R. G. Pearson, "The *Trans* Effect in Metal Complexes," *Prog. Inorg. Chem.*, **1962**, 4, 381–453.

Associative Substitution on 18-Electron Complexes

F. Basolo, *New J. Chem.*, **1994**, 18, 19.

J. M. O'Connor and C. P. Casey, *Chem. Rev.*, **1987**, 87, 307.

F. Basolo, *Inorg. Chim. Acta.*, **1985**, 100, 33.

17- and 19-Electron Complexes

S. Sun and D. A. Sweigert, *Adv. Organomet. Chem.*, **1996**, 40, 171.

Oxidative Addition and Reductive Elimination

F. Ozawa, "Reductive Elimination," In *Fundamentals of Molecular Catalysis*, H. Kurosawa and A. Yamamoto, Eds., Elsevier: Amsterdam, 2003, pp. 479–512.

J. K. Stille, "Oxidative Addition and Reductive Elimination," In *The Chemistry of the Metal–Carbon Bond*, F. R. Hartley and S. Patai, Eds., Wiley: New York, 1985, Vol. 2, pp. 625–787.

C–H and C–C Bond Activation

K. I. Goldberg and A. S. Goldman, Eds., *Activation and Functionalization of C–H Bonds*, ACS Symposium Series 885, American Chemical Society: Washington, D. C., 2004.

R. H. Crabtree and D.-H. Lee, "Activation of Substrates with Non-Polar Single Bonds," In *Fundamentals of Molecular Catalysis*, H. Kurosawa and A. Yamamoto, Eds., Elsevier: Amsterdam, 2003, pp. 65–113.

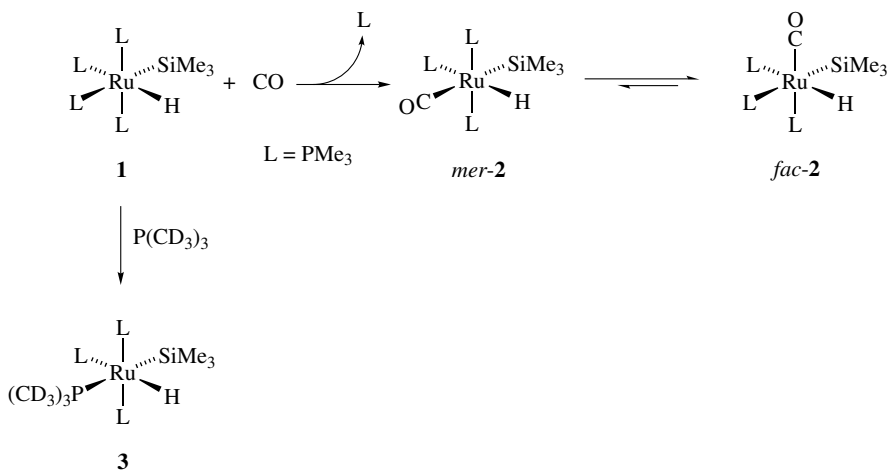
J. A. Labinger and J. E. Bercaw, *Nature*, **2002**, 417, 507.

S. Murai, Ed., *Activation of Unreactive Bonds and Organic Synthesis* (Vol. 3 in the *Topics in Organometallic Chemistry* series), Springer-Verlag: Heidelberg, 1999.

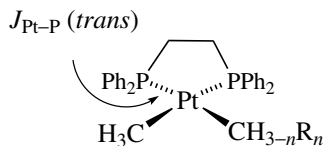
¹²¹For a review of dinuclear REs, see J. P. Collman, L. S. Hegedus, J. R. Norton, and R. G. Finke, *Principles and Applications of Organotransition Metal Chemistry*, University Science Books: Mill Valley, CA, 1987, pp. 333–343.

Problems

- 7-1 Structure **1** below underwent ligand exchange with CO to give only *mer-2*, which later rearranged to *fac-2*. Treatment of **1** with $\text{P}(\text{CD}_3)_3$ gave **3**, showing that ligand exchange occurred only *trans* to the SiMe_3 group. An X-ray analysis of **1** indicated that other than the length of the Ru–P bond located *trans* to H, the next longest Ru–P bond was situated *trans* to the SiMe_3 group.¹²²



- How do the *trans* effect and *trans* influence of the SiMe_3 group compare with those of phosphines? Explain?
 - What is the driving force for the rearrangement of *mer-2* to *fac-2*?
- 7-2 Consider the data shown in the table on the next page. What do these data tell you about the relative *trans* influence of the σ carbon donor ligands ($\text{CH}_{3-n}\text{R}_n$) listed? What is the reason for the trend?¹²³



¹²²V. K. Dioumaev, L. J. Procopio, P. J. Carroll, and D. H. Berry, *J. Am. Chem. Soc.*, **2003**, *125*, 8043.

¹²³T. G. Appleton and M. A. Bennett, *Inorg. Chem.*, **1978**, *17*, 738.

Ligand	n	J_{Pr-P} (trans)
CH ₃	0	1794 Hz
CH ₂ (COCH ₃)	1	2346 Hz
CH(COCH ₃) ₂	2	2948 Hz
C(COCH ₃) ₃	3	4124 Hz

7-3 A ligand substitution reaction, $L_nML^1 + L^2 \longrightarrow L_nML^2 + L^1$, has the rate law rate = $k[L_nML^1][L^2] + k'[L_nML^1]$.

What does this rate law imply about the mechanism of this reaction?

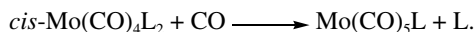
7-4 The rates of exchange of CO (labeled with ¹³C) on *cis*-[M(CO)₂X₂]⁻ complexes—where M = Rh, Ir and X = Cl, Br, I—have been measured, and the results are given in the table below.¹²⁴



M	X	k (L/mol-s at 298 K)	ΔH^\ddagger	ΔS^\ddagger (eu)	ΔV^\ddagger (cm ³ /mol)
Ir	Cl	1100	3.7	-32	-21
	Br	13,000	3.2	-29	
	I	99,000	3.0	-26	
Rh	Cl	1700	4.2	-30	-17
	Br	30,000	2.7	-29	
	I	850,000	2.4	-23	

- What do the data suggest about the mechanistic pathway for CO exchange?
- Why does the rate of exchange increase going from Cl to I?
- Why is the exchange rate faster for Rh complexes compared with Ir?

7-5 In a series of experiments, the rate of phosphine dissociation from *cis*-Mo(CO)₄L₂ (L = phosphine) was determined for several phosphines. The overall reaction in each case was of the form



¹²⁴R. Churlaud, U. Frey, F. Metz, and A. E. Merbach, *Inorg. Chem.*, **2000**, 39, 304.

Rate data:	Phosphine	Rate constant (s^{-1})
	PMe_2Ph	$< 1.0 \times 10^{-6}$
	PMePh_2	1.3×10^{-5}
	PPh_3	3.2×10^{-3}

Account for this trend in reaction rates.

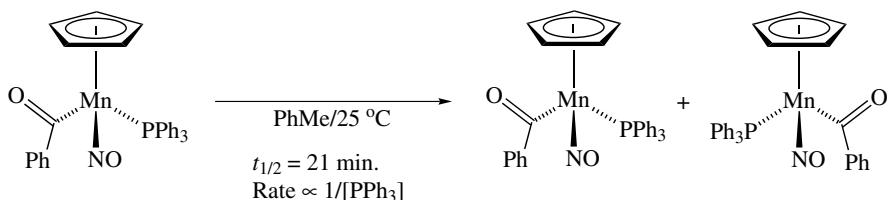
- 7-6** Verify the rate law shown below and expressed in Section 7-1-4, relating to Scheme 7.2.

$$\text{Rate} = k_1 k_2 [\text{M}(\text{CO})_4 \text{diene}] [\text{L}] / (k_{-1} + k_2 [\text{L}]) + k_3 [\text{M}(\text{CO})_4 \text{diene}] [\text{L}]$$

Also verify that when $k_2 [\text{L}]$ is large, the rate law reduces to

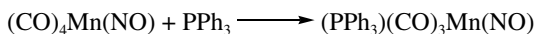
$$\text{Rate} = k_1 [\text{M}(\text{CO})_4 \text{diene}] + k_3 [\text{M}(\text{CO})_4 \text{diene}] [\text{L}].$$

- 7-7** When PEt_3 reacts with $\text{Mo}(\text{CO})_6$ the final product is *fac*- $\text{Mo}(\text{CO})_3(\text{PEt}_3)_3$. Substitution goes no farther than trisubstitution. Give two reasons why this might be so. Account for the stereochemistry of the product. [Hint: Why would production of the *mer*-isomer be not as likely?]
- 7-8** The chiral Mn complex below undergoes racemization according to the equation shown.

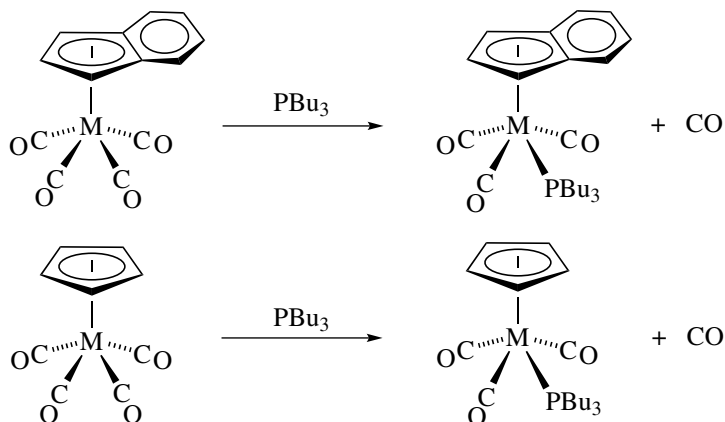


Propose a mechanism that is consistent with the rate being affected inversely by the concentration of PPh_3 .

- 7-9** The reaction below shows a rate law that is second order in substrate metal complex and first order in phosphine. The ΔS^\ddagger is negative, and an intermediate was isolated and shown to be $(\text{PPh}_3)_3(\text{CO})_4\text{Mn}(\text{NO})$. Propose a mechanism for the reaction. What is the nature of the bonding of the NO ligand at each stage of the reaction?



- 7-10** Consider the reactions shown on the next page ($\text{M} = \text{Nb}, \text{Ta}$).



Regardless of the π ligand, the Nb complexes underwent ligand exchange over two times faster than the comparable Ta complex. The sign of the entropy of activation for ligand exchange was positive or slightly negative for the Nb- and Ta-Cp complexes, but highly negative for either indenyl (Ind) complex. Moreover, rates of ligand exchange were generally faster for the indenyl complexes than for the Cp complexes.¹²⁵

Propose mechanistic pathways for ligand exchange that account for the differences in rate between Cp-M and Ind-M complexes.

7-11 Assign the oxidation states and valence electron counts for the transition metals in the following complexes:

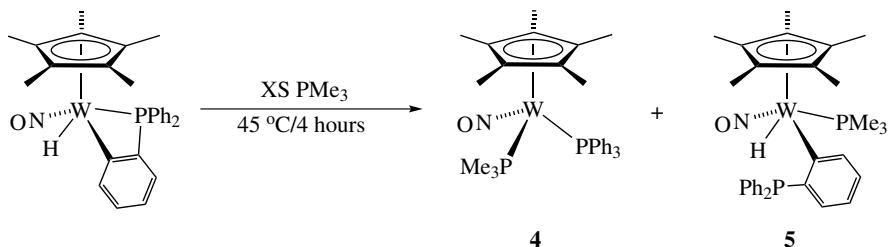
- $\text{Ir}(\text{CO})(\text{PPh}_3)_2\text{Cl}$
- $(\eta^5\text{-C}_5\text{H}_5)_2\text{TaH}_3$
- $[\text{Rh}(\text{CO})_2\text{I}_2]^-$
- $(\eta^5\text{-C}_5\text{H}_5)(\text{CH}_3)\text{Fe}(\text{CO})_2$
- $\text{CH}_3\text{C}(\text{=O})\text{Co}(\text{CO})_3$

7-12 Assign the oxidation states and valence electron counts for the transition metals in the following complexes:

- The reactant and product in equation 7.29
- Structure 8 in Scheme 7.6
- Structure 31 in Figure 7.12
- Structure 33 and its reaction product in equation 7.56

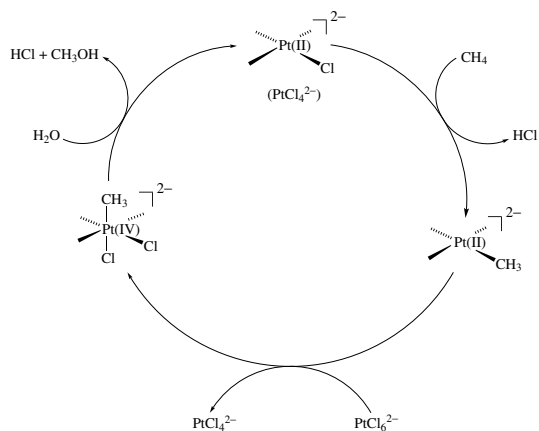
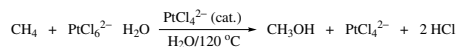
¹²⁵T. E. Bitterwolf, D. Lukmanova, S. Gallagher, A. L. Rheingold, I. A. Guzei, and L. Liable-Sands, *J. Organomet. Chem.*, **2000**, 605, 168.

7-13 Propose a stepwise mechanism for the formation of compounds **4** and **5**.¹²⁶



7-14 Shilov and co-workers were among the first to demonstrate intermolecular C–H bond activation. Consider the reaction of CH_4 to give CH_3OH , which is stoichiometric in the Pt(IV) complex and catalytic in the Pt(II) complex.¹²⁷

Such a reaction could be quite useful on an industrial scale, but unfortunately, it is stoichiometric in highly expensive Pt complex. Since its discovery in 1972, Shilov chemistry has been the focus of numerous investigations, many of which have sought to replace the Pt(IV) stoichiometric oxidant with a cheaper alternative. In the course of this research, the mechanism of the Shilov C–H bond activation has been elucidated. The following scheme shows the catalytic cycle involved.

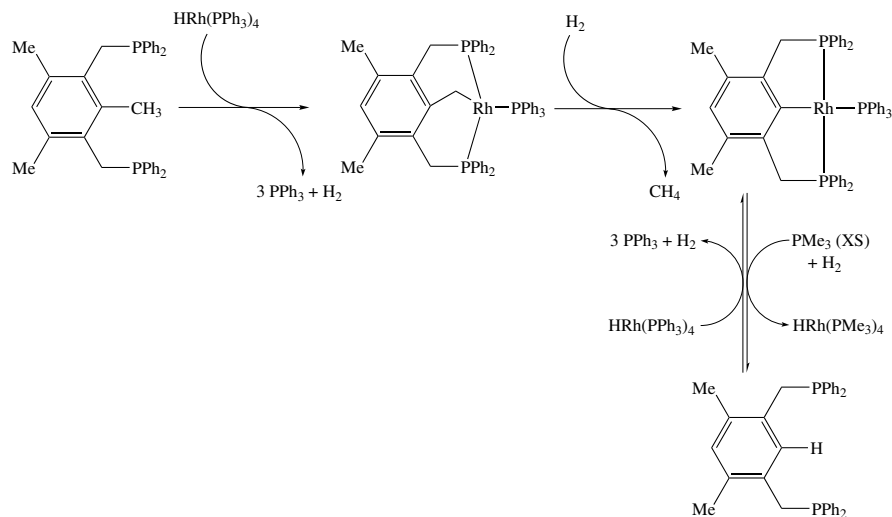


¹²⁶D. J. Burkey, J. D. Debad, and P. Legzdins, *J. Am. Chem. Soc.*, **1997**, *119*, 1139.

¹²⁷N. F. Gol'dshleger, V. V. Es'kova, A. E. Shilov, and A. A. Shteinman, *Zhurnal Fizicheskoi Khimii*, **1972**, *46*, 1353.

For each of the three steps, supply mechanistic detail that describes how the transformation occurs.

7-15 Supply mechanistic details for each of the steps involved in the reaction scheme shown below, which exemplifies the use of pincer ligands:¹²⁸



¹²⁸M. Gozin, A. Weisman, Y. Ben-David, and D. Milstein, *Nature*, **1993**, 364, 699.

Organometallic Reactions II

Reactions Involving Modification of Ligands

Once a ligand is attached to a metal, several events may occur. In Chapter 8 we will consider a few of the most common possibilities for reactions involving changes in the ligand. Such transformations are often integral parts of the catalytic cycles we will examine in Chapter 9. Reactions on ligands bound to a transition metal are also of great interest to the organic chemist, because transformations are now possible that would be difficult or impossible to do using conventional carbon-based chemistry. We will explore the basis for these new possibilities in Chapter 8, and then apply what we learn in Chapters 9, 10, 11, and 12. We will divide our discussion into two major parts: (1) insertion or deinsertion of a ligand with respect to a bond between a metal and another ligand and (2) attack on a ligand by a nucleophile or electrophile.

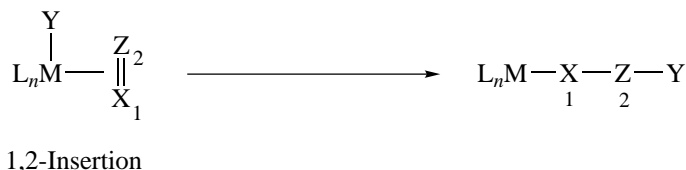
8-1 INSERTION AND DEINSERTION

Equations 8.1 and 8.2 describe the general process of insertion of a ligand into an M–Y bond. The former shows a process known as 1,1-insertion and the latter its 1,2 counterpart. The reverse reactions are known interchangeably as deinsertion, extrusion, or elimination.



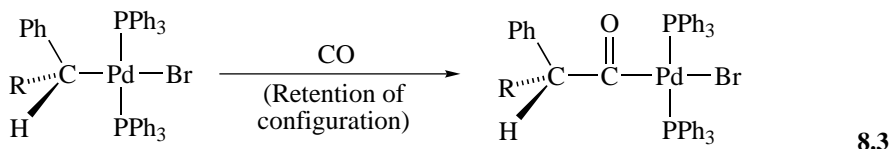
1,1-Insertion

8.1

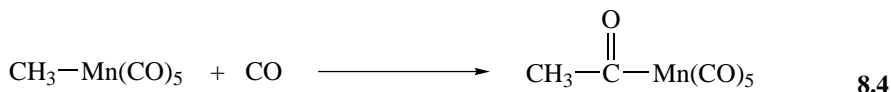


8-1-1 1,1-Insertion: "Carbonyl Insertion" (Alkyl Migration) Reactions

Perhaps the most well-studied example of the insertion–deinsertion reaction is that of the 1,1-insertion of carbon monoxide into a metal–alkyl (or aryl) bond. This reaction figures prominently as a key step in a number of catalytic processes. The numbering designation of 1,1 refers to the numbering on the CO ligand. If we designate the carbon of the CO ligand to be the 1-position, the insertion occurs such that both the metal and the original alkyl ligand are bonded to that carbon when insertion is complete, hence the numbers 1,1. Equation 8.3 illustrates insertion of a carbonyl ligand into a Pd–C bond, one of the reactions shown earlier in Scheme 7.7.



The prototypical example of carbonyl insertion, and the one most thoroughly investigated, involves reaction of CO with $(CH_3)Mn(CO)_5$ to yield the acetyl manganese complex, which is shown in equation 8.4.



From the net equation we might expect that the CO inserts directly into the Mn–CH₃ bond; if such were the case, the label "CO insertion" would be entirely appropriate for this reaction. Other mechanisms, however, are possible that would give the overall reaction stoichiometry while involving steps other than insertion of an incoming CO. The following three mechanisms have been suggested as plausible for this reaction.

Mechanism I: CO insertion

Direct insertion of CO into metal–carbon bond.

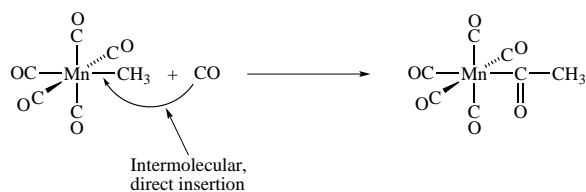
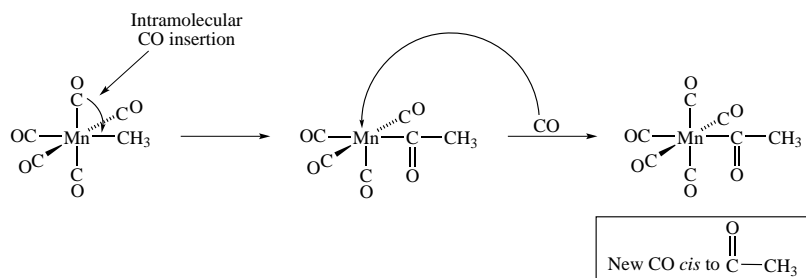
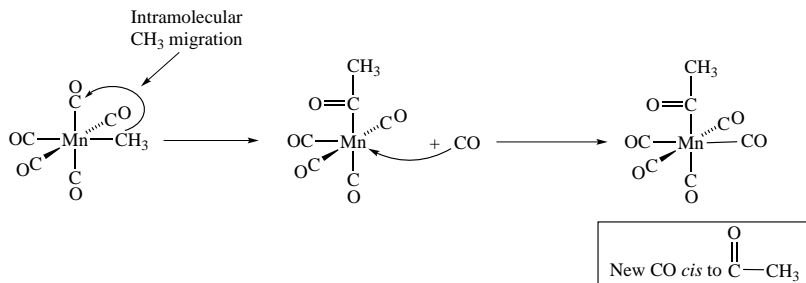
Mechanism 2: CO migration

Migration of CO to give *intramolecular* CO insertion. This would give rise to a 5-coordinate intermediate, with a vacant site available for attachment of an incoming CO.

Mechanism 3: Alkyl migration

In this case the alkyl group would migrate—rather than the CO—and attach itself to a CO *cis* to the alkyl. This would also give a 5-coordinate intermediate with a vacant site available for an incoming CO.

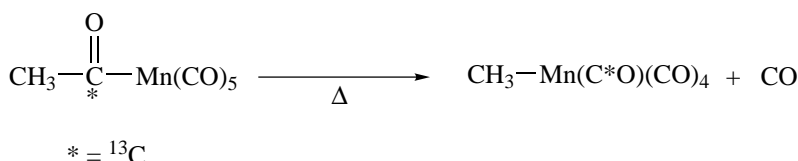
These mechanisms are described schematically in Figure 8-1. In both mechanisms 2 and 3, the intramolecular migration is considered most likely to occur to the migrating group's nearest neighbors, located in *cis* positions.

Mechanism 1:Mechanism 2:Mechanism 3:**Figure 8-1**

Possible
Mechanisms for CO
Insertion Reactions

Experimental evidence that may be applied to evaluating these mechanisms includes the following.¹

- I. Reaction of $\text{CH}_3\text{Mn}(\text{CO})_5$ with ^{13}CO yields a product with the labeled CO in carbonyl ligands only—*none* is found in the acyl $[\text{CH}_3\text{C}(=\text{O})]$ position.
- II. When the reverse reaction (which occurs readily on heating $\text{CH}_3\text{C}(=\text{O})\text{Mn}(\text{CO})_5$) is carried out with ^{13}C in the acyl position, the $\text{CH}_3\text{Mn}(\text{CO})_5$ formed has the labeled CO entirely *cis* to CH_3 . No labeled CO is lost in this reaction.



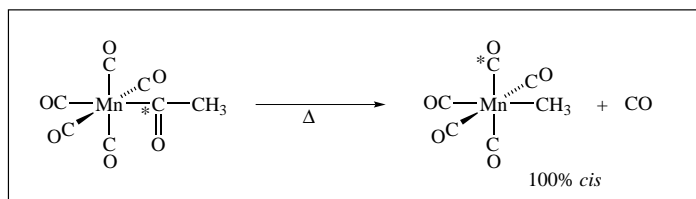
- III. When the reverse reaction is carried out with a ^{13}CO positioned *cis* to the acyl group, the product has a 2:1 ratio of *cis* to *trans* (*cis* and *trans* referring to the position of labeled CO relative to CH_3 in the product). Some labeled CO is also lost in this reaction.

The mechanisms can now be evaluated on the basis of these data. First, mechanism **I** is definitely ruled out by experiment **I**. Direct insertion of ^{13}C must result in ^{13}C in the acyl ligand; since none is found, the mechanism cannot be a direct insertion. Mechanisms **2** and **3**, on the other hand, are both compatible with the results of this experiment.

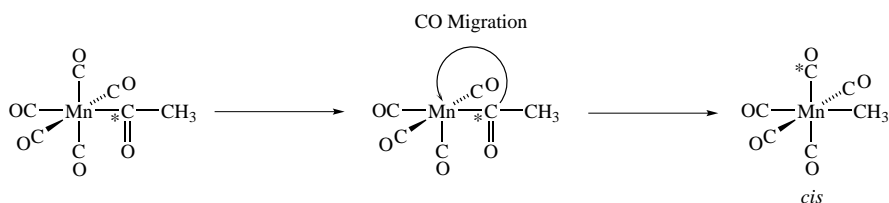
The principle of microscopic reversibility (discussed in Chapter 7) is applicable when considering the information uncovered by experiment **II**. Let us assume that the acyl manganese complex contains a ^{13}C -labeled carbonyl carbon (Figure 8-2). If the forward reaction is carbonyl migration (mechanism **2**), the reverse reaction must proceed by loss of a CO ligand attached directly to the metal, resulting in an empty site, followed by migration of ^{13}CO from the acyl ligand to the empty site. Because this migration is unlikely to occur to a *trans* position, all of the product should show a ^{13}CO in a *cis* position relative to the alkyl ligand. If the mechanism is alkyl migration (mechanism **3**), the reverse reaction must proceed by loss of a CO ligand attached directly to the metal, again providing an empty site, followed by migration of the alkyl portion of the acyl ligand to the vacant site. Because migration of an alkyl group to a *trans* position is also unlikely, all of the product should again show the ^{13}CO situated *cis* to the alkyl group. Since both mechanisms

¹T. C. Flood, J. E. Jensen, and J. A. Stadler, *J. Am. Chem. Soc.*, **1981**, *103*, 4410, and references cited therein.

Mechanism 2 vs. Mechanism 3:



Mechanism 2:



Mechanism 3:

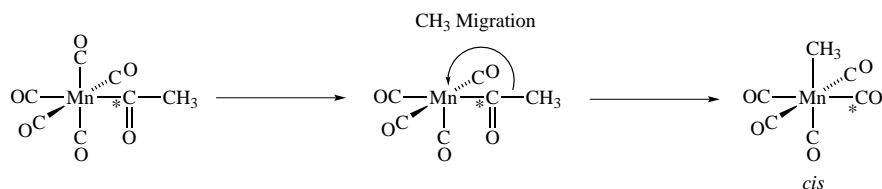


Figure 8-2

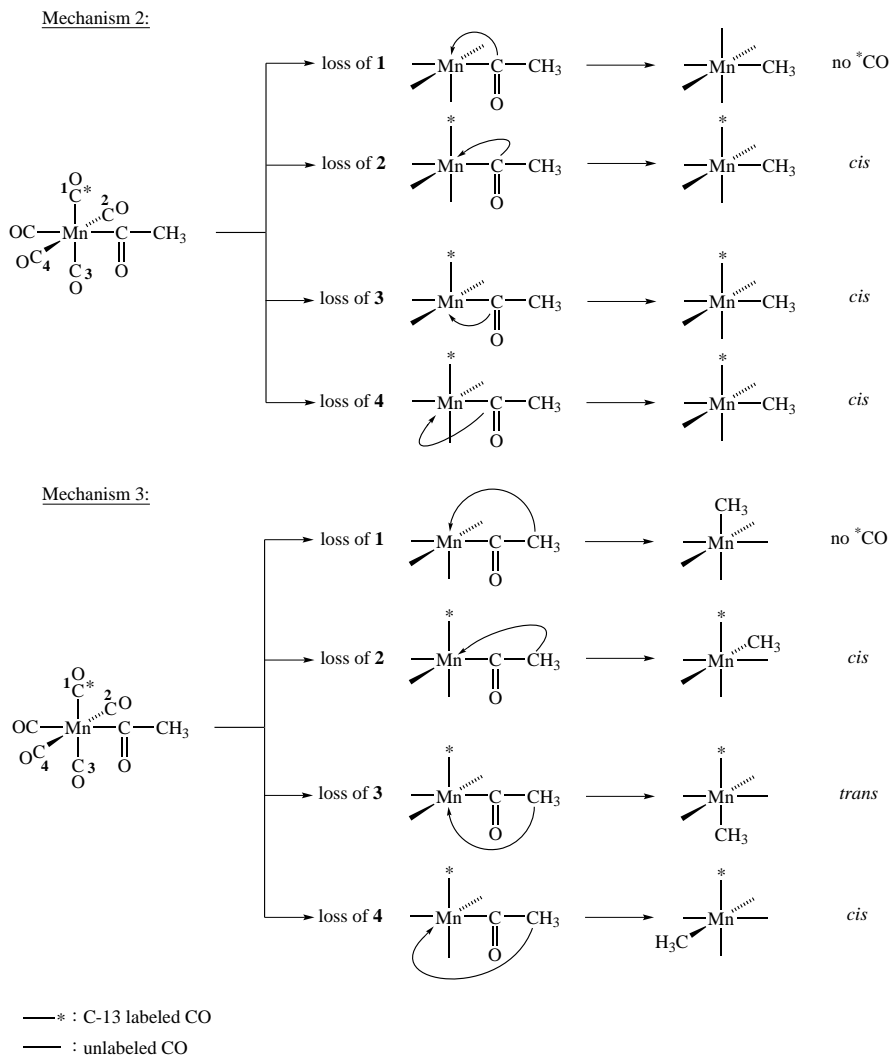
Mechanisms of Reverse Reactions for CO Migration and Alkyl Migration Related to Experiment II

2 and 3 in effect transfer labeled CO in the acyl group to a *cis* position, they are consistent with the experimental data for experiment II.

Exercise 8-1

Show that heating of $\text{CH}_3^{13}\text{C}(=\text{O})\text{-Mn}(\text{CO})_5$ would not be expected to yield the *cis* product by mechanism I.

The third experiment (Figure 8-3), which also invokes the principle of microscopic reversibility, allows a choice between mechanisms 2 and 3. The CO migration of mechanism 2, starting with ^{13}CO *cis* to the acyl ligand, requires migration of CO from the acyl ligand to the vacant site. As a result, 25% of the product should have no ^{13}CO label, and 75% should have the labeled CO *cis* to the alkyl, as shown in Figure 8-3. On the other hand, alkyl migration (mechanism 3) should yield 25% with no label, 50% with the label *cis* to the alkyl, and 25% with the label *trans* to the alkyl. Because this is the ratio of *cis*- to *trans*-products found

**Figure 8-3**

Mechanisms of Reverse Reactions for CO Migration and Alkyl Migration Related to Experiment III

in the experiment, the evidence supports mechanism 3, which continues to be the accepted pathway for this reaction.

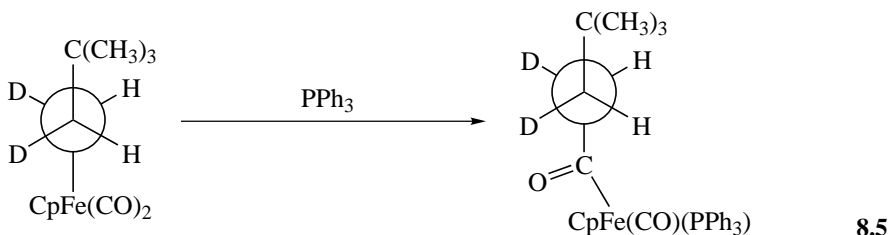
One additional point about the mechanism of these reactions should be made. In the discussion of mechanisms 2 and 3 above, it was assumed that the intermediate was a square pyramid and that no rearrangement to other geometries (such as trigonal bipyramidal) occurred. Other labeling studies, involving reactions of labeled $\text{CH}_3\text{Mn}(\text{CO})_5$ with phosphines, have supported a square-pyramidal intermediate.²

²See Footnote 1.

Exercise 8-2

Predict the product distribution for the reaction of *cis*-CH₃Mn(CO)₄ (¹³CO) with PR₃ (R = C₂H₅) (You may check your answer by consulting Footnote 1).

Stereochemical probes can provide useful information about the course of a reaction (see Section 7-2-3). Reaction of the *threo* iron complex (equation 8.5) with PPh₃ resulted in the *threo* migratory insertion product (95% stereoselectivity), which indicates that the alkyl group migrated with retention of configuration of the migrating center.³ This stereochemical result is consistent with that observed for alkyl migrations to carbocationic centers in organic reactions.



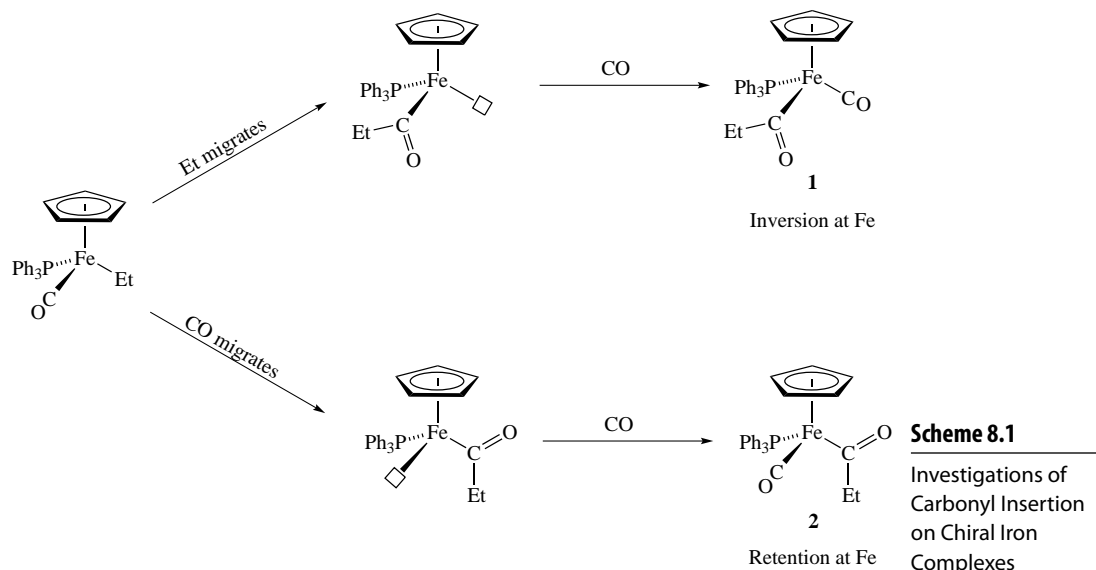
If CO insertion is really alkyl migration to CO, then the configuration of the metal center should not be retained upon migration when all ligands to the metal are different. In the CH₃Mn(CO)₅ complexes studied, it is impossible to tell that the configuration at the metal center changed after alkyl migration and attachment of free CO to the metal. The pseudotetrahedral iron complex shown in Scheme 8.1⁴ could serve as a useful stereochemical probe for examining the mechanism of carbonyl insertion–deinsertion.⁵ If the alkyl group migrates, we would expect **1** to form. If, on the other hand, the CO group migrates, enantiomeric complex **2** should be produced. Note that formation of **1** requires inversion of configuration at the metal, whereas **2** exhibits retention at the iron center. When the reaction was run in nitroethane solvent, **1** formed with 95% ee;⁶ however, when coordinating solvents such as hexamethylphosphoramide (HMPA) and acetonitrile were used,

³G. M. Whitesides and D. J. Boschetto, *J. Am. Chem. Soc.*, **1969**, *91*, 4313 and P. L. Bock, D. J. Boschetto, J. R. Rasmussen, J. P. Demers, and G. M. Whitesides, *J. Am. Chem. Soc.*, **1974**, *96*, 2814.

⁴A comment on notation is in order here. A box (□) attached to a metal signifies an open coordination site available for ligand coordination.

⁵T. C. Flood, *Top. Stereochem.*, **1981**, *12*, 37.

⁶The term “ee” stands for enantiomeric excess, that is the excess of one enantiomer over the other (%R – %S). For example, if a synthesis produced 90% S and 10% R, the ee = 90% – 10% = 80%. This means that the mixture consists of 80% S and 20% racemic modification (R + S). In the example used above, ee = 95% indicates the mixture consists of 97.5% S and 2.5% R.



both **1** and **2** formed. In the latter cases, there was even an excess of product **2** observed compared with **1**.⁷ It appears, unfortunately, that experiments designed to test the stereochemistry of the metal upon alkyl migration have produced conflicting results (see also problem **8-3**). Whether the experiments shown in Scheme **8.1** are the result of alkyl migration in nitroethane and net CO migration using coordinating solvents is unclear. It is also possible under some reaction conditions that the configuration of the intermediate upon alkyl migration is not fixed, thus leading to both inversion and retention of configuration at the metal center.

Other Considerations

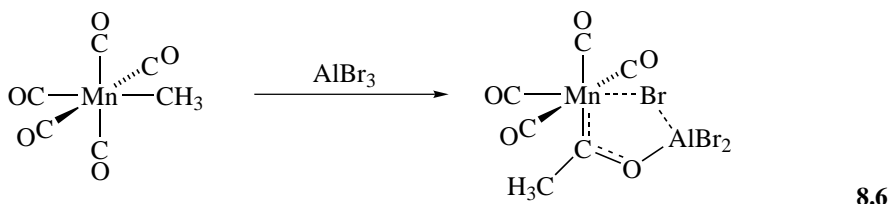
Within groups of transition metals, the tendency for CO insertion usually has the following order of reactivity: row 3 ~ row 4 > row 5.⁸ This trend reflects the strength of the M–C bond, which tends to increase as one goes down a column of the periodic table. Such results again lend support to the mechanism of insertion consisting of alkyl rather than CO migration. The observation that CO insertion into M–H bonds is less facile than insertion into M–C bonds also seems to reflect the typically higher bond strength of M–H bonds compared with M–C.

The presence of Lewis acids enhances CO insertion, not only by increasing the overall rate of reaction, but also by causing an alternative pathway of insertion to occur. The role of the Lewis acid is to complex with a CO ligand (thus making

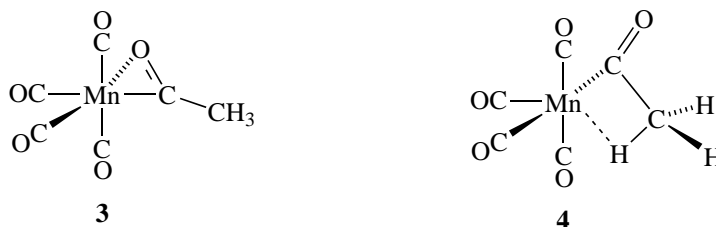
⁷T. C. Flood and K. D. Campbell, *J. Am. Chem. Soc.*, **1984**, *106*, 2853.

⁸See, for example, M. Aubert, G. Bellachioma, G. Cardaci, A. Macchioni, G. Reichenbach, and M. C. Burla, *J. Chem. Soc. Dalton Trans.*, **1997**, 1759.

the carbonyl carbon more positive and more susceptible to attack by the relatively electron-rich alkyl group) and to stabilize the resulting unsaturated acyl complex after alkyl migration. Equation 8.6 shows a specific example of the role of AlBr_3 in promoting CO insertion in alkyl metal carbonyl complexes, which actually occurs in the absence of free CO .⁹



More recently, there have been several investigations of CO insertion using high-level molecular orbital calculations at the DFT level. These have confirmed that CO insertion is indeed alkyl migration, and two intermediates, structures **3** and **4**, have been shown to exist along the reaction path.¹⁰



Structure **3** is termed a coordinatively-saturated η^2 -complex with the carbonyl oxygen also bonding to the metal. Such complexes are especially important during CO insertion with early transition metal complexes, since the metals involved tend to be highly oxophilic.¹¹ The η^2 -complex has also been detected during photochemically induced deinsertion of CO in $\text{CH}_3\text{Mn}(\text{CO})_5$.¹² Structure **4** is a coordinatively unsaturated complex that contains an agostic bond between the metal and the C–H hydrogen. Such interaction produces stabilization of the empty site.

It now seems clear that a reaction that initially appears to involve CO insertion, and is often so designated, does not involve CO insertion at all! In fact, it

⁹S. B. Butts, S. H. Strauss, E. M. Holt, R. E. Stimson, N. W. Alcock, and D. F. Shriver, *J. Am. Chem. Soc.*, **1980**, *102*, 5093 and T. G. Richmond, F. Basolo, and D. F. Shriver, *Inorg. Chem.*, **1982**, *21*, 1272.

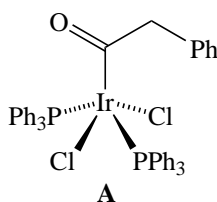
¹⁰A. Derecskei-Kovacs and D. S. Marynick, *J. Am. Chem. Soc.*, **2000**, *122*, 2078 and X. Wang and E. Weitz, *J. Organomet. Chem.*, **2004**, *689*, 2354.

¹¹Oxophilicity is a measure of the affinity of a metal for bonding with oxygen.

¹²P. C. Ford and S. Massick, *Coord. Chem. Rev.*, **2002**, *226*, 39 and S. M. Massick, V. Mertens, J. Marhenke, and P. C. Ford, *Inorg. Chem.*, **2002**, *41*, 3553.

is really analogous to a 1,2-alkyl shift in organic chemistry where a relatively electron-rich alkyl carbon migrates (with retention of configuration) to a relatively electron-poor center in order to produce a more stable carbocation. It is not uncommon for reactions, on close study, to be found to differ substantially from how they might first appear. In this reaction, as in all chemical reactions, it is extremely important for chemists to undertake mechanistic studies and to keep an open mind with regard to possible alternative mechanisms. No mechanism can be proven; it is always possible to suggest alternatives consistent with the known data. It does appear, however, that for the vast majority of carbonyl insertions, the reaction involves migration of the alkyl group to the carbonyl ligand with retention of configuration of the migrating center.

Complex **A** [$\nu(\text{CO}) = 1670 \text{ cm}^{-1}$] rearranges cleanly to the isomeric compound **B** [$\nu(\text{CO}) = 2040 \text{ cm}^{-1}$] at 30° in benzene. Draw a possible structure for **B**.

Exercise 8-3


8-1-2 1,2-Insertion and Deinsertion (β -Elimination)

1,2-Insertion into M–H Bonds

Alkenes and alkynes can undergo 1,2-insertion into M–H bonds. The numbering again refers to the numbers for the carbon atoms on the double or triple bond. A schematic insertion reaction is outlined below:

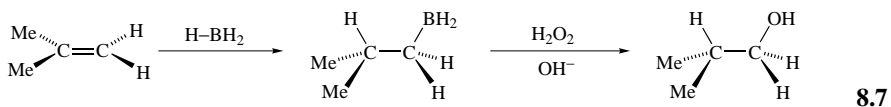


or



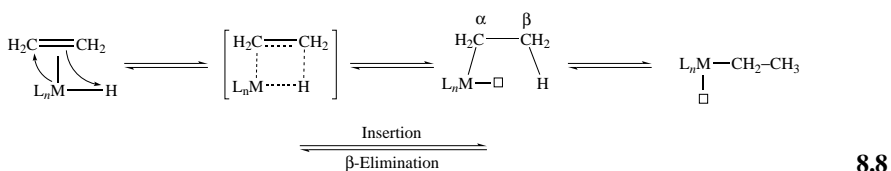
We can also think of 1,2-insertion as migration of the hydride to the β -position on the alkene or alkyne, much the same as we saw for 1,1-CO migratory insertion.

A useful 1,2-insertion reaction encountered in organic chemistry is hydroboration of an alkene to form an alkylborane (equation 8.7), which subsequently undergoes treatment with alkaline H_2O_2 to yield an alcohol.



From the organic chemist's standpoint, hydroboration is considered a *syn* addition of a B–H bond across a C=C or C \equiv C bond. Categorizing the reaction as a 1,2-insertion is, however, equally valid.

We saw in Chapter 6 that a reaction that is the reverse of 1,2-insertion—called 1,2- or β -elimination—may also occur with metal alkyls, the product of insertion.¹³ Equation 8.8 details the insertion–elimination reaction that yields a vacant site for coordination in the forward direction (1,2-insertion) and requires a vacant site for the reverse (β -elimination) pathway.



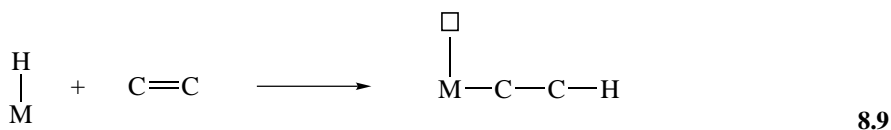
Experimental evidence and computational analysis point to a mechanism in which the alkene (or alkyne) carbons and the M–H bond must be nearly coplanar to react. Once the metal alkene complex has achieved such geometry, 1,2-insertion can occur. During insertion, the reactant proceeds through a four-center transition state.¹⁴ The reaction involves simultaneous breakage of the M–H and C–C π bonds, as well as the formation of an M–C σ bond and a C–H bond at the 2-position of the alkene (or alkyne). The result is a linear compound, $\text{L}_n\text{M}(\text{CH}_2\text{CH}_3)$, in the case of ethene insertion. The reverse reaction, β -elimination, follows the same pathway starting from a metal–alkyl complex with an open coordination site.

¹³The Greek letter α is used to designate the carbon atom (or other non-hydrogen atom) directly attached to the metal. The next position beyond the α -position is designated β and the next one beyond that γ , etc.

¹⁴See H. Wadepohl, U. Kohl, M. Bittner, and H. Köppel, *Organometallics*, **2005**, *24*, 2097, for a recent computational study at the DFT level of the mechanism of C=C insertion into a Co–H bond, which shows a picture of the four-centered transition state determined by high-level MO calculations.

Note that the hapticity of the organic ligand decreases by one (η^2 to η^1) with insertion and increases by one (η^1 to η^2) during β -elimination.

Insertion is generally exothermic (but not highly so) according to the following analysis using the estimated energies of bonds made and broken (see Table 7-6) in the schematic equation 8.9.



Bond Energies:

Broken:

M-H:	65–80 kcal/mol
π -C=C:	50–60 kcal/mol
Total:	115–140 kcal/mol

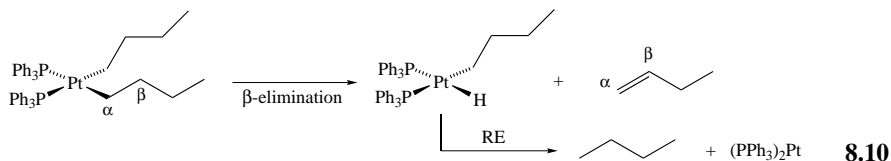
Formed:

M-C:	40–70 kcal/mol
C-H:	90–100 kcal/mol
Total:	130–170 kcal/mol

$$\Delta_r H = -15 \text{ to } -30 \text{ kcal/mol}$$

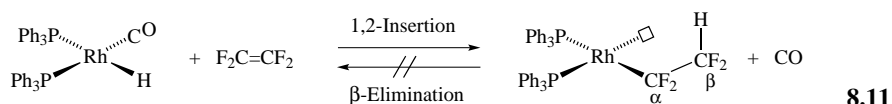
Because $\Delta_r S$ for insertion should be negative, the free energy of the reaction will be slightly negative. This, of course, means that the reverse reaction (β -elimination) should also have a $\Delta_r G$ value that is slightly positive, since the positive $\Delta_r S$ counterbalances the positive $\Delta_r H$. On the basis of thermodynamics, it is thus not surprising that both insertion and deinsertion are common components of catalytic cycles because the free energy barrier of either reaction is not insurmountable. Experiment and theory¹⁵ have demonstrated that 1,2-insertion tends to be more uphill thermodynamically as one goes from third-row to fifth-row transition metal complexes, probably due mainly to increasing M–H bond strength.

Transition metal alkyl complexes tend to be kinetically unstable and rapidly undergo β -elimination. Equation 8.10 shows the decomposition of a dibutylplatinum complex, first through β -elimination and then through the already-familiar mode of reductive elimination.



¹⁵Y. Han, L. Deng, and T. Ziegler, *J. Am. Chem. Soc.*, **1997**, *119*, 5939, and references therein.

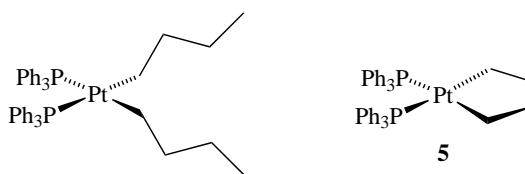
There are several ways to prevent or at least lessen the propensity for β -elimination to occur (especially after 1,2-insertion has occurred). Obviously, if there is no β -hydrogen atom, elimination cannot occur. Electron withdrawing atoms, such as fluorine, placed at the α - or β -alkyl positions (equation 8.11), will also lessen the tendency for β -elimination by strengthening the M–C σ bond.

**Exercise 8-4**

Why does the presence of C–F bonds at the α - or β -positions of an alkyl ligand tend to strengthen the M–C bond of the metal alkyl complex?

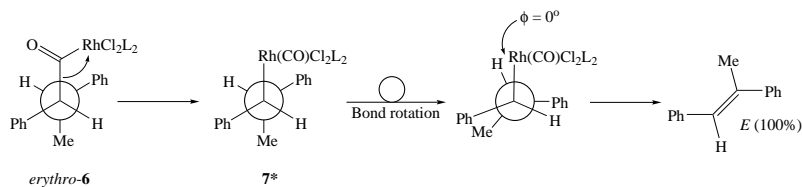
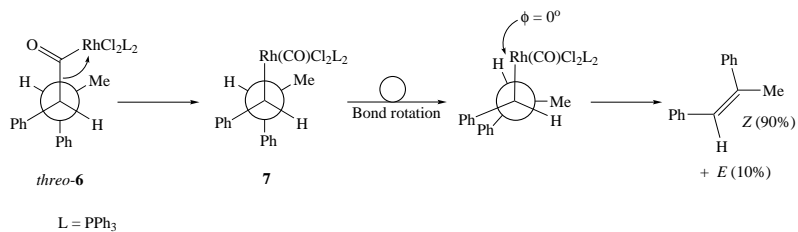
Coordinationally-saturated metal–alkyl complexes tend not to undergo β -elimination, especially if they are in solution in the presence of an excess of L-type ligand, such as CO or PR_3 , or if ligands also bound to the complex, such as Cp or bidentate phosphines, are reluctant to leave and provide an open coordination site.

Metal alkyls in which the metal, C–C bond, and the β -hydrogen cannot become coplanar either do not undergo elimination or do so at a severely retarded rate. For example, the platinacyclopentane¹⁶ (**5**) is kinetically more stable than the corresponding dibutyl complex by a factor of 10^4 .

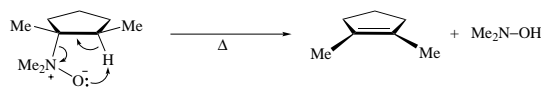


Equation 8.12 illustrates β -elimination from a rhodium complex, a reaction preceded by deinsertion of CO. The reaction is significant in demonstrating that the stereochemistry of the elimination is typically *syn* in which the dihedral angle (ϕ) defined by the C(β)–H bond and the M–C(α) bond is 0° . The stereochemistry of β -elimination is analogous to that observed in organic chemistry with the Cope reaction, which is a useful method of synthesizing alkenes, shown in equation 8.13. The success of this unimolecular, concerted reaction requires that the amine oxide group and the β hydrogen be coplanar (*syn*).

¹⁶J. X. McDermott, J. F. White, and G. M. Whitesides, *J. Am. Chem. Soc.*, **1976**, 98, 6521.



8.12



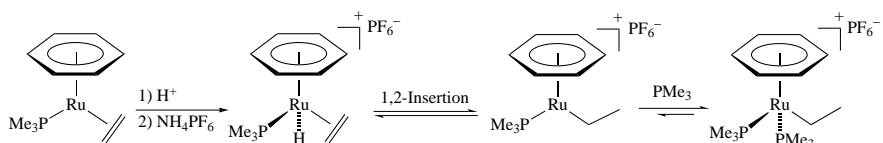
8.13

Elimination from the rhodium complex is another example of the use of stereochemical probes to demonstrate *syn* orientation of the β -hydrogen and the metal–carbon bond. Starting with the *threo*-acylrhodium complex **6**, the reaction first proceeds through 1,1-deinsertion of the CO with retention of configuration to give *threo*-alkylrhodium **7**. β -Elimination yields (*Z*)-1-methyl-1,2-diphenylethene as 90% of the product (10% is the corresponding *E*-isomer). Starting with the *erythro* isomer, 1,1-deinsertion of CO (to give **7***) and elimination provide exclusively the *E*-alkene.¹⁷ The results are entirely consistent with *syn* stereochemistry for β -elimination and also, by virtue of the principle of microscopic reversibility, correspond to a *syn* geometry for 1,2-insertion. The metal complex thus serves as a template allowing stereospecific insertion or deinsertion to occur.

Equation **8.14** illustrates how the equilibrium between insertion and elimination can be shifted in favor of the metal alkyl by adding an electron-rich trialkyl phosphine ligand to a Ru(II) complex.¹⁸ The alkyl complex is positively charged, but electron-rich phosphines stabilize it. This means that loss of one of the phosphines to create an open coordination site necessary for β -elimination is less likely than in a neutral complex.

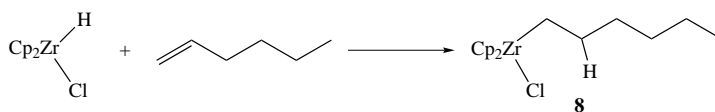
¹⁷J. K. Stille, F. Huang, and M. T. Regan, *J. Am. Chem. Soc.*, **1974**, *96*, 1518.

¹⁸H. Werner and R. Werner, *J. Organometal. Chem.*, **1979**, *174*, C63.



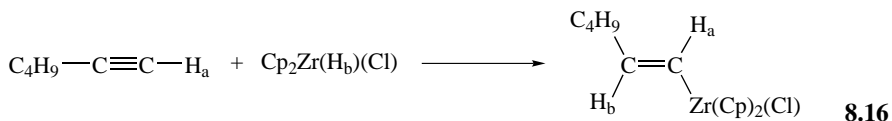
8.14

One of the more synthetically useful 1,2-insertions, hydrozirconation, is shown in equation 8.15. The starting material, known as Schwartz's reagent,¹⁹ readily reacts with 1-alkenes to give the corresponding alkyl zirconium complex **8**. This d^0 Zr(IV) complex is stable and undergoes relatively little useful synthetic chemistry on its own, but ultimately it is a synthetically valuable intermediate. One of the driving forces for β -elimination is thought to be the ability of the metal to donate d electrons to an antibonding σ orbital located mainly at the β C–H bond. Placing electrons in this orbital weakens the C–H bond, an event necessary for elimination to occur. Thus, the lack of d electrons on the Zr,²⁰ which could back-donate into a β -C–H σ^* orbital, serves as a major reason for the kinetic stability of **8**. In addition, 1,2-insertion into M–H bonds tends to be more exothermic for early transition metal complexes compared with that for complexes involving mid- to late-transition metals because the difference between M–H bond energy in the reactant and the M–C bond energy of the product is less (ca. 20 kcal/mol vs. 30 kcal/mol for late transition metals), which results in a more negative $\Delta_r G$.



8.15

Hydrozirconation occurs with *syn*-addition of the Zr–H bond across a C=C or C \equiv C bond (equation 8.16). Due to lower steric hindrance, the addition also tends to be regioselective, with the zirconium attached to the less substituted position (just as in hydroboration). Internal alkenes and alkynes isomerize to 1-alkyl and 1-alkenyl complexes, respectively—presumably by alternating reactions of insertion and deinsertion—until the complex with the least steric hindrance is formed.



8.16

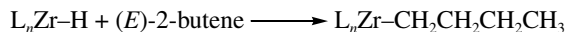
¹⁹J. Schwartz and J. A. Labinger, *Angew. Chem. Int. Ed. Eng.*, **1976**, *15*, 333.

²⁰High-valent, early transition metals such as Zr(IV) in general lack d electrons and M-alkyl complexes tend to be relatively kinetically stable.

1,2-Insertion of alkynes into early transition metal M–H bonds is much more exothermic than corresponding alkene insertion. Explain. [Hint: See section 7-2-1.]

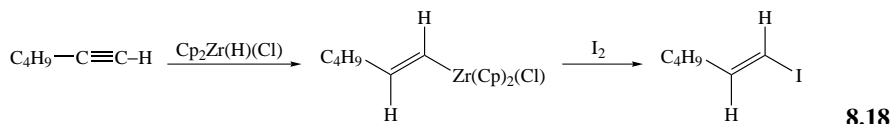
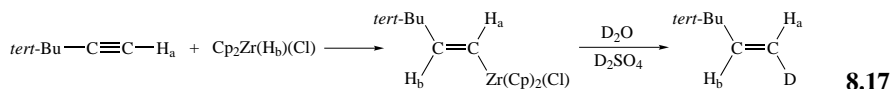
Exercise 8-5

Propose a mechanism for the following reaction.



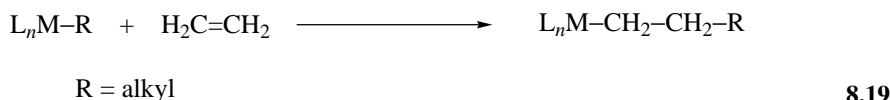
Exercise 8-6

Equations 8.17²¹ and 8.18 indicate that zirconium alkyls do undergo cleavage by electrophiles (see Section 8-4-1), such as protic acids or halogens (X₂), to give the corresponding hydrocarbon or alkyl (alkenyl) halide. Note that retention of configuration occurs at the carbon attached to the metal as the reaction proceeds to the organic product.



1,2-Insertion into an M–C Bond

The insertion of a C=C bond between a metal and a carbon atom is of great importance in building long carbon chains. When the process occurs according to equation 8.19, giant molecules with masses well over 10,000 Da²² can result.

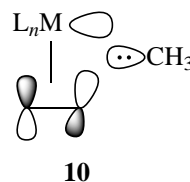
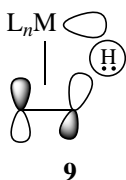


The molecules are then processed into plastics such as polypropylene or high-density polyethylene. Chemists now agree that the key step in such polymerizations involves a “classical” insertion of C=C into an M–C bond analogous to 1,2 M–H insertion.

²¹J. A. Labinger, D. W. Hart, W. E. Seibert, III, and J. Schwartz, *J. Am. Chem. Soc.*, **1975**, 97, 3851.

²²A dalton (Da) is the same as the atomic mass unit, 1/12 the mass of a ¹²C atom.

Although $\Delta_r G$ is more negative than for M–H insertion,²³ M–C insertion appears to be unfavorable kinetically. Computational analysis of M–C insertions indicates a higher kinetic barrier than that for M–H insertion, and this barrier increases as one goes down the periodic table. Why is this the case? If we assume that 1,2-insertion is actually migration of a hydrogen (or more accurately, a hydride) or a carbon (carbanion) to the β -position of the C=C bond (represented by the empty π^* orbital), then the reaction requires that as an M–H (or M–C) bond breaks, a C–H (or C–C) bond must form. The spherical nature of the hydrogen 1s orbital (occupied by two electrons) allows for smooth, continuous overlap among it, the appropriate metal orbital, and the developing sp^3 orbital at the β -position (structure **9**). The directional nature of the sp^3 orbital (also doubly occupied) on the migrating carbon, on the other hand, makes such continuous overlap more difficult (structure **10**).²⁴ This analysis is very similar to that presented in Section 7-2-2 that compared C–H to C–C bond activation.



It appears that *both* thermodynamic and kinetic effects make 1,2-insertion into both M–H and M–C bonds more difficult going from third-row to fourth-row and finally to fifth-row transition metals.

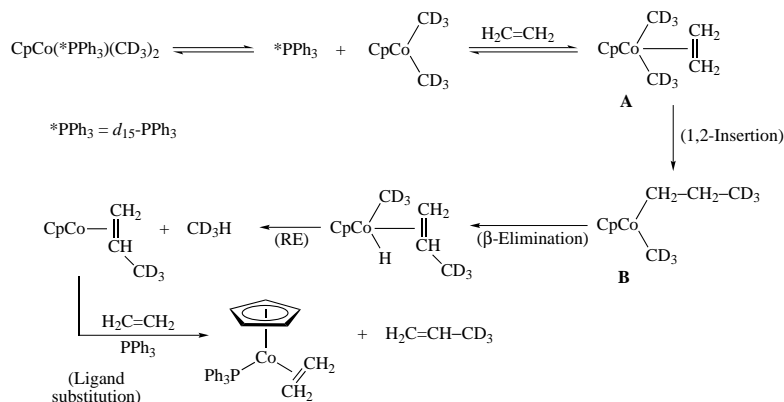
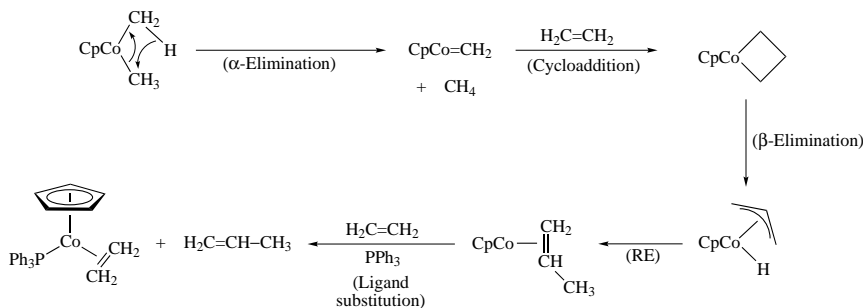
In addition to the relatively high kinetic barrier to 1,2-insertion into M–C bonds, rapid β -elimination of the insertion product would normally preclude direct observation of the insertion. There have been reports, however, of a few examples of C=C insertion into an M–C bond. We will mention a couple of these after describing a key experiment that lent credence to the possibility that C=C insertion can occur in the “classical” manner.

Almost 30 years ago, Bergman²⁵ reported on chemistry that is detailed in Scheme 8.2. Labeled cobalt complex **A** undergoes insertion of ethylene between the metal and CD₃ group to give the intermediate propyl cobalt complex **B**. β -Elimination and subsequent reductive elimination ultimately provide CD₃–CH=CH₂ and CHD₃, products that seem reasonable only as the result of

²³Note that insertion into an M–C bond results in a new M–C bond with about the same energy as that in the starting material. Thus, this insertion is more favorable enthalpy-wise than C=C or C≡C insertion into a relatively strong M–H bond.

²⁴See Footnote 14 for a more complete analysis.

²⁵E. R. Evitt and R. G. Bergman, *J. Am. Chem. Soc.*, **1979**, *101*, 3973.

"Classical" Mechanism:**Alternate Mechanism:****Scheme 8.2**

C=C Insertion into an M-C Bond

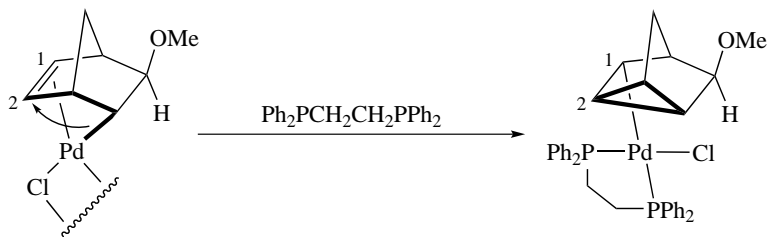
direct insertion by the "classical" pathway. An alternative mechanism, also illustrated in Scheme 8.2, involves an early α -elimination step that would give CD_4 and $\text{CD}_2=\text{CH}-\text{CH}_3$ instead starting from the same deuterated Co complex.

Show how the alternative mechanism in Scheme 8.2 would give CD_4 and $\text{CD}_2=\text{CH}-\text{CH}_3$ starting with the hexadeuterodimethyl cobalt complex and ethene.

Exercise 8-7

If the mechanism of C=C insertion into an M-C bond is truly analogous to that for M-H bonds, then the stereochemistry should be the same (i.e., *syn* addition of M-C to the double bond). If the R group (equation 8.19) constitutes a stereogenic center, moreover, retention of stereochemistry should be observed. Equation 8.20 demonstrates one of the few examples of stereospecific C=C

insertion where the metal and R group have no real alternative but to undergo *syn* addition with retention of configuration at R.²⁶



8.20

The sequence of reactions outlined in Scheme 8.3²⁷ shows a high degree of stereospecificity for C=C insertion.²⁸ (*Z*)-1-Phenyl-1-propene yields finally (*Z*)-1,2-diphenylpropene as 90% of the products collected. Starting with (*E*)-1-phenyl-1-propene, the corresponding (*E*)-1,2-diphenyl-1-propene was obtained as virtually the only product. If one assumes that the last step, which is β -elimination, proceeds with *syn* stereochemistry only, then C=C insertion must also be *syn*.

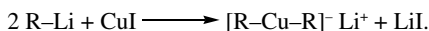
Exercise 8-8

Start with (*E*)-1-phenyl-1-propene instead of the *Z*-isomer in Scheme 8.3 and show that the corresponding *E*-diphenylpropene forms as the result of *syn* C=C insertion and *syn* β -elimination.

Equation 8.21 demonstrates another reaction (this time catalytic in the Rh complex and also using a radical scavenger to prevent polymerization of the vinyl group) where C=C insertion into an M–C bond must have occurred. Scheme 8.4 follows up on this reaction by illustrating the results of an analysis of the mechanism of the catalytic cycle that involved first oxidative addition of one of two possible C–C bonds to Rh, followed by C=C insertion. A labeling experiment using ¹³C indicated that an alternative rhodacyclic intermediate **11** was not involved and suggested that path **a** was the correct mechanism.²⁹

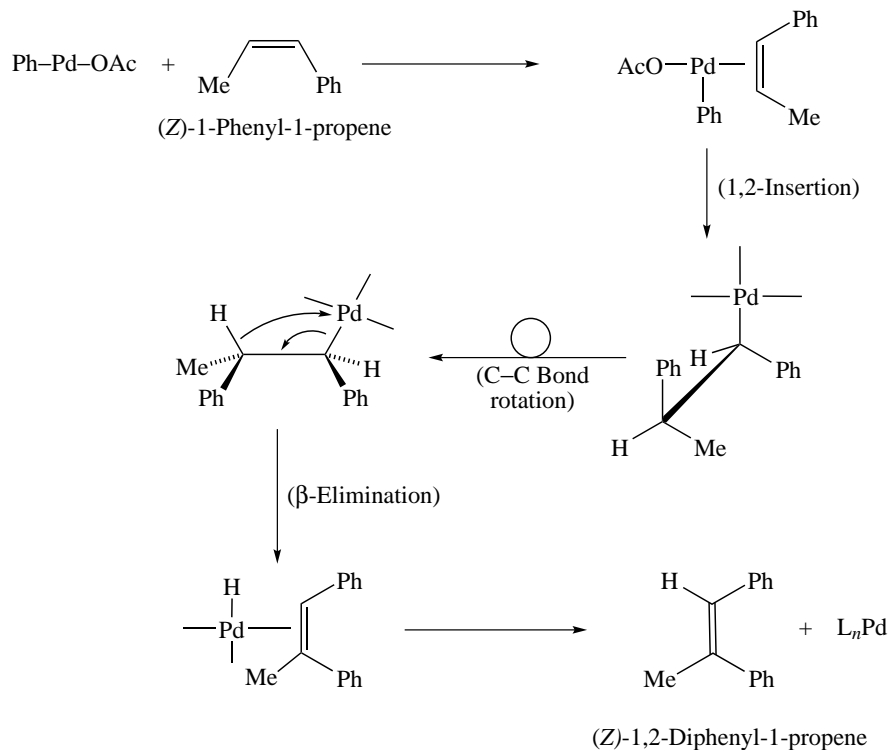
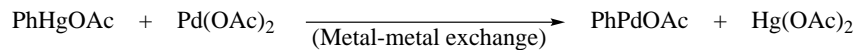
²⁶D. R. Coulson, *J. Am. Chem. Soc.*, **1969**, *91*, 200.

²⁷The first step in Scheme 8.3 shows a metal–metal exchange, a reaction common in organometallic chemistry. Such exchanges will be discussed in Chapter 12. The exchange shown in the scheme is reminiscent of the metal–metal exchange that occurs in the formation of Gilman reagents. For example,

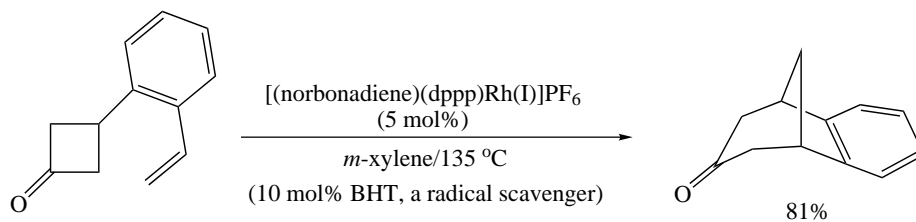


²⁸R. F. Heck, *J. Am. Chem. Soc.*, **1969**, *91*, 6707.

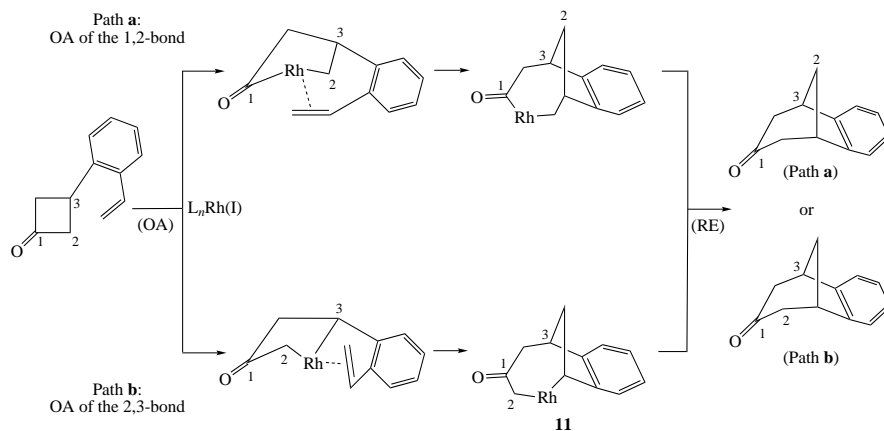
²⁹M. Murakami, T. Itahashi, and Y. Ito, *J. Am. Chem. Soc.*, **2002**, *124*, 13976.

**Scheme 8.3**

C=C Insertion into a Pd-Ph Bond

**8.21**

Scheme 8.4
Rh-Catalyzed
Formation of a
Cyclic Ketone

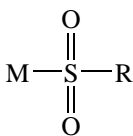
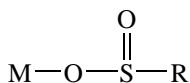
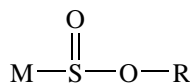
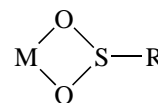
**Exercise 8-9**

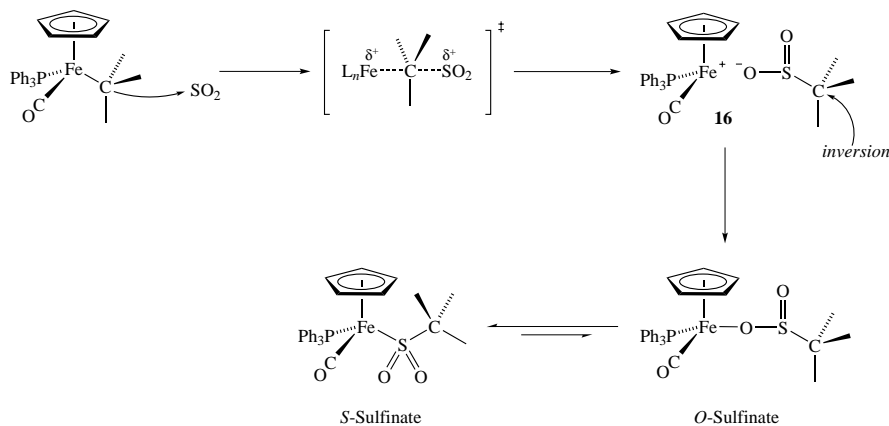
Propose a mechanism for the formation of compound **11** in Scheme 8.4.

Efforts to completely elucidate the mechanism of C=C insertion into an M–C bond remain an active area of research in organometallic chemistry. We shall again consider this reaction when we discuss metal-catalyzed polymerization in Chapter 11.

1,1- and 1,2-Insertion of SO₂

SO₂ may insert into an M–C bond in a variety of ways yielding structures **12–15**. Only the *S*-sulfinate **12** and *O*-sulfinate **13** are usually observed, however. Whether the sulfur or the oxygen binds to the metal depends upon metal softness, with softer metals binding to sulfur and harder metals binding to oxygen (see Section 7-1-2). For most of the transition metals, the *S*-sulfinate form predominates. Complexes of titanium and zirconium, on the other hand, often give the *O*-sulfinate insertion product, owing to the harder, more oxophilic nature of the early transition metals. A reaction to form **12** constitutes a formal 1,1-insertion, whereas overall 1,2-insertion leads to **13**.

**12****13****14****15**

**Scheme 8.5**Mechanism of SO_2
Insertion

The mechanism of SO_2 insertion has been investigated extensively for 18-electron iron complexes.³⁰ Scheme 8.5 outlines the general mechanism for insertion. Note that SO_2 is a Lewis acid (electrophile), and it does not attack the metal in this case.³¹

The reaction is considered to proceed first via an $\text{S}_{\text{E}}2$ ³² pathway where, like its nucleophilic counterpart in organic chemistry, inversion of configuration is observed at the carbon attached to the metal (the α -carbon). After electrophilic attack, a tight or intimate ion pair, **16**, forms that retains stereochemical integrity at the carbon. Collapse of **16** leads to the *O*-sulfinate. The *O*-sulfinate seems to be the kinetically-favored product that ultimately rearranges to the more thermodynamically stable *S*-sulfinate. The rate of the reaction is sensitive to the nature of substituents attached to the metal-bound carbon. Bulky alkyl groups decrease the rate, consistent with a bimolecular, concerted step involving a sterically congested transition state. Electron withdrawing substituents attached to the α -carbon also result in a rate retardation by making the carbon less nucleophilic.

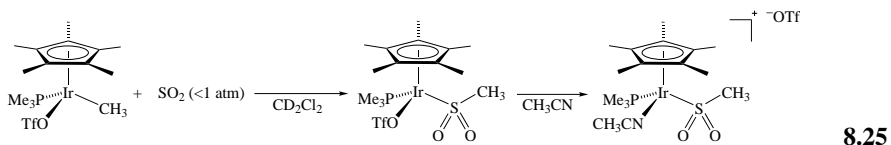
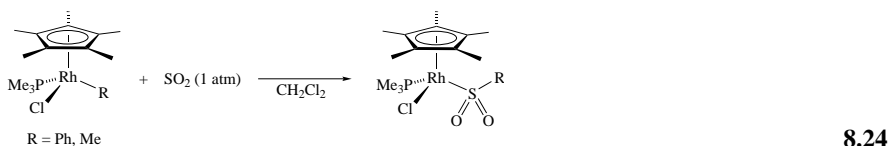
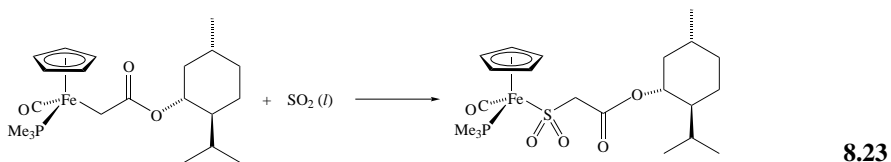
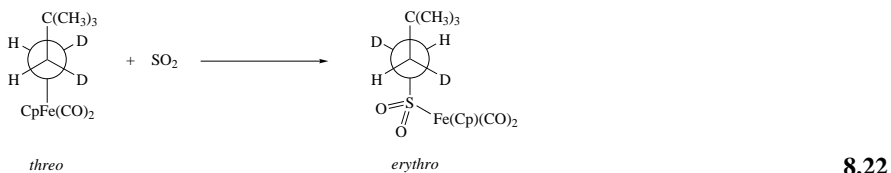
Equations 8.22 and 8.23 illustrate the results of some studies designed to elucidate the stereochemistry involved in SO_2 insertion into iron complexes. In 8.22, the *threo* Fe complex undergoes insertion to yield the corresponding *erythro* *S*-sulfinate with a high degree of stereospecificity. Unlike CO insertion, retention of configuration occurs at the metal center. Equation 8.23 illustrates an experiment designed to correlate stereochemistry of reactant and insertion product.

³⁰A. Wojcicki, "Insertion Reactions of Transition Metal–Carbon σ -Bonded Compounds II. Sulfur Dioxide and Other Molecules." In *Advances in Organometallic Chemistry*, F. G. A. Stone and R. West, Eds., Academic Press: New York, 1974, Vol. 12, pp. 31–81, and references therein.

³¹In some cases, when the metal complex is electron rich, the initial reaction with SO_2 consists of the metal acting as an electron-pair donor to the empty sulfur $3p$ orbital of SO_2 to form an $\text{L}_n\text{M}-\text{SO}_2$ complex, which then undergoes insertion into an $\text{M}-\text{C}$ bond.

³² $\text{S}_{\text{E}}2$ stands for "substitution-electrophilic-bimolecular."

The stereospecificity of the insertion is greater than 90% retention at the metal center.³³ Equations 8.24 and 8.25 show additional examples of SO₂ insertions.³⁴



Insertion of SO₂ occurs with a wide variety of transition metal complexes, almost as commonly as CO insertion. Unlike CO, however, deinsertion of SO₂ (desulfination) is not common. Because SO₂ reacts with 18-electron complexes, the resulting coordinatively saturated insertion complex must lose a ligand to provide an open site for alkyl migration to occur. Apparently, this is a difficult process, and when it does occur, it is accompanied by substantial decomposition.

Several other small molecules undergo “insertion” into M–C bonds. Examples of these are R–NC (1,1-insertion of the C-atom of an isonitrile),³⁵ NO

³³T. C. Flood and D. L. Miles, *J. Am. Chem. Soc.*, **1973**, 95, 6460.

³⁴L. Lefort, R. J. Lachicotte, and W. D. Jones, *Organometallics*, **1998**, 17, 1420.

³⁵Y. Kayaki and A. Yamamoto, “1,1-Insertions into Metal–Carbon Bonds,” In *Fundamentals of Molecular Catalysis*, H. Kurosawa and A. Yamamoto, Eds., Elsevier: Amsterdam, 2003, pp. 390–395.

(1,1-insertion of the N-atom),³⁶ and CO₂ (1,2-insertion).³⁷ Discussion of these and other insertions is beyond the scope of this text.

8-2 NUCLEOPHILIC ADDITION TO THE LIGAND

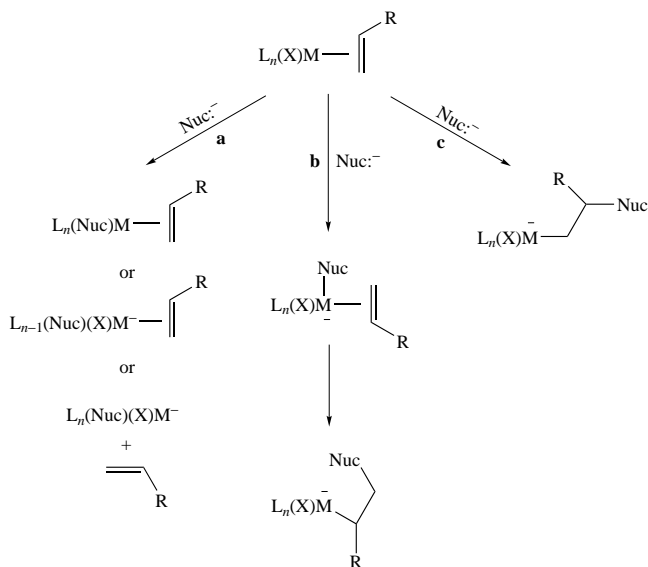
A nucleophile may attack an organometallic complex—substituted with at least one unsaturated ligand (e.g., CO, alkene, polyene, arene)³⁸—in a variety of ways, as shown in Scheme 8.6. Path **a** involves nucleophilic attack at the metal, which was already discussed in Chapter 7. Nucleophilic attack at the metal (via a four-centered transition state) is also of importance with regard to transmetallation reactions in which alkyl, alkenyl, alkynyl, and aryl groups may be transferred from either ionically bonded main group organometallic compounds, such as Grignard reagents, or more covalent compounds, such as R–Hg–Cl. These reactions were discussed in Section 6-1; we will see how they may be applied to organic synthesis in Chapter 12. Path **b** also involves nucleophilic attack at the metal, but instead of displacement, a *syn* insertion of an unsaturated ligand between the metal and the nucleophilic ligand can occur, some of the details of which we discussed earlier in Chapter 8. In contrast to the first two paths, path **c** shows the nucleophile attacking the ligand. It is this route that we shall consider in our discussion of nucleophilic reactions, because such a pathway offers the chemist numerous possibilities for accomplishing synthetic transformations that would be impossible without the presence of the metal. Note that with path **c**, the hapticity of the π ligand decreases by one and the overall charge on the complex becomes more negative by one unit.

Path **c** demonstrates a phenomenon that often occurs in organometallic chemistry—*umpolung*. *Umpolung* is a German word that translates into English approximately to mean “reversal of polarity.” One example of *umpolung* from the realm of organic chemistry is shown in equation 8.26 where an electrophile, CH₃I, adds to a dithiane to give a ketone.

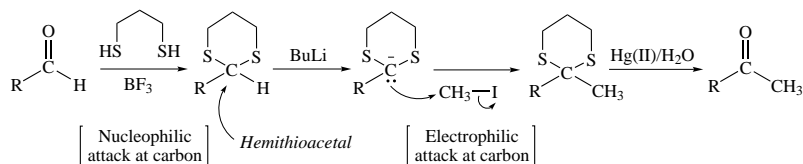
³⁶S. Niu and M. B. Hall, *J. Am. Chem. Soc.*, **1997**, *119*, 3077.

³⁷Transition metal-catalyzed insertion of CO₂ into M–H and M–C bonds could be an important pathway toward utilization of this abundant C₁ molecule in organic synthesis and for industrial-scale processes, potentially replacing the use of CO. For examples of CO₂ insertion, see R. Johansson and O. F. Wendt, *Dalton Transactions*, **2007**, 488; A. R. Cutler, P. K. Hanna, and J. C. Vites, *Chem. Rev.*, **1988**, *88*, 1363; and W. J. Evans, C. A. Seibel, J. W. Ziller, and R. J. Doedens, *Organometallics*, **1998**, *17*, 2103. For another review, which discusses (in part) the utilization of CO₂ by way of M–C insertion, see T. J. Marks, *et al.*, *Chem. Rev.*, **2001**, *101*, 953.

³⁸The latter three groups are generally also known as π ligands.

**Scheme 8.6**

Reactions of
Nucleophiles with
Metal Complexes

**8.26**

The overall transformation represents formally the attack of an electrophile at the carbon of a carbonyl group. Normally, only nucleophiles attack carbonyl carbon atoms (as indicated in the first step of equation 8.26) because these carbons represent electron-deficient sites. By converting the carbonyl to a hemithioacetal and pulling off the now relatively acidic proton with base, the carbonyl carbon becomes nucleophilic instead of electrophilic.

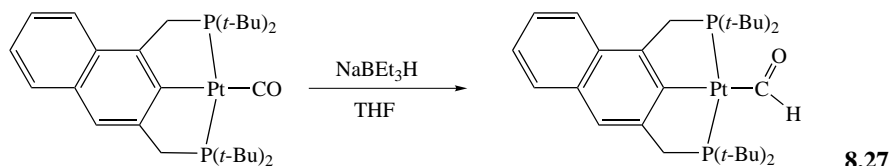
Alkenes, polyenes, arenes, and CO normally do not react with nucleophiles because these species are already electron rich. When these π ligands complex with a metal, however, (especially if the metal is electron deficient due to the presence of other electron-withdrawing ligands or due to a relatively high oxidation state), they are forced to give up some of their electron density to the attached metal complex fragment. The complexed ligands are now electron deficient compared with

their free state. Nucleophilic attack on them is now possible, giving a substituted ligand that can either stay attached to the metal or be released from the metal by numerous methods such as β -elimination or oxidative cleavage (Section 8-4-1).

The tendency for a nucleophile to attack an unsaturated ligand directly is a function of the electron density on the metal (i.e., complexes with a formal positive charge on the metal are more reactive than neutral ones), the degree of coordinative saturation of the metal (unsaturated metals have a higher probability of attack directly at the metal), and the presence of π -electron attracting ligands (such as CO) that can absorb some of the increased electron density on the metal after attack has occurred.

8-2-1 Addition at CO and Carbene Ligands

Equations 8.27 to 8.29 illustrate that carbonyl and carbene ligands can undergo nucleophilic reactions. In equation 8.27, NaBEt_3H delivers a hydride to the carbonyl ligand to yield a relatively rare Pt–formyl complex.³⁹ Attack by OH^- on one of the CO ligands in $\text{Fe}(\text{CO})_5$ liberates CO_2 in equation 8.28.⁴⁰ This is a key step in the iron-catalyzed⁴¹ water–gas “shift reaction,” a process used to produce H_2 from a mixture of CO and H_2O . Equation 8.29 illustrates a Fischer carbene complex⁴² undergoing attack by a I° amine to yield a product that requires replacement of OMe by NRH_2 . This is analogous to a reaction in organic chemistry known as aminolysis (shown also for comparison in equation 8.30), where the amine nucleophile attacks the carbon to produce a tetrahedral intermediate. Breakdown of the intermediate yields the substituted product plus alcohol (or alkoxide) as the leaving group. The carbene complex in this case reacts as if it were a carboxylic acid derivative.

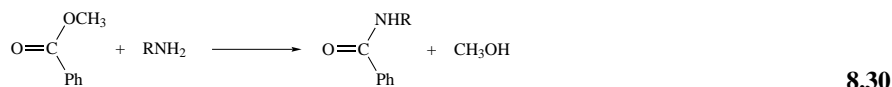
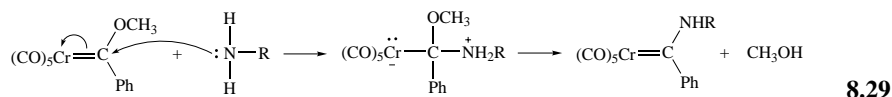
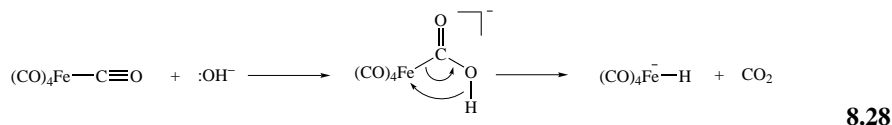


³⁹L. Schwartsburd, E. Poverenov, L. J. W. Shimon, and D. Milstein, *Organometallics*, **2007**, 26, 2931. The steric bulk of the PCP pincer ligand helps to stabilize the Pt–CO complex, and the electronic properties of the naphthyl group enhance the susceptibility of the CO group toward reaction with a nucleophile.

⁴⁰This reaction is analogous to the loss of CO_2 under thermal conditions from a β -carbonyl carboxylic acid such as malonic acid, $\text{CH}_2(\text{COOH})_2$.

⁴¹J. W. Reppe, *Annalen*, **1953**, 582, 121.

⁴²H. Werner, E. O. Fischer, B. Heckl, and C. G. Kreiter, *J. Organomet. Chem.*, **1971**, 28, 367.



8-2-2 Addition to π Ligands

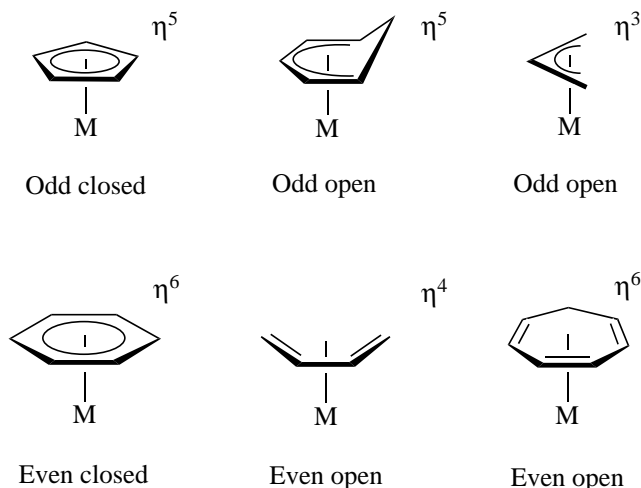
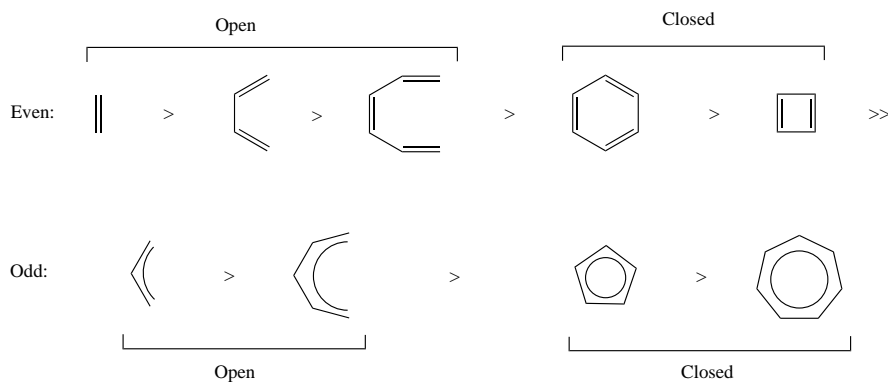
Numerous examples of nucleophilic addition to π hydrocarbonyl ligands exist.⁴³ The regiochemistry of these additions to cationic metal complexes has been well studied and summarized by Davies, Green, and Mingos⁴⁴ (DGM) as a set of rules. These rules can be used to predict where the nucleophile will add to a variety of π -ligands when the reaction is under kinetic control. A summary of the rules follows.

1. Nucleophilic attack occurs preferentially at *even* instead of *odd* coordinated polyenes.
2. Nucleophilic addition to *open* coordinated polyenes is preferred over addition to *closed* polyenes.
3. For *even, open* polyenes, nucleophilic addition occurs preferentially at the terminal position; for *odd, open* polyenes, attack occurs at the terminal positions only if the metal fragment is strongly electron withdrawing.

Figure 8-4 provides some examples of ligands attached to the generic metal, M, according to their classification under the DGM scheme. Note that the DGM system classifies a ligand as *even* or *odd* depending on its hapticity and electron count, assuming that it is a neutral ligand. Thus, η^3 -allyl ($3e^-$) is an *odd, open*

⁴³L. S. Hegedus, "Nucleophilic Attack on Transition Metal Organometallic Compounds," In *The Chemistry of the Metal-Carbon Bond*, F. R. Hartley and S. Patai, Eds., Wiley-Interscience: New York, 1985, pp.401-512.

⁴⁴S. G. Davies, M. L. H. Green, and D. M. P. Mingos, *Tetrahedron*, **1978**, *34*, 3047; a simplified explanation of the rules and several examples are provided in S.G. Davies, *Organotransition Metal Chemistry: Applications to Organic Synthesis*, Pergamon Press: Oxford, 1982, pp. 116-186.

**Figure 8-4**Classification of π Ligands**Figure 8-5**Relative Reactivity of π Ligands

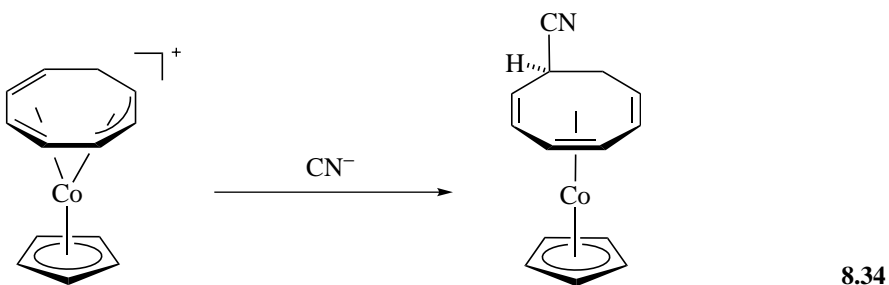
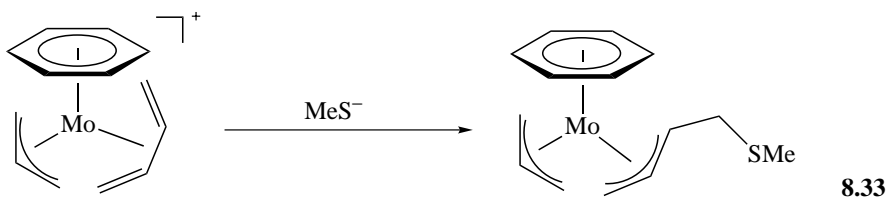
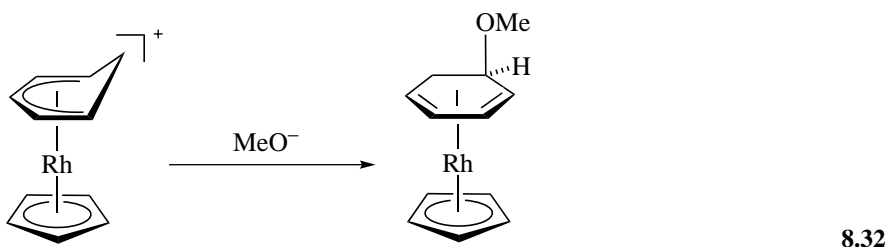
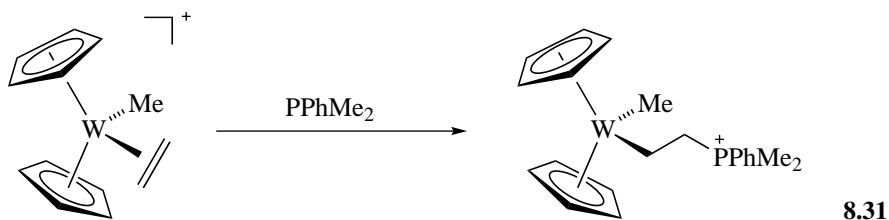
ligand, and η^4 -cyclohexadienyl ($4 e^-$) is *even* and also *open*.⁴⁵ The first two rules may be simplified further.

1. *Even* before *odd*.
2. *Open* before *closed*.

Figure 8-5 expresses rules 1 and 2 another way by ranking the various ligands in terms of their relative reactivity to nucleophilic attack.

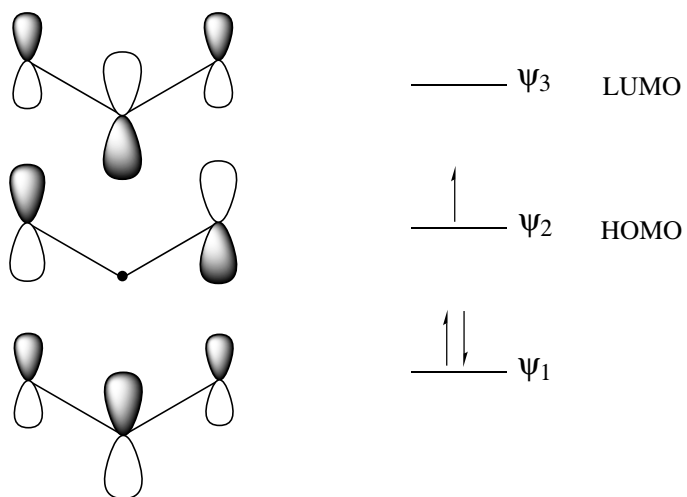
Equations 8.31 to 8.34 provide some examples of some cationic complexes, polysubstituted with π -ligands, that seem to obey the rules.

⁴⁵Note that a cyclic conjugated system involving all atoms of a ring, such as benzene or Cp, is considered *closed*.

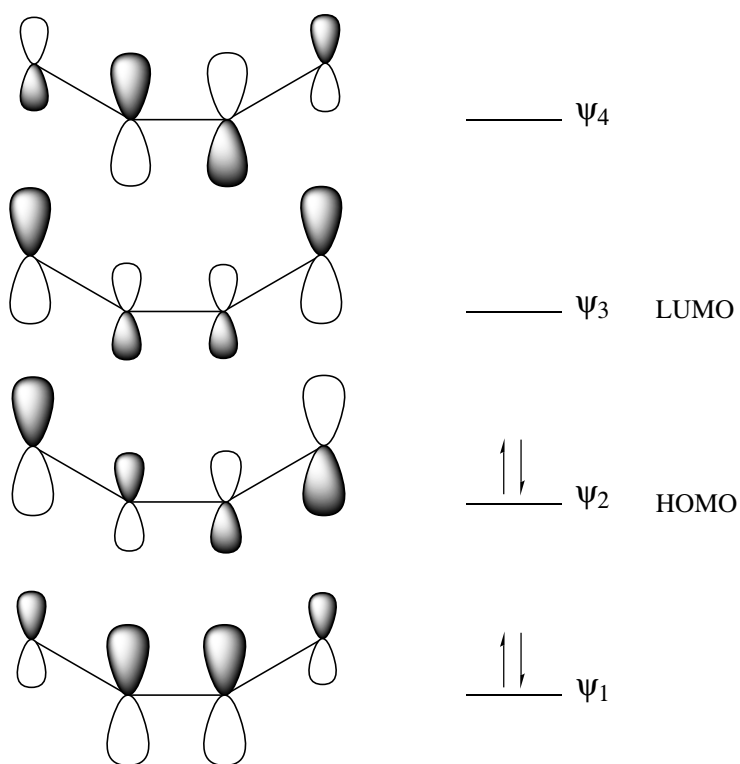


DGM and others have attempted to explain the basis for these rules. Rule 1 may be explained on the basis of the reactions being under charge control. Consider the orbitals of the π ligand once attached to the metal (Figure 8-6). For *even* ligands the HOMO is doubly occupied.⁴⁶ If the metal is quite electron deficient,

⁴⁶One exception to this statement is cyclobutadiene. This molecule has two degenerate (equal energy) HOMOs, each of which is singly occupied with an electron. Nucleophilic attack on other *even* polyenes is preferred according to Rule 1. Cyclobutadiene is, however, attacked in preference to *odd* polyenyl ligands.



Allyl



Butadiene

Figure 8-6

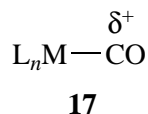
π MOs of Allyl and
1,3-Butadiene

up to two electrons could transfer from the HOMO of the ligand to the metal. The net charge on the ligand could then be as high as +2. *Odd* π ligands are singly occupied in the HOMO. With *odd* ligands, bonding electrons are contributed by both the ligand and the metal. At most, one electron may be transferred from the ligand to the metal, and thus the net charge on the ligand will be maximally +1. In a complex with both an *even* and an *odd* π ligand, the *even* ligand will be more positive (and thus more susceptible to attack by nucleophiles) than the *odd* by up to one unit of positive charge.

Rule 2 states that *open* ligands will undergo nucleophilic attack before *closed* ligands. Although not explicitly proven by DGM, it seems reasonable that, for cyclic, *closed* polyenes, the positive charge on the ring is more evenly distributed due to symmetry. As a consequence, any site on a *closed* ligand will have less positive charge than at least some sites on an *open* ligand with the same number of π electrons.

There does, however, seem to be an empirical basis for the increased reactivity of *open* over *closed* ligands when the reactivity of ethene and benzene ligands is compared. Work reported after DGM's initial investigations by Bush and Angelici⁴⁷ indicates that there is a relation between the tendency of a ligand to undergo nucleophilic attack and the effective force constant,⁴⁸ k_{CO}^* , when reactions are under kinetic control. The reasoning goes as follows:

The electron-withdrawing nature of a positive metal center should have the same effect on a π ligand as it would on a carbonyl group. The IR stretching frequency of a carbonyl (more accurately the force constant, k) is a reflection of the electronic interaction of the carbonyl group and the metal. Electron-poor metals (or metals also coordinated to π acids) do not backbond effectively to the carbonyl. Thus, the Lewis structure **17** makes a substantial contribution to the actual structure of the complex.



The more electron-withdrawing the metal fragment, the more complete the σ donation to the metal. This will increase the triple bond character of the C–O bond and thus increase the force constant. Bush and Angelici analyzed a number of cationic complexes containing π ligands for their tendency to undergo addition with a variety

⁴⁷R. C. Bush and R. J. Angelici, *J. Am. Chem. Soc.*, **1986**, *108*, 2735.

⁴⁸If we assume that bonds are analogous to springs with varying degrees of stiffness, the force constant, k , measures the stiffness of the bond; see Section 4-1 for more details.

of nucleophiles. The force constant, k_{CO}^* , represents the effective force constant if the π ligand were replaced by the equivalent number of carbonyl groups. For instance, $[(\text{C}_2\text{H}_4)\text{Rh}(\text{PMe}_3)_2\text{Cp}]^{2+}$ would be equivalent to $[(\text{CO})\text{Rh}(\text{PMe}_3)_2\text{Cp}]^{2+}$, and $[(\eta^6\text{-benzene})\text{Mn}(\text{CO})_3]^+$ would correspond to three CO ligands grouped in a *facial* arrangement on $[\text{Mn}(\text{CO})_6]^+$. Bush and Angelici found, in general, that addition of a particular kind of nucleophile, such as an amine or a phosphine, would not occur in complexes when k_{CO}^* was below a certain threshold value. One particularly interesting result from this analysis was that the threshold value of k_{CO}^* for addition of a particular kind of nucleophile—phosphines, for instance—was lower when ethene (an *open* ligand) was coordinated to the metal than when benzene was (a *closed* ligand). In other words, the ethene ligand, attached to a number of different metals, seemed to be more susceptible to attack by a variety of nucleophiles than the benzene ligand. We must be careful not to extrapolate this analysis too far since nucleophilic addition could be influenced by both kinetic *and* thermodynamic factors. In this limited case, however, there does seem to be a way of predicting whether a complex containing either a benzene or ethene ligand (or both) will undergo addition. If addition does occur, the ethene reacts preferentially to benzene in accordance with Rule 2.

Rule 3 considers the regiochemistry of attack of the nucleophile. For *even*, *open* ligands, the nucleophile tends to attack at the terminal position of the ligand. Consider 1,3-butadiene as a typical example. The LUMO of butadiene, (Ψ_3) ,⁴⁹ has larger lobes at the termini of the orbital than in the middle (Figure 8-6). The incoming nucleophile (if it is reasonably soft) will be attracted to that part of the orbital with the biggest lobe.⁵⁰

The picture is more complicated when we apply Rule 3 to *odd*, *open* ligands. Attack may occur at the termini or internal positions depending on the electron richness of the attached metal fragment. Usually attack occurs at the terminal carbons of η^3 -allyl ligands, but for relatively electron-rich metal complexes such as $[\text{Cp}_2\text{Mo}(\eta^3\text{-allyl})]^+$ (equation 8.35⁵¹) and $[\text{Cp}^*(\text{PMe}_3)\text{Rh}(\eta^3\text{-allyl})]^+$ (equation 8.36⁵²), addition occurs at C-2 to form metallacyclic products.

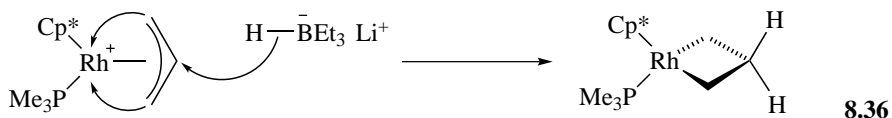


⁴⁹Assuming that there is still electron occupation of Ψ_2 .

⁵⁰R. Pankayatselvan and K. M. Nichols, *J. Organomet. Chem.*, **1990**, 384, 361. Nucleophilic attack at the terminal position of cationic η^4 -diene complexes almost invariably occurs. See J.-S. Fan and R.-S. Liu, *Organometallics*, **1998**, 17, 1002, for an example of addition of Grignard reagents to the internal position of $[\text{CpW}(\text{CO})_2(\eta^4\text{-1,3-cyclohexadiene})]^+$.

⁵¹M. Ephretikine, B. R. Francis, M. L. H. Green, R. E. Mackenzie and M. J. Smith, *J. Chem. Soc. Dalton Trans.*, **1977**, 1131.

⁵²R. A. Periana and R. G. Bergman, *J. Am. Chem. Soc.*, **1984**, 106, 7272.



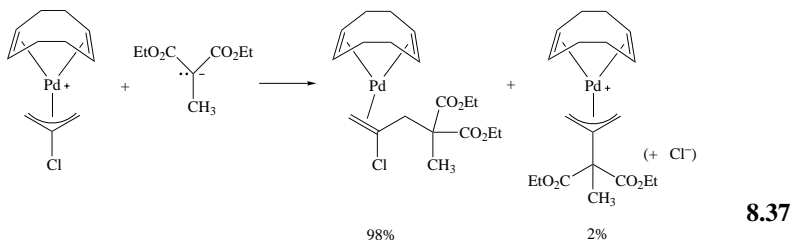
We can understand this difference in regiochemistry if we consider the molecular orbitals of the allyl system in Figure 8-6. For electron-rich metal fragments, the LUMO becomes ψ_3 , which has a large lobe (or high lack of electron density) at C-2. Nucleophiles thus would be attracted to the middle carbon of the allyl ligand in these cases. Electron-poor metal fragments, on the other hand, pull electron density out of the allyl ligand, and the LUMO becomes ψ_2 , an MO with the largest lobes at the ends of the system. Incoming nucleophiles thus tend to attack at these positions.⁵³

The stereochemistry of addition in equation 8.36 is interesting. If LiEt_3BD is used instead of its protium analog, the deuterium ends up at the C-2 of the allyl ligand *syn* to the Cp^* . As we shall see in the examples to follow, nucleophilic addition onto π ligands almost always occurs *anti* to the metal fragment. This seems reasonable because *anti* addition involves a pathway with less steric hindrance than *syn*.

Exercise 8-10

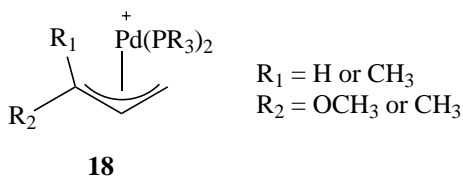
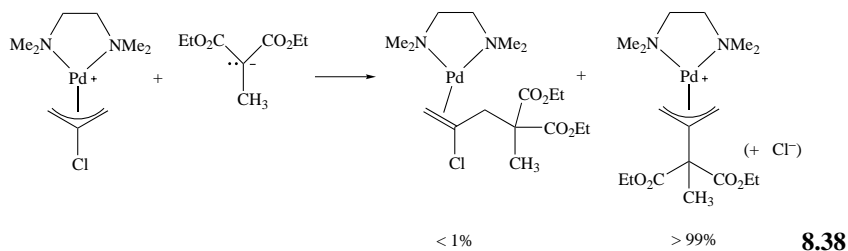
Propose a mechanism that might explain why deuterium adds *syn* to the Cp^* ligand in equation 8.36.

A more recent experimental and computational study of η^3 -allyl-Pd cationic complexes confirmed the tendency of nucleophiles to attack the terminal positions of the allyl ligand as long as π -accepting ligands are present.⁵⁴ If σ -donating ligands are attached to palladium, which would pump electron density into the allyl ligand, attack occurs mainly at the C-2 position. Equations 8.37 and 8.38 summarize these results.



⁵³See also T. Suzuki, G. Okada, Y. Hioki, and H. Fujimoto, *Organometallics*, **2003**, *22*, 3649, for a theoretical treatment of nucleophilic addition to π -allyl-Mo cationic complexes. This study sheds light on the tendency for nucleophiles to attack primarily at the terminal positions of the allyl ligand.

⁵⁴A. Aranyos, K. J. Szabó, A. M. Castano, and J.-E. Bäckvall, *Organometallics*, **1997**, *16*, 1058.



When allyl ligands are unsymmetrically substituted, experiment shows that cationic $(\text{PR}_3)_2\text{Pd}(\eta^3\text{-R}_1\text{-R}_2\text{-allyl})$ complexes **18** (one end of the allyl group is either substituted with two CH_3 groups or one OCH_3 group) undergo attack at the more-substituted terminal position as long as R_1 and R_2 are not sterically bulky. A theoretical study of such complexes ($\text{PR}_3 = \text{PH}_3$) using DFT calculations duplicated experimental results, especially when solvent effects were considered.⁵⁵ Figure 8-7 suggests a qualitative explanation for this regiochemistry by showing the π MOs of the unsymmetrical allyl ligand where one or more electron-donating groups (Y) are substituted at C-1. The occupied π_2 MO (HOMO) of the complex shows a relatively large lobe at C-3, which means an electron-rich ligand would not be attracted to this position compared with C-1 (i.e., the filled–filled repulsive interaction is minimized if the nucleophile attacks at C-1). More important, the LUMO (π_3) has a larger lobe at C-1 than at C-3, which means that there is a stronger HOMO (nucleophile)–LUMO (π_3) interaction at C-1 than at C-3. Taken together, these two interactions direct the nucleophile to the more substituted position, C-1.

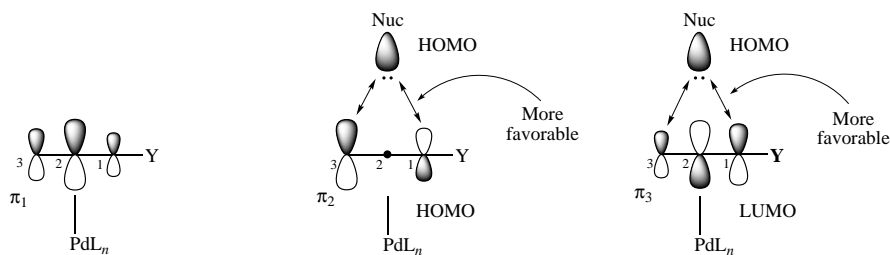
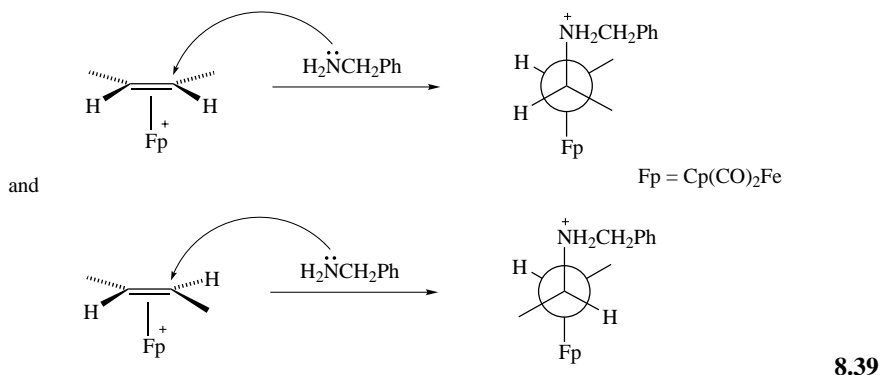


Figure 8-7
 π -MOs of
 Unsymmetrical Allyl
 Ligands

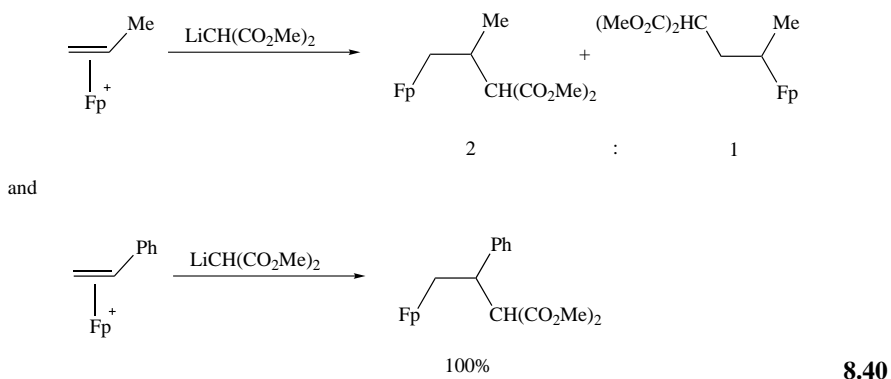
⁵⁵F. Delbecq and C. Lapouge, *Organometallics*, **2000**, *19*, 2716, and references therein that discuss experimental work on these complexes.

$\eta^2 \pi$ Ligands

Addition of a variety of nucleophiles to η^2 -alkene and alkyne ligands has been investigated, particularly when these ligands are complexed with iron and palladium. Reactions shown in equation 8.39 demonstrate well the typical stereochemistry resulting from the *trans* mode of attack by external nucleophiles on η^2 - π systems.⁵⁶ Careful analysis of the reaction of amines with (*E*)- and (*Z*)-2-butenyl iron complexes (the CpFe(CO)₂ group is abbreviated Fp, which is pronounced “fip”) showed the stereochemistry to be cleanly *anti*.⁵⁷



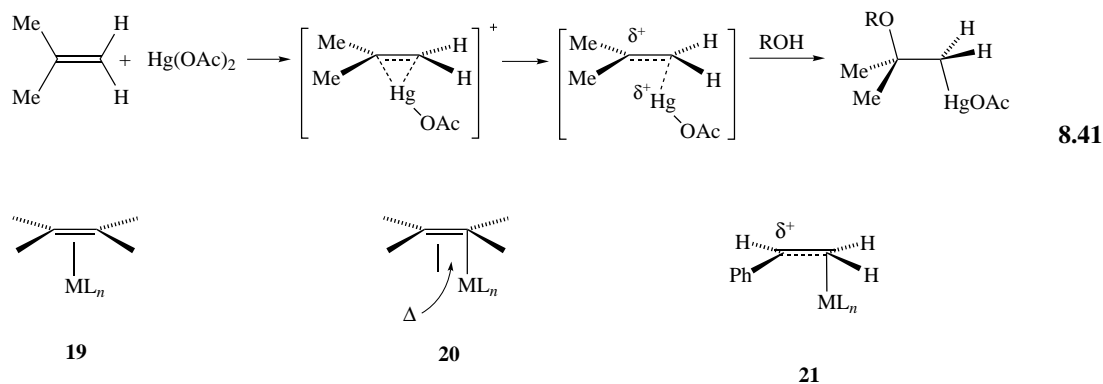
The study also showed that the regioselectivity was low for alkenes substituted with alkyl groups, but was high when styrene was the ligand (equation 8.40).



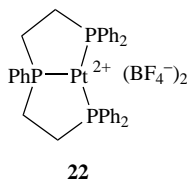
⁵⁶P. Lennon, A. M. Rosan, and M. Rosenblum, *J. Am. Chem. Soc.*, **1977**, *99*, 8426. See A. R. Chianese, S. J. Lee, and M. R. Gagne, *Angewandte Chemie Int. Ed.*, **2007**, *46*, 4042, for a recent review on nucleophilic addition to η^2 -alkene–Pt complexes.

⁵⁷Addition with overall *syn* stereochemistry is a possible outcome. This could result from initial attack of the nucleophile at the metal followed by attack by the nucleophile onto the face of η^2 -alkene ligand nearer to the metal (Scheme 8.6). This mode of addition is relatively rare compared to *anti* addition.

Addition to unsymmetrical η^2 -alkenes seems to occur generally at the more substituted carbon, analogous to a reaction from the realm of organic chemistry known as solvomercuration (equation 8.41). Computational analysis⁵⁸ using extended Hückel theory of attack at alkene ligands has indicated that a “slippage” occurs from the η^2 -complex (**19**) to the η^1 -complex (**20**) along the path to product, where Δ is a measure of the slippage from η^2 ($\Delta = 0$) to η^1 ($\Delta = 0.69$). Calculations show that, for donor substituents such as alkyl groups, the energies of the pathways leading to attack at the more substituted position *vis-a-vis* the less substituted do not differ greatly. A phenyl group, on the other hand, is slightly electron withdrawing yet can effectively stabilize, through resonance, the positive charge that would develop in the η^1 -complex (**21**). Attack, therefore, occurs exclusively at the benzylic position.



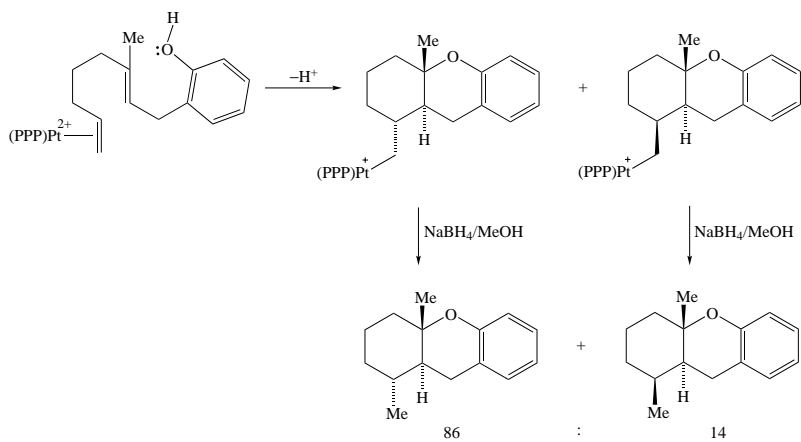
Although Pt-alkene complexes are normally not as reactive as the corresponding Pd complexes toward nucleophilic addition, platinum can serve usefully as a catalyst in these reactions.⁵⁹ The following cyclization was mediated by a Pt-PPP-pincer complex **22**, demonstrating Markovnikov addition at each step of the cyclization (equation 8.42).⁶⁰ The reaction is stereoselective and mimics the cyclization of squalene epoxide to lanosterol, a key step in the biosynthesis of cholesterol.



⁵⁸O. Eisenstein and R. Hoffmann, *J. Am. Chem. Soc.*, **1980**, *102*, 6148, and **1981**, *103*, 4308; A. D. Cameron, V. H. Smith, and M. C. Baird, *J. Chem. Soc. Dalton Trans.*, **1988**, 1037.

⁵⁹A. R. Chianese, S. J. Lee, and M. R. Gagné, *Angew. Chem. Int. Ed.*, **2007**, *46*, 4042.

⁶⁰J. H. Koh and M. R. Gagné, *Angew. Chem. Int. Ed.*, **2004**, *43*, 3459.



8.42

Exercise 8-11

Propose a stepwise mechanism for the polycyclization reaction shown in equation 8.42. Does each ring closure step involve Markovnikov addition to a C=C bond? Explain.

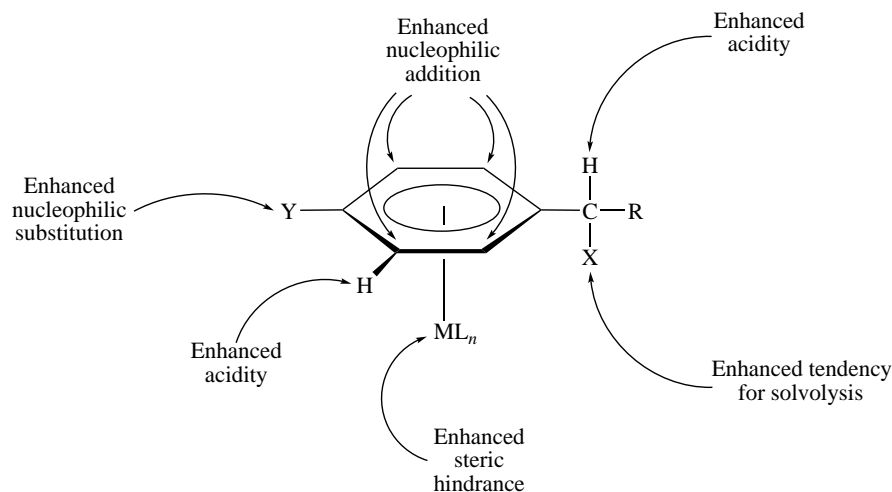
 η^3 -Allyl Ligands

A wide variety of nucleophiles add to an η^3 -allyl ligand. Desirable nucleophiles typically include stabilized carbanions such as $\text{CH}(\text{COOR})_2^-$ or I^\ominus and II^\ominus amines. Unstabilized nucleophiles such as MeMgBr or MeLi often attack the metal first and then combine with the π -allyl by reductive elimination. The Tsuji–Trost reaction, which is typified by the addition of stabilized carbanions to η^3 -allyl ligands complexed to palladium followed by loss of the resulting substituted alkene, comprises an extremely useful method of constructing new C–C bonds, and many applications of this reaction have appeared in the literature.⁶¹ Equation 8.43 illustrates an example of a Pd-catalyzed addition of a stabilized enolate to an allyl acetate.⁶² The initial step in the catalytic cycle is oxidative addition of the allyl acetate to the Pd(0) complex, followed by η^1 - to η^3 -allyl isomerization, and then attack by the nucleophile to a terminal position of the η^3 -allyl ligand. We will discuss the Tsuji–Trost reaction, especially in regard to its utility in chiral synthesis,⁶³ more extensively in Chapter 12.

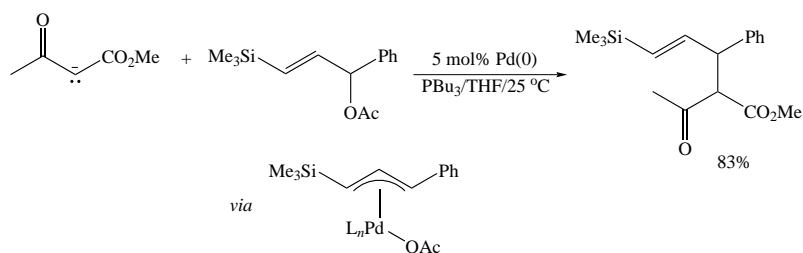
⁶¹B. M. Trost, *Acc. Chem. Res.*, **1980**, *13*, 385; J. Tsuji, *Tetrahedron*, **1986**, *42*, 4361; L. S. Hegedus, *Transition Metals in the Synthesis of Complex Organic Molecules*, 2nd ed., University Science Books: Sausalito, CA, 1999, pp. 250–282; and J. Tsuji, *Palladium Reagents and Catalysts*, Wiley: Chichester, England, 2004, Chap. 4.

⁶²J. Tsuji, *Pure Appl. Chem.*, **1989**, *61*, 1673.

⁶³See B. M. Trost and D. L. Van Vranken, *Chem. Rev.*, **1996**, *96*, 395, for an account of the use of the Tsuji–Trost reaction in chiral synthesis.

**Figure 8-8**

Reactivity at Different Sites on Metal–Arene Complexes



8.43

π -Arene Ligands

π -Arene complexes offer interesting possibilities for demonstrating the utility of *umpolung*. Group 6 (especially Cr) metal–arene compounds⁶⁴ have been particularly well investigated and exploited for their synthetic utility. Complexation of a transition metal to the arene results in the maintenance of the aromaticity of the ring, but this binding also provides enhanced reactivity to not only the metal but also the carbon atoms of the arene that are bonded to the metal and to even more remotely attached atoms.⁶⁵ Figure 8-8 illustrates the changes in reactivity caused by metal complexation.

⁶⁴(a) For reviews on the chemistry of Cr(0)–arene complexes see S. Maiorana, C. Baldoli, and E. Licandro, “Carbonylchromium(0) Complexes in Organic Synthesis,” In *Metal Promoted Selectivity in Organic Synthesis*, A. F. Noels *et al.*, Eds., Kluwer Academic: Amsterdam, 1991, pp. 261–286; (b) R. D. Pike and D. A. Sweigert, *Coord. Chem. Rev.*, **1999**, 187, 183; and (c) for a recent account of the utility of such complexes in organic synthesis, see A. R. Pape, K. P. Kaliappan, and E. P. Kündig, *Chem. Rev.*, **2000**, 100, 2917.

⁶⁵P. v. R. Schleyer, B. Kiran, D. V. Simion, and T. S. Sorenson, *J. Am. Chem. Soc.*, **2000**, 122, 510; for an account of computational studies on the reactivity of η^6 -arene–Cr complexes,

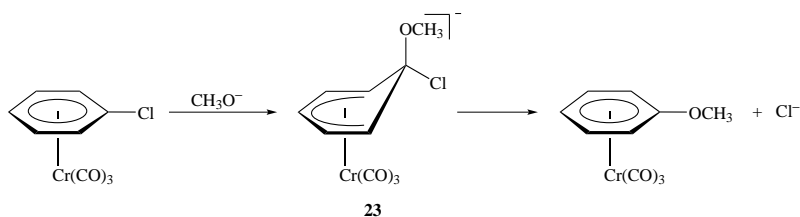
Table 8-1 Acidities of Chromium–Aryl Carboxylic Acids Compared with Noncomplexed Analogs^a

Acid	p <i>K</i> _a	Acid	p <i>K</i> _a
PhCOOH	5.68	PhCH ₂ COOH	5.54
(PhCOOH)Cr(CO) ₃	4.77	(PhCH ₂ COOH)Cr(CO) ₃	5.02
<i>p</i> -NO ₂ -C ₆ H ₄ -COOH	4.48	<i>p</i> -NO ₂ -C ₆ H ₄ -CH ₂ COOH	5.01

^aData taken from Footnote 64a.

When M = Cr, profound effects on the acidity of arene and neighboring protons, electron density of the arene, and steric hindrance at the metal occur. As Table 8-1 indicates, the metal exerts an electron-withdrawing effect on an arene comparable to that of a *para*-NO₂ group. Metallation of the ring using strong bases such as butyllithium occurs at even -78 °C, a much lower temperature than would be required in the noncomplexed arene.

The electron-withdrawing effect of the metal fragment is also manifested in the enhanced ability of complexed arenes to undergo nucleophilic aromatic substitution, a reaction normally requiring strong nucleophiles in noncomplexed arenes. The reaction of methoxide with the chloroarene chromium complex illustrated in equation 8.44 gives the corresponding methoxyarene complex at a rate comparable to that for substitution by methoxide on noncomplexed 1-nitro-4-chlorobenzene. As with their noncomplexed counterparts in organic chemistry, nucleophilic substitutions on coordinated arenes go through an intermediate σ -complex, **23**, known as a Meisenheimer complex.⁶⁶

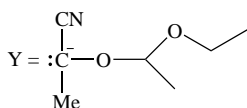
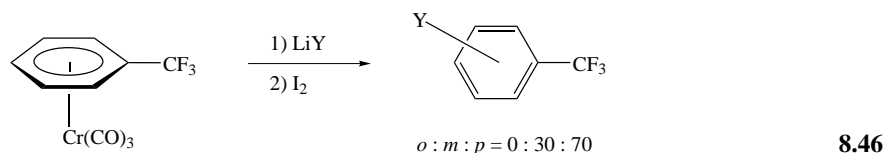
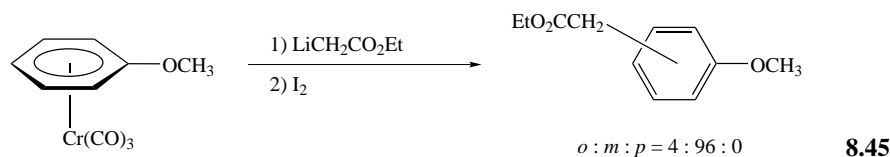
**8.44**

When a substituent is present that is not a good leaving group, the directing effects of that substituent tend to be the reverse of what they would be for electrophilic substitution on the uncomplexed arene. For instance, in equation 8.45 the electron-donating OCH₃ group directs primarily to the *meta* position, whereas in 8.46 the electron-withdrawing CF₃ group directs to the *para* position

see also C. A Merlic, M. M. Miller, B. N. Hietbrink, and K. N. Houk, *J. Am. Chem. Soc.*, **2001**, *123*, 4904.

⁶⁶See J. McMurry, *Organic Chemistry*, 7th ed., Thompson Brooks-Cole: Belmont, CA, 2008, pp. 572–576, for a concise discussion of nucleophilic aromatic substitution.

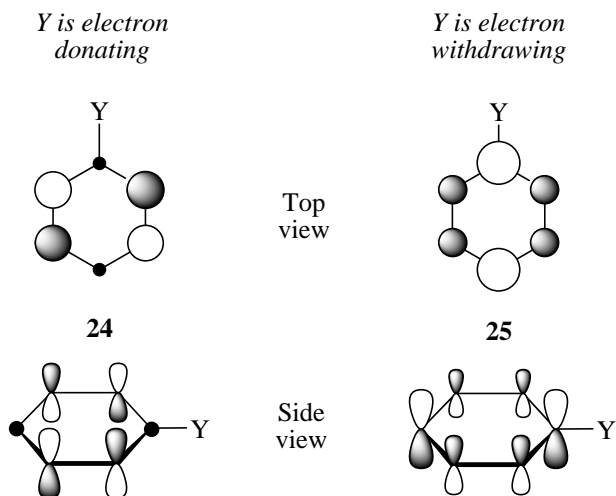
primarily. The last step in these reactions involves oxidative cleavage (using I₂) of the arene–metal bonds.



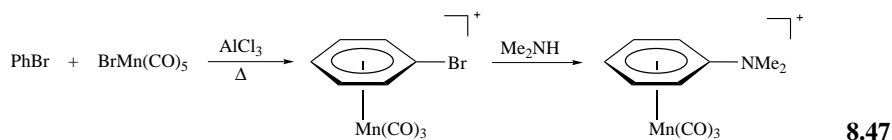
Again, the stereochemistry of attack is such that the nucleophile adds *anti* to the metal.

The rationalization for the regiochemistry of addition when a directing group is present and when the reaction is under kinetic control is based on inspection of the LUMO of the metal arene complex.⁶⁷ If the LUMO of the arene complex and the HOMO of the base are reasonably close in energy, then inspection of the coefficients on the LUMO offers some insight into the orientation of attack on the aromatic ring. The LUMO, when the substituent is electron donating, is given by **24** and shows large coefficients at the *ortho* and *meta* positions. When the substituent is electron withdrawing, however, the coefficients are large mainly at the 1 and 4 positions as shown in **25**. We would expect an incoming nucleophile to attack at the positions where the coefficients are large because this would provide the best overlap with the lobe(s) of the nucleophile's HOMO. This analysis is reasonable, however, only if the reaction is under kinetic control and if considerations of steric hindrance are unimportant.

⁶⁷M. F. Semmelhack, G. R. Clark, R. Farina, and M. Saeman, *J. Am. Chem. Soc.*, **1979**, *101*, 217; for a more recent discussion of orientation effects based on kinetic and thermodynamic control, see E. P. Kunding, V. Desobry, D. P. Simmons, and E. Wenger, *J. Am. Chem. Soc.*, **1989**, *111*, 1804.



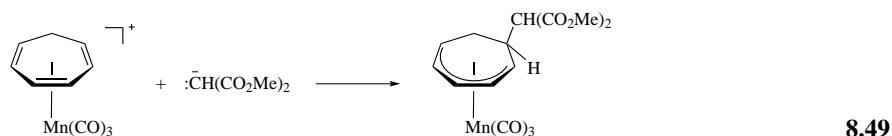
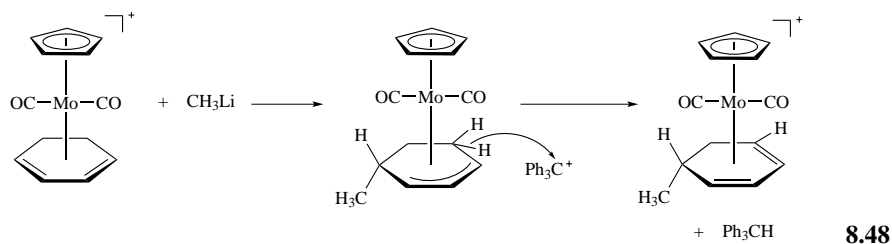
Equations **8.47** to **8.49** illustrate other examples of nucleophilic addition to cyclic π ligands. The cationic Mn–arene complex in **8.47**,⁶⁸ produced by ligand substitution in the presence of a Lewis acid, undergoes nucleophilic substitution by a variety of alkoxide and amine nucleophiles. In equation **8.48**, the molybdenum η^4 –diene complex undergoes attack by methyllithium to give an η^3 –allyl intermediate.⁶⁹ Hydride abstraction with an electrophile known as trityl cation (Ph_3C^+) yields the product with the methyl group *anti* to the metal fragment. Reaction of the η^6 –trieryl Mn complex with a stabilized carbanion such as malonate results in an η^5 –pentadienyl complex, again showing the nucleophile *anti* to the metal (equation **8.49**).⁷⁰ Note that the last two cases explicitly show the typical pattern that accompanies nucleophilic addition to π ligands: the charge on the complex becomes more negative by one unit and the hapticity of the π ligand decreases by one.



⁶⁸P. L. Pauson and J. A. Segal, *J. Chem. Soc. Dalton*, **1975**, 1677, 1683.

⁶⁹J. W. Faller, H. H. Murray, D. L. White, and K. H. Chao, *Organometallics*, **1983**, 2, 400.

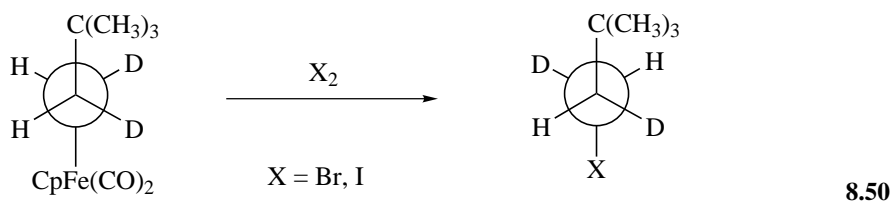
⁷⁰A. J. Pearson, P. Bruhn, and I. C. Richards, *Tetrahedron Lett.*, **1984**, 25, 387.



8-3 NUCLEOPHILIC ABSTRACTION

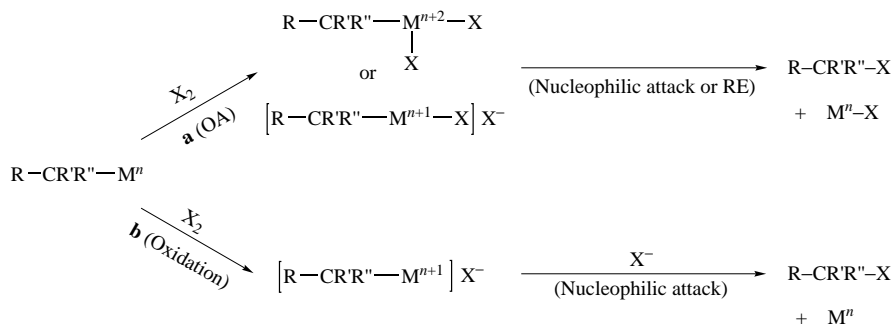
Instead of simply adding to a ligand, the possibility exists for a nucleophile to attack the ligand in such a way that part or all of the original ligand is removed along with the nucleophile. We call this reaction *nucleophilic abstraction*.

Abstraction of alkyl groups by nucleophiles is relatively uncommon, because reduced metals are generally poor leaving groups. If the metal fragment is first oxidized, however, nucleophilic attack on alkyl ligands at the carbon attached to the metal becomes much more feasible. Oxidation makes the leaving metal fragment less basic and also weakens the M–C bond. The halogens Br₂ and I₂ serve effectively as M–C cleaving agents, for example in the oxidatively-driven, nucleophilic abstraction shown in equation 8.50.⁷¹



Note that the reaction proceeds with inversion of configuration at the stereogenic center attached to the metal. It is not clear exactly what the initial function of the halogen is in the reaction, however. Scheme 8.7 presents two possible scenarios for the reaction. In path **a**, the halogen oxidatively adds to the metal to give a cationic complex. The remaining nucleophilic halide ion attacks the complex at the

⁷¹G. M. Whitesides and D. J. Boschetto, *J. Am. Chem. Soc.*, **1971**, 93, 1529.

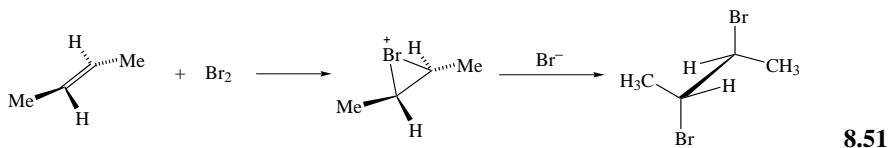
**Scheme 8.7**

Pathways for
Oxidatively-Driven
Nucleophilic
Abstraction

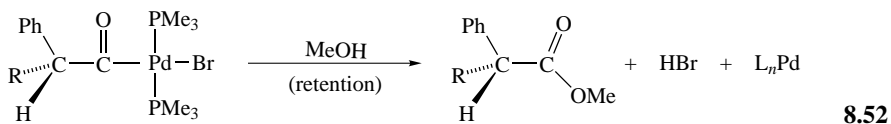
n , $n+1$, and $n+2$ represent different oxidation states of the metal

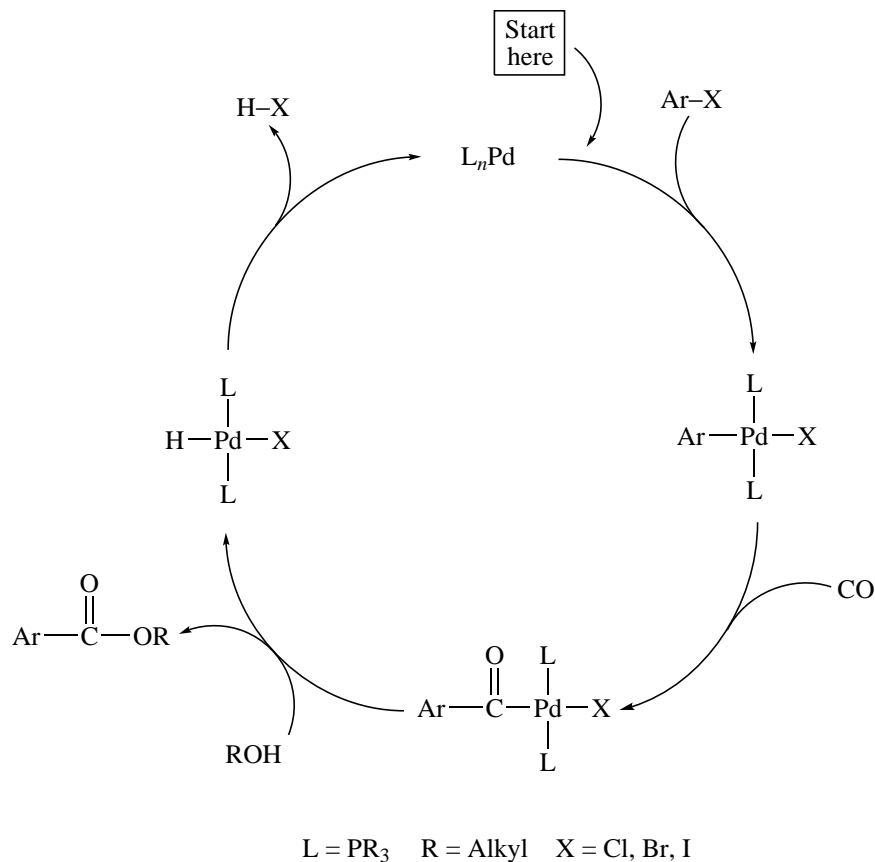
α -carbon of the alkyl group, giving inversion of configuration (note that RE with retention of configuration at the α -carbon is also possible). Path **b**, on the other hand, shows oxidation of the metal without addition, followed by nucleophilic attack by X^- .

We can also envision the overall process of halogen cleavage as an *electrophilic* process if the first step is the addition of X^+ (from X_2) to the metal, analogous to the addition of halogen to a $\text{C}=\text{C}$ bond in organic chemistry. Addition of halogen to alkenes is a two-step process where attack of the electrophile occurs first to form an intermediate halonium ion (equation 8.51), followed by attack by the nucleophile, X^- . We see that sometimes the designation “nucleophilic” or “electrophilic” can be rather arbitrary, and it depends upon one’s perspective in describing the reaction. We shall consider electrophilic processes in more detail in Section 8-4.



Equation 8.52, which is one of the reactions listed in Scheme 7.7, demonstrates an important example of nucleophilic abstraction. Here CH_3OH acts as a nucleophile that attacks the σ -acyl group. Breakdown of the resulting tetrahedral intermediate yields the methyl ester and a reduced Pd complex.



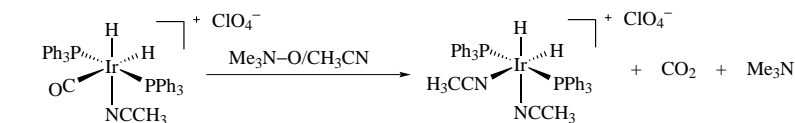
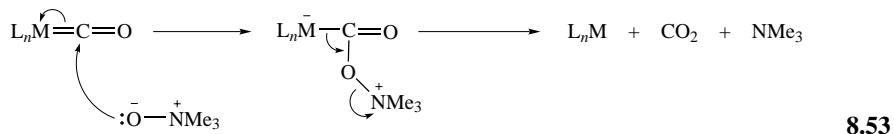
**Scheme 8.8**

Nucleophilic
Abstraction
of σ -Acyl-Pd
Complexes

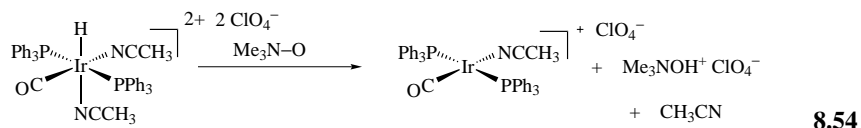
Nucleophilic abstraction of σ -acyl ligands is quite useful synthetically, especially when the metal is Pd. Scheme 8.8 illustrates a sequence of reactions that may be either stoichiometric or catalytic in that metal.⁷² Palladium is the metal of choice here because it readily forms σ -M-C complexes, which then undergo facile CO insertion and subsequent σ -acyl-Pd bond cleavage with a variety of nucleophiles. The first step involves OA of a vinyl or aryl halide to a Pd(0) complex (shown as L_nPd in Scheme 8.8). Migratory insertion of CO (Section 8-1) gives the σ -acyl complex, which undergoes nucleophilic abstraction with MeOH to give the corresponding methyl ester. This sequence of reactions has synthetic applicability, because intermolecular nucleophilic abstraction produces a variety of linear acyl derivatives, and intramolecular attack provides cyclic compounds such as lactones or lactams.

⁷²R. F. Heck, *Pure Appl. Chem.*, **1978**, 50, 691.

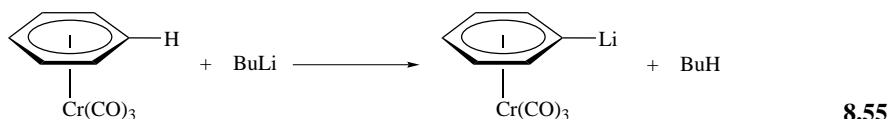
Another example of nucleophilic abstraction is the use of trimethylamine *N*-oxide (Me_3NO), a widely-used reagent for decarboxylation of metal carbonyl complexes (equation 8.53).⁷³ Equation 8.54 describes a reaction where the iridium dihydride complex undergoes CO abstraction while a similar monohydride complex undergoes hydride extraction. The reason for the difference in reactivity of Me_3NO is not clear.⁷⁴



and



Equation 8.55 can be considered a nucleophilic abstraction of H^+ from the arene ligand by a strong nucleophile. An alternate interpretation of this transformation is that it represents a Brønsted–Lowry acid–base reaction. Regardless of the viewpoint of the observer, the reaction is facile mainly because of the electron-withdrawing nature of the metal fragment.



The last example of nucleophilic abstraction shows removal of a methyl group from a Fischer carbene complex (equation 8.56).⁷⁵ The course of this reaction is unusual because normally nucleophiles *add* to the carbene carbon, as we shall see in Chapter 10. In this case, however, the apparent steric bulk of the abstracting

⁷³See, for example, K. Yang, S. G. Bott, and M. G. Richmond, *Organometallics*, **1994**, *13*, 3788 and M. O. Albers and N. Coville, *J. Coord. Chem. Rev.*, **1984**, *53*, 227.

⁷⁴C. S. Chin, M. Oh, G. Won, H. Cho, and D. Shin, *Bull. Korean Chem. Soc.*, **1999**, *20*, 85.

⁷⁵L. M. Toomey and J. D. Atwood, *Organometallics*, **1997**, *16*, 490.

agent directs the course of the reaction toward abstraction rather than addition. The anionic metal carbonyl complex acts as a nucleophile in attacking the methyl group via an S_N2 mechanism. When the methyl group is substituted with ethyl, the reaction is 70 times slower, which would be expected for an S_N2 displacement.



R = Me, Et

8.56

8-4 ELECTROPHILIC REACTIONS

Reactions involving a metal complex and an electron-deficient species (the electrophile, E^+) are common in organometallic chemistry and often useful synthetically. There are several possibilities for interaction of a metal complex and E^+ , some of which we have already encountered. For example, the insertion of SO_2 (equation 8.22), electron deficient at sulfur, begins with attack by the electrophile at the carbon attached to the metal.

Just where and with what stereochemistry the electrophile will attack a metal complex depends upon a number of factors. If the reaction is controlled by frontier orbital interactions, then the point of attack on the complex is dictated by the electron density of the complex's HOMO. Major lobes of the HOMO could be on the ligand or the metal or both. The stereochemistry of attack may depend on such factors as the steric hindrance of the metal fragment or even the nature of the solvent. Extensive study of electrophilic attack on specific metal complexes has uncovered some general trends for use as a basis in predicting how an electrophile will react. We will limit our treatment of electrophilic attack to a few well-defined examples that illustrate the major pathways of a reaction where E^+ either directly or indirectly interacts with a coordinated ligand. Again, we distinguish between *addition* reactions, where all or part of the electrophilic species adds to the coordinated ligand, and *abstractions*, in which E^+ attacks in such a manner that all or part of the ligand is removed from the metal complex (see Table 7-1).

Electrophiles

The term electrophile is synonymous with Lewis acids. Classifying electrophiles on the basis of their "strength" is virtually impossible (see Section 7-2-2). It is useful, however, to point out that we can classify Lewis acids according to the three types as described on the next page.⁷⁶

⁷⁶M. D. Johnson, "Electrophilic Attack on Transition Metal η^1 -Organometallic Compounds," In F. R. Hadley and S. Patai, Eds., *The Chemistry of the Metal-Carbon Bond*, Wiley: London, 1985, Vol. 2, p. 515.

1. *Metallic* electrophiles, such as Hg(II), Tl(I), Ag(I), Ce(IV), Pt(IV), Au(III), or Ir(V)—most of which also have accessible oxidation states one or two units lower in value from those given above
2. *Organic* electrophiles, such as R_3O^+ , Ph_3C^+ , $R-X$, or $(NC)_2C=C(CN)_2$
3. *Non-metallic* electrophiles, such as X_2 , SO_x , CO_2 , NO_x^+ , or H^+

Each of these classes of electrophiles may attack transition metal complexes. We will encounter examples of all three classes during the remainder of the discussion in this section of Chapter 8.

8-4-1 Metal–Carbon σ Bond Cleavage

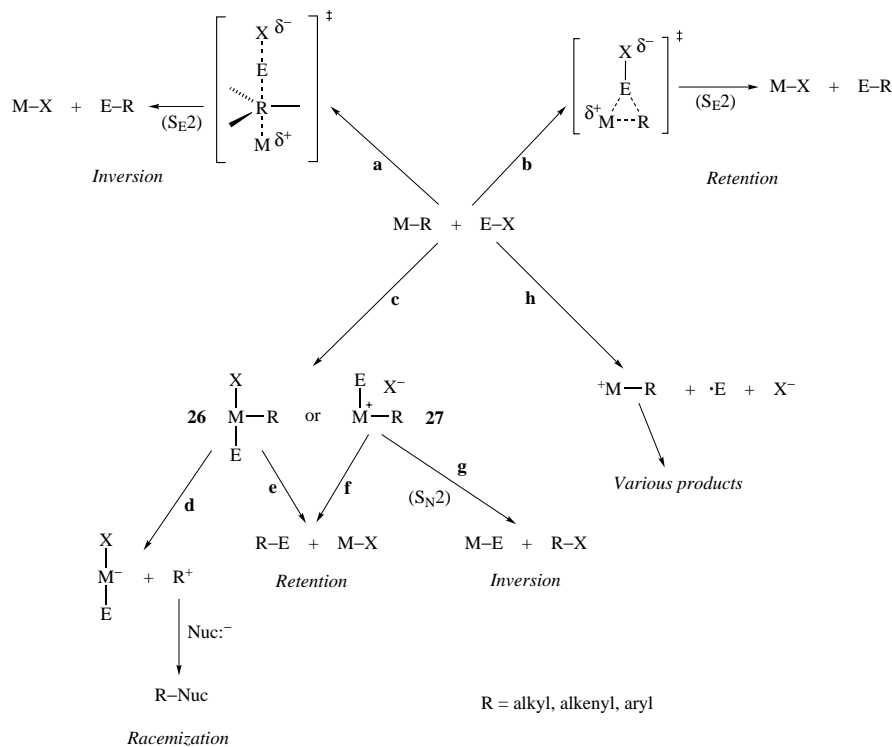
The use of an electrophile (e.g., H^+ or X_2) to remove a σ -bonded hydrocarbyl ligand from a metal is common in organometallic chemistry. Such a reaction constitutes an electrophilic abstraction of the entire ligand. Scheme 8.9 diagrams some of the many pathways available for this type of abstraction. Stereochemical outcomes include retention, inversion, and racemization and depend upon such factors as the nature of the metal, steric hindrance, the nature of E^+ , where the HOMO is located on the complex, and characteristics of the solvent.

- Pathways **a** and **b** represent a mechanism called S_E2 , which we encountered earlier in the discussion on SO_2 insertion. Inversion⁷⁷ (path **a**) or retention (path **b**) of stereochemistry may occur at the stereogenic center⁷⁸ attached to the metal.
- Pathway **c** is oxidative addition to give intermediates **26** and **27**, which may suffer several fates.
- Pathway **d**, emanating from **26**, is ligand dissociation to give a stable carbocation followed by nucleophilic capture to give racemic⁷⁹ product.
- Also originating from **26** is pathway **e**, RE , from which we would expect retention of configuration.

⁷⁷Inversion of configuration means transformation of **R** to **S** (or vice versa) or *erythro* to *threo* (or vice versa) if one or more stereogenic centers is present in the σ -bonded hydrocarbyl ligand.

⁷⁸A “chirality center” (or “chiral center”) is one type of “stereogenic center” or, simply, “stereocenter.” A stereogenic atom is defined as one bonded to several groups of such nature that interchange of any two groups produces a stereoisomer. See E. L. Eliel and S. H. Wilen, *Stereochemistry of Organic Compounds*, Wiley–Interscience: New York, 1994, p. 53.

⁷⁹The term “racemic” applies strictly if only one stereogenic center is present in the hydrocarbyl ligand. A more inclusive term for the stereochemical result upon formation of R^+ would be “stereorandomization.” For example, if the hydrocarbyl ligand had two stereocenters, giving it the stereochemical designation *threo*, stereorandomization would provide roughly equal amounts of two diastereomers, *threo* and *erythro*. In the subsequent discussion we will use the terms “racemic” and “racemization” to indicate that stereorandomization has occurred.

**Scheme 8.9**

Pathways for
Electrophilic
Abstraction of
 σ -bonded M-C
Hydrocarbyl
Ligands

- RE with retention (path **f**) could also lead from **27**; however, direct nucleophilic S_N2 displacement (path **g**) would yield product with inversion of configuration (see equation **8.50**).
- Path **h** represents a general oxidation process of the metal that may occur by a single electron mechanism. It is likely that some electrophilic cleavages occur under these conditions, but experimental evidence is difficult to obtain. Discussion of such mechanisms is beyond the scope of this text.⁸⁰

Table **8-2** summarizes the mechanistic type and stereochemical characteristics of each path.

Cleavage by H^+

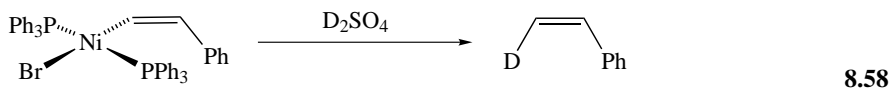
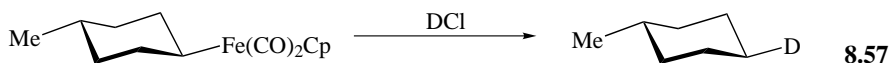
Protonolysis or the use of Brønsted–Lowry acids to cleave σ M–C bonds is an often-used method of σ M–C bond cleavage. The stereochemistry observed invariably seems to be retention of configuration at the stereocenter attached to the

⁸⁰See J. K. Kochi, *Organometallic Mechanisms and Catalysis*, Academic Press: New York, 1978, Chap. 18.

Table 8-2 Characteristics of Electrophilic Abstraction Pathways

Pathway	Reaction Type	Stereochemistry
a	S_E2	Inversion
b	S_E2	Retention
c	OA	Different stereochemistries possible
d	Ligand dissociation followed by nucleophilic capture	Racemization
e	RE	Retention
f	RE	Retention
g	S_N2	Inversion
h	Radical	Several possible

metal. Equations **8.57**⁸¹ and **8.58**⁸² provide two examples of protolytic cleavage using deuterated acids to provide an indication of stereochemistry. The reactions probably occur via paths **c** and then **f**, that is, protonation of the metal followed by reductive elimination.



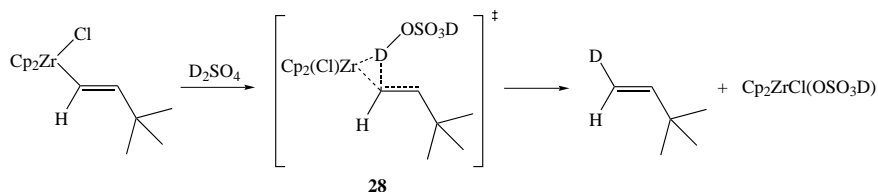
Unlike the metals in equations **8.57** and **8.58**, the metal in equation **8.59**⁸³ is an early d^0 -transition metal. The OA–RE pathway is not possible from such a complex, because it is difficult to remove electrons from a d^0 metal, yet protolysis occurs again with retention. The mechanism for this reaction probably involves path **b**, a concerted S_E2 reaction involving a 3-centered transition state, **28**. *This mechanism seems to be general for electrophilic cleavages involving the early transition metals because the HOMO is centered at the M–C σ bond, and oxidative pathways are not possible.*⁸⁴

⁸¹W. N. Rogers and M. C. Baird, *J. Organomet. Chem.*, **1979**, 182, C65.

⁸²D. Dodd and M. D. Johnson, *J. Organomet. Chem.*, **1973**, 52, 1.

⁸³J. S. Labinger, D. W. Hart, W. E. Seibert, III, and J. Schwartz, *J. Am. Chem. Soc.*, **1975**, 97, 3851.

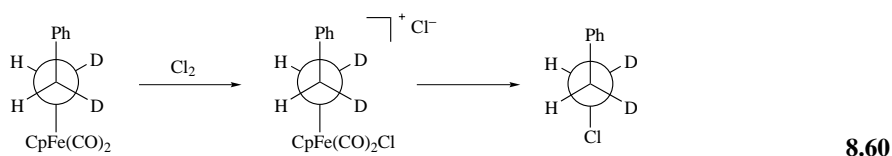
⁸⁴For example, MO calculations performed by the authors at the extended Hückel and DFT level on Cl_3ZrCH_3 show a large lobe centered at the Zr–CH₃ bond.



8.59

Cleavage by Halogens

Cleavage by halogens is a second important method of electrophilic cleavage. We have already encountered an example of this reaction (equation 8.50). Another example is shown in equation 8.60.

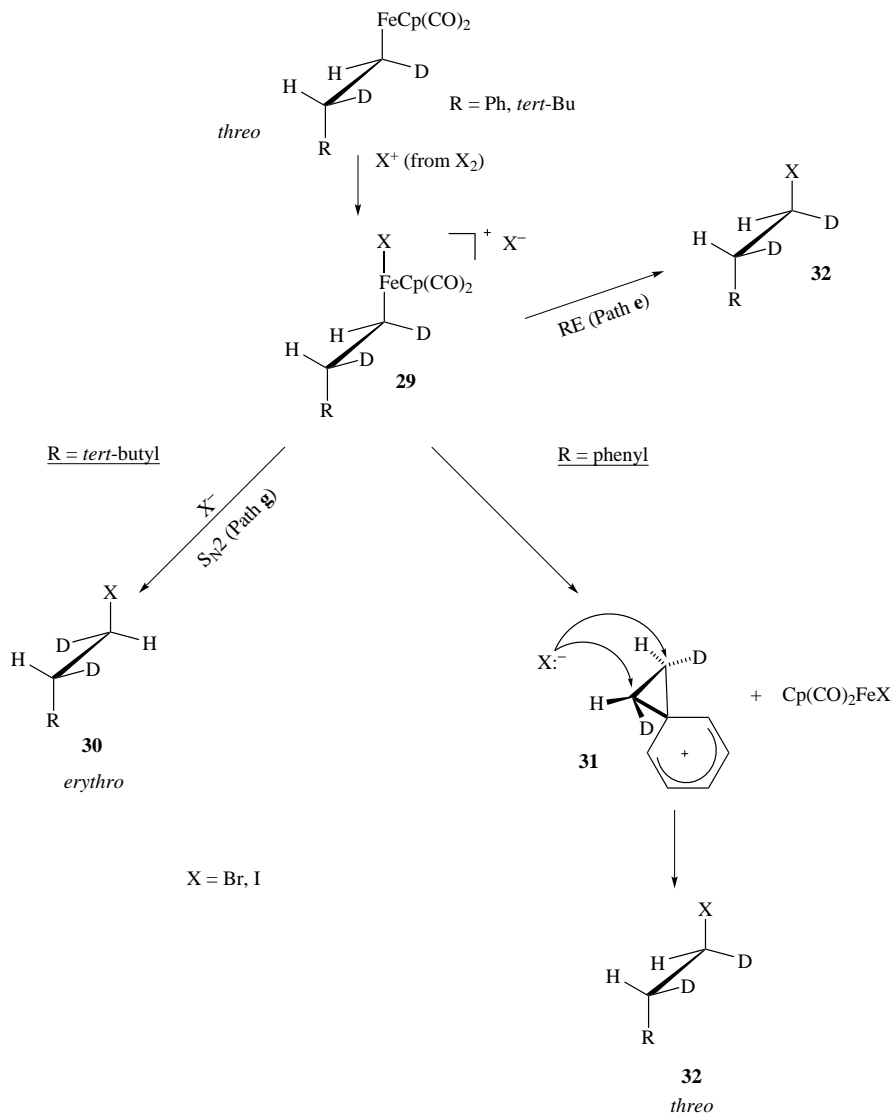


In these reactions, rather different stereochemistry results depending upon the group attached to the β carbon of the σ -hydrocarbyl ligand. When the β group is Ph, retention of configuration is observed. Change the group to *tert*-butyl, and cleavage occurs with inversion of configuration at the carbon originally attached to the metal. Scheme 8.10 details the stereochemistry involved in the two reactions.

The reaction begins by the addition of X^+ to the *threo*-Fe complex to give **29**. If R = *tert*-butyl, then X^- attacks at the α -carbon to produce the *erythro*-alkyl halide (path **g**, Scheme 8.9), **30**. A change in R to Ph results in attack by X^- with retention of configuration to yield *threo*-alkyl halide, **32**. There are actually two pathways to consider when explaining how retention of configuration could occur when R = Ph. Direct reductive elimination (path **e**, Scheme 8.9) would provide **32**, because we know that RE proceeds with retention of configuration. The other possibility proceeds through a symmetrical, bridged carbocation, **31**, known generally as a phenonium ion. Attack by X^- at either alkyl carbon of **31** produces *threo*-alkyl halide. The steric bulk of the bridged phenyl group forces attack from the same side to which the metal fragment was originally attached, thus ensuring retention of configuration.

There is much evidence for phenonium ions in the realm of organic chemistry.⁸⁵ In the case described in equation 8.60, there is experimental support for the presence of **31** based on the following experiment: Analogous cleavage by

⁸⁵See T. H. Lowry and K. S. Richardson, *Mechanism and Theory in Organic Chemistry*, 3rd ed., Harper & Row: New York, 1987, pp. 434–448 and F. A. Carey and R. J. Sundberg, *Advanced Organic Chemistry, Part A*, 5th ed., Springer Scientific: New York, 2007, pp. 423–425, for good discussions on the evidence for the existence of phenonium ions.

**Scheme 8.10**

Stereochemical Possibilities for Metal-Halogen Cleavage

Exercise 8-12

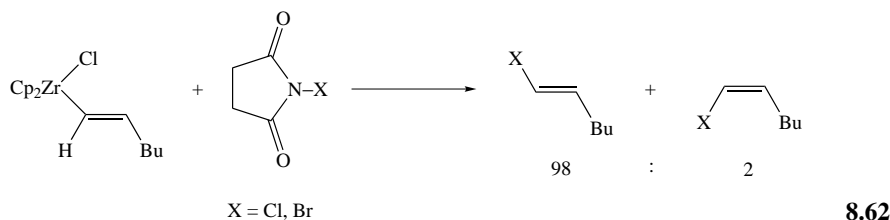
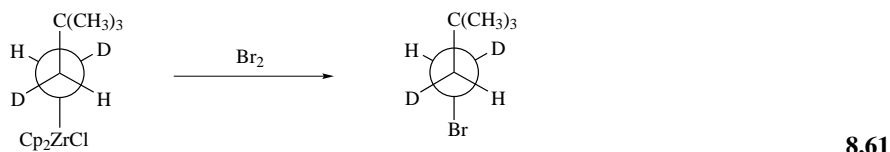
What is the stereochemical relationship between the alkyl halides produced when X^- attacks at the two alkyl positions in **31**? Note, only one isomer (structure **32**) of the alkyl halides is shown in Scheme 8.10.

X_2 of $CpFe(CO)_2CD_2CH_2Ph$ led to the formation of a 1:1 mixture of XCD_2CH_2Ph and XCH_2CD_2Ph .⁸⁶ Had the reaction occurred by concerted, one-step RE, only one isomer would have been observed. With this example we see that an apparent concerted RE with retention probably did not occur, but instead the reaction proceeded through a free carbocation to give the same stereochemical result as we would have expected from RE. This case, moreover, again points out the need for careful experimentation any time a mechanism is proposed.

Show that halogen cleavage of $CpFe(CO)_2CD_2CH_2Ph$ will give two different constitutional isomers in equal amounts if **31** is an intermediate in the reaction.

Exercise 8-13

The dichotomy between retention and inversion during halogenolysis occurs with a number of σ metal–alkyl and metal–alkenyl complexes. The factors mentioned earlier, such as solvent polarity, steric hindrance, and the nature of the HOMO, are influential in directing the stereochemical outcomes. It is only with the early transition metals that rather consistent stereochemical outcomes occur. As in protonolysis, it appears that halogen cleavage occurs by an S_E2 mechanism with retention of configuration (path **b**, Scheme 8.9). Equations 8.61⁸⁷ and 8.62⁸⁸ demonstrate this pathway for σ -alkyl and σ -alkenyl Zr complexes, respectively.



⁸⁶T. C. Flood and F. J. DiSanti, *J. Chem. Soc. Chem. Commun.*, **1975**, 18.

⁸⁷J. S. Labinger, D. W. Hart, W. E. Seibert, III, and J. Schwartz, *J. Am. Chem. Soc.*, **1975**, 97, 3851.

⁸⁸D. W. Hart, T. F. Blackburn, and J. Schwartz, *J. Am. Chem. Soc.*, **1975**, 97, 679.

Cleavage by Metal Ions

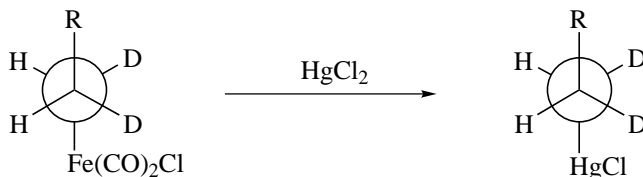
The third and last method of σ M–C cleavage we will consider is that with metal ions. The metal ion most thoroughly studied is Hg(II), which is well known for its ability to reversibly transfer alkyl, alkenyl, and aryl groups to a variety of transition metals. Investigations on the stereochemistry attendant cleavage of σ M–C bonds have been performed on a number of complexes involving Fe, Mn, W, Mo, and Co. There seems to be no single pathway preferred for cleavage, based on stereochemical results, although a pathway involving retention of configuration is common. Our discussion will focus on a few of these investigations.

In Scheme 8.11 the products formed upon treatment of $\text{CpFe}(\text{CO})_2\text{R}$ with HgX_2 ($\text{X} = \text{Cl}, \text{Br}, \text{or I}$) seem to depend on the nature of R. The stereochemistry of the liberated organic group, moreover, also depends on the structure of R. The scheme takes into account the involvement of HgX_2 in the first two steps of the mechanism, giving an observed third-order rate law of

$$\text{Rate} = k[\text{L}_n\text{FeR}][\text{HgX}_2]^2.$$

When the hydrocarbonyl ligand is I° alkyl, the reaction proceeds with overall retention of configuration to produce RHgX and L_nFeX . When $\text{R} = \text{III}^\circ$ or benzyl, racemization is the stereochemical outcome and the products are RX and L_nFeHgX . Apparently two pathways are operative in this example. Path **e** (Schemes 8.9 and 8.11) gives retention by a reductive elimination pathway. As R becomes substituted with groups that can stabilize a carbocation, path **d** (Schemes 8.9 and 8.11) takes over to produce free R^+ that picks up X^- from HgX_3^- .

The equations that follow show actual examples of electrophilic cleavage due to Hg(II) salts. Cleavage of the two iron complexes ($\text{R} = \text{tert-butyl}^{89}$ and phenyl⁹⁰) with retention of stereochemistry is illustrated in equation 8.63. When $\text{R} = \text{phenyl}$, a phenonium ion could also form to give retention of configuration, as demonstrated in Scheme 8.10. The rate law showing second-order involvement of Hg(II), however, argues for the mechanism involving path **e**. The *trans*- $\text{CpW}(\text{CO})_2(\text{PEt})_3(\text{alkyl})$ complex in equation 8.64 also undergoes cleavage with retention.⁹¹



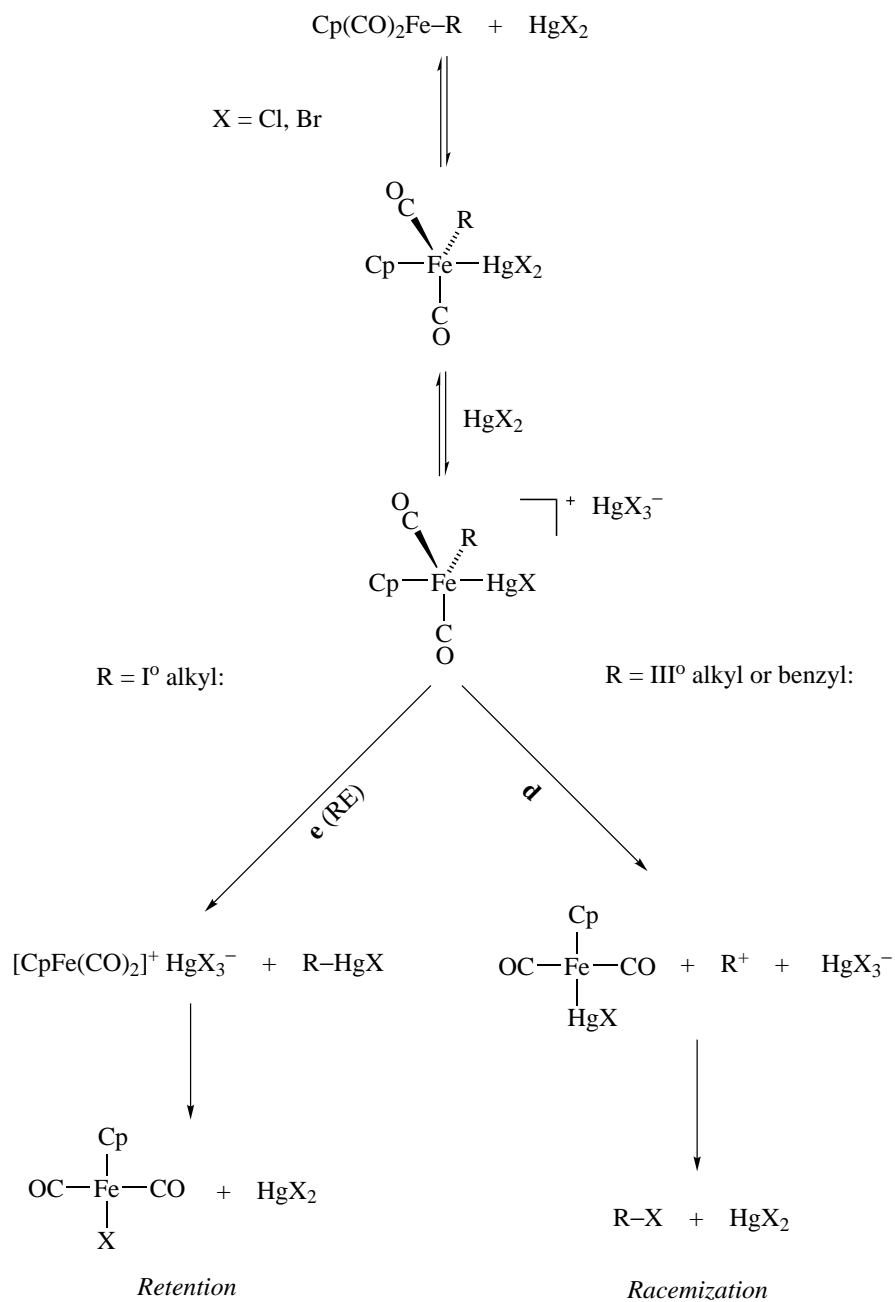
$\text{R} = \text{tert-Bu}, \text{Ph}$

8.63

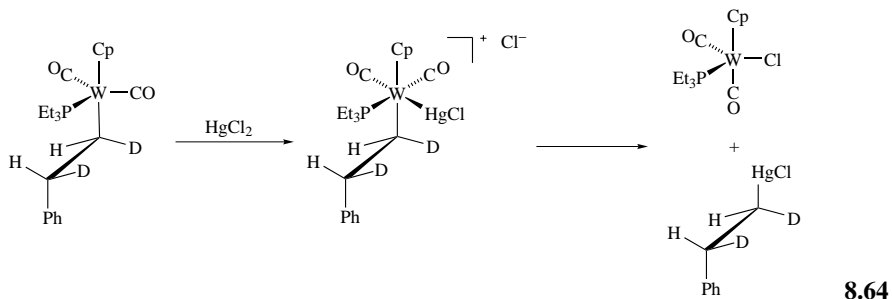
⁸⁹G. M. Whitesides and D. J. Boschetto, *J. Am. Chem. Soc.*, **1971**, 93, 1529.

⁹⁰D. Dong, D. A. Slack, and M. C. Baird, *Inorg. Chem.*, **1979**, 18, 188.

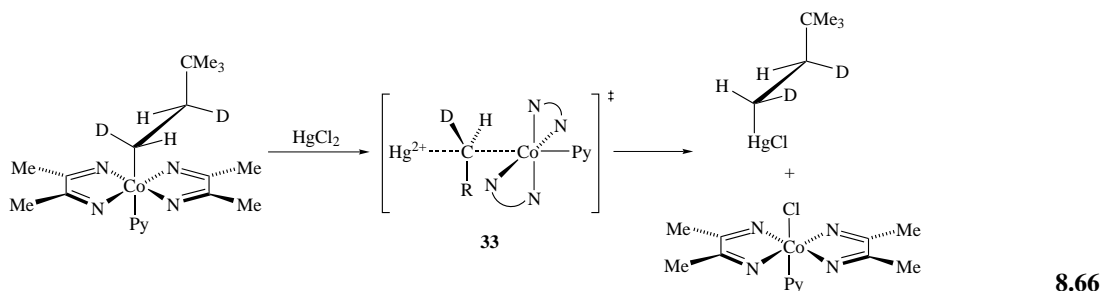
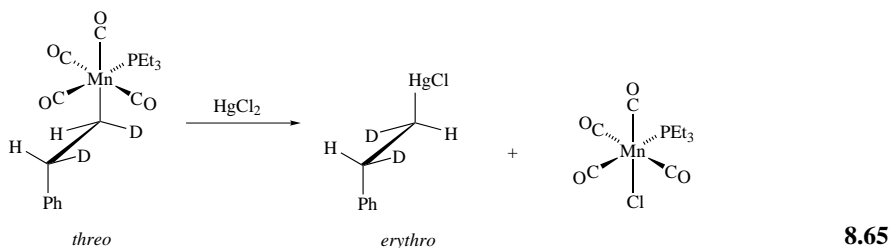
⁹¹See Footnote 90.

**Scheme 8.11**

Hg(II) Cleavage of
Fe-C Bonds



Hg(II) cleavage of the Mn^{92} (equation **8.65**) or the Co^{93} complex (equation **8.66**), on the other hand, results in inversion of configuration, probably via an $\text{S}_{\text{E}2}$ mechanism (path **a**, Scheme **8.9**). Steric hindrance about the metal—especially in the case of the Co complex with its large, bidentate ligands—seems to be the reason that Hg(II) cleavage occurs with inversion of configuration in these cases. The investigators proposed a transition state, **33**, as that involved for the Co complex.



⁹²See Footnote 90.

⁹³H. L. Fritz, J. H. Espenson, D. A. Williams, and G. A. Molander, *J. Am. Chem. Soc.*, **1974**, *96*, 2378.

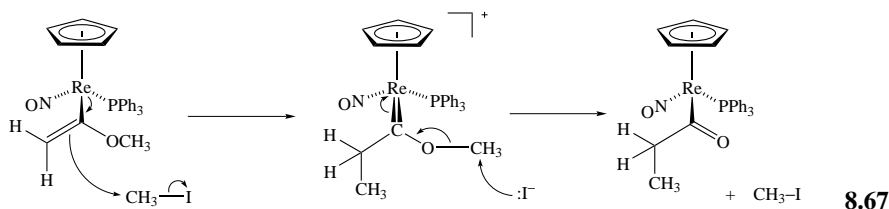
Although electrophilic cleavage of σ -bonded hydrocarbyl ligands constitutes an important method for removing those ligands from the metal, we now see that the pathways available for this process are diverse indeed. A few generalizations regarding the stereochemical course of these abstractions can be made, such as retention of configuration with all electrophiles when early transition metals are involved or retention during protonolysis, but the stereochemistry of most cleavages is difficult to predict and depends on a balance of a number of interrelated factors.

8-4-2 Addition and Abstraction on Ligands with π Bonds

In Section 8-2-2, much of the discussion centered on the attack by nucleophiles on π ligands, such as monoolefins or arenes. In these reactions, hapticity ($\eta^n \rightarrow \eta^{n-1}$) and the overall charge ($+n \rightarrow +n-1$) tended to change by one unit. Similar events can occur with electrophiles, and sometimes the changes in hapticity and overall charge are just the opposite of those found in nucleophilic reactions. Although reports in the chemical literature of electrophilic attack on ligands containing π bonds are fewer than for nucleophilic counterparts, many examples of this kind of reaction do exist.

Addition

In equation 8.67, attack of the electrophile occurs at the β position to give a carbene complex as the intermediate; subsequent loss of CH_3I produces the acyl-Re complex as the final product.⁹⁴



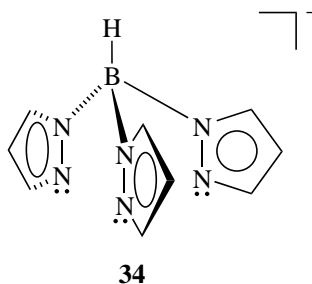
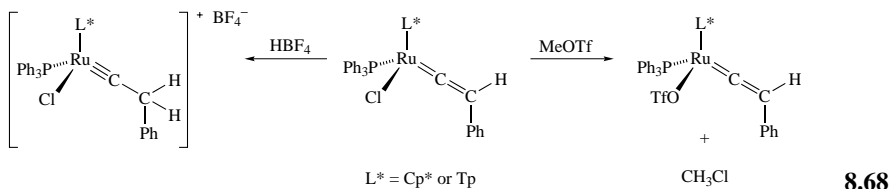
A more recent example of this chemistry is shown in equation 8.68.⁹⁵ Here the sterically-demanding Cp^* and Tp (structure 34)⁹⁶ ligands dictate the course of the

⁹⁴D. E. Smith and J. A. Gladysz, *Organometallics*, **1985**, *4*, 1480.

⁹⁵N. J. Beach, A. E. Williamson, and G. J. Spivak, *J. Organomet. Chem.*, **2005**, *690*, 4640.

⁹⁶The Tp ligand, hydridotris(pyrazoyl)borate, also known as a *scorpionate*, is sometimes abbreviated as $\text{HB}(\text{pz})_3^-$. A related, even more sterically-demanding ligand is known as Tp^* , and its systematic name is hydridotris(3,5-dimethylpyrazoyl)borate. These ligands have a huge cone angle of at least 180° , compared with 146° for Cp^* and 100° for Cp. Because Tp and Tp^* are so sterically hindered, they can stabilize complexes that are electron deficient

electrophilic reaction. Both the Cp* and the Tp ruthenium vinylidene complexes undergo electrophilic addition with H⁺ at the β-position of the vinylidene moiety to give the corresponding carbyne complexes. Use of methyl triflate, on the other hand, results in loss of Cl in the form of CH₃Cl. The investigators determined that the probable mode of reaction here was the electrophilic abstraction of Cl by “CH₃⁺.” The steric hindrance of the Cp* and Tp ligands probably prevented attack either directly at the metal or at the β-position of the vinylidene by the bulkier electrophile.

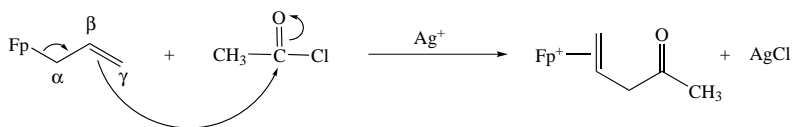


Equation 8.69 demonstrates addition to the γ position of the η¹-allyl complex and represents simply the reverse of nucleophilic addition to [Fe(alkene)]⁺ reagents (see equations 8.39 and 8.40).⁹⁷ The synthetic utility of this reaction is illustrated in equation 8.70, where the iron complex undergoes conjugate addition to the α,β-unsaturated diester. The resulting η²-π ligand then undergoes

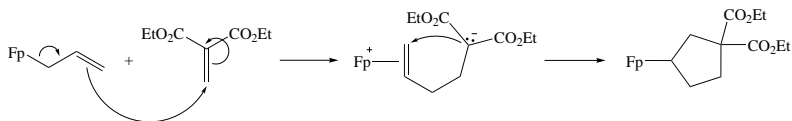
and protect complexes from undergoing reactions such as ligand substitution or decomposition in other ways. Cp* and Tp are isoelectronic ligands (donor-pair method of e⁻ counting) that form half-sandwich complexes. The η⁵ to η³ ring slippage of Cp* is comparable to the η³ to η² (sometimes denoted κ³ to κ², where κ denotes the hapticity of a kryptand ligand) bonding mode of Tp, in which one of the three arms of the ligand dissociates from the metal. The two ligands differ, however, in their mode of bonding to a metal—Cp* is a π-bonding ligand and Tp is a σ-donor. For more information on Tp ligands and other scorpionates, see S. Trofimenko, *Chem. Rev.*, **1993**, 93, 943.

⁹⁷For several examples of this type of electrophilic addition, see S. G. Davies, *Organotransition Metal Chemistry: Applications to Organic Synthesis*, Pergamon Press: Oxford, 1982, pp. 189–192, and references therein.

intramolecular nucleophilic addition by the carbanion to give a substituted cyclopentane that may be converted to a number of different compounds.⁹⁸



8.69



8.70

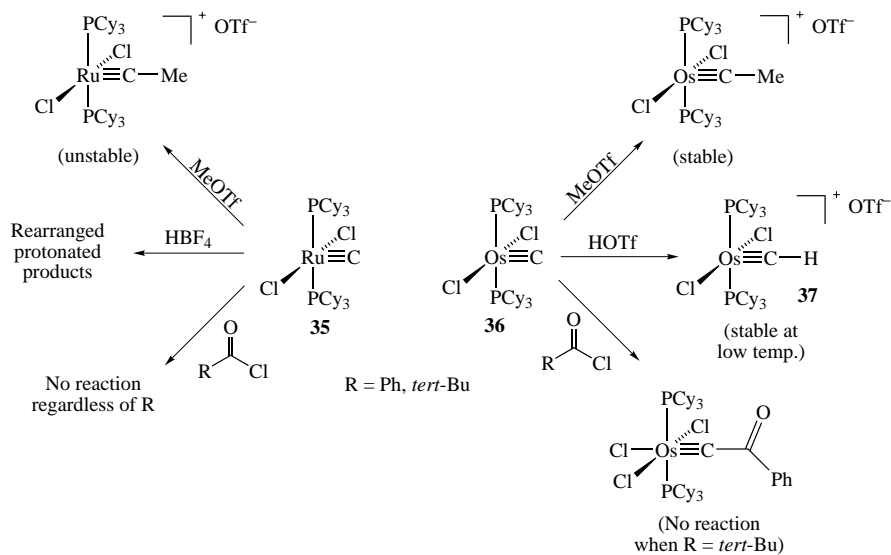
Group 8 carbide complexes, which are relatively rare and were first mentioned in Section 6-1-4, undergo electrophilic addition, and there are subtle differences shown between the reactivities of Ru and Os complexes. Scheme 8.12 details some chemistry whereby metal carbides undergo electrophilic addition to yield carbyne complexes (which readers will encounter in Section 10-4).⁹⁹ Both compounds **35** and **36** undergo methylation by reacting with MeOTf, which is not surprising since the carbide carbon tends to carry a partial negative charge. Both react with strong protic acids, but Ru carbides yield rearranged products upon protonation at the carbide carbon. In one case, however, the Os carbide reacted with HOTf to yield the corresponding electrophilic addition product **37**. Electrophilic addition of acylium ion ($R-C\equiv O^+$) was influenced by both steric hindrance and the Lewis basicity of the carbide carbon. Treatment of **35** with either acetyl chloride or pivaloyl chloride led to no reaction. Compound **36** was also unreactive with pivaloyl chloride but did react with benzoyl chloride to give the expected product of electrophilic addition at the carbide carbon. Johnson and co-workers ascribed the lack of reactivity with pivaloyl chloride to its high steric bulk, and the reactivity of the Os carbide over the Ru analog to the relatively higher Lewis basicity of the carbide carbon.

Equation 8.71 shows attack of the electrophile ("Et⁺") at the carbonyl oxygen, the most electron-rich site on the η^4 -dienone ligand, to yield a product with η^5 hapticity.¹⁰⁰

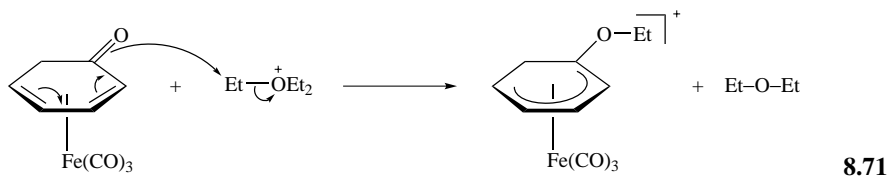
⁹⁸T. S. Abram, R. Baker, and C. M. Exon, *Tetrahedron Lett.*, **1979**, 4103.

⁹⁹M. H. Stewart, M. J. A. Johnson, and J. W. Kempf, *Organometallics*, **2007**, 26, 5102.

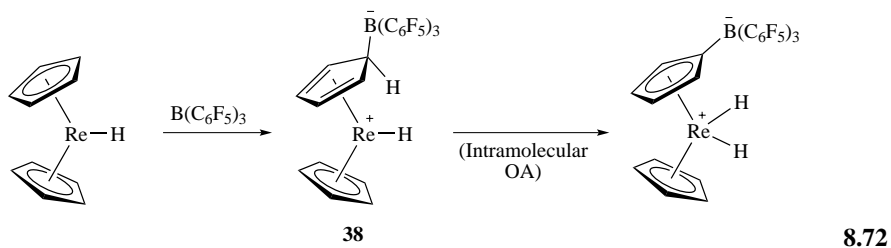
¹⁰⁰A. J. Birch and I. D. Jenkins, *Tetrahedron Lett.*, **1975**, 119.

**Scheme 8.12**

Electrophilic
Addition Reactions
of Group 8 Carbide
Complexes



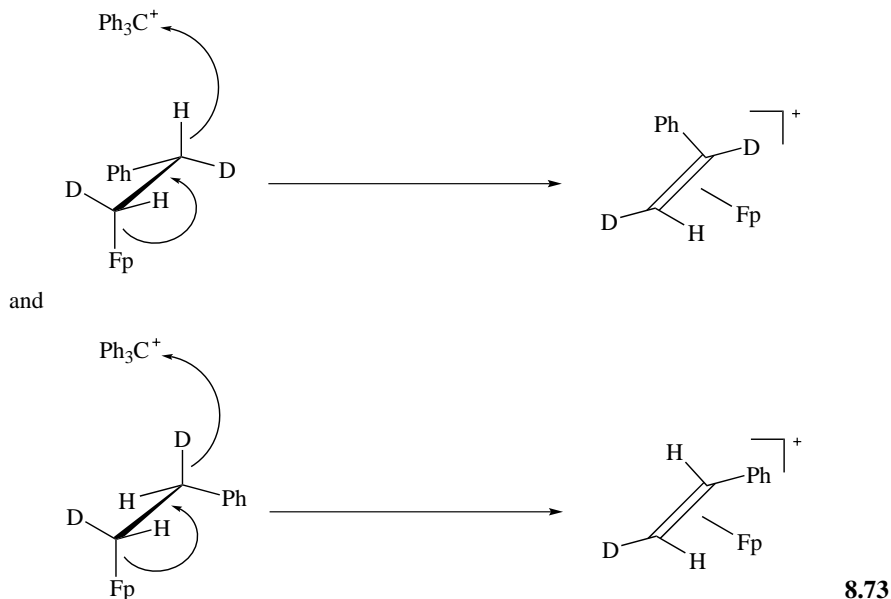
Finally, electrophilic addition of $\text{B}(\text{C}_6\text{F}_5)_3$, a strong Lewis acid, to a Cp ligand yields an η^4 -Cp Re complex **38**. Oxidative addition of a C–H bond (intramolecular C–H bond activation) from the η^4 -Cp ring results in a zwitterionic rhenium dihydride, as shown in equation **8.72**.¹⁰¹



¹⁰¹L. H. Doerrer, A. J. Graham, D. Haussinger, and M. L. H. Green, *J. Chem. Soc., Dalton Trans.*, **2000**, 813.

Abstraction

Electrophilic abstraction of a portion of a σ -bound hydrocarbyl or a coordinated π ligand may occur. The trityl cation, Ph_3C^+ , is a commonly-used electrophile for this task. Equation 8.73 provides an example of abstraction at the β position of an alkyl ligand to provide an η^2 -alkene complex,¹⁰² a useful route for the synthesis of these compounds.

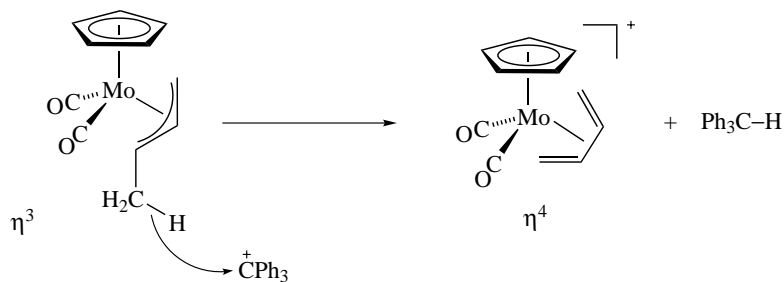


The reaction is stereospecific, as shown by the use of ligand deuterated at the β -position. Formation of these products requires *anti* elimination in a manner analogous to the E_2 pathway in organic chemistry. The difference here, of course, is that abstraction occurs with an electrophile and not with a base, as we find in the organic analog. It is not surprising that trityl cation serves as the premier hydride abstracting agent in reactions such as 8.73. The cation is rather stable (trityl salts are commercially available) and easy to handle. Because of its steric bulk, it does not readily attack the metal directly. Finally, the reaction is thermodynamically feasible in terms of enthalpy change.

Hydride abstraction by Ph_3C^+ also occurs on the η^3 -allyl-Mo complex¹⁰³ shown in equation 8.74, again causing an increase in hapticity of one unit.

¹⁰²D. Slack and M. C. Baird, *J. Chem. Soc., Chem. Commun.*, **1974**, 701.

¹⁰³J. W. Faller and A. M. Rosan, *J. Am. Chem. Soc.*, **1977**, *99*, 4858. For references to other hydride abstractions using Ph_3C^+ , see D. Mandon, L. Toupet, and D. Astruc, *J. Am. Chem. Soc.*, **1986**, *108*, 1320.



Although we will encounter other types of reactions in later chapters, ligand substitution, oxidative addition, reductive elimination, insertion, elimination, and nucleophilic and electrophilic attack on ligands comprise most of the fundamental processes that encompass all of organometallic chemistry. Your understanding of these reactions will enable you to appreciate the many applications of organotransition metal chemistry to other areas of the chemical sciences. In Chapter 9 we consider the role of organometallic compounds as catalysts in pathways leading to industrially useful molecules. The individual steps involved in these transformations are typically the basic reaction types we have just discussed in Chapter 8 and in Chapter 7.

Suggested Reading

1,1- and 1,2-Insertion

- Y. Kayaki and A. Yamamoto, "1,1-Insertion into Metal-Carbon Bond," In *Fundamentals of Molecular Catalysis*, H. Kurosawa and A. Yamamoto, Eds., Elsevier: Amsterdam, 2003, Chap. 7.
- P. Espinet and A. C. Albéniz, "1,2-Insertion and β -Elimination," In *Fundamentals of Molecular Catalysis*, H. Kurosawa and A. Yamamoto, Eds., Elsevier: Amsterdam, 2003, Chap. 6.
- J. M. Andersen and J. R. Moss, *Adv. Organometal. Chem.*, **1995**, 37, 169.
- J. P. Collman, L. S. Hegedus, J. R. Norton, and R. G. Finke, *Principles and Applications of Organotransition Metal Chemistry*, University Science Books: Mill Valley, CA, 1987, Chap. 6.
- F. Calderazzo, *Angew. Chem. Int. Ed. Engl.*, **1977**, 16, 299.

Nucleophilic Additions and Abstractions

- H. Kurosawa, "Additions to Unsaturated Ligands," In *Fundamentals of Molecular Catalysis*, H. Kurosawa and A. Yamamoto, Eds., Elsevier: Amsterdam, 2003, Chap. 8.
- J. P. Collman, L. S. Hegedus, J. R. Norton, and R. G. Finke, *Principles and Applications of Organotransition Metal Chemistry*, University Science Books: Mill Valley, CA, 1987, Chap. 7.

Electrophilic Additions and Abstractions

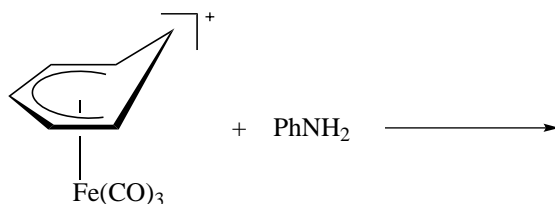
J. P. Collman, L. S. Hegedus, J. R. Norton, and R. G. Finke, *Principles and Applications of Organotransition Metal Chemistry*, University Science Books: Mill Valley, CA, 1987, Chap. 8.

M. D. Johnson, "Electrophilic Attack on Transition Metal η^1 -Organometallic Compounds," In *The Chemistry of the Metal-Carbon Bond*, F. R. Hartley and S. Patai, Eds., Wiley: New York, 1985, vol. 2, Chap. 7.

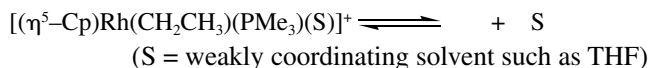
Problems

8-1 Predict the products.

- $cis\text{-Re}(\text{CH}_3)(\text{PR}_3)(\text{CO})_4 + {}^{13}\text{CO} \rightarrow$ [show structures of all products]
- $trans\text{-Ir}(\text{CO})\text{Cl}(\text{PPh}_3)_2 + \text{CH}_3\text{I} \rightarrow \mathbf{A}$; $\mathbf{A} + \text{CO} \rightarrow \mathbf{B}$
- $\text{CH}_3\text{Mn}(\text{CO})_5 + \text{SO}_2 \rightarrow$ [no gases are evolved]
- $\eta^5\text{-CpFe}(\text{CO})_2(\text{CH}_3) + \text{PPh}_3 \rightarrow$
-



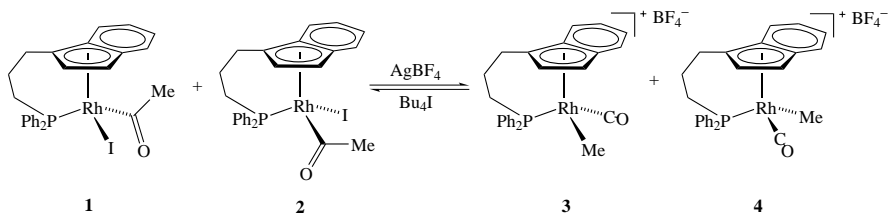
8-2 Predict the structure of the product of the following equilibrium (Note: The product obeys the 18-electron rule).



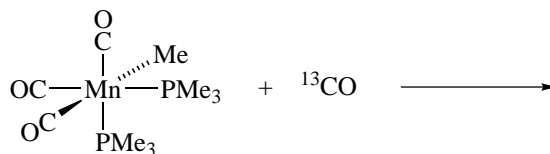
8-3 Rhodium complex **1** and its stereoisomer **2** (ratio of **1:2** = 85:15) were treated with AgBF_4 to give diastereomeric products **3** and **4** (ratio of **3:4** = 84:16).¹⁰⁴

- Was the stereochemistry about the Rh center inverted or retained? Explain.
- What does this experiment show about the nature of the deinsertion reaction? Did the CH_3 group migrate or the CO?

¹⁰⁴Y. Kataoka, A. Shibahara, T. Yamagata, and K. Tani, *Organometallics*, **2001**, 20, 2431.

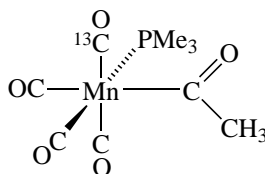


8-4 Predict the products of the following reaction, showing clearly the structure of each and the expected relative distribution of products.

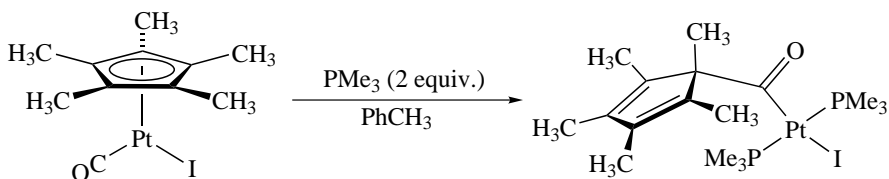


8-5 The ^{13}C -labeled molecule shown loses CO on heating. Predict the products of this reaction assuming that the mechanism is the reverse of:

- a. Direct CO insertion
- b. Intramolecular CO migration
- c. Intramolecular CH_3 migration

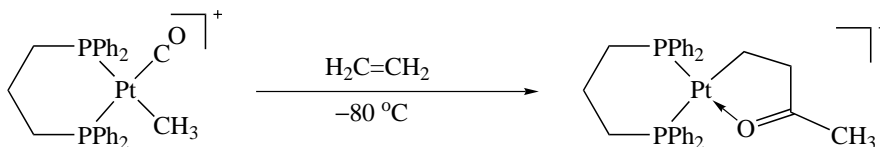


8-6 Propose a mechanism for the following reaction.¹⁰⁵



¹⁰⁵L. Leontyeva, R. P. Hughes, and A. L. Rheingold, *Organometallics*, **2007**, *26*, 5735.

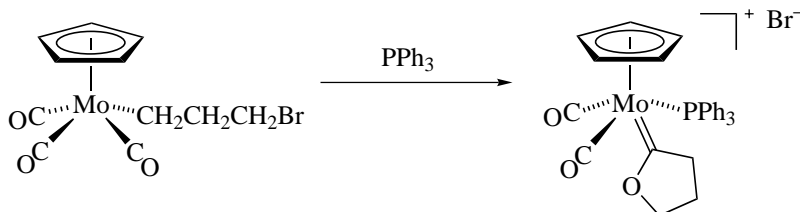
8-7 Propose a mechanism for the following transformation.¹⁰⁶



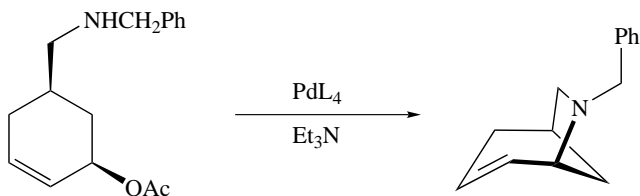
8-8 The complex $[(\eta^6\text{-C}_6\text{H}_6)\text{Mn}(\text{CO})_3]^+$ has carbonyl bands at 2026 and 2080 cm^{-1} and a single ^1H NMR resonance at δ 6.90 ppm. This complex reacts with PBu_3 to give product **5**, which has infrared bands at 1950 and 2028 cm^{-1} and ^1H NMR signals at δ 6.30 (relative area = 1), 5.50 (2), 4.40 (1), 3.40 ppm (2), and signals corresponding to butyl groups. Complex **5** converts photochemically into **6**, which has infrared bands at 1950 and 1997 cm^{-1} and only one signal, at δ 6.42 ppm, other than signals for the butyl groups. Suggest structures for **5** and **6**.

8-9 Propose mechanisms for the two transformations shown.

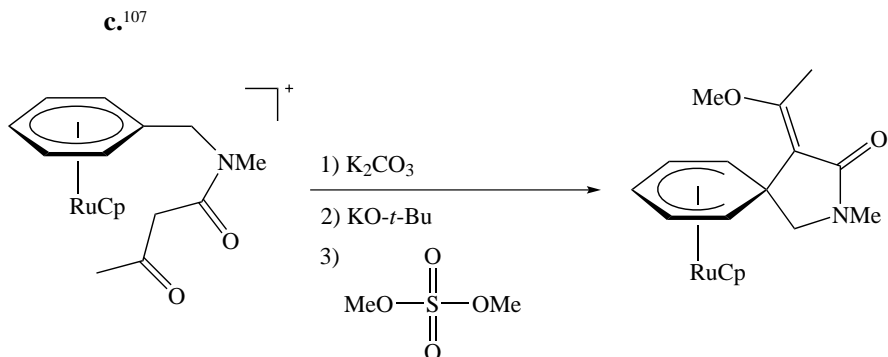
a.



b.

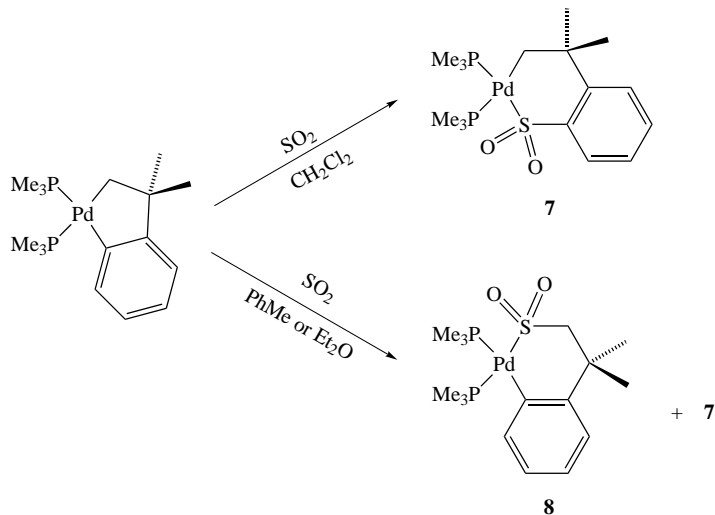


¹⁰⁶C. S. Shultz, J. M. DeSimone, and M. Brookhart, *J. Am. Chem. Soc.*, **2001**, *123*, 9172.



8-10 Consider the transformation shown below. When CH_2Cl_2 is the solvent, formation of **7** occurs exclusively. Use of toluene or diethyl ether as solvent results in a mixture of **7** and **8**, with **7** usually predominating. The investigators postulated a mechanism for SO_2 insertion that was different than the $\text{S}_{\text{E}}2$ pathway discussed in Chapter 8.¹⁰⁸

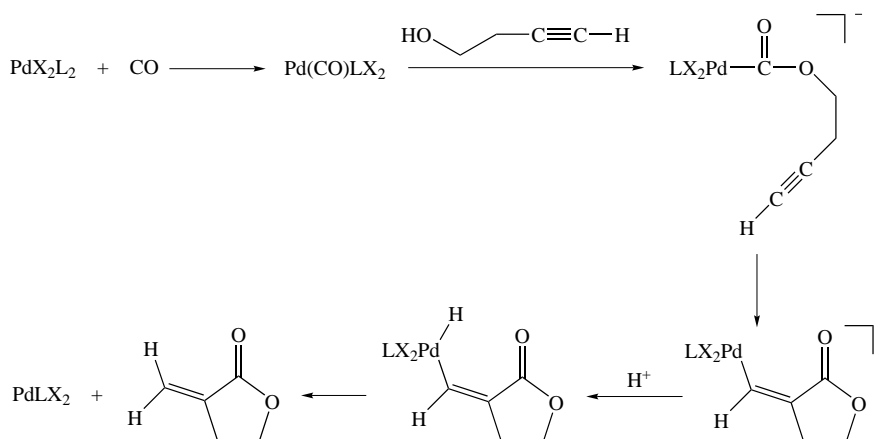
- Propose an alternative step-wise mechanism for this reaction. [Hint: What positions on the Pd complex starting material are attractive for bonding with SO_2 ?]
- Why isn't the $\text{S}_{\text{E}}2$ mechanism a likely pathway for the formation of compound **7**?



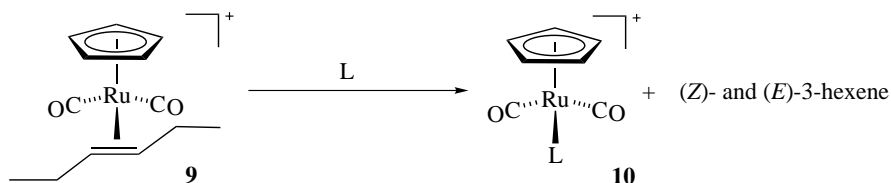
¹⁰⁷F. C. Pigge, J. J. Coniglio, and S. Fang, *Organometallics*, **2002**, *21*, 4505.

¹⁰⁸J. Cámpora, J. A. López, P. Palma, D. del Río, E. Carmona, P. Valerga, C. Graiff, and A. Tiripicchio, *Inorg. Chem.*, **2001**, *40*, 4116.

8-11 Follow the step-wise reaction shown below. For each step, indicate what kind of fundamental organometallic reaction type is taking place.



8-12 *E*-alkenes are more stable than their *Z*-isomers. When the (*E*)-3-hexene Ru complex **9** was treated with an excess of PPh₃ or 4-substituted pyridines, the corresponding substituted complex **10** was produced as well as 3-hexene. If this were a simple ligand substitution, one would expect that only (*E*)-3-hexene would be released. Interestingly, both (*E*)- and (*Z*)-3-hexene were formed using the two types of nucleophiles. In fact, when 4-methoxypyridine was used as the nucleophile, the *E/Z* ratio was 13:87! Propose a mechanism that accounts for the formation of (*Z*)-3-hexene.¹⁰⁹

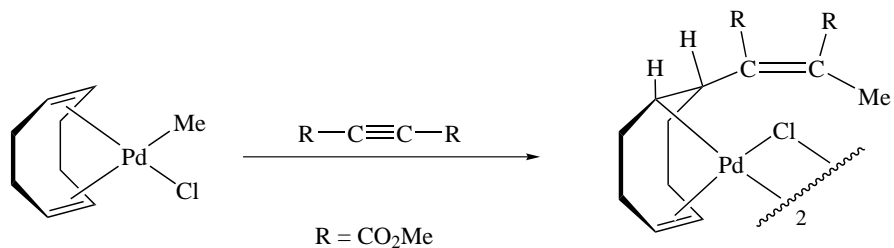


L = PPh₃, 4-picoline, 4-methoxypyridine

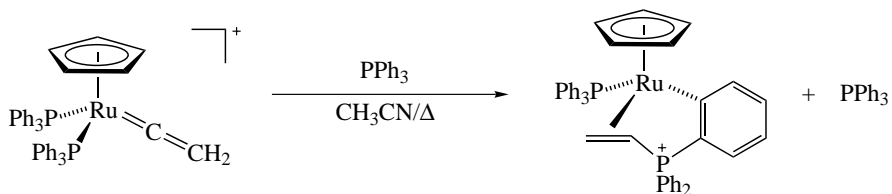
8-13 Propose a mechanism for the following reaction.¹¹⁰

¹⁰⁹K. M. McWilliams and R. J. Angelici, *Organometallics*, **2007**, *26*, 5111.

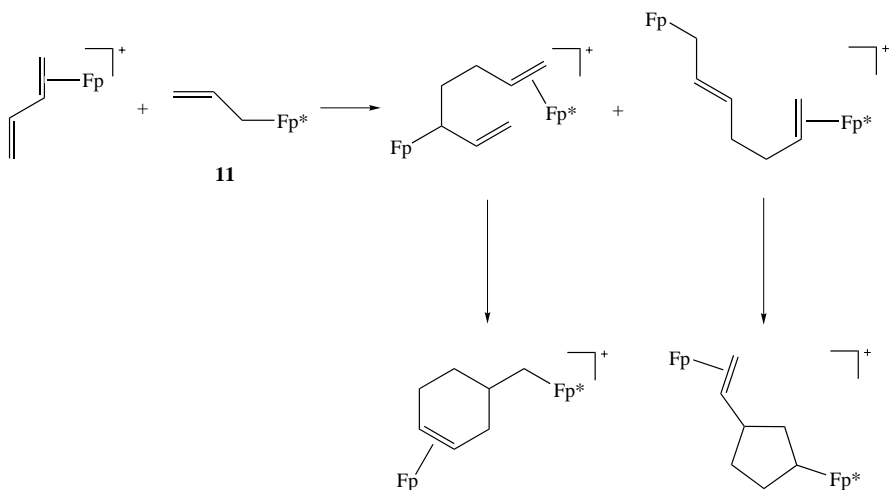
¹¹⁰G. R. Hoel, R. A. Stockland, Jr., G. K. Anderson, F. T. Ladipo, J. Braddock-Wilking, N. P. Rath, and J. C. Mareque-Rivas, *Organometallics*, **1998**, *17*, 1155.



8-14 Propose a mechanism for the following transformation [Hint: the mechanism involves steps that are described in both Chapters 7 and 8.]¹¹¹



8-15 Propose a mechanism for the following multi-step reaction that involves nucleophilic participation of a remote π bond. Assume that in the first step compound **11** acts as a nucleophile. [Fp = CpFe(CO)₂; * = an arbitrary label to distinguish one Fp group from the other]



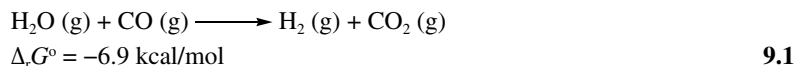
¹¹¹K. Onitsuka, M. Nishii, Y. Matsushima, and S. Takahashi, *Organometallics*, **2004**, *23*, 5630.

Homogeneous Catalysis

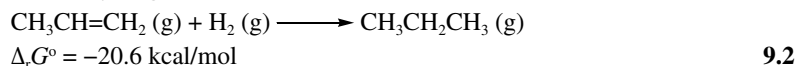
The Use of Transition Metal Complexes in Catalytic Cycles

There are many reactions in chemistry that are favorable thermodynamically, yet they occur extremely slowly at room temperature. A few of these are shown in equations 9.1–9.3.

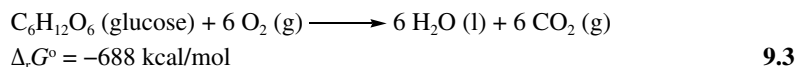
Water gas shift reaction:



Alkene hydrogenation:



Glucose metabolism:



The presence of a *catalyst* dramatically increases the rate of the reactions shown and countless others, even those that may not have negative free energies of reaction. Chapter 9 will consider the role transition metal complexes play as catalysts for several transformations, many of which are important industrially. As catalysts, transition metal complexes undergo most of the reactions we have just discussed in Chapters 7 and 8. We will encounter a number of different catalytic cycles in Chapter 9; other catalytic processes involving transition metals will be described in Chapters 11 and 12.

9-1 FUNDAMENTAL CONCEPTS OF HOMOGENEOUS CATALYSIS

The phenomenon of catalysis was recognized over 150 years ago by Berzelius, who referred to the “catalytic power of substances” that were able to “awake affinities that are asleep at this temperature by their mere presence and not by their own affinity.”¹ Once the principles of thermodynamics were developed and the concept of equilibrium was established by the turn of the 20th century, scientists realized that catalysts are species that increase the rate of a reaction without affecting the equilibrium distribution of reactants and products. Exactly how catalysts are able to speed up reactions without changing the free energy of either reactants or products remained a mystery for many years. Only in the past few decades has it been possible to elucidate mechanistic pathways involving catalysts using such tools as kinetics, stereochemical studies, and spectroscopy. It is clear now that catalysts interact with reactants to provide a reaction pathway with a significantly lower free energy of activation than the corresponding uncatalyzed pathway. Figure 9-1 depicts this phenomenon, with the solid line representing the uncatalyzed reaction and the dashed line the catalyzed reaction path.

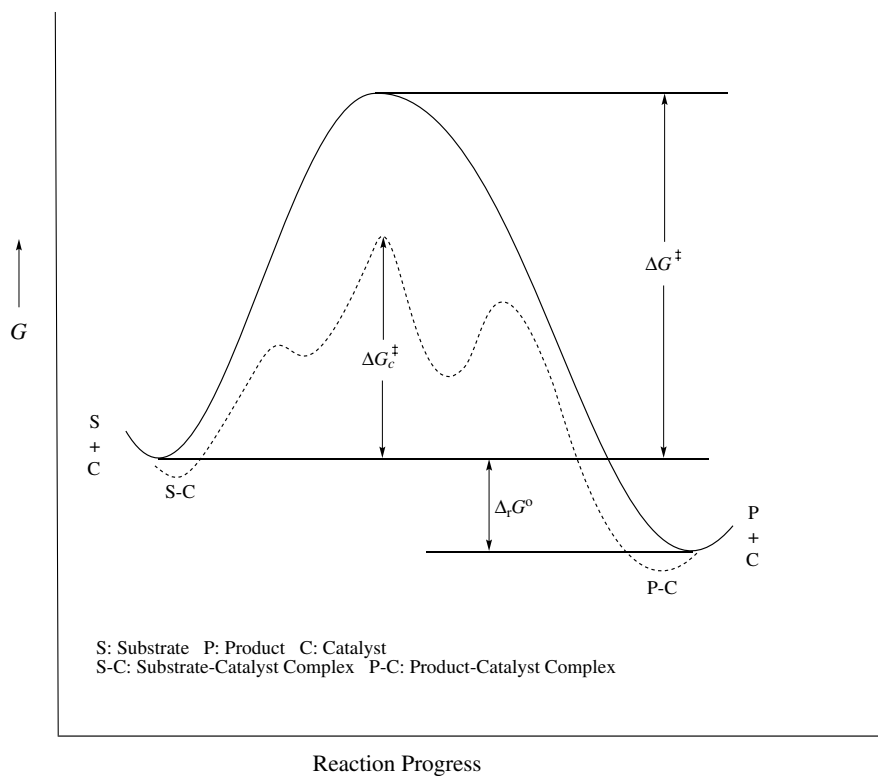
Typically, catalysts are intimately involved with reactants (often called substrates) in a cyclic series of associative (binding), bond making and/or breaking, and dissociative steps (Scheme 9.1). During each cycle, the catalyst is regenerated so that it may go through another cycle. Each cycle is called a *turnover*, and an effective catalyst may undergo hundreds, even thousands of turnovers before decomposing, with each cycle producing a molecule of product. The *turnover number* (abbreviated TON) is defined as the total number of reactant molecules a molecule of catalyst converts to product molecules. This is true if the catalyst is homogeneous and has one active site; if the catalyst has more than one active site, TON is calculated per active site. *Turnover frequency* (TOF) is the TON per unit time.² In a stoichiometric reaction, on the other hand, the “catalyst” (actually reagent) undergoes only *one* turnover per molecule of product produced.

9-1-1 Selectivity

The laws of thermodynamics dictate that the product distribution resulting from a catalyzed or uncatalyzed reaction must be the same if enough time is allowed for the transformation to come to equilibrium. The presence of a catalyst, however, can influence initial product distributions, allowing preferential formation of a product that may be less stable thermodynamically than another. This

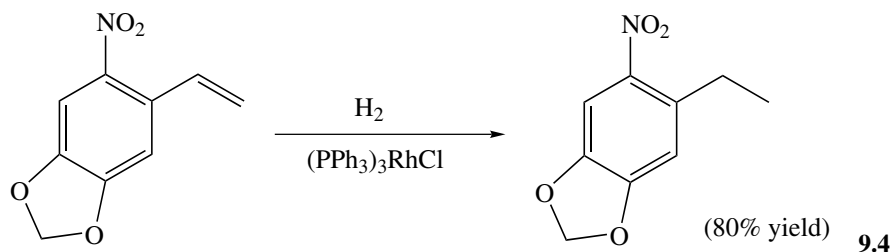
¹Taken from a quotation in G. C. Bond, *Homogeneous Catalysis*, Oxford University Press: Oxford, 1987, p. 2.

²For more information on TON and TOF, see G. P. Chiusoli and P. M. Maitlis, Eds., *Metal Catalysis in Industrial Organic Processes*, RSC Publishing: Cambridge, 2006, p. 270.

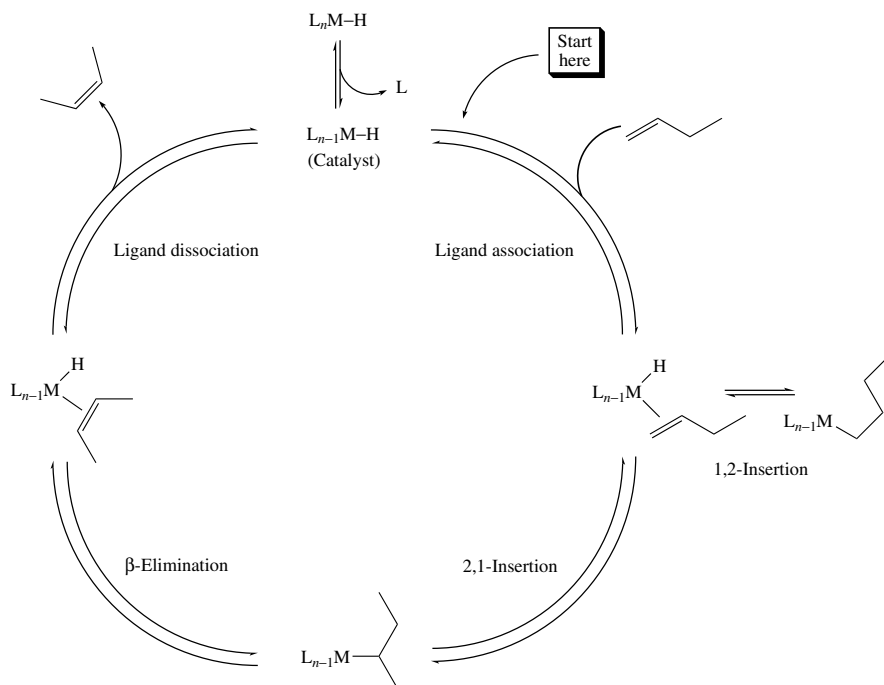
**Figure 9-1**

Reaction Progress versus Energy Diagrams for a Catalyzed and Uncatalyzed Reaction

is a phenomenon known as *selectivity*. There are several kinds of selectivity demonstrated by catalysts, such as chemoselectivity, regioselectivity, and stereoselectivity. Equation 9.4 illustrates an example of chemoselectivity, whereby hydrogenation occurs selectively at only one functional group in the reactant. In principle, hydrogenation could occur at the phenyl ring, the C=C bond, or the nitro group. In the presence of the Rh catalyst, however, H_2 adds only to the alkene group.³

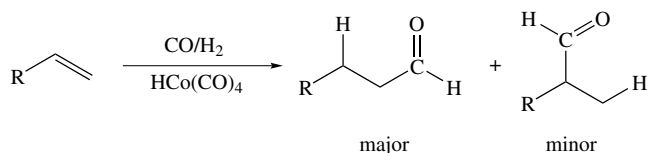


³A. Jourdan, E. González-Zamora, and J. Zhu, *J. Org. Chem.*, **2002**, 67, 3163.

**Scheme 9.1**

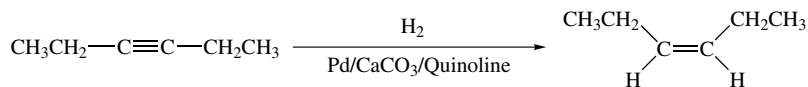
A Schematic Picture of a Catalytic Cycle Showing C=C Bond Isomerization

The hydroformylation reaction (Section 9-2), shown in equation 9.5, demonstrates regioselectivity, whereby one regioisomer forms preferentially over another. The Co catalyst may be modified to increase the proportion of linear (anti-Markovnikov) over branched (Markovnikov) product.



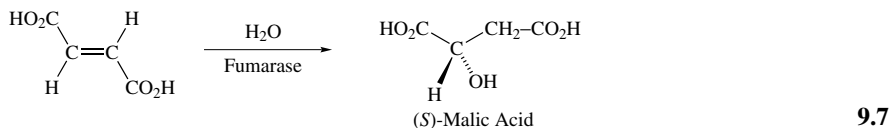
9.5

The hydrogenation of disubstituted alkynes with Lindlar catalyst (equation 9.6) represents an example of the use of a stereoselective catalyst. Such catalysts promote the formation of one stereoisomer in preference to one or more others. In this particular example, the *Z* alkene is formed in great preference to the corresponding *E* isomer.



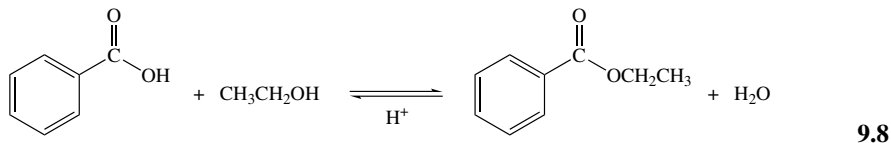
9.6

Catalysts also exhibit selectivity in their initial binding to reactants. Enzymes are well known for their ability to bind selectively to only one member of a pair of stereoisomers. The bound stereoisomer will undergo reaction, and the remaining isomer is inert to the reaction conditions. For example, the enantioselective addition of water to fumaric acid (the *E* isomer), which yields (*S*)-malic acid (equation 9.7), is catalyzed by an enzyme called fumarase. Isomeric maleic acid (the *Z* isomer) fails to react in the presence of fumarase.



9-1-2 Homogeneous versus Heterogeneous Catalysts

In your study of chemistry thus far, you have probably encountered a number of catalyzed reactions. Those who are familiar with organic chemistry will recognize equation 9.2 as an alkene hydrogenation reaction that occurs at a reasonable rate only in the presence of a catalytic amount of Pd or Pt deposited on an inert solid. The synthesis of esters from alcohols and carboxylic acids (equation 9.8) is catalyzed by mineral acids such as H_2SO_4 or HCl .



The catalyst involved in the former reaction is known as a *heterogeneous* catalyst. Equation 9.8, on the other hand, demonstrates the use of a *homogeneous* catalyst. A heterogeneous catalyst exists as another phase in the reaction medium, typically as a solid in the presence of a liquid or gaseous solution of reactants. A homogeneous catalyst is *dissolved* in the reaction medium, along with the reactants. Homogeneous catalysts that are transition metal complexes find increasing importance in the chemical industry, where the use of heterogeneous catalysts has historically been predominant.⁴

⁴Despite the increasing use of homogeneous catalysts in the chemical industry, homogeneous catalysts are involved in processes that yield only about 15% of the total production of chemicals worldwide; J. Hagen, *Industrial Catalysis: A Practical Approach*, 2nd ed., Wiley-VCH Verlag: Weinheim, Germany, 2006, pp. 9 and 425.

Table 9-1 Major Differences between Homogeneous and Heterogeneous Catalysts

Characteristic	Homogeneous	Heterogeneous
1. Catalyst composition and nature of active site	Discrete molecules with well-defined active site	Nondiscrete molecular entities; active site not well defined
2. Determination of reaction mechanism	Relatively straightforward using standard techniques	Very difficult
3. Catalyst properties	Easily modified, often highly selective, poor thermal stability, operates under mild reaction conditions	Difficult to modify, relatively unselective, thermally robust, operates under vigorous reaction conditions
4. Ease of separation from product	Often difficult	Relatively easy

Table 9-1 summarizes the major differences between homogeneous and heterogeneous catalysts. The subsequent discussion assumes that the homogeneous catalysts being discussed contain transition metals.

Catalyst Composition and Nature of the Active Site

The active sites on a heterogeneous catalyst are difficult to characterize because they are not discrete molecular entities. Instead, the active sites may be aggregations of solid support material (e.g., silica gel or zeolites) coated with deposited metal atoms. Not all sites on the surface of the catalyst have the same activity and physical or chemical characteristics. Analytical techniques, such as Auger spectroscopy and electron spectroscopy for chemical analysis, as well as scanning tunneling microscopy, have been applied in attempts to determine the nature of such catalytic surfaces. Much progress has been made, but much more information must be obtained before a complete and cogent understanding of heterogeneous catalysis can emerge.

Homogeneous catalysts, on the other hand, are discrete molecules that are relatively easy to characterize by standard spectroscopic techniques, such as NMR, IR, etc. The active site consists of the metal center and adjoining ligands.

Determination of the Reaction Mechanism

Because the constitution of the active site of a heterogeneous catalyst is difficult to determine, the elucidation of reaction mechanisms involving these catalysts can be troublesome indeed. The field of homogeneous catalysis, in contrast, has advanced rapidly over the past few decades because chemists have developed many techniques that are useful for studying reaction mechanisms. Elucidating the mechanism of a homogeneously-catalyzed reaction requires studying the mechanism of each individual step, in a series of relatively elementary chemical

reactions, by conventional methods. Each step must be shown to be kinetically and thermodynamically reasonable.⁵ Although this can be a daunting task for a reaction involving several catalytic steps, it is not at present as difficult as determining exactly what goes on during a heterogeneous catalysis.

Catalyst Properties: Ease of Modification, Selectivity, Thermal Stability, and Reaction Conditions

Because homogeneous catalysts are typically organotransition metal complexes, it is relatively easy to modify these compounds in order to increase selectivity. As we shall see, phosphines appear commonly as ligands in homogeneous catalysts. Phosphines offer a wide variety of stereoelectronic properties that can substantially influence the course of a catalyzed reaction.

Homogeneous catalysts are often much less thermally stable than their heterogeneous counterparts. The use of a homogeneous catalyst rather than a heterogeneous one requires milder conditions of temperature and pressure. If a sufficiently active homogeneous catalyst can be found that can do the job of a heterogeneous one, substantial savings in energy and initial capital cost (plants that run at high temperature and pressure are very expensive to build) accrue to the manufacturer that chooses to employ a homogeneously-catalyzed process.

Ease of Separation from Reaction Products

Homogeneous catalysts suffer from one key disadvantage when compared with their heterogeneous counterparts. They are often quite difficult to separate from reaction products. Catalyst recovery is clearly important, not only in ensuring product purity but also in conserving often-used precious metals such as palladium and rhodium.

9-1-3 Enzymes: Homogeneous or Heterogeneous Catalysts?

A discussion of catalysis would not be complete without a comparison of the catalysts we normally encounter in the laboratory or in industry with those that occur naturally (i.e., enzymes). Enzymes are proteins that are either soluble in the aqueous medium of the cell or attached to a cellular membrane. Soluble enzymes resemble homogeneous transition metal catalysts in ways other than their solubility characteristics. Enzymes have at least one region that serves as

⁵It should be pointed out that an individual step may be endothermic, even if the overall reaction is exothermic.

an active site (see Figure 9-2) for substrate(s) to bind⁶ and thence to undergo transformation into product(s). Modification of the enzyme's amino acid sequence can drastically alter the catalytic efficiency of the enzyme. Often, enzymes have sites remote from the active site where ligands other than substrate can bind. This binding can alter the nature of the active site by causing a conformational change in the structure of the protein. Binding at these remote sites may be a necessary precursor for catalytic activity. Similarly, transition metal complexes may change significantly in catalytic activity when modifications are made of ligands that are not directly involved in the overall chemical transformation (i.e., phosphines).

The active site of enzymes is not a discrete molecule, such as an organotransition metal complex, but instead is comprised of functional groups from several amino acids that are often positioned in the peptide chain rather distant from one another. These functional groups become neighboring only because of the folding of the polymeric chain of amino acids. Enzymes are large molecules that have a vast surface area compared with transition metal complexes and, as such, may have complex interactions with other cellular entities.

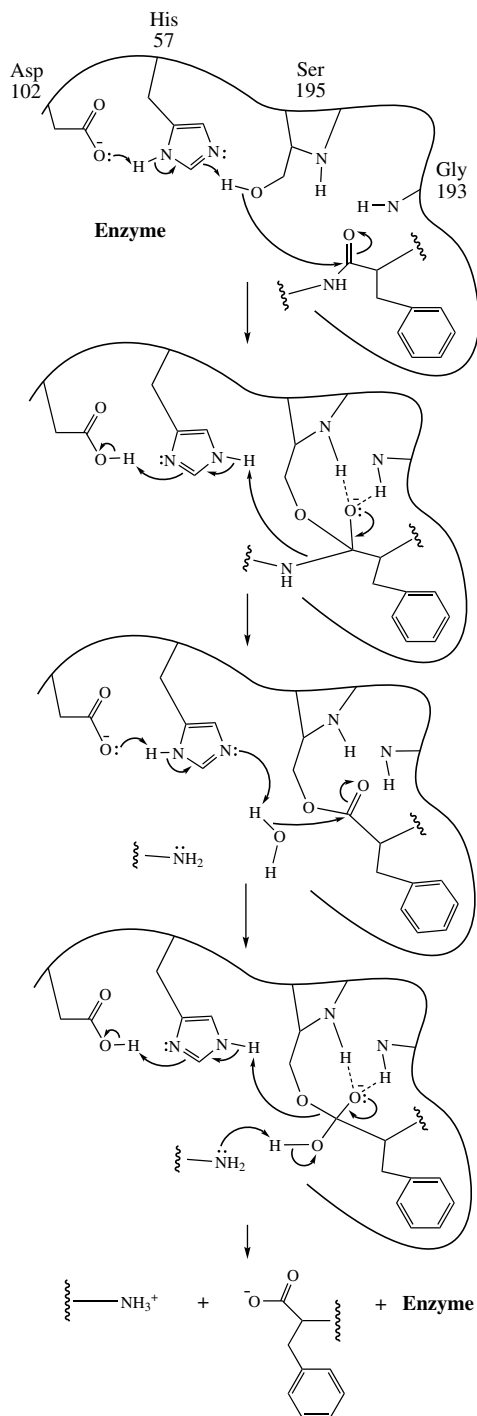
Membrane-bound enzymes loosely represent a hybrid between homogeneous and heterogeneous catalysts. The membrane represents a large surface area that supports catalytically active entities (the enzymes). The enzymes, however, are discrete molecules (although giant ones) in contrast to metal crystallites found in most heterogeneous catalysts.

Interestingly, one of the most active areas in transition metal catalysis concerns the use of a hybrid catalyst that resembles a membrane-bound enzyme. Much work has been reported in which transition metal complexes are bound to solid supports such as silica, alumina, or organic polymers. These catalytic systems have some of the advantages of both types of catalysts. Based on studies in homogeneous media, the transition metal complexes may be easily modified to increase selectivity. The complex, on the other hand, may be readily separated from product because it is bound to a solid support, a useful property indeed, as we discussed above. As promising as these hybrid catalysts are, however, their use in industry has not come to fruition. Such catalysts tend to suffer from "bleeding" of the active transition metal away from the binding surface. Such bleeding lowers activity with time and is prohibitively costly if the active sites involve precious metals.

9-1-4 The Unique Fitness of the Transition Metals

Although many species serve as useful homogeneous catalysts (e.g., H^+ , OH^- , Al^{3+} , imidazole), complexes of transition metals are far and away the most selective.

⁶The binding energies involved in enzyme–substrate interactions are much less than ordinary chemical bonds. The cumulative effect, however, of several weak binding interactions is significant.

**Figure 9-2**

A Schematic View of the Mechanism of Chymotrypsin-Catalyzed Amide Hydrolysis Occurring at the Enzyme Active Site

Why is this so? The discussion in the next paragraphs attempts to shed some light on this very important question, in part by reminding readers of several concepts that we have already encountered.⁷

A Variety of Ligands Will Bind to Transition Metals

Chapters 4–6 have shown that a host of different ligands will bind to metals and that these ligands may be classified as X- or L-type. In fact, transition metals will bind to virtually any other element in the periodic table and to almost all organic molecules. Ligands may either be directly involved in the catalytic process or indirectly affect catalysis by exerting steric and/or electronic effects on the complex.

Transition Metals Have the Ability to Bind to Ligands in a Number of Ways

In Chapters 4–6, we described how various ligands can bind to transition metals. The availability of *d* as well as *s* and *p* orbitals on the metal allows for the formation of σ and π bonds from metal to ligand. A single ligand, such as an allyl group, may bind in an η^1 or η^3 manner, for example. The hapticity of such a ligand may change during a catalytic cycle, and the ease of this change facilitates ligand modification. Carbonyl ligands attach to a metal in a terminal or bridging bonding mode. Groups such as methyl or hydride may react as anionic, neutral (radical), or cationic species depending on the electron density of the metal. Finally, the strength of metal–ligand bonds is moderate (30–80 kcal/mol), allowing bonds between ligand and metal to form or break relatively easily—a necessity for the catalytic cycle to proceed.

A Variety of Oxidation States Is Available

As ligands are added to or removed from the metal by processes such as oxidative addition and reductive elimination, the oxidation state of the metal changes. Transition metals, with their *d* valence electrons, usually have a rather large number of oxidation states available, particularly in comparison to main group metals. The elements in Groups 8–10 especially possess a tendency for rapid, reversible two-electron change (such as from 18 e^- to 16 e^- and back), and thus it is not surprising that they are often involved in homogeneous catalysis.

⁷An excellent discussion on the fitness of the transition metals for catalytic activity is found in C. Masters, *Homogeneous Transition-Metal Catalysis—A Gentle Art*, Chapman & Hall: London, 1981, pp. 5–20; see also J. Hagen, *Industrial Catalysis: A Practical Approach*, 2nd ed., Wiley–VCH Verlag: Weinheim, Germany, 2006, Chap. 2.

Transition Metal Complexes Exhibit Several Different Geometries

Depending on the coordination number, a variety of structural possibilities exists for transition metal complexes. Geometries such as square planar, octahedral, tetrahedral, square pyramidal, and trigonal bipyramidal are common in complexes involving the transition metals. Much is already known about the behavior of ligands attached to metals in these geometries. For example, in square planar complexes, a ligand *trans* to another may cause the latter ligand to be quite labile and thus readily dissociate from the metal. If loss of the latter ligand is required for effective catalysis, then it is desirable to (1) design the catalytic cycle in such a way that a square planar complex is one of the intermediates along the path to the product and (2) have the directing group with a high *trans* effect positioned *trans* to the leaving group. Another example might involve a process where a key step is the reductive elimination of two ligands. We saw in Chapter 7 that RE requires the two leaving groups to be *cis* with respect to each other before the reaction may occur. The catalysis will be successful in this case if an intermediate forms readily, such that the two leaving groups are *cis*.

Transition metal complexes, with their well-defined geometries, serve as “templates” for the occurrence of reliable stereospecific or stereoselective ligand interaction. We know that alkyl migration to a carbonyl group occurs with retention of configuration at carbon, and that reductive elimination involves retention of configuration in the two leaving groups. In this way, transition metal complexes mimic the stereospecific reactions often catalyzed by enzymes.

Transition Metal Complexes Possess the “Correct” Stability

By varying metal and ligands, transition metal complexes can be designed to serve as intermediates that are not too reactive or too unreactive. For a catalytic turnover to occur, each intermediate in the cycle must be reactive enough to proceed to the next stage, yet not so reactive that other pathways (e.g., decomposition or a different bonding mode) become feasible.

We have just seen several reasons for the unique fitness of transition metals and their complexes as catalysts. The take-home lesson from all of this discussion is that the transition metals and the complexes derived from them are versatile. The stage is now set to examine several examples of homogeneous transition metal catalysis.

9-1-5 Catalysis and Green Chemistry

We have already made reference to green aspects of organometallic chemistry in Section 7-2-1, where environmentally-friendly characteristics of the activation of H–H, C–H, and C–C bonds were pointed out. In this section, we focus on the relationship between green chemistry and organometallic chemistry. Green chemistry is defined as the “utilization of a set of principles that reduces or eliminates

the use or generation of hazardous substances in the design, manufacture, and application of chemical products.”⁸ Among the 12 principles of green chemistry is the goal to maximize atom economy (i.e., to ensure that as many atoms of reactant as possible end up in the desired product). Other goals include reducing the use of hazardous materials; using renewable feedstocks for chemical processes (petroleum is not a renewable resource, at least in our lifetimes); using water as a solvent or using no solvent at all; producing useful, non-toxic, and biodegradable materials; and, most important for the discussion at hand, employing catalysts instead of stoichiometric reagents wherever possible.

Organotransition metal compounds play a key role in catalyzing “green” reactions and processes, especially when it comes to maximizing atom economy. The chemical industry has taken a lead role in promoting green chemistry, and we shall see examples of these developments in this and later chapters.

9-2 THE HYDROFORMYLATION REACTION

Among all of the homogeneous processes catalyzed by transition metals, hydroformylation stands out in three respects. It is the oldest process still in use today, it is responsible for producing the largest amount of material resulting from a homogeneous transition metal-catalyzed reaction,⁹ and it can be considered a green process because it proceeds with almost 100% atom economy. The hydroformylation reaction was outlined already in equation 9.5.

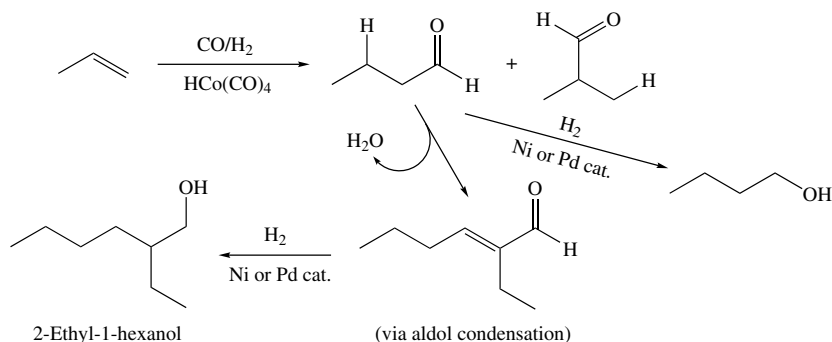
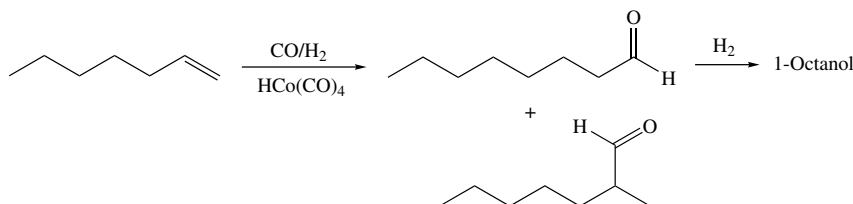
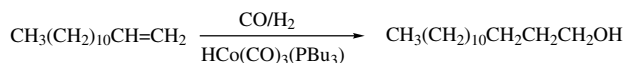
Discovered in 1938 by Otto Roelen¹⁰ (of Ruhrchemie in Germany), cobalt-catalyzed hydroformylation (also known as the *oxo*¹¹ reaction) was used successfully during World War II by the Germans to produce aldehydes from alkenes, H₂, and CO. It was not until the mid 1950s, however, that hydroformylation became a large-scale industrial process worldwide. Two main factors then drove the production of hydroformylation-derived products: (1) the ready availability of 1-alkenes from the petrochemical industry and (2) the large increase in production of plastics, which require plasticizing agents that are derived

⁸P. T. Anastas and J. C. Warner, *Green Chemistry: Theory and Practice*, Oxford University Press: New York, 1998, p. 11. This book is an excellent resource for those new to the field of green chemistry.

⁹In 2005, nearly 9.6 million metric tons (1 metric ton = 1000 kg or 1.1 U.S. tons) of hydroformylation products were produced worldwide; S. Bizzari, M. Blagoev, and A. Kishi, “Oxo Chemicals,” in *Chemical Economics Handbook*, SRI Consulting: Menlo Park, CA, 2006.

¹⁰O. Roelen, Ger. Patent, 849 548, 1938 O. Roelen, *Angew. Chem.*, **1948**, *60*, 62; and J. Falbe, *Carbon Monoxide in Organic Synthesis*, Springer Verlag: New York, 1970.

¹¹The name *oxo* was given to the reaction because in German *oxo* means carbonyl, and carbonyl compounds (especially aldehydes) are the initial products of hydroformylation processes.

Propene:**C₇–C₉ Alkenes:****C₁₁–C₁₅ Alkenes:****Scheme 9.2**

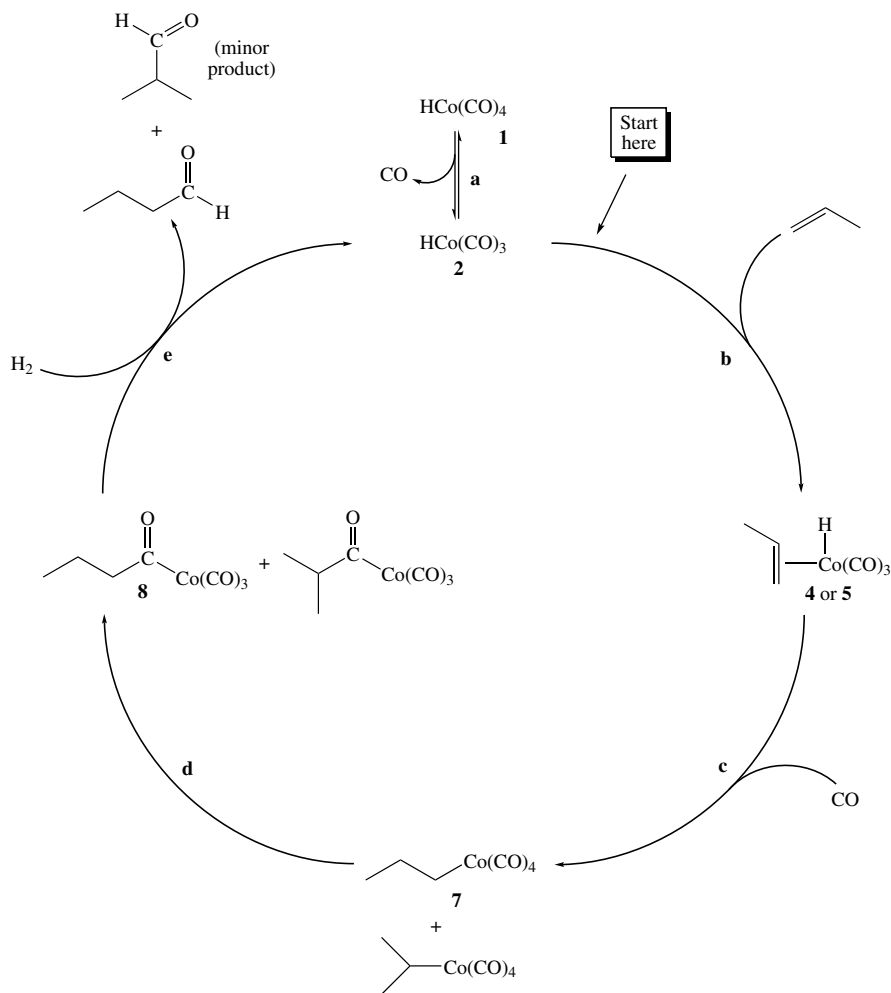
Industrially Useful
Compounds
Produced by
Hydroformylation

from hydroformylation.¹² Scheme 9.2 depicts some of the original applications of Co-catalyzed hydroformylation. Because of its economic importance and because it serves as a prototypical example of homogeneous transition metal catalysis, we will consider hydroformylation in more detail than some other catalytic processes that appear later in Chapter 9.

Propene is the most common feedstock for hydroformylation and is transformed into butanal and 2-methylpropanal, the former being the much more valuable product. Butanal may be hydrogenated in a separate step using a heterogeneous catalyst to give 1-butanol, a useful solvent, or it may undergo aldol condensation followed by hydrogenation to give 2-ethyl-1-hexanol. The substituted hexanol is used to make a diester of phthalic acid, which then serves as an agent (called a plasticizer) for making the normally rigid plastic, polyvinyl chloride (PVC), flexible.¹³ Hydroformylation converts C₇–C₉ alkenes to aldehydes

¹²C. Kohlpaintner, "Hydroformylation-Industrial," in *Encyclopedia of Catalysis*, Vol 3, I. Horváth, Ed., Wiley: Hoboken, NJ, 2003, p. 787.

¹³Tygon tubing, commonly used in laboratories, is an excellent example of plasticized PVC.

**Scheme 9.3**

Heck-Breslow
Mechanism for
Hydroformylation

containing one more carbon atom, which are then hydrogenated to give straight-chain alcohols, also useful as plasticizers. Alcohols containing 12 to 16 carbons result from hydroformylation-hydrogenation of corresponding alkenes with one less carbon atom. These alcohols serve as the basis for surfactant (detergent) compounds with several domestic and industrial uses.

9-2-1 Co-catalyzed Hydroformylation

Scheme 9.3 illustrates the cycle of catalytic steps proposed by Heck and Breslow¹⁴ for cobalt-catalyzed hydroformylation. The mechanism they proposed

¹⁴R. F. Heck and D. S. Breslow, *J. Am. Chem. Soc.*, **1961**, 83, 4023.

resulted from studies on model organocobalt carbonyl complexes. The cycle shown is an excellent example of transition metal catalysis because it contains steps converting a precatalyst to the active complex, it consists of several simple mono- and bimolecular steps involving the fundamental reactions of organometallic chemistry, it demonstrates the validity of the 16- and 18-electron rules, and it shows intermediates with plausible geometries. It must be pointed out, however, that the mechanism for cobalt-catalyzed hydroformylation is not completely understood with regard to kinetic and thermodynamic parameters for each step.¹⁵ We will look at each step, commenting on its relation to the catalytic cycle and to material you have already encountered in this text, and we will also point out some of the more recent work aimed at elucidating the mechanism of hydroformylation.

Step a

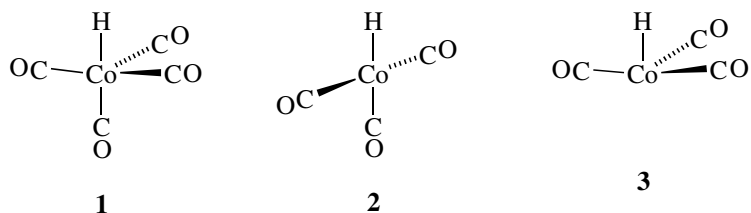
The true catalytically-active species is probably $\text{HCo}(\text{CO})_3$, a 16-electron complex. This intermediate results from 18-electron $\text{HCo}(\text{CO})_4$, **1**, which in turn ultimately comes from $\text{Co}(0)$ or $\text{Co}(\text{II})$, via $\text{Co}_2(\text{CO})_8$, in the presence of a 1:1 mixture of CO and H_2 (synthesis gas).¹⁶ Sometimes **1** is prepared in a separate step and introduced to the alkene in the presence of synthesis gas; this allows the subsequent hydroformylation to be run at a lower temperature (90–120 °C rather than the usual 120–170 °C). The dissociation step to form the active catalyst occurs with a relatively high activation energy, and it is, of course, inhibited by a high concentration of CO (the overall rate law for hydroformylation typically shows the concentration of CO with a negative exponent, n , where $0 > n > -1$). The reaction is run, however, under very high pressure (200–300 bar) to stabilize $\text{HCo}(\text{CO})_3$ and later intermediates in the catalytic cycle, thus demonstrating a balance in reaction conditions between the formation of sufficient $\text{HCo}(\text{CO})_3$ for hydroformylation to occur at a reasonable rate and the enhancement of the stability of catalytic intermediates.¹⁷ Calculations indicate that the preferred geometry

¹⁵For a recent summary of mechanistic work on Co-catalyzed hydroformylation, see P. W. N. M. van Leeuwen, *Homogeneous Catalysis: Understanding the Art*, Kluwer Academic: Dordrecht, The Netherlands, 2004, Chap. 7.

¹⁶Mixtures of CO and H_2 are called synthesis gas (sometimes referred to as “water gas”). Synthesis gas results from reaction of natural gas (or petroleum distillates) and steam over a nickel catalyst, and it is the basis for numerous organic molecules produced in large scale by the petrochemical industry.

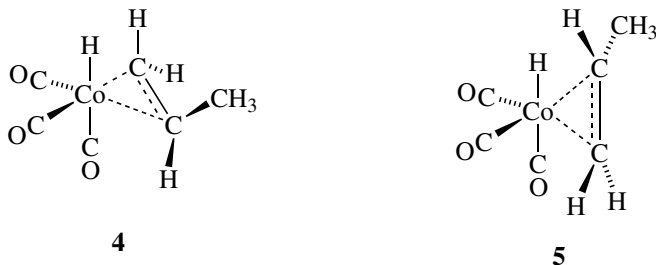
¹⁷For a good discussion of hydroformylation reaction conditions, see Footnotes 12 and 15 (Chapters 7 and 8); see also G. W. Parshall and S. D. Ittel, *Homogeneous Catalysis*, 2nd ed., John Wiley and Sons: New York, 1992, pp. 106–111, for a more concise treatment.

for $\text{HCo}(\text{CO})_3$ is more likely to be **2** (loss of CO from an equatorial position) instead of **3** (loss of CO from an axial position).¹⁸



Step b

The next step involves binding of the alkene to **2**, forming an 18-electron hydridoalkene complex that can have several structures, two of which are shown as **4** and **5**. Theoretical calculations at the DFT-B3LYP level¹⁹ by Jiao and co-workers demonstrated that Structure **4** is about 4 kcal/mol more stable than **5** (probably due to less steric hindrance), although only **5** has the requisite geometry (Co, H, and the double bond carbon atoms all coplanar) for a direct 1,2-insertion step (step c).²⁰ Overall, therefore, steps **a** and **b** constitute a ligand substitution via a D mechanism.



¹⁸(a) T. Ziegler and L. Versluis, "The Tricarbonylhydridocobalt-Based Hydroformylation Reaction," in *Homogeneous Transition Metal Catalyzed Reactions*, W. R. Moser and D. W. Slocum, Eds., American Chemical Society: Washington, D.C., 1992, pp. 75–93, and references therein. (b) For a recent study reaching a similar conclusion to Ziegler but still refining the structures of **2** and **3**, see C.-F. Huo, Y.-W. Li, G.-S. Wu, M. Bellar, and H. Jiao, *J. Phys. Chem. A*, **2002**, *106*, 12161.

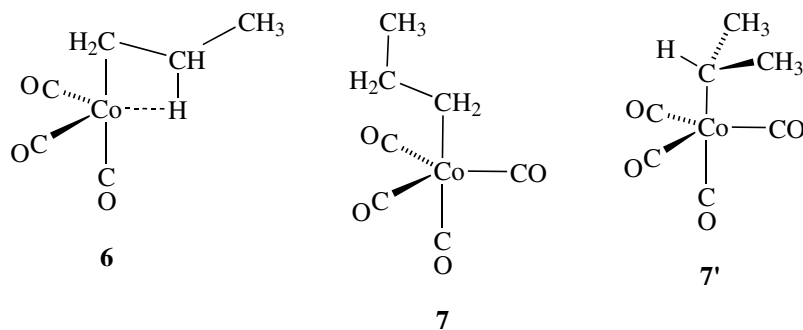
¹⁹C.-F. Huo, Y.-W. Li, M. Beller, and H. Jiao, *Organometallics*, **2003**, *22*, 4665.

²⁰See Footnotes 18a and 19.

Step c

Once complexation of the alkenes occurs, 1,2-insertion is facile and reversible. Insertion gives initially a 16-electron complex, **6**, which shows an agostic hydrogen. The high concentration of CO quickly drives step **c** to completion, resulting in 18-electron intermediate **7**. Structures **6** and **7** show the result of “anti-Markovnikov” insertion from which the linear aldehyde, rather than the branched isomer, will result.

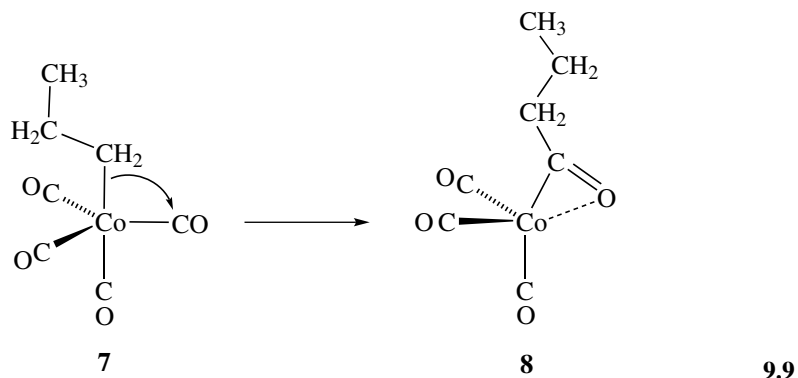
It is this exothermic step that probably is the source of the preference for linear hydroformylation products over branched ones. The structure of the comparable 18-electron branched intermediate **7'** is about 2 kcal/mol less stable than **7**, according to Jiao's calculations. This difference leads ultimately to the anti-Markovnikov, linear aldehyde over the branched-chain isomer. Although β -elimination is possible now, the high partial pressure of CO present in the reaction vessel tends to stabilize **7** and prevent loss of CO that would generate the vacant site necessary for elimination to occur.

**Step d**

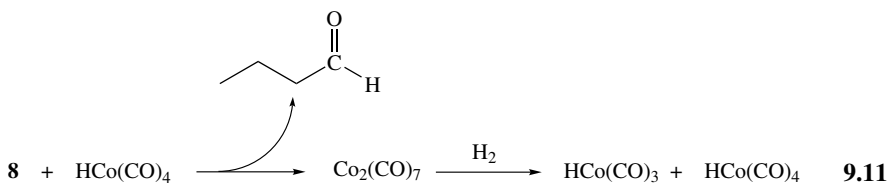
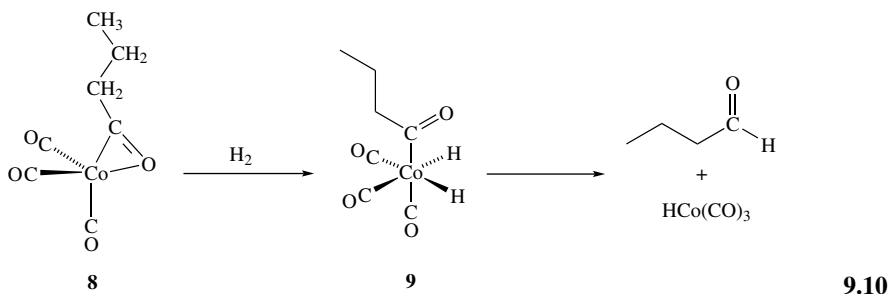
Step **d** involves CO insertion, which really is, as we saw in Chapter 8, a 1,2-migration of the alkyl group to CO (equation 9.9). Calculations indicate that the rearrangement has a low activation energy and is endothermic.²¹ Under the reaction conditions of high CO partial pressure, the 16-electron alkyl η^2 -carbonyl complex (**8**) must reversibly add CO to form (RCO)Co(CO)₄, which is the only detectable intermediate observed when the reaction has been followed using IR spectroscopy.²² The stage is now set for the addition of hydrogen to give the aldehyde mixture as the final products of the catalytic cycle.

²¹See Footnote 19.

²²R. J. Whyman, *J. Organomet. Chem.*, **1974**, 66, C23, and **1974**, 81, 97.

**Step e**

Two pathways have been proposed for step e, which may be the rate-limiting stage in the cycle (this notion is supported by the observed overall rate law for hydroformylation, which is typically first-order in H_2 concentration). Equation 9.10 illustrates an oxidative addition followed by reductive elimination sequence, as originally proposed. Since Heck and Breslow's work, a bimolecular process described by equation 9.11 has been suggested.²³

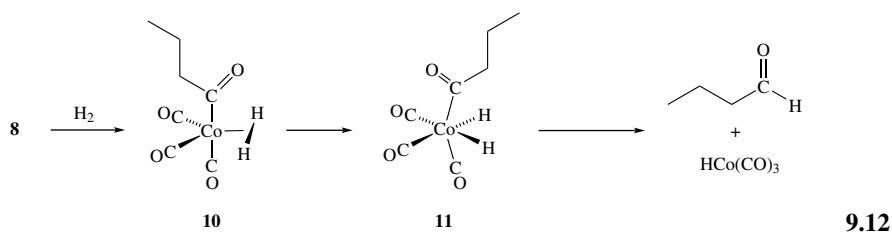


Although the bimolecular process involving reaction of the acylcobalt complex with HCo(CO)_4 occurs readily under stoichiometric conditions, the low

²³N. H. Alemaroglu, J. M. L. Renninger, and E. Oltay, *Monatsh. Chem.*, **1976**, *107*, 1043.

concentration of the two required cobalt complexes under catalytic conditions probably argues against the process shown in equation 9.11 as a catalytic step. It has also been shown using IR spectroscopy that, under normal catalytic conditions in the presence of a mixture of D_2/H_2 , H_2 is the main source of hydrogen in the aldehyde RE step, even in the presence of a high concentration of $HCo(CO)_4$.²⁴

Whether the OA–RE process occurs (equation 9.10) in the usual manner is still a matter of question because calculations indicate that a direct process involving the addition of H_2 to **8** to give dihydride **9** occurs with a rather high activation energy. A lower-energy process seems to be possible according to most recent calculations if an η^2 -dihydrogen complex (**10**, equation 9.12), forms instead. Once **10** forms, bond rotation about the Co–C (carbonyl) bond occurs, followed by conversion of the η^2 - H_2 complex into dihydride **11**. Complex **11** then undergoes exothermic RE to give $HCo(CO)_3$ and linear aldehyde predominantly.²⁵ The detailed experimental verification of theoretical calculations for step e awaits further investigation.



The original hydroformylation process described above is still used, especially for the production of aldehydes and alcohols derived from alkenes with more than four carbon atoms. The process, however, is not without problems in actual practice. Some of these problems include the following.

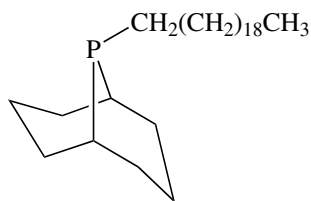
1. The ratio of linear to branched aldehydes is at best only ca. 4 to 1, and because the linear isomer is far more valuable than its branched coproduct, improvement in this regard would be important from an economic standpoint.
2. The active catalyst is unstable, and its separation and recovery are difficult.
3. The high partial pressure of CO required for the process means that plants are expensive to build and operate.

²⁴P. Pino, A. Major, F. Spindler, R. Tannenbaum, G. Bor, and I. T. Horváth, *J. Organomet. Chem.*, **1991**, 417, 65.

²⁵See Footnote 19 and references therein.

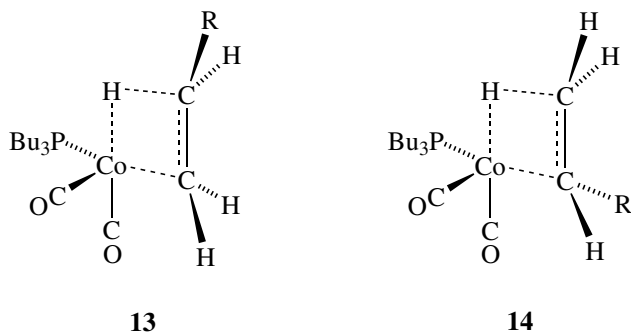
9-2-2 Phosphine-Modified Hydroformylation

In 1968, Slaugh and Mullineaux²⁶ (Shell Oil Company) reported that adding tertiary phosphines, such as PBu_3 or the bicyclo tertiary phosphine **12** (used because this ligand confers thermal stability to the catalyst, allowing the catalyst to be heated to a higher temperature than is possible with PBu_3), resulted in hydroformylation taking place at less than 100 bar (vs. the 200–300 bar normally required). Although the phosphine-modified catalyst was not as active as $\text{HCo}(\text{CO})_3$ toward hydroformylation, it was a better hydrogenation catalyst. Thus, the two stages of hydroformylation and hydrogenation could be combined into one step (using a ratio of $\text{H}_2/\text{CO} = 2:1$). The ratio of linear to branched product, moreover, was as high as 9 to 1. Finally, because the modified catalyst, $\text{HCo}(\text{CO})_3(\text{PR}_3)$, turned out to be more stable than the original, it was easier to separate it from product alcohols. The advantages of the Shell process are diminished somewhat because hydroformylation must occur at a higher temperature (160–200 °C) and some alkene (ca. 15%) is converted directly to the corresponding alkane, owing to the effectiveness of the catalyst in promoting hydrogenation.



The higher selectivity of the modified catalyst in producing anti-Markovnikov product versus branched probably is due mainly to steric factors. The large steric bulk of PBu_3 or phosphine **12** (compared with that of CO), as measured by its cone angle (see Section 6-3), must influence the course of the insertion of the alkene into the $\text{Co}-\text{H}$ bond as shown in transition state structures **13** and **14**. Structure **13** illustrates the occurrence of 1,2-insertion that would lead ultimately to linear aldehyde or alcohol. The phosphine ligand points away from the R group on the alkene. Much more steric hindrance occurs with the other orientation, shown by **14**, in which the R group and the phosphine are on the same side of the structure.

²⁶L. H. Slaugh and R. D. Mullineaux, *J. Organomet. Chem.*, **1968**, *13*, 469 and L. H. Slaugh and R. D. Mullineaux (to Shell Oil Company), U. S. Patents 3,239,569 and 3,239,570, 1966.



Studies with a variety of phosphine ligands have indicated that electronic factors may also play a role in the rate and orientation of phosphine-modified hydroformylation. As σ -donors, phosphines (possessing low χ values; see Section 6-3 for a discussion on χ values) undoubtedly donate electron density to the Co center that can then be taken up by the CO ligands, thus providing overall stability to the catalyst complex.²⁷ Investigations of phosphine-modified hydroformylation have attempted to identify key intermediates in the catalytic cycle. Instead of acyl- and alkylcobalt complexes typical of the unmodified process, only phosphine-substituted cobalt carbonyl species have been observed.²⁸ We can only assume that the steps in the catalytic cycle are analogous to those for the unmodified process (Scheme 9.3), with the first step consisting of loss of a CO ligand, but that the rate-determining step occurs at a different stage, perhaps during alkene complexation.²⁹ The Shell process and related phosphine-modified hydroformylations continue to be used in industry on a large scale to produce C₁₂–C₁₆ detergent alcohols.

9-2-3 Rhodium-Catalyzed Hydroformylation

Monodentate Ligands

As the development of suitable cobalt hydroformylation catalysts occurred, work was also carried out to create corresponding Rh complexes that could also serve as suitable catalysts. Under appropriate conditions in the presence of H₂ and CO, HRh(CO)₄ forms from Rh–carbonyl cluster compounds. The hydrido–Rh

²⁷For a good discussion of the modified hydroformylation process including an analysis of phosphine ligand effects, see C. Masters, *Homogeneous Transition-Metal Catalysis—A Gentle Art*, Chapman & Hall: London, 1981, pp. 114–120.

²⁸F. Piacenti, M. Bianchi, and M. Bendetti, *Chim. Ind. Milan*, **1969**, 49, 245.

²⁹For a recent review on high-pressure NMR studies of phosphine-modified, Co-catalyzed hydroformylation, see C. Dwyer, H. Assumption, J. Coetzee, C. Crause, L. Damoense, and M. Kirk, *Coord. Chem. Rev.*, **2004**, 248, 653.

complex catalyzes hydroformylation, but it also serves as a good alkene hydrogenation catalyst. Ratios of linear to branched hydroformylation products tend to be low also. Several groups³⁰ discovered in the 1960s that the addition of phosphines allowed hydroformylation to occur, even at atmospheric pressure and at relatively low temperature. With the appropriate phosphine and by adjusting other reaction parameters, high linear-to-branched aldehyde product ratios were achieved without extensive hydrogenation of either the alkene starting material or the aldehyde (to give alcohol). In 1976, Union Carbide first commercialized the use of phosphine-modified rhodium catalysts in hydroformylation.

Rhodium–phosphine catalysts offer many advantages over cobalt systems. Rhodium complexes are 100 to 1000 times more active than Co complexes, so much less rhodium needs to be present in the reactor.³¹ The pressure (15–25 bar) and temperature (80–120 °C) required for reaction are significantly lower than for either Co-based process, meaning that initial costs for plant construction are relatively low, as are energy expenses to keep the plant running. If the hydrocarbon starting material consists of only 1-alkenes, linear-to-branched aldehyde product ratios as high as 15 to 1 are obtained. Despite the need to carefully recover expensive catalyst, rhodium–phosphine-catalyzed hydroformylation is clearly the optimal process if linear aldehydes are the desired products. If alcohols are the goal, then using a phosphine-modified Co catalyst is preferred because hydroformylation and hydrogenation occur in the same reaction vessel.³²

Scheme 9.4 illustrates the steps involved in the phosphine–rhodium catalytic cycle. The immediate precursor to the active species is either $\text{HRh}(\text{CO})_2(\text{PR}_3)_2$ or $\text{HRh}(\text{CO})(\text{PR}_3)_3$ ³³ depending on the concentration of CO with respect to phosphine.

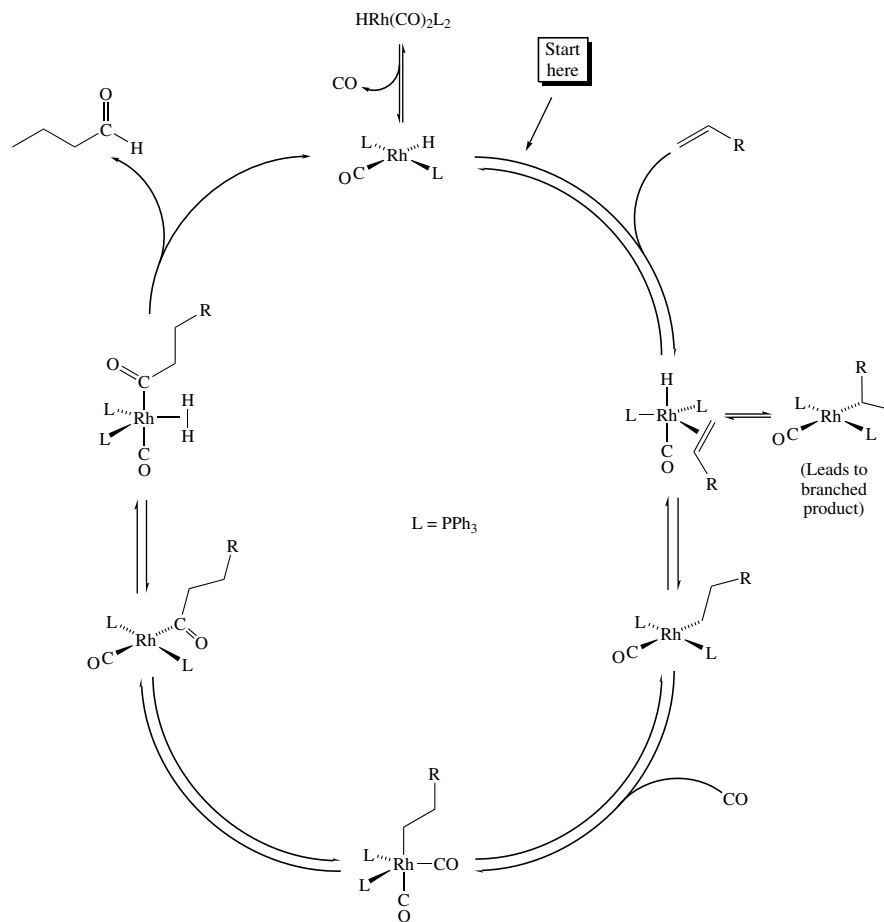
In contrast to PBU_3 , used in the phosphine-modified Co process, the optimal phosphine for Rh-based catalysis appears to be PPh_3 or a similar aryl phosphine. PBU_3 is apparently too effective at donating electron density to the metal in the case of Rh, and the intermediate catalytic species are too stable for effective catalysis.

³⁰J. A. Osborne, J. F. Young, and G. Wilkinson, *J. Chem. Soc., Chem. Commun.*, **1965**, 17; C. K. Brown and G. Wilkinson, *J. Chem. Soc. A*, **1970**, 2753; R. L. Pruett and J. A. Smith, *J. Org. Chem.*, **1969**, *34*, 327; and L. H. Slaugh and R. D. Mullineaux, U.S. Patent 3,239,566, 1966.

³¹This is fortunate, because the cost per gram of Rh is over 1000 times higher than that of Co.

³²C. Masters, *Homogeneous Transition-Metal Catalysis—A Gentle Art*, Chapman & Hall: London, 1981, pp. 127–128.

³³It is interesting to note that $\text{HRh}(\text{CO})(\text{PR}_3)_3$ is an efficient alkene hydrogenation catalyst. It also resembles the very effective hydrogenation catalyst, $\text{ClRh}(\text{PPh}_3)_3$ (Wilkinson's catalyst, Section 9-4-2). Apparently, when the partial pressure of CO exceeds 10 bar, the capability of the complex to hydrogenate alkenes is suppressed.



Scheme 9.4
Catalytic Cycle
for Phosphine-
Modified,
Rh-Catalyzed
Hydroformylation

The triaryl phosphine seems to have the right combination of steric (to induce the formation of linear product at the 1,2-insertion stage) and electronic (to donate electron density to metal in order to stabilize CO ligands) properties. Studies indicate that the rate-determining step is likely to be hydrogenation of the acylrhodium intermediate (as with unmodified Co hydroformylation), but the mechanism of this apparent OA–RE step is not completely understood.³⁴ DFT-level theoretical studies have suggested that the selection for linear versus branched aldehydes

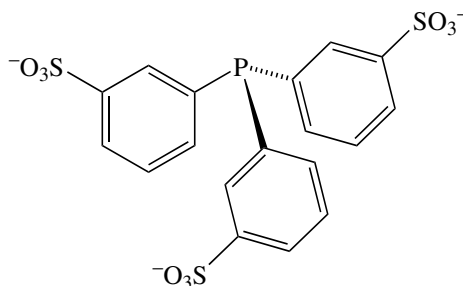
³⁴M. Garland and P. Pino, *Organometallics*, **1991**, *10*, 1693; J. H. Feng and M. Garland, *Organometallics*, **1999**, *18*, 417; G. Liu, R. Volken, and M. Garland, *Organometallics*, **1999**, *18*, 3429; and A. Oswald, D. E. Hendriksen, R. V. Kastrup, and E. J. Mozeleski, "Electronic Effects on the Synthesis, Structure, Reactivity, and Selectivity of Rhodium Hydroformylation Catalysts," in *Homogeneous Transition Metal Catalyzed Reactions*, W. R. Moser and D. W. Slocum, Eds., American Chemical Society: Washington, D.C., 1992, pp. 395–417.

occurs early in the catalytic cycle during the alkene complexation and insertion stages.³⁵

Exercise 9-1

Increasing the concentration of phosphine in the phosphine–rhodium cycle slows the reaction rate, but it also raises the linear/branched product ratio. Explain.

In the 1980s, Ruhr Chemie (now Celanese) and Rhone–Poulenc developed a now well-established Rh-catalyzed formylation involving a highly water-soluble Rh–phosphine complex where the aryl substituents of the phosphine were substituted with sulfonic acid groups at the *meta*-position, giving a ligand known as triphenylphosphinetrisulfonate, or tppts (structure **15**).³⁶ A two-stage process is involved, which is run under mild conditions at 18 bar and 85–90 °C, where the catalyst remains in the aqueous phase and the aldehyde product goes to the organic phase, where it may be easily separated. One major advantage of the two-phase reaction, in addition to producing a high linear-to-branched product ratio under mild conditions, is that catalyst loss is minimal. In contrast to a single-stage process, where a catalyst separation operation is necessary, the two-stage process finds the catalyst already separated from the product as it forms. The initial lack of solubility of alkenes—especially C₅ and above—in the aqueous phase, however, limits the two-phase process to hydroformylation of low-molecular-weight alkenes such as propene and 1-butene.

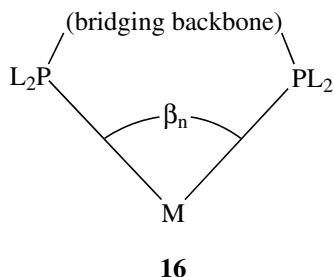
**15**

³⁵M. Sparta, K. J. Børve, and V. R. Jensen, *J. Am. Chem. Soc.*, **2007**, *129*, 8487 and references therein.

³⁶E. Kuntz, *CHEMTECH*, **1987**, *17*, 570 and P. W. N. M. van Leeuwen, *Homogeneous Catalysis: Understanding the Art*, Kluwer Academic: Dordrecht, The Netherlands, 2004, pp. 150–152.

Bidentate Ligands

Over the past 20 years, much research on Rh-catalyzed hydroformylation has focused on the use of bidentate phosphine and phosphite ligands. The presence of such ligands often results in high ratios of linear to branched aldehydes. In addition to the cone angle and electronic factor χ , there is another parameter associated with bidentate ligands called the *bite angle*. Casey and Whiteker³⁷ were the first to define a concept known as the natural bite angle (β_n), which is the P–M–P bond angle (Structure 16) determined from molecular mechanics calculations (see Section 2-4).³⁸



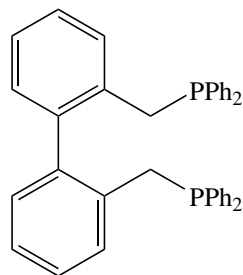
There is potential for error in these calculations, because the value of β_n for a particular ligand will vary as a function of the metal and the force field used in the molecular mechanics calculation. As long as the metal atom remains constant and the same force field is used for the calculation, the values of β_n for a series of related bidentate phosphines and phosphites are self-consistent within the series.

One of the first-reported bidentate ligands that resulted in significant enhancement of the ratio of linear to branched aldehyde was 2,2'-bis[(diphenylphosphino) methyl]-1,1'-biphenyl, which is abbreviated BISBI (structure 17).³⁹

³⁷C. P. Casey and G. T. Whiteker, *Isr. J. Chem.*, **1990**, 30, 299.

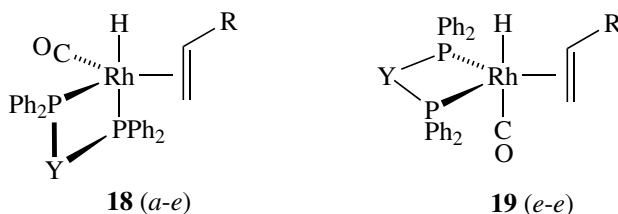
³⁸Crystal structures of diphosphine–metal complexes may show bite angles that are different than β_n , so the calculation of β_n has built in with it the possibility of some flexibility in bond angle as long as the change in bite angle does not result in an increase of more than 3 kcal/mol of strain energy. See Footnote 37 and P. W. N. M. van Leeuwen, *Homogeneous Catalysis: Understanding the Art*, Kluwer Academic: Dordrecht, The Netherlands, 2004, pp. 16–19, and 153–166 for additional discussion of β_n .

³⁹T. J. Devon, G. W. Phillips, T. A. Puckett, J. L. Stavinoha, and J. J. Vanderbilt (to Texas-Eastman), U.S. Patent 4,694,109, 1987.

**17**

Casey observed a linear/branched ratio of 66:1 using a BISBI–Rh complex to hydroformylate 1-hexene. This is a huge increase over the linear/branched ratio of only 2.6, which Casey observed when a Rh–dppe⁴⁰ complex is used for hydroformylation of 1-alkenes.⁴¹ The β_n of BISBI is 113–120°, whereas that of dppe is much lower, at 85°.

One explanation for the regioselectivity is related to the stereochemistry of the diphosphine–Rh catalyst complexed with the alkene. We have seen earlier that high linear-to-branch ratios in Rh-catalyzed hydroformylation, as with Co-catalyzed hydroformylation, stem from the alkene complexation–insertion step of the catalytic cycle, so differences in steric and electronic factors as a function of stereochemistry could play a significant role in the regiochemical result of the reaction. There are two trigonal bipyramidal possibilities for the diphosphine–Rh–alkene complex, which are denoted *a–e* (apical–equatorial isomer **18**) and *e–e* (diequatorial isomer **19**).

**18** (*a–e*)**19** (*e–e*)

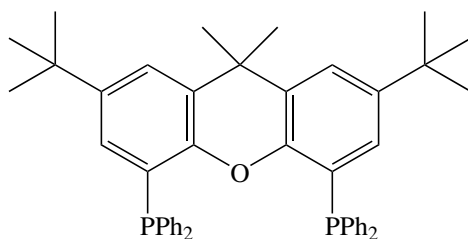
Y = Bridging backbone

Studies have shown that when β_n is large, the bidentate ligand tends to bind with *e–e* stereochemistry. Because the bond angle described by two equatorial ligands in a trigonal bipyramid is expected to be 120°, *e–e* stereochemistry ought

⁴⁰Another abbreviation for dppe is DIPHOS.

⁴¹C. P. Casey, G. T. Whiteker, M. G. Melville, L. M. Petrovich, J. A. Garvey, Jr., and D. R. Powell, *J. Am. Chem. Soc.*, **1992**, *114*, 5535.

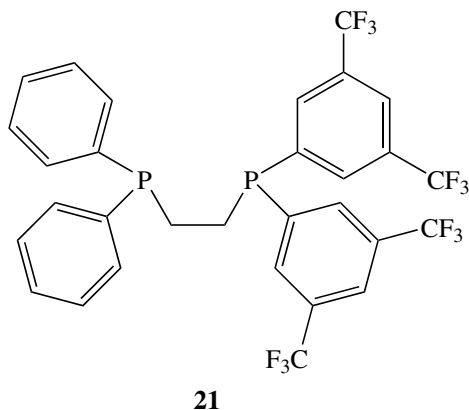
to be more feasible with ligands with large values of β_n . On the other hand, the bond angle expected when two ligands are *a-e* with respect to each other is 90° , so bidentate ligands with β_n values around 90° would tend to bond in that manner. Researchers have suggested that *e-e* bisphosphine complexes introduce more steric congestion than corresponding *a-e* complexes. This congestion, therefore, favors the transition state and product that are less congested, which are those associated with the pathway to produce linear aldehyde. A series of diphosphine ligands, one of which is shown in structure **20**, was synthesized by van Leeuwen.⁴² He observed that there was a strong correlation between a high value of β_n and a high linear-to-branched ratio, which lends support to the hypothesis that the more the catalyst-alkene complex exists as the *e-e* stereoisomer, the higher the likelihood of the formation of linear over branched aldehyde.

**20**

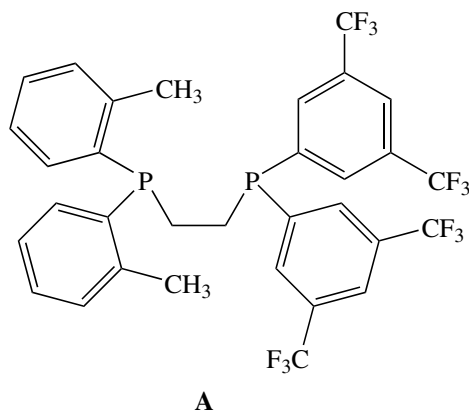
At this time, however, there is still work to be done to completely understand the influence of β_n on the regiochemistry of Rh-catalyzed hydroformylation. For example, studies have demonstrated that electronic factors also play a key role in determining linear-to-branched ratio with substituted DIPHOS ligands, such as **21**, showing a clear preference for linear product when the electron-withdrawing phosphine resided in the equatorial position and the electron-rich phosphine in the apical position of a trigonal bipyramidal Rh complex.⁴³

⁴²M. Kranenburg, Y. E. M. van der Burgt, P. C. J. Kramer, and P. W. N. M. van Leeuwen, *Organometallics*, **1995**, *14*, 3081; L. A. van der Veen, M. D. K. Boele, F. R. Bregman, P. C. J. Kramer, P. W. N. M. van Leeuwen, K. Goubitz, J. Fraanje, H. Schenk, and C. Bo, *J. Am. Chem. Soc.*, **1998**, *120*, 11616; and L. A. van der Veen, P. H. Keeven, G. C. Schoemaker, J. N. H. Reek, P. C. J. Kramer, P. W. N. M. van Leeuwen, M. Lutz, and A. L. Spek, *Organometallics*, **2000**, *19*, 872.

⁴³C. P. Casey, E. L. Paulsen, E. W. Beuttenmueller, B. R. Proft, B. A. Matter, and D. R. Powell, *J. Am. Chem. Soc.*, **1999**, *121*, 63.

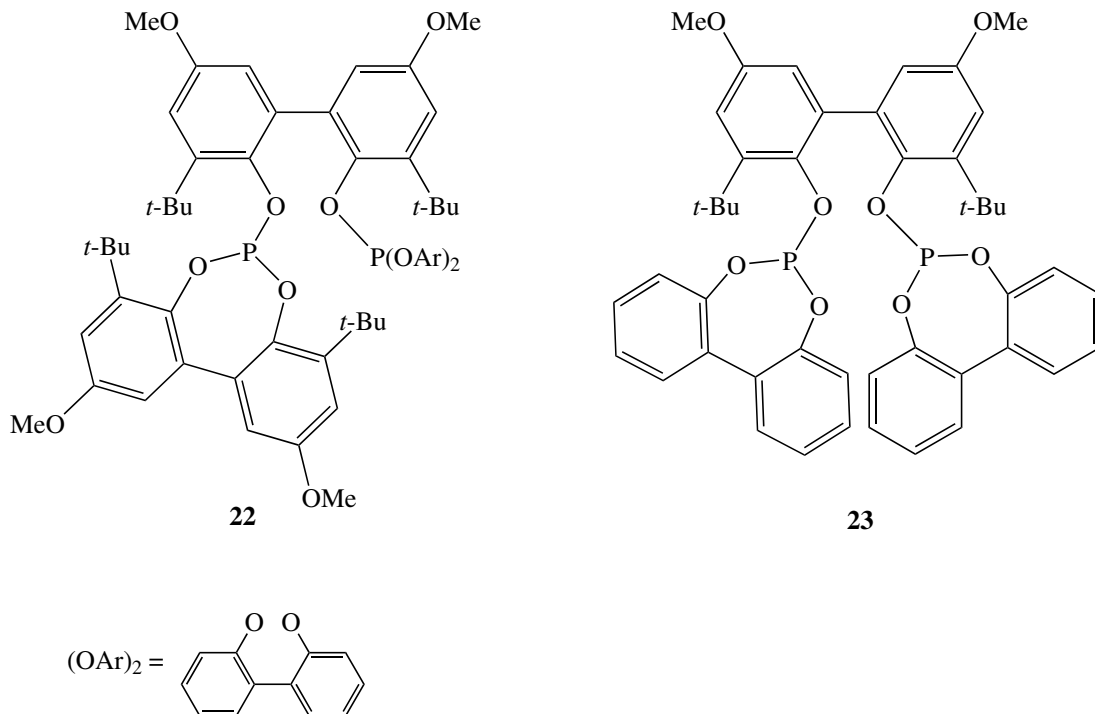
**Exercise 9-2**

How would the linear-to-branched ratio change if DIPHOS ligand **21** were replaced by structure **A**, assuming that the predominant trigonal bipyramidal Rh complex has one phosphino group in the equatorial position and the other in the apical position? Explain.



Beside diphosphines, diphosphites have also been thoroughly explored as ligands that enhance both the linear/branch distribution of product and the TON of Rh-catalyzed hydroformylation. The most recent industrial development, which Union Carbide introduced on an industrial scale in 1995, was the use of highly sterically-hindered diphosphites such as compounds **22** and **23**.⁴⁴

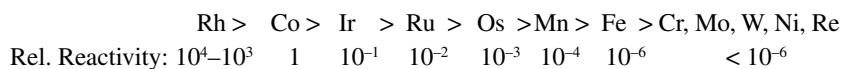
⁴⁴E. Billig, A. G. Abatjoglou, and D. R. Bryant (to Union Carbide), U.S. Patent 4,748,261, 1998.



These ligands allow hydroformylation of propene to occur at 100 °C and less than 20 bar, resulting in a linear/branched ratio of 30:1 and a 98% conversion of propene to product in one pass over the catalyst—truly an impressive achievement.

9-2-4 Other Aspects of Hydroformylation

Other metals may serve as the basis for hydroformylation catalysts. The overall effectiveness of these metals compared with Co and Rh is as follows.⁴⁵

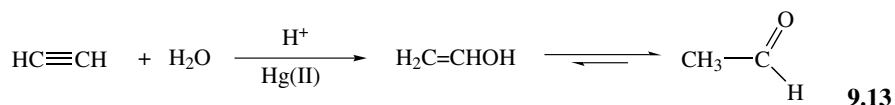


Investigations of mechanistic steps in hydroformylation cycles and the effects of ligands continue to be an active area of interest for organometallic chemists. Later in Chapter 9 there will be an example of the use of hydroformylation in the green synthesis of a popular drug. The use of chiral diphosphine and diphosphite ligands for hydroformylation also shows promise for producing enantioenriched chiral aldehydes (section 12-3-1).

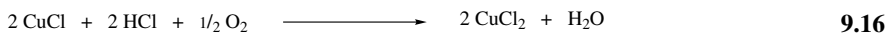
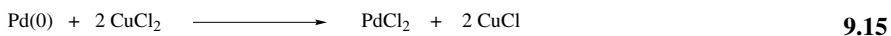
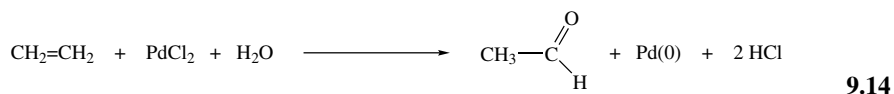
⁴⁵K.-D. Wiese and D. Obst, *Top. Organomet. Chem.*, **2006**, 18, 1.

9-3 THE WACKER–SMIDT SYNTHESIS OF ACETALDEHYDE

Ethanal (more commonly known as acetaldehyde) is another aldehyde of commercial importance. Oxidation to acetic acid and possible subsequent dehydration to form acetic anhydride are the typical fates of this compound. Acetaldehyde was originally prepared by hydration of acetylene according to equation 9.13, a facile and high-yield route. This synthesis is now obsolete because of problems associated with the starting material, acetylene. Acetylene must be produced by heating a hydrocarbon gas stream to high temperature, sometimes in the presence of an electric arc. All processes for producing it require large amounts of energy. Acetylene is also thermodynamically unstable, and it must be handled with extreme care to prevent explosion.



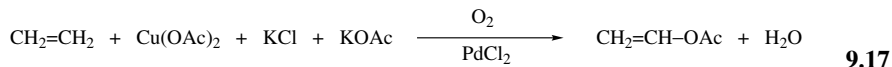
The incentive, therefore, existed to develop a process for producing acetaldehyde from a cheaper and less hazardous starting material. It had long been known that acetaldehyde formed directly from ethylene and water in the presence of a stoichiometric amount of PdCl_2 , according to equation 9.14.⁴⁶ It was not until the 1950s, however, that a commercially-feasible process was developed by Smidt at Wacker Chemie in Germany.⁴⁷ The Wacker–Smidt synthesis of acetaldehyde combines equation 9.14 with steps shown in equations 9.15 and 9.16. This allows deployment of Pd in *catalytic* amount because much less expensive reagents— CuCl_2 , HCl , and O_2 —are used to keep Pd in the proper oxidation state.



⁴⁶F. C. Phillips, *J. Am Chem. Soc.*, **1894**, *16*, 255.

⁴⁷J. Smidt, W. Hafner, R. Jira, J. Sedlmeier, R. Sieber, R. Rütlinger, and H. Kojer, *Angew. Chem.*, **1959**, *71*, 176 and J. Smidt, W. Hafner, R. Jira, R. Sieber, J. Sedlmeier, and S. Sabel, *Angew. Chem. Internat. Edit. Engl.*, **1962**, *1*, 80.

The overall reaction is equivalent to direct oxidation of ethylene by O₂. The process is run in one or two stages depending on whether the catalyst is regenerated *in situ* or in a separate reactor. The former process uses pure oxygen in the presence of ethylene, Pd(II), CuCl₂, and HCl. The latter process uses the chemistry described in equation 9.14 in one reactor and that described in equations 9.15 and 9.16 in another separate reaction vessel. Both processes have their advantages and disadvantages and both were used commercially in the United States and Europe, producing acetaldehyde at about the same production cost. In terms of the amount of product produced, the Wacker–Smidt process represents an economically significant example of the use of transition metal homogeneous catalysis. The technology also has been used to produce vinyl acetate (equation 9.17), a monomer that is subsequently polymerized to give polyvinylacetate films.⁴⁸



The Wacker–Smidt process—hereafter known simply as the Wacker oxidation, reaction, or process—enjoyed considerable success, yet its use has declined dramatically over the past 10 years for at least two reasons.⁴⁹ First, manufacturing plants are expensive to build and maintain because they must be constructed to withstand a corrosive environment. Second, another procedure that yields acetic acid directly from synthesis gas was developed and now supplants the Wacker–Smidt process. This newer route also uses homogeneous catalysis involving Rh and Ir complexes and will be described in Section 9-5.

Although the Pd(II)-catalyzed route to acetaldehyde is no longer important to the chemical industry, the mechanistic basis of the process is interesting because it involves a number of fundamental kinds of organometallic reactions, such as ligand substitution, nucleophilic attack at a π ligand, and 1,2-insertion. The quest for understanding the details of the catalytic mechanism has been extensive, and it has uncovered much useful information concerning not only the Wacker oxidation but also other organopalladium reactions. Moreover, the chemistry of the Wacker process has been adapted by synthesis chemists to convert terminal alkenes to methyl ketones.⁵⁰

⁴⁸For a good discussion of the Wacker–Smidt and related processes, see P. Wiseman, *An Introduction to Industrial Organic Chemistry*, Wiley: New York, 1976, pp. 97–103. A process using palladium-impregnated silica, developed later, is superior to the homogeneously-catalyzed process described in equation 9.17.

⁴⁹Acetaldehyde production via the Wacker process in North America has ceased; only China remains as a significant producer of this compound, presumably using, at least in part, the Wacker process (S. M. Malveda, K. Fujita, and B. Suresh, “Acetaldehyde,” in *Chemical Economics Handbook*, SRI Consulting: Menlo Park, CA, 2007).

⁵⁰For good reviews on the use of Wacker oxidation in organic synthesis, see J. M. Takacs and X.-T. Jiang, *Curr. Org. Chem.*, **2003**, 7, 369 and C. N. Cornell and M. S. Sigman, *Inorg. Chem.*, **2007**, 46, 1903.

Scheme 9.5 illustrates an outline of the catalytic cycle involving organopalladium complexes. It also shows how Cu(II) and O₂ couple with the Pd cycle to regenerate Pd(II). The scheme is consistent with the rate law⁵¹ observed for Wacker–Smidt oxidation:

$$\text{Rate} = \frac{k[\text{CH}_2=\text{CH}_2][\text{PdCl}_4^{2-}]}{[\text{H}^+][\text{Cl}^-]^2}$$

The exact pathway for acetaldehyde formation is still not completely clear. One difficulty rests with the instability of Pd–alkene and –alkyl intermediates (which goes hand in hand with Pd(II) being such an effective catalyst). We shall also see that some experiments involving Pd complexes were reported under conditions that did not exactly duplicate those for the Wacker process. Nevertheless, these experiments provided useful, although indirect, information. More recently, experiments by Henry and co-workers have been performed under conditions that replicate those that occur during the industrial process. These studies also provided key insight into the role of water in the catalytic cycle. Most recently, theoretical calculations have been brought to bear on most aspects of the catalytic cycle. These studies have provided some surprising results that call into question previous assumptions about certain catalytic steps, and reference will be made to them in the following discussion.

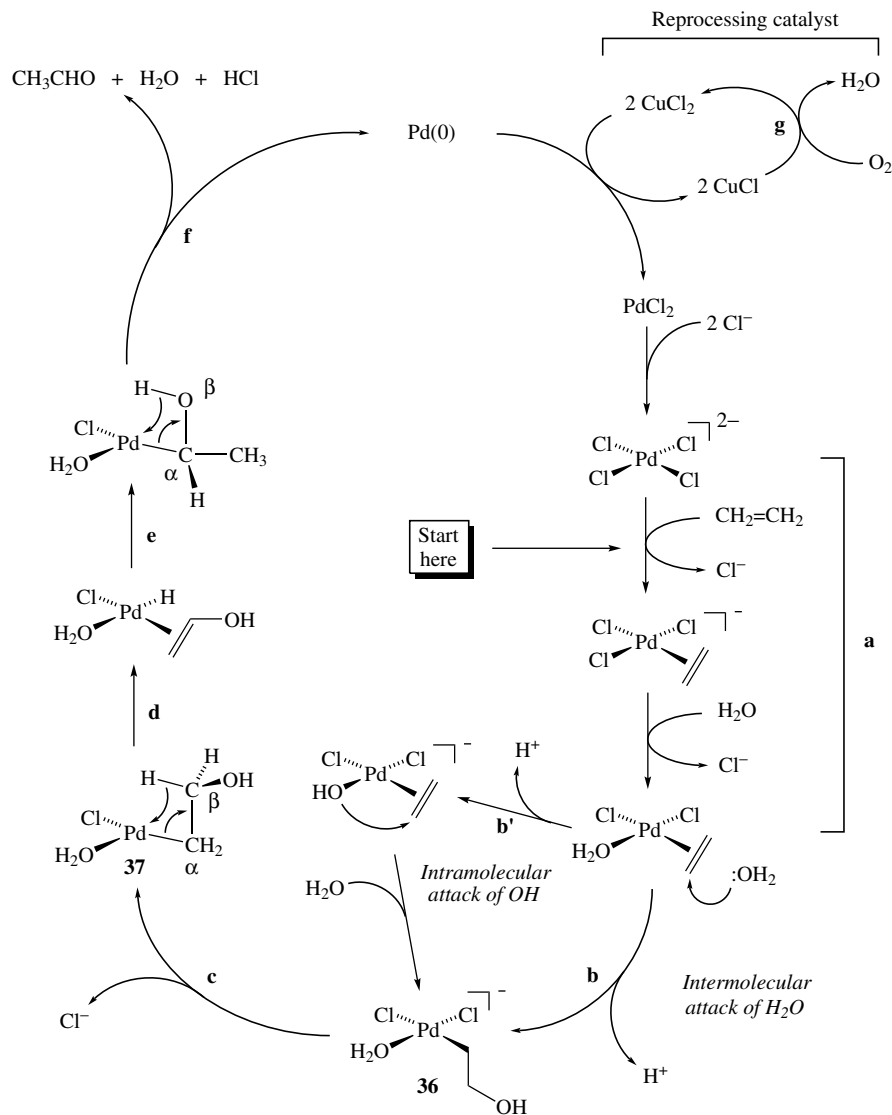
Step a

The first major transformation in the pathway probably consists of two steps in which two Cl[−] ions are displaced and substituted with alkene and H₂O. These set the stage for nucleophilic attack on the bound alkene.

Step b

The mechanism of attack of the nucleophile (H₂O) on the coordinated alkene was unclear for many years. Does the nucleophile attack externally in a manner *trans* to Pd to give the hydroxyalkylpalladium complex (*anti* attack, path **b**, Scheme 9.5) or does intramolecular 1,2-insertion of the alkene between the metal and a coordinated OH group (formed after deprotonation) occur with to OH *cis* to Pd (*syn* attack, path **b'**, Scheme 9.5)? The observed rate law could be consistent with

⁵¹(a) J. E. Bäckvall, B. Åkermark, and S. O. Ljunggren, *J. Am. Chem. Soc.*, **1979**, *101*, 2411 and (b) P. M. Henry, *J. Am. Chem. Soc.*, **1964**, *86*, 3246. Later investigations found that the rate law for conditions of high concentrations of Cl[−] and CuCl₂ was a function of [Cl[−]]^{−1} and zero order in [H⁺] (O. Hamed, C. Thompson, and P. M. Henry, *J. Org. Chem.*, **1997**, *62*, 7082).

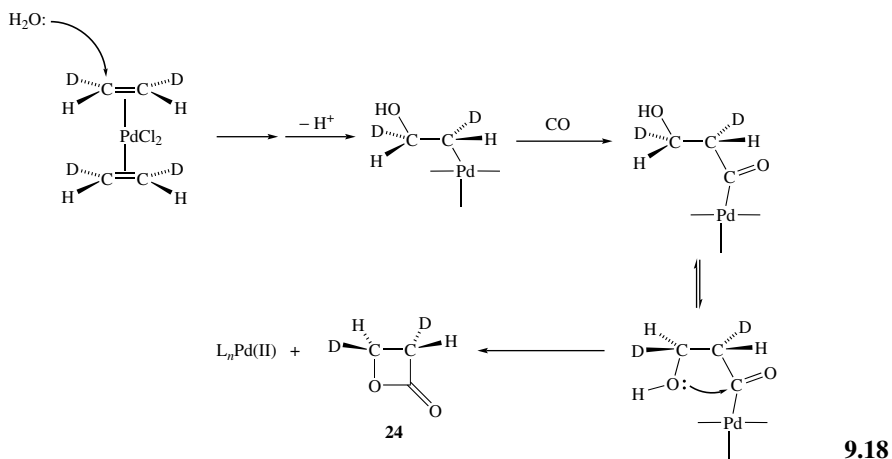


either mechanism, although chemists now know that the rate law depends on the concentrations of Cl^- and CuCl_2 .

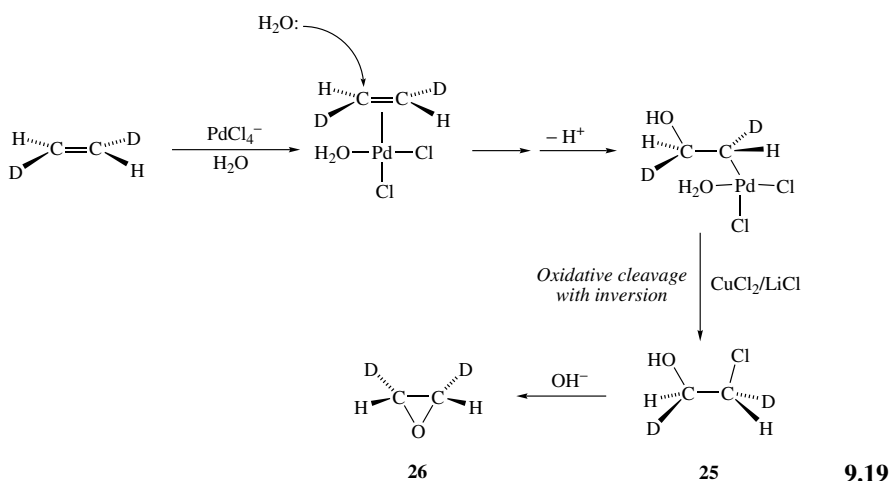
To answer this question, researchers designed rather elegant experiments. The first, reported by Stille and Divakaruni (equation 9.18),⁵² showed *cis*-dideuterioethylene undergoing hydroxypalladation in the presence of CuCl_2 , followed by CO insertion to give lactone **24**. The deuterium atoms in **24** ended

⁵²J. K. Stille and R. Divakaruni, *J. Am. Chem. Soc.*, **1978**, *100*, 1303.

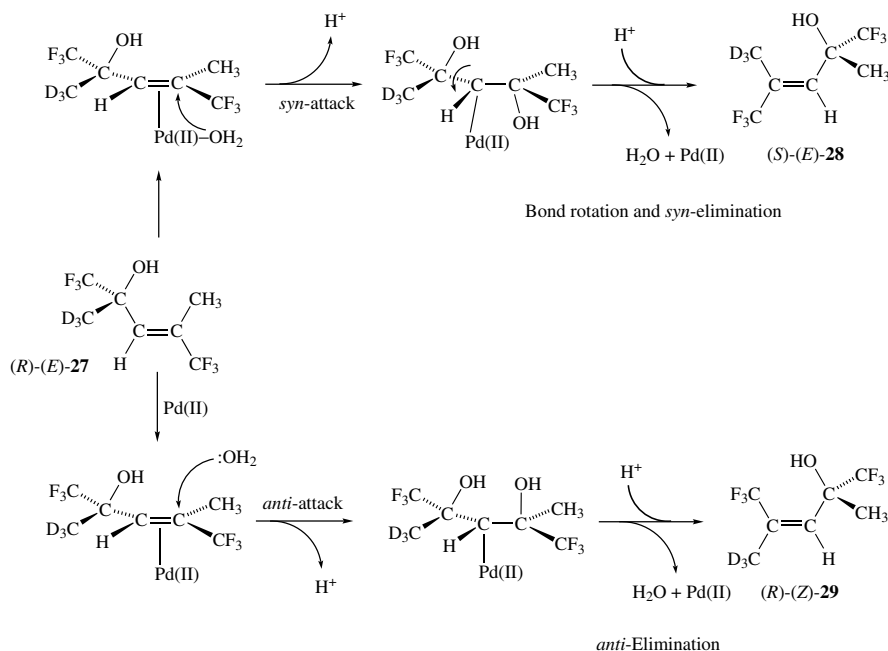
up *trans* to one another, meaning that inversion of configuration occurred. Since CO insertion is known to occur with retention of configuration (Section 8-1), inversion must have taken place during attack by H₂O, which is exactly the result expected when nucleophiles attack π ligands (Section 8-2-1).



Another investigation (equation 9.19), reported by Bäckvall and Åkermark,⁵³ described an *anti* attack on a *trans*-dideuterioethylene Pd complex. In the presence of high concentrations of Cu(II) and Cl⁻, the final product after oxidative cleavage (Section 8-4-1) was the chlorohydrin, **25**, rather than the aldehyde. Treatment of the chlorohydrin with base gave dideuterioethylene oxide, **26**, in which the two deuterium atoms were *cis*. This result is again consistent with attack by an external nucleophile.



⁵³See Footnote 51a.

**Scheme 9.6**

Intramolecular *syn*-
Attack of OH versus
Intermolecular
anti-Attack of H₂O

Fill in the details of equation **9.19** by showing how the *trans* didedeuteroalkene complex ends up as *threo*-**25** and then *cis*-dideuteroethylene oxide **26**. What must be the stereochemistry at the carbon originally attached to Pd after oxidative cleavage by CuCl₂ of the Pd–C bond? What would the stereochemistry of **26** be if intramolecular 1,2-insertion occurred instead?

Exercise 9-3

Despite these two experiments, convincing evidence exists that the *syn*-intramolecular route occurs for hydroxypalladation. Reports by Henry and Francis⁵⁴ described experiments designed to probe both the kinetics and the stereochemistry of the Wacker process. Scheme **9.6** illustrates the two stereochemical outcomes possible starting with allylic alcohol **27**, designed so that oxidation to form the ketone is not possible. When Cl[−] concentrations were low and comparable to Wacker conditions, **28** formed, a compound that indicated *syn* intramolecular attack by a coordinated OH ligand had occurred. At higher Cl[−] concentrations, similar to those used by Bäckvall, compound **29**, a product that must result from *anti* intermolecular attack by H₂O, was produced instead.

⁵⁴J. M. Francis and P. M. Henry, *Organometallics*, **1991**, *10*, 3498; **1992**, *11*, 2832.

Exercise 9-4

Verify that the stereochemical outcomes are those outlined in Scheme 9.6.

Building on his work using the F- and D-labeled allylic alcohols above, Henry studied the Wacker reaction with chiral allylic alcohols that were suitable substrates for both allylic rearrangement (high Cl^- concentration) and oxidation (low Cl^- concentration). These results are shown in Scheme 9.7.⁵⁵

To examine a pathway where only *syn* attack by a nucleophile occurs, Henry used allylic alcohols **30a** and **30b** as starting materials and a phenyl ligand bound to Pd as the nucleophile. He found that configuration of the stereogenic center was preserved regardless of whether the concentration of Cl^- was low (**31a**) or high (**31b**). He used this as a reference system for determining the stereochemical outcomes of his experiments with H_2O (**32** and **33**) or CH_3OH (**34** and **35**) as the nucleophile. At high Cl^- concentrations, *anti* addition from an external nucleophile occurred when either H_2O or CH_3OH were the nucleophiles, which is demonstrated by inversion of stereochemistry at the chirality center. At low Cl^- concentrations, which duplicate the industrial process, *syn*-intramolecular attack was the result, as evidenced by retention of stereochemistry at the chirality center.

Exercise 9-5

Convince yourself that the stereochemistry shown in Scheme 9.7 is consistent with *anti* attack by H_2O at high concentrations of Cl^- and *syn* addition of OH at low Cl^- concentrations.

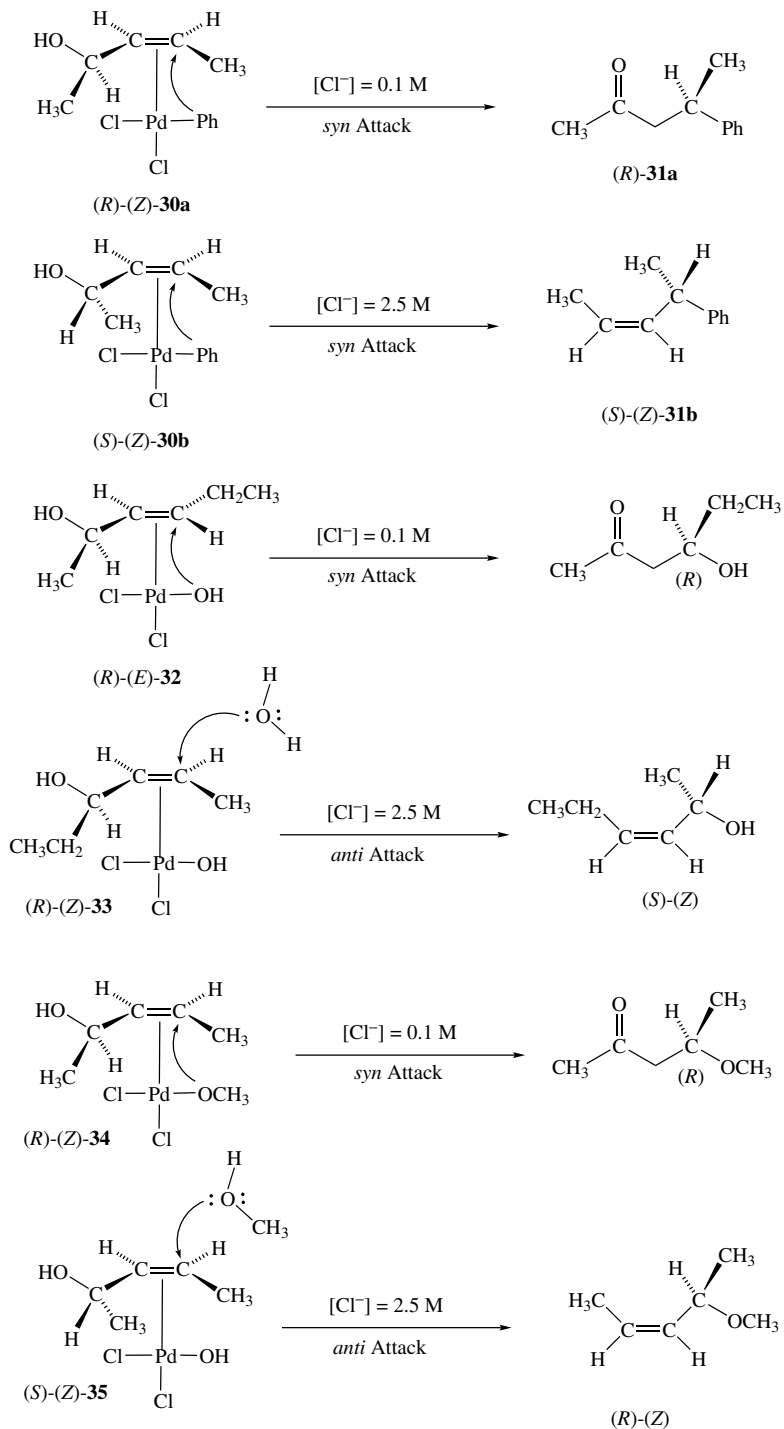
Thus, it would seem that the issue of the stereochemistry associated with hydroxypalladation has been settled and that stereochemistry is dependent on Cl^- concentration. This would explain Backvall's results at high Cl^- concentration and Henry's results shown in Schemes 9.6 and 9.7.⁵⁶

Steps c, d, and e

These steps represent β -elimination and 2,1-insertion reactions that result in Pd becoming attached to more substituted carbon. Loss of Cl^- from 16-electron intermediate **36** (step **c**) to give **37**, a 14-electron complex, could possibly precede β -elimination (step **d**). Once β -elimination has occurred, readers might imagine

⁵⁵O. Hamed, P. M. Henry, and C. Thompson, *J. Org. Chem.*, **1999**, *64*, 7745.

⁵⁶These two mechanistic paths are sometimes termed *outer-sphere* (the *anti* attack by an external molecule of H_2O) and *inner-sphere* (the *syn* attack by an OH group bound to Pd).

**Scheme 9.7**

Stereochemical
 Outcomes for
 Rearrangement and
 Oxidation for the
 Wacker Oxidation

that the complexed enol simply leaves the coordination sphere and goes directly to acetaldehyde by an enol–keto tautomerism. When the Wacker–Smidt reaction is run in D_2O , however, there is no D-incorporation in the aldehyde, thus ruling out ligand dissociation–tautomerism.⁵⁷

Exercise 9-6

Why would deuterium incorporation be expected into acetaldehyde if enol simply dissociates after step c in D_2O solvent?

Step f

Step f represents the last step in the formation of aldehyde, apparently as a result of β -elimination of a proton from the α -OH group. At the same time, the oxidation state of palladium drops from +2 \rightarrow 0, possibly by reductive elimination of HCl.

Step g

The last step in the cycle regenerates Pd(II) at the expense of Cu(II). The Cu(I) species that results is reoxidized to Cu(II) by either pure O_2 (single stage) or air (two stage process).

Theoretical Studies

The Wacker oxidation has been the focus of numerous recent theoretical studies.⁵⁸ The most definitive of these are the work of Goddard and co-workers. They have studied the entire catalytic cycle using high-level DFT calculations, and the results of this work have provided some interesting insights into key mechanistic steps.

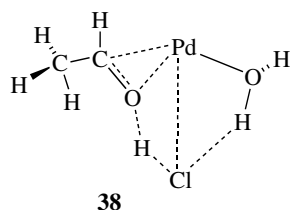
For example, calculations showed (Footnote 58c) that the activation energy barrier for step f (β -elimination of hydride) was about twice as high as the activation energy observed ($\Delta H^\ddagger = 19.8$ kcal/mol)⁵⁹ for the overall oxidation process, strongly indicating that β -elimination could not occur during this step. Further investigation discovered an alternative transition state (structure 38) that was much lower in energy than that for β -elimination and was also less than 19.8 kcal/mol. This transition state shows a process that is akin to RE instead of

⁵⁷See Footnote 47.

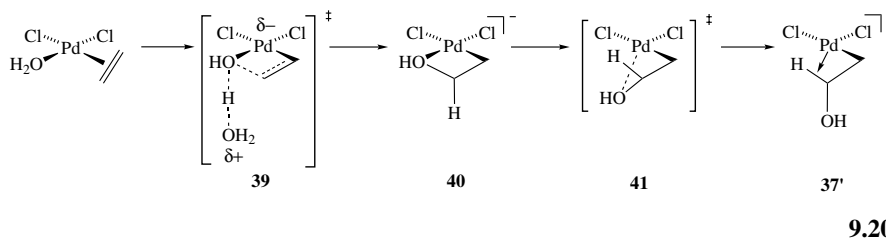
⁵⁸(a) P. E. M. Siegbahn, *J. Phys. Chem.*, **1996**, *100*, 14672; (b) D. J. Nelson, R. B. Li, and C. Brammer, *J. Am. Chem. Soc.*, **2001**, *123*, 1564; (c) J. A. Keith, J. Oxgaard, and W. A. Goddard, III, *J. Am. Chem. Soc.*, **2006**, *128*, 3132; (d) J. A. Keith, R. J. Nielsen, J. Oxgaard, and W. A. Goddard, III, *J. Am. Chem. Soc.*, **2007**, *129*, 12342; and (e) S. A. Beyramabadi, H. Eshtiagh-Hosseini, M. R. Housaindokht, and A. Morsali, *Organometallics*, **2008**, *27*, 72.

⁵⁹P. M. Henry, *J. Am. Chem. Soc.*, **1964**, *86*, 3246.

β -elimination. Here, a molecule of H_2O assists in the RE of HCl and the loss of acetaldehyde from Pd .



A second investigation by the Cal Tech group (Footnote 58d) attempted to discern why reaction products (aldehyde when $[\text{Cl}^-]$ is low and chlorohydrin when $[\text{Cl}^-]$ is high) and rate laws (inverse dependence on $[\text{H}^+]$ and $[\text{Cl}^-]^2$ when $[\text{Cl}^-]$ is low and zero-order dependence on $[\text{H}^+]$ and inverse first-order dependence on $[\text{Cl}^-]$ when $[\text{Cl}^-]$ is high) for Wacker oxidation differ as a function of reaction conditions. The group reported that the mechanism suggested by steps **b'** and **c**, involving *syn* attack by a coordinated OH ligand, could only involve reasonable activation energy barriers if the pathway shown in equation 9.20 occurred.



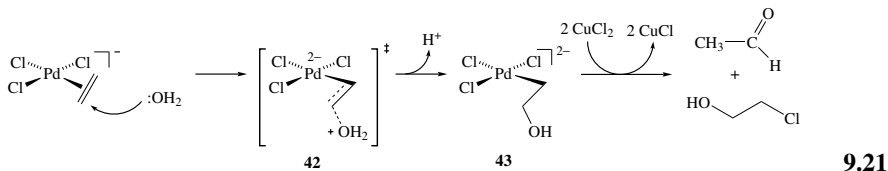
For this alternative pathway to compound **37** (Scheme 9.5), assistance by a molecule of H_2O is essential in lowering the energy of the first transition state **39**. A second barrier involves rate-determining isomerization of intermediate **40** to **37'** (similar to structure **37**, Scheme 9.5) via the second transition state **41**. This analysis is consistent with the rate law for low Cl^- concentration.

Why is the mechanism suggested by Keith and Goddard consistent with the rate law for Wacker oxidation when $[\text{Cl}^-]$ is low?

Exercise 9-7

The external attack by H_2O is also possible during step **a** (Scheme 9.5). Here, H_2O directly attacks the intermediate $[\text{PdCl}_3(\text{CH}_2=\text{CH}_2)]^-$ —in a rate-determining, *anti* manner—to give compound **43** (via transition state **42**), which then goes on to either aldehyde or chlorohydrin (equation 9.21) according to the pathway

already described. Such a process would be consistent with the rate law observed for high concentrations of Cl^- .⁶⁰



At this stage of both computational and experimental analysis, it appears that there is a much clearer picture of the major details of the Wacker oxidation than that existing 10–20 years ago. No doubt additional work will appear that elaborates further details of the catalytic cycle.

9-4 HYDROGENATION

The addition of H_2 across a multiple bond, such as $\text{C}=\text{C}$, $\text{C}\equiv\text{C}$, or $\text{C}=\text{O}$, constitutes an important synthetic procedure both at laboratory and industrial scale. This reaction is usually run in the presence of a heterogeneous catalyst. In the following section, however, we will discuss the use of homogeneous catalysts that are capable of promoting the saturation of multiple bonds (especially $\text{C}=\text{C}$) under mild conditions. Although homogeneously-catalyzed hydrogenation is not used industrially on nearly the scale that is associated with hydroformylation (with the exception being the use of phosphine-modified cobalt catalysts in both hydroformylation and subsequent hydrogenation), it finds increasing use in the production of specialty (fine) chemicals and pharmaceuticals. This is especially true when chiral ligands are attached to the metal, which allows products to form enantioselectively.

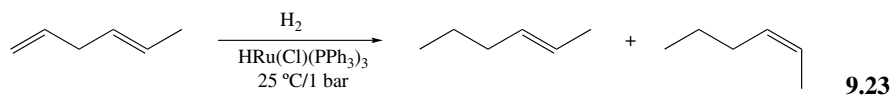
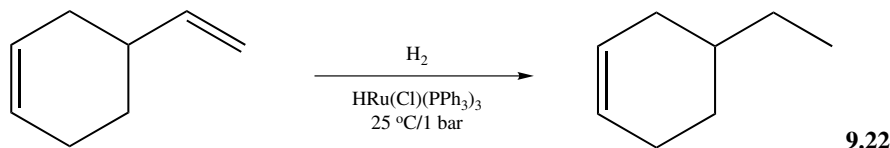
9-4-1 Hydrogenation Involving a Monohydride Intermediate

Two major pathways seem to occur with homogeneously-catalyzed hydrogenation—one involving metal monohydrides ($\text{M}-\text{H}$) and the other dihydrides (MH_2). The $\text{M}-\text{H}$ mechanism will be considered first in a rather limited manner, with much more detailed treatment reserved for the dihydride pathway.

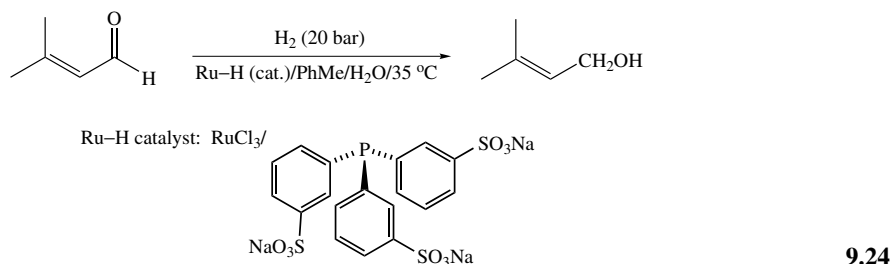
$\text{RuCl}_2(\text{PPh}_3)_3$ and related $\text{Ru}(\text{II})$ complexes serve usefully in the catalytic hydrogenation of alkenes as shown in equations 9.22 and 9.23,⁶¹ showing very high selectivity for terminal over internal double bonds.

⁶⁰Further analysis by Goddard *et al.* provided an explanation for the effects of CuCl_2 concentration on the product distribution and rate laws, but this work is beyond the scope of this text.

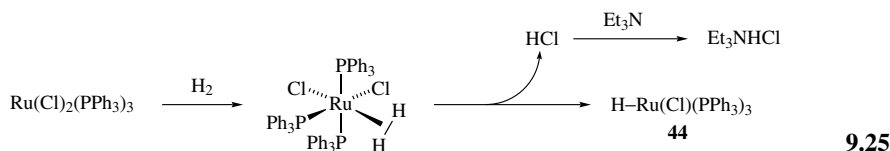
⁶¹P. S. Hallman, B. R. McGarvey, and G. Wilkinson, *J. Chem. Soc., A*, **1968**, 3143.



Equation **9.24** shows the chemoselectivity that the Ru–hydride catalysts offer when both a carbonyl group and a C=C bond exist in the same molecule.⁶² Here, use of a water-soluble Ru catalyst allows reduction of the carbonyl to the alcohol in a two-phase solvent system. Ru–hydride catalysts are often used for the hydrogenation of polar double bonds.

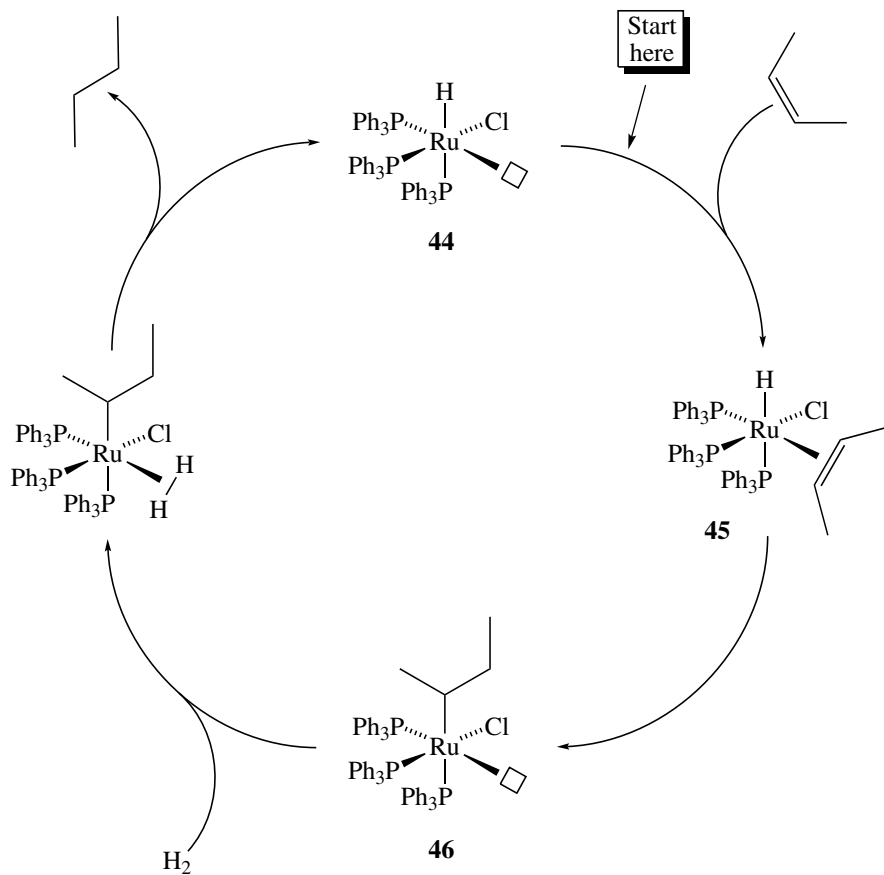


The active catalytic species is probably the 16-electron complex, $\text{HRuCl}(\text{PPh}_3)_3$, **44**, formed according to equation **9.25**. The reaction begins with the addition of H_2 to $\text{RuCl}_2(\text{PPh}_3)_3$ to give a dihydrogen complex and not a dihydride (a dihydride would oblige Ru to take on a relatively unstable oxidation state of +4).⁶³ The presence of Et_3N accelerates the formation of the active species by serving as a proton sponge to trap the HCl that forms by heterolytic cleavage of M–H and M–Cl bonds.



⁶²J. M. Grosselin, C. Mercier, G. Allmang, and F. Grass, *Organometallics*, **1991**, *10*, 2126.

⁶³Hydrogenations involving Ru(IV) are known, however. For a summary of possible modes of Ru–H formation, see S. E. Chapman, A. Hadzovic, and R. H. Morris, *Coord. Chem. Rev.*, **2004**, *248*, 2201. This review also discusses the many different mechanistic pathways available for Ru-catalyzed hydrogenation.

**Scheme 9.8**

A Catalytic Cycle
for Ru-Catalyzed
Hydrogenation of a
C=C Bond

Exercise 9-8

Propose a mechanism for the conversion of the dihydrogen complex to HCl and **44**, described in equation 9.25, and for the mechanism of the last step in Scheme 9.8.⁶⁴

Monohydride **44**, with its vacant site now available, can bind to the alkene, giving **45**, which can then undergo 1,2-insertion to form alkyldihydride complex **46**. Finally, heterolytic cleavage with H₂ regenerates the catalyst and gives the alkane (Scheme 9.8).

In Chapter 12 we shall encounter Ru-hydride hydrogenations again in the context of enantioselective transformations. In this case, chiral ligands provide an

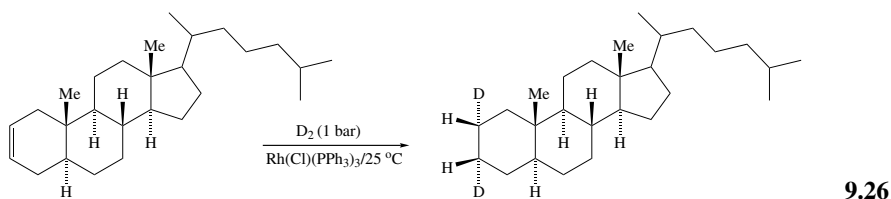
⁶⁴See R. H. Crabtree and D. G. Hamilton, *J. Am. Chem. Soc.*, **1986**, *108*, 3124, for more insight into the mechanism.

asymmetric environment during hydrogenation so that selection of one enantiomer over the other is possible.⁶⁵

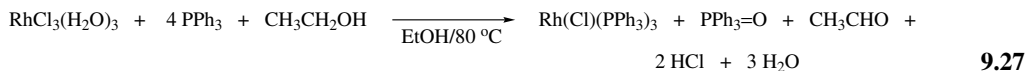
9-4-2 Hydrogenation Involving a Dihydride Intermediate

By far the most well-studied and synthetically-useful catalyst systems involving dihydride (MH_2) intermediates are those based upon Rh(I). The discovery by Wilkinson⁶⁶ (and independently and nearly simultaneously by Coffey⁶⁷) in 1965 that $RhCl(PPh_3)_3$ could catalyze the hydrogenation of alkenes at atmospheric pressure (in the presence of a wide variety of unsaturated functional groups that are unaffected by the reaction conditions) was a momentous event in the history of organometallic chemistry. This breakthrough stimulated a great deal of research on the elucidation of catalytic mechanisms in general and in particular on both the determination of the mechanism and the definition of the synthetic utility of homogeneous hydrogenation using Rh(I) complexes, so much so that today $RhCl(PPh_3)_3$ is known as “Wilkinson’s catalyst.”

Equation 9.26 shows an example of hydrogenation using Wilkinson’s catalyst. The use of D_2 rather than H_2 clearly indicates the stereochemistry of *syn* addition typical of Rh-catalyzed hydrogenation.



The catalyst itself is prepared either from $RhCl_3 \cdot xH_2O$ through treatment with excess PPh_3 in hot ethanol (equation 9.27) or by first making a chlorine-bridged dialkene complex and then allowing it to react with phosphine (equation 9.28). The latter process allows phosphines other than PPh_3 to be coordinated to Rh.



⁶⁵For a review of Ru-catalyzed reactions in organic synthesis, see T. Noata, H. Takaya, and S.-I. Murahashi, *Chem. Rev.*, **1998**, 98, 2599.

⁶⁶J. F. Young, J. A. Osborn, F. H. Jardine, and G. Wilkinson, *J. Chem. Soc., Chem. Commun.*, **1965**, 131.

⁶⁷R. S. Coffey, Imperial Chemical Industries, Brit. Patent 1,121,642,1965.

Table 9-2 Relative Rates for Hydrogenation of C=C Bonds over Wilkinson's Catalyst at 25 °C^a

Substrate	$k \times 10^2$ (L/mol/sec)
cyclohexene	31.6
1-hexene	29.1
2-methyl-1-pentene	26.6
(<i>Z</i>)-4-methyl-2-pentene	9.9
(<i>E</i>)-4-methyl-2-pentene	1.8
1-methylcyclohexene	0.6
3,4-dimethyl-3-hexene	< 0.1

^aF. H. Jardine, J. A. Osborne, and G. Wilkinson, *J. Chem. Soc. A*, **1967**, 1574.

Steric hindrance about the C=C bond of the alkene seems to play a role in influencing the rate of hydrogenation, according to Table 9-2.

Interestingly, the rate of H₂ addition to ethylene, a most sterically uncongested molecule, is quite slow relative to that for mono- and di substituted alkenes. Ethylene apparently binds tightly to Rh early in the catalytic cycle, inhibiting subsequent addition of H₂ (see step **j** of Scheme 9.9).⁶⁸

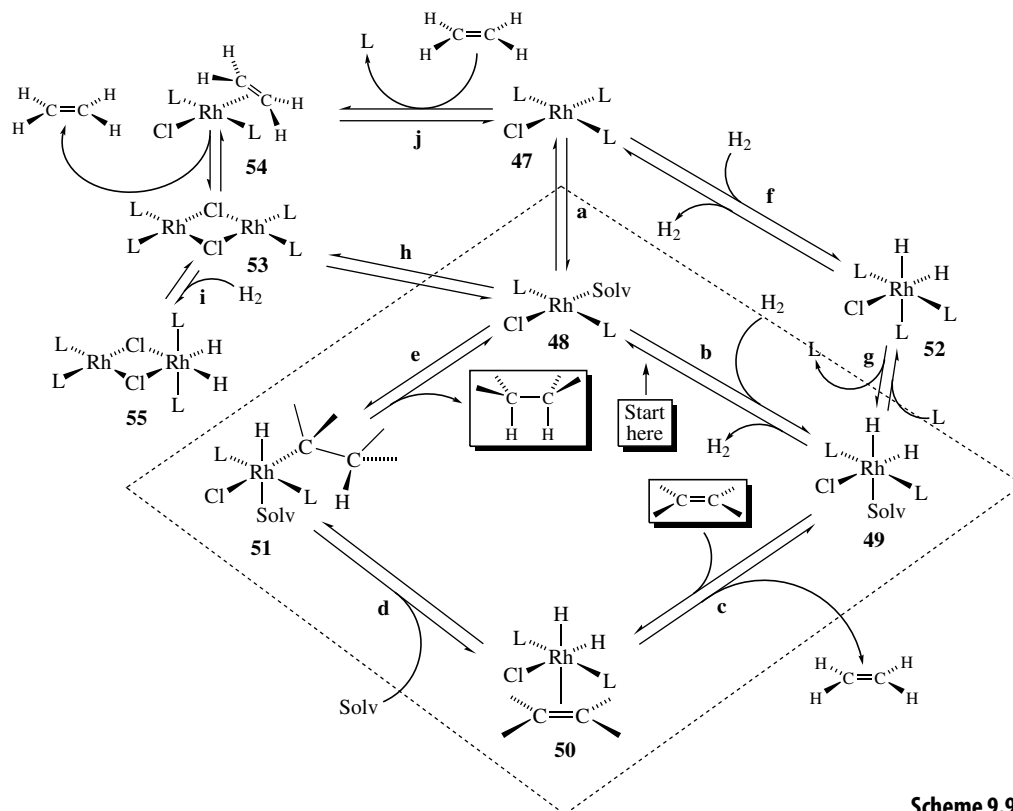
Scheme 9.9 depicts what most consider to be the mechanism for hydrogenation with Wilkinson's catalyst. The inner cycle of reactions (surrounded by the diamond-shaped dotted-line box) represents the key catalytic steps based on the work of Halpern⁶⁹ and Tolman.⁷⁰ They showed that compounds **52** to **55**, while detectable and isolable, were not responsible for the actual catalytic process and, moreover, the buildup of these intermediates during hydrogenation may even slow down the overall reaction.⁷¹ This work provided a valuable lesson for chemists trying to determine a catalytic mechanism—compounds that are readily isolable are probably not true intermediates. Through careful kinetic and spectroscopic

⁶⁸For an excellent discussion of the scope and limitations of Rh(I)-catalyzed hydrogenation, see A. J. Birch and D. H. Williamson, *Org. React.*, **1976**, 24, 1.

⁶⁹J. Halpern, T. Okamoto, and A. Zakhariev, *J. Mol. Cat.*, **1976**, 2, 65.

⁷⁰C. A. Tolman, P. Z. Meakin, D. L. Lindner, and J. P. Jesson, *J. Am. Chem. Soc.*, **1974**, 96, 2762.

⁷¹*Parahydrogen induced polarization* (PHIP) NMR techniques have been used to study intermediates involved in hydrogenations catalyzed by Wilkinson's catalyst, particularly those involved in the OA of H₂ with various Rh species to give compounds such as **55**. Although the detailed explanation of this technique is beyond the scope of this text, PHIP allows the use of ¹H NMR, a relatively insensitive technique normally, to be used to detect intermediates involved in catalytic cycles in low concentration due to enhanced signals resulting from induced polarization of hydrogen nuclei. For more information on this technique and results relevant to Wilkinson's catalyst, see S. A. Colebrooke, S. B. Duckett, J. A. B. Lohman, and R. Eisenberg, *Chem. Eur. J.*, **2004**, 10, 2459 and S. B. Duckett, C. L. Newell, and R. Eisenberg, *J. Am. Chem. Soc.*, **1994**, 116, 10548. The principle of PHIP is reviewed in R. Eisenberg, *Acc. Chem. Res.*, **1991**, 24, 110.



Key steps: **a, b, c, d, and e**

L = PPh₃; Solv = EtOH, THF

Scheme 9.9

Mechanism of Hydrogenation with Wilkinson's Catalyst

studies, Halpern showed by inference that structures **48** to **51** were the true intermediates in the catalytic cycle. The following discussion will include a look at some of the key steps in the catalytic cycle to see how they correspond to the overall hydrogenation process.⁷²

Steps a and b

Dissociation of **47** to **48**, a 14-electron intermediate (unless we count solvent coordination), followed by oxidative addition of H₂ seems at first glance implausible

⁷²For a good discussions of the mechanism of hydrogenation catalyzed by RhCl(PPh₃)₃, see J. P. Collman, L. S. Hegedus, J. R. Norton, and R. G. Finke, *Principles and Applications of Organotransition Metal Chemistry*, University Science Books: Mill Valley, CA, 1987, pp. 531–535; R. Giernoth, “Hydrogenation,” in *Homogeneous Catalysis. A Spectroscopic Approach*, B. Heaton, Ed., Wiley–VCH Verlag: Weinheim, Germany, 2005, p. 359; and D. J. Nelson, R. Li, and C. Brammer, *J. Org. Chem.*, **2005**, *70*, 761.

and unnecessary because the step is endothermic, and a scheme involving 16- and 18-electron intermediates (**47** → **52** → **49**, steps **f** and **g**) could also occur readily. Halpern estimated, however, that the rate of H₂ addition to **48** was 10,000 times greater than to **47**, although he had not actually isolated **48**.⁷³ Several years later, Wink and Ford⁷⁴ generated **48** as a transient species and observed it spectroscopically. They also measured the rate of H₂ addition and found it to be close to Halpern's value.⁷⁵

There is a question regarding the stereochemistry of the phosphine ligands in **48**: Are the groups *cis* or *trans* with respect to each other? Work by Brown suggests that they are *cis*, and that this stereochemistry continues throughout the cycle.⁷⁶ *Ab initio* MO calculations⁷⁷ using a small basis set suggest, however, that if *cis* stereochemistry is associated with later intermediates, the rate-determining step occurs at step **e** rather than a step **d** (see below), which is inconsistent with Halpern's results. It may be that with phosphines bulkier than PH₃ and with alkenes other than those of low molecular weight (the conditions used in the theoretical studies), the pathway involving *cis* phosphines is operative. Also, it is possible that *cis*–*trans* isomerization of phosphine ligands among intermediates in the cycle could occur.

Dimerization of **48** to **53** followed by hydrogen addition to give **55** seems to occur (steps **h** and **i**). Complex **55**, however, does not readily take part in the catalytic cycle. Under normal hydrogenation conditions, **48** reacts rapidly to give **49**.

Step c

Step **c** is a straightforward coordination of alkene ligand onto dihydride **49**. Assuming that solvent only very weakly coordinates to Rh in **49**, addition of the alkene to give 18-electron **50** should be facile. It should be pointed out that strongly coordinating alkenes such as ethylene, however, bind preferentially to **47** to give **54** (step **j**), a stable complex that does participate in the catalytic cycle.

⁷³J. Halpern and C. S. Wong, *Chem. Commun.*, **1973**, 629.

⁷⁴D. A. Wink and P. C. Ford, *J. Am. Chem. Soc.*, **1985**, *107*, 1794, and **1986**, *108*, 4838.

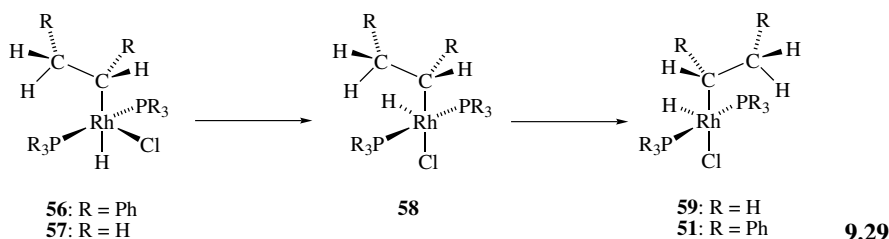
⁷⁵A recent computational study on the OA of the C–H bond of an imidazolium salt to Wilkinson's catalyst indicated that both an associative (similar to **47** to **52** to **49**) or a dissociative (**47** to **48** to **49**) mode of OA could occur, but the dissociative route was favored, especially if a solvent molecule was attached to the site vacated by the departing phosphine ligand. K. J. Hawkes, D. S. McGuinness, K. J. Cavell, and B. F. Yates, *Dalton Trans.*, **2004**, 2505.

⁷⁶J. M. Brown, P. L. Evans, and A. R. Lucy, *J. Chem. Soc. Perkin Trans. 2*, **1987**, 1589 and J. M. Brown, *Chem. Soc. Rev.*, **1993**, 25.

⁷⁷N. Koga and K. Morokuma, *Chem. Rev.*, **1991**, *91*, 823.

Step d

This step is rate-determining and actually is a combination of two fundamental steps. First, 1,2-insertion of the alkene ligand gives **56** (see equation 9.29; structures **56** to **59** may be considered distorted square pyramids), where the alkyl and hydride ligands are *trans*. In order for step e, reductive elimination, to occur, these two ligands must be situated *cis* with respect to each other. This requires that an isomerization occur. Although it is not known just how this happens, *ab initio* MO calculations⁷⁸ on a model system where PH₃ is used instead of PPh₃ indicated that a reasonable scenario for isomerization might take place according to equation 9.29. Here, **57** (**56** if L = PPh₃) undergoes sequential hydride and chloride migration (both occur with low activation energy) to yield **58** before Rh–C bond rotation in the ethyl group occurs to give **59** (**51** if L = PPh₃). The observation of a primary deuterium isotope effect⁷⁹ ($k_{\text{obs}}^{\text{Rh-H}}/k_{\text{obs}}^{\text{Rh-D}} = 1.15$) provides additional evidence that the rate-determining step is one that involves M–H bond breaking.



Based on your knowledge of the *trans* and *cis* effects (Chapter 7), why should the rearrangement of **57** to **59** be energetically reasonable?

Exercise 9-9

⁷⁸C. Daniel, N. Koga, J. Han, X. Y. Fu, and K. Morokuma, *J. Am. Chem. Soc.*, **1988**, *110*, 3773.

⁷⁹Primary kinetic deuterium isotope measurements are useful in determining whether bond breaking between a hydrogen and some other atom has occurred before or during the rate-determining step in a reaction mechanism. If so, the rate of reaction involving X–H bond breaking (X = a heavy atom) will be slower when deuterium is present than the case for hydrogen, and $k_{\text{obs}}^{\text{X-H}}/k_{\text{obs}}^{\text{X-D}} > 1$. If $k_{\text{obs}}^{\text{X-H}}/k_{\text{obs}}^{\text{X-D}} = 1$, then there is no isotope effect and X–H bond breaking likely occurs after the rate-determining step. See T. H. Lowry and K. S. Richardson, *Mechanism and Theory in Organic Chemistry*, 3rd ed., Harper & Row: New York, 1987, pp. 232–244 and F. A. Carey and R. J. Sundberg, *Advanced Organic Chemistry, Part A*, 5th ed., Springer Scientific: New York, 2007, pp. 332–335, for good discussions of kinetic isotope effects.

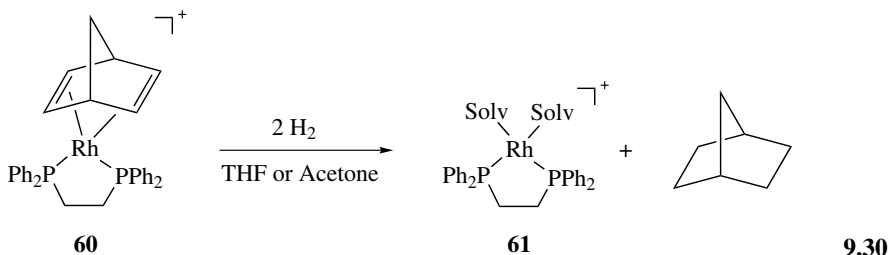
Step e

Now that the hydride and alkyl groups are *cis* with respect to each other, reductive elimination readily occurs to yield alkane and regenerate **48**. We know that RE takes place with retention of configuration. This result, combined with effective *syn* addition of Rh and hydrogen during the 1,2-insertion, means that both hydrogens ultimately add to the same face of the alkene C=C bond.

Molecular orbital calculations,⁸⁰ performed for each step of the catalytic cycle (solvent effects were neglected and L = PH₃), verified that the mechanism postulated by Halpern is reasonable. The caveat to bear in mind with the Halpern mechanism or the mechanism of any catalytic process is that variations in alkene, solvent, and phosphine ligands may change the pathway or the rate-determining step (see above for the discussion regarding steps **a** and **b**).

9-4-3 Cationic Hydrogenation Catalysts**Rh Catalysts**

The discovery of Wilkinson's catalyst led to the development of a new class of complexes capable of promoting hydrogenation; these have the general formula L_{*n*}M⁺ (M = Rh or Ir). The Rh series was first reported by Schrock and Osborn;⁸¹ equation **9.30** demonstrates how such a complex may be prepared. The cationic Rh(I) complex (**60**), interacts with a solvent such as THF or acetone to give a 12-electron, "unsaturated" diphosphine intermediate (**61**), which is considered the active catalyst. The catalytic cycle begins this time with alkene binding, followed by the oxidative addition of H₂.

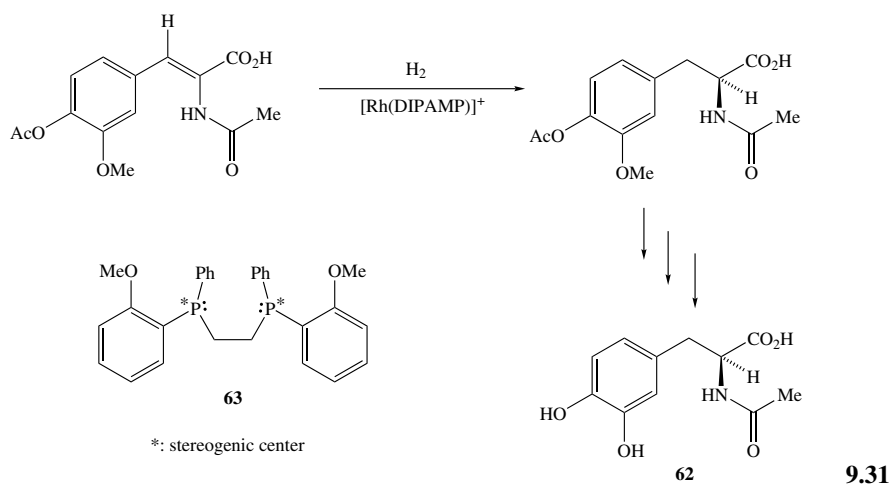


Although cationic Rh complexes have found some use in reducing alkenes to alkanes, converting alkynes to *cis*-alkenes, and transforming ketones to alcohols, the most important function of these catalysts has been to promote asymmetric hydrogenation of a C=C bond. Equation **9.31** shows a key step that Knowles

⁸⁰See Footnotes 77 and 78.

⁸¹R. R. Schrock and J. A. Osborn, *J. Am. Chem. Soc.*, **1976**, 98, 2134, and references therein.

developed in his Nobel Prize-winning work on the industrial-scale synthesis of the drug L-Dopa (**62**), used to treat Parkinson's disease.⁸² The reduction proceeds with remarkable stereoselectivity producing the *S*-enantiomer in 94% ee.⁸³ Note that the diphosphine ligand DIPAMP (**63**) possesses two stereogenic centers at the phosphorus atoms and provides a chiral environment (when complexed with Rh) during the course of the catalytic cycle. A closer examination of the mechanism of asymmetric hydrogenation and its application to organic synthesis will appear in Chapter 12, where it is considered along with other methods for inducing chirality into molecules.



Ir Catalysts

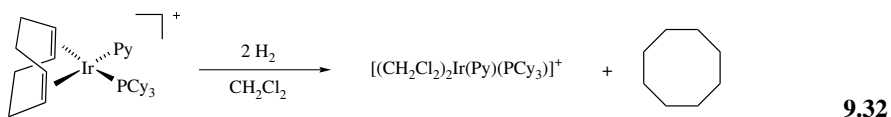
Because Ir resides below Rh in the periodic table, we might expect it to parallel rhodium's behavior as a hydrogenation catalyst. Unfortunately, the Ir analog of Wilkinson's catalyst, $IrCl(PPh_3)_3$, is not effective in saturating C=C bonds because phosphine is more tightly bound to Ir (typical of third-row transition elements) than with Rh, and thus the catalytically active species, $IrCl(PPh_3)_2$, does not readily form. Cationic Ir complexes, on the other hand, are even more active in promoting hydrogenation than Wilkinson's catalyst. Developed initially mainly by Crabtree,⁸⁴ cationic Ir complexes of the general form $(COD)Ir(L)(L')$

⁸²W. S. Knowles, *J. Chem. Ed.*, **1986**, *63*, 222; for a more recent account, which is Knowles' Nobel Lecture, see W. S. Knowles, *Angew. Chem. Int. Ed.*, **2002**, *41*, 1998.

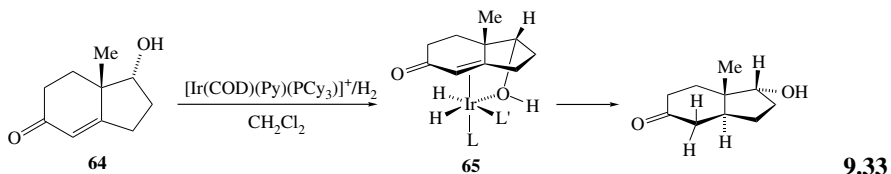
⁸³See Section 8-1-1 for the definition of the term "ee."

⁸⁴R. H. Crabtree, H. Felkin, and G. E. Morris, *J. Organomet. Chem.*, **1977**, *141*, 205 and R. H. Crabtree, *Acc. Chem. Res.*, **1979**, *12*, 331.

catalyze saturation of even tetrasubstituted double bonds almost as fast as that for the mono- and disubstituted variety. Apparently, in the presence of H_2 and a non-coordinating solvent such as CH_2Cl_2 , an active, transient, 12-electron species—“ $Ir(L)(L')^+$ ”—forms along with the conversion of the COD ligand to cyclooctane (equation 9.32).



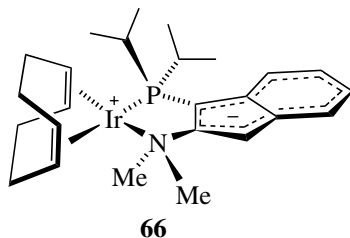
This highly unsaturated complex with its positive charge is a relatively hard Lewis acid, binding not only alkene and hydrogen but also polar ligands such as alcohol and carbonyl oxygen. Equation 9.33 shows⁸⁵ the remarkable stereoselectivity obtained when enone **64** is hydrogenated in the presence of $[Ir(COD)(Py)(PCy_3)]PF_6$. The high preference for the isomer in which the methyl group is *trans* to H at the junction of the two rings is probably caused by the formation of intermediate **65** in which hydrogen, alkene, and alcohol group bind simultaneously to Ir. Such high stereoselectivity is typical in cyclic systems where a polar group resides near a C=C bond.



More recent developments in improving the scope of iridium hydrogenation catalysts have involved the synthesis of ligands that make the Ir complex zwitterionic. One such complex is shown as structure **66**. The complex has an overall charge of zero, yet the metal still retains a cationic center like Crabtree's catalyst. Experiments showed that **66** was soluble in nonpolar solvents such as benzene and hexanes, unlike Crabtree's catalyst. Although **66** is not as active as Crabtree's catalyst in hydrogenating styrene, for example, there is the potential of modifying the P–N ligand structure to allow it and similar compounds to be more active.⁸⁶

⁸⁵G. Stork and D. E. Kahne, *J. Am. Chem. Soc.*, **1983**, 105, 1072.

⁸⁶J. Cipot, R. McDonald, M. J. Ferguson, G. Schatte, and M. Stradiotto, *Organometallics*, **2007**, 26, 594.

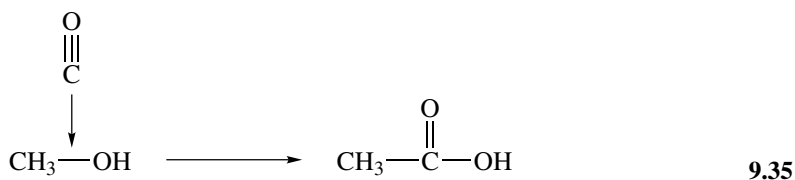


Since the initial discovery of Crabtree's catalyst, the most intense research activity has centered on developing Ir catalysts that will promote asymmetric hydrogenations. This work will be discussed in more detail in Chapter 12.

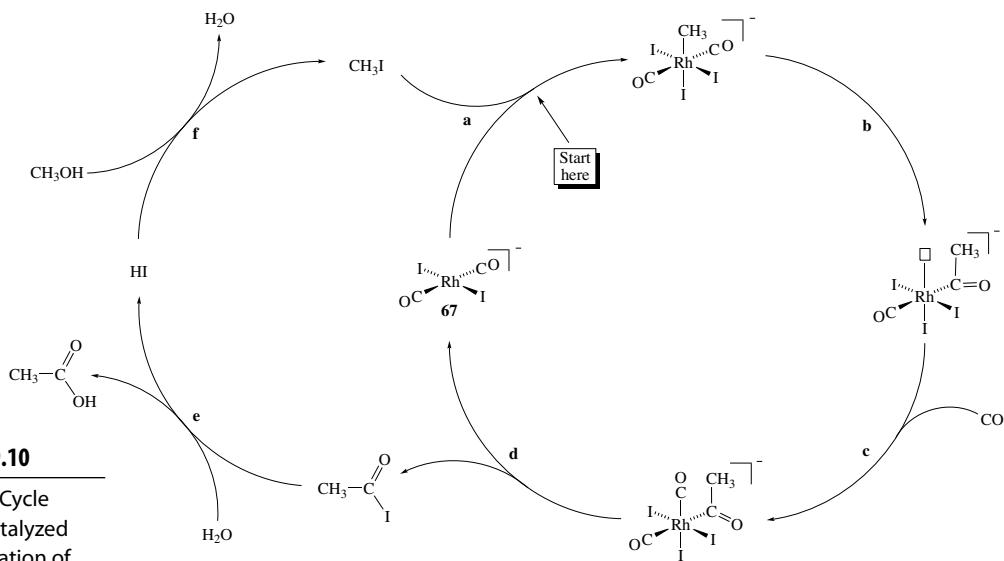
9-5 CARBONYLATION OF METHANOL

9-5-1 Rh-catalyzed Carbonylation

Acetic acid is produced industrially on a large scale. Although useful in some commercial processes as is, most of the acetic acid produced is subsequently converted to acetic anhydride, a valuable acetylating agent employed in synthesizing cellulose acetate films and aspirin. For many years, the major production method of acetic acid was through the Wacker process. The ready availability of CH_3OH from synthesis gas using a heterogeneously-catalyzed reaction (equation 9.34), however, sparked interest in trying to discover a procedure to insert CO directly into the C–O bond of methanol (9.35). Such a process would then be based entirely on synthesis gas if a suitable catalyst could be found. Direct carbonylation of methanol is now a reality, and today almost all of the acetic acid and acetic anhydride produced worldwide results from this process.



In the mid 1960s, the German-based chemical company BASF developed a methanol carbonylation process using a mixture of $\text{Co}_2(\text{CO})_8$ and HI as catalyst. Unfortunately, severe conditions (210 °C and 700 bar) were required to produce $\text{CH}_3\text{CO}_2\text{H}$ rapidly enough and in sufficient amount to be commercially acceptable. A few years later, Monsanto announced a significant breakthrough in the



Scheme 9.10
Catalytic Cycle
for Rh-Catalyzed
Carbonylation of
Methanol

quest to produce acetic acid directly from methanol. Instead of Co, a Rh–HI system provided the necessary catalytic activity to form acetic acid as virtually the sole product at 180 °C and 30–40 bar. The molar concentration of catalyst required, moreover, was about 100 times less than for the Co-catalyzed process. Once Monsanto perfected its new procedure on a tonnage scale, all previous operations became rapidly obsolete. Again, we see an example of how rhodium chemistry is superior to that of cobalt.

Scheme 9.10 diagrams catalytic cycles involved in methanol carbonylation. Note that there are actually two major interlocking cycles—one involving the Rh complex and the other designed to generate CH_3I from CH_3OH . Most any Rh(III) salt and source of I^- are suitable precursors for generating the active catalytic complex, $[\text{Rh}(\text{CO})_2\text{I}_2]^-$ (**67**). The overall rate of carbonylation is independent of the concentration of CO but dependent upon Rh and methyl iodide concentrations according to

$$\text{Rate} = k[\mathbf{67}][\text{CH}_3\text{I}].$$

The rate law is consistent with other observations that indicate oxidative addition of CH_3I to **67** (step **a**) is the rate-determining step, which consists of an $\text{S}_{\text{N}}2$ displacement (Section 7-2-2) of I^- on CH_3I by the negatively charged and highly nucleophilic **67**.⁸⁷ After OA of CH_3I , facile carbonyl insertion (step **b**), the addition of one more CO ligand (step **c**), and reductive elimination occur to

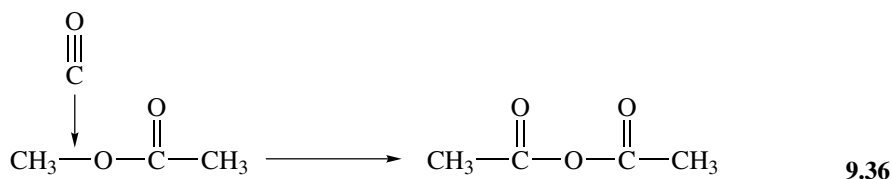
⁸⁷Consistent with the $\text{S}_{\text{N}}2$ mechanism are the observations that the rate of reaction is 10 times slower when Br^- is the co-catalyst instead of I^- and that the rates of carbonylation of methyl, ethyl, and propyl alcohols parallel the rates of ordinary $\text{S}_{\text{N}}2$ substitution of the corresponding alkyl halides with methyl > ethyl > propyl.

regenerate **67** and produce acetyl iodide (step **d**), which subsequently undergoes rapid hydrolysis to acetic acid (step **e**). The by-product of the last step, HI, then reacts with additional CH_3OH to yield CH_3I (step **f**), allowing a new carbonylation cycle to occur.⁸⁸

The rate of carbonylation of 2-propanol to give a mixture of butanoic and 2-methylpropanoic acids is actually a little faster than that for carbonylation of ethanol and up to seven times more rapid than that for 1-propanol. If OA is still the rate-determining step in the pathway, what can be said about the mechanism of that step when 2-propanol is the starting material? [Hint: See Section 7-2-3]

Exercise 9-10

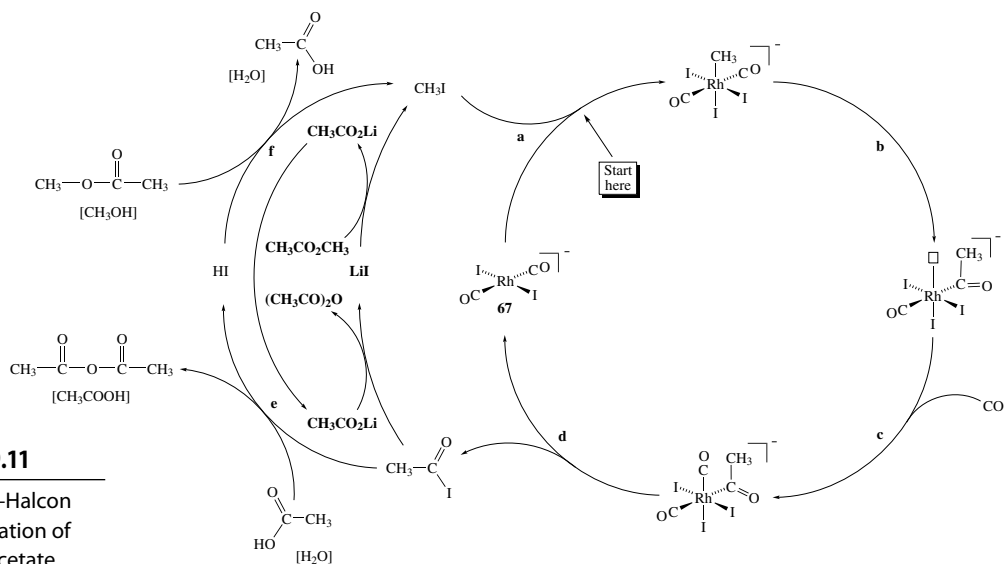
Because acetic anhydride is more useful to the chemical industry than acetic acid, there was economic incentive to develop a process that would yield the anhydride directly without first producing the acid as a separate operation. By the early 1980s, Eastman Chemicals, in conjunction with Halcon Chemical Company, developed a procedure that provided acetic anhydride using technology similar to the Monsanto process, and since 1991 a plant run by Eastman has produced anhydride in excess of 500,000 metric tons per year.⁸⁹ The Eastman–Halcon (E–H) operation amounts formally to inserting CO into the C–O bond of methyl acetate according to equation **9.36**.⁹⁰



⁸⁸For a good discussion of the mechanism of Rh-catalyzed carbonylation, see articles written by chemists who were instrumental in developing the process at Monsanto: D. Forster, *Adv. Organometal. Chem.*, **1979**, *17*, 255 and D. Forster and T. W. Dekleva, *J. Chem. Ed.*, **1986**, *63*, 204, and references therein.

⁸⁹R. G. Smith, "Chemicals from Coal Operations," Gasification Department, Eastman Chemical Company. A report presented at the 2000 Gasification Technologies Conference, San Francisco, Oct. 8–11, 2000.

⁹⁰S. W. Polichnowski, *J. Chem. Ed.*, **1986**, *63*, 206 and J. R. Zoeller, J. D. Cloyd, J. L. Lafferty, V. A. Nicely, S. W. Polichnowski, and S. L. Cook, "Rhodium-Catalyzed Carbonylation of Methyl Acetate," in *Homogeneous Transition Metal Catalysis*, W.R. Moses and D.W. Slocum, Eds., American Chemical Society: Washington, D.C., 1992, pp. 395–418.



We can best understand the process by looking at Scheme 9.11, which is largely a revisit of Scheme 9.10. Note that the reagents in brackets are those for the Monsanto methanol carbonylation. The E–H process uses methyl acetate instead of methanol as one of the starting materials and acetic acid rather than H_2O to react with acetyl iodide at the end.

Despite the similarities between the two carbonylations, there are some significant differences. The E–H scheme requires a reducing atmosphere of H_2 to be present to keep sufficient Rh in the form of **67**.⁹¹ A second difference is that the E–H process uses a cationic promoter.⁹² Exhaustive studies indicated that Li^+ was the best cation for the job, and at low concentration it plays a role in the overall kinetics of the carbonylation. A third cycle in Scheme 9.11, which also produces acetic anhydride showing key intermediates in bold type, attempts to rationalize the role of Li^+ in the overall reaction, based on work by researchers at Eastman.

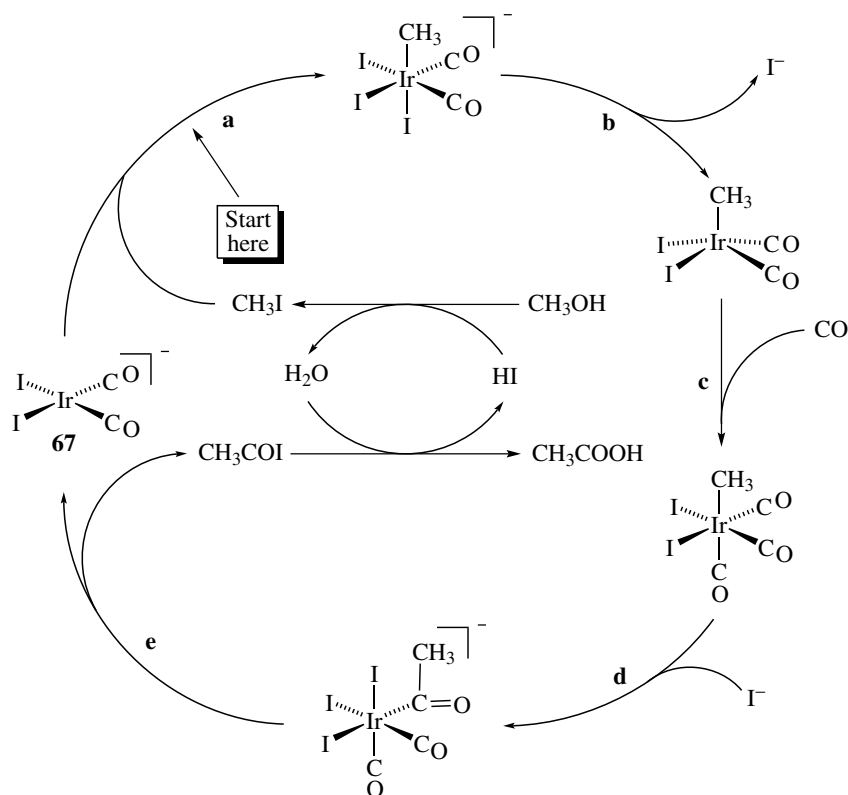
9-5-2 Ir-catalyzed Carbonylation

The latest advance in carbonylation of methanol is the use of an Ir catalyst. Introduced as the *Cativa* process in 1996 by BP Chemicals, Ir-catalyzed production of acetic acid is now used worldwide.⁹³ The catalytic cycle, called the

⁹¹Unless H_2 is present in low concentration, the anhydrous conditions of the E–H process produce $[\text{Rh}(\text{CO})_2\text{I}]^+$, an inactive catalyst.

⁹²The presence of Li^+ apparently serves to maximize the amount of Rh present in the form of **67**.

⁹³*Chem. Br.*, **1996**, 32, 7. For a discussion of the *Cativa* process by some of the scientists who developed it, see G. J. Sunley and D. Watson, *Catal. Today*, **2000**, 58, 293.

**Scheme 9.12**

The Anionic Cycle
for Ir-Catalyzed
Carbonylation of
Methanol

anionic cycle and shown in Scheme 9.12, is quite similar to that for Rh-catalyzed carbonylation. Original work by Forster and others⁹⁴ on the mechanism of Ir-catalyzed carbonylation demonstrated that there is actually an alternative pathway called the *neutral cycle* in which CH_3I undergoes OA with neutral $\text{Ir}(\text{CO})_3\text{I}$ or $\text{Ir}(\text{CO})_2\text{I}$ instead of anionic $[\text{Ir}(\text{CO})_2\text{I}_2]^-$, analogous to the Rh-catalyzed reaction. Chemists consider the anionic cycle to be principally operative under industrial-scale conditions.⁹⁵

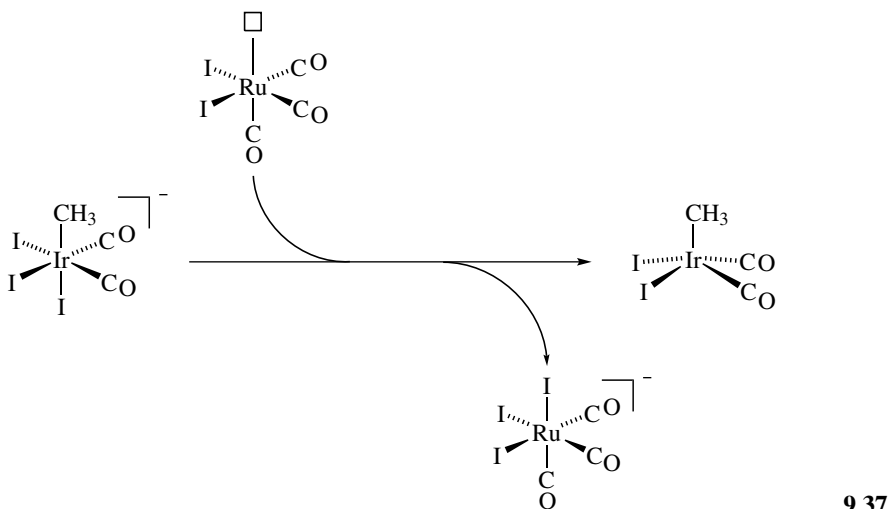
Although the rate-determining step for Rh-catalyzed carbonylation is the OA of CH_3I to $[\text{Rh}(\text{CO})_2\text{I}_2]^-$, the comparable step for the Cativa process (step a) is several hundred times faster. Migratory CO insertion, on the other hand, is very sluggish for $[\text{MeIr}(\text{CO})_2\text{I}_3]^-$, but studies have indicated that it is much faster if the

⁹⁴D. Forster, *J. Chem. Soc., Dalton Trans.*, **1979**, 1639 and A. Haynes, *et al.*, *J. Am. Chem. Soc.*, **2004**, 126, 2847.

⁹⁵M. Volpe, G. Wu, A. Iretskii, and P. C. Ford, *Inorg. Chem.*, **2006**, 45, 1861 and references therein.

neutral intermediate $\text{MeIr}(\text{CO})_3\text{I}_2$ forms first. This requires loss of I^- , which is a slow step (step **b**). It is this loss of I^- that is a bottleneck in the whole catalytic cycle, and until chemists discovered a way to unplug the bottleneck, Ir-catalyzed carbonylation was not feasible on an industrial scale.

A real breakthrough came with the discovery of promoter molecules that could be added to the reaction mixture. One such promoter is $\text{Ru}(\text{CO})_3\text{I}_2$. Its mode of action seems to be in part to act as an I^- abstractor from $[\text{MeIr}(\text{CO})_2\text{I}_3]^-$ (equation 9.37), which has the effect of accelerating steps **c** and **d**. Several other transition metal carbonyl-iodo complexes will work, as will simple iodides of Zn, Cd, and Hg. Studies have shown that the iodinated promoter product is recycled by contributing its extra I^- to the process for producing CH_3I .



The Cativa process offers several advantages over conventional Rh-catalyzed carbonylation, including the following:

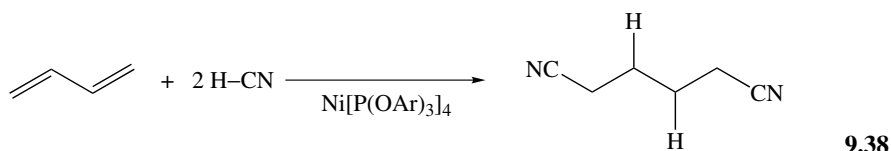
- Employs an inherently more stable catalyst system (Ir–ligand bonds are usually stronger)
- Uses lower concentrations of H_2O , thus minimizing the water gas shift reaction (see equation 9.1), and allows for easier separation of product
- The catalyst can exist over a wider range of conditions than comparable Rh catalysts before precipitating as IrI_3

The Monsanto, E–H, and Cativa processes represent triumphs in the application of organotransition metal chemistry to catalysis, using homogeneous transition metal compounds to promote production of valuable materials cheaply, efficiently, and selectively. Without question, fundamental work accomplished previously on the understanding of basic organometallic reaction types helped

tremendously in the efforts required to unravel the intricacies of these and other cycles we have already considered. These catalytic processes and those considered later in Chapter 9 and in following chapters provide beautiful illustrations of not only the basic reaction types in action, but also how scientific investigations can lead to practical applications of major economic significance.

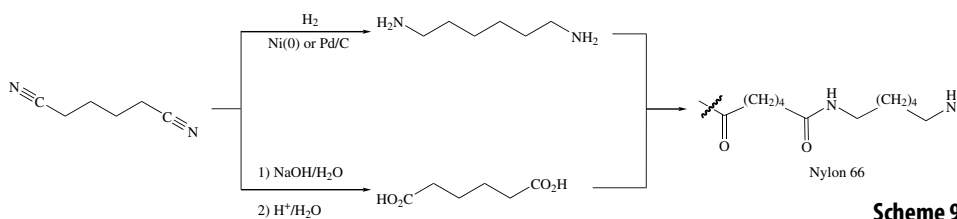
9-6 HYDROCYANATION

Hydrocyanation is the addition of HCN across a C=C bond. In 1971, Dupont reported a new process that added two equivalents of HCN, in an anti-Markovnikov manner, to 1,3-butadiene to yield adiponitrile (equation 9.38).⁹⁶ The process is catalyzed overall by a Ni(0) triarylphosphite complex.



Adiponitrile is an extremely important compound because it may be hydrogenated over a heterogeneous catalyst to give 1,6-hexanediamine or hydrolyzed to yield adipic acid. Both products are used in the production of the polyamide nylon 66, one of the most common nylon polymers used today (Scheme 9.13).⁹⁷

The mechanism of hydrocyanation turns out to be another classic example of a set of catalytic cycles that use many of the fundamental types of organometallic reactions that we have already encountered. In fact, the investigation of the details of this mechanism went hand in hand with the advancement of important general



Scheme 9.13

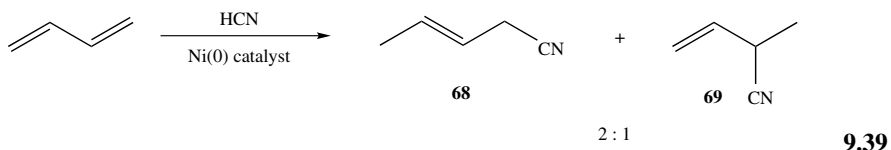
Conversion of
Adiponitrile to
Nylon 66

⁹⁶*Chem. Eng. News*, **1971**, 49, 30.

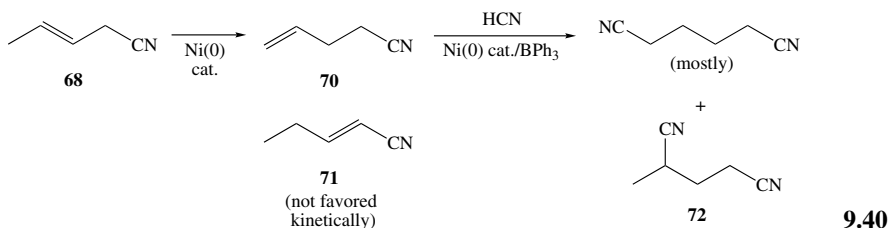
⁹⁷Adipic acid is also made on an industrial scale through oxidation of cyclohexanone. The number 66 represents the number of carbons in the two different monomeric units of nylon 66; both adipic acid and 1,6-hexanediamine contain six carbon atoms. Nylon 6 is made from only one type of monomeric unit, which also contains six carbon atoms.

concepts about basic organometallic reactions and catalytic cycles that we accept as valid today.⁹⁸

Hydrocyanation of 1,3-butadiene occurs in three stages. Equation 9.39 shows the first stage, which produces a 2:1 mixture of the desired 3-pentenitrile (**68**), produced by a 1,4-addition of HCN to 1,3-butadiene, and the branched isomer 2-methyl-3-butenitrile (**69**), which results from Markovnikov 1,2-addition.

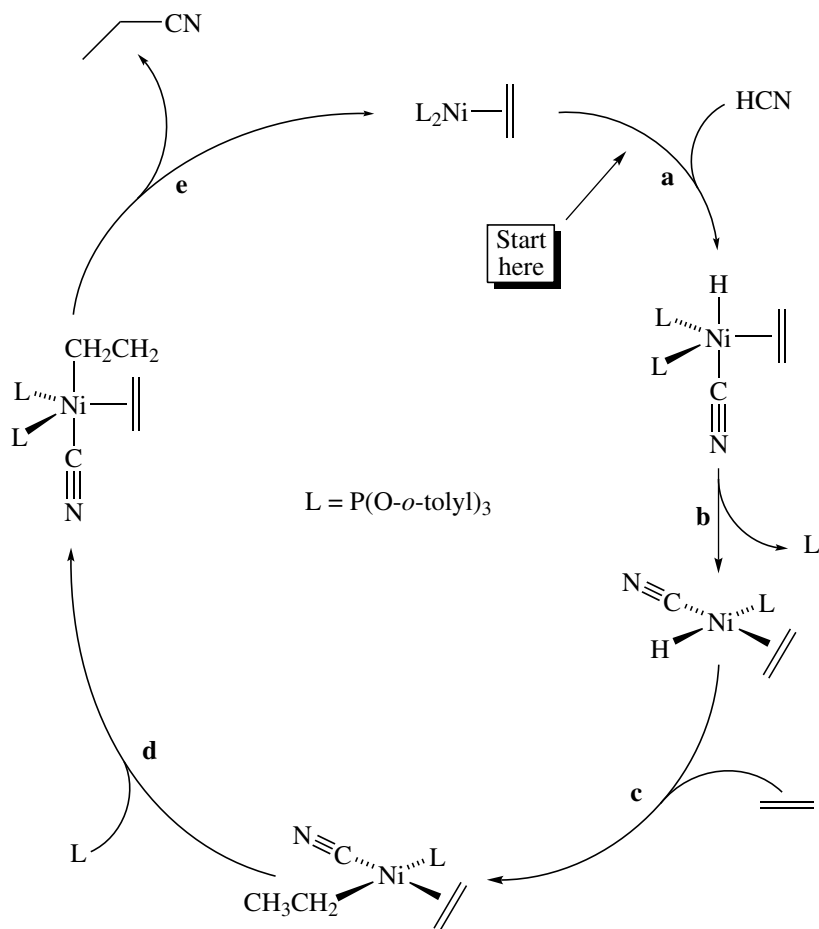


The next stage requires equilibration and isomerization of **69** to **68**, giving a 9:1 ratio of desired to undesired product. A Ni catalyst is also used for this reaction. Finally, the third stage consists of two transformations, where **68** is first isomerized to 4-pentenitrile (**70**) under kinetic control, fortunately without producing much of the thermodynamically more stable 2-pentenitrile (**71**). Compound **70** then undergoes a second hydrocyanation with anti-Markovnikov orientation (equation 9.40). In this last Ni-catalyzed stage of the overall process, a Lewis acid, such as Ph_3B , is added to ensure that linear rather than branched product (**72**) forms.

**Exercise 9-11**

Why is formation of **68** favored over formation of **69**? Why is **68** or **70** less stable than **71**?

⁹⁸For an excellent overview, written by a Dupont chemist, of the development of the adiponitrile process and the investigation of its fundamental chemistry, see C. A. Tolman, *J. Chem. Ed.*, **1986**, 63, 199; for a key research paper on Tolman's work, see C. A. Tolman, W. C. Seidel, J. D. Druliner, and P. J. Domaille, *Organometallics*, **1984**, 3, 33.



Scheme 9.14
Catalytic Cycle for
Hydrocyanation of
Ethene

Although details of the catalytic cycle that converts 1,3-butadiene to **68** remain proprietary information, a thorough study has been reported on the catalytic cycle for hydrocyanation of ethene to give propanenitrile.⁹⁹ The butadiene cycle must be quite similar in most aspects. Scheme 9.14 shows the major steps in propanenitrile formation. The L ligand is typically a phosphite, such as $P(O-o\text{-tolyl})_3$, which possesses a large cone angle ($\theta = 141^\circ$). Such a large value of θ seems to promote the dissociation of L in the precatalyst NiL_4

⁹⁹R. J. McKinney and D. C. Roe, *J. Am. Chem. Soc.*, **1986**, *108*, 5167.

and also assists RE in the last step (step **e**). Phosphites also possess relatively high χ values, which helps to stabilize the electron-rich Ni(0) complex that forms after RE.

Step **a** involves OA of HCN to give an 18-electron complex. Steps **b** and **c** involve loss of phosphite ligand, followed by migratory 1,2-insertion of ethene into a Ni–H bond, which is driven by the presence of excess ethene. Step **e** requires a RE to give product and regenerate the active Ni(0) catalyst species. Investigation showed that step **e** must have been preceded by complexation of L (step **d**) to give an 18-electron intermediate. This amounts to RE by a relatively rare associative mechanism (see Section 7-3). Researchers pointed out that the addition of one more equivalent of phosphite both increased steric hindrance, which is relieved by RE, and provided another electron-withdrawing ligand that stabilized the electron-rich Ni(0) complex resulting from RE.

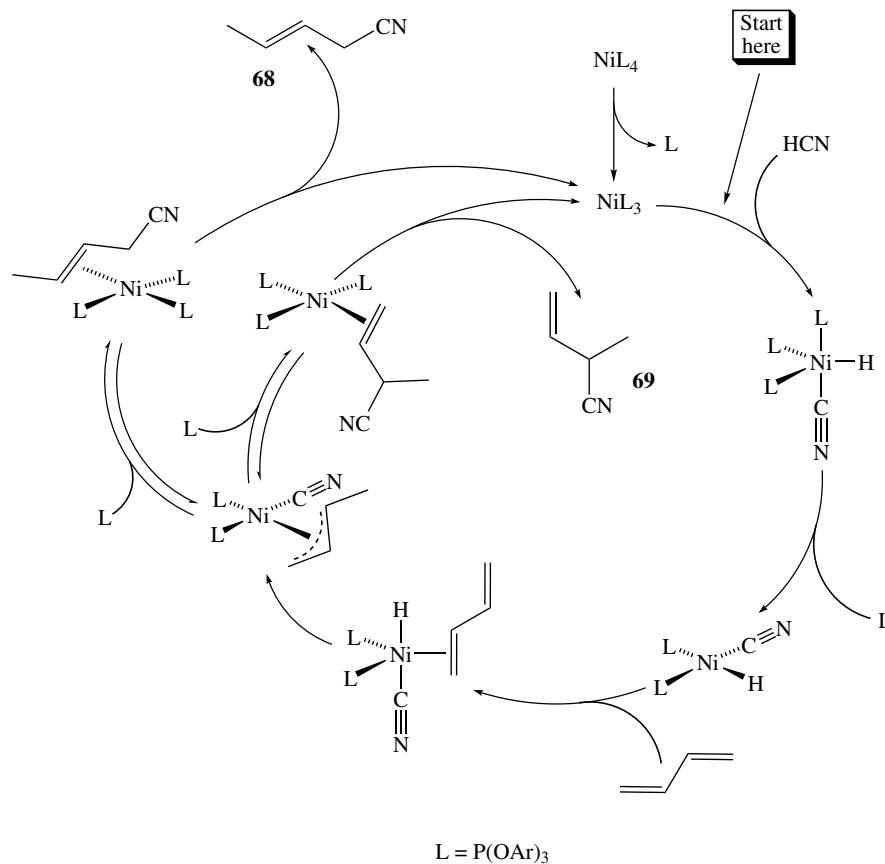
Scheme 9.15 shows the cycles that are assumed to represent conversion of 1,3-butadiene to either **68** or **69**, which are quite similar to that for ethene hydrocyanation.¹⁰⁰ Intermediates in these cycles, however, consist of η^2 -butadiene complexes or η^3 -allyl complexes that form after insertion of one of the C=C bonds of the diene into the Ni–H bond.

The isomerization of **69** to **68** is of interest to chemists. A French group has studied the isomerization using a Ni(II) complex **73**, which they generated *in situ* from a combination of Ni(COD)₂, **69**, and bis(diphenylphosphino)butane (dppb).¹⁰¹ Isomerization of **69** to **68** in the presence of a catalytic amount of **73** occurred with 97% conversion and 83% selectivity for the formation of **68**. DFT-B3LYP MO calculations performed by the same group supported a catalytic cycle shown in Scheme 9.16. Here PH₃ was substituted for dppb to make high-level calculations accessible. Steps **b** and **e** represent C–CN bond breaking (a relatively rare C–C bond activation, see Section 7-2-1) and formation (RE), respectively. Other experimental work has supported the feasibility of step **b**.¹⁰² Although the chemistry shown in Scheme 9.16 may not represent exactly the mechanism that occurs under the real-world circumstances of the Dupont process, it represents a reasonable scenario for a Ni(0)-catalyzed isomerization that could occur under mild conditions.

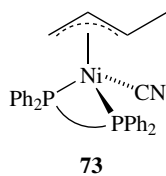
¹⁰⁰See Footnote 99.

¹⁰¹A. Chaumonnot, F. Lamy, S. Sabo-Etienne, B. Donnadieu, B. Chaudret, J.-C. Barthalat, and J.-C. Galland, *Organometallics*, **2004**, 23, 3363.

¹⁰²N. M. Brunkan, D. M. Brestensky, and W. D. Jones, *J. Am. Chem. Soc.*, **2004**, 126, 3627.

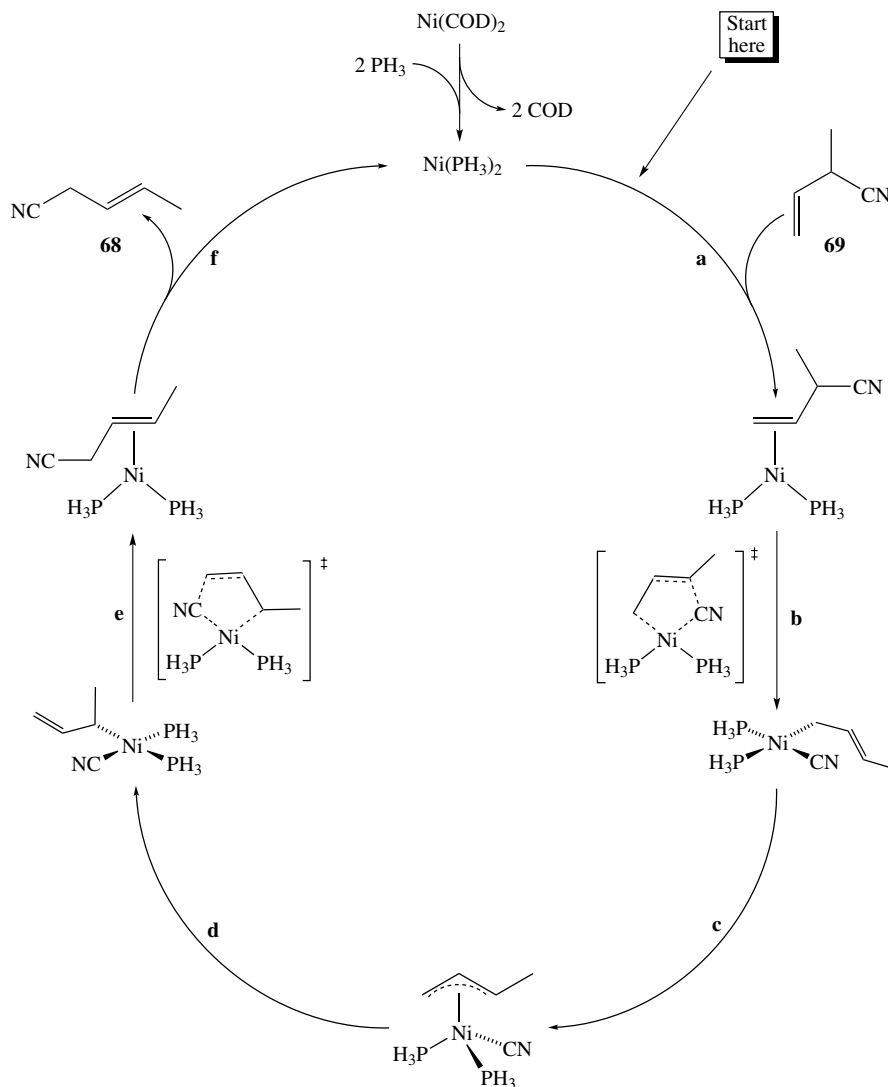


Scheme 9.15
Catalytic Cycles for
Hydrocyanation of
1,3-Butadiene



Studies have shown that bidentate phosphine and phosphite ligands have improved selection for **68** over **69**.¹⁰³ Such ligands, with β_n values of around 109° ,

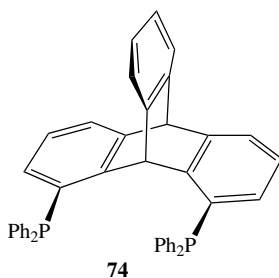
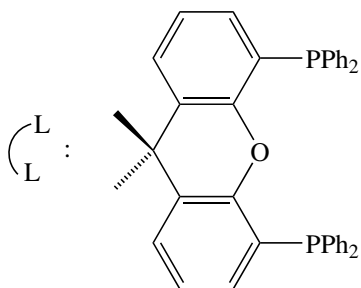
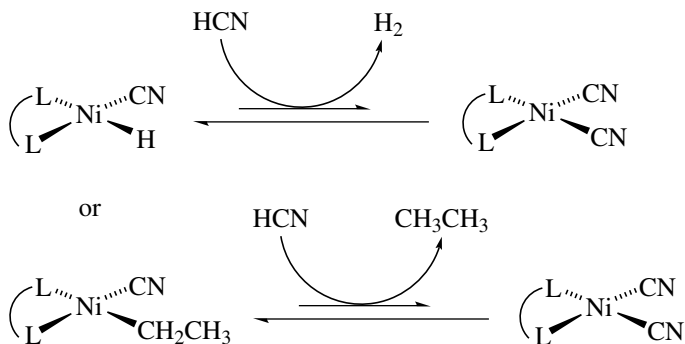
¹⁰³P. W. N. M. van Leeuwen, *Homogeneous Catalysis: Understanding the Art*, Kluwer Academic: Dordrecht, The Netherlands, 2004, pp. 233–236, and references therein.

**Scheme 9.16**

Catalytic Cycle for Isomerization of **69** to **68**

seem to destabilize square planar $\text{Ni}(\text{II})$ complexes that might form according to equation 9.41. The resulting dicyano–Ni complexes that form here after a second OA of HCN are incapable of being regenerated to a catalytically active species, so it is vital that such reactions be suppressed. A $\text{Ni}(0)$ complex of COD and bidentate ligand **74** proved to be particularly successful in catalyzing the conversion of 1,3-butadiene to a 97.5/2.5 ratio of **68** to **69**.¹⁰⁴

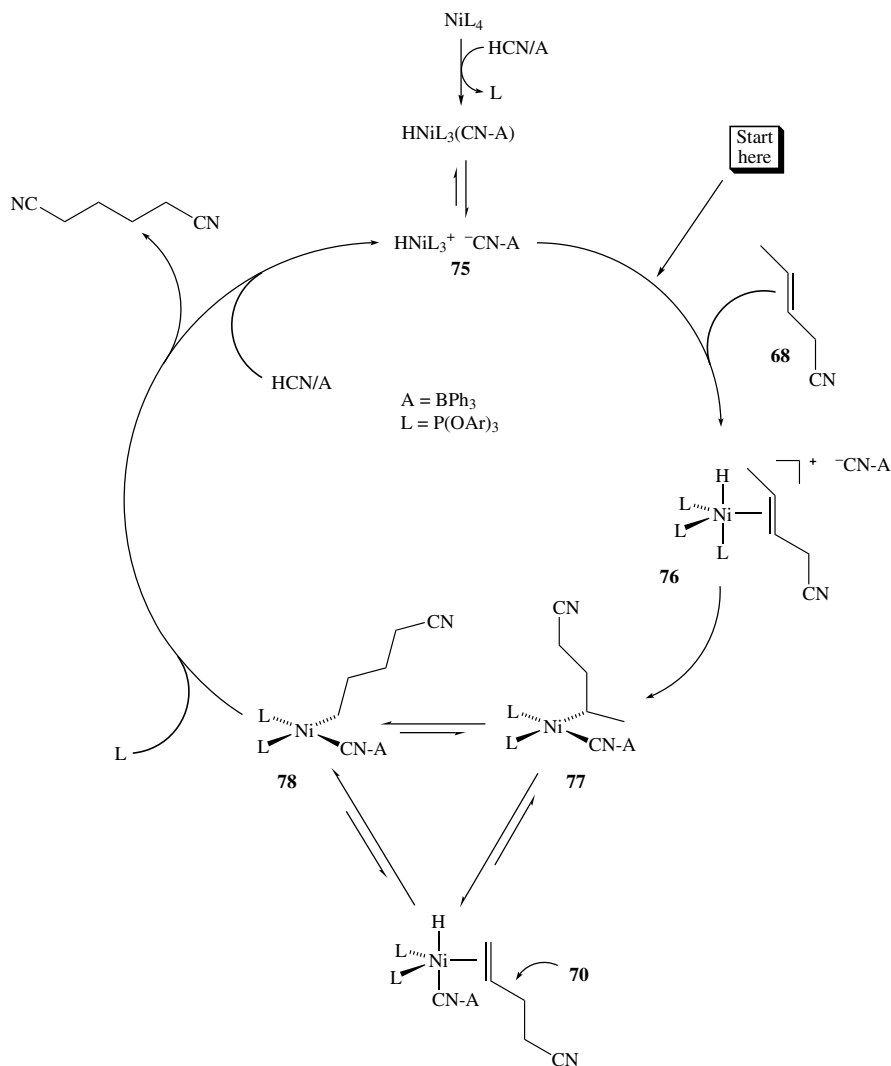
¹⁰⁴L. Bini, C. Müller, J. Wilting, L. von Chrzanowski, A. L. Spek, and D. Vogt, *J. Am. Chem. Soc.*, **2007**, *129*, 12622.



Why does the incorporation of a rigid, diphosphine ligand with β_n of about 110° cause destabilization of square planar Ni(II) complexes?

Exercise 9-12

The last steps in hydrocyanation of 1,3-butadiene involve first isomerization to **70** and then anti-Markovnikov addition of HCN to the remaining C=C bond,

**Scheme 9.17**

The Final Steps in
Hydrocyanation of
1,3-Butadiene

according to a catalytic cycle presumably similar to that shown in Scheme 9.14. The role of a Lewis acid promoter such as BPh_3 in these end steps is not completely clear. BPh_3 may bind to the nitrogen end of a CN ligand (Scheme 9.17), causing dissociation of the CN– BPh_3 ligand from the Ni to give a cationic nickel hydride complex **75** that can bind **68** to yield complex **76**. 1,2-Insertion and β -elimination complete the cycle to give **70**. The presence of the sterically bulky CN– BPh_3 ligand also favors formation of the less sterically hindered complex **78** over more sterically congested **77**, thus allowing adiponitrile to form in the last step as a result of RE.¹⁰⁵

¹⁰⁵G. W. Parshall and S. D. Ittel, *Homogeneous Catalysis*, 2nd ed., Wiley–Interscience: New York, 1992, pp. 42–47.

9-7 SPECIALTY CHEMICALS

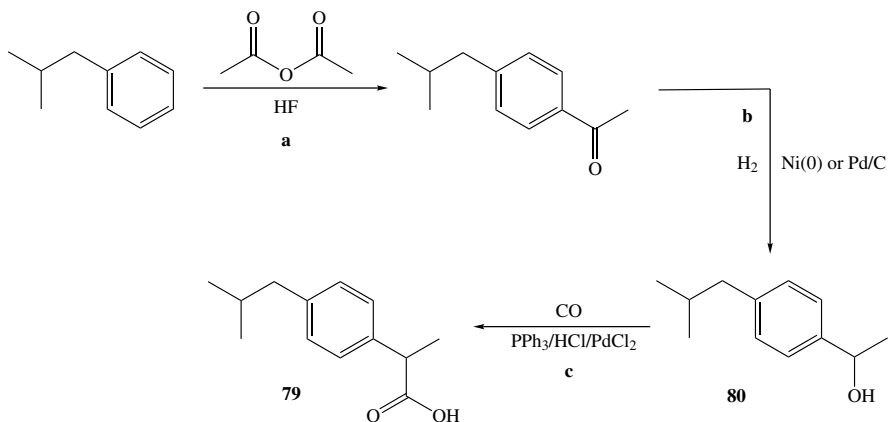
As the science of organometallic chemistry has developed over the past decades, it has become apparent that transition metal complexes can serve as extremely efficient and highly selective catalysts. These catalysts can control not only the chemoselectivity of the reaction but also its regio- and, more important, stereoselectivity.

The demand for new compounds that can alleviate human ailments and safely control agricultural pests continues to increase. Many of these compounds are chiral, sometimes possessing several stereogenic centers. Usually only one enantiomer or diastereomer is active. Racemic modifications are often unacceptable because 50% of the drug or pesticide is at best useless and sometimes even toxic to the patient or the environment. The chemical industry and especially manufacturers of pharmaceuticals and agricultural chemicals have focused their efforts recently on developing homogeneous catalysts that can control the selectivity of key steps in the synthesis of these specialty compounds.¹⁰⁶ Although the expense of catalyst material and the cost of developmental research are both high in designing these selective catalysts, the payoff resulting from successful efforts can be enormous.

In these endeavors, therefore, selectivity becomes ever more important because unselective reactions generate waste products that sometimes cost more to dispose of than the original cost of the starting materials.¹⁰⁷ Moreover, these waste materials are often quite toxic. The atom economy principle of green chemistry dictates that the sustainable approach is to design chemical processes so that all or almost all of the atoms put into a chemical reaction end up in the desired product. The use of homogenous transition metal catalysts can be of tremendous benefit in maximizing atom economy, enhancing all three types of selectivity, and minimizing waste production. The rest of this section will briefly explore three examples where homogeneous catalysis played a major role in the successful synthesis of biologically important molecules of commercial significance.

¹⁰⁶Specialty chemicals are also called fine chemicals. Fine chemicals possess relatively complex structures, sometimes with several stereogenic centers; are produced on a smaller scale than bulk petrochemicals, such as acetic acid (<10,000 tons/year); and their synthesis often involves several chemical steps. For a good summary on the role of Pd catalysts in the synthesis of fine chemicals, see A. Zapf and M. Beller, *Top. Catal.*, **2002**, *19*, 101.

¹⁰⁷There is an inverse relationship between the scale of chemical production and the percentage of waste products generated. Synthesis of petrochemicals on a scale of billions of pounds generates a very small amount of waste compared with the volume of starting material. On the other hand, for every pound of a drug produced there could be hundreds of pounds of waste generated (resulting in a very unfavorable *E*-factor, which is the ratio of the total mass of waste to the total mass of desired product).

**Scheme 9.18**

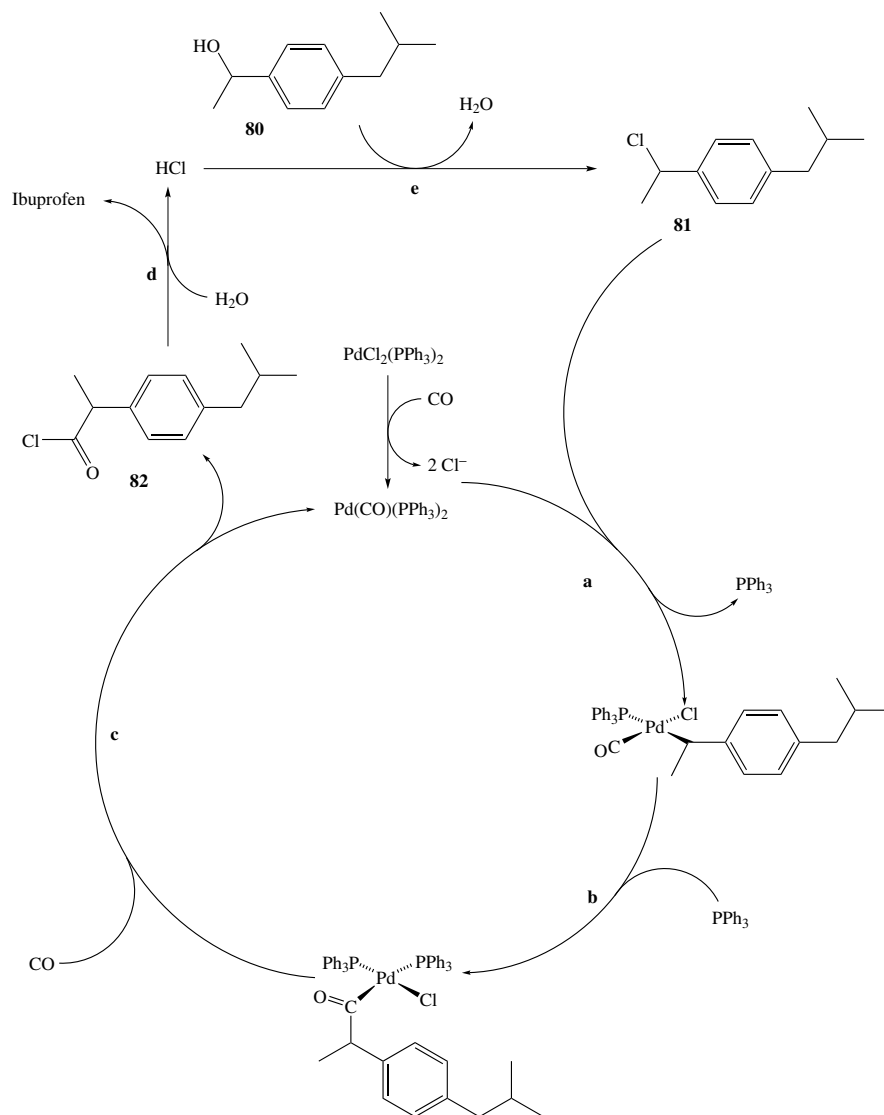
The Boots–Hoechst–Celanese Process for Ibuprofen Synthesis

9-7-1 Ibuprofen

Ibuprofen (**79**) is one of the most useful over-the-counter drugs in the world. Classified as a nonsteroidal anti-inflammatory drug (NSAID), ibuprofen (sometimes called “Vitamin I”) was developed in the 1960s by the Boots Pure Drug Company in England to treat pain and inflammation. The Boots synthesis involved six steps that unfortunately had an overall atom economy of only 40%, meaning that 60% of the starting materials ended up as unrecoverable waste. Once the original patents on the Boots process expired, Boots collaborated with the Hoechst–Celanese Company to develop a much more efficient process. By the early 1990s, this collaboration resulted in a highly efficient three-step process shown in Scheme 9.18.¹⁰⁸

Step **a** involves a Friedel–Crafts acylation where HF serves as the catalyst and the solvent for the reaction. Although HF is highly toxic, it can be contained on an industrial scale and completely recycled. The acetic acid by-product can also be recycled. The second step (**b**) involves heterogeneously-catalyzed hydrogenation of a carbonyl group to give the corresponding alcohol **80** with an atom economy of 100%. Either palladium on charcoal or Raney–nickel can be used as a catalyst. Step **c** is an excellent example of an alcohol carbonylation that we saw earlier in Section 9-5; this process, like carbonylation of methanol, has an atom economy of 100%. The overall atom economy of the new process, which

¹⁰⁸For information on the differences between the Boots and the Boots–Hoechst–Celanese syntheses of ibuprofen, see G. Rothenberg, *Catalysis: Concepts and Green Applications*, Wiley–VCH Verlag: Weinheim, Germany, 2008, pp. 22–23, and M. A. Matthews, “Green chemistry,” in *Kirk-Othmer Encyclopedia of Chemical Technology*, 5th ed., Wiley: New York, 2001, pp. 799–818 (there is an online version of this encyclopedia that is continually upgraded).

**Scheme 9.19**

Catalytic Cycle for the Carbonylation Step of the Boots-Hoechst-Celanese Synthesis of Ibuprofen

produces about 3500 tons/year of ibuprofen, is 77%; however, if the recycling of acetic acid is taken into account, the atom economy is close to 100%.¹⁰⁹

The homogeneously-catalyzed process involved with step **c** will be the focus of the following discussion. Note here that a Pd catalyst was used instead of one containing Rh or Ir, but the steps of the catalytic process are very similar to those for methanol carbonylation. Scheme 9.19 outlines the catalytic cycle.

¹⁰⁹In 1997, the developers of the Boots-Hoechst-Celanese process were awarded the Presidential Green Chemistry Award, sponsored by the U.S. Environmental Protection Agency.

The precatalyst is $\text{PdCl}_2(\text{PPh}_3)_2$, which is converted to $\text{Pd}(\text{CO})(\text{PPh}_3)_2$ under the reducing conditions of the reaction. Once the catalyst is generated, benzyl chloride **81**, generated from a secondary cycle involving steps **d** and **e**, enters the cycle and undergoes OA (step **a**). Migratory CO insertion (step **b**) precedes RE (step **c**), which regenerates the catalyst and produces acid chloride **82**. Hydrolysis of **82** (step **d**) yields ibuprofen and HCl, which then reacts with alcohol **80** to produce **81**.¹¹⁰

Ibuprofen possesses a stereogenic center, and studies have shown that (*S*)-ibuprofen is the active enantiomer. A chiral synthesis of (*S*)-ibuprofen, which is suitable for an industrial scale, has been developed by the Cheminor Company in India.¹¹¹ Subsequent biochemical studies of racemic ibuprofen in mammalian tissue, however, have shown that there is an isomerase enzyme available in the body that can convert the *R*-enantiomer to (*S*)-ibuprofen.¹¹² Since this discovery, enthusiasm for the production of chiral ibuprofen has waned. Racemic ibuprofen is the only form of the drug that is currently readily available.

9-7-2 (*S*)-Metolachlor

(*S*)-Metolachlor is the active ingredient of the herbicides Dual and Bicep, which are widely applied in the United States and were developed by the Swiss company Ciba–Geigy (now Novartis). The steric hindrance near the aryl–N bond restricts rotation about that bond. This restricted rotation results in a type of stereoisomerism called *atropisomerism*, resulting in *aR* and *aS* configurations about the chiral aryl–N bond axis.¹¹³ There is also a stereogenic center (position *I*) on a carbon next to the N-atom in the amino side chain. All four possible stereoisomers of metolachlor are shown in Figure 9-3.

It turns out that only the isomers with the *S*-configuration at position *I* are active herbicides, regardless of the configuration of the chiral axis (*aR* or *aS*).

Scheme 9.20 illustrates the last key steps in the synthesis of (*S*)-metolachlor. Early on, researchers at Novartis turned their attention to creating conditions for an asymmetric, homogeneous, metal-catalyzed hydrogenation of imine **83** to

¹¹⁰For more details on the catalytic cycle, see R. A. Sheldon, I. Arends, and U. Henefeld, *Green Chemistry and Catalysis*, Wiley–VCH Verlag: Weinheim, Germany, 2007, pp. 247–249 and E. J. Jang, K. H. Lee, and Y. G. Kim, *J. Mol. Catal. A*, **1999**, 138, 25.

¹¹¹A. S. Bommarius and B. R. Riebel-Bommarius, *Biocatalysis: Fundamentals and Applications*, Wiley–VCH Verlag: Weinheim, Germany, 2004, p. 578.

¹¹²C. Reichel, R. Brugger, H. Bang, G. Geisslinger, and K. Brune, *Mol. Pharmacol.*, **1997**, 51, 576.

¹¹³The descriptor “a” stands for axis or axial. Molecules that exhibit atropisomerism are chiral because of the presence of a chiral axis rather than a chirality center. For a discussion of chiral axes and atropisomerism, see E. L. Eliel and S. H. Wilen, *Stereochemistry of Organic Compounds*, Wiley–Interscience: New York, 1994, Chap. 14.

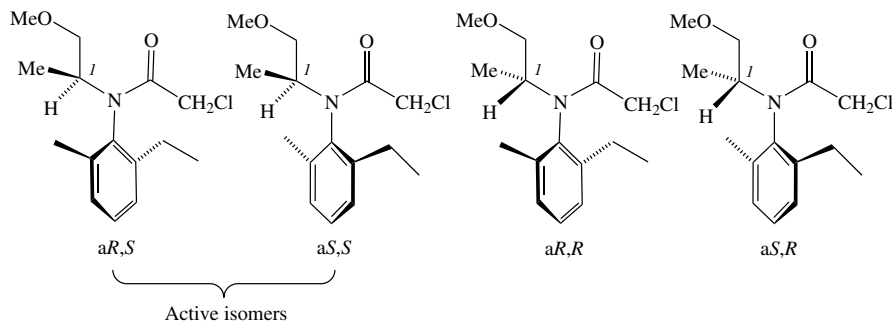
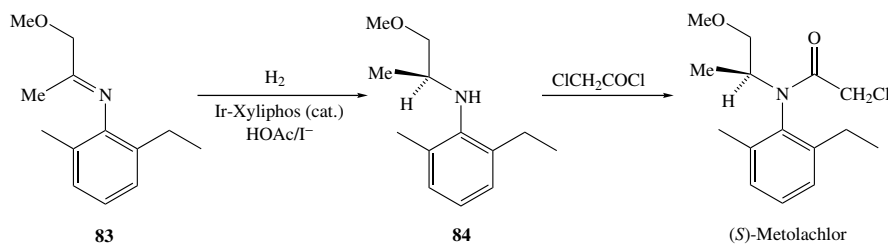


Figure 9-3

Stereoisomers of
Metolachlor

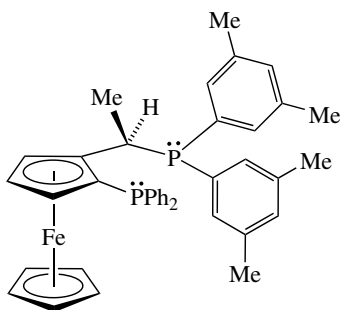
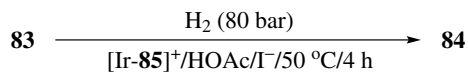
Scheme 9.20

Final Steps in
the Synthesis of
(*S*)-Metolachlor

amine **84**. It took considerable effort over almost a 20-year period for Novartis chemists to determine that a cationic Ir catalyst would be most suitable. For chirality to be induced during the hydrogenation, a chiral environment must exist during the addition of H₂ to the C=N bond. Chiral bisphosphine ligands, such as DIPAMP used in the synthesis of L-Dopa, must be attached to the metal catalyst to provide that environment. A search of possible ligands eventually zeroed in on bisphosphine **85**, a so-called *Josiphos* ligand that is a ligand based on ferrocene and is also known as *xyliphos*.¹¹⁴ Equation 9.42 details the final reaction conditions developed for asymmetric hydrogenation of **83**.

Regardless of the ultimate success of (*S*)-metolachlor as a herbicide, the development of the key asymmetric hydrogenation step was a significant triumph in transition metal homogeneous catalysis on an industrial scale. The process is considered the largest application of asymmetric catalysis in terms of amount of product produced (a production capacity of 10,000 tons/year). The process is characterized by an extremely high TOF (>1.8 × 10⁶/hour) and a very favorable substrate/catalyst ratio of 10⁶ to 1. Even though the ee of the process is only about 80%, this is acceptable for the final application in the field; higher

¹¹⁴For an article on the discovery and development of *Josiphos* ligands, eponymously derived from the first name of the chemist who first synthesized them, see H.-U. Blaser, W. Brieden, B. Pugin, F. Spindler, M. Studer, and A. Togni, *Top. Catal.*, **2002**, *19*, 3.



85: Xyliphos (Josiphos)

9.42

values of ee can be achieved, but with less favorable TOF and substrate/catalyst ratios.¹¹⁵

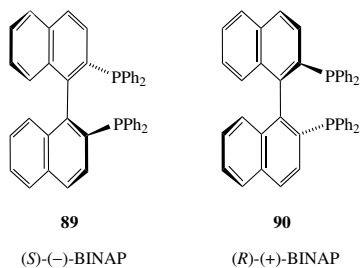
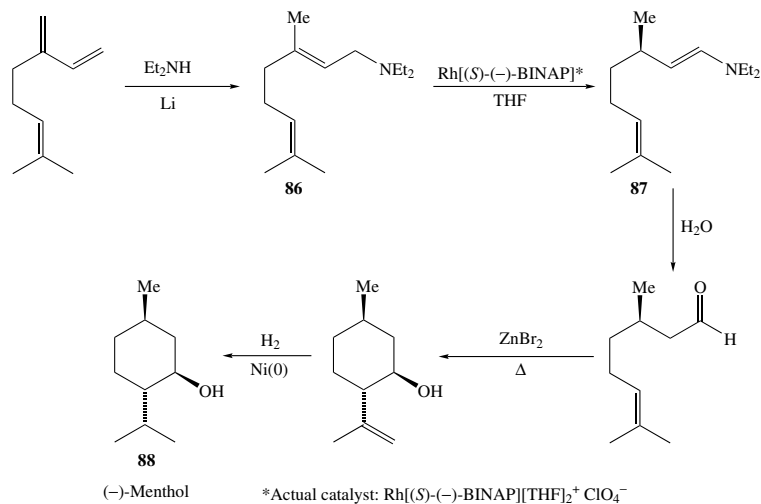
9-7-3 (-)-Menthol

(-)-Menthol (**88**) is an important fragrance ingredient that finds use as a food additive and in cold remedies. Although it is obtainable from natural sources, workers at the Takasago Perfumery in Japan developed a route to **88** outlined in Scheme 9.21.¹¹⁶ Run on a 3000–4000 ton/year scale, the process now accounts for about one third of the world's supply of (-)-menthol. The key step in the synthesis is the stereoselective isomerization of (*E*)-vinylamine **86** to enamine **87**. This step induces chirality at the 3-position and is catalyzed by [Rh(*S*)-(-)-BINAP(COD)]ClO₄, where (*S*)-(-)-BINAP (**89**) is a now well-known chiral bisphosphine ligand. The enantiomeric (*R*)-(+)-ligand is also shown as structure **90** in Scheme 9.21.

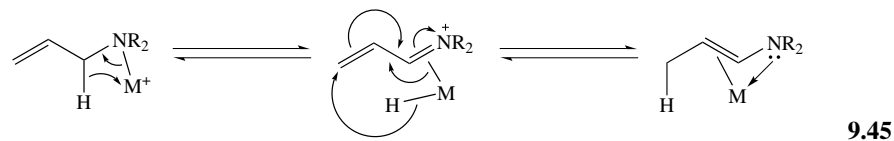
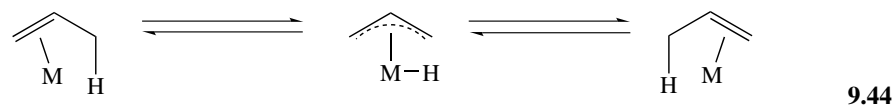
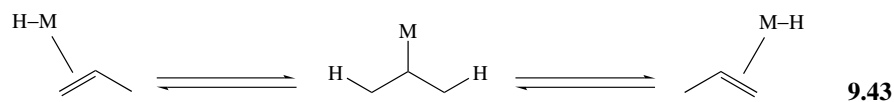
Double bond migration such as that involved in **86** going to **87** is an important reaction, useful on both an industrial and a laboratory scale; its mechanism has been well studied. Equations 9.43 and 9.44 describe two major pathways for migration, the former involving metal hydride insertion and β-elimination steps

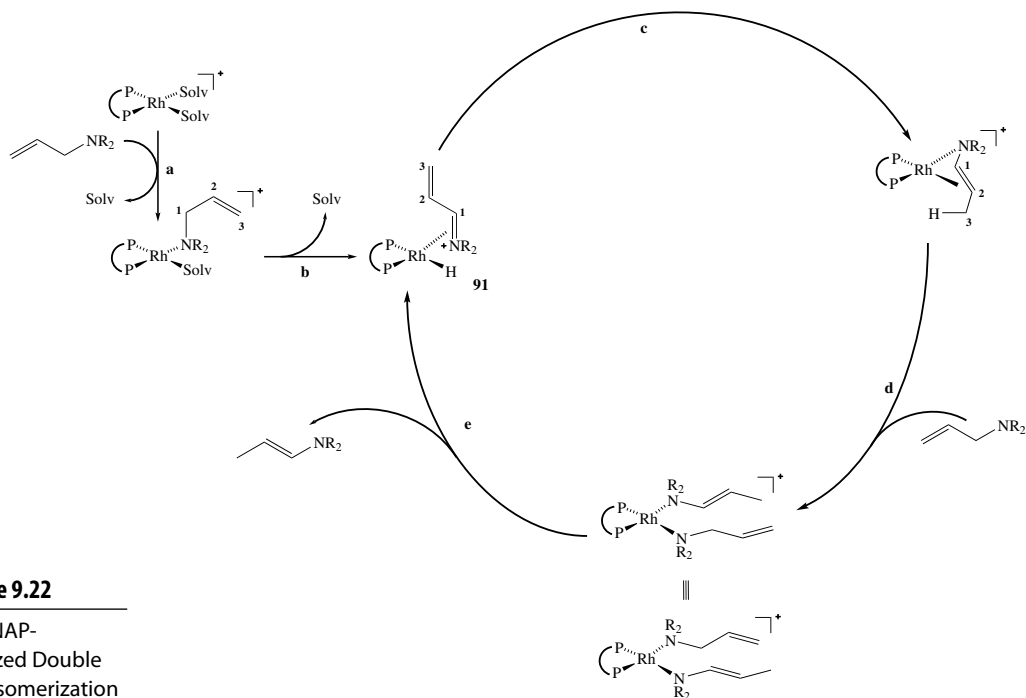
¹¹⁵For a rendition of the story behind the research and development of the asymmetric hydrogenation in the synthesis of (*S*)-mentolachlor, see H.-U. Blaser, *Adv. Synth. Catal.*, **2002**, 344, 17.

¹¹⁶S. Inoue, H. Takaya, K. Tani, S. Otsuka, T. Sato, and R. Noyori, *J. Am. Chem. Soc.*, **1990**, 112, 4897 and R. Noyori and H. Takaya, *Acc. Chem. Res.*, **1990**, 23, 345.

**Scheme 9.21**Chiral Synthesis of
(-)-Menthol

and the latter a 1,3-hydride shift via a $\eta^3 \pi$ -allyl intermediate. The researchers at Takasago proposed a third mechanism for bond migration, outlined in equation 9.45, which they termed “nitrogen triggered.”



**Scheme 9.22**

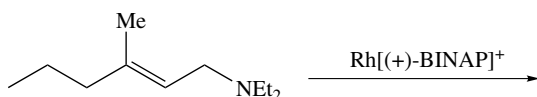
Rh-BINAP-
Catalyzed Double
Bond Isomerization

Scheme 9.22 describes the nitrogen-triggered pathway. Steps **a** and **b** provide an activated Rh-BINAP complex (**91**) by associative substitution of solvent (EtOH or THF) and substrate followed by β -elimination to form an iminium complex. The stereochemically key step, **c**, adds a proton to the 3-position and gives the complexed enamine. In step **d**, the η^3 enamine ligand shifts to η^1 as a new molecule of allyl amine adds to the complex. The nitrogen plays a key role in activating the Rh, particularly in step **d**, the rate-determining step of the overall cycle. Step **e** liberates enamine product and regenerates **91**.¹¹⁷

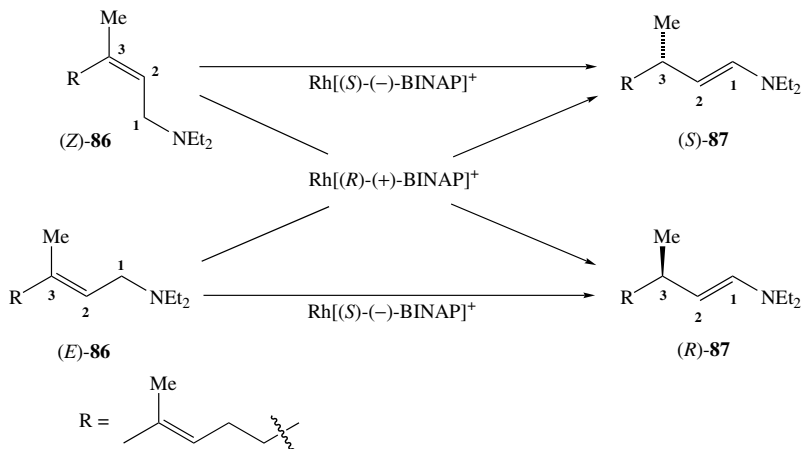
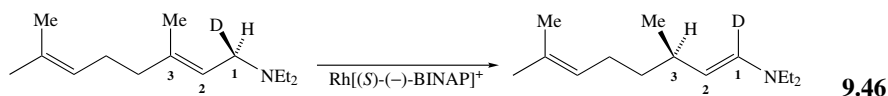
¹¹⁷A later paper by workers associated with the Takasago process reported on *ab initio* MO calculations for the catalytic cycle. Their work suggested that steps **b** and **c** (Scheme 9.22) involved an intramolecular OA of C-H, followed by a RE in which the hydride ligand attached itself to the terminal carbon of the allyl group. See M. Yamakawa and R. Noyori, *Organometallics*, **1992**, *11*, 3167. It is not clear which pathway is correct because the theoretical study used only PH_3 and not BINAP to model the Rh-catalyzed isomerization. See also C. Chapuis, M. Barthe, and J.-Y. de Saint Laumer, *Helv. Chim. Acta*, **2001**, *84*, 230.

Predict the product of the following transformation. Indicate the expected stereochemistry of the product.

Exercise 9-13



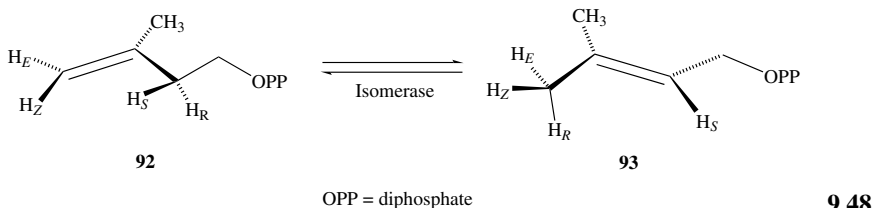
The isomerization of the double bond in the synthesis of (–)-menthol is stereospecific. Evidence obtained using vinyl amine specifically deuterated at C-1 indicates that the transfer of a proton from C-1 to C-3 is suprafacial,¹¹⁸ as indicated by equation 9.46. Equation 9.47 illustrates how the chirality of the BINAP ligand and the stereochemistry of the trisubstituted double bond in **86** control the stereochemistry of the methyl group at C-3 in **87** upon double bond migration.



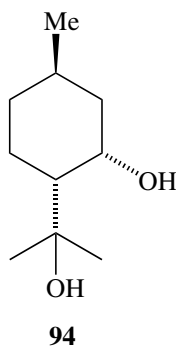
¹¹⁸With regard to sigmatropic shifts such as a 1,3-hydride shift, the word “suprafacial” means that the migrating group moves along the same face of the π system from one end to the other. An “antarafacial” migration results in the movement of the group to the opposite face of the π system. See J.E. McMurry, *Organic Chemistry*, 7th ed., Thompson–Brooks/Cole: Belmont, CA, 2008, Chapter 30, especially pp. 1191–1195, and F. A. Carey and R. J. Sundberg, *Advanced Organic Chemistry Part A*, 5th ed., Springer Scientific: New York, 2007, Chap. 10, especially pp. 911–935, for a more detailed definition accompanied by other examples.

A Biological Double Bond Migration

It is interesting to note that this Rh-catalyzed isomerization mimics a similar double bond migration found in nature in the biosynthesis of cholesterol and terpenes in which isopentenyl diphosphate (**92**) is converted reversibly to dimethylallyl diphosphate (**93**), shown in equation **9.48**.¹¹⁹ The stereochemistry of this reaction is also suprafacial.



The Rh-catalyzed isomerization step of the Takasago synthesis of (–)-menthol is highly efficient. With modification of the catalyst precursor (still based on BINAP and its derivatives), the % ee has risen to 99% with a TON of up to 400,000 (if catalyst recycling occurs). The isomerization step is also useful in producing precursors to (+)-*cis-p*-menthane-3,8-diol (**94**), which shows promise as an insect repellent that could replace DEET, the most common repellent sold today.¹²⁰



¹¹⁹For a good discussion of the role of double bond isomerization in steroid and terpene biosynthesis, see C. D. Poulter and H. C. Rilling, "Prenyl Transferases and Isomerases," In *Biosynthesis of Isoprenoid Compounds*, Vol. 1, J. W. Porter and S. L. Spurgeon, Eds., Wiley: New York, 1981, pp. 161–224.

¹²⁰For more information on the Takasago (–)-menthol synthesis, see H. Kumobayashi, *Recl. Trav. Chim. Pays-Bas*, **1996**, *115*, 201; C. Chapis and D. Jacoby, *Appl. Catal. A*, **2001**, *221*, 93; and G. P. Chiusoli and P. M. Maitlis, *Metal-Catalysis in Industrial Organic Processes*, RSC Publishing: Cambridge, 2006, pp. 103–107.

The syntheses of ibuprofen, (*S*)-metolachlor, and (–)-menthol represent only three of the numerous uses of soluble transition metal complexes to catalyze, often stereoselectively, key steps in the production of biologically important compounds in the laboratory or on an industrial scale. Discussions in Chapter 12, especially with regard to asymmetric conditions, will explore more fully the use of these catalysts in the synthesis of other organic compounds.

Suggested Readings

General References on Homogeneous Catalysis

- G. Rothenberg, *Catalysis: Concepts and Green Applications*, Wiley–VCH: Weinheim, Germany, 2008. An excellent resource for those interested in green chemistry.
- R. A. Sheldon, I. Arends, and U. Hanefeld, *Green Chemistry and Catalysis*, Wiley–VCH: Weinheim, Germany, 2007.
- J. Hagen, *Industrial Catalysis: A Practical Approach*, 2nd ed., Wiley–VCH: Weinheim, Germany, 2006.
- G. P. Chiusoli and P. M. Maitlis, *Metal-Catalysis in Industrial Organic Processes*, RSC Publishing: Cambridge, 2006.
- P. W. N. M. van Leeuwen, *Homogeneous Catalysis: Understanding the Art*, Kluwer Academic: Dordrecht, The Netherlands, 2004.
- Applied Homogeneous Catalysis with Organometallic Compounds: A Comprehensive Handbook in Three Volumes*, 2nd ed., B. Cornils and W. A. Herrmann, Eds., Wiley–VCH: Weinheim, Germany, 2002.

Hydroformylation

- K.-D. Wiese and D. Obst, “Hydroformylation,” *Top. Organometal. Chem.*, **2006**, *18*, 1.
- F. Ungváry, “Hydroformylation—Homogeneous,” in *Encyclopedia of Catalysis*, I. T. Horváth, Ed., Wiley–Interscience: New York, 2003, Vol. 3, pp. 734–787.
- C. Kohlpaintner, “Hydroformylation—Industrial,” in *Encyclopedia of Catalysis*, I. T. Horváth, Ed., Wiley–Interscience: New York, 2003, Vol. 3, pp. 787–808.
- Rhodium Catalyzed Hydroformylation*, P. W. N. M. van Leeuwen and C. Claver, Eds., Kluwer Academic: Boston, 2002.
- J. J. Carbó, F. Maseras, and C. Bo, “Rhodium Diphosphine Hydroformylation,” in *Computational Modeling of Homogeneous Catalysis*, F. Maseras and A. Lledós, Eds., Kluwer Academic: Dordrecht, The Netherlands, 2002, pp. 161–187.

Wacker Oxidation

- P. M. Henry, “Palladium-Catalyzed Reactions Involving Nucleophilic Attack on π -Ligands of Palladium-Alkene, Palladium-Alkyne, and Related Derivatives,” in *Handbook of Organopalladium Chemistry for Organic Synthesis*, E.-i. Negishi, Ed., Wiley–Interscience: New York, 2002, pp. 2119–2139.

Hydrogenation

J. G. de Vries and C. J. Elsevier, Eds., *Homogeneous Hydrogenation*, Wiley-Interscience: New York, 2007, Vol. 1–3.

Carbonylation of Methanol

A. Haynes, “Acetic Acid Synthesis by Catalytic Carbonylation of Methanol,” *Top. Organomet. Chem.*, **2006**, *18*, 179.

Hydrocyanation

K. Huthmacher and S. Krill, “Reactions with Hydrogen Cyanide (Hydrocyanation),” in *Applied Homogeneous Catalysis with Organometallic Compounds*, 2nd ed., B. Cornils and W.A. Herrmann, Eds., Wiley-VCH: Weinheim, Germany, 2002 Vol. 1, pp. 468–490.

Specialty Chemicals

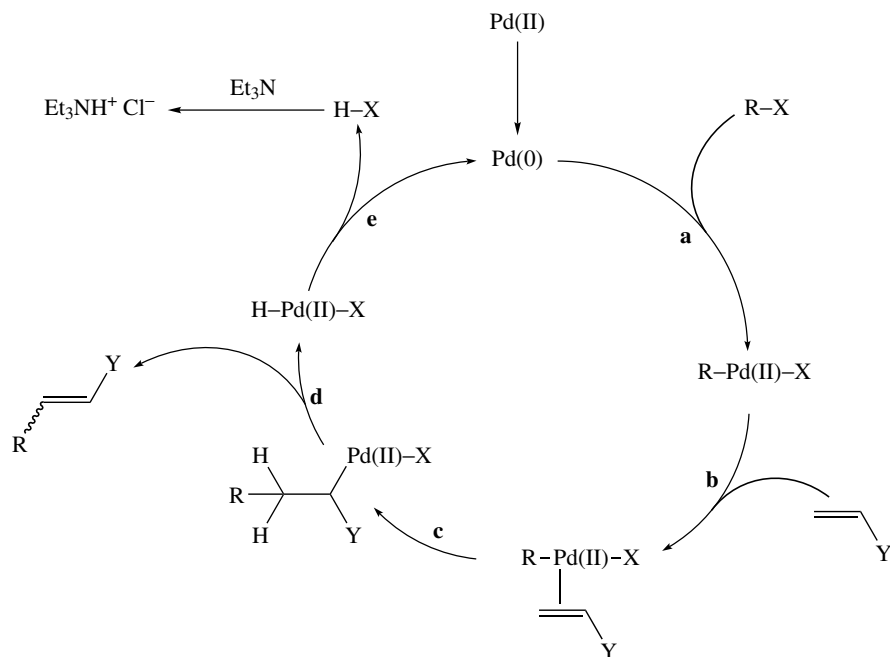
E. J. Jang, K. H. Lee, J. S. Lee, and Y. G. Kim, *J. Mol. Catal. A*, **1999**, *138*, 25 [Ibuprofen].

H.-U. Blaser, *Adv. Synth. Catal.*, **2002**, *344*, 17 [(*S*)-Metolachlor].

S. Otsuka, *Acta Chim. Scand.*, **1996**, *50*, 353 [(–)-Menthol and related compounds].

Problems

- 9-1** The complex $\text{Rh}(\text{H})(\text{CO})_2(\text{PPh}_3)_2$ can be used in the catalytic synthesis of pentanal from an alkene having one less carbon atom. Propose a mechanism for this synthesis. In your mechanism, indicate the reaction type of each step. Identify the catalytic species.
- 9-2** Increasing the concentration of CO during Co-catalyzed hydroformylation not only retards the reaction rate, but also suppresses the tendency of the reaction to add a formyl group (CHO) to a carbon other than those contained in the C=C bond of the starting alkene (i.e., an isomerization of the double bond does not occur during the catalytic cycle). Explain.
- 9-3** Propose a catalytic cycle for hydrogenation step in the production of (*S*)-metolachlor using the cationic Ir complex described in Section **9-7-2**.
- 9-4** Propose a mechanism for step **e** of Scheme **9.22**. This transformation requires more than one step. Be sure to count electrons for each species in your pathway.
- 9-5** On the next page is the catalytic cycle associated with the Heck olefination reaction. For each step marked with a letter, attach the name of one of the fundamental types of organometallic reactions (e.g., nucleophilic abstraction or ligand substitution).

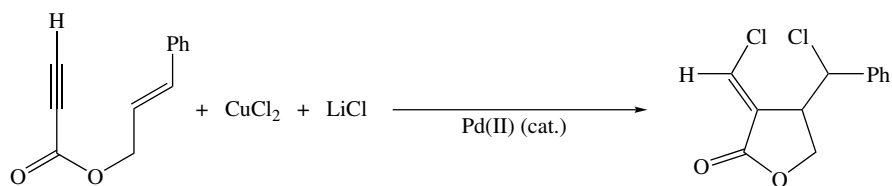


- 9-6** Consider the transformation of an alkyl bromide to an aldehyde shown below.



Assume that the reaction is catalyzed by $\text{HFe}(\text{CO})_4^-$ in an atmosphere rich in CO and H_2 . Propose a catalytic cycle that would show this catalysis and account for the formation of the two products. Label each step in your cycle with terms corresponding to the fundamental organometallic reaction types.

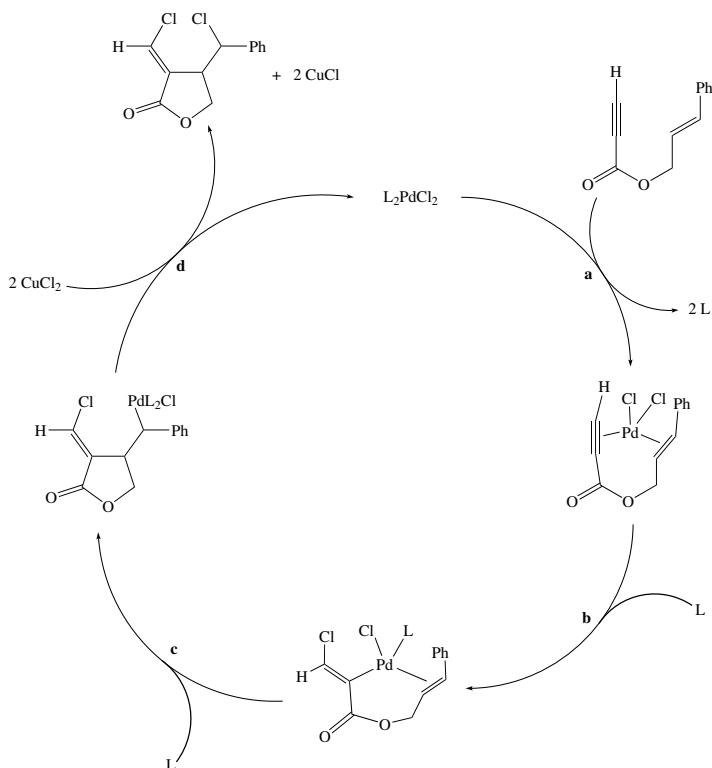
- 9-7** The transformation below is reminiscent of Wacker chemistry described in Chapter 9.



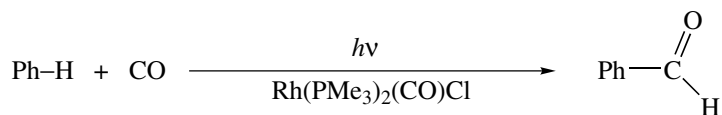
A catalytic cycle has been proposed and is shown on the next page.¹²¹ One of the steps is an example of a relatively rare type of reaction discussed in

¹²¹S. Ma and X. Lu, *J. Org. Chem.*, **1993**, 58, 1245.

Section 8-1-2. Describe in detail what is happening in each of the four major transformations in the cycle. What is the function of CuCl_2 ?



- 9-8 Catalytic, selective functionalization of hydrocarbons is one of the most important goals of organometallic chemistry. A report in the literature describes the Rh-catalyzed conversion of benzene to benzaldehyde under photochemical conditions.¹²²

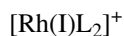
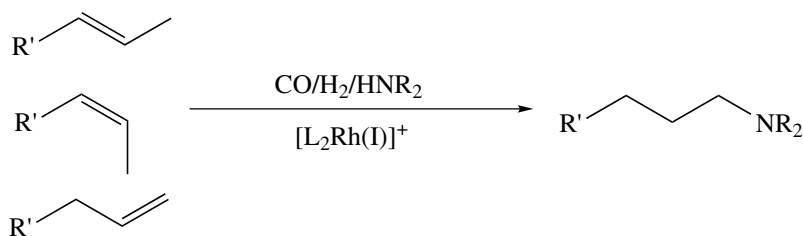


Assuming that the first step in the catalytic cycle is photoactivation of the Rh complex, propose a possible mechanism for the transformation above.

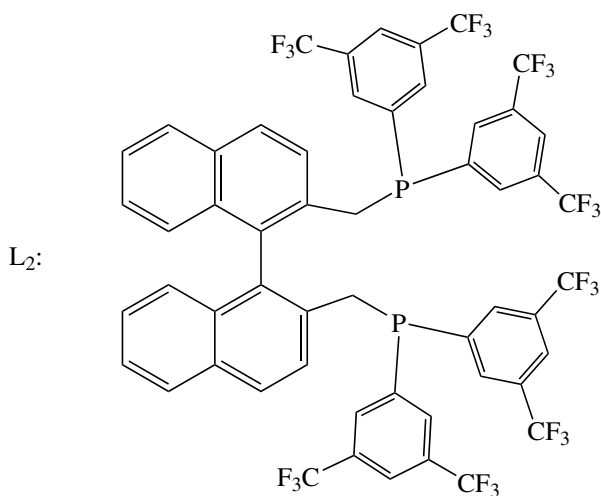
- 9-9 The transformation on the next page is called hydroaminomethylation, first reported by Reppe over 60 years ago. There are four stages to this process,

¹²²G. P. Rosini, W. T. Boese, and A. S. Goldman, *J. Am. Chem. Soc.*, **1994**, *116*, 9498.

all of which occur in the same reaction vessel! Three of these are catalyzed by the same Rh catalyst. First, internal alkenes are isomerized to terminal alkenes. Next, the terminal alkene undergoes hydroformylation with a preference for formation of linear instead of branched aldehyde. Third, the aldehyde reacts with an amine (without catalysis) to give the imine, which undergoes Rh-catalyzed hydrogenation to the amine in the last step. Assuming that the active catalyst is of the form shown in structure **1**, propose mechanisms for the isomerization of internal to terminal alkenes and for hydrogenation of the imine to amine.¹²³

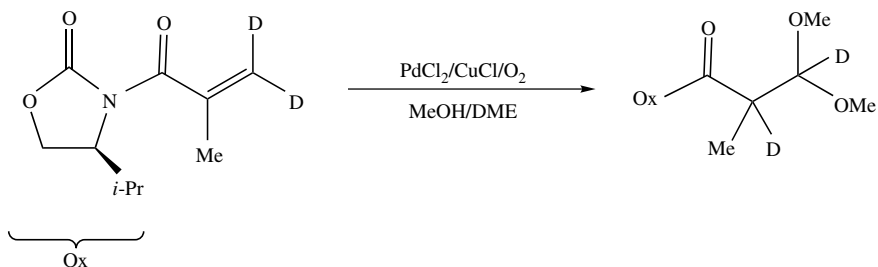


1

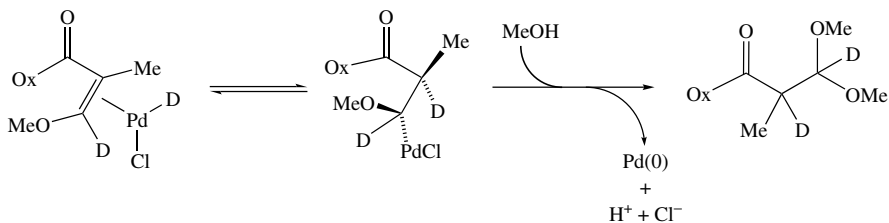


¹²³A. Seayad, M. Ahmed, H. Klein, R. Jackstell, T. Gross, and M. Bellar, *Science*, **2002**, 297, 1676, and references therein. See also J. F. Hartwig, *Science*, **2002**, 297, 1653.

- 9-10** Another promoter for step **b** (Scheme **9.12**) of the Ir-catalyzed carbonylation of methanol (Cativa process) is $[\text{PtI}_2(\text{CO})_2]$. First, draw out the structure of the Pt complex and then show how it could effect promotion of step **b** of Scheme **9.12**. What is the fate of the Pt complex during the promotion process?¹²⁴ [Hint: A diido-bridged Ir–Pt complex first forms.]
- 9-11** An interesting variation of the Wacker oxidation of an alkene is shown below.¹²⁵



A mechanism was proposed for the transformation, the last two steps of which are shown in the following scheme.

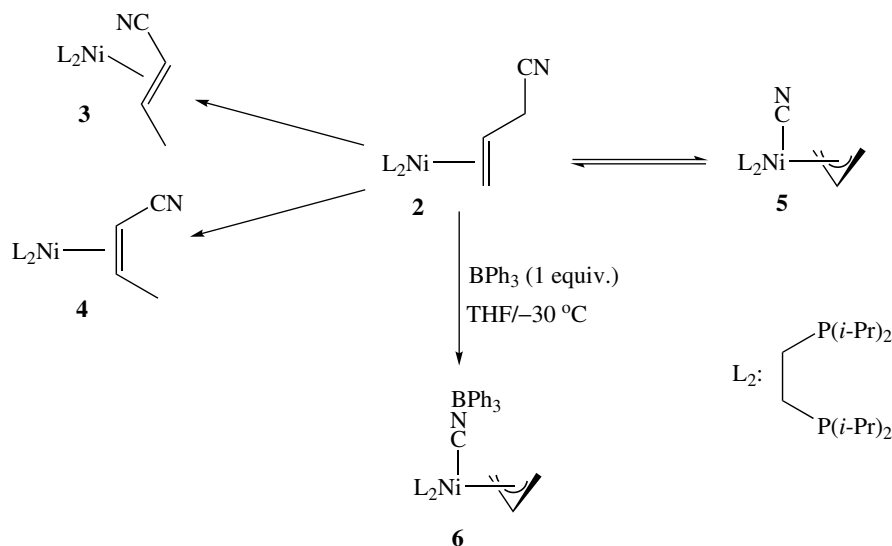


Propose a more detailed, stepwise mechanism for the last two steps. What kind(s) of fundamental organometallic reaction(s) do the steps demonstrate?

- 9-12** Consider the reaction scheme shown on the next page.

¹²⁴S. Gautron, *et al.*, *Organometallics*, **2006**, 25, 5894.

¹²⁵T. Hosakowa, T. Yamanaka, M. Itotani, and S.-I. Murahashi, *J. Org. Chem.*, **1995**, 60, 6159.

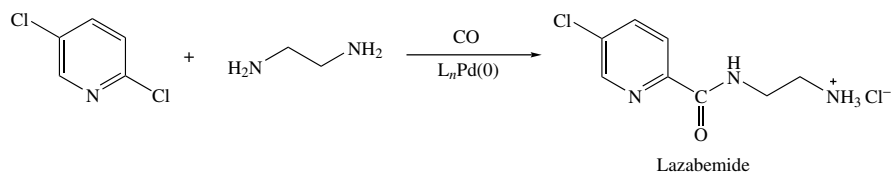


Jones and co-workers used this scheme to study C–C versus C–H bond cleavage reactions involving Ni(0) complex **2**, which is reminiscent of the chemistry involved with hydrocyanation of 1,3-butadiene.¹²⁶ At room temperature, compounds **3** and **4** form more rapidly than **5**. Over time, especially at temperatures above 25 °C, compound **5** disappears from the reaction mixture and compounds **3** and **4** are the only products. When BPh₃ was added to complex **2**, compound **6** formed exclusively and rapidly, even at –30 °C. There was no formation of complexes **3** and **4**, which would involve C–H activation, indicating that in the presence of a Lewis acid, C–C activation is faster than OA of a C–H bond.

- Show with a mechanism how compound **2** goes to **5** involving C–C bond cleavage.
- Show how the transformation of **2** to **3** and **4** involves C–H bond activation.
- Which product, **2** or **3**, ought to predominate under equilibrium conditions?
- How are the results involving the use of BPh₃ important for understanding the mechanism of the final stages of hydrocyanation of 1,3-butadiene?

¹²⁶N. M. Brunkan, D. M. Brestensky, and W. D. Jones, *J. Am. Chem. Soc.*, **2004**, *126*, 3627.

- 9-13** The Pd-catalyzed amidation shown is used to synthesize Lazabemide, a monoamine oxidase inhibitor, in 65% yield.¹²⁷ This transformation replaced an eight-step synthesis route to the same drug. Propose a catalytic cycle for this aminocarbonylation by assuming that the first step is OA of the pyridyl chloride.

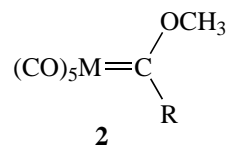
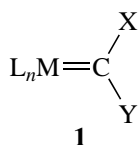


¹²⁷R. Schmid, *Chimia*, **1996**, *50*, 110.

Transition Metal–Carbene and –Carbyne Complexes

Structure, Preparation, and Chemistry

Dⁱsubstituted carbon atoms may bind directly to a transition metal, producing a formal double bond between the metal and the carbon. The divalent carbon ligand possesses distinctive properties in comparison to most of the ligands discussed in Chapters 4–6, not only with regard to its structure and bonding characteristics but also in terms of its chemistry. Complexes containing these ligands are called *metal–carbene complexes*. Metal–carbene complexes have the general structure shown in **1**, where X and Y may be alkyl, aryl, H, or heteroatoms (O, N, S, halogens). The first carbene complex (**2**, M=W) was reported by Fischer and Maasböl in 1964,¹ and since then chemists have learned much about these interesting compounds (see Section 6-1-2 for an introductory discussion of metal–carbene complexes).



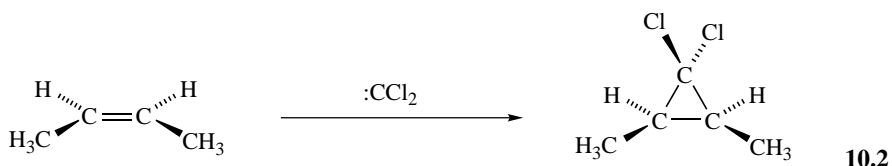
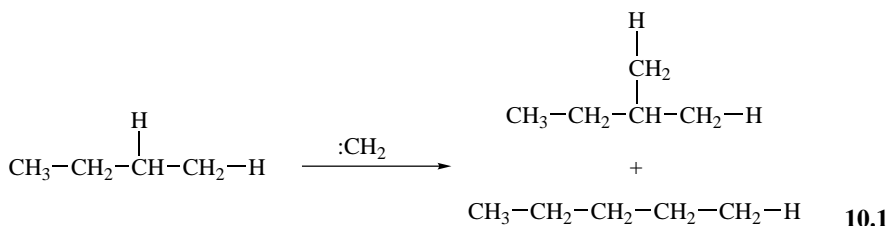
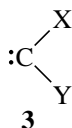
Metal–carbene complexes undergo numerous reactions, several of which are useful in the synthesis of complex organic molecules. These complexes are also intermediates in processes such as *metathesis* and *ring-opening metathesis polymerization* (Chapter 11). In Chapter 10 we will discuss the structure, synthesis, and

¹E. O. Fischer and A. Maasböl, *Angew. Chem. Int. Ed. Engl.*, **1964**, 3, 580.

chemistry of carbene complexes. Metal–carbene complexes will appear again in Chapters 11 and 12, where some of the applications of their chemistry to organic synthesis will be discussed.

10-1 STRUCTURE OF METAL CARBENES

The word “carbene” derives from the name given to free, disubstituted carbon compounds with general structure **3** (X and Y same as in **1**).² Because the central carbon atom does not possess an octet of electrons, free carbenes are electron deficient and extremely reactive. They are so reactive that some carbenes insert themselves into normally inert alkane C–H bonds (equation **10.1**) or react with alkenes to form cyclopropanes (equation **10.2**), a synthetically useful transformation.



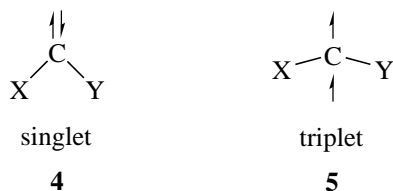
Transition metal–carbene complexes are not normally produced from free carbenes;³ moreover, they do not produce free carbenes. It is, however, useful to think of metal–carbene complexes as a construct of a free carbene and a metal

²We will call such compounds *free carbenes* to distinguish them from metal complexes possessing divalent carbon ligands.

³There is one exception to this statement. One route to the synthesis of *N*-heterocyclic carbene complexes involves complexation of the free carbene with a metal salt. Such complexes will be discussed later in this section.

fragment. Before we actually discuss the structure of carbene complexes, we will review some information regarding free carbenes.

Free carbenes exist in two different electronic states, singlet and triplet,⁴ which are represented in structures **4** and **5**. The singlet state has one lone electron pair, whereas the triplet state has two unpaired electrons.

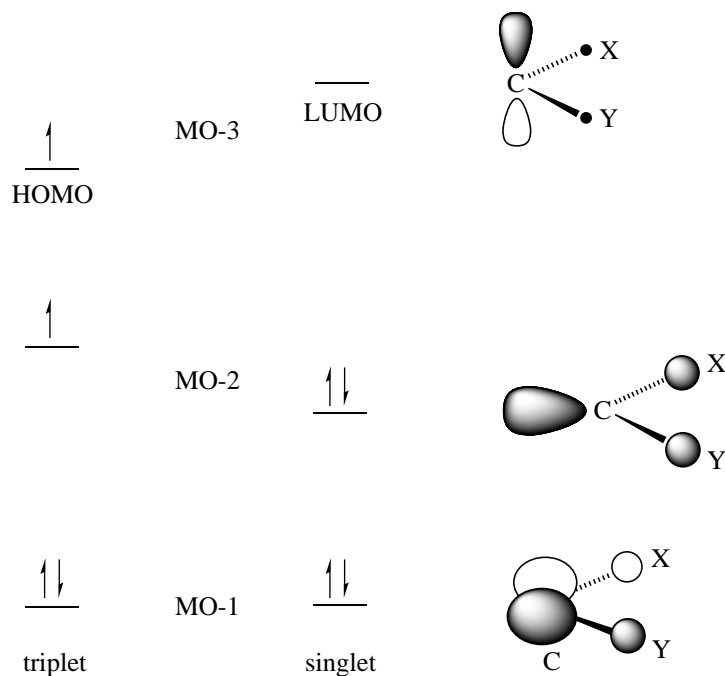


We can think of the singlet state of a free carbene, in terms of localized hybrid orbitals, as a bent molecule (**6**) harboring three sp^2 orbitals (one of which is doubly occupied and non-bonding) and an empty, perpendicularly-situated $2p$ orbital. A triplet carbene (really a diradical) would be a less bent species (**7**) with two singly-occupied, orthogonal $2p$ orbitals and two sp orbitals that are involved in bonding to substituents.



Figure 10-1 illustrates the molecular orbital picture of a free carbene. Note that for the singlet state (shown on the right side of Figure 10-1) there are two bonding orbitals, MO-1 and MO-2 (the HOMO resembles an sp^2 orbital) and a relatively low-lying empty orbital, MO-3 (the LUMO resembles a $2p$ orbital). If MO-2 and MO-3 are close in energy, the two orbitals tend to be singly occupied and a triplet state exists (shown on the left side of Figure 10-1). If the energy gap widens, then the ground state of the carbene consists of a doubly-occupied MO-2 and an empty MO-3, indicating a singlet state.

⁴The designations singlet and triplet refer to the spin multiplicity of the electronic state. Spin multiplicity is calculated by $2S + 1 = \text{multiplicity}$, where S is the total spin for all the electrons. The spin of the first electron in a pair is arbitrarily designated $+\frac{1}{2}$, with the second as $-\frac{1}{2}$. For every electron pair, $S = \frac{1}{2} + (-\frac{1}{2}) = 0$. If all electrons in a species are paired, $S = 0$, and the multiplicity is $2(0) + 1 = 1$, which signifies a singlet. On the other hand, if two electrons are unpaired, $S = \frac{1}{2} + \frac{1}{2} = 1$. The multiplicity is $2(1) + 1 = 3$, which designates a triplet.

**Figure 10-1**

Molecular Orbital
Diagram for Triplet
and Singlet Free
Carbene

X, Y = H, alkyl (usually a triplet)

X, Y = Cl, O, N, S (usually a singlet)

Whether a free carbene exists in the ground state as a singlet or as a triplet depends upon the nature of the substituents, X and Y, which bind to carbon. When X, Y = alkyl or H, the triplet state is usually the ground state. A singlet ground state occurs, on the other hand, when X and Y are heteroatoms such as N, O, S, or the halogens. Figure 10-2 illustrates the influence of a heteroatomic substituent such as Cl (the MOs shown on the left side of Figure 10-2 are the same as those in Figure 10-1). Imagine that a Cl atom mixes with a free carbene ($:\text{CH}_2$ in this case) to give $:\text{CHCl}$. The mixing results in drastic lowering in energy of MO-3 to give a new π MO called MO-3'. MO-2 is lowered slightly because of the electronegativity of Cl to give a new σ MO designated MO-2'. The result is a considerable energy gap between MO-2' (the HOMO) and MO-3' (the LUMO). The gap is large enough that a singlet (no unpaired electrons) now becomes the ground state when Cl is attached to carbon. This effect is general for all heteroatoms such as

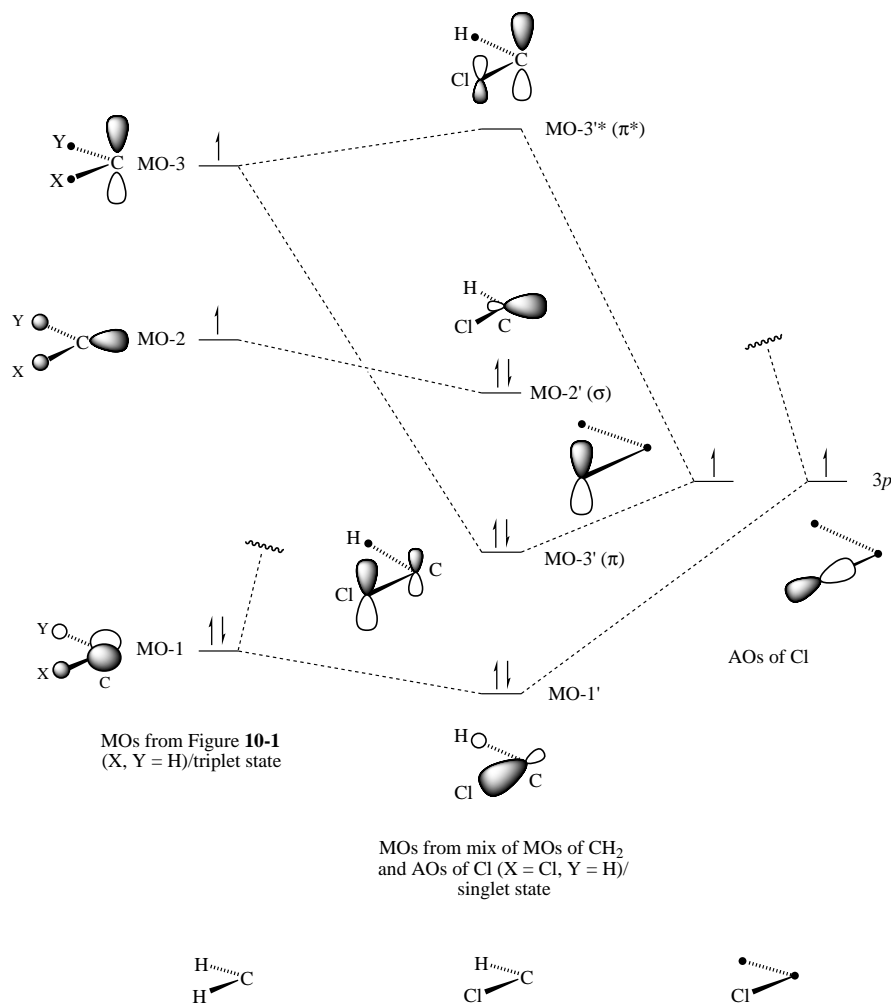


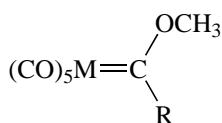
Figure 10-2
Influence of a
Heteroatom
Substituent on the
Electronic State of a
Free Carbene

N, O, S, and the halogens. Substituents such as a hydrogen atom or an alkyl group have approximately the same electronegativity as carbon and also lack filled π orbitals, so the interactions to lower the σ and raise the π MOs do not occur; a triplet state results.

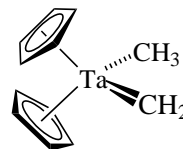
It was mentioned in Section 6-1-2 that, just as there are two types of free carbenes, there are also two fundamental kinds of metal–carbene complexes. As with free carbenes, the two varieties of metal–carbene complexes depend upon the nature of the substituents X and Y. When either substituent bound to C_{carbene}⁵ is

⁵The carbon atom directly attached to the metal in a metal–carbene complex is called C_{carbene}.

heteroatomic, the resulting structure is called a *Fischer* carbene complex (structure **2** below). Several years after the first Fischer-type carbene was reported, Schrock⁶ discovered species where the substituents X and Y attached to C_{carbene} were H or alkyl. Such metal–carbene complexes have since become known as *Schrock* carbene complexes or *alkylidenes*; structure **8** shows an example of a Schrock-type carbene complex. A third type of metal–carbene complex has grown in importance, especially over the past 20 years. This type shows binding of a metal to an *N*-heterocyclic carbene (NHC). Structure **9** illustrates a generalized example of such an NHC–metal complex, which resembles a Fischer carbene in that C_{carbene} is attached to two heteroatomic nitrogen atoms. We will consider the unique properties of NHC–metal complexes in Section **10-1-1**.

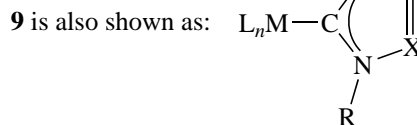
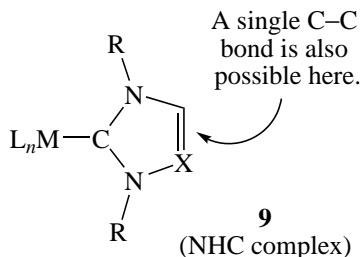


2
(Fischer carbene complex)



8
(Schrock carbene complex)

R = CH₃, Ph



X = C or N
R = alkyl, aryl, or silyl

The three kinds of carbene complexes differ in several ways. As will be discussed in Section **10-3**, Fischer carbene complexes tend to undergo attack at C_{carbene} by nucleophiles and thus are termed *electrophilic* (equation **10.3**). Schrock carbene complexes, on the other hand, undergo attack by electrophiles at C_{carbene} and are considered *nucleophilic* species (equation **10.4**). Because of their

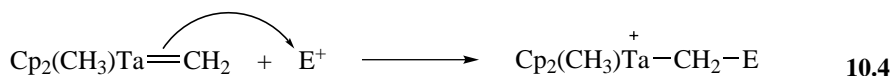
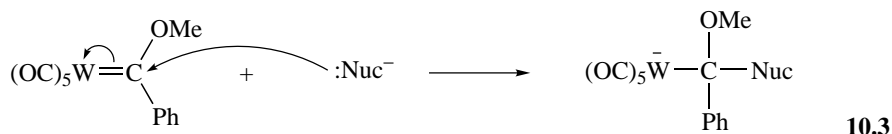
⁶R. R. Schrock, *J. Am. Chem. Soc.*, **1974**, 96, 6796.

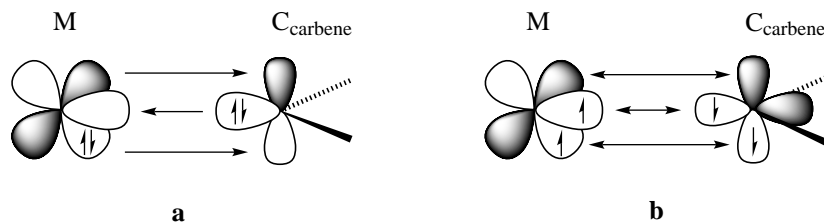
Table 10-1 Fischer, Schrock, and NHC–Carbene Complexes^a

Characteristic	Fischer	Schrock (Alkylidenes)	NHC Metal Complexes
Typical metal [ox. state]	Middle to late transition metal [Fe(0), Mo(0), Cr(0)]	Early- to mid-transition metal [Ti(IV), Ta(V), Mo(VI)]	Variable
Substituents attached to C _{carbene}	At least one electronegative heteroatom, e.g., O or N	H or alkyl	2 N-atoms that are often part of a ring
Typical ligands also attached to metal	Good π acceptor, e.g., CO	Good σ or π donor, e.g., Cp, Cl, alkyl, O-alkyl, PR ₃	Variable
Electron count	18 e ⁻	10–18 e ⁻	Variable, but complexes are usually coordinatively-saturated
Typical chemical behavior	Nucleophile attacks at C _{carbene}	Electrophile attacks at C _{carbene}	Usually unreactive at C _{carbene} ; NHCs serve as supporting ligands
Ligand type	L	X ₂	L
M–C bond order	1–2	2	ca. 1

^aThis table describes limiting cases. Many metal–carbene complexes exist that do not neatly fit into any of these three formalisms.

chemical behavior, Fischer carbene complexes are more properly called *electrophilic metal–carbene complexes* and Schrock carbenes are called *nucleophilic metal–carbene complexes*. Both names for these two carbene types are often seen in the chemical literature. Standing apart in reactivity from Fischer and Schrock carbene complexes are NHC–metal complexes. C_{carbene} is relatively unreactive in these complexes, and the NHC ligand serves more as a supporting ligand for the rest of the metal complex than as a center of reactivity. Table 10-1 summarizes several differences among the three carbene complex types. Finally, we must point out that the fundamental distinctions among carbene complex types shown in Table 10-1 can break down, and it is difficult at times to distinguish among the three fundamental types. Section 10-3-3 will examine some of these less well-defined cases.



**Figure 10-3**

(a) Interaction between a Singlet Free Carbene and a Metal; (b) Interaction between a Triplet Free Carbene and Metal

The picture is quite different for nucleophilic metal–carbene complexes. Here, contributing structures **10** and **13** seem to make the most contribution to the overall structure. Support for this observation comes from temperature-dependent NMR measurements⁸ of the M–C rotational barriers of various Ta–carbene complexes. The values obtained range from 12 to 21 kcal/mol, and seem to indicate considerable double bond character (structure **10**).

Another approach toward understanding the bonding and structure of metal carbenes involves the interaction of localized orbitals of the metal and carbon atom. We may envision electrophilic carbene complexes as the result of bonding of a singlet free carbene to the metal (Figure **10-3a**). The free carbene acts as a σ donor to an empty metal p or d_{z^2} orbital through its filled sp^2 orbital (MO-2, Figure **10-1**) and a π acceptor via back-donation of electrons from a filled metal d orbital to the empty $2p$ orbital (MO-3, Figure **10-1**) of the free carbene. The picture is exactly analogous to bonding of a CO ligand, except that carbene is a better σ donor and poorer π acceptor than CO (which makes the M–C_{carbene} bond weaker than an M–CO bond). The carbon in a Fischer carbene is, therefore, formally an **L-type ligand**, donating two electrons to the metal. Upon addition of the free carbene to the metal, the metal's oxidation state remains unchanged.

Figure **10-3b** illustrates the formation of a Schrock carbene. Here, a triplet free carbene interacts with the metal, and the double bond forms because two singly-occupied $2p$ orbitals from carbon and two singly-occupied metal orbitals contribute one electron to form both a σ and a π bond. Because highly oxidized early transition metals typically are involved, we can think of the carbon fragment as both a σ and a π donor, contributing a total of four electrons to the metal (still two electrons, according to the neutral ligand scheme). The carbon is thus an **X₂-type ligand** that causes an oxidation state change of +2 on the metal.

Ab initio MO calculations have been reported on complexes **15** and **16**; the former is a good example of a Fischer carbene complex and the latter is a Schrock-type.⁹

⁸J. D. Fellmann, G. A. Rupprecht, C. D. Wood, and R. R. Schrock, *J. Am. Chem. Soc.*, **1978**, *100*, 5964.

⁹T. E. Taylor and M. B. Hall, *J. Am. Chem. Soc.*, **1984**, *106*, 1576; see also the following papers, which investigate the structure and bonding of high-valent metal–alkylidene

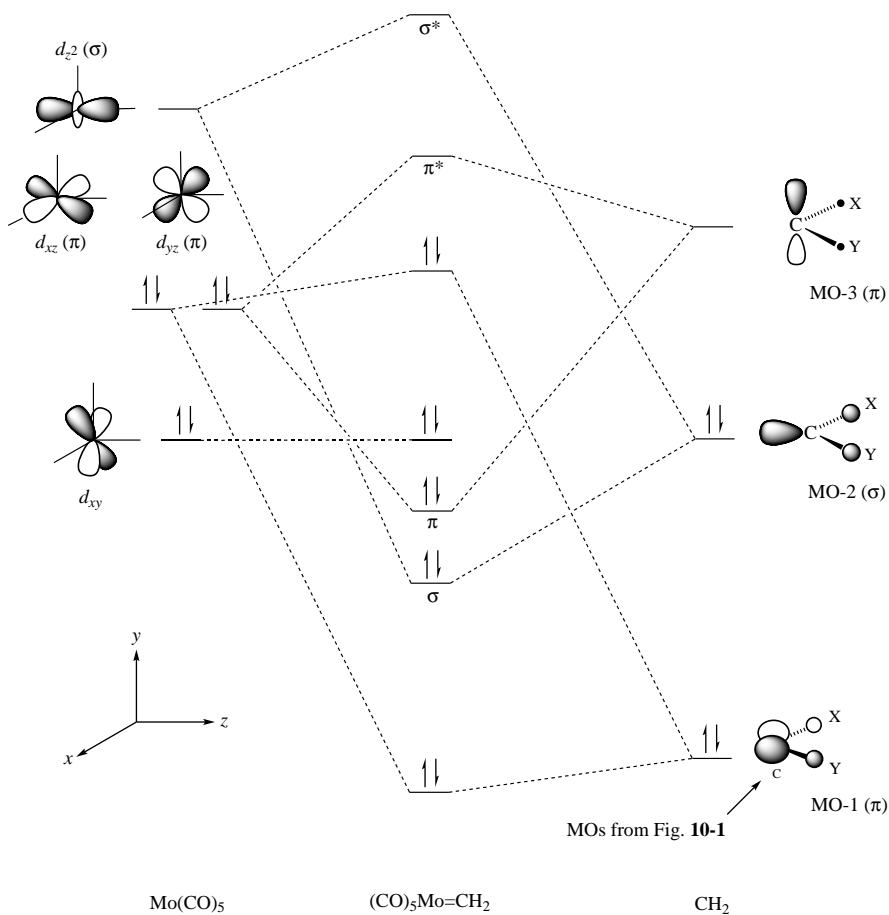


Figure 10-4a
Molecular Orbital
Picture of a Fischer
Carbene Complex

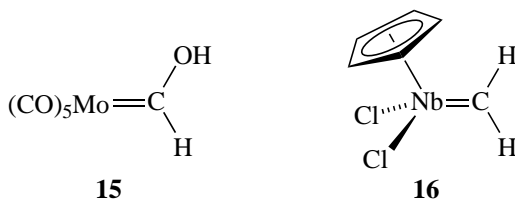


Figure 10-4a shows the interaction of the carbene fragment with appropriate metal orbitals. For the sake of simplification, the free carbene orbitals are shown without interaction of the heteroatom (see Figure 10-1). The key features of this interaction include σ donation from the carbon (MO-2) to the d_{z^2} metal orbital

complexes: T. R. Cundari and M. S. Gordon, *J. Am. Chem. Soc.*, **1991**, *113*, 5231 and **1992**, *114*, 539.

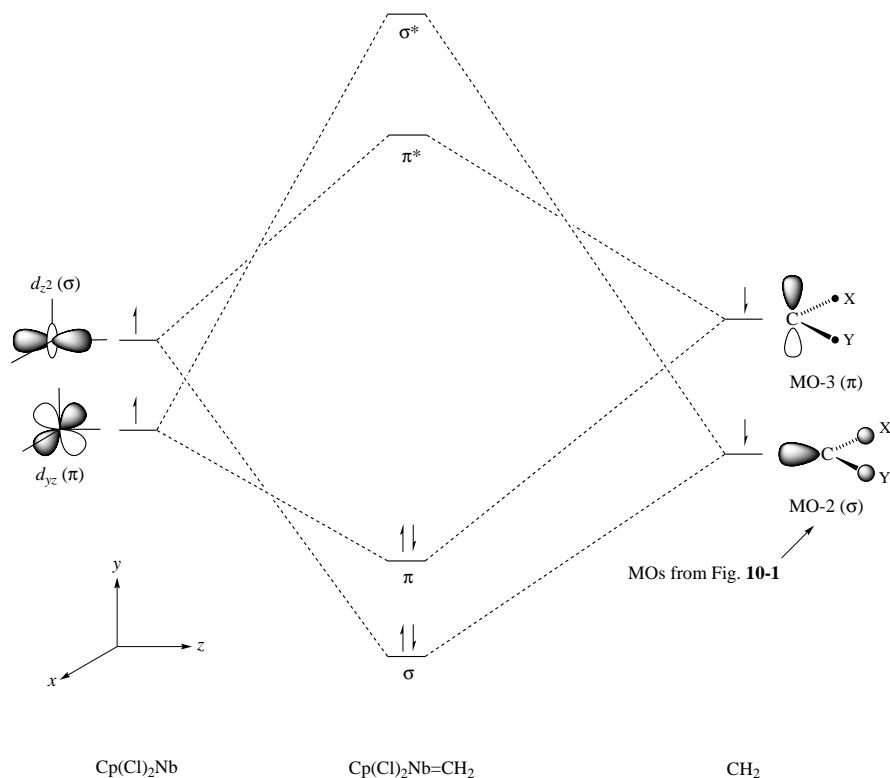


Figure 10-4b

Molecular Orbital
Picture of a Schrock
Carbene Complex

and back-donation of π electrons from the filled d_{yz} metal orbital to the ligand (MO-3). There is significant energy separation of the frontier orbitals¹⁰ in both metal and ligand, which leads to all electrons being paired.

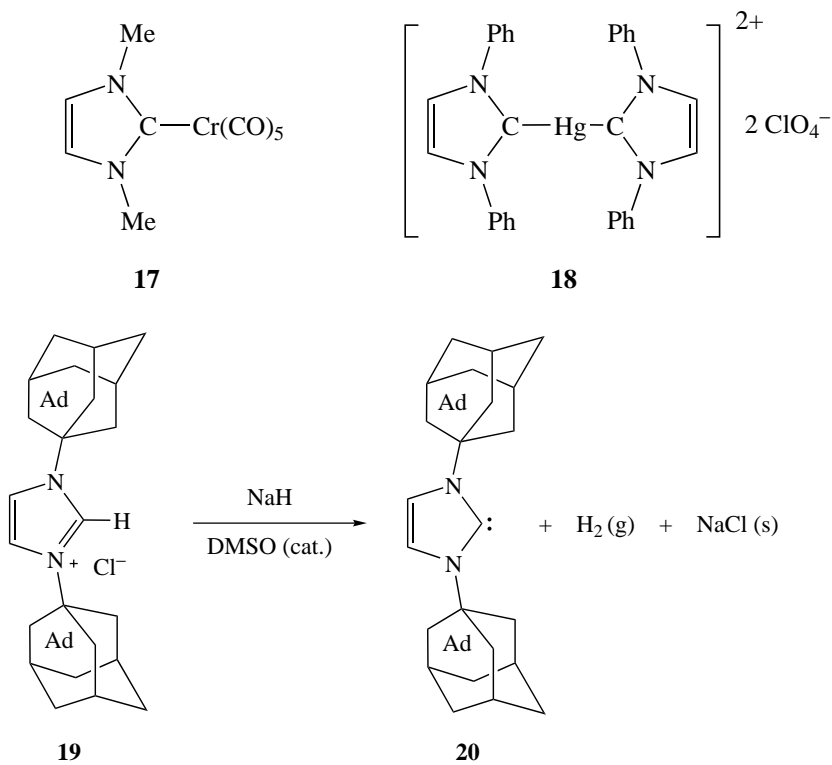
When the metal is niobium, the two metal frontier orbitals, d_{yz} and d_{z^2} , are closer in energy and match the corresponding orbitals of triplet free carbene. Figure 10-4b provides a picture of the interactions involved (only the important orbital interactions are shown). The electrons in the M–C bond are much more equally distributed between the metal and $\text{C}_{\text{carbene}}$ (because the energy levels of the metal and carbon orbitals are comparable) than with an electrophilic carbene complex. In resonance terminology, this means that structure **10** becomes an important contributor to the overall structure of this particular Schrock carbene complex.¹¹

¹⁰The HOMO and the LUMO comprise the frontier orbitals.

¹¹There exists a relevant analogy between Schrock carbene complexes and ylides. The term *yliide* typically refers to a dipolar compound where carbon is attached to a nonmetal such as N, P, or S. An ylide shows nucleophilic character at the carbon, with two resonance structures providing significant contribution to the overall structure of the molecule, (*i.e.*, $\text{R}_n\text{Y}=\text{CR}_2 \leftrightarrow \text{R}_n\text{Y}^+-\text{CR}_2^-$). For an introduction to the chemistry of ylides, see M. B. Smith,

10-1-1 N-Heterocyclic Carbene Complexes

NHC complexes, which are generalized by structure **9**, are seemingly related to Fischer carbene complexes because heteroatoms occupy the two positions next to C_{carbene} . They possess many unique properties, however, that require them to be treated as a separate class. NHC–metal complexes first appeared in the literature in 1968 (compounds **17**¹² and **18**¹³); however, interest in these compounds languished until 1991, when the isolation of the first free NHC carbene (**20**) was reported (equation **10.5**).¹⁴ Amazingly, free carbene **20** is a thermally-stable, crystalline solid with a melting point above 200 °C, and its structure was determined by X-ray crystallography. It is, however, moisture- and air-sensitive. Since the discovery of **20**, there has been a great deal of research activity directed toward exploiting the chemistry of it and more-recently reported, related free carbenes.



Organic Synthesis, 2nd ed., McGraw–Hill: New York, 2002, pp. 656–682, and references therein.

¹²K. Öfele, *J. Organomet. Chem.*, **1968**, *12*, P42.

¹³H.-W. Wanzlick and H.-J. Schönherr, *Angew. Chem., Int. Ed. Engl.*, **1968**, *7*, 141.

¹⁴A. J. Arduengo III, R. L. Harlow, and M. Kline, *J. Am. Chem. Soc.*, **1991**, *113*, 361.

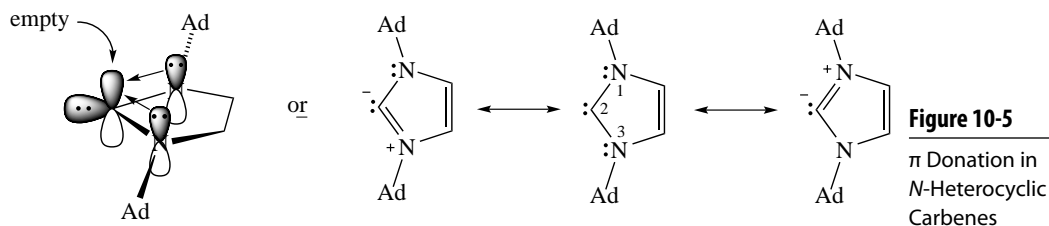


Figure 10-5
 π Donation in
N-Heterocyclic
 Carbenes

Free carbene **20** is stable because the lone pairs on the two adjacent nitrogen atoms can interact with the empty $2p$ orbital on C_{carbene} (considered the 2-position on the ring), resulting in a very effective π donation of electron density (Figure 10-5). The bulky *N*-adamantyl (Ad) groups may donate electron density to the nitrogen atoms, thereby enhancing the ability of the N atoms to donate π -electron density to C_{carbene} , but it is probably the steric bulk of the *N*-adamantyl groups that has the dominant effect.¹⁵ Instead of being electron deficient and electrophilic, properties one associates with free carbenes, NHCs are relatively electron rich and nucleophilic. Thus NHCs are very effective σ donors and relatively poor π acceptors because both the sp^2 and $2p$ orbitals on C_{carbene} are occupied. The pK_a of the parent imidazolium ion (**19**), from which NHC **20** derives, is about 24, so **20** is both a rather strong base and a strong nucleophile.¹⁶

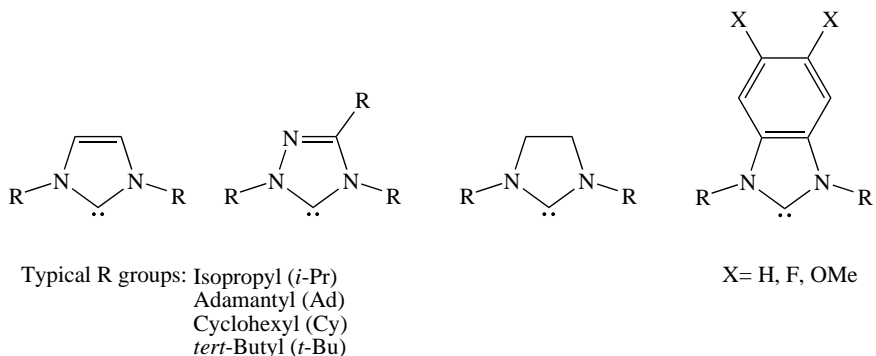
It is this strong nucleophilicity that makes NHCs effective L-type ligands, and their electronic and steric properties rival those of phosphines. Figure 10-6 displays several of the most common NHCs, which are used as ligands in transition metal complexes.

It is possible to modify both the groups attached to the N atoms and the groups attached to the ring. Studies have shown that, as these substituents change, NHCs do not vary as widely in electronic properties (χ) as do phosphines, but steric properties (θ) can be quite variable.¹⁷ In general, NHCs are stronger electron donors than even the most electron-rich phosphines. The steric profile of NHCs is different from that of phosphines, which is conveniently measured by θ , the cone angle. NHCs tend to be flat, fan-like ligands with the substituents on the N-atoms pointing toward the metal rather than generally away, as is the case with most phosphines. Attempts have been made to quantify the steric effects of

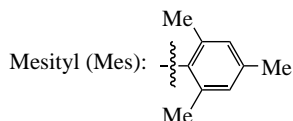
¹⁵The sterically-bulky *N*-adamantyl groups also impart kinetic stability to the carbene by helping to prevent dimerization at the carbene carbon, which is a common reaction of more reactive free carbenes. The successful isolation of Arduengo's carbene was undoubtedly strongly influenced by the ability of the compound to crystallize.

¹⁶R. W. Alder, P. R. Allen, and S. J. Williams, *J. Chem. Soc. Chem. Commun.*, **1995**, 1267.

¹⁷(a) R. A. Kelly III, H. Clavier, S. Giudice, N. M. Scott, E. D. Stevens, J. Bordner, I. Samardjiev, C. D. Hoff, L. Cavallo, and S. P. Nolan, *Organometallics*, **2008**, *27*, 202 and (b) S. Leuthäuser, D. Schwarz, and H. Plenio, *Chem. Eur. J.*, **2007**, *13*, 7195.

**Figure 10-6**

Some Important
N-Heterocyclic
Carbenes



NHCs, but work still remains before a definitive, simple-to-use, and universally-accepted parameter like θ is available to chemists.¹⁸

Exercise 10-1

Why is varying substituents on NHCs, either the groups attached to the N-atoms or the groups attached to the ring, less likely to cause large variation in χ than is the case with phosphines?

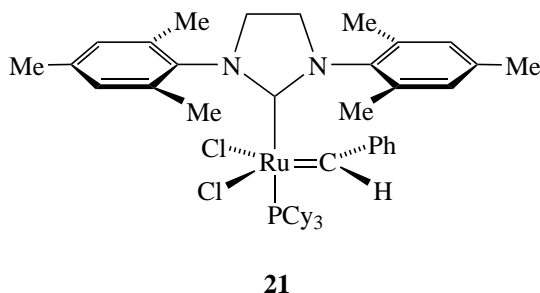
The bonding picture for NHC–metal complexes is rather different than exists for Fischer or Schrock complexes. Calculations show that the amount of back-bonding from the metal to the ligand is quite small, and that bonding is almost entirely due to σ -donation from the relatively electron rich C_{carbene} .¹⁹ As such, most consider the bond between ligand and metal to be closer to a single bond rather than a formal double bond, and NHC–metal complexes are typically drawn with an $M-C_{\text{carbene}}$ single bond. According to the resonance treatment, which was discussed in Section 10-1, the structure of NHC–metal complexes would be most closely approximated by structure 12.

NHC–transition metal complexes find increasing use in the field of organic synthesis. Structure 21, known as a second-generation Grubbs catalyst used in

¹⁸See Footnote 17a.

¹⁹G. Frenking, M. Solà, and S. F. Vyboishchikov, *J. Organomet. Chem.*, **2005**, 690, 6178.

reactions that form C=C bonds, is perhaps the most famous of these compounds.²⁰ Note that this catalyst is both an NHC-complex and an alkylidene. We will consider the role of compound **21** and related complexes in C=C bond formation in Chapter 11.



10-2 SYNTHESIS OF METAL CARBENE COMPLEXES

10-2-1 Fischer (Electrophilic) Carbene Complexes

There are numerous synthetic routes to Fischer carbene complexes.²¹ We may classify these routes as fundamentally of two kinds:

- A. Replacement or modification of an existing non-carbene ligand.
- B. Modification of an existing carbene ligand.

In this section, our discussion focuses on the type A pathway. Because modification of an existing carbene ligand to produce a new carbene is an example of a type of reaction carbenes may undergo, we will postpone discussion of type B reactions until Section 10-3.

Following are a few general methods for the preparation of Fischer-type carbene complexes.

Formation of Carbene Complexes by Nucleophilic Attack at a Carbonyl Ligand

Equation 10.6 shows the original work of Fischer and Maasböl in preparing the first reported metal-carbene complex. Attack by the carbanion (see equation 8.28

²⁰M. Scholl, S. Ding, C. W. Lee, and R. H. Grubbs, *Org. Lett.*, **1999**, *1*, 953.

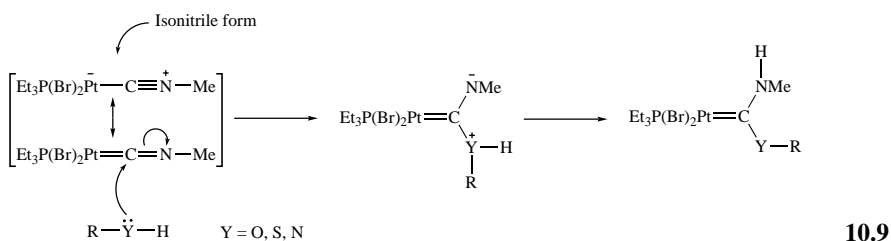
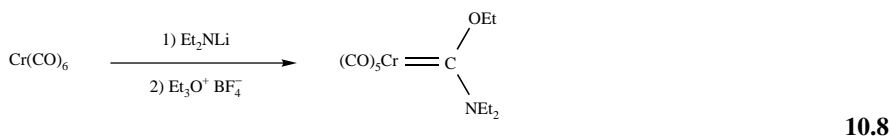
²¹Several good reviews exist that describe synthetic routes to electrophilic carbene complexes. These include F. J. Brown, *Prog. Inorg. Chem.*, **1980**, *27*, 1; K. H. Dötz, *et al.*, *Transition Metal Carbene Complexes*, Verlag Chemie: Deerfield Beach, FL, 1983, pp. 1-68; and M. A. Gallop and W. R. Roper, *Adv. Organomet. Chem.*, **1986**, *25*, 121.

What is the mechanism of the first step in equation 10.7?

Exercise 10-3

Synthesis of N-Substituted Carbene Complexes

Nitrogen often appears attached directly to carbon in Fischer-type carbene complexes. Equations 10.8²³ and 10.9²⁴ provide two examples of N-substituted carbene complex synthesis. The first procedure involves attack by the amide on one of the carbonyls (analogous to equation 10.6) followed by alkylation.



The second case involves attack of R–Y–H on the electron-deficient carbon of the isonitrile ligand, followed by proton transfer. It is adjustable with regard to nucleophile since amines (Y = N), unhindered alcohols (Y = O), and thiols (Y = S) add to the isonitrile carbon to form the corresponding diamino, aminoalkoxy, and aminothio carbenes. Isonitrile complexes of several different metals undergo this reaction, although Pd and Pt complexes have been the most thoroughly investigated.²⁵

10-2-2 Schrock (Nucleophilic) Carbenes

Compared with electrophilic carbene complexes, relatively few procedures exist for preparing nucleophilic carbene complexes (alkylidenes).²⁶ Generally, these

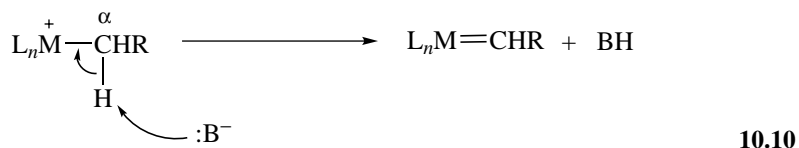
²³E. O. Fischer and H.-J. Kollmeier, *Angew. Chem. Int. Ed. Eng.*, **1970**, 9, 309.

²⁴E. M. Badley, J. Chatt, and R. L. Richards, *J. Chem. Soc., A*, **1971**, 21.

²⁵H. Fischer, In *The Chemistry of the Metal-Carbon Bond*, F. R. Hartley and S. Patai, Eds., Wiley-Interscience: New York, 1982, Vol. 1, p. 185.

²⁶For a recent survey on the synthesis of high-valent metal-alkylidene and -alkylidyne complexes, see R. R. Schrock, *Chem. Rev.*, **2002**, 102, 145.

complexes are more reactive than corresponding Fischer carbene complexes because of the lack of stabilizing heteroatom substituents. Obvious precursors for alkylidenes ought to be alkyl ligands; loss of an α -H would give the corresponding carbene, as shown in equation 10.10.

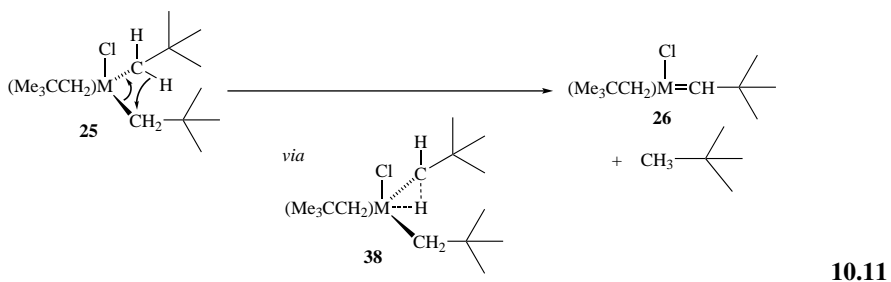


One problem with this approach is the ever-present, rapid, competing side reaction of β -elimination (Section 8-1-2). As we shall see, α -elimination is indeed used to produce alkylidenes, but the circumstances of this reaction are unique. Other approaches that we will discuss include decomposition of bridged alkylidenes and direct attack of a free carbene precursor on a metal.

Loss of the α Hydrogen

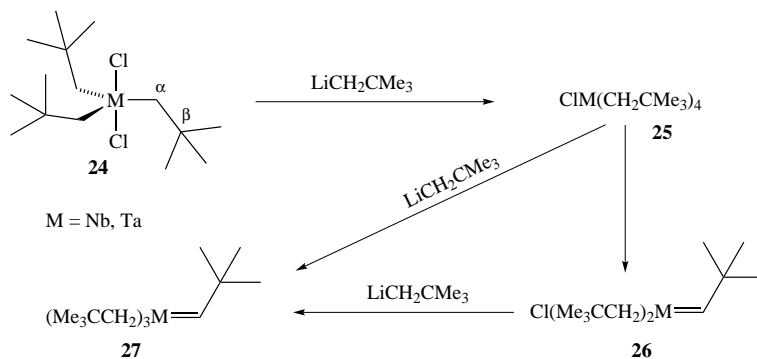
The early work of Schrock and co-workers²⁷ involved the synthesis and characterization of Group 5 alkylidenes involving Ta and Nb. Scheme 10.1 describes some of the first preparations of alkylidenes. The key reaction here is loss of a proton attached to C_α to form an $\text{M}=\text{C}$ bond (α -elimination). In all cases, β -elimination is blocked because of the lack of a β -hydrogen.

Sequence 1. The first sequence of reactions in the scheme begins when 10-electron **24** reacts with neopentyl lithium to give the tetraalkylchloro complex **25** via a ligand substitution reaction. Intermediate **25** either reacts directly with additional neopentyl lithium to give **27** [via $(\text{neopentyl})_5\text{M}$] or it decomposes to the chloroalkylidene complex **26**, which then reacts with another equivalent of neopentyl lithium, replacing the chloro group with a neopentyl ligand. Regardless of the pathway, the reaction is remarkable because somehow an alkane (2,2-dimethylpropane) and an alkylidene form as products. Equation 10.11 shows how this may occur.

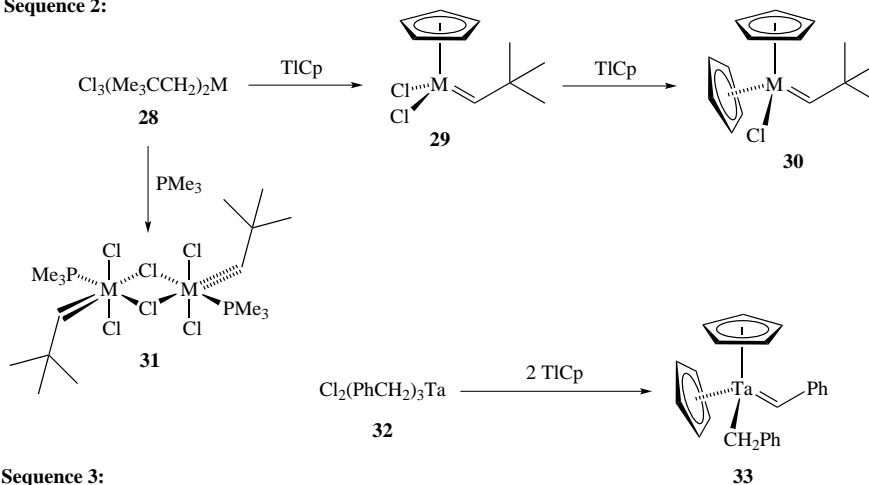


²⁷For a good summary of this work, see R. R. Schrock, *Acc. Chem. Res.*, **1979**, *12*, 98, and references therein.

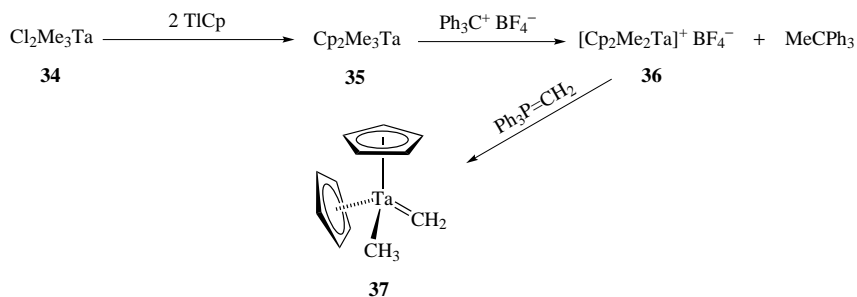
Sequence 1:



Sequence 2:



Sequence 3:



Scheme 10.1

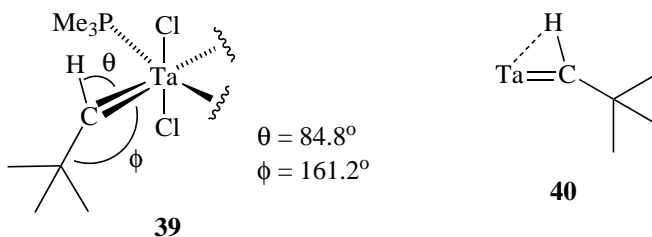
Preparation of
Group 5 Schrock
Carbene Complexes

The driving force for the reaction clearly must be the reduction of steric hindrance that occurs upon expulsion of one of the sterically-demanding neopentyl groups. Protons attached at the α -position of the neopentyl groups also may be somewhat agostic (structure **38**; see Section 6-2-3), because the Group 5 metal is

electron deficient [M(V) and d^0]. If so, the α C–H bond would already be weakened, making hydrogen transfer to alkyl more favorable energetically.

Sequence 2. Treatment of the dineopentyl complex (**28**) with cyclopentadienylidene ion displaces one of the chloro groups with a Cp ligand with simultaneous expulsion of alkane to give **29**. Again, the steric bulkiness of the Cp group actuates the loss of alkane by α -elimination. A second Cp–Cl ligand exchange results in formation of **30** (an 18- e^- complex). Conversion of **32** to **33** is analogous and demonstrates that the reaction also occurs with a benzyl ligand.

Conversion of **28** to **31** is possible because of the steric and electronic properties of PMe_3 . The dimeric **31** contains 14 electrons/metal atom, and its electron deficiency is stabilized by the presence of the phosphine, a strong σ donor. The phosphine also has sufficient steric bulk so that, as it attaches to the metal, steric hindrance increases sufficiently to allow *intramolecular* α -elimination to occur. An X-ray structure of **31** (shown partially as structure **39**, M = Ta) is interesting.²⁸ It shows that the bond angle involving the metal, α -, and β -carbons is 161.2° , much higher than the expected 120° for the sp^2 alkylidene α carbon. The bond angle involving metal, $\text{C}_{\text{carbene}}$, and attached hydrogen is 84.8° —significantly less than 120° ! The bond distance between Ta and C is only 189.8 pm, considerably shorter than Ta=C bond distances in other Ta–carbene complexes (average distance = 204 pm). Structure **40** illustrates a possible explanation for these observations. Steric hindrance apparently forces the M– $\text{C}_{\text{carbene}}$ – C_β bond angle to increase beyond that expected for an sp^2 -hybridized carbon. The electron deficiency at Ta (14 e^-) provides an opportunity for extra electron density to be supplied through an agostic interaction between the α -hydrogen and an empty d orbital on the metal. In effect, the bond between Ta and carbon is a three-center, six-electron bond.²⁹

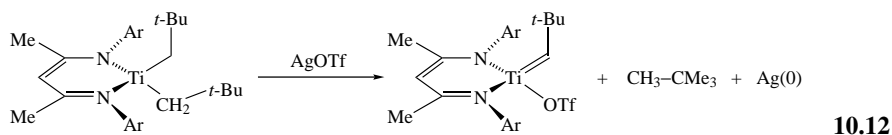


²⁸A. J. Schultz, J. M. Williams, R. R. Schrock, G. A. Rupprecht, and J. D. Fellmann, *J. Am. Chem. Soc.*, **1979**, *101*, 1593.

²⁹For a recent review on agostic interactions of early- to mid-transition metal methylidenes, see L. Andrews and H.-G. Cho, *Organometallics*, **2006**, *25*, 4040.

Sequence 3. The last reaction sequence in Scheme 10.1 details the preparation of a methyldiene complex (**37**) starting with **34**. Attempts to observe α -elimination analogous to the reactions described above in **35** were unsuccessful; only decomposition was observed. Electrophilic abstraction of a methyl group from **35** using trityl cation (Ph_3C^+), however, produced tantalonium salt **36**. Schrock realized here the analogy between the tantalonium salt and phosphonium salts, the precursors to ylides in the Wittig reaction. Protons attached to the α -carbon in phosphonium salts are relatively acidic and may be abstracted with bases of varying strength depending upon the nature of other substituents attached to the α -carbon. Schrock reasoned that a methyl proton (the α -proton) in **36** could be removed by a strong base. Use of a phosphorus ylide,³⁰ $(\text{CH}_3)_3\text{P}=\text{CH}_2$, as well as other bases successfully confirmed his prediction, yielding methyldiene **37** as a pale-green crystalline solid.

A more recent example involving α -elimination is shown in equation 10.12. Here, Ag(I) is used to induce alkylidene formation by first oxidizing Ti to a d^0 state, which is followed by α -elimination and then RE of alkane. Similar chemistry occurs with vanadium and niobium complexes.³¹



Decomposition of Bridged Alkylidene Complexes

Another approach to alkylidenes involves Group 4 metals, particularly Zr. Treatment of a vinyl Cp_2Zr complex (**41**) with diisobutylaluminum hydride gives bridged alkylidene **42** where the alkylidene group is shared (μ -bonding) between Zr and Al (equation 10.13).³² The dialkylaluminum hydride's Al-H bond adds across the vinyl C=C in a manner analogous to hydroboration such that the chloro ligand (attached to Zr) can act as a Lewis base complementary to electron-deficient Al.

³⁰See Footnote 11.

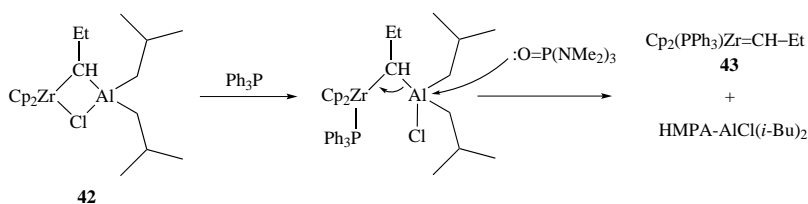
³¹F. Basuli, B. C. Bailey, L. A. Watson, J. Tomaszewski, J. C. Huffman, and D. J. Mindiola, *Organometallics*, **2005**, *24*, 1886; for a review of oxidatively induced alkylidene formation involving Ti and other early transition metals, see D. J. Mindiola, *Acc. Chem. Res.*, **2006**, *39*, 813.

³²F. W. Hartner Jr. and J. Schwartz, *J. Am. Chem. Soc.*, **1981**, *103*, 4979.



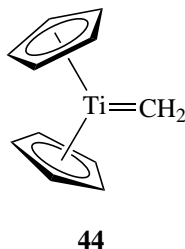
10.13

Once **42** forms, treatment first with Ph_3P and then with hexamethylphosphoramide (HMPA) results in the formation of alkylidene **43** (phosphines are good ligands for electron-deficient Zr(IV) complexes such as **42**). First the phosphine binds to Zr, and then HMPA (a highly polar molecule and a Lewis base) attacks Al (equation 10.14).³³ Fragmentation results in formation of the alkylidene and an HMPA–Al complex.



10.14

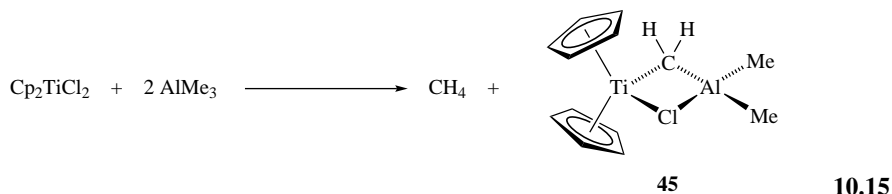
One of the most famous Ti carbene complexes is methylidene **44**. Although **44** probably occurs fleetingly as an intermediate in Schrock carbene reactions, it is too reactive to be isolated or observed spectroscopically. Two related compounds, however, have been synthesized:³⁴ $\text{Cp}_2\text{TiCH}_2(\text{PET}_3)$, in which the phosphine donates electrons to Ti to stabilize the complex, and the immediate precursor to **44**, known as Tebbe's reagent (**45**, equation 10.15³⁵).



³³F. W. Hartner Jr., J. Schwartz, and S. M. Clift, *J. Am. Chem. Soc.*, **1983**, 105, 640.

³⁴S. H. Pine, *Org. Reactions*, **1993**, 43, 1.

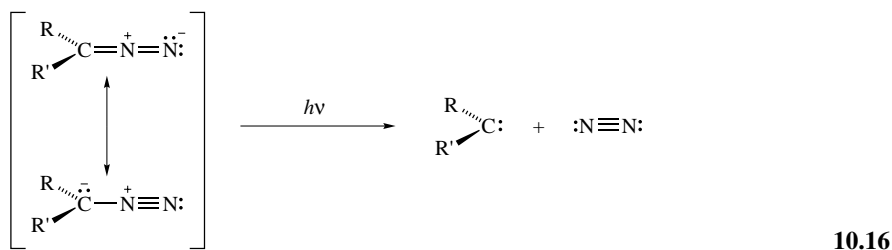
³⁵F. N. Tebbe, G. W. Parshall, and G. S. Reddy, *J. Am. Chem. Soc.*, **1978**, 100, 3611.



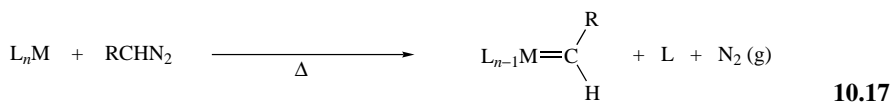
Equation **10.15** provides another example of the use of Al compounds to form bridging alkylidenes, providing stabilization for the very reactive Group 4 carbene complexes. Later in Chapter 10 (Section **10-3-2**), we shall encounter some of the synthetically useful chemistry of Tebbe's reagent.

Direct Attack of a Free Carbene Precursor onto a Metal

Diazoalkanes, $\text{RR}'\text{C}=\text{N}=\text{N}$ ($\text{R}, \text{R}' = \text{H}, \text{alkyl}, \text{aryl}$), serve as precursors to free carbenes through thermal- or photochemical-induced loss of N_2 , according to equation **10.16**.

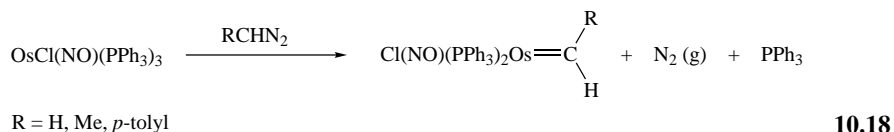


Although transition metal complexes do not usually react directly with free carbenes (with the exception of the formation of NHC–metal complexes, Section **10-2-3**), low-valent Group 7 to 9 metal complexes in particular react with diazoalkanes to produce alkylidenes. Equation **10.17** shows a general example of this reaction. The complex must either be unsaturated or possess a labile L-type ligand so that the reaction can occur. The intermediate in this reaction is unlikely to be a free carbene.



A good example of this type of metal carbene synthesis appears in equation **10.18**, which shows that a variety of diazoalkanes react with the Os complex.³⁶ We will encounter more diazoalkane chemistry in Section **10-3-3**.

³⁶A. F. Hill, W. R. Roper, J. M. Waters, and A. H. Wright, *J. Am. Chem. Soc.*, **1983**, *105*, 5939; see also M. A. Gallop and W. R. Roper, *Adv. Organomet. Chem.*, **1986**, *25*, 121–198, especially pp. 156–159.

**Exercise 10-4**

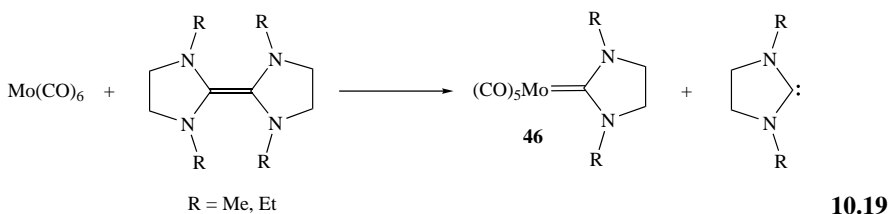
Propose a synthesis of $(\text{NO})(\text{PMe}_3)_3\text{Ir}=\text{C}(\text{H})(\text{Me})$ starting with an appropriate Ir complex.

10-2-3 Synthesis of *N*-Heterocyclic Carbene Complexes

There are many approaches to the synthesis of NHC–metal complexes, and a few of these will be discussed in this section. Among the most commonly-used strategies for producing these complexes are the following: 1) inserting a metal into the C=C bond of an NHC dimer, 2) allowing a metal complex to react with a protected form of the NHC, 3) generating an NHC *in situ* via a Brønsted–Lowry acid–base reaction in the presence of a metal complex, and 4) directly combining a free NHC with a metal complex.³⁷

Metal Insertion into the C=C Bond of an NHC Dimer

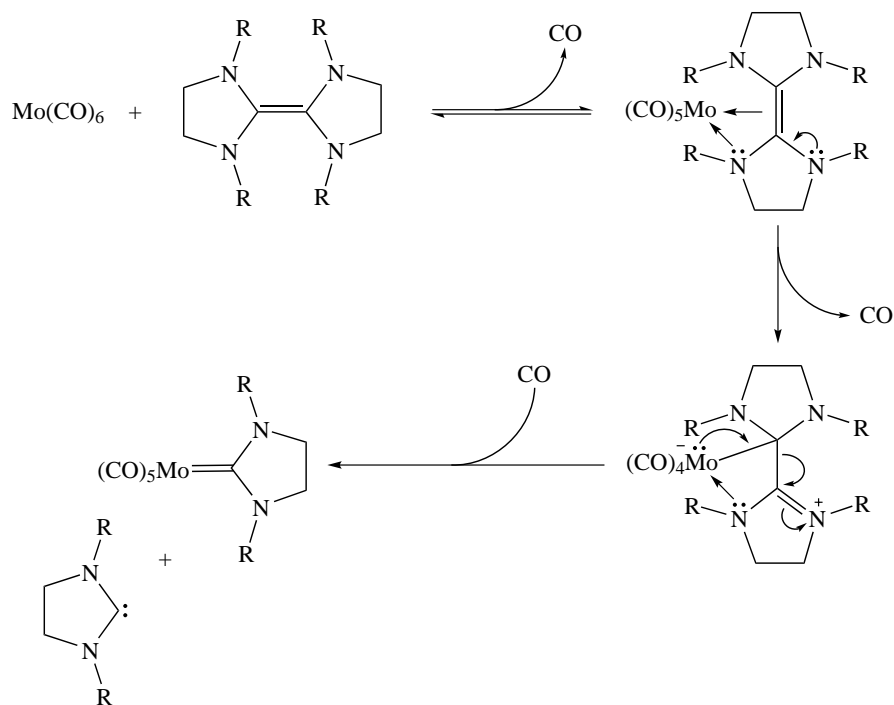
Producing NHC–metal complexes by C=C scission of an NHC dimer is one method that is fairly general and interesting mechanistically. Equation 10.19 indicates the overall pathway to complex **46**.³⁸



A plausible mechanism for this reaction is shown in Scheme 10.2, which consists of a stepwise sequence of several fundamental types of organometallic reactions.

³⁷A fifth method, which now sees increasing use, involves first formation of a Ag–NHC complex, which then undergoes reaction with another metal complex (typically involving a Group 10 metal). The NHC ligand is transferred from the Ag complex to the other metal. For a review of this method and the others mentioned above, see E. Peris, *Top. Organomet. Chem.*, **2007**, 21, 83 and J. C. Garrison and W. J. Youngs, *Chem. Rev.*, **2005**, 105, 3978.

³⁸For a review of this method for formation of NHC–metal complexes, see M. F. Lappert, *J. Organomet. Chem.*, **1988**, 358, 185.

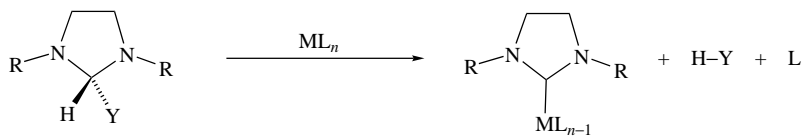
**Scheme 10.2**

A Possible
Mechanistic
Pathway for Alkene
Scission

Beside complexes of the Group 6 triad, Ru, Os, and Ir carbonyl complexes also undergo this reaction.

Reaction of Protected NHCs with Metal Complexes

NHC precursors **47a** and **47b** may be used to generate the corresponding free carbene because an alcohol or chloroform readily eliminates from carbon (equation 10.20). Chemists can synthesize and isolate these precursors before allowing them to react with metal complexes or simply generate them *in situ* in the presence of the metal complex.



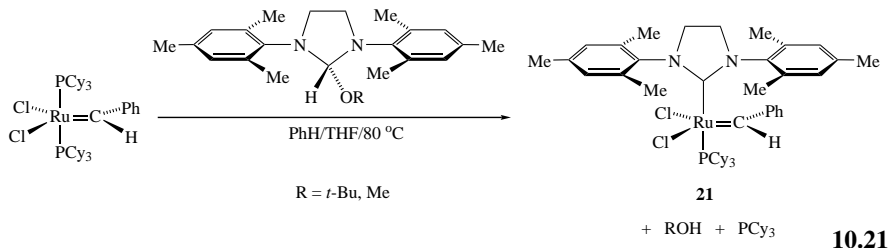
47a: Y = OR' (R' = alkyl)

47b: Y = CCl₃

10.20

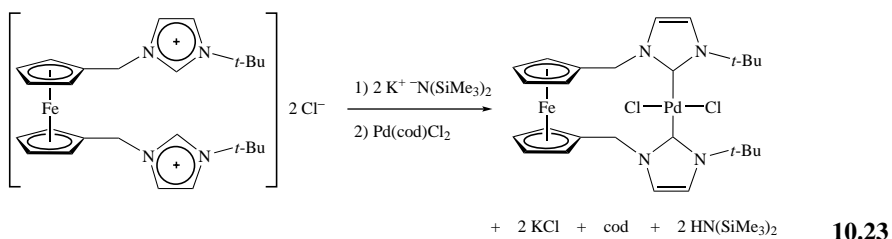
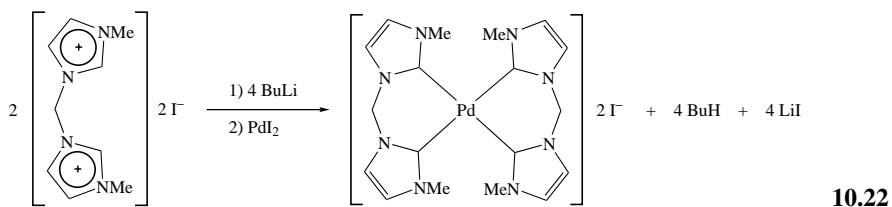
Equation 10.21 shows how Grubbs and co-workers used this method to generate compound **21**, the second-generation catalyst mentioned earlier. Here, the

NHC precursor was generated *in situ* from the corresponding imidazolium salt.³⁹



Generation of an NHC from the Corresponding Azolium Salt

The use of an external base to pull off a proton of an imidazolium or triazolium salt can generate the corresponding NHC, allowing it to react immediately with a metal complex already present. Equations 10.22⁴⁰ and 10.23⁴¹ illustrate this method.



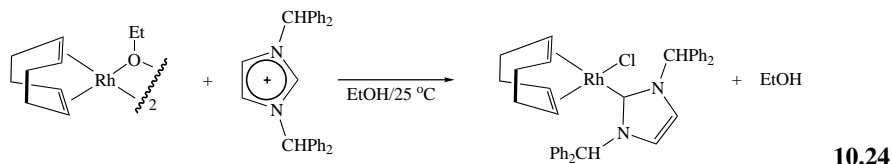
Sometimes the presence of a basic ligand, such as an acetoxy or alkoxy group, will cause deprotonation of the azolium salt. Equation 10.24 shows this variation of *in situ* generation of an NHC followed by complexation.⁴²

³⁹See Footnote 20.

⁴⁰W. P. Fehlhammer, T. Bliss, U. Kernbach, and I. Brudgam, *J. Organomet. Chem.*, **1995**, 490, 149.

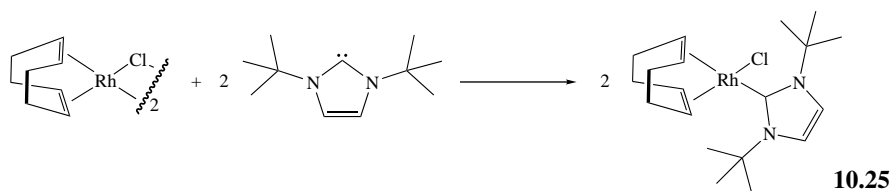
⁴¹K. S. Coleman, S. Turberville, S. I. Pascu, and M. L. H. Green, *J. Organomet. Chem.*, **2005**, 690, 653.

⁴²C. Köcher and W. A. Herrmann, *J. Organomet. Chem.*, **1997**, 532, 261 and T. Weskamp, V. P. W. Böhm, and W. A. Herrmann, *J. Organomet. Chem.*, **2000**, 600, 12 (a review of several methods for synthesizing NHC–metal complexes).

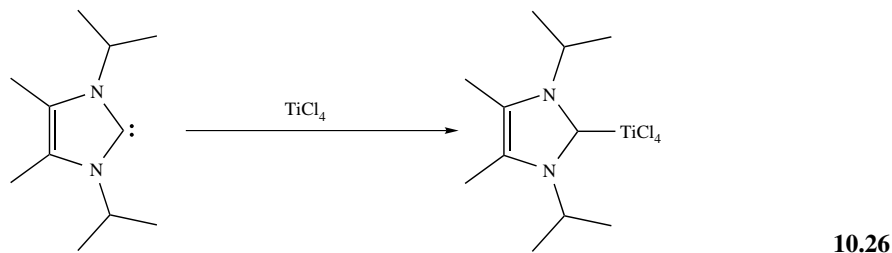


Reaction of a Free NHC with a Metal Complex

Because free NHCs bind so strongly to a metal, it is not necessary to use an excess amount of these ligands to make NHC–metal complexes. This contrasts with the synthesis of metal phosphine complexes, where often an excess of the ligand is required for success. There are numerous examples of simple combination of the free carbene and a suitable metal complex. Equation **10.25** illustrates one example.⁴³



Because back-donation of electron density to ligands is not likely with high-valent, early transition metals, it seems reasonable that complexes between such metals and strong σ donor ligands such as NHCs, which are not good π acceptors, could be synthesized. Synthesis of such complexes is indeed possible, as equation **10.26** demonstrates.⁴⁴



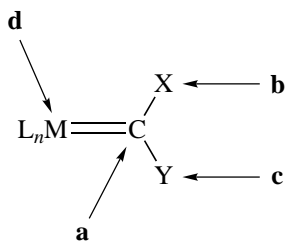
10-3 REACTIONS OF METAL–CARBENE COMPLEXES

Transition metal–carbene complexes possess several sites where nucleophiles, electrophiles, oxidizing agents, and protic acids might attack; these are depicted

⁴³See Footnote 17a.

⁴⁴N. Kuhn, T. Kratz, D. Blaser, and R. Boese, *Inorg. Chim. Acta*, **1995**, 238, 179.

Figure 10-7
Reactive Sites of
Transition Metal–
Carbene Complexes



in Figure 10-7. In the following discussion, we will focus primarily on the reaction of nucleophiles at C_{carbene} (site **a**), at the substituents attached to C_{carbene} (sites **b** and **c**), and at the metal (site **d**). We will also discuss reactions of electrophiles at sites **a** and **d**.

A Caveat Regarding the Reactivity of Metal Carbenes

As mentioned in Section 10-1, it is convenient to classify carbene complexes on the basis of their reactivity at C_{carbene} (site **a**). Fischer carbene complexes tend to undergo nucleophilic attack at this position, whereas Schrock carbene complexes (alkylidenes) undergo attack by electrophiles at site **a**. Although this is a useful generalization, applicable in most cases, there are several exceptions to this pattern of reactivity. For example, we shall encounter alkylidenes that undergo attack by nucleophiles at C_{carbene} , indicating that there is a spectrum of reactivities possessed by metal–carbene complexes. Metal oxidation state, overall charge on the complex, position of the metal in the periodic table, and electronic properties of ligands all influence the reactivity of the metal carbene such that the line of demarcation between the reactivity patterns of Fischer and Schrock carbene complexes is indistinct at times.

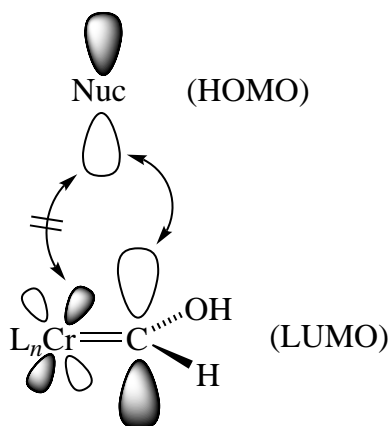
10-3-1 Nucleophilic Reactions⁴⁵

Site a

Despite the caveat expressed above, the most common reaction that Fischer carbene complexes undergo is attack by a nucleophile at C_{carbene} . It is interesting that such reactivity should occur, because partial charge calculations typically indicate a higher positive charge at the carbon in CO ligands than at C_{carbene} .⁴⁶ The key to understanding the electrophilicity of these complexes, however, is the

⁴⁵For a recent, comprehensive discussion on the mechanism of reactions of Fischer carbene complexes, see C. F. Bernasconi, *Adv. Phys. Org. Chem.*, **2002**, 37, 137.

⁴⁶T. F. Block, R. F. Fenske, and C. P. Casey, *J. Am. Chem. Soc.*, **1976**, 98, 441 and N. M. Kostić and R. F. Fenske, *Organometallics*, **1982**, 1, 974.

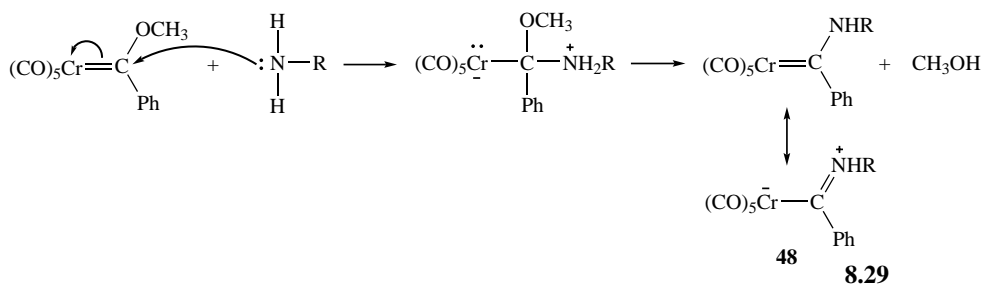
**Figure 10-8**

Frontier Orbital Interaction in Nucleophilic Attack on Fischer Carbene Complexes

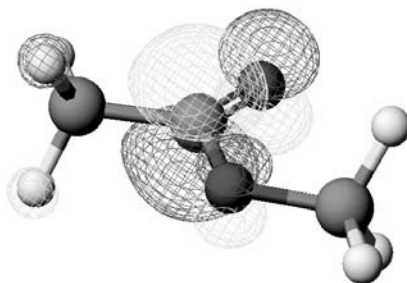
application of frontier molecular orbital theory. Electrophilic carbene complexes usually have a relatively low-energy LUMO with a large lobe on C_{carbene} and a much smaller lobe on M . Thus, as the nucleophile approaches the carbene complex, there is a much better bonding overlap between the HOMO of the nucleophile and the carbene LUMO at C_{carbene} than at the metal. Figure 10-8 illustrates this concept for attack on $(\text{CO})_5\text{Cr}=\text{C}(\text{H})(\text{OH})$.

It is noteworthy that the LUMO of a Fischer type carbene resembles the LUMO (determined using semi-empirical MO theory) of a typical ester such as methyl acetate (Figure 10-9a) or a ketone such as acetone (Figure 10-9b). In fact, the analogy between Fischer carbenes and carbonyl compounds should be useful to readers already familiar with organic chemistry. Indeed, the chemistry of these two types of compounds, seemingly so different in structure, is similar in several ways.

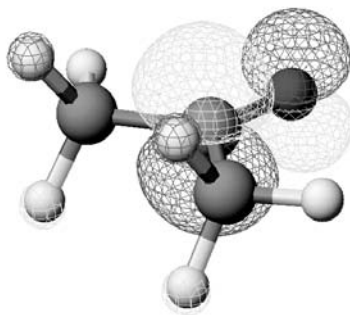
Equation 8.29 (Section 8-2-1 and reproduced below) already has provided an illustration of nucleophilic attack on a Fischer-type carbene and the analogy with aminolysis.



The driving force for the exchange of groups at C_{carbene} is formation of a C–N bond that is stronger than C–O. Structure 48 (comparable to resonance contributor 11 in Section 10-1), which shows considerable double bond character between C_{carbene} and the heteroatom, takes on increasing importance when nitrogen is



a



b

Figure 10-9

The LUMOs of
(a) Methyl Acetate
and (b) Acetone

present instead of oxygen because a positively-charged nitrogen atom is more stable than the correspondingly charged oxygen.

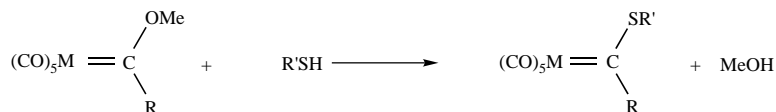
Fischer measured the kinetics of carbene aminolysis (specifically for the reaction shown in equation 8.29) and derived a rate law according to the following:⁴⁷

$$\text{Rate} = k[\text{MeNH}_2][\text{HX}][\text{Y}][\text{carbene}].$$

where HX = a proton donor e.g., the amine or a protic solvent

Y = a proton acceptor e.g., the amine or solvent

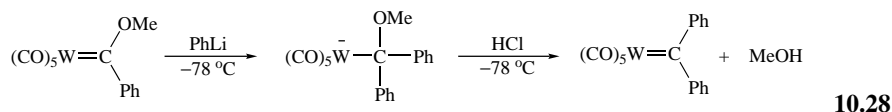
⁴⁷B. Heckl, H. Werner, and E. O. Fischer, *Angew. Chem. Int. Ed. Eng.*, **1968**, 7, 817 and H. Werner, E. O. Fischer, B. Heckl, and C. G. Kreiter, *J. Organomet. Chem.*, **1971**, 28, 367.



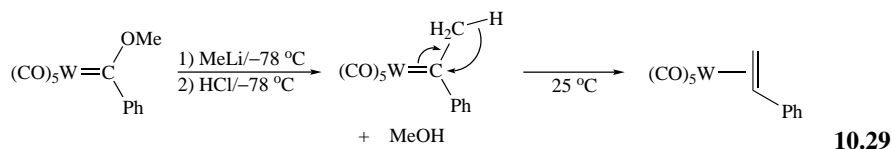
M = Cr, W; R = Me, Ph; R' = Me, Et, Ph

10.27

Organolithium compounds can serve as sources of carbon nucleophiles to drive substituent group exchange at $\text{C}_{\text{carbene}}$ —thus providing a route to alkylidenes—according to equation 10.28.⁴⁹ The reaction is limited to lithium reagents that do not possess H atoms attached to the carbon bonded to Li; otherwise, rearrangement (equation 10.29) occurs to give an alkene.⁵⁰



10.28



10.29

Sites b and c

In organic chemistry, carbonyl compounds can undergo reaction at the carbon next to a $\text{C}=\text{O}$ group (the α carbon) as well as nucleophilic attack on the carbonyl carbon. The electron-withdrawing nature of the carbonyl group renders protons at the α -position acidic. In Fischer carbene complexes, hydrogen atoms α to $\text{C}_{\text{carbene}}$ are analogously acidic. Such reactivity is synthetically useful. Loss of an α -hydrogen generates a carbanion analogous to an enolate ion that then undergoes reaction with electrophiles such as D^+ , R^+ , or $\text{R}-\text{C}=\text{O}^+$, the last two affording routes to new carbenes. Equation 10.30⁵¹ shows specific deuteration, 10.31⁵² alkylation using allyl bromide, and 10.32⁵³ an aldol condensation.

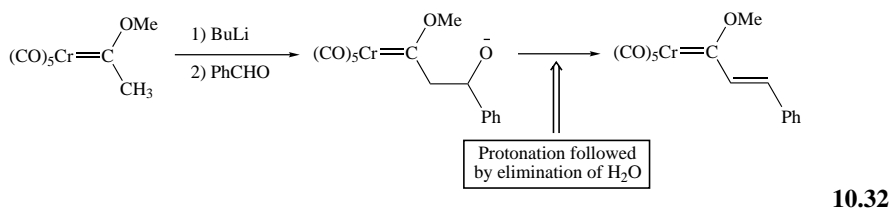
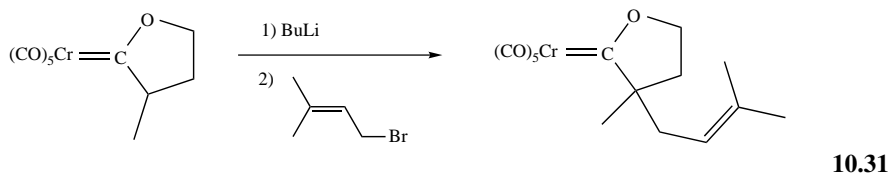
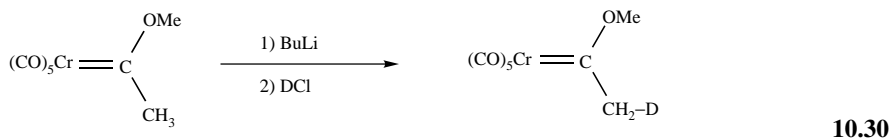
⁴⁹C. P. Casey and T. J. Burkhardt, *J. Am. Chem. Soc.*, **1973**, 95, 5833.

⁵⁰C. P. Casey, L. D. Albin, and T. J. Burkhardt, *J. Am. Chem. Soc.*, **1977**, 99, 2533.

⁵¹C. P. Casey, R. A. Boggs, and R. L. Anderson, *J. Am. Chem. Soc.*, **1972**, 94, 8947.

⁵²C. P. Casey, "Metal–Carbene Complexes in Organic Synthesis," in *Transition Metal Organometallics in Organic Synthesis*, H. Alper, Ed., Academic Press: New York, 1976, Vol. 1., pp. 189–233.

⁵³C. P. Casey and W. R. Brunsvold, *J. Organomet. Chem.*, **1974**, 77, 345.



Propose a synthesis of spirocyclic carbene complex **B** starting from **A**.

Exercise 10-5



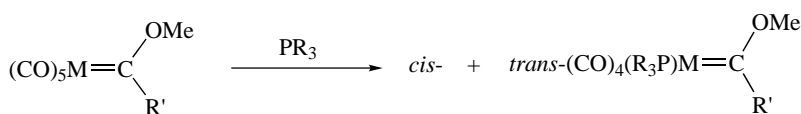
Site d

Carbonyls are the most common ligand found in electrophilic carbene complexes. They may be exchanged readily for other ligands, usually by a dissociative substitution pathway (see Section 7-1-3). Equation 10.33 describes studies involving ligand substitution with phosphines, perhaps the most typical nucleophile used. Interestingly, the reaction shows two mechanistic pathways: (1) dissociative substitution of CO by PR_3 ($\text{S}_{\text{N}}1$ -like) and (2) rate-determining attack by PR_3 at $\text{C}_{\text{carbene}}$ to produce a tetrahedral intermediate (the phosphorus analogue of structure 50), which is followed by rearrangement to the product shown in equation 10.33 ($\text{S}_{\text{N}}2$ -like).⁵⁴

⁵⁴H. Fischer, E. O. Fischer, C. G. Kreiter, and H. Werner, *Chem. Ber.*, **1974**, *107*, 2459; see also Footnote 45.

Table 10-2^a Rate Parameters for Ligand Dissociation of Cr Complexes

L	k_{rel}	ΔH (kcal/mol)
=C(OMe)(Me)	240,000	27.6
CO	11	38.7
P(Cy) ₃ ^b	1	40.4

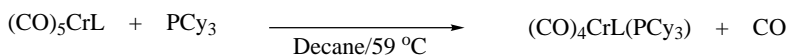
^aF. J. Brown, *Prog. Inorg. Chem.* **1980**, 27, 1 (especially p. 45).^bCy = cyclohexyl.

M = Cr, Mo, W; R' = Ph, Me; R = Me, Et, Bu, Ph

10.33

It is worth noting that the presence of a carbene ligand in Cr carbonyl complexes provides a kinetic stimulus toward CO dissociation, especially compared with non-carbene analogs. Table 10-2 illustrates the effect of the carbene ligand on the tendency for CO to dissociate in Cr complexes according to equation 10.34.

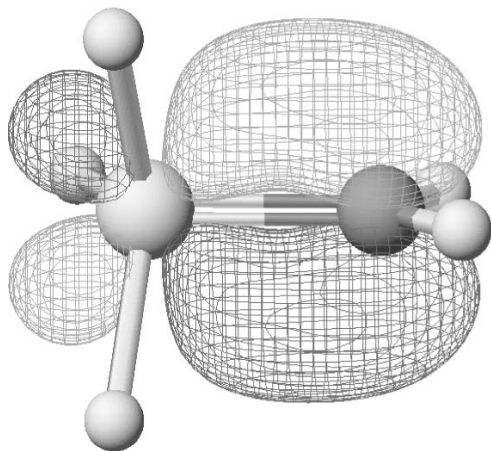
The driving force for such high CO ligand lability probably rests with the ability of the heteroatom attached to C_{carbene} to donate electrons by resonance to the metal, which becomes electron deficient upon loss of CO.



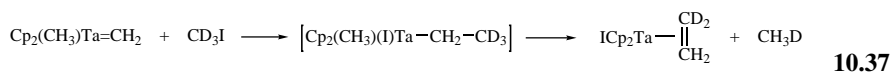
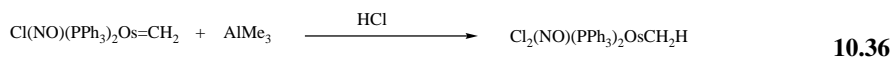
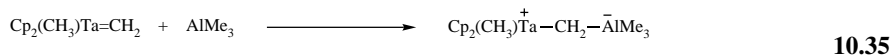
10.34

10-3-2 Electrophilic Reactions

Certain metal–carbene complexes, especially alkylidenes involving the early-transition metals, behave as nucleophiles, reacting with electron-deficient species at C_{carbene}. Figure 10-10 illustrates the HOMO (determined using DFT) of F₃Nb=CH₂, a hypothetical Schrock-type carbene. Note the high electron density at C_{carbene}, indicating a position readily susceptible to attack by electrophiles. Resonance theory also indicates that Schrock-type metal carbenes possess substantial negative charge density at C_{carbene}, with structures 9 and 12 (Section 10-1) having the greatest contribution to the overall structure. We again emphasize that it is useful to think of alkylidenes as behaving like phosphorus ylides (see Footnote 11).

**Figure 10-10**The HOMO of
 $\text{F}_3\text{Nb}=\text{CH}_2$

In our discussion we will focus on electrophilic reactions that occur at $\text{C}_{\text{carbene}}$, site **a**. Equations **10.35**, **10.36**, and **10.37** provide some examples of alkylidene chemistry.

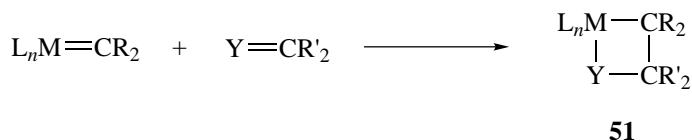


In equation **10.35**, the Ta–carbene complex is a Lewis base (at $\text{C}_{\text{carbene}}$), complexing strongly with the acidic AlMe_3 . The metal in the Os complex (**10.36**) is relatively electron rich and bonded to a carbon lacking heteroatom substituents. AlMe_3 either complexes directly with Os, followed by protonation with HCl, or reacts with HCl to give $\text{AlMe}_3\text{Cl}^- \text{H}^+$, which then protonates $\text{C}_{\text{carbene}}$. The alkylidene behaves, therefore, as a nucleophilic Schrock carbene. In equation **10.37**, a Ta complex again reacts with an electrophile initially via $\text{S}_{\text{N}}2$ substitution at $\text{C}_{\text{carbene}}$.

In equation **10.37**, some steps are missing. Provide these steps, emphasizing the transformation from the intermediate to the final products.

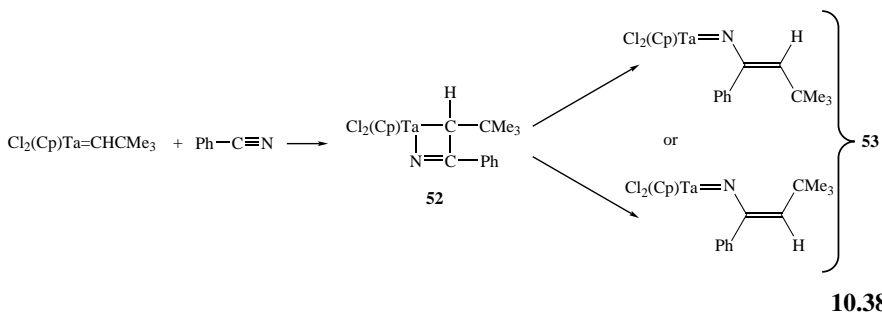
Exercise 10-6

Schrock carbene complexes undergo reaction with multiple bonds via four-center metallacyclic intermediates (**51**). Chapter 11 will consider what occurs when alkylidenes react with alkenes, a reaction known as alkene *metathesis*. Below are examples of Schrock carbenes reacting with polar multiple bonds such as C–N and C=O.

**Exercise 10-7**

Assuming that alkylidenes act as nucleophiles, show how metallacycles such as **51** could form when an organic compound containing a C=O bond reacts with $L_nM=CR_2$.

Equation **10.38** shows a Ta alkylidene reacting with benzonitrile to give **53** as a mixture of *E* and *Z* isomers. Presumably, the reaction goes through metallacycle **52** as an intermediate. Ring opening of **52** gives **53**. The driving force behind this last step is probably because Ta, as an early transition metal, prefers to bond to the more electronegative nitrogen rather than the less electronegative carbon.⁵⁵

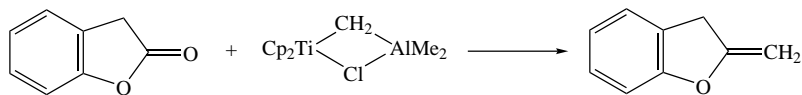


In Section **10-2-2**, we discussed the synthesis of Tebbe's reagent, a bridged Ti methylene complex. This reagent converts a C=O group to an alkene in a manner analogous to that of a phosphorus ylide (Wittig reagent).⁵⁶ Conversion of a carbonyl to a terminal alkene may seem to be of limited utility until one realizes that, unlike phosphorus ylides that react only with aldehydes and ketones, Tebbe's

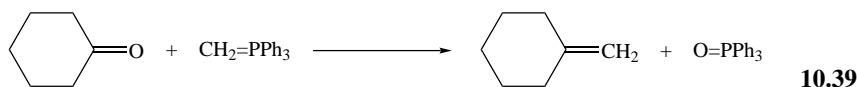
⁵⁵R. R. Schrock, *Acc. Chem. Res.*, **1979**, *12*, 98.

⁵⁶Over 30 years ago, Schrock reported that Ta alkylidenes react with a variety of carbonyl compounds—including aldehydes, ketones, and carboxylic acid derivatives—to give alkenes in exactly the same manner as Wittig reagents (except that Wittig reagents do not give alkenes from carboxylic acid derivatives). See R. R. Schrock, *J. Am. Chem. Soc.*, **1976**, *98*, 5399.

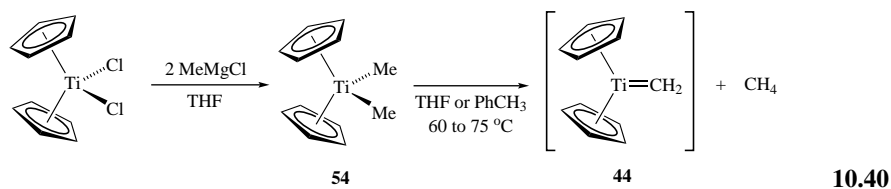
reagent will react with a variety of carbonyl compounds such as esters, thioesters, and amides, in addition to aldehydes and ketones. Equation 10.39 provides an example of alkene formation from an ester reacting with Tebbe's reagent.⁵⁷



Wittig reaction:



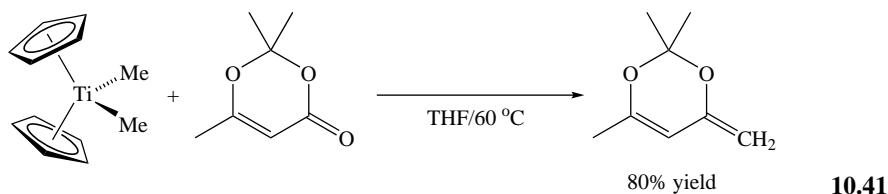
There are disadvantages associated with the use of Tebbe's reagent, however. It is air- and moisture-sensitive and pyrophoric; moreover, products resulting from its use are contaminated with aluminum salts. Attempts to extend the scope of this reagent to formation of higher alkenes, such as ethylidenes using triethylaluminum, have been unsuccessful.⁵⁸ Fortunately, more recent work has indicated that dimethyltitanocene (compound **54**, now known as Petasis reagent) is relatively stable in the presence of air and moisture and is not pyrophoric; it is easily produced from titanocene dichloride and methylmagnesium chloride or methylmagnesium chloride (equation 10.40).⁵⁹ Compound **54** then forms $\text{Cp}_2\text{Ti}=\text{CH}_2$ (**44**) *in situ* upon heating, which goes on to react with carbonyl compounds to form methylenes that are free of Al contamination. Equation 10.41 shows an example of this process.



⁵⁷For a comprehensive review detailing the scope and utility of methylenation of carbonyl compounds using Tebbe's reagent, see S. H. Pine, *Org. React.*, **1993**, *43*, 1; for a more recent review, see R. H. Hartley and G. J. McKiernan, *J. Chem. Soc., Perkin Trans. 1*, **2002**, 2763.

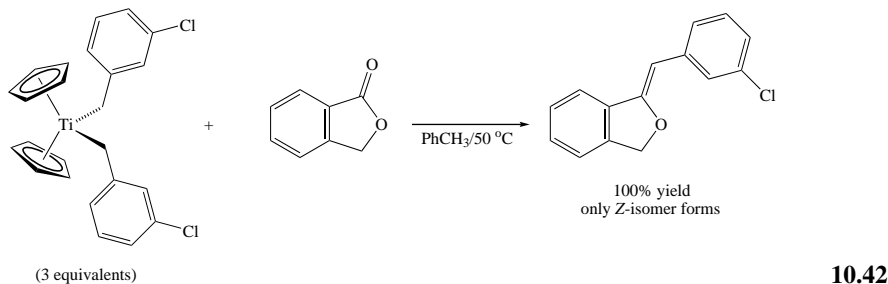
⁵⁸F. N. Tebbe and L. J. Guggenberger, *J. Chem. Soc., Chem. Commun.*, **1973**, 227.

⁵⁹N. A. Petasis and E. I. Bzowej, *J. Am. Chem. Soc.*, **1990**, *112*, 6392 and J. F. Payack, D. L. Hughes, D. Cai, I. F. Cottrell, and T. R. Verhoeven, *Org. Synth.*, **2002**, *79*, 19.

**Exercise 10-8**

Propose a mechanism for how Petasis reagent, upon heating, forms $\text{Cp}_2\text{Ti}=\text{CH}_2$.

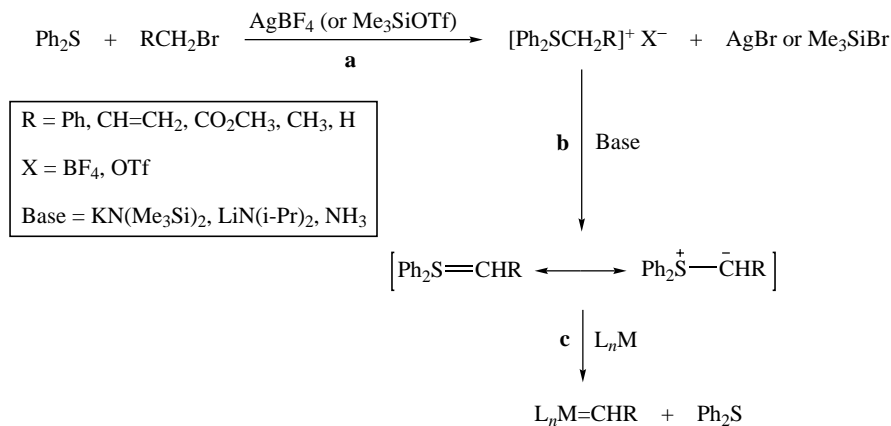
The use of Petasis reagent extends beyond methylenation. Equation **10.42** shows a transformation where it is possible to convert a lactone carbonyl group to a benzylidene.⁶⁰



10-3-3 The Chemistry of Mid- to Late Transition Metal Fischer Carbene Complexes and Alkylidenes

Although early transition metal–alkylidene complexes have rather well-defined chemistry involving the nucleophilicity of $\text{C}_{\text{carbene}}$, mid- to late transition metal alkylidenes and Fischer carbene complexes sometimes have a different chemistry associated with them. In this section, we will look at some of this chemistry, some of which has significant impact on modern organic synthesis methodology. We will compare the chemistry of these complexes with that of traditional Fischer carbene complexes.

⁶⁰N. A. Petasis and E. I. Bzorej, *J. Org. Chem.*, **1992**, 57, 1327.

**Scheme 10.4**

A General Synthesis of Metal–Alkylidene Complexes

Synthesis

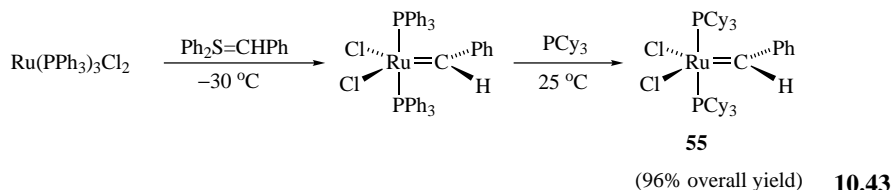
One of the most general approaches has already been mentioned and exemplified by equation 10.16. In this approach, diazoalkanes are used as free carbene precursors. These are photochemically or thermally decomposed to the free carbene, which reacts with a low-valent, mid- to late transition metal complex to give the alkylidene. Although general, this method suffers from the difficulty in handling often unstable diazo compounds.

Milstein and co-workers recently developed a general metal alkylidene synthesis that is outlined in Scheme 10.4.⁶¹ The carbon attached to sulfur (the ylide carbon) is transferred to the metal in key step c, which is called transylidation.

This method has several advantages over previously reported methodology: (1) Sulfur ylides are easy to prepare; simple variation of the R group yields several different ylides and subsequent carbene complexes. (2) All of the reaction steps, from sulfonium salt to alkylidene, occur in one reaction vessel under very mild conditions. (3) The overall transformation exhibits high atom economy because Milstein's group demonstrated that the Ph₂S by-product can be recycled.⁶² Equation 10.43 shows the near-quantitative synthesis of Grubbs' first-generation catalyst (55), which we will later encounter in Chapter 11.

⁶¹M. Gandelman, B. Rybtchinski, N. Ashkenazi, R. M. Gauvin, and D. Milstein, *J. Am. Chem. Soc.*, **2001**, *123*, 5372 and M. Gandelman, K. M. Naing, B. Rybtchinski, E. Poverenov, Y. Ben-David, N. Ashkenazi, R. M. Gauvin, and D. Milstein, *J. Am. Chem. Soc.*, **2005**, *127*, 15265.

⁶²Recycling occurs in the following way. Ph₂S is tethered to a polymeric resin so that the sulfonium salt and subsequent ylide are made in the usual way, but they are also tethered to the resin. Once the ylide has been made, the metal complex is introduced and the alkylidene forms. The Ph₂S by-product that also appears, however, is tethered to the resin and may be reused in the next cycle. This method also allows for facile separation and purification of the desired alkylidene because by-product is not in the same phase as product. The



A Spectrum of Reactivity

At the beginning of Section 10-3, we commented that metal–carbene complexes exhibit a spectrum of reactivities with nucleophiles and electrophiles, especially at $\text{C}_{\text{carbene}}$. Carbene complexes of mid-transition metals (Groups 7–9) without heteroatomic substituents at $\text{C}_{\text{carbene}}$ may show electrophilic behavior depending upon the nature of other ligands, oxidation state of the metal, and overall charge on the complex. From some observations listed below, we may be able to discern a pattern of reactivity.⁶³

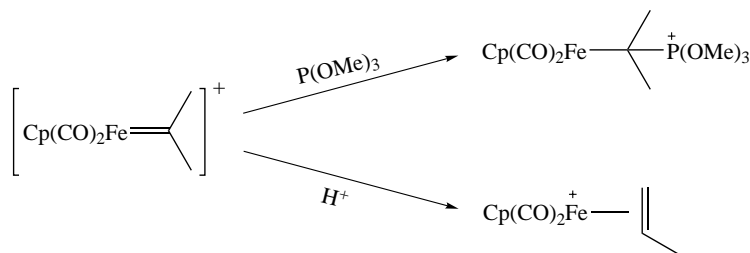
1. $\text{Cl}(\text{NO})(\text{PPh}_3)_2\text{Os}=\text{CH}_2$ reacts with the electrophile H^+ (equation 10.36) but not with CH_3I , indicating a relatively weak reactivity toward electrophiles. $[\text{I}(\text{CO})_2(\text{PPh}_3)_2\text{Os}=\text{CH}_2]^+$ readily reacts with nucleophiles.
2. $(\text{CO})_2(\text{PPh}_3)_2\text{Ru}=\text{CF}_2$ reacts with electrophiles, but $\text{Cl}_2(\text{CO})(\text{PPh}_3)_2\text{Ru}=\text{CF}_2$ reacts with nucleophiles and not at all with electrophiles.
3. $[\text{Cp}(\text{NO})(\text{PPh}_3)\text{Re}=\text{CH}_2]^+$ and $[\text{Cp}(\text{CO})_2\text{Re}=\text{C}(\text{H})(\text{alkyl})]^+$ ⁶⁴ react with both electrophiles and nucleophiles.
4. $[\text{Cp}(\text{CO})_3\text{M}=\text{CH}_2]^+$ ($\text{M} = \text{Cr}, \text{Mo}, \text{W}$) reacts with nucleophiles but not electrophiles, although neutral methylene complexes involving these metals are nucleophilic.

Observation 1 indicates that the overall charge is important in determining the reactivity of Group 7–9 carbene complexes; adding a positive charge makes the Os complex electrophilic. The Ru complexes compared in observation 2 differ in oxidation state of Ru (assuming that the carbene is an L-type ligand), with the latter an electrophilic Ru(II) complex and the former nucleophilic and Ru(0). The Re complex, described in observation 3, is transitional between nucleophilic and electrophilic reactivity. There apparently is a balance

Milstein procedure is thus analogous to the use of heterogeneous catalysts, where separation of reaction product from catalyst is straightforward.

⁶³M. A. Gallop and W. R. Roper, *Adv. Organomet. Chem.*, **1986**, 25, 121 (especially pp. 127–129).

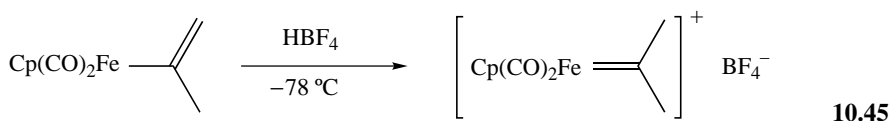
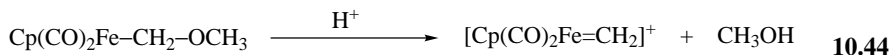
⁶⁴Such carbene complexes are called *amphiphilic*; see C. P. Casey, P. C. Vosejka, and F. R. Askham, *J. Am. Chem. Soc.*, **1990**, 112, 3713.

**Scheme 10.5**

Reactions of
Electrophilic Fe
Alkylidenes

between the electron-donating properties of the Cp and phosphine ligands and the overall charge on the complex, giving the carbene borderline reactivity. Simply increasing the overall charge to +1 in normally nucleophilic Group 6 metal carbenes causes these complexes to be electrophilic, according to observation 4. On the basis of these observations, the largest influence upon reactivity at C_{carbene} is the overall charge on the complex; the more positive the charge, the more electrophilic the species.

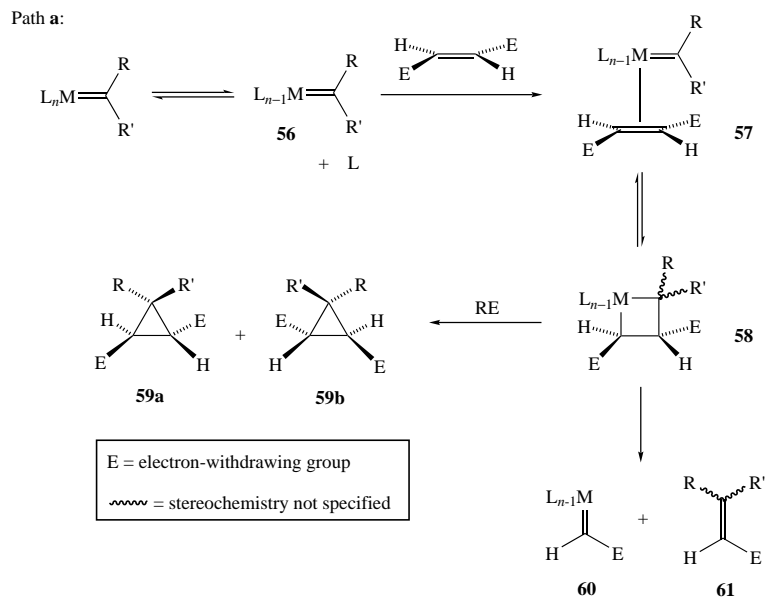
Another example of electrophilic alkylidene chemistry involves cationic Fe species, which typically react with a variety of nucleophiles at C_{carbene} . Several routes are available to synthesize these carbene complexes; equations 10.44⁶⁵ and 10.45⁶⁶ demonstrate two of these.



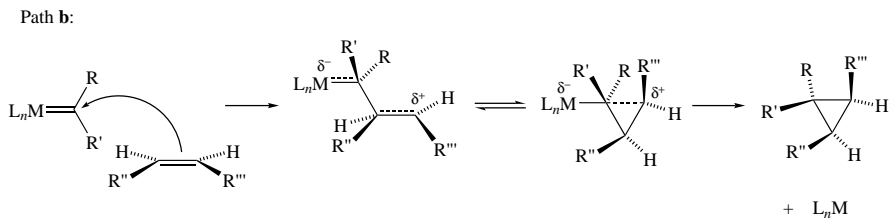
The first procedure involves ionization of a leaving group attached to C_{carbene} (perhaps more accurately described as an electrophilic abstraction, Section 8-4-2). The second procedure occurs when an electrophile (usually H^+) undergoes electrophilic addition (Section 8-4-2) to a η^1 -vinyl complex. The cationic iron complexes produced are usually thermally unstable and may either react with a nucleophile or rearrange at low temperature to an alkene complex via a 1,2-H-shift (Scheme 10.5).

⁶⁵P. W. Jolly and R. Pettit, *J. Am. Chem. Soc.*, **1966**, 88, 5044.

⁶⁶C. P. Casey, W. H. Miles, and H. Tukada, *J. Am. Chem. Soc.*, **1985**, 107, 2924.

**Scheme 10.6**

Mechanistic Pathways for Metal–Carbene-Promoted Cyclopropanation



Cyclopropane Formation

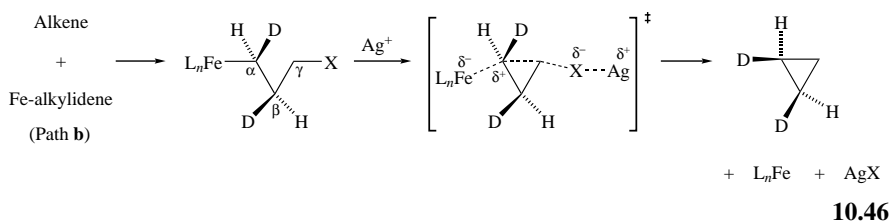
The cycloaddition of free carbenes to alkenes to give cyclopropanes is well known (see equation **10.2**). Transition metal–carbene complexes, acting either stoichiometrically or catalytically, promote cyclopropanation, sometimes in a synthetically-useful manner. Several mechanistic pathways have been observed, some of which involve mid-transition metal alkylidenes. Two of the most common of these are outlined in Scheme **10.6**.⁶⁷

⁶⁷For discussions on pathways available for cyclopropanation, see (a) C. P. Casey, “Metal–Carbene Complexes in Organic Synthesis,” in *Transition Metal Organometallics in Organic Synthesis*, H. Alper, Ed, Academic Press: New York, 1976, Vol. 1, pp. 189–233; (b) M. Brookhart and W. B. Studabaker, *Chem. Rev.*, **1987**, 87, 411; and (c) R. H. Grubbs, T. M. Trnka, and M. S. Sanford, “Transition Metal–Carbene Complexes in Olefin Metathesis and Related Reactions,” in *Fundamentals of Molecular Catalysis*, H. Kurosawa and A. Yamamoto, Eds, Elsevier: Amsterdam, 2003, pp. 187–231.

Path **a** shows loss of an L-type ligand first (giving complex **56**), which allows complexation of the alkene to the metal to yield **57**. Rearrangement of **57** to metalocyclobutane **58** amounts to a formal 2+2 cycloaddition of alkene to compound **56**. Intermediate **58** can then undergo RE to give cyclopropane **59**, or it may decompose to give **60** and a new alkene **61**. Cyclopropanation is stereospecific with respect to the substitution pattern of the alkene, but two stereomeric products (**59a** and **59b**) are possible if two different substituents were originally attached to C_{carbene} .

The sequence of steps from **56** to **61** is the pathway that occurs during π bond metathesis. We will consider closely the mechanism and importance of this important transformation in Chapter 11.

A more common, alternative path (**b**) is a direct cycloaddition mechanism, which involves interaction with C_{carbene} with one or both carbons of the $C=C$ bond of the alkene. Here, C_{carbene} acts as a “carbenoid” species in a manner analogous to what occurs in the Simmons–Smith reaction, which involves addition of CH_2 (derived from an organozinc complex) to alkenes.⁶⁸ Again, stereochemistry originally associated with the $C=C$ bond is generally preserved in the cyclopropane. Studies by Casey⁶⁹ and Brookhart,⁷⁰ using cationic Fe–alkylidene complexes, have shown that inversion of configuration, similar to an $\text{S}_{\text{E}}2$ mechanism (Chapter 8), occurs at C_{carbene} during cyclopropanation resulting from attack of the more remote γ -carbon (equation **10.46**).



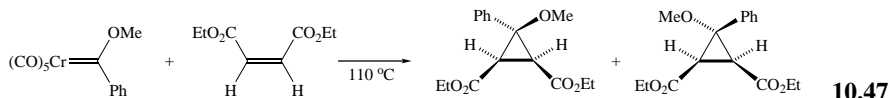
Equations **10.47** to **10.51** demonstrate several examples of cyclopropanation reactions. As shown in equation **10.47**, reaction of Group 6 Fischer carbene complexes with an electron-poor alkene—at a temperature high enough to promote CO dissociation—gives diastereomeric mixtures of cyclopropanes.⁷¹ Path **a** (Scheme **10.6**) is the likely mechanism for this reaction, and the first of the two diastereomeric products tends to be favored.

⁶⁸For a brief discussion of the Simmons–Smith reaction, see M. B. Smith, *Organic Synthesis*, 2nd ed., McGrawHill: New York, 2002, pp. 1212–1215.

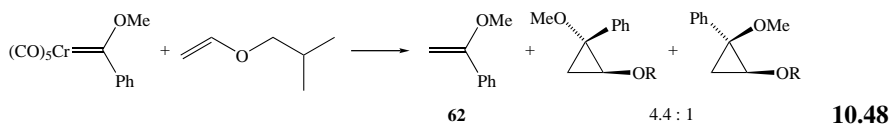
⁶⁹C. P. Casey and L. J. Smith Vosejka, *Organometallics*, **1992**, *11*, 738.

⁷⁰M. Brookhart, *et al.*, *J. Am. Chem. Soc.*, **1991**, *113*, 927 and M. Brookhart and Y. Liu, *J. Am. Chem. Soc.*, **1991**, *113*, 939.

⁷¹K. H. Dötz and E. O. Fischer, *Chem. Ber.*, **1972**, *105*, 1356.



Electron-rich alkenes also react with electrophilic carbene complexes, as equation **10.48** shows. Although reaction temperatures tend to be lower than necessary for cyclopropanation of electron-poor alkenes, the distribution of products is a function of CO pressure. In the absence of CO, alkene **62** forms predominantly.⁷² At 100 bar CO pressure, cyclopropane formation predominates. Presumably, at low CO pressure a metathesis pathway (Chapter 11) can occur. At high CO pressure, loss of CO is unlikely, so RE elimination to form cyclopropane predominates.

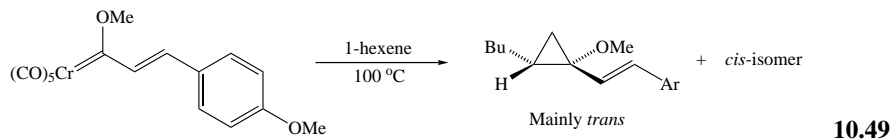
**Exercise 10-9**

Path a in Scheme 10.6 shows two initial steps whereby a CO ligand is replaced by the alkene. Why are these steps unlikely for the reaction of electrophilic carbenes with electron-rich alkenes at high CO pressure?

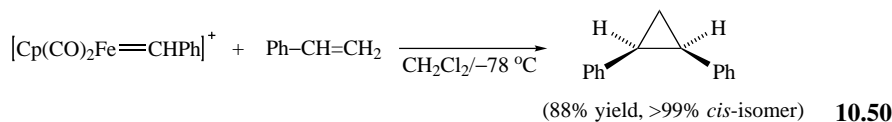
Fischer carbene complexes do not normally react with simple alkenes that are not substituted with either electron-donating or withdrawing groups. Recently, work with α,β -unsaturated carbene complexes, which also possess π electron-rich substituents such as *p*-methoxyphenyl or ferrocenyl, has shown that cyclopropanation of unactivated alkenes is possible. Equation **10.49** (using *p*-methoxyphenyl as the electron-rich substituent) shows an example of this kind of cyclopropane formation that seems to occur via path **a** (Scheme **10.6**).⁷³ Barluenga proposed that the Fischer carbene complex is more reactive than is typical because the ferrocenyl and *p*-methoxyphenyl groups act as electron donors. This donated electron density ends up on C_{carbene} and the $\text{Cr}(\text{CO})_5$ fragment, which can absorb any extra negative charge.

⁷²E. O. Fischer and K. H. Dötz, *Chem. Ber.*, **1972**, *105*, 3966; for a more recent paper on reactions of Fischer carbene complexes with electron-rich alkenes, see W. D. Wulff, D. C. Yang, and C. K. Murray, *Pure Appl. Chem.*, **1988**, *60*, 137.

⁷³J. Barluenga, S. López, A. A. Trabanco, A. Fernandez-Acebes, and J. Flórez, *J. Am. Chem. Soc.*, **2000**, *122*, 8145.



Although the use of Fischer carbene complexes for cyclopropanation is somewhat limited, there are other procedures that are more general. One such method is the use of cationic alkylidene complexes, with Fe complexes being perhaps the most thoroughly studied. These react at low temperature with a variety of alkenes bearing alkyl and aryl substituents; equation **10.50** shows a typical example with the cationic alkylidene precursor usually generated *in situ*.⁷⁴ Path **b** (Scheme **10.6**) has been shown to be the operative mechanism for these reactions.⁷⁵



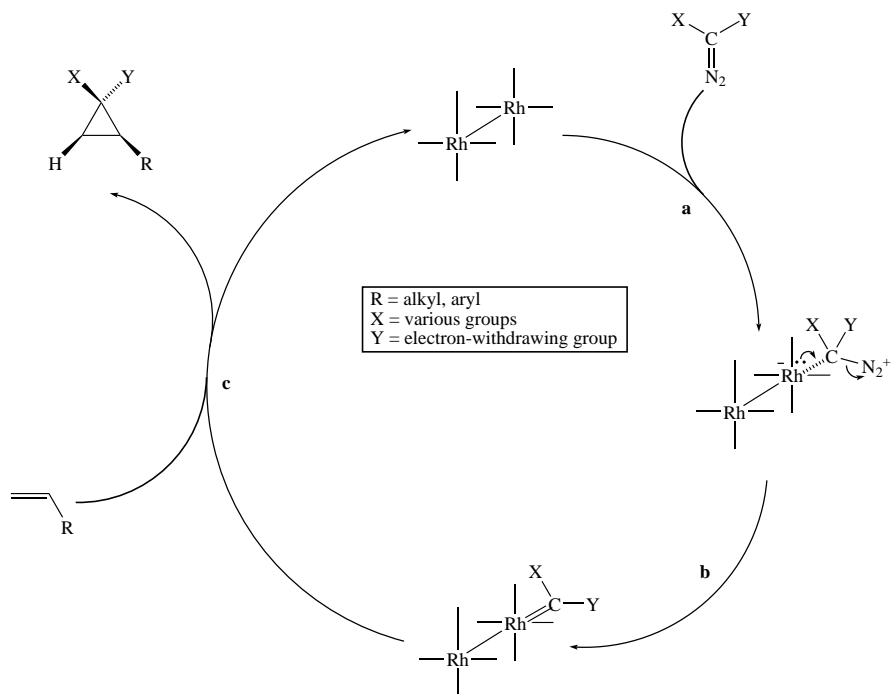
Another cyclopropanation procedure that is quite general involves the use of Rh–carbene complexes, which can act catalytically to effect ring formation. Scheme **10.7** shows some of the details of this method. C_{carbene} is derived from corresponding diazo compounds, which were traditionally used directly as sources of free carbenes. The scheme includes a catalytic cycle for conversion of the diazo compound to the Rh–carbene complex, which then delivers C_{carbene} to the alkene. Transfer of C_{carbene} regenerates an active catalyst that can react with another mole of diazo compound. The detailed mechanism of step **c** in the cycle resembles path **b** from Scheme **10.6**.

The precursor to the Rh–carbene complex is a dirhodium system that typically has four bidentate ligands attached. One example of the dirhodium complex is shown as structure **63**, which was discovered by Doyle and co-workers and is abbreviated $\text{Rh}_2(5S\text{-MEPY})_4$.⁷⁶ Here the 5*S*-MEPY ligand is chiral carboxamidate, which is derived from the amino acid L-proline. The use of **63** and similar complexes makes it possible to induce chirality into the cyclopropane product. Equation **10.51** is an example of an intramolecular chiral cyclopropanation

⁷⁴M. Brookhart, M. B. Humphrey, H. J. Kratzner, and G. O. Nelson, *J. Am. Chem. Soc.*, **1980**, *102*, 7802.

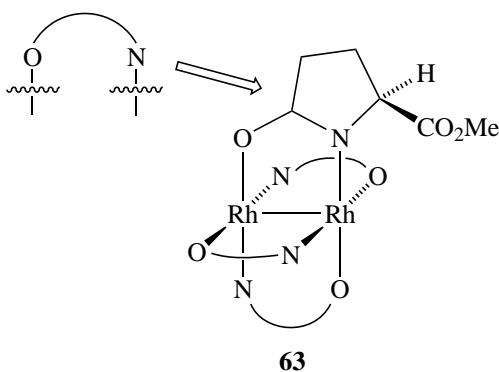
⁷⁵For information on the scope and synthetic utility of cyclopropanation using electrophilic alkylidenes, see Footnote 67b.

⁷⁶M. P. Doyle, W. R. Winchester, J. A. A. Hoorn, V. Lynch, S. H. Simonsen, and R. Ghosh, *J. Am. Chem. Soc.*, **1993**, *115*, 9968.

**Scheme 10.7**

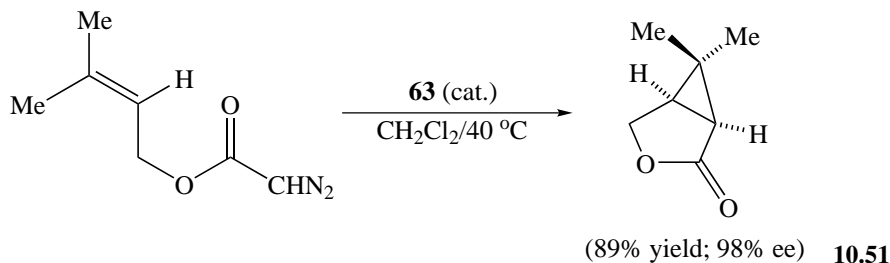
Catalytic Cycle
for Rh-Catalyzed
Cyclopropanation

catalyzed by compound **63**.⁷⁷ The use of diazo alkanes to generate both Rh and Cu carbene catalysts to effect intermolecular and intermolecular cyclopropanation is now a widely-used method in synthesis.⁷⁸



⁷⁷M. P. Doyle, et al., *J. Am. Chem. Soc.*, **1995**, *117*, 5763.

⁷⁸For comprehensive reviews that provide numerous examples of cyclopropanation based on Rh- and Cu-carbene catalysis, see M. P. Doyle, M. A. McKervey, and T. Ye, *Modern Catalytic Methods for Organic Synthesis with Diazo Compounds*, Wiley: New York, 1998; M. P. Doyle and D. C. Forbes, *Chem. Rev.*, **1998**, *98*, 911; and M. P. Doyle, *J. Org. Chem.*, **2006**, *71*, 9254.



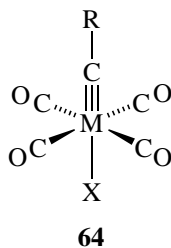
10-3-4 Chemistry of NHC–Metal Complexes

Metal complexes of NHCs are extremely important as catalysts in reactions of importance to the field of organic synthesis. Section 10-1-1 has already addressed the electronic and steric properties of NHC ligands that enhance the catalytic activity of NHC–metal complexes, and section 10-2-3 discussed methods of synthesis. Very little chemistry, however, occurs at C_{carbene} . Instead, NHCs act mainly as supporting ligands, so that useful chemistry can take place at other positions on the catalyst complex. We will see applications of the use of NHC–metal complexes for synthesis in Chapters 11 and 12.

10-4 METAL–CARBYNE COMPLEXES

10-4-1 Structure

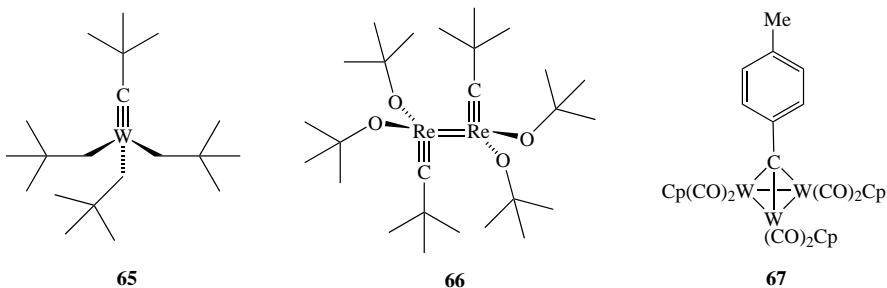
Following his pioneering work in the preparation of the first stable metal–carbene complexes, Fischer⁷⁹ reported the first syntheses of complexes containing an $M\equiv C$ bond nine years after his metal–carbene articles appeared. Complexes **64**, called *metal–carbyne complexes* or *alkylidynes* (if $R = \text{alkyl or aryl}$), were discovered serendipitously in the course of attempts to develop new methods for preparing carbene complexes.



$M = \text{Cr, Mo, W}; X = \text{Cl, Br, I}; R = \text{Me, Et, Ph}$

⁷⁹E. O. Fischer, G. Kreis, C. G. Kreiter, J. Müller, G. Huttner, and H. Lorenz, *Angew. Chem. Int. Ed. Eng.*, **1973**, *12*, 564.

Since Fischer's breakthrough, numerous new carbyne complexes involving mainly Group 5, 6, 7, 8, and 9 metals have been prepared, their structures determined, and their chemistry explored. Some examples of metal carbynes appear as structures **65**, **66**, and **67**.



Tungsten alkylidyne **65** was first reported by Schrock⁸⁰ in 1978, and it represents a very different type of carbyne complex than that first synthesized by Fischer. Structure **66** portrays a dirhenium–dicarbyne complex, also prepared by Schrock,⁸¹ and is rather unusual in that it lacks bridging ligands that support the metal–metal bonding. The μ_3 -bridging carbyne complex⁸² (**67**) demonstrates that the carbyne ligand may bond to more than one metal atom. Although **67** is interesting structurally,⁸³ we will confine our discussion to *terminal* carbyne complexes (non-bridging) as represented by structures **64–66**.

There are several parallels between the chemistries of the carbene and carbyne ligands. The classification of carbyne complexes into two major structural types—Fischer and Schrock—is perhaps the most obvious of these parallels. Complex **64** represents the prototypical Fischer carbyne complex: C_{carbyne} bonded to a low-valent metal with π -accepting CO ligands attached. Structure **65**, on the other hand, is a classic example of a Schrock carbyne complex because a high-valent metal is present with electron-donating ligands attached. Atoms attached to C_{carbyne} , helpful in distinguishing between Fischer and Schrock carbene complexes (i.e., heteroatoms for the former and H and C for the latter), are less important in the case of carbyne complexes. It is convenient to classify carbyne complexes

⁸⁰D. N. Clark and R. R. Schrock, *J. Am. Chem. Soc.*, **1978**, *100*, 6774.

⁸¹R. Toreki, R. R. Schrock, and M. G. Vale, *J. Am. Chem. Soc.*, **1991**, *113*, 3610.

⁸²M. Green, S. J. Porter, and F. G. A. Stone, *J. Chem. Soc., Dalton Trans.*, **1983**, 513.

⁸³Bridging carbynes are important ligands in metal cluster compounds (Chapter 13) and may play a role in surface-catalyzed reactions. Methine (C–H), bound to more than one metal atom, is considered to be involved in intermediate stages of the Fischer–Tropsch reaction, which is used to convert basic hydrocarbon starting materials, such as those from coal, into gasoline and diesel fuel (M. J. Overett, R. O. Hill, and J. R. Moss, *Coord. Chem. Rev.*, **2000**, *206–207*, 581).

according to these two types, but some caution must be exercised because the scheme breaks down for some of these complexes. For example, the metal in tungsten–benzylidyne complex **68** is low valent and relatively electron rich, yet the ligands attached are neither strong π donors nor π acceptors.⁸⁴ Another example of a carbyne complex intermediate between the classical Fischer and Schrock structural types would be $\text{Cl}(\text{CO})(\text{PPh}_3)_2\text{Os}\equiv\text{C}-\text{Ph}$, which is analogous to the Group 8 carbene complexes mentioned in Section 10-3-3.

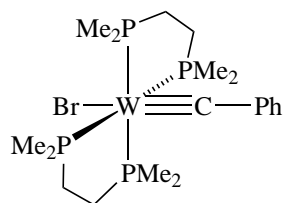
**68**

Figure 10-11a provides a rationalization for the bonding of a univalent carbon fragment to a metal in Fischer carbyne complexes. The carbon fragment possesses three electrons,⁸⁵ two in an sp orbital and one distributed between two degenerate $2p$ orbitals. The metal fragment has filled and unfilled orbitals of comparable symmetry such that one σ and two π bonds form. Under the neutral ligand method of electron counting, the carbyne ligand is considered an LX ligand.

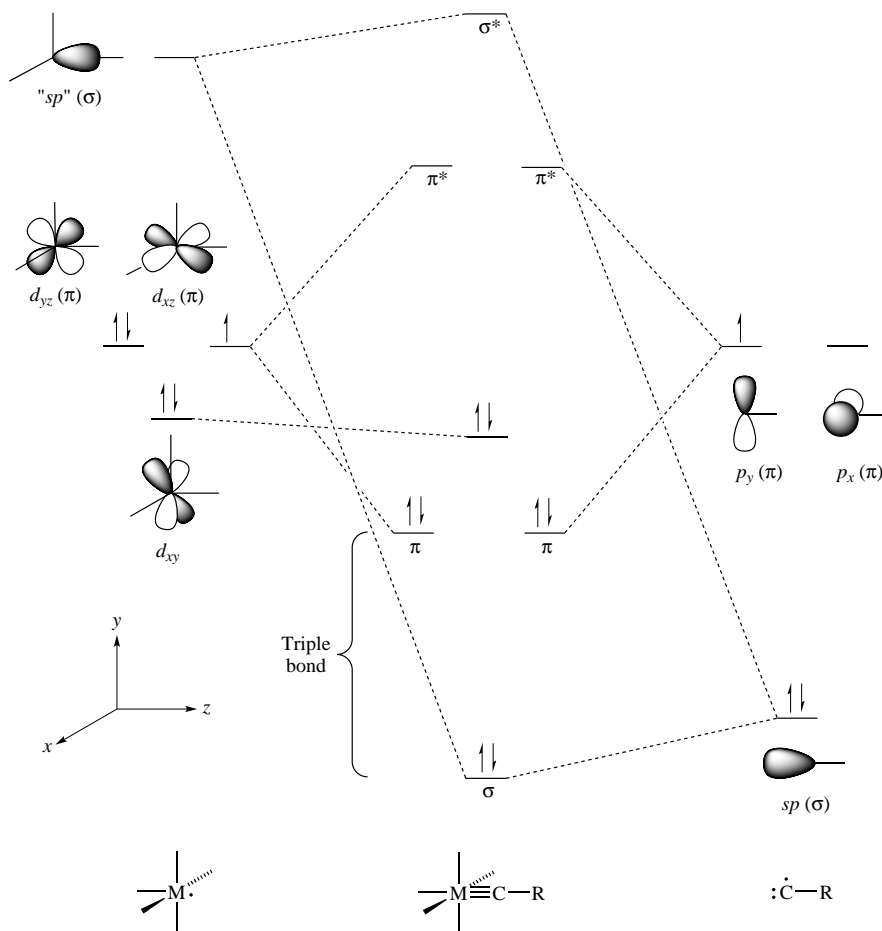
A similar bonding scheme could accommodate Schrock carbyne complexes involving high-oxidation-state metals. In this case, we consider the carbyne ligand to be $\text{R}-\text{C}^3-$ or an X_3 ligand (still a $3-e^-$ ligand according to the neutral ligand model). Acting as both a σ and a π donor, the carbyne fragment forms three bonds to the electron-deficient metal (Figure 10-11b).⁸⁶

The triple bond in metal carbynes is shorter than the comparable double bond in metal carbenes (ca. 165–185 pm vs. >200 pm). The $\text{M}-\text{C}-\text{R}$ bond angle, although not exactly 180° , is usually larger than 170° .

⁸⁴J. Manna, T. M. Gilbert, R. E. Dallinger, S. J. Geib, and M. D. Hopkins, *J. Am. Chem. Soc.*, **1992**, *114*, 5870.

⁸⁵Some models for carbyne bonding use a two-electron $^+\text{C}-\text{R}$ ligand bonded to a L_nM^- fragment. Use of a three-electron carbon ligand is more consistent with the electron count (a $3-e^-$ LX ligand according to the neutral ligand method) associated with carbyne ligands.

⁸⁶For a recent summary of the use of MO calculations on carbyne complexes, see G. Frenking and N. Fröhlich, *Chem. Rev.*, **2000**, *100*, 717; see also H. Fischer, P. Hofmann, F. R. Kreissl, R. R. Schrock, U. Schubert, and K. Weiss, *Carbyne Complexes*, VCH Publishers: New York, 1988, pp. 60–98.

**Figure 10-11a**

Molecular Orbital Bonding Scheme for a Fischer Carbyne Complex

Exercise 10-10

The $M\equiv C$ bond distance for $Br(CO)_4Cr\equiv C-Ph$ is 168 pm, whereas that for $Br(CO)_4Cr\equiv C-NEt_2$ is 172 pm. Consider the nature of the two substituents attached to C_{carbyne} and explain the difference in bond lengths in terms of resonance theory.

10-4-2 Synthesis

Equation 10.52 shows the chemistry used to produce **64** and similar complexes; this not only is the original procedure employed by Fischer, but also constitutes perhaps the most versatile method for the preparation of Fischer carbyne complexes. The reaction begins with an electrophilic abstraction of the alkoxy group from starting carbene **69** to give the cationic carbyne **70**. Carbyne ligands are such powerful π acceptors that they exert a strong *trans* effect (Section 7-1-1). If

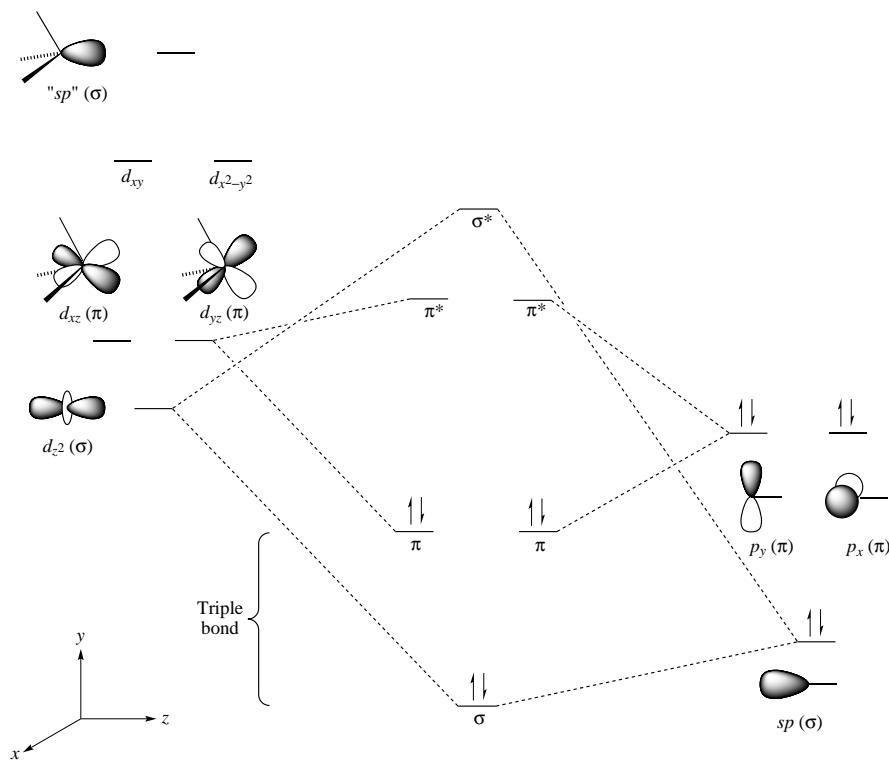
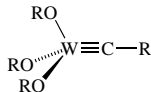
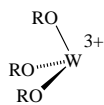
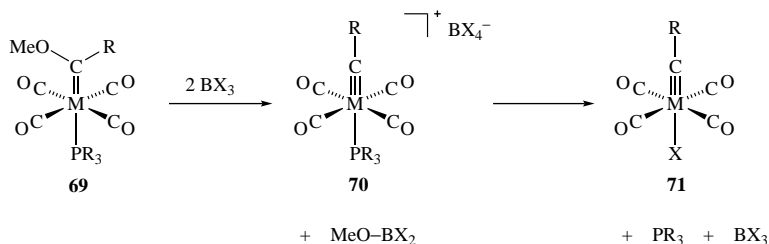


Figure 10-11b

Molecular Orbital Bonding Scheme for a Schrock Carbyne Complex

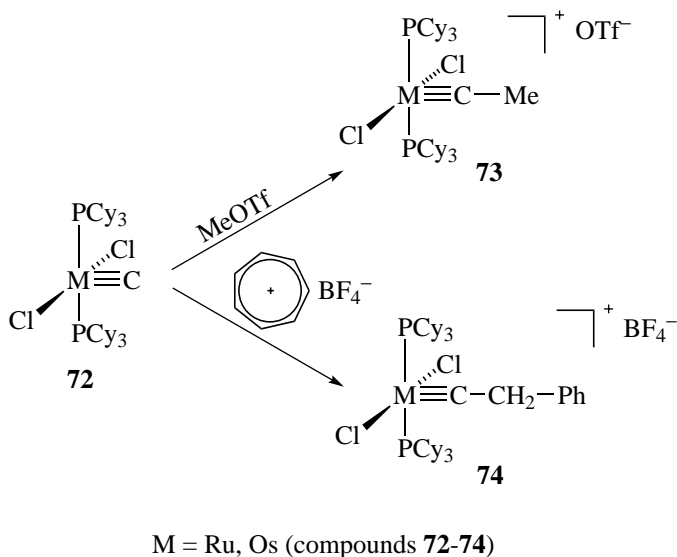


the group *trans* to C_{carbyne} is a π acceptor such as CO or PR_3 , the M–CO or M–P bond is relatively weak. A halide displaces the phosphine ligand to give the final neutral carbyne complex **71**. Now a π -donating halogen group is situated *trans* to the carbyne ligand, which stabilizes the complex overall.



R = alkyl, aryl; M = Mo, W; X = Cl, Br

10.52

**Scheme 10.8**

Use of Carbide
Complexes as
Precursors to
Alkydynes

Exercise 10-11

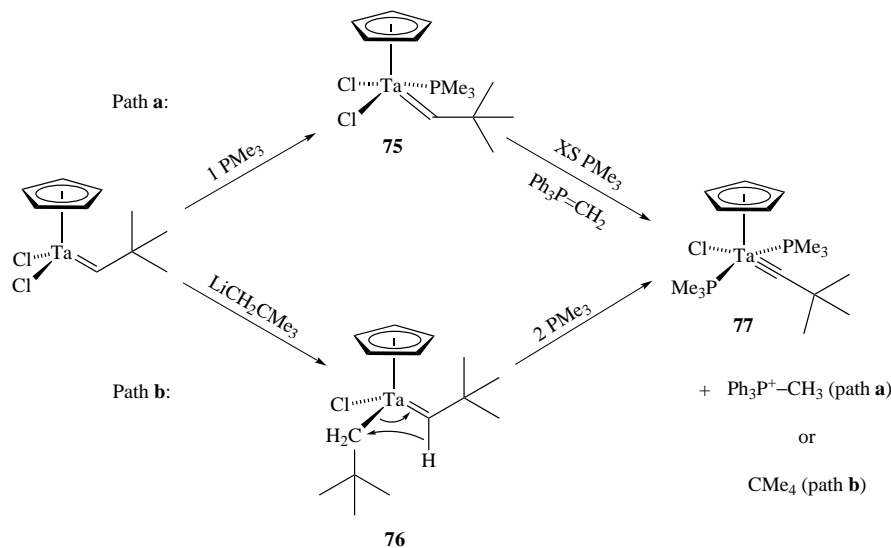
If the ligand *trans* to C_{carbide} in **69** is NR₂ (R = alkyl, aryl), a stable, cationic carbyne analogous to **70** may be isolated. Explain.

In Chapter 8 we described how metal carbides (first mentioned in Section 6-1-4) could serve as precursors to carbyne complexes by way of electrophilic addition. Scheme 10.8 revisits a portion of Scheme 8.12, showing Os–carbide complex **72**—with its nucleophilic C_{carbide} atom—reacting with methyl triflate or tropylium ion to give alkydynes **73** and **74**, respectively. Comparable reactions occur with the corresponding Ru–carbide complex.⁸⁷ This method may become more general after the synthesis of additional carbide complexes occurs.

Scheme 10.9 shows routes that Schrock⁸⁸ used to produce Ta–carbyne complex **77** involving either α-hydrogen abstraction or α-elimination, two widely-used methods for producing alkydynes. Path **a** involves addition of one equivalent of PMe₃ to give **75**. Deprotonation of **75** with an ylide in the presence of excess PMe₃ yields **77**. Path **b** involves displacement of one Cl ligand with neopentyl to give **76**. Attachment of PMe₃ to Ta creates sufficient steric hindrance for an intramolecular α-elimination to occur yielding **77** and one equivalent of 2,2-dimethylpropane.

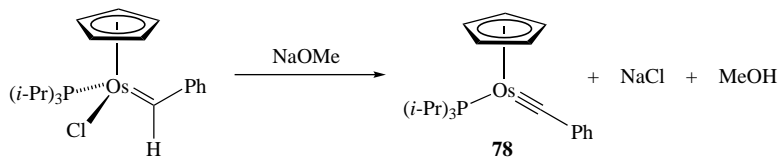
⁸⁷M. H. Stewart, M. J. A. Johnson, and J. W. Kampf, *Organometallics*, **2007**, *26*, 5102.

⁸⁸S. J. McLain, C. D. Wood, L. W. Messerle, R. R. Schrock, F. J. Hollander, W. J. Youngs, and M. R. Churchill, *J. Am. Chem. Soc.*, **1978**, *100*, 5962.

**Scheme 10.9**

Two Routes to
Schrock Carbyne
Complexes

A route to Os alkylidyne (**78**), which has both Schrock and Fischer characteristics, is shown in equation **10.53**. The reaction resembles an E2 elimination from the corresponding alkylidene complex.⁸⁹



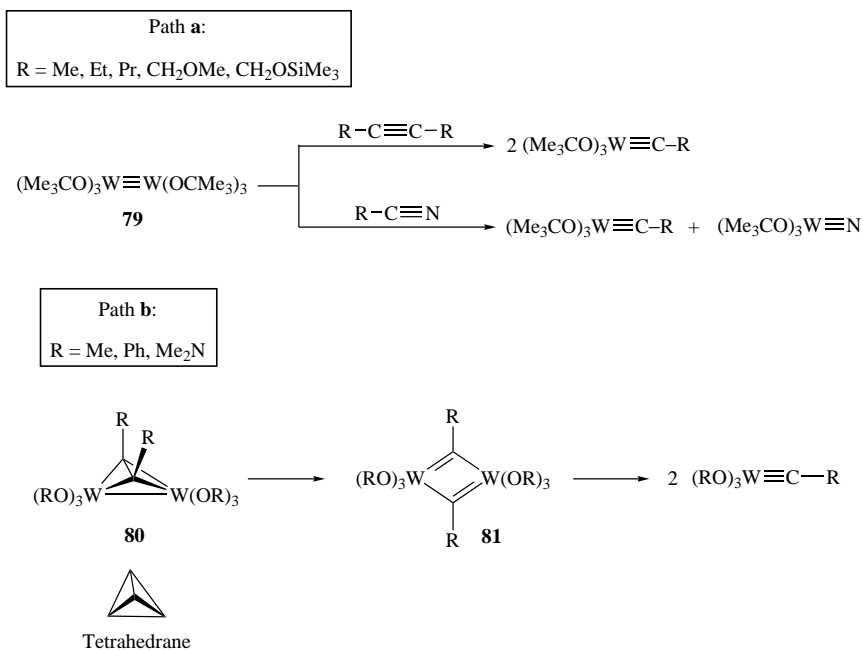
A route to alkylidynes containing metals with high oxidation states involves a metathesis exchange reaction that we have referred to briefly in earlier sections of Chapter 10. Scheme **10.10** shows the triply-bonded ditungsten complex **79** reacting with either alkynes or nitriles to give the corresponding metal carbyne (path **a**)⁹⁰ or metal–carbyne plus nitride complex (path **b**).⁹¹ Scheme **10.10** also shows results of molecular orbital calculations at the DFT level.⁹² In the case

⁸⁹M. A. Esteruelas, A. I. González, A. M. López, and E. Oñate, *Organometallics*, **2003**, *22*, 414, and **2004**, *23*, 4858.

⁹⁰(a) R. R. Schrock, M. L. Listemann, and L. G. Sturgeoff, *J. Am. Chem. Soc.*, **1982**, *104*, 4291 and (b) M. L. Listemann and R. R. Schrock, *Organometallics*, **1985**, *4*, 74.

⁹¹M. H. Chisholm, J. C. Huffman, and N. S. Marchant, *J. Am. Chem. Soc.*, **1983**, *105*, 6162, and reference 90a.

⁹²S. Fantacci, N. Re, M. Rosi, A. Sgamellotti, M. F. Guest, P. Sherwood, and C. Floriani, *J. Chem. Soc., Dalton Trans.*, **1997**, 3845.

**Scheme 10.10**

Synthesis of
Carbyne Complexes
Using Metathesis

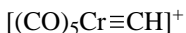
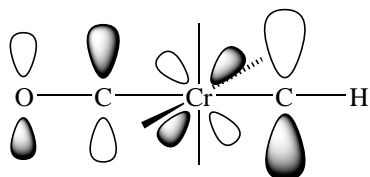
of the reaction of **79** with the alkyne, the preferred pathway involves first addition of the alkyne to the W≡W bond to give bridging complex **80**. Complex **80** resembles a flattened analog of tetrahedrane (shown below **80** for comparison). The pathway continues to a 1,3-tungstacyclobutadiene **81** before fragmenting to two equivalents of the metal carbyne.

10-4-3 Reactions

As with carbene complexes, metal carbynes display a range of reactivity with electrophiles and nucleophiles. Molecular orbital calculations show that even cationic Fischer carbyne complexes are polarized as $\text{M}^{\delta+}\equiv\text{C}^{\delta-}$; neutral Fischer- and Schrock carbyne complexes have an even greater negative charge on $\text{C}_{\text{carbyne}}$.⁹³ If all reactions between carbyne complexes and other species were charge-controlled, we would predict that nucleophiles would always attack at the metal and electrophiles at $\text{C}_{\text{carbyne}}$. As we should expect by now, the picture is more complicated in practice.

Cationic Fischer-type carbyne complexes react with nucleophiles exclusively at $\text{C}_{\text{carbyne}}$. Calculations show that the LUMO of these complexes possess

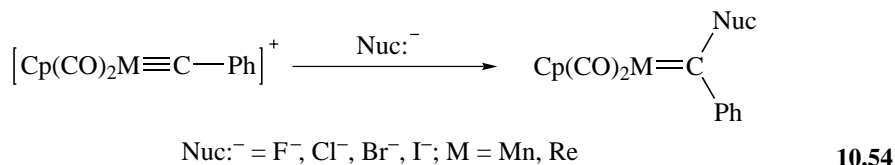
⁹³S. F. Vyboishchikov, and G. Frenking, *Chem. Eur. J.*, **1998**, *4*, 1439 and J. Ushio, H. Nakatsuji, and T. Yonezawa, *J. Am. Chem. Soc.*, **1984**, *106*, 5892.



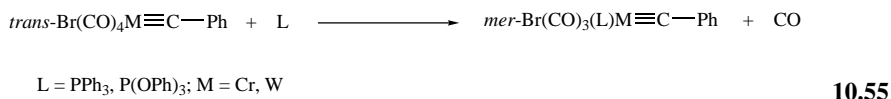
Figures 10-12a

LUMO of a Cationic
Fischer Carbyne
Complex

a large lobe centered about $\text{C}_{\text{carbyne}}$ and a much smaller lobe at the metal (Figure 10-12a). Instead of being controlled by charge density, such reactions are frontier orbital controlled. Equation 10.54⁹⁴ shows an example of cationic Group 7 metal carbynes reacting with a variety of nucleophiles, a transformation that is also an excellent method for converting carbynes to carbenes.



Nucleophiles react differently with neutral Fischer carbyne complexes because now the LUMO and next higher unoccupied orbital (close to the LUMO in energy) of these complexes do not show a distinct region of electron deficiency at $\text{C}_{\text{carbyne}}$. In addition to $\text{C}_{\text{carbyne}}$, the metal and the ligands (such as the carbon of a CO ligand) offer sites suitable for nucleophilic attack (Figure 10-12b, which shows only the lobes on $\text{C}_{\text{carbyne}}$ and Cr). Equation 10.55 shows the attack of a phosphine or phosphite on the metal of neutral Group 6 carbynes.⁹⁵



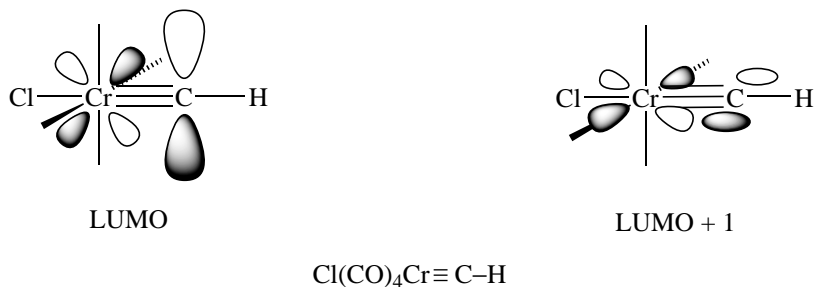
The reaction is first order in the presence of excess phosphine with a positive entropy of activation, suggesting that ligand substitution occurs via a dissociative pathway.

⁹⁴E. O. Fischer, C. Jiabi, and S. Kurt, *J. Organomet. Chem.*, **1983**, 253, 231 and E. O. Fischer and J. Chen, *Huaxue Xuebao*, **1985**, 43, 188.

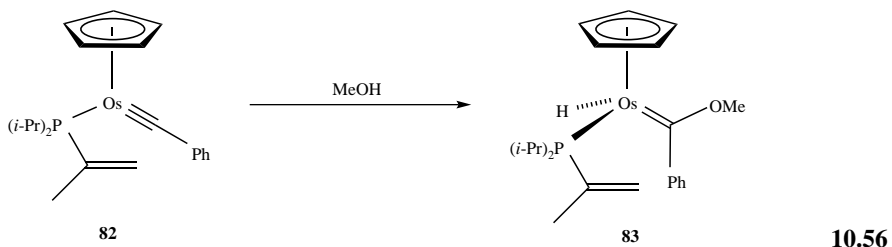
⁹⁵M. H. Chisholm, K. Folting, D. M. Hoffman, and J. C. Huffman, *J. Am. Chem. Soc.*, **1984**, 106, 6794.

Figure 10-12b

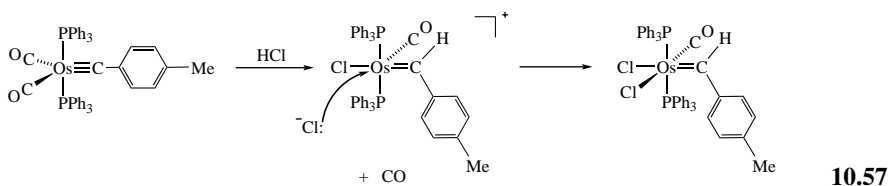
LUMOs of a Neutral Fischer Carbyne Complex Showing Only the M–C_{carbyne} Interactions



On the other hand, neutral Os alkylidyne **82** undergoes reaction with methanol to give carbene complex **83** (equation 10.56).⁹⁶ It would appear that **82** undergoes reaction with nucleophilic methanol at C_{carbyne} first, which is followed by proton transfer to Os. Such reactivity would be consistent with that associated with Fischer carbyne complexes, yet the metal center is more electron-rich than the group 6 metal complex reactant in equation 10.55.



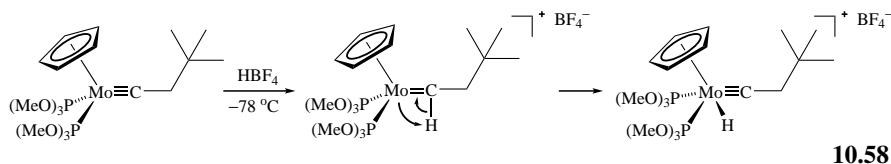
Schrock carbynes and Group 8 (M = Os, Ru) alkylidynes react with electrophiles, typically at C_{carbyne}. Equation 10.57 shows the electrophilic addition of HCl across the M≡C of an Os carbyne complex in a manner reminiscent of Markovnikov addition of HCl across an unsymmetrical C≡C bond. The reaction presumably begins by attack of H⁺ at C_{carbyne}, followed by ligand attachment of Cl⁻.⁹⁷



⁹⁶See Footnote 89.

⁹⁷G. R. Clark, K. Marsden, W. R. Roper, and L. J. Wright, *J. Am. Chem. Soc.*, **1980**, *102*, 6570.

Reaction of the Mo Schrock carbyne complex in equation 10.58 with HBF_4 results in protonation at $\text{C}_{\text{carbyne}}$, followed by rearrangement to the thermodynamically more stable Mo–H complex. The BF_4^- ion is such a weakly coordinating ligand that substitution at the metal does not occur.⁹⁸



Other Lewis acids react with metal carbynes. Although the initial attack often occurs at $\text{C}_{\text{carbyne}}$, the final product may be the result of subsequent reactions that may be difficult to rationalize mechanistically.⁹⁹ Some of the problems at the end of Chapter 10 will depict more of the chemistry of carbyne complexes. Perhaps the most significant reaction of carbyne complexes is π bond metathesis, which has been alluded to in the discussion on procedures for metal–carbyne synthesis. We will see more consideration of this reaction in Chapter 11.

Suggested Readings

Metal Carbene Complex Structure

- G. Frenking, M. Solà, and S. F. Vyboishchikov, “Chemical Bonding in Transition Metal Carbene Complexes,” *J. Organomet. Chem.*, **2005**, 690, 6178.
- T. Strassner, “Electronic Structure and Reactivity of Metal Carbenes,” *Top. Organomet. Chem.*, **2004**, 13, 1.
- G. Frenking and N. Fröhlich, “Bonding in Transition–Metal Compounds,” *Chem. Rev.*, **2000**, 100, 717.

Fischer Carbene Complexes

- C. F. Bernasconi, “The Physical Organic Chemistry of Fischer Carbene Complexes,” *Adv. Phys. Org. Chem.*, **2002**, 37, 137.
- K.-H. Dötz, H. Fischer, P. Hofmann, F. R. Kreissl, U. Schubert, and K. Weiss, *Transition Metal Carbene Complexes*, Verlag Chemie: Weinheim, Germany, 1983.

⁹⁸M. Bottrill, M. Green, A.G. Orpen, D. R. Saunders, and I. D. Williams, *J. Chem. Soc., Dalton Trans.*, **1989**, 511.

⁹⁹The synthesis and reactivity of metal carbynes has been comprehensively reviewed. See M. A. Gallop and W. R. Roper, *Adv. Organomet. Chem.*, **1986**, 25, 121; H. P. Kim and R. J. Angelici, *Adv. Organomet. Chem.*, **1987**, 27, 51; and A. Mayr and H. Hoffmeister, *Adv. Organomet. Chem.*, **1991**, 32, 227. More recent summaries of carbyne reactions appear annually in the journal *Coordination Chemistry Reviews*; see, for example, G. Jia, *Coord. Chem. Rev.*, **2007**, 251, 2167, for a recent review of the chemistry of Os carbyne complexes.

F. J. Brown, “Stoichiometric Reactions of Transition Metal Carbene Complexes,” *Prog. Inorg. Chem.* **1980**, *27*, 1.

Schrock Carbene Complexes (Alkylidenes)

R. R. Schrock, “High Oxidation State Multiple Metal–Carbon Bonds,” *Chem. Rev.*, **2002**, *102*, 145.

R. C. Hartley and G. J. McKiernan, “Titanium Reagents for the Alkylidene of Carboxylic Acids and Carbonic Acid Derivatives,” *J. Chem. Soc., Perkin Trans. 1*, **2002**, 2763.

N-Heterocyclic Carbene Complexes

F. E. Hahn and M. C. Jahnke, “Heterocyclic Carbenes: Synthesis and Coordination Chemistry,” *Angew. Chem. Int. Ed.*, **2008**, *47*, 3122.

E. Peris, “Routes to N-Heterocyclic Carbene Complexes,” *Top. Organomet. Chem.*, **2007**, *21*, 83.

F. Glorius, “N-Heterocyclic Carbenes in Catalysis—An Introduction,” *Top. Organomet. Chem.*, **2007**, *21*, 1.

Cyclopropanation

M. P. Doyle, M. A. McKervey, and T. Ye, *Modern Catalytic Methods for Organic Synthesis with Diazo Compounds*, Wiley: New York, 1998.

Metal Carbyne Complexes

P. F. Engel and M. Pfeffer, “Carbon–Carbon and Carbon–Heteroatom Coupling Reactions of Metallacarbynes,” *Chem. Rev.*, **1995**, *95*, 2281.

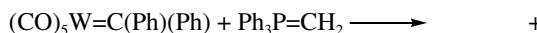
H. Fischer, P. Hofmann, F. R. Kreissl, R. R. Schrock, U. Schubert, and K. Weiss, *Carbyne Complexes*, VCH Publishers: New York, 1988.

H. P. Kim and R. J. Angelici, “Transition Metal Complexes with Terminal Carbyne Ligands,” *Adv. Organomet. Chem.*, **1987**, *27*, 51.

See also the Schrock *Chemical Review* (2002) paper from above.

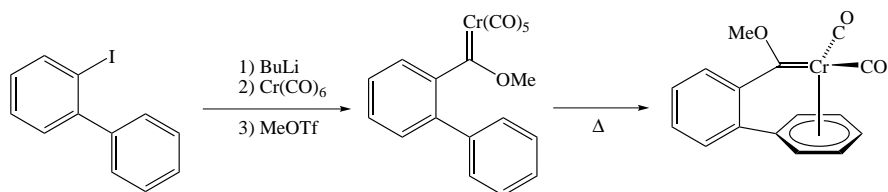
Problems

10-1 Assuming that Fischer-type carbene complexes react similarly to ketones and that phosphorus ylides are good carbon nucleophiles, predict the products in the following reaction:



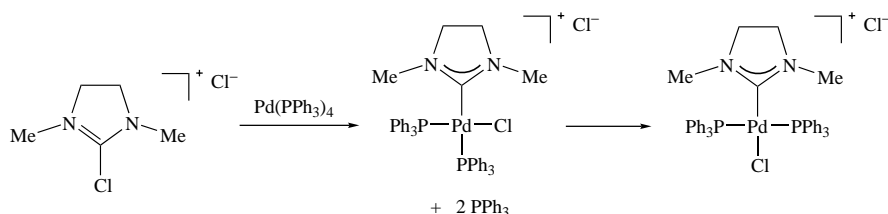
10-2 The chemistry outlined on the next page was used to produce a cyclic arene–chromium carbene complex.¹⁰⁰

¹⁰⁰C. A. Merlic, D. Xu, and S. I. Khan, *Organometallics*, **1992**, *11*, 412.



- a. Describe in detail what happens in each reaction step.
- b. The carbene complex above is interesting because it was unreactive toward nucleophiles under conditions that cause ordinary Fischer-type carbene complexes to react readily (for example, it did not undergo the chemistry shown in equations **10.27–10.29**). X-ray analysis showed that the $M-C_{\text{carbene}}$ bond distance was 195.3 pm and the bond distance between the metal and carbonyl carbon ($M-CO$) was 184 pm. This contrasts with $M-C_{\text{carbene}}$ and $M-CO$ bond distances of 200–210 pm and 180 pm, respectively, for Fischer carbene complexes such as $(CO)_5Cr=C(OCH_3)(Ph)$. Explain why the cyclic arene-Cr carbene complex is not electrophilic in its chemical behavior.

10-3 A method for producing Group 10 metal-NHC complexes is the following. What kind of fundamental organometallic reaction is involved in each step with this method?¹⁰¹

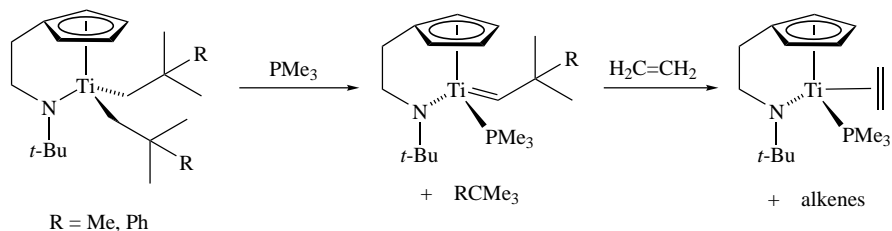


10-4 Propose a reasonable mechanism for the transformation shown below. Assume that the first step is protonation at C_{carbyne} .

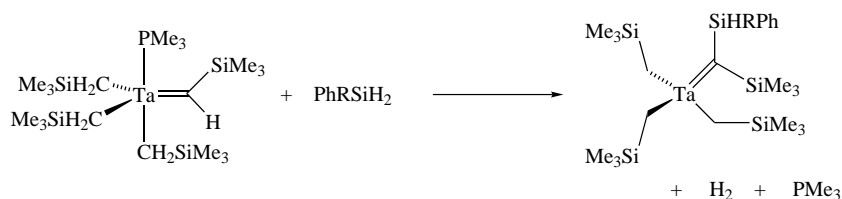


¹⁰¹D. Kremzow, G. Seidel, C. W. Lehmann, and A. Fürstner, *Chem. Eur. J.*, **2005**, *11*, 1833.

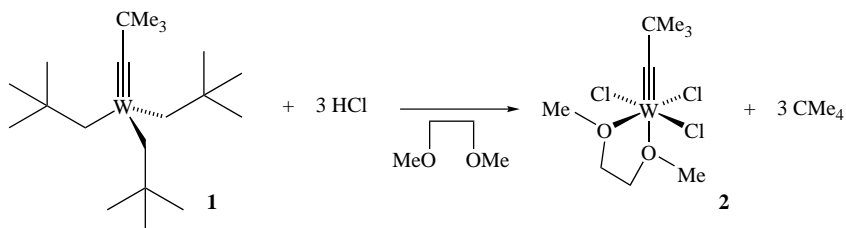
- 10-5** Propose a stepwise mechanism for the transformation shown.¹⁰² Suggest a structure for one of the alkene by-products that form in the second step.



- 10-6** Suggest a mechanistic pathway that would account for the following transformation.¹⁰³



- 10-7** Although alkylidyne **1** appears to resist protonation in the reaction shown below, other evidence indicates that protonation does occur initially. Propose a mechanism that accounts for the formation of alkylidyne **2** and the accompanying stoichiometry of the overall transformation.¹⁰⁴

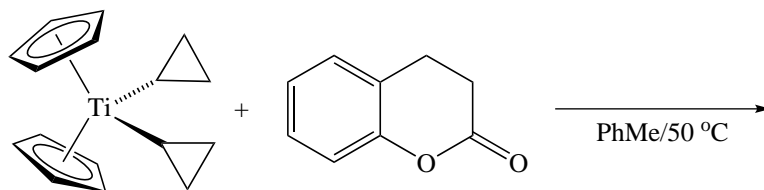


¹⁰²P.-J. Sinnema, L. van der Veen, A. L. Spek, N. Veldman, and J. H. Teuben, *Organometallics*, **1997**, *16*, 4245.

¹⁰³J. B. Dimminie, J. R. Blanton, H. Cai, K. T. Quisenberry, and Z. Xue, *Organometallics*, **2001**, *20*, 1504.

¹⁰⁴R. R. Schrock, *J. Chem. Soc., Dalton Trans.*, **2001**, 2541.

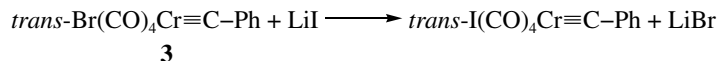
- 10-8** Predict the organic product that would result from the following reaction.¹⁰⁵



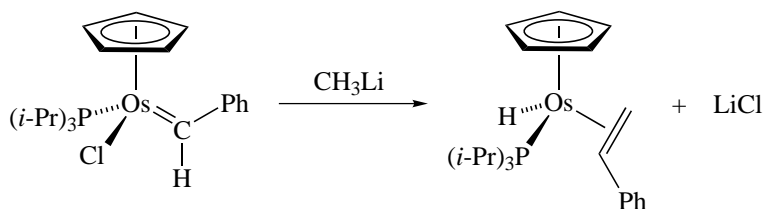
- 10-9** Consider the reaction shown in which I⁻ replaces the *trans* Br⁻ in complex **3**. The rate law for this reaction was determined to be

$$\text{rate} = k[\mathbf{3}][\text{I}^-].$$

Kinetic parameters measured included $\Delta H^\ddagger = 13.5$ kcal/mol and $\Delta S^\ddagger = -7.9$ eu. The rate of reaction was insensitive to the leaving group, so when the relative rate of reaction (1,1,2-trichloroethane solvent) when Br⁻ was the leaving group was compared with I⁻ as the leaving group, $k(\text{Br})/k(\text{I}) = 1.2$. What kind of fundamental organometallic reaction occurs here? Propose a mechanism for this reaction.¹⁰⁶



- 10-10** Propose a mechanism for the transformation shown.¹⁰⁷



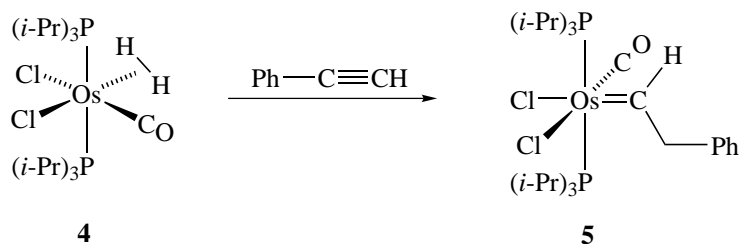
- 10-11** Reaction of dihydrogen complex **4** with phenylethyne gives vinylidene **5** as shown. No other reagents are required for this reaction. Propose a pathway from **4** to **5**. [Hint: The first step probably involves elimination of HCl.]¹⁰⁸

¹⁰⁵N. A. Petasis and E. I. Bzowej, *Tetrahedron Lett.*, **1993**, 34, 943.

¹⁰⁶H. Fischer and S. Friedrich, *J. Organomet. Chem.*, **1984**, 275, 83.

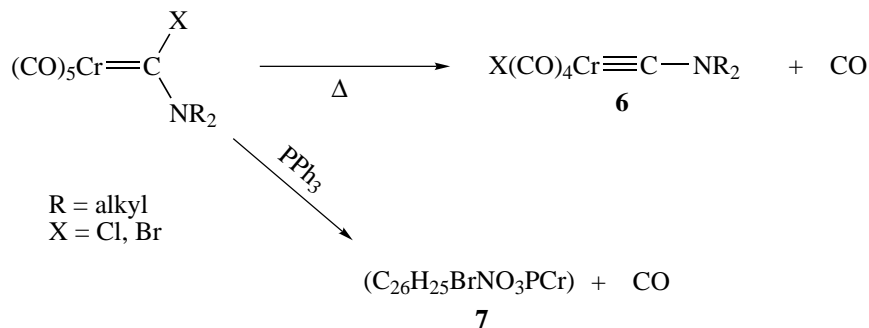
¹⁰⁷See Footnote 89.

¹⁰⁸M. L. Buil, O. Eisenstein, M. A. Esteruelas, C. García-Yebra, E. Gutiérrez-Puebla, M. Oliván, E. Oñate, N. Ruiz, and M. A. Tajada, *Organometallics*, **1999**, 18, 4949.



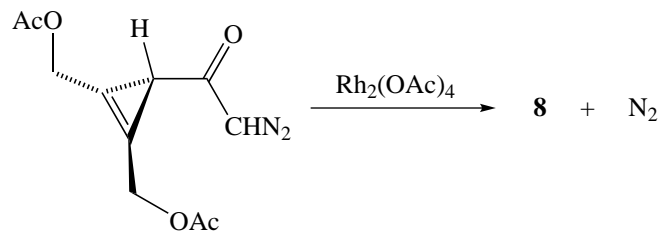
10-12 The reaction below follows a first-order rate law to form carbyne complex **6**, and it is faster when X = Br than when X = Cl. When R is changed from methyl to isopropyl, the rate increases by a factor of 10^7 . Although increases in rate occur when solvents become more polar, these rate enhancements are modest compared with solvent effects on reactions that generate intermediates with full-fledged charges. Adding more Cl⁻ or increasing the pressure of CO has no effect on reaction rate. Finally, the addition of high concentrations of PPh₃ does not affect reaction rate, but it does result in the formation of compound **7** (R = Et, X = Br). Spectral characteristics of **7** were as follows: IR: $\nu = 2043, 1980, 1950,$ and 1570 cm^{-1} (1575 cm^{-1} in the starting material when X = Br and R = Et); NMR: $\delta = 7.6$ (multiplet, 15 H), 3.1 (quartet, 4 H), and 1.2 ppm (triplet, 6 H). The rate of reaction for treatment of **6** with PPh₃ to form **7** is much faster than the rate of formation of **7** from the carbyne complex starting material.¹⁰⁹

- Propose a structure for compound **7**.
- Propose a stepwise mechanism for the formation of compound **6** and for the formation of compound **7** from both the starting material and compound **6**.



¹⁰⁹C. F. Bernasconi, *Adv. Phys. Org. Chem.*, **2002**, 37, 137.

10-13 Predict the structure of product (**8**) for the following dirhodium-catalyzed reaction.¹¹⁰



Spectral characteristics of compound **8**:

IR: $\nu = 1795$ and 1751 cm^{-1}

¹H NMR: $\delta = 4.93$ (singlet, 4H), 2.16 (singlet, 2H), and 2.02 ppm (singlet, 6 H)

¹¹⁰P. Dowd, P. Garner, R. Schappert, H. Irgartinger, and A. Goldman, *J. Org. Chem.*, **1982**, 47, 4240.

Metathesis and Polymerization Reactions

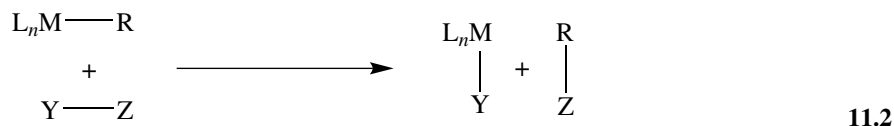
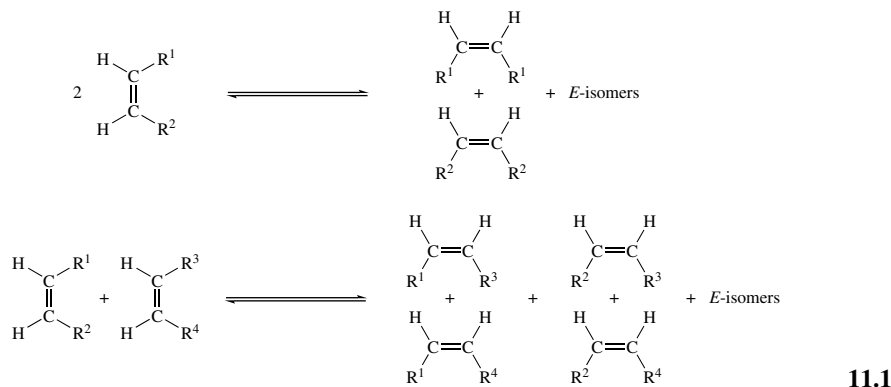
In Chapter 11 we will see how metal–carbene complexes are involved in a process known as metathesis, which we encountered briefly in Chapter 10. Metathesis is now used to synthesize everything from low-molecular-weight hydrocarbons to complex drugs to high-molecular-weight materials that are useful in everyday life. We will discover in Chapter 11 that these giant molecules result from polymerization reactions, which are catalyzed not only by metal–carbene complexes but also by early- and late-transition metal compounds that are not metal carbenes.

11-1 π BOND METATHESIS

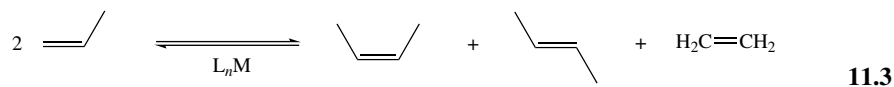
Equation 11.1 shows a formal interchange of substituent groups (typically alkyl groups or H) attached to the C=C bond of either the same or two different alkenes. Such a reaction is termed π bond metathesis, *olefin*¹ metathesis, or simply *metathesis*.² Alkynes can also undergo these interchange reactions by a similar pathway; these transformations will be discussed in a subsequent section in Chapter 11. Another type of metathesis (equation 11.2), which involves reorganization of single bonds, is called σ bond metathesis; we will discuss this reaction toward the end of Chapter 11.

¹Olefin is an older, but still commonly-used term for alkene. The name derives from two Latin words—*oleum* (oil) and *ficare* (to make)—that were combined to describe the reaction of ethene (a gas) with Cl₂ to give ClCH₂–CH₂Cl (a liquid or “oil”). Chemists, especially those employed in industrial settings, often use the word olefin interchangeably with alkene.

²The word metathesis was coined from two Greek words: *meta* (change) and *thesis* (position).



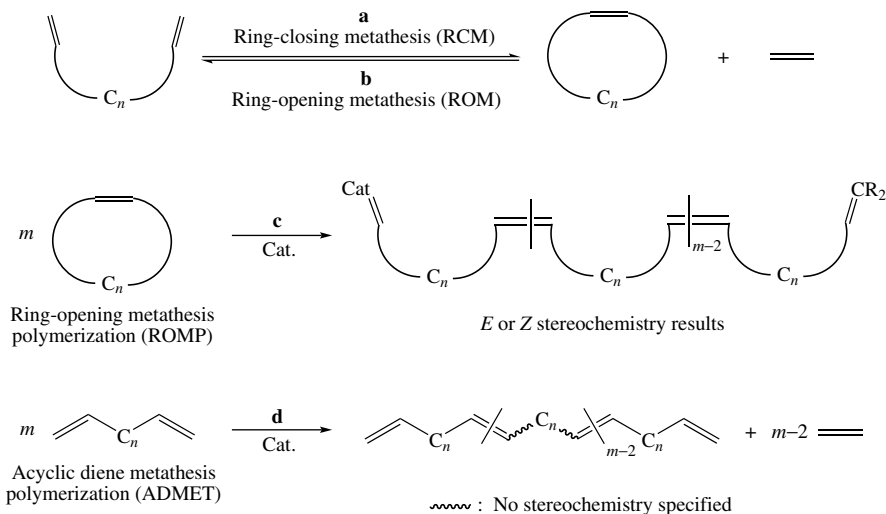
Discovered independently in the mid 1950s by workers at DuPont, Standard Oil of Indiana,³ and Phillips Petroleum,⁴ olefin metathesis is a reaction catalyzed, either homo- or heterogeneously, primarily by complexes of Ru, Mo, W, Re, and some Group 4 and 5 metals. The reaction often occurs under very mild conditions (room temperature and pressure). The original metathesis reactions involved the transformation of low-molecular-weight alkenes into other simple alkenes. Equation 11.3 shows conversion of propene to ethene and 2-butenes (known as the Triolefin Process) which was commercialized in 1966. Later the Triolefin Process was discontinued because ethylene and butenes became available less expensively from other processes.⁵ Today, chemical engineers take advantage of the reversibility of this and most other olefin metathesis reactions, and they run the Triolefin Process (now also known as *Olefin Conversion Technology* or OCT) such that the more economically valuable propene is produced from mixtures of ethene and 2-butenes.



³E. F. Peters and B. L. Evering, US Patent 2,963,447, assigned to Standard Oil of Indiana, 1960.

⁴R. L. Banks and G. C. Bailey, *Ind. Eng. Chem. Prod. Res.*, **1964**, 3, 170 (Phillips Petroleum).

⁵For a summary of the history of the metathesis reaction written by two of its co-discoverers, see R. L. Banks, *Chemtech*, **1986**, 16, 112 and H. Eleuterio, *Chemtech*, **1991**, 21, 92 (DuPont).



Equations **11.1** and **11.3** depict a type of metathesis known as *cross-metathesis* (CM). Several other types are known, and these are summarized in Scheme **11.1**. Path **a** in Scheme **11.1** outlines *ring-closing metathesis* (RCM), which has become extremely useful in making rings of many different sizes. The reverse reaction (path **b**), known as *ring-opening metathesis* (ROM), is most useful when run under conditions that allow polymerization of the diene monomer to occur (path **c**). Under such conditions, we have a transformation called *ring-opening metathesis polymerization* (ROMP). Path **d** shows a type of CM, but this time the starting material is a diene that can undergo polymerization under a process known as *acyclic diene metathesis polymerization* (ADMET). Later in Chapter 11 we shall encounter several examples and applications of these types of metathesis reactions.

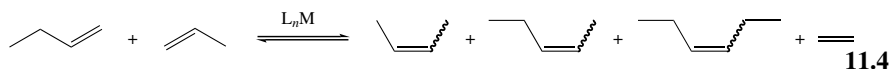
Metathesis is now used in the production of specialty chemicals, agricultural chemicals, drugs, and polymers with unique properties, and interest in using it as a means to generate other new materials remains strong. The economic importance of olefin metathesis to the chemical industry has been a stimulus for research on the mechanism of this reaction. In addition to providing obvious monetary benefits, basic study on the metathesis reaction promoted a synergistic melding of the disciplines of catalysis and organometallic chemistry, the result of which was significant advancement of our knowledge of the chemical properties of metal carbene complexes and of understanding their role in alkene interchange and polymerization. Green benefits of metathesis reactions are high atom economy and mild reaction conditions. On an industrial scale, it is often possible to recycle by-products in subsequent metathesis exchange reactions so that the highest possible yields of desired products result.⁶

⁶C. L. Dwyer, "Metathesis of Olefins," in *Metal-Catalysis in Industrial Organic Processes*, G. P. Chiusoli and P. M. Maitlis, Eds., Royal Society of Chemistry: Colchester, UK, 2006, pp. 201–217.

In 2005, Yves Chauvin, Robert Grubbs, and Richard Schrock were awarded the Nobel Prize in Chemistry for their fundamental studies on the mechanism and applications of metathesis. We will encounter much of their work in the following sections.

11-1-1 The Mechanism of π Bond Metathesis

Equation 11.1 shows only two possibilities for exchange of alkyl substituents during CM. Several other product combinations are possible and, given enough time for the reaction to reach equilibrium, all possible products form in amounts based upon their relative free energies (see equation 11.4 below and Exercise 11-1 for examples). The reaction may be manipulated to achieve desired product combinations, however. For example, a self-metathesis of a terminal alkene will produce ethene as one of the products. The reaction may be driven toward formation of ethene and an internal alkene by collecting volatile ethene as it forms. The presence of high concentrations of ethene during metathesis, on the other hand, converts an internal alkene to a terminal one.



Assume 2-pentene and 2-hexene undergo metathesis. At equilibrium, what are all the possible alkenes that could be present, neglecting stereochemistry about the double bond? Remember to consider self-metathesis reactions.

Exercise 11-1

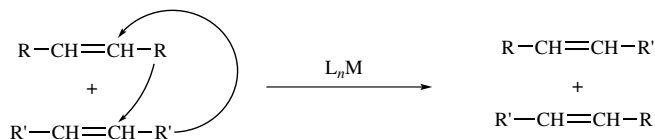
Elucidation of the mechanism of metathesis, as with any mechanistic pathway, requires knowing which bonds are broken and which are formed. Over the years, investigators of this mechanism have considered several pathways, three of which are:⁷

1. Mechanism *I*: Transfer of alkyl groups from one C=C bond to another as shown in equation 11.5.⁸

⁷See also R. Grubbs and T. K. Brunck, *J. Am. Chem. Soc.*, **1972**, *94*, 2538 and C. G. Biefield, H. A. Eick, and R. H. Grubbs, *Inorg. Chem.*, **1973**, *12*, 2166, for an alternative proposal for involvement of a metallocyclopentane as an intermediate in CM.

⁸N. Calderon, H. Y. Chen, and K. W. Scott, *Tetrahedron Lett.*, **1967**, 3327. Calderon was the first to coin the term olefin metathesis for the olefin exchange reaction that is typified by the Trioolefin Process.

Mechanism 1:

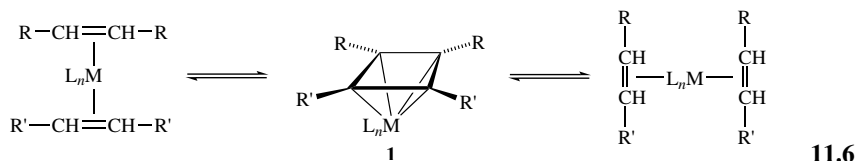


(Only one exchange possibility shown)

11.5

2. Mechanism 2: A *pairwise* breakage of C=C bonds followed by the construction of new C=C bonds, pictured in equation 11.6.⁹

Mechanism 2:



11.6

3. Mechanism 3: A *non-pairwise* breakage of C=C bonds followed by formation of new C=C bonds outlined in Scheme 11.2.

A single experiment (Scheme 11.3), involving self metathesis of a symmetrical alkene, clearly indicated that Mechanism 1 could not occur.¹⁰ A mechanism involving alkyl group transfer by C–C bond cleavage should give several different labeled 2-butene isomers, whereas cleavage of the C=C bond would give only one structure (neglecting stereoisomers). Because the only product isolated upon equilibrium contained four deuterium atoms (*d*₄-2-butene), the results are consistent with cleavage of the double bond (Mechanisms 2 or 3).

The study of organic chemistry, however, tells us that C=C bonds are rather strong (145–150 kcal/mol), and yet metathesis, remarkably, is a reaction capable of breaking these bonds and forming new ones under rather mild conditions. The question remains: **how do C=C bonds break and then reform?**

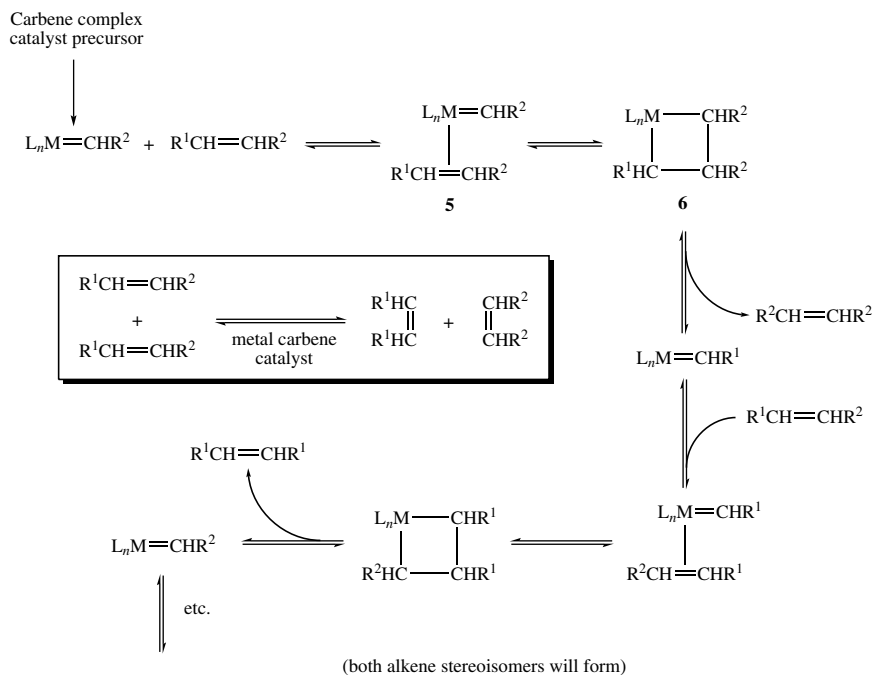
In 1967, Bradshaw¹¹ proposed (equation 11.6) that metathesis occurs first by coordination of the two alkenes to the metal followed by cycloaddition of

⁹C. P. C. Bradshaw, E. J. Howman, and L. Turner, *J. Catal.* **1967**, 7, 269.

¹⁰N. Calderon, E. A. Ofstead, J. P. Ward, W. A. Judy, and K. W. Scott, *J. Am. Chem. Soc.*, **1968**, 90, 4133.

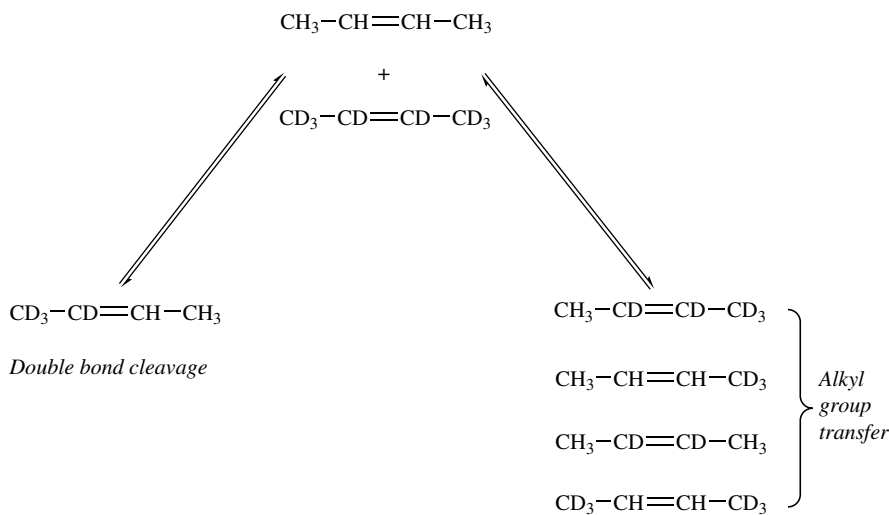
¹¹See Footnote 9.

Mechanism 3:



Scheme 11.2

Non pairwise
Mechanism for
Metathesis

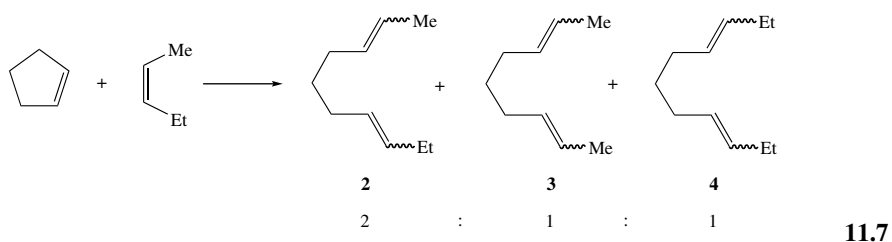


Scheme 11.3

Self Cross-
Metathesis of
Labeled and
Unlabeled 2-Butene

the alkenes to form a metal-coordinated cyclobutane (1). Finally, the four-membered ring breaks apart in a retrocycloaddition to give two new alkenes. Chemists soon labeled Bradshaw's pathway the "pairwise" or "diolefin" mechanism (Mechanism 2).

In 1971, Hérisson and Chauvin¹² performed an experiment described in equation 11.7. They isolated three major products, **2** (C₁₀), **3** (C₉), and **4** (C₁₁), upon tungsten-catalyzed CM of cyclopentene and 2-pentene. Product **2** is expected as the direct result of pairwise metathesis of the two starting materials; the other two products could result from subsequent reactions of **2** with 2-pentene. At equilibrium, all products would be present in nearly statistical distribution according to the pairwise mechanism. What troubled Hérisson and Chauvin, however, was the observation that, **upon quenching the reaction well before equilibrium could be achieved, a statistical distribution of the three products was already present.**

**Exercise 11-2**

Show how **3** and **4** (equation 11.7) could form using the pairwise mechanism for metathesis.

Mechanism 3 shows a pathway that was strongly influenced by the results of Hérisson and Chauvin and is outlined in Scheme 11.2. Two key intermediates in this pathway are an alkene–metal carbene complex (**5**) and a metallacyclobutane (**6**), formed through concerted cycloaddition of the M=C and C=C bonds. A highly significant feature of the mechanism, caused by the unsymmetrical structure of **6**, is its explanation of randomization early in the course of reaction. **The Hérisson–Chauvin mechanism does not require a specific pair of alkenes to interact directly for metathesis to occur, hence the name “non-pairwise” mechanism.**

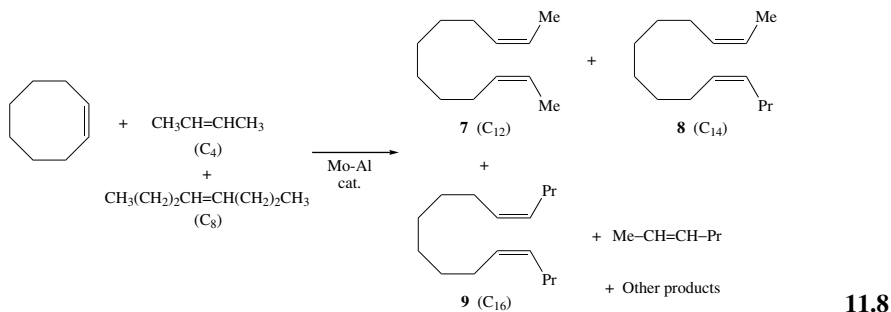
¹²J. L. Hérisson and Y. Chauvin, *Makromol. Chem.*, **1971**, 141, 161. This paper does not propose the discrete intermediates, **5** and **6**, but it does suggest that carbene complexes could interact with alkenes separately in a non-pairwise manner such that a new alkene and a new carbene complex could form after a bond reorganization. The mechanism shown in Scheme 11.2 is the non-pairwise mechanism that was elucidated after much work by other chemists, and it is discussed later in this section and in Section 11-1-2.

Starting with $L_nM=CH-Me$ or $L_nM=CH-Et$, cyclopentene, and 2-pentene, show how the non pairwise mechanism could account for initial formation of **3** and **4** as well as **2** (equation 11.7).

Exercise 11-3

The early development of Mechanism **3** was bold for its day because Fischer carbene complexes had just been discovered a few years earlier, and alkylidenes were not yet known. The carbene complexes prepared before 1971 also did not catalyze olefin metathesis. With the discovery of Schrock carbene complexes and the demonstration that some alkylidenes could promote metathesis, the non-pairwise mechanism became more plausible (Section 11-1-2). It was, however, the elegant work of Katz and co-workers that provided early substantial support for the Hérisson–Chauvin mechanism.

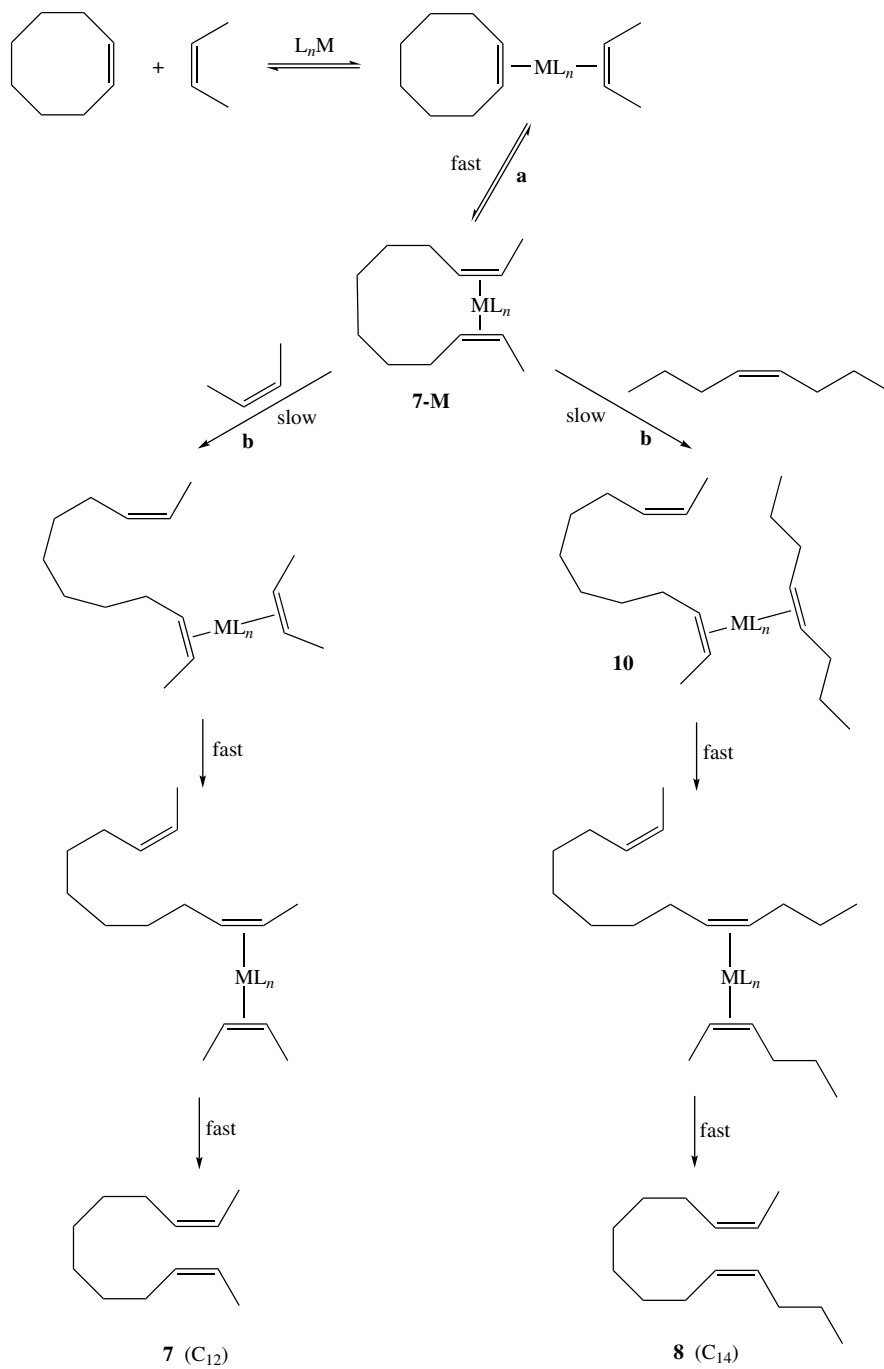
First, Katz¹³ conducted an experiment similar to that of Hérisson and Chauvin (equation 11.8), which he termed the “double cross” metathesis. If Mechanism **2** were operative, the product ratios $[8]/[7]$ and $[8]/[9]$ should be zero when concentrations were extrapolated back to the very beginning of the reaction (t_0), because **8**—the double cross product—would have to form after the symmetrical products **7** and **9**.



The non-pairwise mechanism (Mechanism **3**) should provide some of the unsymmetrical **8** quickly, thus making the ratios $[8]/[7]$ and $[8]/[9]$ non-zero at t_0 . When the experiment was run, Katz found values of $[8]/[7] = 0.40$ and $[8]/[9] = 11.1$ at t_0 .

Despite this strong evidence supporting the non-pairwise mechanism, others objected that the pairwise mechanism could explain the results of Katz's experiment if another step in the pairwise mechanism were rate determining. Consider Scheme 11.4, in which initial “single cross” metathesis is rapid to form the C₁₂ alkene (**7**). If **7** sticks to the metal and 4-octene attacks in a rate-determining step

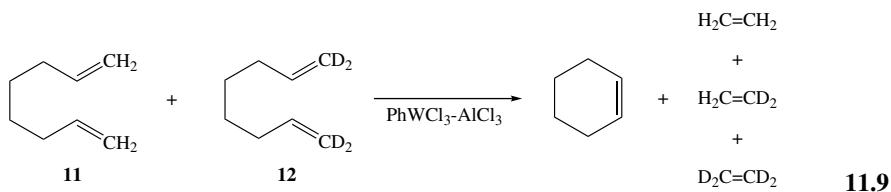
¹³T. J. Katz and J. McGinness, *J. Am. Chem. Soc.*, **1975**, 97, 1592, and **1977**, 99, 1903.



Scheme 11.4
 "Sticky Olefin"
 Hypothesis

(step **b**) to displace one of the alkene groups to give **10**, then metathesis would give double cross product **8**. If **7** sticks to the metal long enough, several displacements and subsequent metatheses could occur, providing a statistical distribution of products even at the beginning of the reaction. If, on the other hand, pairwise metathesis (step **a**) is rate determining, even this modified pairwise mechanism fails to explain the results of Katz and the earlier results of Hérisson and Chauvin, because the rate-determining step would produce only the single cross-product. The proposition that an alkene could stick to the metal and subsequently be displaced by another alkene was called the “sticky olefin” hypothesis, and it constitutes a modification of Mechanism 2.¹⁴

At this point, the non-pairwise (Mechanism 3) and sticky olefin-modified pairwise process (Mechanism 2) both could explain the double cross experiment. More definitive proof was required, and this was provided independently by Grubbs and Katz through some clever experiments. In one experiment,¹⁵ metathesis of a 1:1 mixture of dialkene **11** and deuterated partner **12** gives cyclohexene and three ethenes with different amounts of deuterium incorporation (equation **11.9**). The design of the experiment was astute in at least two respects. First, cyclohexene, although a simple disubstituted alkene, is a notable exception to the rule that sterically unhindered alkenes undergo metathesis; in this case, it does not react with starting material or other products in the presence of the W-catalyst. Second, the ethenes are sufficiently volatile that they could be removed and collected as formed, thus preventing their reaction with starting material. Because of these constraints, the initial products observed would truly be those formed during the first metathesis. For example, secondary reactions that could occur via the sticky olefin-modified pairwise pathway (Mechanism 2) and lead to scrambled products would not take place at the initial stages of the reaction. A non-pairwise mechanism predicts that the ratio of $d_0:d_2:d_4$ -ethenes should be 1:2:1, whereas the sticky-olefin-metathesis mechanism does not; experiment showed results close to the 1:2:1 ratio.

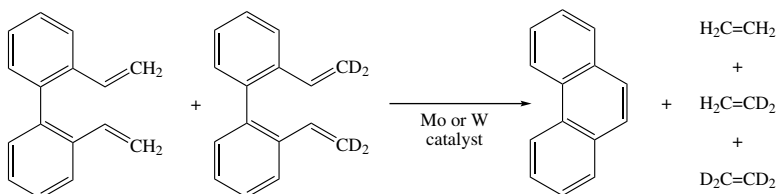


¹⁴N. Calderon, *Acc. Chem. Res.*, **1972**, 5, 127.

¹⁵R. H. Grubbs, P. L. Burk, and D. D. Carr, *J. Am. Chem. Soc.*, **1975**, 97, 3265.

Addition of excess d_0 -ethene to the reaction mixture did not affect the ethene- d_2/d_4 product ratio, which means that the ethene products do not react with each other once formed. Moreover, mass spectral analysis of **11** and **12** both before the reaction started and after a short reaction time showed no scrambling of label between the two starting materials. This suggests that **11** and **12** must interact separately with the metal catalyst during metathesis and do not interact with each other before metathesis. Mechanism **3** best explains all of these results.

Equation **11.10** describes another experiment, performed by Katz, which is similar to Grubbs' earlier work.¹⁶ A 1:1 ratio of d_0 - and d_4 -divinylbiphenyls gave a 1:2:1 ratio of ethenes as above. Again, the products are such that secondary metatheses do not occur.



Mo or W catalyst: $M(\text{NO})_2\text{Cl}_2[\text{P}(\text{octyl})_3]_2/\text{Al}_2\text{Me}_3\text{Cl}_3$

11.10

Since the definitive experiments of Katz and Grubbs appeared in the literature, the non-pairwise mechanism has become the accepted pathway for metathesis. Subsequent investigations have supported this pathway.^{17,18} Key intermediates in the non-pairwise mechanism are metal-carbene and metallacyclobutane complexes. Both have been prepared and shown to catalyze metathesis, and more recently both species have actually been observed in the same reaction mixture and shown to interconvert during it, thus offering additional support for Mechanism **3**.¹⁹ The next section will cover the discovery of discrete metal-carbene complexes that do serve as metathesis catalysts.

¹⁶T. J. Katz and R. Rothchild, *J. Am. Chem. Soc.*, **1976**, 98, 2519.

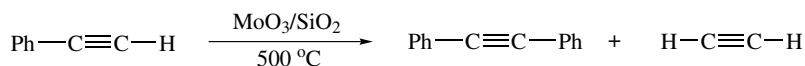
¹⁷For general reviews covering the mechanism of metathesis, see R. H. Grubbs, *Prog. Inorg. Chem.*, **1978**, 24, 1; T. J. Katz, *Adv. Organomet. Chem.*, **1977**, 16, 283; and R. H. Grubbs, "Alkene and Alkyne Metathesis Reactions," in *Comprehensive Organometallic Chemistry*, G. Wilkinson, Ed., Pergamon Press: New York, 1982, Vol. 8, pp. 499–551.

¹⁸For more modern reviews on the development of the mechanism of metathesis, see the following: A. M. Rouhi, *Chem. Eng. News*, **2002**, 80, 34; D. Astruc, *New J. Chem.*, **2005**, 29, 42; T. J. Katz, *New J. Chem.*, **2006**, 30, 1844; D. Astruc, *New J. Chem.*, **2006**, 30, 1848; and C. P. Casey, *J. Chem. Ed.*, **2006**, 83, 192.

¹⁹J. Kress, J. A. Osborn, R. M. E. Greene, K. J. Ivin, and J. J. Rooney, *J. Am. Chem. Soc.*, **1987**, 109, 899.

Based upon your knowledge of alkene metathesis, what is the mechanism of the following transformation?

Exercise 11-4

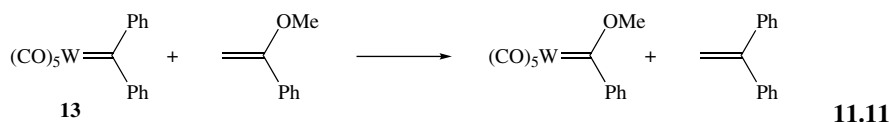


11-1-2 Metathesis Catalysts

Metathesis catalysts may be either homo- or heterogeneous. Although complexes of Ru, Mo, and W seem to show the most activity, metathesis may be catalyzed in some instances by Ti and Ta species. Heterogeneous substances, such as $\text{WO}_3/\text{silica}$ or MoO_3 and $\text{Mo}(\text{CO})_6$ supported on alumina, catalyze the Triolefin Process and others performed on an industrial scale. Mechanistic studies of the type described in the previous section were essentially impossible to do with heterogeneous catalysts because the nature of these catalysts was so ill defined. Further discussion of the mechanism of metathesis under heterogeneous catalysis is beyond the scope of this textbook.

The work on elucidating the mechanism of metathesis that occurred during the 1970s involved use of homogeneous catalysts, but even these were often mixtures of compounds, such as $\text{WCl}_6/\text{AlEt}_2\text{Cl}$ or WCl_6/BuLi . Even today, it is not clear how these mixtures, let alone heterogeneous catalysts, react to form the meta-carbene and metallacyclobutane intermediates that are now accepted as part of the mechanism of metathesis. Chauvin and Hérisson never observed carbene complexes or metallacyclobutanes in their seminal research, so it was not until later that other workers determined that these species were indeed intermediates in the metathesis reaction and that carbene complexes did, in fact, catalyze metathesis.

The first definitive work that showed that a metal-carbene complex could promote metathesis was that of Casey and Burkhardt.²⁰ They synthesized diphenyl tungsten-carbene complex **13** and demonstrated that the stoichiometric exchange process in equation **11.11** occurred.

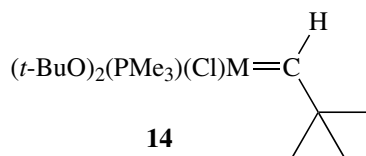


²⁰C. P. Casey and T. J. Burkhardt, *J. Am. Chem. Soc.*, **1974**, *96*, 7808.

Casey and Burkhardt reasoned that the metathesis mechanism influenced by Chauvin and Hérisson's work was sufficient to explain their results. Complex **13** is interesting in that the pentacarbonyl substitution makes it similar to a traditional Fischer carbene complex, yet it also possesses Schrock character because both substituents at C_{carbene} are hydrocarbon fragments.

In a series of papers that appeared in the mid to late 1970s, Katz and co-workers showed that complex **13** could catalyze metathesis reactions,²¹ not only CM reactions but also ROMPs of small-ring cycloalkenes.²² Although **13** was not a highly active catalyst, its use clearly demonstrated that metal–carbene complexes could be the true catalytically active species.

Up to this time, because complex **13** was not a highly active catalyst, there was concern that it may not be the true catalytic species in Katz's CM and ROMP experiments. It was suspected that **13** could first transform to a carbene complex with W in a high oxidation state before metathesis occurred. Further advancement in the field occurred a few years later, with Schrock's report in 1980 of alkylidenes **14** (M = Nb and Ta), which were active catalysts that led to productive metathesis.²³ It was Schrock's opinion that true metathesis catalysts consisted of alkylidenes with metals in high oxidation states and that the discovery of complex **14** was significant because it was the first carbene complex to catalyze productive metathesis. To this day, there is disagreement about who can claim to have first discovered a metal–carbene complex that was a true metathesis catalyst.²⁴



Me = Nb, Ta

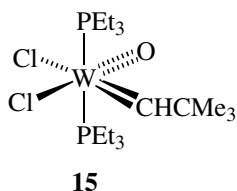
²¹See Footnote 13.

²²(a) T. J. Katz, S. J. Lee, and N. Acton, *Tetrahedron Lett.*, **1976**, 4247; (b) T. J. Katz and N. Acton, *Tetrahedron Lett.*, **1976**, 4251; and (c) T. J. Katz, S. J. Lee, and M. A. Shippey, *J. Mol. Catal.*, **1980**, 8, 219.

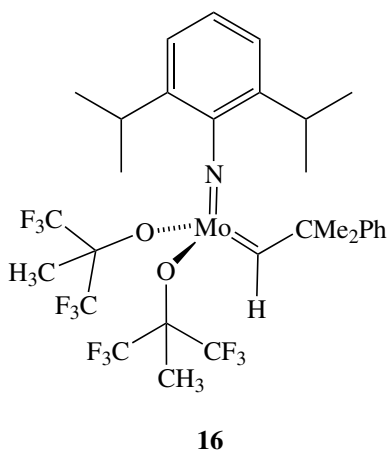
²³R. Schrock, S. Rocklage, J. Wengrovius, G. Rupprecht, and J. Fellmann, *J. Mol. Catal.*, **1980**, 8, 73 and S. M. Rocklage, J. D. Fellmann, G. A. Rupprecht, L. W. Messerle, and R. R. Schrock, *J. Am. Chem. Soc.*, **1981**, 103, 1440.

²⁴See Footnote 18.

Schrock's group also looked into tungsten catalysts, such as compound **15**. Although **15** also catalyzed metathesis, it required the presence of a Lewis acid such as AlCl_3 to be effective.²⁵



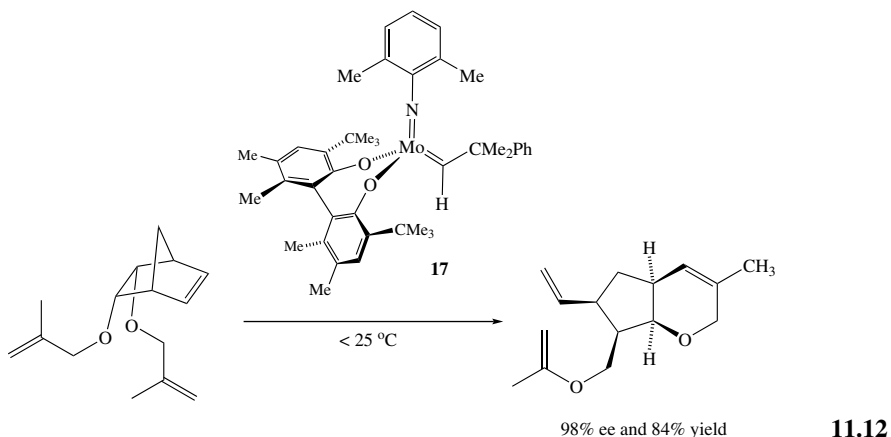
Continued work by Schrock's group led to some very active catalysts. By replacing the oxo group of **15** with an imido ligand (to enhance steric hindrance), changing the metal to Mo, and replacing some ligands with finely-tuned alkoxy groups (containing fluorinated alkyl fragments to modify the electronic nature of these groups), Schrock was able to construct alkyldiene **16** and numerous other structurally-related complexes, some of the most active catalysts for all types of metathesis detailed in Scheme **11.1**.²⁶



²⁵J. H. Wengrovius, R. R. Schrock, M. R. Churchill, J. R. Missert, and W. J. Youngs, *J. Am. Chem. Soc.*, **1980**, 102, 4515.

²⁶J. H. Oskam, H. H. Fox, K. B. Yap, D. H. McConville, R. O'Dell, B. J. Lichtenstein, and R. R. Schrock, *J. Organomet. Chem.*, **1993**, 459, 185.

A chiral version of **16** (alkylidene **17**), containing a biphenyldiolate ligand, is effective in producing metathesis products that exhibit high yields and excellent % ee values under mild conditions (equation **11.12**).²⁷



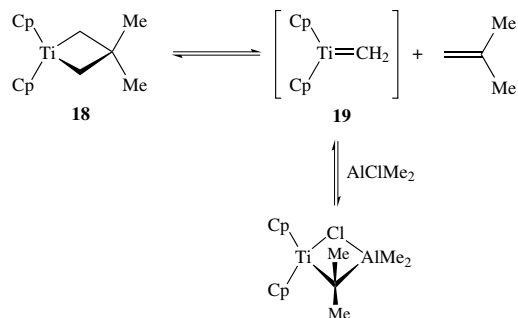
Parallel to Schrock's efforts were those of Grubbs and co-workers.²⁸ They studied Tebbe's reagent and found that titanacyclobutanes derived from the reagent could be isolated. For example, they found that titanacycle **18** was in direct equilibrium with metal carbene **19** (equation **11.13**). This system was not an active metathesis catalyst, but the work showed that both intermediates were important in the metathesis pathway. Further work found that reaction of Tebbe's reagent with norbornene resulted in metallacycle **20**, which promoted ROMP of additional equivalents of norbornene and produced a polymer that was relatively *monodisperse*²⁹ (equation **11.14**).³⁰

²⁷G. S. Weatherhead, J. G. Ford, E. J. Alexanian, R. R. Schrock, and A. H. Hoveyda, *J. Am. Chem. Soc.*, **2000**, *122*, 1828.

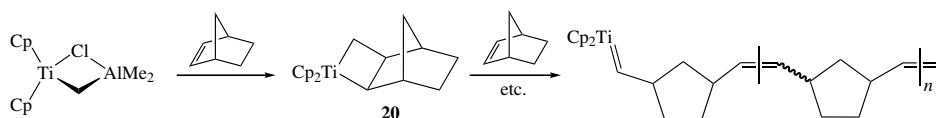
²⁸For a nice summary of metathesis catalysis development from the Grubbs research group, see R. H. Grubbs, *Tetrahedron*, **2004**, *60*, 7117.

²⁹Polymers are often characterized by their *polydispersity index* (PDI), which is determined by dividing the weight average molecular weight (M_w) of a polymer sample by its number average molecular weight (M_n). The value of the PDI is ≥ 1 , and large values of the PDI correspond to a polymer sample containing highly variable chain lengths for the individual polymer strands. A polymer is said to be relatively monodisperse when its PDI approaches the value of unity, indicating that all chain lengths are about the same. The mechanical properties of a polydisperse polymer may be quite different from the same polymer whose PDI approaches unity.

³⁰L. R. Gilliom and R. H. Grubbs, *J. Am. Chem. Soc.*, **1986**, *108*, 733.



11.13



11.14

Although the Ti complexes served to help elucidate the true nature of metathesis catalysts, they were not useful in a practical sense because they were not as active as other catalysts and the oxophilic nature of Ti prevented their use in metathesis of alkenes containing oxygen groups.

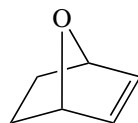
It was Grubbs' work with ruthenium, however, that led to numerous metathesis catalysts that are especially useful in the field of organic synthesis. Grubbs showed that ROMP of 7-oxanorbornene (**21**) amazingly could occur using a RuCl₃ catalyst in H₂O,³¹ and this work led to the development of Ru-alkylidene catalysts, the first of which was complex **22**.³² Further modification produced alkylidene **23**,³³ which is now called the first-generation Grubbs' catalyst. A more active form of **23** is complex **24**,³⁴ which has an NHC (Section 10-1-1) as one of its ligands and is known as a second-generation catalyst. Organic chemists have made extensive use of the last two catalysts for CM and RCM reactions.

³¹B. M. Novak and R. H. Grubbs, *J. Am. Chem. Soc.*, **1988**, *110*, 960.

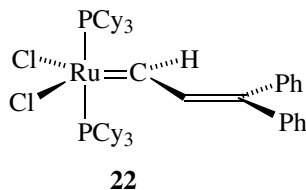
³²S. T. Nguyen, L. K. Johnson, R. H. Grubbs, and J. W. Ziller, *J. Am. Chem. Soc.*, **1992**, *114*, 3974 and S. T. Nguyen, R. H. Grubbs, and J. W. Ziller, **1993**, *115*, 9858.

³³P. Schwab, R. H. Grubbs, and J. W. Ziller, *J. Am. Chem. Soc.*, **1996**, *118*, 100.

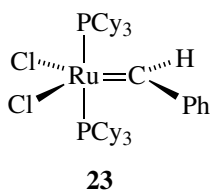
³⁴M. Scholl, T. M. Trnka, J. P. Morgan, and R. H. Grubbs, *Tetrahedron Lett.*, **1999**, *40*, 2247.



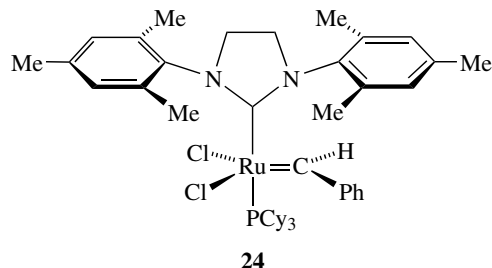
21



22



23



24

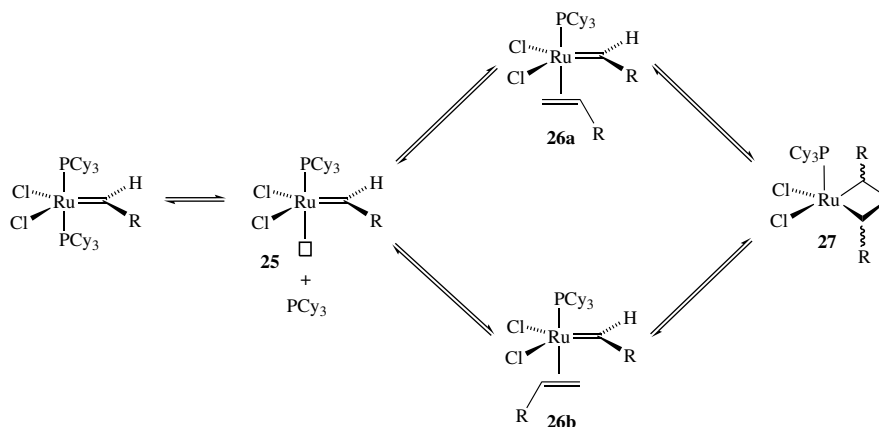
It is interesting that the Ru alkylidenes that Grubbs discovered are both alkylidenes and complexes with the metal in a relatively low oxidation state (+2).³⁵ As Grubbs has mentioned in his writings and conversations, there is a whole spectrum of reactivity in metal–carbene complexes, and it is difficult to classify the reactivity of many of these as being either Fischer type or Schrock type.³⁶

The mechanism of Ru–alkylidene-catalyzed reactions has been investigated. Note that Grubbs' first- and second-generation catalysts are 16-electron species, so if the first step involves complexation of an alkene to the metal, this process could occur in an associative or dissociative manner. Evidence suggests (see Scheme 11.5) that this occurs in a dissociative manner, however, first forming a 14-electron intermediate **25** and then **26a** or **26b** after complexation of the alkene. Gas-phase mass spectral evidence supports the initial formation of **25**. Complexes similar to **26a** and **b** have been isolated from reaction mixtures under appropriate conditions, but ruthenacyclobutane **27** has not been directly observed until quite recently.³⁷

³⁵It can be argued that, if one considers Grubbs catalysts to be true alkylidenes (Schrock carbene complexes), the oxidation state of Ru is +4.

³⁶R. H. Grubbs, T. M. Trnka, and M. S. Sanford, "Transition Metal–Carbene Complexes in Olefin Metathesis," in *Fundamentals of Molecular Catalysis*, H. Kurosawa and A. Yamamoto, Eds., Elsevier: Amsterdam, 2003, pp. 187–193.

³⁷A recent NMR study characterized a ruthenacyclobutane analog related to structure **27** starting with the methyldiene analog of Grubbs' second-generation catalyst. See E. F. van der Eide, P. E. Romero, and W. E. Piers, *J. Am. Chem. Soc.*, **2008**, *130*, 4484.

**Scheme 11.5**

Mechanism of
Catalysis for
Ru-Alkylidene
Complexes

There was speculation that this species existed as a transition state rather than a discrete intermediate.³⁸

RCM and cross metathesis, using both Grubbs Ru-alkylidenes and Schrock's Mo-catalysts, are routinely used in both academic and industrial research laboratories to produce complex organic molecules.³⁹ These reactions constitute one of the greatest advances in synthetic methodology to occur in the past 15 years, and they play a significant role in the synthesis of molecules that exhibit pharmaceutical activity. Although the Schrock catalysts are often more active than the Grubbs variety, the latter complexes are more tolerant of different functional groups already in place on substrates and are easier to use. For example, Schrock catalysts typically must be used in glove boxes or manipulated on Schlenk lines, and Grubbs catalysts may be employed under standard conditions for running organic reactions.

11-1-3 Industrial Uses for Metathesis: Small Molecules

Besides the Triolefin Process or OCT, metathesis is a key step in a number of other industrial transformations used to produce small molecules. By far the most important application of metathesis for this task is connected with the Shell

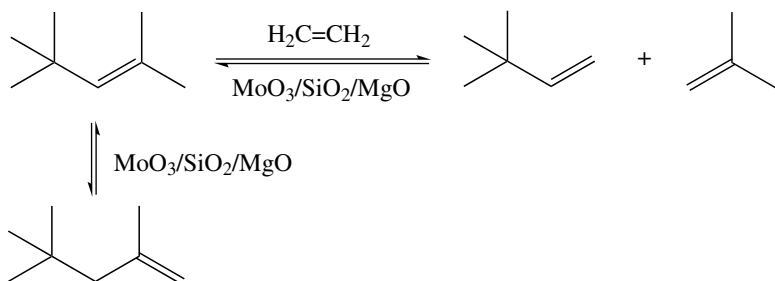
³⁸For a discussion of mechanistic studies of Ru-alkylidene catalysis of metathesis, see M. S. Sanford and J. A. Love, "Mechanism of Ruthenium-Catalyzed Olefin Metathesis Reactions," in *Handbook of Metathesis*, Vol. 1, R. H. Grubbs, Ed., Wiley-VCH: Weinheim, Germany, 2003, pp. 112–131.

³⁹For a comprehensive review on the use of metathesis for the synthesis of complex organic molecules, see J. A. Love, "Olefin Metathesis Strategies in the Synthesis of Biologically Relevant Molecules," in *Handbook of Metathesis*, Vol. 2, R. H. Grubbs, Ed., Wiley-VCH: Weinheim, Germany, 2003, pp. 296–360.

Higher Olefin Process (SHOP), which was developed over 30 years ago by the Shell Oil Company and produces about a million tons per year of linear C_{12} – C_{15} alcohols derived from C_{11} – C_{14} alkenes.⁴⁰ Most of these alcohols are subsequently converted into detergents and plasticizers.

Scheme 11.6 diagrams this process, which begins with a Ni-catalyzed⁴¹ oligomerization⁴² to give alkenes of various chain lengths. These are distilled into three different fractions corresponding to short-, medium-, and long-chain alkenes. The medium chains are used in the later stages of the process, but the short- and long-chain olefins are isomerized from terminal to internal alkenes. These then undergo metathesis over a heterogeneous catalyst of MoO_3/Al_2O_3 or one that is Re-based. The resulting medium-weight alkenes (combined with a medium-length fraction from above) finally undergo hydroformylation, using a phosphine-modified Co catalyst, for which Shell is renowned (see Section 9-2-2). The catalyst promotes isomerization of internal double bonds to terminal before hydroformylation and subsequent hydrogenation occur.

A metathesis similar to OCT came on stream about the same time as the SHOP process. *Ethenolysis*⁴³ of a mixture of 2,4,4-trimethyl-2-pentene and 2,4,4-trimethyl-1-pentene yields 3,3-dimethyl-1-butene (commonly called neohexene) plus isobutylene (equation 11.15).

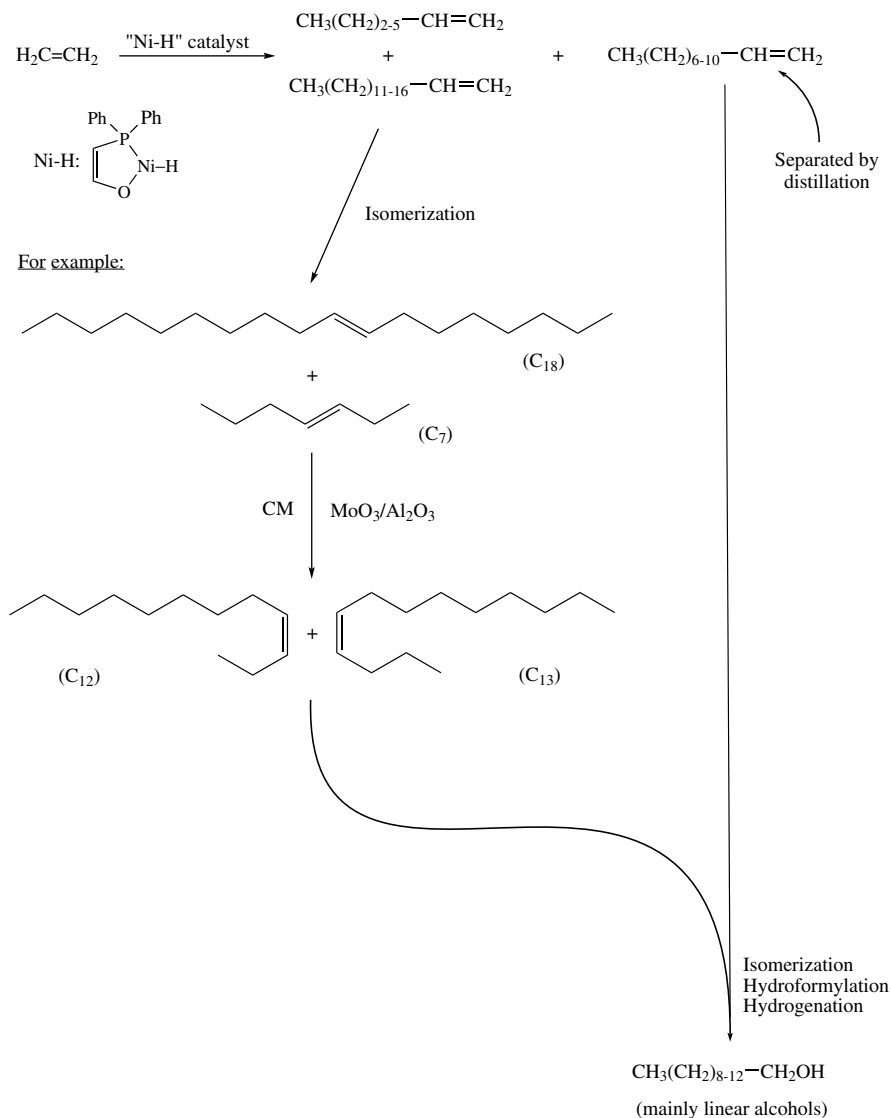


⁴⁰A. J. Berger, U.S. Patent 3,726,938, 1973; P. A. Verbrugge and G. J. Heiszwolf, U.S. Patent, 3,776,975, 1973; E. R. Freitas and C. R. Gum, *Chem. Eng. Progr.*, **1979**, 75, 73; W. Keim, F. H. Kowaldt, R. Goddard, and C. Krüger, *Angew. Chem. Int. Ed. Eng.*, **1978**, 17, 466; and B. Reuben and H. Wittcoff, *J. Chem. Ed.*, **1988**, 65, 605.

⁴¹For a discussion of the nature of the Ni oligomerization catalyst, see W. Keim, *Angew. Chem.*, **1990**, 102, 251.

⁴²Oligomers are low-molecular-weight polymers. They are analogous to peptides in the realm of biochemistry whereas proteins would be analogous to high-molecular-weight polymers.

⁴³Ethenolysis refers to metathesis involving ethene as one of the reactants. Such a reaction will liberate two terminal alkenes from the non-ethenylinic metathesis partner.

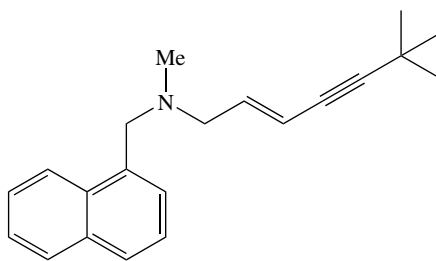


The process is quite atom economical because the isobutylene is recycled to undergo dimerization to the starting mixture of trimethylpentene isomers, and the metathesis catalyst, typically a mixture of $\text{WO}_3/\text{silica}$ and MgO , also promotes isomerization of the 1-pentene to the desired 2-isomer.⁴⁴

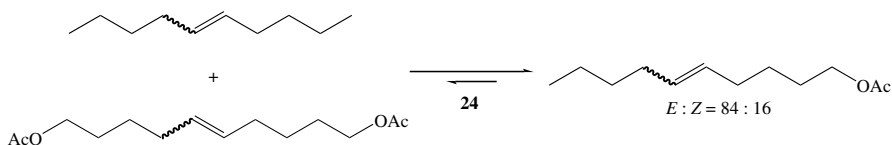
This process, now run by the Chevron Phillips Chemical Company, produces over a million pounds of neohexene annually. Neohexene is a raw material used

⁴⁴R. L. Banks, D. S. Banasiak, P. S. Hudson, and J. R. Norell, *J. Mol. Catal.*, **1982**, *15*, 73.

for production of synthetic perfume ingredients (called musks) and Terbinafine, an antifungal pharmaceutical that is also called Lamisil (**28**).⁴⁵

**28**

Pheromones are chemicals that are used by animals and plants for communication. Insects utilize pheromones extensively to indicate their availability for reproduction, to sound alarms, and to make known the presence of food. The use of pheromones in small amounts in traps can interfere with the reproduction of harmful insects in an environmentally friendly manner. Recently, Grubbs' second-generation catalyst (**24**) was used to synthesize on an industrial scale the sex attractant pheromone of the peach twig borer, a pest that attacks peach, plum, nectarine, and almond crops.⁴⁶ Equation **11.16** shows how Ru-catalyzed metathesis of 5-decene and 1,10-diacetoxy-5-decene produces a 50% yield of *E-Z* mixture (the desired *E*-isomer predominates, and the presence of small amounts of *Z*-isomer does not lower the activity of the pheromone) of the desired pheromone at low temperature. The unreacted starting materials are recovered by vacuum distillation and recycled.

**11.16**

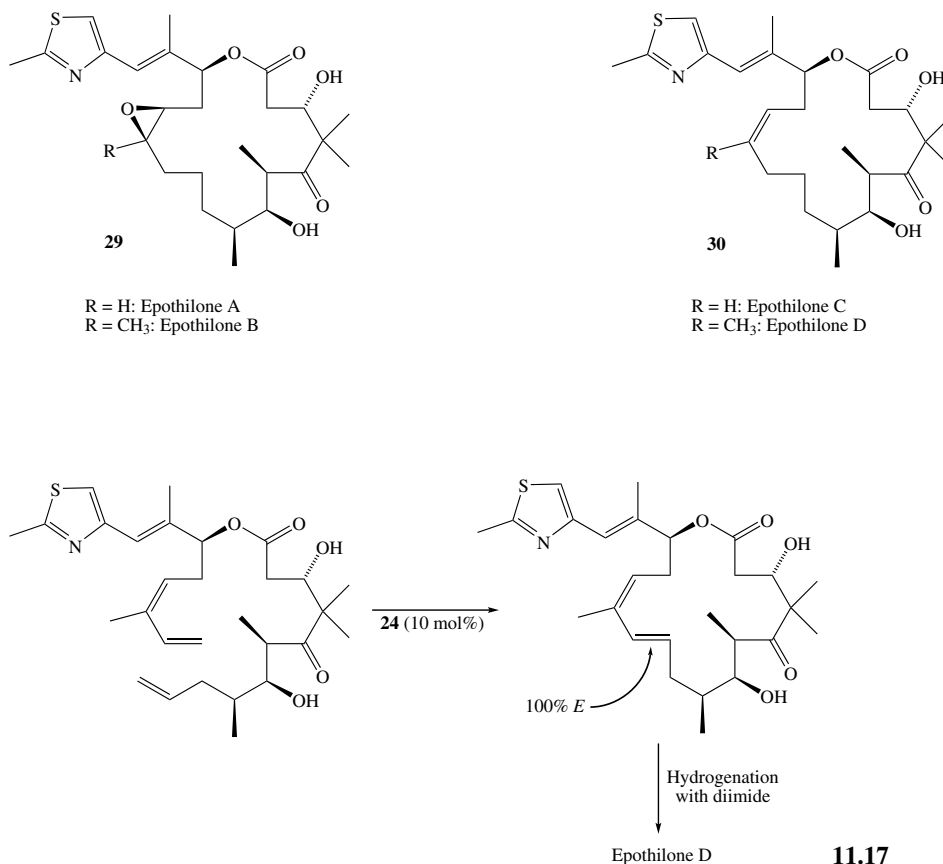
Other pheromones have been synthesized using this technology.

Over the past 15 years, chemists have vigorously investigated the synthesis and reactivity of one important class of cancer-fighting drugs called epothilones (**29** and **30**), which show more promise in treating stubborn breast and uterine

⁴⁵L. Delaude and A. F. Noels, "Metathesis," in *Kirk-Othmer Encyclopedia of Chemical Technology*, Wiley: New York, 2005, Vol. 26, pp. 939–941.

⁴⁶R. L. Pederson, I. M. Fellows, T. A. Ung, H. Ishihara, and S. P. Hajela, *Adv. Synth. Catal.*, **2002**, *344*, 728.

cancers than the highly touted taxols that are already in use.⁴⁷ RCM has been used by different research groups as a means of constructing 16-membered rings that are a characteristic part of the epothilone family of related compounds. Equation 11.17 shows one spectacular use of RCM.⁴⁸

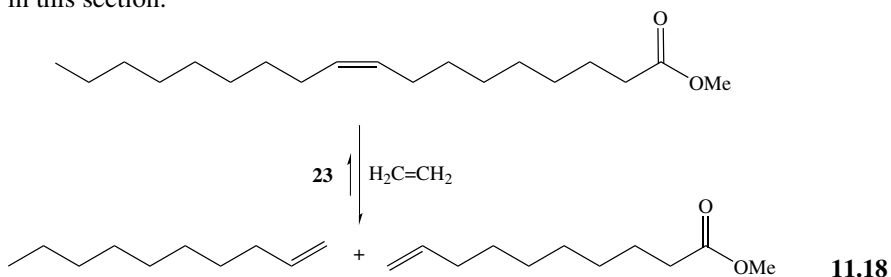


Up to this point, our discussion has centered on industrial applications of metathesis in which petrochemical-derived starting materials have been used.

⁴⁷For reviews on the biology and chemistry of the epothilones, see K. C. Nicolaou, F. R. Roschangar, and D. Vourloumis, *Angew. Chem. Int. Ed.*, **1998**, 37, 2014; M. Wartmann and K.-H. Altmann, *Curr. Med. Res.-Anti-Cancer Agents*, **2002**, 2, 123; and R. Zhang and Z. Liu, *Curr. Org. Chem.*, **2004**, 8, 267.

⁴⁸K. Biswas, S. J. Danishefsky, *et al.*, *J. Am. Chem. Soc.*, **2002**, 124, 9825.

Naturally-occurring fatty acids, such as oleic acid, could serve as feedstocks for metathesis-centered transformations. For example, workers at Dow Chemical Company explored the use of Grubbs' first-generation catalyst (**23**) to promote ethenolysis of methyl oleate (equation **11.18**) to form C_{10} alkenes, which might serve as feedstocks for some of the processes that have already been mentioned in this section.⁴⁹

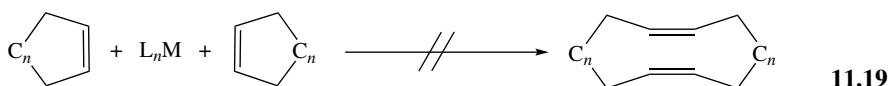


Although issues of catalyst activity, stability, and selectivity have not yet allowed such processes to be economically feasible, the Dow study provided a basis for development of these transformations on an industrial scale in the near future. With the price and availability of petroleum fluctuating rapidly, the use of plant-derived starting materials is especially attractive and, under the right conditions, ultimately a good example of green chemistry.

11-1-4 Industrial Uses for Metathesis: Polymers

ROMP

Most cyclic alkenes (cyclohexene being the notable exception because of its stability) undergo metathesis, but instead of dimerizing to form cyclodienes (equation **11.19**), they usually polymerize instead to form polyalkenamers (path **c**, Scheme **11.1**). Because this kind of metathesis involves rupturing the $C=C$ and opening up the ring, the process is called ROMP.



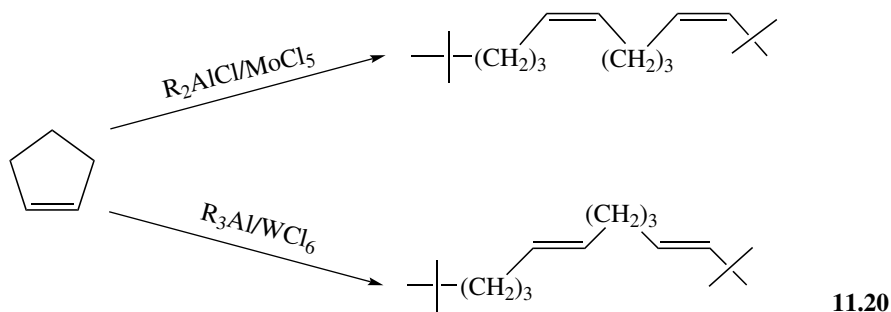
This remarkable reaction is used today in the chemical industry and continues to be an important means toward the production of interesting new materials.

The first good example of ROMP involved cyclopentene.⁵⁰ Depending upon the catalyst, good stereoselectivity was possible, producing either all *cis* (catalyzed

⁴⁹K. A. Burdett, L. D. Harris, P. Margl, B. R. Maughon, T. Mokhtar-Zadeh, P. C. Saucier, and E. P. Wasserman, *Organometallics*, **2004**, *23*, 2027.

⁵⁰G. Natta, G. Dall'asta, and G. Mazzanti, *Angew. Chem. Int Ed. Engl.*, **1964**, *3*, 723 and N. Calderon and R. L. Hinrichs, *Chemtech*, **1974**, *4*, 627.

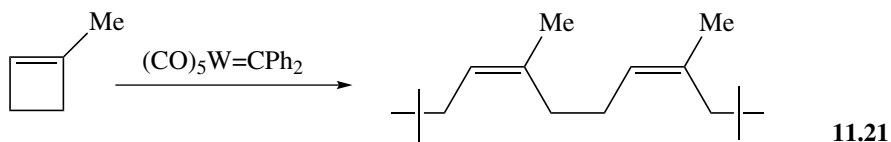
by $\text{MoCl}_5/\text{AlEt}_3$ or all *trans* (catalyzed by $\text{WCl}_6/\text{AlEt}_3$) polymer (equation 11.20). The reasons for this selectivity are not well understood, although several research groups have proposed models that explain how *cis* or *trans* double bonds may form.⁵¹



Draw the structure of the polymer that would result from ROMP of 2,5-dihydrofuran. Show at least three repeating units and assume that the C=C bonds that form have *trans*-stereochemistry.

Exercise 11-5

Equation 11.21 shows another example, where 1-methylcyclobutene polymerizes to form polyisoprene primarily with *cis* stereochemistry about the C=C. The properties of this polymer are quite similar to those of natural rubber, which is also *cis*-polyisoprene.⁵² In this case, Katz used a discrete metal-carbene complex to catalyze the polymerization. One reason why there has been general interest in ROMP is because cycloalkenes often polymerize to give materials with elastomeric (rubber-like) properties.



Among the most interesting examples of ROMP is the polymerization of norbornene (**31**, Scheme 11.7), which is also shown in part in equation 11.14 but is worth revisiting. There is much more ring strain in norbornene compared with cyclopentene, so the real driving force for this polymerization is the release of

⁵¹N. Calderon, J. P. Lawrence, and E. A. Ofstead, *Adv. Organomet. Chem.*, **1979**, *17*, 449; see especially pp. 481–482.

⁵²T. J. Katz, J. Mcginnis, and C. Altus, *J. Am. Chem. Soc.*, **1976**, *98*, 606.

that strain. Using a variation of Tebbe's reagent as a catalyst, Grubbs⁵³ was able to prepare titanobicyclopentane **32**. Complex **32** is a catalyst for polymerization of **31**, but there is an interesting twist to this special kind of chain-growth polymerization.⁵⁴ Grubbs termed the process an example of a "living" polymerization because chain growth continued until the supply of monomer was exhausted. Chain growth was also linear as a function of the number of equivalents of **31**, providing polymer chains with PDIs close to unity.⁵⁵ Chain termination in this case was very slow compared with initiation and chain propagation. Therefore, lacking any factors that could interfere with chain growth (presence of oxygen or moisture) and once all monomer was consumed, the polymer chain awaited "feeding" with additional monomer. This process makes it possible to create polymers that have homogeneous blocks. For instance, after a certain number of equivalents of **31** were added, another substituted norbornene (**33**) could be introduced to give a polymer consisting of two different blocks. Block copolymers often have properties entirely different from those consisting of only one type of monomer (homopolymers). Scheme 11.7 also shows a block polymerization process starting with **31**.

Exercise 11-6

Chain-growth polymerization can cease or be highly modified by chain transfer processes, which may occur in an intra- or intermolecular manner. Propose mechanistic pathways that show the following:

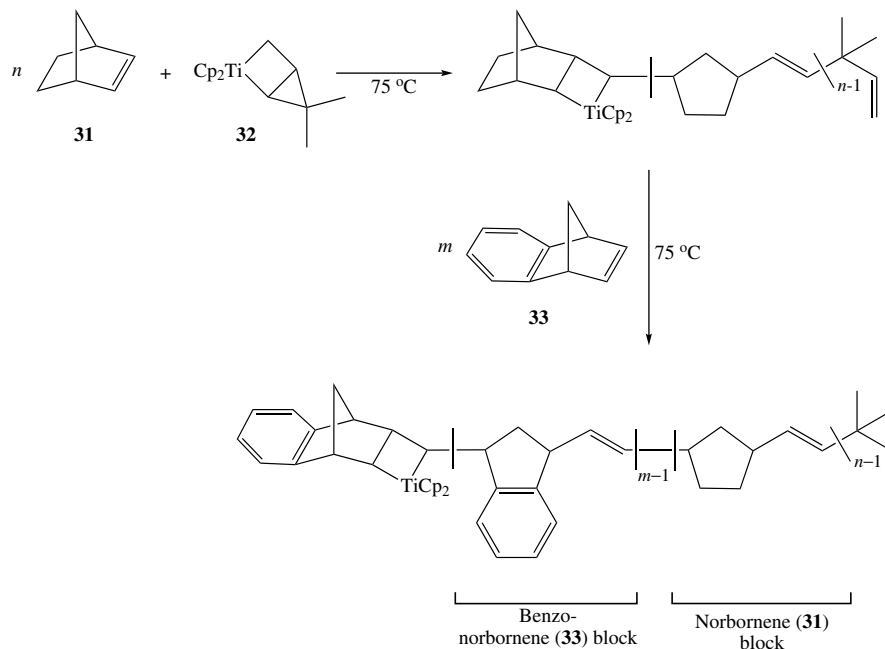
1. Metathesis of a metal carbene at the end of a growing polymer chain with a C=C bond in the middle of another polymer chain.
2. Metathesis of a terminal metal carbene with a C=C bond in the same chain.

Recent years have seen rapid advancements in development of W, Mo, and Ru carbene complexes that serve not only as catalysts for metathesis of small molecules (Section 11-1-3) but also as ROMP catalysts. Grubbs' use of a Ru(III) catalyst for ROMP in aqueous medium helped pave the way for development of his first- and second-generation Ru alkylidenes, which also catalyze ROMP. The Schrock catalysts that we have encountered already (compounds **15**

⁵³R. H. Grubbs and W. Tumas, *Science*, **1989**, 243, 907, and references therein.

⁵⁴Chain-growth polymers form in linear fashion by growing, one monomer at a time, from one end of the polymer chain.

⁵⁵Schrock has prepared alkylidene complexes of Mo and W whose activity is tuned so that they are unreactive to ordinary internal alkenes but actively catalyze polymerization of strained cyclic alkenes, such as norbornene. See R. R. Schrock, *Acc. Chem. Res.*, **1990**, 23, 158, and references therein.

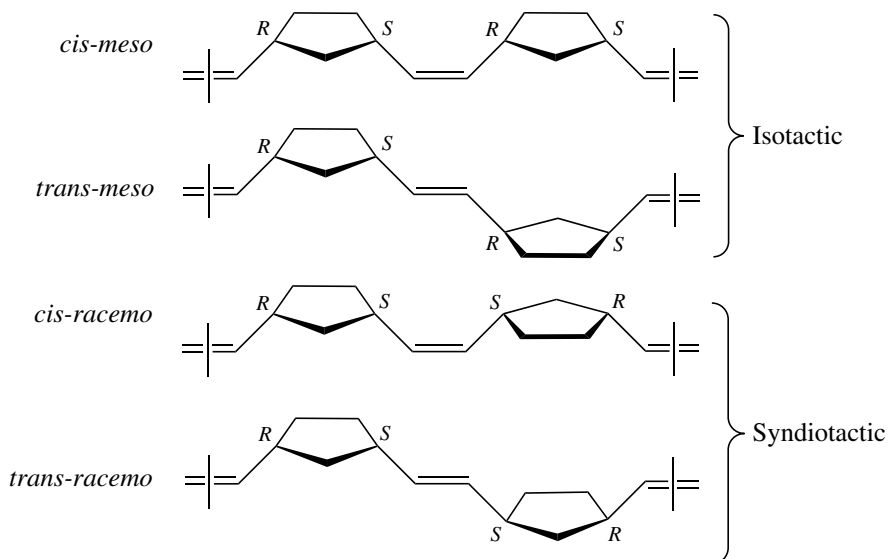
**Scheme 11.7**

"Living" ROMP of
Norbornenes

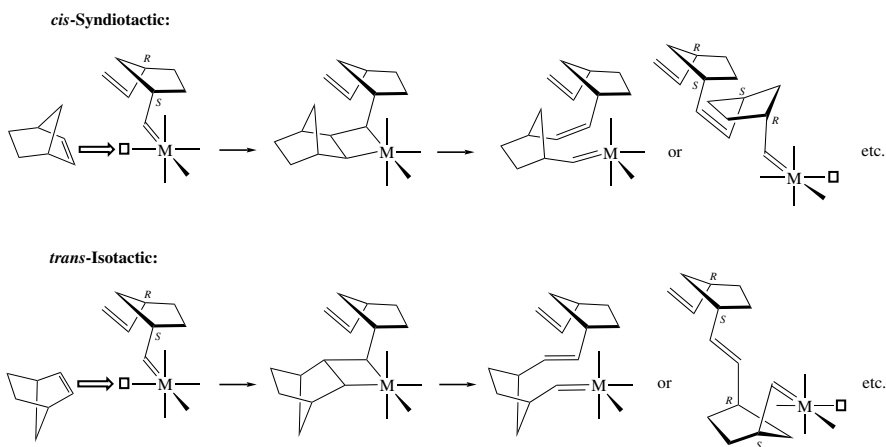
and **16**) are also effective. Some of the newer catalysts, especially the Ru-alkylidenes, permit the presence of polar substituents in the molecules undergoing metathesis, which is difficult with older catalysts because of their strong Lewis acidity.

The stereochemistry resulting from ROMP is of interest because this can influence the properties of the material produced. For polymerization of norbornene and related bicyclic alkene, there are four possible stereochemical results (other than random stereochemistry). These are presented in Figure **11-1**, which shows stereochemical relationships for two adjacent monomeric units (dyads).

Both the *cis*- and the *trans-racemo* arrangements are termed *syndiotactic*, whereas the two *meso* possibilities are considered *isotactic* stereochemistries. We will see isotactic-syndiotactic terminology again in Section **11-3**. The stereochemistry of the C=C bond and the tacticity can be determined by spectroscopic means, primarily NMR. When alkenamer chains have mainly *trans* C=C bonds, the melting point of the polymer tends to be higher than is the case with *cis*-polymers. The influence of the tacticity is less clear, but certainly there are some effects. It should be noted that most polyalkenamers do not have only one C=C configuration or tacticity throughout the polymer chain, but there seems to be a tendency to produce *cis*-syndiotactic and *trans*-isotactic stereochemistries instead of the other two possibilities. Figure **11-2**

**Figure 11-1**

Possible Dyad Tacticity and Double Bond Configuration Associated with ROMP of Norbornene

**Figure 11-2**

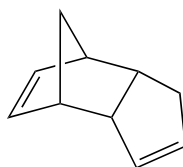
Cis-Syndiotactic and *trans-Isotactic* Configurations during ROMP of Norbornene

diagrams how *cis-syndiotactic* or *trans-isotactic* stereochemistry could result during ROMP of norbornene.⁵⁶

⁵⁶For good discussions of ROMP and the stereochemistry associated with it, see G. Black, D. Maher, and W. Risse, "Living Ring-Opening Olefin Metathesis Polymerization," in *Handbook of Metathesis*, Vol. 3, R. H. Grubbs, Ed., Wiley-VCH: Weinheim, Germany, 2003, pp. 2–71 and J. G. Hamilton, "Stereochemistry of Ring-Opening Metathesis Polymerization," in *Handbook of Metathesis*, Vol. 3, R. H. Grubbs, Ed., Wiley-VCH: Weinheim, Germany, 2003, pp. 143–179.

Commercial applications of ROMP do exist, but their scale is limited compared with the volume of polymers produced by Ziegler–Natta (Z–N) catalysis or those formed by radical, cationic, or anionic mechanisms. These applications, however, serve as unique and useful niches within the entire polymer industry because ROMP of cyclopentene, cyclooctene (sold as Vestenemer), and norbornene (Norsorex) produces elastomeric materials that act as shock insulators, for example. Like polyisoprene in natural rubber, some of these polyalkenamers can undergo vulcanization, which gives the resulting polymer a memory upon stretching and adds to the durability of the elastomer. Although well-defined Schrock and Grubbs carbene complexes can catalyze ROMP to produce polyalkenamers, industrial-scale applications typically use ill-defined heterogeneous catalysts or a homogeneous catalyst such as RuCl_3/HCl .

One area where Grubbs' first- and second-generation catalysts play a role in a commercial application of ROMP is in the polymerization of dicyclopentadiene (**34**), often abbreviated DCPD. Although polyDCPD could exist as a single chain polymer, it more likely undergoes ROMP to give a highly branched and cross-linked material. As such, polyDCPD may be formed *in situ* as a fairly rigid, tough material that exhibits, for instance, impenetrability to bullets. PolyDCPD also has unique properties that find use in sporting goods, where toughness and corrosion resistance are important.⁵⁷



34

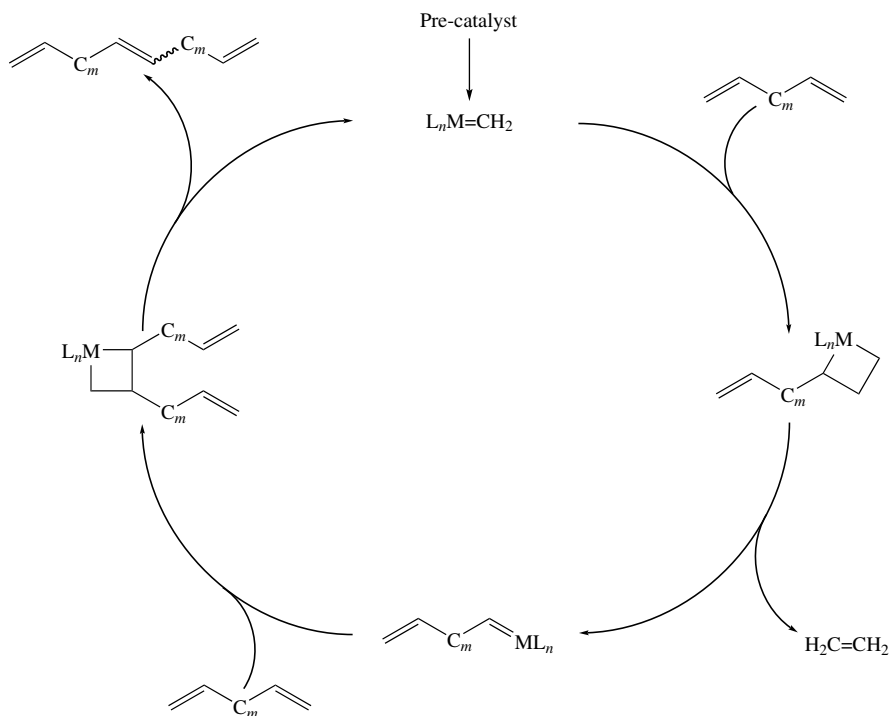
Suggest a structure for a portion of polyDCPD that shows chain branching and cross-linking.

Exercise 11-7

Acyclic Diene Metathesis Polymerization

Another means of metathesis polymerization involves an intermolecular CM of terminal diene monomers, and this pathway is called ADMET. Path **d** of Scheme 11.1 outlines the general process, which has a positive value of $\Delta_r S^\circ$ to

⁵⁷For more information about commercial applications for ROMP, see M. S. Trimmer, "Commercial Applications of Ruthenium Olefin Metathesis Catalysis in Polymer Synthesis," in *Handbook of Metathesis*, Vol. 3, R. H. Grubbs, Ed., Wiley–VCH: Weinheim, Germany, 2003, pp. 407–418; and J. C. Mol, *J. Mol. Catal.*, **2004**, 213, 39.

**Scheme 11.8**

A Mechanistic
Pathway for ADMET
Polymerization

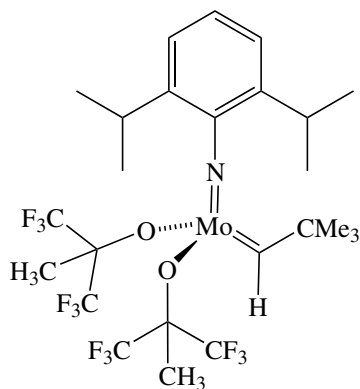
serve as a thermodynamic driving force. Moreover, if ethene can be removed during polymerization, Le Chatelier's principle dictates that the equilibrium will be shifted toward the production of polymer. Scheme **11.8** outlines a mechanism for ADMET polymerization that is fully consistent with the Chauvin mechanism for metathesis.

ADMET differs from ROMP in one major respect. Whereas ROMP is a chain-growth polymerization, ADMET is a step-growth, condensation process.⁵⁸ Manifestation of this difference lies in both the molecular weights and the molecular weight distributions of polymer chains that result from the two path-

⁵⁸Step-growth (or condensation) polymers result from reaction of monomers that have functional groups at two or three positions on the molecule (such as the diester of succinic acid, $RO_2CCH_2CH_2CO_2R$). These functional groups react with functional groups on another monomer (ethylene glycol, $HOCH_2CH_2OH$, for example) such that growth can occur at two or three positions on the original monomeric unit. The new, larger molecule that results still has multiple functional groups available for further reaction with additional monomers or polymer fragments. The process continues in steps such that high-molecular-weight polymers form only at the end of the reaction. The reaction of two molecules to produce a larger molecule plus a small molecule, such as H_2O , an alcohol, HCl , or ethene is called a condensation.

ways. Early in ROMP processes, the molecular weights of the polymer chains are large, even while the degree of polymerization is small. Just the opposite is true with ADMET polymerizations, where the degree of polymerization must be high before high-molecular-weight polymer chains form. Because both ROMP and ADMET can produce the same polyalkenamer, the lower-molecular-weight distributions that usually occur under ADMET can result in different properties, such as lower melting point and mechanical strength but more flexibility, than are attainable with ROMP. The PDIs of polymers resulting from ADMET tend to be larger as well.

The stereochemistry of the C=C bond in the polymer chains that result from ADMET of dienes of the type $\text{H}_2\text{C}=\text{CH}-(\text{CH}_2)_n-\text{CH}=\text{CH}_2$ tends to be mostly *trans* in contrast to the result from ROMP of simple cycloalkenes, where *trans* C=C bond content may not be the predominant stereochemistry. For example, ADMET polymerization of 1,5-hexadiene gave a linear polymer with a *trans* C=C bond content of over 70% (catalyzed by Schrock catalyst **35**), which is close to the value expected on the basis of thermodynamics.⁵⁹ Earlier (equation **11.21**), we saw that a similar polyalkenamer results from ROMP of methylcyclobutene (catalyzed by $(\text{CO})_5\text{W}=\text{CPh}_2$); this time the stereochemistry of the C=C bond was 93% *cis*.⁶⁰

**35**

The ADMET process involves metathesis of terminal dienes just like RCM. Why does ADMET occur and not RCM? The answer is that RCM can be quite competitive with ADMET unless reaction conditions are adjusted properly. Because RCM is an intramolecular process and ADMET is intermolecular, one obvious solution is to run ADMET polymerizations at high concentrations of

⁵⁹K. B. Wagener, J. M. Boncella, and J. G. Nel, *Macromolecules*, **1991**, *24*, 2649.

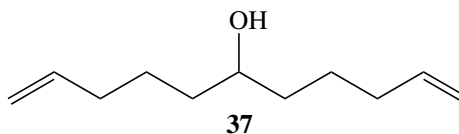
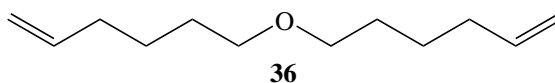
⁶⁰See Footnotes 22b and 52.

monomer. Another option is to avoid use of dienes that will undergo RCM to form stable rings (e.g., C₅, C₆, and C₇ cycloalkenes).

Exercise 11-8

Which cycloalkene using ROMP and which terminal diene using ADMET polymerization will both produce poly(1-octene)?

ADMET polymerization of dienes containing functional groups has been explored to some extent. It appears that diene ethers such as **36** are tolerant of Schrock's W-alkylidene catalysts when undergoing ADMET polymerization, but Grubbs' first-generation catalyst is required to successfully polymerize diene alcohol **37**,⁶¹ because the OH group is too Lewis basic for catalysis by W- and Mo-alkylidenes.⁶²



Chemists continue to explore ADMET using well-defined carbene complex catalysts, but the use of this mode of metathesis polymerization on a significant industrial scale awaits further research and development.⁶³

11-2 ALKYNE METATHESIS

Mechanism and Catalysts

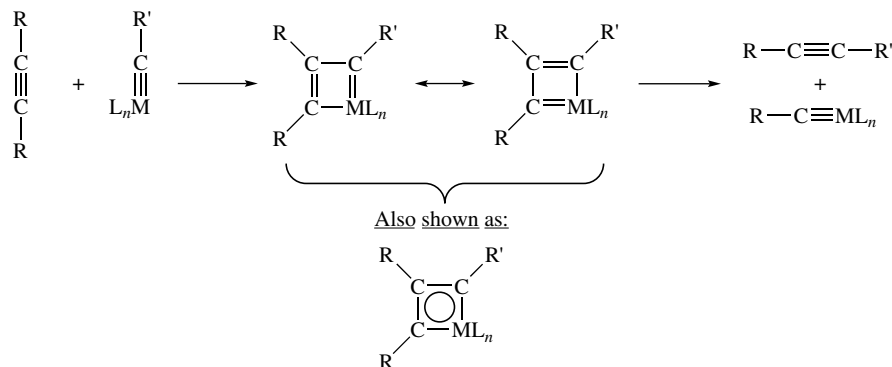
We first encountered alkyne metathesis in Chapter 10 in connection with reactions of metal-carbyne complexes. The mechanism of alkyne metathesis, first proposed by Katz,⁶⁴ is analogous to that for alkenes, and it is shown in Scheme 11.9.

⁶¹K. Brzezinska and K. B. Wagener, *Macromolecules*, **1991**, 24, 5273.

⁶²D. J. Valenti and K. B. Wagener, *Macromolecules*, **1998**, 31, 2764.

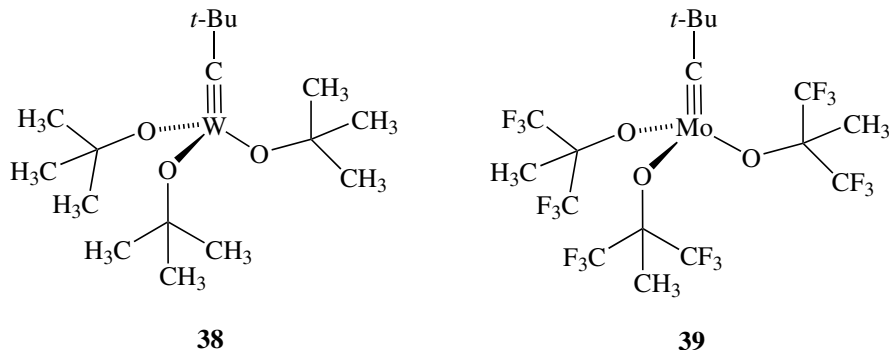
⁶³For more information on ADMET, see S. E. Lehman Jr. and K. B. Wagener, "ADMET Polymerization," in *Handbook of Metathesis*, Vol. 3, R. H. Grubbs, Ed., Wiley-VCH: Weinheim, Germany, 2003, pp. 283–353.

⁶⁴T. J. Katz and J. McGinnis, *J. Am. Chem. Soc.*, **1975**, 97, 1592.

**Scheme 11.9**

The Mechanism of Alkyne Metathesis

Parallel to the development of catalysts for olefin metathesis, the first alkyne metathesis catalysts were W and Mo metal oxides or carbonyls suspended on alumina or silica.⁶⁵ The first homogeneous catalysts were developed by Mortreux and consisted of a mixture of Mo(CO)₆ and substituted phenols.⁶⁶ It was not until the work of Schrock and his collaborators, however, that a well-defined, isolable alkylidyne catalyst (**38**) was synthesized, characterized, and shown to catalyze alkyne metathesis.⁶⁷ Later modifications on **38** included substituting the alkoxy groups with fluorinated analogs, and for the corresponding Mo alkylidynes (**39**), the fluorinated alkoxy groups are essential for catalytic activity.⁶⁸



To this day, the most effective alkyne metathesis catalysts are Group 6 alkylidynes; however, there are drawbacks to use of these carbyne complexes.

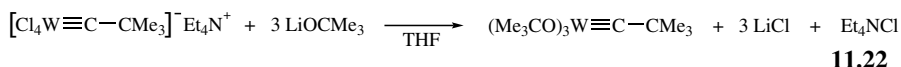
⁶⁵F. Pennella, R. L. Banks, and G. C. Bailey, *Chem. Commun.*, **1968**, 1548.

⁶⁶A. Mortreux and M. Blanchard, *J. Chem. Soc., Chem. Commun.*, **1974**, 786.

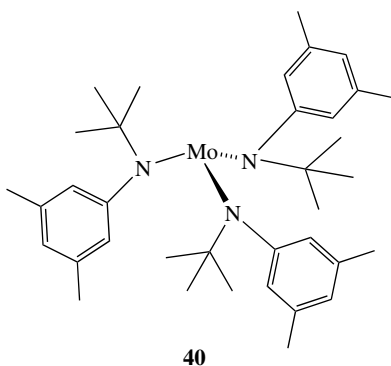
⁶⁷J. H. Wengrovius, J. Sancho, and R. R. Schrock, *J. Am. Chem. Soc.*, **1981**, *103*, 3932.

⁶⁸L. G. McCullough, R. R. Schrock, J. C. Dewan, and J. C. Murdzek, *J. Am. Chem. Soc.*, **1985**, *107*, 5987.

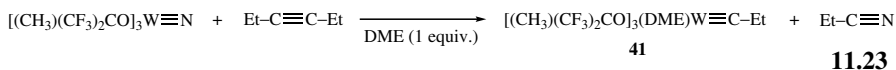
Although synthesis of **38** and related W-alkylidyne is relatively straightforward according to equation 11.22, the analogous Mo alkylidyne like **39** are more difficult to synthesize.



One approach to synthesis of active Mo catalysts was reported by Fürstner. Complex **40** is not an alkylidyne, but it is instead considered a precatalyst, which, when placed in CH_2Cl_2 solvent, actively promotes metathesis. There is some evidence that during the course of the reaction, the precatalyst converts to some ill-defined, high-oxidation-state Mo complex that could be an alkylidyne. One advantage of the Fürstner catalysts is that they are tolerant of the presence of polar functional groups on substrates, which the Schrock alkylidyne are not.⁶⁹



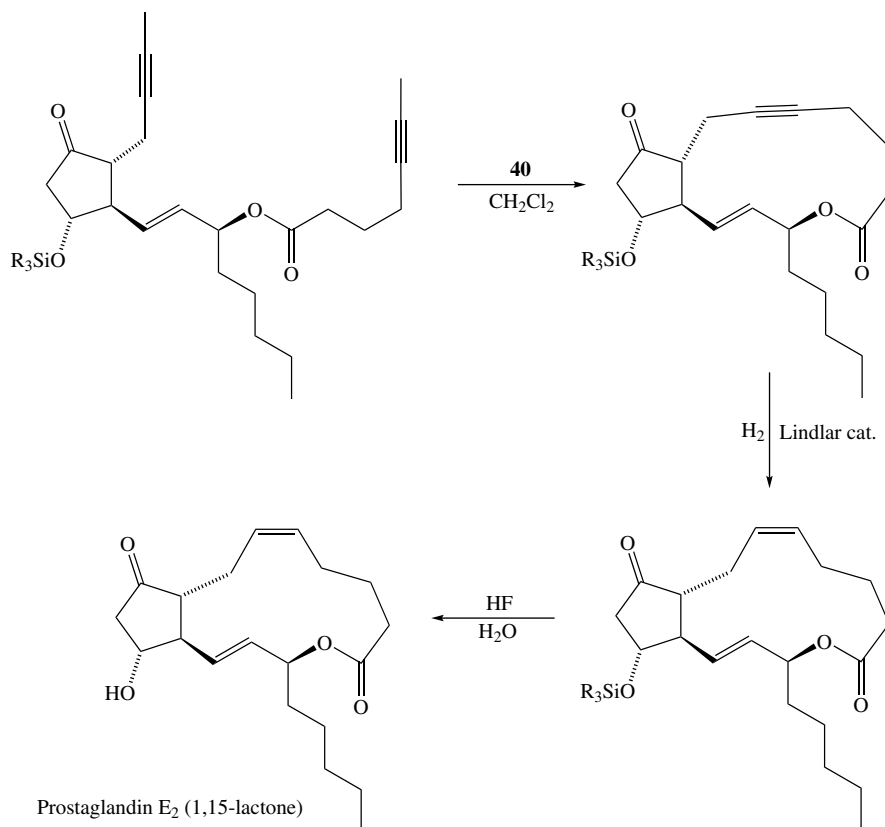
Another method for producing an analog to **39** was developed recently by Gdula and Johnson.⁷⁰ Here, a Mo nitride, which is easier to synthesize than an alkylidyne, reacts (equation 11.23) with a sacrificial, symmetrical, and inexpensive alkyne to produce the corresponding Mo alkylidyne complexed with dimethoxyethane (DME) (**41**). Alkylidyne **41**, first synthesized by Schrock,⁷¹ is an active metathesis catalyst that can be produced on a multigram scale.



⁶⁹A. Fürstner, C. Mathes, and C. W. Lehmann, *J. Am. Chem. Soc.*, **1999**, *121*, 9453 and A. Fürstner, C. Mathes, and C. W. Lehmann, *Chem. Eur. J.*, **2001**, *7*, 5299.

⁷⁰R. L. Gdula and M. J. A. Johnson, *J. Am. Chem. Soc.*, **2006**, *128*, 9614.

⁷¹See Footnote 68.



Scheme 11.11
 Synthesis of
 Prostaglandin
 E₂-1,15-lactone

appropriate catalyst. First reported by Katz in 1985,⁷³ it is finding increasing use in organic synthesis. Scheme 11.12 diagrams a reasonable mechanism for the transformation. Most alkene metathesis catalysts will promote this reaction, but Grubbs' first- and second-generation Ru-alkylidenes seem to be most commonly employed.

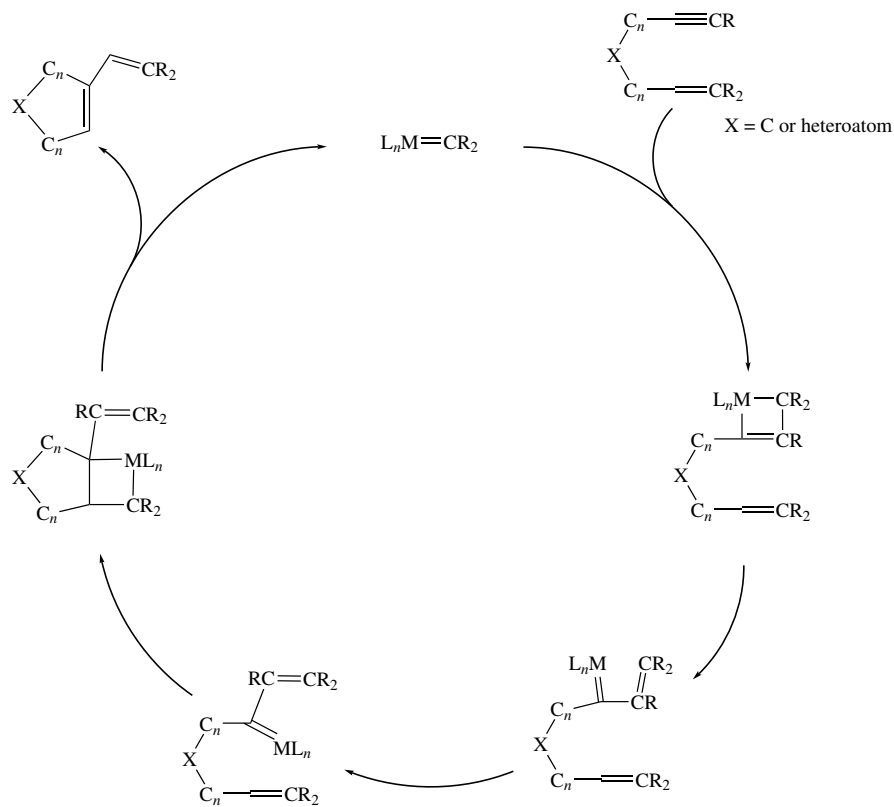
The most likely scenario for enyne metathesis is an intramolecular combination of the alkene and alkyne moieties to form a ring, which is really a variation of RCM. Examples of intermolecular enyne metathesis (CM) have been successful if they are run in an atmosphere of ethene, using it as the alkene component. Even for some intramolecular enyne metatheses, preequilibration of the catalyst with ethene caused vastly improved yields.⁷⁴ Equations 11.24⁷⁵ and 11.25⁷⁶ show

⁷³T. J. Katz and T. M. Sivavec, *J. Am. Chem. Soc.*, **1985**, 107, 737.

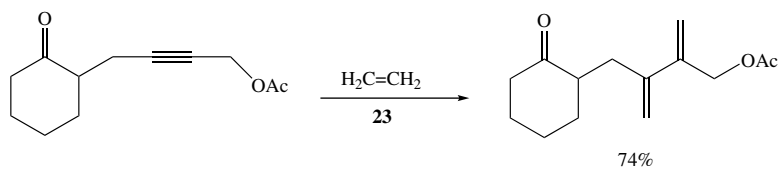
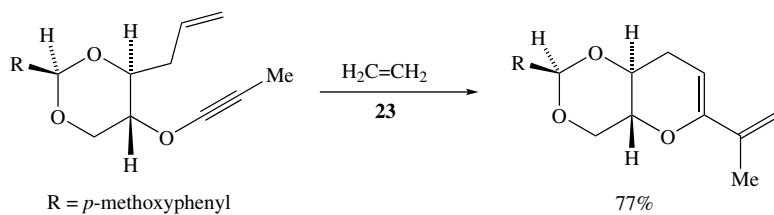
⁷⁴A. Mori, N. Sakakibara, and A. Kinoshita, *J. Org. Chem.*, **1998**, 63, 6082.

⁷⁵J. S. Clark, G. P. Trevitt, D. Boyall, and B. Stammen, *Chem. Commun.*, **1998**, 2629.

⁷⁶A. Kinoshita, N. Sakakibara, and M. Mori, *J. Am. Chem. Soc.*, **1997**, 119, 12388.



examples of intra- and intermolecular enyne metathesis, respectively; in both cases Grubbs' first-generation catalyst (**23**) was used.



under the same high-temperature, radical conditions possible to make PE always produced low-molecular-weight, goeey material (often called “road tar” by frustrated chemists) with no commercial value. The years that followed Ziegler and Natta’s original discoveries brought the commercialization of processes to manufacture both “high density”⁷⁸ PE and polypropylene (PP), as well as other polyolefins, using early-transition metals as cocatalysts mixed with alkylaluminum compounds. The scientific and commercial importance of their work was so significant that in 1963 Ziegler and Natta shared the Nobel Prize in chemistry.

11-3-1 The Mechanism of Ziegler–Natta Polymerization

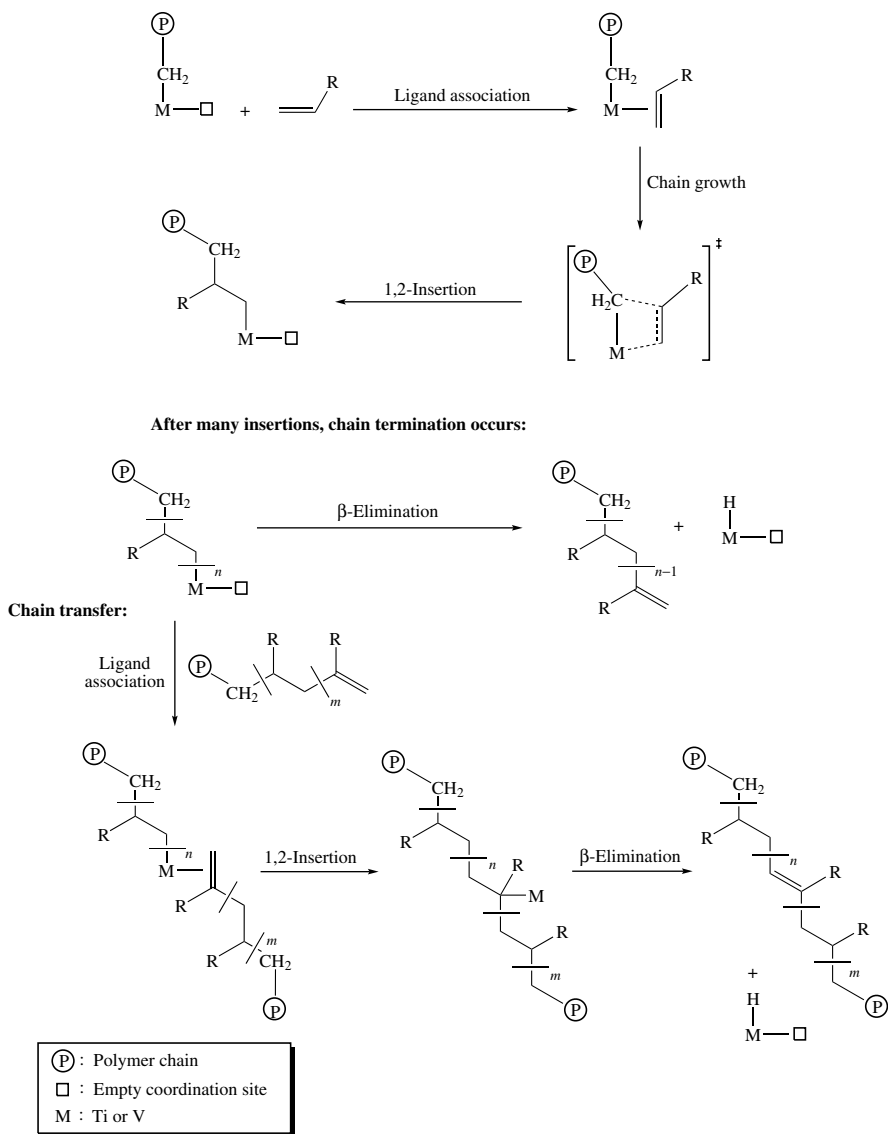
The mechanism of Z–N catalysis was unclear for decades after the original reports by Ziegler and Natta. The active catalyst forms from a mixture of high-valent Ti or V halides and an alkyl or chloroalkylaluminum compound, with either component being an ineffective catalyst when present alone. Catalysis may either be homogeneous⁷⁹ or heterogeneous, with the latter preferred on an industrial scale. Cossee proposed a mechanism in 1964⁸⁰ that is outlined in Scheme 11.13a. The essential features of Cossee’s mechanism require that a coordinatively unsaturated Ti- or V-alkyl (the alkyl group arising from the aluminum alkyl cocatalyst) complex forms followed by 1,2-insertion of an alkene into the Ti–C bond. Eventually, chain termination occurs, most likely by β -elimination or chain transfer. Chain transfer occurs by complexation of another chain, 1,2-insertion, and β -elimination (see Scheme 11.13a).

Although the Cossee mechanism accounted for much of the experimental data related to Z–N polymerization, it was a bold proposal because 1,2-insertions into M–C bonds of early transition metal complexes were unknown at the time. Metal alkyls, should they form by 1,2-insertion into an M–C bond, ought to have a high propensity to undergo loss of a β -hydrogen by 1,2-elimination. Thus,

⁷⁸PE produced under high-temperature, radical conditions (called “low-density” PE) has lower density, poorer mechanical strength, and a lower temperature range for use than the PE resulting from Z–N catalysis. Low-density PE has a great deal of chain branching along the polymer backbone, whereas the high-density variety is much more linear. The lack of chain branching in high-density PE means that carbon chains can fit together into regular, repeating “crystalline” regions similar to the regular packing patterns of monomeric crystals. The “crystalline” regions of high-density PE provide high mechanical strength and higher density because of the close packing of atoms in the aligned chains. For more information about the relationship between the molecular structure and physical properties of polymers, see H. R. Alcock and F. W. Lampe, *Contemporary Polymer Chemistry*, 2nd ed., Prentice Hall: Englewood Cliffs, NJ, 1990, Chapter 17.

⁷⁹There are indications that even catalysts that appear to be soluble are actually present as small aggregate particles.

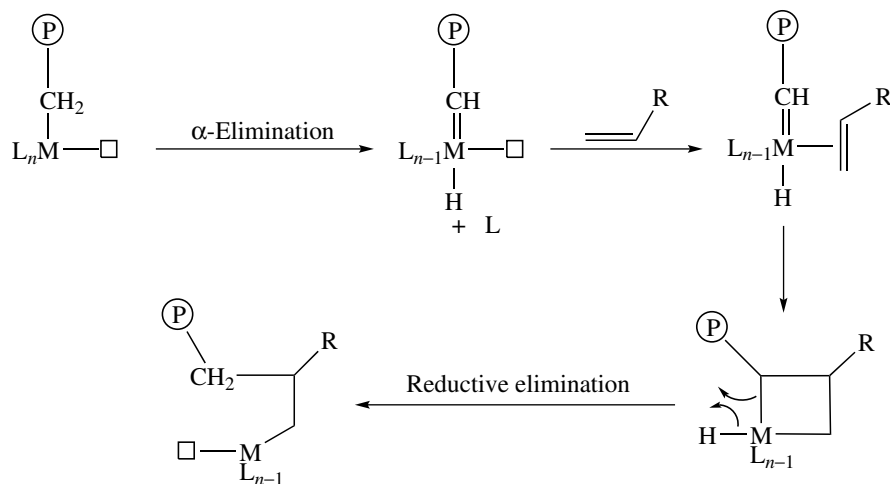
⁸⁰P. Cossee, *J. Catal.*, **1964**, 3, 80 and E. J. Arlman and P. Cossee, *J. Catal.*, **1964**, 3, 99.

**Scheme 11.13a**

The Cossee
 Mechanism for Z-N
 Polymerization

chemists asked, even if insertion could occur into the M–C bond, how could the polymer grow in light of facile β -elimination? The answer, we now know, probably rests in the reluctance of some high-valent, early transition metal alkyls to undergo β -elimination due to the lack of *d* electrons (see Section 8-1-2).

Nevertheless, the paucity of evidence for direct M–C alkene insertion was a nagging problem associated with the Cossee mechanism. Several years later,

**Scheme 11.13b**

The Green–Rooney
Mechanism for Z–N
Polymerization

Green and Rooney⁸¹ proposed an alternative mechanism (Scheme 11.13b) that also accounted for Z–N catalysis. The mechanism resembles a metathesis-like pathway by starting with α -elimination to give a metal–carbene hydride followed by cycloaddition with the alkene monomer to form a metallacyclobutane. Reductive elimination finally yields a new metal alkyl with two more carbon atoms in the growing chain. The Green–Rooney mechanism, although plausible overall, requires an α -elimination, a process that is difficult to demonstrate.

Elucidating mechanistic pathways for catalytic processes is always demanding work, but trying to make sense of Z–N catalysis was especially difficult because the structures of neither the active catalysts nor the intermediates and products were completely determined when Cossee and later Green and Rooney proposed their routes. In recent years, the efforts of several research groups strongly support the Cossee mechanism as the correct pathway. For instance, Watson⁸² reported that an alkyl Lu(III) complex⁸³ could undergo a 1,2-insertion of propene. The new Lu–alkyl could continue to grow in length or undergo reversible reactions of both β -hydride and β -alkyl elimination (Scheme 11.14).

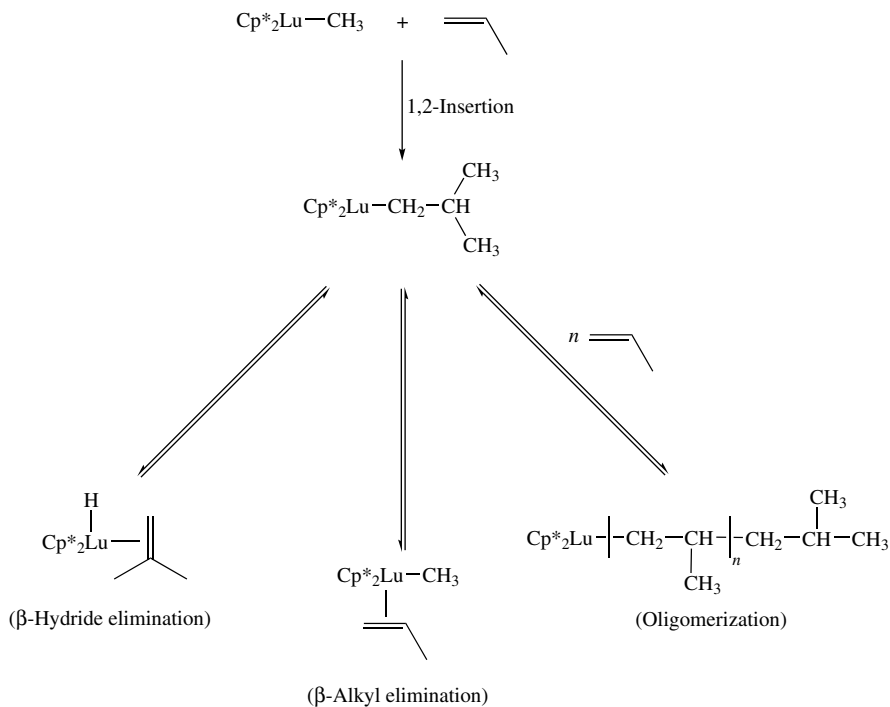
Eisch⁸⁴ showed that an alkyne could insert into a Ti–C bond under Z–N-like conditions, the first such demonstration of this phenomenon (equation 11.26).

⁸¹K. J. Ivin, J. J. Rooney, C. D. Stewart, M. L. H. Green, and J. R. Mahtab, *J. Chem. Soc., Chem. Commun.*, **1978**, 604 and M. L. H. Green, *Pure Appl. Chem.*, **1978**, 100, 2079.

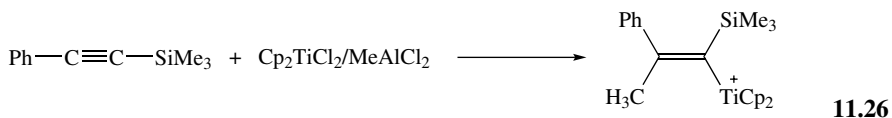
⁸²P. L. Watson, *J. Am. Chem. Soc.*, **1982**, 104, 337.

⁸³Lanthanides resemble early transition metals in their chemistry.

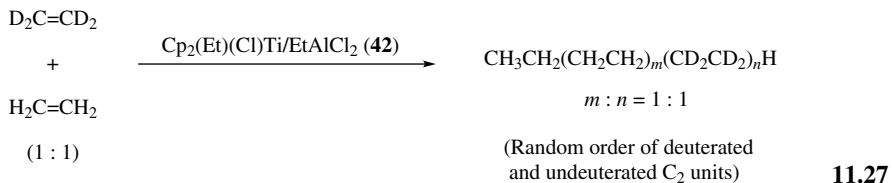
⁸⁴J. J. Eisch, A. M. Piotrowski, S. K. Brownstein, E. J. Gabe, and F. L. Lee, *J. Am. Chem. Soc.*, **1985**, 107, 7219.



Scheme 11.14
Insertion of Propene
into a Lu–C Bond



The experiments just described point out the feasibility of the 1,2-M–C insertion described by the Cossee mechanism, but they fail to distinguish between it and the Green–Rooney pathway. Grubbs⁸⁵ reported definitive evidence in support of the Cossee mechanism when he measured the rate of polymerization (in the presence of catalyst **42**) of a 1:1 mixture of $\text{H}_2\text{C}=\text{CH}_2$ and $\text{D}_2\text{C}=\text{CD}_2$ (equation **11.27**). There was no kinetic isotope effect, thus supporting the Cossee mechanism.

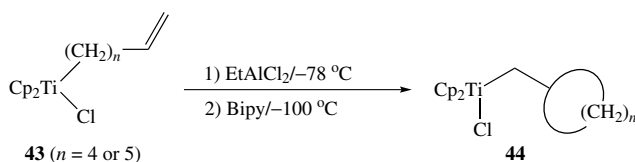


⁸⁵J. Soto, M. Steigerwald, and R. H. Grubbs, *J. Am. Chem. Soc.*, **1982**, *104*, 4479.

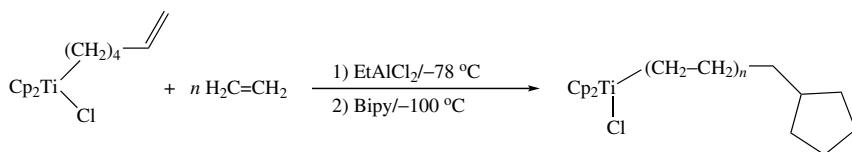
Explain how Grubbs' observation of a lack of deuterium isotope effect during polymerization in the presence of **42** would argue for the Cossee mechanism and against that of Green and Rooney.

Exercise 11-10

Although the lack of a kinetic isotope effect argued against the Green–Rooney pathway, the conclusion was based upon negative evidence rather than direct support for the Cossee scheme. Later, Grubbs⁸⁶ reported an ingenious experiment that clearly supported the Cossee mechanism and excluded the other. Schemes **11.15a** and **b** show the experiment in some detail. The starting material was alk-1-enyl titanocene **43**, which, in the presence of EtAlCl₂, cyclized to give **44** by intramolecular insertion of the remote alkene group into the Ti–C bond (equation **11.28**). The mixture of **43** and EtAlCl₂ was an appropriate catalyst mimic of Z–N polymerization because the system also reacted with ethene to give ethene oligomers capped with a ring (equation **11.29**).



11.28



11.29

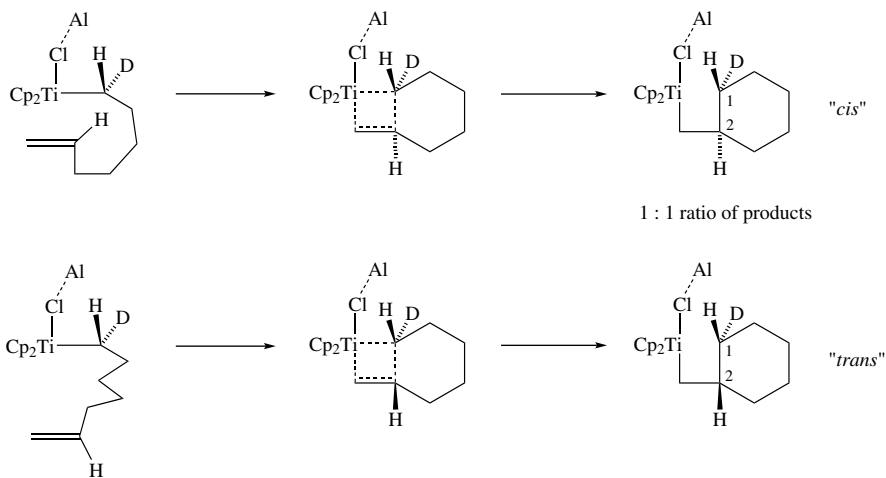
Grubbs reasoned that the tethered alkene group would react at the Ti center by either a direct insertion of the alkene into the Ti–C bond (the Cossee mechanism, Scheme **11.15a**) or by an α -hydrogen-activated pathway (the Green–Rooney mechanism, Scheme **11.15b**). The experiment was designed to measure a “stereochemical” isotope effect as well as a kinetic isotope effect according to the following logic:

If α -elimination to the metal is the required first step, then it *will* make a difference whether H or D is lost at the α -position. The resulting monosubstituted cyclohexanes will form according to the ease of loss of H with respect to D. In other words, the ratio of *cis*

⁸⁶L. Clawson, J. Soto, S. L. Buchwald, M. L. Steigerwald, and R. H. Grubbs, *J. Am. Chem. Soc.*, **1985**, *107*, 3377.

Scheme 11.15a

The Grubbs
Stereochemical
Isotope Experiment:
The Cossee
Mechanism



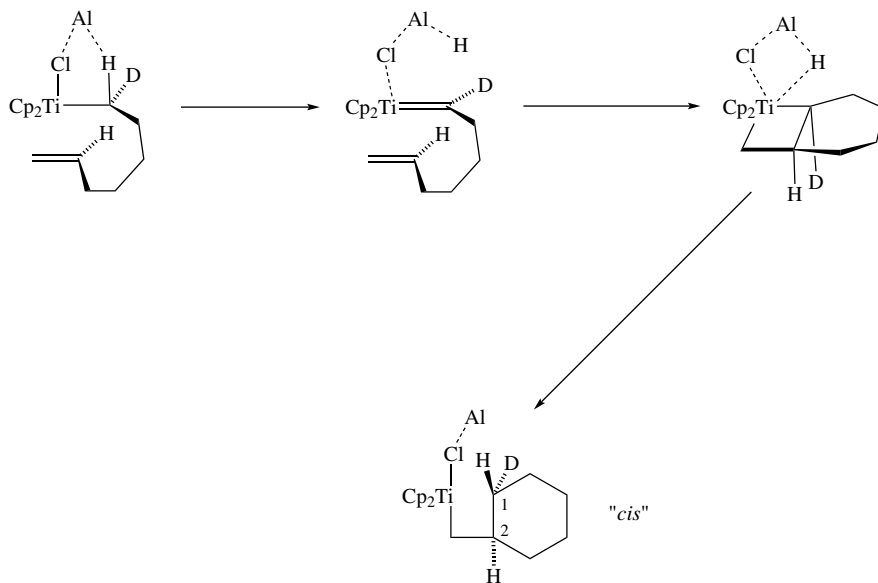
to *trans* (for example, *cis* means the D at the 1-position is *cis* with respect to H at the 2-position) will not be 1:1. If direct insertion occurs (the Cossee mechanism), on the other hand, the preference for H over D is irrelevant because a C–H(D) is not broken. The ratio of *cis* to *trans* should be 1:1. Schemes 11.15a and b follow the two mechanistic pathways when $n = 5$ and for only one of the two possible α -deuterio enantiomers.

In all cases, Grubbs found that the *cis*–to–*trans* ratio was always 1:1, thus demonstrating that α -activation does not influence the rate or stereochemistry of alkene insertion. The result of the experiment was the key piece of evidence supporting the Cossee mechanism for *Z*–N polymerization long sought after by chemists. The experiment allowed researchers to make a clear distinction between metathesis and *Z*–N polymerization, the former involving the chemistry of the M=C bond and the latter that of the M–C bond.⁸⁷

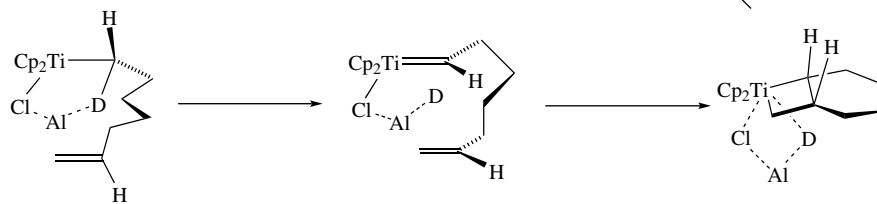
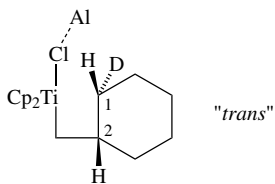
Since this work, Grubbs and others have suggested that the evidence shows that there is a modification of the Cossee mechanism that may occur, depending on the catalyst system.⁸⁸ Further work indicates an agostic interaction of an

⁸⁷In at least one case, there is an example of ethene polymerization using a Ta–carbene complex in which there is strong evidence for a metathesis-based mechanism. See H. W. Turner and R. R. Schrock, *J. Am. Chem. Soc.*, **1982**, *104*, 2331, a paper that describes oligomerization of up to 35 ethene units in the presence of Ta[=CH(*t*-Bu)](H)(PMe₃)₃I₂. It seems clear that although the Cossee mechanism is operative when polymerization occurs in the presence of *Z*–N-type catalysts, some polymerizations may involve metathesis, especially when hydrido–metal carbenes can form readily.

⁸⁸(a) R. H. Grubbs and G. W. Coates, *Acc. Chem. Res.*, **1996**, *29*, 85, and references therein and (b) M. Brookhart, M. L. H. Green, and L. L. Wong, *Prog. Inorg. Chem.*, **1988**, *36*, 1.

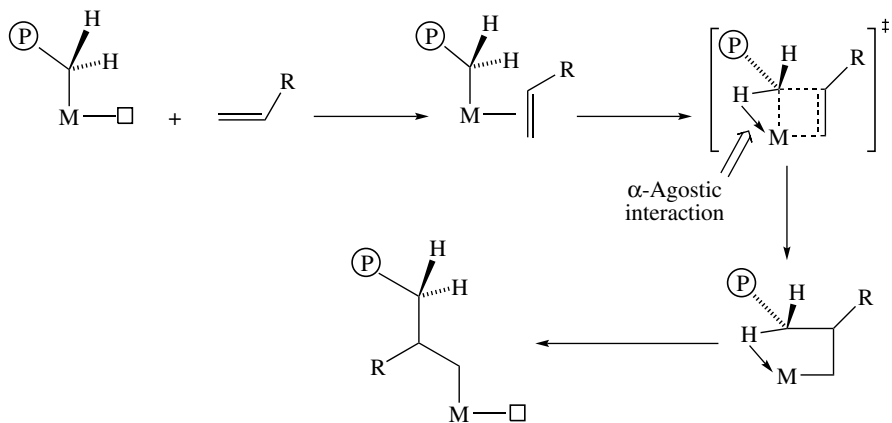


Product ratio is not 1 : 1



Scheme 11.15b

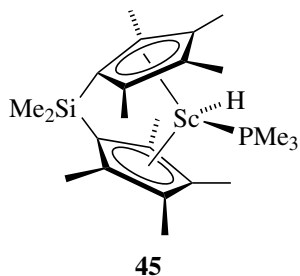
The Grubbs
Stereochemical
Isotope Experiment:
The Green–Rooney
Mechanism

**Scheme 11.16**

Modified Cossee
Mechanism
Showing an
 α -Agostic
Interaction

α -hydrogen may occur before or during the M–C insertion step. Scheme 11.16 shows this modification.

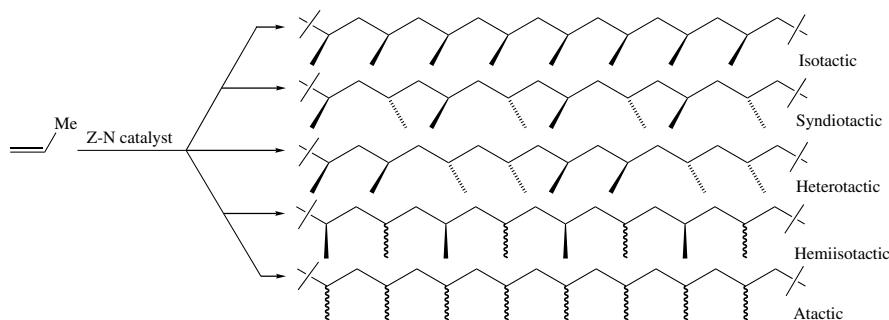
For example, use of a neutral Sc–metallocene catalyst (**45**) shows kinetic deuterium isotope effects that were not present with Grubbs Ti system.⁸⁹ It appears that deuterium isotope effects occur if insertion is rate-determining and if overall the rate of polymerization is relatively slow.

**11-3-2 Stereochemistry of Z–N Polymerization**

Polymerization of monosubstituted alkenes introduces stereogenic centers along the carbon chain at every other position. When, for example, propene undergoes Z–N polymerization, several possible geometries are possible, including *isotactic*, *syndiotactic*, *heterotactic*, *hemiisotactic*, and *atactic* (Figure 11-3).⁹⁰

⁸⁹W. E. Piers and J. E. Bercaw, *J. Am. Chem. Soc.*, **1990**, *112*, 9406 and J. E. Bercaw, et al., In *Ziegler Catalysts*, G. Fink, R. Mühlhaupt, and H. H. Brintzinger, Eds., Springer-Verlag: Berlin, 1995, pp. 317–331.

⁹⁰G. W. Coates, *Chem. Rev.*, **2000**, *100*, 1223.

**Figure 11-3**

Some Common Stereochemistries Resulting from Z–N Polymerization of Propene and Other 1-Alkenes

Note that isotactic polymers have all substituent groups (called *pendant* groups) on the same side of the chain; syndiotactic polymers maintain alternating stereochemistry for the pendant groups; heterotactic chains have alternating stereochemistry for each dyad, hemiisotactic polymers show the same stereochemistry at every other pendant group, but the intervening pendant group has random stereochemistry; and atactic polymers display a random stereochemical arrangement of substituents throughout the polymer chain (the stereochemistries that are perhaps most common and well studied are isotactic and syndiotactic). All of these types of PP have been prepared, each with rather different mechanical properties. The potential existed early on to produce hundreds of polyalkenes, not only with different composition caused by change in pendant group, but also with several different kinds of tacticities. In the years since Natta's first discovery of isotactic PP, progress in the design of catalysts capable of producing polymers with specific stereochemistry has been substantial.

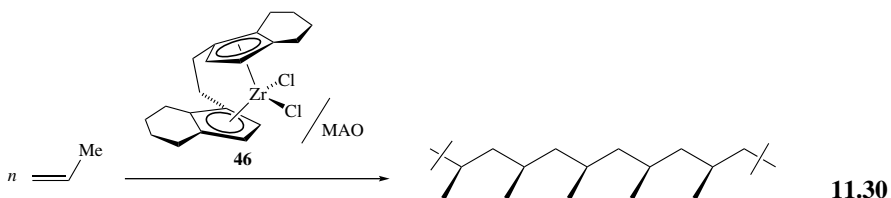
Even today, however, there is not complete understanding of how different stereochemistries result from different catalyst systems, especially under heterogeneous conditions. In general, Ti–Al catalysts tend to give isotactic and atactic PP, whereas VCl_4 – $AlEt_2Cl$ gives mainly the syndiotactic polymer.

A real advancement in the development of Z–N catalysts came when metallocene catalysts were discovered.⁹¹ Now discrete, single-site complexes of early-transition metal metallocenes could be synthesized and characterized. These not only were potentially useful on an industrial scale, but also served as useful model systems for studying the mechanism and stereochemistry of Z–N catalysis. With the advent of high-level DFT–MO methods that were parameterized for all transition metals, metallocene catalysts and the attendant polymerization processes could be easily modeled to help understand the stereochemical outcomes of Z–N

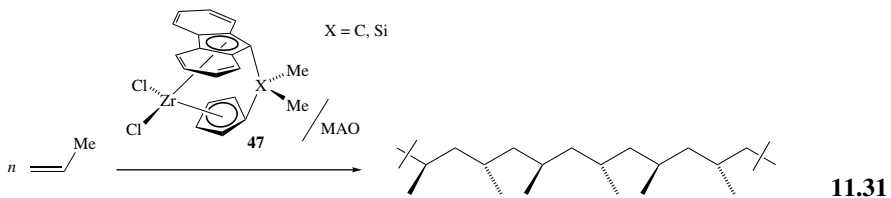
⁹¹For some reviews on metallocene Z–N catalysts, see H. Sinn, W. Kaminsky, H.–J. Vollmer, and R. Woldt, *Angew. Chem. Int. Ed. Engl.*, **1980**, *19*, 390; H. H. Brintzinger, D. Fischer, R. Mühlhaupt, B. Rieger, and R. M. Waymouth, *Angew. Chem. Int. Ed. Engl.*, **1995**, *34*, 1143; and G. G. Hlatky, *Coord. Chem. Rev.*, **1999**, *181*, 243.

catalysis and to verify the mechanistic work of Cossee, Green and Rooney, and Grubbs.

For example, homogeneous Zr complexes, with rigid, cyclic π ligands, mixed with methylalumoxane ($[\text{Al}(\text{CH}_3)_2\text{O}]_n$, abbreviated MAO) catalyze Z-N polymerization to give stereoregular polymers. MAO acts as an *in situ* methylating agent that replaces a Cl ligand on Zr with CH_3 . Equation 11.30 shows formation of isotactic PP using the chiral, ethano-bridged, *bis*-tetrahydroindenyl Zr complex **46**.⁹²



Syndiotactic polymerization, shown in equation 11.31, occurs with the Cp-fluorenyl Zr complex **47**.⁹³ Note that **47** possesses a plane of symmetry bisecting the two cyclic π ligands, whereas **46** is a chiral molecule, possessing a C_2 symmetry axis⁹⁴ but no symmetry plane.

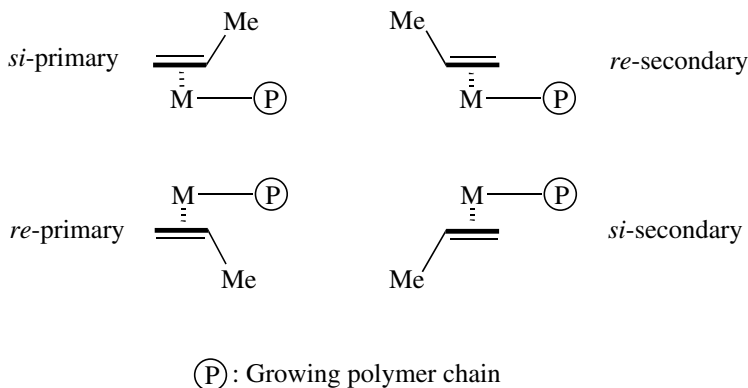


There has been a great deal of effort reported designed to make sense of how different metallocene complexes regulate polymer tacticity as a function of the symmetry properties of the catalyst. To begin to understand this, we must look at stereochemical possibilities of approach by propene to the metal. Figure 11-4 shows four such options, which may be classified as *re*-primary, *si*-primary, *si*-secondary, and *re*-secondary. The designations *re* and *si* refer to the faces of the propene C=C bond, and Figure 11-4 also details the difference between *si*

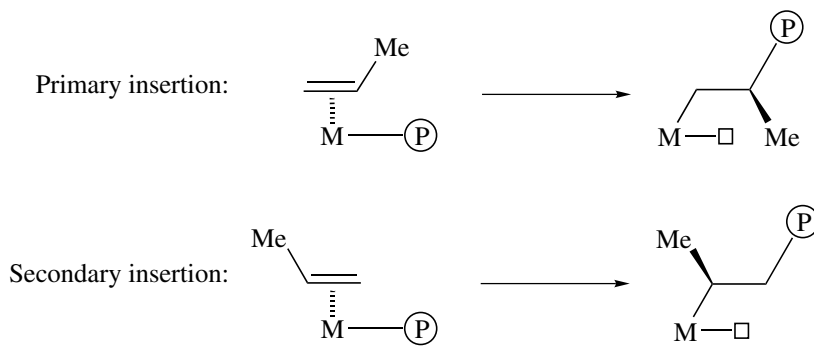
⁹²W. Kaminsky, W. K. Kulper, H. H. Brintzinger, and F. R. W. P. Wild, *Angew. Chem. Int. Ed. Engl.*, **1985**, 24, 507.

⁹³J. A. Ewen, R. L. Jones, and A. Razavi, *J. Am. Chem. Soc.*, **1988**, 110, 6255.

⁹⁴A molecule that possesses a C_2 symmetry axis may be rotated by $360^\circ/2$ (or 180°) to obtain a geometry equivalent to the starting geometry. In general, a C_n axis corresponds to rotation by $360^\circ/n$. Chiral molecules typically possess no elements of symmetry or only C_n axes. Molecules that possess a plane of symmetry are necessarily achiral.

**Figure 11-4**

Modes of Approach and Insertion of Prochiral Propene onto a Metal Site and Growing Polymer Chain

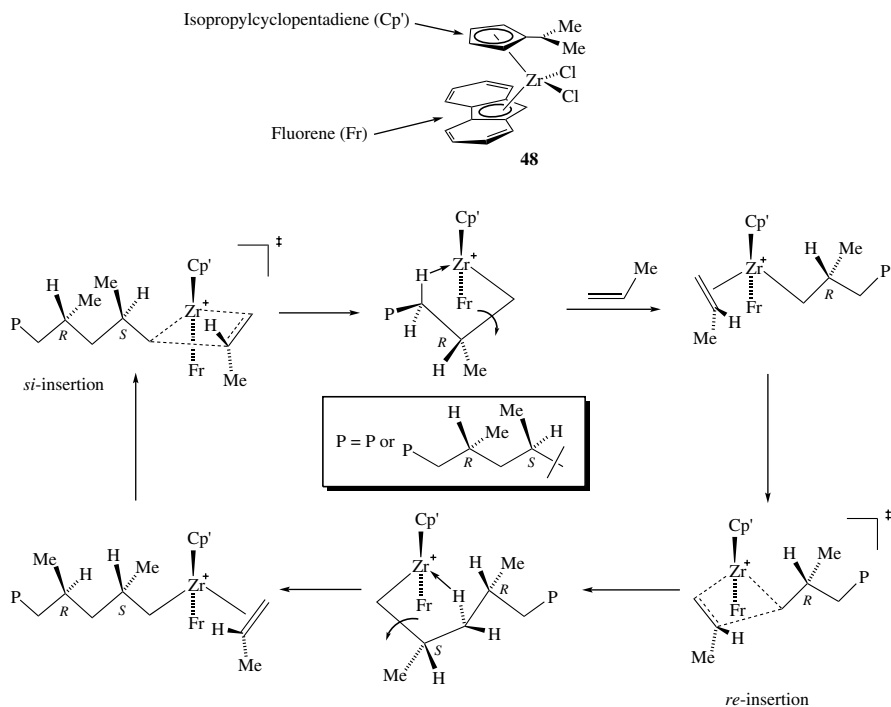
**Figure 11-5**

Primary and Secondary Insertion of Propene in a Growing Polymer Chain

and *re*.⁹⁵ The primary and secondary descriptors designate whether the polymer chain grows with a primary carbon attached to the metal or a secondary carbon (Figure 11-5). The primary approach seems more likely, based on a lower steric effect, for metallocene catalysts.

We can generalize, based on our understanding of the different approach modes of the alkene to the metal, by saying that isotactic polymers result from multiple insertions of the alkene to the same enantioface (*re* or *si*) and syndiotactic chains form from regular alternations for complexation and insertion

⁹⁵The terms *re* and *si* describe the prochiral nature of the two faces of an alkene such as propene. To determine which term applies, one looks at a face of the alkene and assigns priorities (using the Cahn–Ingold–Prelog rules) to the substituents attached to the more substituted carbon of the C=C bond. The =CH₂ group has the highest priority, followed by CH₃, and finally by H. If a clockwise motion connects these groups on the basis of highest, medium, and lowest priorities, then the face that the observer is looking at is designated *re*. A counterclockwise motion would give *si*. For additional information, see E. L. Eliel and S. H. Wilen, *Stereochemistry of Organic Compounds*, Wiley: New York, 1994, pp. 484–486.

**Scheme 11.17**

A Possible Mechanism for Syndiotactic Polymerization of Propene

of the alkene at the metal enantioface (*re* then *si* then *re*, etc.).⁹⁶ Scheme **11.17** shows a possible mechanism for the origin of syndiotacticity in a polymerization catalyzed by Zr metallocene **48**, which is similar in structure to **47**.⁹⁷ Isotactic polymerization shows influence of both the metal enantioface and the steric bulk of the growing polymer chain.⁹⁸

Metallocene-catalyzed Z–N polymerization is finding increased use on an industrial scale. One application is the production of linear low-density polyethylene (mLLDPE),⁹⁹ which is a linear polymer with short branches incorporated deliberately at various points along the chain. Short branches are produced by Z–N copolymerization of ethene with 1-butene, 1-pentene, and 1-hexene rather than through radical mechanisms of chain transfer and backbiting. Thus, the process is

⁹⁶P. Corradini, G. Guerra, and L. Cavallo, *Acc. Chem. Res.*, **2004**, *37*, 231.

⁹⁷See Footnote 88a.

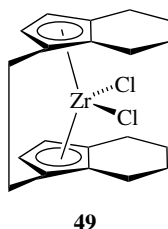
⁹⁸For additional discussion of the factors that direct either isotacticity or syndiotacticity, see Footnotes 88a, 90, 96, and A. Motta, I. L. Fragalà, and T. J. Marks, *J. Am. Chem. Soc.*, **2007**, *129*, 7327.

⁹⁹The letter m refers to the use of metallocene catalysts for the production LLDPE. Other Z–N catalysts could also be used, but metallocenes provide LLDPE with superior mechanical properties.

a linear polymerization, except there is more than one monomer present. Several oil and petrochemical companies have invested heavily in this technology to produce mLLDPE, a material that has better properties than low-density PE for use as films and packaging materials.

Using the transformations described in equations 11.30 and 11.31 as a guide, what stereochemistry would you expect for PP when **49** (the *meso* form of **46**) is used as a co catalyst instead of one of the enantiomers of **46**? Explain (see Footnote 90).

Exercise 11-11



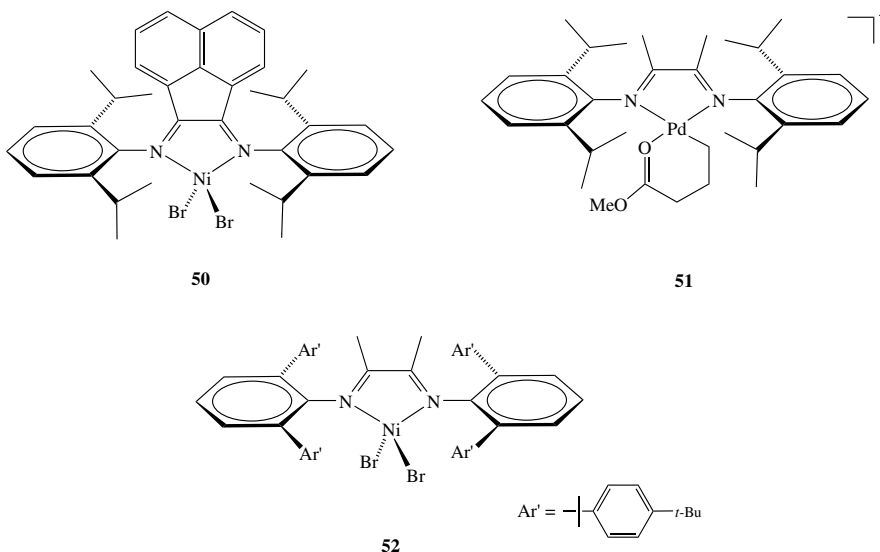
11-3-3 Polymerizations Catalyzed by Late Transition Metal Complexes

Over the past 15 years, a very active area of organometallic chemistry has developed, which has the goal of using late transition metal catalysts to promote polymerization of ethene and 1-alkenes.¹⁰⁰ We have seen already in the SHOP process the use of a Ni catalyst in the oligomerization of ethene. Extending this to the polymerization of ethene to high molecular weights could have several advantages over other means of polymerization: (1) unlike Z–N catalysts, late transition metal catalysts should be tolerant of oxygen and nitrogen functional groups on monomers. Thus, copolymerization with acrylate esters or vinyl acetate, which is normally done using radical catalysts and which produces commercially useful materials, could be accomplished by such catalysts. (2) Late transition metal catalysts also accommodate the presence of air and moisture, which is not the case with Z–N catalysts. (3) Highly active late-transition metal catalysts should allow polymerization of ethene under mild conditions, which is in contrast to the high temperature and pressures used to do this reaction using radical catalysts.

Late-transition metal catalysts became a reality as a result of the efforts of Brookhart and co-workers, who discovered a number of highly active cationic Ni

¹⁰⁰Also known as α -olefins.

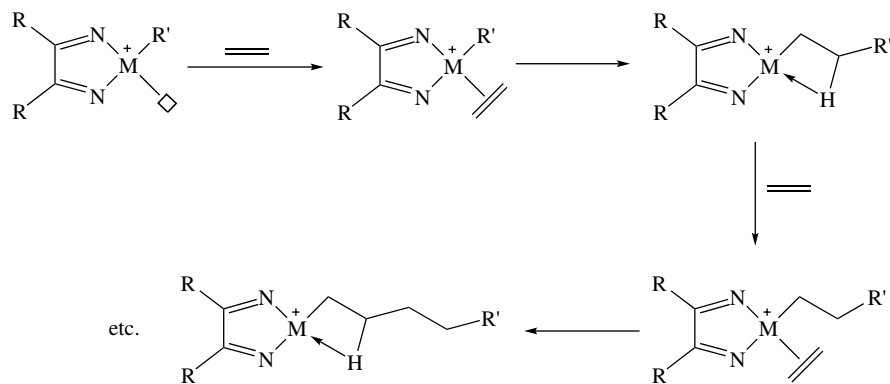
and Pd catalysts and first reported on these in 1995.¹⁰¹ These compounds promoted polymerization of ethene to materials of high molecular weight and were well suited for this task for several reasons: (1) the soft, cationic metal centers are of sufficient electrophilicity that they readily bind to π bonds and subsequently allow for 1,2-insertion. (2) The presence of sterically bulky diimine ligands helps to prevent β -elimination, which normally occurs with late transition metal alkyl ligands. (3) The presence of a non- or weakly-coordinating ligand allows for ease of binding of ethene. Structures **50**, **51**, and **52** show examples of these catalysts or precatalysts (MAO or Na[B(Ar_F)₄], where Ar_F = 3,5-bis(trifluoromethyl)phenyl, is also present as needed to remove a halide ligand and to create an open coordination site).



Scheme **11.18** shows a reasonable mechanism for polymerization that consists of first complexation of alkene, followed by 1,2-insertion. Ideally, the two steps will continue until synthesis of high-molecular-weight polymer occurs. Chain growth will cease if chain transfer occurs. Scheme **11.19** indicates two possible mechanisms for chain transfer, both of which are reasonable and indistinguishable by experiment. In both cases, the steric bulk of the diimine ligand seems to hinder the transfer process.¹⁰²

¹⁰¹L. K. Johnson, C. M. Killian, and M. Brookhart, *J. Am. Chem. Soc.*, **1995**, *117*, 6414.

¹⁰²S. D. Ittel, L. K. Johnson, and M. Brookhart, *Chem. Rev.*, **2000**, *100*, 1169 and S. Mecking, *Angew. Chem. Int. Ed.*, **2001**, *40*, 534.

**Scheme 11.18**

Mechanism
of Ethene
Polymerization
Catalyzed by Late-
Transition Metal
Complexes

Chain branching in ethene polymerization is catalyzed by Ni and Pd complexes through a process called “chain migration” or “walking.” A series of β -eliminations and 2,1-insertions occurs as the metal “walks” along the growing polymer chain. A pause in this process allows 1, 2-insertion to continue from the point of metal attachment along the polymer chain; thus, branching results. Show with a mechanism how this could give chain branches of three ethylene units.

Interestingly, as the pressure of ethene increases, the amount of chain branching decreases. Explain.

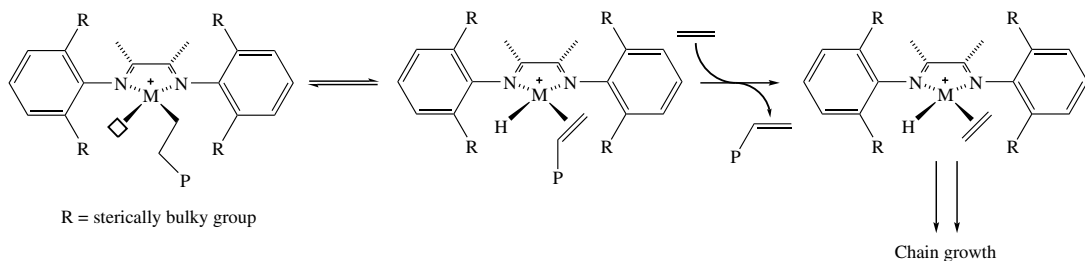
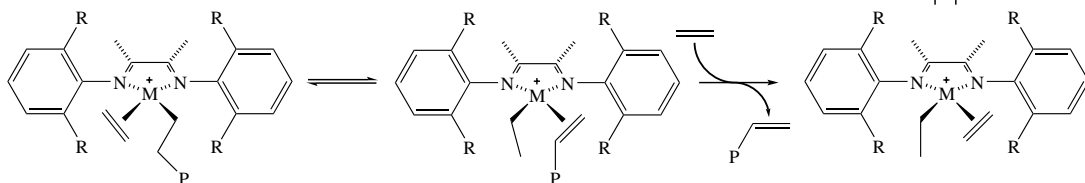
Exercise 11-12

α -Olefins also polymerize in the presence of Ni and Pd catalysts, and the properties of these materials are quite different from those resulting from Z-N polymerization. So far, there has not been a significant commercial application of Ni- or Pd-catalyzed α -olefin or ethene polymerization. On the other hand, there has been much serious and useful collaboration already between industry and academia on the use of such processes. The ease of producing materials that could have useful commercial application suggests that there will be industrial uses for this process in the future.¹⁰³

11-4 σ BOND METATHESIS

In Chapter 7 (Section 7-2-1), we discussed activation of nonpolar bonds, such as C-H, C-C, and H-H via oxidative addition to a metal center, as having

¹⁰³For additional information on olefin polymerization, catalyzed by late transition metals, see G. W. Coates, P. D. Hustad, and S. Reinartz, *Angew. Chem. Int. Ed.*, **2002**, *41*, 2236.

β -Elimination followed by ligand exchange: **β -Hydride transfer to monomer followed by ligand exchange:****Scheme 11.19**

Chain Transfer
Processes That
Inhibit Chain
Growth

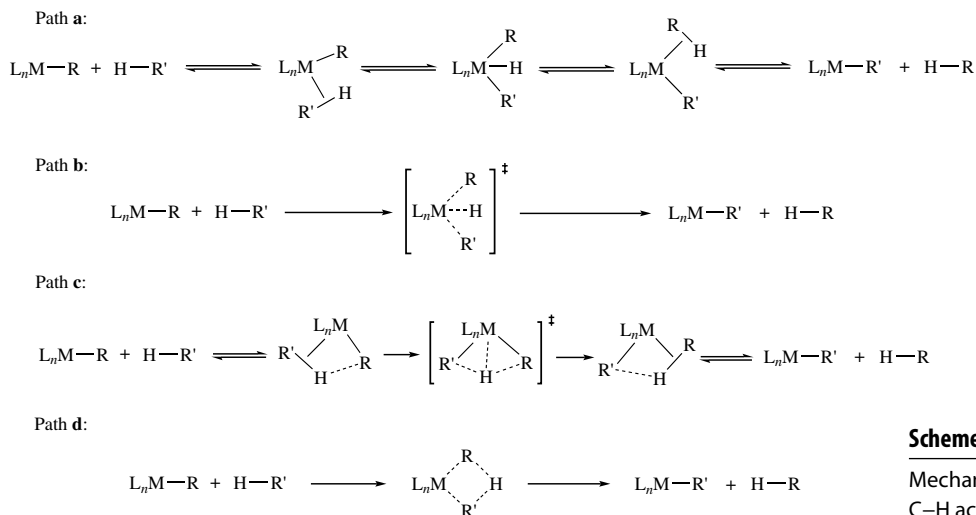
great synthetic and economic importance. One way of demonstrating that C–H activation has occurred is through exchange reactions of the type shown in equation **11.32**.



Several mechanisms have been proposed for such a reaction, and these are described in Scheme **11.20**.

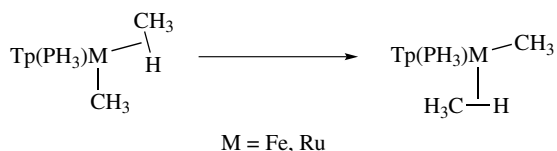
Path **a** shows the traditional OA–RE sequence already discussed in Chapter 7, which we would expect to operate with mid- to late transition metal complexes where the metal is in a low oxidation state. Path **b** details a mechanism that goes in one step to products through a transition state that shows an increase in coordination number and oxidation state of the metal before reorganization to products.¹⁰⁴ A mechanism termed *σ -complex-assisted metathesis* (σ -CAM) is

¹⁰⁴Z. Lin, *Coord. Chem. Rev.*, **2007**, 251, 2280.

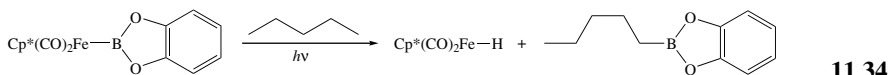
**Scheme 11.20**Mechanisms for
C–H activation

outlined in path **c**. This pathway shows no change in oxidation state of the metal, and it requires the presence of discrete intermediates.¹⁰⁵ Finally, path **d** portrays a one-step pathway that goes through a four-center transition state where the oxidation state of the metal does not change. This last pathway, called σ -bond metathesis (SBM), is associated with d^0 complexes of early transition metals as well as lanthanides and actinides, which cannot undergo OA. It is clear from intense research interest in SBM as well as in other paths to C–H and C–C bond activation over the past 20 years that a continuum of mechanistic possibilities exists for the type of exchange reaction that is shown in equation 11.32, with paths **a** and **d** existing at the two ends of the mechanistic spectrum.

Although it is not obvious that the following reaction (equation 11.33) actually occurs via path **b**, theoretical analysis using DFT of the reaction ($PR_3 = PH_3$) indicates that a one-step OA pathway occurs that goes through a transition state as shown in Scheme 11.20.¹⁰⁶

**11.33**¹⁰⁵R. N. Perutz and S. Sabo-Etienne, *Angew. Chem. Int Ed.*, **2007**, *46*, 2578.¹⁰⁶W. H. Lam, G. Jia, Z. Lin, C.P. Lau, and O. Eisenstein, *Chem. Eur. J.*, **2003**, *9*, 2775.

Reactions of the type shown in equation **11.34** have been run by Hartwig and thoroughly analyzed by theory at the DFT level. A reasonable explanation for the borylation of alkanes and arenes is the σ -CAM mechanism via path **c**.¹⁰⁷



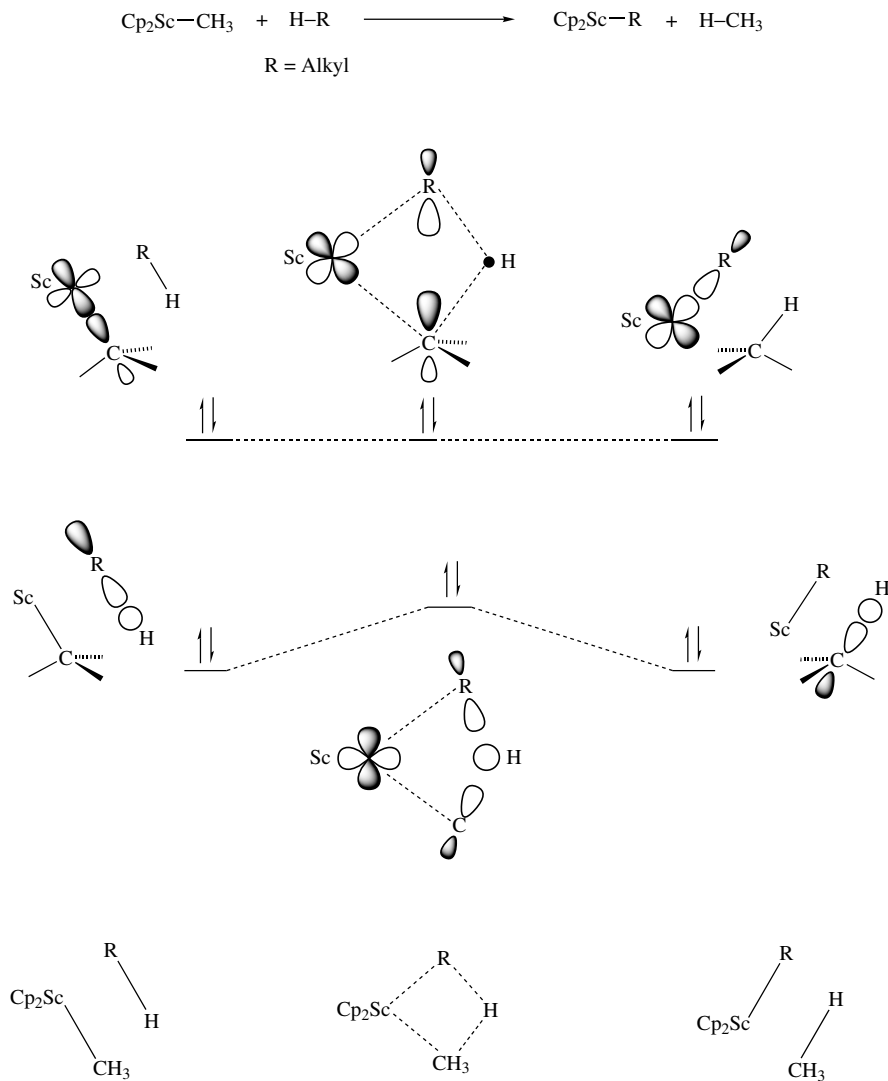
The remainder of this section will focus on true SBMs, which have been the subject of vigorous research. Despite the electron deficiency of early transition metal, lanthanide, and actinide complexes, several groups reported that some of these d^0f^n complexes do react with the H–H bond from dihydrogen and C–H bonds from alkanes, alkenes, arenes, and alkynes in a type of exchange reaction shown in equation **11.32**. So many examples of SBM involving early, middle, and late transition metal complexes have appeared in the chemical literature over the past 20 years that chemists now consider this reaction to be another fundamental type of organometallic transformation along with oxidative addition, reductive elimination, and others that we have already discussed.

As with olefin metathesis, we may consider a true SBM to be formally a 2 + 2 cycloaddition, but unlike its π bond counterpart, SBM does not require the formation of a four-membered ring intermediate. Instead, a four-center, four-electron transition state occurs along the reaction coordinate, which calculations have shown to be kite-shaped. In ordinary organic reactions, 2 + 2 cycloadditions—whether they involve σ or π bonds—are disallowed¹⁰⁸ under thermal conditions. Organometallic metatheses, on the other hand, involve a metal that has the ability to utilize not only s and p orbitals but also d and f (in the case of the lanthanides and actinides) orbitals, singly or in combination. Figure **11-6** shows how molecular orbitals of starting material, transition state, and products correlate well in a pathway involving a low-energy transition state.¹⁰⁹ There is continuous bonding along the reaction coordinate for all the occupied orbitals, the hallmark of

¹⁰⁷C. E. Webster, Y. Fan, M. B. Hall, D. Kunz, and J. F. Hartwig, *J. Am. Chem. Soc.*, **2003**, *125*, 858 and J. F. Hartwig, K. S. Cook, M. Hapke, C. D. Incarvito, Y. Fan, C. E. Webster, and M. B. Hall, *J. Am. Chem. Soc.*, **2005**, *127*, 2538.

¹⁰⁸The term “disallowed” means that, for the reaction to occur in a concerted fashion, the reaction coordinate must pass through a high-energy transition state. Lower-energy paths may be possible, but these would involve a non-concerted mechanism with radical or charged intermediates.

¹⁰⁹Note that the MOs for the transition state represent a σ bond analogy to the bonding and non-bonding π MOs of the allylic system.

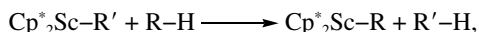
**Figure 11-6**

Molecular Orbital
Correlation
Diagram for σ Bond
Metathesis

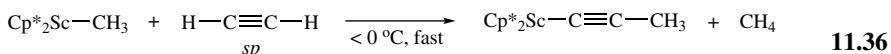
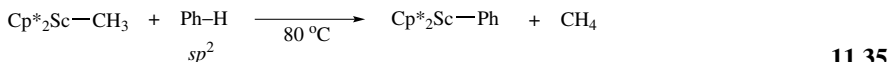
a concerted, thermally allowed reaction. Note how the hydrogen appears at the position farthest to the right or the top of the “kite,” also known as the B-position, in the transition state. This is caused by the spherical nature of the hydrogen s orbital that can best accommodate the angular overlap required at that position. Were carbon to occupy this position, the orbitals available would be shaped to point in a specific direction and thus unable to overlap smoothly with other orbitals

at the kite's side positions (see also the discussion on C–H and C–C activation in Chapter 7).¹¹⁰

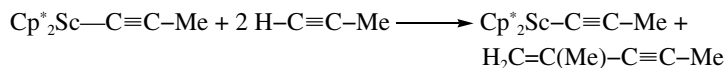
Bercaw¹¹¹ first coined the term σ bond metathesis in 1987. For the general reaction



he found that the order of reactivity was $\text{R} = \text{R}' = \text{H} \gg \text{R} = \text{H}, \text{R}' = \text{alkyl} \gg \text{R}-\text{H} = sp \text{ C}-\text{H}, \text{R}' = \text{alkyl} > \text{R}-\text{H} = sp^2 \text{ C}-\text{H}, \text{R}' = \text{alkyl} > \text{R}-\text{H} = sp^3 \text{ alkyl}, \text{R}' = \text{alkyl}$. The trend seems counter to what one might expect based on bond energies. It does, however, reflect a relationship that suggests that the greater the s character of a σ bond, the greater its reactivity. Equations 11.35 and 11.36 provide examples of his work with d^0 Sc–alkyl complexes.

**Exercise 11-13**

Some alkynes undergo M–C insertion as well as metathesis. Provide a mechanism for the following transformation:



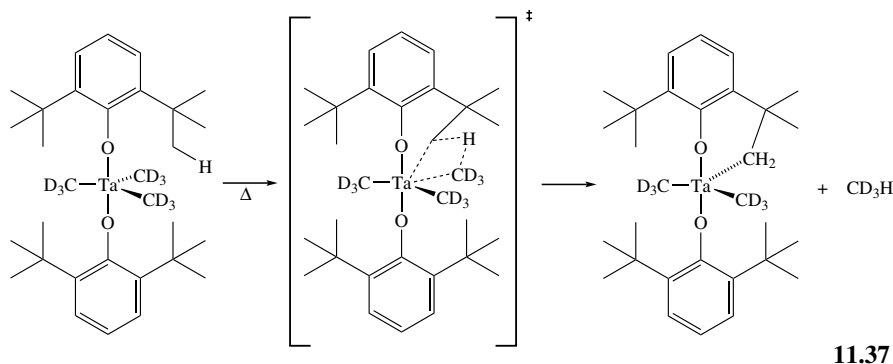
[Hint: The reaction involves two major steps.]

SBM may also occur intramolecularly, as equation 11.37 shows.¹¹²

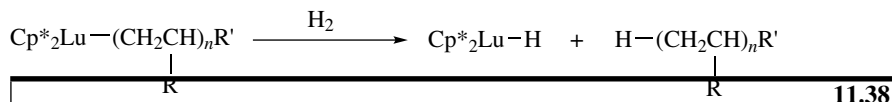
¹¹⁰For articles describing DFT MO calculations relating to SBM, see P. A. Hunt, *Dalton Trans.*, **2007**, 1743; N. Barros, O. Eisenstein, and L. Maron, *Dalton Trans.*, **2006**, 3052; T. Ziegler, E. Folga, and A. Berces, *J. Am. Chem. Soc.*, **1993**, 115, 636; and A. K. Rappé, *Organometallics*, **1990**, 9, 466.

¹¹¹M. E. Thompson, S. M. Baxter, A. R. Bulls, B. J. Burger, M. C. Nolan, B. D. Santarsiero, W. P. Schaefer, and J. E. Bercaw, *J. Am. Chem. Soc.*, **1987**, 109, 203.

¹¹²L. R. Chamberlain, I. P. Rothwell, and J. C. Huffman, *J. Am. Chem. Soc.*, **1986**, 108, 1502; see also I. P. Rothwell, *Acc. Chem. Res.*, **1988**, 21, 153, for more examples of intramolecular SBM.



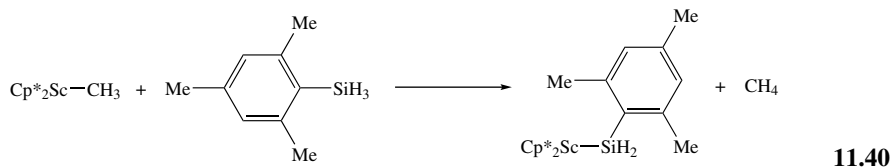
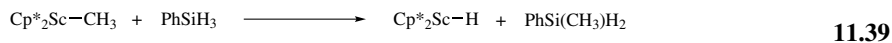
The involvement of SBM in alkene polymerization is another area of research interest. Although chain growth in Z-N polymerization occurs by 1,2-insertion into an M-C bond, chain termination may involve SBM. For example, H₂ is sometimes added to curtail the length of polymer chains. Watson¹¹³ observed that H₂ reacts with Lu-alkyls according to equation **11.38**. The reaction is undoubtedly a SBM and, as such, may provide a good model for what actually occurs when H₂ is used to limit polyalkene chain length.



Besides β -elimination and the addition of dihydrogen, another mechanism to limit chain length during Z-N polymerization is called chain transfer (see Scheme **11.13a**). In this process, the growing polymer detaches from the metal center by exchanging places with monomer or another free polymer chain. Could a mechanism involving SBM rationalize this phenomenon? Explain.

Exercise 11-14

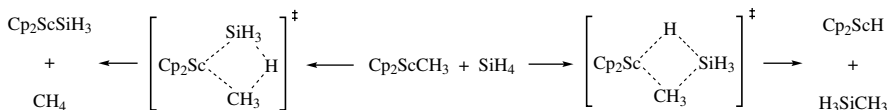
Silyl hydrides also undergo SBM, and equations **11.39** and **11.40** show some recent results. In the second example the silane is more sterically hindered.



¹¹³P. L. Watson and G. W. Parshall, *Acc. Chem. Res.*, **1985**, *18*, 51, and references therein.

Scheme 11.21

Two Product
Outcomes from SBM
of $\text{Cp}_2\text{ScCH}_3 + \text{SiH}_4$



DFT calculations showed that a four-center transition state was involved in both cases, but the transition states must be different for there to be two different sets of products. For the simplified reactions shown in Scheme 11.21, these calculations also showed that the transition states (structures **53** and **54**) leading to the two different product outcomes are remarkably similar in energy.¹¹⁴

Exercise 11-15

Reexamine the two different outcomes shown in equations 11.39 and 11.40. Propose an explanation for this difference.

Metathesis reactions that involve carbene complexes as intermediates have many useful industrial applications, and they play a key role in the synthesis of a large number of molecules of biological interest. Metathesis polymerizations lead to the production of materials with unique physical and chemical properties. Although we now know that the production of stereoregular polymers by *Z*-N catalysis does not involve metal–carbene complexes, the chemistry associated with this type of polymerization is linked to that of metal carbenes through early mechanistic investigations. The last section of Chapter 11 demonstrated that another type of metathesis exists in which σ M–C bonds, especially those involving the early-transition metals, interact with other σ bonds. σ Bond metathesis now ranks with oxidative elimination and 1,2-insertion as a fundamental organo-metallic reaction type.

Suggested Readings **π Bond Metathesis—General**

L. Delaude and A. F. Noels, “Metathesis,” in *Kirk–Othmer Encyclopedia of Chemical Technology*, Wiley: New York, 2005, Vol. 26, pp. 920–958.

R. H. Grubbs, *Tetrahedron*, **2004**, 60, 7117.

Handbook of Metathesis, R. H. Grubbs, Ed., Wiley–VCH: Weinheim, Germany, 2003, Vol. 1–3. This compendium has chapters on all aspects of π bond metathesis.

¹¹⁴The silicon atom is bigger than carbon, so it can exist at the position at the top of the “kite” more readily than carbon. For more details, see A. D. Sadow and T. D. Tilley, *J. Am. Chem. Soc.*, **2005**, 127, 643.

R. H. Grubbs, T. M. Trnka, and M. S. Sanford, "Transition Metal–Carbene Complexes in Olefin Metathesis and Related Reactions," in *Fundamentals of Molecular Catalysis*, H. Kurosawa and A. Yamamoto, Elsevier: Amsterdam, 2003, Chap. 4.
A. M. Rouhi, *Chem. Eng. News*, December 23, 2002, pp. 29–33.

π Bond Metathesis Mechanism and Catalysts

C. P. Casey, *J. Chem. Ed.*, **2006**, 83, 192.
D. Astruc, *New J. Chem.*, **2005**, 29, 42.
R. R. Schrock and A. H. Hoveyda, *Angew. Chem. Int. Ed.*, **2003**, 42, 4592.
A. M. Rouhi, *Chem. Eng. News*, December 23, 2002, pp. 34–38.

π Bond Metathesis Applications

A. H. Hoveyda and A. R. Zhugralin, *Nature*, **2007**, 450, 243.
J. C. Mol, *J. Mol. Catal. A*, **2004**, 213, 39.
K. J. Ivin and J. C. Mol, *Olefin Catalysis and Metathesis Polymerization*, Academic Press: New York, 1997.

Alkyne Metathesis

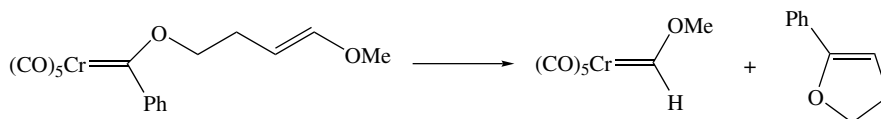
See Chap. 1.12, 2.5, 2.12, 3.10, and 3.11 in the *Handbook of Metathesis* listed above.

Ziegler–Natta and Related Olefin Polymerizations

P. Corradini, *J. Polym. Sci., Part A. Polym. Chem.*, **2004**, 42, 391.
R. Blom, A. Follestad, E. Rytter, M. Tilset, and M. Ystenes, Eds., *Organometallic Catalysts and Olefin Polymerization*, Springer Verlag: New York, 2001.
S. D. Ittel, L. K. Johnson, and M. Brookhart, *Chem. Rev.*, **2000**, 100, 1169.

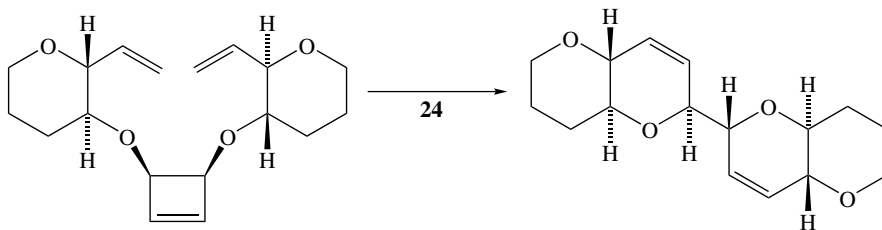
Problems

11-1 Propose a mechanism that would explain the following transformation. Note that no other reagents are required for the reaction.

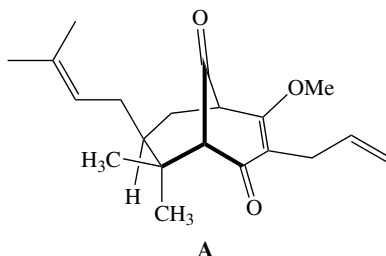


11-2 Propose a mechanism for the following transformation, which was catalyzed by Grubbs' second-generation catalyst (structure **24**, Section **11-1-2**).¹¹⁵

¹¹⁵K. C. Nicolaou, J. A. Vega, and G. Vassiliannakis, *Angew. Chem. Int. Ed.*, **2001**, 40, 4441.



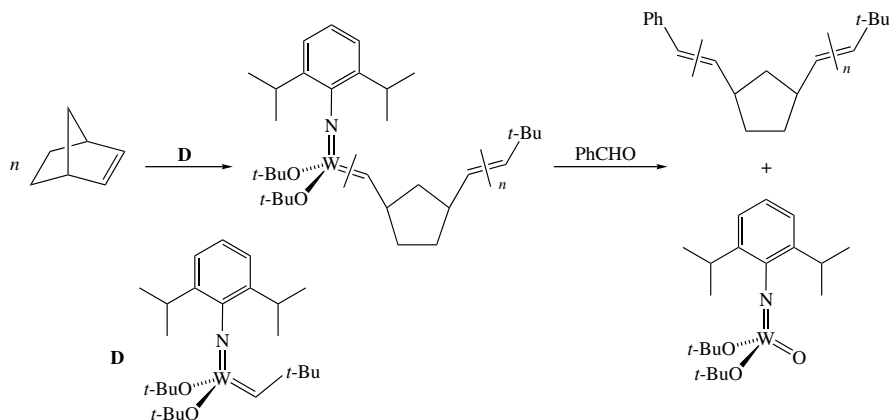
- 11-3** Grubbs' second-generation catalyst also catalyzes cross metathesis of compound **A** with 2-methyl-2-butene. Predict the products of this transformation. The ^1H NMR spectrum of one of the products (**B**) showed four singlets, each integrating to three protons, in the range δ 1.55 to 1.71 ppm in addition to a three-proton singlet at δ 4 ppm. The other product (**C**) gave a simple ^1H NMR spectrum with only four signals. Propose structures for compounds **B** and **C**.¹¹⁶



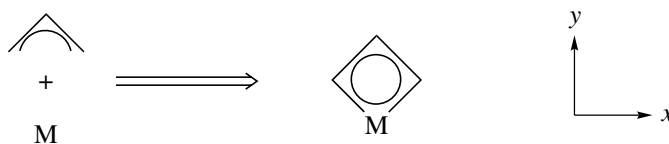
- 11-4** The ROM polymerization of norbornene, catalyzed by Schrock catalyst **D**, is a living polymerization that can be halted by the addition of benzaldehyde. This gives a polymer terminated at one end by $\text{CH}=\text{CH}-\text{Ph}$ and at the other end by $\text{CH}=\text{CH}-t\text{-Bu}$. The byproduct is a tungsten oxide complex. Propose an explanation for the chain termination step.¹¹⁷

¹¹⁶S. J. Spessard and B. M. Stoltz, *Org. Lett.*, **2002**, *4*, 1943.

¹¹⁷G. Black, D. Maher, and W. Risse, "Living Ring-Opening Metathesis Polymerization," in *Handbook of Metathesis*, Vol. 3, R. H. Grubbs, Ed., Wiley-VCH: Weinheim, Germany, 2003, p. 20.



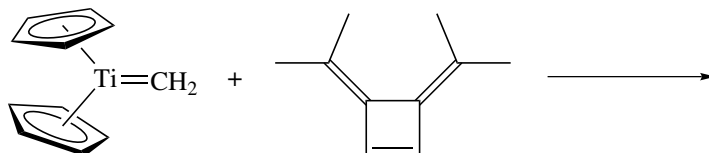
- 11-5** Metallacyclobutadienes are proposed as intermediates in metathesis reactions of alkynes. They formally may be considered derived from a metal and an allyl group.¹¹⁸



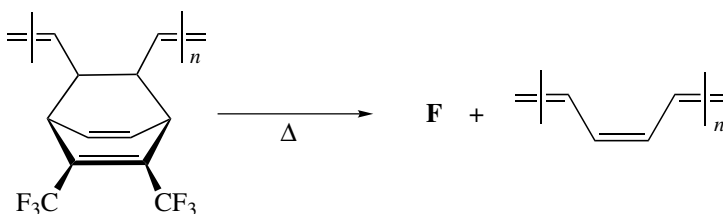
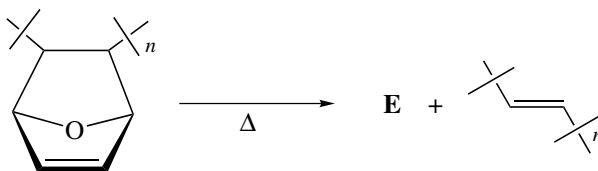
- Sketch the π orbitals of the allyl group. Also indicate the relative energies of these orbitals.
 - For each of the π orbitals, determine the metal orbitals suitable for interaction.
 - Which orbital on the metal would you expect to be most strongly involved in σ bonding with the end carbons?
- 11-6** The reaction conditions on the next page were used to produce a polymer by ROMP. Predict what the structure of the polymer will be.¹¹⁹

¹¹⁸Although there are two more hydrogen atoms in the system $L_nM + \text{allyl}$ than are present in a metallacyclobutadiene, the operative word in this problem is "formal." Here, you are asked to interact only the orbitals from the metal and the allyl system that would produce the corresponding orbitals in the metallacyclobutadiene.

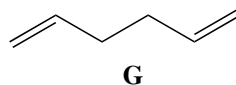
¹¹⁹T. M. Swager and R. H. Grubbs, *J. Am. Chem. Soc.*, **1987**, 109, 894.

(generated *in situ*)

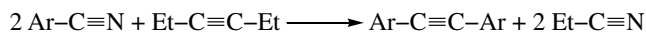
- 11-7** Propose a reasonable catalytic cycle for the Ni-catalyzed oligomerization of ethene that occurs during the first stage of SHOP. Assume that the active catalyst is $L(X)Ni-H$.
- 11-8** Polyacetylene synthesis has long been a goal of polymer chemists and materials scientists because its rigid conjugated system could be an organic electrical conductor. Two approaches are outlined below. Propose mechanisms for how polyacetylene forms in both approaches. What are the structures of byproducts **E** and **F**?¹²⁰



- 11-9** Draw the structure of a copolymer that could result from reaction with diene **G** and cyclooctene. Assume that the polymerization is catalyzed by Grubbs', second-generation catalyst.



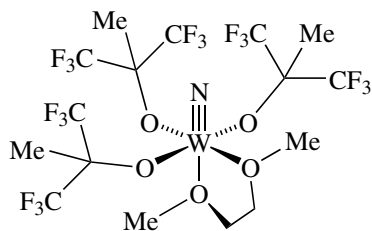
- 11-10** Consider the following transformation:



¹²⁰A. L. Safir and B. M. Novak, *Macromolecules*, **1993**, *26*, 4072 and L. Y. Park, R. R. Schrock, S. G. Stieglitz, and W. E. Crowe, *Macromolecules*, **1991**, *24*, 3489.

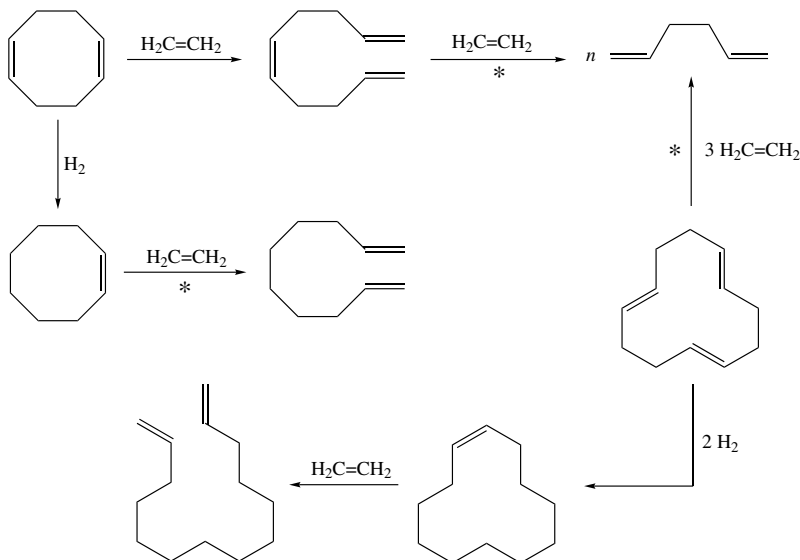
Ar = *p*-methoxyphenyl

The reaction is catalyzed by W complex **H**. Propose a mechanism for the reaction that accounts for both products and the overall stoichiometry.¹²¹



H

- 11-11** Terminal dienes (also called α,ω -diolefins) are useful in ADMET polymerization. The scheme below shows a number of processes that were patented by Shell Oil Company and were designed to produce terminal dienes. The name FEAST (Further Exploitation of Advanced Shell Technology) was coined to describe these reactions, most of which involve metathesis. Assume that the catalyst is a generic carbene complex, $L_nM=CRR$. Propose mechanisms for the transformations indicated by an asterisk near the reaction arrow.

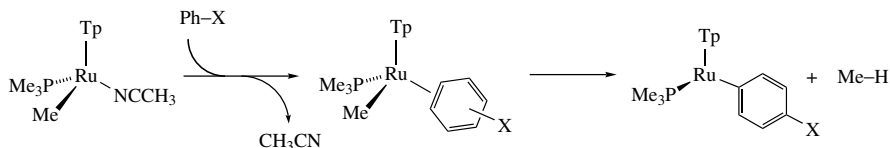


¹²¹A. M. Geyer, R. L. Gdula, E. S. Wiedner, and M. J. A. Johnson, *J. Am. Chem. Soc.*, **2007**, *129*, 3800.

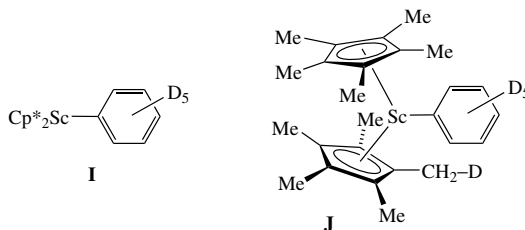
11-12 The copolymerization of ethene and CO produces an interesting polar material with alternating C_2 alkane and carbonyl groups. If a monosubstituted alkene is used, isotactic and syndiotactic polymers can result. The usual catalyst for such a process is a Pd–phosphine complex. If the phosphine ligand is chiral, stereoregularity with reference to the pendant group from the alkene can result.

- Propose a mechanism for the copolymerization of ethene and CO, assuming that the catalyst is one of the cationic Brookhart complexes shown in Section 11-3-3.
- Draw pictures of the isotactic and syndiotactic versions of a copolymer of styrene and CO.

11-13 Consider the C–H bond activation reaction involving a Tp–Ru complex shown. As the substituent X varies from an electron-donating group to an electron-withdrawing group, the rate of exchange increases. The authors of the study concluded that this result ruled out a classical OA–RE mechanism and instead supported a mechanism resembling a SBM. Why did the researchers reach that conclusion? Explain.¹²²

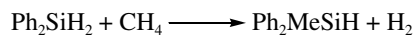


11-14 When Cp^*_2Sc-Me was allowed to react with d_6 -benzene (C_6D_6) at $125^\circ C$, a 1:1:1:1 mixture of CH_3D , CH_4 , **I**, and **J** was obtained. Explain.



¹²²N. J. DeYonker, N. A. Foley, T. R. Cundari, T. B. Gunnoe, and J. L. Petersen, *Organometallics*, **2007**, 26, 6604.

11-15 The following reaction is catalyzed by Cp^*_2ScH .



Two catalytic cycles were proposed for the overall transformation, one of which involved participation of one of the Cp^* methyl groups and the other that did not. Draw the two possible catalytic cycles.¹²³

¹²³See Footnote 114.

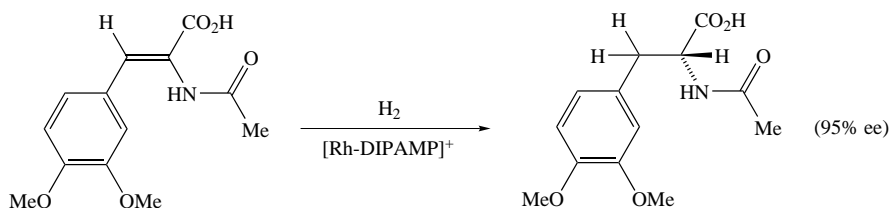
Applications of Organometallic Chemistry to Organic Synthesis

Organic synthesis is the science *and* art practiced by chemists who concern themselves with the construction of carbon-containing molecules, many of which possess biological significance. Nature, of course, constitutes the premier laboratory for the creation of organic compounds. Natural products—representing targets for laboratory synthesis—have provided chemists with tremendous challenges, which have been difficult and even impossible to meet using yesterday's technology. The past 2 decades have seen an explosion of papers reporting new synthetic methods and descriptions of successful total syntheses of highly complex molecules. Of considerable assistance to synthesis chemists has been the development of new reagents and reaction conditions involving organometallic compounds, particularly complexes of the transition metals.

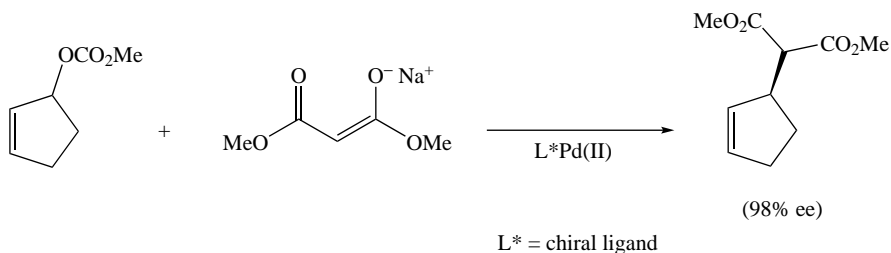
There are several approaches to describing the application of organotransition metal chemistry to organic synthesis. For example, one could examine the field—metal by metal—reporting on uses for each element. Another strategy might be to scrutinize several syntheses of interesting molecules, each of which includes the use of organometallic reagents in key steps. The approach of Chapter 12, however, will be different. It will build upon the coverage in previous chapters of fundamental reaction types, catalytic processes, and metal–carbene complex chemistry and then use that knowledge to discuss some basic kinds of synthetic transformations. These transformation types are not necessarily tied to the use of only one of the transition metals; usually several different ones could work. Although coverage of the entire field of synthetic applications is impossible in

one chapter,¹ it is possible for the reader to appreciate the utility of transition metals by considering the following kinds of transformations, which are accompanied by a typical example:

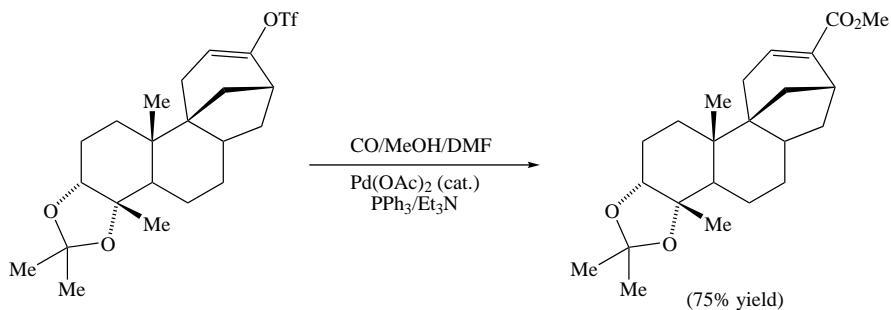
1. *Enantioselective functional group interconversions.*



2. *Carbon-carbon bond formation via nucleophilic attack on a π ligand.*

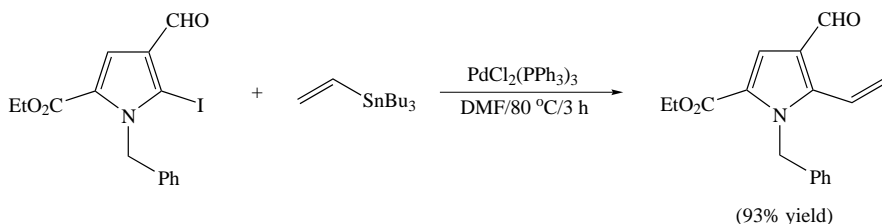


3. *Carbon-carbon bond formation via carbonyl or alkene insertion*

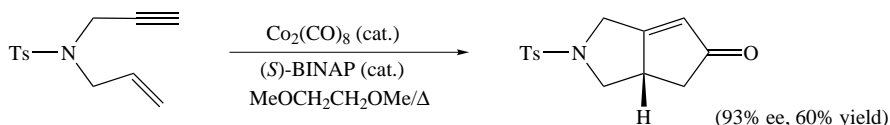


¹Entire books or major parts of some books cover the application of organometallic chemistry to organic synthesis. For some examples, see J. P. Collman, L. S. Hegedus, J. R. Norton, and R. G. Finke, *Principles and Applications of Organotransition Metal Chemistry*, University Science Books: Mill Valley, CA, 1987; Chap. 13–20; L. S. Hegedus, *Transition Metals in the Synthesis of Complex Organic Molecules*, 2nd ed., University Science Books: Mill Valley, CA, 1999; *Handbook of Organopalladium Chemistry for Organic Synthesis*, E. Negishi and A. DeMeijere, Eds., Wiley: New York, 2002; and *Comprehensive Asymmetric Catalysis*, E. N. Jacobsen, A. Pfaltz, and H. Yamamoto, Eds., Supplement 1, Springer: New York, 2003. See the **Suggested Readings** section at the end of Chapter 12 for more sources on this topic.

4. Carbon-carbon bond formation via transmetalation reactions



5. Carbon-carbon bond formation through cyclization reactions

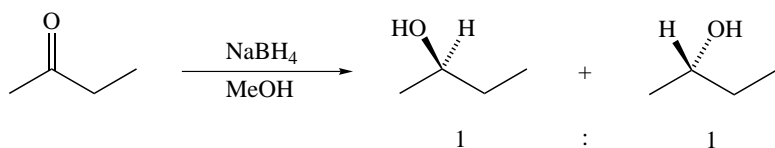


12-1 ENANTIOSELECTIVE FUNCTIONAL GROUP INTERCONVERSIONS

The ability to interconvert one functional group into another is of fundamental importance in organic synthesis. Often, these interconversions involve reduction or oxidation of a functional group, and such transformations also may either create or destroy a stereogenic center. The first part of Section 12-1 will explore transition metal-catalyzed hydrogenations of C=C and C=O bonds, which can exhibit a high degree of stereoselectivity. The second part will consider oxidation reactions that are also catalyzed by transition metal complexes, which can lead to enantioenriched products.

12-1-1 Asymmetric Hydrogenations

The double bond in an alkene is rich in its chemistry, and it undergoes transformation to alcohols, alkyl halides, and alkanes depending upon reaction conditions. Although C=O and C=C bonds are planar and provide an achiral reaction site, the interaction of these functional groups with specific reagents often creates one or more stereogenic centers in the reaction product, as reaction 12.1 shows.



In this case, the achiral reagents reacting via an achiral (or racemic) intermediate in an achiral solvent should produce racemic product. Over 40 years ago, this is all we could expect of such a reaction in terms of stereoselectivity. If the purpose of the transformation was to obtain one or the other enantiomer, then special and often tedious methods were required to resolve the racemic product. Today, the goal of synthesis chemists often is to produce molecules that are not only chiral, but also enantiomerically pure. Biologically active molecules typically exist in only one enantiomeric form. Efficacious drugs are also often most effective if they exist as only one enantiomer in order to interact properly with a chiral active site. A racemic drug is a mixture of enantiomers, only 50% of which is usually efficacious. The other 50% is at best worthless and at worst toxic, sometimes severely so.²

With the goal in mind of mimicking Nature or producing materials even more efficacious than those naturally occurring, chemists have discovered several methods for obtaining a particular enantiomer of a chiral compound. Among these are the following:

1. Chemical resolution of a racemate
2. Chiral chromatography
3. Use of chiral natural products as starting materials
4. Stoichiometric use of chiral auxiliaries
5. Asymmetric catalysis

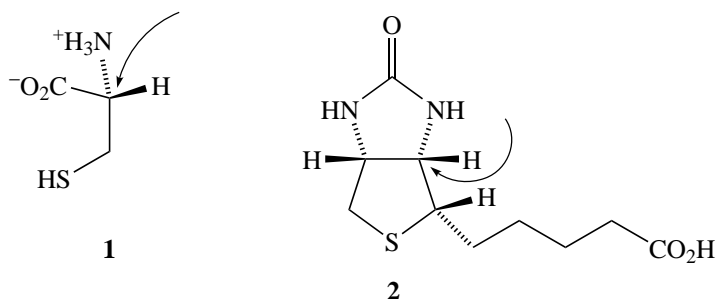
Method 1 represents the oldest technique for producing selectively one enantiomer, and readers should already be familiar with it.³ A chromatography column normally is an achiral environment; elution of a racemate through the column should result in no separation into enantiomers. In Method 2, however, columns are modified by attaching chiral, enantioenriched groups to the solid support. Now a chiral environment does exist such that the two enantiomers exhibit diastereomerically different interactions with the column; this is the basis for separation. Chiral column chromatography can sometimes resolve

²The classic example of a racemic drug, one enantiomer of which is beneficial and the other toxic, is thalidomide. The efficacious enantiomer is a tranquilizer and the other isomer causes severe birth defects when given to pregnant women. Another example is naproxen, the (*S*)-enantiomer of which is an effective NSAID; the (*R*)-enantiomer, although modestly effective, is also a liver toxin at its therapeutically effective dose (which is much higher than the dose for the (*S*)-isomer). It was necessary to design a synthesis of naproxen that produced the (*S*)-enantiomer with high stereoselectivity. One approach to synthesis of (*S*)-naproxen involves an asymmetric hydrogenation as a key step.

³For a brief discussion, see P. Y. Bruice, *Organic Chemistry*, 5th ed., Pearson Prentice Hall: New York, 2007, pp. 232–233, or almost any other current undergraduate-level organic chemistry textbook for similar information.

racemates quite effectively, providing either enantiomer with a high degree of enantio purity.⁴

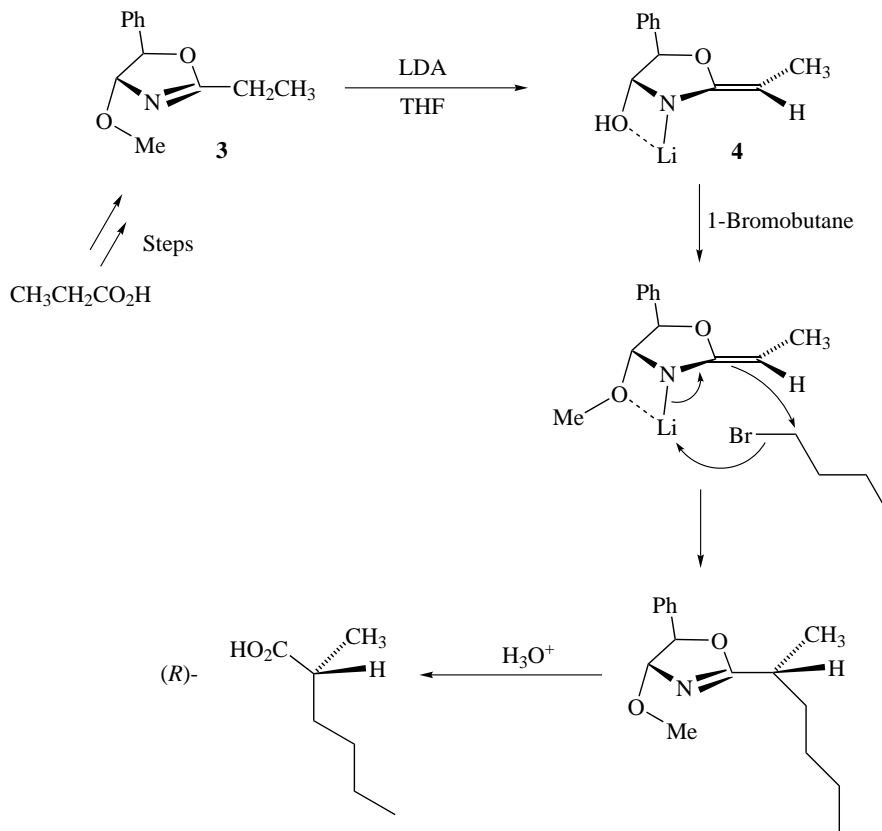
Allowing Nature to do part of the work is the central theme of Method 3. Numerous chiral molecules, isolated from natural sources and often available commercially, already contain much of the appropriate stereochemistry required in an enantioselective synthesis. These compounds are called the pool of chiral compounds. One reported synthesis of biotin (**2**), a molecule involved in enzymatic transfer of CO₂, used the methyl ester of the amino acid cysteine (**1**) as starting material.⁵ Note how **1** possesses a key stereocenter that later appears in biotin.



Attaching a chiral group to a reagent and then performing a reaction that goes through two possible diastereomeric transition states is the basis for Method 4. The presence of a *chiral auxiliary* provides an environment in which two pathways—diastereomerically related—are possible between reactant and product. One pathway is usually lower in energy due to steric hindrance, and it is more favorable. The result, upon removal of the chiral auxiliary, is selection for one enantiomer over the other. Absence of the chiral auxiliary during the transformation would produce a racemate because the transition state would be racemic. Scheme 12.1 shows an alkylation of a carboxylic acid to yield preferentially the R-enantiomer. The acid is first converted to a derivative, known as an oxazoline (**3**), which is non-racemic. Treatment of **3** with lithium diisopropyl amide (LDA), a very strong base, provides the enolate (**4**) that is then allowed to react with an electrophile (1-bromobutane in this case). The lithium ion can coordinate not only to the nitrogen and to the methoxy group but also to the halide ion of the incoming electrophile (if it attacks on the bottom face of the enolate). The bulky phenyl group, pointing upward, also tends to prevent attack on the top face of **4**. These two factors raise the energy of the transition state that involves top face attack.

⁴For a discussion on chiral chromatography, see E. Juaristi, *Introduction to Stereochemistry and Conformational Analysis*, Wiley: New York, 1991, pp. 132–136.

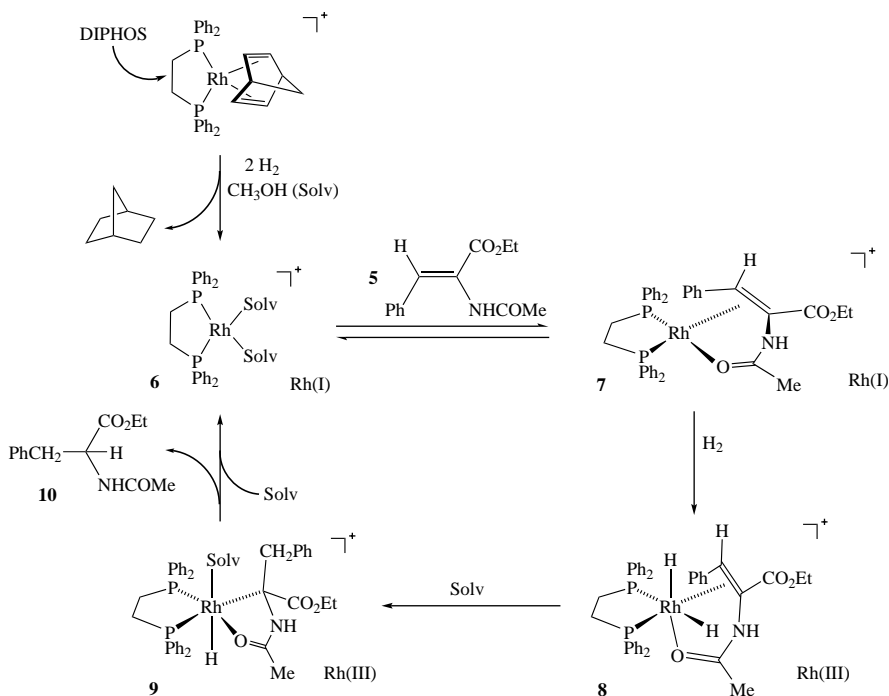
⁵E. J. Corey and M. M. Mehrotra, *Tetrahedron Lett.*, **1988**, 29, 57.



The result, upon removal of the chiral auxiliary by hydrolysis, favors selection of the *R*-enantiomer in this case. There are several examples of use of Method 4 in the chemical literature,⁶ but the technique does suffer from one disadvantage—one reaction is required to add the chiral auxiliary and another to remove it.

Method 5, asymmetric catalysis, is similar to the fourth technique except that enantioselectivity results *catalytically* without requisite separate stoichiometric steps for adding and later removing a chiral auxiliary. In light of increasing interest in applying the principles of green chemistry to organic transformations, Method 5 is perhaps the most environmentally benign approach to enantioselectivity. Atom economy is maximized, and the *E*-factor (see Section 9-1-5 for a

⁶For a review on the use of oxazoline chiral auxiliaries, see K. A. Lutonski and A. I. Meyers, "Asymmetric Syntheses via Chiral Oxazolines," in *Asymmetric Syntheses*, Vol. 3, J. D. Morrison, Ed., Academic Press: San Diego, 1984, pp. 213-274; A. I. Meyers, *Asymmetric Synth.*, **2007**, 37, 37; and H. Nishiyama, J. Ito, T. Shiomi, T. Hashimoto, T. Miyakawa, and M. Kitase, *Pure Appl. Chem.*, **2008**, 80, 743.

**Scheme 12.2**

Rh-DIPHOS-Catalyzed Hydrogenation of EAC

discussion of atom economy and *E*-factor) is minimized. Method 5, moreover, mimics Nature such that enzymes serve as giant chiral auxiliaries that bind substrates to active sites where chemical transformation can occur enantioselectively before the release of product. Organotransition metal catalysts in some cases duplicate the high stereoselectivity of enzymatic systems, and the remainder of Section 12-1 and later sections in Chapter 12 (see also some examples in Sections 9-7-2 and 9-7-3) will describe some of the most successful examples of asymmetric catalysis using organometallic complexes.

Asymmetric Hydrogenation Using Rhodium Complexes

Section 9-4-3 discussed an example of asymmetric hydrogenation in the synthesis of L-Dopa, pioneered by Knowles.⁷ We now have a good understanding of how Rh (I) complexes can catalyze the enantioselective addition of H_2 across an unsymmetrical $\text{C}=\text{C}$ bond, thanks to the work of Halpern and Brown.⁸ Scheme 12.2

⁷W. S. Knowles, *Acc. Chem. Res.*, **1983**, *16*, 106, and references therein to his earlier work.

⁸J. Halpern, *Science*, **1982**, *217*, 401; J. M. Brown and P. A. Chaloner, *J. Am. Chem. Soc.*, **1980**, *102*, 3040; and J. M. Brown and D. Parker, *Organometallics*, **1982**, *1*, 950.

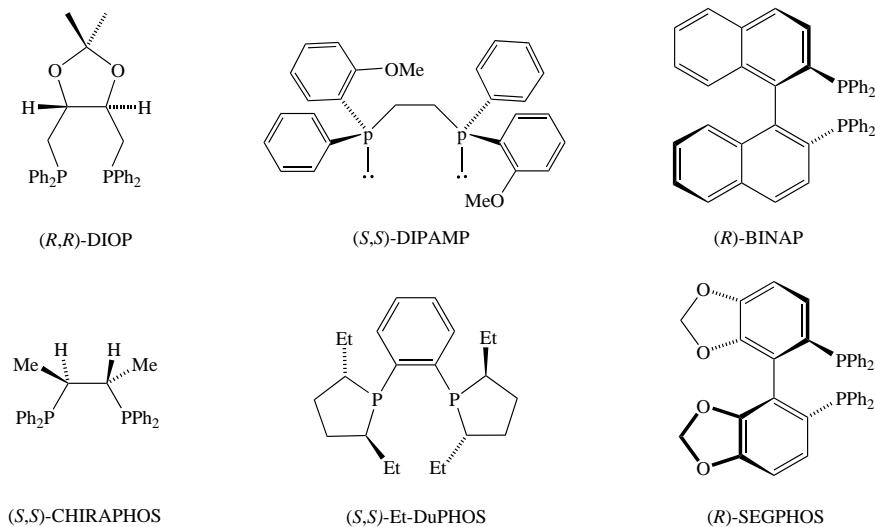


Figure 12-1
Chiral Diphosphine
Ligands

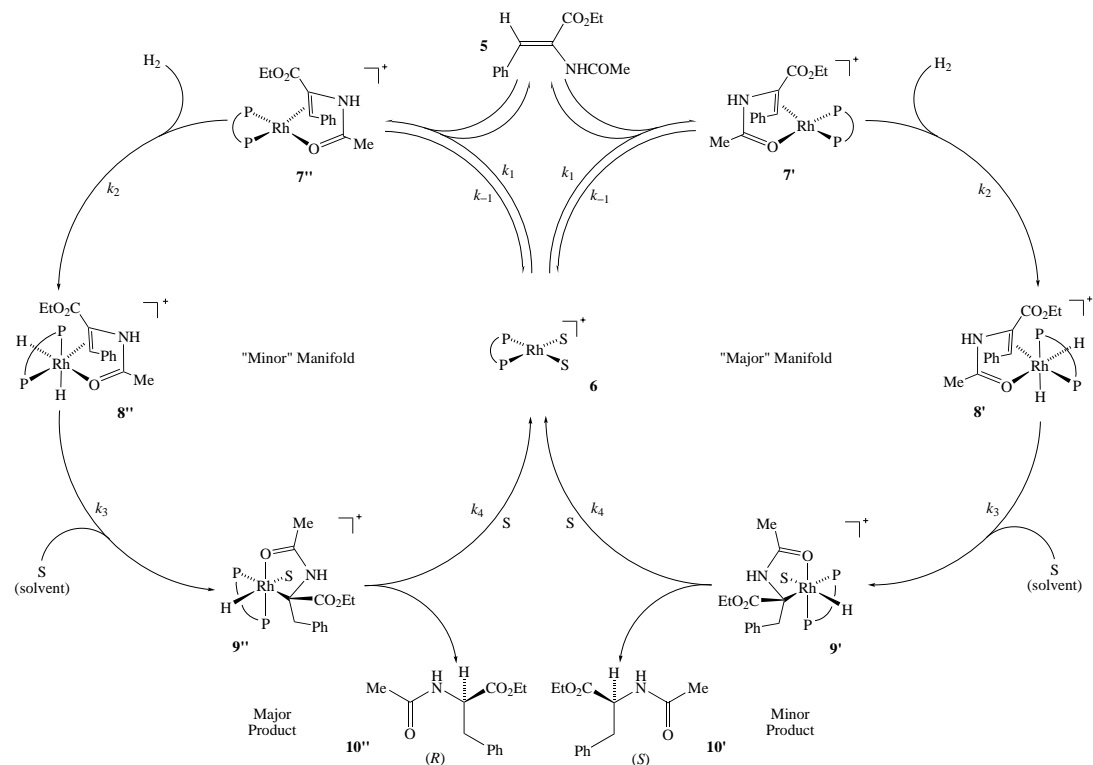
shows the catalytic cycle for hydrogenation of ethyl (*Z*)-1-acetamidocinnamate (EAC, **5**) using a cationic Rh(I)–DIPHOS complex (**6**) as the catalyst.

Because DIPHOS (or dppe) is an achiral ligand, the environment at the initial stages in the cycle is racemic, and no enantioselectivity is possible. The most common ligands used in asymmetric hydrogenation are, however, chiral diphosphines that usually possess a *C*₂ symmetry axis; Figure 12-1 shows just a few of the hundreds and hundreds of diphosphine and related ligands that have been reported in the literature.

Halpern reasoned that if he could work out the essential features of the catalytic cycle using readily available DIPHOS, he could then apply this knowledge to hydrogenations using chiral ligands. Employing a combination of techniques, he was able to determine the rate constant for each step in the cycle and to characterize all intermediates except dihydride **8**, formed during the rate-determining step. The formation of **8** does seem reasonable, however, based upon previous studies encountered already in Chapter 7 on the oxidative addition of H₂ to square planar Rh complexes. The other steps in the cycle should be quite familiar by now: **6** to **7** (ligand binding), **8** to **9** (1,2-insertion), and **9** to **6** (reductive elimination).

The presence of a chiral ligand, such as CHIRAPHOS, complicates the cycle because now there are two parallel pathways that are diastereomeric,⁹

⁹Because the CHIRAPHOS ligand possesses two stereocenters, the intermediates **7'** and **7''** are diastereomeric and not mirror images.

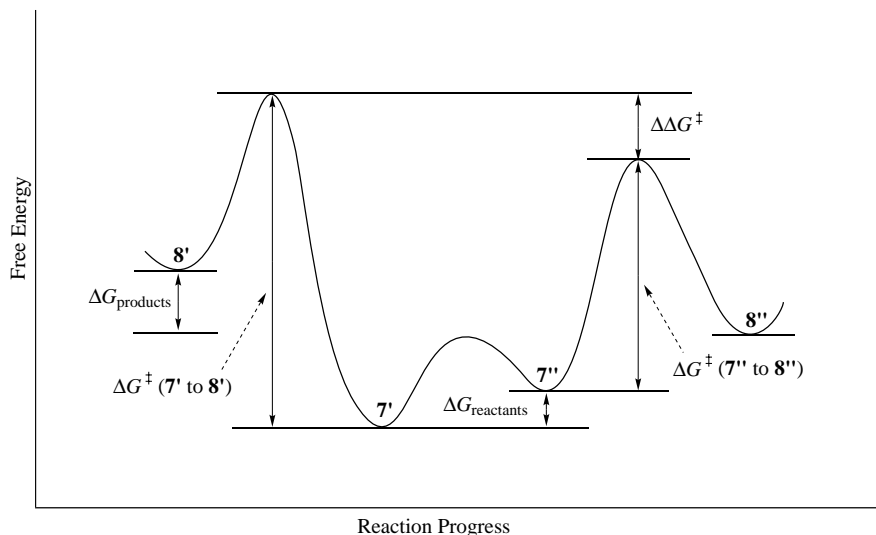


Scheme 12.3

Mechanism of
Asymmetric
Hydrogenation
Using
Rh-CHIRAPHOS

as shown in Scheme 12.3. Efforts to understand the chiral catalytic cycle were boosted by Halpern's success in isolating 7' and obtaining its crystal structure.

If hydrogen adds to 7' in accord with the mechanism depicted in Scheme 12.2, then the final hydrogenation product should be *N*-acetyl-(*S*)-phenylalanine ethyl ester (10, Scheme 12.3). Halpern found, however, that the predominant product in the presence of CHIRAPHOS was the *R*-enantiomer (10'', Scheme 12.3)! Based on this result and other evidence, it was possible for Halpern to say that 7' and 7'' form as an equilibrium mixture rapidly and reversibly from reaction of 5 and 6. Although 7' is more stable than 7'', and thus is part of what Halpern termed the "major" manifold shown in Scheme 12.3, the less stable "minor" manifold isomer (7'') reacts much faster during rate-determining oxidative addition of H_2 , eventually leading to the *R*-amino acid derivative.

**Figure 12-2**

Free-Energy versus Reaction Progress Diagram for the Rate-Determining Step of Asymmetric Hydrogenation

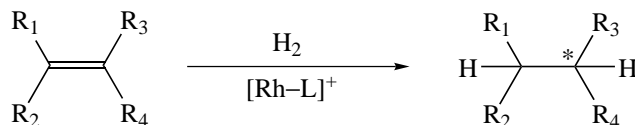
Based on the stereochemistry associated with 1,2-insertion and reductive elimination, verify that, in Scheme 12.3, **8'** will transform ultimately into the *S*-amino acid derivative and **8''** into the *R*-enantiomer.

Exercise 12-1

The origin of enantioselectivity is thus the lower ΔG^\ddagger for the path **7''** to **8''** than for **7'** to **8'**. Figure 12-2 shows a free-energy versus reaction progress diagram for the rate-determining step.

Calculations show that **7'** is probably more stable than **7''** because the alkene ligand fits better into the pocket formed by the phenyl groups of the CHIRAPHOS ligand in **7'**. The difference in free energy alone between **7'** and **7''** is insufficient to explain the relative rate difference leading to an enantiomeric excess of *R*- versus *S*-amino acid of 96%, that is if one assumes that ΔG is approximately equal to $\Delta\Delta G^\ddagger$. To explain an ee of 96%, Halpern also speculated that there was a reversal in stability of the two products **8'** and **8''**, with **8''** being more stable than **8'**. More recent calculations show this to be the case.¹⁰ As Figure 12-2 shows, the higher energy of **7''** and the lower energy of **8''**, when compared with their diastereomers, act synergistically to provide a much lower pathway for **7''** going to **8''** than for **7'** to **8'** (this is in agreement with the Hammond Postulate, see Section 7-1-3).

¹⁰Calculations performed using a different bisphosphine ligand showed a similar kinetic preference for the less stable diastereomer of the type shown above as **7''**. See S. Feldgus and C. R. Landis, *J. Am. Chem. Soc.*, **2000**, 122, 12714.

Table 12-1 Asymmetric Rh-catalyzed Hydrogenation of Alkenes

Entry No.	R ₁	R ₂	R ₃	R ₄	L	% ee	Configuration at * position
1 ^a	H	Ph	CO ₂ H	NHCOMe	(<i>S,S</i>)-CHIRAPHOS	99	<i>R</i>
2 ^a	H	Ph	CO ₂ H	NHCOMe	(<i>R,R</i>)-DIPAMP	96	<i>S</i>
3 ^b	H	Ph	CO ₂ H	NHCOPh	(<i>R</i>)-BINAP	100	<i>S</i>
4 ^a	H	Ph	CO ₂ H	NHCOMe	(<i>S,S</i>)-DIOP	82	<i>S</i>
5 ^b	Ph	H	CO ₂ H	NHCOPh	(<i>S</i>)-BINAP	87	<i>S</i>
6 ^a	H	H	CO ₂ H	NHCOMe	(<i>S,S</i>)-CHIRAPHOS	92	<i>R</i>
7 ^a	H	H	CO ₂ H	NHCOMe	(<i>R,R</i>)-DIOP	71-88	<i>R</i>
8 ^a	H	Ph	CO ₂ Me	NHCOMe	(<i>R,R</i>)-DIPAMP	97	<i>S</i>
9 ^a	Me	Me	CO ₂ Me	NHCOMe	(<i>R,R</i>)-DIPAMP	55	<i>S</i>
10 ^c	H	<i>i</i> -Pr	CH ₂ CO ₂ H	CO ₂ Et	(<i>R,R</i>)-Et-DuPHOS	99	<i>R</i>

^a Data taken from K. E. Koenig, "The Applicability of Asymmetric Homogeneous Catalytic Hydrogenation in Asymmetric Syntheses," in *Asymmetric Synthesis*, Vol. 5, J. D. Morrison, Ed., Academic Press: San Diego, 1985, pp. 71–101.

^b Data taken from S. L. Blystone, *Chem. Rev.*, **1989**, 89, 1663.

^c Data taken from M. J. Burk, F. Bienewald, M. Harris and A. Zanotti-Gerosa, *Angew. Chem. Int. Ed.*, **1998**, 37, 1931.

Later, Halpern conducted the same experiments using a Rh–DIPAMP complex to catalyze hydrogenation of methyl-(*Z*)-1-acetamidocinnamate (MAC), and the results were entirely analogous to the CHIRAPHOS system.¹¹ The important lesson learned in Section 9-4-2 again applies in the mechanism for asymmetric hydrogenation—isolable intermediates such as 7' are typically *not* the active species involved in a catalytic cycle.¹²

Exercise 12-2

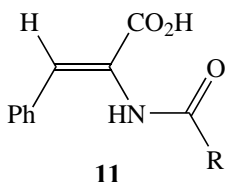
Based upon the mechanism depicted in Schemes 12.2 and 12.3, what would the effect on enantioselectivity be if the pressure of H₂ were increased?

Table 12-1 lists several early examples of asymmetric hydrogenations. The highest enantioselectivity seems to result when the substrate is a (*Z*)- α -amidocinnamic

¹¹C. R. Landis and J. Halpern, *J. Am. Chem. Soc.*, **1987**, 109, 1746.

¹²Some have termed the kinetic preference for the less stable diastereomer—that is, the diastereomer characterized by a poorer substrate-metal fit than is the case with the more stable isomer—the “anti-lock-and-key behavior” of catalytic asymmetric hydrogenation. See also Footnote 10.

acid derivative (**11**), as shown below. Entry 3 shows perfect enantioselection, which was achieved through use of the BINAP ligand that Noyori and co-workers synthesized almost 30 years ago.¹³ Unfortunately, the finicky reaction conditions necessary to achieve this remarkable result and the overall rate of the hydrogenation were too slow for it to have practical use.¹⁴



Divergence from this “ideal” substrate tends to lower % ee values (entries 7 and 9, Table **12-1**). For catalysis to be efficient, it is necessary to have a group attached to the alkene double bond that can bind to the metal (e.g., the amide carbonyl group). This secondary binding helps to lock the C=C in a rigid conformation in the presence of the chiral diphosphine ligand, thus enabling stereoselection to occur. Ordinary unsymmetrical alkenes, with only alkyl substituents attached to the double bond, usually undergo hydrogenation with much less enantioselectivity. Substituents attached to the carboxyl and amido groups may have some effect on the overall enantioselectivity, but their impact is relatively difficult to predict. Despite the limited number of alkenes that undergo highly stereoselective hydrogenation, it is amazing that in some cases enantioselectivity can be greater than 95%. This selectivity is possible sometimes under mild conditions (ca. 1 atm. H₂ and 25–50 °C) at rates that are quite high for transition metal catalysis (over 100 turnovers/s). Such results compare well with those obtained from enzymatic systems.

More recent work on new Rh-based catalysts indicates that even better enantioselectivity, especially on reactions run on large scale, is possible during hydrogenation under mild conditions of α -amidoacrylic acid derivatives. Burk at DuPont¹⁵ synthesized several chiral diphosphines (**12a–d**)—the first three collectively called DuPHOS ligands and the last termed Me-BPE (methyl bisphospholanoethane)¹⁶—that promote high enantioselectivity when bound to Rh(I). When R = Et (**12b**), protected amino acids of either absolute configuration (obtained with an ee of at least 99%) result depending on whether the (*S,S*)- or

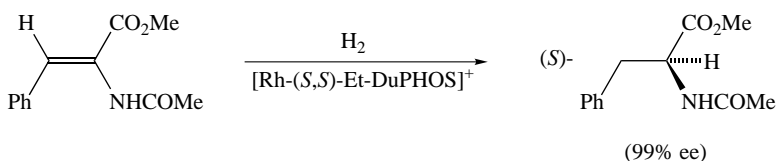
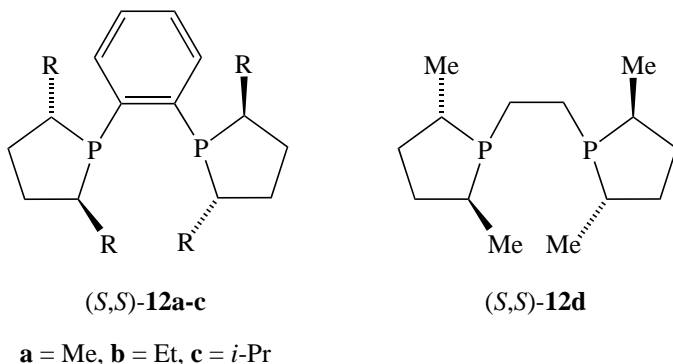
¹³A. Miyashita, A. Yasuda, H. Takaya, K. Toriumi, T. Ito, T. Souchi, R. Noyori, *J. Am. Chem. Soc.*, **1980**, *102*, 7932.

¹⁴R. Noyori, M. Kitamura, and T. Ohkuma, *Proc. Natl. Acad. Sci. U.S.A.*, **2004**, *101*, 5356.

¹⁵M. J. Burk, *J. Am. Chem. Soc.*, **1991**, *113*, 8518.

¹⁶The cyclic phosphine group is known as a phospholane.

the (*R,R*)-form of DuPHOS is used (equation 12.2). Note also entry 10 in Table 12-1. Here the substrate did not contain an amido group, and still the ee was 99%. Although the past 15 years have seen a spate of reports on new chiral ligands, the DuPHOS ligands have stood the test of time and remain among the best in their ability to promote highly enantioselective asymmetric hydrogenation of acrylic acid derivatives, especially on an industrial scale.¹⁷

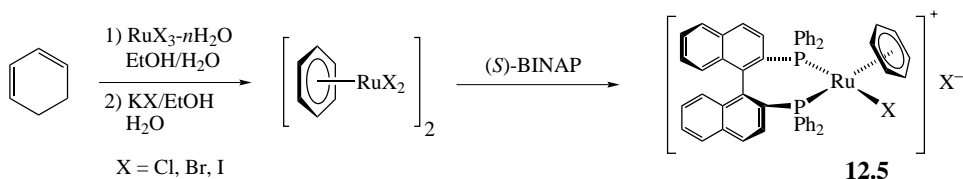
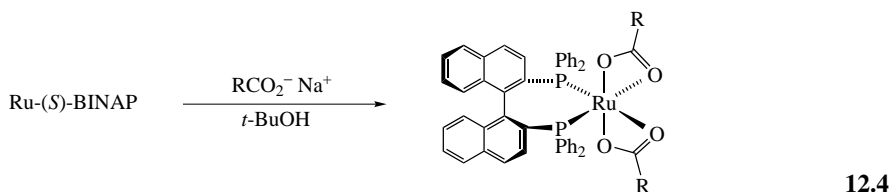
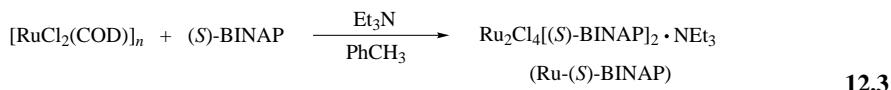


Asymmetric Hydrogenation of C=C Bonds Using Ru-Based Catalysts

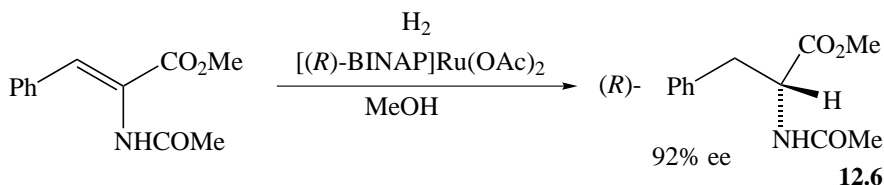
For many years, the field of asymmetric hydrogenation was dominated by the use of Rh-based catalysts. More recent breakthroughs using Ru(II) complexes have been especially fruitful, however, leading to enantioselective reduction of either C=C or C=O bonds in a number of compounds. One of the most efficient catalyst systems involves complexation of Ru(II) salts with (*S*)- or (*R*)-BINAP (see Figure 12-1). Equations 12.3–12.5 describe the steps involved in producing a number of Ru–BINAP catalysts.¹⁸

¹⁷For a report on the utility of DuPHOS ligands in asymmetric hydrogenation, see M. J. Burk, *Acc. Chem. Res.*, **2000**, *33*, 363.

¹⁸H. Takaya, T. Ohta, and K. Mashima, “New 2,2’-Bis(diphenylphosphino)-1,1’-binaphthyl-Ru(II) Complexes for Asymmetric Catalytic Hydrogenation,” in *Homogeneous Transition Metal Catalyzed Reactions*, W.R. Moser and D.W. Slocum, Eds., American Chemical Society: Washington, DC, 1992, pp. 123-142. It should also be noted that one advantage of Ru-based catalysts over Rh-based is that the cost of Ru is about 10% that of Rh.



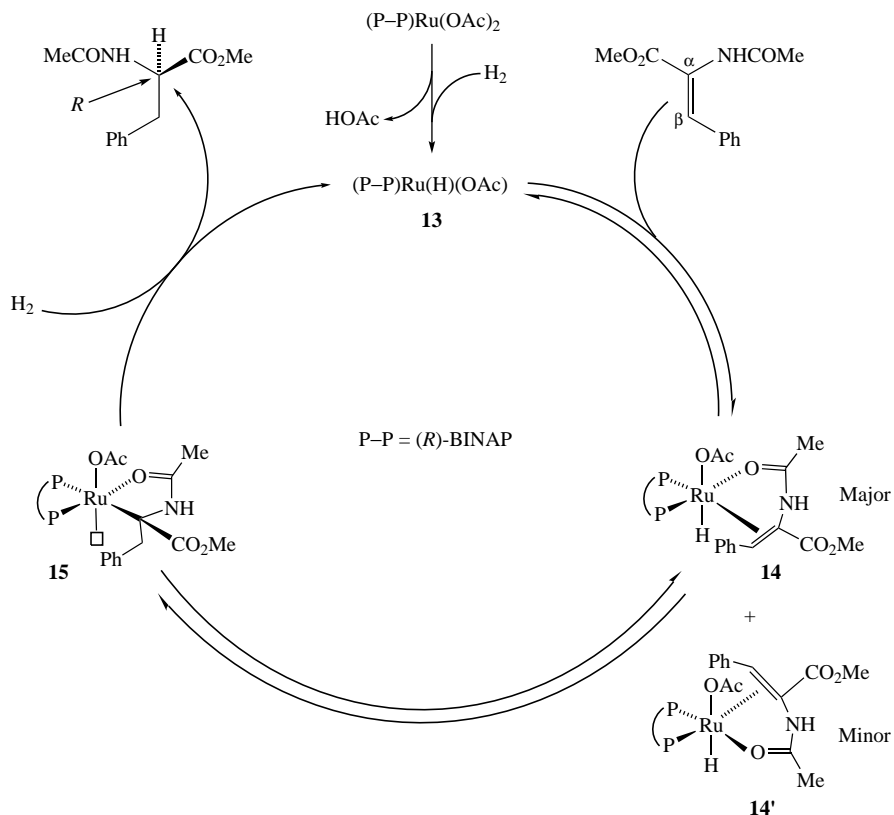
We encountered Rh–BINAP as a hydrogenation catalyst earlier in Chapter 12 (Table 12-1) and as a catalyst for double bond isomerization in Section 9-7-3. As the examples below will show, Ru–BINAP catalysts are indeed even more versatile and selective than corresponding Rh complexes. In general, like Rh(I) catalysts, Ru(II) catalysts usually must have a chelating heteroatom (O or N) positioned close to the C=C bond undergoing saturation for effective stereoselection to occur. Equation 12.6 shows an early example of the work of Noyori,¹⁹ who pioneered in the development of Ru(II) hydrogenation catalysts, showing enantioselective hydrogenation of an amidocinnamate ester.²⁰



The mechanism of asymmetric C=C hydrogenation, shown in Scheme 12.4, probably involves the formation of a Ru–H species 13 (see also Scheme 9.8

¹⁹R. Noyori shared the Nobel Prize in Chemistry in 2001 with W. S. Knowles, who pioneered the use of Rh-catalyzed asymmetric hydrogenation, and K. B. Sharpless, who is known for fundamental work on asymmetric epoxidation and dihydroxylation of alkenes involving transition metal catalysis.

²⁰T. Ohta, H. Takaya, and R. Noyori, *Inorg. Chem.*, **1988**, 27, 566 and M. Kitamura, M. Tokunaga, and R. Noyori, *J. Org. Chem.*, **1992**, 57, 4053.

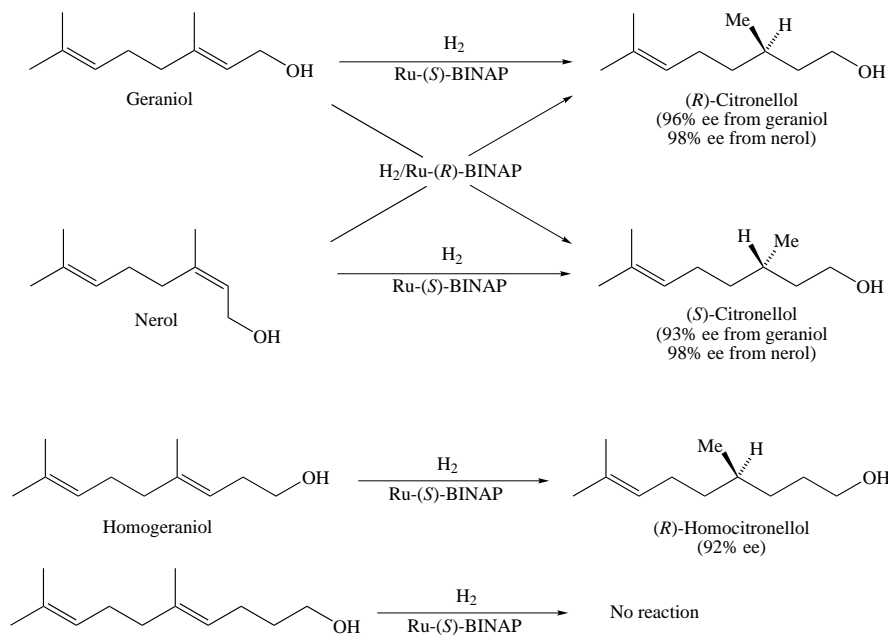
**Scheme 12.4**

Mechanism of
Asymmetric
Hydrogenation of
C=C Bonds

for non-asymmetric hydrogenation by the monohydride mechanism), which contrasts with the dihydride mechanism that is prevalent with hydrogenation by cationic Rh(I) complexes. The carbonyl oxygen atom also coordinates to the Ru.

The stereochemistry of the stereogenic center is fixed in going from structure **15** to **13**. It appears that, unlike the case with Rh-catalysis, the stereochemistry of the major product corresponds to the *higher* stability of one of the diastereomeric complexes **14** compared with **14'**. The relative stability of **14** results from lack of steric interactions between the CO₂Me group at the α-position and one of the phenyl groups attached to P, and this diastereomer goes on smoothly to give the (*R*)-dihydrocinnamate.²¹ In general, Ru-(*R*)-BINAP catalyzes formation of (*R*)-hydrogenated product and Ru-(*S*)-BINAP gives (*S*)-product, which is opposite to the results for Rh-BINAP hydrogenation catalysts.

²¹See Footnote 14.



Scheme 12.5
Ru(II)-BINAP-
Catalyzed
Hydrogenation
of Allylic and
Homoallylic
Alcohols

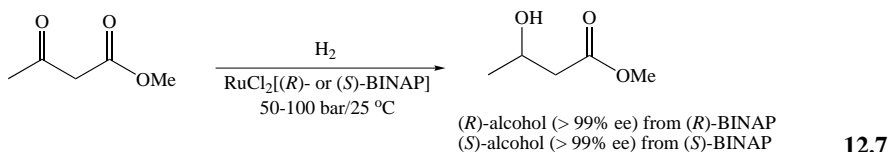
Allylic and homoallylic²² alcohols undergo asymmetric hydrogenation (Scheme 12.5).²³ The $\text{Ru}(\text{O}_2\text{C}-\text{CF}_3)_2$ -BINAP catalyst (equation 12.4) used in these reactions is extremely specific in many respects. Both enantiomers of citronellol result with high % ee starting with either geraniol or nerol, depending on whether (*S*)- or (*R*)-BINAP is the ligand. The reaction shows double bond face selectivity, since the same catalyst, Ru-(*S*)-BINAP, transforms geraniol into (*R*)-citronellol and nerol into (*S*)-citronellol. Note that the remote double bond is unreactive to the hydrogenation conditions, indicating that the allylic alcohol group probably provides necessary secondary chelation during the reaction. Further demonstration of this chelation is also shown in Scheme 12.5, whereby homogeraniol reacts to give (*R*)-homocitronellol. Extending the carbon chain by just one more carbon, however, results in no reaction because the OH group is too far removed from the C=C double bond to effectively also bind to Ru.

²²Homoallylic systems have one more carbon atom than allylic systems. For example, $\text{CH}_2=\text{CH}-\text{CH}_2-$ is allylic, whereas $\text{CH}_2=\text{CH}-\text{CH}_2-\text{CH}_2-$ is homoallylic.

²³H. Takaya, T. Ohta, N. Sayo, H. Kumobayashi, S. Akutagawa, S. Inoue, I. Kasahara, and R. Noyori, *J. Am. Chem. Soc.*, **1987**, *109*, 1596.

Asymmetric Hydrogenation of C=O Using Ru(II) Catalysts

Ketones also undergo asymmetric hydrogenation using Ru(II) catalysts. Early work showed that Ru(OAc)₂-BINAP, which was excellent in catalyzing asymmetric C=C bond hydrogenation, showed no effectiveness in hydrogenating the β-C=O group in β-ketoesters. Merely replacing the acetoxy groups with halogen (Cl, Br, or I) caused such catalysts to be extraordinarily enantioselective, as shown in equation 12.7.



Depending upon whether (*S*)- or (*R*)-BINAP was chosen, either enantiomer of the β-hydroxyester (in >97% yield with ee > 99%) formed.²⁴ These results are comparable to the enantioselectivity achieved using enzymes from baker's yeast!

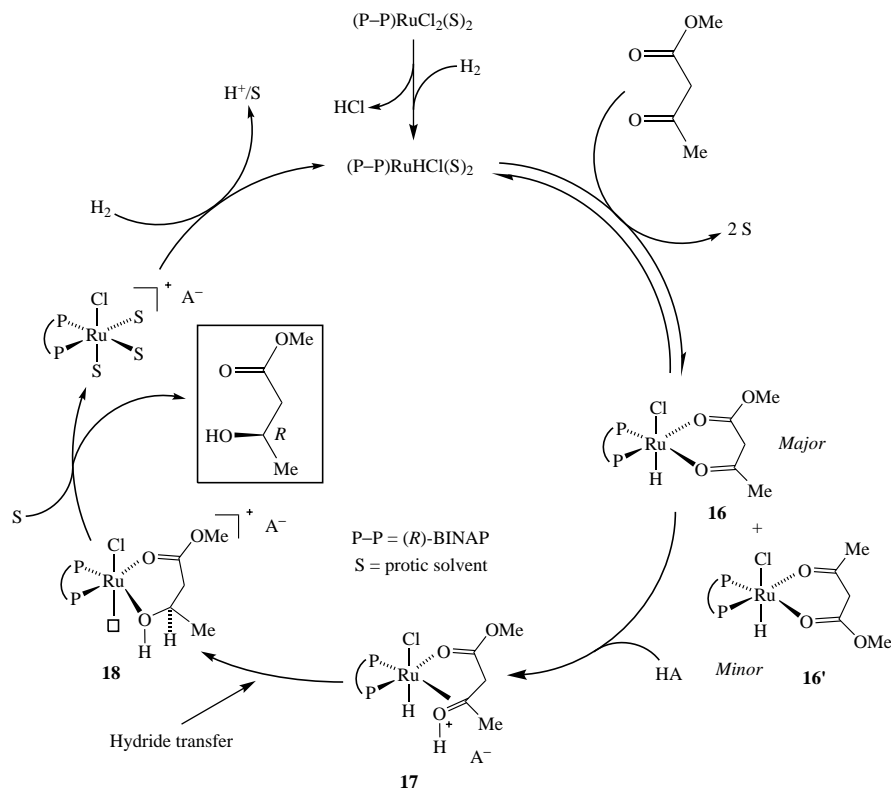
Noyori and co-workers have postulated a mechanism for this hydrogenation (Scheme 12.6). This scheme shows a mechanism that is similar to Ru-catalyzed hydrogenation of C=C bonds in the beginning stage. As with hydrogenation of acrylate esters, complexation of a neighboring C=O groups is important. Interestingly, hydrogen comes from two sources: (1) H₂ ultimately and (2) an external proton, derived from either mineral acid or protic solvent. Formation of diastereomerically different complexes **16** or **16'** leads to stereodifferentiation later in the cycle. Protonation of the ketone oxygen atom in complex **16** gives **17**, which now shows a change in C=O bonding from σ to π. This bonding change now makes the carbonyl carbon more susceptible to attack by hydride onto the bottom face of the C=O bond, yielding **18** with weakly bound hydroxyester now attached to Ru. The cycle is complete when ligand exchange with solvent liberates the (*R*)-β-hydroxyester and subsequent OA of H₂ regenerates the catalyst.²⁵

Although β-ketoesters undergo asymmetric hydrogenation with high enantioselectivity, the utility of this method would be greatly enhanced if ordinary ketones could also be reduced to chiral alcohols. Another major discovery by Noyori's group paved the way for asymmetric hydrogenation of C=O groups to become much wider in scope when a series of bifunctional catalysts shown in Figure 12-3 was reported.²⁶ Note that the complex contains both BINAP and a chiral diamine.

²⁴R. Noyori, T. Ohkuma, M. Kitamura, H. Takaya, N. Sayo, H. Kumobayashi, and S. Akutagawa, *J. Am. Chem. Soc.*, **1987**, *109*, 5856.

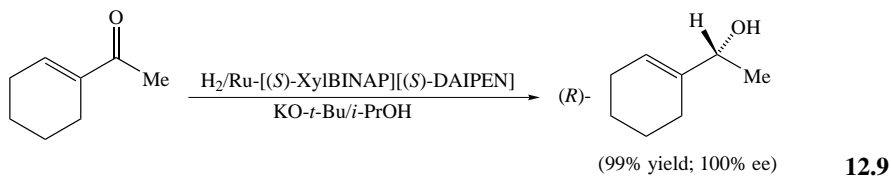
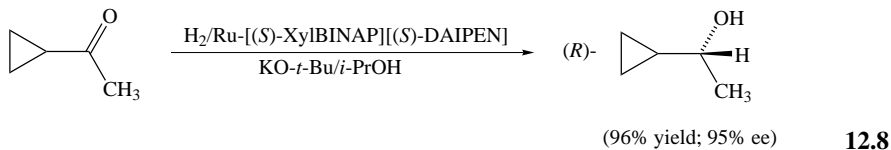
²⁵See footnote 14 and references therein.

²⁶R. Noyori and T. Ohkuma, *Angew. Chem. Int. Ed.*, **2001**, *40*, 40, and references therein.

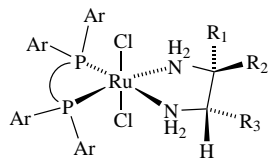
**Scheme 12.6**

Mechanism of
Asymmetric
Hydrogenation of
 β -Ketoesters

Equations 12.8, 12.9, and 12.10 demonstrate the range of ketones that undergo asymmetric hydrogenation using bifunctional catalysts.²⁷



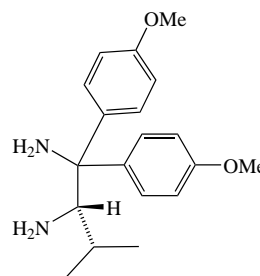
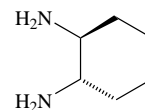
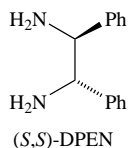
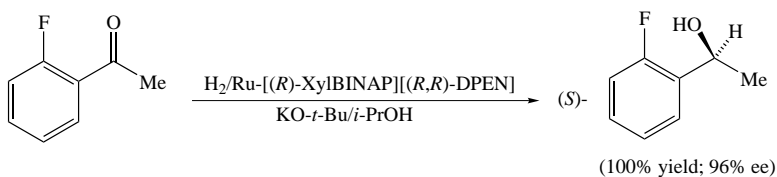
²⁷T. Ohkuma, M. Koizumi, H. Doucet, T. Pham, M. Kozawa, K. Murata, E. Katayama, T. Yokozawa, T. Ikariya, and R. Noyori, *J. Am. Chem. Soc.*, **1998**, *120*, 13529.



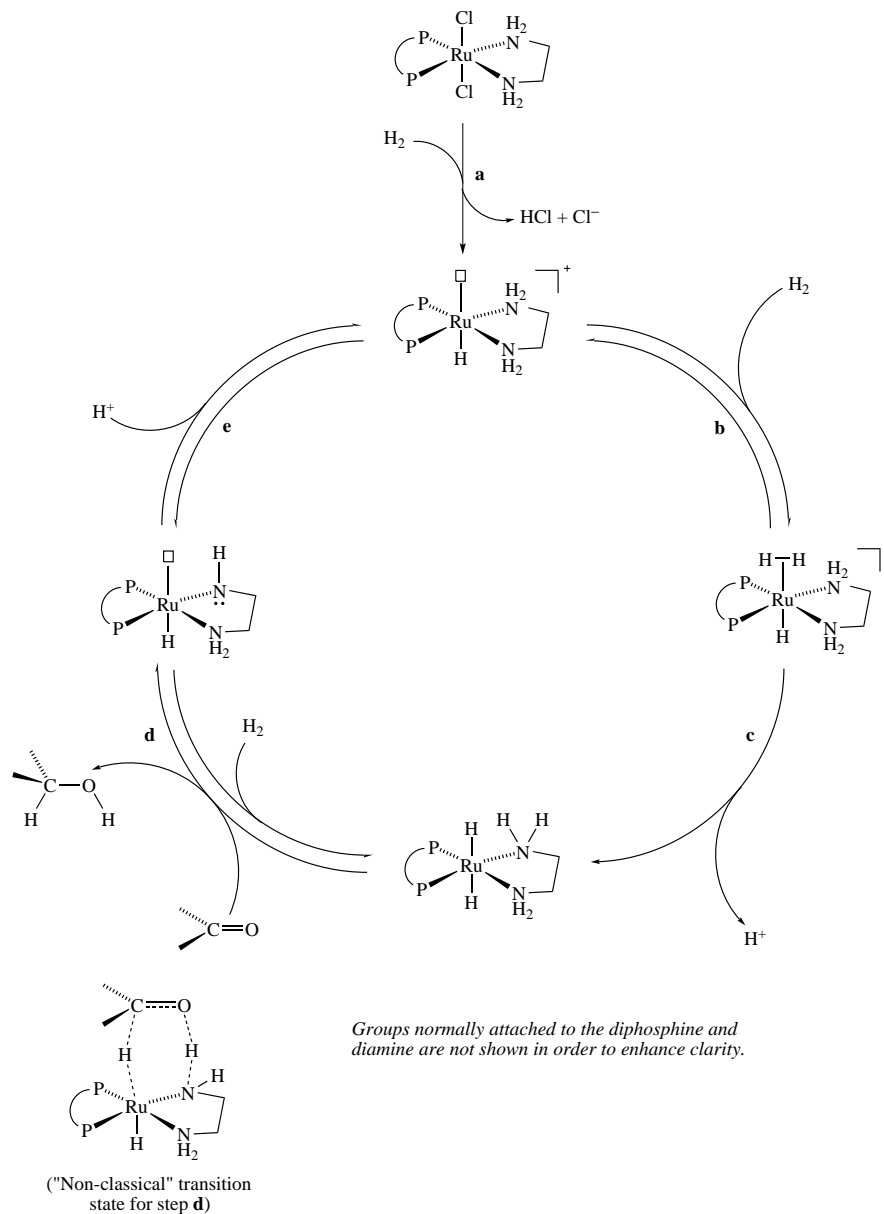
Ru(II)-diphosphine-diamine catalyst

Diphosphines:

- (*S*)-BINAP (Ar = Ph)
- (*S*)-TolBINAP (Ar = 4-MePh)
- (*S*)-XylBINAP (Ar = 3,5-(Me)₂Ph)
- (*S,S*)-DIOP
- (*S,S*)-CHIRAPHOS

Diamines:**Figure 12-3**Ru(II)-BINAP/
Diamine Catalysts

Equation **12.9** exemplifies excellent chemoselectivity, whereby a C=C bond conjugated with a C=O bond does not undergo hydrogenation under these conditions. There is a good reason for this effect. When bifunctional catalysts are used to hydrogenate the C=O bond, the mechanism of C=O hydrogenation is different than that we have seen earlier using monofunctional catalysts. Scheme **12.7** shows a catalytic cycle for C=O hydrogenation in which two H atoms are transferred to the C=O group by an “outer sphere” mechanism that takes place through a six-membered ring transition state during step **d**, a mechanism termed “non-classical” by Noyori. The diamine ligand can donate a proton to the carbonyl oxygen while a hydride ligand attaches to one or the other face of the carbonyl

**Scheme 12.7**

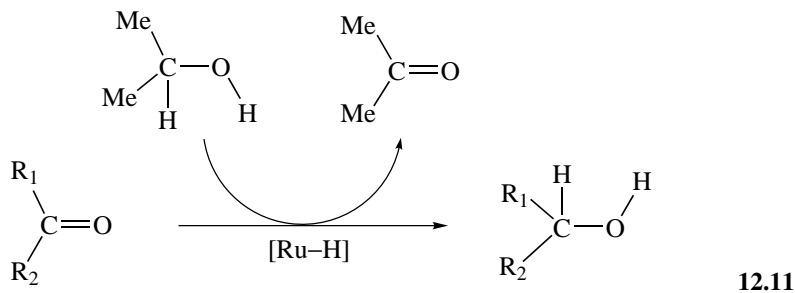
Mechanism for Asymmetric Hydrogenation of C=O Bonds in the Presence of Bifunctional Ru(II) Catalysts

group at carbon. At no time is binding of the C=O bond to the Ru required during hydrogenation, yet stereoselectivity is governed by the asymmetric bias of both the BINAP and the diamine.²⁸

²⁸Previous catalytic pathways for hydrogenation have involved transfer of a metal-bound hydride to the substrate containing the double bond, which is also bonded to the metal. This

Hydrogenation is an excellent example of green chemistry. Atom economy is high because the addition of H₂ across a multiple bond yields only one constitutional isomer. Under conditions of asymmetric catalysis, one enantiomer is strongly preferred, so little material is wasted in separation procedures (resulting in a low *E*-factor). Often, such reactions are also carried out under mild conditions involving low temperature and pressure, which means that energy consumption is minimized. Recent research has shown that water, the premier example of an environmentally benign solvent, can serve as a reaction medium for asymmetric hydrogenation of ketones under conditions of *transfer hydrogenation* (TH or ATH when the hydrogenation is asymmetric).

TH is an indirect form of hydrogenation that can be catalyzed by transition metal complexes.²⁹ Equation 12.11 outlines the concept where 2-propanol is the hydrogen transfer agent, which means that H₂ does not have to be present. Two hydrogens are transferred from 2-propanol, and the by-product is acetone.

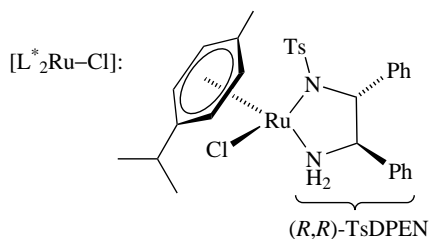
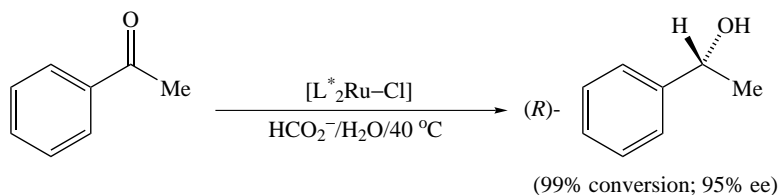


Another source of hydrogen is formate ion, HCOO⁻, which can donate its hydrogen atom to a substrate, forming CO₂ as a by-product. Xiao has shown that acetophenone can undergo ATH with nearly quantitative conversion when it is converted to the corresponding (*R*)-alcohol in 95% ee (equation 12.12).³⁰ The reaction only takes one hour when it is run at 40°C in aqueous formate solution using a chiral η⁶-arene-Ru catalyst with a modified DPEN ligand, mild conditions indeed. The most likely mechanism involves transfer of two hydrogen atoms to the ketone via a transition state that was already shown in Scheme 12.7.

is called an “inner-sphere” mechanism. For more details on this non-classical hydrogenation, see Footnote 26.

²⁹For a recent review on transfer hydrogenation involving Ru complexes, see S. E. Clapham, A. Hadzovic, and R. H. Morris, *Coord. Chem. Rev.*, **2004**, 248, 2201.

³⁰(a) X. F. Wu, X. G. Li, W. Hems, F. King, and J. Xiao, *Org. Biomol. Chem.*, **2004**, 2, 1818; and (b) X. G. Li, X. F. Wu, W. P. Chen, F. E. Hancock, F. King, and J. Xiao, *Org. Lett.*, **2004**, 6, 3321.

**12.12**

Other alkyl aryl ketones show similar results with this catalyst. Because the catalyst is mostly water insoluble, it is possible that catalysis occurs *on* water rather than *in* water.

Even Rh(I) and Ir(I) complexes of diamines similar to that shown in equation 12.12 are very effective catalysts for ATH of C=O groups. At present, however, the scope of the reaction is limited to aryl ketones and imines. Nevertheless, the potential for the success of ATH under green chemistry conditions remains strong.³¹

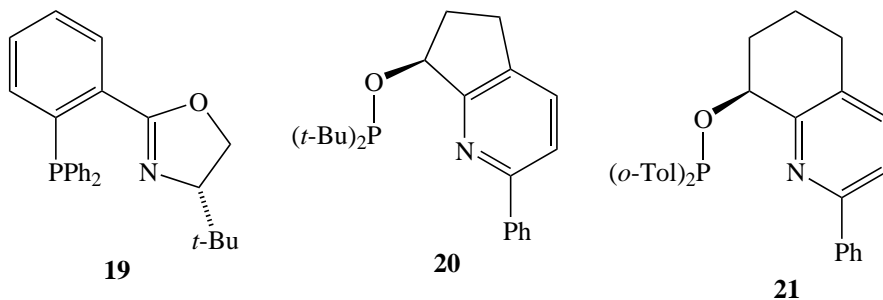
Asymmetric Hydrogenation Using Cationic Ir(I) Catalysts

In Section 9-4-3, we mentioned that cationic Ir catalysts (sometimes called Crabtree catalysts) are quite active for hydrogenation of highly substituted C=C bonds. Moreover, asymmetric Ir-catalyzed hydrogenation of an imine is a key step in the industrial-scale synthesis of the herbicide (*S*)-metolachlor (Section 9-7-2). In addition to these applications, relatively recent work has shown that cationic Ir(I) complexes bonded to chiral ligands can catalyze asymmetric hydrogenation of unfunctionalized C=C bonds (i.e., C=C bonds to which no polar functional groups, such as C=O, are attached).

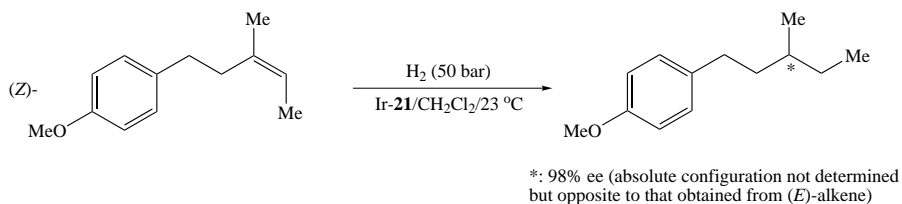
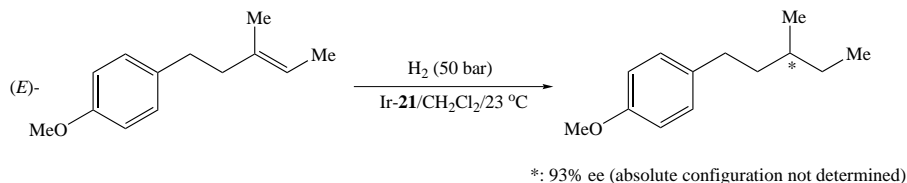
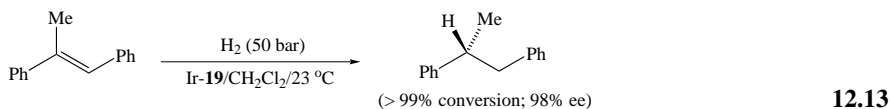
Largely through efforts of Pfaltz and co-workers, a series of chiral ligands was developed that allowed unfunctionalized alkenes to undergo asymmetric hydrogenation;³² structures 19 (*t*BuPHOX ligand), 20, and 21 show a few of these.

³¹For a recent summary of ATM in green solvents, see X. Wu and J. Xiao, *Chem. Comm.*, **2007**, 2449.

³²For recent reviews of this work, see (a) S. J. Roseblade and A. Pfaltz, *C. R. Chemie*, **2007**, *10*, 178 and (b) K. Källström, I. Munslow, and P. G. Andersson, *Chem. Eur. J.*, **2006**, *12*, 3194.



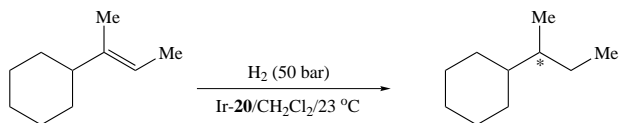
Initially, the Pfaltz ligands were effective only in catalyzing asymmetric hydrogenation of alkenes substituted with phenyl groups (equation **12.13**).³³ Further refinement of the ligand produced a significant improvement in the scope of asymmetric hydrogenation of unfunctionalized alkenes. Equations **12.14**³⁴ and **12.15**³⁵ show highly enantioselective reduction of alkenes where either the aromatic substituent is attached at a position remote from the C=C or is not present at all.

**12.14**

³³A. Lightfoot, P. Schnider, and A. Pfaltz, *Angew. Chem. Int. Ed.*, **1998**, 37, 2897.

³⁴A. Pfaltz, J. Blankenstein, R. Hilgraf, E. Hörmann, S. McIntyre, F. Menges, M. Schönleber, S. P. Smit, B. Würstenberg, and N. Zimmermann, *Adv. Synth. Catal.*, **2003**, 345, 33.

³⁵S. Bell, B. Würstenberg, S. Kaiser, F. Menges, T. Netscher, and A. Pfaltz, *Science*, **2006**, 311, 642.



*: 92% ee (absolute configuration not determined)

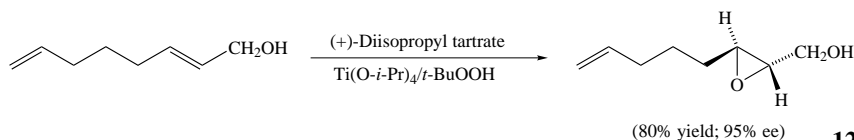
12.15

One proposal for the catalytic cycle involves an Ir(III)–dihydride intermediate that forms after OA of H₂ onto an Ir(I)–alkene complex. Experimental results seem to support this cycle,³⁶ but computational studies suggest that the cycle involves Ir(III) and Ir(V) intermediates.³⁷ The details of neither proposal have been elucidated. Work continues to expand the scope of this reaction to include asymmetric hydrogenation of any unfunctionalized alkene that could yield a chiral alkane.

Propose a catalytic cycle for Ir-catalyzed asymmetric hydrogenation that involves Ir(I) and Ir(III) complexes as intermediates. Assume that the starting point of the cycle is a cationic Ir(I) complex, which is bonded to a general aminophosphine ligand and solvent molecules as needed to form a square planar complex. OA of H₂ is then followed by ligand displacement of solvent by alkene. Which step introduces a stereogenic center?

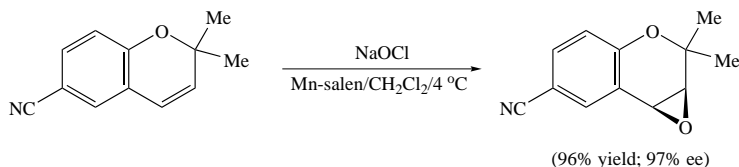
Exercise 12-3**12-1-2 Asymmetric Oxidations**

One of the most exciting developments in asymmetric catalysis over the past 25 years has been the discovery of transition metal complexes that catalyze the oxidation of alkenes to chiral epoxides and 1,2-diols. Equations **12.16**, **12.17**, and **12.18** show examples of epoxidation and 1,2-dihydroxylation.

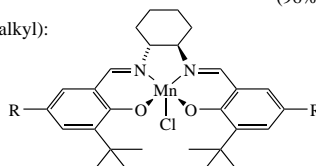
**12.16**

³⁶R. Dietiker and P. Chen, *Angew. Chem. Int. Ed.*, **2004**, *43*, 5513.

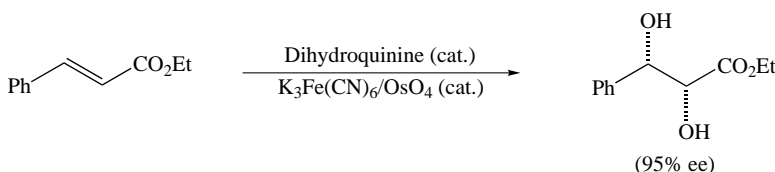
³⁷Y. Fan, X. Cui, K. Burgess, and M. B. Hall, *J. Am. Chem. Soc.*, **2004**, *126*, 16688 and P. Brandt, C. Hedberg, and P. G. Andersson, *Chem. Eur. J.*, **2003**, *9*, 339.



An example of a Mn-salen ligand (R = alkyl):



12.17



12.18

Equation **12.16** is an example of the Sharpless–Katsuki asymmetric epoxidation of allylic alcohols, which is catalyzed by a Ti complex bound to a chiral tartrate ligand.³⁸ A Mn–salen³⁹ complex serves as catalyst for asymmetric epoxidation (Jacobsen–Katsuki reaction) of a wide variety of unfunctionalized alkenes, shown in equation **12.17**.⁴⁰ OsO₄ complexed with chiral alkaloids, such as quinine derivatives (equation **12.18**), catalyzes asymmetric 1,2-dihydroxylation of alkenes (known as the Sharpless asymmetric dihydroxylation).⁴¹ The key step of all these transformations is the transfer of metal-bound oxygen, either as a single atom or as a pair, to one face of the alkene.

It should be pointed out, however, that these heteroatom transfer reactions do not typically involve true organometallic complexes; traditional carbon-based

³⁸T. Katsuki and K. B. Sharpless, *J. Am. Chem. Soc.*, **1980**, *102*, 5974 and B. E. Rossiter, T. Katsuki, and K. B. Sharpless, *J. Am. Chem. Soc.*, **1981**, *103*, 464; for a comprehensive review of the reaction, see T. Katsuki and V. S. Martin, *Org. React.*, **1996**, *48*, 1; for the Sharpless Nobel Prize in Chemistry (2001) lecture, see K. B. Sharpless, *Angew. Chem. Int. Ed.*, **2002**, *41*, 2024.

³⁹Salen is an abbreviation for the name of a ligand composed of salicylic acid (sal) and ethylenediamine (en).

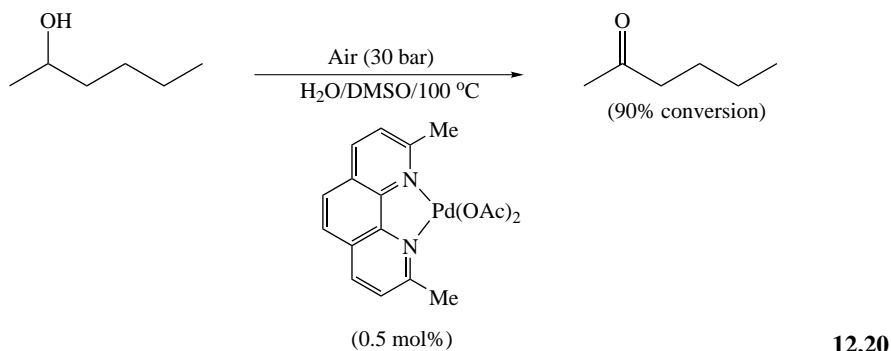
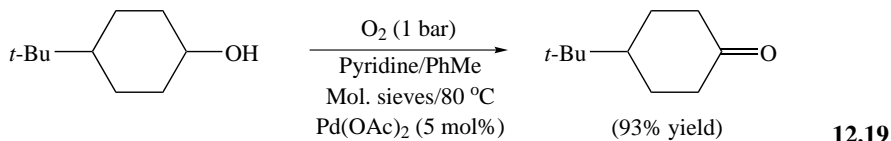
⁴⁰W. Zhang, J. L. Loebach, S. R. Wilson, and E. N. Jacobsen, *J. Am. Chem. Soc.*, **1990**, *112*, 2801; E. N. Jacobsen, W. Zhang, A. R. Muci, J. R. Ecker; and L. Deng, *J. Am. Chem. Soc.*, **1991**, *113*, 7063; T. P. Yoon and E. N. Jacobsen, *Science*, **2003**, *299*, 1691; and R. Irie, K. Noda, Y. Ito, and T. Katsuki, *Tetrahedron Lett.*, **1991**, *32*, 1055.

⁴¹E. N. Jacobsen, I. Marko, W. S. Mungall, G. Schroeder, and K. B. Sharpless, *J. Am. Chem. Soc.*, **1988**, *110*, 1968 and H. C. Kolb, M. S. VanNieuwenhze, and K. B. Sharpless, *Chem. Rev.*, **1994**, *94*, 2483.

ligands (e.g., CO, alkenes, and Cp, or other ligands considered “organometallic,” such as hydride or PR_3), are not bound to the metal during the catalytic cycle. Despite the high significance of these reactions to the field of organic synthesis, we will limit our discussion of asymmetric oxidation to reactions in which traditional organometallic complexes are involved during catalysis.⁴²

Pd-Catalyzed Oxidation of Secondary Alcohols

Over the past 10 years, there have been great strides reported in the Pd-catalyzed oxidation of secondary alcohols to ketones using O_2 as the ultimate oxidizing agent. Often, these reactions exhibit many of the tenets of green chemistry by occurring under very mild conditions, even using air instead of pure O_2 . Reactions **12.19**⁴³ and **12.20**⁴⁴ reveal typical conditions for such reactions, which were developed by Uemura and Sheldon almost simultaneously. Primary alcohols also react to give aldehydes, but lower yields and overoxidation are problems. Recently reported work by Sigman has shown, by replacing pyridine with triethylamine, that a wide range of secondary and primary alcohols can be oxidized to ketones and aldehydes in very high yield using O_2 or even air as the ultimate oxidant.⁴⁵ These reactions seem general enough to obviate the use of carcinogenic and environmentally hazardous Cr(VI) reagents, which have been used traditionally for alcohol oxidations.



⁴²The references cited above should point readers to current work in the chemical literature that is associated with asymmetric heteroatom transfer oxidations.

⁴³For a review of Uemura's work, see T. Nishimura and S. Uemura, *Synlett*, **2004**, 2, 201.

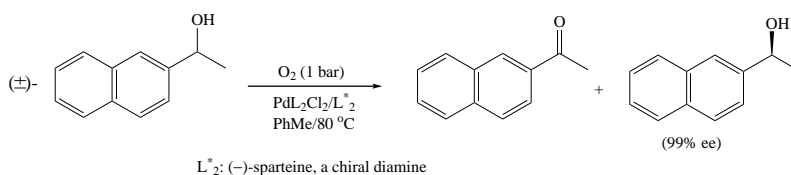
⁴⁴For a review of green oxidations by Sheldon's group, see G.-J. ten Brink, I. W. C. E. Arends, M. Hoogenraad, G. Verspuil, and R. Sheldon, *Adv. Synth. Catal.*, **2003**, 345, 1341.

⁴⁵M. J. Schultz, S. S. Hamilton, D. R. Jensen, and M. S. Sigman, *J. Org. Chem.*, **2005**, 70, 3343.

Over the last several years, Stoltz and Sigman simultaneously reported on the potential of using asymmetric versions of such oxidations to selectively oxidize racemic secondary alcohols so that one enantiomer undergoes conversion to the corresponding ketone and the other remains unreacted. This process, called a kinetic resolution, allows isolation of one enantiomer in up to 50% yield,⁴⁶ and it mimics enzyme-catalyzed resolution (whereby the enzyme interacts with only one enantiomer). It is thus typically more efficient than chemical resolution processes that form diastereomeric derivatives of each enantiomer, which then must be laboriously separated and purified. The method also is often superior to separation on chiral chromatography columns, which is usually amenable to use only on a small scale. If the unreacted enantiomer is the one desired, the technique is even more attractive when there is a way of recycling the ketone product back to racemic alcohol and then oxidizing this material. Yields higher than 50% can then be realized.

Exercise 12-4

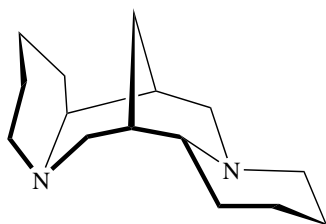
Consider Stoltz's stereoablative kinetic resolution of a naphthyl secondary alcohol shown in the following equation.



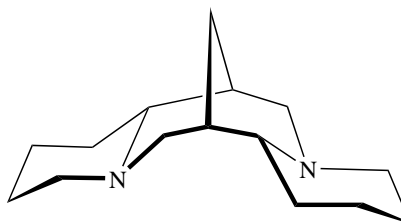
Suggest a means for recycling the unreacted ketone back to racemic alcohol so that overall yield of the desired (*S*)-alcohol is greater than 50% (see Footnote 46).

To incorporate a chiral environment into the oxidation, both Stoltz and Sigman employed (-)-sparteine (**22a**) as a bidentate ligand to replace pyridine, which was used for the achiral versions of alcohol oxidation mentioned above.

⁴⁶Stoltz terms such reactions *stereoablative*. Ablation is the effect of taking something away. For example, the heat shield of the Space Shuttle burns away (ablates) sacrificially during reentry after a mission in order to preserve the spacecraft. An ablative reaction is one where an existing stereogenic element in a molecule is eliminated. For more information on ablative reactions, see J. T. Mohr, D. C. Ebner, and B. M. Stoltz, *Org. Biomol. Chem.*, **2007**, *5*, 3571.



22a: (-)-Sparteine

22b: (-)- α -Isosparteine

Careful work on the mechanism of Pd(-)-sparteine oxidation has pinned down most of the details of the process, resulting in the catalytic cycle shown in Scheme 12.8.⁴⁷

The rate-determining step occurs during β -hydride elimination. One model for enantioselection is shown in Figure 12-4, where the diamine ligand, (-)-sparteine, exhibits C_1 symmetry⁴⁸ instead of C_2 . C_2 symmetry is associated with diastereomeric structure 22b, (-)- α -isosparteine). C_2 is also the inherent symmetry of chiral bisphosphine ligands used for asymmetric hydrogenation.⁴⁹

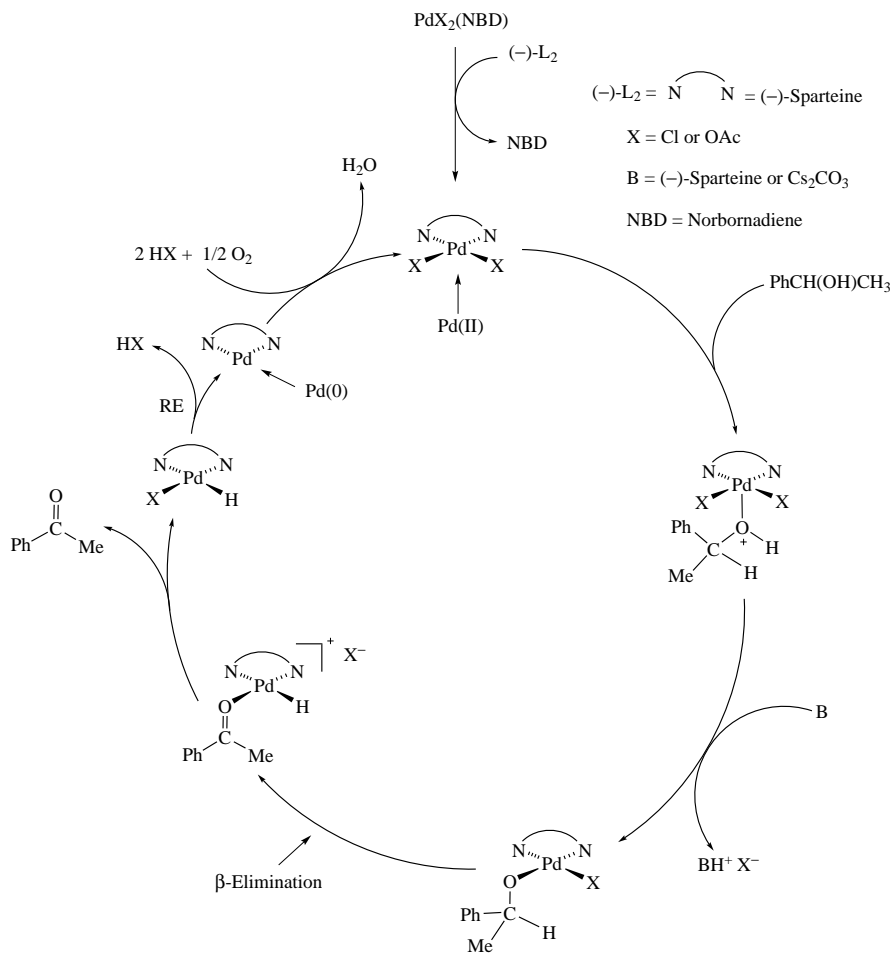
In this model, only one enantiomer of the racemic alcohol yields a complex that is readily suitable for β -elimination, whereas the diastereomerically related complex, with the other enantiomer bonded to Pd, is energetically unfavorable. An energetically unsuitable complex (23a) is shown by the interference of the larger group G_L , attached to C-1 of the alcohol, interfering with sterically encumbered quadrant III of the (-)-sparteine ligand. The energetically more favorable diastereomeric complex (23b) shows the smaller group, G_S , pointing to quadrant III and G_L filling the void denoted in Figure 12-4 as quadrant IV. It is this complex that is set up favorably for β -elimination to form the corresponding ketone. The energetically unsuitable complex breaks apart under the reaction conditions and releases unreacted, but enantiomerically pure, alcohol. Table 12-2 (on p. 552) shows the range and enantioselectivity of this oxidation.

There are challenges that remain for optimization of the Pd(-)-sparteine-catalyzed asymmetric oxidation of secondary alcohols—including accelerating the relatively slow reaction rate, finding a general method for recycling oxidized product, and using air rather than O_2 as oxidant in all cases. Nonetheless, this

⁴⁷R. J. Nielsen, J. M. Keith, B. M. Stoltz, and W. A. Goddard, III, *J. Am. Chem. Soc.*, **2004**, *126*, 7967 and M. J. Schultz, R. S. Adler, W. Zierkiewicz, T. Primolov, and M. S. Sigman, *J. Am. Chem. Soc.*, **2005**, *127*, 8499.

⁴⁸Meaning that there are no elements of symmetry present except rotation about an axis by 360°.

⁴⁹R. Trend and B. M. Stoltz, *J. Am. Chem. Soc.*, **2004**, *126*, 4482; see also J. A. Mueller, A. Cowell, B. D. Chandler, and M. S. Sigman, *J. Am. Chem. Soc.*, **2005**, *127*, 14817 for additional work on the origin of enantioselectivity.

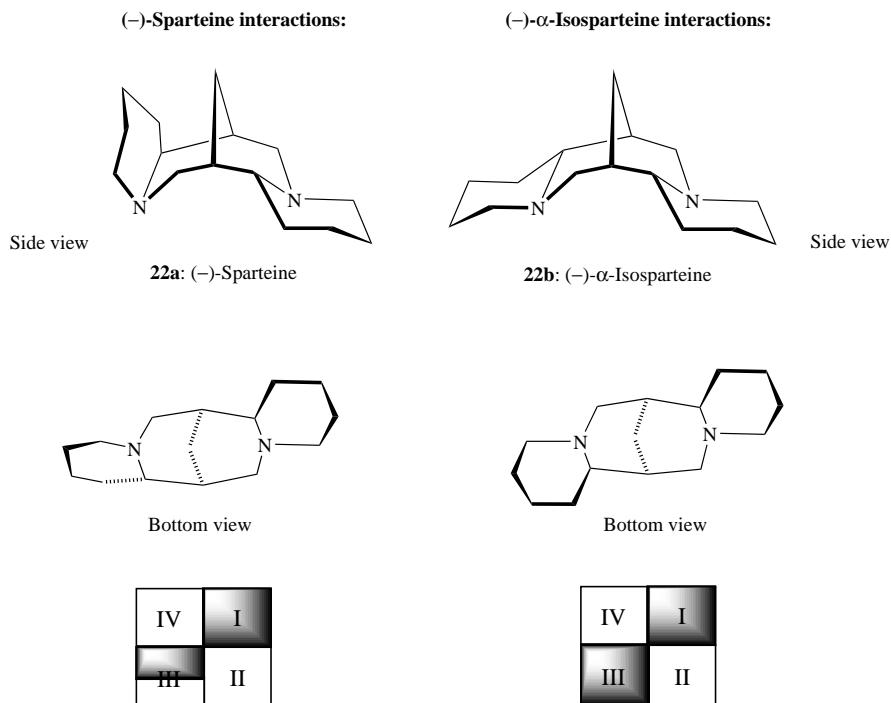
**Scheme 12.8**

Catalytic Cycle for
Pd-(-)-Sparteine
Asymmetric
Oxidation of
Secondary Alcohols

method has promise as a means of kinetic resolution of secondary alcohols with enantioselectivities approaching those achieved using enzymes.

Oxidative Cyclizations

As we saw in Chapter 9 (Section 9-3), the Wacker Chemie process converts ethene to ethanal under Pd(II) catalysis. This process has potential in the realm of organic synthesis as a general means of converting alkenes to aldehydes or ketones. Since the original discovery of the Wacker Chemie process, there has been recent, renewed interest in making the process simpler and greener by using only O_2 as the ultimate and sole oxidizing agent. Recall that the original Wacker process required the use of stoichiometric amounts of Cu(II), which served to oxidize Pd(0) back to Pd(II) in a connected, separate cycle. The use of



Bottom view translated into quadrants: shaded areas depict the steric bulk of the carbon framework of (-)-sparteine or (-)- α -isosparteine; unshaded areas indicate the lack of steric hindrance.

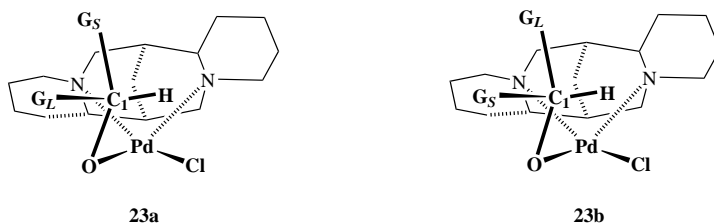


Figure 12-4

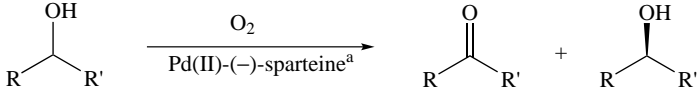
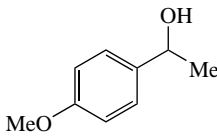
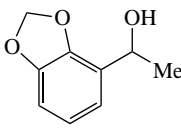
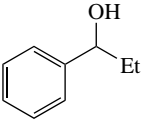
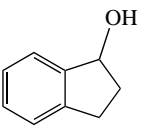
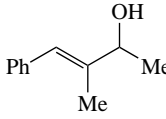
A Predictive Model for Enantioselection in Asymmetric Oxidation of Secondary Alcohols

O₂ as the sole oxidant would obviate the use of relatively expensive Cu(II) as a co-oxidant and would be consistent with the tenets of green chemistry, especially if air instead of pure O₂ were employed.

Kaneda recently reported a major step toward this goal, which involved running the oxidation using O₂ at a pressure of 6 bar and at a temperature 80 °C in dimethylacetamide(DMA)–H₂O solvent (equation 12.21).⁵⁰

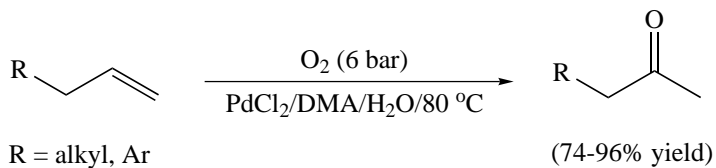
⁵⁰T. Mitsudome, T. Umetani, N. Nosaka, K. Mori, T. Mizugaki, K. Ebitani, and K. Kaneda, *Angew. Chem. Int. Ed.*, **2006**, 45, 481.

Table 12-2 Enantioselective Oxidation of Secondary Alcohols

		
(±)-RR'CHOH	% conversion ^b	% ee ^b
	67	99.5
	56	99.7
	63	98.0
	74	99.5
	65	87.9

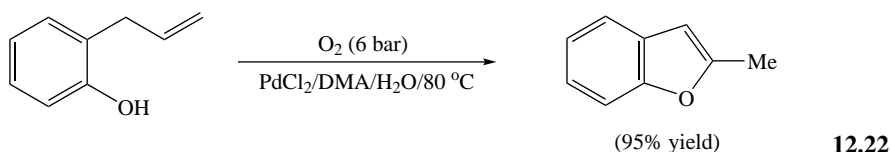
^aReaction conditions: 5 mol% PdCl₂(NBD); 20 mol% (-)-sparteine; 0.5 equiv. Cs₂CO₃; 1.5 equiv. *t*-BuOH; 1 bar O₂/60-80 °C

^bData taken from J. T. Bagdanoff, E. M. Ferreira, and B. M. Stoltz, *Org. Lett.*, **2003**, 5, 835.



A wide range of terminal alkenes were converted to methyl ketones in 70–90% yield under the same reaction conditions. Shortly after Kaneda published his results, Sigman reported that using a $\text{PdCl}_2((-)\text{-sparteine})$ as catalyst allowed the reaction to occur, albeit more slowly, under a balloon of O_2 at 70 °C, also in $\text{DMA-H}_2\text{O}$.⁵¹

A variation on Kaneda's Wacker oxidation of terminal alkenes involves oxidative cyclization, shown generally in equation 12.22. Although this process does not show conversion of an alkene to a ketone, a formal oxidation occurs because there is a net loss of two hydrogen atoms in going to the cyclic ether.

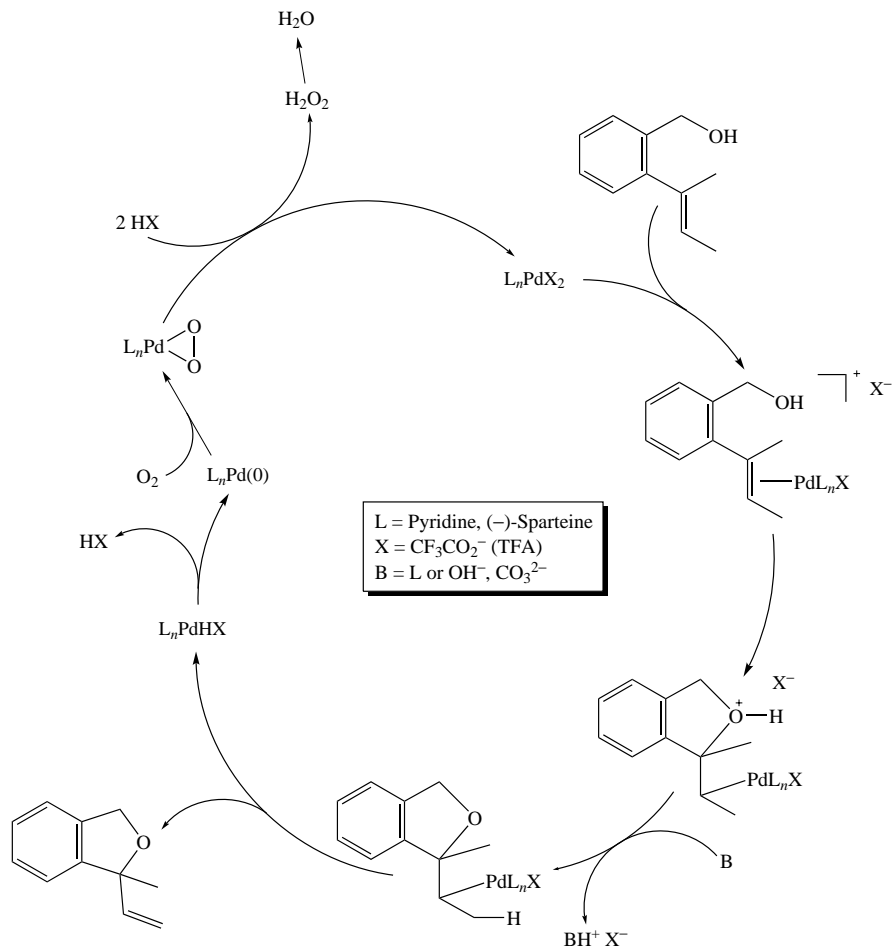


Presumably the reaction is Wacker-like because the tethered OH group must act as a nucleophile to attack the alkene group attached to Pd, which is analogous to H_2O or Pd-bound OH attacking the ethene in the Wacker process. Recently, Stoltz and co-workers⁵² developed an elegant, mild Pd(II)-catalyzed cyclization process involving both cycloxygenation and cycloamination under 1 bar of O_2 at 80 °C in anhydrous toluene. Equation 12.23 outlines the scope of the reaction, and Scheme 12.9 shows a plausible mechanism for cyclization, along with an additional cycle designed to convert Pd(0) back to Pd(II) (see also Scheme 12.8). The details of the second cycle were elaborated on by Stahl⁵³ for a similar Pd-catalyzed oxidation involving O_2 as the sole oxidant. Stoltz reported that the cycloxygenations involved *syn* attack of the OH group (attached as an alkoxide ligand to Pd) onto the complexed alkene, which is reminiscent of a Wacker oxidation. For reasons that remain unclear, the cyclization involving carboxyl OH proceeded with *anti* attack onto the alkene.

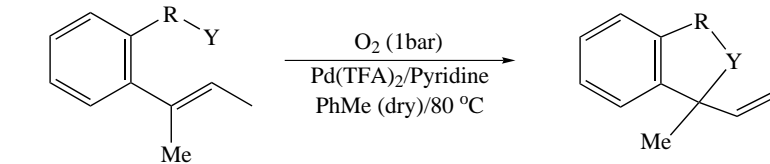
⁵¹C. N. Cornell and M. S. Sigman, *Org. Lett.*, **2006**, *8*, 4117; for a summary of the progress to date in developing Wacker oxidations where O_2 is the sole oxidant, see C. N. Cornell and M. S. Sigman, *Inorg. Chem.*, **2007**, *46*, 1903.

⁵²R. M. Trend, Y. K. Ramtohol, E. M. Ferreira, and B. M. Stoltz, *Angew. Chem. Int. Ed.*, **2003**, *42*, 2892.

⁵³B. A. Steinhoff, S. R. Fix, and S. S. Stahl, *J. Am. Chem. Soc.*, **2002**, *124*, 766; B. A. Steinhoff and S. S. Stahl, *Org. Lett.*, **2002**, *4*, 4179; and S. S. Stahl, J. L. Thorman, R. C. Nelson, and M. A. Kozee, *J. Am. Chem. Soc.*, **2001**, *123*, 7188.

**Scheme 12.9**

Pd(II)-Catalyzed,
Wacker-Type
Oxidative
Cyclizations Where
 O_2 Is the Sole
Oxidant



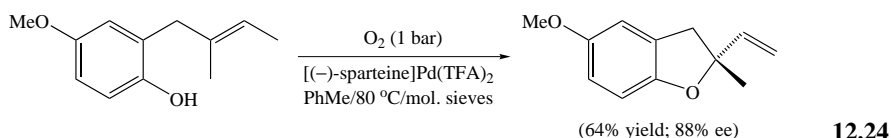
$R = \text{C}=\text{O} \text{ or } \text{CH}_2$
 $\text{YH} = \text{NHTs, NHOBn, OH}$

(63-90% yield)

The stereochemical course of Wacker-type cyclization, when the nucleophile OH comes from an alcohol or a phenol, is different than it is when the OH originates from a carboxylic acid. How does the OH group of a carboxyl group differ from that of a phenol or alcohol? Consider in your answer such factors as pK_a , stereochemical constraints, and nucleophilicity.

Exercise 12-5

The cyclizations reported by Stoltz typically produce a stereogenic center. Accordingly, he was able to develop an asymmetric version of this cyclization in the case where the OH group is phenolic.⁵⁴ Equation 12.24 shows an example of this cyclization, again using (–)-sparteine to create a chiral environment during the cyclization process.



Although this cyclization is not yet general, there is potential for expanding the scope of this reaction to other systems. At present, the details of asymmetric oxidations are not as well characterized as those of hydrogenation, but the range of synthetically useful possibilities for transition metal catalyzed oxidation is larger.

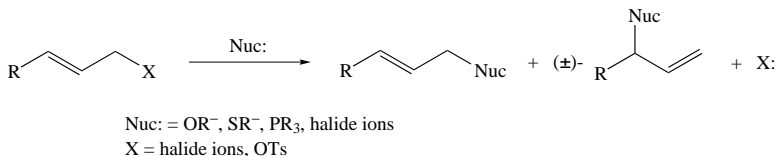
12-2 CARBON–CARBON BOND FORMATION VIA NUCLEOPHILIC ATTACK ON AN η^3 - π LIGAND: THE TSUJI–TROST REACTION

The remainder of Chapter 12 will explore how organotransition metal complexes are particularly useful in promoting the formation of a C–C bond, which is the most important reaction in organic synthesis. In the course of this treatment, we will see how fundamental types of organometallic reactions are involved in C–C bond formation. Section 12-2 considers a particularly useful and widely applicable method of C–C bond creation that features nucleophilic attack by carbanions on η^3 -allyl ligands. Later sections will draw attention to (1) 1,1- and 1,2-migratory insertion; (2) a sequence of oxidative addition, transmetalation, and reductive elimination; and (3) a variety of multiple C–C bond formations that produce rings, all involving fundamental organometallic reaction types and occurring in one grand chemical step.

⁵⁴R. M. Trend, Y. K. Ramtohol, and B. M. Stoltz, *J. Am. Chem. Soc.*, **2005**, *127*, 17778.

12-2-1 General Considerations: Mechanism and Achiral Examples

In organic chemistry, allylic substrates are relatively reactive toward some nucleophiles, as shown in equation 12.25. The reaction suffers, however, from a number of disadvantages, including unpredictable stereochemistry, poor control of regiochemistry, and the possibility of carbon-skeleton rearrangements.



12.25

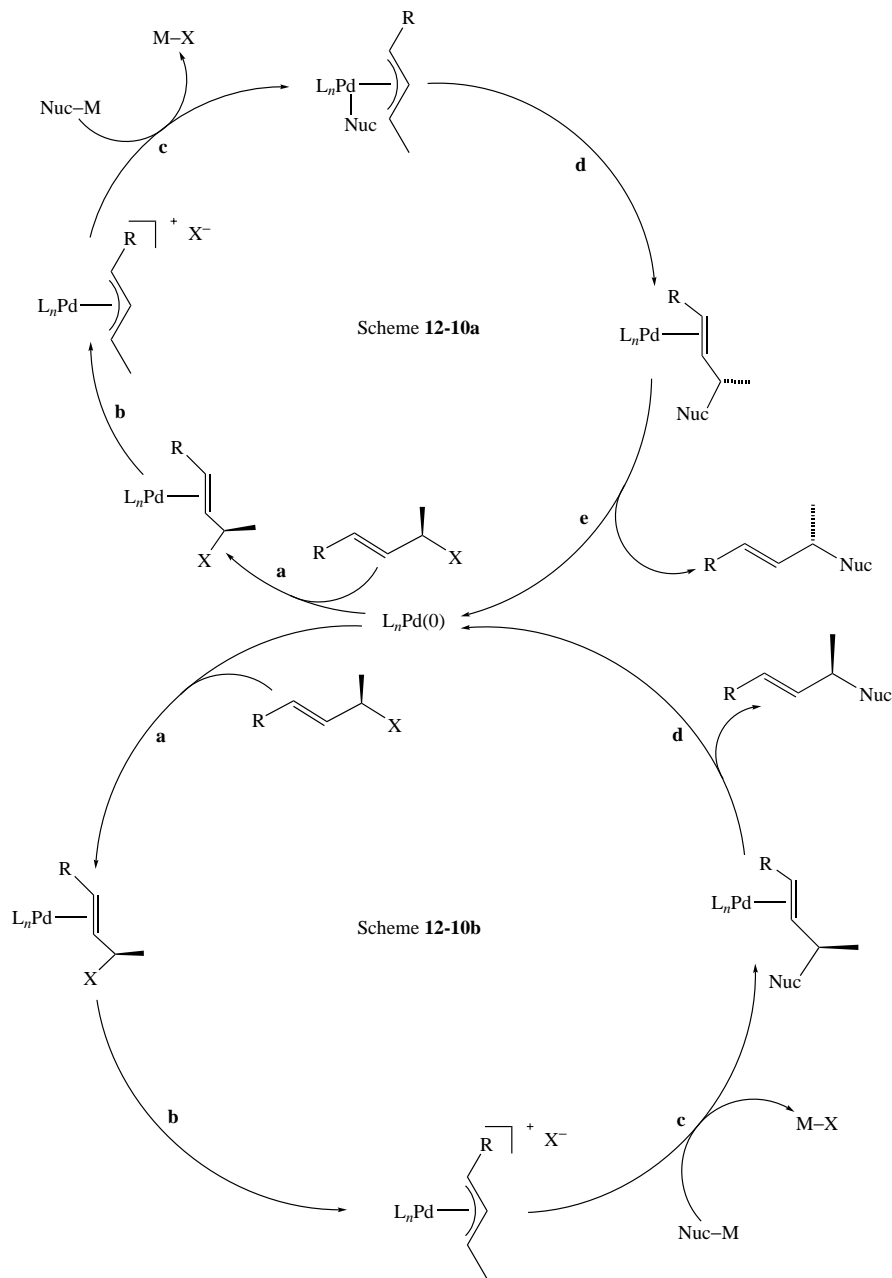
In contrast, η^3 - π -allyl metal complexes—especially cationic ones—are more reactive toward a variety of nucleophiles, usually with predictable regio- and stereochemistry. Carbon nucleophiles, moreover, react with these complexes, forming the all-important C–C bond. Since its discovery over 40 years ago, this transformation, now termed the Tsuji–Trost reaction (see Section 8-2-2 for a brief introduction to the Tsuji–Trost reaction and some leading early references), has seen increasing use as a means of enantioselective synthesis of chiral molecules. Palladium is by far the metal of choice to bind to η^3 -allyl ligands, forming relatively stable (but not too stable for catalytic reactions) complexes that are potentially isolable but rarely isolated.⁵⁵ Commonly used leaving groups are listed below on the basis of their relative reactivity.



Considerations of stereochemistry and regiochemistry resulting from complexation of the allylic system and subsequent attack by a nucleophile are of great importance to the utility of the Tsuji–Trost reaction in organic synthesis. Schemes 12.10a and b show two catalytic cycles for the Tsuji–Trost allylation reaction that result in two different stereochemical outcomes depending on the basicity of the nucleophile.⁵⁶ Allylation by unstabilized or “hard” nucleophiles ($\text{p}K_{\text{a}}$ of the conjugate acid > 25 —typically organometallic compounds of Mg, Li, and Zn) generally results in an overall inversion of configuration at the allylic site (Scheme 12.10a), whereas stabilized or “soft” nucleophiles ($\text{p}K_{\text{a}}$ of the conjugate acid < 25 —typically stabilized enolate ions such as the one derived from diethylmalonate) react to give net retention of configuration (Scheme 12.10b).

⁵⁵Other metals that bond to allylic substrates with subsequent, synthetically useful nucleophilic attack include Mo, W, Fe, and especially Ni.

⁵⁶B. M. Trost and D. L. Van Vranken, *Chem. Rev.*, **1996**, 96, 395.



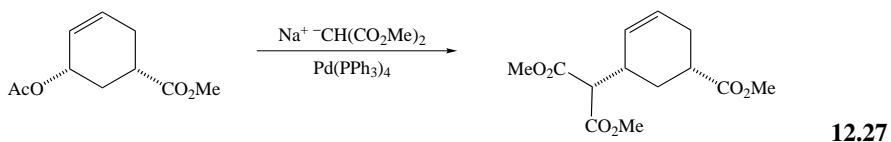
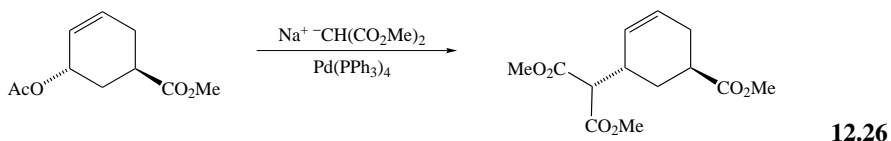
**Schemes 12.10a
and 12.10b**

Catalytic Cycles
Showing the
Stereochemistry
Associated with the
Tsuji–Trost Reaction

The steps leading to net inversion follow after complexation of the π ligand (step **a**, Scheme **12.10a**) and begin with OA (Section **7-2-2**) of the allyl–X bond onto Pd (inversion of configuration, step **b**), which is followed by a transmetalation (retention of configuration via possibly a σ bond metathesis, step **c**) and then reductive elimination of the nucleophile and allyl ligands (retention of

configuration, step **d**). Decomplexation (step **e**) involves retention of stereochemistry, so overall the one inversion step sets the stereochemistry for the entire cycle.

With soft nucleophiles, steps **a** and **b** of Scheme 12.10b are the same as those in Scheme 12.10a. The crucial difference between the two pathways originates in the next steps. Soft nucleophiles attack the η^3 -allyl complex *anti* to the metal (step **c**, Scheme 12.10b), which results in another inversion of configuration. This is followed by decomplexation (step **d**), which occurs with retention of configuration. Overall, therefore, two inversions followed by retention result in a net retention of configuration. Equations 12.26 and 12.27 illustrate the stereochemistry attendant to the reaction of diastereomeric allylic acetates with malonate ion.⁵⁷

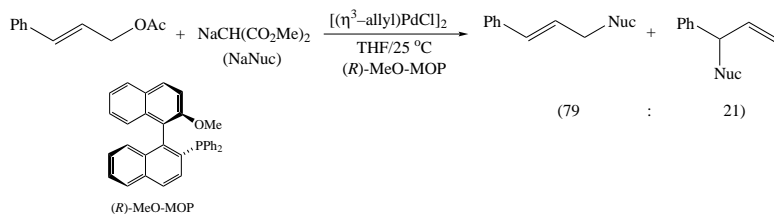


Nucleophiles, especially those that are sterically bulky and soft, tend to attack at the less substituted terminal position of unsymmetrically substituted η^3 -allyl ligands. This tendency is enhanced if substituents at a terminal allylic position are also bulky. Unfortunately, this is not a “hard and fast rule” (see discussion in Section 8-2-2 on regiochemistry at the terminal positions of η^3 -allyl ligands when electron donating groups occupy one of the terminal positions), and the regiochemistry of attack is complicated by a phenomenon chemists have termed a *memory effect*. Sometimes leaving groups seem to be reluctant to depart before nucleophilic attack, so attack occurs predominantly at the position where the leaving group was originally attached, although this position is more sterically hindered. Equations 12.28 and 12.29⁵⁸ show the typical preference for nucleophilic attack at the less substituted allylic position, when either the nucleophile is a separate molecule or it is already tethered to the allylic substrate, whereas equation 12.30 demonstrates a memory effect. Studies of memory effects as a function of leaving groups are ongoing.⁵⁹

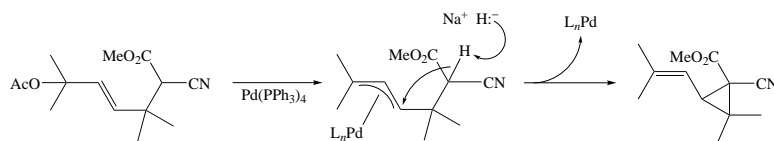
⁵⁷B. M. Trost and T. R. Verhoeven, *J. Org. Chem.*, **1976**, *41*, 3215.

⁵⁸Loss of the carboxy group and conversion of CN to COOH in the product leads ultimately to synthesis of chrysanthemic acid, derivatives of which serve as effective insecticides known as pyrethrins. J. P. Genet and F. Piau, *J. Org. Chem.*, **1981**, *46*, 2414.

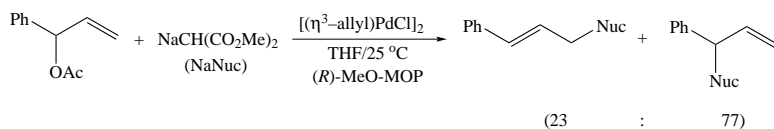
⁵⁹For a recent study of memory effects in Tsuji–Trost allylation reactions, see P. Fristrup, T. Jensen, J. Hoppe, and P.-O. Norrby, *Chem. Eur. J.*, **2006**, *12*, 5352; for some experimental



12.28



12.29



12.30

12-2-2 Asymmetric Tsuji–Trost Allylations

It was not long after the original work on the Trost–Tsuji reaction that asymmetric examples were reported.⁶⁰ In recent years, numerous cases have appeared where this reaction was used to create chiral substituted allylic compounds in high % ee. Enhancement of chirality in allyl substrates is challenging because chemistry on the allylic ligand occurs remotely from the chiral ligand also attached to the metal. There are several different points in the catalytic cycles depicted in Schemes **12.10a** and **b** where asymmetric induction could occur.⁶¹ These scenarios include the following:

1. Enantiotopic faces of the alkene: initial selective complexation of one or the other prochiral faces of the π bond of the allyl group to Pd will lead to one or the other enantiomer of the product (step **a**, Scheme **12.10a** or **b**).⁶²
2. Enantiotopic leaving groups: enantioselective ionization of the allylic leaving group during OA of a *meso* allylic system will lead to one or the other enantiomer of the product (step **b**, Scheme **12.10a** or **b**).

studies, see T. Hayashi, M. Kawatsura, Y. Uozumi, *J. Am. Chem. Soc.*, **1998**, *120*, 1681.

⁶⁰For accounts of early efforts in asymmetric Tsuji–Trost reactions, see B. M. Trost and P. E. Strege, *J. Am. Chem. Soc.*, **1977**, *99*, 1650 and G. Consiglio and R. M. Weymouth, *Chem. Rev.*, **1989**, *89*, 257.

⁶¹See Footnote 56.

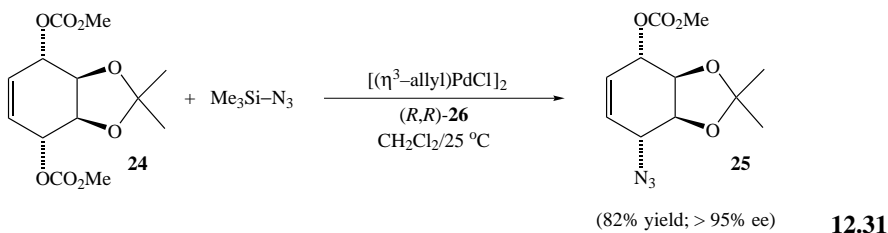
⁶²See Footnote 95 in Chapter 11 for a brief discussion on prochiral faces of a π bond.

3. Enantioface exchange in the η^3 -allyl complex: enantioselection occurs because only one of the two π faces of the η^3 -allyl ligand is presented to the attacking nucleophile (just prior to step **c**, Scheme **12.10a** or **b**).
4. Attack at enantiotopic termini of the η^3 -allyl ligand: when the η^3 -allyl ligand is symmetrically substituted at the two terminal positions, the two allylic positions are equivalent except in the chiral environment of the Pd complex and one position is more reactive (step **d**, Scheme **12.10a**, or step **c**, Scheme **12.10b**).
5. Attack by different enantiofaces of prochiral nucleophiles: if the nucleophile is an enolate ion, it has two prochiral faces that could attack the η^3 -allyl ligand; attack from the top face will lead to one enantiomer and attack from the bottom face will lead to the other (step **c**, Scheme **12.10a** or **b**).

We will consider a couple of these scenarios; readers are directed to literature references in Footnote 56 and the **Suggested Readings** section at the end of Chapter 12 for additional examples.

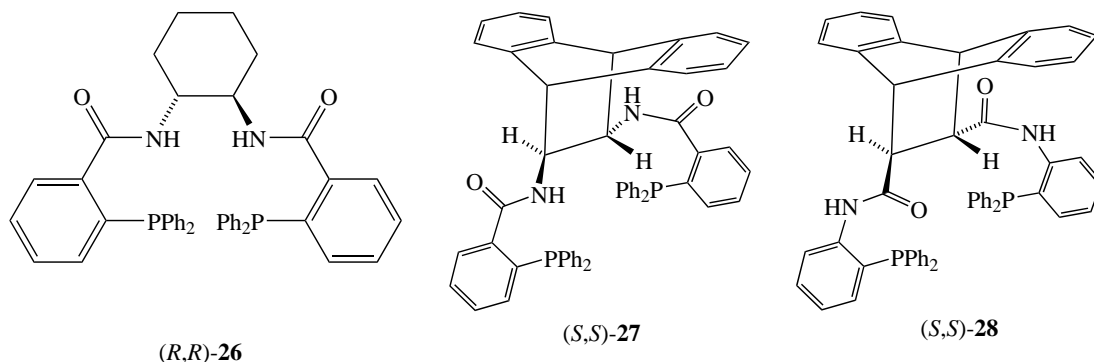
Enantioselective Ionization of Leaving Groups in *meso*-Disubstituted Allylic Compounds

Equation **12.31** shows an example of enantioselective displacement (desymmetrization) by azide ion of one of the two methyl carbonate ligands of *meso* compound **24** to yield **25** in 82% yield with >95% ee.⁶³ This was accomplished using a Pd complex also bound to chiral diamide–diphosphine ligand (**26**).⁶⁴ Other Trost ligands include structures **27** and **28**.



⁶³B. M. Trost and S. R. Pulley, *J. Am. Chem. Soc.*, **1995**, *117*, 10143.

⁶⁴Trost and co-workers have synthesized a series of these ligands, and now they are often called “Trost ligands.” For reports on the synthesis and reactivity of these ligands, see B. M. Trost, D. L. Van Vranken, and C. Bingel, *J. Am. Chem. Soc.*, **1992**, *114*, 9327 and B. M. Trost, B. Breit, S. Peukert, J. Zambrano, and J. W. Ziller, *Angew. Chem. Int. Ed. Engl.*, **1995**, *34*, 2386.



Trost has developed a predictive tool for deciding which prochiral leaving group reacts in *meso*-disubstituted allylic systems. This mnemonic is based on whether the relationship of the two phosphine groups is clockwise or counterclockwise (Figure 12-5) as one sights along the major C–C bond axis in the ligand that is perpendicular to its C_2 axis. A “clockwise” ligand (**27**) gives rise to clockwise ionization, and a counterclockwise ligand (**26**) induces “counterclockwise” ionization according to Figure 12-5.⁶⁵

Interestingly, when the order of the amide linkage was reversed to give ligand **28**, the enantioselectivity with respect to sense of orientation was just the opposite as obtained by the “normal” Trost ligands such as **26** and **27**.⁶⁶ It is apparent that work remains to be done in developing a predictive model that works for all C_2 -symmetric ligands.

Attack at Enantiotopic Termini of the η^3 -Allyl Complex

The symmetric 1,3-diphenyl allylic substrate **29** is typically used as a standard for testing the enantioselection potential of chiral ligands. Table 12-3 shows some results for a variety of ligands for this standard reaction. The reaction is quite sensitive to reaction conditions and the method of generating the nucleophile from diester **30**.

Good results were obtained with one of the PHOX ligands, which were developed by Pfaltz, Helmchen, and Williams and also used in Ir-catalyzed

⁶⁵(a) B. M. Trost and C. Lee, “Asymmetric Allylic Alkylation Reactions,” in *Catalytic Asymmetric Synthesis*, 2nd ed., I. Ojima, Ed., Wiley–VCH: New York, 2000, pp. 593–649 and (b) B. M. Trost and D. L. Van Vranken, *Chem. Rev.*, **1996**, 96, 395.

⁶⁶See Table 2 in footnote 65b.

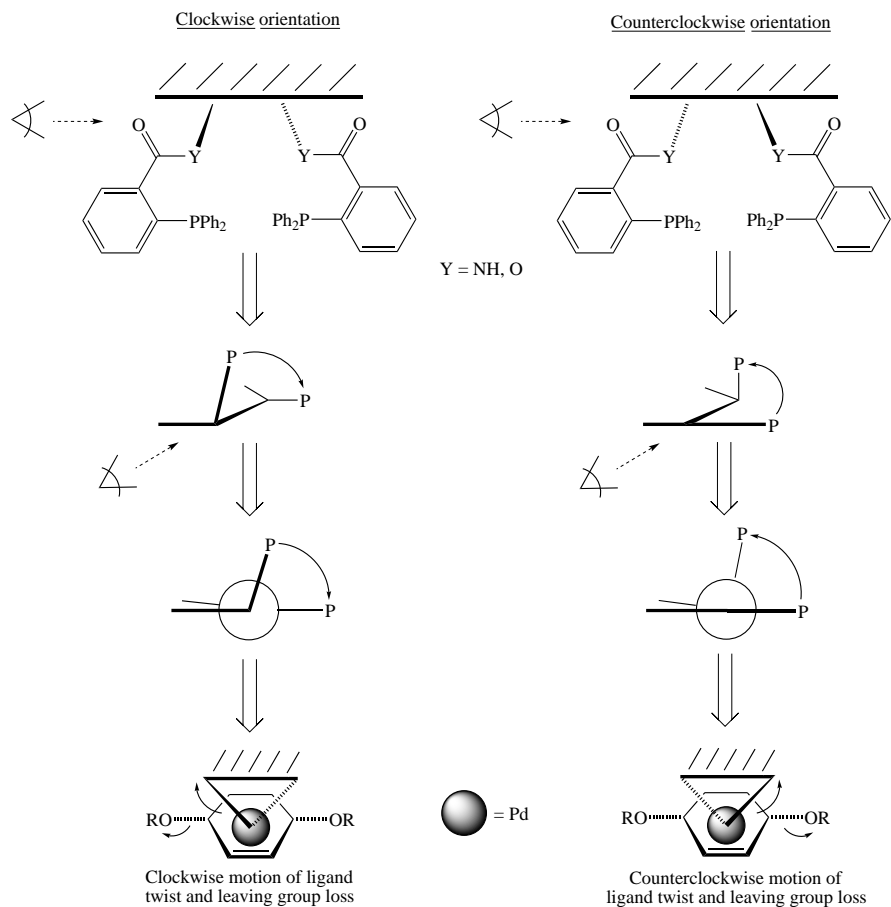
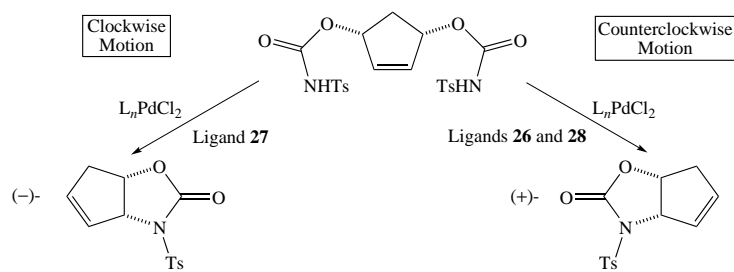


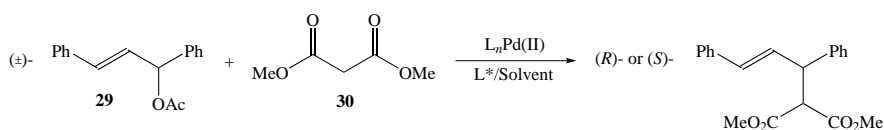
Figure 12-5
The Relationship of Enantioselective Desymmetrization to Sense of Phosphine Orientation in C_2 -Symmetric Bisphosphine-Bisamide Ligands

Example:



asymmetric hydrogenation (Section 12-1-1).⁶⁷ (*S*)-BINAP and (*S,S*)-Chiraphos also gave good results. C_1 -symmetric sparteine produced somewhat better

⁶⁷G. Helmchen and A. Pfaltz, *Acc. Chem. Res.*, **2000**, 33, 336 and J. M. J. Williams, *Synlett*, **1996**, 705.

Table 12-3 Yield and Enantioselectivity for Allylic Alkylation of a substrate that Binds to Pd as a η^3 -Allyl Ligand^a

Ligand (L*)	Nuc:	Solvent	% Yield	% ee
(S,S)-Chiraphos	Na-enolate of 30	THF	86	90
(–)-Sparteine	Na-enolate of 30	DMF	81	95
(–)- α -Isosparteine	Na-enolate of 30	DMF	87	82
(S)- <i>i</i> -Pr-PHOX	30 /BSA ^b	DMF	98	98
(S)-(–)-BINAP	Na-enolate of 3-NHAc- 30	CD ₂ Cl ₂	92	95

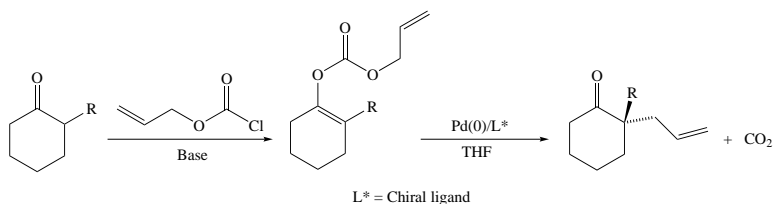
^aData taken from Table 8, Footnote 65b.

^bBSA: *N,O*-bis(trimethylsilyl)acetamide.

results than its C_2 -symmetric diastereomer (–)-isosparteine. It has been pointed out, however, that high % ee values obtained using the standard reaction do not always translate to other systems that are similar.⁶⁸

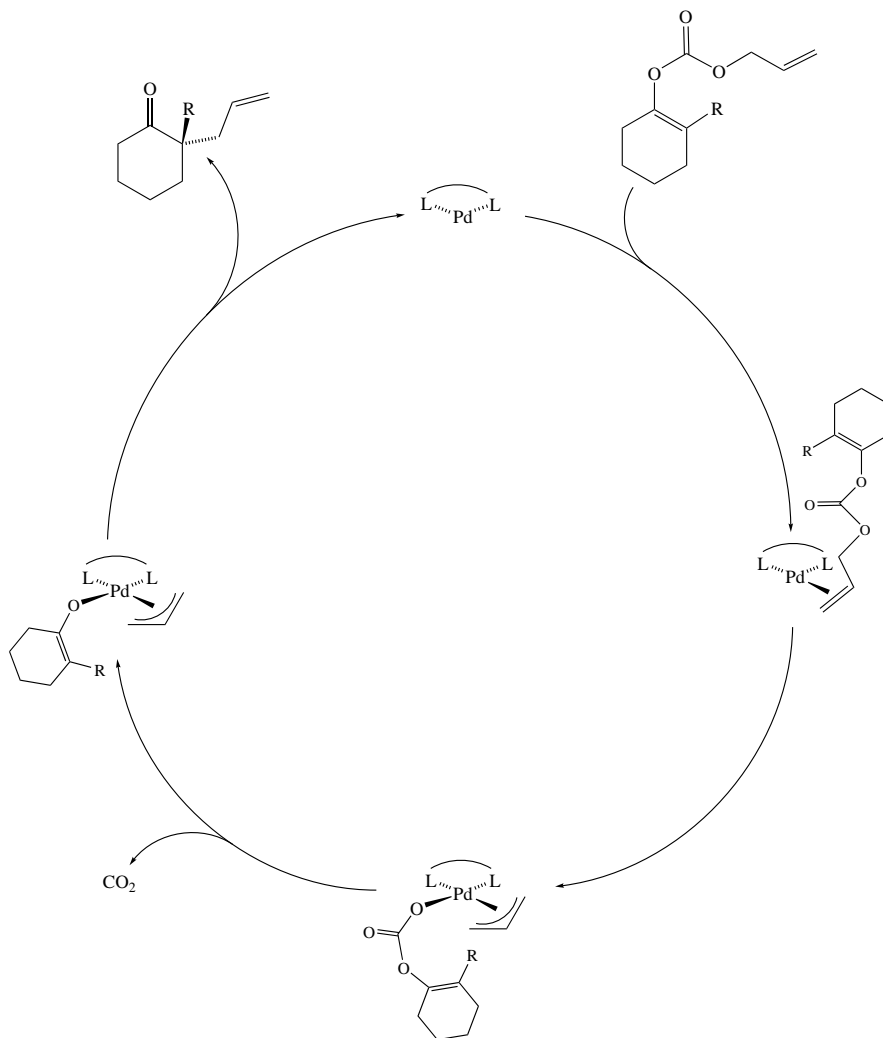
Use of the Tsuji–Trost Reaction for Asymmetric Creation of Quaternary Centers

One of the most challenging tasks in organic synthesis has long been the installation of quaternary centers, especially if that center is also a chirality center. The inherent high degree of steric hindrance associated with quaternary carbon atoms present a daunting challenge to chemists who attempt to create them. One recent and exciting development associated with research on the Tsuji–Trost reaction has been the development of a general means of enantioselectively creating quaternary centers adjacent to carbonyl groups. Equation 12.32 outlines the general procedure.⁶⁹

**12.32**

⁶⁸J. Tsuji, *Palladium Reagents and Catalysts*, Wiley: Chichester, England, 2004, p. 446.

⁶⁹D. C. Behanna and B. M. Stoltz, *J. Am. Chem. Soc.*, **2004**, *126*, 15044.

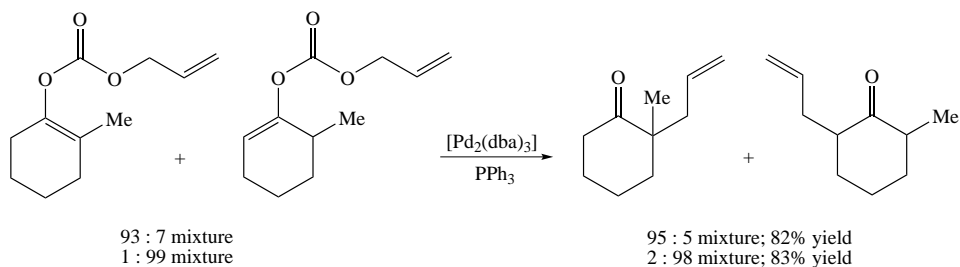
**Scheme 12.11**

General Mechanism for Tsuji-Trost Synthesis of Quaternary Carbons via Intramolecular Allylation of Enolates

In this reaction, the nucleophile (an enolate ion) comes from the enol ester part of the system, which is connected to the allyl group by a carbonate ester. Scheme 12.11 shows the steps in the catalytic process.

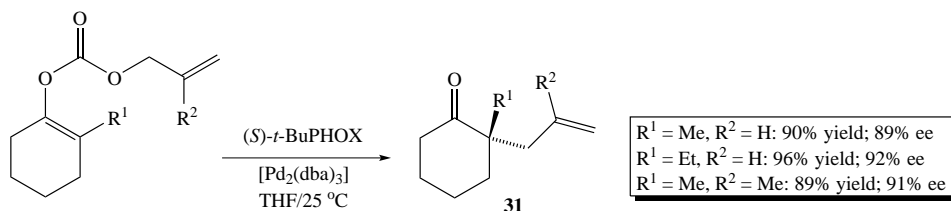
Complexation of allyl C=C bond to Pd is followed by OA and decarboxylation, which also produces an equivalent of CO₂ and an enolate. The enolate ion then complexes with Pd, so that both the η³-allyl group and the enolate are in close proximity to each other. RE of these two groups produces the quaternary center. Equation 12.33 shows that the position of the C=C bond in the enol group is preserved during allylation.⁷⁰

⁷⁰J. Tsuji, I. Minimani, and I. Shimizu, *Tetrahedron Lett.*, **1983**, 24, 1793.



12.33

In 2004, Stoltz reported the first asymmetric synthesis of ketone **31** (equation 12.34) in 90% yield with an ee of 89%, using the (*S*)-*t*-BuPHOX ligand.⁷¹

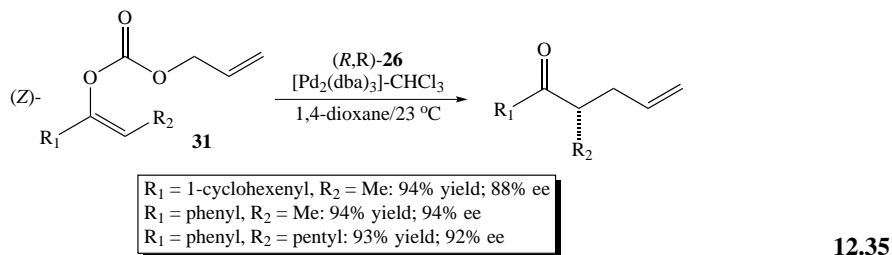


12.34

This procedure was extended to a number of related starting materials where the R^1 group, the substitution on the ring, and even the ring size were varied. In all cases studied, both the yield and the % ee were generally very high.

Shortly after Stoltz's report, Trost also showed that Pd catalysis in presence of Trost ligands such as **26** could also convert a wide variety of enol allyl carbonates into ketones with quaternary centers at the α -position in an analogous manner to that demonstrated in equation 12.34. In almost all cases reported, both yield and % ee values were high.

Trost was able to extend the scope of this reaction by investigating use of acyclic (*Z*)-enolate starting materials, such as compound **31** in equation 12.35.⁷² Again, both yield and % ee were quite good. Stoltz expanded his work to determine that β -ketoesters also give ketones with highly enantioenriched quaternary centers at the α -position (equation 12.36).⁷³

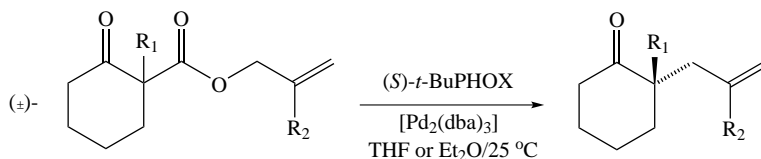


12.35

⁷¹D. C. Behenna and B. M. Stoltz, *J. Am. Chem. Soc.*, **2004**, *126*, 15044.

⁷²B. M. Trost and J. Xu, *J. Am. Chem. Soc.*, **2005**, *127*, 17180.

⁷³J. T. Mohr and B. M. Stoltz, *Chem. Asian J.*, **2007**, *2*, 1476.

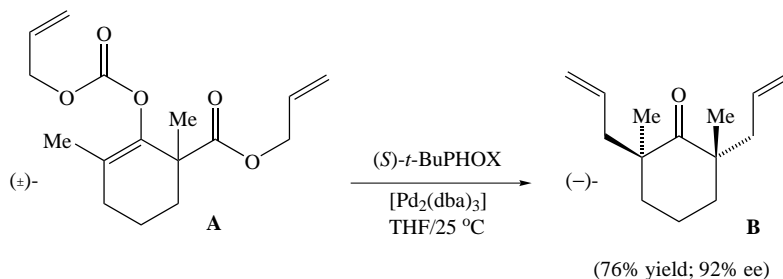


R₁ = Me, R₂ = H: 89% yield; 88% ee
 R₁ = Me, R₂ = Cl: 87% yield; 91% ee
 R₁ = CH₂Ph, R₂ = H: 99% yield; 85% ee

12.36

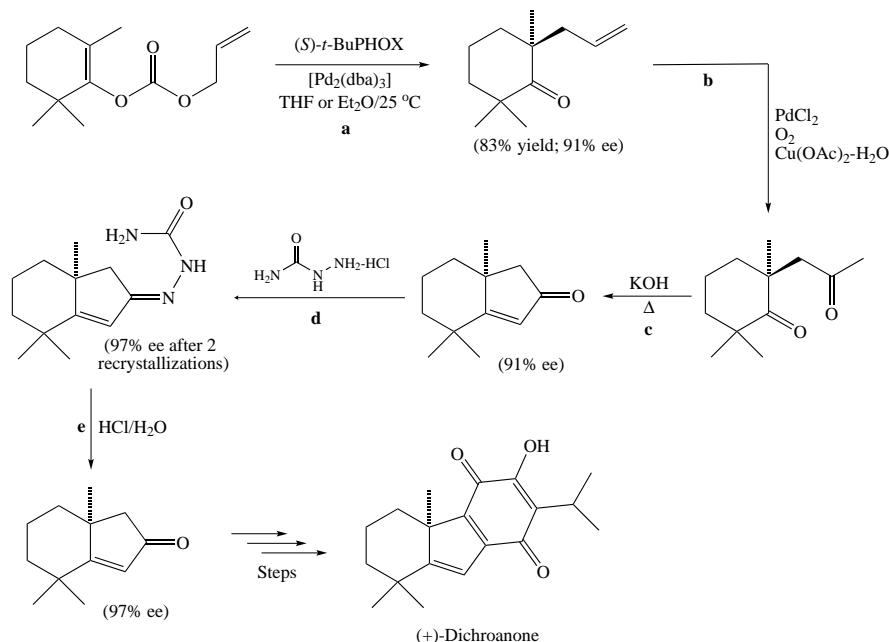
Exercise 12-6

Propose a stepwise mechanism that shows how compound **A** goes to **B**, which is a 4:1 mixture of two diastereomers, the more abundant of which has a ee of 92% and the other is achiral. What is the structure of the achiral diastereomer?



The enantioselectivity associated with quaternary allylation is connected with scenario 5 above (one of the five points associated in the catalytic cycles shown by Schemes **12.10a** and **b** where chirality could be induced), which is where enantioselection of one of two faces of the nucleophile (the enolate ion) occurs. Theoretical studies of the transformation using the PHOX ligand have shown support for an inner sphere mechanism, where nucleophilic attack of the enolate onto the η^3 -allyl ligand occurs from the Pd-bound enolate and not from an external nucleophile.⁷⁴ These studies have not been able to definitively determine the step that defines the enantioselectivity of the reaction, and it is not clear how these results would carry over to reactions involving the Trost ligands. At this time, selection of which ligand one should use not only to induce enantioselectivity but also to predict the sense of absolute configuration of any asymmetric Tsuji–Trost allylation is mostly based on empirical results. Work continues on this

⁷⁴J. A. Keith, D. C. Behenna, J. T. Mohr, S. Ma, S. C. Marinescu, J. Oxgaard, B. M. Stoltz, and W. A. Goddard III, *J. Am. Chem. Soc.*, **2007**, *129*, 11876.



useful transformation to widen its scope with respect to determining the range of starting materials allowed and leaving groups harboring sufficient reactivity.

Scheme 12.12 shows an example of where asymmetric installation of a quaternary center was a key step in the synthesis of the enantiomer of a chiral natural product, which occurred in 4% overall yield without the use of protecting groups.⁷⁵

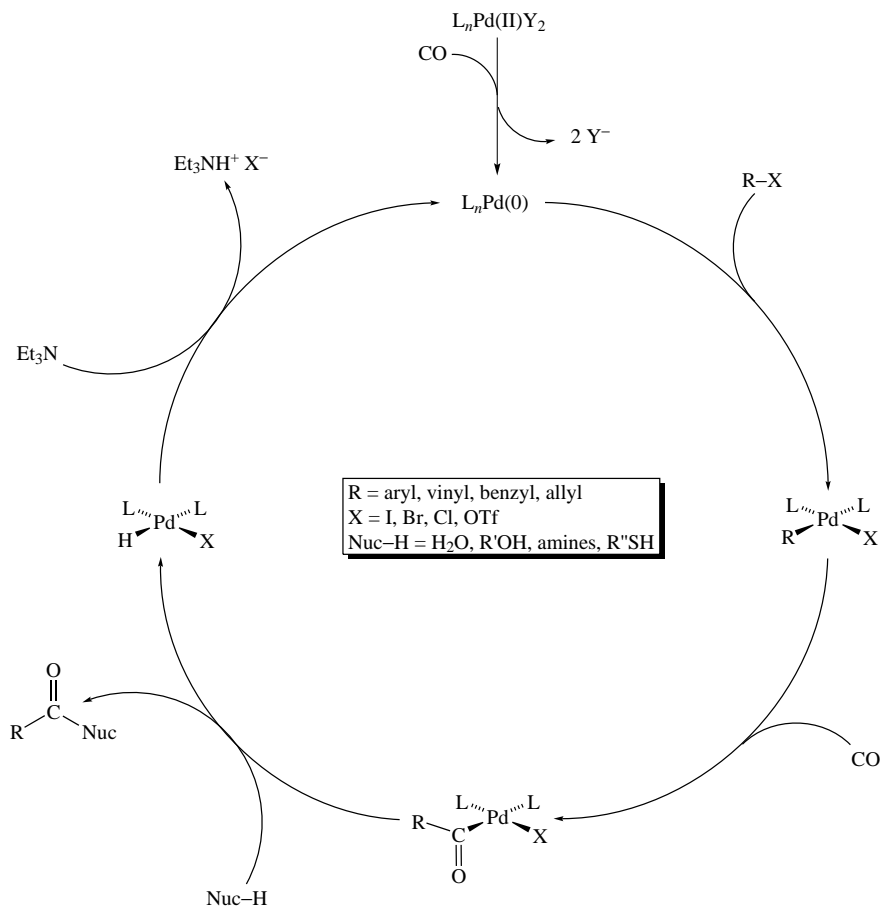
- a. What kind of reaction occurs during step **b** of Scheme 12.12?
b. Propose a mechanism for the transformation described in step **c**.

Exercise 12-7

12-3 CARBON–CARBON BOND FORMATION VIA CARBONYL AND ALKENE INSERTION

This section focuses on the second important means of C–C bond construction: migratory insertion. As discussed in Chapter 8, transition metal-catalyzed 1,1-carbonyl insertion (more properly called alkyl migration to a carbonyl ligand)

⁷⁵R. M. McFadden and B. M. Stoltz, *J. Am. Chem. Soc.*, **2006**, *128*, 7738.

**Scheme 12.13**

Catalytic Insertion
of CO into a Pd-C
Bond

and 1,2-migratory alkene insertion are general, stereospecific methods of forming new C-C bonds.

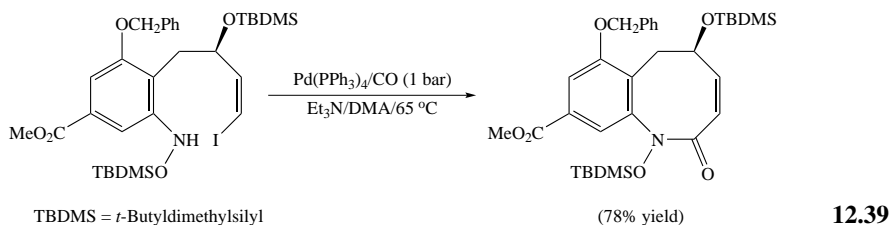
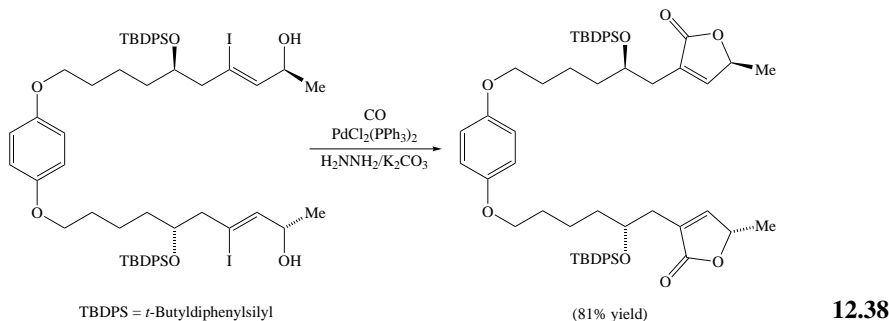
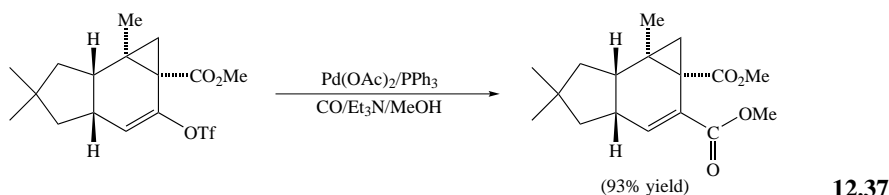
12-3-1 Carbonyl Insertions

Pd-Catalyzed Formation of Derivatives of Carboxylic Acids

σ -Alkyl (lacking β hydrogens), -alkenyl, and -aryl complexes of Pd readily undergo carbonyl insertion. In principle, any species with a C-X (X = leaving group) bond that can undergo oxidative addition with Pd(0) (without readily undergoing subsequent β -elimination) is capable of conversion to a product containing a C(C=O)Nuc (Nuc = nucleophile) functionality. This extremely versatile reaction is catalytic in Pd and occurs both inter- and intramolecularly. Scheme 12.13 depicts the likely catalytic cycle, involving a series of steps that should be familiar.⁷⁶

⁷⁶A. M. Trzeciak and J. J. Ziolkowski, *Coord. Chem. Rev.*, **2005**, 249, 2308.

Although Pd(0) complexes are catalytically active as is, Pd(II) salts have also been used; the reducing atmosphere of CO converts Pd(II) to Pd(0) *in situ*. A “proton sponge” such as Et₃N also must be present to tie up the acidic byproduct, HX. Equations 12.37,⁷⁷ 12.38,⁷⁸ and 12.39⁷⁹ provide a few examples of Pd-catalyzed carbonylation.



Equation 12.37 shows an intermolecular carbonylation of a vinyl group and subsequent nucleophilic attack by alcohol to form an ester. Intramolecular carbonylation occurs in dual fashion (equation 12.38) to yield lactones at the ends of the carbon skeleton. This reaction was the key step in the synthesis of the natural product (+)-parviflorin, which is a plant-derived compound possessing significant antitumor activity. Carbonylation also occurred in the cycloamidation

⁷⁷S. K. Thompson and C. H. Heathcock, *J. Org. Chem.*, **1990**, 55, 3004.

⁷⁸T. R. Hoye and Z. Ye, *J. Am. Chem. Soc.*, **1996**, 118, 1801.

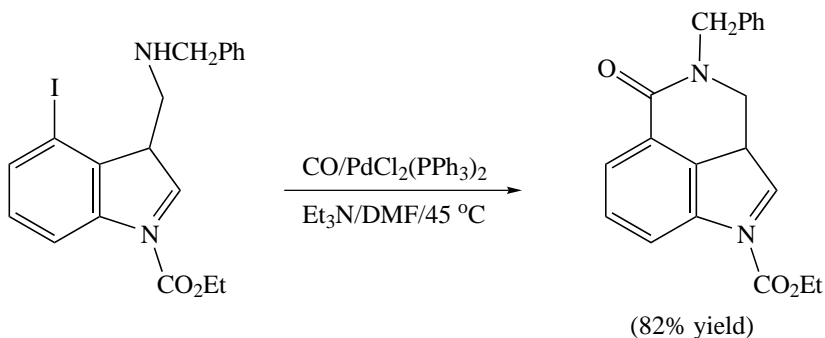
⁷⁹B. M. Trost and M. K. Ameriks, *Org. Lett.*, **2004**, 6, 1745.

reaction shown in equation 12.39. The resulting eight-membered ring lactam is considered a strategic precursor in the synthesis of a series of compounds that have activity against solid tumors.

The examples above are just a few of the countless applications of Pd-catalyzed carbonylation that have been reported. Although other metals will catalyze carbonylation, catalytic systems involving Pd continue to be the most widely used.⁸⁰

Exercise 12-8

Propose a stepwise mechanism for the transformation shown below.

**Asymmetric Hydroformylation**

We considered at length in Chapter 9 the hydroformylation reaction, which is the largest application of organometallic homogeneous catalysis on an industrial scale and is also a reaction involving carbonylation. Moreover, hydroformylation generally is a green reaction because it exhibits high atom economy, uses cheap and readily available starting materials, and occurs under close to neutral conditions.⁸¹ Much of the past efforts to improve this process have focused on enhancing hydroformylation's regioselectivity, ensuring that the linear-to-branched ratio of products is as high as possible while at the same time trying to maintain the mildest possible reaction conditions.

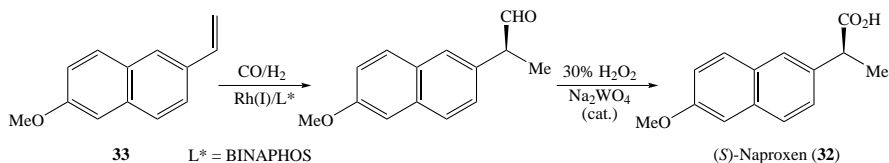
If, on the other hand, the regiochemistry of hydroformylation of mono-substituted alkenes were adjusted so that the branched aldehyde now becomes the predominant product, the possibility then exists to create enantioenriched aldehydes (equation 12.40) through catalysis in the presence of chiral, bidentate ligands. Hydroformylation of 1,1- and 1,2-disubstituted alkenes (equations 12.41 and 12.42) can also lead to chiral aldehydes, and these reactions present

⁸⁰J. Tsuji, *Palladium Reagents and Catalysts*, Wiley: Chichester, England, 2004, pp. 265–288.

⁸¹J. Klosin and C. R. Landis, *Acc. Chem. Res.*, **2007**, *40*, 1251.

Scheme 12.14

A Chiral Synthesis Route to Naproxen Using Asymmetric Hydroformylation



has been only modestly successful so far (low % ee values and low branched-to-linear ratios), but continued development of chiral ligands may make the process more amenable to industrial scale.

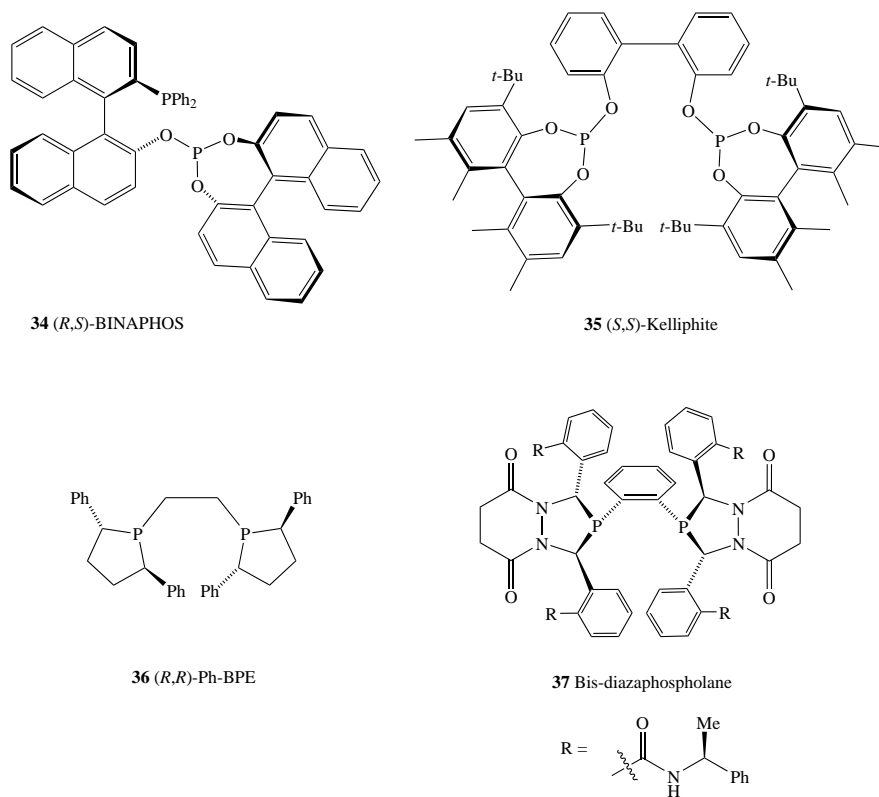
The most successful AHs have indeed involved use of styrene and related vinyl aromatic compounds as the starting material. Here, branched-to-linear ratios generally favor the branched aldehyde, for reasons that are not clear at this time.⁸⁴ The mechanism of AH is presumed to be the same as the achiral variety of Rh-catalyzed hydroformylation in the presence of bidentate ligands (Section 9-2-3). Three steps in the catalytic cycle are points where asymmetric induction could occur: (1) complexation of the alkene with the metal with π facial selection, (2) migratory insertion of the alkene to form the metal-alkyl complex, and (3) migratory insertion of the alkyl group onto a CO ligand. It seems likely that there is no one mechanistic step that produces asymmetric induction in all cases, although calculations have supported a model for predicting enantioselectivity of AH of styrene in the presence of specific bidentate ligands. This model correlates the sense of enantioselectivity as a function of which face of the prochiral alkene approaches the metal.⁸⁵

Some chiral ligands that have shown the most promise in providing both high regio- and enantioselectivity are illustrated in Figure 12-6. Phosphine-phosphite ligand **34** (*R,S*-BINAPHOS) was reported in 1993, and that event represented a breakthrough in AH, which up to that time had been relatively unsuccessful.⁸⁶ Ligand **35**, (*S,S*)-kelliphite, demonstrates an example of a chiral version of the diphosphites developed by Union Carbide in 1995 to promote linear

⁸⁴The aryl group attached to a C=C bond, of course, presents to the bidentate ligand attached to Rh different steric and electronic effects than would occur with small linear alkyl groups, so factors that favored hydroformylation to give linear aldehydes with simple, monosubstituted alkenes may not be applicable to monosubstituted aryl alkenes. Studies have shown that the most favorable enantio- and regioselectivities for AH of styrene result when bidentate chiral ligands bind to Rh in an *e-e* fashion (see related material in Section 9-2-3, **Bidentate Ligands**, for a discussion on *e-a* versus *e-e* trigonal bipyramid intermediates during Rh-catalyzed hydroformylation. See also M. Diéguez, O. Pàmies, and C. Claver, *Tetrahedron: Asymmetry*, **2004**, *15*, 2113).

⁸⁵For a brief discussion on the origin of enantioselectivity during AH, see footnote 82, pp. 437–439.

⁸⁶N. Sakai, S. Mano, K. Nozaki, and H. Takaya, *J. Am. Chem. Soc.*, **1993**, *115*, 7033.

**Figure 12-6**

Chiral Ligands
That Promote
Asymmetric
Hydroformylation

hydroformylation of propene and other low-molecular-weight alkenes at low temperature and pressure.⁸⁷ One of the DuPHOS family of phospholanes (*R,R*-Ph-DPE, **36**), which we encountered earlier in Section 12-1 as a very effective ligand for Rh-catalyzed asymmetric hydrogenation, has also been used successfully for AH. The last example (**37**) is known as a diazaphospholane, which is a member of a class of ligands created by Landis and co-workers.⁸⁸

Table 12-4 shows both regio- and enantioselectivity attendant Rh-catalyzed AH using the ligands shown in Figure 12-6. In addition to styrene, AH of other vinyl compounds listed in Table 12-4 shows something of the scope of the reaction. The results indicate that ligand **34** is an effective regio- and enantioselective ligand overall, but the reactions it promotes are rather sluggish compared with those run in the presence of ligands **36** or **37**, which also seem to possess the

⁸⁷C. J. Cobley, J. Klosin, C. Qin, and G. T. Whiteker, *Org. Lett.*, **2004**, 6, 3277.

⁸⁸C. R. Landis, W. Jin, J. S. Owen, and T. C. Clark, *Angew. Chem. Int. Ed.*, **2001**, 40, 3432 and T. C. Clark and C. R. Landis, *Tetrahedron: Asymmetry*, **2004**, 15, 2123.

Table 12-4 The Scope of Regio- and Enantioselectivity of Asymmetric Hydroformylation^a

$$\text{R-CH=CH}_2 \xrightarrow[\text{RhL}^*/3 \text{ hr}/80 \text{ }^\circ\text{C}/\text{PhMe}]{1 : 1 \text{ CO}/\text{H}_2 (10 \text{ bar})} \text{R-CH(Me)-CHO} + \text{R-CH}_2\text{-CH}_2\text{-CHO}$$

R = Ph, NCCH₂, OAc (branched) (linear)

Ligand	Styrene			Allyl cyanide			Vinyl acetate		
	Conversion %	b/l ^b	% ee	Conversion %	b/l	% ee	Conversion %	b/l	% ee
34	35	4.6	81 (<i>R</i>)	58	2.1	68 (<i>R</i>)	23	7.1	58 (<i>S</i>)
35	32	9.2	3 (<i>S</i>)	99	10.1	66 (<i>R</i>)	32	100	75 (<i>R</i>)
36	33	45.0	92 (<i>R</i>)	67	7.6	90 (<i>R</i>)	34	263	82 (<i>S</i>)
37	73	5.7	80 (<i>R</i>)	100	3.9	80 (<i>R</i>)	92	47	95 (<i>S</i>)

^aData taken from Footnote 81; percent conversion obtained after 3 hours of reaction time.

^bb/l: branched-to-linear ratio.

broadest scope of effectiveness of any ligands tested. Diphosphite ligand **35** also successfully promotes AH of styrene, but its activity is not general.

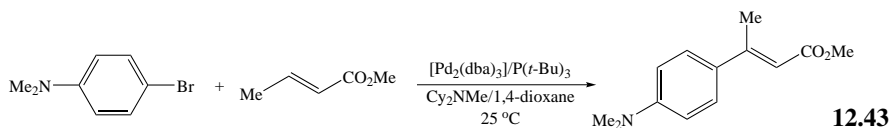
AH of other simple alkenes has also been studied, but the results have not been as promising as we have seen above. Although enantioselectivities can be high, depending on the bidentate ligand chosen, branched-to-linear aldehyde ratios generally are unfavorable. Overall, AH offers an attractive means of producing chiral aldehydes from some monosubstituted alkenes with enantioselectivities comparable to asymmetric hydrogenation. The reaction, however, still does not have the broad substrate scope that chemists have seen with asymmetric hydrogenation.

12-3-2 Carbon–Carbon Double Bond Insertion: The Heck Reaction

Chapters 8 and 11 emphasized that there are relatively few instances of insertion of a C=C bond into an M–C bond, with Z–N polymerization serving as the most significant example. Perhaps the migratory C=C insertion most useful to synthesis chemists is the Heck reaction, which is also known as Heck olefination.⁸⁹

⁸⁹The first report of C–C bond formation by C=C insertion, which we now call Heck olefination, was reported by Mizoroki in Japan in 1971 about a year before Heck's first paper appeared. Some refer to the Heck reaction as the Mizoroki-Heck reaction, but Mizoroki unfortunately died shortly after his original work was published. Since Heck and his co-workers vigorously pursued research on the mechanism and scope of this transformation after 1972, Heck's name is the only one usually attached to the process. T. Mizoroki, K. Mori, and A. Ozaki, *Bull. Chem. Soc. Jpn.*, **1971**, *44*, 581 and R. F. Heck and J. P. Nolley, Jr., *J. Org. Chem.*, **1972**, *37*, 2320.

Equation **12.43** shows an example of the reaction. The transformation is similar in scope to Pd-catalyzed carbonylation, only instead of CO insertion, migratory insertion C=C into a Pd–C bond occurs.



One approach to discussing Heck olefination is to link it to cross-coupling reactions, another very useful C–C bond forming transformation that we will cover in Section **12-4**. Like the Heck reaction, cross-couplings involve oxidative addition as the first step in the catalytic cycle. This is followed by transmetalation and reductive elimination to form new a C–C bond. After OA, the Heck olefination, on the other hand, proceeds through olefin coordination, migratory insertion of a C=C bond, and β -elimination. Because insertion is a key step in the overall process, the Heck reaction will be considered in the same section along with migratory carbonyl insertion.

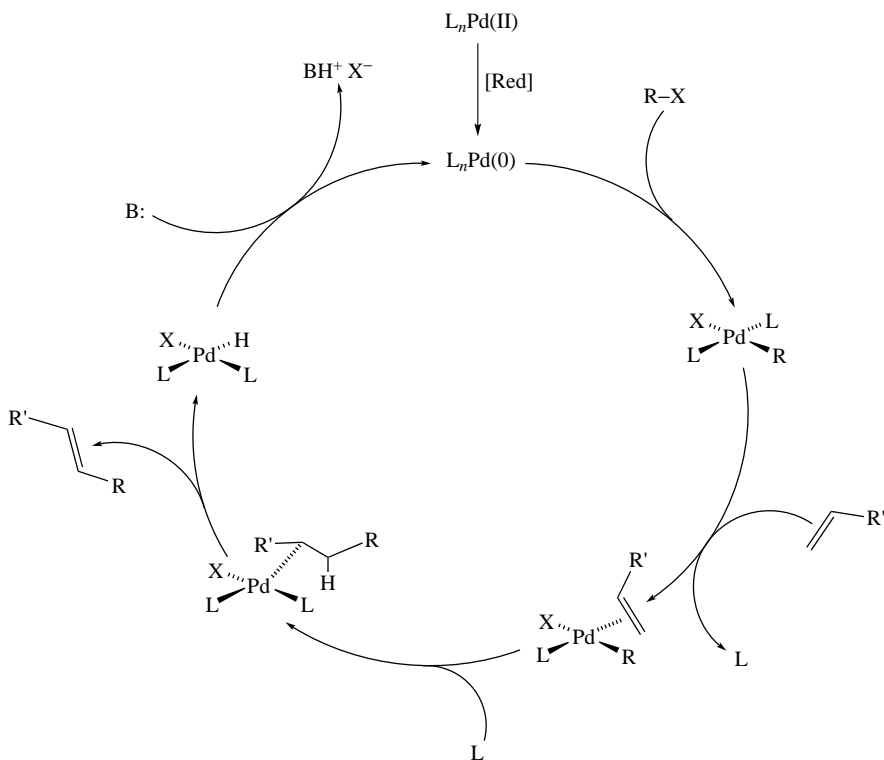
Heck olefination typically involves the oxidative addition of R–X—where R = aryl, vinyl, benzyl, or allyl (i.e., a substrate lacking β hydrogens attached to an sp^3 hybridized carbon) and X = Cl, Br, I, or OTf—followed by alkene complexation and 1,2-insertion of an alkene.⁹⁰ The last step is β -elimination. The Heck reaction is catalytic in Pd, and Scheme **12.15a** shows what is traditionally considered the catalytic cycle under most reaction conditions (known as the neutral pathway). Complete understanding of some aspects of the mechanism, however, still awaits further experimentation, and the large variability in reaction conditions used means that a universal, all-encompassing mechanism for the reaction is quite unlikely.⁹¹ Scheme **12.15b** shows a very similar cycle, called the cationic cycle, which occurs when the substrate is an unsaturated triflate. Vinyl or aryl halides, allowed to react in the presence of a halide scavenger such as Ag(I), also transform via the cationic cycle.⁹² This seems to be the pathway of choice when, in addition to the leaving group characteristics mentioned above, the reaction is set up to undergo intramolecular Heck olefination in the presence of a Pd–bisphosphine catalyst.

Recent work suggests that there could be even another version of the cycle, when Pd(OAc)₂ is used as the Pd source, which involves formation of anionic Pd

⁹⁰For most Heck reactions, the order of reactivity is I > OTf > Br >> Cl.

⁹¹(a) For a recent, lucid discussion of the mechanism, see J. P. Knowles and A. Whiting, *Org. Biomol. Chem.*, **2007**, *5*, 31. For two reviews of some of the early mechanistic work on the Heck reaction that include summaries of its scope, see (b) R. F. Heck, *Acc. Chem. Res.*, **1979**, *12*, 146 and (c) R. F. Heck, *Org. React.*, **1982**, *27*, 345.

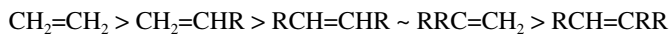
⁹²W. Cabri, I. Candiani, S. DeBernardis, F. Francalanci, and S. Penco, *J. Org. Chem.*, **1991**, *56*, 5796 and F. Ozawa, A. Kubo, and T. Hayashi, *J. Am. Chem. Soc.*, **1991**, *113*, 1417.

**Scheme 12.15a**

The Neutral
Catalytic Cycle of
the Heck Reaction

complexes along the pathway to the final product.⁹³ These findings also suggest that anionic, pentacoordinate Pd complexes are involved in the mechanism, but this is counter to the known reluctance of Pd to form five-coordinate structures with monodentate ligands.⁹⁴ The anionic variation does not seem to apply, however, when other sources of Pd are used and when common leaving groups such as X = I or OTf are present.

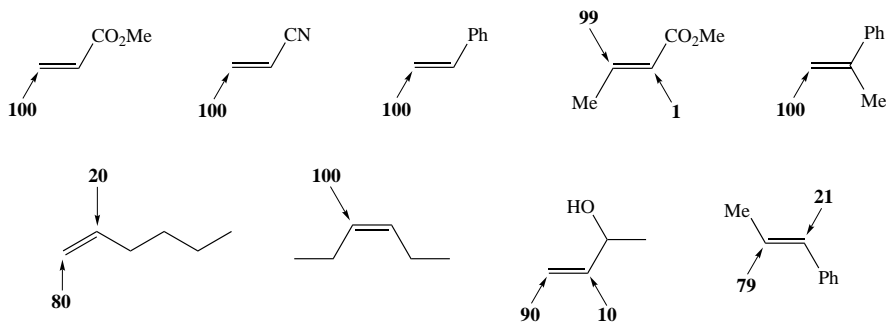
The rate of reaction and regioselectivity of Heck olefination are sensitive to steric hindrance about the C=C bond of the vinylic partner. For simple aryl halides reacting with alkenes, the rate of reaction as a function of alkene substitution varies⁹⁵ according to



⁹³C. Amatore and A. Jutand, *Acc. Chem. Res.*, **2000**, 33, 314.

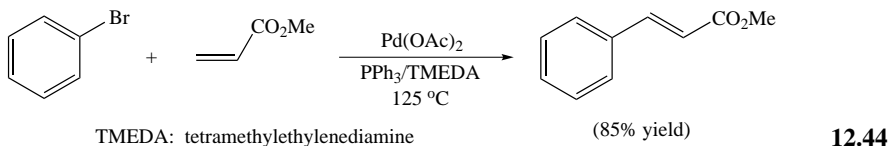
⁹⁴M. Bröring and C. D. Brandt, *Chem. Commun.*, **2003**, 2156 and S. Hansson, P.-O. Norrby, M. P. T. Sjögren, B. Åkermark, M. E. Cucciolito, F. Giordano, and M. Vitagliano, *Organometallics*, **1993**, 12, 4940.

⁹⁵See Footnote 91c.

**Figure 12-7**

Regioselectivity of Addition of an Aryl Halide to Various Alkenes during Heck Olefination

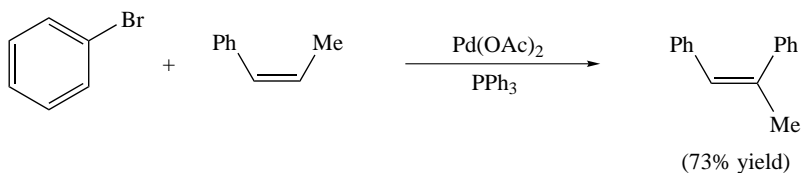
alkenes react with aryl halides, the β hydrogen removed (Scheme **12.15a**) is the one that leads preferentially to an *E*-double bond (equation **12.44**).⁹⁷



1,2-Disubstituted alkenes insert to give a mixture of *E*- and *Z*-trisubstituted olefins, with usually the more stable isomer predominating. If a choice of β hydrogens is available, the most acidic is lost in the β -elimination step.

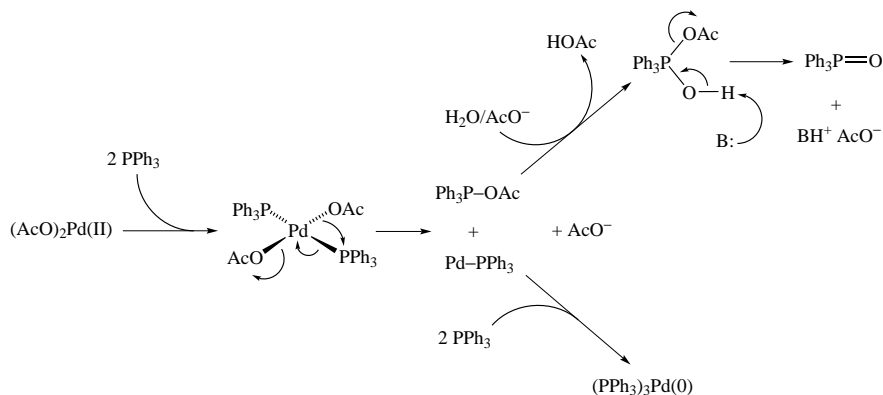
Exercise 12-9

Consider the mechanistic pathway shown in Scheme **12.15a** and show that (*E*)-1,2-diphenyl-1-propene ought to result as the major product, analogous to the conversion shown in the equation below, if the starting material is (*E*)-1-phenyl-1-propene.



Although Pd(0) is the active oxidation state for catalysis and some procedures use Pd(0) catalysts such as Pd(PPh₃)₄ or [Pd₂dba₃], typical Heck olefination procedures utilize Pd(II) salts (such as PdCl₂, Pd(OAc)₂, or Na₂PdCl₄) and a reducing

⁹⁷See Footnote 91b and H. A. Dieck and R. F. Heck, *J. Am. Chem. Soc.*, **1974**, 96, 1133.

**Scheme 12.16**Reduction of Pd(II)
to Pd(0) by PPh₃

agent to generate Pd(0) *in situ*. When Pd(OAc)₂ is used as the Pd source, phosphines are often present. They serve two purposes: (1) they act as stabilizing ligands to Pd and (2) they reduce Pd(II) to Pd(0) by a pathway proposed by Jutand and Hayashi.⁹⁸ Scheme 12.16 shows this pathway. Other pathways for reduction are possible, including reduction by Et₃N.⁹⁹

Since its discovery over 35 years ago, the Heck reaction has undergone several modifications. The use of DMF as a solvent is usually preferable to that originally employed, CH₃CN.¹⁰⁰ The presence of Bu₄NCl with Pd(OAc)₂, especially accompanied by KHCO₃ or K₂CO₃ in DMF, increases the reaction rate and allows the reaction to proceed at room temperature instead of 80–130 °C, as normally required.¹⁰¹ Originally thought to serve as a phase transfer catalyst,¹⁰² the quaternary ammonium salt probably serves also as a source of Cl⁻, which tends to bind to Pd and stabilize intermediate metal complexes involved in the catalytic cycle.

⁹⁸C. Amatore, A. Jutand, and M. A. M'Barki, *Organometallics*, **1992**, *11*, 3009 and F. Ozawa, A. Kubo, and T. Hayashi, *Chem. Lett.*, **1992**, 2177.

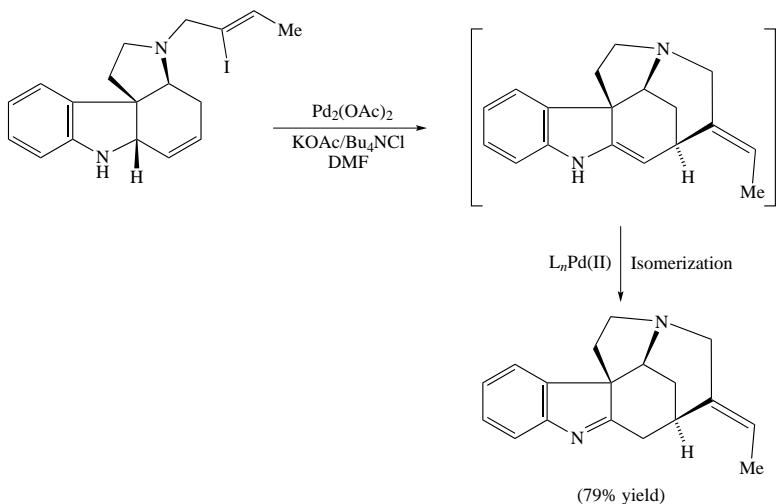
⁹⁹See Footnote 91a.

¹⁰⁰A. Spencer, *J. Organomet. Chem.*, **1984**, *270*, 115, which includes references to his earlier work.

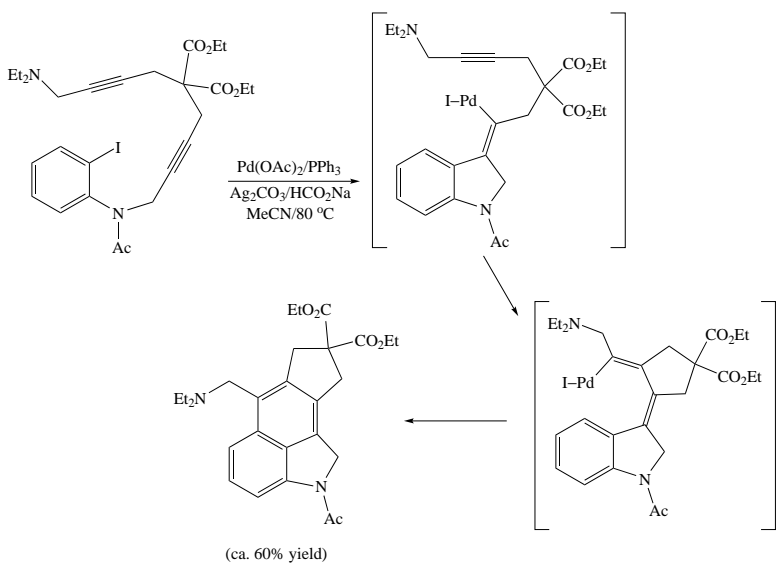
¹⁰¹T. Jeffery, *Tetrahedron Lett.*, **1985**, *26*, 2667; *J. Chem. Soc., Chem. Commun.*, **1984**, 1287; and R. Larock and B. E. Baker, *Tetrahedron Lett.*, **1988**, *29*, 905. These reaction parameters are sometimes referred to as “Jeffery’s ligandless conditions.”

¹⁰²A phase transfer catalyst is typically a quaternary ammonium salt with medium to long hydrocarbon chains attached to the nitrogen. The hydrocarbon region is hydrophobic and thus compatible with nonpolar organic solvents. The charged nitrogen end of the molecule is hydrophilic or water compatible. Because of these properties, phase transfer catalysts function as anion carriers capable of transporting nucleophiles or bases from an aqueous phase to an organic liquid phase. Reactions that require the presence of the salt of a strong nucleophile, base, or oxidizing agent—normally not soluble in a non-polar solvent—proceed considerably faster in the presence of such catalysts. See M. B. Smith and J. March, *Advanced Organic Chemistry*, 5th ed., Wiley: New York, 2001, pp. 454–456.

Equations 12.45¹⁰³ and 12.46¹⁰⁴ show two examples of intramolecular Heck olefination. In the first case, under Jeffrey's ligandless conditions, the Pd catalyst also acts to isomerize a C=C bond to give a final product that has the C=N bond in conjugation with the aromatic ring. The second example demonstrates how the Heck reaction can cause alkynes as well as alkenes to undergo 1,2-insertion. The transformation is also a nice application of tandem Pd-catalyzed reactions to create a rather complex ring system.



12.45



12.46

¹⁰³V. H. Rawal and C. Michoud, *J. Org. Chem.*, **1993**, 58, 5583.

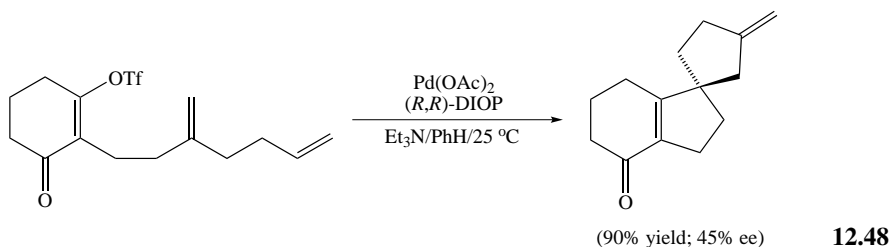
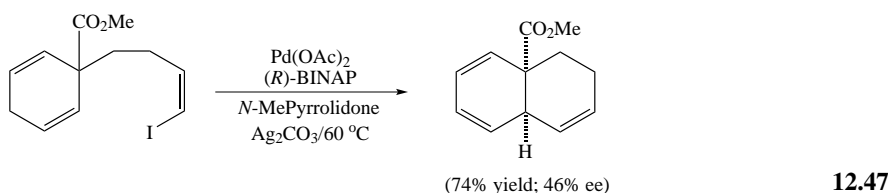
¹⁰⁴R. Grigg, V. Loganathan, and V. Sridharan, *Tetrahedron Lett.*, **1996**, 37, 3399.

How does the last intermediate in equation **12.46** transform to the final product? What kind of reaction must occur in this step?

Exercise 12-10

Asymmetric Heck Reactions

The first examples of asymmetric Heck reactions (AHRs) appeared around 20 years ago, reported almost simultaneously by Shibasaki and Overman. Equations **12.47**¹⁰⁵ and **12.48**¹⁰⁶ show these first efforts. Despite the modest enantioselectivities observed, the transformations are notable because they show that tertiary and especially difficult to build quaternary centers can be constructed in a stereo- and regioselective manner. Equation **12.48** also shows an example of tandem Heck reactions in which two cyclizations occur in sequence.

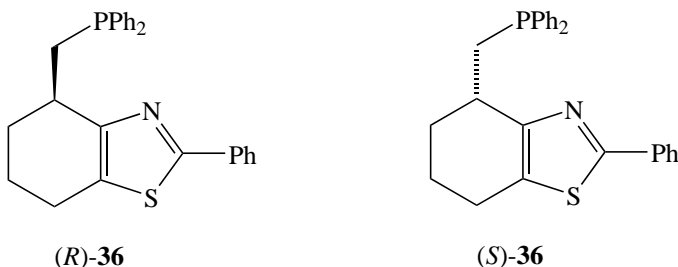


Studies suggest that the mechanism of AHRs is quite similar to the achiral version, which includes the same fundamental steps in the catalytic cycles that we have seen already. The major difference is the presence of chiral bidentate ligands, such as bisphosphines [$R_2P-Y-PR_2$], phosphine-phosphites [$R_2P-Y-P(OR)_2$], bisphosphites [$(RO)_2P-Y-P(OR)_2$], aminophosphines [$R_2N-Y-PR_2$], or diamines (such as (–)-sparteine), which we encountered earlier in Chapter 12. The bidentate variation of the cationic cycle, shown in Scheme **12.15b**, seems to explain most aspects of the mechanism of AHR when $X = OTf$ or I (in the presence of halide scavengers). Throughout the cycle, the ligand remains bidentate, and this factor seems to enhance enantioselectivity. The neutral cycle variant, which ought to be

¹⁰⁵Y. Sato, M. Sodeoka, and M. Shibasaki, *J. Org. Chem.*, **1989**, *54*, 4738.

¹⁰⁶N. E. Carpenter, D. J. Kucera, and L. E. Overman, *J. Org. Chem.*, **1989**, *54*, 5846.

similar to Scheme 12.15a, may involve the dissociation of one chelating atom from Pd, and this could diminish enantioselectivity. Although either coordination of the alkene to Pd or migratory insertion could lead to enantiodifferentiation, a recent theoretical (DFT) and experimental study, using chiral aminophosphines (*R*)- and (*S*)-**36** as the bidentate ligand, indicated that the migratory insertion of alkene is the step responsible for asymmetric induction.¹⁰⁷ The study also found that the less favored of the diastereomeric complexes leading to insertion was more reactive than the more stable complex, exactly the same kind of situation observed by Halpern in his investigation of asymmetric hydrogenation. It is not clear at this time whether these results apply to other systems.



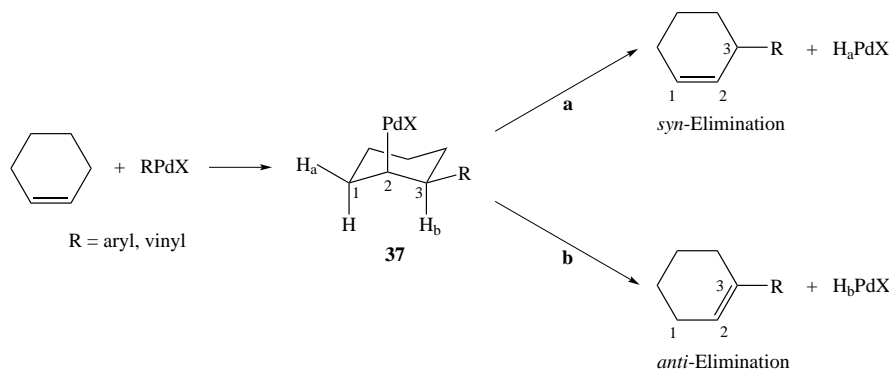
Besides enantioselectivity, another concern in AHRs is the regioselectivity of β -hydride elimination. Scheme 12.17 shows two scenarios that could result once migratory alkene insertion occurs to give intermediate **37**.¹⁰⁸ Path **b** results in the destruction of the chirality center, whereas path **a** preserves it. This is a serious problem for intermolecular AHRs, but less so for the intramolecular version. Thus, it is not surprising that most good examples of AHR involve intramolecular cyclization to form five- and six-membered rings, as Scheme 12.17 (path **a**) shows. Elimination of HPdX from carbons 2 and 3 gives the more substituted alkene, which destroys the chirality center, but this is not likely because that would involve *anti* elimination.¹⁰⁹ Loss of hydrogen from C₁, on the other hand, involves *syn* elimination; the chirality center is preserved.

Another scenario for AHRs is the formation of quaternary chirality centers. Here, β -elimination via path **b** is impossible (when H _{β} is replaced by a hydrocarbyl group). The downside, however, is that construction of such centers is difficult because it requires the insertion of trisubstituted C=C bonds, which normally react sluggishly in Heck reactions. Some of this lack of reactivity, however, can

¹⁰⁷S. T. Henriksen, P.-O. Norrby, P. Kaukoranta, and P. G. Andersson, *J. Am. Chem. Soc.*, **2008**, *130*, 10414.

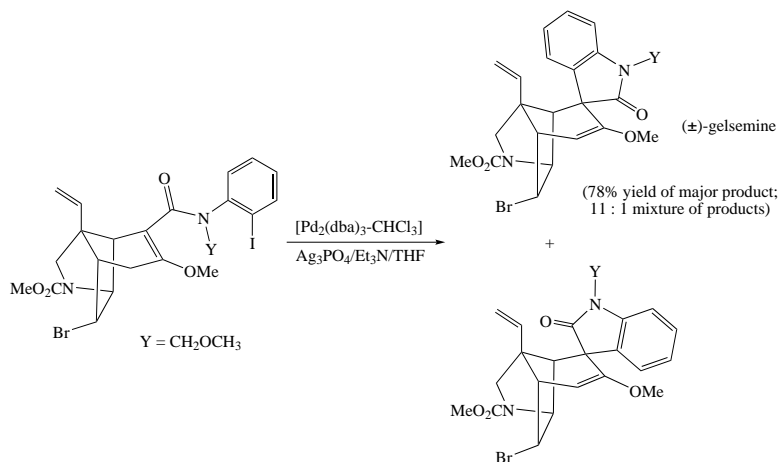
¹⁰⁸A. B. Dounay and L. E. Overman, *Chem. Rev.*, **2003**, *103*, 2945, and Footnote 91a.

¹⁰⁹In the intermolecular process, rotation about the C₂-C₃ bond could occur, leading to *syn*-elimination. With a rigid ring system as shown in Scheme 12.17, this is not possible.



Scheme 12.17
Regioselectivity and
the Heck Reaction

be overcome in intramolecular Heck reactions because entropy constraints are minimized. Judicious choice of solvent and coreactants can also enhance yields, making this transformation one of the best ways of creating quaternary centers (see also Section **12-1-2**). A rather spectacular demonstration of the use of Heck olefination to create a quaternary center, albeit a racemic transformation, was used in the synthesis of the alkaloid (\pm)-gelsemine (equation **12.49**).¹¹⁰



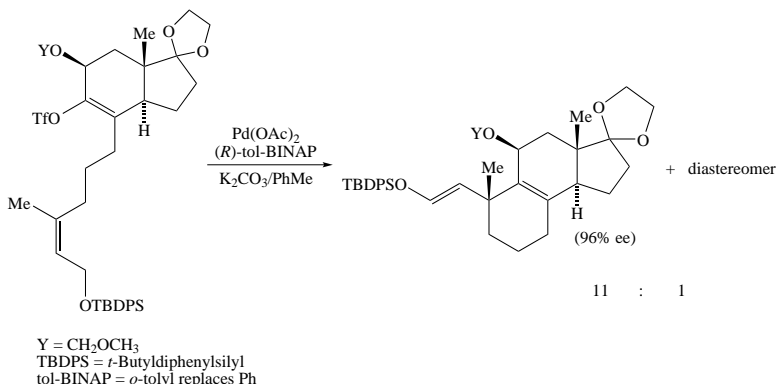
12.49

Equation **12.50** demonstrates an application of AHR to form a quaternary chiral center using (*R*)-tol-BINAP (same as BINAP except *o*-tolyl replaces Ph) as the bidentate ligand.¹¹¹ Another good example is shown in equation **12.51**, where

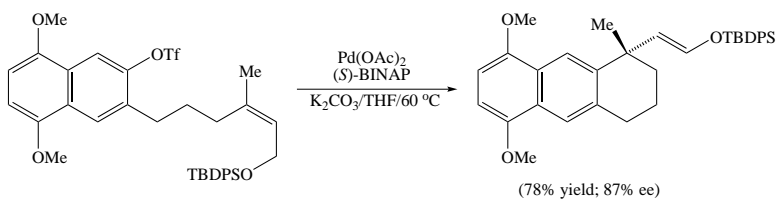
¹¹⁰A. Madin, C. J. O'Donnell, T. Oh, D. W. Old, L. E. Overman, and M. J. Sharp, *J. Am. Chem. Soc.*, **2005**, *127*, 18054.

¹¹¹S. Honzawa, T. Mizutani, and M. Shibasaki, *Tetrahedron Lett.*, **1999**, *40*, 311 and T. Mizutani, S. Honzawa, S.-Y. Tosaki, and M. Shibasaki, *Angew. Chem. Int. Ed.*, **2002**, *41*, 4680.

(*S*)-BINAP is used as the chiral ligand.¹¹² The AHR continues to find wide use in synthesis as a means of installing tertiary and quaternary chirality centers.¹¹³



12.50



12.51

12-4 CARBON-CARBON BOND FORMATION VIA TRANSMETALATION REACTIONS (CROSS-COUPLING REACTIONS)

12-4-1 Introduction

Representing the third important method of C–C bond formation covered in Chapter 12, *cross-coupling* reactions constitute one of the most powerful and widely used tools available today to the synthesis chemist. Equation **12.52** shows the general overall reaction, which involves combination of two carbon fragments (R and R'), one typically originating from an organohalide and the other from a metal hydrocarbyl compound. A transition metal complex serves as catalyst and template for the coupling to occur.



¹¹²A. Kojima, T. Takemoto, M. Sodeoka, and M. Shibasaki, *J. Org. Chem.*, **1996**, *61*, 4876.

¹¹³For reviews of the AHR, see Footnote 108 and M. Shibasaki, E. M. Vogl, and T. Oshima, *Adv. Synth. Catal.*, **2004**, *346*, 1533.

The variety of carbon fragments that can join and the general tolerance of the reaction conditions to functional groups already present on these fragments lead to countless possibilities for rapid construction of complex molecules, especially biologically active compounds. One key difference between cross-coupling reactions and the Tsuji–Trost allylation or Heck olefination is the occurrence of a transmetalation step during the catalytic cycle.

Transmetalation, according to general equation **12.53**, is an excellent method for introducing σ -bonded hydrocarbon ligands into the coordination sphere of transition metals. The equilibrium is thermodynamically favorable from left to right if the electronegativity of M (usually a mid- to late-transition metal) is greater than that of M' (often a main group or early-transition metal) and is kinetically favorable if an empty orbital is available on both metals.¹¹⁴

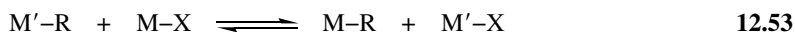


Table **12-5** shows a portion of the periodic table with Pauling electronegativities listed below each element.¹¹⁵ Use of these electronegativity values in conjunction with equation **12.53** allows one to predict whether a particular transmetalation is favorable or unfavorable.

Organolithium and magnesium reagents (containing highly electropositive metals, M') are the most reactive transmetalation reagents. Unfortunately, these compounds are too reactive toward many functional groups, which might also be present in the substrates that are joined in cross-coupling. Less reactive organozirconium, zinc, tin, boron, and aluminum compounds often possess just the right amount of reactivity to be useful in transferring σ -bonded hydrocarbyl ligands to M without affecting functional groups on ligands already attached to M. Even if transmetalation is not favorable thermodynamically, based on electronegativity differences between M and M', the reaction is often useful because even small concentrations of transmetalation product can react in a subsequent irreversible step, thus driving the equilibrium.

¹¹⁴E-i. Negishi, *Organometallics in Organic Synthesis*, Wiley: New York, 1980, pp. 54–56.

¹¹⁵It should be pointed out that the Pauling electronegativities listed in Table **12-5** indeed support the theory that transmetalation among Pd, Rh, Ru, or Pt and a variety of more electropositive metals should readily occur based on thermodynamic grounds. It must also be emphasized, however, that more recent determinations of electronegativities, based on both high-level theoretical calculations and experiment, indicate that Pauling-scale electronegativity values of second- and third- row transition metals of Groups 8, 9, and 10 are probably too high (see J. B. Mann, *et al.*, *J. Am. Chem. Soc.*, **2000**, *122*, 5132, and references therein). It may be that transmetalations to Pd, for example, which appear to be infeasible on the basis of electronegativity differences, are feasible because of the irreversibility of subsequent steps in a catalytic cycle.

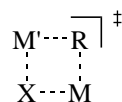
Table 12-5 Electronegativities^a of Selected Elements Useful in Synthesis

Li												B	C
0.98												2.04	2.55
Na	Mg											Al	Si
0.93	1.31											1.61	1.90
K	Ca	Sc	Ti	V	Cr	Mn	Fe	Co	Ni	Cu	Zn		
0.82	1.00	1.36	1.54	1.63	1.66	1.55	1.83	1.88	1.91	1.90	1.65		
			Zr		Mo		Ru	Rh	Pd	Ag			Sn
			1.33		2.16		2.2 ^b	2.28	2.20	1.93			1.96
					W		Os	Ir	Pt	Au	Hg	Tl	Pb
					2.36		2.2 ^b	2.20	2.28	2.54	2.00	1.62	2.33

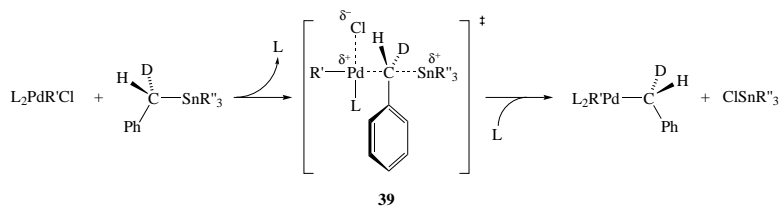
^aPauling electronegativities taken from A.L. Allred, *J. Inorg. Nucl. Chem.*, **1961**, 17, 215.

^bEstimated.

Transmetalation may proceed via a concerted σ bond metathesis, involving a four-center transition state (**38**) (or even a metallacyclobutane intermediate) that leads to transfer of the organic group R to M with retention of configuration.

**38**

Other mechanisms are possible, however. For example, the original mechanism proposed for the transmetalation step in Stille coupling (Section 12-4-2) involved an acyclic S_E2 (Section 8-4-1) pathway (equation 12.54), which proceeds through transition state **39** such that R is transferred with inversion of configuration.¹¹⁶ We will further discuss this dichotomy in Section 12-4-2.

**12.54**

Palladium is by far the most useful transition metal (M) involved as the acceptor metal in synthetically useful cross-coupling reactions. There are several different types of cross-couplings involving transmetalation to Pd, and the rest of this section will consider four of the most commonly used and useful of these.

¹¹⁶J. K. Stille, *Angew. Chem. Int. Ed. Engl.*, **1986**, 25, 508.

Table 12-6 Synthetically Useful Pd-Catalyzed Cross Coupling Reactions^a

$$\text{R}'\text{-X} + \text{M}'\text{-R} \xrightarrow{\text{L}_n\text{Pd}(0)} \text{R}'\text{-R} + \text{M}'\text{-X}$$

Name	M'	L	First reported
Stille	Sn	PY ₃ ^b	1976–1978
Suzuki	B	PY ₃ ^c	1979
Sonogashira	Cu	PY ₃ ^d	1975
Negishi	Zn	PY ₃ ^e	1977

^aX = I, Br, Cl, OTf, or OPO(OR'')₂ (R'' = simple alkyl group); R and R' are typically aryl, vinyl, allyl, benzyl, or acyl (R only), although alkyl groups can be used if β-elimination can be suppressed.

^bY = Ph, 2-furyl; PdCl₂(MeCN)₂ and [Pd₂(dba)₃] are also useful catalysts.

^cY = Ph, *o*-tolyl; PdCl₂(dppf) is also a useful catalyst [dppf = 1,1'-bis(diphenylphosphino)ferrocene].

^dY = Ph; PdCl₂(MeCN)₂ and PdCl₂(PPh₃)₂ are also widely used.

^eY = Ph, 2-furyl; [Pd₂(dba)₃] is also widely used.

Table 12-6 lists these four types, showing both the differences and the similarities among them.

Scheme 12.18 outlines the general catalytic cycle for cross-coupling, the key steps of which are (a) oxidative addition of R'–X to Pd(0), (b) *cis*–*trans* isomerization of a square planar Pd complex (if necessary), (c) transmetalation of R–M' to give R'–Pd–R, (d) *trans*–*cis* isomerization (if necessary), and (e) reductive elimination of R'–R and regeneration of Pd(0).

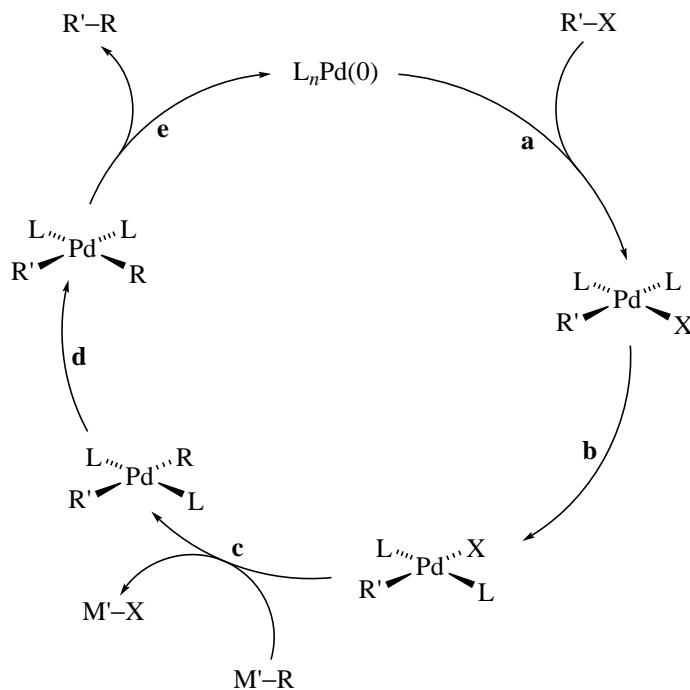
12-4-2 Stille Cross-Coupling

Early efforts by Eaborn¹¹⁷ and Kosugi,¹¹⁸ who independently studied transmetalations between Pd and organotin compounds, laid the groundwork for extensive research by Stille into the mechanism and scope of Pd-catalyzed cross-coupling involving stannanes as transmetalating agents.¹¹⁹ In honor of his widely encompassing investigations, the reaction is now known as Stille cross-coupling, or the Stille reaction. In addition to allowing a variety of carbon fragments to join, Stille cross-coupling is broadly useful as a means of constructing new C–C bonds for

¹¹⁷D. Azarian, S. S. Dua, C. Eaborn, and D. R. M. Walton, *J. Organometal. Chem.*, **1976**, 117, C55.

¹¹⁸M. Kosugi, K. Sasazawa, Y. Shimizu, and T. Migita, *Chem. Lett.*, **1977**, 301 and M. Kosugi, Y. Shimizu, and T. Migita, *Chem. Lett.*, **1977**, 1423.

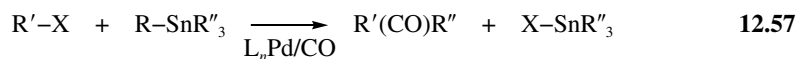
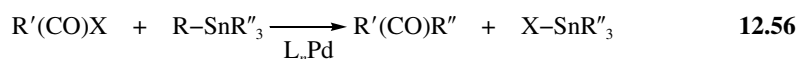
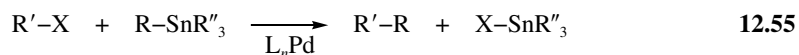
¹¹⁹First report: D. Milstein and J. K. Stille, *J. Am. Chem. Soc.*, **1978**, 100, 3636; see also Footnote 116.

**Scheme 12.18**

The General
Catalytic Cycle for
Pd-Catalyzed Cross-
Coupling Reactions

several reasons: (1) the reaction conditions are highly tolerant of many organic functional groups, which means that protection–deprotection steps are minimized; (2) organotin compounds are relatively easy to synthesize by a number of routes, and some are commercially available; (3) organotin compounds are relatively stable and easily handled by conventional techniques because the Sn–C bond energy is ca. 50 kcal/mol; and (4) organotin compounds are not particularly air or moisture sensitive, which reduces considerably the need to use sophisticated laboratory techniques.

Equations 12.55–12.57 outline the general types of coupling transformations that are possible using organotin reagents in the presence of Pd.

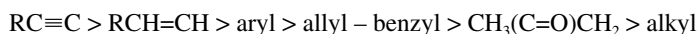


As with Heck olefination or Pd-catalyzed CO insertion, almost any organic bromide or iodide (without hydrogens attached to an sp^3 -hybridized β carbon,

Table 12-7 Electrophiles and Organotin Reagents Suitable for Coupling Reactions

Electrophile	Organotin reagent
R'(C=O)Cl	H–SnR ₃
R'R''C=CR'''–CH ₂ –X (allyl)	R'''C≡C–SnR ₃
ArCH ₂ –X (benzyl)	R'R''C=CR'''–SnR ₃
R'R''C=CR'''–X	Ar–SnR ₃
Ar–X	R'R''C=CR'''–CH ₂ –SnR ₃
R'–C(H)(X)–CO ₂ R''	Ar–CH ₂ –SnR ₃
	R'–SnR ₃ (R' = alkyl)
X = Br, I (Cl also works, but special conditions are required)	R', R'', R''' = a wide variety of hydrocarbyl groups; R = Me, Bu

of course) will serve as an electrophile and undergo coupling with the organotin reagent (equation 12.55). Usually, the organotin compound is designed so that one group will transfer preferentially over the rest. The order of transfer is approximately as follows.



Methyl or butyl groups typically comprise the remaining, nontransferable groups in the stannane (the R'' groups in equations 12.55–12.57).¹²⁰ Acyl chlorides react to give ketones (equation 12.56), or alternatively, R'–X reacts in the presence of CO to yield the same result (equation 12.57). Use of the alternate path to ketones works when the acid chloride is not readily available or if the presence of an acyl chloride group is incompatible with the presence of protic functional groups such as OH or NH₂. Pd(PPh₃)₄ or PdCl₂(MeCN)₂ are particularly useful catalysts for Stille coupling (the latter Pd(II) complex is likely reduced *in situ*). Table 12-7 summarizes the broad scope of Stille cross-coupling. In general, any electrophile listed in the first column will couple with any stannane from the second column.

Propose a catalytic cycle for the cross-coupling plus carbonylation described by equation 12.57.

Exercise 12-11

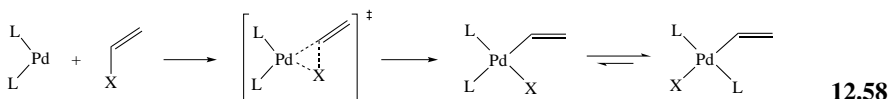
Reaction Mechanism

Among all four cross-coupling reactions we will consider, the Stille reaction has been the most investigated. Although any of the five steps in the general cycle

¹²⁰Tetraalkyltin reagents will react—albeit more slowly than those containing Sn–C(sp²) or Sn–C(sp) bonds—if the transfer of a simple alkyl group is desired.

shown in Scheme 12.18 could be the slow step, transmetalation is most often rate determining. If that is the case, transferable groups attached to Sn may have β -hydrogens attached to sp^3 carbons, because steps subsequent to transmetalation are rapid.

Experimental evidence points to two different modes of oxidative addition. For $R'-X$, when R' is sp^2 hybridized, a three-centered mechanism seems to apply (see also Section 7-2-2). This leads to an intermediate where R' and X are *cis*. Because of the high *trans* effect of R' , a rapid *cis*-*trans* rearrangement likely occurs to give the more stable stereoisomer (equation 12.58).¹²¹



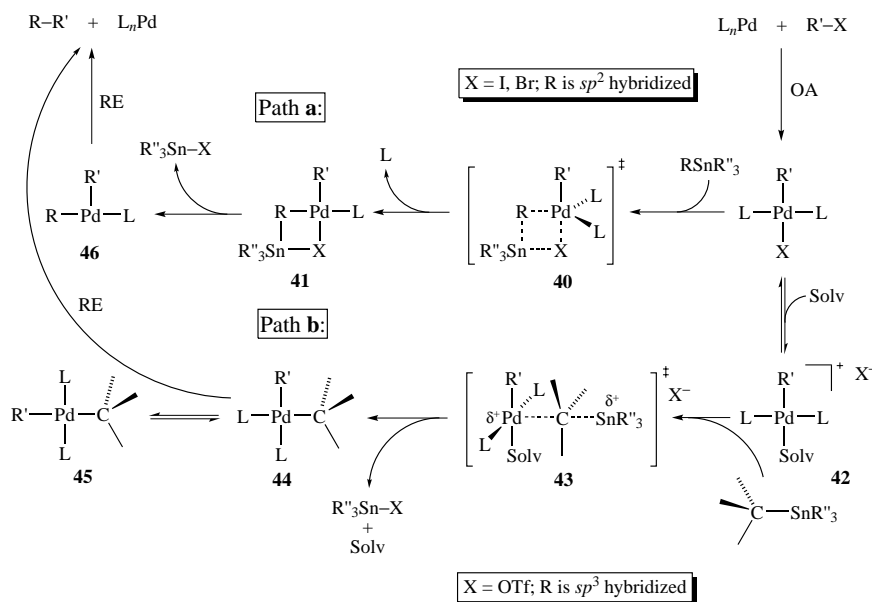
When R = allyl, OA seems to involve either an S_N2 mechanism (inversion of configuration) or a mechanism that goes through a three-centered transition state (retention of configuration). Inversion is the stereochemical outcome in polar, coordinating solvents such as DMSO or acetonitrile, whereas retention is found with use of less polar and less coordinating solvents such as THF, benzene, and CH_2Cl_2 .¹²²

The attachment of a new carbon ligand to Pd during transmetalation amounts to a ligand substitution, and mechanistic studies show support for an associative mechanism overall, which is typical for square planar Pd complexes. Details of the transmetalation step have been elucidated experimentally and computationally at the DFT level, and two major pathways seem to be operative.¹²³ Transmetalations run in less coordinating solvents, such as toluene, CH_2Cl_2 , or THF, go via path **a** (Scheme 12.19), which involves cyclic transition state **40** and intermediate **41**. This route results in retention of configuration at the α carbon of R . This path seems especially favorable for $X = Br$ or I and also when C_α is sp^2 hybridized. For Stille couplings run in coordinating polar, aprotic solvents, such as HMPA or DMSO, an “open” pathway (path **b**, Scheme 12.19) is prevalent, especially if $X = OTf$. The stereochemical consequence of path **b** is inversion

¹²¹A. L. Casado and P. Espinet, *Organometallics*, **1998**, *17*, 954.

¹²²H. Kurosawa, S. Ogoshi, Y. Kawasaki, S. Murai, M. Miyoshi, and I. Ikeda, *J. Am. Chem. Soc.*, **1990**, *112*, 2813; H. Kurosawa, H. Kajimura, S. Ogoshi, H. Yoneda, K. Miki, N. Kasai, S. Murai, and I. Ikeda, *J. Am. Chem. Soc.*, **1992**, *114*, 8417; and A. Vitagliano, B. Åkermark, and S. Hansson, *Organometallics*, **1991**, *10*, 2592.

¹²³(a) A. Nova, G. Ujaque, F. Maseras, A. Lledós, and P. Espinet, *J. Am. Chem. Soc.*, **2006**, *128*, 14571; (b) R. Álvarez, O. N. Faza, A. R. de Lera, and D. J. Cárdenas, *Adv. Synth. Catal.*, **2007**, *349*, 887; (c) M. H. Pérez-Temprano, A. Nova, J. A. Casares, and P. Espinet, *J. Am. Chem. Soc.*, **2008**, *130*, 10518; and (d) R. Álvarez, M. Pérez, O. N. Faza, and A. R. de Lera, *Organometallics*, **2008**, *27*, 3378.

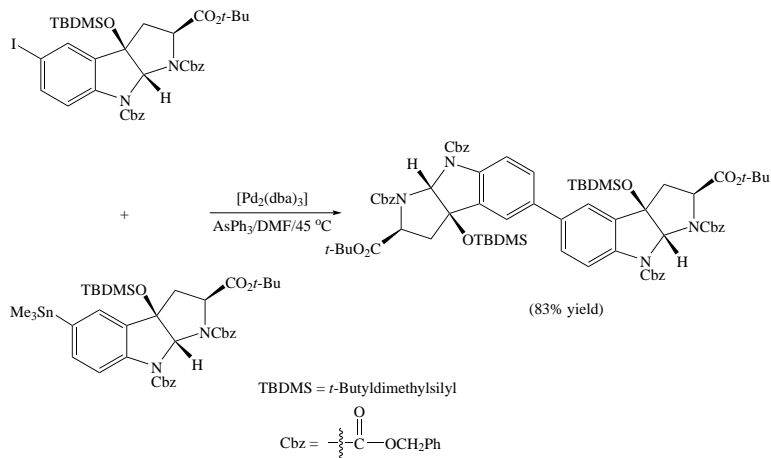


Scheme 12.19
A Mechanism
for Stille Cross-
Coupling

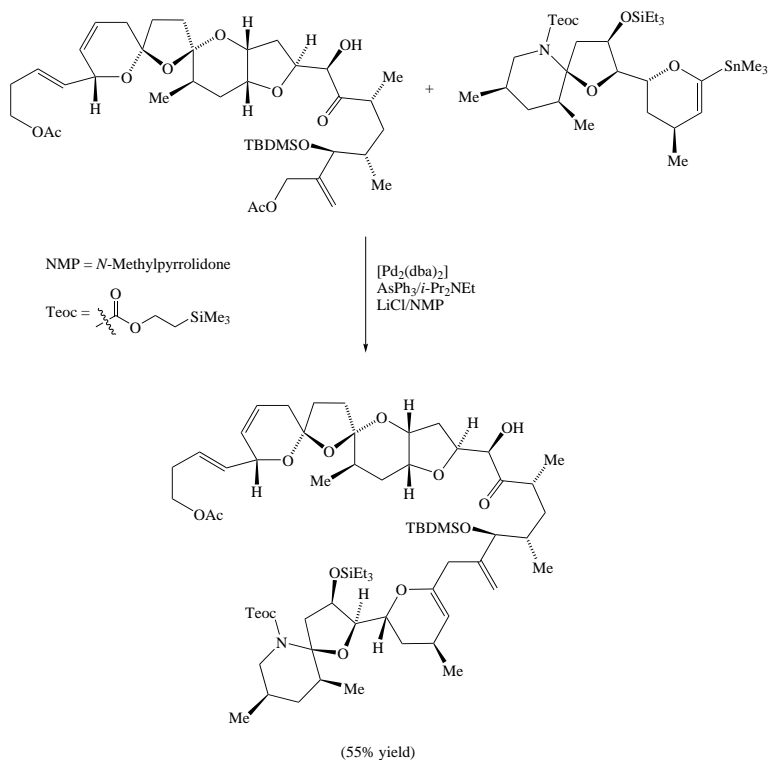
of configuration. The poor coordinating ability of triflate ion and the presence of highly polar solvents lend support to formation of cationic intermediate **42** and *cis*- and *trans*-transmetalation products **44** and **45**. Transition state **43** connects intermediate **42** with these products via an S_E2 transmetalation route.

Reductive elimination (Section 7-3) must necessarily proceed from an intermediate where R' and R are *cis* to each other. Between transmetalation and reductive elimination, *trans*–*cis* isomerization (**45** \rightarrow **44**) must occur, although it is interesting to note that path **a** in Scheme 12.19 yields reactive T-shaped complex **46** directly from cyclic intermediate **41**. We would, therefore, expect that RE would not be the rate-determining step in cross-coupling reactions going through path **a**. RE as a result of path **b** may be slow, especially if the carbon group transferred from Sn is allyl.¹²⁴ Although the general scheme for cross-coupling (Scheme 12.18) gives a good overview of the catalytic cycle for Stille cross-coupling, it does not explain many of the subtleties of the transformation including different stereochemical outcomes as a function of reaction conditions. Scheme 12.19 sheds some light on the stereochemical characteristics of the transmetalation step, such as retention of configuration throughout coupling of two vinyl

¹²⁴It may be that the relatively weak allyl– R' bond makes RE less favorable both thermodynamically and kinetically. For an excellent summary of recent mechanistic studies of the Stille cross-coupling reaction, see P. Espinet and A. M. Echavarren, *Angew. Chem. Int. Ed.*, **2004**, *43*, 4704.



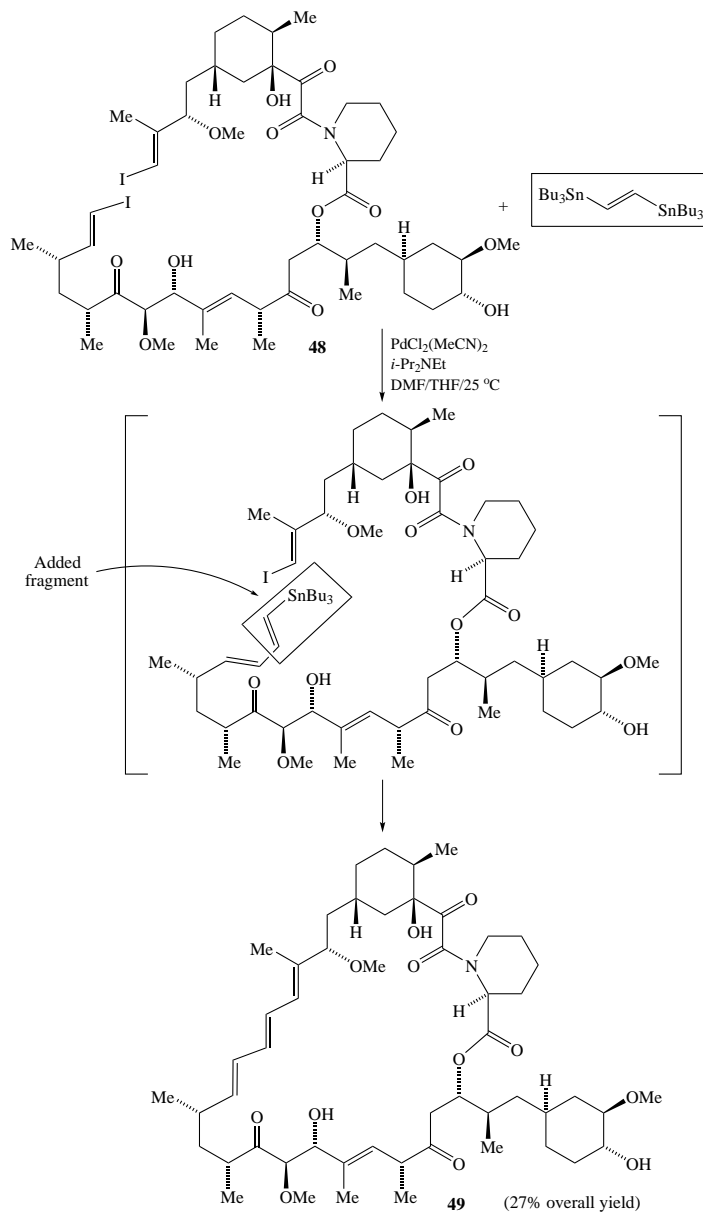
12.60



12.61

Equation 12.59 shows an intramolecular cross-coupling combined with a carbonylation, which was used in the synthesis of (\pm)-*epi*-jatrophone (**47**), a diterpene that possesses antitumor activity.¹²⁶ Early in investigations on the reactivity

¹²⁶A. C. Gyorkos, J. K. Stille, and L. S. Hegedus, *J. Am. Chem. Soc.*, **1990**, *112*, 8465.



12.62

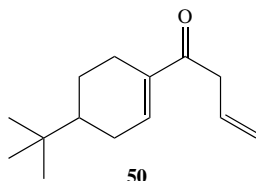
of triflate esters, the addition of LiCl was found to enhance reactivity of $\text{R}'\text{-OTf}$, but the reason for this is still not completely understood.¹²⁷ An intermolecular

¹²⁷Some recent work has shed light on the efficacy of LiCl. Theoretical investigation of the reaction of vinyl triflates in Stille cross-coupling has shown that LiCl reacts with $\text{L}_n\text{Pd}(0)$ to

aryl–aryl coupling is pictured in equation 12.60.¹²⁸ This transformation was an important step in the synthesis of himastatin, a microbial metabolite with antibacterial and antitumor properties. Another intermolecular Stille reaction is detailed in equation 12.61.¹²⁹ Here coupling involves R'–X attaching to Pd in an η^3 -manner, so the reaction demonstrates features of both Stille cross-coupling and the Tsuji–Trost reaction. A rather spectacular example of cascading inter- and intramolecular Stille reactions appears in equation 12.62,¹³⁰ and this was used to synthesize the antibiotic rapamycin (49). Note the lack of protecting groups on the oxygen functional groups attached to diiodide 48.

What are the starting materials required to synthesize compound 50 using a Stille cross-coupling reaction?

Exercise 12-13



12-4-3 Suzuki Cross-Coupling

First reported in 1979 by Suzuki and Mayaura, Suzuki cross-coupling (also called the Suzuki–Mayaura reaction) is an extremely versatile and useful means of forming C–C bonds.¹³¹ Typical reaction conditions are shown in equation 12.63. Although the transmetalating agent, R–B(R'')₂, is different, the scope of the reaction is quite similar to that of Stille cross-coupling (see Table 12-7). This is not surprising on the basis of electronegativity differences between Pd and M' because the electronegativities of B and Sn are nearly equal according to Table 12-5.

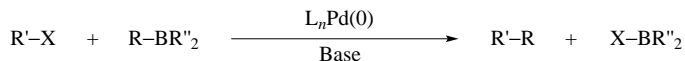
form an anionic complex $[L_2PdCl]^-$, which then is more reactive in OA of vinyl triflates than $L_nPd(0)$. See Footnote 123d.

¹²⁸T. M. Kamenecka and S. J. Danishefsky, *Chem. Eur. J.*, **2001**, 7, 41. Note that Ph_3As is used in this reaction. Sometimes it is used instead of phosphine ligands because it is less strongly coordinating to Pd. Because L-type ligands must attach and depart from Pd during the catalytic process, use of Ph_3As can sometimes speed up cross-coupling.

¹²⁹K. C. Nicolaou, T. V. Koftis, S. Vyskocil, G. Perovic, T. Ling, Y. M. A. Yamada, W. Tang, and M. O. Frederick, *Angew. Chem. Int. Ed.*, **2004**, 43, 4318.

¹³⁰K. C. Nicolaou, A. D. Piscopio, P. Bertinato, T. K. Chakraborty, N. Minowa, and K. Koide, *Chem Eur. J.*, **1995**, 1, 318.

¹³¹N. Miyaura and A. Suzuki, *J. Chem. Soc. Chem. Comm.*, **1979**, 866 and N. Miyaura, K. Yamada, and A. Suzuki, *Tetrahedron Lett.*, **1979**, 3437.



R, R', L: see Tables 12-6 and 12-7

R'': alkyl, OH, O-alkyl

Base: MOH (M = Na, Tl), M₂CO₃ (M = Na, K, Cs), MF (M = K, Cs), NaOMe, K₃PO₄

12.63

Organoboranes, borates, and boronic acids are readily available (hundreds are sold commercially) or they are easily synthesized (for example, hydroboration of the 1-position of terminal alkynes yields 1-borylalkenes). These compounds react with R'-X under mild Pd-catalyzed conditions, and the inorganic byproducts are easily removed at the end of the reaction. Moreover, boranes, borate esters, and boronic acids are tolerant of most common functional groups and are sometimes even compatible with water, which is one of the green aspects of Suzuki cross-coupling. Another important characteristic of organoboron reagents, which makes the Suzuki cross-coupling a greener reaction than the Stille version, is their relatively low toxicity, especially compared with highly toxic organotin compounds.¹³² Although Stille cross-coupling still finds wide use among synthesis chemists, the Suzuki reaction has become the method of choice in recent years.¹³³

Reaction Mechanism

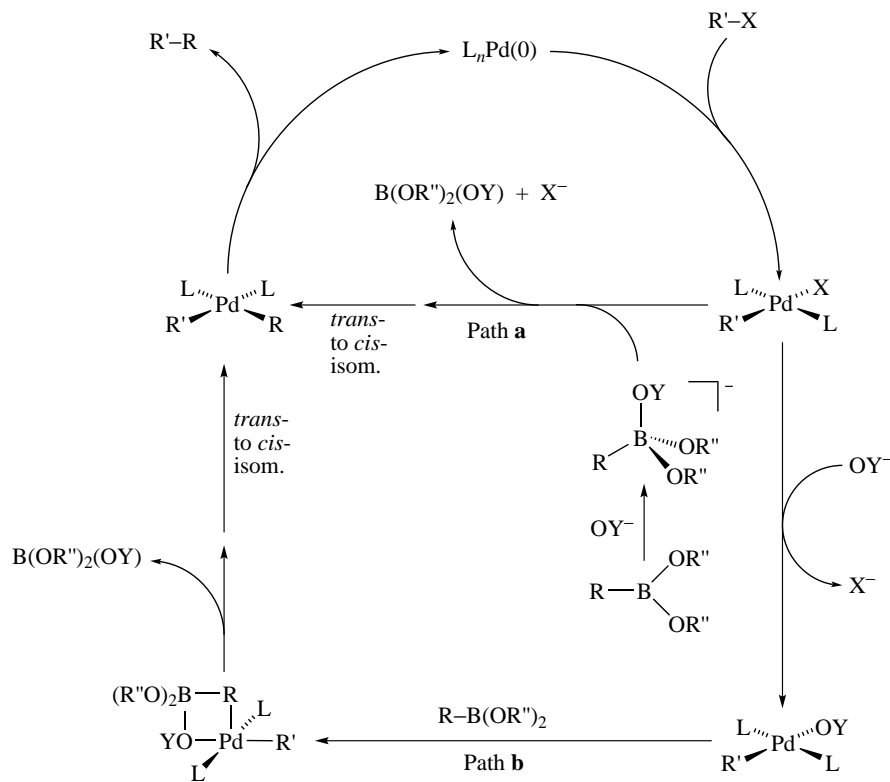
The first two and last two steps for the catalytic cycle of Suzuki cross-coupling are much the same as those for the Stille reaction (Scheme 12.18); the transmetalation step, however, is unique. Transmetalation involves transfer of R to Pd from a borane, borate ester, or boronic acid. Both recent experimental investigations and analysis using DFT calculations indicate that transmetalation is not simply a concerted process as suggested by transition state structure 38.

Early in his investigation of the reaction, Suzuki determined that the addition of base was necessary for smooth cross-coupling.¹³⁴ Although many different bases will work, the simplest bases (OY⁻), OH⁻, and alkoxides, seem to act in either of two ways. Scheme 12.20 shows how OY⁻ can either react with the borate

¹³²Recent research has uncovered reaction conditions that allow coupling of vinyl and aryl halides with a vinyltin partner, which is generated *in situ* using a catalytic amount of Me₃SnCl. These conditions drastically reduce the toxic hazard posed by handling, use, and disposal of stoichiometric amounts of organotin compounds. Although it remains to be seen whether this method will be general, preliminary results were encouraging. See W. P. Gallagher and R. E. Malezcka Jr., *J. Org. Chem.*, **2005**, *70*, 841.

¹³³A search of the literature by one of the authors for years 2006–2008 found 176 hits for Stille cross-coupling and 961 hits for the Suzuki reaction.

¹³⁴For a brief summary of Suzuki's work in discovering and developing Suzuki cross-coupling, see A. Suzuki, *Chem. Commun.*, **2005**, 4749.

**Scheme 12.20**

Pathways for the Action of Base during Transmetalation

or boronic acid to give an anionic species, which then undergoes transmetalation with Pd (path **a**), or react directly with $\text{L}_n\text{R}'\text{PdX}$, displacing X^- and giving $\text{L}_n\text{R}'\text{PdOY}$.¹³⁵ This latter path continues via transmetalation of R-B(OY)_2 to Pd to yield $\text{L}_n\text{PdRR}'$ and B(OY)_3 (path **b**).

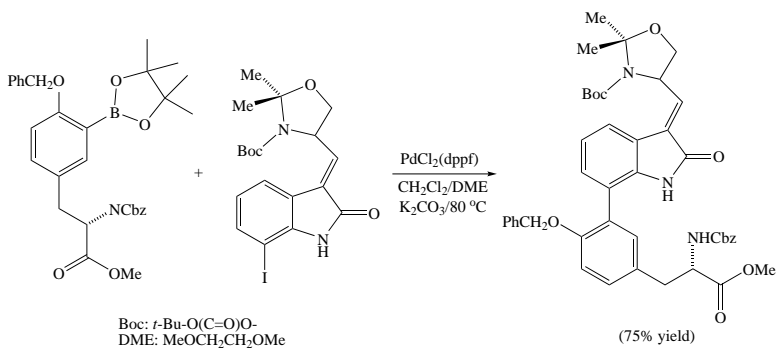
Several steps are apparently involved in transmetalation according to calculations, and these investigations also suggest that different mechanistic pathways exist during transmetalation beginning with either a *cis*- or *trans*- $\text{L}_2\text{R}'\text{PdX}$ intermediate.¹³⁶ As we found with Stille cross-coupling, transmetalation seems more likely to proceed through an associative pathway rather than dissociative. At some point during transmetalation, a cyclic transition state occurs (not necessarily a four-centered one) that allows transfer of R to Pd.

¹³⁵N. Miyaura, *Top. Curr. Chem.*, **2002**, 219, 11.

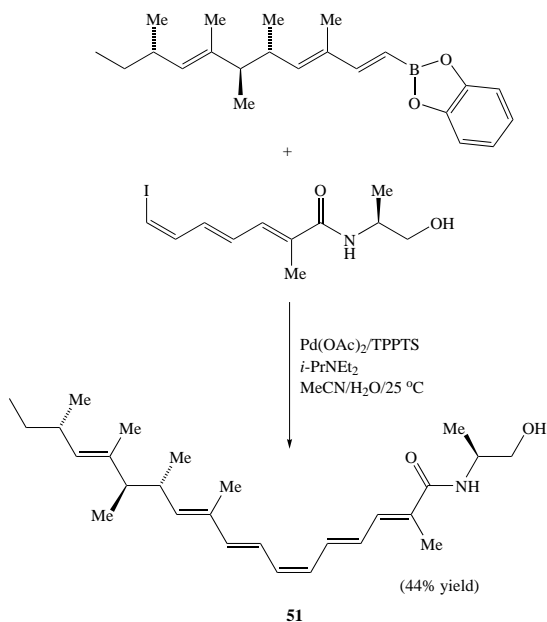
¹³⁶(a) A. A. C. Braga, G. Ujaque, and F. Maseras, *Organometallics*, **2006**, 25, 3467; (b) L. J. Goossen, D. Koley, H. Hermann, and W. Thiel, *Organometallics*, **2006**, 25, 54; (c) C. Sirce, A. A. C. Braga, F. Maseras, and M. M. Cid, *Tetrahedron*, **2008**, 64, 7437; and (d) Y.-L. Huang, C.-M. Weng, and F.-E. Hong, *Chem. Eur. J.*, **2008**, 14, 4426.

Synthesis Applications

As with Stille cross-coupling, use of the Suzuki reaction has had a dramatic effect on organic synthesis.¹³⁷ The chemo-, regio-, and stereoselectivity observed with Suzuki cross-coupling are quite similar to those observed for the Stille reaction. Equations 12.64–12.67 show some of the scope of Suzuki cross-coupling.

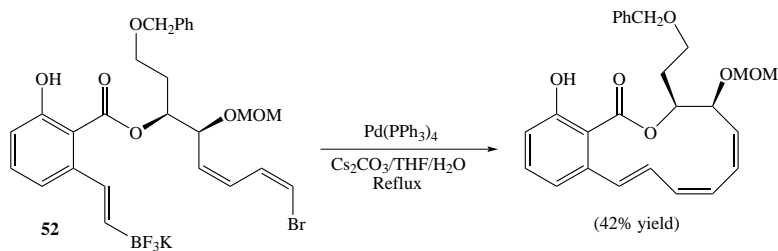


12.64

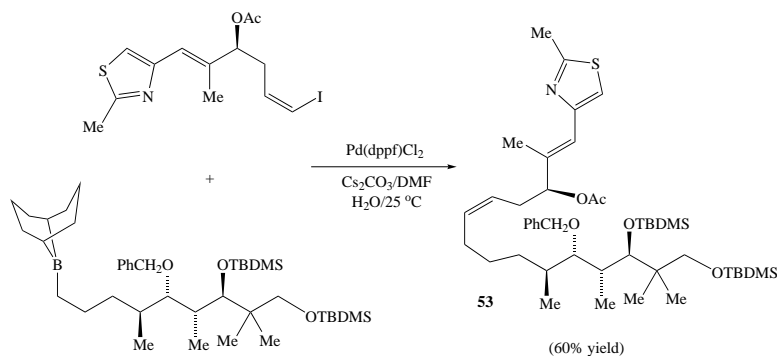


12.65

¹³⁷For example, Suzuki cross-coupling was a key step in the synthesis of *palytoxin*, perhaps the most potent nonpeptide toxin known, which is isolated from coral. Palytoxin possesses over 70 stereogenic centers (which means that the number of stereoisomers possible approaches Avogadro's number!) and has a molecular weight of 2680 Da, making it the heaviest secondary metabolite to be synthesized to date. For a report on the synthesis of palytoxin, see E. M. Suh and Y. Kishi, *J. Am. Chem. Soc.*, **1994**, *116*, 11205.



12.66



12.67

The Suzuki reaction is today the most widely used method for aryl–aryl coupling, and equation 12.64 demonstrates one example. In this case, aryl–aryl coupling was a key step in the synthesis of proteasome inhibitor TMC-95A.¹³⁸ Equation 12.65 shows a vinyl–vinyl coupling that leads to myxalamide A (51), a potent antibacterial and antifungal compound.¹³⁹ Here, the R group is transferred from a borate ester. Intramolecular Suzuki cross-coupling is readily feasible, and equation 12.66 shows a nice example, which was employed for the synthesis of the antitumor compound oximidine II.¹⁴⁰ Fluoroborate salt 52 found use here, instead of the usual borate ester or boronic acid, because it is relatively stable and easily handled. Suzuki cyclization occurred under mild conditions at high dilution of substrate in order to prevent intermolecular cross-coupling.

¹³⁸S. Lin and S. J. Danishefsky, *Angew. Chem. Int. Ed.*, **2002**, *41*, 512. Proteasome inhibitors block the breakdown of proteins in the cell, and these may be effective in fighting the growth of tumor cells.

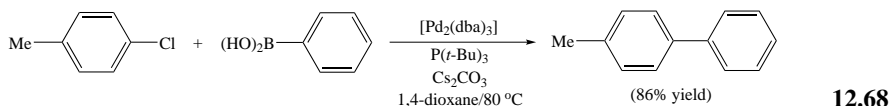
¹³⁹A. K. Mapp and C. H. Heathcock, *J. Org. Chem.*, **1999**, *64*, 23.

¹⁴⁰G. A. Molander and F. Dehmel, *J. Am. Chem. Soc.*, **2004**, *126*, 10313; see also G. A. Molander and N. Ellis, *Acc. Chem. Res.*, **2007**, *40*, 275, for a recent review on the use of organotrifluoroborates in Suzuki cross-coupling.

The last example (equation **12.67**) shows so-called *B*-alkyl cross-coupling in which an sp^3 hybridized carbon is transferred from boron to Pd.¹⁴¹ This reaction produced fragment **53**, which was used to synthesize epothilone A. Epothilones were mentioned in Section **11-1-3**, and they are a family of macrocyclic compounds that appear to be very effective in fighting breast and uterine cancers. Reaction conditions were adjusted for *B*-alkyl cross-coupling such that β -elimination of the alkyl group transferred to Pd was suppressed. One way of doing this is to use the diphosphine complex $\text{PdCl}_2(\text{dppf})$. The naturally large bite angle (β_n) of dppf is such that when R and R' are *cis* to one another, they are closer than would be in the case when monodentate or other bidentate phosphines are attached to Pd. Reductive elimination is then quite facile and occurs before β -elimination can occur. R-BBN derivatives are also quite reactive during transmetalation if the base is carefully chosen. Note that the group transferred in equation **12.67** is primary. Secondary alkyl groups will transfer, although at a much slower rate, thus making this reaction not nearly as useful synthetically. This is, however, an active area of research.

Further Developments

One of the key problems associated with the Suzuki cross-coupling was the lack of reactivity of aryl chlorides. This is unfortunate, because chlorinated aromatics are usually much cheaper and more readily available than other haloarenes. Equation **12.68** shows a solution to this problem where the addition of the base Cs_2CO_3 and $\text{P}(t\text{-Bu})_3$, a sterically hindered and electron-rich phosphine, led to successful coupling of an aryl chloride and arylboronic acid.¹⁴²

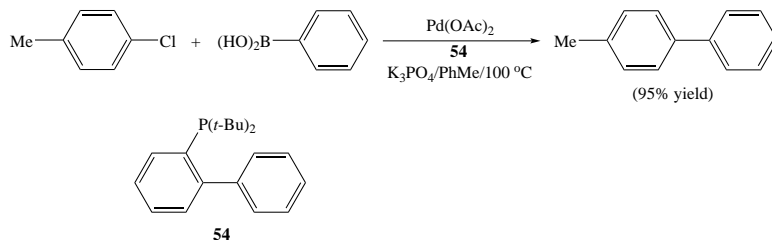


Buchwald also developed favorable conditions for coupling aryl chlorides. Instead of using $\text{P}(t\text{-Bu})_3$, which is pyrophoric, he reported that phosphine **54** in the presence of the base K_3PO_4 allowed cross-coupling of aryl chlorides and arylboronic acids (equation **12.69**).¹⁴³

¹⁴¹B. Zhu and J. S. Panek, *Org. Lett.*, **2000**, 2, 2575.

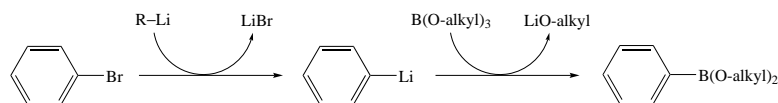
¹⁴²A. F. Littke and G. C. Fu, *Angew. Chem. Int. Ed.*, **1998**, 37, 3387 and A. F. Littke, C. Dai, and G. C. Fu, *J. Am. Chem. Soc.*, **2000**, 122, 4020.

¹⁴³J. P. Wolfe and S. L. Buchwald, *Angew. Chem. Int. Ed.*, **1999**, 38, 2413; for more recent work, see S. D. Walker, T. E. Barder, J. R. Martinelli, and S. L. Buchwald, *Angew. Chem. Int. Ed.*, **2004**, 43, 1871.



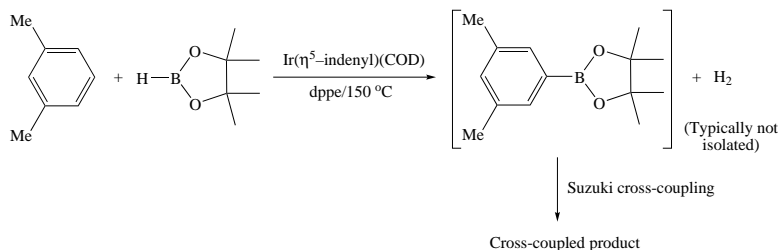
12.69

Aryl borate esters are usually produced from the corresponding aryl halide by first metalating the carbon bearing the halide (typically with R–Li) and then treating the metalated arene with B(O-alkyl)₃ (equation 12.70).



12.70

More recently, a protocol was elucidated by Maleczka and Smith to produce aryl borate esters directly without first producing aryl halides.¹⁴⁴ The reaction involves an Ir-catalyzed C–H activation (Section 7-2-1) to yield the aryl borate, which can then be used directly in Suzuki cross-coupling (equation 12.71). This new development adds another green aspect to Suzuki cross-coupling, which is already a relatively green synthesis tool.



12.71

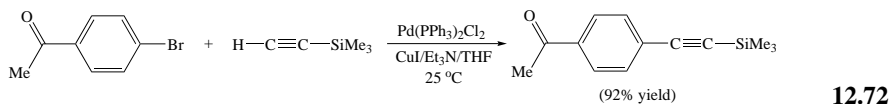
12-4-4 Sonogashira Cross-Coupling

Sonogashira reported in 1975 the first synthetically useful transfer of a terminal alkyne to *sp*² hybridized carbons.¹⁴⁵ His discovery, which consists of a

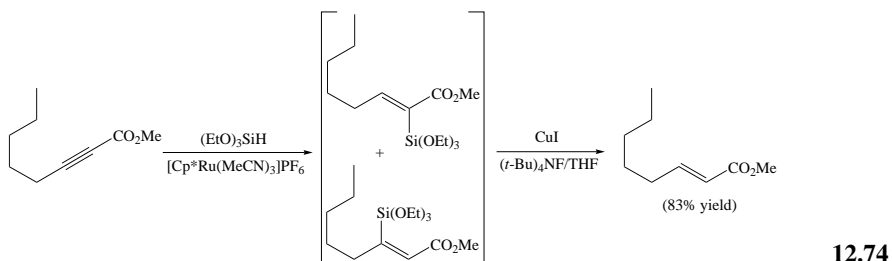
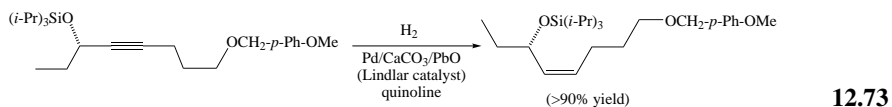
¹⁴⁴V. A. Kallepalli, S. M. Preshlock, P. C. Roosen, R. E. Maleczka, Jr., and M. R. Smith, III, "Iridium-Catalyzed C–H Borylation: Recent Synthetic Advances," Abstracts of Papers, 237th ACS National Meeting, Salt Lake City, UT, March 22–26, 2009. See also G. A. Chotana, V. A. Kallepalli, R. E. Maleczka Jr., and M. R. Smith, *Tetrahedron*, **2008**, *64*, 6103. Maleczka and Smith were honored in 2008 as winners of the Presidential Green Chemistry Challenge Award.

¹⁴⁵K. Sonogashira, Y. Tohda, and N. Hagihara, *Tetrahedron Lett.*, **1975**, 4467.

Cu-catalyzed alkylation of L_nPd and cross-coupling with $R'-X$, has developed into a widely used method for forming new C–C bonds between alkynyl and aryl or vinyl groups. This transformation is now called Sonogashira cross-coupling. Equation 12.72 shows a typical example of the Sonogashira reaction.¹⁴⁶



Because one partner must be a terminal alkyne, the scope of Sonogashira cross-coupling is more limited than that of either the Stille or the Suzuki reactions. Overall, the reaction often requires fairly high loadings of the Cu and Pd catalysts and relatively high reaction temperature, so $R'-X$ is generally limited to $R' =$ aryl, heteroaryl, or vinyl and $X = I, Br,$ or OTf (vinyl and aryl chlorides usually react sluggishly). Within these parameters, however, the reaction is extremely useful. For example, although R is limited to terminal alkynes, the installed triple bond upon cross-coupling is a versatile functional group. Such bonds may be readily hydrogenated stereoselectively to either *Z*- or *E*-alkenes, as shown in equations 12.73¹⁴⁷ and 12.74.¹⁴⁸

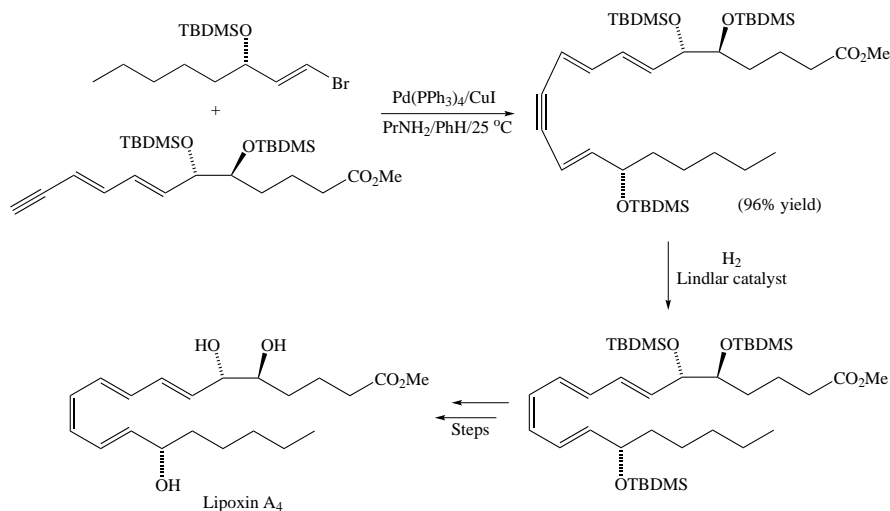


Sometimes organoboranes or stannanes are either unavailable or too unstable under Suzuki or Stille cross-coupling conditions. The Sonogashira reaction, however, does not involve the synthesis or handling of stoichiometric amounts of $M'-R$

¹⁴⁶S. Thorand and N. Krause, *J. Org. Chem.*, **1998**, 63, 8551.

¹⁴⁷D. S. Coffey, A. I. McDonald, L. E. Overman, M. H. Rabinovitz, and P. A. Renhowe, *J. Am. Chem. Soc.*, **2000**, 122, 4893.

¹⁴⁸For recent work on the stereoselective transition metal-catalyzed hydrogenation of alkynes to *E*-alkenes, see B. M. Trost, Z. T. Ball, and T. Jöge, *J. Am. Chem. Soc.*, **2002**, 124, 7922 and A. Fürstner and K. Radkowski, *Chem. Commun.*, **2002**, 2182.



Scheme 12.21
Use of Sonogashira
Coupling in the
Stereoselective
Synthesis of
Polyenes

transmetalating agents. Instead, Cu–alkynes are formed in catalytic amounts *in situ*, and then the terminal alkyne is transferred over to Pd. The two-step protocol of first Sonogashira alkene–alkyne coupling followed by stereoselective hydrogenation can be a highly useful alternative to formation of conjugated polyenes, as Scheme 12.21 shows.¹⁴⁹

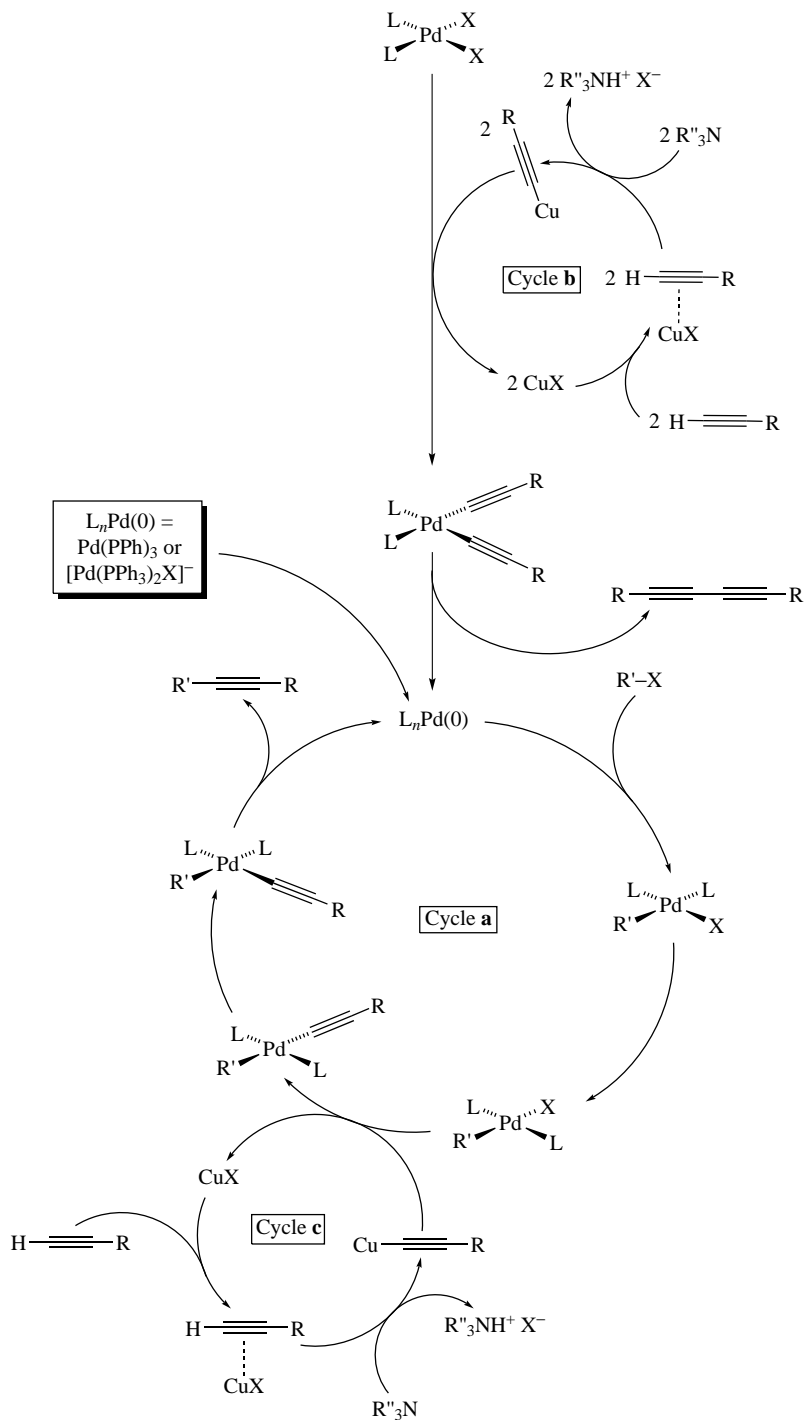
Reaction Mechanism

Scheme 12.22 shows the generally accepted mechanism for Sonogashira coupling. It features three interconnecting cycles.¹⁵⁰ Cycle **a** lies at the heart of the mechanism and should by now be quite familiar. Cycle **b** shows a plausible scheme for converting Pd(II) complexes, the usual form of the precatalyst, to Pd(0). Other mechanisms for this reduction may apply, however, especially since tertiary amine bases are commonly present in the reaction (see Section 12-3-2). Cycle **c** connects with cycle **a**, and it suggests how Cu catalyzes the formation of the Cu–alkyne, which then transmetalates with Pd.

As we have seen before, we should expect that the mechanistic details of the first two and last two steps of cycle **a** are similar to what we have seen earlier in the first two cross-coupling reactions. Again, mechanistic information on

¹⁴⁹K. C. Nicolaou, C. A. Veale, S. E. Webber, and H. Katerinopoulos, *J. Am. Chem. Soc.*, **1985**, *107*, 7515; see also footnote 129.

¹⁵⁰(a) For a concise historical account of the Sonogashira reaction, including a discussion of the mechanism, see K. Sonogashira, *J. Organomet. Chem.*, **2002**, *653*, 46 and (b) for a good recent review of the use of Sonogashira cross-coupling in synthesis, which includes a discussion of mechanism, see R. Chinchilla and C. Nájera, *Chem. Rev.*, **2007**, *107*, 874.

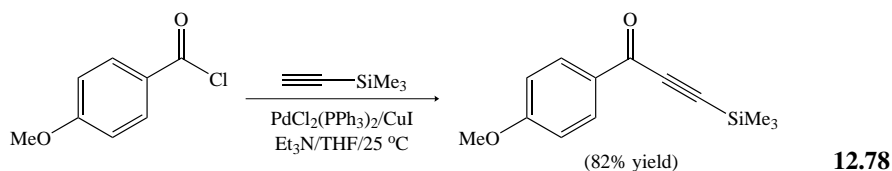
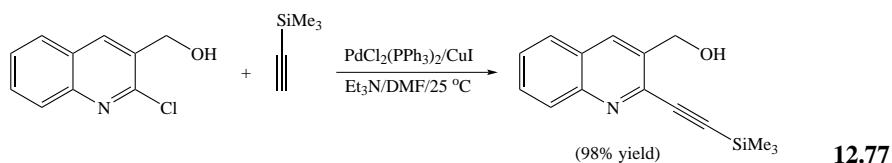
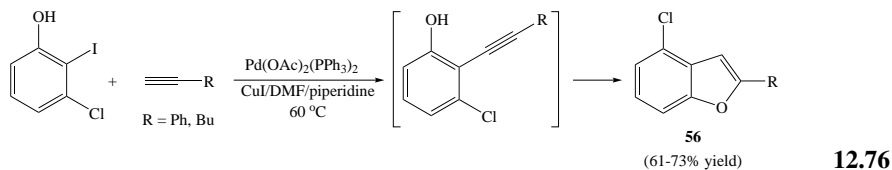
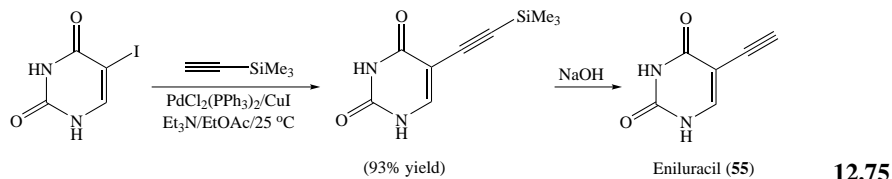
**Scheme 12.22**

Mechanism of the
Sonogashira Cross-
Coupling Reaction

transmetalation is sketchy.¹⁵¹ It seems reasonable that the alkyne must complex with Cu (cycle **c**)—making the terminal hydrogen more acidic—before the relatively weak amine base can pull off the proton (a nucleophilic abstraction). Otherwise, acid–base reaction between a tertiary amine and a terminal alkyne ($pK_a \sim 25$) is quite unlikely. The overall mechanism pictured above also accommodates the presence of $[\text{Pd}(0)\text{L}_2\text{X}]^-$, which could form in the presence of excess halide ion or if $\text{Pd}(\text{OAc})_2$ were used as the precatalyst.

Synthesis Applications

Over the past 25 years, there have been numerous uses of Sonogashira cross-coupling in synthesis. Equations 12.75–12.78 highlight a small sampling of these applications.



¹⁵¹For a recent study of the mechanism of Sonogashira cross-coupling, see M. R. an der Heiden, H. Plenio, S. Immel, E. Burello, G. Rothenberg, and H. C. J. Hoefsloot, *Chem. Eur. J.*, **2008**, *14*, 2857.

Sonogashira cross-coupling is key to the synthesis on an industrial scale of eniluracil (**55**), an anticancer drug used to treat breast and colorectal cancers (equation **12.75**).¹⁵² Halogenated heterocyclic aromatic compounds are often used as the R'-X component of these coupling reactions. Equation **12.76** shows the relative reactivity of Cl vs. I in the regioselective alkynylation of 3-chloro-2-iodophenol.¹⁵³ After cross-coupling occurs, the catalyst system also promotes cyclization to produce benzofuran **56**. Even aryl chlorides can react under Sonogashira reaction conditions (equation **12.77**), but the electron-withdrawing nitrogen atom in the pyridine ring is most likely the reason that the Ar-Cl bond is reactive toward facile oxidative addition.¹⁵⁴ The last example shows that acyl chlorides can undergo cross-coupling to form ynones, which are useful intermediates in synthesis (equation **12.78**).¹⁵⁵

Exercise 12-14

Propose a mechanism for the second step in equation **12.76**, which converts the arylalkyne to benzofuran **56**.

Further Developments

Numerous researchers have investigated modifications of Sonogashira cross-coupling, mainly to determine whether both catalytic metals must be in place. The so-called Cu-free and Pd-free versions of this reaction have been reported, but concern has been expressed by others that the reaction conditions are not really free of one or the other element. For example, a Pd-free Suzuki cross-coupling using Na₂CO₃ as the base was reported, but it was later determined that the carbonate contained trace amounts of Pd.¹⁵⁶ The same situation obtains for some Cu-free versions.¹⁵⁷ Even if these modifications are not entirely free of Pd or Cu, however, they serve as useful reactions because the amount of at least one metal present is drastically reduced. Sonogashira reactions run using microwave heating have become popular of late, allowing standard cross-coupling reactions to be run

¹⁵²J. W. B. Cooke, R. Bright, M. J. Coleman, and K. P. Jenkins, *Org. Process Res. Dev.*, **2001**, 5, 383.

¹⁵³R. Sanz, M. P. Castroviejo, Y. Fernández, and F. J. Fañanas, *J. Org. Chem.*, **2005**, 70, 6548.

¹⁵⁴M. Toyota, C. Komori, and M. Ihara, *J. Org. Chem.*, **2000**, 65, 7110.

¹⁵⁵A. S. Karpov, and T. J. J. Müller, *Org. Lett.*, **2003**, 5, 3451.

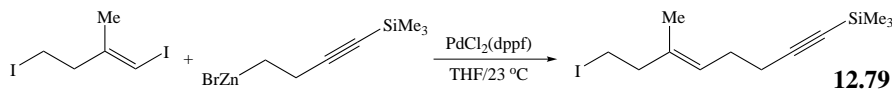
¹⁵⁶R. K. Arveda, N. E. Leadbeater, M. S. Sangri, V. A. Williams, P. Granados, and R. D. Singer, *J. Org. Chem.*, **2005**, 70, 161.

¹⁵⁷J. Gil-Moltó and C. Nájera, *Adv. Synth. Catal.*, **2006**, 348, 1874.

much more quickly than under conventional heating methods.¹⁵⁸ Greener solvents have been used, such as poly(ethylene glycol), with good results.¹⁵⁹ Although there is still much work to be done to fill in the mechanistic details of Sonogashira coupling, continued effective application of this reaction in synthesis, especially in light of the further developments just mentioned, ensures that this mode of cross-coupling will long remain a useful synthesis tool.

12-4-5 Negishi Cross-Coupling

Although the Negishi cross-coupling reaction¹⁶⁰ is less used in synthesis applications than the Suzuki reaction, it is a versatile method for joining two carbon fragments together. It is often the method of choice for synthesis of acyclic di-, tri-, and higher-order terpenoid systems. Organozinc reagents are typically involved in Negishi cross-coupling, but the reaction is also interesting from an organometallic chemistry standpoint because other metals beside Zn also can be involved in a cascade of transmetalations that finally yield the cross-coupled product. Equation 12.79 shows a typical example of the Negishi reaction.¹⁶¹



The scope of the Negishi reaction is broad, similar to that of Stille and Suzuki cross-coupling. The reaction seems to work if $R' =$ aryl, vinyl, alkynyl, acyl, allyl, benzyl, homoallyl ($-\text{CH}_2-\text{CH}_2-\text{CH}=\text{CH}_2$) and homobenzyl ($-\text{CH}_2-\text{CH}_2-\text{Ph}$), or even primary alkyl, and if $X = \text{I}, \text{Br},$ or OTf (Cl works, but often sluggishly). Correspondingly, $R =$ aryl, vinyl, alkynyl, allyl, benzyl, and primary alkyl. The organozinc reagent may either be used as a preformed compound, such as R_2Zn

¹⁵⁸For some examples of Sonogashira cross-coupling reactions under microwave heating, see N. E. Leadbeater and M. Marco, *Org. Lett.*, **2002**, *4*, 2973; G. W. Kabalka, L. Wang, V. Nambodiri, and R. M. Pagni, *Tetrahedron Lett.*, **2000**, *41*, 5151; and E. Petricci, M. Radi, F. Corelli, and M. Botta, *Tetrahedron Lett.*, **2003**, *44*, 9181.

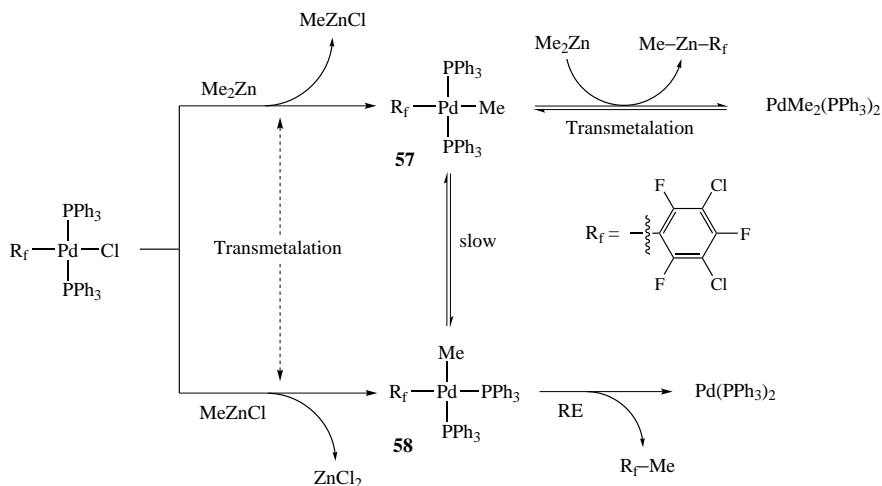
¹⁵⁹G. O. Spessard, "Recent developments in green chemistry education at St. Olaf College." Abstracts of Posters, 1st International IUPAC Conference on Green-Sustainable Chemistry, Dresden, Germany, September 10–15, 2006, Poster V-002 and G. O. Spessard, T. Drake, D. Harris, and D. Vock, "Use of polyethylene glycols as green solvents in organic reactions," Gordon Research Conference on Green Chemistry, Oxford, England, August 27–September 1, 2006.

¹⁶⁰First reports of the Negishi cross-coupling: E. Negishi and S. Baba, *J. Chem. Soc. Chem. Commun.*, **1976**, 596 and S. Baba and E. Negishi, *J. Am. Chem. Soc.*, **1976**, *98*, 6729; for historical accounts of the discovery and development of the reaction, see E. Negishi, *J. Organomet. Chem.*, **2002**, *653*, 34 and E. Negishi, *Bull. Chem. Soc. Jpn.*, **2007**, *80*, 233.

¹⁶¹E. Negishi, S. Y. Liou, C. Xu, and S. Huo, *Org. Lett.*, **2002**, *4*, 261.

Scheme 12.23

Different Stereochemical Outcomes for Transmetalation as a Function of the Type of Organozinc Reagent



or $RZnX$ ($X = I, Br, \text{ or } Cl$), or $RZnX$ may be generated *in situ* by first allowing $R-X$ to react with Zn dust. Nickel compounds catalyze Negishi cross-coupling reactions, but Pd -phosphine complexes seem to give higher yields and better selectivity, thus, they are the catalysts most commonly employed.

Reaction Mechanism

The cycle for Pd -catalyzed Negishi cross-coupling is most likely quite similar to the other three examples that we have already considered (see Scheme 12.18), but little mechanistic work has been reported, especially with regard to the transmetalation step. Recently, there have been theoretical investigations published on the Ni -catalyzed version, but these have indicated a different sequence of steps than is likely for the Pd -catalyzed cross-couplings.¹⁶² A limited study on the difference between transmetalation by Me_2Zn or $MeZnCl$ on a fluorinated aryl- Pd complex revealed that the stereochemistry of the resulting transmetalated Pd complex was different depending on which organozinc compound was used.¹⁶³ These results are shown in Scheme 12.23. It is not clear why Me_2Zn yields mainly *trans*-isomer **57**, whereas $MeZnCl$ gives the *cis*-complex **58**.

Synthesis Applications

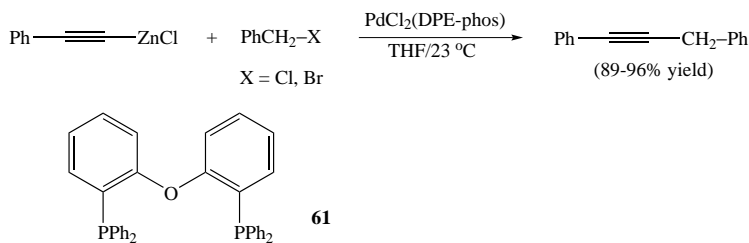
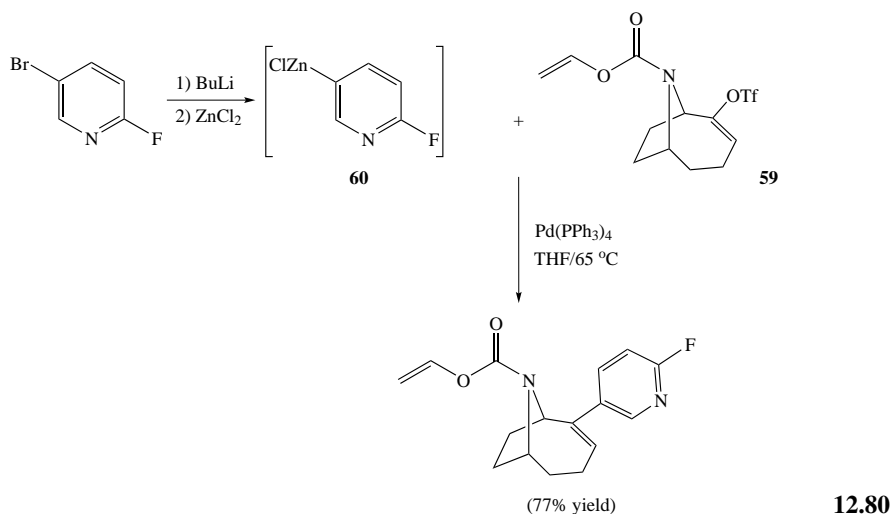
Negishi cross-coupling has sometimes been used when either the Stille or the Suzuki reactions either proceeded sluggishly or would not work at all.¹⁶⁴ The

¹⁶²G. D. Jones, C. McFarland, T. J. Anderson, and D. A. Vicic, *Chem. Commun.*, **2005**, 4211 and X. Lin and D. L. Phillips, *J. Org. Chem.*, **2008**, 73, 3680.

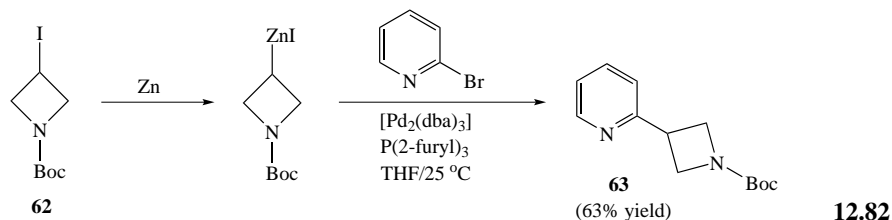
¹⁶³J. A. Casares, P. Espinet, B. Fuentes, and G. Salas, *J. Am. Chem. Soc.*, **2007**, 129, 3508.

¹⁶⁴See Footnote 129.

reaction, however, is often less tolerant of acidic or carbonyl-containing functional groups already present on R and R'. Organozinc reagents are also sensitive to oxygen and moisture, which is not too surprising because Zn is more electropositive than either B or Sn. Equations 12.80–12.82 hint at the utility of Negishi cross-coupling.



Bis(2-(diphenylphosphino)phenyl) Ether (DPE-Phos)



Equation 12.80 shows a vinyl–aryl cross-coupling, which is apparently tolerant of the vinyl carbamate group on compound 59. The organozinc reagent (60)

was prepared by first treatment of 5-bromo-2-fluoropyridine with BuLi to give the corresponding 5-lithiopyridine, which then was allowed to react with ZnCl₂ to produce **60** (a typical procedure for making aryl and vinylzinc compounds).¹⁶⁵ An alkynylzinc reagent combines with benzyl bromide in equation **12.81** to yield coupled product.¹⁶⁶ The best precatalyst for this transformation was the complex Pd(DPE-phos)Cl₂ (**61**), which was far superior to Pd(dppf)Cl₂—a normally very effective, general catalyst for stubborn cross-couplings. A highly strained alkyl iodide (**62**) reacts with Zn dust in equation **12.82** to give the corresponding organozinc reagent. Cross-coupling with 2-bromopyridine, catalyzed by Pd[P(2-furyl)₃]₂, yields the *N*-protected pyridylazetidine **63**.¹⁶⁷

Scheme **12.24** highlights a spectacular cascade of transmetalations that begins with Zr-catalyzed formation of alkynylalane **64**, followed by transmetalation to the corresponding organozinc reagent, which then undergoes Negishi cross-coupling with a vinyl bromide. The resulting product **65** was deprotected to give terminal alkyne **66**, then the transmetalation cascade was repeated, and the final step was a bis-Negishi cross-coupling to yield β-carotene (**67**). The overall yield going from the starting point in the scheme to β-carotene was 48%, truly a remarkable example of the power of the Negishi reaction and a nice demonstration of a Zr → Al → Zn → Pd transmetalation cascade.¹⁶⁸

Exercise 12-15

Propose a mechanism for Zr-catalyzed methyl-alumination of the terminal alkyne starting material in Scheme **12.24**. Your mechanism should account for the stereochemistry of the transformation.

Further Developments

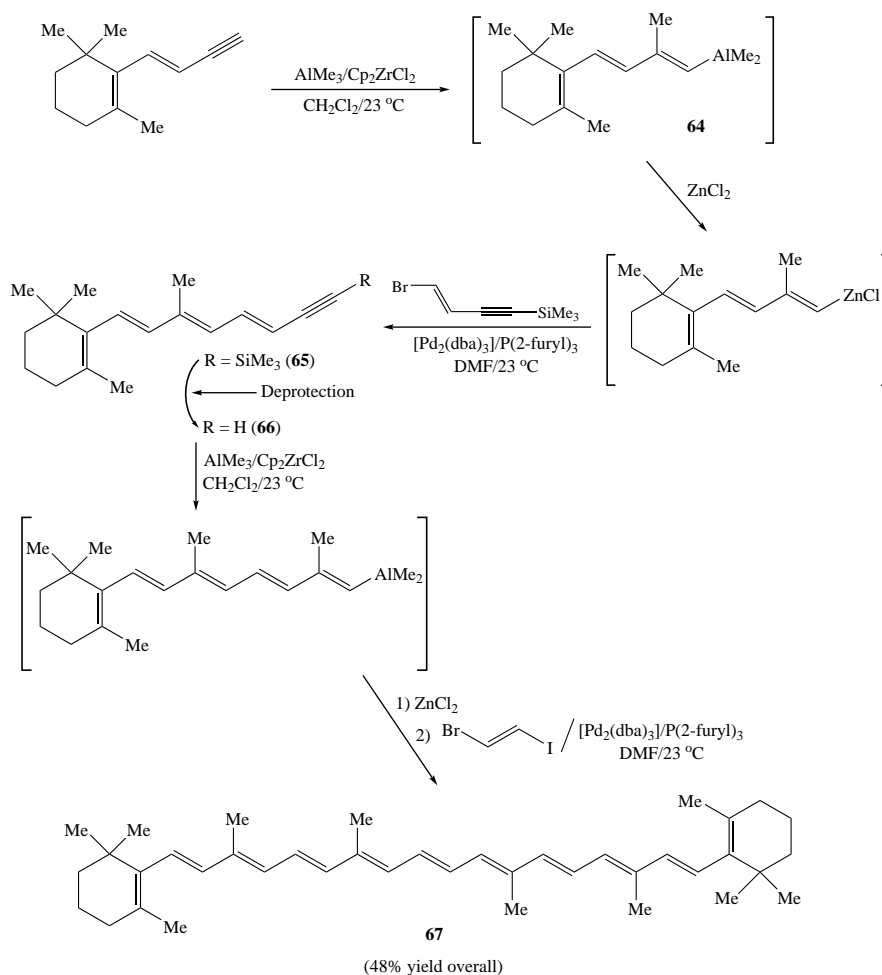
Research is active to produce precatalysts that are stable in air, highly active, well-defined, and possess a broad spectrum of activity. One such precatalyst is complex **68**, which consists of Pd complexed with a sterically hindered NHC carbene (Section **10-1-1**). Also present is a substituted pyridine ligand (a so-called “throw-away” ligand). Complex **68** is a member of the PEPPSI (pyridine-enhanced precatalyst preparation, stabilization, and initiation) family

¹⁶⁵A. Sutherland, T. Gallagher, C. G. V. Sharples, and S. Wonnacott, *J. Org. Chem.*, **2003**, *68*, 2475.

¹⁶⁶M. Qian and E. Negishi, *Tetrahedron Lett.*, **2005**, *46*, 2927.

¹⁶⁷S. Billotte, *Synlett*, **1998**, 379.

¹⁶⁸F. Zeng and E. Negishi, *Org. Lett.*, **2001**, *3*, 719.

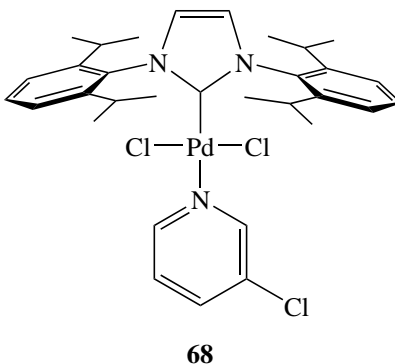
**Scheme 12.24**

Cascading Transmetalations and Negishi Cross-Coupling Used in the Synthesis of β -Carotene

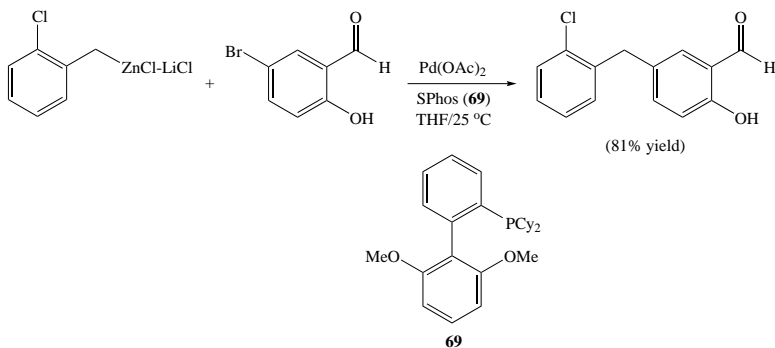
(“generation”) of precatalysts. This particular precatalyst is active in promoting Negishi cross-coupling between a wide variety of aryl and alkyl groups ($\text{R}' = \text{aryl or alkyl}$; $\text{R} = \text{aryl or alkyl}$).¹⁶⁹ PEPPSI catalysts have also shown activity for Suzuki cross-coupling,¹⁷⁰ so their versatility will no doubt increase over the years.

¹⁶⁹M. G. Organ, S. Avola, I. Dubovyk, N. Hadei, E. A. B. Kantchev, C. J. O'Brien, and C. Valente, *Chem. Eur. J.*, **2006**, *12*, 4749.

¹⁷⁰C. J. O'Brien, E. A. B. Kantchev, C. Valente, N. Hadei, G. A. Chass, A. Lough, A. C. Hopkinson, and M. G. Organ, *Chem. Eur. J.*, **2006**, *12*, 4743.



It is now possible to couple chlorophenols, haloanilines, and halovinyl alcohols with organozinc reagents without concern that protic groups found in $R'-X$ will react with the transmetalating agent. Equation **12.83** outlines this procedure, which also shows another variation in the synthesis of organozinc compounds—direct insertion of Zn into a C–X bond in the presence of LiCl.¹⁷¹



A key to the success of this transformation is the use of a relatively new ligand for Pd called SPhos (**69**), which Buchwald found especially useful for speeding up normally sluggish cross-coupling reactions.¹⁷²

The discovery, use, and further development of cross-coupling reactions have mightily advanced the field of organic synthesis. Today, chemists routinely use Stille, Suzuki, Sonogashira, and Negishi reactions to construct new C–C bonds, and this step is often the key to successful synthesis of incredibly complex

¹⁷¹G. Manolikakes, M. A. Schade, C. M. Hernandez, H. Mayr, and P. Knochel, *Org. Lett.*, **2008**, *10*, 2765.

¹⁷²S. D. Walker, T. E. Barder, J. R. Martinelli, and S. L. Buchwald, *Angew. Chem. Int. Ed.*, **2004**, *43*, 1871.

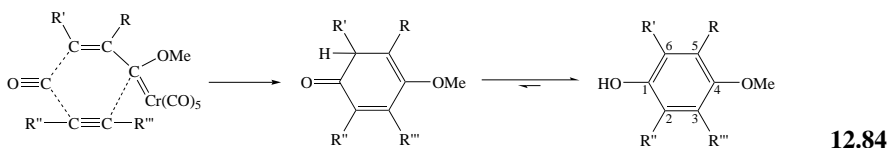
molecules. It is clear that investigations on the utility of cross-coupling reactions will continue to be an active area of research for many years to come.

12-5 CARBON–CARBON BOND FORMATION THROUGH CYCLIZATION REACTIONS

Previously in Chapter 12 we have seen several examples of cyclization reactions that have involved transition metal catalysis. In Chapter 11, we introduced Mo- and Ru-catalyzed RCM as a means of converting acyclic dienes, alkene–alkynes, and dialkynes into rings containing carbon–carbon double and triple bonds. Section 12-5 will cover a few cases where organotransition metal complexes effectively promote the construction of rings where two or more C–C bond connections occur during the same transformation. Some examples will be extensions of reactions already covered, whereas others will entail “new” chemistry.

12-5-1 Cyclizations Involving Fischer Carbene Complexes: The Dötz Arene Synthesis

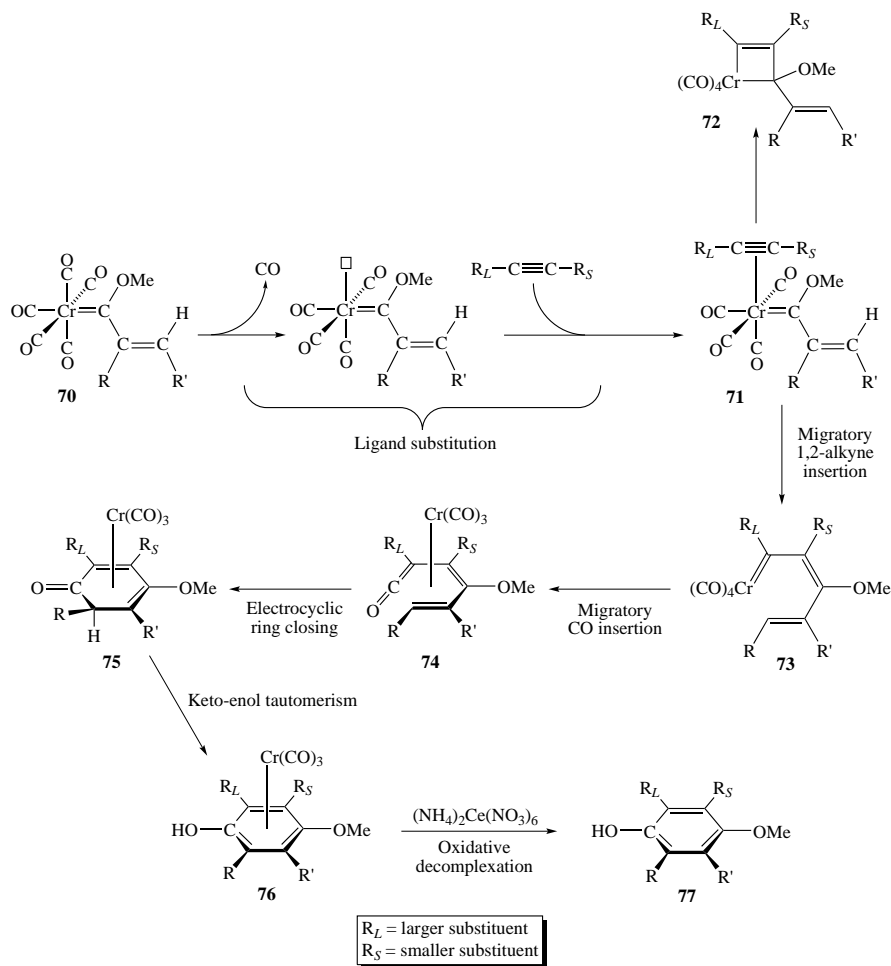
Fischer chromium carbene complexes have numerous applications to organic synthesis. Beginning about 25 years ago, Dötz,¹⁷³ Wulff,¹⁷⁴ and several other groups discovered and developed a procedure for synthesizing substituted phenols, naphthols, and higher polycyclic aromatic homologs that amounts to a [3 + 2 + 1] cyclization involving three partners: a Cr–carbene complex (contributing three of the ring atoms), an alkyne (contributing two ring atoms), and CO (contributing the sixth ring atom). Equation 12.84 shows a schematic representation of the cyclization, indicating how the reactant fragments fit together. Note that the methoxy group attached to C_{carbene} ends up *para* to the phenolic OH group. If the alkyne is unsymmetrically substituted, the larger substituent usually ends up *ortho* to the phenolic OH.¹⁷⁵



¹⁷³For a summary of work on the use of Cr carbenes to synthesize arenes, see K. H. Dötz, *Angew. Chem. Int. Ed. Engl.*, **1984**, 23, 587.

¹⁷⁴W. D. Wulff, P.-C. Tang, K.-S., Chan, J. S. McCullum, D. C. Yang, and S. R. Gilbertson, *Tetrahedron*, **1985**, 41, 5813.

¹⁷⁵Electronic effects also play a role in directing regiochemistry. Electron-withdrawing substituents tend to end up *ortho* to the phenol group, whereas electron-donating groups (such as ethers) prefer the *meta* position. See F. J. McQuillan, D. J. Parker, and G. R. Stephenson, *Transition Metal Organics for Organic Synthesis*, Cambridge University Press: Cambridge, 1991, pp. 419–420.

**Scheme 12.25**

Mechanism of the
Dötz Reaction

Scheme 12.25 shows the generally accepted mechanism for the cyclization. First, carbene complex **70** loses one CO ligand, which provides an open coordination site for the incoming alkyne and formation of **71** (overall a dissociative ligand substitution, which is considered the rate-determining step).¹⁷⁶ An early proposal for the next step suggested that rearrangement of **71** would lead to chromacyclobutene **72**, a reaction that should be familiar from Chapters 10 and 11. Calculations indicated, however, that this was not likely,¹⁷⁷ and instead direct

¹⁷⁶H. Fischer and P. Hofmann, *Organometallics*, **1999**, *18*, 2590, and references therein.

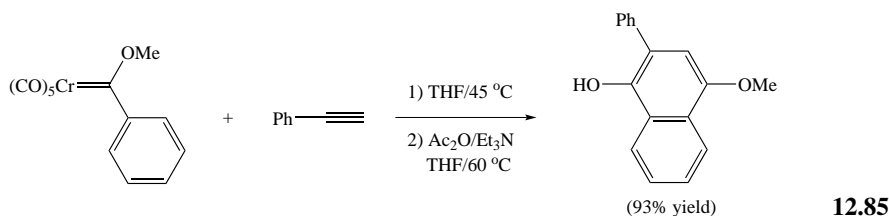
¹⁷⁷P. Hofmann and M. Hämmerle, *Angew. Chem. Int. Ed. Engl.*, **1989**, *28*, 908; for an examination of the entire mechanism of the Dötz reaction at the DFT level of theory, see

insertion of the alkyne between Cr and C_{carbene} occurs to yield **73**. Next, migratory CO insertion occurs to produce ketene **74**, which is followed by electrocyclic ring closure to give cyclohexadienone complex **75**.¹⁷⁸ The driving force for the reaction, regardless of prior mechanistic steps, is the highly exothermic and rapid keto–enol tautomerism to yield phenol–Cr complex **76**.¹⁷⁹ Several methods exist to remove the metal from the η^6 - π ligand of **76** to produce highly substituted aromatic compound **77**. These include oxidative treatment with air or Ce(IV) and carbonylation of Cr in an atmosphere of CO.¹⁸⁰

For unsymmetrical alkynes, there are two orientations possible for the alkyne substituents in the final six-membered ring product. Assume that 1-hexyne reacts with $(\text{CO})_5\text{Cr}=\text{C}(\text{OMe})(\text{Ph})$ to give a naphthol derivative. Follow the reaction through according to Scheme 12.25 and determine the predominant regioisomer based upon the difference in steric hindrance of the substituents attached to the triple bond of the alkyne.

Exercise 12-16

The Dötz arene synthesis is an excellent technique for construction of complex, densely functionalized aromatic ring systems. Equations 12.85–12.87 present three examples.

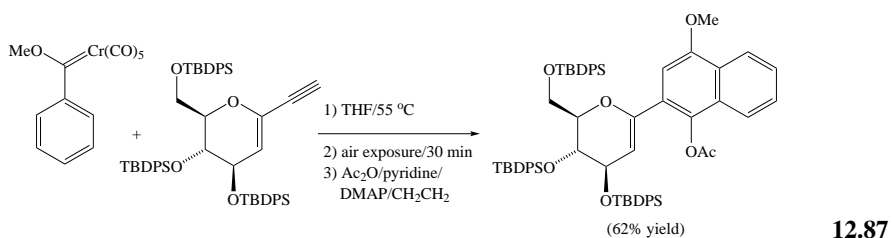
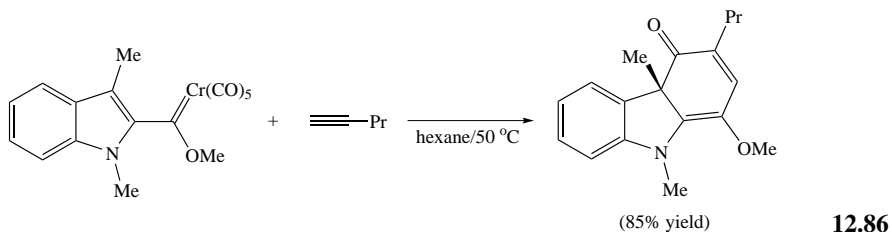


M. M. Gleichmann, K. H. Dötz, and B. A. Hess, *J. Am. Chem. Soc.*, **1996**, *118*, 10551. For a recent theoretical investigation of the Dötz reaction, which supports earlier work, see S. Ketrat, S. Müller, and M. Dolg, *J. Phys. Chem. A*, **2007**, *111*, 6094.

¹⁷⁸For additional information on electrocyclic ring openings and closures, see P. Y. Bruice, *Organic Chemistry*, 5th ed., Pearson/Prentice Hall: Upper Saddle River, NJ, 2007, pp. 1269–1275 and F.A. Carey and R.J. Sundberg, *Advanced Organic Chemistry, Part A*, 5th ed., Springer Scientific: New York, 2007, Chap. 10, especially pp. 892–911.

¹⁷⁹Keto–enol tautomerism will not occur if there are two substituents at C-6.

¹⁸⁰For a good summary of mechanistic investigations on the Dötz reaction, see A. de Meijere, H. Schirmer, and M. Duetsch, *Angew. Chem. Int. Ed.*, **2000**, *39*, 3964, and references therein; see also M. L. Waters, M. E. Bos, and W. D. Wulff, *J. Am. Chem. Soc.*, **1999**, *121*, 6403.



Equation **12.85**¹⁸¹ shows a benzoannulation to produce a substituted naphthalene in very good yield. The phenol is acetylated in the same reaction vessel, and apparently the reaction conditions, including the presence of acetic anhydride and Et₃N, cause the chromium carbonyl fragment to depart. Formation of a substituted indole occurs in equation **12.86**.¹⁸² Because a methyl group resides at the 3-position on the indole–carbene complex, the keto form is the end product. A naphthyl glycoside results in the reaction shown by equation **12.87**, which also demonstrates that monosaccharide units survive typical Dötz reaction conditions. Again, the phenolic group is intercepted by acetic anhydride to form the phenyl acetate product. Exposure to air is used for decomplexation.¹⁸³

12-5-2 Cyclizations Involving Palladium

Discovered over 60 years ago¹⁸⁴ and analogous to the renowned Diels–Alder reaction, the *ene reaction* (equation **12.88**) is a concerted transformation that brings together two partners, one of which is a simple π system, called the *ene* (typically an isolated C=C or C=O bond with at least one hydrogen at the allylic position) and the other an isolated π bond, termed the *enophile* (enophiles with electron-withdrawing groups attached to the π system work best). The reaction resembles a cycloaddition, proceeding through a six-electron, six-membered-ring transition state (**78**), and both intra- and intermolecular versions are known. Because the reaction

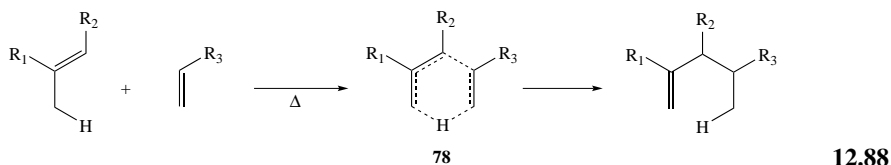
¹⁸¹J. Bao, W. D. Wulff, *et al.*, *J. Am. Chem. Soc.*, **1996**, *118*, 3392.

¹⁸²W. E. Bauta, W. D. Wulff, S. F. Pavkovic, and E. J. Zaluzec, *J. Org. Chem.*, **1989**, *54*, 3249.

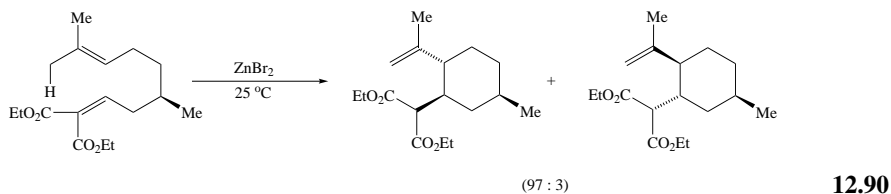
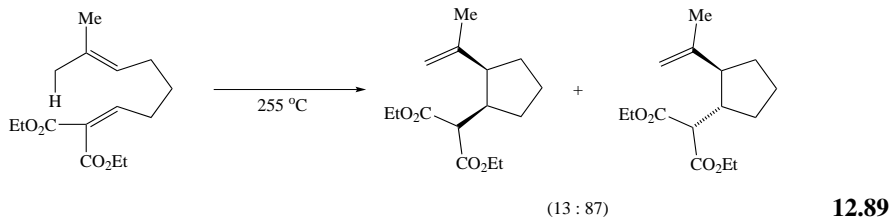
¹⁸³S. R. Pulley and J. P. Carey, *J. Org. Chem.*, **1998**, *63*, 5275.

¹⁸⁴K. Alder, F. Pascher, and A. Schmitz, *Chem. Ber.*, **1943**, *76*, 27.

results in the formation of a new C–C bond with the stereoselectivity attendant concerted processes, the ene reaction has great potential as a useful synthetic procedure. Intramolecular versions, moreover, produce rings. The utility of the transformation was limited for many years, however, because of the high temperatures required compared with those used for its more famous analog, the Diels–Alder reaction.



The discovery that Lewis acids catalyze ene reactions greatly increased the utility of the transformation.¹⁸⁵ Equations **12.89**¹⁸⁶ and **12.90**¹⁸⁷ demonstrate the effect of a Lewis acid, ZnBr₂, in not only decreasing the severity of reactions conditions required, but also increasing the stereoselectivity observed.



Palladium is effective as a catalyst for the ene reaction. Two research groups, Trost's¹⁸⁸ in the United States and Oppolzer's¹⁸⁹ in Switzerland, used slightly different approaches to synthesize five-membered rings via a Pd-catalyzed ene reaction. Scheme **12.26** shows an example of Trost's procedure. The starting

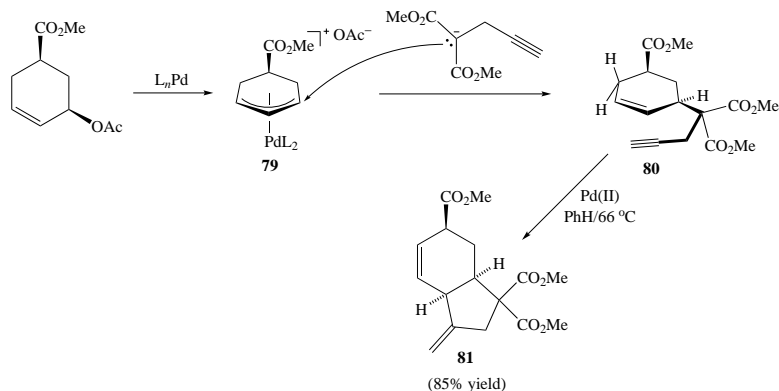
¹⁸⁵For a review of acid-catalyzed ene reactions, see B. B. Snider, *Acc. Chem. Res.*, **1980**, *13*, 426.

¹⁸⁶S. K. Ghosh and T. K. Sarkar, *Tetrahedron Lett.*, **1986**, *27*, 525.

¹⁸⁷L. F. Tietze, V. Beifuss, and M. Ruther, *J. Org. Chem.*, **1989**, *54*, 3120.

¹⁸⁸B. M. Trost, *Acc. Chem. Res.*, **1990**, *23*, 34, and references therein.

¹⁸⁹W. Oppolzer, *Angew. Chem. Int. Ed. Engl.*, **1989**, *28*, 38.

Scheme 12.26Trost's Pd-Catalyzed
Ene Reaction

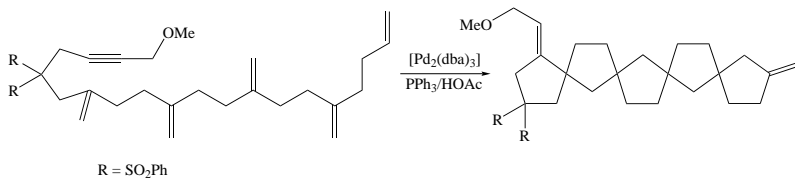
material for the ene reaction is a 1,6-enyne (**80**), which results from a nice application of chemistry we have already seen—attack of a stabilized carbanion on a Pd–allyl complex (**79**) (the Tsuji–Trost reaction, Section 12-2). Once formed, **80** undergoes the ene reaction in the presence of Pd(II) to give **81**.

Research on the mechanism of the Pd(II)-catalyzed ene reaction points to a hypopalladation cycle shown in Scheme 12.27, which first involves complexation of Pd to both π ligands of the substrate to yield **82** (step a). Migratory 1,2-insertion of the alkyne into the Pd–H bond provides **83** (step b), and then 1,2-insertion of the η^2 -coordinated double bond occurs to yield **84** (step c). Finally, step d is β -elimination, which yields two possible regioisomers (**85** and **86**).

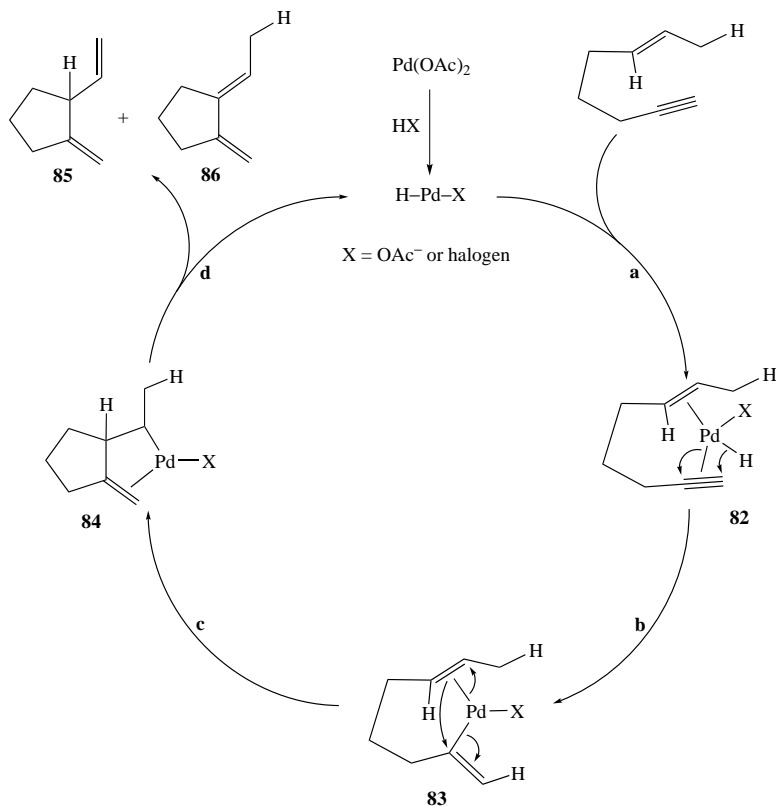
Several applications of the Trost ene reaction have appeared in the literature. A spectacular extension of this reaction involves a cascade of reactions, first using the ene reaction to construct a five-membered ring and then utilizing the remaining functionality to initiate a subsequent ene reaction followed by an electrocyclic ring closure.¹⁹⁰ Scheme 12.28 describes this transformation in which an acyclic molecule is transformed in one operation into a tricyclic species.

Exercise 12-17

The reaction below is another impressive example of cascading intramolecular ene reactions. Show how the transformation occurs by writing down all the intermediates formed after each ene reaction.



¹⁹⁰B. M. Trost and Y. Shi, *J. Am. Chem. Soc.*, **1992**, *114*, 791.

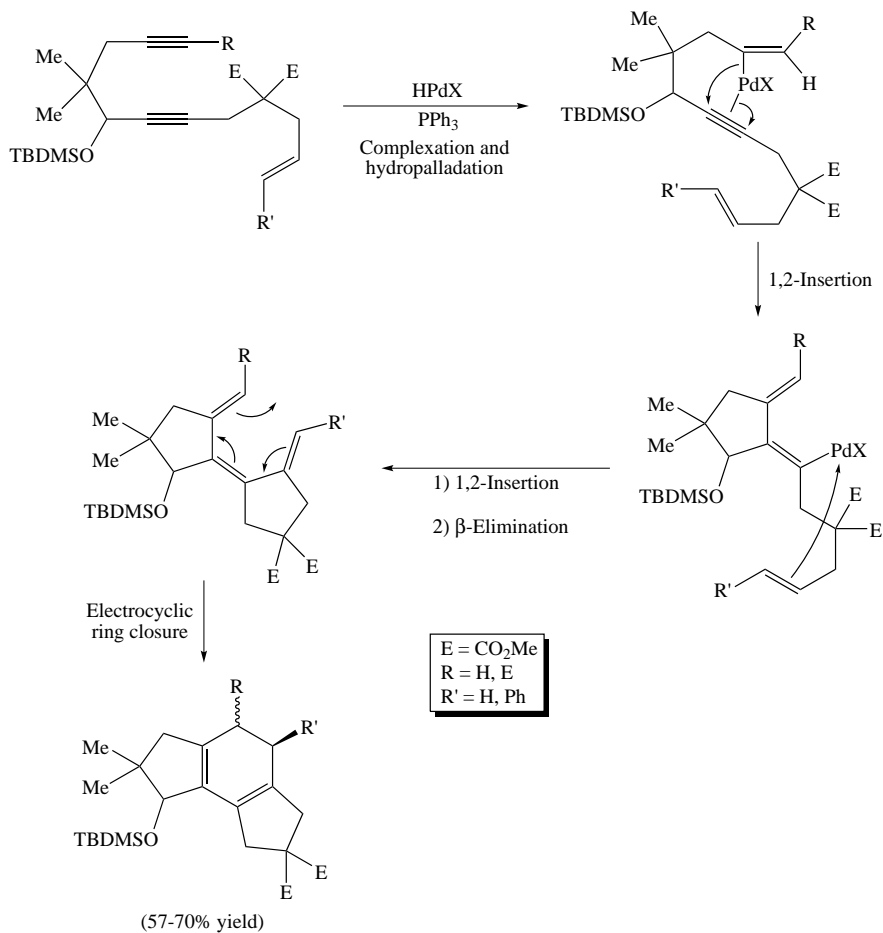
**Scheme 12.27**

The
Hydropalladation
Mechanism for the
Ene Reaction

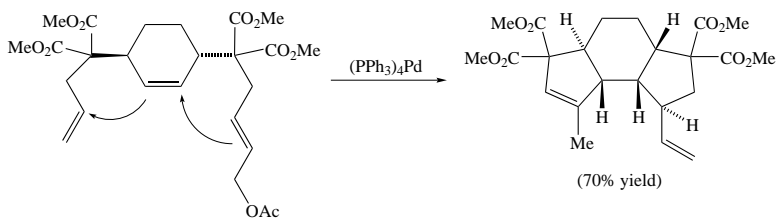
Oppolzer's approach to Pd-catalyzed ene reactions starts with an allyl acetate that is part of a 1,6-diene system. Scheme 12.29 details a plausible mechanism that involves a Pd(0) species as the active catalyst. The cycle begins with oxidative addition of the allyl acetate portion of **87** to give **88**. Next, η^1 - to η^3 -allylic rearrangement leads to **89**, and allylic rearrangement again gives **90**. Insertion of a 1,2-C=C bond follows, yielding **91**. The last step, as in the Trost procedure, is β -elimination.

Equation 12.91 shows an application of Oppolzer's approach in which two five-membered rings result from consecutive ene reactions.¹⁹¹

¹⁹¹W. Oppolzer and R. J. DeVita, *J. Org. Chem.*, **1991**, 56, 6256. Oppolzer has also used Rh(I) complexes to catalyze the ene reaction. Yields are similar, but the stereochemical results are opposite those obtained with Pd catalysts. This difference may be a function of the octahedral geometry of Rh(III) intermediates, presumably generated during the catalytic cycle. See W. Oppolzer and A. Fürstner, *Helv. Chim. Acta.*, **1993**, 76, 2339.

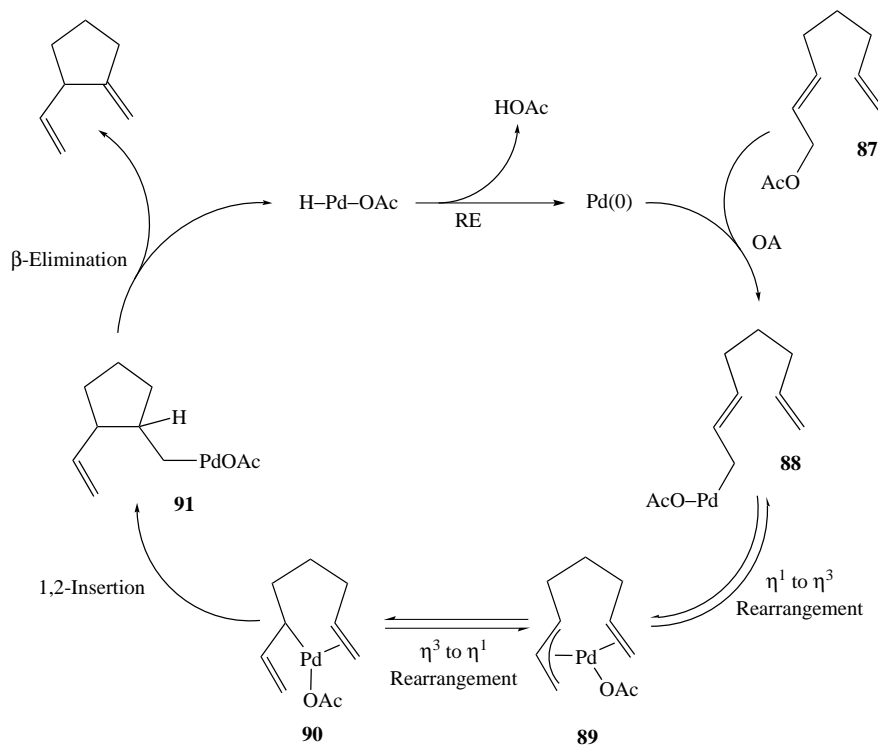
**Scheme 12.28**

Pd-Catalyzed
 Ene Cascade
 of Cyclization
 Reactions

**12.91**

An Oppolzer cyclization was used in the stereoselective synthesis of (–)-erythrodiene (**95**), a sesquiterpenoid isolated from Caribbean coral (Scheme **12.30**).¹⁹²

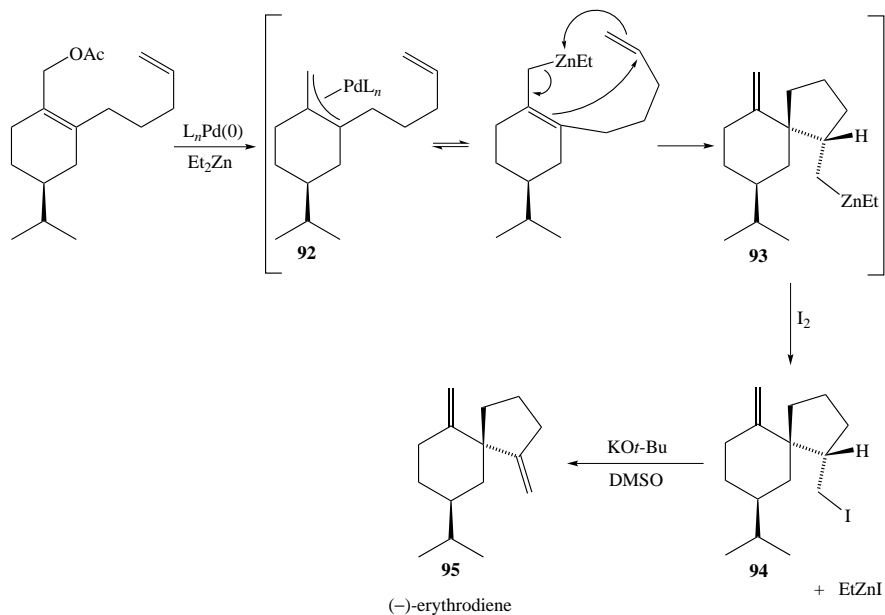
¹⁹²W. Oppolzer and F. Flaschmann, *Tetrahedron Lett.*, **1998**, 39, 5019.



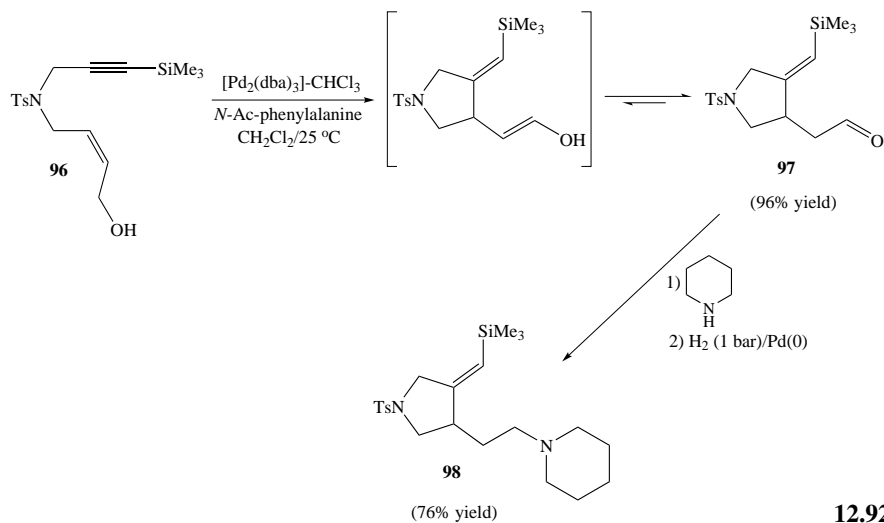
An interesting twist here is to use a stoichiometric excess of Et_2Zn to transmetalate the η^3 -allyl-Pd intermediate **92**, which can then react with a variety of electrophiles (see Section 8-4). In this case, iodination of dialkylzinc compound **93** yields alkyl halide **94**, which is nicely set up to give only one E2 elimination product—(–)-erythrodiene. The use of Et_2Zn allowed Oppolzer to run the metal-ene cyclization at a low temperature.

Equation 12.92 highlights a recent example of Trost metal-ene cyclization where enyne **96** yielded azacyclopentane **97**.¹⁹³ The addition of a catalytic amount of an acetylated amino acid (*N*-acetylphenylalanine) provides just the right amount of acidity to speed up the reaction. If the reaction occurs in the presence of a secondary amine, the ketone that initially forms from the cyclization becomes an enamine. Subsequent hydrogenation over the Pd catalyst already present produces amine **98**.

¹⁹³C. J. Kressierer and T. J. J. Müller, *Org. Lett.*, **2005**, 7, 2237.

**Scheme 12.30**

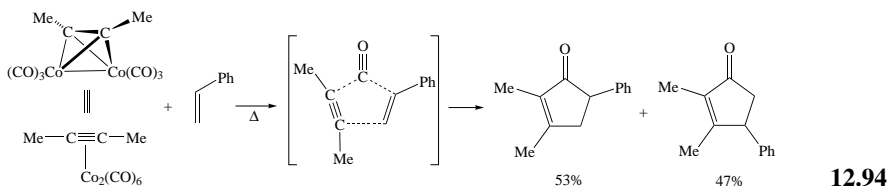
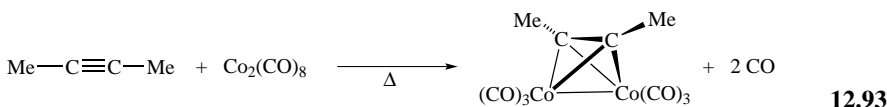
Use of the Oppolzer Metal–Ene Reaction for the Synthesis of (-)-Erythrodiene

**12.92****Exercise 12-18**

Propose a mechanism to explain how the metal–ene cyclization followed by reaction with piperidine and subsequent hydrogenation, shown in equation **12.92**, produced amine **98**.

12-5-3 Cobalt-Promoted Formation of Five-Membered Rings— The Pauson–Khand Reaction

Alkynes react with $\text{Co}_2(\text{CO})_8$ to form stable dicobalt complexes according to equation **12.93**. Reaction of these complexes with alkenes at elevated temperature and high CO pressure results in the formation of cyclopentenones (equation **12.94**). The transformation, formally a $[2 + 2 + 1]$ cycloaddition (the connecting fragments are shown in equation **12.94**), was first reported in the early 1970s by Pauson, Khand, and co-workers.¹⁹⁴ It is now formally called the Pauson–Khand (P–K) reaction. The reaction forms three new C–C bonds in one fell swoop. There are few other reactions promoted by transition metals that can create complex five-membered ring systems in one step (see Chapter 11 and Sections **12-5-2** for other good examples of this kind of transformation). Additionally, the P–K reaction tolerates the presence of many organic functional groups.



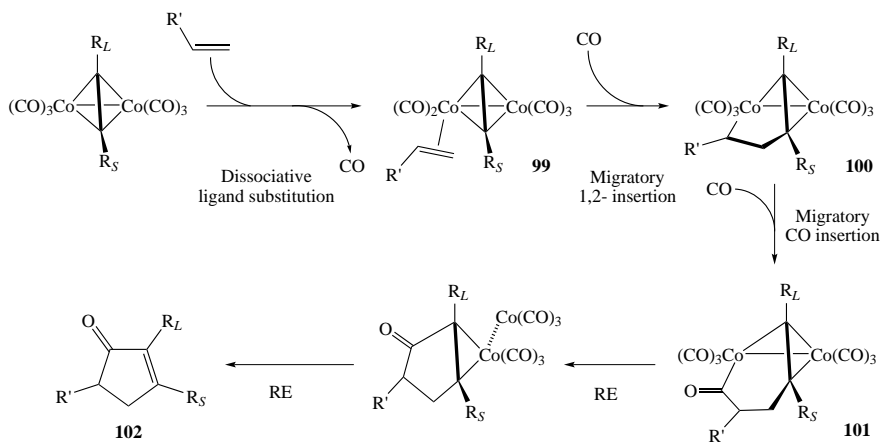
Unlike most of the reactions involving organotransition metals that we have already mentioned, this transformation was initially discovered and developed as *stoichiometric* in Co, not catalytic. More recent investigations of the P–K reaction have uncovered a catalytic method, which will be covered briefly later in this section. The mechanism is not completely known at this time; however, Magnus proposed a stepwise mechanism over 20 years ago (Scheme **12.31**),¹⁹⁵ which is still accepted today as the most likely pathway. After loss of CO and complexation of the alkyne to form the alkyne – $\text{Co}_2(\text{CO})_6$ complex, CO is lost as part of a dissociative ligand substitution to make way for binding of the alkene to one of the Co atoms (intermediate **99**). Migratory 1,2-insertion of the alkene, driven by the presence of extra CO, yields cobaltacycle **100**. Migratory CO insertion into the ring produces intermediate **101**, which sets up two consecutive reductive

¹⁹⁴I. U. Khand, G. R. Knox, P. L. Pauson, and W. E. Watts, *J. Chem. Soc. Chem. Commun.*, **1971**, 36 and I. U. Khand, G. R. Knox, P. L. Pauson, W. E. Watts, and M. I. Foreman, *J. Chem. Soc., Perkin Trans. I*, **1973**, 977.

¹⁹⁵P. L. Magnus, C. Exon, and P. Albaugh-Robertson, *Tetrahedron*, **1985**, *41*, 5861 and P. L. Magnus and M. Principe, *Tetrahedron Lett.*, **1985**, *26*, 4851.

Scheme 12.31

Mechanism of the
Pauson–Khand
Reaction



eliminations to finally give cyclopentenone **102**. Finally, it should be noted that although the P–K reaction occurs primarily at only one of the two Co atoms, the other cobalt carbonyl fragment seems to serve as an anchor to stabilize the reactions occurring at the reactive Co center.¹⁹⁶

Theoretical studies demonstrated that the Magnus mechanism is a reasonable pathway, and they further indicated that the loss of CO before alkene complexation, as is the case with the Dötz cyclization, is probably the rate-determining step. Calculations showed that 1,2-alkene insertion also has a relatively high energy barrier, is irreversible, and may be rate limiting in some cases.¹⁹⁷ It is this step that determines both the regio- and the stereoselectivity of the alkene fragment in the cyclopentenone. Special mass spectrometric techniques have observed in the gas phase some of the intermediates postulated by Magnus.¹⁹⁸

The P–K reaction is regioselective for cycloaddition of substituted alkynes, yielding a cyclopentenone in which the larger alkyne substituent is usually adjacent to the keto group. Stereochemistry about 1,2-disubstituted alkenes is typically preserved upon cycloaddition; however, if the substituents are different, both regioisomers will form. The reaction is quite sensitive to the nature of the alkene. Tri- and tetra-substituted olefins are unreactive, and the order of

¹⁹⁶For a good review of the mechanism of the P–K reaction, see S. Laschat, A. Becheanu, T. Bell, and A. Baro, *Synlett*, **2005**, 2547.

¹⁹⁷(a) M. Yamanaka and E. Nakamura, *J. Am. Chem. Soc.*, **2001**, 123, 1703 and (b) T. J. M. de Bruin, A. Millet, A. E. Greene, and Y. Gimbert, *J. Org. Chem.*, **2004**, 69, 1075.

¹⁹⁸Y. Gimbert, D. Lesage, A. Milet, F. Fournier, A. E. Greene, and J.-C. Tabet, *Org. Lett.*, **2003**, 5, 4073.

reactivity for cycloalkenes is the following: cyclohexene < cyclopentene < norbornene (bicyclo[2.2.1]hept-2-ene); cyclopropenes are also reactive.¹⁹⁹

The first examples of the P–K reaction required high temperatures and pressures to succeed. Several improvements in yield and reaction rate have resulted from continued research efforts over the past 30 years. These include the addition of silica gel²⁰⁰ to the reaction mixture (adsorption of the alkyne–Co complex onto silica may restrict molecular motion, allowing the ene–yne system to interact more readily; also, lack of solvent would allow bimolecular reactions to proceed faster); the use of tertiary amine *N*-oxides;^{201,202} the application of photochemical conditions to ease departure of CO in the rate-determining step; and the inclusion of various Lewis bases, which help stabilize intermediate Co complexes.²⁰³

Despite various improvements and enhancements, the intermolecular P–K reaction suffers from a number of problems including relatively harsh reaction conditions, poor regioselectivity at the alkene region of the five-membered ring, and diversion of product into side reactions.²⁰⁴ The intramolecular version of the P–K reaction is much more useful as a means of five-membered ring synthesis for several reasons: (1) the problem of regiochemistry is eliminated because only one orientation of the alkene with respect to the alkyne–Co complex is possible; (2) both reactants are positioned in the same molecule, so unfavorable entropy effects are diminished and the need for high concentrations of reactants is removed; (3) stereochemistry in the alkene region of the new ring is easier to

¹⁹⁹There is a correlation between the energy of the LUMO of the alkene (the π^* orbital) and its reactivity. The lower the LUMO energy, the faster the reaction. When a LUMO is low in energy, it is easier for Co to back-donate some of its electron density into the π^* orbital of the alkene. This means less electron density that is available for back-donation to the CO ligands. The CO ligands are thus less tightly bound to Co, which means they come off the metal more rapidly as needed and the overall reaction speeds up. See Footnote 197b for more explanation.

²⁰⁰S. O. Simonian, W.A. Smit, A. S. Gybin, A. S. Shashkov, G. S. Mikaelian, V. A. Tarasov, I. I. Ibragimov, R. Caple, and D. E. Froen, *Tetrahedron Lett.*, **1986**, 27, 1245.

²⁰¹S. Shambayani, W. E. Crowe, and S. L. Schreiber, *Tetrahedron Lett.*, **1990**, 31, 5289.

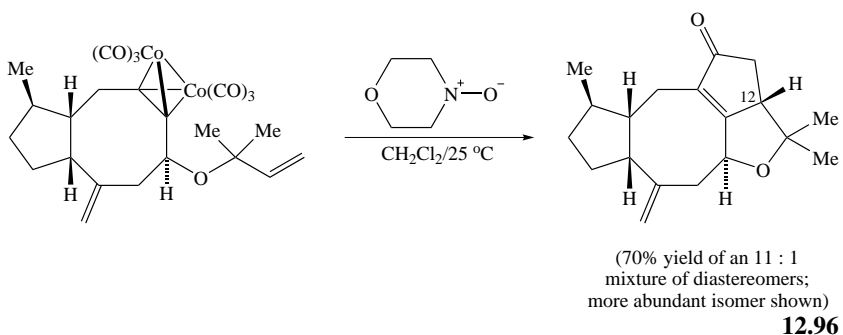
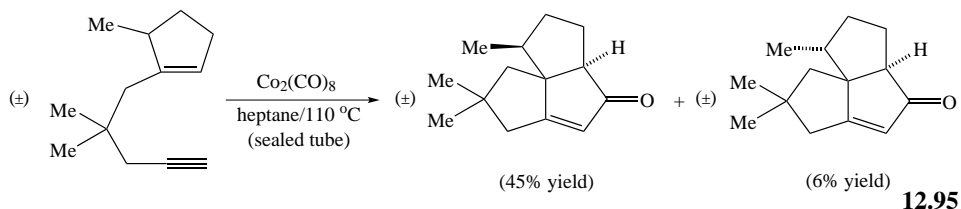
²⁰²Remember that *N*-oxides remove CO ligands by formation of CO₂ (Section 8-3); this probably opens a site on Co for complexation of the alkene fragment. More recent advances here include tethering the amine *N*-oxide onto a polymer support, which obviates the necessity of using 3–6 equivalents of amine *N*-oxide in solution. See W. J. Kerr, D. M. Lindsay, and S. P. Watson, *Chem. Commun.*, **1999**, 2551.

²⁰³For good reviews on recent advances in improving the efficacy of intermolecular P–K reactions, see Footnote 196 and S. E. Gibson and N. Mainolfi, *Angew. Chem. Int. Ed.*, **2005**, 44, 3022.

²⁰⁴For a review focusing on P–K side reactions, see L. V. R. Boñaga and M. E. Krafft, *Tetrahedron*, **2004**, 60, 9795.

control; and (4) depending on the structure of the enyne, it is possible to construct polycyclic ring systems in one step.

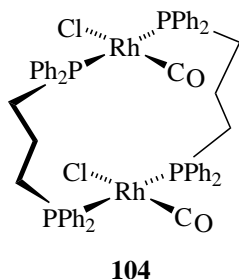
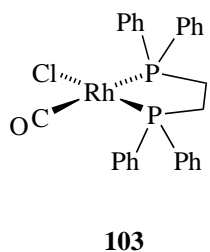
Stereoselective formation of a complex, tricyclic molecule with three five-membered rings fused together is straightforward using the P–K reaction according to equation **12.95**.²⁰⁵ Equation **12.96** illustrates the construction of a highly complex tetracyclic ring system, which was a key intermediate in the synthesis of a diterpene called epoxydictymene. Very high diastereoselectivity was demonstrated in the cyclization at C-12, and the use of an amine *N*-oxide allowed the reaction to proceed at room temperature.²⁰⁶



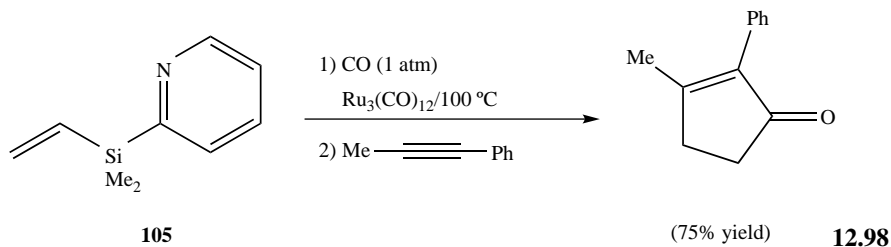
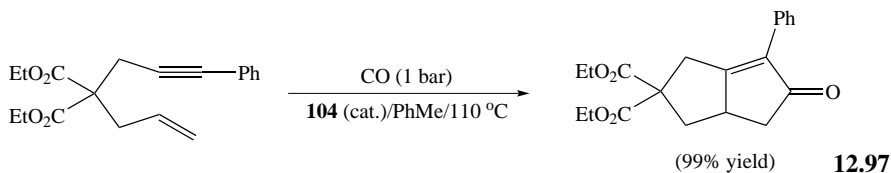
Two relatively recent advancements that have increased the utility of the P–K reaction include (1) allowing the reaction to run with catalytic amounts of transition metal and (2) making the transformation asymmetric. Several metals beside Co will catalyze the P–K reaction, including Rh, Ir, Fe, Ru, Group 6 metals, and Ti. Much of the work in catalyst development has focused on use of Rh(I) and Ru(II) complexes, which seem to be most effective. Many Rh precatalysts have been used, such as $\text{Rh}_3(\text{CO})_{12}$, Wilkinson's catalyst, and complexes **103** and **104**. AgOTf is often used in conjunction with the last three catalysts to remove Cl, which then produces more catalytically active cationic Rh(I) species.

²⁰⁵N. E. Schore and E. G. Rowley, *J. Am. Chem. Soc.*, **1988**, *110*, 5224.

²⁰⁶T. F. Jamison, S. Shambayati, W. E. Crowe, and S. L. Schreiber, *J. Am. Chem. Soc.*, **1997**, *119*, 4353.



Equation **12.97** illustrates use of catalyst **104** in the synthesis of a bicyclic ring system.²⁰⁷ Note that the presence of a catalyst also allows the transformation to occur under a CO pressure of 1 bar. Equation **12.98** demonstrates a clever application of the so-called “traceless tether” method for running a Ru-catalyzed P–K reaction.²⁰⁸ Although this is an intermolecular P–K reaction, the alkene is tethered to a pyridylsilyl group (compound **105**), which directs regioselective reaction of the alkene fragment with the alkyne. The presence of residual H₂O in the reaction mixture removes the silyl group, which can be recycled.

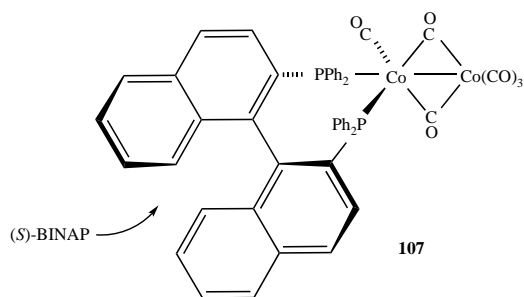
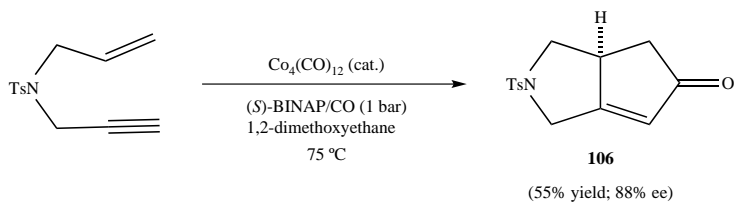


Chemists have investigated asymmetric P–K reactions, using chiral diphosphine and diphosphite ligands to induce enantioselectivity. When (*S*)-BINAP was added to a catalytic amount of Co₄(CO)₁₂, (*S*)-bicyclic ketone **106** formed in 55% yield with an ee of 88% (equation **12.99**). Experimental evidence suggested that the active catalyst was dicobalt complex **107**, in which BINAP binds in bidentate

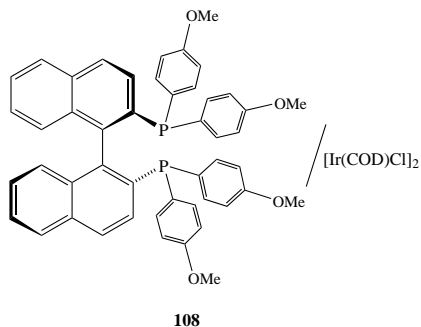
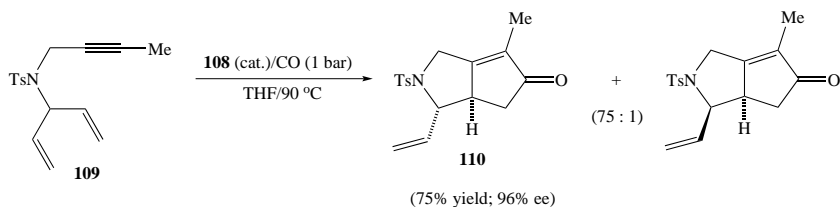
²⁰⁷N. Jeong, B. K. Sung, J. S. Kim, S. B. Park, S. D. Seo, J. Y. Shin, K. Y. In, and Y. K. Choi, *Pure Appl. Chem.*, **2002**, 74, 85.

²⁰⁸K. Itami, K. Mitsudo, K. Fujita, Y. Ohashi, and J. Yoshida, *J. Am. Chem. Soc.*, **2004**, 126, 11058.

fashion to one of the Co atoms.²⁰⁹ Equation 12.100 shows an asymmetric P–K reaction in which a chiral Ir catalyst (**108**), based on a modified (*R*)-BINAP ligand, was used to desymmetrize *meso*-dienyne **109**; the resulting bicycloketone **110** formed with an ee of 96%.²¹⁰



12.99



12.100

²⁰⁹S. E. Gibson, K. A. C. Kaufmann, J. A. Loch, and A. Miyazaki, *Pure Appl. Chem.*, **2008**, *80*, 903.

²¹⁰N. Jeong, D. H. Kim, and J. H. Choi, *Chem. Commun.*, **2004**, 1134.

Chapter 12 serves as an introduction to a huge area of chemistry devoted to the use of organometallic compounds for the construction of complex molecules. The material covered in Chapter 12 exemplifies several of the most important applications of organotransition metal chemistry to organic synthesis. Thousands of articles have appeared over the past 10 years that report on either the use of transition metal compounds in key steps of syntheses, which would be difficult or even impossible to carry out without transition metals, or on the development of novel methodology that may have many applications to synthesis down the road. Research on the connection between organometallic chemistry and synthesis remains active and fruitful, and there is every indication that this endeavor will continue to hold the interest of chemists for many years to come.

Suggested Readings

General References on Organometallic Synthesis

- J. J. Li and G. W. Gribble, *Palladium in Heterocyclic Chemistry*, 2nd ed., Elsevier: Amsterdam, 2007.
- F. A. Carey and R. J. Sundberg, *Advanced Organic Chemistry Part B: Reactions and Synthesis*, 5th ed., Springer: New York, 2007, Chap. 8.
- C. Elschenbroich, *Organometallics*, 3rd. ed., Wiley–VCH: Weinheim, Germany, 2006, Chap. 18.
- J. Tsuji, *Palladium Catalysts and Reagents*, Wiley: Chichester, UK, 2004.
- L. F. Tietze, H. Ila, and H. P. Bell, *Chem. Rev.*, **2004**, *104*, 3453.
- M. B. Smith, *Organic Synthesis*, 2nd ed., McGraw–Hill: New York, 2002, Chap. 12.
- L. S. Hegedus, *Transition Metals in the Synthesis of Complex Organic Molecules*, 2nd ed., University Science Books: Sausalito, CA, 1999.

Enantioselective Functional Group Interconversions

- W. S. Knowles and R. Noyori, *Acc. Chem. Res.*, **2007**, *40*, 1238, and references therein.
- J. T. Mohr, D. C. Ebner, and B. M. Stoltz, *Org. Biomol. Chem.*, **2007**, *5*, 3571.
- R. Noyori, *Chem. Commun.*, **2005**, 1807.
- B. M. Trost, *Proc. Natl. Acad. Sci.*, USA, **2004**, *101*, 5348.
- R. Noyori, *Angew. Chem. Int. Ed.*, **2002**, *41*, 2008.

Carbon–Carbon Bond Formation via Nucleophilic Attack on a π Ligand

- L. F. Tietze and T. Kinzel, *Pure Appl. Chem.*, **2007**, *79*, 629.
- J. T. Mohr and B. M. Stoltz, *Chem. Asian J.*, **2007**, *2*, 1476.
- B. M. Trost and M. Crawley, *Chem. Rev.*, **2003**, *103*, 2921.
- J. Tsuji, *Tetrahedron*, **1986**, *42*, 4361.

Carbon–Carbon Bond Formation via Carbonyl and Alkene Insertion

- C. Claver, M. Diéguez, O. Pàmies, and S. Castillón, *Top. Organomet. Chem.*, **2006**, *18*, 35.
 A. M. Trzeciak and J. J. Ziolkowski, *Coord. Chem. Rev.*, **2005**, *249*, 2308.
 A. B. Dounay and L. E. Overman, *Chem. Rev.*, **2003**, *103*, 2945.

Carbon–Carbon Bond Formation via Transmetalation Reactions

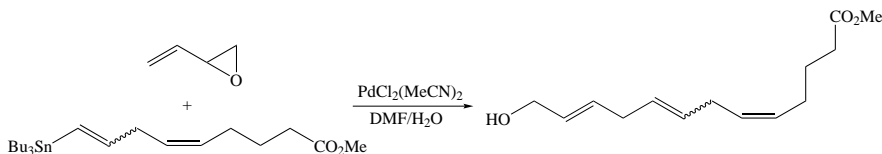
- J. B. Johnson and T. Rovis, *Angew. Chem. Int. Ed.*, **2008**, *47*, 840.
 R. Chinchilla and C. Nájera, *Chem. Rev.*, **2007**, *107*, 874.
 E. Negishi, *Bull. Chem. Soc. Jpn.*, **2007**, *80*, 233.
 K. C. Nicolaou, P. G. Bulger, and D. Sarlah, *Angew. Chem. Int. Ed.*, **2005**, *44*, 4442.
 A. de Meijere and F. Diederich, Eds., *Metal-Catalyzed Cross-Coupling Reactions*, 2nd ed., Wiley–VCH: Weinheim, Germany, 2004.
 S. Kotha, K. Lahiri, and D. Kashinath, *Tetrahedron*, **2002**, *58*, 9633.
 N. Miyaura, *Top. Curr. Chem.*, **2002**, *219*, 11.

Carbon–Carbon Bond Formation through Cyclization Reactions

- D. Strübling and M. Beller, *Top. Organomet. Chem.*, **2006**, *18*, 165.
 K. H. Dötz and J. Stendel Jr., “The Chromium-Templated Carbene Benzannulation Approach to Densely Functionalized Arenes,” In *Modern Arene Chemistry*, D. Astruc, Ed., Wiley–VCH: Weinheim, Germany, 2002, pp. 250–296.
 N.E. Schore, *Org. React.*, **1991**, *40*, 1.
 B. M. Trost, *Angew. Chem. Int. Ed. Engl.*, **1989**, *28*, 1173.

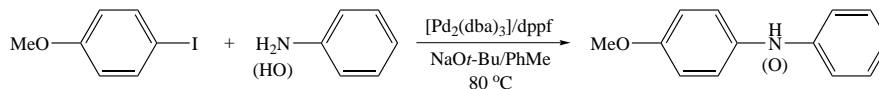
Problems

- 12-1** Calculate the difference in free energies of activation, $\Delta\Delta G^\ddagger$, at 25 °C for conversion of **7'** to **8'** and **7''** to **8''** that would be required to lead to an enantiomeric excess (ee) of 96% for the *R*-amino acid ester, **10''** (Scheme **12.3**).
- 12-2** Propose a stepwise mechanism for the following transformation.²¹¹

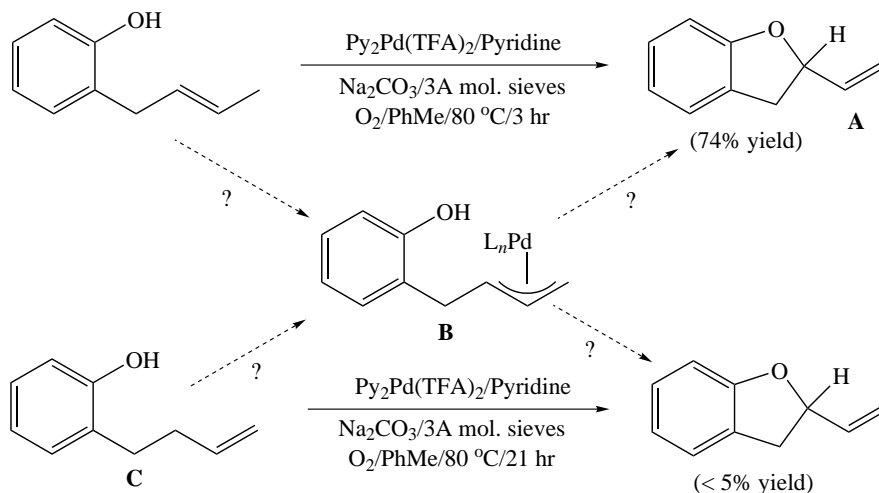


²¹¹J. D. White and M. S. Jensen, *Synlett*, **1996**, 31.

12-3 The equation below shows a very useful method for converting aryl halides to aryl amines (or phenol derivatives). Propose a mechanism for this transformation.²¹²



12-4 Consider the first oxidative cyclization shown to produce **A**. It was proposed originally that the cyclization proceeded through η^3 -allyl-Pd intermediate **B**. Treatment of **C**, however, which was predicted to form **B** under the same reaction conditions, led to **A** in less than 5% yield, even after 21 hours of reaction time. The researchers involved were forced to come up with another mechanism. Propose an alternate catalytic pathway that involves complexation of the phenolic oxygen and side chain C=C bond to Pd and then oxypalladation of the C=C bond.²¹³



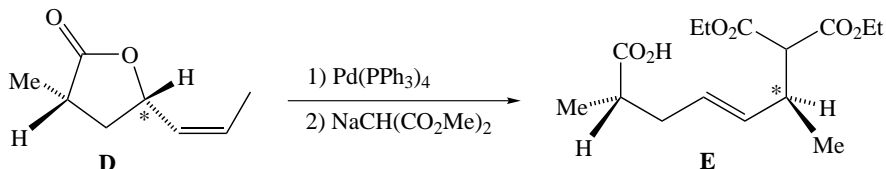
12-5 The equation on the next page demonstrates a clever transfer of the chirality at one stereocenter to another during a Pd(0)-catalyzed nucleophilic attack on an allyl ligand.²¹⁴ Try to correlate the stereochemistry of the starting material **D** with that of the final product **E**. Is the stereochemistry of the new stereocenter in **E** the result of overall retention or

²¹²J. F. Hartwig, *Angew. Chem. Int. Ed.*, **1998**, 37, 2046.

²¹³R. M. Trend, Y. K. Ramtohul, and B. M. Stoltz, *J. Am. Chem. Soc.*, **2005**, 127, 17778.

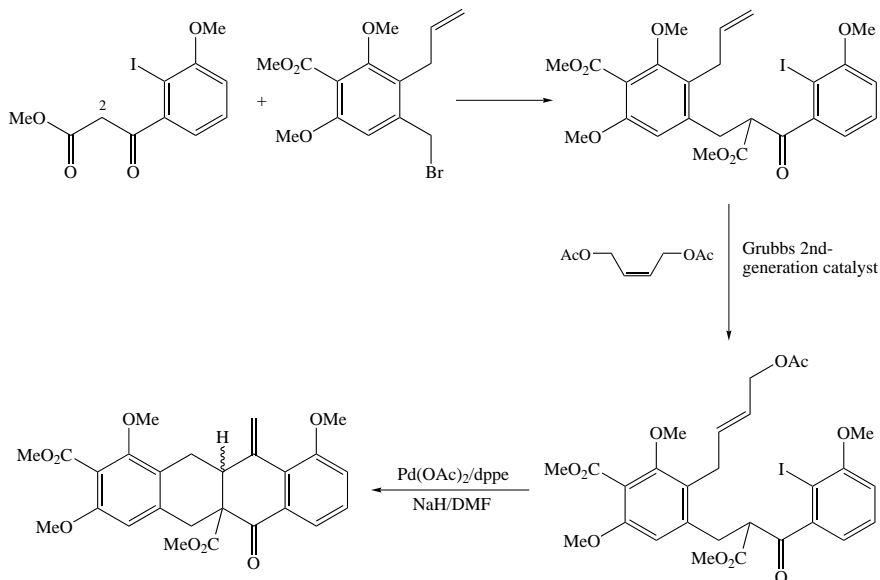
²¹⁴B. M. Trost and T. P. Klun, *J. Am. Chem. Soc.*, **1979**, 101, 6756.

inversion of configuration? Explain. [Hint: consider lactone **D** to be a masked allyl acetate.]



12-6 The reaction scheme shown is a nice application of the use of several important transition metal-catalyzed methods for producing C–C and C=C bonds.²¹⁵

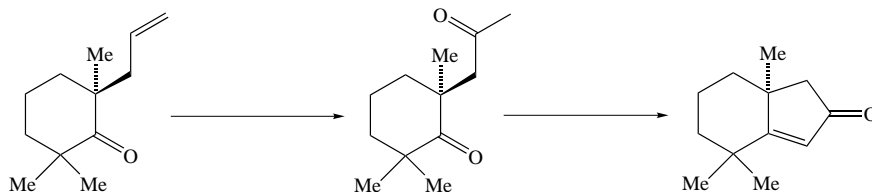
- For step 1, supply the reagents that would be necessary to complete the reaction. [Hint: Note that the hydrogen atom at C-2 is rather acidic.]
- For step 2, name the reaction type that occurs.
- For step 3, propose a mechanism for the transformation.



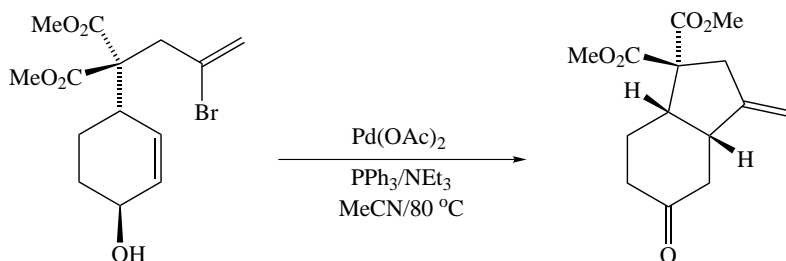
12-7 Supply the reagents necessary to carry out the two-step transformation shown on the next page.²¹⁶

²¹⁵L. F. Tietze, T. Redert, H. P. Bell, S. Hellkamp, and L. M. Levy, *Chem. Eur. J.*, **2008**, *14*, 2527.

²¹⁶J. T. Mohr and B. M. Stoltz, *Chem. Asian J.*, **2007**, *2*, 1476.

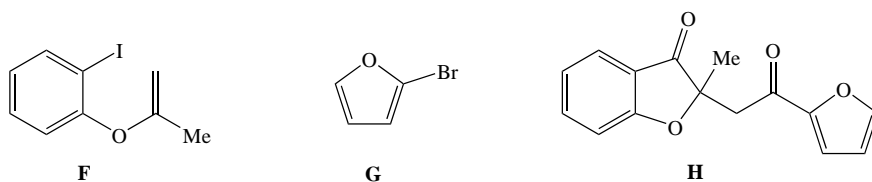
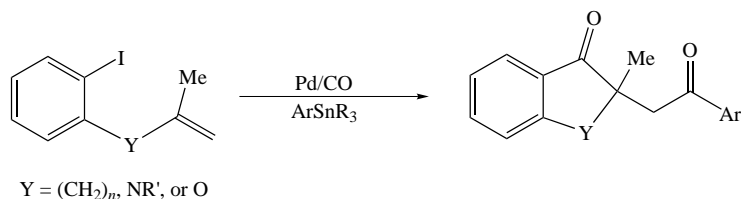


12-8 For the intramolecular olefination shown below, provide a pathway that accounts for the formation of the ketone.



12-9 Transmetalation and CO insertion reactions play key roles in the following Pd-catalyzed transformation, shown below in general form.²¹⁷

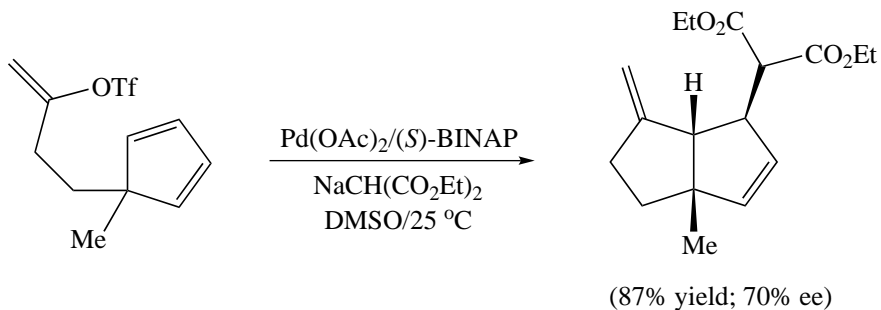
- Propose a mechanism for this transformation.
- Starting with **F** and **G**, propose a synthesis of compound **H**.



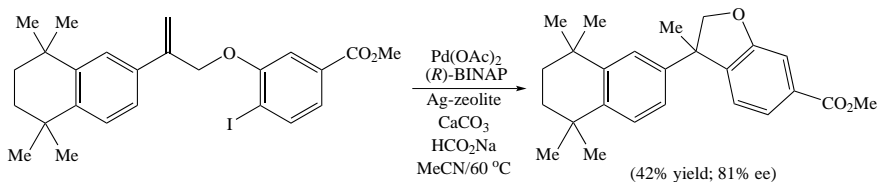
12-10 The transformation shown on the next page has been described as a Heck olefination followed by nucleophilic attack by the enolate on the η^3 -allyl-Pd

²¹⁷R. Grigg, J. Redpath, V. Sridharan, and D. Wilson, *Tetrahedron Lett.*, **1994**, 35, 7661.

intermediate. Propose a mechanism that is consistent with the above description.²¹⁸

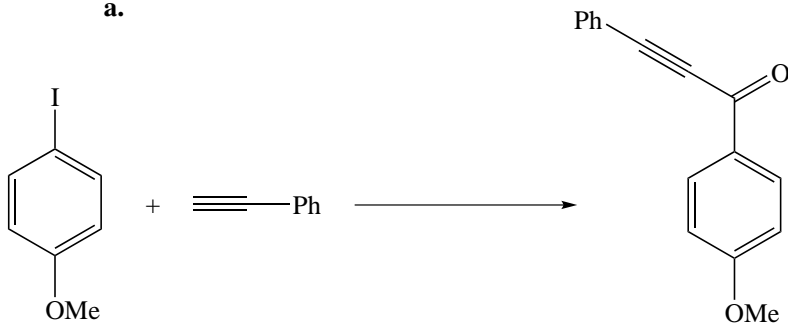


12-11 The cyclization shown below is another example of Heck olefination; however, because a quaternary center forms that makes β -elimination impossible, a reducing agent (HCO_2^-) was also required to reduce Pd(II) to Pd(0).²¹⁹ Propose a catalytic cycle for the reaction. How does HCO_2^- act as a reducing agent?



12-12 Propose two synthesis routes for each transformation, all of which use Pd chemistry.

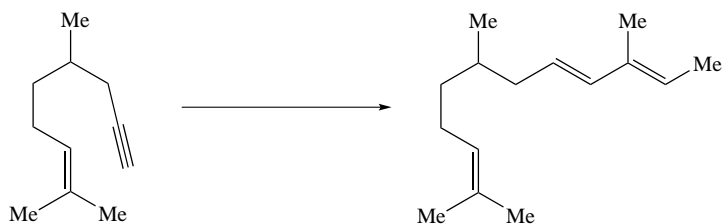
a.



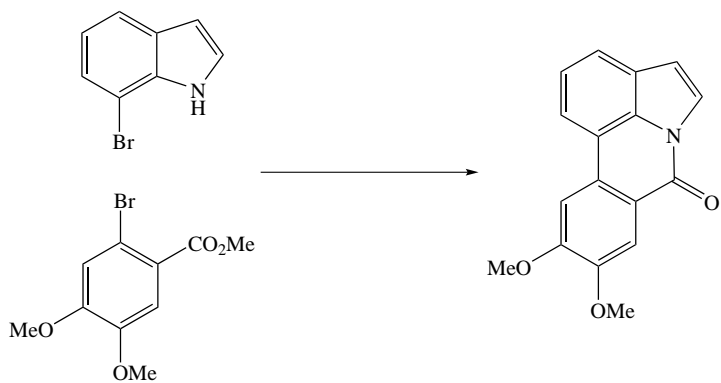
²¹⁸T. Ohshima, K. Kagechika, M. Adachi, M. Sodeoka, and M. Shibasaki, *J. Am. Chem. Soc.*, **1996**, *118*, 7108.

²¹⁹P. Diaz, F. Gendre, L. Stella, and B. Charpentier, *Tetrahedron*, **1998**, *54*, 4579.

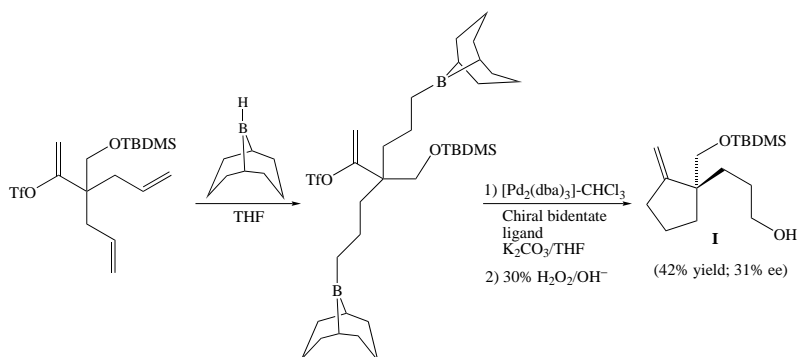
b.



c.

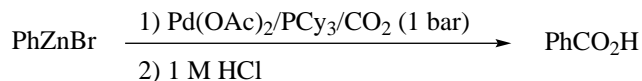


12-13 The transformation shown below is a desymmetrization that provides product **I** in modest % ee.²²⁰ Propose a mechanism-based explanation for the reaction assuming that only one *B*-alkyl side chain participates in the first step. What is the purpose of the second step?

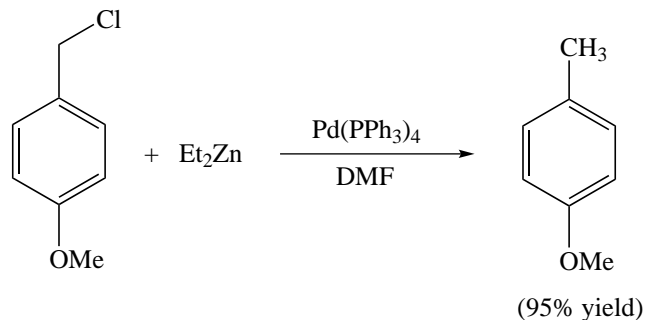


²²⁰S. Y. Cho and M. Shibasaki, *Tetrahedron: Asymmetry*, **1998**, 9, 3751.

- 12-14** CO_2 is potentially an excellent carbon source for the petrochemical industry. Unfortunately, it is rather inert chemically, and it is difficult to convert it readily to a form that is useful for further transformations. Under certain conditions, however, the CO_2 activation occurs in very good yield.²²¹ An example of recent research, which has combined organozinc chemistry with Ni- and Pd-catalyzed CO_2 activation, is shown below. A catalytic cycle has been postulated, beginning with oxidative addition of CO_2 to Pd(0) or Ni(0) to form $\text{L}_2\text{M}(\text{II})$ ($\eta^2\text{-CO}_2$), where $\text{L} = \text{PCy}_3$. The initial product is PhCO_2ZnBr , which is acidified by 1 M HCl. Propose a complete catalytic cycle for this transformation.



- 12-15** In an unusual twist to the Negishi cross-coupling reaction, *p*-substituted benzyl halides undergo reduction to *p*-substituted toluenes in the presence of Et_2Zn (one or two equivalents) and catalytic amounts of Pd(0).²²² Consider the reaction below, and propose a catalytic cycle that explains how it might occur. Assume that a $\text{L}_n\text{Pd-H}$ species forms and the by-products of the reaction are ethene and EtZnCl .

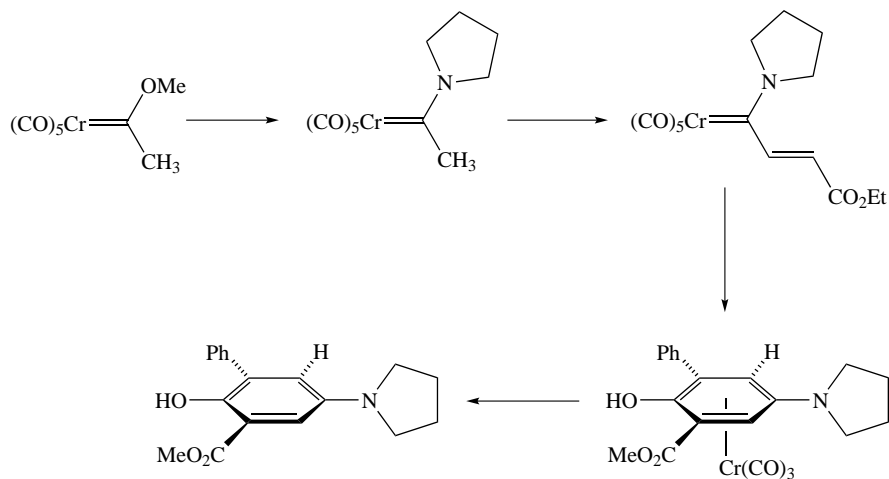


- 12-16** Consider the synthesis scheme shown. Supply missing reagents as required.²²³ [Hint: Review Section 10-2 as needed.]

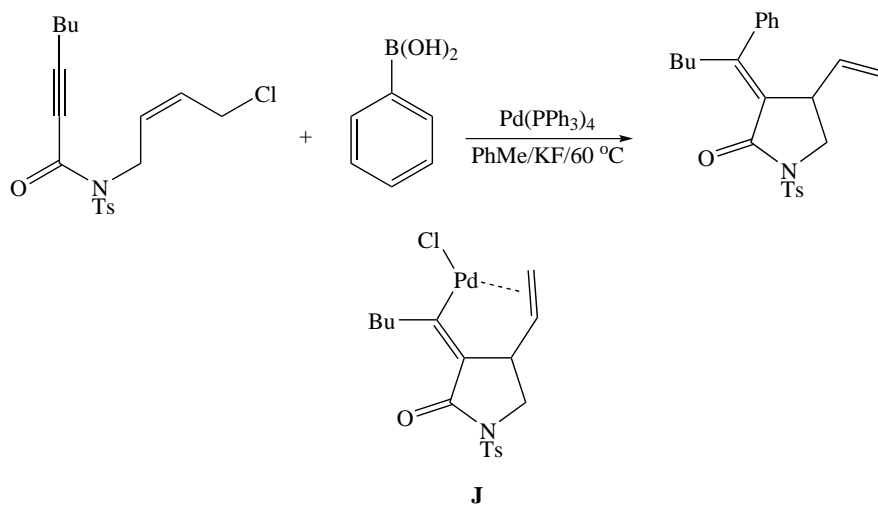
²²¹C. S. Yeung and V. M. Dong, *J. Am. Chem. Soc.*, **2008**, *130*, 7826.

²²²K. A. Agrios and M. Srebnik, *J. Org. Chem.*, **1993**, *58*, 6908.

²²³J. Barluenga, L. A. López, S. Martínez, and M. Tomás, *J. Org. Chem.*, **1998**, *63*, 7588.



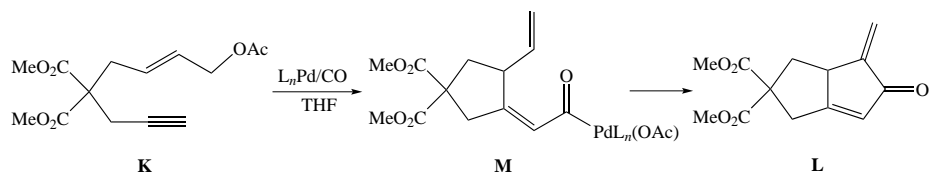
12-17 The reaction shown can be considered a combination of a Pd-catalyzed ene reaction and a Suzuki cross-coupling.²²⁴ Propose a catalytic cycle for the reaction. One of the key intermediates is structure **J**.



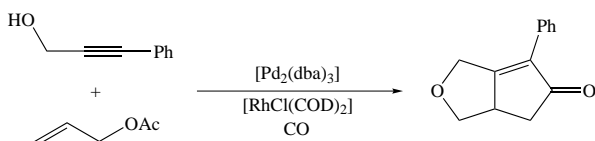
12-18 The ene reaction was used to convert acyclic compound **K** to bicyclic ketone **L**, as shown on the next page.²²⁵ The reaction is catalytic in Pd(0). Propose a catalytic cycle that accounts for the formation of two fused five-membered rings. Assume that one of the intermediates in the cycle is **M**.

²²⁴G. Zhu, X. Tong, J. Cheng, Y. Sun, D. Li, and Z. Zhang, *J. Org. Chem.*, **2005**, *70*, 1712.

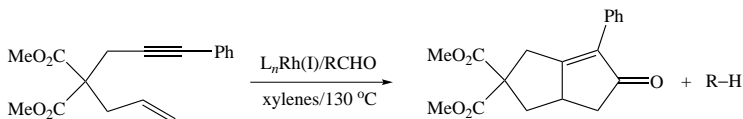
²²⁵N. H. Ihle and C. H. Heathcock, *J. Org. Chem.*, **1993**, *58*, 560.



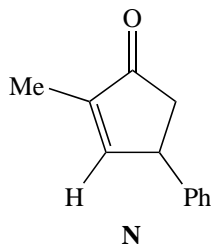
- 12-19** Two different catalysts were required for the transformation shown.²²⁶ Propose a mechanism-based explanation for the transformation, clearly stating what the role of each catalyst is.



- 12-20** A Rh-catalyzed Pauson–Khand reaction is shown below. Sometimes an aldehyde (RCHO) is used as a source of CO.²²⁷ Assume that the Rh catalyst is of the form $\text{L}_n\text{Rh(I)}$, and the by-product of the P–K reaction is R–H.



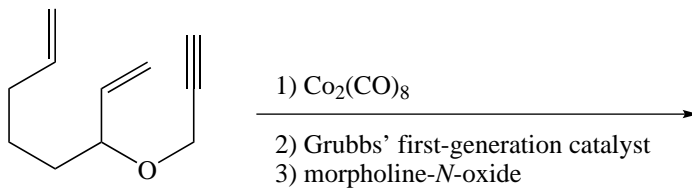
- Propose a catalytic cycle for the carbonylation of the Rh catalyst by RCHO prior to the P–K reaction.
- It is possible to achieve maximum atom economy if the aldehyde is not only the source of CO, but also is one of the reacting partners in the P–K reaction. What two reactants are necessary to produce cyclopentenone **N**?



²²⁶N. Jeong, S. D. Seo, and J. Y. Shin, *J. Am. Chem. Soc.*, **2000**, *122*, 10220.

²²⁷T. Shibata, *Adv. Synth. Catal.*, **2006**, *348*, 2328.

- 12-21** Show the intermediates and final product that result after the reagents shown are used.²²⁸



The final product was determined to be tricyclic with the following spectral information observed:

IR: $\nu = \text{ca. } 1700$ (strong) and 1100 cm^{-1} (medium)

$^1\text{H-NMR}$: δ 5.97 (singlet, 1H), 4.5 (doublet of doublets, 2H, $J = 15\text{--}20 \text{ Hz}$), 4.35 ppm (multiplet, 1H); several other peaks

$^{13}\text{C-NMR}$: δ 213, 182, 122, 75, 65, 48, 47, 29, 25, 21 ppm

Elemental analysis: %C = 73.01; %H = 7.25

²²⁸M. Rosillo, L. Casabubios, G. Domínguez, and J. Pérez-Castells, *Org. Biomol. Chem.*, **2003**, *1*, 1450.

Isolobal Groups and Cluster Compounds

13-1 THE ISOLOBAL ANALOGY

In earlier chapters, there have been a variety of examples of similarities between organometallic chemistry and organic chemistry. Such similarities can be envisioned on a broader scale by considering frontier orbitals of the molecular fragments of which organometallic compounds are composed. In his 1981 Nobel lecture, Hoffmann described molecular fragments as isolobal,

if the number, symmetry properties, approximate energy and shape of the frontier orbitals and the number of electrons in them are similar—not identical, but similar.¹

To illustrate this definition, we will use one of Hoffmann's examples, comparing fragments of methane with fragments of an octahedrally coordinated transition metal complex ML_6 . For simplicity, we will consider only σ interactions between the metal and the ligands in this complex.² The fragments to be considered are shown in Figure 13-1.

The parent compounds have filled valence-shell electron configurations, eight electrons (an "octet") for CH_4 and 18 electrons for ML_6 . Methane is considered to use sp^3 hybrid orbitals in bonding, with eight electrons occupying bonding pairs formed from interactions between the hybrids and $1s$ orbitals on the hydrogens. The metal in ML_6 , by similar reasoning, uses d^2sp^3 hybrids to bond to the ligands, with 12 electrons occupying bonding orbitals and six

¹R. Hoffmann, *Angew. Chem. Int. Ed. Engl.*, **1982**, *21*, 711.

²Pi interactions can also be considered; see Footnote 1 and H.-J. Krause, *Z. Chem.*, **1988**, *28*, 129.

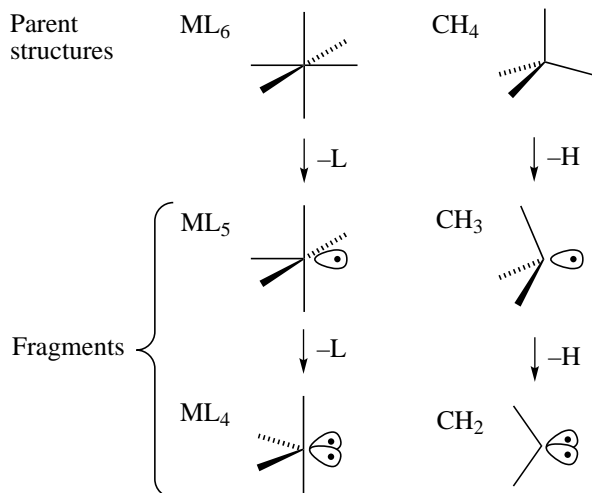


Figure 13-1

Octahedral and Tetrahedral Fragments

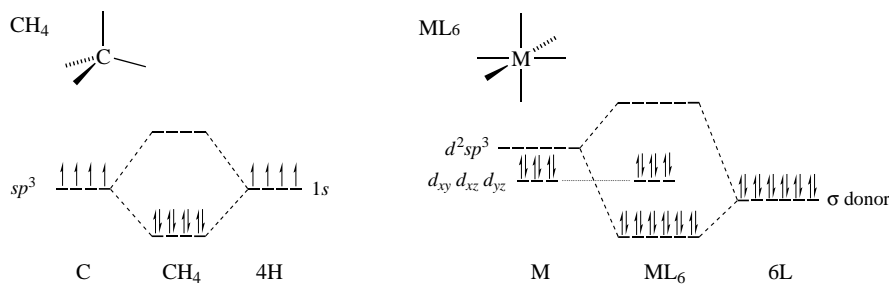


Figure 13-2

Orbitals of Parent Structures CH_4 and ML_6

nonbonding electrons occupying d_{xy} , d_{xz} , and d_{yz} orbitals. These orbitals are shown in Figure 13-2.

Molecular fragments containing fewer ligands than the parent polyhedra can now be described; for the purpose of the analogy, these fragments are assumed to preserve the original geometry of the remaining ligands.

Tetrahedral CH_4 and octahedral ML_6 can form 7- and 17-electron fragments having the orbital characteristics shown in Figure 13-3. To form the fragments used in this example, the C–H and M–L bonds are assumed to cleave homolytically.

For example, in the 7-electron fragment CH_3 , three of the sp^3 orbitals of carbon are involved in σ bonding with the hydrogens. The fourth hybrid is singly occupied and at higher energy than the σ bonding pairs of CH_3 , as shown in Figure 13-3. The frontier orbitals of the 17-electron fragment $Mn(CO)_5$ are similar to those of CH_3 . The σ interactions between the ligands and Mn in this fragment may be considered to involve five of the metal's d^2sp^3 hybrid orbitals. The sixth hybrid is singly occupied and at higher energy than the five σ bonding orbitals; in this respect, it is similar to the singly occupied hybrid in CH_3 .

Figure 13-3

Seven- and 17-Electron Fragments

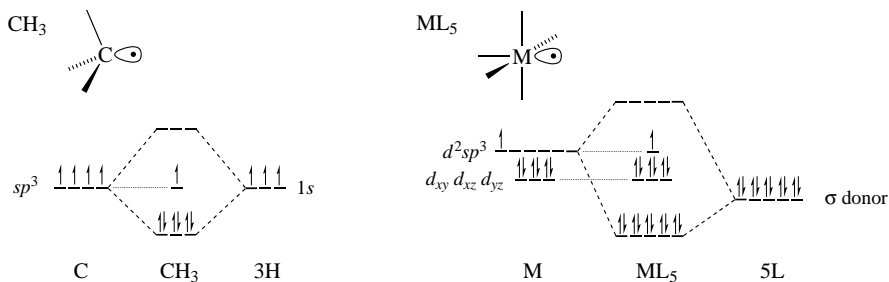
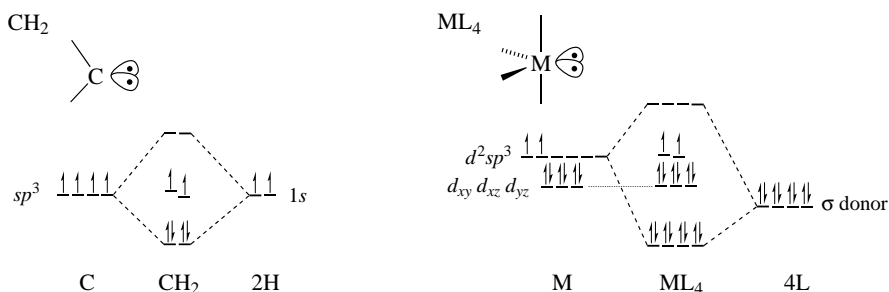
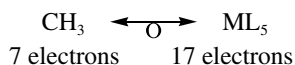


Figure 13-4

Six- and 16-Electron Fragments

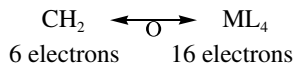


Each of these fragments has a single electron in a hybrid orbital at the vacant site of the parent polyhedron. These orbitals are sufficiently similar to meet Hoffmann's isolobal definition. Using Hoffmann's symbol \longleftrightarrow to designate groups as isolobal, we may therefore write the following.

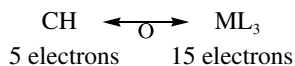


Similarly, 6-electron CH_2 and 16-electron ML_4 are isolobal, as shown in Figure 13-4.

Each of these fragments represents the parent polyhedron, with single electrons occupying two hybrid orbitals at otherwise vacant sites; each fragment also has two electrons fewer than the filled shell octet or 18-electron configurations.



The absence of a third ligand from the parent polyhedra also gives a pair of isolobal fragments, CH and ML_3 .

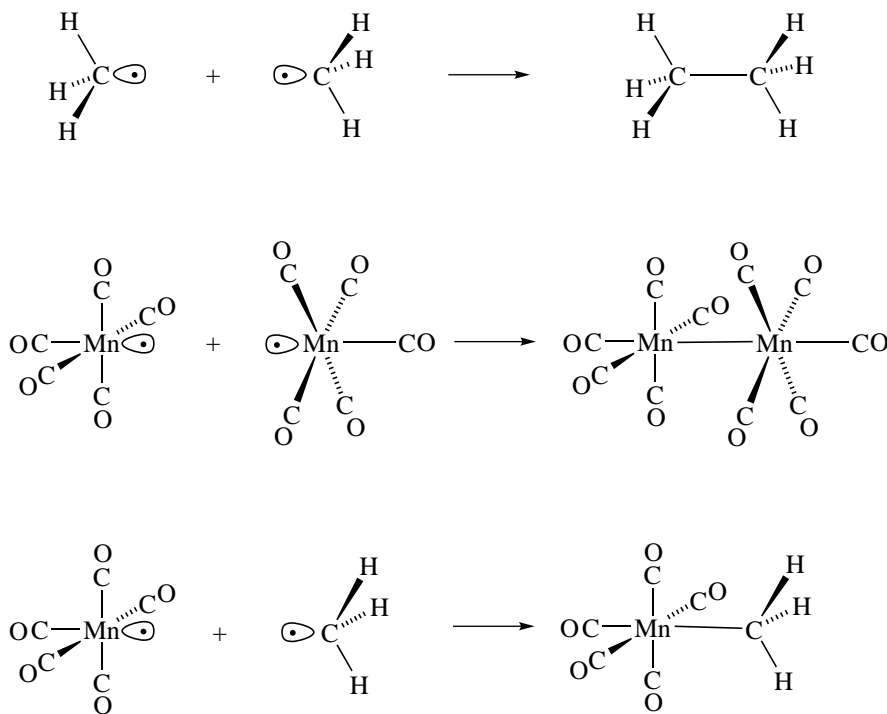


These relationships are summarized in Table 13-1.

Table 13-1 Isolobal Fragments

	Organic	Inorganic	Vertices missing from parent polyhedron	Electrons short of filled shell	Organometallic example ^a
Parent:	CH₄	ML₆	0	0	Cr(CO)₆
Fragments:	CH ₃	ML ₅	1	1	Mn(CO) ₅
	CH ₂	ML ₄	2	2	Fe(CO) ₄
	CH	ML ₃	3	3	Co(CO) ₃

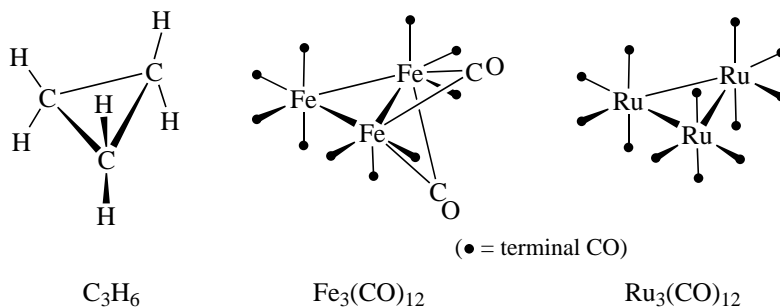
^aThese examples involve π interactions between the metal and the ligands (affecting the energies of the d_{xy} , d_{xz} , and d_{yz} orbitals); however, the overall electronic structures of the fragments shown are still consistent with their being considered isolobal.

**Figure 13-5**

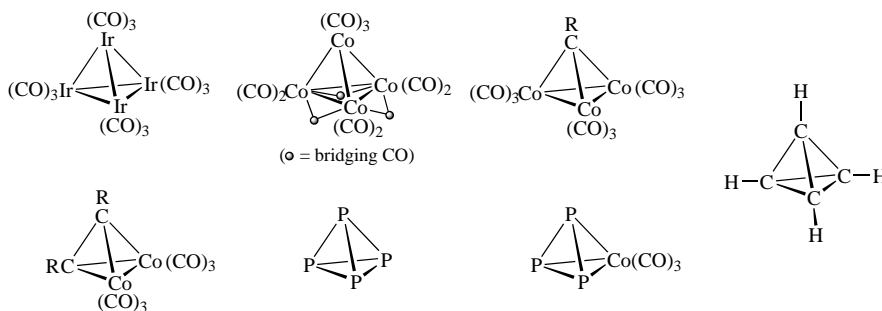
Molecules
Resulting from the
Combination of
Isolobal Fragments

Isolobal fragments can be formally combined into molecules, as shown in Figure 13-5. For example, two CH₃ fragments, when linked, form ethane, and two Mn(CO)₅ fragments form the dimeric (OC)₅Mn–Mn(CO)₅. Furthermore, organic and organometallic fragments can be intermixed; an example is H₃C–Mn(CO)₅, also a known compound.

Organic and organometallic parallels are not always this complete. For example, whereas two 6-electron CH₂ fragments form ethylene, H₂C=CH₂, the dimer of the isolobal Fe(CO)₄ is not nearly as stable; it is known as a transient

**Figure 13-6**

Isolobally Related
Three-Membered
Rings

**Figure 13-7**

Isolobally Related
Tetrahedral
Molecules

species obtained thermally or photochemically from $Fe_2(CO)_9$.³ Both CH_2 and $Fe(CO)_4$, however, form three-membered rings: cyclopropane and $Fe_3(CO)_{12}$. Although cyclopropane is a trimer of CH_2 fragments, $Fe_3(CO)_{12}$ has two bridging carbonyls and is therefore not a perfect trimer of $Fe(CO)_4$. The isoelectronic $Ru_3(CO)_{12}$, on the other hand, is a trimeric combination of three $Ru(CO)_4$ fragments (which are isolobal with both $Fe(CO)_4$ and CH_2) and can correctly be described as $[Ru(CO)_4]_3$. These structures are shown in Figure 13-6.

The 15-electron fragment $Ir(CO)_3$ forms $[Ir(CO)_3]_4$, which has an Ir_4 core in the shape of a regular tetrahedron. In this complex all the carbonyl groups are terminal. The isoelectronic complexes $Co_4(CO)_{12}$ and $Rh_4(CO)_{12}$ have nearly tetrahedral arrays of metal atoms, but three carbonyls bridge one of the triangular faces in each of these clusters. Compounds are also known having a central tetrahedral core, with one or more $Co(CO)_3$ fragments [isolobal and isoelectronic with $Ir(CO)_3$] replaced by the isolobal CR fragment (shown in Figure 13-7). More simply, individual phosphorus atoms, with five valence electrons, may also be considered isolobal with 15-electron organometallic fragments. Phosphorus atoms readily arrange themselves into tetrahedra; tetrahedral P_4 is in fact the most

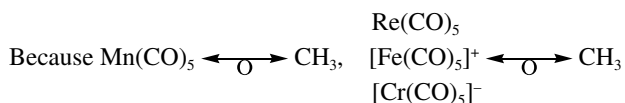
³M. Poliakoff and J. J. Turner, *J. Chem. Soc. A*, **1971**, 2403.

common molecular form of this element. Tetrahedral combinations of phosphorus atoms and isolobal 15-electron organometallic fragments such as $\text{Co}(\text{CO})_3$ have also been prepared; one example is shown in Figure 13-7.

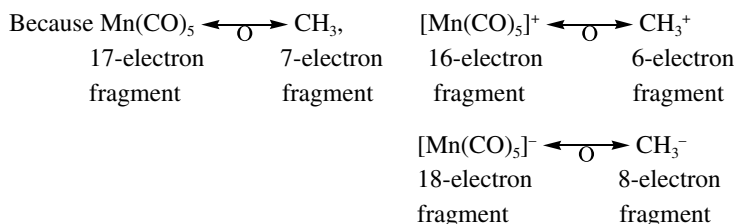
13-1-1 Extensions of the Analogy

The concept of isolobal fragments can be extended beyond the examples given so far, to include charged species, a variety of ligands other than CO, and organometallic fragments based on structures other than octahedral. Some of the ways of extending the isolobal parallels can be summarized as follows.

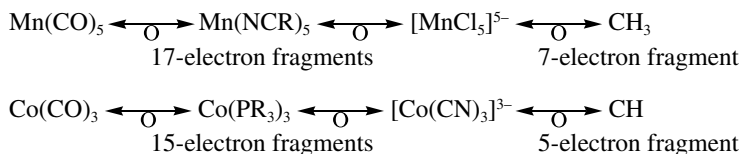
1. The isolobal definition may be extended to isoelectronic fragments having the same coordination number. For example,



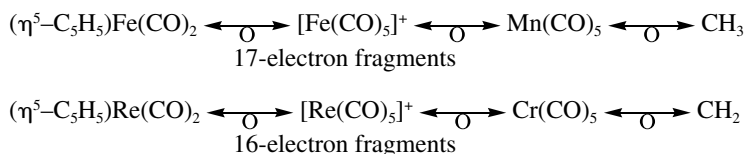
2. Gain or loss of electrons from two isolobal fragments yields isolobal fragments. For example,



3. Other two-electron donors are treated similarly to CO.



4. $\eta^5\text{-Cp}$ is considered to occupy three coordination sites and to be a six-electron donor (as C_5H_5^-).



Examples of isolobal fragments containing CO and $\eta^5\text{-Cp}$ ligands are given in Table 13-2.

Table 13-2 Examples of Isolobal Fragments

	Number of Electrons Short of Parent Configuration (8 or 18)			
	0	1	2	3
Neutral hydrocarbon	CH₄	CH₃	CH₂	CH
Isolobal fragments	Cr(CO) ₆ [V(CO) ₆] ⁻ [Re(CO) ₆] ⁺ CpMn(CO) ₃	Mn(CO) ₅ [Cr(CO) ₅] ⁻ [Os(CO) ₅] ⁺ CpFe(CO) ₂	Fe(CO) ₄ [Mn(CO) ₄] ⁻ [Ir(CO) ₄] ⁺ CpCo(CO)	Co(CO) ₃ [Fe(CO) ₃] ⁻ [Pt(CO) ₃] ⁺ CpNi
Anionic hydrocarbon fragments^a	CH₃⁻	CH₂⁻	CH⁻	
Isolobal fragments	Fe(CO) ₅	Co(CO) ₄	Ni(CO) ₃	
Cationic hydrocarbon fragments^b		CH₄⁺	CH₃⁺	CH₂⁺
Isolobal fragments		V(CO) ₆	Cr(CO) ₅	Mn(CO) ₄

^aAnionic hydrocarbon fragments were obtained by removing H⁺ from the neutral hydrocarbons at the top of the columns.

^bCationic hydrocarbon fragments were obtained by adding H⁺ to the neutral hydrocarbons at the top of the columns.

Exercise 13-1

For the following, propose examples of isolobal organometallic fragments other than those given so far in Chapter 13:

- A fragment isolobal with CH₃⁻
- A fragment isolobal with CH₂⁺
- Three fragments isolobal with CH

Exercise 13-2

Give organic fragments isolobal with each of the following:

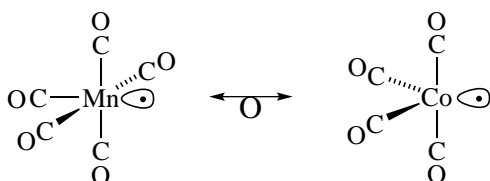
- (η⁵-C₅H₅)Mo(CO)₂
- (η⁶-C₆H₆)Fe(PH₃)
- [Co(CO)₃Br]⁻

Analogies are by no means limited to organometallic fragments of octahedra; similar arguments can be used to derive fragments of different polyhedra. For example, Co(CO)₄, a 17-electron fragment of a trigonal bipyramid, is isolobal with Mn(CO)₅, a 17-electron fragment of an octahedron, and the compound composed of these two fragments, (CO)₅Mn—Co(CO)₄, is known.

Table 13-3 Isolobal Relationships for Fragments of Polyhedra

Organic fragment	Coordination number of transition metal for parent polyhedron			Valence electrons of transition metal fragment
	5	6 ^a	7	
CH ₃	<i>d</i> ⁹ -ML ₄	<i>d</i> ⁷ -ML ₅	<i>d</i> ⁵ -ML ₆	17
CH ₂	<i>d</i> ¹⁰ -ML ₃	<i>d</i> ⁸ -ML ₄	<i>d</i> ⁶ -ML ₅	16
CH		<i>d</i> ⁹ -ML ₃	<i>d</i> ⁷ -ML ₄	15

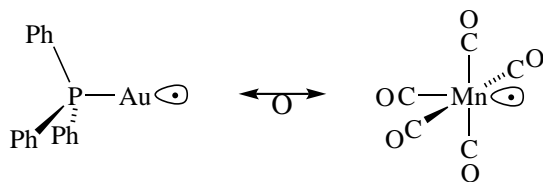
^aExamples have already been considered (Table 13-2).



Examples of electron configurations of isolobal fragments of polyhedra having five through seven vertices are given in Table 13-3.⁴

13-1-2 Examples of Applications of the Analogy

The isolobal analogy can, in principle, be extended to *any* molecular fragment having frontier orbitals of suitable size, shape, symmetry, and energy. In many cases, the characteristics of frontier orbitals are not as easy to predict as in the examples cited above, and calculations are necessary to determine the symmetry and energy of molecular fragments. For example, Au(PPh₃), a 13-electron fragment, has a single electron in a hybrid orbital pointing away from the phosphine.⁵ This electron is in an orbital that has similar symmetry but somewhat higher energy than the singly occupied hybrid in the Mn(CO)₅ fragment.

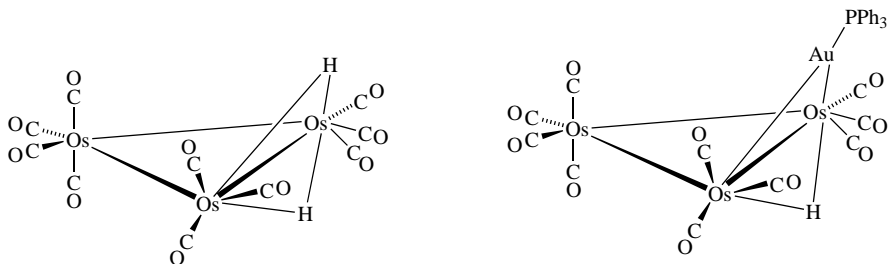


⁴For analysis of the energies and symmetries of fragments of a variety of polyhedra, see R. Hoffmann, Footnote 1; M. Elain and R. Hoffmann, *Inorg. Chem.*, **1975**, *14*, 1058; and T. A. Albright, R. Hoffmann, J. C. Thibeault, and D. L. Thorn, *J. Am. Chem. Soc.*, **1979**, *101*, 3801.

⁵D. G. Evans and D. M. P. Mingos, *J. Organomet. Chem.*, **1982**, *232*, 171.

Figure 13-8

Isolobal $\text{Au}(\text{PPh}_3)$
and H



The $\text{Au}(\text{PPh}_3)$ fragment can be combined with the isolobal $\text{Mn}(\text{CO})_5$ and CH_3 fragments to form $(\text{OC})_5\text{Mn}-\text{Au}(\text{PPh}_3)$ and $\text{H}_3\text{C}-\text{Au}(\text{PPh}_3)$.

Even a hydrogen atom, with a single electron in its $1s$ orbital, can in some cases be viewed as a fragment isolobal with such species as CH_3 , $\text{Mn}(\text{CO})_5$, and $\text{Au}(\text{PPh}_3)$. Hydrides of the first two [i.e., CH_4 and $\text{HMn}(\text{CO})_5$] are very well known. In addition, in some cases $\text{Au}(\text{PPh}_3)$ and H show surprisingly similar behavior, such as in their ability to bridge triosmium clusters^{6,7} (Figure 13-8) and the capacity of a gold phosphine fragment to replace hydrogen in fluorescent organic molecules.⁸

A practical use of isolobal analogies is in suggesting syntheses of new compounds. For example, CH_2 is isolobal with 16-electron $\text{Cu}(\eta^5\text{-Cp}^*)$ (extension 4 of the analogy, as described previously) and with 14-electron PtL_2 ($\text{L} = \text{PR}_3, \text{CO}$);⁹ all three of these fragments are two ligands and two electrons short of their parent polyhedra. Recognition that these fragments are isolobal has been exploited in preparing new organometallic compounds composed of fragments isolobal with fragments of known compounds. Examples of compounds obtained in these studies are shown on the next page.^{10,11}

⁶A. G. Orpen, A. V. Rivera, E. G. Bryan, D. Pippard, G. Sheldrick, and K. D. Rouse, *J. Chem. Soc., Chem. Commun.*, **1978**, 723.

⁷B. F. G. Johnson, D. A. Kaner, J. Lewis, and P. R. Raithby, *J. Organomet. Chem.*, **1981**, 215, C33.

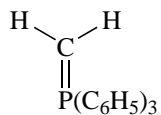
⁸T. G. Gray, *Comments Inorg. Chem.*, **2007**, 28, 181.

⁹In a manner similar to the relationship between the “18-electron rule” for octahedra and other structures, and the “16-electron rule” for square planar complexes, isolobal relationships between 16-electron fragments of octahedra and 14-electron fragments of square planar structures can also be demonstrated.

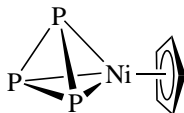
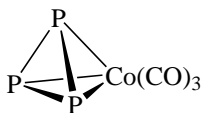
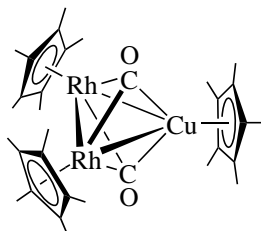
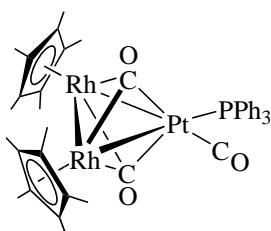
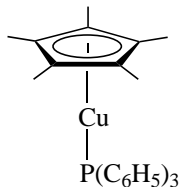
¹⁰G. A. Carriedo, J. A. K. Howard, and F. G. A. Stone, *J. Organomet. Chem.*, **1983**, 250, C28.

¹¹N. J. Fitzpatrick, P. J. Groarke, and N. M. Tho, *Polyhedron*, **1992**, 11, 2517.

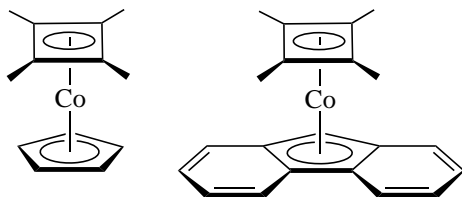
*Previously
known compounds*



*New compounds
composed of isolobal fragments*



Another example is provided by recognition of the isolobal nature of the $(\eta^5\text{-C}_5\text{H}_5)$ Fe^+ and $(\eta^4\text{-C}_4\text{H}_4)\text{Co}^+$ fragments¹² as background for the synthesis of a variety of cyclobutadiene cobalt analogues of ferrocene, including the examples shown below.¹³



¹²R. Gleiter, H. Schimanke, S. J. Silverio, M. Büchner, and G. Huttner, *Organometallics*, **1996**, *15*, 5635.

¹³E. V. Mutseneck, D. A. Loginov, D. S. Perekalin, Z. A. Starikova, D. G. Golovanov, P. V. Petrovskii, P. Zanello, M. Corsini, F. Laschi, and A. R. Kudinov, *Organometallics*, **2004**, *23*, 5944.

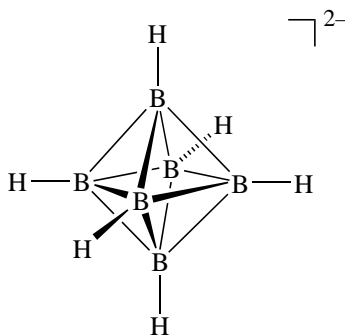
13-2 CLUSTER COMPOUNDS

Transition metal cluster chemistry has developed rapidly during the past several decades. Beginning with simple dimeric molecules such as $\text{Co}_2(\text{CO})_8$ and $\text{Mn}_2(\text{CO})_{10}$,¹⁴ chemists have developed syntheses of far more complex clusters, some with interesting and unusual structures and chemical properties. Large clusters have been studied with the objective of developing catalysts that may duplicate or improve upon the properties of heterogeneous catalysts; the surface of a large cluster may in these cases mimic in some degree the behavior of the surface of a solid catalyst.

Before considering organometallic clusters, we will find it useful to examine the capacity of boron to form clusters. The types of orbital interactions involved in boron-based clusters will provide useful background to understand the types of interactions that occur in organometallic clusters containing transition metals.

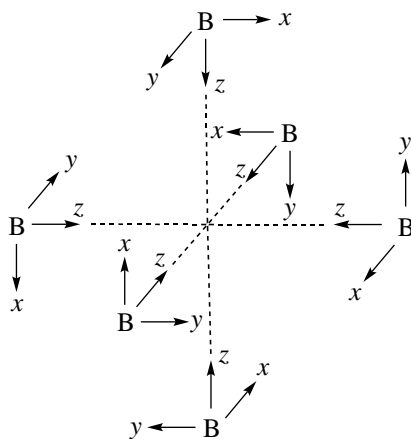
13-2-1 Boranes

There are a great many neutral and ionic species composed of boron and hydrogen, far too numerous to consider in this text.¹⁵ For the purposes of illustrating parallels between these species and transition metal organometallic clusters, we will first consider one category of boranes, *closo* (“cage-like”) boranes, which have the formula $\text{B}_n\text{H}_n^{2-}$. These boranes are closed polyhedra having n corners; their faces are all triangular (triangulated polyhedra). Each corner is occupied by a BH group; an example, the highly symmetric $\text{B}_6\text{H}_6^{2-}$, is shown below.



¹⁴Some chemists define clusters as having at least three metal atoms.

¹⁵For a more detailed introductory outline of boron cluster chemistry, see N. N. Greenwood and A. Earnshaw, *Chemistry of the Elements*, 2nd Ed., Butterworth-Heinemann: Oxford, 1997, pp. 141–181.

**Figure 13-9**

Coordinate System for Bonding in $B_6H_6^{2-}$ (Adapted with permission from G.L. Miessler and D.A. Tarr, *Inorganic Chemistry*, 3rd ed., Pearson Education: Upper Saddle River, NJ, 2004, p. 573.)

Molecular orbital calculations have shown that *closo* boranes have two types of molecular orbitals that are instrumental in holding the boron framework together:

- n orbitals involving interactions between boron orbitals in the outer framework (or skeleton) of the structure
- 1** orbital involving interactions of boron orbitals at the center of the cluster

In total, therefore, there are $n + 1$ bonding orbitals in the central core.¹⁶ These orbitals, occupied by electron pairs, are primarily responsible for holding the core framework of the cluster together.

In addition, there are n boron–hydrogen bonding orbitals involved in the σ bonds between these atoms on the outside of the cluster. Adding these to the $n + 1$ bonding orbitals in the central core gives a total of $2n + 1$ bonding orbitals overall in the cluster.

The $B_6H_6^{2-}$ ion is a useful example; a convenient set of coordinate axes for its boron atoms is shown in Figure 13-9. Each boron has four valence orbitals (s , p_x , p_y , and p_z), a total of 24 boron valence orbitals for the cluster. It is convenient to assign the z axis of each boron to point toward the center of the octahedron, with the x and y axes oriented as shown.

The p_z and s orbitals of the borons collectively have the same symmetry and may therefore be considered to combine to form sp hybrid orbitals. These hybrid orbitals point in toward the center of the cluster and out toward the hydrogen atoms. The unhybridized $2p$ orbitals (p_x and p_y) of the borons remain to participate in bonding within the B_6 core.

¹⁶K. Wade, *Electron Deficient Compounds*, Nelson: London, 1971, pp. 50–59.

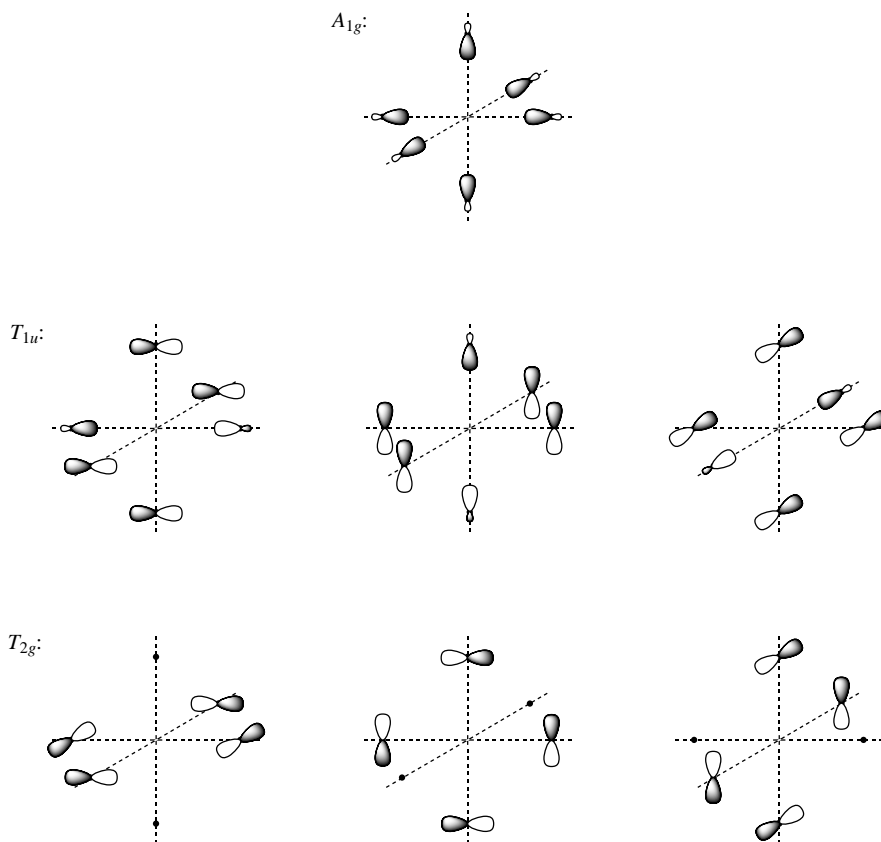


Figure 13-10
Bonding in $B_6H_6^{2-}$

Seven orbital combinations ($n + 1$) lead to bonding interactions within the B_6 core; these are shown in Figure 13-10. Constructive overlap of all six hybrid orbitals at the center of the octahedron yields one framework bonding orbital, labeled A_{1g} .¹⁷ Additional bonding interactions are of two types: overlap of two sp hybrid orbitals with parallel p orbitals on four boron atoms (three such interactions, symmetry label T_{1u}) and overlap of p orbitals on four boron atoms within the same plane (three interactions, symmetry label T_{2g}). The remaining orbitals form antibonding molecular orbitals or are nonbonding. A summary follows.

¹⁷The symmetry label A_{1g} designates the highly symmetric interaction that occurs when all sp hybrids point toward the center of the polyhedron. For an explanation of symmetry labels, see F. A. Cotton, *Chemical Applications of Group Theory*, 3rd ed., Wiley: New York, 1990, pp. 231–238.

Table 13-4 Bonding Pairs for *Closo* Boranes

Formula	Framework bonding pairs			
	Total valence electron pairs	A Symmetry ^a (overlap at center)	Other framework	B–H bonding pairs
B ₆ H ₆ ²⁻	13	1	6	6
B ₇ H ₇ ²⁻	15	1	7	7
B ₈ H ₈ ²⁻	17	1	8	8
B _n H _n ²⁻	2n + 1	1	n	n

^aThese are bonding pairs occupying the highly symmetric orbital that results from the combination of all *sp* hybrid orbitals pointing directly toward the center of the polyhedron. The actual designation (such as A_{1g}) depends on the overall symmetry of the cluster.

From the 24 valence atomic orbitals of boron the following are formed:

13 bonding orbitals (2n+1), consisting of:

7 framework molecular orbitals (n+1):

1 bonding orbital from overlap of *sp* hybrid orbitals

6 bonding orbitals from overlap of *p* orbitals of boron with *sp* hybrid orbitals or with other boron *p* orbitals

6 boron–hydrogen bonding orbitals (*n*)

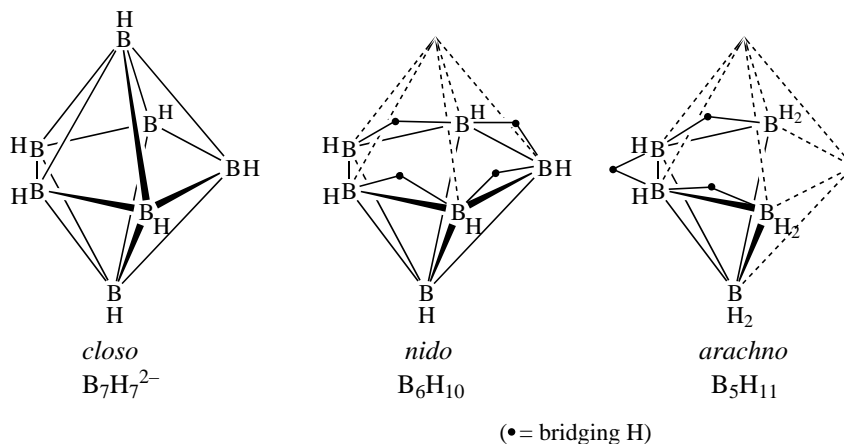
11 antibonding or nonbonding orbitals

Similar descriptions of bonding can be derived for other *closo* boranes. In each case, one particularly useful similarity can be found: there is one more framework bonding pair than the number of vertices in the polyhedron. The extra framework bonding pair is in a highly symmetric orbital resulting from overlap of atomic (or hybrid) orbitals at the center of the polyhedron, similar to the interaction labeled A_{1g} in Figure 13-10. In addition, there is a significant gap in energy between the HOMO and the LUMO.¹⁸ The numbers of bonding pairs for several *closo* boranes are shown in Table 13-4.

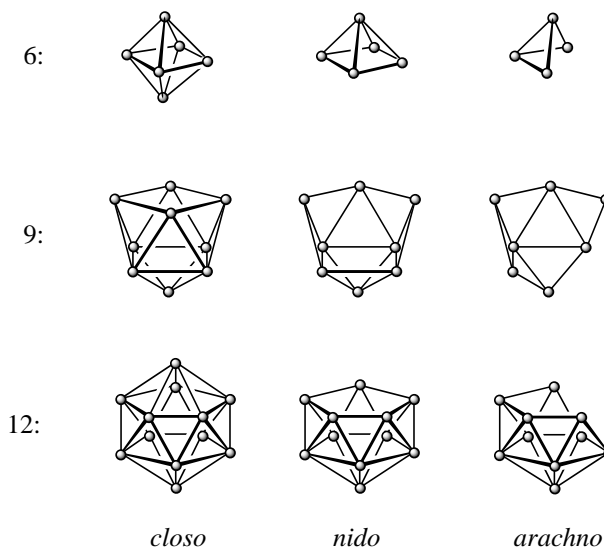
Together, the *closo* structures make up only a small fraction of all known borane species. Additional structural types can be obtained by removing one or more corners from the *closo* framework. Removal of one corner yields a *nido* (“nest-like”) structure, removal of two corners an *arachno* (“spiderweb-like”) structure, and removal of three corners a *hypho* (“net-like”) structure.¹⁹ Examples

¹⁸K. Wade, “Some Bonding Considerations” in B.F.G. Johnson, Ed., *Transition Metal Clusters*, Wiley: New York, 1980, p. 217.

¹⁹Detailed rules for classifying boranes and related compounds are provided in G. J. Leigh, Ed., *Nomenclature of Inorganic Chemistry*, Blackwell Scientific: Oxford, England, 1990, pp. 207–237.

**Figure 13-11**

Closo, *Nido*, and *Arachno* Borane Structures

**Figure 13-12**

Structures of *Closo*, *Nido*, and *Arachno* Boranes

of three related *closo*, *nido*, and *arachno* borane structures are shown in Figure 13-11, and the structures of the boron core of selected additional boranes are shown in Figure 13-12.

The classification of structural types can often be done more conveniently on the basis of valence electron counts. Various schemes for relating electron counts to structures have been proposed, with most proposals based on the set of rules formulated by Wade in 1971.²⁰ A classification scheme based on these rules is summarized in Table 13-5.

²⁰K. Wade, *Adv. Inorg. Chem. Radiochem.*, **1976**, *18*, 1.

Table 13-5 Classification of Cluster Structures

Label	Corners occupied	Pairs of framework bonding electrons	Empty corners
<i>closo</i>	n corners of n -cornered polyhedron	$n + 1$	0
<i>nido</i>	$(n - 1)$ corners of n -cornered polyhedron	$n + 1$	1
<i>arachno</i>	$(n - 2)$ corners of n -cornered polyhedron	$n + 1$	2
<i>hypho</i>	$(n - 3)$ corners of n -cornered polyhedron	$n + 1$	3

Table 13-6 Examples of Electron Counting in Boranes

Vertices in parent polyhedron	Classification	Boron atoms in cluster	Valence electrons	Framework electron pairs	Examples	Formally derived from
6	<i>closo</i>	6	26	7	$B_6H_6^{2-}$	$B_6H_6^{2-}$
6	<i>nido</i>	5	24	7	B_5H_9	$B_5H_5^{4-}$
6	<i>arachno</i>	4	22	7	B_4H_{10}	$B_4H_4^{6-}$
12	<i>closo</i>	12	50	13	$B_{12}H_{12}^{2-}$	$B_{12}H_{12}^{2-}$
12	<i>nido</i>	11	48	13	$B_{11}H_{13}^{2-}$	$B_{11}H_{11}^{4-}$
12	<i>arachno</i>	10	46	13	$B_{10}H_{15}^-$	$B_{10}H_{10}^{6-}$

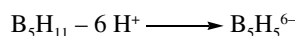
In addition, it is sometimes useful to relate the total valence electron count in boranes (and, as we shall see, organometallic clusters) to the structural type. In *closo* boranes, the total number of valence electron pairs is equal to the sum of the number of vertices in the polyhedron (at each boron, one electron pair is involved in boron–hydrogen bonding) and the number of framework bond pairs. For example, in $B_6H_6^{2-}$ there are 26 valence electrons, or 13 pairs ($=2n + 1$, as mentioned previously). The number of vertices in the parent polyhedron (an octahedron) is six, and the number of framework bond pairs is seven ($n + 1$; see Figure 13-10). The total of 13 pairs corresponds to the 6 pairs involved in bonding to the hydrogens (one per boron) and the 7 pairs involved in framework bonding. These electron counts are summarized for two sets of examples, based on six and 12 vertices in parent polyhedra, in Table 13-6.

13-2-2 Method for Classifying Structures

From a practical standpoint, it is useful to have a classification scheme based on molecular formulas rather than parent polyhedra (which may not immediately be obvious). In addition, such a classification scheme should ideally be adaptable to other clusters, whether or not they involve the element boron. Here is one such scheme.

<i>Classification</i>	<i>Formally derived from</i> ²¹
<i>closo</i>	$B_nH_n^{2-}$
<i>nido</i>	$B_nH_n^{4-}$
<i>arachno</i>	$B_nH_n^{6-}$
<i>hypho</i>	$B_nH_n^{8-}$

For boranes, the matching formulas above can be obtained by subtracting a sufficient number of H^+ ions (such that the number of boron atoms becomes equal to the number of hydrogen atoms) from the actual formulas (except for the *closo* clusters, the number of hydrogen atoms in general is greater than the number of boron atoms). For example, to classify B_5H_{11} , subtract six H^+ ions from the formula



The resulting formula matches the *arachno* classification.

Example 13-1

The following examples illustrate this method for classifying boranes according to structural type:

- | | | | |
|-------------------|------------------------|-----------------------|--------------------------------|
| a. $B_{10}H_{14}$ | $B_{10}H_{14} - 4 H^+$ | $= B_{10}H_{10}^{4-}$ | Classification: <i>nido</i> |
| b. $B_2H_7^-$ | $B_2H_7^- - 5 H^+$ | $= B_2H_2^{6-}$ | Classification: <i>arachno</i> |
| c. B_8H_{16} | $B_8H_{16} - 8 H^+$ | $= B_8H_8^{8-}$ | Classification: <i>hypho</i> |

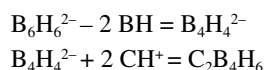
Exercise 13-3

Classify the following boranes by structural type.

- a. $B_5H_8^-$ b. $B_{11}H_{11}^{2-}$ c. $B_{10}H_{18}$

13-2-3 Heteroboranes

The electron counting schemes described for boranes can be extended to isoelectronic species such as carboranes,²² clusters containing both carbon and boron as framework atoms. The CH^+ unit is isoelectronic with BH ; many compounds are known in which one or more BH groups have been formally replaced by CH^+ (or by C , which has the same number of electrons as BH). For example, the replacement of two BH groups in *closo*- $B_6H_6^{2-}$ with CH^+ yields *closo*- $C_2B_4H_6$.



²¹This is a formalism only and does not, except for the *closo* classification, imply that ions of the given formula (such as $B_nH_n^{8-}$) actually exist.

²²Also known as carboranes.

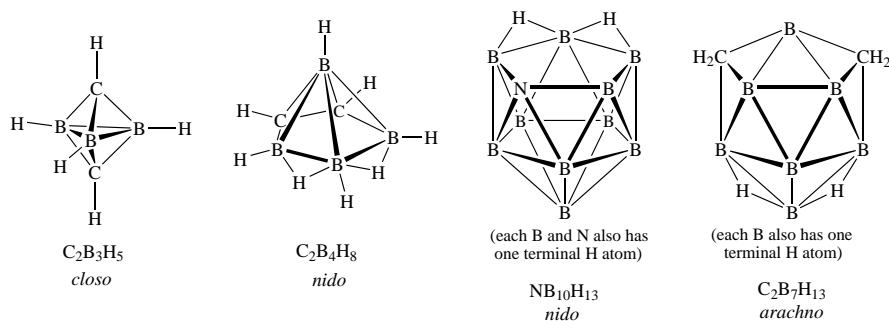


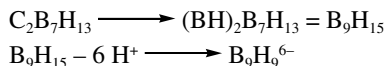
Figure 13-13

Examples of Heteroboranes

Closo, *nido*, and *arachno* carboranes are all known, most commonly containing two carbon atoms; examples are shown in Figure 13-13. Examples of chemical formulas corresponding to these designations are as follows.

Type	Borane	Example	Carborane	Example
<i>closo</i>	$B_nH_n^{2-}$	$B_{12}H_{12}^{2-}$	$C_2B_{n-2}H_n$	$C_2B_{10}H_{12}$
<i>nido</i>	$B_nH_{n+4}^{23}$	$B_{10}H_{14}$	$C_2B_{n-2}H_{n+2}$	$C_2B_8H_{12}$
<i>arachno</i>	$B_nH_{n+6}^{24}$	B_9H_{15}	$C_2B_{n-2}H_{n+4}$	$C_2B_7H_{13}$

Carboranes may be classified structurally using the same method as for boranes. Because a carbon atom has the same number of valence electrons as a boron atom plus a hydrogen atom, each C can be converted to BH in the classification scheme. For example, for a carborane having the formula $C_2B_7H_{13}$,



The classification of $C_2B_7H_{13}$ is therefore *arachno*.

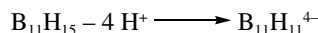
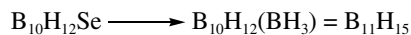
Many derivatives of boranes containing other main group atoms (heteroatoms) are also known. These “heteroboranes” may be classified by formally converting the heteroatom to a BH_x group having the same number of valence electrons and then proceeding as in previous examples. For some of the most common heteroatoms, the following substitutions can be used.

Heteroatom	Replace with
C, Si, Ge, Sn	BH
N, P, As	BH_2
S, Se	BH_3

²³*Nido* boranes may also have the formulas $B_nH_{n+3}^-$ and $B_nH_{n+2}^{2-}$.

²⁴*Arachno* boranes may also have the formulas $B_nH_{n+5}^-$ and $B_nH_{n+4}^{2-}$.

For example, to classify the heteroborane having the formula $B_{10}H_{12}Se$,



The classification of $B_{10}H_{12}Se$ is therefore *nido*.

Exercise 13-4

Determine formulas of boranes isoelectronic with the following.

- closo*- $C_2B_3H_5$
- nido*- CB_5H_9
- SB_9H_9 (classify as *closo*, *nido*, or *arachno*)
- $CPB_{10}H_{11}$ (classify as *closo*, *nido*, or *arachno*)

Although it may not be surprising that the same set of electron counting rules can be used to satisfactorily describe such similar compounds as boranes and carboranes, it is of interest to examine how far the comparison can be extended. Can Wade's rules, for example, be used effectively on compounds containing organometallic fragments in place of boron, carbon, or other atoms? Can the rules be extended even further, to describe the bonding in polyhedral organometallic clusters?

13-2-4 Metallaboranes and Metallacarboranes

The CH group of a carborane is isolobal with 15-electron fragments of an octahedron such as $Co(CO)_3$ and $Ni(\eta^5-Cp)$. Similarly, BH, which has four valence electrons, is isolobal with 14-electron fragments such as $Fe(CO)_3$ and $Co(\eta^5-Cp)$. These organometallic fragments have been found in substituted boranes and carboranes in which the organometallic fragments substitute for the isolobal CH and BH groups. For example, the organometallic derivatives of B_5H_9 , shown in Figure 13-14 have been synthesized.

Theoretical calculations on the iron derivatives have supported the view that $Fe(CO)_3$ bonds in a manner isolobal with BH.²⁵ In both fragments, the orbitals involved in framework bonding within the cluster are similar (Figure 13-15). In BH, the orbitals participating in framework bonding are an sp_z hybrid pointing toward the center of the polyhedron and p_x and p_y orbitals tangential to the surface of the cluster. In $Fe(CO)_3$, an $sp_z d_{z^2}$ hybrid points toward the center, and pd hybrid orbitals are oriented tangentially to the cluster surface.

²⁵R. L. DeKock and T. P. Fehlner, *Polyhedron*, **1982**, *1*, 521.

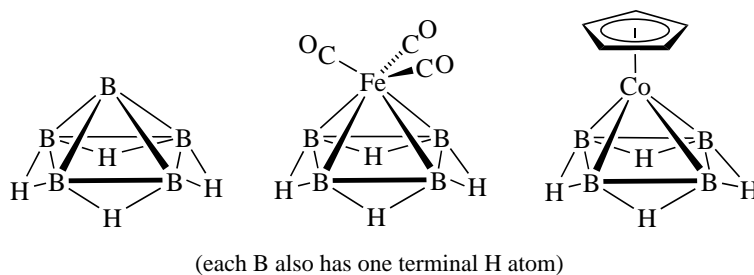


Figure 13-14

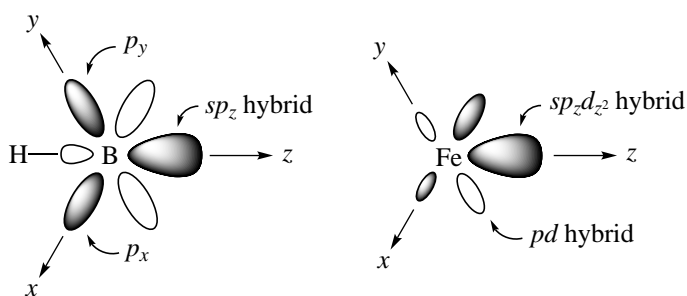
Organometallic
Derivatives of B_5H_9 

Figure 13-15

Orbitals of Isolobal
Fragments BH and
 $Fe(CO)_3$

Examples of metallaboranes and metallocarboranes are numerous.²⁶ Selected examples with *closo* structures are given in Table 13-7.

Anionic boranes and carboranes can also act as ligands toward metals in a manner resembling that of cyclic organic ligands. For example, *nido* carboranes of formula $C_2B_9H_{11}^{2-}$ have *p* orbital lobes pointing toward the “missing” site of the icosahedron (remember that the *nido* structure corresponds to a *closo* structure [which in this case is the 12-vertex icosahedron] with one vertex missing). This arrangement of *p* orbitals can be compared with the *p* orbitals of the cyclopentadienyl ring, as shown in Figure 13-16.

The similarity between these ligands is sufficient that $C_2B_9H_{11}^{2-}$ can bond to iron to form a carborane analogue of ferrocene, $[Fe(\eta^5-C_2B_9H_{11})_2]^{2-}$. A mixed ligand sandwich compound containing one carborane and one cyclopentadienyl ligand, $[Fe(\eta^5-C_2B_9H_{11})(\eta^5-C_5H_5)]$, has also been made (Figure 13-17),²⁷ and the chemistry of sandwich compounds involving carboranes as ligands is now extensive.²⁸ Numerous other examples of boranes and carboranes serving as ligands to transition metals are also known.²⁹

²⁶A useful brief review of boranes as ligands is in N. N. Greenwood, *Coord. Chem. Rev.*, **2002**, 226, 61.

²⁷M. W. Hawthorne, D. C. Young, and P. A. Wegner, *J. Am. Chem. Soc.*, **1965**, 87, 1818.

²⁸M. Corsini, F. Fabrizi de Biani, and P. Zanello, *Coord. Chem. Rev.*, **2006**, 250, 1351.

²⁹K. P. Callahan and M. F. Hawthorne, *Adv. Organomet. Chem.*, **1976**, 14, 145.

Table 13-7 Metallaboranes and Metallacarboranes with *Closo* Structures





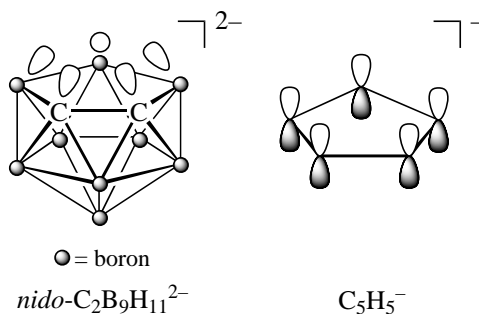
Number of framework atoms	Shape		Examples
6	Octahedron		$B_4H_6(CoCp)_2$ $C_2B_3H_5Fe(CO)_3$
7	Pentagonal bipyramid		$C_2B_4H_6Ni(PPh_3)_2$ $C_2B_3H_5(CoCp)_2$
8	Dodecahedron		$C_2B_4H_4[(CH_3)_2Sn]CoCp$
12	Icosahedron		$C_2B_7H_9(CoCp)_3$ $C_2B_9H_{11}Ru(CO)_3$

Figure 13-16

Comparison of $C_2B_9H_{11}^{2-}$ with $C_5H_5^-$. Each B and C atom also has a terminal H atom, not shown.



Metallaboranes and metallacarboranes can be classified structurally by a procedure similar to that for boranes and their main group derivatives.³⁰ In this scheme, the valence electron count of the metal-containing fragment is first determined and then compared with the requirements of the 18-electron rule. This fragment can then be considered equivalent to a BH_x fragment needing the same number of electrons to satisfy the octet rule. For example, a 15-electron fragment

³⁰D. M. P. Mingos, *Acc. Chem. Res.*, **1984**, *17*, 311.

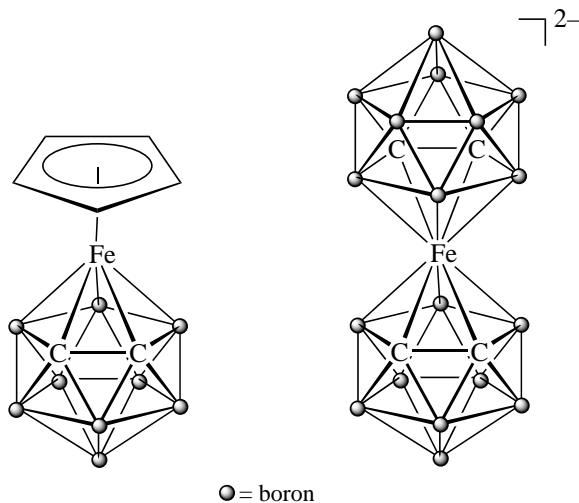


Figure 13-17

Carborane
Analogues of
Ferrocene

Table 13-8 Organometallic and Borane Fragments

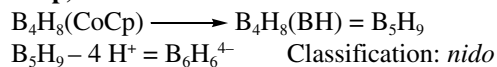
Valence electrons in organometallic fragment	Example	Valence electrons in borane fragment	Borane fragment
13	Mn(CO) ₃	3	B
14	Co(η ⁵ -Cp)	4	BH
15	Co(CO) ₃	5	BH ₂
16	Fe(CO) ₄	6	BH ₃

such as Co(CO)₃ is three electrons short of 18; this fragment may be considered the equivalent of the five-electron fragment BH₂, which is three electrons short of an octet. Examples of organometallic fragments and their corresponding BH_x fragments are given in Table 13-8.

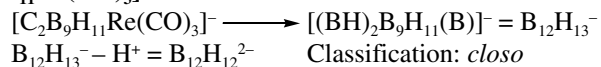
The following examples illustrate that the method described previously for classifying boranes can also be used for metallaboranes.

Example 13-2

B₄H₈(CoCp)



[C₂B₉H₁₁Re(CO)₃]⁻



Exercise 13-5

Classify the following by structural type.

**13-2-5 Carbonyl Clusters**

Many carbonyl clusters have structures similar to boranes; it is therefore of interest to determine to what extent the approach used to describe bonding in boranes may also be applicable to bonding in carbonyl clusters.

According to Wade, in addition to the obvious relation shown in equation **13.1** below, the valence electrons in a cluster can be assigned to framework and metal–ligand bonding, as shown in equation **13.2**.³¹

$$\begin{array}{l} \text{Total number of} \\ \text{valence electrons} \\ \text{in cluster} \end{array} = \begin{array}{l} \text{Number of valence} \\ \text{electrons contributed} \\ \text{by metal atoms} \end{array} + \begin{array}{l} \text{Number of valence} \\ \text{electrons contributed} \\ \text{by ligands} \end{array} \quad \mathbf{13.1}$$

$$\begin{array}{l} \text{Total number of} \\ \text{valence electrons} \\ \text{in cluster} \end{array} = \begin{array}{l} \text{Number of electrons} \\ \text{involved in framework} \\ \text{interactions} \end{array} + \begin{array}{l} \text{Number of electrons} \\ \text{involved in metal-} \\ \text{ligand interactions} \end{array} \quad \mathbf{13.2}$$

As we have seen previously, the number of electrons involved in framework interactions in boranes is related to the classification of the structure as *closo*, *nido*, etc. Rearranging equation **13.2** gives the following.

$$\begin{array}{l} \text{Number of electrons} \\ \text{involved in framework} \\ \text{interactions} \end{array} = \begin{array}{l} \text{Total number of} \\ \text{valence electrons} \\ \text{in cluster} \end{array} - \begin{array}{l} \text{Number of electrons} \\ \text{involved in metal-} \\ \text{ligand interactions} \end{array} \quad \mathbf{13.3}$$

For a borane, two electrons are assigned to each boron–hydrogen bond (including each 3-center, 2-electron bond for bridging hydrogens). For a transition metal–carbonyl complex, Wade suggests that 12 electrons per metal are either involved in metal–carbonyl bonding (to all carbonyls on a metal) or are nonbonding and therefore unavailable for participation in framework bonding. The result is that there is a net difference of 10 electrons per framework atom in comparing boranes with transition metal carbonyl clusters. A metal–carbonyl analogue of *closo*- $B_6H_6^{2-}$, which has 26 valence electrons, would therefore need a total of 86 valence electrons to adopt a *closo* structure. An 86-electron cluster that satisfies this requirement is $Co_6(CO)_{16}$. Like $B_6H_6^{2-}$, $Co_6(CO)_{16}$ has an octahedral framework. As in the case of boranes, *nido* structures correspond to *closo*

³¹K. Wade, *Adv. Inorg. Chem. Radiochem.*, **1976**, 18, 1.

Table 13-9 Electron Counting in Main Group and Transition Metal Clusters

Structure type	Main group cluster	Transition metal cluster
<i>closo</i>	$4n + 2$	$14n + 2$
<i>nido</i>	$4n + 4$	$14n + 4$
<i>arachno</i>	$4n + 6$	$14n + 6$
<i>hypho</i>	$4n + 8$	$14n + 8$

geometries from which one vertex is empty; *arachno* structures lack two vertices, and so on. The valence electron counts corresponding to the various structural classifications for main group and transition metal clusters are summarized in Table 13-9.

Examples of *closo*, *nido*, and *arachno* borane and transition metal clusters are given in Table 13-10. In each case, the transition metal cluster has an electron count exceeding the matching borane cluster by 10 valence electrons per framework atom. For example, for four framework atoms per cluster, the transition metal clusters exceed the matching borane clusters by 40 valence electrons.

Transition metal clusters formally containing seven metal–metal framework bonding pairs are among the most common; examples illustrating the structural diversity of these clusters are given in Table 13-11³² and Figure 13-18.

Predicted structures of transition metal–carbonyl complexes using Wade's rules are often, but not always, accurate.³³ For example, the clusters $M_4(CO)_{12}$ ($M = Co, Rh, Ir$) have 60 valence electrons and are predicted to be *nido* complexes ($14n + 4$ valence electrons). A *nido* structure would be a trigonal bipyramid (the parent structure) with one position vacant. X-ray crystallographic studies, however, have shown these complexes to have tetrahedral metal cores.³⁴

13-2-6 Carbon-Centered Clusters

In recent years, many compounds have been synthesized, often fortuitously, in which one or more atoms have been partially or completely encapsulated within

³²K. Wade, "Some Bonding Considerations," In B.F.G. Johnson, Ed., *Transition Metal Clusters*, Wiley: New York, 1980, p. 232.

³³Limitations of Wade's rules are discussed in R. N. Grimes, "Metallacarboranes and Metallaboranes," In G. Wilkinson, F. G. A. Stone, and W. Abel, Eds., *Comprehensive Organometallic Chemistry*, Vol. 1, Pergamon Press: Elmsford, NY, 1982, p. 473.

³⁴The metal cores of $Co_4(CO)_{12}$ and $Rh_4(CO)_{12}$ are slightly distorted; as mentioned earlier in Chapter 13 (see Figure 13-4), these complexes have three bridging carbonyls on one triangular face.

Table 13-10 *Closo*, *Nido*, and *Arachno* Borane and Transition Metal Clusters

Framework atoms in cluster	Vertices in parent polyhedron	Framework electron pairs	Valence electrons (boranes)				Valence electrons (transition metal clusters)				
			<i>Closo</i>	<i>Nido</i>	<i>Arachno</i>	Example	<i>Closo</i>	<i>Nido</i>	<i>Arachno</i>	Example	
4	4	5	18			^a	58				
	5	6		20				60		Co ₄ (CO) ₁₂	
	6	7			22				62	[Fe ₄ C(CO) ₁₂] ²⁻	
5	5	6	22			C ₂ B ₃ H ₅ ^a	72				
	6	7		24				74		Os ₅ (CO) ₁₆	
	7	8			26				76	Os ₅ C(CO) ₁₅ [Ni ₅ (CO) ₁₂] ²⁻	
6	6	7	26			B ₆ H ₆ ²⁻	86				
	7	8		28				88		Co ₆ (CO) ₁₆ Os ₆ (CO) ₁₇ [P(OMe) ₃] ₃	
	8	9			30				90	[Os ₆ (CO) ₁₈ P] ⁻	

^aIons having the formulas B₄H₄²⁻ and B₃H₃²⁻, which would be classified as *closo*, have not been isolated.

Table 13-11 Clusters That Formally Contain Seven Metal–Metal Framework Bond Pairs

Number of framework atoms	Cluster type	Shape	Examples	
7	Capped <i>closo</i> ^a	Capped octahedron	$[\text{Rh}_7(\text{CO})_{16}]^{3-}$	
6	<i>closo</i>	Octahedron	$\text{Rh}_6(\text{CO})_{16}$	
6	Capped <i>nido</i> ^b	Capped square pyramid	$\text{H}_2\text{Os}_6(\text{CO})_{18}$	
5	<i>nido</i>	Square pyramid	$\text{Ru}_5\text{C}(\text{CO})_{15}$	
4	<i>arachno</i>	Butterfly	$[\text{HFe}_4(\text{CO})_{13}]^{-c}$	

^aA capped *closo* cluster has a valence electron count equivalent to neutral B_nH_n .

^bA capped *nido* cluster has the same electron count as a *closo* cluster, equivalent to $\text{B}_n\text{H}_n^{2-}$.

^cThis complex has an electron count matching a *nido* cluster, but it adopts the butterfly structure expected for *arachno*. This is one of many examples in which structures of metal complexes are not predicted accurately by Wade's rules.

metal clusters. The most common of these cases have been carbon-centered clusters (sometimes called carbide clusters), with carbon exhibiting coordination numbers and geometries not found in classical organic structures. Other nonmetals

such as nitrogen have also been found encapsulated in clusters. Examples of these unusual coordination geometries are shown in Figure 13-18.

Encapsulated atoms contribute their valence electrons to the total electron count. For example, carbon contributes its four valence electrons in $\text{Ru}_6\text{C}(\text{CO})_{17}$ to give a total of 86 electrons, corresponding to a *closo* electron count.

How is it possible for carbon or other atoms having only four valence orbitals to form bonds to more than four surrounding transition metal atoms? $\text{Ru}_6\text{C}(\text{CO})_{17}$ is again a useful example. The octahedral Ru_6 core has framework

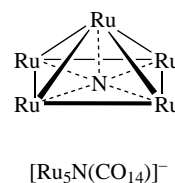
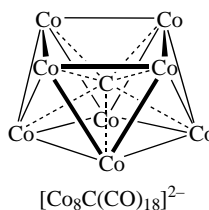
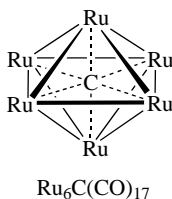
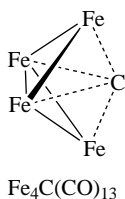
Exercise 13-6

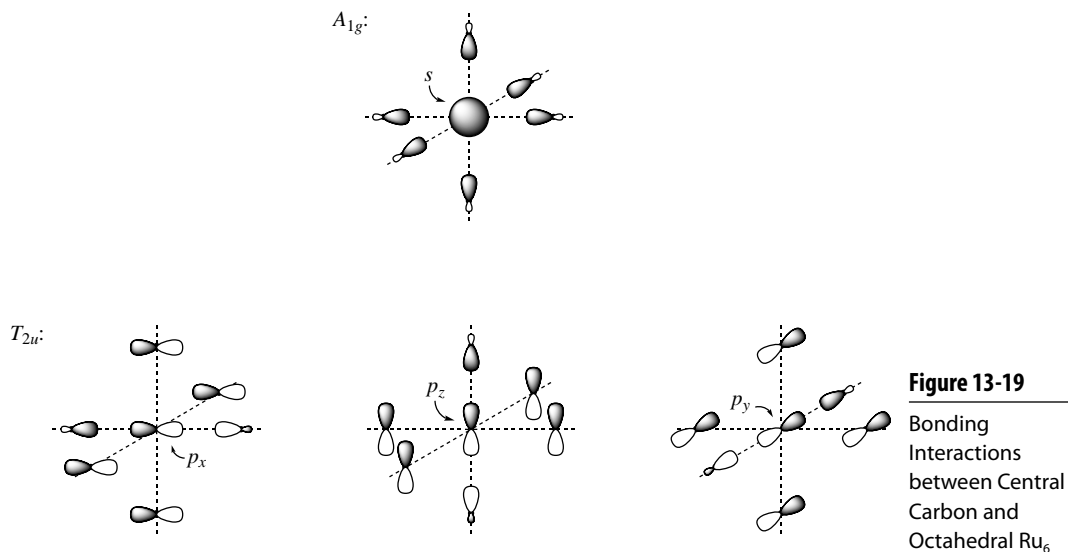
Verify the electron counts and cluster type of the clusters listed in Table 13-11.

molecular orbitals (Figure 13-19) similar to those of $\text{B}_6\text{H}_6^{2-}$ (Figure 13-10). The key point is that carbon is not restricted to forming bonds with individual atoms (as is commonly described in organic compounds of carbon), but can participate in the formation of molecular orbitals extending through carbon from the surrounding metals. Figure 13-19 shows the orbitals from which four of the most important bonding orbitals in the central Ru_6C core are derived. The $2s$ orbital of carbon can interact with six metal orbitals (hybrid orbitals, involving significant d character) in a σ fashion, as shown in the top diagram in Figure 13-19 (labeled A_{1g}). In addition, each of the carbon's $2p$ orbitals can participate in more complex interactions, as shown in the three lower diagrams in Figure 13-19 (labeled T_{2u}). The net result of these interactions is the formation of four C–Ru bonding orbitals, occupied by electron pairs to hold the carbon in the center of the “cage.”

Figure 13-18

Carbon- and Nitrogen-Centered Clusters (Adapted with permission from G.L. Miessler and D.A. Tarr, *Inorganic Chemistry*, 3rd ed., Pearson Education: Upper Saddle River, NJ, 2004, p. 587.)





Suggested Readings

The Isolobal Analogy

R. Hoffmann, *Angew. Chem. Int. Ed. Engl.*, **1982**, *21*, 711–724 (Nobel lecture).

Boranes

K. Wade, *Electron Deficient Compounds*, Nelson: New York, 1971.

N. N. Greenwood and A. Earnshaw, *Chemistry of the Elements*, 2nd ed., Butterworth-Heinemann: Oxford, 1997, pp. 141–181.

As ligands: N. N. Greenwood, *Coord. Chem. Rev.*, **2002**, *226*, 61–69.

Metallacarboranes

R. N. Grimes, in E. W. Abel, F. G. A. Stone, and G. Wilkinson, eds., *Comprehensive Organometallic Chemistry II*, Pergamon Press: Oxford, 1995, Vol. 1, Chap. 9, pp. 373–430.

Analogues of metallocenes

M. Corsini, F. Fabrizi de Biani, P. Zanello, *Coord. Chem. Rev.*, **2006**, *250*, 1351.

Problems

13-1 Propose organic fragments isolobal with the following:

- a. $[Re(CO)_4]$
- b. $Tc(CO)_4(PPh_3)$

- c. $(\eta^5\text{-Cp})\text{Ir}(\text{CO})$
 d. $(\eta^4\text{-C}_4\text{H}_4)\text{Co}(\text{PMe}_3)_2$
 e. The ligands in the carbon-centered cluster $[\text{C}(\text{SiMe}_3)_2(\text{AuPPh}_3)_3]^+$, an example of pentacoordinate carbon.
- 13-2** Propose an organometallic fragment, not mentioned in Chapter 13, isolobal with the following:
- a. CH_3^+
 b. CH_2
 c. CH_2^-
 d. CH_3^-
- 13-3** a. On the basis of the isolobal analogy, propose a synthesis of $(\eta^5\text{-Cp})(\text{CO})_2\text{Fe}\text{---}\text{Mn}(\text{CO})_5$.
 b. Predict the main product of the reaction between $[(\eta^5\text{-Cp})\text{Mn}(\text{CO})_3]_2$ and $\text{Re}_2(\text{CO})_{10}$.
- 13-4** Organoimido ligands (NR^-) may be viewed as isolobal with the cyclopentadienyl ligand C_5H_5 (alternatively, NR^{2-} may be considered isolobal with C_5H_5^- ; like C_5H_5^- , which has three electron pairs in π orbitals, NR^{2-} has three valence electron pairs that can be involved in ligand-metal bonding).³⁵ Thus, a transition metal complex containing C_5H_5 may have chemical parallels with an organoimido complex of the same charge involving a metal from the following group in the periodic table. (For example, $[\text{WCp}]^{5+}$ would be analogous with $[\text{Re}(\text{NR})]^{5+}$.) On this basis, predict formulas of organoimido complexes isolobal with the following.
- a. Cp_2Zr and $\text{Cp}_2\text{Nb}(\text{NR})$.³⁶
 b. The zwitterionic complex $\text{CpZr}(\text{CH}_3)_2[(\eta^6\text{-C}_6\text{H}_5\text{CH}_2\text{B}(\text{C}_6\text{F}_5)_3)]$.³⁷
- 13-5** The 15-electron $\text{Co}(\text{CO})_3$ fragment has a number of chemical parallels with the phosphorus atom.
- a. Propose structures for the compounds formed by replacing one or more phosphorus atoms of the tetrahedral P_4 cluster with $\text{Co}(\text{CO})_3$ fragments.

³⁵D. S. Glueck, J. C. Green, R. I. Michelman, and I. N. Wright, *Organometallics*, **1992**, *11*, 4221.

³⁶J. Sundermeyer and D. Runge, *Angew. Chem. Int. Ed. Engl.*, **1994**, *33*, 1255.

³⁷R. Arteaga-Müller, J. Sánchez-Nieves, J. Ramos, P. Royo, and M. E. G. Mosquera, *Organometallics*, **2008**, *27*, 1417.

b. Like $\text{Co}(\text{CO})_3$, the $(\eta^5\text{-Cp})\text{Mo}(\text{CO})_2$ fragment may substitute for phosphorus atoms in P_4 . Propose formulas and structures for the clusters that would result from such substitution.³⁸

13-6 Classify as *closo*, *nido*, or *arachno*.

- $\text{B}_{10}\text{H}_{14}^{2-}$
- $\text{C}_3\text{B}_5\text{H}_7$
- $\text{PCB}_{10}\text{H}_{11}$
- $\text{B}_4\text{H}_6(\text{RhCp})_2$
- $\text{B}_3\text{H}_8\text{Re}(\text{CO})_3$
- $\text{C}_2\text{B}_9\text{H}_{11}\text{Os}(\text{CO})_3$

13-7 Classify as *closo*, *nido*, or *arachno*.

- B_8H_{12}
- $\text{C}_2\text{B}_7\text{H}_{12}^-$
- $\text{AsCB}_9\text{H}_{11}^-$
- $\text{B}_4\text{H}_6(\text{CoCp})_2$
- $\text{C}_2\text{B}_7\text{H}_9(\text{CoCp})_3$
- $\text{C}_2\text{B}_4\text{H}_6\text{Ni}(\text{PPh}_3)_2$

13-8 Azaboranes are derivatives of boranes in which nitrogen atoms occupy one or more structural positions. Classify the following azaboranes as *closo*, *nido*, or *arachno*.³⁹

- $\text{B}_3\text{H}_2(\text{CMe}_3)_3(\text{NCMe}_3)$
- $\text{B}_3\text{H}_2(\text{CMe}_3)_2(\text{NEt}_2)(\text{NCMe}_3)$

13-9 Determine the electron counts for the clusters in Figure 13-18 (except for $\text{Ru}_6\text{C}(\text{CO})_{17}$), and classify as *closo*, *nido*, or *arachno*.

13-10 The fragment $\text{Co}(\eta^4\text{-C}_4\text{H}_4)$ is isolobal with $\text{Fe}(\eta^5\text{-C}_5\text{H}_5)$.

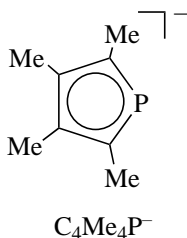
- What compound would result by replacing part of ferrocene by this cobalt fragment?
- A solution of sodium cyclopentadienide in THF was added to a stirred solution of $(\eta^4\text{-C}_4\text{Me}_4)\text{Co}(\text{CO})_2\text{I}$, also in THF. After reaction, the solvent was removed under vacuum, and the residue was extracted into petroleum ether. Removal of solvent and purification by sublimation yielded a yellow–orange solid. This product showed two ^1H NMR resonances, at chemical shifts of 1.55 and 4.53 ppm; it had no

³⁸T. Kilthau, B. Nuber, and M. L. Ziegler, *Chem. Ber.*, **1995**, 128, 197.

³⁹M. Müller, T. Wagner, U. Englert, and P. Paetzold, *Chem. Ber.*, **1995**, 128, 1.

infrared bands between 1800 and 2100 cm^{-1} . Suggest a structure of this product.

- c. In a separate reaction, a solution containing the ion $\text{C}_4\text{Me}_4\text{P}^-$ was added to a stirred solution of $(\eta^4\text{-C}_4\text{Me}_4)\text{Co}(\text{CO})_2\text{I}$, with THF again used as the solvent. Isolation by a similar procedure as in **b** gave a product with a single ^{31}P NMR resonance and no infrared bands between 1800 and 2100 cm^{-1} . Elemental analysis gave 62.91% C and 8.05% H by mass. Propose a structure of this product.⁴⁰



- 13-11** The ligand $\text{In}[\text{C}(\text{SiMe}_3)_3]$ is known to occupy positions similar to terminal carbonyl ligands; for example, like $\text{Ni}(\text{CO})_4$, the complex $\text{Ni}[\text{In}\{\text{C}(\text{SiMe}_3)_3\}_4]$ is tetrahedral.⁴¹ Are CO and $\text{In}[\text{C}(\text{SiMe}_3)_3]$ isolobal? [Suggestion: Consider the potential donor and acceptor orbitals of the ligands.]
- 13-12** Ligands having the formula GaR (R = alkyl) exhibit similarities to the carbonyl ligand. Show how a GaR ligand could act as both a σ donor and a π acceptor. What would be the formula of an 18-electron Zr complex containing only $\eta^5\text{-Cp}$ and GaR ligands?⁴²
- 13-13** Identify the first-row transition metal in the following *closo* complexes:⁴³
- $[\text{CB}_7\text{H}_8\text{M}(\text{CO})_3]^-$
 - $\text{C}_2\text{B}_9\text{H}_{11}\text{M}(\text{CO})_2$
- 13-14** $\text{Cp}_2\text{Zr}(\text{CH}_3)_2$ reacts with the highly electrophilic borane $\text{HB}(\text{C}_6\text{F}_5)_2$ to form a product having stoichiometry $(\text{CH}_2)[\text{HB}(\text{C}_6\text{F}_5)_2]_2(\text{ZrCp}_2)$; the product is an example of pentacoordinate carbon.⁴⁴

⁴⁰E. V. Mutseneck, D. A. Loginov, D. S. Perekalin, Z. A. Starikova, D. G. Golovanov, P. V. Petrovskii, P. Zanello, M. Corsini, F. Laschi, and A. R. Kudinov, *Organometallics*, **2004**, *23*, 5944.

⁴¹W. Uhl, M. Pohlmann, and R. Wartchow, *Angew. Chem. Int. Ed.*, **1998**, *37*, 961.

⁴²X. Yang, B. Quillian, Y. Wang, P. Wei, and G. H. Robinson, *Organometallics*, **2004**, *23*, 5119.

⁴³A. Franken, T. D. McGrath, and F. G. A. Stone, *Organometallics*, **2005**, *24*, 5157; B. E. Hodson, T. D. McGrath, and F. G. A. Stone, *Inorg. Chem.*, **2004**, *43*, 3090.

⁴⁴R. E. von H. Spence, D. J. Parks, W. E. Piers, M.-A. MacDonald, M. J. Zaworotko, and S. J. Rettig, *Angew. Chem. Int. Ed. Engl.*, **1995**, *34*, 1230.

- a. Propose a structure for this product. [Useful information: The ^1H NMR spectrum has singlets at $\delta = 5.23$ (relative area = 5) and 2.29 ppm (rel. area = 1) and a broad signal at $\delta = -2.05$ ppm (rel. area = 1); the ^{19}F NMR spectrum has three resonances; and the ^{11}B NMR has a single peak.]
- b. An isomer of this product, $[\text{Cp}_2\text{ZrH}]^+[\text{CH}_2\{\text{B}(\text{CF}_3)_2\}_2(\mu\text{-H})]^-$, has been proposed as a potential Z-N catalyst. Suggest a mechanistic pathway by which this isomer might serve as a catalyst for the polymerization of ethylene.⁴⁵

13-15 Refluxing $\text{Ru}_3(\text{CO})_{12}$ with the tetramethyldisilylene compound shown below in xylene solvent gives several products. The most interesting of these has the following characteristics:

IR (cm^{-1}): 1934–1985 (4 peaks), 1807, 1779

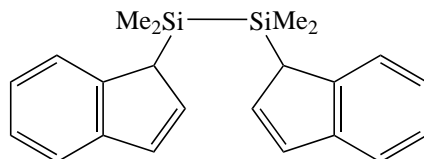
^1H NMR: multiple peaks between 6.82 and 4.41 ppm; no peaks in the range 0–1 ppm

Composition by mass: 25.67% C, 0.914% H, 14.51% O

Additional information: each oxygen is attached to carbon; one carbon is significantly different from all the rest.

Finally, some would say that this molecule wears three caps!

Propose a structure for this product.⁴⁶



⁴⁵See also L. Jia, X. Yang, C. Stern, and T. J. Marks, *Organometallics*, **1994**, *13*, 3755.

⁴⁶D. Chen, B. Mu, S. Xu, and B. Wang, *J. Organomet. Chem.*, **2006**, *691*, 3823.

APPENDIX A

List of Abbreviations

\square	Empty coordination site
\longleftrightarrow	Isolobal symbol
\sim	A bond line that indicates stereochemistry is not specified
I ^o , II ^o , III ^o	Primary, secondary, tertiary
α	Position on carbon chain attached to metal; α denotes carbon directly attached to metal
β	Position on carbon chain attached to metal; β denotes one carbon beyond the α position
β_n	Natural bite angle; a measure of the P–M–P bond angle of diphosphine and diphosphite ligands
η^n	Descriptor of hapticity (the number of binding sites on a ligand); the superscript designates the number of binding sites
θ	Cone angle; a measure of the steric bulk of phosphine ligands
μ	Descriptor for bridging ligand(s)
ν	Frequency
χ	A measure of the electronic properties of PR ₃ ligands; each R group has a different χ value. The lower the value of χ , the more electron donating the R group and thus the phosphine.
A	Associative substitution
ADMET	Acyclic diene metathesis
Ar	Aryl
Bn	Benzyl (PhCH ₂ -)
Boc or <i>t</i> -Boc	<i>tert</i> -butoxycarbonyl; a protecting group, typically used to protect amines
Bu	Butyl (previously known as <i>n</i> -butyl)

A-2 Appendix A List of Abbreviations

<i>t</i> -Bu	<i>tert</i> -Butyl or <i>tert</i> -Bu
CO	Carbonyl ligand
COD (or cod)	1,5-Cyclooctadiene
COT (or cot)	1,3,5,7-Cyclooctatetraene
Cp	Cyclopentadienide ion, C ₅ H ₅ ⁻
Cp*	Pentamethylcyclopentadienide ion, C ₅ (Me) ₅ ⁻
Cp'	Ethyltetramethylcyclopentadienide ion, C ₅ (Et)(Me) ₄ ⁻
Cy	Cyclohexyl
D	Dissociative substitution
dba	Dibenzylideneacetone (Ph-CH=CH-C(=O)-CH=CH-Ph); a useful ligand for Pd-catalyzed reactions in organic synthesis
DMA	<i>N,N</i> -Dimethylacetamide
DMAP	4-Dimethylaminopyridine; used as a basic catalyst
DMF	<i>N,N</i> -Dimethylformamide
DMSO	Dimethylsulfoxide
dppf	[1,1'-bis(Diphenylphosphino)ferrocene, Fe(C ₅ H ₄ PPh ₂) ₂]; a useful bidentate ligand
<i>dⁿ</i>	Formal <i>d</i> -electron configuration
E or E ⁺	Electrophile
<i>E</i> -factor	The environmental factor (the ratio of the total mass of waste to the mass of the desired product); a measure of how green a reaction or process is
ee or % ee	Percent enantiomeric excess
Et	Ethyl
Et ₂ O	Diethyl ether
EtOH	Ethanol
eu	Entropy units (cal/mol K)
en	Ethylenediamine
<i>fac</i>	Facial stereochemistry (three ligands occupy the same face of an octahedral complex)
Fp	CpFe(CO) ₂ ; pronounced "fip"
HMPA	Hexamethylphosphoric triamide or, commonly, hexamethylphosphoramide, (Me ₂ N) ₃ P-O

HOMO	Highest occupied molecular orbital
I	Interchange mechanism of ligand substitution
IR	Infrared
L	A generalized ligand, most often a 2-e ⁻ neutral ligand
LDA	Lithium diisopropylamide
L _n M	A generalized metal complex fragment with <i>n</i> L-type ligands attached
Ln	Lanthanide
LUMO	Lowest unoccupied molecular orbital
M	Central metal in a complex
Me	Methyl
MeOH	Methanol
<i>mer</i>	Meridional stereochemistry (three ligands arranged to define a plane through an octahedral complex)
MO	Molecular orbital
MOM	Methoxymethyl; a protecting group for alcohols
NHC	<i>N</i> -heterocyclic carbene
NMR	Nuclear magnetic resonance
Nuc or Nuc: ⁻	Nucleophile
OA	Oxidative addition
OAc ⁻	Acetate ion
O.S.	Oxidation state
OMs	Mesylate, CH ₃ SO ₃ ⁻
OTf	Triflate, CF ₃ SO ₃ ⁻
OTs	Tosylate, <i>p</i> -CH ₃ -C ₆ H ₄ -SO ₃ ⁻ (Ts = tosyl)
PE	Polyethylene
Ph	Phenyl
pm	Picometer
PP	Polypropylene
Pr	Propyl
<i>i</i> -Pr	Isopropyl

A-4 Appendix A List of Abbreviations

PR ₃	Phosphine
Py	Pyridine
R	Usually a generalized alkyl group
RE	Reductive elimination
ROMP	Ring-opening metathesis polymerization
S or Solv	Solvent
SBM	σ bond metathesis
SHOP	Shell higher olefin process
TBDMS	<i>tert</i> -Butyldimethylsilyl [(CH ₃) ₃ C(CH ₃) ₂ Si-]
TBDPS	<i>tert</i> -Butyldiphenylsilyl [(CH ₃) ₃ C(Ph) ₂ Si-]
TFA	Trifluoroacetic acid
THF or thf	Tetrahydrofuran
TMS	Trimethylsilyl, (CH ₃) ₃ Si-
Tp	A trispyrazolylborate ligand ([HB(C ₃ N ₂ H ₃) ₃], hydridotris(pyrazoyl)borate); a highly sterically bulky ligand used to protect metals from attack by other ligands
Tp*	Hydridotris(3,5-dimethylpyrazoyl)borate; similar to Tp but sterically more bulky
X	A generalized X-type ligand (1 e ⁻ in the neutral ligand counting method)
Z-N	Ziegler–Natta

INDEX

Index Terms

Links

A

<i>Ab initio</i> MO calculations	45–49			
Absolute rate theory	185			
Acceptor ligand (π)	62–64			
Acetaldehyde (from Wacker Chemie process)	340–341			
Acetic acid process (Monsanto)	361–363			
Acetic anhydride	340	363–364		
Acetone, LUMO	422			
Actinides	125–126	509–510		
Activation enthalpy (ΔH^\ddagger)	185			
Activation entropy (ΔS^\ddagger)	185			
Activation of ligands				
C-C	215–218			
C-H	209–215			
Activation volume (ΔV^\ddagger)	185			
Acyclic diene metathesis (ADMET) polymerization	458	483–486		
Acyl complexes	149–150	245–253		
Agostic interaction	154–155	252–253	327	411–412
	498	500		
Alkene-metal complexes	103–104			
Reactions of	278–280			
Alkenes				
Hydroformylation of	314	322–339	570–574	
(asymmetric)				

Index Terms

Links

Alkenes (<i>Cont.</i>)				
Hydrogenation of (asymmetric)	313	350–361	524–545	
Isomerization of (<i>N</i> -triggered)	314	259	380–384	
Metathesis of (<i>see also</i> π -Bond metathesis)	456–492			
Oligomerization of	474	492	496–498	505
Polymerization of	9	478–486	492–507	
Alkenyl (vinyl)-metal complexes	140			
Alkylidene complexes (<i>see also</i> Metal-carbene complexes)	141–142	398–399		
Bridged	413–414			
Electrophilic, reactions of	426–430			
Synthesis of	409–416			
Alkylidyne complexes (<i>see also</i> Metal-carbyne complexes)	137 439 ff	141	145	148
Alkyl migration	245–253			
Stereochemistry	245–251			
Alkynes				
Hydrogenation of	314	602		
Metal-alkyne complexes	150			
Use in synthesis (metathesis)	489–492 601–607			
(Sonogashira cross coupling)	623–628			
(Pauson-Khand reaction)				
Alkyne metathesis	486–492			
Synthesis applications	489–492			
Allowed and disallowed reactions	510–511			

Index Terms

Links

Allyl ligand, nucleophilic attack on	276–277	280–281		
Alpha(α)-elimination (<i>see</i> Elimination, α)				
Alpha(α)-hydrogen abstraction	410–413	444–445		
Aminolysis	269–270	422–423		
Arene-metal complexes	122–123	281–285		
Bonding	42			
Cr complexes	122–123	282–283		
Nucleophilic reactions of	282–285			
Organic synthetic applications	282–285			
Preparation	122			
Aryl-metal complexes	140			
Associative (A) ligand substitution	178–180	184–190		
Eighteen-electron complexes	188–190			
Kinetics	190–192			
Mechanism	178–180	184	190	197–198
Seventeen-electron complexes	201–202			
Stereochemistry	187–188	202		
<i>trans</i> Effect	179–184			
Asymmetric C=C migration	381–384			
Asymmetric Heck reaction (AHR)	581–584			
Asymmetric hydroformylation (AH)	570–574			
Asymmetric hydrogenation	7	524 ff		
Cationic Ir(I) complexes	543–545			
C=O, using Ru(II)	538–543			
Rh catalysts	528–534			
Ru catalysts	534–543			
Asymmetric metathesis	470			
Asymmetric oxidations	545–555			
Green aspects	547			
Asymmetric Pauson-Khand reaction	627–628			
Asymmetric Tsuji-Trost reaction	559–567			

Index Terms

Links

Atactic polymers	500–501		
(<i>see also</i> Ziegler-Natta polymerization)			
B			
Back bonding (back donation)	64		
To carbene ligands	401		
To CO	63–64	95	
To NO	90		
To phosphines	156–157		
To pi ligands	104–107		
Bidentate ligands in hydroformylation	335–339		
BINAP ligand	7–8	381	529
BINAPHOS ligand	571–573		
Binary carbonyls	70	83–86	
Biotin	526		
BISBI (2,2'-bis[(diphenylphosphino) methyl]-1,1'-biphenyl) ligand	335		
Bite angle (β_n)	335		
(also known as natural bite angle)			
Block copolymers	480–481		
Bond energies			
M-C	210	255	
M-H	210	255	
Boots-Hoechst-Celanese ibuprofen synthesis	376–378		
Borane clusters	650–661		
Heteroboranes	656–658		
Metallaboranes and metallacarboranes	658–661		
Born-Oppenheimer approximation	44		

Index Terms

Links

Bridging ligands			
Alkylidene	440		
CO	79–82		
Hydride	648	654	
NO	91		
μ -symbol	79		
Brookhart ligands	506		
Buckyball (<i>see</i> Fullerenes)			
Buckminsterfullerene (<i>see</i> Fullerenes)			
η^4 -Butadiene-metal complexes	106–107	272–273	
C			
Carbene (also known as a free carbene)	394–397		
Influence of heteroatom on MO diagrams for	396–397		
Carbene complexes (<i>see</i> Metal-carbene complexes)			
Carbide clusters	3	663–667	
Carbide ligands	148–149	301–302	
Carbon-carbon bond formation via			
CO and C=C insertion	567–584		
Cross coupling	584–613		
Cyclization	613–628		
Metathesis	473–478		
Tsuji-Trost reaction	555–567		
Carbon-centered (carbide) clusters	3	663–667	
Carbon monoxide			
Bonding of (MO picture)	24–26	63	75–76
Ligand properties (<i>see</i> Carbonyls)			
Carbonyl clusters	662–667		

Index Terms

Links

Carbonyl insertion		
(<i>see also</i> 1,1-insertion)	245–253	
Carbonyls, metal	75–87	92–96
Back bonding to metal	64	95
Binary	70	83–86
Bridging	79–82	
Infrared spectra	77–80	92–96
Metal carbonyl cluster compounds	83	662–667
Migratory insertion to	245–253	
Nucleophilic attack on		
ligand	269–270	288
Number of IR bands and		
symmetry	92–95	
Oxygen-bonded	86–87	
Preparation of	84–87	
Reactions of	85–86	
Semibridging complexes	81–82	
Special bridging in $[(\eta^5\text{-Cp})$		
$\text{Mo}(\text{CO})_2]_2$	82	
Stretching frequencies of CO	77–80	
Carbonylation of methanol	361–367	
Cativa Process	364–365	
Ir-catalyzed	364–367	
Rh-catalyzed	361–364	
Carbonylation of methyl acetate		
(Eastman-Halcon Process)	363–364	
Carbonylation, use in synthesis	568–574	
Asymmetric hydroformylation	570–574	
Carboxylic acid derivative formation (Pd-catalyzed)	568–570	
Carbynes (alkylidynes) (<i>see</i> Metal-carbyne complexes)		
Cascade carbometallations	611	622

Index Terms

Links

Catalysis	311 ff			
Active site	316			
Catalytic cycles	312–314			
C=C bond isomerization	314			
Chemoselectivity	313			
Enzymes	315	317–319		
Fitness of transition				
metals for	318–321			
General principles of	311–321			
Green chemistry in				
relation to	321–322			
Heterogeneous	315–318			
Homogeneous	315–318			
Hydrocyanation	367–374			
Hydroformylation	314	322 ff		
Hydrogenation	350–361			
Mechanistic studies	316–317			
<i>(see also mechanistic aspects of various reactions catalyzed by organometallic compounds)</i>				
Selectivity	312–315			
Cativa process	364–366			
C-C bond activation	215–218			
C-F bond interactions with metal	150	255–256		
CF ₃ group (stability as alkyl group)	150	255–256		
C-H bond activation	209–215			
Chain transfer (in polymerization)	493–494	504–506	508	513
Chelate effect	230	232		
Chemoselectivity	313			
Chi (χ) factor for phosphines	159–160			
Chiral auxiliary	526–527			

Index Terms

Links

Chiral chromatography	525–526			
Chiral ligands	529	534	543	561
	573			
Chiral synthesis	8	524–528		
(see also various other sections of Chapter 12)				
CHIRAPHOS ligand	529–532			
Chymotrypsin	319			
<i>cis</i> Effect	192–194			
Citronellol	557			
Cluster compounds	2–3	650 ff		
<i>Arachno</i>	654			
Boranes	650–664			
Carbide	2–3	663–667		
Carbonyl	662–663			
Carboranes	658–662			
Classification of structures	654–657	660–663		
<i>Closo</i>	654			
Electron counting in	651 ff			
Encapsulated atoms	663–666			
<i>Hypho</i>	655			
Metallaboranes	659–661			
<i>Nido</i>	654			
Cobalticinium ion	115			
Cobaltocene $[(\eta^5\text{-Cp})_2\text{Co}]$	113–115			
CO complexes (see Carbonyls, metal)				
Coenzyme B ₁₂	9–10			
Collman's reagent	85–86			
σ -Complex-assisted metathesis (σ -CAM)	508–509			
Computational organometallic chemistry	42–49			
Cone angle (θ) of phosphine ligands	157–159			

Index Terms

Links

Coordination geometries	64–71			
Coordination number	59			
Coordinative saturation and unsaturation	266			
Cope reaction (elimination)	256–257			
Cossee mechanism for Ziegler-Natta polymerization	493–500			
Covalent bond classification (L-X notation)	59–60	176–177		
L-type ligand	59			
X-type ligand	59			
Cr(CO) ₆	54–55	64–67		
Cr(NO) ₄	91			
Crabtree's catalyst	359–360			
Cross coupling reactions	584 ff			
Negishi	607–613			
Sonogashira	601–607			
Stille	587–595			
Suzuki	595–601			
Transmetalation	584–587			
Cross metathesis (CM)	458			
Crossover experiments	232–233			
Crystal field theory	69			
Cyano (CN) complexes	89			
Cyclization	613 ff			
Dötz reaction	613–616			
Pauson-Khand reaction	623–628			
Pd-catalyzed	616–622			
Ring-closing metathesis (RCM)	458	477		
Cyclobutadiene complexes	118–121			
Cycloheptatriene complexes	123–124			
Cyclometalation	140	203	209	212

Index Terms

Links

Cyclooctatetraene (COT) complexes	125–126	
Cyclopentadienyl ligand (Cp)	107–117	
Bonding in	41	109–114
Cp vs Cp*	107	
Cp'	107	
Synthesis of Cp-metal complexes	121	
Cyclopropane formation	434–439	
Using Rh-carbene complexes	437–439	
Cyclopropenyl complexes	118–119	
D		
<i>d</i> ⁿ Configuration	60	
Davies-Green-Mingos (DGM) rules		
for nucleophilic reactions on π		
ligands	270–277	
Deinsertion (<i>see</i> Elimination)		
Density functional theory (DFT)	47–49	
Kohn-Sham equations	48	
Deuterium isotope effect (primary kinetic		
isotope effect)	357	
Dicyclopentadiene (DCPD)		
polymerization	483	
Dibenzenechromium [$(\eta^6\text{-C}_6\text{H}_6)_2\text{Cr}$]	122	
Diels-Alder reaction	616–617	
Dienes (<i>see</i> η^4 -Butadiene-metal complexes)		
Diffusion-controlled rate processes	197	
Dihydrogen metal complexes	152–154	204–208
Dimethyltitanocene (Petasis reagent)	429–430	
Dinitrogen as a ligand	89	
Dioxygen, bonding in	23–24	
DIPAMP ligand	529	532

Index Terms

Links

DIPHOS (diphos, also known as dppe)				
ligand	157	336	528	
Diphosphine ligands (chiral)	529			
Diphosphite ligands	338–339	573		
Dissociative (D) ligand				
substitution	190–196			
<i>cis</i> Effect	192–194			
Effect of cone angle	193	196		
Kinetics	190–191			
Mechanism	178	190–191		
Nineteen-electron complexes	201–202			
Stereochemistry	192–193	202		
Donor ligands				
π	62			
σ	61			
L-Dopa	359			
Dötz-Wulff synthesis of arenes	613–616			
Double bond isomerization (migration)	258–259	312	314	380–384
(<i>N</i> -triggered)				
Double cross experiment (in olefin metathesis)	463–466			
dppe (also known as DIPHOS)				
ligand	157	336	528	
duPHOS ligand	533–534	573–574		

E

e_g^* orbital	68			
Eastman-Halcon process	363–364			
Effective atomic number (EAN) rule	53			
Eighteen electron rule	53–60			
Covalent bond classification (L-X notation)	59–60			

Index Terms

Links

Eighteen electron rule (<i>Cont.</i>)			
Donor pair method	53–55		
Exceptions to	67		
Justification for	60–69		
L-X notation (<i>see</i> Covalent bond classification)			
Molecular orbital theory and	60–71		
Neutral ligand method	55–58		
Pi-acceptor ligands	62–64		
Pi-donor ligands	62	64	
Sigma donor ligands	61	64	
Sixteen electron rule	69–71		
Electrocyclic ring closure	614–615	618	620
Electron correlation	46–47		
Electron counting (<i>see</i> Eighteen electron rule, Cluster compounds)			
Electronegativities of transition metals (table of)	586		
Electrophilic abstraction and addition	116	124	289–304
Hapticity change	299		
M-C Cleavage by H ⁺	291–293		
M-C Cleavage by halogens	293–295		
M-C Cleavage by Hg(II)	296–298		
Mechanistic pathways for M-C cleavage	290–293		
Reactions on π ligands	299–304		
Stereochemistry of	291–303		
With trityl (Ph ₃ C ⁺) cation	303–304		
Electrophilic carbene			
complexes	401	403	
Reactions of	420–426		

Index Terms

Links

Electrophilic carbene (<i>Cont.</i>)			
Synthesis of	407–408		
Electrophilic reagents	289–290		
Elimination (Deinsertion)	139	253–259	
α -	261	410–413	
β -	139–140	253–259	263
Mechanism	254		
Stereochemistry	254–257		
Enantiomer isolation	525–528		
Enantiomeric (ee) excess (% ee)	251		
Enantioselective reactions	524 ff		
Ene reaction	616–622		
Lewis acid-catalyzed	617		
Pd-catalyzed Oppolzer			
approach	619–622		
Pd-catalyzed Trost approach	617–619		
Enthalpy of activation (<i>see</i> Activation			
enthalpy)			
Entropy of activation (<i>see</i> Activation			
entropy)			
Enyne metathesis	489–492		
Mechanism	490–491		
Use in synthesis	490–492		
Enzymes	317–319		
Epothilones	476		
Biological activity	476–477		
Synthesis	477	599–600	
<i>Erythro</i>	224	257	
Ethenolysis	474–476		
Ethylene-metal complexes	103–104		
Ethyltetramethylcyclopentadienyl ligand (Cp')	107		

Index Terms

Links

Extended Hückel theory	46	49
F		
<i>fac</i> vs <i>mer</i> stereochemistry	85	
Fe(CO) ₅	67	
Ferrocene [(η ⁵ -Cp) ₂ Fe]	6–7	108–116
Bonding	109–113	
Discovery of	6	
Isomer	127	
Reactions of	115–116	
Synthesis	6	121
Fischer-Hafner synthesis of		
dibenzenechromium	122	
Fischer carbene complexes	141–142	398–400
(<i>see also</i> Metal-carbene complexes or Electrophilic carbene complexes)		
Fischer-Tropsch reaction	440	
Fluxional processes	131–132	
Force constant	77	275
Related to nucleophilic attack	274–275	
Fp [(η ⁵ -Cp)(CO) ₂ Fe] (Fip)	278	301 303
Free carbene (<i>see</i> Carbene)		
Free energy of activation (ΔG [‡])	312–313	
Frontier orbitals	186–187	207
Frost circle trick (mnemonic)	39–40	
Fullerenes	160–165	
As ligands	162–165	
Buckminsterfullerene (C ₆₀)	160–161	
C ₇₀ -fullerenes	161–162	
Metal complexes	162–165	
Structure	160–162	

Index Terms

Links

Fumarase	315			
Further Exploitation of Advanced Shell Technology (FEAST)	519			
G				
Geraniol	537			
Green chemistry	208–209	321–322	375	
Applications in catalysis	322	478	542	547
	551	596		
Applications in synthesis				
design	376–378	527	571	601
	607			
Atom economy	322			
C-H Activation	209			
<i>E</i> -factor	375	527–528	542–543	673
(definition)				
Green solvents	208	543	607	
Hydroformylation	322	570–571		
Hydrogenation	542–543			
Pd-Catalyzed oxidation of secondary alcohols	547–550			
Presidential Green Chemistry				
Awards	377	601		
Green-Rooney mechanism				
for Ziegler-Natta				
polymerization	495–500			
Grignard reagents	5–6	202–203		
Group orbitals	29 ff			
Grubbs' catalyst	471–473			
1 st Generation	471–472			
2 nd Generation	406–407	471–472		

Index Terms

Links

Grubbs' catalyst (*Cont.*)

Mechanism of catalysis

472–473

Synthesis applications

476–478

Use as a polymerization
catalyst

483–486

H

H₂

21–22

(*see* Dihydrogen metal complexes)

H₃⁺

29–30

37–38

Half sandwich compounds

117

Hammond Postulate

194–196

205

Hapticity

54–55

Hard and soft acids and bases (HSAB)

186–187

Hartree-Fock theory

45

Hartwig C-N coupling

631

Heck-Breslow mechanism

324–329

(*see also* Hydroformylation)

Heck reaction (olefination)

574–584

Anionic cycle

576

Asymmetric

581–584

Cationic cycle

577

Intramolecular

417

Neutral cycle

576

Regioselectivity

577–578

Hemiisotactic polymers

500–501

Hérrison-Chauvin experiment

relating to the mechanism of
alkene metathesis

462

Heteroatoms

393

Heteroboranes

141–145

656–658

Index Terms

Links

Heterogeneous catalyst	315–317			
Heterotactic polymers	500–501			
Homogeneous catalyst	315–317			
Homoleptic complexes	91	138		
Hund's rule	24	27–28		
Hydride complexes	152–154			
Acidity	96–97			
Agostic	154–155			
Bonding	152			
Bridging	648	654		
Preparation	152			
Hydride mechanism for				
hydrogenation	350–353	535–539		
Hydroboration	254	258		
Hydrocarbyl	211	270	290	292–293
	296	299	303	
Hydrocyanation	367–374			
Butadiene	370–371			
DuPont process	367			
Ethene as a model	369–370			
Mechanism	367–374			
Nylon synthesis	367			
Hydroformylation	314	322–339		
Asymmetric	570–574			
Bidentate phosphines and phosphites	335–339			
Bite angle	335			
Catalytic cycle	324	333		
Green chemistry aspects	322	570		
Linear to branched ratio	329–330	332	335–338	
Phosphine-modified	330–331			

Index Terms

Links

Hydroformylation (*Cont.*)

Rhodium-catalyzed	331–339	
Synthetic applications	570–574	
Hydrogenation	350–361	
Asymmetric	358–359	524–545
Dihydride mechanism	353–361	
Iridium-catalyzed	359–361	
Monohydride mechanism	350–353	
Rhodium-catalyzed	353–359	
Ruthenium-catalyzed	351–353	
Using cationic complexes	358–360	
Using Wilkinson's catalyst	353–358	
Hydrozirconation	258	

I

Ibuprofen	376–378	
Boots-Hoechst-Celanese process	377–378	
Green aspects	376–377	
Pd-catalyzed carbonylation of an alcohol	377	
Indenyl complexes (slippage in)	189–190	
Indenyl ligand effect	189	
Infrared spectroscopy		
Carbonyls	77–78	
Nitrosyls	91	
Symmetry of structure and number of IR bands	92–95	
Insertion	177	244–267
1,1-	244–253	264–267
1,2-	245	253–264 265–267

Index Terms

Links

Insertion (*Cont.*)

Alkenes into M-C	259–264			
Alkenes into M-H	253–259			
Applications to organic synthesis	258–259	567–584		
CO into M-C	244–253			
Involving lanthanides	496			
Mechanism	245–256			
SO ₂ into M-C	264–267			
Stereochemistry	245–251	254	257	262
Interchange mechanism for ligand substitution	178	196–200		
I _a mechanism	199–200			
I _d mechanism	196–200			
Ionic liquids	186			
Ir(PPh ₃) ₂ (CO)Cl (Vaska's compound)	204–207			
Isolobal analogy	640–649			
Applications	647–649			
Isolobal molecular fragments	641–645			
Isotactic polymers	482	500–503		
(<i>see also</i> Ziegler-Natta polymerization)				
Isotope effect (<i>see</i> Kinetic isotope effect)				

J

Jacobsen-Katsuki asymmetric epoxidation	546			
(±)- <i>epi</i> -Jatrophone	592–593			

K

K[Pt(η ² -CH ₂ =CH ₂)Cl ₃]XH ₂ O (Zeise's salt)	4	103–104		
---	---	---------	--	--

Index Terms

Links

Karplus relation	225		
Kinetic isotope effect	357	496–497	500
Kinetic resolution of enantiomers	548		
Kinetic <i>trans</i> effect	181–182		
Kinetics, use in elucidating mechanisms	190–200		
Kinetic vs. thermodynamic control	265		
Kohn-Sham equations	48		

L

L-X notation (<i>see</i> Covalent bond classification)			
Lanthanides	495	509–510	
Late transition metal-catalyzed polymerization	505–507		
Leaving group ability	186	220	
Ligands (<i>see individual ligands</i>)			
Definition	1		
Ligand substitution	178–202		
Lindlar catalyst	314	602–603	
Linear low density polyethylene (mLLDPE)	504–505		
Living polymerization	480		

M

Main group chemistry and organotransition metal complexes	96–99		
Mass spectra	165–169		
APCI mass spectra	166	169	
Fragmentation	166–167		

Index Terms

Links

Mass spectra (<i>Cont.</i>)		
Isotope patterns	167–169	
Observing molecular ions	169	
Techniques	166	
Me ₃ N-O	288	625–626
(-)-Menthol	380–383	
5S-MEPY ligand	437	
Mercury		
Cleavage of M-C bond	296–298	
Solvomercuration	279	
Metal-alkyl complexes	136–141	
Agostic	154–155	
Bridging	414–415	
<i>d</i> ⁰	258	292–293
Electrophilic abstraction	290–299	
β-Elimination	139–140	253–259
Metallacycles	140	
Preparation of	138	
Stability of	138–139	
Metal-allyl complexes	104–106	
η ¹ - to η ³ -Rearrangement	106	
Molecular orbital description of	104–105	
Nucleophilic addition to	275–278	280–281
Preparation of	106	
Synthetic applications	280–281	555–567
Metal-carbene complexes	141–145	393 ff
Bonding in	142–145	394–407
Classification	399	
Diazomethane as a reagent for synthesis of	415	
Electrophilic (Fischer)	398	
Fischer	141–145	398–399

Index Terms

Links

Metal-carbene complexes (*Cont.*)

Fischer vs. Schrock (table of characteristics)	399			
Involvement in metathesis	467–473			
Metallacyclobutanes (formation of from carbene complexes)	428	462	466–467	495
Mid- to late-transition metal carbene complexes	430–439			
<i>N</i> -heterocyclic (NHC)	398–399	404–407	416–419	
Nucleophilic (Schrock)	398–399	403		
Reactions of	419 ff			
Electrophilic reactions	426–430			
Nucleophilic reactions	420–426			
Reactive sites	419–420			
Rotation of M=C bond	400			
Schrock	141–142	398–403	409–415	426–420
Synthesis of	407–419			
Synthetic applications of	473–478			
Use in polymerization	478–486			
Metal-carbyne complexes (alkylyl-dynes)	145–148	439–449		
Bonding and structure	146–148	441–443		
Bridging	440			
Fischer	145	439		
Involvement in metathesis	486–489			
Reactions	446–449			
Schrock	145	440		
Synthesis	145–146	442–446		
Metallaboranes	658–662			
Metallacarboranes	658–662			
Metallacumulene complexes	150–151			

Index Terms

Links

Metallacycles	140	209	217	
(<i>see also</i> Cyclometalation)				
Formation in carbene complexes	428	462	466–467	495
In alkyne metathesis	487			
In enyne metathesis	490–491			
Metalloenes	108	113–116	126	
“All-inorganic”	116			
Bonding	109–114			
Catalysts for Ziegler-Natta polymerization	501–505			
Reactions of	115–116			
Metal-metal bonds				
Cluster compounds	467–472			
Electron counting	56–57	662–666		
Metathesis	8	456 ff		
ADMET polymerization	483–486			
Alkene	456–459			
Alkyne	486–492			
Catalysts	467–473			
σ -Complex-assisted (CAM)	508–509			
Cross metathesis (CM)	457–458			
Enyne	489–492			
Industrial uses for	473–486			
Mechanisms for	459–467			
Hérisson and Chauvin (non-pairwise)	462–467			
Pair-wise (diolefin)	460–462			
Sticky olefin hypothesis	464–465			
Ring-opening metathesis polymeriza- tion (ROMP)	478–483			
(<i>see also</i> Polymerization)				

Index Terms

Links

Metathesis (<i>Cont.</i>)			
Sigma bond	507–514		
Methyl acetate, LUMO	422		
Methylmalonyl-CoA	9		
(<i>S</i>)-Metolachlor	378–380		
Stereoisomers	379		
Xyliphos (Josiphos) ligand	380		
Microscopic reversibility			
principle	226	235	
Migratory insertion involving carbonyls			
(<i>see also</i> 1,1-Insertion)	245–253		
Molecular mechanics (MM)	43–44	49	
Use in bite angle calculation	44	335	
Molecular orbital theory	17 ff		
Alkenes	34	104	
Allyl	34–36	273	277
Atomic orbital interactions	17–20		
Bond order	22		
Butadiene	34	36–37	273
Carbonyl ligands	24–25	76	81
C-C activation	216		
C-H activation	211		
CO ₂	31–34		
Cr(CO) ₆	64–68		
Cyclic π ligands	33 ff		
C ₃ H ₃	40–41		
C ₄ H ₄	39–40		
C ₅ H ₅	41	109–114	
C ₆ H ₆	40–42		
C ₇ H ₇	51–52		
C ₈ H ₈	40	106–107	

Index Terms

Links

Molecular orbital theory (*Cont.*)

Cyclopentadienyl	41	109–114	
Diatomic molecules	23–29		
Dihydrogen	21–22	153	
Dioxygen	23–24		
Ferrocene	108–113		
Group orbitals	29 ff		
H ₃ ⁺	29–31	37–39	
HOMO and LUMO	186–187	272–276	
Metal-carbene complexes	143	401–403	
Metal-carbyne complexes	146	442–443	
MO diagrams	18 ff		
N ₂	76		
NO ligands	89–90		
Nonbonding molecular orbitals	20	30	
Pi molecular orbitals	19	23	34 ff
Procedure for generating molecular orbitals	21 ff		
Sigma bond metathesis	511		
Sigma molecular orbitals	16–18		
Multiple-decker sandwich compounds	2	127	
Myxalamide A	598–599		

N

Naproxen synthesis	571–572		
Natural bite angle (<i>see</i> Bite angle)			
Negishi cross coupling	607–613		
Further developments	610–613		
Mechanism	608		
Scope	607–608		

Index Terms

Links

Negishi cross coupling (<i>Cont.</i>)				
Synthesis applications	608–610			
Neopentyl ligands	411–412			
Nerol	537			
<i>N</i> -heterocyclic carbene (NHC) complexes	398–399	404–407	416–419	
Synthesis	416–419			
Ni(CO) ₄	5	75	84	91
Nickelocene [(η ⁵ -Cp) ₂ Ni]	114–115			
Nineteen-electron complexes				
substitution of	201–202			
Nobel Prize in Chemistry	7–9	359	459	493
	535	546	640	
NO (nitrosyl) ligands	89–92			
Bent vs. linear	90–91			
Bonding	89–91			
Bridging	91			
Electron counting	89–90			
IR spectrum	91			
Related ligands (NS, NSe)	91–92			
Norbornene (polymerization of)	481–482			
Nuclear magnetic resonance				
spectroscopy	127–132			
Carbon-13	128–129			
Chemical shift values	129–130			
Fluxional processes	130–132			
Karplus relation	225			
Phosphorus-31	160			
Proton	129–130			
Temperature-dependent	130–131			
<i>trans</i> -Influence	180–181			

Index Terms

Links

Nucleophilic metal-carbene				
complexes	399	426–430		
Nucleophilic reactions on				
ligands	115	267–289		
Abstraction	285–289			
Addition	267–285			
Carbonyl ligands	269–270			
DGM rules for predicting				
reactivity	270–277			
Influence of force constants on				
selectivity	274–275			
Metal carbene complexes	269–270			
On alkenes	278–280			
On allyl complexes	275–277	280–281		
On arenes	281–285			
On polyenes	270–274			
Oxidatively-driven abstraction	285–286			
Regiochemistry	270–285			
Stereochemistry	275–282	285–286		

O

Octahedral complexes	64–69			
Olefin (<i>see</i> Alkenes)				
Definition	456			
Olefin Conversion Technology (OCT)	457	474		
Oligomers	474	492	496	505
Open (vacant) coordination site	266			
Oppolzer cyclization	619–622			
Orbitals				
Antibonding	18–20			
Atomic	13–16			

Index Terms

Links

Orbitals (<i>Cont.</i>)		
Bonding	18	
Molecular	17 ff	
Nonbonding	20	
Potential energy	26	
Organoaluminum reagents	611	
Organocopper reagents (Gilman reagents)	262	
Organolanthanide chemistry (<i>see</i> Lanthanides)		
Organolithium reagents	137–138	141
Organomagnesium reagents (<i>see also</i> Grignard reagents)	5–6	202–203
Organotin reagents	588–589	
Organozinc reagents	607–608	
Oxidation (<i>see</i> Pd-catalyzed oxidation)		
Oxidation state	54	60
Oxidative addition (OA)	202–226	
Addition of C-C	215–218	
Addition of C-H	209–215	
Addition of H-H	204–208	
Addition of halogens	219	
Addition of R-X	219–222	
Binuclear	203	
Intramolecular	203	
Pathways, table of	226	
Polar	219–222	
Radical mechanism	222–226	
Substitution (S _N 2) mechanism	219–222	
Stereochemistry	208	219–225
Three-center mechanism	204–218	

Index Terms

Links

Oxidative cleavage of M-C bonds	285–286			
Oxidative cyclization	550–555			
Oximidine II	599			
Oxophilic species	252			
Oxo reaction (<i>see also</i> Hydroformylation)	322			
Oxymercuration (solvomercuration)	279			
P				
Palytoxin	598			
Paramagnetic	23–24			
Parkinson's disease	359			
Pauli Exclusion Principle	15	27–28	48	
Pauson-Khand reaction	623–628			
Asymmetric	627–628			
Catalytic	626–628			
Intermolecular	623–625			
Intramolecular	625–628			
Pd-catalyzed oxidation	547–555			
Asymmetric	548–552			
Cyclization	550	553–555		
Green aspects	547			
Oxidation of secondary alcohols	547–550			
Wacker-type	552–555			
Pentamethylcyclopentadienyl (Cp*) ligand	107			
Petasis reagent (dimethyltitanocene)	429–430			
Pfaltz (PHOX) ligands	543–545	561	563	566

Index Terms

Links

Phase transfer catalyst	579			
Phenonium ion	293–296			
Pheromone synthesis	476			
Phosphine ligands	155–160			
(see also DIPHOS, Diphosphine ligands)				
Bidentate	335–338			
Bonding	155–157			
Chiral	529			
Cone angle (θ)	157–159			
Electron-donating properties	155			
Electronic effects (χ factor)	159–160			
Involvement in				
hydroformylation	330–338			
P-31 NMR	160			
Photochemical reactions	85	252	307	388
	415	431	625	
PHOX ligands	543–544	561	563	566
Pi-bond metathesis	456 ff			
(see also Metathesis for detailed subcategories)				
Pi ligand complexes	103 ff			
Bonding (see particular ligand)				
Chemistry of (see Chapters 8 and 11)				
Pincer ligands	217–218	269		
Polyene (<i>odd, even, open closed</i>)	270–272			
Polyethylene (PE)	492			
Polyethylene glycol (PEG)	607			
Polymerization	478–486	492 ff		
Alkene (see Ziegler-Natta polymerization)				
Block	480–481			
Dicyclopentadiene (DCPD)	483			

Index Terms

Links

Polymerization...(Cont.)

Living	480–481		
Ring-opening metathesis (ROMP)	478–483		
Tacticity	481–482	500–505	
Using late transition metal (Brookhart) catalysts	505–507		
Ziegler-Natta	9	492–505	
Polypropylene (PP)	9	492–493	500–504
Prostaglandin E ₂ (1,15-lactone)	489–490		
Protection-deprotection in organic synthesis	588		
Pseudohalogen	97		
Pseudotetrahedral Fe complexes	250–251		

Q

Quantum numbers	14–15		
-----------------	-------	--	--

R

Racemization	224	291	
Radical pathways (in oxidative addition)	222–226		
Chain	223		
Non-chain	223	225–226	
Stereochemical test for Rapamycin	224–225		
Stereochemical test for Rapamycin	594–595		
<i>re</i> and <i>si</i> terminology	502–503		
Reaction types	177		
Reductive elimination (RE)	226–237		
C-C elimination	228–234		
(<i>see also</i> Cross coupling reactions)			

Index Terms

Links

Reductive elimination (RE) (*Cont.*)

C-H elimination 235–236

Dinuclear 236–237

Mechanism of 228–234

Stereochemistry of 228–234

Regiochemistry

In electrophilic and nucleophilic reactions at ligands 272–280 281–285

In hydroformylation 335–339 570–574

Regioselectivity 313–314

Resolution of enantiomers 525

Rh(PPh₃)₃Cl (Wilkinson's compound) 70 353–354

Ring-closing metathesis (RCM) 458 471 473 477

485–486 489–490

Ring fusion 122

Ring-opening metathesis (ROM) 458

Ring-opening metathesis polymerization (ROMP) 458 470–471 478–486

(*see also* Polymerization)

Ring whizzers 131–132

Ru₆C(CO)₁₇ 666

S

Sandwich compounds 1–2 7 108 119

126–127

Schrock carbene complexes 141–142 396–397

(*see also* Metal-carbene complexes;

Nucleophilic metal-carbene complexes)

Schrödinger wave equation 13–15 45

Schwartz' reagent [Zr(η⁵-Cp)₂(H)(Cl)] 258–259

Index Terms

Links

Scorpionate ligand	299–300			
Tp (hydridotris(pyrazoyl)borate)	299–300	509		520
Tp* (hydridotris(3,5-dimethylpyrazoyl) borate)	299–300			
Selenocarbonyl complexes	87–88			
Semibridging CO complexes	82			
Semi-empirical MO theory	45–46	49		
Seventeen electron complexes	200–202			
Sharpless-Katsuki asymmetric epoxidation	545–546			
Shell Higher Olefin Process (SHOP)	473–475			
Shell hydroformylation process (phosphine-modified hydroformylation)	330–331			
1,2-Shifts (CO insertion)	9	245–253		
Sigma bond metathesis Intramolecular Mechanism MO diagram for	211 513 508–511 511	507–514		
Sigmatropic shifts	383			
Singlet state	395			
Sixteen electron complexes	69–71			
Slippage in π ligands	189	279		
S _E 2 reaction	262	290–291		
S _N 1 reaction	179	185	191	194
S _N 2 reaction	178–179	184	187	291
SO ₂ insertion Stereochemistry	264–267 265–266			
Solvents as ligands	199–200	230	355	358
Solvomercuration (oxymercuration)	279			

Index Terms

Links

Sonogashira cross coupling	601–607		
Further developments	606–607		
Mechanism	603–605		
Scope	601–602		
Synthesis applications	605–606		
Specialty (fine) chemicals	375–385		
Ibuprofen	376–378		
(-)-Menthol	380–384		
(S)-Metolachlor	378–380		
Square planar complexes	69–71		
Stability of alkyls	139–141		
Stannanes	588–589		
Steady state approximation	190–191	197–198	
Stereochemical isotope effect	497–498		
Stereochemical probes	224–225	250	257
Stereochemistry (<i>see reaction type, e.g.</i> Insertion)			
Stereogenic center (stereocenter, stereo- genic atom)	290		
Stereorandomization	225	290	
Stereoselectivity	314		
Steric effects (cone angle)	157–159		
Stille cross coupling	587–595		
Mechanism	589–592		
Scope	588–589		
Synthesis applications	592–595		
Succinyl-CoA	9		
<i>O</i> -Sulfinate	264–265		
<i>S</i> -Sulfinate	264–265		
Sulfur dioxide insertion (<i>see SO₂ insertion</i>)			

Index Terms

Links

Suzuki cross coupling	595–601		
Further developments	600–601		
Mechanism	596–597		
Scope	595–596		
Synthesis applications	598–600		
Symmetry and number of IR stretching bands	93–95		
Syndiotactic polymers (<i>see also</i> Ziegler-Natta polymerization)	9	482	500–505
Synthesis gas (H ₂ /CO)	325	361	
T			
<i>t</i> _{2g} orbital	65–66		
T vs. Y geometry (in reductive elimination)	228		
Tacticity of polymers	481–482	500–504	
Takasago process for (-)-menthol synthesis	380–381		
Tebbe's Reagent [Ti(η ⁵ -Cp) ₂ (μ-CH ₂)(μ-Cl) AlMe ₂]	414–415		
Structure	415		
Use in organic synthesis	428–429		
Use in polymerization	470	480	
Tellurocarbonyl complexes	87–88		
Terpenes	384	593	626
Tetrahedral complexes	67–70		
Thalidomide	525		
Thiocarbonyl complexes	87–88		
Thionitrosyl ligand	91–92		
<i>Threo</i>	224	257	
[Ti(η ⁵ -P ₅) ₂] ²⁻	116		

Index Terms

Links

Tolman χ factor	159–160			
tppts ligand (triphenylphosphinesulfonate)				
ligand	334			
<i>trans</i> Effect	179–184	442		
Kinetic <i>trans</i> effect	181–182			
<i>trans</i> Influence	179–181			
Transition metal complex analogs	96–99			
Transition state theory	185			
Transmetalation	584–587			
Electronegativity and	585–586			
Use in organic synthesis	587 ff			
<i>TRANS</i> PHOS ligand	231–232			
Triflate (OSO ₂ CF ₃)	214			
As leaving group	214			
Use in cross coupling	575	591	594–595	
Use in Heck reaction	575–577			
Trigonal bipyramid geometry	67	181–182	187–188	195
	219	233		
Trigonal prismatic geometry	139			
Trimethylamine- <i>N</i> -oxide	288	625–626		
Triolefin process	457			
Triple decker sandwich compounds	2	127		
Triplet state	395			
Tropylium (C ₇ H ₇) complexes	51	123–124	271	
Trost ligands	560–561			
Tsuji-Trost reaction	280–281	556–567		
Asymmetric version	559–563			
Creation of quaternary centers	563–567			
Mechanism	555–559			
Turnover frequency (TOF)	312			
Turnover in catalysis	312			

Index Terms

Links

Turnover number (TON)

312

U

Umpolung

267

281

Uranocene $[(\eta^8\text{-COT})_2\text{U}]$

125–126

V

$\text{V}(\text{CO})_6$

192

200–201

Vacant coordination site

246–248

254

Valence orbital potential energy

26

Vaska's compound $[\text{Ir}(\text{PPh}_3)_2(\text{CO})\text{Cl}]$

204–207

Vinyl-metal complexes

140

Vinylidene-metal complexes

150–151

(see also Metallacumulene complexes)

Vitamin B₁₂ coenzyme

9–10

W

Wacker Chemie (Wacker-Smidt) oxidation

process

340–350

Catalytic cycle

343

Industrial significance

340–341

Mechanism

342–350

Stereochemistry

346–348

Synthesis applications

341

553

Theoretical studies

348–350

Wade's rules

654–655

662–663

(see also Cluster compounds, Electron counting in)

Water Gas Shift (WGS) Reaction

269

311

366

Wilkinson's catalyst $[\text{Rh}(\text{PPh}_3)_3\text{Cl}]$

70

204

Index Terms

Links

Wittig reagents (*see* Ylides)

X

Xyliphos (Josiphos) ligand 380

Y

Ylides 403 413

- Comparison with nucleophilic carbene complexes 403 426
- Comparison with Tebbe's reagent 428–430
- Use in synthesis of alkylidenes 431–432
- Use in synthesis of alkylidynes 444–445

Z

Zeise's salt, $K[Pt(\eta^2-CH_2=CH_2)C_{13}]XH_2O$ 4 103–104

Ziegler-Natta polymerization 9 492–505

- Catalysts for 492–493 501–505
- Cossee mechanism 495
- Green-Rooney mechanism 495
- Grubbs' stereochemical isotope experiment 497–500
- Industrial importance 492–493
- Metallocene catalysts 501–505
- Modified Cossee mechanism 500
- Stereoregular polymers (atactic, isotactic syndiotactic, etc.) 500–505

Index Terms

Links

Zr(η^5 -Cp)₂(H)(Cl) (Schwartz' reagent)

258–259